Nenad Blau · Marinus Duran · K. Michael Gibson
Editors

Laboratory Guide to the Methods in Biochemical Genetics

CD-ROM
INCLUDED

Springer

Nenad Blau · Marinus Duran
K. Michael Gibson

Laboratory Guide to the Methods in Biochemical Genetics

Foreword by C. R. Scriver

With 176 Figures and 113 Tables

Springer

Nenad Blau
Division of Clinical Chemistry
and Biochemistry
University Children's Hospital
Steinwiesstrasse 75
8032 Zurich
Switzerland
E-mail: nenad.blau@kispi.unizh.ch

Marinus Duran
Academic Medical Centre
Laboratory Genetic Metabolic Diseases
University Amsterdam
Meibergdreef 9
1105 AZ Amsterdam
The Netherlands
E-mail: m.duran@amc.nl

K. Michael Gibson
Biochemical Genetics Laboratory
University of Pittsburgh Medical Center
and Children's Hospital of Pittsburgh
Rangos Research Building Room 2111
Pittsburgh, PA 15213
USA
E-mail: michael.gibson@chp.edu

ISBN 978-3-540-76697-1 e-ISBN 978-3-540-76698-8

Library of Congress Control Number: 2008925138

Cover design: Frido Steinen-Broo, eStudio Calamar, Spain
Production: le-tex publishing services oHG

Printed on acid-free paper

9 8 7 6 5 4 3 2 1

springer.com

Foreword

This book, which is authored by numerous authorities, presents as a stand-alone handbook for those working in the field of human biochemical genetics. It is a far cry from the day when there were rather simple descriptions of "side room tests", as Garrod called them.

Garrod recognized patients in whom there were disruptions of dynamic biochemistry, that is of pathways, as we now know them. He also recognized that the disruption could be inherited; hence his descriptive term "inborn errors of metabolism". Garrod used his tests to reveal "chemical individuality", a theme that dominated his writing and thinking throughout his lifetime. Garrod described chemical phenotypes as they were revealed in his patients with inborn errors of metabolism. Garrod's observations introduced a new paradigm in medical thinking.

The range and sophistication of the methods used to describe the chemical phenotype at the beginning of the 21st century are very different from those that were available to Garrod at the beginning of the 20th century. This new book describes a spectrum of tests, from simple screening methods that we could all do, to analytical methods that are dependent on technologies that very few of us will ever use.

Behind the chemical phenotype is a "biochemical phenotype". The latter describes disorder in a dynamic function; any function that modifies a molecule or moves it from here to there. How to measure a function that can be disrupted by a mutant gene is an important part of this laboratory guide.

The present laboratory guide goes beyond the chemical phenotype, beyond the biochemical phenotype, to examine the genotype, where instructions to maintain normal biochemical function and the normal metrical trait values begin. In my own experience, for example, I have witnessed the power of methods that can identify a novel chemical phenotype by chromatography, then confirmed the corresponding biochemical phenotype by using the appropriate functional analysis, and finally revealed the actual mutant allele in the gene in question.

Authors of this book, and certainly many of its readers, will recall the series called "Methods in Enzymology"; this laboratory guide could become a counterpart. In the post-genome era, when one can talk about the metabolome and the phenome, or refer to networks, nodes, hubs, edges and exemplars, it is likely that this laboratory guide only begins to describe the methods we will soon be using in human biochemical genetics. And surely we will need to have colleagues who can create the mathematical models and algorithms to describe the complexity of the phenotype.

Last, but not least, there is always the need for interpretation of results and assessment of outcomes, particularly now that tandem mass spectrometry is increasingly embedded in newborn screening. This laboratory guide serves the expertise upon which interpretation depends. Accordingly, the correct use of a laboratory guide is certain to be multidisciplinary, and at the end of the inquiry and analysis, one will know better why this person has this disease, now.

Charles R. Scriver

Preface

Experienced chefs may harbor several recipes for delicious entrees in their memory banks. The rest of us, who cook either for enjoyment or sustenance, often follow recipes, where lists of ingredients are meticulously described, accompanied by details for mixing and baking that are key to a successful outcome. Which of us hasn't realized that the omission of one small item such as baking powder can lead to a very "flat" cake? We learn that adherence to the recipe is the key to good results, and this is the basis of the usefulness of "cookbooks."

So follows the current tome entitled "Laboratory Guide to the Methods in Biochemical Genetics". The last methodology-driven book on this subject was edited by Dr. Frits Hommes in 1991, a comprehensive and well-referenced manual that is found in the laboratories of most biochemical geneticists and clinical biochemists. While a stalwart in the laboratory, Hommes' tome has become dated due to methodological advances and the addition of high-throughput, high-sensitivity equipment. The current endeavor is geared to fill the "methodological" gap in laboratory techniques that has developed over the last several years. Together with two previous books "Physician's Guide to the Diagnosis of Metabolic Diseases" and "Physician's Guide to the Treatment and Follow-Up of Metabolic Diseases", this book completes the trilogy.

In recent years, biochemical genetics has witnessed enhanced exposure as a laboratory discipline because of the advent of expanded newborn screening around the world. Sample numbers in most biochemical genetics laboratories are growing because of the required evaluation of positive newborn screening results. Accordingly, it is in everyone's interest (physician, patient, metabolic specialist, and other healthcare providers) that biochemical genetics laboratories have the most up-to-date methods available on their test menu.

The editors of this new book have thereby attempted a compilation of laboratory tests that will be useful in most laboratories. Each chapter has been developed by experts, with the goal of making each chapter "self-sufficient." The utility of such a structure will prevent the need to reference other technique papers, enabling a more rapid implementation of techniques in the laboratory. The majority of methods in biochemical genetics are labor-intensive and complex, especially when compared to the automated testing laboratory, and therefore a laboratory-based compendium should be a useful and valuable adjuvant. This has been our goal in compiling this edition.

To those of our readers and colleagues who are well-versed in the biochemical genetics laboratory, we hope that this book will serve to augment already established protocols or to fill gaps in the test menu. To others just starting a laboratory, we wish you happy biochemical cooking!

Nenad Blau
Marinus Duran
K. Michael Gibson

Contents

List of Contributors

Nico G.G.M. Abeling
Academic Medical Center
Laboratory Genetic Metabolic Diseases
Meibergdreef 9
1105 AZ Amsterdam
The Netherlands
Email: n.g.abeling@amc.nl

Johannes M.F.G. Aerts
Department of Biochemistry
Academic Medical Center
K1-157 Meibergdreef 9
NL1105 AZ Amsterdam
The Netherlands
Email: j.m.aerts@amc.nl

Matthias Baumgartner
Division of Metabolism and Molecular Pediatrics
University Children's Hospital
Steinwiesstrasse 75
8032 Zurich
Switzerland
Email: matthias.baumgartner@kispi.zh.ch

Nenad Blau
Division of Clinical Chemistry and Biochemistry
University Children's Hospital
Steinwiesstrasse 75
8032 Zurich
Switzerland
Email: nenad.blau@kispi.zh.ch

Jim R. Bonham
Department of Clinical Chemistry
Sheffield Children's Hospital
Western Bank
Sheffield, S10 2TH
UK
Email: jim.bonham@sch.nhs.uk

Nils Bosshard
Division of Metabolism and Molecular Pediatrics
University Children's Hospital
Steinwiesstrasse 75
8032 Zurich
Switzerland

Donald H. Chace
Pediatrix Analytical
Center for Pediatrix/Obstetrix
Research and Education
Pediatrix Medical Group
P.O. Box 559001
Ft. Lauderdale
FL 33355-9001
USA
Email: donald_chace@pediatrix.com

Katrina M. Dipple
Departments of Human Genetics and Pediatrics
David Geffen School of Medicine at UCLA
Gonda Center 5506B
695 Charles E. Young Drive South
Los Angeles, CA 90095-7088
USA
Email: kdipple@mednet.ucla.edu

Marinus Duran
Laboratory Genetic Metabolic Diseases
Academic Medical Center
University of Amsterdam
P.O. Box 22700
1100 DE Amsterdam
The Netherlands
Email: m.duran@amc.nl

Udo F.H. Engelke
Laboratory of Pediatrics and Neurology
University Medical Centre Nijmegen
Institute of Neurology
Reinier Postlaan 4
6525GC Nijmegen
The Netherlands

Giorgio Federici
Department of Laboratory Medicine
University Hospital "Policlinico Tor Vergata"
via Oxford 81
00133 Roma
Italy
Email: giorgio.federici@uniroma2.it,
giorgio.federici@ptvonline.it

Brian Fowler
UKBB Kinderspital
Stoffwechsellabor
Römergasse 8
4005 Basel
Switzerland
Email: brian.fowler@unibas.ch

K. Michael Gibson
Division of Medical Genetics
Departments of Pediatrics and Pathology
Children's Hospital Pittsburgh
University of Pittsburgh School of Medicine
Rangos Research Center, Room 2111
Pittsburgh, PA 15213
USA
Email: michael.gibson@chp.edu

Simon J.R. Heales
Neurometabolic Unit
National Hospital and Institute of Neurology (UCL)
National Hospital
Queen Square
London WC1N 3BG
UK
Email: sheales@ion.ucl.ac.uk

Martin Hersberger
Division of Clinical Chemistry and Biochemistry
University Children's Hospital Zurich
Steinwiesstrasse 75
8032 Zurich
Switzerland
Email: martin.hersberger@kispi.uzh.ch

Cornelis Jakobs
VU University Medical Center
Clinical Chemistry, Metabolic Unit
P.O. Box 7057
1007 MB Amsterdam
The Netherlands
Email: c.jakobs@vumc.nl

Bart Janssen
Univeristy of Heidelberg
Department of Human Genetics
Im Neuenheimer Feld 366
69120 Heidelberg
Germany

Erwin E.W. Jansen
VU University Medical Center
Clinical Chemistry, Metabolic Unit
P.O. Box 7057
1007 MB Amsterdam
The Netherlands

Christian Körner
Universitäts-Kinderklinik
Abteilung I
Im Neuenheimer Feld 153
69120 Heidelberg
Germany
Email: christian.koerner@med.uni-heidelberg.de

Jürgen Lübbehusen
Universitäts-Kinderklinik
Abteilung I
Im Neuenheimer Feld 153
69120 Heidelberg
Germany

Zoltan Lukacs
Department of Pediatrics
University Hospital of Hamburg
Metabolic Laboratory
Martinistraße 52
20246 Hamburg
Germany
Email: lukacs@uke.uni-hamburg.de

Dietrich Matern
Division of Laboratory Genetics
Departments of Laboratory Medicine and Pathology
Medical Genetics, and Pediatric and Adolescent Medicine
Mayo Clinic College of Medicine
200 First Street SW
Rochester, MN 55902
USA
Email: matern@mayo.edu

Edward R.B. McCabe
Department of Pediatrics
David Geffen School of Medicine at UCLA
10833 LeConte Ave
Los Angeles, CA 90095-1752
USA
Email: emccabe@mednet.ucla.edu

Elisabeth Minder
Stadtspital Triemli
Chemie Zentrallabor
8000 Zurich
Switzerland
Email: elisabeth.minder@triemli.stzh.ch

Thomas Opladen
Zentrum für Kinder- und Jugendmedizin Heidelberg
Im Neuenheimer Feld 153
69120 Heidelberg
Germany
Email: thomas.opladen@med.uni-heidelberg.de

R.J. Pollitt
UK Cystic Fibrosis Screening Programme
Children's Hospital
Western Bank
Sheffield, S10 2TH
UK
Email: rodney.pollitt@sch.nhs.uk

Ben J.H.M. Poorthuis
Department of Medical Biochemistry, K1
University of Amsterdam
Meibergdreef 9
1105 AZ Amsterdam
The Netherlands
Email: b.j.poorthuis@amc.uva.nl

Piero Rinaldo
Biochemical Genetics Laboratory – Hilton 360C
Division of Laboratory Genetics
Department of Laboratory Medicine and Pathology
Mayo Clinic College of Medicine
200 First Street SW
Rochester MN 55905
USA
Email: rinaldo@mayo.edu

Lucia Rohner
Institute of Clinical Chemistry
University Hospital Zurich
Raemistrasse 100
8091 Zurich
Switzerland

Pierre Rustin
INSERM U676
Hopital Robert Debre
48, Boulevard Serurier
75019 Paris
France
Email: rustin@rdebre.inserm.fr

X. Schneider-Yin
Stadtspital Triemli
Chemie Zentrallabor
8000 Zurich
Switzerland

Adrian C. Sewell
Zentrum der Kinderheilkunde
JWG Universität Frankfurt
Theodor-Stern-Kai 7
60596 Frankfurt
Germany
Email: adrian.sewell@kgu.de

Cedric Shackleton
Children's Hospital
Oakland Research Institute
5700 Martin Luther King Jr Way
Oakland, CA 94609
USA
Email: cshackleton@chori.org

Beat Steinmann
Division of Metabolism and Molecular Pediatrics
University Children's Hospital
Steinwiesstrasse 75
8032 Zurich
Switzerland
Email: beat.steinmann@kispi.unizh.ch

Eduard A. Struys
VU University Medical Center
Clinical Chemistry, Metabolic Unit
P.O. Box 7057
1007 MB Amsterdam
The Netherlands
Email: e.struys@vumc.nl

Terttu Suormala
UKBB Kinderspital
Stoffwechsellabor
Römergasse 8
4005 Basel
Switzerland
Email: terttu.suormala@ukbb.ch

Christian Thiel
Universitäts-Kinderklinik
Abteilung I
Im Neuenheimer Feld 153
69120 Heidelberg
Germany

Beat Thöny
Division of Clinical Chemistry and Biochemistry
University Children"s Hospital
Steinwiesstrasse 75
8032 Zurich
Switzerland
Email: beat.thony@kispi.unizh.ch

Arno van Cruchten
Academic Medical Centre
Laboratory Genetic Metabolic Diseases
Meibergdreef 9
1105 AZ Amsterdam
The Netherlands

André B.P. van Kuilenburg
Academic Medical Centre
Laboratory Genetic Metabolic Diseases
Meibergdreef 9
1105 AZ Amsterdam
The Netherlands
Email: a.b.vankuilenburg@amc.nl

Anne J. Vassault
Laboratoire de Biochimie B
Hopital Necker Enfants Malades
149 Rue de Sevres
75015 Paris
France
Email: anne.vassault@nck.ap-hop-paris.fr

Nanda Verhoeven-Duif
Department of Metabolic and Endocrine Diseases
University Medical Center Utrecht, KC 02 069.1
Lundlaan 6
3584 EA Utrecht
The Netherlands
Email: n.verhoeven@umcutrecht.nl

Frans W. Verheijen
Department of Clinical Genetics
Erasmus MC
PO Box 1738
3000 DR Rotterdam
The Netherlands
Email: f.verheijen@erasmusmc.nl

Arnold von Eckardstein
Institute of Clinical Chemistry
University Hospital Zürich
Raemistrasse 100
8091 Zurich
Switzerland
Email: arnold.voneckardstein@usz.ch

Mirjam M.C. Wamelink
Metabolic Laboratory
Department of Clinical Chemistry
VU University Medical Center
De Boelelaan 1117
1081 HV Amsterdam
The Netherlands
Email: m.wamelink@vumc.nl

Ronald J.A. Wanders
University Hospital Amsterdam
Department of Pediatrics and Clinical Chemistry
AMC
Meibergdreef 9
1105 AZ Amsterdam
The Netherlands
Email: r.j.wanders@amc.nl

Hans Waterham
Academic Medical Centre
Laboratory Genetic Metabolic Diseases
Meibergdreef 9
1105 AZ Amsterdam
The Netherlands
Email: h.r.waterham@amc.nl

Ron A. Wevers
Laboratory of Pediatrics and Neurology
University Medical Centre Nijmegen
Institute of Neurology
Reinier Postlaan 4
6525GC Nijmegen
The Netherlands
Email: r.wevers@cukz.umcn.nl

Johannes Zschocke
University Heidelberg
Department of Human Genetics
Im Neuenheimer Feld 366
69120 Heidelberg
Germany
Email: johannes.zschocke@med.uni-heidelberg.de

Abbreviations

^{1}H NMR	proton nuclear magnetic resonance
2-AB	2-aminobenzamide
3α5β	3α-hydroxy-5βH
3-MD	3-methyldopa
3OHB	3-hydroxybutyrate
4-MU	4-methylumbelliferone
5α-RD-2	5α-reductase-2
5αTHF	5α-tetrahydrocortisol
5HIAA	5-hydroxyindoleacetic acid
5-OH-Me-ura	5-hydroxymethyluracil
5PD	5-pregnene-3β,20α-diol
5PT	5-pregnene-3β,17α,20α-triol
7DHC	7-dehydrocholesterol
7DHPT	5β-pregn-7-ene-3α,17α,20α-triol
8DHPT	5β-pregn-8-ene-3α,17α,20α-triol
18-oxo-THF	18-oxo-tetrahydrocortisol
6-MPH$_4$	6-methyltetrahydropterin
17HP	17α-hydroxypregnenolone
17-OHP	17-hydroxyprogesterone
18-OHF	18-hydroxycortisol
18-OH-THA	18-hydroxytetrahydro-11-dehydrocorticosterone
AA	arachidonic acid
AAA	amino acid analyzer
AADC	aromatic amino acid decarboxylase
AASA	α-aminoadipic semialdehyde
AA-TLC	amino acid thin layer chromatography
ABCA1	ATP-binding cassette transporter A
ABL	abetalipoproteinemia
ACAC	acetoacetate
ACRS	amplification-created restriction site
ACTH	adrenocorticotrophic hormone
AdoHcy	S-adenosylhomocysteine
AdoMet	S-adenosylmethionine
AGAT	L-arginine:glycine amidinotransferase
AIP	acute-intermittent pophyria
ALAD	δ-aminolevulinate dehydratase

ALAS	δ-aminolevulinic acid synthese
ALD	adrenoleucodystrophy
ALD	aldehyde dehydrogenase
AME	apparent mineralocorticoid excess syndrome
AMACR	2-methyl acyl-CoA racemase
AMN	adrenomyeloneuropathy
An	androsterone
APCI	atmospheric pressure chemical ionization
apoA-1	apolipoprotein A1
apoA-IV	apolipoprotein AIV
apoB100	apolipoprotein B-100
apoC	apoliprotein C
apoCII	apolipoprotein CII
ApoC-III	apolipoprotein C III
ApoE	apolipoprotein E
ApoE2	apolipoprotein E-2
APPI	atmospheric pressure photoionization
AR	aldose reductase
ASA	argininosuccinate
BAs	bile acids
BE	Bond-Elut
BH_2	7,8-dihydrobioperin
BH_4	tetrahydrobiopterin
BME	2-mercaptoethanol
bp	base pairs
B-PABA	biotinyl-p-aminobenzoic acid
Br-AMN	2-bromoacetyl-6-methoxynaphthalene
BSA	bovine serum albumin
BSTFA	N,O,-bis-(trimethylsilyl)trifluoroacetamide
CA	cholic acid
CAH	congenital adrenal hyperplasia
CACT	carnitine acylcarnitine translocase
CDCA	chenodeoxycholic acid
CDG	congenital disorders of glycosylation
CDPX2	Conradi-Hunermann syndrome
CE	capillary electrophoresis
CEP	congenial erythropoitic prophyria
CER	cholesterol esterification rate
CETP	cholesteryl ester transfer protein
CFD	cerebral folate deficiency
CMP	cytidine-5'-monophosphate
CNS	central nervous system
COMT	catechol-O-methyltransferase
CPA UK	UK Clinical Pathology Accreditations
CPC	cetylpyridinium chloride
CPT-I	carnitine palmitoyltransferase type I
CPT-II	carnitine palmitoyltransferase type II
Cr	creatine
CR	carbonyl reductase

CSF	cerebrospinal fluid
CTX	cerebrotendinous xanthomatosis
CV	coefficient of variance
d_2CDCA	[11,12-d_2] chenodeoxycholic acid
D_2O	deuterium oxide
DABCO	1,4-diazabicyclo(2,2,2)octane
DCA	deoxycholic acid
DEAE	diethylaminoethyl
DGGE	denaturing gradient gel elecrophoresis
DHA	docosahexaenoic acid
DHA-P	dihydroxyacetone phosphate
DHB	2,5-dihydroxybenzoic acid
DHCA	dihydroxycoprostanic acid
DHCR7	7-dehydrocholesterol reductase
DHEA	dehydroepiandrosterone
DHPLC	denaturing high-pressure liquid chromatography
DHPR	dihydropteridine reductase
DHT	dihydrotestosterone
DMAB	dimethyl-aminobenzaldehyde
DMB	1,9-dimethylene blue
DMEM	Dulbecco`s Modified Eagle Medium
DMG	N,H-dimethylglycine
DMSO	dimethyl sulfoxide
DNPH	dinitrophenylhydrazine
DOC	deoxycorticosterone
DRD	dopa-responsive dystonia
DTE	dithioerythriol
DTNB	dithionitrobenzoic acid
DTPA	diethylenetriaminepentaacetic acid
DTT	dithiothreitol
ECL	enhanced chemiluminescence
EDTA	ethylenediaminetetraacetic acid
EIC	extracted-ion chromatogram
ELISA	enzyme-linked immunosorbent assay
ELSD	evaporative light scattering detector
EPA	eicosapentaenoic acid
EQA	external quality assurance
ERNDIM	European Research Network for evaluation and improvement of screening, Diagnosis and treatment of Inherited disorders of Metabolism
ES	electrospray
ESI	electrospray ionization
Et	etiocholanolones
F-1,6-P	D-fructose 1,6-6 bisphosphate
F-1-P	D-fructose-1-phosphate
F-6-P	fructose-6-phosphate
FAO	fatty acid β-oxidation
Fb	fibroblasts
FCS	fetal calf serum

FDB	familial defective apolipoprotein B-100
FH	familial hypercholesterolemia
FHBL	familial hypobetalipoproteinemia
FIGLU	formiminoglutamate
FRET	fluorescence resonance energy transfer
G-3-P	glycerol-3-phosphate
G-6-P	glucose-6-phosphate
G6-PDH	glucose-6-phosphate dehydrogenase
GABA	gamma-aminobutryc acid; 4-aminobutyric acid
GABA-T	GABA-transaminase
Gal-DH	galactose dehydrogenase
GALT	galctose-1-phosphate uridyltransferase
GAMT	guanidinoacetate methyltransferase
GC	gas chromatography
GCA	glycocholic acid
GC-EI-MS	gas chromatography coupled with electron impact ionization mass spectrometry
GC/FID	gas chromatography with flame ionization detection
GCDCA	glycochenodeoxycholic acid
GC-MS	gas chromatography-mass spectrometry
GDCA	glycodeoxycholic acid
GDH	α-glycerophosphate dehydrogenase
GEMO	glycerol-ether-monooxygenase
GK	glycerol kinase
GKD	glycerol kinase deficiency
GLCA	glycolithocholic acid
GRA	glucocorticoid remediable aldosteronism
GSD	glycogen storage disease
GTP	guanosine triphosphate
GTPCH	GTP cyclohydrolase I
GUDCA	glycoursodeoxycholic acid
H_2NTP	7,8-dihydroneopterin triphosphate
H6PDH	hexose-6-phosphate dehydrogenase
Hb	hemoglobin
HBDH	hydroxybutyrate dehydrogenase
HC	hereditary coproporphyria
HCA	hyocholic acid
HCS	holocarboxylase synthetase
Hcy	homocysteine
HDCA	hyodeoxycholic acid
HEPES	4-(2-hydroxyethyl)-1-piperazineethanesulfonic acid
HDL	high-density lipoproteins
HFB	heptafluorobutyric acid
HFI	hereditary fructose intolerance
HL	hepatic lipase
HMP	2-hydrazino-1-methylpyridine
HMBS	hydroxymethylbilane-synthase
HPA	hyperphenylalaninemia
HPLC	high performance liquid chromatography

HPIC	ion-exchange chromatography
HRP	horseradish peroxidase
HSDH2	3α-hydroxysteroid dehydrogenase type 2
HTLC	high-turbulence liquid chromatography
HTP	hexamethyl disilazane/chlorotrimethyl silane/pyridine
HVA	homovanillic acid
IDL	intermediate-density lipoproteins
IEF	isoelectric focusing
ILBP	ileal lipid-binding protein
INF-γ	interferon-γ
IQC	internal quality control
IS	internal standard
ISSD	infantile sialic acid storage disease
IVPM	in vitro probe medium
KB	ketone body
LAH	lipoid adrenal hyperplasia
LC-MS/MS	liquid chromatography mass spectrometry/mass spectrometry
LCA	lithocholic acid
LCAT	lecithin:cholesterol acyltransferase
LCHAD	long-chain 3-hydroxyacyl-coenzyme A dehydrogenase
LDH	lactate dehydrogenase
LDL	low-density lipoprotein
LDLR	low-density-lipoprotein receptor
L-dopa	3,4-dihydroxy- L-phenylalanine
LLO	lipid-linked oligosaccharides
LOD	lower detection limit
LOQ	lower reporting levels
LPDS	lipoprotein-deficient medium
LPL	lipoprotein lipase
Lp(X)	lipoprotein X
MALDI-TOF	matrix assisted laser desorption ionization – time of flight mass spectrometry
ManNAc	N-acetylmannosamine
MAO	monoamine oxidase
MAT	methionine adenosyltransferase
MCA	muricholic acid
MCAD	medium-chain acyl-CoA dehydrogenase
MEM	minimum essential medium
MLPA	multiplex ligation-dependent probe amplification
MnO_2	manganese dioxide
MoM	multiples of the median
MO-TMS	methoximetrimethylsilyl
MPH	male pseudohermaphroditism
MPS	mucopolysaccharidosis
MPS I	mucopolysaccharidosis type I, Hurler syndrome
MPS II	mucopolysaccharidosis type II, Hunter syndrome
MPS III	mucopolysaccharidosis type III, Sanfilippo syndrome
MPS IV	mucopolysaccharidosis type IV, Morquio syndrome
MPS V	mucopolysaccharidosis type V, Scheie syndrome

MPS VI	mucopolysaccharidosis type VI, Maroteaux-Lamy syndrome
MPS VII	mucopolysaccharidosis type VII, Sly syndrome
MPS-EP	mucopolysaccharide electrophoresis
MRC	mitochondrial respiratory chain
MRI	magnetic resonance imaging
MRM	multiple reaction monitoring
MS	mass spectrometry
MS/MS	tandem mass spectrometry
MSUD	maple syrup urine disease
MTBSTFA	N-methyl-N-(tert-butyldimethylsilyl) trifluoroacetamide
MtDNA	mitochondrial DNA
MTHF	5,10-methylene-tetrahydrofolate
MTHFR	5,10-methylene-tetrahydrofolate reductase
MTP	microsomal triglyceride transfer protein
MU-Gal	4-methylumbelliferyl-β-D-galactopyranoside
MU-NeuAc	4-methylumbelliferyl-α-D-N-acetylneuraminic acid
MW	molecular weight
NAD	nicotinamide adenine dinucleotide
NADPH	nicotinamide adenine dinucleotide phosphate
NCBI	National Center for Biotechnology Information
NCI	negative chemical ionisation
NEQAS	National External Quality Assessment Service
NeuAC	N-acetylneuraminic acid
NeuGc	N-glycolylneuraminic acid
NKH	nonketotic hyperglycinemia
NMR	nuclear magnetic resonance
NPC	Niemann-Pick disease type C
OD	optical density
ODS	octadecylsilyl
OGS	oligosaccharide
OMIM	Online Mendelian Inheritance in Man
OPA	orthophthalaldehyde
ORD	oxidoreductase deficiency
OSS	octane sulphonic acid
PA	pipecolic acid
PAGE	polyacrylamide gel electrophoresis
PABA	4-aminobenzoic acid
PAH	phenylalanine-4-hydroxylase
PBC	primary biliary cirrhosis
PBG	porphobilinogen
PBS	phosphate-buffered saline
PC	pyruvate carboxylase
PCA	perchloric acid
PCD	pterin-4a-carbinolamine dehydratase
PCR	polymerase chain reaction
PCSK9	proprotein convertase subtilisin/kexin 9
PCT	porphyria cutanea tarda
PDA	pentadecanoic acid

p-DABA	p-dimethylaminobenzaldehyde
PDH	pyruvate dehydrogenase
PFB	pentafluorobenzyl bromide
PFBBr	pentafluorobenzylbromide
PGDH	3-phosphoglycerate dehydrogenase
PGI	phosphoglucose isomerase
PH-I	primary hyperoxaluria type I
PH-II	primary hyperoxaluria type II
PKU	phenylketonuria
PLP	pyridoxal phosphate
PMI	phosphomannose isomerase
PMM	phosphomannomutase
PNPO	pyridox(am)ine-5'-phosphate oxidase
PT	pregnanetriol
PTONE	pregnanetriolone
PTP	6-pyruvoyltetrahydrobiopterin
PTPS	6-pyruvoyltetrahydrobiopterin synthase
PUFA	polyunsaturated fatty acids
PV	porphyria variegata
PVDF	polyvinylidene fluoride
QC	quality control
RBC	red blood cells
RCDP	rhizomelic chondrodysplasia punctata
RIA	radioimmunoassay
RO	reverse osmosis
RPA	relative peak area
RPI	ribose-5-phosphate isomerase
rpm	revolutions per minute
RXLI	recessive X-linked ichthyosis
SASD	free sialic acid storage disease
SBDF	ammonium 7-fluorobenzo-2-oxa-1,3-diazole-4-sulphonate
SCAD	short-chain acyl-CoA dehydrogenase
SD	Salla disease
SDS	sodium dodecylsulfate
SIM	single ion monitoring
SLC6A8	Na^+-Cl^--dependent creatine transporter
SLOS	Smith-Lemli-Opitz syndrome
SPE	solid-phase extraction
SR	sepiapterin reductase
SR-BI	scavenger receptor B1
SSA	sulfosalicylic acid
SSADH	succinate semialdehyde dehydrogenase
SSCP	single-stranded conformational polymorphism
StAR	steroidogenic acute regulatory
STSD	steroid sulfatase deficiency
TAE	Tris-acetate-EDTA buffer
TALDO	transaldolase
TBA	thiobarbituric acid

TBE	Tris-borate-EDTA buffer
TCA	taurocholic acid
TCA	trichloroacetic acid
TCDCA	taurochenodeoxycholic acid
TDCA	taurodeoxycholic acid
TDeABr	Tetrakis (decyl) ammonium bromide
TEa	total error allowable
TEA	triethanolamine
TFA	trifluoroacetic acid
TH	tyrsosine-3-hydroxylase
THA	tetrahydro-11-dehydrocorticosterone
THAldo	tetrahydroaldosterone
THB	tetrahydrocorticosterone
THE	tetrahydrocortisone
THF	tetrahydrocortisol
THCA	trihydroxycoprostanic acid
THcy	total homocysteine
THS	tetrahydro-11-deoxycortisol
TIC	total ion current
TIM	triosephosphate
TLC	thin-layer chromatography
TLCA	taurolithocholic acid
TMA	trimethylamine
TMCA	tauromuricholic acid
TMCS	trimethylchlorosilane
TMR	tetramethylrhodamine
TMS	trimethylsilyl
TMSI	trimethylsilylimidazole
TNF-α	tumor necrosis factor-α
TOCSY	total correlated spectroscopy
TOF	time of flight
TPH	tryptophan-5-hydroxylase
Tris	tris(hydroxymethyl)-amino-methane
TSP	trimethylsilyl-2,2,3,3-tetradeuteropropionic acid
TUDCA	tauroursodeoxycholic acid
UDCA	ursodeoxycholic acid
UDP	uridine diphosphate
UDP-GlcNAc	UDP-N-acetyl-D-glucosamine
uE_3	unconjugated estriol
UEFA	unesterified fatty acids
UFE	urinary free cortisone
UFF	urinary free cortisol
VLCFA	very-long-chain fatty acids
VLDL	very-low-density lipoproteins
X-ALD	X-linked adrenoleukodystrophy
ZSDs	Zellweger spectrum disorders

1.1 Laboratory Strategies in Biochemical Genetics

Rodney Pollitt

1.1.1 Introduction

For the first 50 years after Archibald Garrod outlined the concept of an inborn error of metabolism in 1904 the number of such conditions identified grew only slowly. Thereafter, the pace of discovery quickened, powered by the successive emergence of new laboratory techniques such as paper chromatography, gas chromatography and gas chromatography-mass spectrometry (GC-MS), techniques that were all rapidly taken up by routine diagnostic laboratories. Simultaneously, laboratory automation and the commercial availability of a wider variety of biochemicals were bringing enzyme assays, for lysosomal disorders in particular, within the range of a routine service. In the last decade the application of electrospray ionisation tandem mass spectrometry (MS/MS) has opened up additional prospects. Even more recently, the automation of DNA analysis has developed to the stage where it is practicable to use gene sequencing for primary diagnosis. A quick glance at the contents page of this book indicates the scope of what is now possible. The problem is how to incorporate these new capabilities into routine healthcare provision in a rational and cost-effective manner. This entails both an informed approach to test requesting and a laboratory service organised appropriately for the range and volume of work thus generated.

1.1.2 Selection for Investigation

Unless there is a population-wide screening programme in place, the first steps in the diagnosis of an inherited metabolic disease are clinical suspicion and putting in train the appropriate laboratory investigations. The number of samples submitted and the range of tests being requested are both increasing.

In some disorders there is a clearly recognisable phenotype, often a named syndrome that has later been linked to a specific biochemical cause. However, once the biochemical basis of such a syndrome has been recognised it often becomes apparent that milder variants, *formes frustes* showing only some of the features of the classical syndrome, are relatively common. The diagnostic assay then changes from being a rarely used confirmatory test to one that is requested relatively frequently for a variety of less specific indications. The same phenomenon is seen where the abnormal phenotype develops progressively, as in most of the lysosomal disorders, and a bat-

tery of specific enzyme assays may be requested for any child showing possible early signs.

At the other end of the scale, many of the acutely presenting metabolic disorders give few clinical indicators of their underlying biochemical cause, and a rather non-selective approach to laboratory investigation is appropriate. Where time is of the essence, there is a natural tendency to order broad-spectrum "screening" tests and more specific investigations simultaneously, with little attempt to follow a logical diagnostic sequence. There is particular pressure with investigations such as organic acid or amino acid chromatography where results may be required "immediately", but most laboratories find that the proportion of samples giving a diagnostic result is extremely low. However, suggestions that such investigations should be performed in an acutely ill child only if other biochemical indications such as hypoglycaemia or hyperammonaemia are present have been strongly opposed [1]. Another approach to limiting demand is to proscribe common clinical presentations where metabolic investigations are usually unproductive. In the opening page of their "Vademecum Metabolicum" [2], Zschocke and Hoffmannn list six categories of patient where special metabolic investigations are not required. The trouble with either of these proposals is that they will result in a small proportion of cases being diagnosed late or not at all. This may not only compromise the effective treatment of the patient concerned, but also result in further affected children being unwittingly born into the family.

A more structured approach has been devised by Saudubray and Charpentier [3] that is based on the careful consideration of clinical detail and uses an extensive series of diagnostic algorithms. However, the editors' note that accompanies that article warns that the chapter is "an experiment", that patients have derangements in complex, overlapping, "non-categorical biological systems", and that we are "currently faced with the classical dilemma of balancing the practicality of categorical thinking against the reality of biologic variation". Perhaps clinical judgement is still as much an art as a science, and therefore any attempt on the laboratory's part to manage work-load by systematically restricting access would be highly problematical. A better solution is to increase laboratory capacity, although, depending on the financial structures in place, this may not always be a practical proposition.

1.1.3 Choosing the Biological Level

In classical inborn errors of metabolism there is a causal thread linking the defect in the gene with defective function or absence of an enzyme or transporter protein, the consequent excess or lack of one or more metabolites, and the clinical phenotype. Correspondingly, laboratory investigation can be at the nucleotide, protein or metabolite levels. Selecting the appropriate level at which to begin an investigation is an important component of the dialogue that should exist between laboratory and clinical services. In general (the lysosomal disorders being a notable exception), the metabolite level is to be preferred because a single analysis of urinary organic acids or plasma steroids, for example, has the potential to uncover many different disorders. Measurement of overall metabolite flux through a pathway using cultured cells can also be a useful group test, as in fatty acid oxidation disorders. Assays of enzymic activity are specific to individual disorders and are often most useful as con-

firmatory tests. Analysis at the DNA/RNA level is even more specific. Most disorders are heterogeneous with many disease-causing mutations, only a small proportion of which are covered by commercially available test kits. One can readily confirm a diagnosis by analysing for such mutations, but total exclusion is seldom possible. However, techniques that can quickly check for mutations in long stretches of DNA are passing into routine diagnostic use and will overcome this problem. In some of the glycogenoses, where the metabolic indicators are rather non-specific and enzyme assays are difficult and require a liver sample, gene sequencing is proving to be a practicable alternative, even though there are sometimes several candidate genes to be investigated.

The apparent simplicity of the one gene, one protein, one disease paradigm has long been discounted, but we are only now beginning to appreciate fully the complexity of the biological systems involved. Interpretational problems abound. A priori prediction of the clinical effect of a new mutation may be difficult, as apparently benign mutations can affect gene splicing or exert other effects. Even with well-known mutations there are limitations. Databases linking genotype to phenotype are available for several disorders, but there is often a considerable range of clinical expression. Siblings concordant for the same mutant genes may be affected to very different degrees and we have only slight inklings as to what the modifying factors might be. Newborn screening for cystic fibrosis or for medium-chain acyl-CoA dehydrogenase deficiency both suffer from the resulting uncertainty. In both disorders "mild" and "severe" genotypes have been identified, correlating with phenotype in cystic fibrosis and with varying degrees of residual enzyme activity in vitro in medium-chain acyl-CoA dehydrogenase deficiency, respectively. In theory, this additional information should help to refine the screening process. In practice, defining appropriate management schemes for presymptomatic cases with "mild" genotypes presents a major challenge. Similar problems arise in some disorders that are normally diagnosed and characterised only at the metabolite level, phenylketonuria being a prime example.

It is important that molecular genetic tests are integrated properly with other investigations and it is unfortunate that in some health systems molecular genetics has evolved in isolation from other diagnostic services. Some molecular genetics laboratories offer highly specific tests, for the common 985A>G mutation of the medium-chain acyl-CoA dehydrogenase gene in cases of unexplained infant death, for example, without any assurance that appropriate preliminary investigations have been performed and they are at least examining the right gene. In unselected cases of sudden infant death, for every definitive diagnosis (two copies of the 985A>G mutation) there will be approximately two cases where only one copy of the mutant gene is found. In only a minority of the latter will a second disease-causing mutation be present; most will be unaffected carriers – a situation that must be explained to the parents and requires very delicate handling.

The undoubted successes of molecular genetics have lead to exaggerated perceptions of its predictive powers.[1] The resulting sensitivity that legislators and the general public now attach to "genetic information" is an additional, extraneous complication when investigating metabolic disease. Genetic testing has been variously

1 "A smudge of spit on a beer glass leaves a person as vulnerable as if they had left their medical dossier, business card and personal journal lying on the bar top." Science correspondent – The Guardian (UK), February 2002

defined, from the very general "tests that provide information used for diagnosing an inherited disorder" to the more specific "a test to detect the presence or absence of, or change in, a particular gene or chromosome". Thus, even amino acid chromatography could be classed as a genetic test and, according to some official guidelines, be the subject of a formal informed consent process before the sample is collected, seemingly out of place in the context of emergency investigation of an acutely ill child. In practice, attention is generally focussed on analysis of the gene itself; equally specific information at the protein level, in sickle cell anaemia for example, is seen as less threatening – a good example of "genetic exceptionalism". Legal requirements vary from country to country, but in most it would be unwise to proceed to DNA analysis without explicit patient or parental permission.

1.1.4 Laboratory Provision

There is huge diversity in the way that specialist laboratory services in biochemical genetics are provided. Configurations often owe as much to historical chance as to rational planning. At one time, most laboratories serving the larger hospital centres would offer a selection of test-tube and chromatographic tests for the classical inborn errors of metabolism. With the growing sophistication and complexity of the field, the introduction of external quality-assessment schemes, and an ever-increasing workload in other areas, such investigations have tended to migrate progressively to more specialised biochemical genetics centres. However, clinical chemistry departments serving acute paediatric units still need to perform at least a limited range of tests, such as ammonia or lactate in plasma, on a 24 h/day emergency basis. A rapid turn-around service for plasma amino acids and urinary organic acids chromatography would also be advantageous. However, adequate local provision is not always feasible and external quality assessment has shown that laboratories carrying out such work on an occasional basis often perform poorly. It is usually better to have a more comprehensive service organised on a regional basis with rapid courier transport of samples.

Regional centres need to be of a certain size with sufficient sample throughput to justify the capital investment required, the effort needed to ensure technical reliability of the assays offered, and to give staff sufficient on-going experience of specialist interpretation. As a minimum, each centre requires a quantitative amino acid analyser, GC-MS for organic acids analysis and, increasingly, a tandem mass spectrometer with an electrospray ion source. Mixed usage, combining paediatric work with a toxicology service, for example, has in general not proved a satisfactory solution. The larger biochemical genetics laboratories will cover a wider range of activities including newborn screening, tissue culture, enzymatic assays, and molecular genetics, although few, if any, will offer the full range of investigations described in this "Laboratory Guide". Thus, at all levels, a collaborative networking approach is required.

Many of the larger biochemical genetics laboratories are in academic medical centres and make a significant contribution to research. They have collectively been responsible for much of the progress made in recent years. However, there is always a tension between research, where data need to be accumulated into publishable packets and a degree of secrecy prevails, and clinical care, where results need to reported immediately, perhaps to distant clinicians with their own publication needs.

The belief in some quarters that patients have proprietary rights over their samples and any information generated therefrom, and that even anonymised data should not be divulged without permission may cause difficulties even for routine services with no overt research brief, putting interlaboratory audits and external quality assessment schemes at risk.

Particular problems arise when a laboratory attached to some other academic discipline such as paediatrics or pure biochemistry has become the world centre for investigating some extremely rare or difficult disease. Such laboratories are unlikely to satisfy the increasingly arduous demands of accreditation and are by nature evanescent, depending on the research interests of the academic head and supported by time-limited research funds. They tend to work at a different tempo to the routine service and new information, perhaps obtained months or years after the sample was first received, does not always find its way back into the patient's clinical notes. At some stage in the life cycle of such projects the balance will have shifted from new, cutting-edge research to routine service provision, calling for some form of technology-transfer partnership with a larger diagnostic centre.

1.1.5 Impact of New Technologies

The workload is increasing in both volume and scope in all branches of laboratory medicine. In mainstream clinical chemistry, the past 25 years have seen astonishing developments in assay technology and instrumentation; assays that were performed manually with a few dozen assays a day can now be accomplished automatically by the thousands. In biochemical genetics (molecular genetics aside), automation has had a less dramatic impact.

Instrumental developments in GC-MS have brought this technique into routine diagnostic service. It is no longer necessary, as in the early 1970s, to sit by the machine and press a button when a mass scan is required, but sample preparation and interpretation of the output remain labour-intensive. For urinary organic acids, for example, the maximum daily throughput is still only a dozen or so samples per instrument, and attempts to automate interpretation of the resulting profiles by pattern recognition [4] or deviation of prescribed metabolites from a defined range [5] have so far have not resulted in general use. Other more traditional investigations, qualitative and quantitative amino acid chromatography, for example, also remain low-volume and labour-intensive investigations.

More recently, MS/MS and related ion-trap techniques have opened up groups of metabolites that have previously been difficult to analyse, acylcarnitines being the prime example. High throughput (40 or more samples per hour) is achievable and very little sample preparation is required. However, this will do little to reduce the workload elsewhere in the laboratory, as plasma acylcarnitine analysis is complementary to urinary organic acid analysis rather than replacing it. Amino acids are also amenable to MS/MS, but the technique has significant limitations for this group of metabolites and can not completely replace the more time-consuming traditional methods.

High-resolution nuclear magnetic resonance spectroscopy also has the potential for rapid sample throughput and could expand the range of metabolites readily detectable. The instrumentation is expensive and interpretation requires considerable

experience, restricting the technique at present to a few academic centres. If this technique does become affordable for routine diagnostic laboratories it, like GC-MS and MS/MS, is likely to increase the overall workload rather than reduce it.

Newborn screening is a special case where automation has considerable potential. In several countries screening is being concentrated in laboratories screening between 50,000 and 100,000 births per year, this being regarded as the optimum range for economical operation of a single-tandem mass spectrometer. Such a throughput has only become achievable through automatic data handling; specimens where a metabolite concentration or a particular concentration ratio falls outside the specified range are flagged for individual attention. Microarray technology is also being introduced into newborn screening, with a commercial laboratory in the USA screening over 300,000 babies per year, making extensive use of microarray mutation analysis as a second-tier screen.

Centralisation on this scale is out of the question for most biochemical genetics investigations, as the cost of developing the systems required can not be supported by the overall level of demand. There may be some scope for laboratory networks to rationalise test repertoires and invest in a more limited degree of automation, an approach most suited to assays giving simple, readily interpretable, numerical results. More complex tests, particularly related group tests such as organic acids, acylcarnitines and amino acids, are best performed and evaluated together in the same centre. The range of options available will vary with the healthcare environment in which laboratories operate; only free-standing commercial laboratories are able to adopt an outright business-lead approach. Many existing laboratories are embedded within hospitals that provide tertiary paediatric services and, as discussed in the previous section, would need to maintain a substantial core of investigations for urgent use. The quest for micro-economic "efficiency" should not be allowed to destroy the essentially interactive nature of biochemical genetics, where relationships between clinic and laboratory at different levels provide not just a more effective service, but also the intellectual and emotional stimulation that has made this such a rewarding field in which to work.

References

1. Holton JB. Diagnosis of inherited metabolic disease in acutely ill children. Ann Clin Biochem 1982; 19:389–395
2. Zschocke J, Hoffmann GF. Vademecum Metabolicum. A Manual of Metabolic Paediatrics. Stuttgart and New York: Milupa-Schattauer, 1999
3. Saudubray JM, Charpentier C. Clinical phenotypes: diagnosis/algorithms. In: Scriver CR, Beaudet AL, Sly WS, et al. (eds) The Metabolic and Molecular Bases of Inherited Disease, 8th edn, New York: McGraw Hill, 2001, pp 1327–1403
4. Karjalinen EJ, Karjalinen UP. Speeding up the identification of anomalies in urinary organic acids. J Inherit Metab Dis 2003; 26 Suppl 2:49
5. Kimura M, Yamamoto T, Yamaguchi S. A personal computer-based system for interpretation of gas chromatography mass spectrometry in the diagnosis of organic acidaemias. Ann Clin Biochem 1999; 36:671–672

1.2 Quality Control and Quality Assurance in the Biochemical Genetic Laboratory

Jim R. Bonham

1.2.1 Introduction

When using medical laboratories, physicians frequently assume that the results provided are accurate and precise. Those working in the laboratory environment know that this is true only within the constraints of the methods, technology and processes available. In this chapter we will explore how internal quality control (IQC) and external quality assurance (EQA) procedures can inform both the analyst and the physician about the limitations of laboratory testing and permit a more intelligent use of laboratory data, while at the same time indicating areas where improvement is required.

1.2.2 Laboratory Accreditation

While the specialist physician may develop an in-depth knowledge of the strengths and limitations of the laboratory that they use regularly, the occasional user and the patient require the reassurance offered by accreditation systems. In general, accreditation systems follow the principles of healthcare assessment described by Donabedian [5]:

1. Providing guidance concerning the appropriate structures to be in place, for example staffing, equipment and buildings.
2. Ensuring that suitable processes are employed to guarantee reliable testing, for example the use of standard operating procedures, the conduct of IQC and participation in EQA.
3. Requiring examination of outcomes, for example audit and user survey.

The way in which accreditation is organised varies in different countries with organisations such as the Clinical Pathology Accreditation (CPA UK) in the UK and CCKL Test in The Netherlands. Accreditation may be optional or may be mandatory, as in the USA, and mediated by "deemed authorities" such as the College of American Pathologists. However, the standards to which these accreditation bodies operate are usually cross referenced to internationally agreed formulae such as:

1. ISO 9001:2000, which covers: the design of quality management systems; the role and practice of management; equipment, infrastructure and staffing; product realisation; monitoring, including audit and incident reporting. It is worth noting

that ISO 9001:2000 does not provide specifications relevant to reporting or pre-or post-analytical aspects of service provision.
2. ISO 17025:1999, which covers the general requirements for the competence of testing and calibration laboratories, or ISO 15189:2002, which includes particular requirements for quality and competence in medical laboratories extending to post-analytical aspects including the reporting of results.

In complying with the ISO 17025:1999, it is assumed that the organisation will also adopt quality management systems that ensure compliance with ISO 9001:2000.

Member states within the European Union are committed to ensuring a uniformity of laboratory-based diagnostic quality in biochemical genetic testing and consider that laboratory accreditation is the main route by which this may be accomplished. The current Eurogentest project (www.eurogentest.org) seeks to facilitate this approach by providing resources, guidelines and procedures that could ensure a greater degree of harmony and facilitate more rigorous and relevant accreditation standards. As part of this approach, the project will develop EQA provision and uptake and will consider aspects of laboratory reporting, seeking to ensure that results are both reliable and clearly understood.

1.2.3 EQA and IQC in Biochemical Genetics

The purposes of laboratory testing in Biochemical Genetics are usually either:
1. To diagnose or exclude inherited metabolic disorders in individual patients. In this situation the increased concentration of the key metabolite may be quite prominent and is typically at least one order of magnitude greater than the reference range (e.g. phenylalanine > 1000 μmol/l compared with a reference range of 42–110 μmol/l [4].
2. To monitor patients who have already been diagnosed and are receiving treatment designed to avoid the accumulation of key compounds to toxic concentrations while ensuring nutritional adequacy. In this situation, a patient's diet may be modified if the concentration of phenylalanine changes from 200 to 400 μmol/l. Clearly, the requirements of the analytical systems used to quantify the compounds of interest may be quite different in these two situations and this must be considered when designing suitable quality monitoring systems.

The unusual demands placed upon biochemical genetic laboratories make it particularly important to have robust quality management systems in place. In particular:
1. Samples are often only analysed once in a particular patient, unlike the serial or repeated analyses undertaken when monitoring urea and electrolytes in some patients. On the basis of that single result, the possibility of a metabolic disorder in a particular patient is often excluded and the test may not be repeated.
2. It is often unclear which key compounds may prove important at the time when the analysis is requested. Consequently, chromatographic techniques such as gas chromatography, thin-layer chromatography or high-performance liquid chromatography are frequently employed, as these provide a means of "profiling" several functionally or structurally related compounds in a complex biological matrix as part of a single analytical process. Unfortunately, it may be impossible to optimise

the technique for individual compounds of interest while maintaining the ability to detect the range of metabolites required.
3. The analyses are often qualitative rather than quantitative and the interpretation is therefore somewhat subjective.
4. The conditions to be diagnosed are frequently heterogeneous in their biochemical expression as a result of varying residual enzyme activity and other confounding genetic and environmental factors.
5. The amount of sample available is very often limited when the patient, often a young child or neonate, is ill.
6. The results are frequently required urgently to guide important clinical management decisions.
7. The conditions to be diagnosed are rare and few laboratories can maintain extensive experience in all of the conditions that they may occasionally encounter.
8. Many samples are received from non-specialist physicians who may not be familiar with the limitations of testing.

In these circumstances, rigorous adherence to IQC procedures and membership of relevant EQA or proficiency schemes are essential to provide both education and assurance of competent performance.

1.2.4 The Conduct of IQC

1.2.4.1 Quantitative Assays – Defining the Goals

There are three main approaches to setting the goals for the quality that must be achieved. First, a consensus agreement [7] formulated at the 1999 conference "Strategies to Set Global Analytical quality Specifications in Laboratory Medicine" gave primacy to variation in analytical performance that would affect clinical outcomes in specific clinical settings as the highest level indicator on which to base analytical requirements. In the context of biochemical genetics, this may be the performance required to reliably achieve diagnosis. In the newborn with phenylketonuria this would not demand a high level of performance from the phenylalanine assay. However, the performance required to detect reliably significant changes in response to treatment for the patient with phenylketonuria on diet would require a much higher standard of performance. In practice it is difficult to achieve reliable information to define a clinically significant change during patient monitoring in most situations. Many of the action limits used to modify treatment are somewhat arbitrary and reflect local practice without a good evidence base. In my own laboratory we would attempt to review and intervene in a patient with classical homocystinuria whose plasma total homocysteine exceeded 100 μmol/l, whereas a similar patient whose homocysteine was 90 μmol/l may be treated in a more relaxed way. Clearly, it is important that where possible the locally agreed rules should be based upon evidence and that the reliability of the analytical results should support the validity of the planned clinical action.

The second level used to define the requirement for analytical quality is often cited as the Cotlove model [2], defining acceptable analytical imprecision as less than 0.5 times the within-subject biological variation measured as the coefficient of variation

(CV, %). The difficulty in applying this in the context of biochemical genetics is that the concentration required to diagnose disease, or indeed the maximum concentration considered as an acceptable control, may far exceed the mean in the normal population, and the within-subject variation in metabolically ill patients, even with the same condition, is difficult to define. For example, the patient with homocystinuria receiving treatment may exhibit total homocysteine values of 70–80 μmol/l, whereas the normal population mean may be 7–8 μmol/l. Consequently, the requirements based on a within-subject variation of 8.1% [14] at "normal" concentrations may exceed clinically acceptable changes at a mean of 75 μmol/l. It is useful, however, to know both the usual biological variability in the patient being monitored and the characteristics of the assay to guide interpretation.

The third means often used to define acceptable analytical performance is the total error allowable (TEa), which is determined from external quality assessment programs. As an example, a TEa based on retrospective EQA analysis for cholesterol has been agreed as 10% by the United States Clinical Laboratory Improvement Amendments regulations. Such approaches have the virtue of providing clearly defined and achievable targets, but may lack, or in some cases needlessly exceed clinically driven targets. It is possible to identify these targets from inspection of the modal variation of individual analytes at varying concentrations included within the European Research Network for evaluation and improvement of screening, Diagnosis and treatment of Inherited disorders of Metabolism (ERNDIM) EQA system (www.erndimqa.nl).

1.2.4.2 Quantitative Assays – Monitoring Performance

It is assumed that before the analyst has considered using the assay for patient samples, it has been analytically validated (i.e. the recovery, sensitivity, linearity and reproducibility have been determined) and that the method is able to reproduce results, under ideal conditions, so that its variation is sufficiently predictable to apply statistical quality control.

Subsequently, at least two "control" samples are usually included in each batch, one with a concentration in the physiological range and one in the pathological range. The results obtained can be used in real time to determine whether any particular batch of results can be reported safely. The initial description of "charting" such results graphically as a tool for control was made in 1950 by Levey and Jennings [12]. Stable performance is first established by assaying the control materials over a period of time, then calculating the mean and standard deviation (s.d.). Subsequent results are then plotted in relation to the mean, plus or minus 2 or 3 s.d.s. The crucial design feature when monitoring performance is the definition of the control rules (i.e. the set of conditions must be met for a run to be rejected). If a simplistic rule is used where the run is rejected, if any one of two controls falls outside the 2-s.d. limit then this will result in a high false run rejection rate (9%); conversely, if 3-s.d. limits are used, the false rejection rate will be less than 1%. However, by using the wider 3-s.d. limits, the probability of "true" error detection will fall from 85% to 45% for the same "critical systematic error", a performance measure calculated from the assay bias, reproducibility and the total error allowable [15]. It is generally accepted that a rule should be used that will ensure a probability of 90% of detecting medically

important errors combined with a probability of 5% or less that a run will be rejected falsely [15]. It may not be possible to achieve these performance criteria without using a combination of rules when analysing quality control results. This generally includes combining rules that are sensitive to random error (e.g. $x > 2$ s.d. and $x_1 < -2$ s.d. in the same run when these are consecutive control measurements) with those rules that would more sensitively identify systematic error (e.g. x, x_1, x_2, x_3 exceeds + 1 s.d. or is less than –1 s.d. when these are consecutive measurements, or x_1 x_2……..x_9 all fall on the same side of the mean when these are consecutive). Using this multi-rule approach it is possible to reduce the false run rejection rate, thereby increasing efficiency while maintaining a high level of true error detection. Whatever approach is adopted, it is important that:

1. The specific quality requirement for the test is properly understood and defined.
2. The method precision and bias is known.
3. The goals for assay performance are established.
4. The appropriate IQC procedure and rules are used.

It is extremely unlikely that all quantitative tests in a laboratory will be appropriately serviced by a single rule for IQC and this should not be attempted. Properly trained analysts can adapt readily to differing control rules for different tests; this also reinforces the particular requirements of individual tests related to their clinical use.

1.2.4.3 Qualitative Assays – Monitoring Performance

Qualitatively interpreted assays such as mucopolysaccharide electrophoresis (MPS-EP), urinary organic analysis and amino acid thin-layer chromatography (AA-TLC) are extremely important in biochemical genetics and yet are difficult to quality control. Some useful control measures often used include:

1. The use of known normal samples and samples from patients with proven disorders contained within the run. This can add considerably to the analytical workload, but it is the author's view that at least one "normal" and one "pathological" sample should be included at least once per week. In practice, some of these assays (e.g. MPS-EP and AA-TLC) may only be run once per week and this would mean inclusion within each batch. It is increasingly easy to record and store the results as dated sequential digital images (e.g. MPS-EP or AA-TLC), recording changes in the results obtained from aliquots of a single normal pooled urine or a range of pathological samples that have been repeatedly tested. This can then be used to track changes related to the stain, media or operator, for example, and can guide the analyst regarding whether a particular batch falls within or outside acceptable variation. It may also be a useful training resource.
2. The inclusion of known quantities of non-naturally occurring internal standards with varying extraction and analytical characteristics (e.g. heptoanoylglycine and margarate as "internal standards" in urinary organic acid analysis). The abundance of the resulting peaks (corrected for any changes in extraction volume and loading) can be assessed and charted using quantitative quality control procedures.
3. Visual inspection of key naturally occurring peaks from a gas chromatograph trace in relation to the usual baseline variation, reflecting the sensitivity or the

shape and size of bands on thin-layer chromatography, in turn reflecting the skill of application, are also valuable indicators of analytical performance.

The subjectivity of qualitative assays and the unavailability of rigorous IQC procedures place additional demands on the analyst and on laboratory organisation. Consequently:

1. All equipment used should be checked regularly and monitored carefully to reduce random and systematic errors. The checking and maintenance should be documented and reviewed regularly.
2. Detailed standard operating procedures should be in place, reviewed regularly and followed carefully in practice.
3. Analysts should be adequately trained and experienced before undertaking and interpreting these assays.
4. A two-step process (i.e. analysis followed by interpretation by a different person) provides an important and practical way of monitoring both analytical and interpretive quality.
5. Rotation of staff, provided that this is not too frequent, can help identify practices that have diverged from those first established.
6. Continual professional development including attendance at scientific meetings helps to maintain and improve both analytical and interpretive competence and quality.

The lack of adequate IQC for subjectively interpreted qualitative assays is a real cause for concern, but with properly documented methods, carefully maintained infrastructure and good training, clinically reliable results are achievable, and we will explore this further in the following section on EQA.

1.2.5 The Conduct of EQA

While IQC can be operated in "real time" to provide a means of deciding whether or not to report a given set of analytical results, EQA is, by its nature, retrospective. While IQC can provide valuable data on imprecision and may indicate its potential causes, EQA compares performance between laboratories and provides information about the accuracy and bias of the results obtained. This additional information can be used to:

1. Aid method selection.
2. Assess linearity, calibration and recovery.
3. Identify changes in bias dependant upon concentration.
4. Reveal imprecision shown as a lack of consistency of bias by including in the scheme design multiple pairs of samples.
5. Reveal constant blanking errors, resulting in a consistent bias.

Participation in EQA schemes with adequate performance is usually one of the criteria required by external accreditation bodies assessing the competence of laboratories to provide a service. It is also a powerful educational tool that has improved both the awareness of potential problems and the overall performance of laboratories since its inception in the 1950s.

1.2.5.1 EQA for Quantitative Assays

The concept underlying most quantitative EQA schemes is straightforward.

1. The same sample in a stable form is sent simultaneously to all participating laboratories.
2. The laboratories analyse the sample in the same way as a patient sample and report the results within a predefined timescale.
3. The results are analysed to reveal individual variation from a target value.

In practice this is often shown graphically as a histogram illustrating the distribution of results in which the result submitted by the individual participant is clearly shown. This is often refined further into method related groups. It is then possible to begin the mathematically manipulate this data and use it to assess performance over time. One popular approach is to:

1. Determine the percentage bias (for a given result) $= \dfrac{(\text{result}-\text{target})}{\text{target}} \times 100$
2. Use the result, when normalised against an assumed coefficient reflecting the difficulty of the assay, to provide an accuracy index that allows a comparison between analytes and laboratories. In the UK National External Quality Assessment Service (NEQAS; www.ukneqas.org.uk) system, 100 is arbitrarily set as average, with a lower score indicating better performance. Using this approach it is possible to compare directly, on a similar scale, assays with widely differing inherent imprecision, for example thyroid stimulating hormone, where a bias of 5% may be acceptable, and plasma sodium, where 1% would be more usual.

The accuracy index, the untransformed average bias and the statistical variation in bias can be displayed as a running average to reveal trends in performance with time or can be shown in relation to concentration to reveal concentration-dependent analytical performance.

An effective EQA scheme design requires:

1. Reliable and stable samples with target values relevant to the clinical situation.
2. Sufficiently frequent distributions to ensure an adequate data record and regular testing; this is usually defined as a least 12 samples per year.
3. Rapid turnaround of reports to maintain interest and momentum.
4. A formally constituted steering committee to assess scheme design and reporting arrangements.
5. Systems for ensuring the identification and notification of poor performers.
6. Informative and intelligible reports with clear information for the participant explaining the way in which the data is handled and manipulated. Any interpretative comments should be clearly presented and explained.
7. EQA scheme accreditation.

Most of these requirements are explicit or implicit within ISO 43–1:1997-Development and operation of proficiency testing schemes and in the Standards for EQA Schemes in Laboratory Medicine, issued by CPA (UK) [3]. It is appropriate for participants to ensure that the schemes to which they belong, or are considering membership, comply with these basic requirements.

1.2.5.2 Scheme Availability

In Europe, quantitative schemes exist for most common metabolites measured in biochemical genetics laboratories (see Table 1.2.1).

1.2.5.3 Performance Within the Schemes

Amino Acids (2005 Data)

Typical median recovery is 97% and is satisfactory for most of the 26 amino acids analysed, ranging from 92 to 110%. Two amino acids fall outside these limits: cystine (75%) and proline 89%. The median intra-laboratory imprecision is 6.0% (range 4.0–10.5 for the commonly measured amino acids, excluding cystine). Phenylalanine shows a median intra-laboratory imprecision of 4.0% at a concentration of 347 μmol/l and a median inter-laboratory imprecision of CV = 12.8% (range 6.4–32.7). These results underline the difficulty in applying literature values to local use; a phenylalanine result of 400 μmol/l in one laboratory and 300 μmol/l in another are within the 95% confidence limits revealed by this survey.

Special Assays (2005 Data)

The range of recovery and the inter- and intra-laboratory imprecision in some assays is listed in Table 1.2.2. It is salutary to note that when measuring homocysteine in a patient whose true concentration may be 64.0 μmol/l, within the same laboratory the results obtained may range from 55 μmol/l to 73 μmol/l and that in different centres the same patient could be given results ranging from 50 to 78 μmol/l. This perfor-

Table 1.2.1 *Examples of quantitative external quality assurance (EQA) schemes available in Europe in biochemical genetics*

Scheme	Scheme organiser	Samples per year	Participants
Amino acids	ERNDIM	8	172
Special assays (urine and plasma): lactate, orotidine, thiosulphate, carnitine, succinylacetone, hydroxyproline, urate, orotate, sialic acid, MPS, guanidinoacetate, HVA, pyroglutamate, 5H1AA, pipecolate, pyruvate, 3-hydroxybutyrate, phytanate, VLCFA, homocysteine, 7-dehydrocholesterol, phenylalanine	ERNDIM	8	148
Quantitative organic acids	ERNDIM	8	56
Purines and pyrimidines	ERNDIM	8	40
Cystine in white blood cells	ERNDIM	8	27
Orotic acid	UKNEQAS	18	11

Table 1.2.2 *Recovery and laboratory imprecision in quantitative EQA schemes*

Metabolite	Mean concentration	Mean recovery (%)	Mean intra-laboratory imprecision (%)	Mean inter-laboratory imprecision (%)
Urine				
Free carnitine	246 μM	99	7.4	12.7
Lactate	5.1 mM	100	8.0	59.0
Orotate	46.3 μM	99	7.0	90.4
Thiosulphate	11.1 μM	52	94.4	197.9
Succinylacetone	11.7 μM	65	46.6	80.4
Serum				
Free carnitine	90.0 μM	104	6.4	11.4
Homocysteine	64.0 μM	103	7.1	11.0
Lactate	5.9 mM	109	3.5	6.4
Pyruvate	250 μM	81	8.9	15.1
3-Hydroxybutyrate	2.48 mM	123	5.3	21.7
7-Dehydrocholesterol	122 μM	127	16.8	116.3

mance fails to meet the notional target of 0.5 times the within-subject variation proposed by Cotlove et al. [2]. The lack of agreement between laboratories, reflected in the poor inter-laboratory imprecision may impair international multi-centre clinical trials or research. This is perhaps a useful reminder that the design of any multi-centre study should include a component assessing EQA in the participating centres during the period of study.

Quantitative Organic acids (2005 Data)

Many laboratories use quantitative urinary organic acid analysis as an alternative to a qualitative approach and may not use stable isotope dilution as a more rigorous means of quantitation. The results from EQA schemes in the area reflect this variability of practice and the lack of internationally agreed standardisation.

Intra-laboratory CVs range from 9.9% for ethylmalonate (at 102 μmol/l) to 40.7% for suberylglycine (at 48.6 μmol/l) and inter-laboratory CVs from 42.5% for ethylmalonate (at 102 μmol/l) to 757.4% for tiglylglycine at 83.5 μmol/l. This wide variation is also accompanied by marked variability in the reference ranges used by different laboratories; an example is shown (Fig. 1.2.1) for a single return from 18 respondents who quantitated ethylmalonate in a single sample (sample 109) and reported both the result and the upper limit of normal used by their laboratory. Clearly the clinical significance of this apparently extreme variability depends upon the clinical context

and may be less problematic than the results would suggest. Nevertheless, it is a reminder that these limitations should be considered when viewing results from the literature.

Purines and Pyrimidines (2005 Data)

The mean recovery of 100% (range 63% for orotidine to 124% for 2,8 dihydroxyadenine) is probably acceptable; similarly, the mean intra-laboratory imprecision (CV = 11.9%, range 6.0 for pseudouridine to 21.9% for succinyl adenosine) is likely to be adequate for most clinical applications. However, the interlaboratory imprecision is somewhat disturbing: mean CV = 126% (range 16.8% for pseudouridine to 295% for orotidine). This variation indicates the need to harmonise standardisation.

White Cell Cystine (2005 Data)

The mean recovery is 99% and the inter-laboratory CV for cystine is 10%. The mean inter-laboratory CV for cystine expressed per gram of protein is 26.8%. This may reflect a lack of standardisation, but may be acceptable to meet the needs of current clinical practice.

Urinary Orotate (2005 Data)

The range of results returned by participants near to commonly used "cut-off" values is quite wide (e.g. mean 4.8 μmol/mmol creatinine, range 3.5–6.5 μmol/mmol creatinine; mean 5.8 μmol/mmol creatinine, range 3.0–7.0 μmol/mmol creatinine). When

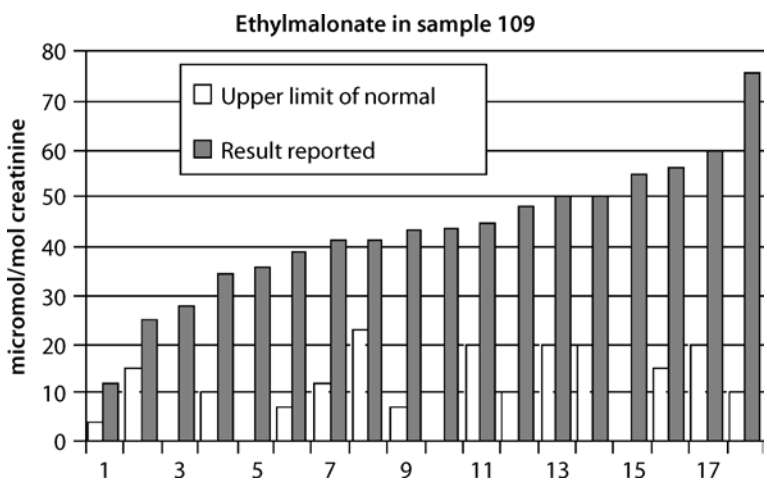

Fig. 1.2.1 Variation in the result reported and the reference range used in 18 laboratories reporting quantitative results for ethylmalonate in a proficiency scheme

participants were asked to classify the results as "normal", "equivocal" or "high", assuming that they were obtained in a 1-year-old child, then perhaps not surprisingly there is an unwelcome degree of variability. In the first example, three participants considered their results normal, six equivocal and two high, and in the second example, four participants considered their results normal, six equivocal and one high. This variability probably reflects differences in methods, standardisation and reference ranges, but clearly may adversely affect patient care.

1.2.5.4 EQA for Qualitative Assays

Some important assays commonly used in biochemical genetics laboratories do not provide quantitative data (e.g. MPS-EP, qualitative urinary organic acid analysis, AA-TLC). In addition, all successful investigations depend heavily upon selection of the correct analytes to measure and the appropriate interpretation of the quantitative or qualitative results in their clinical context. These challenges suggest a requirement for external quality assessment or proficiency testing schemes that can inform participants about their performance in these areas when compared with other centres.

1.2.5.5 Scheme Availability

Several such schemes exist (Table 1.2.3). The design of these schemes share some common features:

1. All use genuine patient urine or blood samples.
2. In all of these schemes participants are invited to report significant analytical findings, comment upon their significance, determine a likely diagnosis from the findings and indicate the need for further testing or investigation.
3. All schemes attempt to "score" the response of the participants, paying attention to these categories.

Table 1.2.3 *Examples of qualitative EQA schemes available in Europe in biochemical genetics*

Scheme	Scheme organiser	Samples per year	Participants
Urinary organic acid analysis	ERNDIM	9	137
Diagnostic proficiency testing	ERNDIM		
	Northern Europe	6	26
	Southern Europe	6	20
	Eastern Europe	6	24
	Central Europe	6	22
Acylcarnitine analysis	ERNDIM	9	67

The diagnostic proficiency testing schemes offer the additional feature of test selection. Participants are provided with brief clinical details and are required to select the investigations to undertake and when completed, report their findings.

1.2.5.6 Performance Within the Schemes

Urinary Organic Acid Analysis (1997–2004 Data)

Nine samples are distributed to participants each year and results scored on the basis: 2 satisfactory; 1 helpful but incomplete; 0 unhelpful; –1 slightly misleading; –2 misleading. It is therefore possible for the best-performing laboratories to achieve an annual score of 18.

Experience over an 8-year period (Fig. 1.2.2) suggests that several laboratories perform consistently well, with average annual scores ranging from 16 to 18 and with little variability of performance from year to year (s.d. = 1; eight laboratories). At the other extreme, some participants (six laboratories) consistently perform significantly less well, with mean annual scores of 5–12 and with considerable year to year variation (s.d. = 5; Fig. 1.2.2). The majority ($n = 39$) perform in the mid-range, with an average score of approximately 15 but with some variation in performance year to year (mean s.d. = 3).

It is tempting to scrutinise different aspects of laboratory practice in this spectrum to determine whether key factors can be identified that predict or are cor-

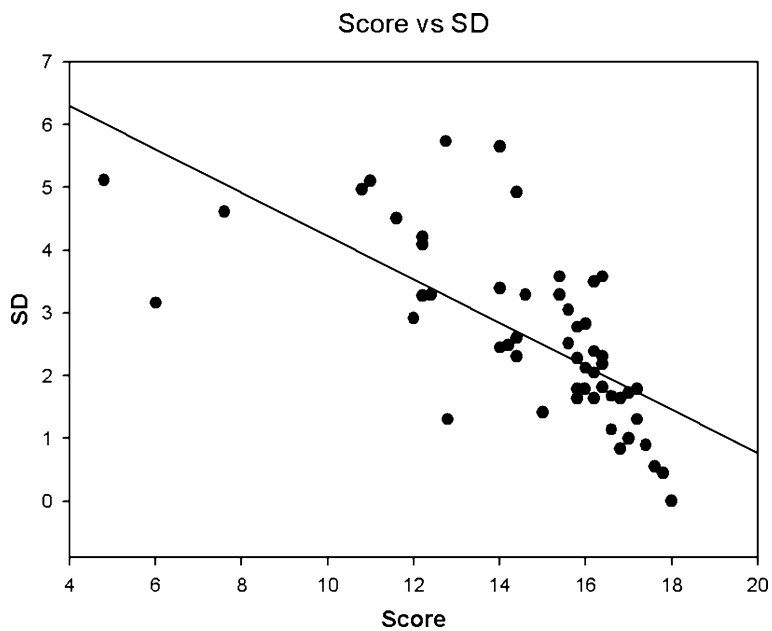

Fig. 1.2.2 The average annual score obtained by participants in the qualitative organic acid scheme and their year-to-year variation shown as standard deviation (*SD*)

related with performance. While retrospective group analysis of the methods used by participants does not demonstrate a convincing link between performance and equipment, staffing, or analytical approach, it is possible to identify some important factors that do influence performance:

1. Poor performance, signified by an average annual score of < 9 (< 50%) was observed only among those participants who performed fewer than 500 analyses per year; this may reflect experience [1].
2. The total number of peaks annotated per sample showed a highly significant correlation with performance, $p = 0.002$, $r = 0.62$; this reflects the degree of attention to detail shown by the analyst [1].
3. Attendance at scientific meetings (exemplified by attendance at the International Society for the Study of Inborn Errors of Metabolism Symposium) showed a correlation with performance ($p = 0.08$, Student's t-test); this reflects scientific awareness and the commitment to training shown by the participating laboratory [1].

The educational role fulfilled by active participation in EQA is demonstrable. Redistribution of the same sample following a gap of several years indicated a detection rate that improved by 20% for mevalonic aciduria, L-2-hydroxyglutaric aciduria, Canavan disease, 4-hydroxybutyric aciduria and long-chain hyroxy-acyl CoA dehydrogenase deficiency [6]. These results probably reflect the fact that many participants encounter rarer conditions for the first time as a member of an EQA scheme. Stored residual samples from such EQA schemes and unlabelled chromatograms can also be used as a valuable training aid or even a competency test for analysts.

Diagnostic Proficiency Testing

The proportion of laboratories correctly diagnosing a range of disorders when supplied with a urine sample and relevant clinical details is shown in Table 1.2.4 from the Northern European experience. The results indicate that even in situations when centres are provided with an adequate sample volume and up to 2 weeks in which to undertake testing, not all achieve a diagnosis. Clearly, the prior index of suspicion of abnormality is high in EQA samples and most analysts would be alerted to the possibility of a disorder. These results therefore probably represent the best performance achievable. The findings suggest that the best results are obtained for those disorders with a relatively high incidence and prominent biochemical findings (e.g. methylmalonic aciduria, medium-chain acyl CoA dehydrogenase deficiency and isovaleric aciduria); the worst performance is obtained for rare disorders or those in which the biochemical abnormalities are more subtle (e.g. fumarase deficiency, prolidase deficiency and sialidosis).

1.2.6 Current and Future Development

The ease with which laboratories can share information over a wide geographical area has improved with the development of the Internet. A greater number of formal and informal national and international networks are developing and seeking to establish best-practice guidelines to achieve consensus agreement concerning test

Table 1.2.4 *The proportion of laboratories reporting a "correct" diagnosis as part of the participation of a diagnostic proficiency scheme (Northern Europe Diagnostic Proficiency Scheme)*

Disorder	Proportion of laboratories giving the correct diagnosis	Disorder	Proportion of laboratories giving the correct diagnosis
Methylmalonic aciduria	100%	2-OH glutaric aciduria	92%
Medium-chain acyl CoA dehydrogenase deficiency	100%	Malonic aciduria	92%
Isovaleric aciduria	100%	Morquio disease	92%
Ornithine aminotransferase deficiency	100%	4-hydroxybutyric aciduria	91%
Hunter disease	100%	Tyrosinaemia type 1	89%
Alkaptonuria	100%	Multiple acyl CoA dehydrogenase deficiency	88%
Ethylene glycol ingestion	96%	Hurler disease	87%
Tyrosinaemia type 2	96%	Homocystinuria	82%
Mevalonic aciduria	96%	Biotinidase deficiency	82%
Maple syrup urine disease	96%	Hypophosphatasia	69%
Glutaric aciduria type 1	94%	Fumarase deficiency	53%
Cystinuria	93%	Peroxisomal disorder	46%
D-glyceric aciduria	93%	Prolidase deficiency	38%
Phenylketonuria	92%	Sialidosis	27%

selection in the investigation of common conditions such as hypoglycaemia, hyperammonaemia and seizures (www.metbio.net).

Similarly, there is an increasing degree of consistency of methodological approach between laboratories. For instance, a recent survey of those undertaking qualitative urinary organic acid analysis revealed that more than 90% (83 of 91) of laboratories indicated that they extracted the samples with ethylacetate or ethylacetate/ether, formed trimethylsilyl derivatives and employed gas chromatography-mass spectrometry as a means of analysis.

Post-analytically, schemes are beginning to emerge specifically to compare practice and performance between laboratories pertaining to the interpretation of test results. For instance, in the UK, NEQAS in conjunction with the National Biochemical Genetic network, MetBio.Net, are offering a scheme that provides the opportunity, when given relevant clinical details, to interpret quantitative amino acid results. This proficiency scheme can compare interpretive skills without the need to circulate scarce clinical samples.

The Internet, perhaps, has most to offer in facilitating the organisation and conduct of EQA schemes. Participants can return results electronically and the resulting data can be analysed and displayed with a very short turnaround time. This could

even be used to merge some aspects of internal quality control and EQA and should also serve to make EQA schemes more accessible and more cost effective to operate.

1.2.7 Conclusions

There is convincing evidence that the proper use of IQC and participation in EQA schemes improve laboratory performance [13] and can help avoid interpretive errors. However, the ultimate goals for quality need to be carefully and properly defined and linked more closely to clinical objectives. It seems that those offering analytical services are keen to participate in EQA schemes regardless of whether these are mandatory or voluntary; this reflects the valuable educational nature of these schemes for those working the field of biochemical genetics. However, while it is encouraging that the rate of participation is high and that performance is improving, the lack of agreed reference methods, reference ranges or commercially available standard material is a serious drawback that limits the accuracy and interpretive reliability for some metabolites.

Widespread consensus agreement on analytical approach, the adoption of peer-reviewed investigational guidelines and the dissemination of standard operating procedures should, together with the drive to laboratory accreditation, improve the consistency of practice in biochemical genetics. It is important that this harmonisation is appropriate and does not inhibit innovation; it is essential that it is undertaken in the service of the clinical needs of the patient and not solely for the sake of governmental regulation. This will be best achieved by the continued growth of professionally organised EQA schemes in which laboratories are encouraged to participate on a voluntary basis.

References

1. Bonham JR, Downing M, Pollitt RJ, Manning NJ, Carpenter KH, Olpin SE, Allen JC, Worthy E (1994) Quality assessment of urinary organic acid analysis. Ann Clin Biochem 31:129–133
2. Cotlove E, Haris EK, Williems GZ (1970) Biological and analytical components of variation in long-term studies of serum constituents in normal subjects. 3, Physiological and medical implications. Clin Chem 16:1028–1032
3. CPA (UK) Ltd. Standards for EQA schemes in Laboratory Medicine 2004. Version 4.02, 45 Rutland Park, Sheffield, S10 2PB, United Kingdom
4. Dickenson JC, Rosenblum H, Hamilton PB (1965) Ion exchange chromatography of the free amino acids in the plasma of newborn infants. Pediatrics 36:2–13
5. Donabedian A (1998) The quality of care. How can it be assessed? J Am Med Assoc 260:1743–1748
6. Downing M, Bonham JR, Allen JC, Heap SJ, Manning NJ, Olpin SE, Pollitt RJ (1999) Is quality assurance for quality urinary organic acid analysis improving performance? J Inherit Metab Dis 22:148
7. Fraser CG, Kallner A, Kenny D, Peterson PH (1999) Strategies to set global analytical quality applications in laboratory medicine. Scand J Clin Lab Invest 59:477–478
8. ISO9001:2000 Quality management systems – Requirements. International Organization for Standardization (ISO), 1, Rue de Varentie, Case Postals 56, CH–2111 Geneva 20, Switzerland

9. ISO/IEC 17025:1999 General requirements for the competence of testing and calibration laboratories. International Organization for Standardization (ISO), 1, Rue de Varentie, Case Postals 56, CH–2111 Geneva 20, Switzerland
10. ISO 15189:2002 Medical laboratories – Particular requirement for quality and competence. International Organization for Standardization (ISO), 1, Rue de Varentie, Case Postals 56, CH–2111 Geneva 20, Switzerland
11. ISO/IEC 43–1:1997 Proficiency testing by interlaboratory comparisons – Part 1. Development and operations and proficiency testing schemes. International Organization for Standardization (ISO), 1, Rue de Varentie, Case Postals 56, CH–2111 Geneva 20, Switzerland
12. Levey S, Jennings ER (1950) The use of control charts in the clinical laboratory. Am J Clin Path 20:1059–1066
13. McGovern MM, Benach M, Wallenstein S, Boone J, Lubin IM (2003) Personnel standards and quality assurance practices of biochemical genetic testing laboratories in the United States. Arch Path Lab Med 127:71–76
14. Rasmussen K, Maller J, Lyngbak M (1999) Within person variation of plasma homocysteine and effects of posture and tourniquet application. Clin Chem 45:1850–1855
15. Westgard JO (2003) Internal quality control: planning and implementation strategies. Ann Clin Biochem 40:593–611

1.3 Simple Metabolic Screening Tests

K. Michael Gibson, Marinus Duran

1.3.1 Cyanide Nitroprusside Test

1.3.1.1 Principle

The cyanide nitroprusside test determines the presence of free sulfhydryl or disulfide compounds in urine samples [1, 3, 4]. During the first step of the assay, cyanide reduces any disulfides that are present to free sulfhydryl compounds. In the second step, a reddish color reaction results when the free sulfhydryl groups complex with nitroprusside. A positive result is most usually due to cystine in the urine. Familial cystinuria is among the most common aminoacidurias. Disulfides are also excreted in other metabolic disorders such as homocystinuria and β-mercaptolactate-cysteine disulfiduria. Both will also produce positive results according to the following reaction: RSH + $Na_2Fe(CN)_5NO$ (sodium nitroprusside) → chromophore + NO.

1.3.1.2 Specimen Requirements

The specimen requirements for this test are as follows:

1. 1.0 ml of clear urine.
2. Store and transport specimen frozen.
3. Gloves and a laboratory coat should be worn. Use the proper technique to avoid aerosols.

1.3.1.3 Reagents

1. Sodium cyanide (NaCN), 5% in H_2O. Weigh out 25 g of NaCN carefully; avoid creating dust. Add NaCN to 500 ml H_2O and stir. Store the reagent in a plastic bottle at room temperature under a fume hood. This reagent is stable for up to 1 year. The reagent bottle must be stored in a container large enough to hold the bottle's contents. Dispose of any unused 5% solution appropriately. Always perform the assay in a fume hood; protect the eyes and skin with glasses and gloves. Discard any completed assay mixture (liquid in tubes) down the drain in the fume hood after adding 70/30 (v:v water) bleach solution into each tube and allowing it to stand for 1 h. Avoid inhalation, contact with skin/mucous membranes, and ingestion.

2. Sodium nitroprusside (sodium nitroferricyanide), 0.5% in H_2O. Carefully weigh out 0.5 g of the reagent; avoid creating dust. Add the reagent to 100 ml H_2O. The reagent is light sensitive, so store it in a dark bottle at +4°C. The solution is stable for up to 4 months. Dispose of any unused standard reagent appropriately. Always perform the assay in a fume hood; protect the eyes and skin with glasses and gloves. Discard any completed assay mixture (liquid in tubes) down the drain in the fume hood after adding 70/30 (v:v water) bleach solution into each tube and allowing it to stand for 1 h.

1.3.1.4 Procedure

1. Set up one 12 × 100 mm test tube per patient. Label the tubes with the patient number/name. Thaw one tube each of pre-made positive and negative controls.
2. Aliquot 1.0 ml of clear patient urine to the corresponding test tubes. If the urine is not clear, spin at ~ 500 × *g* for 3 min.
3. In the fume hood, add 0.4 ml NaCN to each patient's specimen and control tube and vortex.
4. Incubate at room temperature for 20 min.
5. After 20 min, add 0.2 ml sodium nitroprusside to each patient's specimen and control tube one at a time, vortex, and read the results immediately.
6. Note that color develops immediately and fades quickly. A pink to red, or beet color, indicates a positive. Grade the positives on a scale of trace to 4+.
7. Record the results.
8. Add 70/30 bleach solution into each tube and allow to stand for 1 h to ensure that the sodium cyanide will not be reactive when disposed of down the drain.

1.3.1.5 Linearity/Calculations

Not applicable for this test.

1.3.1.6 Interference

The urine sample used should be at neutral pH. If the sample has been preserved with acid, a false positive may occur. Drugs such as N-acetylcysteine, 2-mercaptoethanesulfonate, 2-mercaptopropionylglycine, captopril, penicillamine, and large amounts of synthetic penicillin metabolites and acetoacetate will give positive results. Bacterial contamination may also give a false positive.

1.3.1.7 Quality Control

Positive and negative controls (pooled urine supplemented with and without cysteine, respectively; 50 mg/dl) are run with each batch of patient samples.

1.3.1.8 Normal/Therapeutic Ranges

A slight pink color may be detected from a normal urine that is concentrated; however, the detection of any positive result warrants further investigation.

1.3.1.9 Notes

Cystathionine, methionine, and taurine are not detected by this assay. In addition, this assay may be helpful for the detection of heterozygotes of cystinuria types 2 and 3.

1.3.2 Ehrlich's Aldehyde Reagent

1.3.2.1 Principle

Ehrlich's test is used to identify the presence of porphobilinogen (PBG) or urobilinogen in the urine [1–3]. PBG in urine reacts with Ehrlich's aldehyde reagent to give a red color in samples with acute porphyria. Except for PBG-synthase deficiency, acute porphyria is generally associated with increased urinary excretion of PBG. Urobilinogen, a component of heme degradation, results when bilirubin derivatives are secreted in the bile and further degraded by bacterial enzymes in the large intestine. In the normal patient, some of the urobilinogen is reabsorbed and transported to the kidneys where it is converted to urobilin (yellow) and excreted. However, the majority of urobilinogen is converted microbially to sterobilin (deep red-brown). Urobilin is responsible for the characteristic color of urine, while sterobilin is the main pigment of feces.

1.3.2.2 Specimen Requirements

The specimen requirements for this test are as follows:
1. 1.0 ml of urine.
2. Store and transport the specimen frozen.
3. Gloves and a laboratory coat should be worn. Use the proper technique to avoid aerosols.

1.3.2.3 Reagents

1. 2% (w/v) p-dimethylaminobenzaldehyde (p-DABA) in 2N HCL. Mix 2 g p-DABA in 100 ml 2N HCl. Store in a brown bottle at 4°C. Note: this reagent is an irritant and is corrosive; avoid inhalation and contact with skin/mucous membranes. Dispose of the reagent in the drain at a concentration below 10% in an aqueous solution.
2. Reagent-grade chloroform and butanol.

1.3.2.4 Procedure

1. Set up one 12 × 100 mm test tube per patient and a control. Label each tube with the patient's number/name or control name.
2. Aliquot 1.0 ml each of well-mixed patient and control urine to the corresponding tubes.
3. Add 0.1 ml p-DABA reagent to each tube and vortex.
4. Incubate at room temperature for 10 min.
5. After 10 min, examine the color of tube mixture. A deep orange, pink, or red color is considered positive.
6. If positive, add 1.0 ml chloroform to the tube, vortex, and allow to settle for a few minutes.
7. After it has settled, if the bottom layer is pink, the sample is urobilinogen positive and PBG negative. Grade the color intensity (trace, 1 +, 2 +, 3 +, 4 +) and record the results.
8. If the top layer is pink, pipette it out and place it into a clean tube.
9. Extract by adding 1.0 ml butanol to the removed layer (top layer). Vortex and allow the suspension to settle for a few minutes.
10. Upon settling, if the bottom layer in the tube is pink, the sample is PBG positive. Grade the color intensity (trace, 1 +, 2 +, 3 +, 4 +) and record the results.

1.3.2.5 Linearity/Calculations

Not applicable for this assay.

1.3.2.6 Interference

Clinical samples often contain complex mixtures of different porphyrins. Porphyrin solubility in organic solvents is inversely proportional to the number of acid side chains. Indoles in the urine may also give a positive result.

1.3.2.7 Quality Control

A negative and positive control sample (pooled urine, spiked with urobilinogen/PBG) is run with each batch of patient samples.

1.3.2.8 Normal/Therapeutic Ranges

The range is determined visually by observing the mixture color. A deep orange, pink, or red color is considered positive and is graded on a scale of trace to 4 +. A grade of 3–4 + should be acted on immediately. The range for normal tube test results may include results of negative to 1 + potentially due to the natural occurrence of small amounts of urobilinogen/PBG in urine, and/or interfering substances.

1.3.2.9 Notes

Individuals affected with porphyria present with acute attacks, skin lesions, or both. The onset of these attacks rarely occurs before puberty. An attack usually consists of severe abdominal pain and often neurological sequelae. During and after such attacks, excessive amounts of aminolevulinic acid and PBG are excreted in the urine. The most common porphyria is PBG deaminase deficiency (acute intermittent porphyria), which primarily affects liver function. A positive result coupled with a clinical indication of hepatosplenomegaly suggests that evaluation for tyrosine metabolites in the urine should be pursued (using the nitrosonaphthol test).

1.3.3 Dinitrophenylhydrazine Assay

1.3.3.1 Principle

The dinitrophenylhydrazine (DNPH) assay detects α-keto acids in the urine [1, 4]. 2,4-DNPH reacts with α-keto acids to form hydrazones, which precipitate out of solution. Several metabolic disorders can be detected, including phenylketonuria (PKU), maple syrup urine disease (MSUD), tyrosinosis, tyrosyluria, histidinemia, and methionine malabsorption (Oasthouse syndrome). The presence of acetone also gives a positive result and may suggest a metabolic disorder. A positive result due to acetone is consistent with the diagnosis of disorders such as hyperglycinemia, isovaleric acidemia, and glycogen storage diseases. A 2N HCl test is performed on all DNPH positives to determine the presence of false-positive results.

1.3.3.2 Specimen Requirements

For this assay, 1.0 ml of random, void urine (morning void preferable) is required, stored and transported frozen.

1.3.3.3 Reagents

1. 0.2% 2,4-DNPH in 2N HCL. Store at 4°C. Stable for 1 year. This reagent is corrosive.
2. 2N HCl. Store at room temperature in an acid storage area. Use in a fume hood.
3. 2-Ketoacid standard (3-methyl-2-oxobutyric acid, 2-ketoisovaleric); mix 50 mg in 25 ml (2 mg/ml) deionized water. Store the solution at 4°C.

1.3.3.4 Procedure

1. Label one 13 × 100 mm test tube with the patient's number or name. Add 1.0 ml clear urine. If the urine is turbid, spin at 500 × *g* for 3 min.
2. Prepare a positive control of 20 mg/dl. For this, add to a 13 × 100 mm test tube, 100 μl of 2-ketoacid standard and 900 μl of H_2O. The amount of precipitate that

will occur in this positive control is considered to be approximately 2 +. This aids in judging the amount of precipitate in patient samples.
3. Add 1 ml DNPH reagent to each patient and control tube and vortex. Incubate at room temperature for 10 min.
4. After 10 minutes, examine the samples. The presence of a yellow or whitish precipitate indicates a positive result.
5. If no precipitate occurs, the patient sample is recorded as negative. Grade the samples with a precipitate on a trace–4 + scale and record the results
6. For positive samples, test to ensure that the reaction did not produce a false positive. Label a clean 13 × 100 mm test tube with the patient's name or number and place 1 ml of the patient's clear urine into the tube. Add 1 ml of 2N HCl, vortex, and allow to incubate at room temperature for 10 min.
7. The presence of a precipitate after 10 min indicates a positive result. This suggests that the original positive DNPH result observed was probably a false positive.
8. Record the 2N HCl results as either negative, or grade on a trace–4 + scale if a precipitate is present. Generally, results of 2 + or more are considered a concern.

1.3.3.5 Interfering Substances

Substances with low solubility in acid can interfere with the DNPH assay. Mandelamine (methenamine mandelate), an antibacterial medication, and radiopaque contrast material will form a precipitate immediately upon addition of the DNPH reagent. The color and immediacy of formation of this precipitate distinguishes it from the yellowish precipitate of α-keto acid hydrazones. It is very important to have information on patient medications prior to evaluation of the DNPH test.

1.3.3.6 Quality Control

Control urines are run with each batch of patient samples, consisting of pooled negatives (no appreciable precipitate) in addition to a spiked pool urine containing significant exogenous α-keto acid standard.

1.3.3.7 Affected/Unaffected Values

An unaffected patient will have a negative DNPH result. Mildly affected or partially treated patients may also yield negative results. Patients with a blood phenylalanine level (indicative of PKU) over 1 mmol/l should generate positive DNPH results. Patients with a blood leucine level (indicative of MSUD) of 0.8 mmol/l or higher usually show a positive DNPH result. Patients with pyruvate metabolic disorders may also give positive results, as will patients with true and transient disorders of tyrosine degradation.

1.3.4 Multistix Reagent Strips for Urinalysis

1.3.4.1 Principle

Multistix 10 SG and Multistix PRO 11 (Bayer HealthCare, Elkhart, IN, USA) are reagent test strips that provide qualitative colorimetric analysis of several intermediates in urine, including protein, blood, leukocytes, nitrite, glucose, ketones (acetoacetic acid), pH, specific gravity, creatinine, bilirubin, and urobilinogen. The methodology, interpretation, and characteristics of the approximate linearity of these procedures are provided in the package insert with each reagent bottle. In addition, for each test, sensitivity parameters, expected values, limitations, and interfering substances in urine are described. Results obtained from this screening procedure can provide insight into the status of a patient's kidney and liver function, acid-base balance, and/or carbohydrate metabolism.

1.3.4.2 Specimen Requirements

Fresh void urine is the sample of choice for this analysis, enough to saturate all reagent patches on one strip; the minimum requirement is 1.0 ml of urine. The sample should be stored and transported frozen.

1.3.4.3 Reagents

Reagent strips for urinalysis, manufactured by Bayer HealthCare. Each strip contains reagent patches for the testing of glucose, bilirubin, ketone (acetoacetic acid), blood, pH, and protein. See the package insert for exact reagent compositions.

1.3.4.4 Procedure

1. Dip one strip into well-mixed, thawed urine to ensure saturation of reagent patches, then remove the strip from the urine. The strip should remain in the urine only briefly to reduce the potential for leaching of reagents from the patches.
2. Place the strip onto a paper towel (reagent patch side facing up) and allow it to develop for an appropriate time period; the development times of the specific patches are listed on the package insert.

1.3.4.5 Interferences

Certain medications may induce discoloration of the urine sample, which may interfere with the results. The colorimetric reaction may be affected by riboflavin or drugs containing azo dyes, or by nitrofurantoin. Other interferences may include:

1. Glucose: False negatives may occur when the urine contains small amounts of glucose (75–125 mg/dl) and/or ascorbic acid concentrations of 50 mg/dl or more. Sensitivity may also be decreased by the presence of ketone bodies.

2. Bilirubin: A false negative may occur when the sample contains ascorbic acid concentrations of 25 mg/dl or more. The yellow/orange-to-red color produced by the presence of indican (indoxyl sulfate) is also problematic.
3. Ketone: False positive results may occur in highly pigmented samples, samples containing levodopa metabolites, or samples containing significant amounts of sulfhydryls.
4. Blood: False positives may arise from oxidizing contaminants (such as hypochlorite), or microbial peroxidase (e.g., as a result of a urinary tract infection).
5. Protein: False positives may occur with highly buffered or alkaline samples or from contamination with quaternary ammonium compounds (antiseptics, detergents).

1.3.4.6 Quality Control

A control urine is run with each batch of patient samples. In most instances, this is a pooled control urine that has been aliquoted.

1.3.4.7 Normal/Therapeutic Ranges

1. Glucose: The small amount of glucose excreted normally by the kidneys generally produces a result considered negative to trace.
2. Bilirubin: The detection of even trace amounts of bilirubin in the urine is abnormal.
3. Ketone: A negative result is typical. Positive results can indicate physiological stress (e.g., fasting, pregnancy). Ketoacidosis and other abnormalities of carbohydrate, lipid, and amino acid metabolism may yield high levels of ketones in the urine and positive strip results.
4. Blood: The development of nonhemolyzed blood (intact erythrocytes) or a green color (free hemoglobin/myglobin) on the strip is not typically normal and may warrant further investigation.
5. pH: Urinary pH may range from 5 to 9 for both normal and abnormal samples.
6. Protein: A result beyond trace amounts is suggestive of proteinuria and renal dysfunction.

1.3.4.8 Notes

Refer to the package insert for details concerning the chemical principles of each reagent patch. If samples are allowed to sit at room temperature for prolonged periods before testing, microbial proliferation may occur and alter the results.

1.3.5 Tyrosine Metabolites – the Nitrosonaphthol Test

1.3.5.1 Principle

In the presence of nitric acids, 4-hydroxylated phenolic acids (and to some extent also hydroxylated indoles from tryptophan) conjugate with 1-nitroso-2-naphthol to yield orange/red chromophores [4]. The structure of 1-nitroso-2-naphthol is shown in Fig. 1.3.1.

1.3.5.2 Specimen Requirements

This test requires 1 ml of clear voided urine that is free of particulate matter. If present, any precipitate is removed by centrifugation for 5 min at 3,000 × *g*. The urine sample is stored frozen.

1.3.5.3 Reagents

1. Reagent A: 2.63N nitric acid (one volume of concentrated nitric acid in five volumes of deionized H_2O). Store the solution at 4°C; it is stable for 1 year. Avoid inhalation and contact with skin or mucous membranes.
2. Reagent B: 2.5 g sodium nitrite dissolved in 100 ml H_2O. Store at 4°C. Avoid inhalation and contact with skin or mucous membranes.
3. Reagent C: 100 mg 1-nitroso-2-napthol dissolved in 100 ml 95% ethanol. Store at 4°C in a brown glass bottle; it remains stable for 3 months. Avoid inhalation and contact with skin or mucous membranes. This reagent is an irritant and possible carcinogen.
4. Standard: 0.01M N-acetyl-L-tyrosine in 1M HCl: 40 mg/100 ml 1M HCl. Use only L-tyrosine (human form). Store at 4°C.

1.3.5.4 Procedure

1. Label a 13 × 100 mm test tube with the patient's number or name. Add three drops of their urine to the test tube.
2. Prepare the positive controls. Label four 13 × 100 mm test tubes as "10", "20", "40", and "60", respectively. These correspond to the amount of standard in microliters added to the tubes and provide a range of positive controls from trace to 4 +.
3. Add 10 µl standard to the tube labeled "10", 20 µl to that labeled "20" tube, 40 µl to the "40" tube, and 60 µl to the "60" tube.
4. Add three drops of water to each control tube.

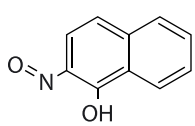

Fig. 1.3.1 Structure of 1-nitroso-2-naphthol

5. Add 1 ml of reagent A to each patient and control tube.
6. Quickly add 1 drop of reagent B to each tube.
7. Quickly add 200 μl of reagent C to each tube.
8. Vortex all tubes and incubate them at room temperature for 15 min.
9. After 15 min, observe the color in each tube. The "10" control tube yields the color intensity of a trace positive. Any patient tube color that is less intense than the "10" control tube is a negative result. Grade any positives according to the range given by the control tubes. Positive controls should yield results as listed in Table 1.3.1.

1.3.5.5 Quality Control

A control urine is run with each batch of patient samples. As for other control samples in this section, this is generally a pooled urine sample that has been aliquoted and stored frozen.

1.3.5.6 Normal/Therapeutic Ranges and Interpretations

An orange-red color suggests the presence of hydroxylated tyrosine analogs (e.g., 4-hydroxyphenylpyruvate, 4-hydroxyphenyllactate, and 4-hydroxyphenylacetate), as well as tyrosine. A key limitation is the occurrence of transient tyrosinemia of the newborn, a not uncommon finding as the hepatic enzymes involved in tyrosine metabolism are not well developed in the newborn. 4-Hydroxyphenylacetate levels may be elevated due to intestinal bacterial metabolism, malabsorption, and other disorders, and may lead to false positives. Some disorders of carbohydrate metabolism, and unassociated liver dysfunction, may alter tyrosine metabolism with artifactual results. Patients undergoing parenteral nutrition are often supplemented with tyrosine analogs, which can lead to difficulties in the interpretation of this test. Patients with tumors may excrete increased homovanillic acid and/or 5-hydroxyindoleacetic acids (end products of dopamine and serotonin metabolism, respectively), which produce pink and purple colorimetric reactions in the nitrosonaphthol reaction. Any positive should be correlated with clinical history and/or followed-up with more specialized testing (blood amino acids/urine organic acids).

Table 1.3.1 *Nitrosonaphthol test results*

Tyrosine control	Qualitative grade	Color
40	Trace	Light orange-red
80	1+	Orange-red
120	2+	Deep orange-red
240	3+/4+	Red/immediate red

References

1. Buist NR (1968) Set of simple side-room urine tests for detection of inborn errors of metabolism. Br Med J 22:745–749
2. Elder GH, Smyth SJ (1991) Porphyrins and porphobilinogen. In: Hommes FA (ed) Techniques in Diagnostic Human Biochemical Genetics. Wiley-Liss, New York, pp 327–344
3. O'Brien D, Ibbott FA, Rodgerson DO (1968) Laboratory Manual of Pediatric Microbiochemical Techniques (4th edn). Harper and Row, New York, p 70
4. Shih VE, Mandell R, Sheinhait I (1991) General metabolic screening tests. In: Hommes FA (ed) Techniques in Diagnostic Human Biochemical Genetics. Wiley-Liss, New York, pp 45–68

1.4 Lactate, Pyruvate, Acetoacetate and 3-Hydroxybutyrate

Anne Vassault

1.4.1 Introduction

Lactate, pyruvate, acetoacetate (ACAC) and 3-hydroxybutyrate (3OHB) are intermediary metabolites that normally occur in blood and play an essential role in energy production. Their accumulation in blood is a frequent cause of metabolic acidosis in children. The determination of these metabolites in biological fluids is useful in the early detection, diagnosis and treatment follow-up of abnormalities such as those of:

1. Enzymes of pyruvate "metabolism" (pyruvate dehydrogenase, PDH, or pyruvate carboxylase, PC, defects).
2. Enzymes of the Krebs cycle.
3. Enzymes of gluconeogenesis.
4. Liver glycogenolysis.
5. Oxidation of fatty acids.
6. Ketogenesis, ketolysis.
7. Mitochondrial respiratory chain.

Their relative blood concentrations are an expression of nutritional balance, providing a view of the metabolic disturbances arising in a patient. In conjunction with the measurement of unesterified fatty acids (UEFA) and glucose, they are useful tools with which to investigate intermediary metabolism in health and disease, particularly in inherited metabolic diseases.

During fasting, hormonal or metabolic modifications mobilise energy stored in adipose tissue as fat. Evaluation of different metabolite concentrations in blood provides insight into the different steps of fat metabolism.

Determinations of lactate, pyruvate, 3OHB and ACAC in biological fluids are run at different times during the day according to different periods of fasting. They are usually performed before and after meals (1 h). They are also performed after loading tests (e.g. glucose, proteins or triglycerides.)

1.4.2 Properties of Analytes

The plasma lactate (CH_3-CHOH-COOH) levels reflect the equilibrium between its production and its consumption by different tissues. Lactate is the end product of

anaerobic glycolysis, which is the main energy source for tissues such as the heart, muscles and kidney. Accumulation of lactate in blood to levels higher than 7 mmol/l leads to lactic acidosis. Hyperlactataemia can be observed either in ischaemic conditions or in many inherited metabolic diseases (e.g. PDH deficiency, PC deficiency).

During fasting, lactate is used by the liver and kidneys to provide glucose (gluconeogenesis). Blood lactate decreases during the first 15 h of fast (about 30% regardless of age). In the postprandial period, lactate is oxidised in mitochondria, producing energy for the heart, muscles and kidneys. The different metabolic pathways of pyruvate and lactate interconversion are shown in Fig. 1.4.1. The ratio of lactate to pyruvate remains unchanged independent of the fasting state.

Lactate and pyruvate are interconverted within the cytoplasm, depending upon the NAD:NADH ratio. In the cytoplasm, the ratio of lactate to pyruvate reflects the oxidoreduction state.

Pyruvate (CH_3-CO-COOH) is an intermediate metabolite, the product of carbohydrate, fat or protein metabolism. Pyruvate is the end point of glycolysis. In mitochondria, pyruvate may be oxidized to CO_2 and H_2O, reduced to acetyl coenzyme A (acetyl CoA) by PDH, or carboxylated by PC into oxaloacetate (Fig. 1.4.2).

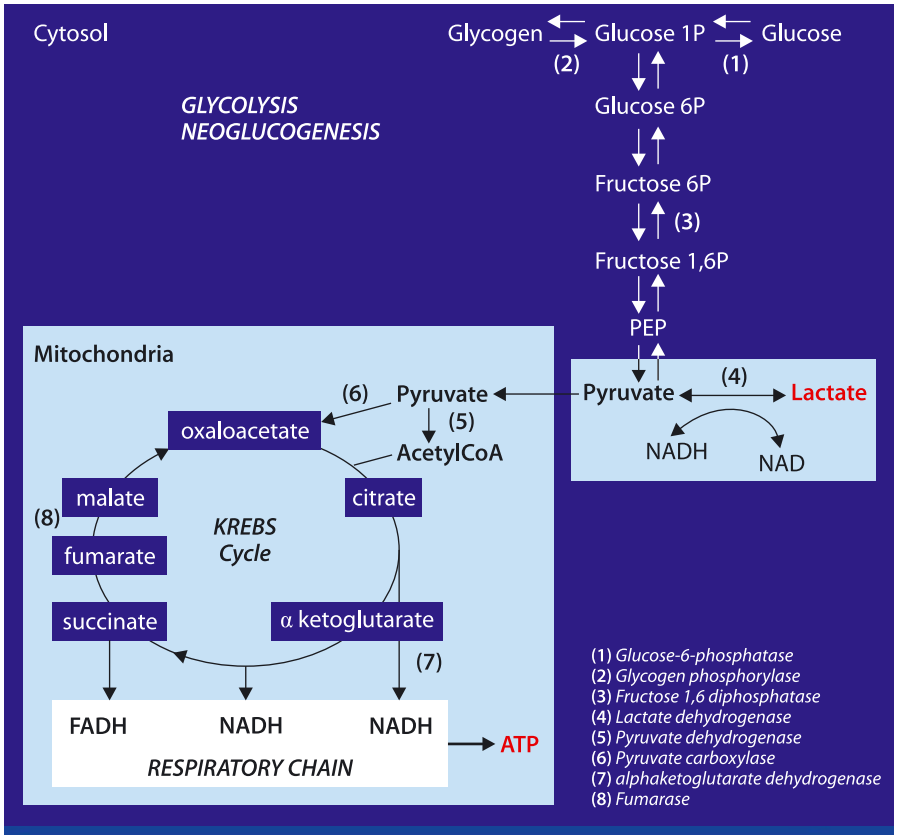

Fig. 1.4.1 Lactate and pyruvate metabolic pathway. (*P* Phosphate, *PEP* phosphoenolpyruvate)

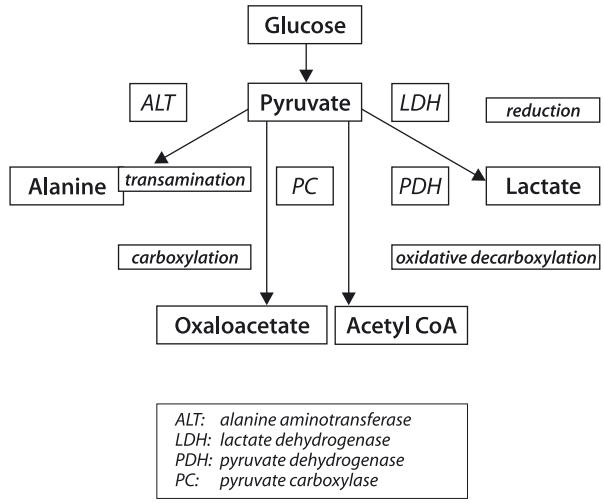

Fig. 1.4.2 Pyruvate pathways

Pyruvate is transformed to lactate by lactate dehydrogenase (LDH) under anaerobic conditions.

Ketone bodies (KBs) circulate in the blood as 3OHB (CH_3-CHOH-CH_2-COOH) and ACAC (CH_3-CO-CH_2-COOH). The blood concentrations of these two metabolites depend upon the equilibrium between their production by the liver (ketogenesis) and consumption at the peripheral level (ketogenolysis). Abnormalities of KB metabolism manifest as ketosis, hypoketotic hypoglycaemia and inversion of the 3OHB:arachidonic acid (AA) ratio [12].

In the fed state, the KB concentrations do not usually exceed 0.2 mmol/l, except during the neonatal period, where higher concentrations are observed. The level of ACAC increases more quickly than that of 3OHB. The blood concentration of KBs increases during the fasted state, with an associated increase in the 3OHB:ACAC ratio, the result of PDH inhibition by mitochondrial acetyl CoA and NADH. KBs are primarily synthesised in the liver from acetyl CoA, the product of fatty acid oxidation.

Interconversion between ACAC and 3OHB is dependent upon the NAD:NADH ratio. Hydroxybutyrate dehydrogenase (HBDH) is localised mainly in the mitochondria. During fasting, fatty acids are transported to the liver to undergo beta oxidation.

Acyl coenzyme As are introduced into mitochondria following coenzyme A esterification in the cytoplasm. Mitochondrial entry depends upon a double membrane transport involving carnitine acyltransferases II and I. Excess acetyl CoA is used for KB synthesis. KBs are transported in the blood and ultimately metabolized via the Krebs cycle. KBs are necessary to provide energy to the brain during fasting, a true alternative substrate to glucose.

1.4.3 Methods

1.4.3.1 Principle

For simultaneous blood measurement of the four metabolites (lactate, pyruvate, ACAC and 3OHB), blood that has been deproteinised with perchloric acid is used as a sample. Spectrophotometric enzymatic methods according to reactions given in Fig. 1.4.3 were developed for automated analysers to minimise sample volume and improve precision [1, 10, 11, 17].

1.4.3.2 Pre-analytical

Specimen

Lactate and 3OHB can be measured in blood, plasma, urine and the cerebrospinal fluid (CSF). Pyruvate and ACAC are highly unstable, so deproteinisation is performed immediately after sampling. Lactate, pyruvate, 3OHB and ACAC determination can be measured in the same sample after deproteinisation using perchloric acid [17].

Patient Preparation

Patient preparation includes evaluation of clinical indications, and nutritional conditions (i.e. fed state, fast state, fasting duration) must be precisely defined. The patient must be fully informed of all procedures and at rest prior to blood sampling or invasive procedure. If fasting is required, the fast is scheduled for 24 h, but can be interrupted. Beginning at night, sampling is performed at 2, 15, 20 and 24 h of the fast.

Blood collection

Blood is collected as follows:

1. Blood sampling (venipuncture) must be performed without tourniquet, venestasis or muscular hand activity. Use of a catheter is recommended. Once the catheter (Cathelon; Critikon, Tampa, Florida, USA) is installed, the first milliliter (1 to 2 volumes of the catheter) should be discarded before a blood sample is taken.
2. Blood volume: 0.6–1 ml is collected into a heparinised tube.
3. The period of the blood collection is determined according to the diagnostic and therapeutic processes chosen, in accord with the suspected disease (i.e. before meals, after meals, fasting state, fasting test, loading test). For example, when screening for mitochondrial cytopathy, redox has to be evaluated in the fed state or after a glucose loading test, and after 10 h of fast.
4. Document in the patient's charts and requests the exact time of sampling and delays after last meals.
5. Avoid capillary blood.
6. Choose venous or arterial blood and document which has been taken.

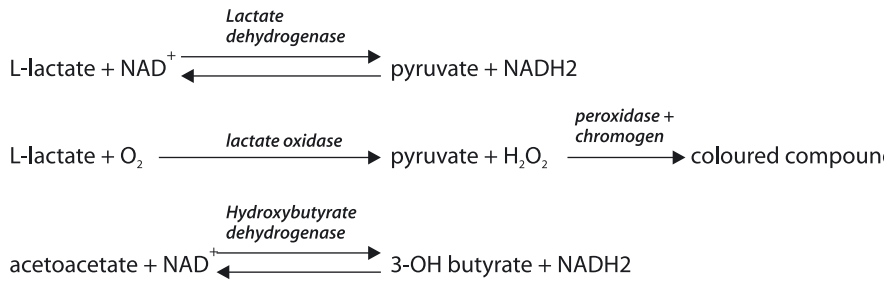

Fig. 1.4.3 Reactions involved in the enzymatic measurement of 3-hydroxybutyrate, acetoacetate, lactate and pyruvate

Sampling volume

Blood lactate, pyruvate, ACAC, 3OHB, glucose and redox ratio should be measured using the same sample for a reliable calculation of redox status.

Blood Pre-treatment

Deproteinisation using acids is required to avoid glycolysis, but has to be performed as soon as possible after sampling (within 5 min). Simultaneous determination of lactate, pyruvate, ACAC and 3OHB is possible using this sample.

Different procedures are described for pre-treatment of blood, but perchloric acid is the most widely used agent: blood collected in a tube containing heparin is immediately deproteinised with a perchloric acid solution (1 mol/l) that has been refrigerated at + 4°C (two volumes for one volume of blood). Deproteinised samples may be frozen for up to 5 days.

Plasma Lactate and 3OHB

Lactate and 3OHB can be measured in plasma. Blood is collected in a tube with an anticoagulant (heparin, EDTA, oxalate) and antiglycolytic agent (fluoride – without which there is an artefactual increase in lactate levels). The tube is transported in ice water and plasma is separated from the blood within 15 min following sampling.

Lactate levels in plasma sampled according to the aforementioned conditions are stable for up to 1 week at + 4°C and for up to 1 month at –20°C.

Lactate in CSF

CSF sampling is performed by lumbar puncture, avoiding haemolysis. No pre-treatment of the sample thus obtained is necessary.

Specimen Preparation Procedure

Deproteinisation

Deproteinisation is carried out immediately after collection (< 5 min) as follows:

1. Measure accurately 1 ml (0.5 ml) blood collected in a tube containing heparin; transfer this to a tube containing 2 ml (1 ml) perchloric acid 1 M (which was measured accurately and refrigerated at 4°C previously).
2. Agitate the blood/perchloric acid mixture thoroughly to obtain a brown coagulum.
3. Keep the tube frozen (–20°C) for a period less than 5 days.

Neutralisation

1. After thawing, deproteinised samples are centrifuged (+ 4°C) for 10 min at $3000 \times g$.
2. Mix 1 ml of the supernatant with 0.5 ml of phosphate buffer. If the volume of the supernatant available is < 1 ml, keep the ratio at one volume of supernatant to half a volume of buffer.
3. Mix. Place the tubes for 10 min at –20°C.
4. Check that the pH is 7 with pH paper (range 1–14.).
5. If needed, adjust pH as follows, noting the added volume for future calculation:
   a. if pH< 7 add phosphate buffer M (50 µl to 100 µl) (see reagent preparation)
   b. if pH> 7add $HCl0_4$ M (50 µl to100 µl).
6. Centrifuge for 5 min at $3500 \times g$ at + 4°C.
7. The deproteinised sample is thawed and centrifuged and the supernatant has to be neutralised using tripotassium phosphate buffer.

The stability in the filtrate of lactate, pyruvate, 3OHB and ACAC is 5 days at –20°C.

Reagents and Chemicals

Lists of reagents, and recipes for working solutions and reagents are provided in Tables 1.4.1 and 1.4.2, respectively. The lactate reagent is prepared as per the manufacturer's instructions. The reagent required for the deproteinisation step is a solution of perchloric acid 1 mol/l (dilute 8.6 ml of $HCLO_4$ 70% in 100 ml distilled water or 11 ml of $HCLO_4$ 60% in 100 ml distilled water). That required for the neutralisation is phosphate tripotassic buffer 1 mol/l: add 5.3 g of phosphate tripotassic in 25 ml distilled water. This solution will be stable for 1 year at 25°C.

Instrumentation and Calibration

An automated method can be run after validation using multiparametric open analysers [1, 11, 17], For example, KONELAB 30 (Thermo Fisher Scientific, Waltham, USA). There is no standard for pyruvate, ACAC or 3OHB. The results are calculated taking into account the molecular extinction coefficient of NADH ($6.3\ mmol^{-1} \cdot cm^{-1}$). A lactate standard is provided in the kit.

■ ***Table 1.4.1*** *List of reagents.* 3OHB *3-Hydroxybutyrate,* ACAC *acetoacetate,* HBDH *hydroxybutyrate dehydrogenase,* LDH *lactate dehydrogenase*

Name	Provider	Reference	Storage temperature
Perchloric acid 70–72%	Merck	100591000	20–25°C
Lactic acid	Sigma	L2250	+4°C
ß NAD grade I	Sigma	N 1511	–20°C
ß NADH grade II	Sigma	N 8129	+4°C
Lactate	Randox	LC 2389	+4°C
Phosphate tripotassic buffer	Sigma	04347	20–25°C
Tris buffer	Merck	1083820500	20–25°C
Paper pH 1–14	MN	902 04	20–25°C
ACAC powder	Sigma	A8509	–20°C
D,L-3OHB powder	Sigma	H6501	+4°C
3-HBDH	Roche	127841	+4°C
LDH	Roche	107069	+4°C
$NaHCO_3$	Merck	1063290500	+4°C
Pyruvate powder	Sigma	P8574	+4°C

■ ***Table 1.4.2*** *Reagent preparation and working solutions. Lactate reagent was prepared according to the manufacturer's instructions*

	ACAC	3OHB	Pyruvate
Tris 0.1 mol/l buffer	pH 6.98: dissolve 3.0285 g of Tris buffer into 200 ml distilled water. Adjust pH to exactly 6.98 with 1.2 M HCl, then adjust the volume to 250 ml.	pH 9.5. dissolve 3.0285 g of Tris buffer into 200 ml distilled water. Adjust the pH to exactly 9.5 with 1.2 M HCl, then adjust the volume to 250 ml.	pH 7.4: dissolve 3.082 g of Tris buffer into 200 ml distilled water. Adjust the pH to exactly 7.4 with 1.2 M HCl, then adjust the volume to 250 ml.
Stability at +4°C	1 month	1 month	1 month
β NADH reduced, stock solution, 0.6 mmol/l			Dissolve 0.85 mg of NADH into 2 ml $NaHCO_3$ 5%
Stability			7 days at +4°C
Working solutions: R1	*β* NADH reduced solution at 0.4 mmol/l: dissolve 2.8 mg of NADH in 10 ml of Tris buffer (pH 6.98)	Solution of NAD 12 mmol/l: dissolve 80 mg of NAD in 10 ml of Tris buffer (pH 9.5)	Solution of NAD 0.12 mmol/l: dilute 1.2 ml stock solution NADH in 4.8 ml Tris buffer pH 7.4
R2	Mix: 750 µl Tris pH 6.98 + 250 µl HBDH (> 15 U/ml)	Mix: 750 µl Tris buffer pH 9.5 + 250 µl HBDH (> 15 U/ml)	Mix: 80 µl of LDH solution (7500 U/ml) + 4720 µl of Tris buffer pH 7.4

Quality Control

The quality control samples are prepared as described in Table 1.4.3. Target values are calculated according to the amount of weighed product, and values obtained must be within ± 15% of the target value.

1.4.4 Analytical

1.4.4.1 Methods

The same deproteinised blood as used for lactate, pyruvate, 3OHB, and ACAC assays described above is used for enzymatic methods employing spectrophotometric measurement (Fig. 1.4.3) [10, 17]. The enzymes involved are LDH for pyruvate, lactate oxidase for lactate and HBDH for ACAC and 3OHB.

Procedure

The operating procedure for this method is given in Table 1.4.4. Note that lactate is quantified according to the manufacturer's instructions.

Calculation

For the filtrate samples, results have to be recalculated according to the dilution ratio (e.g. × 4.5). If acid base or buffer was added to correct the pH, an additional correction must be made according to the following equation:

$$\frac{\text{observed result} \times \text{final volume}}{\text{initial volume}}$$

Validation of the Methods

The results of method validation are given in Table 1.4.5.

1.4.4.2 Post-analytical

Interpretation – Biological Variation

Blood lactate values are usually lower than plasma levels (–15 %) depending upon haematocrit values. KB concentration depends on whether the patient is in a fed or fasted state and age; the concentration is low in the fed state, increasing as the fasting period increases, with some variability according to age in children (e.g. KB elevations are higher in younger, more precocious children; see Fig. 1.4.4) [7]. In the fed state, KB levels are less than 0.2 mmol/l and the ratio 3OHB:ACAC is less than 1. The blood concentration of KBs increases during fasting. The 3OHB:ACAC ratio increases with the concentration of KBs during fasting (2.5–3.5). Plasma values of

■ ***Table 1.4.3*** *Preparation of quality control samples*

	Lactate	Pyruvate	ACAC	3OHB
Stock solution	50 mmol/l	10 mmol/l	20 mmol/l	10 mmol/l
Dissolve into 10 ml albumin 50 g/l solution	0.048 g of lactate (sodium salt)	11 mg of pyruvate (sodium salt)	25.5 mg ACAC	25.7 mg of D-l, 3OHB
Stability	6 months at – 20°C	6 months at – 20°C	6 months at – 20°C	6 months at – 20°C
Prepare three different level solutions				
Level 1	10 µmol/l	100 µmol/l	10 µmol/l	0.25 mmoll
Level 2	50 µmol/l	200 µmol/l	50 µmol/l	0.5 mmol/l
Level 3	100 µmol/l	400 µmol/l	100 µmol/l	1 mmol/l
Stability	Do not store	Do not store	Do not store	Do not store
Target values and acceptable limits	10 µmol/l ± 1.5 50 µmol/l ± 7.5 100 µmol/l ± 15	100 µmol/l ± 15 200 µmol/l ± 30 400 µmol/l ± 60	10 µmol/l ± 1.5 50 µmol/l ± 7.5 100 µmol/l ± 15	0.25 mmol/l ± 0.03 0.5 mmol/l ± 0.075 1 mmol/l ± 0.15

■ ***Table 1.4.4*** *Operating procedure*

	Pyruvate	ACAC	3OHB
Sample (neutralised supernatant)	60 µl	60 µl	40 µl
R1 (buffer + coenzyme)	100 µl	105 µl	120 µl
Mix thoroughly, incubate at 37°C, measure absorbance at 340 nm A1			
R2 (enzyme)	20 µl	12 µl	10 µl
Wait time at 37°C	300 s	450 s	600 s
Measure absorbance at 340 nm A2			
Calculation factor (µmol/l) taking into account the sample dilution (×4.5)	475 2142	466 2686	671 3019

■ ***Table 1.4.5*** *Analytical performances of the methods [17].* CV *Coefficient of variation*

	Lactate	Pyruvate	ACAC	3OHB
Reproducibility within run (CV%)	< 3	< 3	< 3	< 3
range (mmol/l)	0.8–8	0.1–0.5	01–2	0.4–5
Reproducibility run to run (CV%)	< 5	< 5	< 5	< 5
range (mmol/l)	0.8–8	0.1–0.5	0.1–2	0.4–5
Linearity limits (mmol/l)	0–15	0–15	0–15	0–9
Detection limit (mmol/l)	0.1	0.01	0.02	0.02

KBs are 10–20% higher than blood values. No difference has been observed between venous and arterial blood in this regard.

Interpretation – Reference Values

Reference values are given according to age, fed state, fasting state, diet and nutritional status (Table 1.4.6). Figure 1.4.4 shows the evolution of KB level as a function of fasting time and age [4, 17]. The reference values for lactate/creatinine/pyruvate are as follows:

1. Urine: lactate: creatinine ratio < 0.2 mmol/mmol creatinine.
2. CSF [2, 9]:
   a. Lactate: 1.1–2.2 mmol/l
   b. Pyruvate: 0.05–0.15 mmol/l
   c. Lactate:pyruvate ratio: 15–20

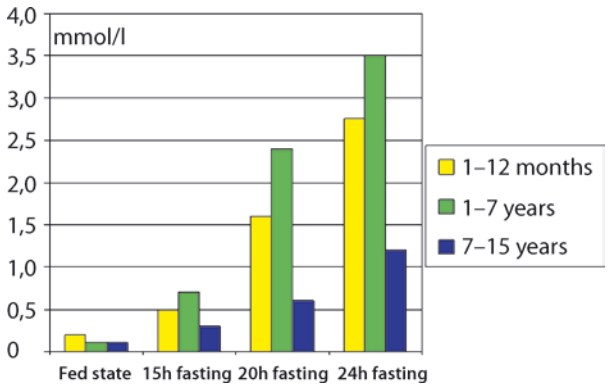

Fig. 1.4.4 Ketone body levels according to fasting time and age

Table 1.4.6 *Reference values for blood lactate, pyruvate, ACAC and 3OHB according to age, fed state and fasting state.* L:P *lactate:pyruvate ratio*

	Lactate (L) (mmol/l)	Pyruvate (P) (mmol/l)	L:P	3OHB (mmol/l)	ACAC (mmol/l)	Ketone bodies (mmol/l)	Ratio 3OHB: ACAC
Children (0–1 year)							
Fed state, 1 h after meals	0.6–2.2	0.04–0.14	6–14	0.10–0.2	0.10–0.25	0.10–0.30	< 1
Children (1–7 years)							
Fasting 10 h	0.7–1.8	0.09–0.17	6–14	0.02–0.3	0.04–0.20	0.02–0.6	< 2.5
Fed state	0.9–1.8	0.08–0.17	6–14	0.02–0.1	0.04–0.13	0.02–0.2	< 1
Children (7–15 years) and adults							
Fasting 10 h	0.7–0.9	0.04–0.12	6–14	0.02–0.3	< 0.2	0.1–0.4	0.4–2.3
Fed state	1.0–1.55	0.08–0.16	6–14	0.02–0.1	0.04–0.13	< 0.20	< 1

1.4.4.3 Main Causes of Hyperlactataemia, Hyperketonaemia and Hypoketonaemia

The main causes of acquired hyperlactataemia and hereditary hyperlactataemia are given in Tables 1.4.7 and 1.4.8, respectively. The main causes of hyperketonaemia and hypoketonaemia are given in Tables 1.4.9 and 1.4.10, respectively.

Table 1.4.7 *Main aetiologies for hereditary hyperlactataemias [3]*

Primary hyperlactataemias	Secondary hyperlactataemias
Glycogen metabolism disorders Amylo-1,6-glucosidase defect Liver phosphorylase defect Glycogen synthetase defect	Organic acidaemias Methylmalonic aciduria Propionic aciduria Isovaleric aciduria
Gluconeogenesis defects Glucose-6-phosphatase defect Fructose-1,6-biphosphatase defect Phosphoenol pyruvate carboxykinase defect	Congenital hyperammonaemia: citrullinaemia Fat oxidation disorders
Pyruvate disorders Pyruvate carboxylase defect Pyruvate dehydrogenase defect	
Krebs cycle abnormalities Ketoglutarate dehydrogenase defect Fumarase defect	
Respiratory chain abnormalities NADH coenzyme Q reductase defect (complex I) Succinate coenzyme Q reductase defect (complex II) Coenzyme Q cytochrome C reductase defect (complex III) Cytochrome oxidase C defect (complex IV) ATPase defect (complex V)	

Table 1.4.8 *Main causes for acquired hyperlactataemia [3, 6]*

With anoxia, resulting in tissue hypoperfusion	**Without anoxia**
Heart stroke, endotoxins or haemorrhagic	Diabetes
Serious anaemia	Renal insufficiency
Intensive muscular disease	Intoxications: salicylate, cyanide, alcohol, antiretroviral drugs, biguanides
Left ventricular insufficiency	
Convulsions	
Hypocapnia	

Table 1.4.9 *Causes for hyperketonaemias*

Over-production	Decreased ketone body utilisation at the peripheral level
Diabetes – insulin dependent	Ketolysis defects: Succinyl coenzyme A:3-keto acid transferase ACAC coenzyme A thiolase
Methyl malonic, propionic or isovaleric acidaemias	
Pyruvate carboxylase and multiple carboxylase deficiency	
Gluconeogenesis enzyme deficiency: glucose-6-phosphatase, fructose-1,6-diphosphatase or abnormality of glycogen synthesis (glycogen synthase)	

Table 1.4.10 *Hypoketonaemic states*

Hyperinsulinism
Multiple acyl coenzyme A dehydrogenase
Long chain fatty acid oxidation defect
Carnitine palmitoyl transferase I and II
Systemic carnitine deficiency
Long-chain acyl coenzyme A dehydrogenase defect
Long-chain 3-hydroxy-acyl coenzyme A dehydrogenase defect
Medium chain acyl coenzyme A dehydrogenase deficiency
Hydroxymethyl glutaryl coenzyme A lyase defect

1.4.4.4 Typical Pathological Values

Respiratory Chain Abnormalities

Data from a patient affected with mitochondrial respiratory chain abnormalities (complex I, III and IV deficiencies) are given in Table 1.4.11. Permanent hyperlactataemia is associated with an increased lactate:pyruvate ratio and postprandial ketosis with an increased 3OHB:AA ratio. Pyruvate, the product of glycolysis, is metabolised in the mitochondria to acetyl CoA by PDH. Pyruvate can be reduced to lactate by LDH or may be utilized for gluconeogenesis. Mitochondrial respiratory chain dysfunction results in decreased acetyl CoA metabolism. Pyruvate metabolism shifts towards other metabolic routes, including reduction to lactate and gluconeogenesis. Lactate cannot be cleared as rapidly as it is being produced, resulting in acidosis. Increased gluconeogenesis results in hyperglycaemia.

A fully functional PDH complex leads to acetyl CoA accumulation. Overproduction of acetyl CoA, without utilisation in the respiratory chain complex, results in accumulation of acetyl CoA in the cytoplasm, where it serves as a substrate for fat production. An inability to metabolise acetyl CoA also leads to increased circulating levels of ACAC and 3OHB [8, 13].

Table 1.4.11 *Data from a patient affected with a complex I, III and IV deficiency*

	Lunch		Dinner	
	Before meals	After meals	Before meals	After meals
Lactate (mmol/l)	6.00	8.50	5.00	8.90
Pyruvate (mmol/l)	0.24	0.31	0.18	0.28
L:P	24.00	27.50	28.00	32.00
ACAC (mmol/l)	0.22	0.14	0.16	0.20
3OHB (mmol/l)	1.53	0.90	1.10	1.27
Ketone bodies (mmol/l)	1.75	1.04	1.26	1.45
3OHB:AA	7.00	6.40	6.90	6.40
Glycaemia (mmol/l)	5.00	5.80	3.30	5.20

PC Defect

In the initial step of gluconeogenesis, pyruvate is carboxylated to oxaloacetate by PC (Fig. 1.4.2). Two forms of PC deficiency are observed. Patients with type B disease develop symptoms in the neonatal period, including severe lactic acidaemia, hypotonia, seizures, failure to thrive, psychomotor retardation and hepatomegaly. The lactate:pyruvate ratio is increased due to a deficiency in aspartate, which is involved in maintaining the mitochondrial redox status. Hypoglycaemia is mild and helps to distinguish this condition from type I glycogen storage disease (glucose-6-phosphatase deficiency), which also produces lactic acidosis. Most patients with type B disease do not synthesize any PC protein. Death usually occurs within the first 6 months of life. Type A disease manifests as less severe lactic acidaemia (3–6 mmol/l) with acute metabolic decompensation usually observed in association with an illness or fasting. These patients demonstrate low muscle tone and developmental delays, mental retardation with cerebral atrophy, and abnormalities of brain myelinisation.

Metabolically, acetyl CoA that is generated is diverted to ketogenesis, and urea cycle activity is decreased, leading to hyperammonaemia associated with fasting hypoglycaemia, increased lactataemia associated with an increased lactate:pyruvate ratio, and increased ketonaemia with a 3OHB:AA ratio < 1. Data from a patient affected with a PC defect are presented in Table 1.4.12.

PDH Defect

Data from a patient affected with a PDH defect are presented in Table 1.4.13. In general, hyperlactataemia (increasing with meals) associated with a normal lactate: pyruvate ratio and normal ketonaemia is observed. The ketogenic diet is a rational treatment for PDH complex deficiency.

■ ***Table 1.4.12*** *Fed and fasting state for a patient affected with a pyruvate carboxylase defect (type B)*

	Before meals	After meals
Lactate (mmol/l)	22.00	11.00
Pyruvate (mmol/l)	0.55	0.22
L:P	40.00	50.00
ACAC (mmol/l)	0.80	0.50
3OHB (mmol/l)	0.35	0.25
Ketone bodies (mmol/l)	1.15	0.80
3OHB:AA	0.40	0.50
Glucose (mmol/l)	2.40	5.60

■ **Table 1.4.13** *Data from a patient affected with a pyruvate dehydrogenase defect*

	Breakfast		Lunch	
	Before meals	After meals	Before meals	After meals
Lactate (mmol/l)	9.30	13	8.80	10.00
Pyruvate (mmol/l)	1.07	1.50	0.66	0.90
L:P	8.70	8.70	13	11.00
ACAC (mmol/l)	0.07	0.03	0.04	0.06
3OHB (mmol/l)	< 0.02	< 0.02	< 0.02	< 0.02
Ketone bodies (mmol/l)	< 0.20	< 0.20	< 0.20	< 0.20
3OHB:AA	< 1	< 1	< 1	< 1

Beta Oxidation Defect

Hypoketotic hypoglycaemia was observed in a patient with consanguinity and a history of hypotrophy and neonatal hypoglycaemia. She was hospitalised at 6 months of age for anorexia, hypotonia, progressive asthenia and failure to thrive [15, 16]. Associated findings included liver insufficiency, icterus and hepatomegaly. Metabolic evaluation of lactate, pyruvate, ACAC and 3OHB (associated with increased UEFA; Table 1.4.14) resulted in an evaluation of a fatty acid oxidation defect. Characterization of plasma acylcarnitines and oxidation of long-chain fatty acids (myristic and palmitic acid) in cultured fibroblasts demonstrated a long-chain 3-hydroxyacyl-coenzyme A dehydrogenase defect.

Table 1.4.14 *Data from a patient affected with a long-chain 3-hydroxyacyl coenzyme A dehydrogenase defect.* UEFA *Unesterified fatty acids*

	Before meals	1 h after	3 h after	4 h after
Lactate (mmol/l)	1.50	2.20	1.50	2.30
Pyruvate (mmol/l)	0.15	0.18	0.15	0.18
L:P	10.00	12.00	10.00	13.00
ACAC (mmol/l)	0.06	0.07	0.07	0.05
3OHB (mmol/l)	0.05	0.02	0.04	0.04
Ketone bodies (mmol/l)	< 0.20	< 0.20	< 0.20	< 0.20
3OHB:AA	< 1	< 1	< 1	< 1
UEFA (mmol/l)	1.00	0.07	1.20	3.50
Glucose (mmol/l)	4.00	5.80	2.50	2.40

Table 1.4.15 *Data from a patient affected with succinyl coenzyme A:3-oxo acid transferase deficiency*

	Fed state	After 20 h fasting
Lactate (mmol/l)	1.50	1.30
Pyruvate (mmol/l)	0.15	0.11
L:P	10.00	12.00
ACAC (mmol/l)	0.25	4.20
3OHB (mmol/l)	0.20	6.00
Ketone bodies (mmol/l)	0.45	10.00
3OHB:AA	< 1	1.40
UEFA (mmol/l)	0.10	3.00
Glucose (mmol/l)	4.50	3.00

Ketolysis Disorder

Succinyl Coenzyme A:3-Oxo Acid Transferase Defect

Succinyl coenzyme A:3-oxo acid transferase catalyses the transformation of ACAC into acetoacetyl coenzyme A in the mitochondria of extra-hepatic tissues. This enzyme defect may be suggested in cases of severe ketoacidosis often associated with neurologic dysfunction [16].

The data presented in Table 1.4.15 are derived from a 2-year-old child in the fed and fasting states and document the results of a metabolic evaluation of this patient. Permanent hyperketonaemia increased with fasting, in comparison to UEFA, which are lower in comparison to the KB concentration, suggests a defect in utilizing KBs in the periphery, not overproduction of KBs from UEFA.

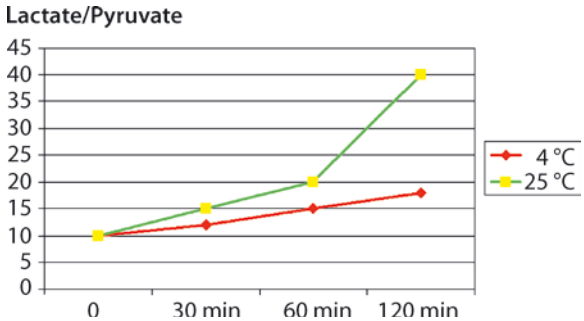

Fig. 1.4.5 Effects of blood storage temperature and delay between sample preparation and measurement on the lactate:pyruvate ratio

1.4.5 Pitfalls

1.4.5.1 Pre-analytical Pitfalls

The main sources of variation are linked to the time of collection, conditions of treatment and the transport and storage of the sample [5, 14].

Deproteinisation

1. An increased lactate:pyruvate ratio is observed when the delay between the moment of blood collection and deproteinisation exceeds 5 min (Fig. 1.4.5).
2. Inappropriate volume of the deproteinised sample will lead to errors in measurement.
3. Inappropriate pH of the filtrate may reflect a non-uniform dilution ratio between the blood sample volume and $HClO_4$ volume, or can be due to errors in $HClO_4$ molarity or instability due to inappropriate storage of the acid.
4. Lactate, pyruvate, 3OHB and ACAC must be measured using the same deproteinised sample; if not, the lactate:pyruvate ratio may be incorrect.

Sample Stability

Pyruvate and ACAC are not stable at 20–25°C.

References

1. Artuch R, Vilaseca MA, Farre C, Ramon F (1995) Determination of lactate, pyruvate, beta-hydroxybutyrate and acetoacetate with a centrifugal analyser. Eur J Clin Chem Clin Biochem 33:529–533
2. Benoit JF, Alberti C, Leclercq S, Rigal O, Jean-Luois R, Ogier de Baulny H, Porquet D, Biou D (2003) cerebrospinal fluid lactate and pyruvate concentration and their ratio in children: age-related reference intervals. Clin Chem 49:487–494
3. Bonnefont JP, Saudubray JM, Vassault A (1991) Dosage des acides lactique, pyruvique et des corps cétoniques. Application au diagnostic des hyprerlactacidémies et des états d'acidocétose chez l'enfant. In: Saudubray JM (ed) Progrès en Pédiatrie, Maladies Métaboliques. Doin Editeurs, Paris, pp 29–40
4. Bonnefont JP, Specola NB, Vassault A, Lombes A, Ogier H, de Klerk JB, Munnich A, Coude M, Paturneau-Jouas M, Saudubray JM (1990) The fasting test in paediatrics: application to the diagnosis of pathological hypo- and hyperketotic states. Eur J Pediatr 150:80–85
5. Carragher FM, Bonham JR, Smith JM (2003) Pitfalls in the measurement of some intermediary metabolites. Ann Clin Biochem 40:313–320
6. Duke T (1999) Dysoxia and lactate. Arch Dis Child 81:343–350
7. Francois B, Colomb V, Bonnefont JP, Goulet O, Benhariz M, Vassault A, Rabier D, Ricour C (1997) Tolerance to starvation in children on long-term total parenteral nutrition. Clin Nutr 16: 113–117
8. Garcia Silva MT, Bonnefont JP, Rotig A, Romero N, Vassault A, Colonna M, Coude M, Rabier D, Munnich A, Fardeau M, et al (1989) Respiratory chain diseases in infancy. Clinical presentation and diagnosis. An Esp Pediatr 31:421–430
9. Hutchesson A, Preece MA, Gray G, Green A (1997) Measurement of lactate in cerebrospinal fluid in investigation of inherited metabolic disease. Clin Chem 43:158–161
10. Kientsch-Engel RI, Siess EA (1985) D(-)-3-hydroxybutyrate and acetoacetate. In: Bergmeyer HU, Bergmeyer J, Graßl M (ed) Methods of Enzymatic Analysis, 3rd edn, vol VIII. Verlag Chemie, Weinheim, Germany, pp 60–69
11. Li PK, Lee JT, Mac Gillivray MH, Schaefer PA, Siegel JH (1980) Direct, fixed-time kinetic assays for beta-hydroxybutyrate and acetoacetate with a centrifugal analyser or a computer-backed spectrophotometer. Clin Chem 26:1713–1717
12. Mitchell GA, Kassovska-Bratinova S, Boukaftane Y, Robert MF, Wang SP, Ashmarina L, Lambert M, Lapierre P, Potier E (1995) Medical aspects of ketone body metabolism. Clin Invest Med 18:193–216
13. Munnich A, Rustin P, Rotig A, Chretien D, Bonnefont JP, Nuttin C, Cormier V, Vassault A, Parvy P, Bardet J, et al (1992) Clinical aspects of mitochondrial disorders. J Inherit Metab Dis 15:448–455
14. Payne B (2004) Pitfalls in the measurement of some intermediary metabolites: stabilization of lactate and pyruvate. Ann Clin Biochem 41:83
15. Saudubray JM, Mitchell G, Bonnefont JP, Schwartz G, Nuttin C, Munnich A, Brivet M, Vassault A, Demaugre F, Rabier D, et al (1992) Approach to the patient with a fatty acid oxidation disorder. Prog Clin Biol Res 375:271–288
16. Saudubray JM, Specola N, Middleton B, Lombes A, Bonnefont JP, Jakobs C, Vassault A, Charpentier C, Day R (1987) Hyperketotic states due to inherited defects of ketolysis. Enzyme 38:80–90
17. Vassault A, Bonnefont. JP, Specola N. Saudubray JM (1991) Lactate, pyruvate and ketone bodies. In: Hommes FA (ed) Techniques in Diagnostic Human Biochemical Genetics XIX. Wiley-Liss, New York, pp 285–308

2.1 Amino Acids

Marinus Duran

2.1.1 Introduction

Amino acids constitute the building blocks of our proteins and peptides and, as such, they are the most important low-molecular-weight substances in the human organism. The name amino acid stems from its chemical structure: in general these substances contain one or two primary amino groups and one or two carboxyl groups. For almost a century the detection of amino acids in biological fluids depended on its reaction with ninhydrin: the colored reaction product can be visualized on filter paper or quantified by its light absorption at 400–600 nm. The invention of the amino acid analyzer (AAA) in the 1950s marked the start of large-scale investigations into inborn errors of metabolism and constituted a scientific development that is still going on. From that time onwards it also became possible to monitor the dietary therapy of amino acid disorders, thereby improving the quality of life for the patients. Furthermore, sensitive amino acid analysis of amniotic fluid enabled the prenatal diagnosis of selected disorders, an important preventive action.

Protein consists of some 20 different amino acids, of which half can be synthesized endogenously; the other half (the essential amino acids) are derived from the diet. Protein synthesis then takes place for a large part in the liver; every protein has a highly constant amino acid composition. Although there are only 20 protein amino acids, numerous alternative reactions take place, resulting in the formation of "unusual" amino acids. The classic book of Bremer et al. [2] mentions more than 100 amino acids occurring in human urine, and the actual number may even be higher. The recent application of tandem mass spectrometry (MS/MS) analysis of human amino acids [8] tells us to take at least 76 amino acids of biological interest into account.

Inherited defects of amino acid catabolism, biosynthesis, or transport have been known for many years; the number of novel defects is only slowly increasing [1, 3, 4, 10, 12]. In this respect, cystinuria was among the first four inherited metabolic diseases described by Garrod 100 years ago. The disease with the highest impact on the community – phenylketonuria (PKU) – was discovered as early as the 1930s. Despite its early discovery, PKU remains a mysterious disease in several aspects, and patient-oriented research of this condition continues today.

Amino acids are precious components of the human organism and therefore urinary losses are small due to an efficient renal tubular reabsorption system. Because of this, and because the analytical approach is aimed at detecting catabolic

disorders and anabolic disorders, there is a necessity to correctly identify increased and decreased amino acid levels. The low levels of amino acids in the cerebrospinal fluid (CSF) and the neurotransmitter action of several amino acids adds an extra dimension to this analytical problem.

Amino acids are not only associated with inborn errors of metabolism; they may also serve as sensitive markers of the nutritional state and of the function of various organs such as the liver, the kidneys, the intestine, and the muscles. The changes in amino acid concentrations in (acquired) malfunctioning of these organs may be subtle, therefore the amino acid analysis should have a fairly high level of accuracy in order to interpret these changes. Internal and external quality assurance programs such as the ones offered by European Research Network for evaluation and improvement of screening, Diagnosis and treatment of Inherited disorders of Metabolism (ERNDIM) are an indispensable aid in the improvement of one's analytical systems in this area.

2.1.2 Properties of Analytes

Amino acids are by definition low-molecular-weight mono- or dicarboxylic acids with one or more amino groups. A few imino acids (proline, hydroxyproline, pipecolic acid) are also considered to belong to this group of biologically important substances.

The carboxylic acid group of the amino acid has a loosely bound proton and thus tends to have a slightly negative electric charge. On the other hand, the amino group – having a free electron pair at the nitrogen atom – is prone to bind a proton, thereby becoming positively charged. The net effect is a neutral substance with a bipolar, extremely hydrophilic character ("Zwitterion"). In spite of the hydrophilic nature of the amino acids, some of them are only slightly soluble in water. These amino acids are cystine and tyrosine, and care should be taken to fully dissolve these substances in the urine prior to amino acid analysis.

Amino acids with two carboxylic groups or those with two amino groups behave slightly differently in that they are not entirely neutral, but may be acidic or basic. All amino acids therefore have a different isoelectric point (see Table 2.1.1). These differences in polarity form the basis of the separation of amino acids: the neutral amino acids are in the middle part of the chromatogram and the dibasic amino acids elute late. In addition, the length of the aliphatic chain of the molecule makes the amino acid less polar, causing later elution (e.g., ornithine, which has five carbon atoms, elutes before its homolog lysine, which has six carbon atoms).

None of the amino acids are bound to protein, with exception of the sulfur amino acids cysteine and homocysteine and the heterocyclic amino acid tryptophan. Care should be taken in the deproteinization of biological samples in order to preserve these amino acids.

The ionic and hydrophilic nature of the amino acids precludes their isolation from biological fluids by solvent/solvent extraction. Modification of the amino group, for example the formation of an N-acetyl group, makes solvent extraction accessible.

There is a way of bringing amino acids from the biological matrix into an aqueous/organic surrounding – by deproteinization with acetonitrile or alcohol. This is the preferred method of preparing samples for MS/MS.

Table 2.1.1 *Some properties of the most relevant amino acids.* m.w. *Molecular weight,* pI *isoelectric point*

Amino acid	Structure	m.w.	pI
S-Adenosylhomocysteine	4-(adenosylthio)-2-aminobutanoic acid	384.4	
S-Adenosylmethionine	4-(adenosyl-methylthio)-2-aminobutanoic acid	399.4	
Alanine	2-aminopropanoic acid	89.1	6.00
β-Alanine	3-aminopropanoic acid	89.1	
Alloisoleucine	(2S,3R)-3-methyl-2-aminopentanoic acid	131.2	
α-Aminoadipic acid	2-aminohexanedioic acid	161.1	
α-Aminobutyric acid	2-Aminobutanoic acid	103.1	6.08
γ-Aminobutyric acid	4-aminobutanoic acid	103.1	9.20
β-Aminoisobutyric acid	3-amino-2-methylpropanoic acid	103.1	
Arginine	5-guanidino-2-aminopentanoic acid	174.2	11.15
Argininosuccinic acid	(N-4-amino-4-carboxybutyl) carbamimidoyl-aminobutanedioic acid	290.3	3.50
Asparagine	2-amino-3-carbamidopropionic acid	132.1	5.41
Aspartic acid	2-aminobutanedioic acid	133.1	2.77
Citrulline	5-(carbamoylamino)-2-aminopentanoic acid	175.2	5.92
Cystathionine	4-(S-2-aminocarboxypropyl)-2-aminobutanoic acid	222.3	
Cystine	3,3-dithiobis-(2-aminopropionic acid)	240.3	
Ethanolamine	2-hydroxyethylamine	61.1	
FIGLU	2-(iminomethylamino)pentanedioic acid	174.2	
Glutamic acid	2-aminopentanedioic acid	147.1	3.22
Glutamine	2-amino-4-carbamidobutanoic acid	146.2	
Glycine	Aminoacetic acid	75.1	5.97
Histidine	1-H-imidazole-4-(2-aminopropionic acid)	155.2	7.47
Homoarginine	2-amino-6-guanidinohexanoic acid	188.2	
Homocarnosine	N^2-(4-aminobutanoyl) histidine	240.3	
Homocitrulline	2-amino-6-ureidohexanoic acid	189.2	
Homocystine	4,4^1-Dithiobis(2-aminobutanoic acid)	268.3	5.58
Hydroxylysine	2,6-diamino-5-hydroxyhexanoic acid	162.2	9.15
Hydroxyproline	4-hydroxy-2-pyrrolidinecarboxylic acid	131.1	5.74
Isoleucine	(2S,3S)-3-methyl-2-aminopentanoic acid	131.2	5.94
Leucine	4-methyl-2-aminopentanoic acid	131.2	5.98
Lysine	2,6-diaminohexanoic acid	146.2	9.59
Methionine	4-methylthio-2-aminobutanoic acid	149.2	
Ornithine	2,5-diaminopentanoic acid	132.1	
Phenylalanine	3-phenyl-2-aminopropanoic acid	165.2	5.48

■ ***Table 2.1.1*** (continued) *Some properties of the most relevant amino acids.* m.w. *Molecular weight,* pI *isoelectric point*

Amino acid	Structure	m.w.	pI
Phosphoethanolamine	2-aminoethane-1-phosphoric acid	141.1	
Pipecolic acid	2-piperidinecarboxylic acid	129.1	
Proline	2-pyrrolidinecarboxylic acid	115.1	6.30
Saccharopine	N^6-(glutar-2-yl)-2,6-diaminohexanoic acid	276.3	
Sarcosine	N-methylaminoacetic acid	89.1	6.12
Serine	3-hydroxy-2-aminopentanoic acid	105.1	5.68
Sulfocysteine	S-(3-amino-3-carboxypropane)sulfonic acid	201.2	
Taurine	2-aminoethanesulfonic acid	125.2	
Tryptophan	3-indole-2-aminopropanoic acid	204.2	5.89
Tyrosine	3-(4-hydroxyphenyl)-2-aminopropanic acid	181.2	5.66
Valine	3-methyl-2-aminobutanoic acid	117.2	5.96

2.1.3 Specimens for Analysis

As indicated earlier, amino acids are transported across various membranes by a variety of specific transporters. In order to gain insight into defects affecting any of these transporters, one may have to analyze different body fluids, cells, or tissues. However, the initial samples for investigation disorders of amino acid metabolism are a fasting plasma sample combined with a 24-h urine. In daily practice one will observe that many blood samples will be taken in an outpatient clinic situation during mid-morning or after lunch. This may result in mildly increased levels of a range of amino acids; the pattern is considered non-specific. It should be emphasized here that the diagnosis of amino acid biosynthesis defects (glycine, serine, methionine, proline, citrulline) does require testing of a fasting plasma sample to avoid erroneous interpretations.

2.1.3.1 Plasma

Plasma should be separated from the blood cells within a few hours. For most amino acids the levels in plasma and red cells are comparable, but glutamate, aspartate, and taurine have extremely high intracellular levels and thus tend to rise in plasma upon hemolysis. A second effect of red cell degradation is the liberation of the enzyme arginase, which will convert arginine into ornithine.

Sulfur-containing amino acids such as cystine and homocystine tend to bind to plasma proteins. This binding is irreversible; hence, these amino acids will be severely underestimated unless the plasma is deproteinized immediately following its separation from red cells. Blood should be left standing for as short a time as possible to avoid binding of cystine to proteins and hemolysis.

Tryptophan is another amino acid that tends to bind with protein; it is also sensitive to the deproteinization process. The use of sulfosalicylic acid (SSA) in particular is contraindicated. Trichloroacetic acid, on the other hand, leaves tryptophan unaffected.

Plasma that cannot be analyzed instantaneously should be kept frozen at –20°C. Glutamine is particularly liable to decomposition, thereby yielding glutamic acid, but also the ninhydrin-negative pyroglutamic acid. It has even been claimed that γ-aminobutyric acid can be formed from glutamine. Even at –20°C the decomposition of glutamine cannot be stopped completely.

2.1.3.2 Urine

Amino acids in urine may be preserved by a bacteriostatic such as chloroform or toluene during the 24-h collection. Aliquots of urine should be stored subsequently at –20°C. Heat inactivation at 55°C for 20 min has proven to be effective in suppressing bacterial activity; consequently, the sample can be shipped at room temperature.

2.1.3.3 Cerebrospinal Fluid

CSF should be free of any blood contamination because of the marked differences between plasma and CSF amino acid levels. Usually the first milliliter of CSF is used for routine measurements and the second milliliter is used for amino acid analysis. CSF samples are routinely stored at – 80°C.

2.1.4 Tandem Mass Spectrometry

Liquid chromatographic separation of amino acids is one thing, but specific and accurate detection of the column effluent is equally important for the performance of the analytical system. In this respect, the electrospray MS/MS approach is extremely powerful. It allows the unequivocal identification of not only the 20 protein amino acids, but also a variety of other characteristic substances. Careful selection of a high-performance liquid chromatography (HPLC) technique has enabled Piraud et al. [8] to separate 79 diagnostically important amino acids. Their method should be applicable to all body fluids. One of the limitations of the detailed method is the amount of time involved in the analysis and the amount of work associated with the interpretation of the mass chromatograms (C. Vianey-Saban, personal communication). The other end of the spectrum of analytical approaches is the analysis of amino acids in dried blood spots, such as performed in neonatal population screening programs [9]. High-throughput analysis requires speed of analysis, hence no chromatographic separation of analytes and detection by making use of a common fragmentation reaction (neutral loss).

Here we describe a concise method for the analysis of the 20 or so most important plasma amino acids by positive-ion liquid chromatography-(MS/MS). The method is especially useful for the follow-up of dietary treatment.

2.1.4.1 Principle of Assay

Following extractive deproteinization of the plasma, the amino acids (and their stable-isotope-labeled internal standards) are separated by HPLC and introduced into the mass spectrometer. Electrospray ionization results in the formation of electrically charged molecules, which are separated on the basis of their mass/charge (m/z) ratio in the first quadrupole. Following fragmentation in the collision cell, the characteristic fragment for each amino acid is selected in the second quadrupole. This process is named multiple reaction monitoring.

2.1.4.2 Specimen

A minimum volume of 100 µl plasma is needed.

2.1.4.3 Reagents and Chemicals

All chemicals should be of the highest purity available or HPLC-grade. The following reagents and chemicals are required:

1. Amino acid standard (Pierce 20088); this is diluted tenfold with water prior to use.
2. Glutamine (Merck 289).
3. Asparagine (Merck 1566).
4. Tryptophan (Sigma T-0254).
5. $^{2}H_{3}$-Serine (ARC lab DLM-1073).
6. $^{2}H_{4}$-Alanine (ARC lab DLM-1276).
7. $^{2}H_{5}$-Phenylalanine (ARC lab DLM-1258).
8. $^{2}H_{4}$-Tyrosine (ARC lab DLM-451).
9. $^{2}H_{3}$-Methionine (ARC lab DLM-431).
10. $^{2}H_{3}$-Tryptophan (ARC lab DLM-1092).
11. Acetonitrile (Merck M30).
12. Heptafluorobutyric acid (HFB; Pierce 25003).
13. MilliQ water (Millipore).
14. HCl 35% (Merck 316).
15. Eluent A: prepared by adding water to 1 ml of HFB to a final volume of 1 l.
16. Eluent B: prepared by mixing eight parts of acetonitrile and two parts of water. The mixture is sonicated for 15 min.
17. 0.1 M HCl: made by diluting 13 ml 35% HCl with water to a final volume of 1 l. The internal standard mixture is made up in such a way as to enable normal plasma level determinations.

2.1.4.4 Instrumentation

The analysis is carried out on a Micromass Quattro II tandem mass spectrometer, coupled to a Hewlett Packard HP1100 HPLC system. All other laboratory equipment is standard equipment,with exception of a Centrivap vacuum concentrator (Labconco).

Separation of the amino acids is achieved on a Synergy Hydro-RP column (250 × 4.6 mm, 4-µm particles; Phenomenex 00G-4375-E0) with a 20 × 4.0 mm C18-DB guard column (Supelco 59565).

2.1.4.5 Procedure

A 50-µl aliquot of plasma, control plasma, or calibration standard is pipetted into an Eppendorf vial. Add 20 µl of the internal standard mixture and 500 µl of acetonitrile. Mix on a Vortex mixer and allow deproteinization at 4°C for 15 min. Centrifuge at 12,000 rpm (12,000 × g) in a refrigerated microcentrifuge for 10 min. Transfer the supernatant to a glass vial and evaporate the solvent in the Centrivap vacuum concentrator (50°C, 60 min). Redissolve the residue in 200µl of water and mix. Finally, add 20 µl of 0.1% HFB, mix again, and transfer the sample to an autosampler vial. The sample is ready for injection and can be kept in the refrigerator for 3 days. Ten microliters of the sample are injected into the HPLC equipment. Gradient elution of the amino acids is carried out as shown in Table 2.1.2.

The electrospray -MS/MS instrument is set in such a way that pairs of ions are recorded, each with a dwell time of 0.05 s with an interchannel delay of 0.03 s. The collision energy and the cone voltage are adjusted for each analyte (Table 2.1.3). An example of an MS/MS profile is shown in Fig. 2.1.1.

2.1.4.6 Quality Control

Each series of analyses has one control plasma (a mix of anonymized plasmas), which is also being used for the AAA approach. The observed values of ten individual amino acids are displayed in a Shewhart-card and thus constitute the internal quality control system.

External quality control involves participation in the ERNDIM scheme for quantitative amino acids in plasma. Four pairs of samples with four concentration levels are analyzed throughout the year and their results give an indication of accuracy, precision, linearity, and recovery.

Table 2.1.2 *Gradient elution of the amino acids for tandem mass spectrometry*

Time (min)	%A	%B	Flow (ml/min)
0	100	0	1.2
2	95	5	1.2
10	50	50	1.2
11	0	100	1.2
12	0	100	1.2
12.01	100	0	1.2
13	100	0	1.2

Table 2.1.3 *Multiple reaction monitoring of amino acids for their tandem mass spectrometry quantitation. In daily practise not all mentioned amino acids are measured in one run, but a set of ten dedicated evaluation programs has been developed, covering groups of amino acids associated with groups of disorders. Amino acids presented in italics indicate stable-isotope-labeled internal standards*

Amino-acid	Parent	Daughter	Cone voltage (V)	Collision energy (eV)
Glycine	76.05	30.40	20	10
$^{2}H_5$-Glycine	81.05	35.40	20	10
Alanine	90.05	44.30	20	20
Sarcosine	90.10	44.30	20	15
β-Alanine	90.10	72.20	20	10
^{15}N-β-alanine	91.10	73.20	20	10
$^{2}H_4$-alanine	94.05	48.30	20	20
β-Amino-isobutyric acid	104.05	86.00	20	5
Serine	106.00	60.30	20	15
$^{2}H_3$-Serine	109.00	63.30	20	15
Proline	116.00	70.15	20	15
Valine	118.00	72.15	20	10
Threonine	120.10	74.25	20	15
$^{2}H_7$-Proline	123.00	77.15	20	15
$^{2}H_8$-Valine	126.00	80.15	20	10
Taurine	126.10	108.05	30	10
$^{13}C_2$-Taurine	128.10	110.05	30	10
Leucine	132.05	43.25	20	30
Alloisoleucine	132.05	69.10	20	20
Isoleucine	132.05	86.15	20	15
δ-Amino-laevulinic acid	132.05	114.15	20	10
Ornithine	133.05	70.20	20	20
Asparagine	133.05	74.15	20	20
Aspartic acid	134.20	74.20	20	20
$^{2}H_3$-Leucine	135.05	46.25	20	30
Homocysteine	135.95	90.05	20	10
$^{2}H_3$-Aspartic acid	137.20	77.20	20	20
$^{2}H_6$-Ornithine	139.05	76.20	20	20
$^{2}H_4$-Homocysteine	139.95	94.05	20	10
$^{2}H_{10}$-Isoleucine	142.05	96.15	20	15

Table 2.1.3 (continued) *Multiple reaction monitoring of amino acids for their tandem mass spectrometry quantitation. In daily practise not all mentioned amino acids are measured in one run, but a set of ten dedicated evaluation programs has been developed, covering groups of amino acids associated with groups of disorders. Amino acids presented in italics indicate stable-isotope-labeled internal standards*

Amino-acid	Parent	Daughter	Cone voltage (V)	Collision energy (eV)
Lysine	147.10	84.15	20	20
Glutamine	147.15	129.95	20	10
Glutamic acid	148.05	84.15	20	20
Methionine	150.00	104.10	20	10
$^{2}H_3$-Glutamic acid	151.05	87.15	20	20
$^{2}H_4$-Lysine	151.10	88.15	20	20
$^{2}H_5$-Glutamine	152.15	134.95	20	10
$^{2}H_3$-Methionine	153.00	107.10	20	10
Histidine	156.20	110.10	25	15
α-Amino-adipic acid	162.10	98.10	20	10
Phenylalanine	166.10	120.15	20	15
$^{2}H_5$-Phenylalanine	171.10	125.15	20	15
Arginine	175.15	70.20	25	30
Citrulline	176.10	159.00	15	10
^{13}C-Citrulline	177.10	160.00	15	10
Tyrosine	182.10	165.05	20	10
$^{2}H_7$-Arginine	182.15	77.20	25	30
$^{2}H_4$-Tyrosine	186.10	169.05	20	10
Homocitrulline	190.10	173.05	20	10
Tryptophan	205.25	188.05	20	10
Kynurenine	209.15	192.10	20	10
$^{2}H_5$-Tryptophan	210.25	193.05	20	10
3-OH-Kynurenine	225.00	208.00	20	10
Cystathionine	222.95	134.00	20	15
Cystine	241.00	74.05	25	30
Argininosuccinic acid	291.05	70.10	30	40

2.1.4.7 Validation Data

The lower detection limit in plasma of the aromatic amino acids was at a level of 1 µmol/l, whereas those for alanine and glycine were 5 µmol/l and 10 µmol/l, respectively. The interassay variation was established by analyzing the pool plasma on seven consecutive days. The coefficient of variation ranged from 1.9% for phenylalanine (at a level of 50 µmol/l) to 11.9% for glycine at a level of 230 µmol/l.

The recovery of added amino acids ranged from 91 to 116%, based on the results of the analyses of ERNDIM quality assurance samples. In general there was good agreement between the MS/MS data and the results obtained with the AAA.

2.1.4.8 Postanalysis

Reference values of this approach are not different from those for other amino acid analyses. An example of a mass chromatogram, representing the plasma of a PKU patient, is shown in Fig. 2.1.1. When evaluating the results of MS/MS amino acid analyses, one has to realize that the liquid chromatographic separation is by far less efficient that the AAA separation. For this reason, any amino acid may (partly) co-elute with other amino acid(s), which potentially interferes with its mass spectrometric behavior. This effect is known as quenching. In order to overcome this as much as possible, stable-isotope-labeled internal standards (as many as possible) should be used. However, this matrix effect of ion suppression is the major pitfall in the MS/MS analysis of amino acids. Consequently, the MS/MS analysis of amino acids cannot be regarded as a reference method, similar to all other amino acid analytical methods.

2.1.5 Amino Acid Analyzer

Amino acids can be separated without prior derivatization on a cation-exchange resin column. The elution buffers are classically lithium citrate buffers with different pH values and salt concentrations, which are applied stepwise. There is usually a programmed increase in column temperature. Consequently, there are numerous variables affecting the separation of the individual amino acids [6]. For the detection of the amino acids, the column effluent is mixed with the ninhydrin reagent. Nowadays there are only very few manufacturers of AAAs left. The considerable cost of purchase and the operation costs are a potential threat to the widespread application of this technique, although it is still considered to be the definitive method for diagnosing disorders of amino acid metabolism.

The basis of the separation of amino acids by AAA lies in the interaction between acids – present in the elution buffer – and the stationary phase. This resin is made up of small sulfonated polystyrene particles. The negative charge of the sulfonic acid residues is counterbalanced by the Li^+ -cations of the elution buffer. As the whole separation process takes place at a weakly acidic pH, the carboxylic acid residues are protonated and the interaction with the stationary phase of the column is achieved by the protonated (and thus positively charged) amino group(s) of the amino acids. The more basic the amino acid is, the stronger the interaction with the stationary phase and – consequently – the longer the retention time. So it is easily understood

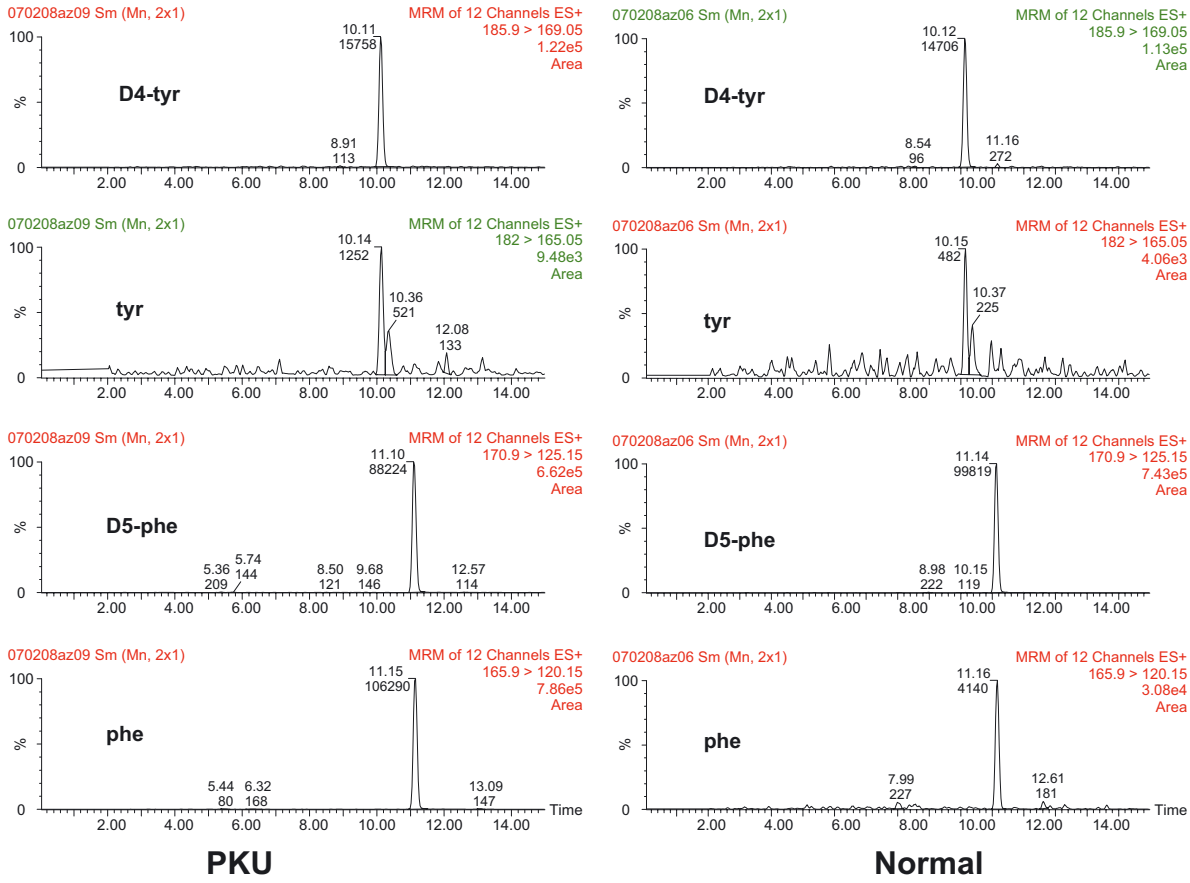

Fig. 2.1.1 Tandem mass spectrometry analyses of plasma phenylalanine (*phe*) and tyrosine (*tyr*) in a patient with phenylketonuria (*PKU*; left panel: phe 793 µmol/l, tyr 70 µmol/l) and in a control (right panel: phe 27 µmol/l, tyr 28 µmol/l). The stable-isotope-labelled internal standards are D4-tyrosine (*D4-tyr*), containing four deuterium atoms and D5-phenylalanine (*D5-phe*), which has five deuterium atoms.

that lysine, having two amino groups, elutes much later than the structurally related leucine, which only has one amino group. The general order of elution is: acidic, neutral, basic. Modification of the predicted order of elution is mainly caused by the nonpolar interaction between the column beads and the secondary functional groups of the amino acids.

2.1.5.1 The Column

Quality of the resin is the basis of good separation and reproducibility of the retention times. In this respect one is highly dependent upon the manufacturer of the instrument, who also supplies the column (and sometimes the resin). During the analysis, the resin is confronted with various buffers of increasing strength and temperature, a fierce regeneration step, and trace amounts of protein that cannot be

totally removed from the biological sample. It is not surprising that the performance of the column seriously deteriorates after some 2000 injections. Cleaning and regeneration procedures have always been popular, but modern column technology often requires a complete replacement of the column, similar to the HPLC approach. A good separation is characterized by 100% valley separation between threonine and serine as well as a clear distinction of the peaks representing alanine and citrulline (the sizes of which differ enormously). Separation problems are usually tackled by modulating the temperature of the column and the switch time of the buffers, as individual changes of the buffer composition have become virtually impossible nowadays.

2.1.5.2 The Buffers

The buffers are uniformly made up of lithium citrate solutions of various pH and salt concentrations. The composition of the buffers is absolutely essential for a reproducible analysis and the supply companies are expected to meet the highest criteria in this respect. Due to impurities in the chemicals, the water, and the mixing devices, different lot numbers of buffers may have slightly different properties. A few tricks have been added over the years to improve the quality of the analysis, including the addition of methylcellosolve (methoxy ethanol) to the first buffer, and antioxidants to preserve methionine from oxidation to methionine sulfoxide.

Temperature changes will result in a shift of the pH of the buffer, and the AAA readily makes use of this property for improving separations. This is applicable mainly to the later part of the analysis. An increase of the column temperature may also influence the binding characteristics of the amino acids with the resin.

So, the analyst has several opportunities to intervene with separation problems. Needless to say, long-standing experience with an AAA is of great value for the continuing quality of the analytical results.

Quantitation of the amino acids proceeds through the postcolumn reaction with ninhydrin at 120–135°C, yielding a purple complex for the primary amino acids (absorbance measured at 570 nm) and a yellow complex for the amino acids proline and hydroxyproline (absorbance at 440 nm).

Secondary amino acids such as sarcosine have some color development with ninhydrin, but its sensitivity is considerably less than that of the primary amino acids.

The AAA thus has two photometers in series. Since for every eluting amino acid both signals are recorded, the so-called 570/440 absorbance ratio may be of help in the identification process. As an example the “simple” primary amino acids have a 570/440 ratio of approximately 6, whereas the sulfur amino acids (cystine, sulfocysteine) have much lower ratios, approaching a value of 1. Small peptides and glycyl-amino acids will react with ninhydrin, an important fact for the diagnosis of prolidase deficiency and aspartylglycosaminuria.

Reduced ninhydrin in solution tends to be unstable, therefore all kinds of precautions have to be taken, such as storage in the cold, in the dark, with a reducing agent added, and exclusion of oxygen. The condition of the ninhydrin solution has to be checked at regular intervals by running an aqueous amino acid standard mixture (Sigma) and adjustment of the response factors.

2.1.5.3 Principle of the Assay

As described above, the amino acids are separated at a constant flow on a high-resolution cation-exchange column using buffer and temperature gradients. The postcolumn reaction with the ninhydrin reagent is carried out at 135°C and the absorbances of the reaction products are read at both 570 and 440 nm. Amino acids are identified by comparing their retention time and 570/440 ratio with that of authentic reference substances (see Fig. 2.1.2).

2.1.5.4 Specimen

See section 2.1.3 for general considerations. The AAA requires a minimum amount of 300 µl plasma or urine; other body fluids can also be used.

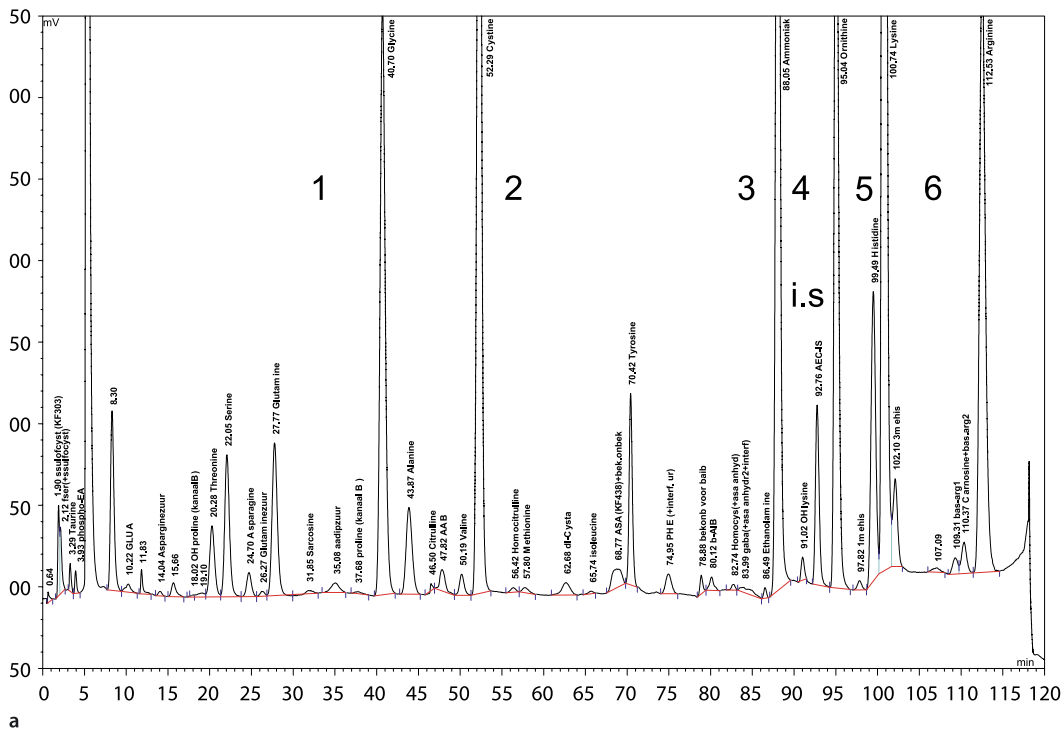

a

Fig. 2.1.2a–c A Urine amino acids in a patient with cystinuria; assayed by an amino acid analyzer (AAA). The indicated peaks are: *1* glycine, *2* cystine, *3* ammonia, *4* ornithine, *5* lysine, *6* arginine, *i.s.* internal standard (S-amino thyl-cysteine). Cystinuria treatment is best followed-up by analyzing an early morning urine specimen, which usually shows the highest amino acid concentrations. **b–c** *see next page*

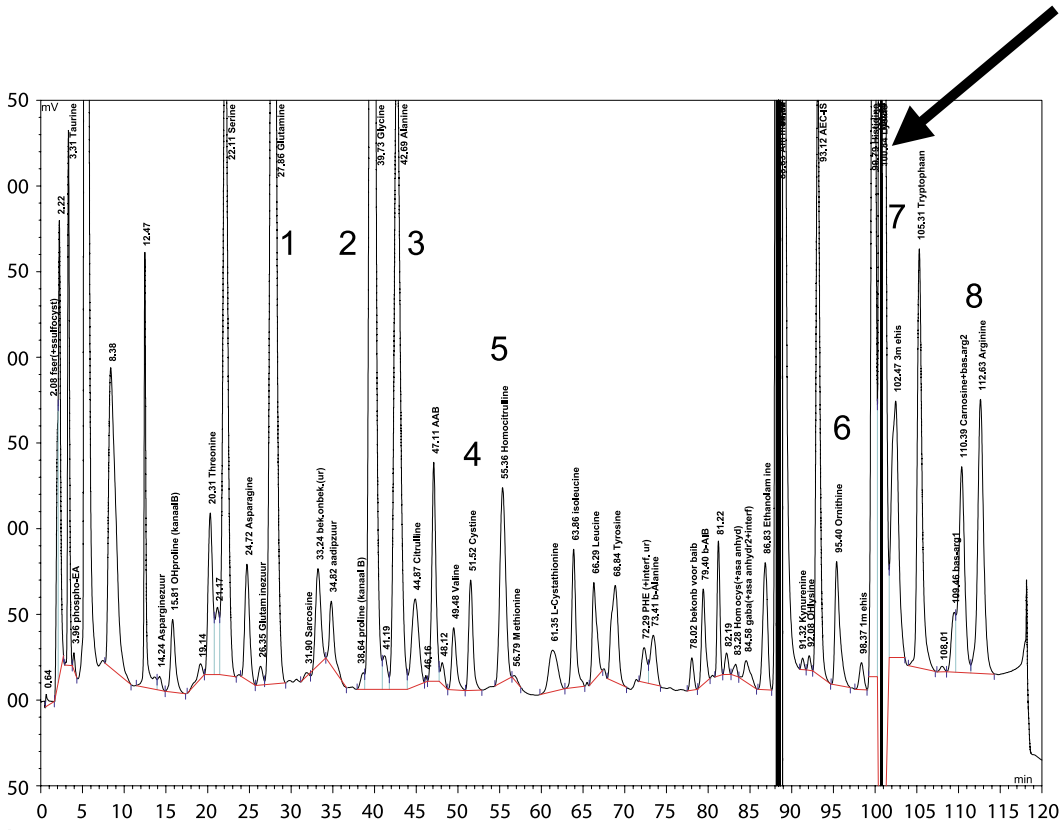
mV
2.08 fseri(+sauflocyst)
2.22
3.31 Taurine
3.96 phospho-EA
8.38
12.47
14.24 Asparginezuur
15.81 Ohproline (kanaalB)
19.14
20.31 Threonine
21.17
22.11 Serine
24.72 Asparagine
26.35 Glutam inezuur
27.86 Glutamine
31.90 Sarcosine
33.24 hek.onbek.(ur)
34.92 aadipzuur
38.64 proline (kanaal B)
39.73 Glycine
41.19
42.69 Alanine
44.87 Citrulline
46.16
47.11 AAB
48.12
49.48 Valine
51.52 Cystine
55.36 Homocitrulline
56.79 M ethionine
61.35 L-Cystathionine
63.86 isoleucine
66.29 Leucine
68.84 Tyrosine
72.29 PHE (+interf. ur)
73.41 b-Alanine
78.02 bekonb voor baib
79.40 b-AIB
81.22
82.19
83.28 Hom ocys(+asa anhyd)
84.58 gaba(+asa anhydr2+interf)
86.83 Ethanolam ine
93.12 AEC-IS
94.23 Kynurenine
95.40 Ornithine
98.37 1m ehis
99.86 Histidine
100.89 Lysine
102.47 3m ehis
105.31 Tryptophaan
108.01
109.46 bas-arg1
110.39 Carnosine+bas.arg2
112.63 Arginine
1
2
3
4
5
6
7
8
min

b

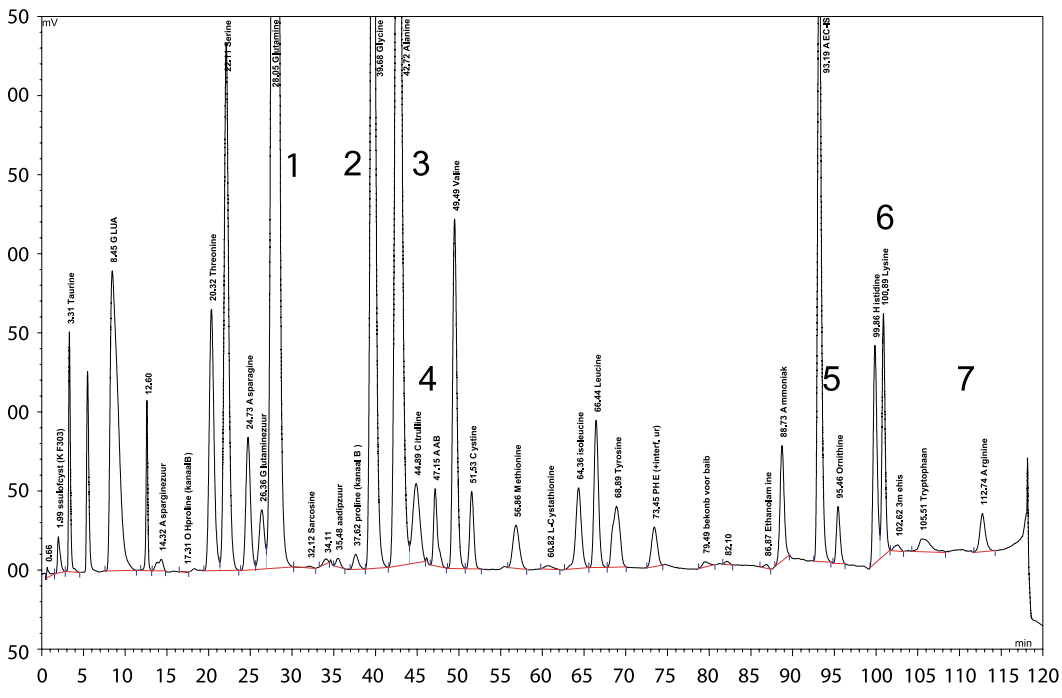
mV
0.66
1.99 saulerlocyst (K F303)
3.31 Taurine
8.45 G LUA
12.60
14.32 A sparginezuur
17.31 O Hproline (kanaalB)
20.32 Threonine
22.11 Serine
24.73 A sparagine
26.36 G lutaminezuur
28.05 Glutamine
32.12 Sarcosine
34.11
35.48 aadipzuur
37.62 proline (kanaal B)
38.68 Glycine
42.72 Alanine
44.98 C itrulline
47.15 A AB
49.49 Valine
51.53 C ystine
56.86 Methionine
60.82 L-Cystathionine
64.36 isoleucine
66.44 Leucine
68.89 Tyrosine
73.45 PH E (+interf. ur)
79.49 bekonb voor baib
82.10
86.87 Ethanolam ine
88.73 A mmoniak
93.19 A EC-IS
95.46 Ornithine
99.86 H istidine
100.89 Lysine
102.62 3m ehis
105.51 Tryptophaan
112.74 A rginine
1
2
3
4
5
6
7
min

c

◄ **Fig. 2.1.2a–c** (*continued*) **b** AAA analysis of urine amino acids in a patient with lysinuric protein intolerance. The denoted peaks are: *1* glutamine, *2* glycine, *3* alanine, *4* cystine, *5* homocitrulline, *6* ornithine, *7* lysine, *8* arginine. Note that the level of cystine is entirely normal. The malfunctioning of the urea cycle in this defect causes ammonia to accumulate. This neurotoxin is subsequently disposed of by the formation of glutamine and alanine. **c** AAA analysis of plasma amino acids in a patient with lysinuric protein intolerance. The denoted peaks are: *1* glutamine, *2* glycine, *3* alanine, *4* citrulline, *5* ornithine, *6* lysine, *7* arginine. Note that levels of the dibasic amino acids lysine, ornithine, and arginine are decreased, whereas that of citrulline is moderately increased

2.1.5.5 Reagents and Chemicals

All chemicals should be of the highest purity available or HPLC grade. The following chemicals and reagents are required:

1. Sulfo-5-salicylic acid dihydrate (Merck 691).
2. Standard amino acids (Sigma A9906).
3. Lithium citrate buffer 1 (P-21 pH 2.98; Jeol).
4. Lithium citrate buffer 2 (P-12 pH 3.28; Jeol).
5. Lithium citrate buffer 3 (P-13 pH 3.46 - Jeol).
6. Lithium citrate buffer 4 (P-14 pH 2.83; Jeol).
7. Lithium citrate buffer 5 (P-15 pH 3.65; Jeol).
8. Lithium hydroxide 0.4 M (P-19; Jeol).
9. Ninhydrin reagent (WAKO 142-04711; includes acetate buffer): this is prepared by first mixing three flasks of acetate buffer for 10 min and bubbling with nitrogen, then adding the flask with ninhydrin and repeat the flushing with nitrogen. This solution is stable for 2 weeks.
10. Methanol (Merck 6007).
11. Sodium bisulfite (Merck 6528).
12. HCl 25% (Merck 316).
13. HCl 37% (Merck 314).
14. Nitrogen gas.
15. Brij-35 30% (polyoxyethylene lauric ether; Sigma 430AG-6).
16. SSA 15%: dissolve 15 g SSA in water and make up to 100 ml.
17. HCl 0.1M: dilute 13 ml HCl 25% with water to 1 l.
18. Internal standard: dissolve 156.1 mg S-2-aminoethylcysteine (AEC) HCl in 10 ml SSA 15%. This solution is stable for 2 years in a refrigerator. For daily use, this standard is diluted 1:25 with SSA 15%

2.1.5.6 Instrumentation

A Jeol Aminotac AAA is used in the author's laboratory. There are several other brands of instruments available that may give comparable results. In general the instrument is equipped with a PC-based operating system that controls the order of the buffers and the temperature of the column. The manufacturer will supply a basic separation program for physiologic fluids, which has to be adapted personally

according to the quality of the column. The order of elution of the amino acids is virtually the same in all systems, hence it is possible for the experienced analyst to interpret results of "foreign" instruments.

Computation of the results will be achieved by a chromatography data system such as the Chromeleon system by Dionex.

2.1.5.7 Procedure

All physiological fluids have to be deproteinized prior to application on the column as the resin is extremely sensitive to pollution by protein. The most useful procedure combines deproteinization with the addition of the internal standard. In brief as follows:

1. Plasma: Put 300 µl of plasma and 30 µl of the internal standard AEC in 35% SSA into an Eppendorf tube. Vortex and put the mixture into a refrigerator for 30 min. Centrifuge at 11000 × *g* in the cold for 10 min. Filter the supernatant through a 0.2-µm filter and subsequently mix 140 µl of the filtrate with 140 µl of lithium citrate buffer 1 (P-21). Mix on a Vortex mixer and place the sample into the refrigerated autosampler, where it is stable for 3 days.
2. Urine/CSF: A 500-µl aliquot of urine or CSF is mixed with 50 µl of internal standard AEC in 15% SSA. Following mixing on a Vortex, the deproteinization proceeds at 4°C for 30 min. The remainder of the procedure is identical to that for plasma.

2.1.5.8 Calibration

The response of the system is calibrated using a commercial standard solution (Sigma) to which known amounts of freshly made solutions of some of the unstable amino acids are added (glutamine, asparagine, tryptophan). In special circumstances, all kinds of other amino acids can be added. It is good practice to check the performance of the system at the end of a series with another commercial standard mix (e.g., Pierce).

Calibration is essential every time a new ninhydrin batch is taken or when the results of the internal quality control samples (see below) are out of range.

2.1.5.9 Quality Control

A pool of plasma is composed by mixing residual amounts of plasma left over from analyses, thereby ensuring the anonymity of the pool sample. Each series of analyses should contain at least one pool plasma sample. The results of 8–10 selected amino acids of the pool are plotted in a Shewhart plot to make deviations from the previously established target values visible. Actions following these deviations will have to be devised by the laboratory staff according to standard quality control rules.

National or international quality control schemes for plasma amino acids exist, such as the ERNDIM scheme. Virtually all schemes use consensus values as the most likely target values and an intelligent scheme adds to that information about repro-

ducibility, recovery, and linearity. This will enable the laboratory to adapt its procedures for individual amino acids. Since the discovery of defects in the biosynthesis of amino acids it has become important to be able to quantify amino acids not only at the supraphysiological level, but also at the subphysiological level. Furthermore, the addition of unusual amino acids to the scheme will force the lab to be more than careful in its interpretations.

2.1.5.10 Validation Data

The linearity of the AAA was tested with an aqueous mixture. In general the assay was linear up to 2500 µmol/l, for glutamine even 5000 µmol/l. Some amino acids were tested at a lower level (cystine, taurine, citrulline) and were found to be linear up to 625–1250 µmol/l.

The interassay variation was assessed in a plasma pool, which was stored at –20°C and analyzed 26 times over an 8-month period. The coefficients of variation (CVs) ranged from 6.1 to 8.9% with the following exceptions: glutamine decreases steadily from 587 to 447 µmol/l with a concomitant increase of glutamic acid from 62 to 164 µmol/l. Cystine decreased from 35 µmol/l to undetectable. Tryptophan, arginine, methionine, asparagine, and proline had CVs slightly in excess of 10%.

The intra-assay variation for plasma was performed in a tenfold analysis and gave CVs of 0.8–4.1% with the exception of tryptophan, methionine, and the imino acids (6.7–8.9%). Urine behaved similarly to plasma in the sense of reproducibility, with CVs between 3.6 and 8.6% in 23 analyses over a 6-month period. Exceptions in this respect were the amino acids with a low ninhydrin color yield, such as β-alanine and sarcosine.

2.1.6 High-Performance Liquid Chromatography

The use of HPLC for amino acid analysis was taken up more than 30 years ago and has resulted in applications that are faster, more reproducible, and more sensitive than the classical AAA –approach [5, 11]. However, there are considerable drawbacks when analyzing physiological fluids. In particular, the wide variation in the composition of urine, with contributions from diet and drugs, has precluded a satisfactory use of the method. In addition, most derivatizing agents do not react in a quantitative way with all amino acids. One major advantage of the HPLC system for amino acids is its cost of operation. A regular HPLC instrument with a run-of-the-mill reversed-phase column and a fluorescence detector will do the job. The sensitivity of the detection makes it ideally suited for CSF analysis, although most of the reported applications deal with plasma.

Orthophthalaldehyde (OPA) in combination with a thiol is the reagent of choice for derivatization, despite its inability to react with proline, hydroxyproline, and the sulfur-containing amino acids. Another drawback of the reagent is the instability of the reaction products, making an automated derivatization system coupled to an automated injector, and constant retention times an absolute necessity. Taking into account these considerations, the HPLC analysis will be of use to every biochemical genetics laboratory for biological fluids other than urine. The system has also a

role as a back-up for the AAA when there are mechanical problems. Several well-established laboratories prefer the HPLC approach for the CSF analysis because of the high sensitivity enabling the detection of lowered levels of glycine, serine, and homocarnosine (see Fig. 2.1.3).

2.1.6.1 Specimens

The same specimen is needed for HPLC as for MS/MS (see section 2.1.4.2.

2.1.6.2 Reagents and Chemicals

1. OPA 97% (Aldrich): prepared by dissolving 20 mg of the salt in 0.5 ml methanol. Add to this solution 3 ml of the potassium borate buffer and 2 ml H_2O, followed by 30 µl mercaptoethanol. This reagent is stable for 1 week when stored in the dark.
2. Methanol 99.8% (Merck)
3. Potassium borate buffer 1.0 M (Pierce)
4. 2-mercaptoethanol (BioRad)
5. Sodium acetate p.a. (Merck): stock solution sodium acetate (1 M) is prepared by dissolving 82 g of sodium acetate and 375 mg ethylenediaminetetraacetic acid (EDTA) in 1000 ml H_2O.
6. Acetic acid 100% (Merck).
7. Lithium citrate buffer B (Pharmacia).
8. HCl 35% (Merck).
9. Isopropanol (Merck).
10. EDTA (Merck).
11. 5-SSA (Merck): 5-SSA 5% is made by dissolving 5 g of the solid in 100 ml H_2O.
12. Eluent A: 0.01 M sodium acetate + 9.1% methanol, pH 5.75 is prepared by diluting 100 ml of the stock sodium acetate to 1 l and adding 100 ml of methanol; the pH is adjusted to 5.75 with acetic acid. This solution is stable at room temperature under helium for 2 weeks.
13. Eluent B: methanol (1 l) with 20 ml isopropanol and 100 ml H_2O. Stable for 4 weeks.

The internal standard is carboxymethylcysteine (10 mg in 10 ml SSA 5%). This should be diluted 1:20 prior to use. Calibration standards containing the usual physiological amino acids may be purchased from Sigma or Pierce. Labile amino acids such as tryptophan, glutamine, asparagine, and homocarnosine should be prepared fresh at each calibration step, but can be stored at –20°C for at least 4 weeks.

2.1.6.3 Procedure

As a consequence of the limited stability of the OPA derivatives, the derivatization procedure should be carried out in an intelligent autosampler such as the Gilson 231XL sampler, equipped with a temperature-controlled sample holder (Gilson 832).

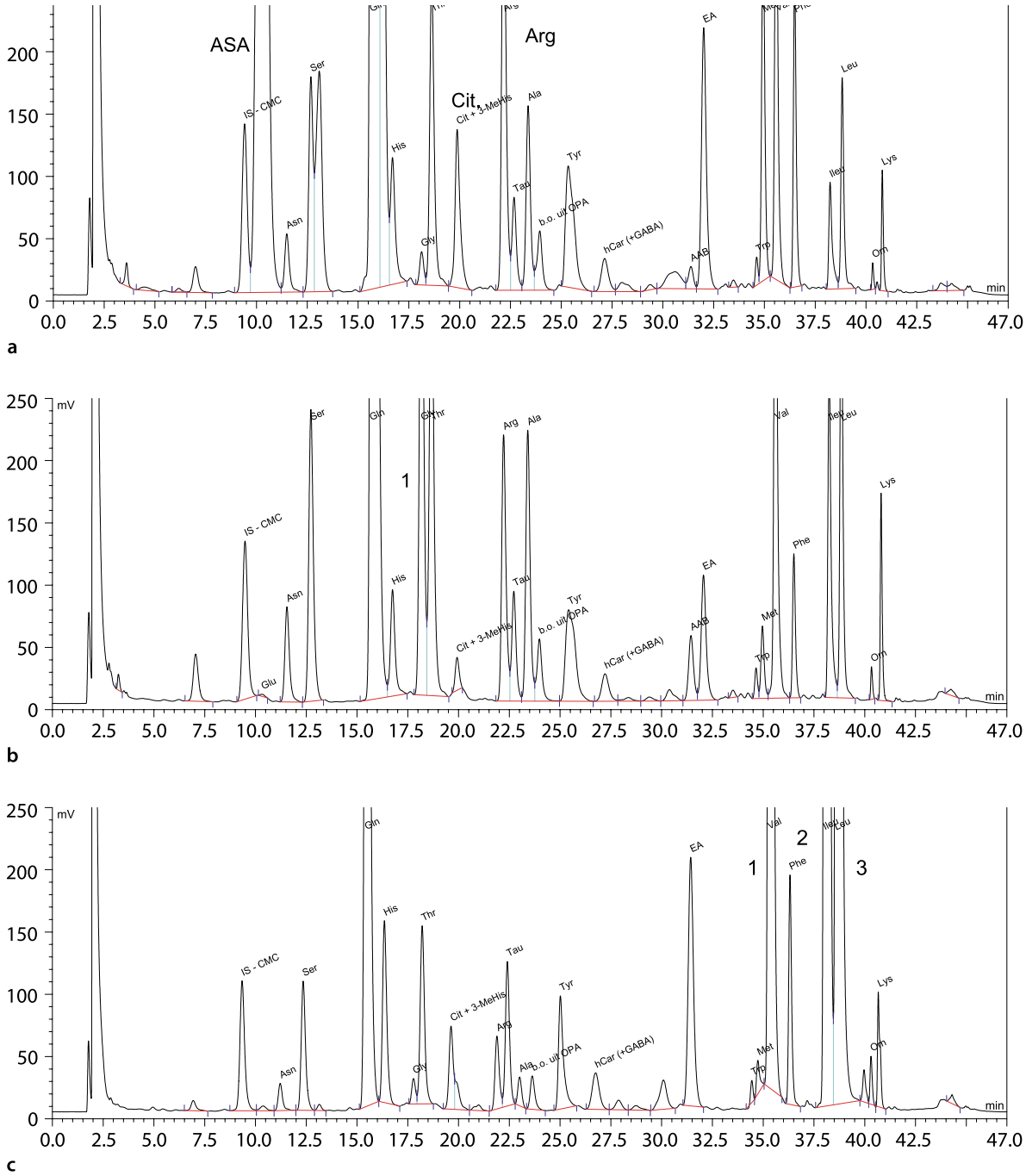

Fig. 2.1.3 **a** Cerebrospinal fluid amino acids assayed by high-performance liquid chromatography (HPLC) in a patient with argininosuccinate lyase deficiency. Note the extremely high level of argininosuccinate (*ASA*), which is higher than the plasma level. In addition, the concentration of citrulline, a precursor of ASA in the urea cycle, was increased. The patient was on arginine supplementation treatment, hence the increased level of that amino acid in this fluid. **b** Cerebrospinal fluid (CSF) amino acids analyzed by HPLC in a patient with nonketotic hyperglycinemia (NKH). Levels of glycine (peak 1) were extremely high (~100 µmol/l); no other changes were observed. CSF is the fluid of choice for the diagnosis of NKH. **c** CSF levels of amino acids assayed by HPLC in a patient with maple syrup urine disease (untreated). High levels of leucine (peak 3), isoleucine (peak 2), and valine (peak 1) are the hallmarks of this disorder. The HPLC approach is unable to separate isoleucine and alloisoleucine

In brief, a 200-µl sample will be deproteinized with 20 µl 5% SSA containing internal standard. Following precipitation and centrifugation, 150 µl supernatant is diluted with 150 µl of the lithium citrate buffer and placed in the autosampler. The derivatization step takes 40 µl of sample and 20 µl of the OPA reagent, which are mixed and left to react for 30 s. A 20-µl aliquot is injected.

HPLC separation is achieved on an Alltech OPA-HR LC-8 column (5 µm; 150 × 4.6 mm) protected by a Supelco LC-18 pellicular guard column (20 µm; 20 × 4.6 mm). Fluorescence detection (Jasco FP-1520) comprises an excitation wavelength of 330 nm and an emission wavelength of 450 mm. A good separation is achieved at 21°C using the elution program provided in Table 2.1.4

2.1.6.4 Validation Data

A CSF sample was analyzed 11-fold. The within-run variation coefficient ranged from 1 to 3.5% with two exceptions: tryptophan (5%) and methionine (7%), which partially coeluted. The interassay coefficients of variation were calculated from a series of 11 analyses over a 7-month period. The median CV was 8%; only taurine, arginine, and glutamate had CVs slightly in excess of 10%. The recovery of added amino acids to three CSF samples ranged form 83% (taurine) to 101% (isoleucine). Most recoveries were between 90 and 100%. At the lower end of the concentration range for CSF, a level of 1 µmol/l can be safely detected.

2.1.7 Interpretation and Follow-Up

The analysis of amino acids has been the first-line approach for the diagnosis of inborn errors of metabolism in most laboratories ever since the end of the 1950s, and it is expected to continue to play this role for a long time. Both the plasma and the CSF amino acid profile are now well known and interpretation should not pose any problems. A correct diagnosis requires adequate pattern recognition [7].

Table 2.1.4 *High-performance liquid chromatography elution program*

Step	Time (min)	Flow (ml/min)	%A	%B
0	0	0.5	95	5
Injection				
1	8	1.0	95	5
2	17	1.0	65	35
3	15	0.6	20	80
4	1	1.0	10	90
5	2	1.0	0	100
6	8	1.0	95	5

Urine amino acid profiles may suffer from the interference of drugs and dietary constituents and, more seriously, knowledge about unusual metabolic products such as formiminoglutamic acid tends to get lost as less and less laboratories have the facility to perform secondary, but highly informative techniques such as thin-layer chromatography or high-voltage paper electrophoresis. New laboratories should not hesitate to collect a fairly large amount of old amino acid literature as the information contained therein is invaluable.

Every amino acid concentration in a given body fluid should be matched against the relevant reference range, preferably constructed within the same laboratory environment. However, the reference ranges in the literature are reassuringly consistent, enabling the correct identification of major abnormalities.

2.1.8 Normal Profiles/Physiological Changes

Amino acids are preferably analyzed in plasma taken after an overnight fast and in a 24-h urine collection. The fasting plasma amino acids levels have a quite narrow range and are somewhat dependent on the general nutritional status of the subject and his/her age (Table 2.1.5)

2.1.8.1 Age

Age does not have a major influence on amino acid levels, with exception of the neonatal period. Premature babies may have underdeveloped hepatic and renal function, leading to increased tyrosine and methionine in their plasma as well as enhanced urinary losses of cystine, lysine, glycine, proline, hydroxyproline, and cystathionine. Taurine levels are generally increased in the first days of life.

2.1.8.2 Nutrition

Nutrition may have a considerable effect. A high intake of milk protein in neonates will result in an increase in most plasma amino acids, especially methionine and tyrosine. Canned infant formulae may contain homocitrulline, which may appear in the patient's urine. White meat (chicken!) will contain carnosine, anserine, and 3-methylhistidine; these substances will appear unchanged in the patient's urine following the ingestion of this type of meat.

Severe protein malnutrition (kwashiorkor) leads to decreased plasma levels of the essential amino acids (branched-chain, phenylalanine, tyrosine, lysine) with a concomitant increase in glycine, serine, and proline. The amino acid gradient across the placenta is such that the fetus in utero does not suffer from amino acid imbalance of an undernourished mother. As an example, fetal plasma phenylalanine is twice as high as maternal plasma phenylalanine. This positive effect has a negative side for pregnant PKU patients, who, unless they maintain a strict diet, will cause brain damage to their unborn children as a result of continuously high phenylalanine during pregnancy.

■ ***Table 2.1.5*** *Reference values for plasma amino acids in different age groups (µmol/l)*

Plasma Amino acid	1st week	1 week–1 month	1–4 months	4 months–2 years	2–10 years	10–18 years	>18 years
Taurine	14–238	9–201	19–139	19–139	24–92	10–162	6–126
Aspartate	1–21	5–37	6–30	0–16	3–15	4–28	1–9
Hydroxyproline	18–66	20–72	22–54	6–30	0–16	0–44	0–33
Threonine	53–141	55–187	66–182	36–136	48–140	72–192	102–190
Serine	62–206	60–240	85–221	42–174	77–169	75–175	68–160
Asparagine	38–114	22–94	28–80	26–70	24–64	32–64	35–63
Glutamate	32–104	0–109	29–81	24–68	11–51	11–59	1–57
Glutamine	198–886	178–670	368–652	337–709	373–709	396–740	435–721
Proline	120–344	65–457	98–254	53–201	93–221	75–307	88–290
Glycine	101–317	20–356	73–241	74–290	113–261	148–324	123–319
Alanine	108–448	116–376	182–378	144–348	158–314	192–508	182–552
Citrulline	5–33	10–50	16–32	6–34	18–50	17–49	16–46
2-Aminobutyrate	3–39	10–26	9–33	10–46	12–40	10–38	7–32
Valine	65–201	59–199	96–228	79–267	133–273	142–278	144–269
Cystine	20–60	28–52	33–57	43–67	24–52	32–64	35–63
Methionine	6–50	13–53	19–51	9–29	11–27	16–36	12–32
Isoleucine	22–82	22–94	28–84	32–92	31–83	38–94	34–84
Leucine	47–175	47–167	55–155	53–149	64–164	76–168	78–160
Tyrosine	38–178	40–160	31–115	14–114	34–82	40–92	35–84
Phenylalanine	21–85	21–93	29–85	26–70	35–67	38–78	39–74
Ethanolamine	26–93	10–50	5–25	1–9	0–10	0–12	0–11
Ornithine	31–207	10–214	51–123	9–105	24–64	20–84	27–98
Histidine	25–113	33–121	55–115	30–110	54–106	58–106	67–109
Lysine	67–291	42–242	56–172	56–148	77–181	105–221	111–248
Tryptophan	16–72	25–65	32–92	27–59	5–57	27–75	30–95
Arginine	12–116	12–104	38–102	18–78	38–98	45–125	46–128

2.1.8.3 Starvation

Starvation for more than a few hours will cause upregulated gluconeogenesis from muscle amino acids. As a consequence, most amino acids will show a steady decrease during prolonged fasting, with the exception of the branched-chain amino acids. The latter substances may even increase. Fasting also induces the breakdown of nucleotides. Beta-aminoisobutyric acid is a nucleotide breakdown marker and will always be increased in the urine following a period of fasting.

2.1.8.4 Gender

Gender is not an important determinant of plasma amino acid levels. Females have a tendency toward small changes of their amino acid levels during the menstrual cycle. However these changes are barely distinguishable from the normal diurnal changes and dietary influences.

2.1.8.5 Muscle Activity

Muscle activity involves processes such as aerobic and anaerobic glycolysis and is therefore accompanied by an increased pyruvate production. Consequently, the pyruvate transamination product alanine will be increased after exercise. Heavy exercise may be associated with an increased need of creatine biosynthesis from arginine. Ornithine is a by-product of this pathway and may be increased under these conditions.

2.1.8.6 Urine

Reference values for amino acids in the urine show a rather sharp decrease from the neonatal period to adulthood (Table 2.1.6). This is mainly due to the maturation of the renal tubular reabsorption system, but is also the result of increasing muscle mass with age, giving rise to increasing creatinine production.

2.1.8.7 Cerebrospinal Fluid

CSF amino acids do not show an important age dependence (Table 2.1.7). Levels of most amino acids in the CSF are much lower than in the plasma, the exception being glutamine. The low CSF values bear a certain analytical risk: a traumatic lumbar puncture will result in the presence of small amounts of blood in the CSF. This readily influences the CSF amino acid levels and should be interpreted with care. In contrast with some of the neurotransmitter metabolites, no ventral/dorsal gradient for the amino acid is observed.

Table 2.1.6 *Reference values for amino acids in urine in different age groups (mmol/mol creatinine)*

Plasma Amino acid	1st week	1 week – 1 month	1–4 months	4 months – 2 years	2–4 years	4–6 years	2–10 years	10–18 years	>18 years
Taurine	0–638	2–61	0–79	0–79	0–79	0–79	0–79	0–79	22–80
Phosphoethanolamine	10–51	10–51	10–5	10–51	5–27	5–27	4–10	4–10	0–5
Aspartate	0.43	8–46	2–23	0–53	4–21	4–21	4–21	3–7	3–5
Hydroxyproline	0–282	36–478	2–384	0–41	0–3	0–3	0–3	0–3	0–3
Threonine	6–55	10–139	19–140	9–100	10–89	1–73	2–45	0–36	1–48
Serine	21–204	23–308	41–288	30–191	30–148	19–112	1–95	12–78	5–69
Asparagine	0–47	1–60	0–67	0–54	0–53	0–74	0–29	0–27	3–9
Glutamate	0–52	0–55	0–51	0–69	0–48	0–38	0–31	1–6	1–3
Glutamine	0–182	41–216	40–239	28–253	23–187	13–151	7–137	18–98	19–57
2-Aminoadipate	0–21	3–59	4–49	3–55	0–47	5–23	1–23	0–16	0–16
Proline	4–142	2–233	3–341	0–34	0–26	0–13	0–7	0–6	0–7
Glycine	0–1046	78–1259	105–796	40–616	76–516	24–397	20–201	18–252	12–199
Alanine	0–135	41–308	58–297	34–189	18–175	8–111	8–80	10–85	5–59
Citrulline	0–2	0–2	0–2	0–8	0–1	0–1	4–18	0–5	1–2
2-Aminobutyrate	0–2	0–11	0–16	2–13	1–4	0–1	0–7	0–7	0–7
Valine	9–15	2–28	6–27	4–32	6–20	4–11	1–12	2–11	2–7

■ ***Table 2.1.6*** (continued) *Reference values for amino acids in urine in different age groups (mmol/mol creatinine)*

Plasma Amino acid	1st week	1 week – 1 month	1–4 months	4 months – 2 years	2–4 years	4–6 years	2–10 years	10–18 years	>18 years
Cystine	0–65	2–52	7–54	0–36	5–25	4–22	3–17	5–16	1–19
Homocitrulline	0–135	0–15	0–15	0–4	1–26	1–11	0–8	0–8	0–8
Methionine	5–25	0–8	2–20	2–20	2–9	2–9	0–8	0–8	0–8
Isoleucine	3–9	1–18	0–26	0–10	4–14	2–12	0–7	0–7	1–5
Leucine	3–24	1–25	0–25	3–21	2–21	2–12	1–12	1–9	2–6
Tyrosine	0–29	9–55	13–75	10–72	0–71	8–51	6–42	6–37	5–27
Phenylalanine	0–34	3–34	3–40	5–37	0–41	2–25	1–20	1–17	2–11
3-Aminoisobutyrate	0–310	0–147	0–222	0–120	8–66	5–78	0–49	0–57	0–57
Ethanolamine	0–361	0–480	84–277	8–175	13–131	40–71	26–61	44–53	44–53
Hydroxylysine	0–14	0–1	0–1	0–1	0–1	0–2	0–2	0–2	0–1
Lysine	0–82	10–172	18–148	0–182	0–92	0–52	0–64	0–20	12–52
Tryptophan	0–1	0–1	0–1	0–1	0–1	0–1	0–1	0–1	2–10
Arginine	2–8	0–20	0–19	0–19	1–13	1–7	0–9	0–8	1–7

Table 2.1.7 *Reference values for amino acids in cerebrospinal fluid of subjects of different age groups (µmol/l)*

Cerebrospinal fluid			
Amino acid	**0–1 year**	**1–18 years**	**>18 years**
Taurine	4–14	4–14	4–14
Aspartate	3.7–10.5	2–4.4	1–5
Threonine	15–130	14–50	14–50
Serine	29.6–86	21.44	21–44
Asparagine	4.5–16.4	3–9	3–17
Glutamate	0.8–11	1.2–11	1.2–11
Glutamine	390–824	352–680	352–680
Glycine	3–8.3	3–8.3	1–14
Alanine	13.–48	13–48	13–48
Citrulline	1.2–7.8	1–6	1–6
2-Aminobutyrate	1–7	1–7	1–7
Valine	12–29	9–18	5–38
Methionine	1.6–7.4.	1–5	1–9
Isoleucine	5–12	2.5–6.5	3.4–13.4
Leucine	12.4–20	6.5–16	4.2–27
Tyrosine	7–25	8–14	8–14
Phenylalanine	5–22.5	4–14	24–19
Ethanolamine	3.3–32	9–26	9–26
Ornithine	2.8–19	2.4–9	2.4–9
Histidine	10.5–30	9–22	9–22
Lysine	12–36	10–28	15–43
Tryptophan	2.1–7.5	1–4	1–4
Arginine	12–32	13–35	13–35
β-Alanine	0.025–0.09	0.008–0.05	0.008–0.035
β-AIB	0–0.06	0–0.03	0–0.03
γ-Aminobutyric acid	0.02–0.3	0.02–0.5	0.02–0.6
Homocarnosine	5.5–12	2.5–10.6	2.5–10.6

Table 2.1.8 *The primary defects of amino acid metabolism and the corresponding changes of plasma or urine amino acid levels.* AA *amino acid,* AAA *α-amino-adipic acid,* AASA *α-aminoadipic semialdehyde,* AdoHcy *S-adenosylhomocysteine,* AdoMet *S-adenosylmethionine,* Ala *alanine,* Arg *arginine,* aIle *alloisoleucine,* Apo *aminopiperidone,* ASA *argininosuccinate,* Asn *asparagine,* Asp *aspartate,* BAIB *β-aminoisobutyric acid,* Carn *carnosine,* Cbl *cobalamin,* CBS *cystathionine β-synthase,* Cit *citrulline, csf cerebrospinal fluid,* Cysta *cystathionine,* FIGLU *formiminoglutamate,* GABA *γ-aminobutyric acid,* Gln *glutamine,* GlcNAc *N-acetylglucosamine,* Glu *glutamate,* GSH *reduced glutathione,* GSSG *oxidised glutathione,* Haw *hawkinsin,* Hcar *homocarnosine,* Hcit *homocitrulline,* Hcy *homocysteine,* HHH *hyperornithinemia-hyperammonemia-homocitrullinemia,* His *histidine,* Hkyn *3-OH-kynurenine,* Hyl *hydroxylysine,* Hyp *hydroxyproline,* Ile *isoleucine,* Kyn *kynurenine,* Leu *leucine,* Lys *lysine,* Met *methionine,* MTHFR *5,10-methylene tetrahydrofolate reductase,* Orn *ornithine,* p *plasma,* P5C *pyrroline-5-carboxylic acid,* PEA *phosphoethanolamine,* Phe *phenylalanine,* P-Hyl *O-phosphohydroxylysine,* Pip *pipecolic acid,* Pro *proline,* Sacch *saccharopine,* Sar *sarcosine,* Ser *serine,* Sulfocys *sulfocysteine,* Thr *threonine,* Tyr *tyrosine,* u *urine,* Val *valine*

1.	N-Acetylglutamate synthase deficiency	p: Glu↑, Cit↓, Arg↓, Lys↑
2.	S-Adenosylhomocysteine hydrolase deficiency	p: Met↑, AdoHcy↑, Adomet↑
3.	α-Aminoadipic semialdehyde dehydrogenase deficiency	u,p: AASA↑, Pip↑
4.	α-Aminoadipic aciduria	u,p: AAA↑
5.	Argininemia	u,p: Arg↑
6.	Argininosuccinic aciduria	p: ASA↑, Cit↑, Gln↑, Arg↓
7.	Aspartylglucosaminuria	u: GlcNAc-Asn↑
8.	γ-Aminobutyric acid transaminase deficiency	u,p,csf: GABA↑
9.	β-Aminoisobutyric aciduria	u: BAIB↑
10.	Δ-Aminolevulinate dehydratase deficiency	u: Δ-aminolevulinic acid ↑
11.	Carbamyl phosphate synthase deficiency	p: Gln↑, Cit↓, Ala↑, Lys↑
12.	Carnosinemia	u: Carn↑
13.	Citrullinemia type 1	p: Cit↑, Gln↑, Ala↑, Arg↓
14.	Citrullinemia type 2 (citrin)	p: Cit↑, Met↑, Thr↑, Tyr↑
15.	Cystathioninuria	u: Cysta↑
16.	Cystinosis	u: All AA↑ (renal Fanconi)
17.	Cystinuria	u: Cys↑, Lys↑, Arg↑, Orn↑
18.	Dicarboxylic aminoaciduria	u: Glu↑, Asp↑
19.	Formiminoglutamic aciduria	u: FIGLU↑
20.	γ-Glutamylcysteine synthase deficiency	u: All AA↑
21.	γ-Glutamyl transpeptidase deficiency	u: GSH/GSSG↑

Table 2.1.8 (continued) *The primary defects of amino acid metabolism and the corresponding changes of plasma or urine amino acid levels.* AA *amino acid,* AAA *α-amino-adipic acid,* AASA *α-aminoadipic semialdehyde,* AdoHcy *S-adenosylhomocysteine,* AdoMet *S-adenosylmethionine,* Ala *alanine,* Arg *arginine, aIle alloisoleucine,* Apo *aminopiperidone,* ASA *argininosuccinate,* Asn *asparagine,* Asp *aspartate,* BAIB *β-aminoisobutyric acid,* Carn *carnosine,* Cbl *cobalamin,* CBS *cystathionine β-synthase,* Cit *citrulline, csf cerebrospinal fluid,* Cysta *cystathionine,* FIGLU *formiminoglutamate,* GABA *γ-aminobutyric acid,* Gln *glutamine,* GlcNAc *N-acetylglucosamine,* Glu *glutamate,* GSH *reduced glutathione,* GSSG *oxidised glutathione,* Haw *hawkinsin,* Hcar *homocarnosine,* Hcit *homocitrulline,* Hcy *homocysteine,* HHH *hyperornithinemia-hyperammonemia-homocitrullinemia,* His *histidine,* Hkyn *3-OH-kynurenine,* Hyl *hydroxylysine,* Hyp *hydroxyproline,* Ile *isoleucine,* Kyn *kynurenine,* Leu *leucine,* Lys *lysine,* Met *methionine,* MTHFR *5,10-methylene tetrahydrofolate reductase,* Orn *ornithine,* p *plasma,* P5C *pyrroline-5-carboxylic acid,* PEA *phosphoethanolamine,* Phe *phenylalanine,* P-Hyl *O-phosphohydroxylysine,* Pip *pipecolic acid,* Pro *proline,* Sacch *saccharopine,* Sar *sarcosine,* Ser *serine,* Sulfocys *sulfocysteine* Thr *threonine,* Tyr *tyrosine,* u *urine,* Val *valine*

22.	Glutamine synthetase deficiency	p: Gln↓
23.	Glycine N-methyltransferase deficiency	p: Met↑, AdoMet↑
24.	Hyperglycinemia	u,p,csf: Gly↑
25.	Hartnup disorder	u: All neutral AA↑
26.	Histidinemia	u,p: His↑
27.	Homocarnosinosis	csf: Hcar↑
28.	HHH-syndrome	p: Orn↑ u: Hcit↑
29.	Hawkinsinuria	u: Haw↑
30.	Homocystinuria/CBS	p: Hcy↑, Met↑, Cys↓, AdoMet↑, AdoHcy↑
31.	Homocystinuria/MTHFR	p: Hcy↑, Met↓
32.	Homocystinuria/Cbl E or G	p: Hcy↑, Met↓ u: FIGLU↑
33.	Hydroxykynureninuria	u: Kyn↑, Hkyn↑
34.	Hydroxylysinuria	u,p: Hyl↑
35.	Hypophosphatasia	u: PEA↑
36.	Iminoglycinuria	u: Pro↑, Hyp↑, Gly↑
37.	Iminopeptiduria (prolidase deficiency)	u: prolylpeptides↑
38.	Lowe syndrome	u: most AA↑
39.	Hyperlysinemia	u,p: Lys↑, Acetyllys↑ u: Hcit↑
40.	Lysinuric protein intolerance	u: Lys↑, Arg↑, Orn↑ p: Lys↓, Arg↓, Orn↓

Table 2.1.8 (continued) *The primary defects of amino acid metabolism and the corresponding changes of plasma or urine amino acid levels.* AA *amino acid,* AAA *α-amino-adipic acid,* AASA *α-aminoadipic semialdehyde,* AdoHcy *S-adenosylhomocysteine,* AdoMmet *S-adenosylmethionine,* Ala *alanine,* Arg *arginine, aIle alloisoleucine,* Apo *aminopiperidone,* ASA *argininosuccinate,* Asn *asparagine,* Asp *aspartate,* BAIB *β-aminoisobutyric acid,* Carn *carnosine,* Cbl *cobalamin,* CBS *cystathionine β-synthase,* Cit *citrulline, csf cerebrospinal fluid,* Cysta *cystathionine,* FIGLU *formiminoglutamate,* GABA *γ-aminobutyric acid,* Gln *glutamine,* GlcNAc *N-acetylglucosamine,* Glu *glutamate,* GSH *reduced glutathione,* GSSG *oxidised glutathione,* Haw *hawkinsin,* Hcar *homocarnosine,* Hcit *homocitrulline,* Hcy *homocysteine,* HHH *hyperornithinemia-hyperammonemia-homocitrullinemia,* His *histidine,* Hkyn *3-OH-kynurenine,* Hyl *hydroxylysine,* Hyp *hydroxyproline,* Ile *isoleucine,* Kyn *kynurenine,* Leu *leucine,* Lys *lysine,* Met *methionine,* MTHFR *5,10-methylene tetrahydrofolate reductase,* Orn *ornithine,* p *plasma,* P5C *pyrroline-5-carboxylic acid,* PEA *phosphoethanolamine,* Phe *phenylalanine,* P-Hyl *O-phosphohydroxylysine,* Pip *pipecolic acid,* Pro *proline,* Sacch *saccharopine,* Sar *sarcosine,* Ser *serine,* Sulfocys *sulfocysteine* Thr *threonine,* Tyr *tyrosine,* u *urine,* Val *valine*

41.	Methionine adenosyltransferase deficiency	p: Met↑, Hcy(↑)
42.	β-mercaptolactate-cysteine disulfiduria	u: β-mercaptolactate cysteine disuflide↑
43.	MSUD	p: Leu↑, Ile↑, Val↑, aIle↑
44.	Ornithine carbamoyltransferase deficiency	p: Gln↑, Cit↓, Ala↑, Lys↑, Arg↓
45.	Ornithinemia	p: Orn↑, Apo↑
46.	Hyperphenylalaninemias	p: Phe↑, Tyr (↓)
47.	3-Phosphoglycerate dehydrogenase deficiency	p,csf: Ser↓, Gly↓
48.	Phosphohydroxylysinuria	u: P-Hyl↑
49.	Prolinemia type 1	p: Pro↑ u: Pro↑, Hyp↑, Gly↑
50.	Prolinemia type 2	p: Pro↑, Δ^1P5C↑ u: Pro↑, Hyp↑, Gly↑, Δ^1P5C↑
51.	Pyrroline-5-carboxylate synthase deficiency	p: Pro↓, Orn↓, Cit↓, Arg↓
52.	Saccharopinuria	u,p: Lys↑, Sacch↑
53.	Sarcosinemia	u,p: Sar↑
54.	Sulfite oxidase deficiency (+Mo-cofactor)	u: Sulfocys↑, Tau↑
55.	Tyrosinemia type 1	p: Tyr↑, Met↑ u: all AA, Δ-aminolevulinec acid ↑
56.	Tyrosinemia type 2	p: Tyr↑ u: Tyr↑
57.	Tyrosinemia type 3	p: Tyr↑ u: Tyr↑

2.1.9 Primary and Secondary Defects; Interference

Some 57 different primary inherited defects of amino acid metabolism that result in changes of plasma or urine amino acid levels have been distinguished thus far (see Table 2.1.8.). These encompass not only defects of the catabolic and anabolic pathways, but also defective transport systems. In this respect, no general rules for the preferred first-line diagnostic fluid can be given. Both plasma and urine have their advantages: moderate metabolic amino acid degradation defects will give elevations of plasma amino acid levels, but as a consequence of the efficient tubular reabsorption, the urine profile may be normal. On the other hand, transport defects usually affect renal function and are best picked up by urine analysis.

Not all disorders of amino acid metabolism are associated with clinical symptoms. Only clinically preselected patients are enrolled in selective screening programs. This led to the erroneous conclusion in the 1960s that conditions such as cystinuria and histidinemia are associated with mental retardation. It was only after the introduction of newborn screening programs that the medical community realized that histidinemia is a harmless condition, a nondisease. For several amino acid disorders the clinical/biochemical relationship has not been resolved, as there are as many clinically affected as "healthy" patients. Examples are the hyperlysinemias, α-aminoadipic aciduria, and formiminoglutamic aciduria.

Table 2.1.9 lists the usual amino acids and their concentration changes in primary inherited defects, but also secondary changes in various conditions such as ketosis. In addition, there are several endogenous or exogenous toxins that may interfere with amino acid catabolizing enzymes or transport systems. Good examples are the short-chain fatty acids (propionic acid), which interfere with the glycine cleavage system and cause ketotic hyperglycinemia. The same effect is exerted by the antiepileptic drug sodium valproate (dipropyl acetate).

Sugar phosphates such as fructose-1-phosphate in fructose intolerance and galactose-1-phosphate in galactosemia are nephrotoxic and cause a renal Fanconi syndrome with a generalized aminoaciduria. Identical findings can be seen in Wilson disease (copper toxicity) and ifosfamide therapy of solid tumors. Lactic acid inhibits proline oxidase, hence patients with lactic acidosis will show secondary hyperprolinemia in addition to the hyperalaninemia. The first step of lysine catabolism requires one molecule of 2-ketoglutaric acid. Consequently, hyperammonemic patients sequestering 2-ketoglutaric acid in the formation of glutamic acid and glutamine will develop a moderate hyperlysinemia.

The liquid chromatography profile of amino acids, especially that of urine, may reveal all kinds of unusual peaks. Table 2.1.10. lists a series of unusual amino acids and their approximate positions in the AAA chromatogram. Many of these unusual substances are not commercially available. In order to establish an idea about the occurrence of these substances, it is advisable to analyze samples from patients with proven defects. Not every laboratory has access to all proven defects, but small aliquots may be available from the Quality Assurance (Diagnostic Proficiency Testing) schemes or from laboratories that have a long-standing experience. The diagnostic work in the area of inborn errors benefits greatly from the experience of having seen "true patient samples".

■ ***Table 2.1.9*** *Changes of blood amino acids in various primary inherited defects and as a result of secondary changes. ASA Argininosuccinic acid,* CPS *carbamoyl phosphate synthase,* LPI *Lysinuric protein intolerance,* MAD *multiple acyl-CoA dehydrogenation,* MSUD *maple syrup urine disease,* NAGS *N-acetylglutamate synthase,* NKH *nonketotic hyperglycinemia,* NTBC *2-(2-nitro-4-3 trifluoro-methylbenzoyl)-1,3-cyclohexanedione,* OCT *Ornithine carbamoyltransferase,* SAH *S-adenosylhomocysteine*

Blood physiological Amino acid	Increase in:	Decrease in:
S-Adenosylhomocysteine	CBS deficiency	
S-Adenosylhomocysteine	SAH hydrolase deficiency	
S-Adenosylmethionine	CBS deficiency	
S-Adenosylmethionine	SAH hydrolase deficiency	
S-Adenosylmethionine	Glycine N-methyltransferase deficiency	
Alanine	Pyruvate/lactate defects	Fasting Prolonged fasting, ketosis
	Hyperammonemias	
β-Alanine	GABA-transaminase deficiency	Ureidopropionase deficiency
	Vigabatrin treatment*	
Alloisoleucine	MSUD	
α-Aminoadipic acid	α-Ketoadipic aciduria	
β-Aminoisobutyric acid	Fasting, catabolism *	Pyrimidine degradation defects
Arginine	Hyperargininemia	LPI
		Urea cycle defects, HHH syndrome
		Hemolytic plasma*
Argininosuccinic acid	ASA-lyase deficiency	
Aspartic acid	Hemolytic plasma*	
Citrulline	Citrullinemia 1 and 2	NAGS, CPS, OCT deficiency
	ASA-lyase deficiency	Pyrroline-5-carboxylate synthase deficiency
	Pyruvate carboxylase deficiency*	
	LPI	
Cystathionine	Cystathionase deficiency	
Cystine		Sulfite oxidase deficiency homocystinuria

* Secondary change

■ ***Table 2.1.9*** (continued) *Changes of blood amino acids in various primary inherited defects and as a result of secondary changes.* ASA *Argininosuccinic acid,* CPS *carbamoyl phosphate synthase,* LPI *Lysinuric protein intolerance,* MAD *multiple acyl-CoA dehydrogenation,* MSUD *maple syrup urine disease,* NAGS *N-acetylglutamate synthase,* NKH *nonketotic hyperglycinemia,* NTBC *2-(2-nitro-4-3 trifluoro-methylbenzoyl)-1,3-cyclohexanedione,* OCT *Ornithine carbamoyltransferase,* SAH *S-adenosylhomocysteine*

Blood physiological Amino acid	Increase in:	Decrease in:
GABA	GABA transaminase deficiency	
Glutamic acid	Hemolytic plasma *	
	Stored plasma*	
	Ca-levulinate treatment	
Glutamine	Hyperammonemias	Glutamine synthase deficiency
Glycine	NKH	Serine bosynthesis defects
	Ketotic hyperglycinemia * Valproate treatment	Hypoglycinemia (?)
Histidine	Histidinemia	
Homocyst(e)ine	CBS deficiency	Sulfite oxidase deficiency
	Cobalamin defects/deficiency	
	MTHFR deficiency	
	Methionine adenosyltransferase deficiency	
	Hyperhomocysteinemia	
Hydroxylysine	Hydroxylysinemia	
Hydroxyproline	Prolinemia type 2	
Isoleucine	MSUD	Severe protein malnutrition
	Lipoamide dehydrogenase deficiency	
Leucine	MSUD	Severe protein malnutrition
	Lipoamide dehydrogenase def.	
Lysine	Hyperlysinemia 1 and 2	LPI
	Saccharopinuria	HHH syndrome
Lysine	Urea cycle defects *	Hyperornithinemia
	Organic acidemias *	

* Secondary change

Table 2.1.9 (continued) *Changes of blood amino acids in various primary inherited defects and as a result of secondary changes.* ASA *Argininosuccinic acid,* CPS *carbamoyl phosphate synthase,* LPI *Lysinuric protein intolerance,* MAD *multiple acyl-CoA dehydrogenation,* MSUD *maple syrup urine disease,* NAGS *N-acetylglutamate synthase,* NKH *nonketotic hyperglycinemia,* NTBC *2-(2-nitro-4-3 trifluoro-methylbenzoyl)-1,3-cyclohexanedione,* OCT *Ornithine carbamoyltransferase,* SAH *S-adenosylhomocysteine*

Blood physiological Amino acid	Increase in:	Decrease in:
Methionine	Methionine adenosyltransferase deficiency	Cobalamin defects
	Glycine N-methyltransferase deficiency	MTHFR deficiency
	SAH hydrolase deficiency	Severe protein malnutrition
	CBS deficiency	
	Tyrosinemia type 1*	
	Liver disease*	
Ornithine	Hyperornithinemia	Urea cycle defects
	HHH syndrome	P5C synthase deficiency
	Hemolytic plasma*	
Phenylalanine	PKU and BH_4-defects	NTBC treatment*
	Severe liver disease*	
Pipecolic acid	Peroxisomal disease	
	AASA dehydrogenase deficiency	
	Hyperlysinemia	
Proline	Prolinemia type 1 and 2	P-5-C synthase deficiency
	Lactic acidemias*	
Saccharopine	Saccharopinuria	
Sarcosine	Sarcosinemia	
	MAD defect	
Serine		Serine biosynthesis defects
Taurine	Sulfite oxidase deficiency	
	Mo-cofactor deficiency	
	Hemolytic plasma*	
Tryptophan	Tryptophanemia (?)	
Tyrosine	Tyrosinemia type 1,2,3	PKU
	Liver disease*	
	Prematurity*	

*Secondary change

■ ***Table 2.1.9*** (continued) *Changes of blood amino acids in various primary inherited defects and as a result of secondary changes.* ASA *Argininosuccinic acid,* CPS *carbamoyl phosphate synthase,* LPI *Lysinuric protein intolerance,* MAD *multiple acyl-CoA dehydrogenation,* MSUD *maple syrup urine disease,* NAGS *N-acetylglutamate synthase,* NKH *nonketotic hyperglycinemia,* NTBC *2-(2-nitro-4-3 trifluoro-methylbenzoyl)-1,3-cyclohexanedione,* OCT *Ornithine carbamoyltransferase,* SAH *S-adenosylhomocysteine*

Blood physiological Amino acid	Increase in:	Decrease in:
Valine	MSUD	Severe protein malnutrition
	Lipoamide dehydrogenase def.	
	Prolonged fasting, ketosis *	
	Leucine, isoleucine	

* Secondary change

■ ***Table 2.1.10*** *Unusual (mainly urinary) amino acids and related substances that may be encountered in metabolic disease. The position of the neighboring components is not always well defined for each instrument, therefore the analytical biochemist will try and collect as many reference substances as possible*

Usual component	Neighboring/coeluting component(s)
Cysteic acid	Sulphocysteine Phosphoserine Cysteine-2-mercaptoethanesulfonic acid disulfide
Taurine	Hypotaurine
Phosphoethanolamine	
Urea	Hawkinsin AADG (aspartylglucosaminuria) Reduced glutathione
Aspartic acid	Δ^1-Pyrroline-3-hydroxy-5-carboxylic acid
4-Hydroxyproline	Methionine sulfoxide Methionine sulfone
Threonine	
Serine	Phosphohydyroxylysine Cysteine-β-mercaptolactate disulfide
Asparagine	

Table 2.1.10 (continued) *Unusual (mainly urinary) amino acids and related substances that may be encountered in metabolic disease. The position of the neighboring components is not always well defined for each instrument, therefore the analytical biochemist will try and collect as many reference substances as possible*

Usual component	Neighboring/coeluting component(s)
Glutamic acid	
Glutamine	Δ^1-P5C S-carboxyisopropylcysteine (isobuteine)
Sarcosine	
2-Aminoadipic acid	Oxidized glutathione Cysteine
Proline	Penicillamine
Glycine	
Alanine	
Citrulline	Formiminoglutamic acid Galactosamine
2-Aminobutyric acid	N^{ε}-acetyllysine Lanthionine
Valine	
Cystine	Saccharopine Pipecolic acid γ-Glutamylphenylalanine
Methionine	Homocitrulline Alloisoleucine Penicillamine-cysteine disulfide
Isoleucine	Dihydroxyphenylalanine N^{ε}-carboxylmethyllysine
Leucine	Argininosuccinic acid Glycylproline
Tyrosine	Cysteine-homocysteine disulfide 3-Methoxytyrosine Erythromycin glucoheptonate
Phenylalanine	N^{α}-acetyllysine Acetaminophen metabolite
β-Alanine	Δ-Aminolevulinic acid
β-Aminoisobutyric acid	GABA ASA-anhydride 1 ASA-anhydride 2 Homocystine Ethanolamine

■ ***Table 2.1.10*** (continued) *Unusual (mainly urinary) amino acids and related substances that may be encountered in metabolic disease. The position of the neighboring components is not always well defined for each instrument, therefore the analytical biochemist will try and collect as many reference substances as possible*

Usual component	Neighboring/coeluting component(s)
Ammonia	Kynurenine γ-vinyl-GABA Cysteinylglycine
Hydroxylysine	
Ornithine	
1-Me-Histidine	
Histidine	Methyllysine (3)
Lysine	
3-Methyl-histidine	
Tryptophan	Carnosine Anserine Homocarnosine
Arginine	Homoarginine 3-Aminopiperidone Methylarginine(s)

References

1. Blau N, Duran M, Blaskovics ME, Gibson KM (2003) Physician's Guide to the Laboratory Diagnosis of Metabolic Diseases. Springer Verlag, Berlin, pp 1–716
2. Bremer HJ, Duran M, Kamerling JP, Przyrembel H, Wadman SK (1981) Disturbances of Amino Acid Metabolism: Clinical Chemistry and Diagnosis. Urban Schwarzenberg, München, pp 1–525
3. Clarke JTR (2006) A Clinical Guide to Inherited Metabolic Diseases. Cambridge University Press, Cambridge, UK, pp 1–338
4. Fernandes J, Saudubray JM, Van den Berghe G, Walter J (2006) Inborn Metabolic Diseases. Springer Verlag, Berlin, pp 1–438
5. Leah JM, Palmer T, Griffin M, Wingad CJ, Briddon A, Oberholzer VG (1986) Urine amino acid analysis by HPLC in the investigation of inborn errors of metabolism. J Inherit Metab Dis 9:250–253
6. Mayne PD, Roche G, Deverell D (2001) Amino acids: analytical aspects, Workshop report. J Inherit Metab Dis 24:305–308
7. Parvy P, Bardet J, Rabier D, Kamoun P (1995) A scheme for the interpretation of primary and secondary disturbances of plasma and urinary amino acid profiles. A possible way to an expert system. Clin Chim Acta 235:1–10

8. Piraud M, Vianey-Saban C, Bourdin C, Acquavica-Bourdain C, Boyer S, Elfakir C, Bouchu D (2005) A new reversed-phase liquid chromatographic/tandem mass spectrometric method for analysis of underivatized amino acids: evaluation for the diagnosis and the management of inherited disorders of amino acid metabolism. Rapid Commun Mass Spectrom 19:3287–3297
9. Schulze A, Lindner M, Kohlmuller D, Olgemoller K, Mayatepek E, Hoffmann GF (2003) Expanded newborn screening for inborn errors of metabolism by electrospray ionization – tandem mass spectrometry: results, outcome, and implications. Pediatrics 111:1399–1406
10. Scriver CR, Beaudet AL, Sly WS, Valle D, Childs B (2001) The Metabolic and Molecular Basis of Inherited Disease. McGraw-Hill, New York, pp 1–6338
11. Walker V, Mills GA (1995) Quantitative methods for amino acid analysis in biological fluids. Ann Clin Biochem 32:28–57
12. Zschocke J, Hoffmann GF (2004) Vademecum Metabolicum. Schattauer, Milupa, Friedrichsdorf, pp 1–164

2.2 Homocysteine, S-adenosylmethionine and S-adenosylhomocysteine

Brian Fowler

2.2.1 Introduction

Homocysteine (Hcy) metabolism is closely linked to that of the essential amino acid methionine and thus plays a central role in several vital biological processes. Methionine itself is needed for protein synthesis and donates methyl groups for the synthesis of a broad range of vital methylated compounds. It is also a main source of sulphur and acts as the precursor for several other sulphur-containing amino acids such as cystathionine, cysteine and taurine. In addition, it donates the carbon skeleton for polyamine synthesis [1, 2]. Hcy is also important in the metabolism of folate and in the breakdown of choline. Hcy levels are determined by its synthesis from methionine, which involves several enzymes, its remethylation to methionine and its breakdown by trans-sulphuration.

The metabolism of Hcy-related pathways in man are shown in Fig. 2.2.1. Methionine is converted to its active form S-adenosylmethionine (AdoMet) by methionine adenosyltransferase (MAT). AdoMet is the compound donates a methyl group as co-substrate for at least 39 methyltransferases involved in the formation of important methylated compounds, for example creatine, epinephrine, dopamine, phosphatidylcholine, methylated proteins and methylated DNA [3]. The highly abundant glycine methyltransferase, which transfers a methyl group to glycine, forming sarcosine (N-methylglycine) [4], is a particularly important methyltransferase that fulfils the need for a high-capacity utilisation of AdoMet and is considered to be an integral enzyme in the trans-sulphuration sequence.

The loss of a methyl group from AdoMet in each of the reactions yields S-adenosylhomocysteine (AdoHcy) and this is subsequently hydrolysed to adenosine and Hcy by AdoHcy-hydrolase. Hcy sits at a metabolic branch point and can be remethylated to methionine by way of two reactions. One is the 5-methyltetrahydrofolate dependent reaction catalysed by methionine synthase, which itself is reductively methylated by cobalamin (vitamin B_{12}) and AdoMet, requiring methionine synthase reductase. 5-Methyltetrahydrofolate is generated from 5,10-methylenetetrahydrofolate (MTHF) by MTHF reductase. The second remethylation reaction is catalysed by betaine methyltransferase, which is restricted to the liver, kidney and brain, while methionine synthase is widely distributed.

As well as remethylation, Hcy can be degraded in the trans-sulphuration pathway, which first involves condensation of Hcy with serine forming cystathionine, then breakdown of this compound to cysteine and α-oxo-butyrate. These reactions

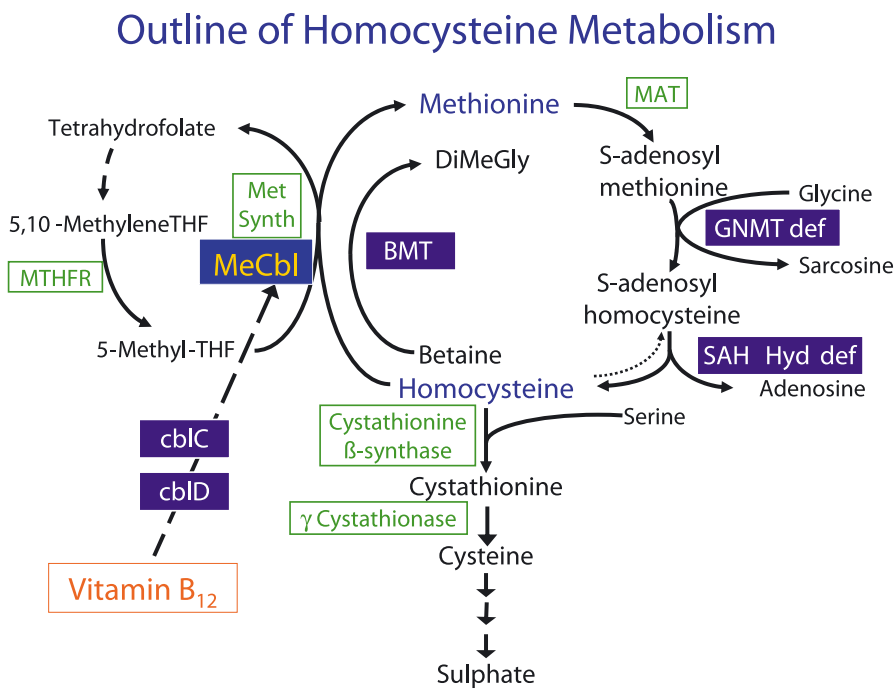

Fig. 2.2.1 Outline of homocysteine metabolism in man. *BMT* Betaine methyltransferase, *cblC* cobalamin defect type C, *cblD* cobalamin defect type D, *GNMT def* glycine N-methyltransferase deficiency, *MAT* methionine adenosyl transferase, *MeCbl* methylcobalamin, *Met Synth* methionine synthase, *MTHFR* methylenetetrahydrofolate reductase, *SAH Hyd def* S-adenosylhomocysteine hydrolase deficiency

are catalysed by cystathionine β-synthase and γ-cystathionase, respectively, both requiring pyridoxal 5'phosphate (vitamin B_6) as a coenzyme. Cysteine is needed for both protein synthesis and as the precursor of the important antioxidant glutathione. Several enzymatic reactions [5] lead to oxidation of the sulphur atom and further breakdown of cysteine, ultimately forming inorganic sulphate.

The metabolic control of methionine metabolism is complex and involves, for example, changes of enzyme levels in particular tissues, mechanisms linked to the kinetic properties of the various enzymes and their interaction with metabolic effectors [6, 7]. A particularly important metabolic effector is AdoMet. This inhibits the low K_m isoenzymes of MAT, and MTHF reductase, inactivates betaine methyltransferase, but activates MAT III (the high-K_m isoenzyme) and cystathionine β-synthase. Therefore, high methionine intake and thus higher AdoMet levels favour trans-sulphuration, and when levels are low methionine is conserved. AdoHcy potently inhibits AdoMet-dependent methyltransferases and both Hcy remethylating enzymes. Another important control mechanism is the export of Hcy from cells into the extracellular space and plasma, which occurs as soon as intracellular levels increase [8].

Elevated Hcy occurs in a wide range of disease processes. This is not surprising bearing in mind the central role of this metabolite in several closely related pathways and because of its links to processes such as polyamine synthesis, methylation and redox potential.

A large elevation of Hcy in body fluids and tissues is found in several genetic enzyme deficiencies, the homocystinurias. These include cystathionine β-synthase deficiency [9], the remethylation defects due to deficiency of MTHF reductase [10], methionine synthase and methionine synthase reductase deficiencies, as well as defects of intracellular cobalamin metabolism [11], namely the cblF, cblC and cblD defects. It is noteworthy that low levels of total Hcy (tHcy) have been described in sulphite oxidase deficiency [12].

Elevated Hcy levels can also occur in nutritional deficiencies of vitamin B_{12} (cobalamin) and folate. Folate or vitamin B_{12} deficiency can even lead to tHcy levels as high as those seen in the genetic homocystinurias [13]. In addition, a reciprocal relationship between blood levels or intake of these vitamins and tHcy concentrations [14] has been shown in many studies.

Several drugs, such as the antifolate compound methotrexate or the anaesthetic gas nitrous oxide, may interfere with methionine metabolism and lead to mild increases of Hcy [2]. Abnormal renal function has been shown to lead to increased plasma Hcy, for example, in end-stage renal disease patients [15].

During the last two decades, much evidence has emerged linking moderately elevated Hcy to several diseases, particularly various forms of vascular disease [16]. Less strong links have also been shown with neural-tube defects, neuropsychiatric disorders, impaired cognitive function, dementia, cancer and osteoporosis. The scope and relevance of the measurement of Hcy has been recently reviewed by Refsum et al. [17].

Because of these ever-widening interests, the measurement of plasma tHcy is undertaken in many clinical chemistry and routine laboratories. Various methods are employed, including high-performance liquid chromatography (HPLC) assays, conventional amino acid analysis, capillary electrophoresis, gas chromatography with or without mass spectrometry, liquid chromatography with tandem mass spectrometry, and in many routine clinical chemistry laboratories immunoassays. In this chapter, those methods that are often available in laboratories involved in the investigation of inborn errors of metabolism are described, namely HPLC and tandem mass spectrometry.

The laboratory measurement of AdoMet and AdoHcy is not routinely performed, but plays an increasing role in studies of pathogenesis of elevated Hcy as well as the differential diagnosis of hypermethioninaemia due to deficiency of MAT, glycine methyltransferase or AdoHcy hydrolase.

Until the middle 1990s, AdoMet and AdoHcy had been studied almost exclusively in tissues or cerebrospinal fluid (CSF). Recent studies have shown that AdoMet and AdoHcy are readily detectable in isolated erythrocytes or whole blood, and reduced levels of AdoMet have been reported in whole blood from patients with coronary artery disease [18]. Application of HPLC with fluorescence detection has allowed the detection of these two compounds in plasma, although levels are in the nanomolar range and clearly much lower than those in tissues [19, 20]. Clear increases were shown in normal subjects following the administration of methionine [20] or AdoMet [21]. Subsequently, several studies have confirmed the ability to measure

these two key compounds in plasma [22, 23]. The measurement of both compounds in CSF can also be useful in the diagnosis of remethylation defects as well as in monitoring their treatment.

2.2.2 Properties of Hcy, AdoMet and AdoHcy

Hcy is a sulphydryl amino acid of molecular weight 135.2. It oxides readily to its disulphide form homocystine, and can be converted to the thiolactone form in acid solution. In normal plasma, Hcy exists in various forms: the sulphydryl form (approximately 1%), bound to the cysteine residues of proteins (approximately 70%), and bound to free cysteine as cysteine-Hcy mixed disulphide (approximately 30%). When levels are elevated, the disulphide form homocystine is formed. All of these forms can be converted to Hcy by chemical reduction and then measured as tHcy.

AdoHcy comprises an adenosyl moiety attached to Hcy through the latter's S atom. Its molecular weight is 384.4 and it absorbs ultraviolet light strongly with a maximum absorbance (λ_{max}) at 260 nm at pH 7.

AdoMet comprises an adenosyl moiety attached to methionine at the sulphur atom. The presence of three substituent groups on the sulphur atom produces a positively charged sulphonium compound that is thermodynamically unstable, resulting in high reactivity of AdoMet. Its molecular weight is 399.4 and it absorbs ultraviolet light strongly with a λ_{max} of 260 nm at pH 7. The compound is unstable under many conditions. Stable solid forms include the hydrogen sulphate and disulphate di-*p*-toluene sulphate salts. Four stereoisomers exist and the active form is L at the 2-carbon and – at the sulphonium centre.

2.2.3 Methods

2.2.3.1 Measurement of tHcy in Plasma Using Isocratic HPLC-Fluorescence Detection

Principle of Assay

Thiols exist in biological systems in various oxidised and reduced forms. Very little Hcy in the free sulphydryl form is found in plasma and it exists mainly as cysteine-Hcy mixed disulphide, bound to cysteine residues of plasma proteins, or as its disulphide homocystine, but the latter only when levels are high. Routinely measured tHcy constitutes all of these forms together and is produced by chemical reduction.

The method described here is based on two reactions: first, the reduction of the disulphide bond between Hcy and other thiols or the cysteine residue of proteins by the reducing compound tri-n-butylphosphine (Fig. 2.2.2a) followed by the reaction of Hcy and other thiols with the flourogenic thiol-specific reagent ammonium 7-fluorobenzo-2-oxa-1,3-diazole-4-sulphonate (SBDF; see Fig. 2.2.2b). The derivatives are separated by reverse-phase HPLC using isocratic elution, and detection and quantification by fluorescence [24, 25].

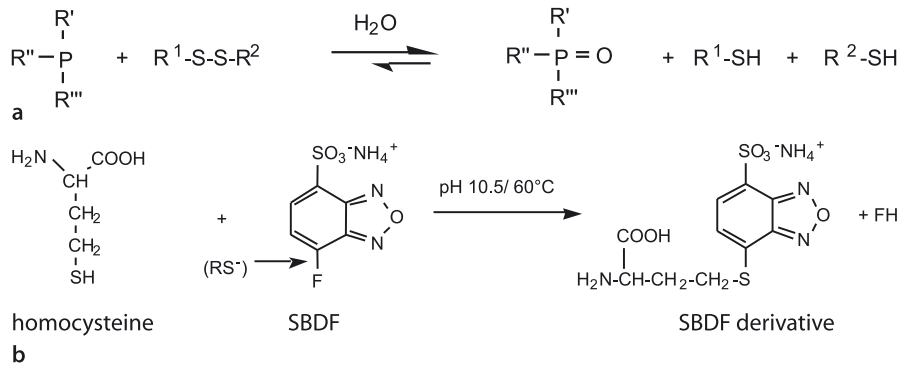

Fig. 2.2.2 **a** Reaction of tri-n-butylphosphine as a reducing agent. **b** Reaction of the derivatisation of Hcy with ammonium 7-fluorobenzo-2-oxa-1,3-diazole-4-sulfonate (*SBDF*), which is a fluorescent derivatising reagent

Pre-analytical

Specimen

A minimum volume of 400 µl plasma is required. Ethylenediaminetetraacetic acid (EDTA) blood, collected after overnight fasting, is separated within 30 min by centrifugation at 2000 × g for 10 min at 4°C. If separation cannot be performed within 30 min, blood can be kept on ice for a maximum of 1 h. Plasma is stored frozen at –20°C until analysis. Hcy is stable in plasma at room temperature for 24 h, at 4°C for 1 week and at –20°C for many years. Serum should not be used, since allowing blood to coagulate leads to a delay in centrifugation.

Pooled plasma collected from healthy subjects is used for standards preparation to avoid matrix effects and for internal control. Pooled plasma is kept in 0.5-ml aliquots at –20 C until required.

Reagents and Chemicals

All chemicals should be of the highest purity available or HPLC grade. Solutions for reduction and derivatisation are:

1. Reduction buffer (0.1 mol/l borate, pH 9.5): Dissolve 6.11 g $K_2B_4O_7 \cdot 4\,H_2O$ (Sigma, O-5754) in H_2O. Adjust the pH to 9.5 with 2 mol/l NaOH and make up to 20 ml with demineralised water.
2. Internal standard (0.25 mmol/l cysteamine in 0.1 mol/l borate buffer): Dissolve 3.78 mg cysteamine (Sigma, M-6500) and 93.55 mg NaEDTA (2 mmol/l, Merck 1.08418) in 0.1 mol/l borate buffer in a final volume of 125 ml.
3. Tri-n-butylphosphine, 10%: one volume of tri-n-butylphosphine (Sigma P-6918) is added to nine volumes of N,N-dimethylformamide (Aldrich 31,993-7). This solution must always be freshly prepared.
4. Perchloric acid 0.6 mol/l: 5 ml 70% $HClO_4$ (Merck, cat. no. 519) and 37.2 mg NaEDTA are made up to 100 ml with demineralised water.
5. Derivatising buffer (0.2 mol/l borate, pH 10.5): Dissolve 6.11 g $K_2B_4O_7 \cdot 4\,H_2O$ and 186 mg NaEDTA in H_20. Adjust the pH to 10.5 with 1 mol/l NaOH and make up to 100 ml with demineralised water.

6. SBDF: Dissolve 1 mg SBDF ammonium salt (Sigma F-4383) in 1 ml of borate buffer, 1 mol/l, pH 9.5 made up by dissolving 61.1 g $K_2B_4O_7 \cdot 4\ H_2O$, adjusting the pH to 9.5 with 2 mol/l NaOH and making up to 200 ml with demineralised water.

Mobile phase for HPLC:
1. Dissolve 13.61 g KH_2PO_4 in about 900 ml H_2O and add 45 ml acetonitrile (= 45%). Adjust the pH to 2.1 with about 6 ml of 85% orthophosphoric acid and make up to 1 l with demineralised water. Vacuum filter the solution (0.45 µM filter, Schleicher and Schuell, reference 10410212).
2. Hcy standards: Both stock and working standards are stable for at least 1 year stored in aliquots at –20°C:
   a. Hcy stock solution, 4 mmol/l: dissolve 5.4 mg DL-Hcy (Fluka 54501) in 10 ml 0.1 mol/l borate buffer solution containing internal standard.
   b. Standards of 6.3–400 µmol/l are prepared by serial dilution of the stock solution in internal standard solution.

Instrumentation

1. General laboratory equipment.
2. Heating block at 60°C for sample derivatisation.
3. Laboratory centrifuge, microcentrifuge, vortex mixer.
4. HPLC system consisting of a buffer pump, preferably with degasser, autosampler with cooling system, fluorescence detector (excitation 384 nm, emission 516 nm) and an integration and data handling system.
5. HPLC column: Nucleosil 120 C18, 5 µm (4.6 × 250 mm) with a guard column (4.6 × 20 mm) containing the same column packing material.

Calibration

Calibration is performed using three standards selected to cover the range expected in the sample batch (usually 4.2, 8.4 and 33.6 µmol/l), together with pooled plasma to allow for any matrix effect, plus a pooled plasma blank.

Quality Control

Quality assessment is performed by including pooled plasma as an internal control in every run. External quality control is achieved using samples obtained from the European Research Network for evaluation and improvement of screening, Diagnosis and treatment of Inherited disorders of Metabolism (ERNDIM) Special Assays Scheme, run according the scheme schedule.

Commercially available control plasma samples level I + II obtained from Chromosystems München are included with each batch of samples.

Detection Limit

Sample concentration of 1 µmol/l.

■ Precision

The within-run coefficient of variation (CV; $n = 10$) was shown to be 4.5% and 2.5% for standards of 16 and 67 µmol/l, respectively. The between-run CV ($n = 20$) was 6.1% and 1.9% for standards of 16 µmol/l and 67 µmol/l, respectively.

■ Recovery

Over a concentration range of 4–67 µmol/l, the recovery was 98.9%±6.0.

Analytical

Procedure

The reduction reaction is carried out in 1.5-ml Eppendorf tubes. Frozen samples are thawed out, thoroughly mixed and, if necessary, centrifuged to remove particulate material. For samples and the pooled plasma blank, 150 µl plasma and 50 µl internal standard in 0.1 mol/l borate buffer are added to 20 µl of 10% tri-n-butylphosphine. For each Hcy standard, 150 µl of pooled plasma and 50 µl of Hcy standard (internal standard is included) are mixed with 20 µl of tri-n-butylphosphine. Tubes are left to stand on ice for 30 min. Samples are deproteinised by the addition of 125 µl of 0.6 mol/l perchloric acid, thorough vortex mixing and centrifugation at 13,000 rpm (11,000 × g) for 5 min (Eppendorf centrifuge). The supernatant is reserved for further processing.

Derivatisation is performed in 5-ml glass tubes by mixing 100 µl of the supernatant with 200 µl of 0.2 mol/l, pH 10.5, borate buffer and 100 µl freshly prepared SBDF solution. After thorough vortex mixing, the tubes are sealed with plastic stoppers and incubated at 60°C for 60 min in a heating block. The reaction is stopped by placing tubes on ice. Samples are filtered through a 0.45-µm membrane (4 mm, Titan PVDF filters, Infochroma, reference 8804-PV-4) using a 1-ml plastic syringe filters, and used for HPLC analysis. If the analysis is not performed immediately, samples can be stored at –20°C.

HPLC conditions

The HPLC analysis is performed isocratically with a flow rate of 2.0 ml/min and a run time of 10 min. The usual pressures are between 22 and 24 MPa (230–240 bar). The injection volume is 25 µl. The fluorimeter is set with an excitation wavelength of 384 nm and emission at 516 nm.

Calculation

A four-point linear regression plot is constructed for calibration, where the x-axis represents added Hcy concentration (µmol/l) and the y-axis represents the ratio of areas of added Hcy:internal standard (IS). Concentrations of Hcy in samples are calculated by dividing the ratio of the area of Hcy:IS area by the slope of the calibration line. Thus, tHcy concentration = Hcy:IS/slope (Fig. 2.2.3).

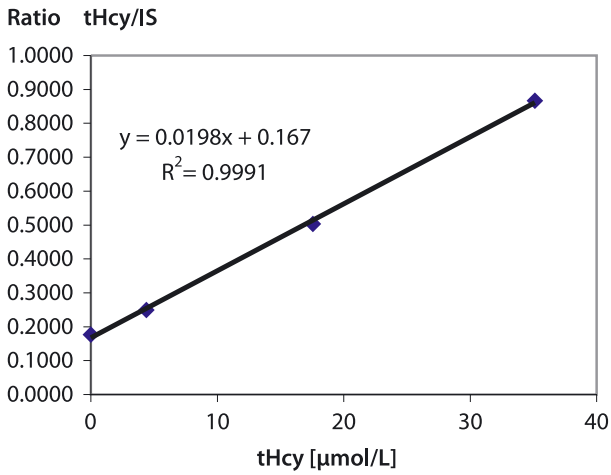

Fig. 2.2.3 Standard curve of total homocysteine (*tHcy*) in human plasma. *IS* Internal standard

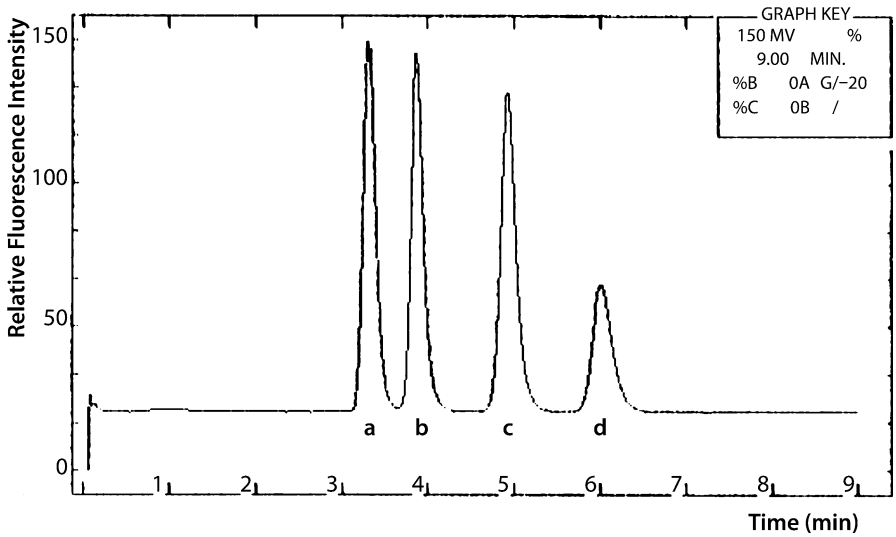

Fig. 2.2.4 Chromatogram of SBDF-derivatised thiols in human plasma. *a* Cysteine, *b* cysteamine, *c* cysteinylglycine, *d* Hcy

Post-analytical

Interpretation

The separation obtained with a normal plasma sample is shown in Fig. 2.2.4. The order of elution is cysteine (3.5 min), cysteamine (4.0 min), cysteinylglycine (5.0 min) and Hcy (6.5 min) with a peak width of under 1 min and complete resolution of peaks.

Chromatogram

An HPLC chromatogram of SBDF-derivatised thiols in human plasma is shown in Fig. 2.2.4.

Reference and Pathological Values of tHcy

Ideally, each laboratory should obtain it's own reference values. Those obtained in our own laboratory are summarised in Table 2.2.1. Typical pathological values of tHcy are given in Table 2.2.2.

Pitfalls

1. There is a time- and temperature-dependent increase of plasma tHcy in the presence of erythrocytes; for example 5–15% per hour at room temperature [27]. Thus, delay in separation of the plasma after blood drawing must be avoided to prevent a falsely elevated Hcy level.
2. Low purity of N,N-dimethylformamide may result in the presence of a negative peak immediately preceding the cysteine peak, although this should not interfere with integration.

Table 2.2.1 *Reference values.* tHcy *Total homocysteine*

		tHcy (µmol/l)		
	n	mean	SD	Range
Men and women age 21–64 years	65	8.1	2.5	3.3–13.3
Men [a]				8–18
Pre-menopausal women [a]				6–15
Post-menopausal women [a]				6–19
Children aged 2 months to 18 years [b]				3.3–8.3
Children aged 11–15 years [b]				4.7–10.3

[a] Values from Dr. Ries Duran
[b] Reference [26]

Table 2.2.2 *Typical pathological values of* tHcy

Pathological state	tHcy (µmol/l)
Vitamin B_{12} deficiency	40–100
Folate deficiency	25–65
Renal failure	23–30
Severe renal failure	30–100
Cystathionine-beta-synthase defect	100–500
MTHF reductase defect	100–250
Methionine synthase deficiency (cblC, cblD, cblF, cblE, cblG defects)	100–250

2.2.3.2 Measurement of tHcy in Plasma using HPLC and Tandem Mass Spectrometry

Principle of Assay

As described in 2.2.3.1, "Principles of Assay", tHcy must be produced by chemical reduction, which is achieved in the method described here by dithiothreitol. tHcy is analysed by HPLC separation followed by electrospray ionisation and then separation of the ionised molecule in the first mass spectrometer, then fragmentation into a specific ion fragment in the second. Quantification is based on comparison of the signal from natural Hcy (transition m/z 135.9 → m/z 89.9) with that of the stable isotope internal standard (transition m/z 139.9 → m/z 93.9).

Pre-analytical

Specimen

This is as in 2.2.3.1, "Specimen", except that a minimum volume of 300 µl plasma is required.

Reagents and Chemicals

All chemicals should be of the highest purity available or HPLC grade.

1. Reducing reagent: dissolve 77 mg dithiothreitol (Roche 708984) in 1 ml demineralised water.
2. Deproteinising solution: mix 800 ml acetonitrile (Merck 10030) with 200 ml demineralised water and add 1 ml of 98–100% formic acid (Merck 122).
3. HPLC mobile phase: mix 70 ml acetonitrile (Merck 10030) with 20 ml demineralised water and add 0.1 ml of 98–100% formic acid (Merck 122).
4. Internal standard: D8-DL-homocystine: weigh out 5.56 mg D8-DL-homocystine (ARC/CLI DLM 3619) and dissolve in 20 ml demineralised water, adding one drop of formic acid (1.007 mmol/l). A 2-ml aliquot of this solution is made up to 20 ml with water (100 µmol/l). This is then diluted 1 in 4 (25 µmol/l) with demineralised water (stable for at least 1 year at 4°C).
5. Calibration standard, 25 µmol/l homocystine: accurately weigh out 33.6 mg L-homocystine (Sigma H-6010) and dissolve in 50 ml demineralised water. This stock is diluted 1 in 100 with phosphate-buffered saline and stored at –20°C in 150-µl aliquots; it is stable for at least 1 year.

Instrumentation

1. General laboratory equipment, laboratory centrifuge, vortex mixer.
2. Tandem mass spectrometer with an HPLC pump, pre-column (Phenomex CN; Bester, AJO-4304), column (LC-CN; Supelco 58979), autosampler and data-handling system. Standard instrumentation such as the Micromass micro (Waters, Milford MA, USA) has sufficient sensitivity.

Calibration

Calibration is performed according to the manufacturer's instructions

Quality Control

Quality assessment is performed by including three control plasmas (low, normal, high levels) as internal controls in every run. External quality control is achieved using samples obtained from the ERNDIM Special Assays Scheme, run according to the scheme schedule.

- Detection Limits

2–150 µmol/l

- Precision

The within-run CV ($n = 12$) was shown to be 8.8%, 3.6% and 1.7% for standards of concentrations 0.9, 10.1 and 51.5 µmol/l, respectively. The between-run CV ($n = 50$) was 9.1%, 6.4% and 6.4% for plasma control samples with average values of 0.9, 9.1 and 48.8 µmol/l, respectively.

- Recovery

The recovery of Hcy standard of 20 µmol/l added to normal plasma containing 14 µmol/l was 96% ($n = 10$, CV = 5%).

Analytical

- Procedure

Samples of 50 µl plasma, standard or control plasma, 20 µl internal standard and 10 µl dithiothreitol solution are thoroughly mixed (vortex) in 1-ml Eppendorf tubes. The tubes are left to stand at room temperature for 15 min. Samples are then deproteinised by the addition of 500 µl deproteinising acetonitrile solution, with thorough vortex mixing followed by centrifugation at 14,000 rpm (11,000 × *g*) for 5 min (4°C). Tandem mass spectrometry analysis is performed on 200 µl of the supernatant reserved in appropriate vials. If the analysis is not performed immediately, samples can be stored at –20°C until analysis.

The instrument is used in the positive ion mode. Multiple-reaction monitoring of the ions 135.9 → 89.9 and 139.9 → 93.9 is used for the quantitative evaluation of Hcy and d_4-Hcy, respectively.

Calculation

Calculation of the Hcy concentration is performed using the internal standard method:

$$\text{Conc. (Hcy)} = \frac{\text{Area (Hcy) } s}{\text{Area (IS) } s.} \times \frac{\text{Area (IS) } std.}{\text{Area (Hcy) std.}} \times \text{Conc. (Hcy) std. in µmol/l}$$

Where Conc. is concentration, *s* is sample chromatogram, IS is the internal standard and std. is the standard chromatogram.

Post-analytical

Interpretation

As this is a single-peak/one-analyte procedure, there are no interpretational complications.

- Chromatogram

See Fig. 2.2.5

- Reference Values and Typical Pathological Values

See Tables 2.2.1 and 2.2.2

- Pitfalls

The pitfalls are the same as those for HPLC with fluorescence detection (see 2.2.3.1, "Pitfalls").

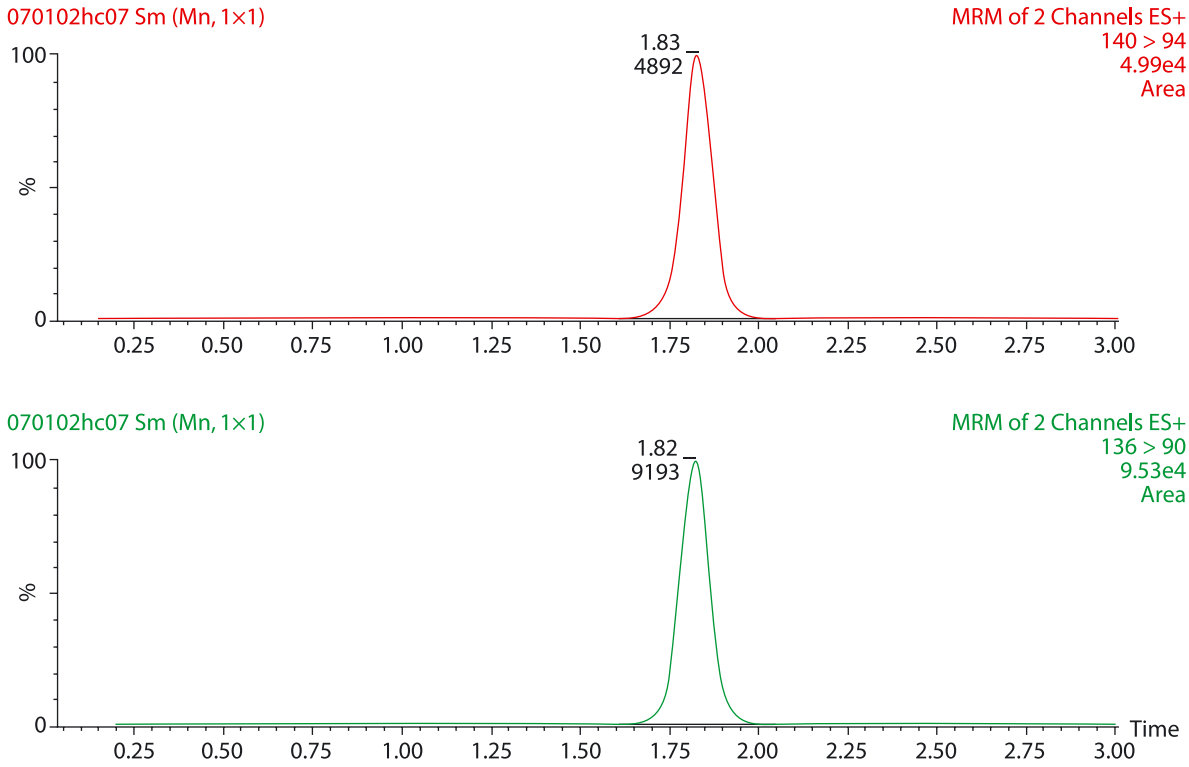

Fig. 2.2.5 Upper panel: transition 139.9 → 93.9 for d_4-Hcy. Lower panel: transition 135.9 → 89.9 for Hcy (Figure courtesy of Dr. Ries Duran, Amsterdam)

2.2.3.3 Measurement of AdoMet and AdoHcy in Plasma and CSF by HPLC with Fluorescence Detection

Principle of Assay

The reaction of AdoMet and AdoHcy with monochloroacetaldehyde produces the etheno derivatives, which are strongly fluorescent (Fig. 2.2.6). These derivatives are separated by isocratic HPLC and detected and quantified by fluorescence. Our methods have been modified from those of Wagner et al. [28].

Pre-analytical

Specimen

A minimum of 2 ml EDTA blood is placed immediately on ice and centrifuged within 30 min at 2000 × *g* for 5 min at 4°C. Plasma is immediately deproteinised by adding 1 ml to 0.625 ml of 10% $HClO_4$ and mixing thoroughly by vortex. The mixture is frozen and stored at –70°C until analysis. 1-ml aliquots of pooled plasma collected from healthy subjects are prepared and stored in the same way and are used to prepare AdoMet and AdoHcy calibration standards to allow for matrix effects and also as an internal quality control. CSF is collected in plain tubes and kept at –70°C until analysis.

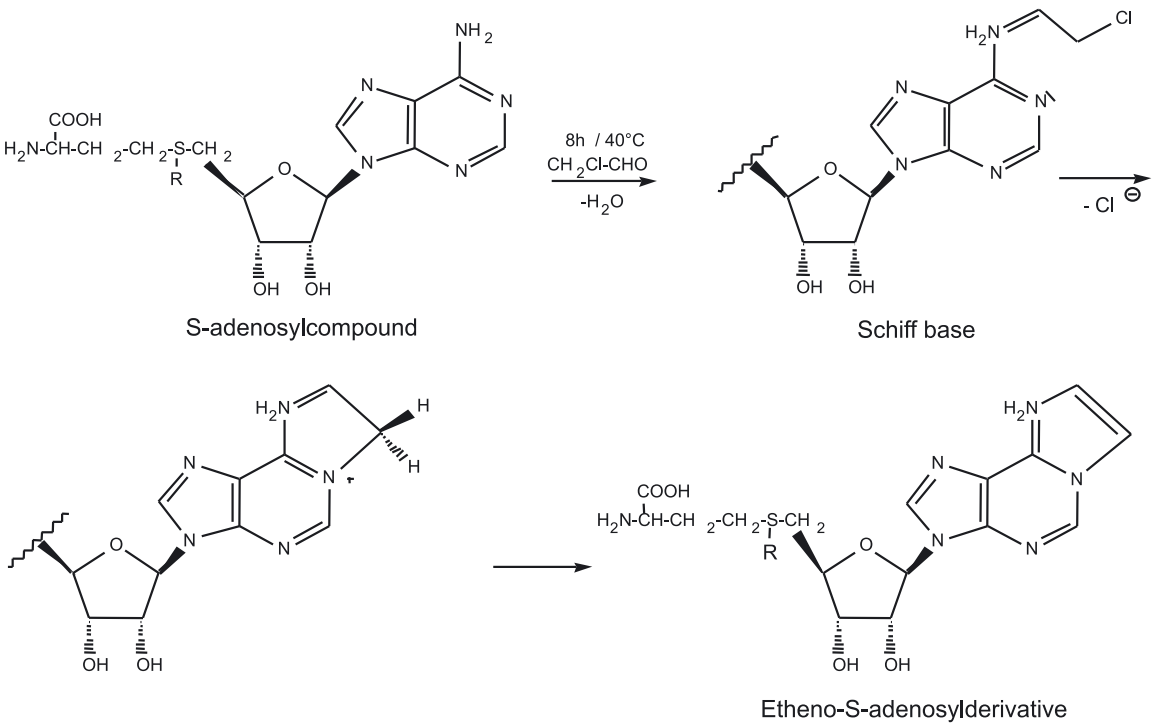

Fig. 2.2.6 Mechanism of the derivatisation of S-adenosylmethionine (AdoMet), S-adenosylhomocysteine (AdoHcy) and chloroacetaldehyde

Reagents and Chemicals

All chemicals should be of the highest purity available or HPLC grade. Solutions for derivatisation and deproteinisation:

1. 55% Chloroacetaldehyde: mix 55 ml chloroacetaldehyde (Fluka, cat. no. 22760) with 45 ml demineralised water.
2. 3 mol/l sodium acetate buffer: dissolve 40.82 g sodium acetate trihydrate (Merck cat. no. 1.06267) in 100 ml demineralised water
3. 10% perchloric acid: make 14.28 ml of of 70% $HclO_4$ (Merck, cat. no. 519) up to 100 ml with demineralised water.
4. 0.4 mol/l perchloric acid: make 3.33 ml of 70% $HClO_4$ (Merck, cat. no. 519) up to 100 ml with demineralised water.
5. Mobile phases for HPLC:
   a. for AdoMet. 0.1 mol/l sodium acetate/2.3% acetonitrile with 10 mmol/l heptanesulphonic acid. Dissolve 13.61 g sodium acetate trihydrate GR (Merck cat. no. 1.06267) in 900 ml demineralised water and add 2 g 1-heptanesulfonic acid, sodium salt (Sigma, cat. no.H2766/H8109) and 23 ml acetonitrile (Fisher Scientific A/0630/PB15). Adjust the pH to 4.3 with 100% glacial acetic acid, make up to 1000 ml with demineralised water and vacuum filter as above.
   b. for AdoHcy. 0.1 mol/l sodium acetate/2.5% acetonitrile: Dissolve 13.61 g sodium acetate trihydrate GR (Merck cat. no. 1.06267) in 900 ml demineralised water and add 25 ml acetonitrile. Adjust the pH to 4.2 with glacial acetic acid, make up to 1000 ml with demineralised water and vacuum filter as above.

AdoMet and AdoHcy Standards

AdoMet/AdoHcy Stock Solutions

Accurately weigh 1.18 mg of S-adenosylmethionine hydrogen sulphonate (Boehringer Mannheim, cat. no. 102 407, MW: 496.2 g/mol) or 1.32 mg of S-adenosylhomocysteine (Sigma cat. no. A 9384, MW 384.4 g/mol). These are dissolved in demineralised water (usually approximately 5 ml) to give a concentration for AdoMet of 0.342 mmol/l (after correction for the purity declared for the particular batch) and for AdoHcy of 0.686 mmol/l. These solutions are immediately diluted ten-fold with 0.4 mol/l perchloric acid and can be stored in aliquots at –20 C for at least 6 months.

Calibration standards are prepared fresh by serial dilution of the stock solutions in 0.4 mol/l perchloric acid (3.43–0.0267 μmol/l). Standards are stable for at least 6 months at –20°C.

Instrumentation

1. General laboratory equipment.
2. Heating block at 60°C for sample derivatisation.
3. Laboratory centrifuge, micro centrifuge.
4. HPLC system consisting of two separate HPLC pumps or a single pump with gradient-forming facility, preferably with degasser, autosampler with cooling system, fluorescence detector (excitation 270 nm, emission 410 nm) and an integration and data-handling system.

■ HPLC columns

1. AdoMet: Hydrosphere C-18, 3 µm (150 × 3 mm) with a guard column (10 × 3 mm) containing the same packing material.
2. AdoHcy: Phenomenex, Gemini C-18, 3 µm (150 × 3 mm) with a guard column (4 × 2 mm) containing the same packing material.

Calibration

For both AdoMet and AdoHcy, calibration is performed using three standards: 53, 106 and 210 nmol/l for AdoMet and 40, 80 and 160 nmol/l for AdoHcy, each added to pooled plasma supernatant fluid, plus a pooled plasma blank. Higher concentrations can be used if sample levels are expected to be high.

Quality Control

Neither AdoMet nor AdoHcy have so far been included in any external quality control scheme. Control samples are not commercially available. A pooled plasma sample is included in each batch as internal quality control.

■ Detection Limit

This depends greatly on the sensitivity of the fluorimeter used, but the following levels should be achievable: AdoMet and AdoHcy, 2–5 nmol/l per sample.

■ Precision

1. For AdoMet standards of 27 nmol/l and 107 nmol/l, the within-run CV ($n = 10$) was shown to be 5.5% and 2.5%, respectively, with a between-run CV ($n = 20$) of 7.1% and 1.8%, respectively.
2. For AdoHcy standards of 20 nmol/l and 81 nmol/l, the within-run CV ($n = 10$) was 3.6% and 2.0%, respectively, and the between-run CV ($n = 20$) was 8.2% and 1.7%, respectively.

■ Recovery

1. AdoMet: 103 ± 9.8% over a concentration range of 27–528 nmol/l.
2. AdoHcy: 92 ± 3.0% over a concentration range of 20–160 nmol/l.

Analytical

AdoMet and AdoHcy are separated and measured as their etheno derivatives using reverse-phase HPLC with isocratic elution in separate runs, using ion-pairing for AdoMet. In both runs the column is flushed with 100% acetonitrile followed by re-equilibration with the mobile phase between sample injections.

Procedure

■ Derivatisation Procedure for AdoMet and AdoHcy

Frozen deproteinised samples are thawed out, thoroughly mixed and then centrifuged at 2000 × *g* for 5 min at 4°C. If the supernatant is turbid it should be clarified by filtration as described earlier. Derivatisation is performed in 5-ml Pyrex tubes. For plasma samples, 200 µl supernatant is added to 50 µl chloracetaldehyde and thoroughly mixed, followed by addition of 45 µl of 3 mol/l sodium acetate to ad-

just the pH to 3.5–4.0. Standards are prepared by adding 100 µl of pooled plasma supernatant to 100 µl of each standard solution or 100 µl of 0.4 mol/l perchloric acid for the blank. To each tube is added 50 µl of 55% chloracetaldehyde with thorough mixing, followed by addition of 45 µl of 3 mol/l sodium acetate to adjust the pH to 3.5–4.0. Tubes are sealed with plastic stoppers and incubated at 39°C for 8 h in a heating block. The reaction is stopped by placing the tubes on ice. The samples can be immediately analysed by HPLC or kept at –20°C until analysis.

■ HPLC Conditions for AdoMet

The HPLC analysis is performed by pumping 100% mobile phase for 54 min at 0.45 ml/min then changing to 100% acetonitrile for 9 min. The column is re-equilibrated with mobile phase for 8 min prior to the subsequent injection. Usual pressures are between ~20 and 21 MPa (210 bar). Samples of 25 µl are injected. The fluorimeter is set with an excitation wavelength of 270 nm and emission at 410 nm.

■ HPLC Conditions for AdoHcy

The HPLC analysis is performed isocratically with a flow rate of 0.5 ml/min and a run time of 71 min. Usual pressures are between ~20 and 21 MPa (210 bar). Samples of 25 µl samples are injected. The fluorimeter is set with an excitation wavelength of 270 nm and emission at 410 nm.

Calculation

Concentrations of AdoMet or AdoHcy in plasma samples are determined by dividing the peak area in the unknown run by the slope of the calibration line and multiplying by 1.625 to allow for the dilution of plasma. Thus, AdoMet or AdoHcy concentration = Area/slope × 1.625. (see Fig. 2.2.7).

Post-analytical

Interpretation

■ Chromatogram: Peak Identification

Chromatography of one or two samples spiked with AdoMet (210 nmol/l) and AdoHcy (160 nmol/l) is performed within each batch to aid in identification of peaks. Typical elution times are 28–34 min for etheno-AdoMet and 8–10 min for etheno-AdoHcy. The separations obtained for AdoMet and AdoHcy obtained with a normal plasma sample are shown in Fig. 2.2.8.

Reference Values

These have been reported by several groups, but it is preferable to produce own values in each laboratory. Our control values are listed in Table 2.2.3.

Typical Pathological Values

A list of typical values for several pathological conditions is given in Table 2.2.4.

Pitfalls

1. AdoMet and AdoHcy are unstable in neutral and alkaline solution; they must be kept acidified.

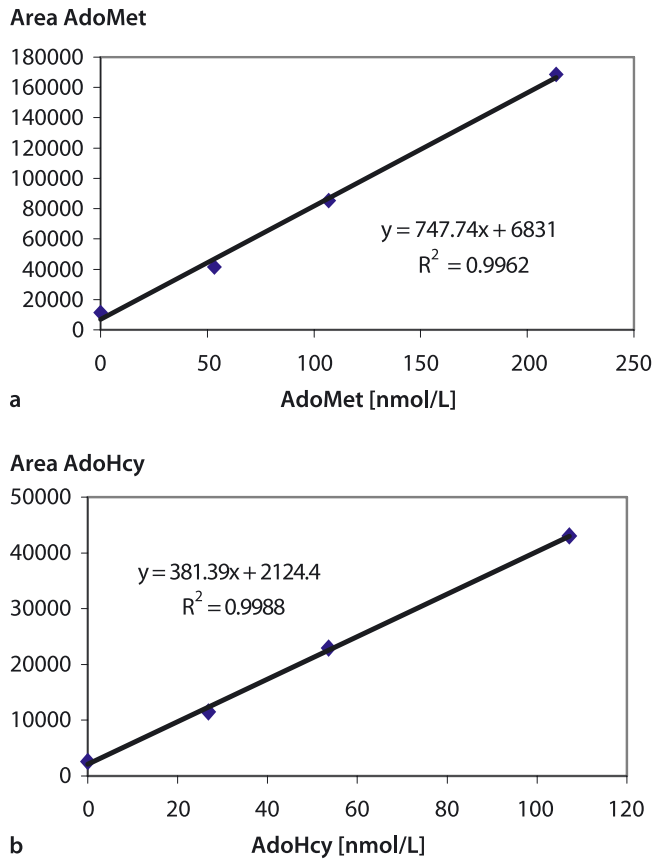

Fig. 2.2.7 **a** Standard curve of AdoMet in human plasma. **b** Standard curve of AdoHcy in plasma

2. Collected plasma has to be immediately deproteinised with 10% perchloric acid.
3. Delayed deproteinisation may result in decomposition of AdoMet/AdoHcy.
4. To achieve optimal pH, which is crucial for the derivatisation step, control the pH with the indication paper after adding 3 mol/l sodium acetate.
5. Care needs to be taken in distinguishing the true AdoMet and AdoHcy peaks from closely eluting substances.

2.2.3.4 Measurement of AdoMet and AdoHcy Using Plasma HPLC and Tandem Mass Spectrometry

Principle of Assay

AdoMet and AdoHcy are separated by HPLC and analysed by electrospray ionisation-tandem mass spectrometry. Quantification is based on comparison of the signal from natural AdoMet (transition m/z 399 → m/z 250) and AdoHcy (transition m/z 385 → m/z 135 and 134) with that from analogous transitions of the stable isotope internal standards.

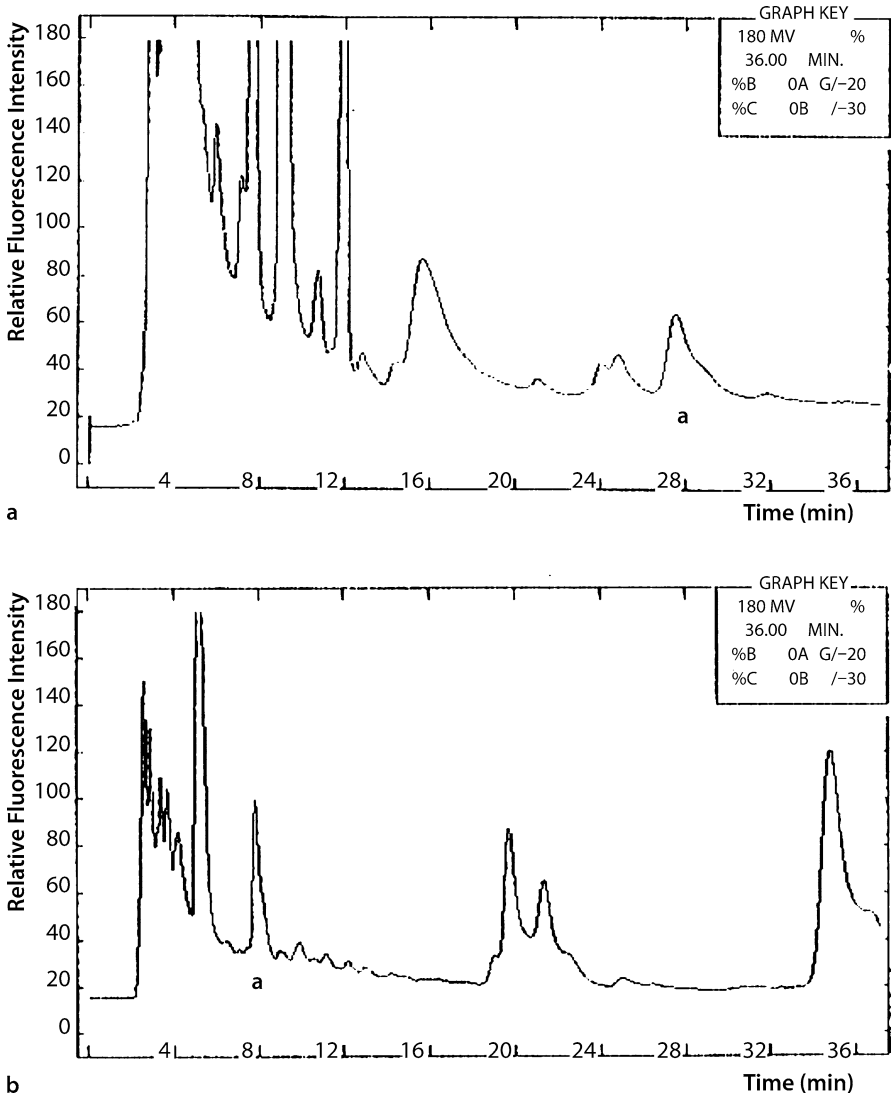

Fig. 2.2.8 **a** Chromatogram of etheno-AdoMet (a) in plasma (a). **b** Chromatogram of etheno-AdoHcy (a) in plasma

■ ***Table 2.2.3*** *Control values for S-adenosylmethionine (AdoMet) and S-adenosylhomocysteine (AdoHcy) in plasma*

	Plasma AdoMet (nmol/l)	Plasma AdoHcy (nmol/l)
Range	29.6–118.2	9.6–48.7
mean ± SD	56.4 ± 17.4	25.5 ± 7.9
n	64	66

Table 2.2.4 *Typical pathological values for AdoMet and AdoHcy*

Pathological condition	AdoMet (nmol/l)	AdoHcy (nmol/l)
Renal disease	220–840	530–1590
Methionine:S-adenosyltransferase deficiency	48–120	10–15
Glycine *n*-methyltransferase deficiency	1000–4000	Normal
S-adenosyl-homocysteine hydrolase deficiency	800–3000	330–5000
Cystathionine *β*-synthase deficiency	900–2000	150–1700

Pre-analytical

Specimen

A minimum volume of 300 µl plasma obtained from EDTA or heparinised blood is required. Plasma must be frozen as soon as possible after collection (–20°C for a maximum of 1 month, longer at –80°C). Since AdoMet is rapidly degraded in plasma, immediate deproteinisation with perchloric acid is recommended.

Reagents and Chemicals

All chemicals should be of the highest purity available or HPLC grade.

1. HPLC mobile phase A: Make 1 ml *n*-heptafluorobutyric acid (Pierce, 25003) up to 1000 ml with demineralised water.
2. HPLC mobile phase B: Methanol gradient grade (Merck, M6007). Check that no turbidity is present.
3. 5 mol/l K_2CO_3: Dissolve 691 g K_2CO_3 (Sigma, 5833) in 1000 ml demineralised water. (take care because of heat production).
4. 1 mmol/l HCl: Make up 0.083 ml concentrated HCl (Merck, M100317) to 1000 ml with demineralised water.
5. Stock standard solutions: weigh out accurately about 5–10 mg AdoMet (Sigma A7007) and AdoHcy (Sigma A9384) and dissolve in 1 ml of 1 mmol/l HCl. These can be stored at –20°C for at least 2 years. Sonication may be needed to ensure complete dissolution. Note that AdoMet can break down into AdoHcy and this can be tested by HPLC with either ultraviolet or tandem mass spectrometry detection.
6. Calibration standards: Prepare serial dilutions of stock standards in 1 mmol/l HCl to give concentrations of 0, 25, 50, 100, 250 and 500 nmol/l, and in the case of samples with very high levels also 1000 nmol/l.
7. Stable isotope internal standard stock solutions:
   a. AdoMet: weigh out accurately about 5–10 mg of AdoMet-methl-D_3 (CDN isotopes, D4903) in 1 ml of 1 mmol/l HCl. Store at –20°C, at which temperature it is stable for at least 2 years. Note that breakdown of AdoMet-D_3 produces unlabelled AdoHcy, but this is unlikely to influence the results since 1% contamination of the 200-nmol/l AdoMet-D_3 used would lead to an increase of AdoHcy of only approximately 2 nmol/l, compared with endogenous levels of about 18–39 nmol/l.

b. AdoHcy: $^{13}C_5$-labelled AdoHcy was synthesised from [ribo-$^{13}C_5$]-adenosine (Ado) by mixing 1 ml of 3.6 mM $^{13}C_5$-Ado with 250 µl of 72.5 mM Hcy, 100 µl AdoHcy hydrolase (22 U/ml) and 13 µl 0.1 M dithiothreitol. The reaction is complete after 5.5 h at 37°C. The $^{13}C_5$-AdoHcy solution is deproteinised by passing the mixture through a 10 KD filter. The yield is approximately 35%. Purification of the standard is carried out by preparative HPLC on a 10 cm × 4.6 mm LC-18S column using a 0.1% heptafluorobutyric acid/methanol gradient. The combined fractions are evaporated and the residue taken up in 0.5 ml H_2O.

8. Internal standards working solution: Prepare a solution containing 2 µmol/l of each internal standard in 1 mmol/l HCl from the stock solutions. Store in 2-ml aliquots at –20°C.

Instrumentation

1. General laboratory equipment, laboratory centrifuge, vortex mixer.
2. Tandem mass spectrometer with HPLC pump, analytical column (LC-18S, 200 × 4.6 mm; Supelco 59630), autosampler and data-handling system.

Calibration

Calibration standards of 0, 25, 50, 100, 250 and 500, and possibly 1000 nmol/l, prepared by serial dilution of the stock solutions, are included with each batch of samples.

Quality Control

Internal Quality Control

1. The area of the internal standard peaks must remain constant throughout a series. If not, the cause must be determined and corrected and, if necessary, the analysis repeated. One possible cause is quenching due to incorrect injection. If the signal of the internal standard is more than 50% reduced, the sample can be re-injected as soon as possible after dilution. Note that the AdoMet-D_3 signal in samples is usually 1.5 times higher than that in standard runs.
2. If the measured concentration is far removed from the reference range, the original sample should be accordingly diluted and re-analysed.
3. The retention times of AdoMet and AdoHcy must remain constant throughout a series. Variations of retention times may indicate deterioration of the column packing material.
4. Quality assessment is performed by including three control plasmas (low, normal and high levels) as internal controls in every run.

External Quality Control

None is available.

Detection Limits

The lower limit of detection is 1 nmol/l for AdoMet and 3 nmol/l for AdoHcy, and the linear range is up to 500 nmol/l for both compounds.

Precision

The within-run CV ranged from 0.6 to 5% for AdoMet and from 2 to 6% for AdoHcy for five injections of a plasma sample spiked with 0, 25, 50 and 100 nmol/l of each standard. The between-run CV ranged from 9 to 12% for AdoMet and from 8 to

11% for AdoHcy for ten measurements of a plasma sample spiked with 0, 25, 50 and 100 nmol/l of each standard.

■ Recovery

Recovery of AdoMet and AdoHcy added to six different plasmas at concentrations of 0, 25, 50 and 100 nmol/l was 94–102% and 102–105%, respectively.

Analytical

Procedure

Each working standard is prepared for HPLC-tandem mass spectrometry analysis by adding 10–100 µl of working internal standard mixture in an HPLC vial. Plasma samples (100 µl) are added to 10 µl of internal standard in 1.5-ml Eppendorf tubes. Samples are deproteinised by addition of 5 µl of 70% perchloric acid (Merck, M514) with vortex mixing, then centrifuged at 14,000 rpm (11,000 × *g*) at 4°C. A 3-µl aliquot of 5 mol/l K_2CO_3 is added to the supernatant to partially neutralise the solution, and precipitated $KClO_4$ is removed by re-centrifugation for 1 min at 14,000 rpm (4°C). Supernatant is transferred to an HPLC vial and 50 µl is injected into the HPLC-tandem mass spectrometry system. Samples can be stored at –20°C for at least 10 days. If insufficient sample is available and analyses with smaller volumes are performed, the same ratio of sample to internal standard must be maintained.

The analysis is performed on a Thermo TSQ Quantum AM instrument. The total analysis time is 8 min. The analytes are quantified by selected reaction monitoring using the decays listed in Table 2.2.5 (See Fig. 2.2.9).

Calculation

Calculation of the AdoMet and AdoHcy concentration is performed using the internal standard method:

$$\text{Conc. } (X) = \frac{\text{Area } (X)\ s}{\text{Area (IS) } s} \times \frac{\text{Area (IS) std.}}{\text{Area } (X) \text{ std.}} \times \text{Conc. (X) std. in µmol/L}$$

Where Conc. is concentration, *X* is AdoMet or AdoHcy, *s* is the sample chromatogram, IS is the internal standard and std. is the standard chromatogram.

■ ***Table 2.2.5*** *Decays used for the quantification of analytes*

Sample	Decay (m/z ratio)
AdoMet	399 → 250
$^2H_3$-AdoMet	402 → 250
AdoHcy	382 → 134
$^2H_5$-AdoHcy	390 → 134

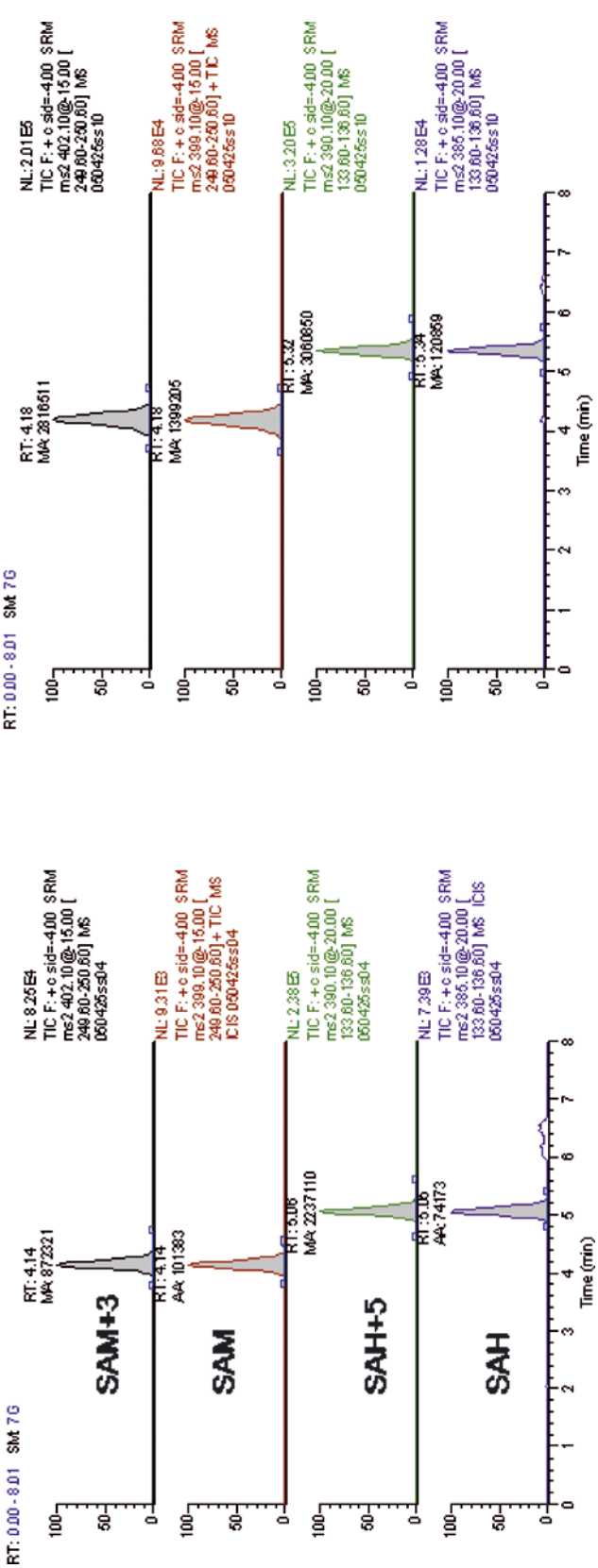

Fig. 2.2.9 High-performance liquid chromatography–tandem mass spectrometric analysis of AdoMet and AdoHcy. The analytes were evaluated by multiple reaction monitoring with the following transitions: m/z 399 → 250 for AdoMet; m/z 402 → 250 for the internal standard, tridenterated AdoMet (AdoMet +3); m/z 385 → 135 for AdoHcy; m/z 390 → 135 for the internal standard, pentadenterated AdoHcy (AdoHcy+5). Mass spectrometric conditions are described in the text. TIC total ion current, SRM selected reaction monitoring (Figure courtesy of Dr. Ries Duran, Amsterdam)

Post-analytical

Interpretation

- Chromatograms

Please refer to Fig. 2.2.9.

- Reference Values

See Table 2.2.3

- Typical Pathological Values

Changes of AdoMet and AdoHcy may be associated with any of the defects of methionine and Hcy metabolism (see 2.2.3.3 and Table 2.2.5). As such, the measurement of these two metabolites cannot be detached from the Hcy assay.

References

1. Finkelstein JD (1990) Methionine metabolism in mammals. J Nutr Biochem 1:228–237
2. Fowler B (2005) Homocysteine: overview of biochemistry, molecular biology, and role in disease processes. Semin Vasc Med 5:77–86
3. Clarke S, Banfield K (2001) S-adenosylmethionine-dependent methyltransferases. In: Carmel R, Jacobsen D (eds) Homocysteine in Health and Disease. Cambridge University Press, Cambridge UK, pp 63–78
4. Yeo E, Wagner C (1994) Tissue binding of glycine N-methyltransferase, a major folate-binding protein of liver. Proc Natl Acad Sci U S A 91:210–214
5. Johnson JL, Duran M (2001) Molybdenum cofactor deficiency and isolated sulfite oxidase deficiency. In: Scriver CR, Beaudet AL, Sly WS, Valle D (eds) The Metabolic and Molecular Bases of Inherited Disease, 8th edn. McGraw-Hill, New York, NY, pp 3163–3177
6. Finkelstein JD (2000) Pathways and regulation of homocysteine metabolism in mammals. Semin Thromb Hemost 26:219–225
7. Finkelstein JD (1998) The metabolism of homocysteine: pathways and regulation. Eur J Pediatr 157:S40–44
8. Fowler B (2001) Transport and tissue distribution of homocysteine and related S-adenosyl compounds. In: Carmel R, Jacobsen D (eds) Homocysteine in Health and Disease. Cambridge University Press, Cambridge UK, pp 163–174
9. Mudd. SH, Levy HL, Kraus JP (2001) Disorders of transsulfuration. In: Scriver CR, Beaudet AL, Sly WS, Valle D (eds) The Metabolic and Molecular Bases of Inherited Disease, 8th edn. McGraw-Hill, New York, NY, pp 2007–2056
10. Rosenblatt DS, Erbe RW (2001) Inherited disorders of folate and cobalamin transport and metabolism. In: Scriver CR, Beaudet AL, Sly WS, Valle D (eds) The Metabolic and Molecular Bases of Inherited Disease, 8th edn. McGraw-Hill, New York, NY, pp 3897–3933
11. Fenton WA, Gravel RA, Rosenblatt DS (2001) Disorders of propionate and methylmalonic acid metabolism. In: Scriver CR, Beaudet AL, Sly WS, Valle D (eds) The Metabolic and Molecular Bases of Inherited Disease, 8th edn. McGraw-Hill, New York, NY, pp 2165–2193
12. Sass JO, Nakanishi T, Sato T, Shimizu A (2004) New approaches towards laboratory diagnosis of isolated sulphite oxidase deficiency. Ann Clin Biochem 41:157–159
13. Stabler SP, Marcell PD, Podell ER, Allen RH, Savage DG, Lindenbaum J (1988) Elevation of total homocysteine in the serum of patients with cobalamin or folate deficiency detected by capillary gas chromatography-mass spectrometry. J Clin Invest 81:466–474
14. Selhub J, Jacques PF, Wilson PW, Rush D, Rosenberg IH (1993) Vitamin status and intake as primary determinants of homocysteinemia in an elderly population. JAMA 270:2693–2698

15. Löhrer FMT, Angst CP, Brunner FP, Haefeli WE, Fowler B (1998) Evidence for disturbed S-adenosylmethionine:AdoHcy ratio in patients with end-stage renal failure: a cause for disturbed methylation reactions? Nephrol Dial Transplant 13:656–661
16. Homocysteine Studies Collaboration (2002) Homocysteine and risk of ischemic heart disease and stroke: a meta-analysis. JAMA 288:2015–2022
17. Refsum H, Smith AD, Ueland PM, Nexo E, Clarke R, McPartlin J, Johnston C, Engbaek F, Schneede J, McPartlin C, Scott JM (2004) Facts and recommendations about total homocysteine determinations: an expert opinion. Clin Chem 50:3–32
18. Loehrer FMT, Angst CP, Haefeli WE, Jordan PP, Ritz R, Fowler B (1996) Low whole-blood S-adenosylmethionine and correlation between 5-methyltetrahydrofolate and homocysteine in coronary artery disease. Arter Thromb Vasc Biol 16:727–733
19. Capdevila A, Wagner C (1998) Measurement of plasma S-adenosylmethionine and A-adenosylhomocysteine as their fluorescent isoindoles. Analyt Biochem 264:180–184
20. Loehrer FMT, Haefeli WE, Angst CP, Browne G, Frick G, Fowler B (1996) Effect of methionine loading on 5-methyltetrahydrofolate, S-adenosylmethionine and S-adenosylhomocysteine in plasma of healthy humans. Clin Sci 981:79–86
21. Loehrer FMT, Schwab R, Angst CP, Haefeli WE, Fowler B (1997) Influence of oral S-adenosylmethionine on plasma 5-methyltetrahydrofolate, S-adenosylhomocysteine, homocysteine and methionine in healthy humans. J Pharmacol Exp Therapeut 282:845–850
22. Castro R, Rivera I, Struys EA, Jansen EE, Ravasco P, Camilo ME, Blom HJ, Jakobs C, Tavares de Almeida I (2003) Increased homocysteine and S-adenosylhomocysteine concentrations and DNA hypomethylation in vascular disease. Clin Chem 49:1292–1296
23. Gellekink H, van Oppenraaij-Emmerzaal D, van Rooij A, Struys EA, den Heijer M, Blom HJ (2005) Stable-isotope dilution liquid chromatography-electrospray injection tandem mass spectrometry method for fast, selective measurement of S-adenosylmethionine and S-adenosylhomocysteine in plasma. Clin Chem 51:1487–1492
24. Araki A, Sako Y (1987) Determination of free and total homocysteine in human plasma by high-performance liquid chromatography with fluorescence detection. J Chromatogr 422:43–52
25. Ubbink JB, Hayward Vermaak WJ, Bissbort S (1991) Rapid high-performance liquid chromatographic assay for total homocysteine levels in human serum. J Chromatogr 565:441–446
26. Ueland PM, Refsum H, Stabler SP, Malinow MR, Andersson A, Allen RH (1993) Total homocysteine in plasma or serum: methods and clinical applications. Clin Chem 39:1764–79
27. Vilaseca MA, Moyano D, Ferrer I, Artuch R (1997) Total homocysteine in pediatric patients. Clin Chem 43:690–692
28. Wagner J, Hirth Y, Claverie N, Danzin C (1986) A sensitive high-performance liquid chromatographic procedure with fluorimetric detection for the analysis of decarboxylated S-adenosylmethionine and analogues in urine samples. Anal. Biochem 154:604–617

2.3 GABA, Homocarnosine, and β-Alanine

Erwin E.W. Jansen, Cornelis Jakobs,
K. Michael Gibson

2.3.1 Introduction

γ-Aminobutyric acid (4-aminobutyric acid, GABA), β-alanine (2-aminopropanoic acid), and homocarnosine (γ-aminobutyryl-L-histidine) represent bioactive amines with diverse roles in intermediary metabolism and central neurotransmission. In adults, GABA is the primary central inhibitory neurotransmitter derived from excitatory glutamate in a reaction that is catalyzed by glutamic acid decarboxylase. Its neuronal disposal is mediated by GABA transaminase (GABA-T) and succinate semialdehyde dehydrogenase (SSADH) [8]. In the transamination step, 2-oxoglutarate serves as a nitrogen acceptor to generate glutamate, thus forming what is historically referred to as the "GABA shunt" pathway. Perhaps one-third of mammalian synapses employ GABA as neurotransmitter, but it also has a pronounced role in nonneural tissues [22]. In the developing central nervous system (CNS), GABA acts trophically in an excitatory fashion, with important roles in synapse formation, dendritic outgrowth and maturation, and synaptic developmental roles [18].

β-alanine is derived from uracil and the decarboxylation of aspartic acid, and is a precursor of acetyl-CoA [7]. It may also be found as the β-alanyl-L-histidine conjugate carnosine (an antiglycation agent), in analogy to the GABA-histidine conjugate homocarnosine (see below) [16]. A preponderance of data (presynaptic localization, calcium-dependent release and/or transmitter-induced release, and postsynaptic receptors) suggest that β-alanine is also a neurotransmitter in mammals, but it is present in much lower concentrations in the brain than is GABA [7]. Recent evidence indicates that quantities of β-alanine are modulated by the stress response, with a resultant downstream effect on excitotoxic and antiapoptotic responses [16].

Homocarnosine is a brain-specific dipeptide that is synthesized by carnosine synthetase in glial cells and hydrolyzed by carnosinase. In some brain regions, concentrations exceed 1 mM, and there is evidence that specific neuronal tracts employ homocarnosine as a storage form of GABA [7]. The specific function of homocarnosine in brain has been widely explored, and the predominance of data suggest a role as an osmoregulator [23]. However, other studies have suggested that homocarnosine is neuroprotective (e.g., similar to β-alanine), especially with respect to ischemic damage, antioxidant damage, and protection from carbonyl toxicity [9]. The mechanism(s) by which these functions occur remain largely undefined.

2.3.2 Analyte Properties and Formulae

The analytes quantified in this chapter (Fig. 2.3.1) are bifunctional, with both amine and carboxyl moieties, which lend themselves to derivatization with several compounds. The physiological fluid of choice for determination is cerebrospinal fluid (CSF) although all species can be quantified in plasma, sera, urine, and even tissue extracts when necessary [9]. It is still unclear as to whether GABA and β-alanine share the same transaminase and nitrogen acceptor (2-oxoglutarate, pyruvate, etc), or if there are different enzymes with distinct specificities [7]. However, arguing in favor of only a single transaminase is the observation that body fluids from a documented patient with GABA-T deficiency had significantly increased β-alanine in addition to GABA [10].

GABA is significantly increased in both GABA-T and SSADH deficiencies; thus, quantitation in CSF has diagnostic importance [8, 11]. GABA levels in CSF derived from SSADH-deficient individuals may also have therapeutic ramifications in gauging the biochemical response to treatment [6]. Quantitation of β-alanine in CSF has diagnostic value for detecting GABA-T deficiency, but this disorder is rare. Isolated homocarnosinemia/homocarnosinosis has been detected in two families, a rare disorder linked to serum carnosinase deficiency [7, 14]. Homocarnosine is also increased in CSF derived from SSADH-deficient individuals (see below).

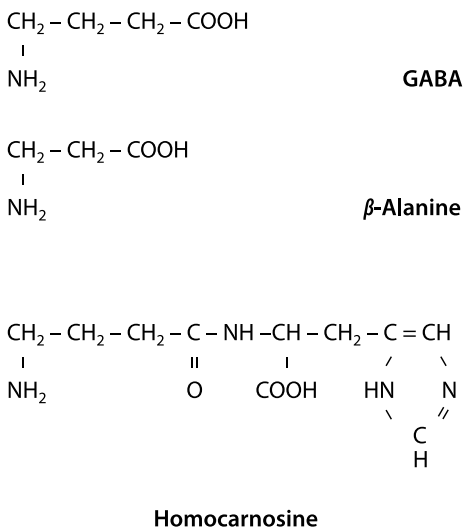

Fig. 2.3.1 Structures of the metabolites γ-aminobutyric acid (*GABA*), β-alanine, and homocarnosine

2.3.3 Methods

2.3.3.1 Quantification of GABA and β-alanine in CSF

Principle

GABA and β-alanine occur in CSF in their free and peptide-linked forms. Hydrolysis of peptide-linked forms of GABA- and β-alanine-conjugates yield the free amino acids. To isolate the amino acids from CSF and achieve good separation on gas chromatography (GC), the amino groups are derivatized with methylchloroformate under basic conditions. Methylchloroformate derivatives are extracted into ethylacetate after acidifying the sample to a pH below 2. Following evaporation, carboxyl moieties (Fig. 2.3.2) are derivatized with pentafluorobenzylbromide (PFB-Br). The resulting

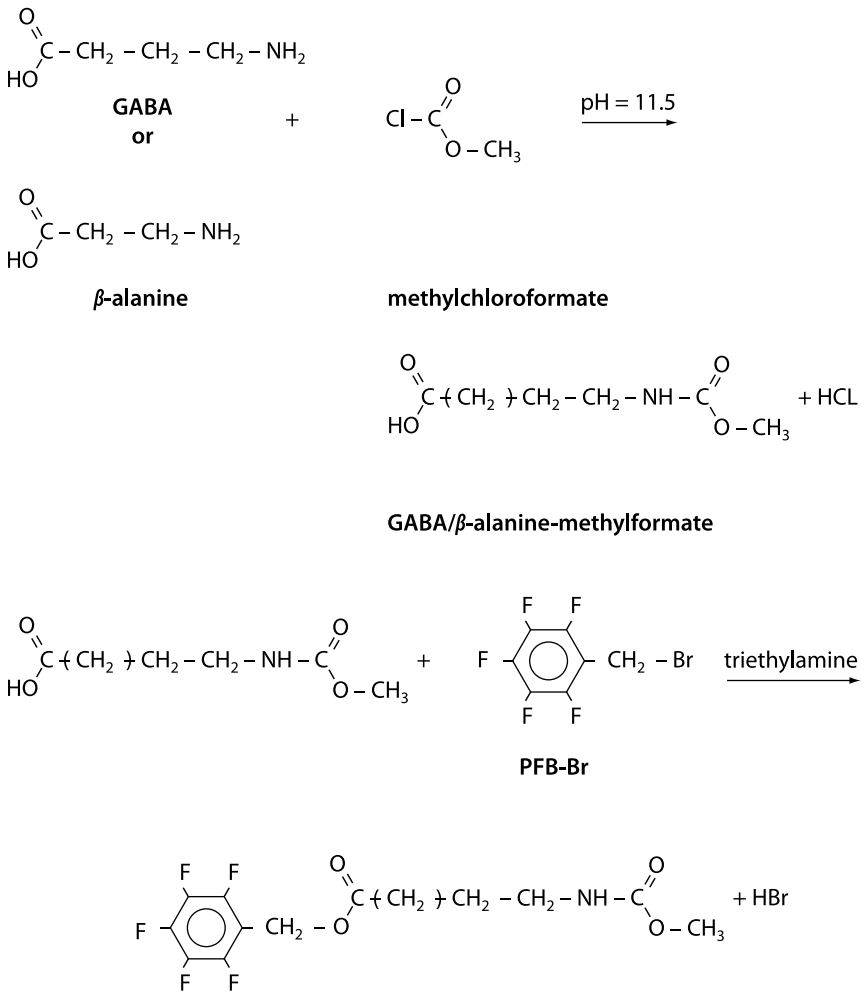

Fig. 2.3.2 Formation of GABA/β-alanine-methylformate and GABA/β-alanine-methylformate-pentafluorobenzyl derivative

methylformate-pentafluorobenzyl derivatives of GABA and β-alanine are quantified using GC electron-capture negative-ion mass fragmentography. Utilizing single ion monitoring (SIM), the response of the unlabeled components at m/z 160 (160.06) for GABA and m/z 146 (146.05) for β-alanine and the labeled internal standards at 162 (162.07) for $^{2}H_2$-GABA and 149 (149.06) for $^{13}C_3$-β-alanine are quantified.

Pre-analytical

Specimen

Lumbar CSF (1–2 ml) is collected and immediately stored at –20°C. Since there is a rostrocaudal gradient for CSF, the first 2 ml that emerges from the spinal tap is not suitable for quantification of GABA and β-alanine. Otherwise, false negative values can occur.

Reagents and Chemicals

1. 1 M phosphate buffer pH = 11.5:
   a. Solution A: 17.8 g $Na_2HPO_4 \cdot 2H_2O$ dissolved in 100 ml demineralized water (1 mol/l).
   b. Solution B: 10.6 g Na_2CO_3 dissolved in 100 ml demineralized water (1 mol/l).
   Mix solutions A and B and adjust the pH to 11.5 with 4 M NaOH; store at 4°C.
2. Methylchloroformate.
3. 6 M HCl.
4. 12 M NaOH.
5. Ethylacetate, p.a. (analytical purity).
6. Triethylamine.
7. Pentafluorobenzylbromide in acetonitrile (7% v/v).
8. 0.05 M HCl.
9. Hexane, p.a.
10. Standard mixture GABA/β-alanine 0.01 mmol/l:
    a. GABA (99%; MW = 103.1): weigh 4-aminobutyric acid and make a dilution of 0.1 mmol/l in demineralized water.
    b. β-alanine (99%,;MW = 89.09): weigh β-alanine and make a dilution of 0.1 mmol/l in demineralized water.
    Mix 1 ml of 0.1 mmol/l GABA and 1 ml of 0.1 mmol/l β-alanine and adjust the volume to 10 ml with demineralized water.
11. Fill Eppendorf tubes with 400 µl of the 0.01 mmol/l standard mixture and store at –20°C.
12. Internal standard (IS) mixture $^{2}H_2$-GABA/$^{13}C_3$-β-alanine 0.001 mmol/l:
    a. $^{2}H_2$-4-aminobutyric acid ($^{2}H_2$-GABA; 98%, MW = 105.1): weigh $^{2}H_2$-4-aminobutyric acid and make a dilution of 0.2 mmol/l in demineralized water.
    b. 62 mmol/l $^{13}C_3$-β-alanine (MW = 92.1): dilute 62 mmol/l $^{13}C_3$-β-alanine in demineralized water, resulting in a solution of 0.3 mmol/l.
    Mix 100 µl of 0.2 mmol/l $^{2}H_2$-GABA and 67 µl of 0.3 mmol/l $^{13}C_3$-β-alanine and adjust the volume to 20 ml with demineralized water.

Instrumentation

1. Gas-chromatograph mass spectrometer operating in the negative chemical ionization mode.
2. GC-column: CP-Sil-88-coated WCOT fused silica 25 m × 0.25 mm inner diameter (i.d.) column (df = 0.2; Varian/Chrompack).

Calibration

A calibration curve is established and quantified for each batch of samples. The calibration curve for free GABA/*β*-alanine: 0 nmol, 0.02 nmol, 0.05 nmol, 0.1 nmol, and 0.2 nmol. The calibration curve for total GABA/*β*-alanine: 0 nmol, 0.1 nmol, 0.2 nmol, 0.5 nmol, and 1.0 nmol. The curves are plotted and results are calculated. The calibration curve is linear up to 1.0 nmol. Linearity beyond these concentrations has not been established.

Quality Control

A CSF pool is analyzed for internal control in every batch of samples.

Analytical

Procedure

The procedure is fully described by Kok et al. [13]. Bring the 1 M phosphate buffer pH 11.5 to room temperature and redissolve the crystals. Add to every tube 0.2 nmol $^{2}H_{2}$-GABA and $^{13}C_{3}$-*β*-alanine (200 µl of 0.001 mmol/l IS mixture). Make a 0.001-mmol/l solution of the GABA/*β*-alanine standard mixture by mixing 100 µl of the 0.01 mmol/l standard mixture and 900 µl demineralized water. Make calibration curves with the amounts of GABA/*β*-alanine listed in Table 2.3.1.

The samples and the CSF pool (quality control) are thawed and placed on ice water. Apply a CSF pool at the beginning of a batch as well as at the end of a batch of samples. Add 1 ml of sample for free GABA/*β*-alanine and, if necessary, add demineralized water to obtain a final volume of 1 ml. Add 50 µl of sample for the determination of total GABA/*β*-alanine and add demineralized water to obtain a total volume of 400 µl.

Free GABA/*β*-Alanine Samples

1. Directly add 800 µl of 1 M phosphate buffer pH 11.5 and 50 µl methylchloroformate. Gently shake the mixture for 10 min.
2. Add 150 µl of 6 M HCl and extract the samples with 4 ml of ethylacetate for at least 1 min. Centrifuge for 2 min at 3300 × *g*.
3. Pipette the organic layer (upper layer) into a new tube.

Total GABA/*β*-Alanine Samples

1. Acidify the samples by adding 400 µl of 6 M HCl.
2. Hydrolyze at 110°C for 4 h (longer heating leads to conversion of $^{2}H_{2}$-GABA into GABA).
3. After cooling, neutralize the samples by adding 200 µl of 12 M NaOH.
4. Add 800 µl of 1 M phosphate buffer pH 11.5 and 50 µl methylchoroformate. Check the pH at random after adding the phosphate buffer. The pH must have a value of > 10. Add more 12 M NaOH if necessary. Gently shake the mixtures for 10 min.

■ ***Table 2.3.1*** *Calibration curve for free γ-aminobutyric acid (GABA)/β-alanine and total GABA/β-alanine*

Free GABA/β-alanine			
Amount	Volume	Standard solution	Demi. water
blank	–	–	1000 µl
0.02 nmol	20 µl	0.001 mmol/l	980 µl
0.05 nmol	50 µl	0.001 mmol/l	950 µl
0.1 nmol	100 µl	0.001 mmol/l	900 µl
0.2 nmol	200 µl	0.001 mmol/l	800 µl
Total GABA/β-alanine			
Amount	Volume	Standard solution	Demi. water
blank	–	–	400 µl
0.1 nmol	100 µl	0.001 mmol/l	300 µl
0.2 nmol	200 µl	0.001 mmol/l	200 µl
0.5 nmol	50 µl	0.01 mmol/l	350 µl
1.0 nmol	100 µl	0.01 mmol/l	300 µl

Abbreviation: demi, demineralized

5. Add 150 µl of 6 M HCl and check the pH randomly.
6. Extract with 4 ml ethylacetate for at least 1 min. Centrifuge at 3300 × *g* for 2 min.
7. Pipette the organic layer into a new tube.

Evaporate the organic layers of the "free" and "total" samples to dryness at 40°C under a gentle stream of nitrogen. Add 10 µl triethylamine and 100 µl of 7% pentafluorobenzylbromide in acetonitrile and derivatize at room temperature for 15 min. Add 150 µl of 0.5 M HCl and extract with 1 ml hexane for at least 1 min. Centrifuge the samples for 2 min at 835 × *g*. Pipette the hexane into a sample vial and evaporate to dryness at 40°C. Add 50 µl hexane and redissolve the residue. Samples are ready for quantification with GC-mass spectrometry (GC-MS).

■ GC-MS Methodology

Under negative chemical ionization conditions, methane or ammonia is used as a moderating gas. A 1- to 2-µl aliquot of sample is injected onto the GC-MS and separation of GABA and β-alanine from other compounds is achieved by employing a CP-Sil 88-coated WCOT fused silica 25 m × 0.25 mm i.d. column (df = 0.2; Varian/Chrompack). The injection temperature of the GC-MS is 220–240°C and the temperature program of the GC is as follows: start temperature 60–80°C, rate of increase in temperature 5–30°C/min to a final temperature of 240°C. The temperature program of the GC should be changed if GABA and β-alanine are not separated well from coeluting components. The temperature of the source is 150–250°C and the temperature of the interface is set to 240°C.

Calculation

The concentration of the CSF analyte is calculated by interpolation of the observed analyte:IS peak-area ratio into the linear regression line for the calibration curve, which is obtained by plotting the peak-area ratios against analyte concentration.

Post-analytical

Interpretation

Calculated concentrations of GABA and β-alanine are compared with the reference values. Increased quantities of GABA, β-alanine, and/or homocarnosine may suggest a defect in the catabolic pathway of GABA (e.g., GABA-T and/or SSADH deficiencies). Elevated levels of β-alanine may also suggest the rare disorder hyper-β-alaninemia, which may be a specific transamination disorder (GABA-T?) or a transport disorder, but this is very rare [7]. Hyper-β-alaninemia is also variably associated with Cohen syndrome [17]. SSADH deficiency may be treated by inhibition of GABA-T with γ-vinyl-GABA (vigabatrin; Sabril), which may lead to artifactual increases in free and total GABA in the CSF.

- Chromatograms

See Fig. 2.3.3.

- Reference Values

Reference values of GABA and β-alanine are age-dependent (see Table 2.3.2).

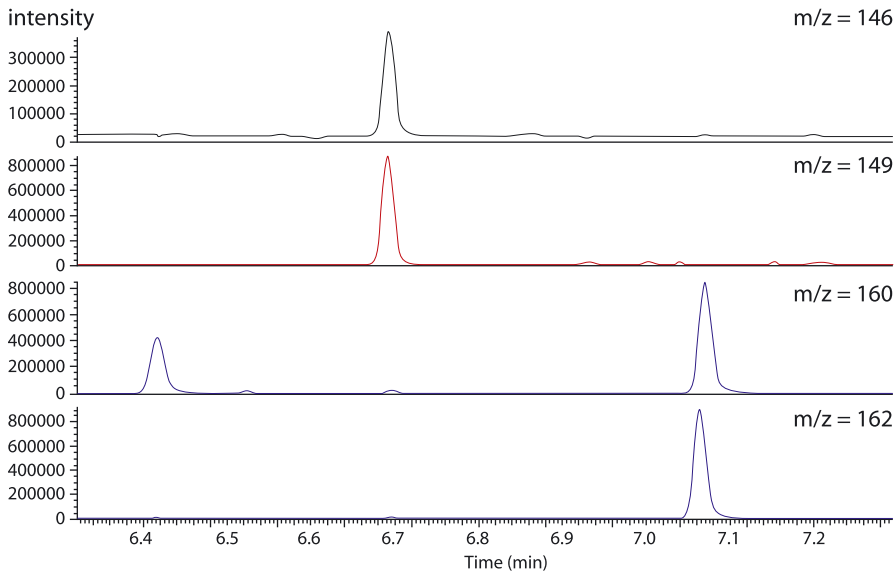

Fig. 2.3.3 Chromatogram of a pooled cerebrospinal fluid (CSF) sample (free β-alanine and free GABA). Trace m/z = 146 represents unlabeled β-alanine (retention time 6.7 min); trace m/z = 149 for $^{13}C_3$-β-alanine (retention time 6.7 min); trace m/z = 160 for unlabeled GABA (retention time 7.07 min); trace m/z = 162 for $^{2}H_2$-GABA (retention time 7.06 min)

■ ***Table 2.3.2*** *Reference values of GABA and β-alanine according to age*

GABA	Free	< 2 years	0.017–0.067 µmol/l
		≥ 2 years	0.032–0.167 µmol/l
	Total	< 2 years	4.2–13.4 µmol/l
		≥ 2 years	3.3–12.2 µmol/l
β-Alanine	Free	< 2 years	0.049–0.108 µmol/l
		≥ 2 years	0.021–0.058 µmol/l
	Total	< 2 years	2.08–4.64 µmol/l
		≥ 2 years	0.91–3.47 µmol/l

■ Pitfalls

Following collection of CSF, and during storage and thawing of the sample, bound GABA may be converted into free GABA yielding false positive values. Freezing of the sample immediately after collection, and thawing just prior to extraction, is necessary for reliable values of free GABA. Heating $^{2}H_2$-GABA in the presence of HCl can cause exchange between ^{2}H and ^{1}H, resulting in ^{1}H-GABA and unlabeled GABA. This results in artifactually high blanks. Thus, do not heat for longer than necessary during the hydrolysis step.

2.3.3.2 Quantification of Homocarnosine in CSF

Principle

Homocarnosine is a dipeptide of GABA and L-histidine. After deproteinizing the sample with ethanol, the mixtures are centrifuged. The clear supernatant is evaporated to dryness and derivatized with butanol. The sample is evaporated to dryness and redissolved in the mobile phase. The homocarnosine-butyl derivatives (Fig. 2.3.4) are quantified using liquid chromatography mass spectrometry/mass spectrometry (LC-MS/MS) operating in the positive mode. With multiple reaction monitoring (MRM), the transitions of m/z 297.0 to m/z 212.0 for homocarnosine and m/z 299.0 to m/z 212.0 for $^{2}H_2$-L-homocarnosine are quantified.

Pre-analytical

Specimen

Lumbar CSF (0.5 ml) is collected and subsequently stored at –20°C.

Reagents and Chemicals

1. Ethanol (minimum 99%).
2. Methanol (HPLC grade).
3. Ammonium acetate.

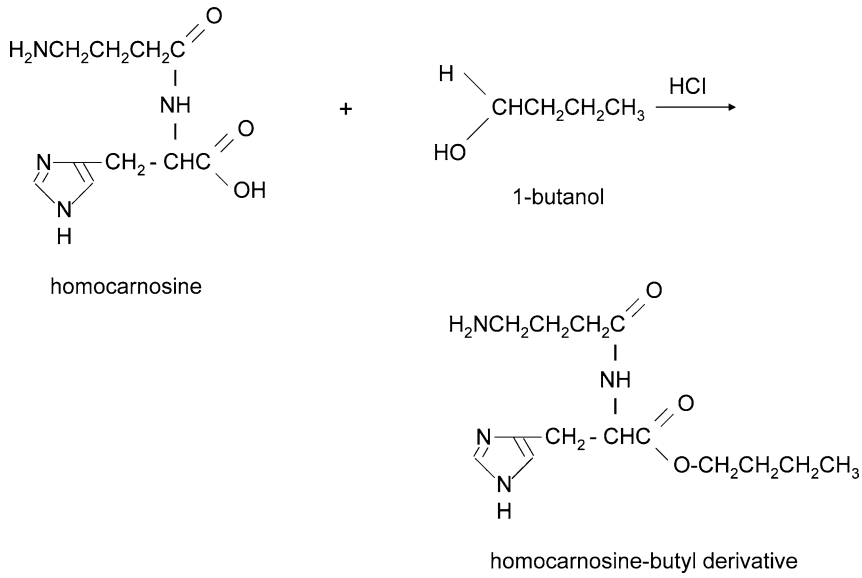

Fig. 2.3.4 Formation of the homocarnosine-butyl derivative from homocarnosine and 1-butanol

4. 10% 6 M HCl in butanol solution.
5. *γ*-Aminobutyryl-L-histidine (L-homocarnosine; MW = 240.3).
6. $^{2}H_{2}$-L-Homocarnosine (93%; MW = 242.3).

Instrumentation

1. Cooled centrifuge.
2. HPLC system with triple quadrupole tandem mass spectrometer.
3. Symmetry C_{18} analytical column (3.9 × 150 mm; 5 μm bead size, Waters)

Calibration

A calibration curve with aqueous calibrators containing 0, 0.1, 0.5, 1.0, and 5.0 nmol homocarnosine are measured. The curve is plotted and results determined. The calibration curve is linear to at least 5.0 nmol.

Quality Control

A CSF pool is measured for internal control in every batch of samples.

Analytical

Procedure

The procedure is well described by Jansen et al. [12]. Prepare a calibration curve by adding the amounts of homocarnosine listed in Table 2.3.3. Add to 100 μl CSF, 10 μl of 0.1 mM $^{2}H_{2}$-L-homocarnosine in water. Deproteinize the samples by adding 300 μl ethanol (99%). Mix the mixtures thoroughly and centrifuge at 20,000 × *g* for

■ ***Table 2.3.3*** *Calibration curve for homocarnosine*

Amount	Volume of standard solution	Concentration of standard solution
Blank	–	
0.1 nmol	10 µl	0.01 mmol/l
0.5 nmol	50 µl	0.01 mmol/l
1.0 nmol	100 µl	0.01 mmol/l
5.0 nmol	50 µl	0.10 mmol/l

5 min at 4°C. Transfer the clear supernatant to a vial and evaporate to dryness under a gentle steam of nitrogen at 40°C. Add 100 µl of 10% 6 M HCl in butanol solution and derivatize the samples at 60°C for 15 min. After cooling, evaporate the samples to dryness at 40°C under a stream of nitrogen. Redissolve the residues in 100 µl mobile phase consisting of H_2O-methanol (50:50, by volume) containing 25 mM ammonium acetate. Transfer the solutions to new tubes and centrifuge for 5 minutes at 10,000 × *g* at 4°C. Approximately 1–10 µl of the clear supernatant is injected onto the LC-MS/MS system.

■ LC-MS/MS Methodology

Separation of homocarnosine is achieved employing a Symmetry C_{18} analytical column (3.9 × 150 mm; 5-µm bead size; Waters) using H_2O-methanol (50:50, by volume) containing 25 mM ammonium acetate as the mobile phase. The flow rate is set to 0.9 ml/min and is split into a ratio of 1:4, producing an inlet flow of 180 µl/min into the mass spectrometer. Detection of the homocarnosine-butyl derivatives is performed on a triple quadrupole tandem mass spectrometer with the turbo ion electrospray source operating in the positive mode. The temperature of the source is set to 400°C; turbo ion gas (nitrogen) is used at a flow rate of 8 l/min and the ion spray voltage is set at 4,200 V; the declustering potential is set at 30 V and the collision energy is 20 V. Data is acquired and processed using Analyst for Windows NT (version 1.3.1). For the MRM, the following transitions are performed: m/z 297.0 to m/z 212.0 for homocarnosine and m/z 299.0 to m/z 212.0 for $^2H_2$-L-homocarnosine.

Calculation

The CSF homocarnosine concentration is calculated by interpolating the observed analyte:IS peak-area ratio into the linear regression line for the calibration curve, which is obtained by plotting the peak-area ratios against analyte concentration.

Post-analytical

Interpretation

Calculated homocarnosine concentrations are compared with the reference values. Large quantities of GABA and GABA conjugates, including homocarnosine, are

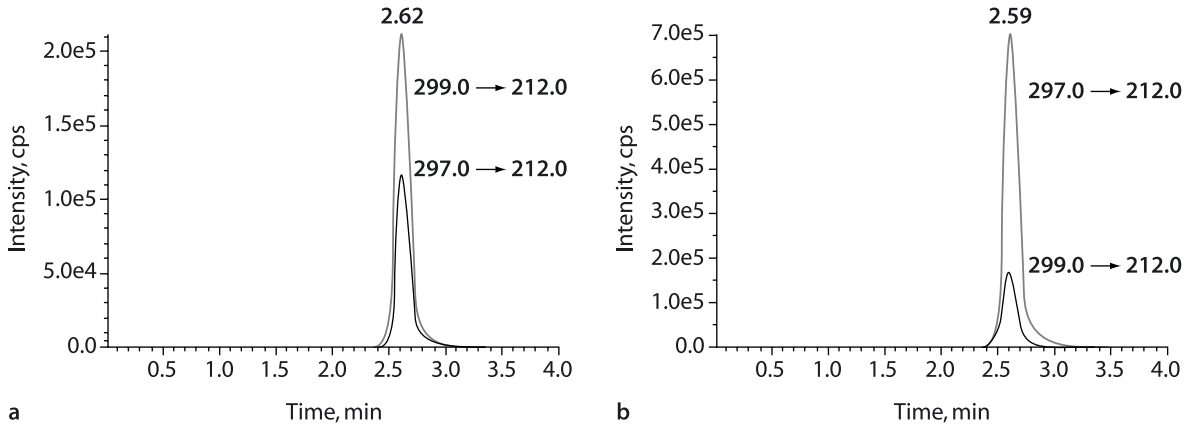

Fig. 2.3.5 Chromatograms of a pooled CSF sample (**a**) and from a succinate-semialdehyde-dehydrogenase-deficient patient aged 4 years (**b**). Transition m/z 297.0 → m/z 212.0 for homocarnosine; transition m/z 299.0 → m/z 212.0 for $^{2}H_{2}$-L-homocarnosine

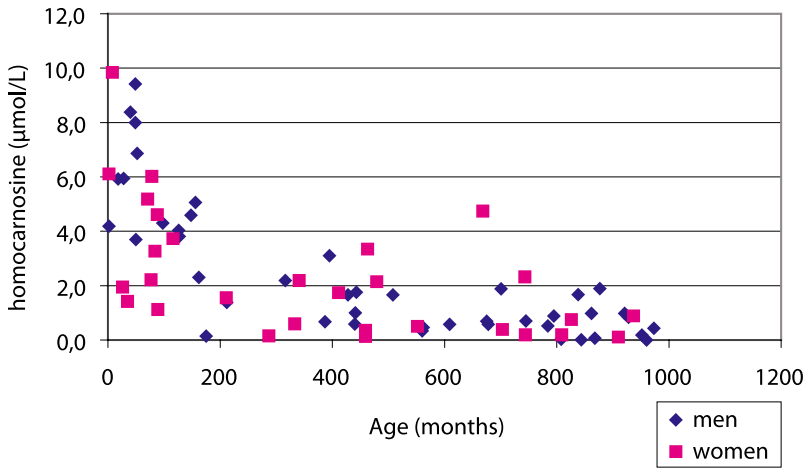

Fig. 2.3.6 Reference values for homocarnosine: at < 10 years = 1.12–9.84 µmol/l ($n = 21$); at > 10 years = < 0.02–5.06 µmol/l ($n = 52$)

found in CSF derived from patients with GABA-T and SSADH deficiencies. CSF homocarnosine can also be elevated in patients with homocarnosinosis.

Chromatograms

See Fig. 2.3.5.

Reference Values

No significant gender difference is observed in CSF homocarnosine concentrations. Homocarnosine concentration is highly age-dependent. A comparison between two control groups should be made, individuals < 10 years and individuals > 10 years of age (Fig. 2.3.6).

■ Pitfalls

The same pitfalls for homocarnosine determination may be applied as for the case of total GABA. Avoid excessive freeze-thaw cycles for CSF; thaw only prior to aliquoting for measurement, and freeze CSF immediately upon isolation.

2.3.3.3 Alternative Methodology: the Amino Acid Analyzer

GABA, β-alanine, and homocarnosine may be quantified with the amino acid analyzer [21]. Sensitivity is much lower (μmol/l vs nmol/l for the methods described in this chapter). GABA and β-alanine are quantified directly. Conversely, homocarnosine is not easily quantified because of its size and hydrophobicity. Following acid hydrolysis, however, homocarnosine content may be estimated via measurement of free histidine and GABA [2].

2.3.3.4 Follow-Up Enzyme Assays

GABA-T and SSADH enzyme activities may be reliably quantified in leukocytes isolated from whole blood. In both disorders, GABA elevation is expected in CSF, while in GABA-T deficiency, β-alanine and homocarnosine are also elevated [10].

GABA-T has been previously quantified by employing a radiometric analysis and HPLC quantification [15]. In this system, ^{14}C-GABA is incubated with cell extract in the presence of α-ketoglutarate to conjugate NH_4^+ ion. Radiolabeled ^{14}C-succinate semialdehyde is converted to the methoxime derivative and quantified following HPLC separation by liquid scintillation spectrometry. More recently, Schor and colleagues [20] developed an elegant stable isotope dilution GC-MS assay for quantifying GABA-T activity. These investigators employed ^{15}N-GABA with cell extracts in the presence of α-ketoglutarate as an acceptor for ^{15}N. The resulting ^{15}N-glutamate was quantified by GC-MS employing $^{2}H_5$-glutamate as the IS. Of interest, in these studies Schor and coworkers provided evidence that β-alanine and GABA transaminases are identical. SSADH activity is readily measured by fluorometric enzyme analysis, using unlabeled succinate semialdehyde as the substrate and NAD^+ as a cofactor. Production of NADH in the reaction is quantified fluorometrically using the NAD^+/NADH couple at excitation 355 nm/emission 470 nm [3]. Prenatal diagnosis of SSADH deficiency may also be reliably performed in chorionic villus and cultured chorion tissue, and mutation analysis is available in cDNA and genomic DNA samples [1, 5].

β-Alanine occupies a central role in intermediary metabolism, primarily as the metabolic breakdown product of pyrimidine (uracil, cytidine) metabolism [7]. Increases in β-alanine may also be detected in hyper-β-alaninemia, GABA-T deficiency (see above), and putative combined semialdehyde dehydrogenase deficiency [4]. Serum carnosinase activity is readily measured as a marker for carnosinosis, homocarnosinosis and in instances of β-alanine elevation in physiological fluids [7]. For quantification, carnosine is incubated with sera samples, and the histidine liberated in the reaction is quantified as the fluorescent *o*-phthalaldehyde derivative [19]. To estimate the activity of methylmalonate semialdehyde dehydrogenase (direct enzyme determination methods have not been reported), fibroblast extracts are incubated with 1-^{14}C-β-alanine and trapping of $^{14}CO_2$.

References

1. Akaboshi S, Hogema BM, Novelletto A, Malaspina P, Salomons GS, Maropoulos GD, Jakobs C, Grompe M, Gibson KM (2003) Mutational spectrum of the succinate semialdehyde dehydrogenase (ALDH5A1) gene and functional analysis of 27 novel disease-causing mutations in patients with SSADH deficiency. Hum Mutat 22:442–450
2. Ferraro TN, Hare TA (1985) Free and conjugated amino acids in human CSF: influence of age and sex. Brain Res 338:53–60
3. Gibson KM, Lee CF, Chambliss KL, Kamali V, Francois B, Jaeken J, Jakobs C (1991) 4-Hydroxybutyric aciduria: application of a fluorometric assay to the determination of succinic semialdehyde dehydrogenase activity in extracts of cultured human lymphoblasts. Clin Chim Acta 196: 219–222
4. Gibson KM, Lee CF, Bennett MJ, Holmes B, Nyhan WL (1993) Combined malonic, methylmalonic and ethylmalonic acid semialdehyde dehydrogenase deficiencies: an inborn error of beta-alanine, L-valine and L-alloisoleucine metabolism? J Inherit Metab Dis 16:563–567
5. Gibson KM, Baumann C, Ogier H, Rossier E, Vollmer B, Jakobs C (1994) Pre- and postnatal diagnosis of succinic semialdehyde dehydrogenase deficiency using enzyme and metabolite assays. J Inherit Metab Dis 17:732–737
6. Gibson KM, Jakobs C, Ogier H, Hagenfeldt L, Eeg-Olofsson KE, Eeg-Olofsson O, Aksu F, Weber H-P, Rossier E, Vollmer B, Lehnert W (1995) Vigabatrin therapy in six patients with succinic semialdehyde dehydrogenase deficiency. J Inherit Metab Dis 18:143–146
7. Gibson KM, Jakobs C (2001) Disorders of beta- and gamma-amino acids in free and peptide-linked forms. In: Scriver CR, Beaudet AL, Sly WS, Valle D (eds) The Metabolic and Molecular Bases of Inherited Disease, 8th edn. McGraw-Hill, New York, pp 2079–2105
8. Gibson KM, Jakobs C, Pearl PL, Snead OC (2005) Murine succinate semialdehyde dehydrogenase deficiency, a heritable disorder of GABA metabolism with epileptic phenotype. IUBMB Life 57:639–644
9. Gupta M, Polinsky M, Senephansiri H, Snead OC, Jansen EEW, Jakobs C, Gibson KM (2004) Seizure evolution and amino acid imbalances in murine succinate semialdehyde dehydrogenase (SSADH) deficiency. Neurobiol Dis 16:556–562
10. Jaeken J, Casaer P, de Cock P, Corbeel L, Eeckels R, Eggermont E, Schechter PJ, Brucher JM (1984) Gamma-aminobutyric acid-transaminase deficiency: a newly recognized inborn error of neurotransmitter metabolism. Neuropediatrics 15:165–169
11. Jakobs C, Jaeken J, Gibson KM (1993) Inherited disorders of GABA metabolism. J Inherit Metab Dis 16:704–715
12. Jansen EEW, Gibson KM, Shigematsu Y, Jakobs C, Verhoeven N (2006) A novel, quantitative assay for homocarnosine in cerebrospinal fluid using stable-isotope dilution liquid-chromatography mass spectrometry. J Chromatogr B Analyt Technol Biomed Life Sci 18:196–200
13. Kok RM, Howells DW, van den Heuvel CC, Guerand WS, Thompson GN, Jakobs C (1993) Stable isotope dilution analysis of GABA in CSF using solvent extraction and electron-capture negative-ion mass fragmentography. J Inherit Metab Dis 16:508–512
14. Kramarenko GG, Markova ED, Ivanova-Smolenskaya IA, Boldyrev AA (2001) Peculiarities of carnosine metabolism in a patient with pronounced homocarnosinemia. Bull Exp Biol Med 132:996–999
15. Medina-Kauwe LK, Tobin AJ, De Meirleir L, Jaeken J, Jakobs C, Nyhan WL, Gibson KM (1999) 4-Aminobutyrate aminotransferase (GABA-transaminase) deficiency. J Inherit Metab Dis 22:414–427
16. Mehta AD, Seidler NW (2005) Beta-alanine suppresses heat inactivation of lactate dehydrogenase. J Enzyme Inhib Med Chem 20:199–203
17. Okamoto N, Hatsukawa Y, Arai H, Goto M (1998) Cohen syndrome with high urinary excretion of hyaluronic acid. Am J Med Genet 76:387–388
18. Represa A, Ben-Ari Y (2005) Trophic actions of GABA on neuronal development. Trends Neurosci 28:278–283

19. Schoen P, Everts H, de Boer T, van Oeveren W (2003) Serum carnosinase activity in plasma and serum: validation of a method and values in cardiopulmonary bypass surgery. Clin Chem 49:1930–1932
20. Schor DS, Struys EA, Hogema BM, Gibson KM, Jakobs C (2001) Development of a stable-isotope dilution assay for gamma-aminobutyric acid (GABA) transaminase in isolated leukocytes and evidence that GABA and beta-alanine transaminases are identical. Clin Chem 47:525–531
21. Shih VE (2003) Amino acid analysis. In: Blau N, Duran M, Blaskovics ME, Gibson KM (eds) Physician's Guide to the Laboratory Diagnosis of Metabolic Diseases. Springer, Berlin, pp 11–26
22. Tanaka C, Taniyama K (1992) The role of GABA in peripheral nervous system. In: Erdo SL (Ed) GABA outside the CNS. Springer-Verlag, Berlin, pp 3–17
23. Vaughan-Jones RD, Spitzer KW, Swietach P (2005) Spatial aspects of intracellular pH regulation in heart muscle. Prog Biophys Mol Biol 90:207–224

2.4 Pipecolic Acid

Marinus Duran

2.4.1 Introduction

The essential amino acid lysine (2,5-diaminohexanoic acid) can be degraded via two pathways, viz. the so-called saccharopine pathway and the pipecolic acid (PA) pathway. Both pathways merge at the level of α-aminoadipic acid semialdehyde (AASA). It is generally accepted that the saccharopine pathway constitutes the major breakdown pathway. However, the PA pathway has attracted much attention since the discovery of the association between the presence of elevated PA levels and Zellweger syndrome almost 40 years ago. Mainly because the analysis of amino acids was the primary biochemical approach for studying presumed inborn errors of metabolism, PA in Zellweger syndrome was discovered even before it was realized that this disorder was based on a defect of peroxisomal functions.

The clinical importance of PA remained limited for a long time until it was realized that this imino acid was elevated in all patients with so-called pyridoxine-responsive convulsions. Following the discovery of a genetic defect of AASA dehydrogenase as the underlying cause of this disorder – leading to a secondary increase of PA – the analysis of this imino acid again became an important diagnostic tool.

Historically, PA was analyzed with the aid of the amino acid analyzer. The sensitivity of this method is insufficient for reliable determinations in plasma or cerebrospinal fluid (CSF); therefore, more specific and sensitive methods were developed.

2.4.2 Properties of the Analyte

PA (piperidine-2-carboxylic acid) is a nitrogen-containing heterocyclic compound with a molecular weight of 129.2. Its structure is shown in Fig. 2.4.1.

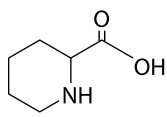

Fig. 2.4.1 Chemical structure of pipecolic acid

2.4.3 Specimens for Analysis

PA can be analyzed in urine, plasma, and CSF. The conditions for sampling are similar to those of the other amino acids (see Chap. 2.1). As PA is a stable compound, no special precautions for its preservation have to be taken.

2.4.4 Tandem Mass Spectrometry Assay

2.4.4.1 Introduction

The availability of stable isotope-labeled PA makes an accurate quantitative determination of this imino acid possible. A short high-performance liquid chromatography (HPLC) run prior to the mass spectrometer inlet will result in a discrete peak of PA. For the definitive diagnosis of AASA dehydrogenase deficiency, a simultaneous determination of AASA would be preferred. The absence of a commercially available labeled standard leaves this analysis in the experimental stage.

2.4.4.2 Principle of the Assay

Following the extractive deproteinization of the plasma, urine, or CSF, PA is derivatized with methyl chloroformate. The analyte is measured in the tandem mass spectrometer in the positive ion mode using multiple reaction monitoring (MRM; Fig. 2.4.2).

2.4.4.3 Sample

A minimum volume of 50 µl plasma/urine or 200 µl CSF is required.

2.4.4.4 Reagents and Chemicals

1. Acetonitrile (Merck M30).
2. Acetic acid (Merck 100063).
3. Disodiumhydrogenphosphate-dihydrate (Merck 106580).

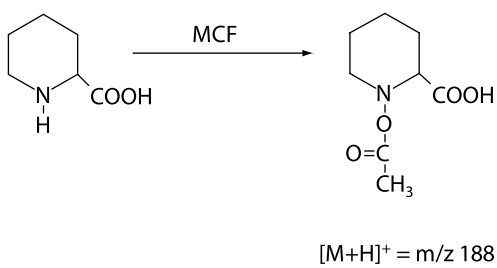

Fig. 2.4.2 Derivatization of pipecolic acid with methyl chloroformate (*MCF*)

4. Methyl chloroformate (Merck 802357).
5. Sodium hydroxide (Merck 106842).
6. Pipecolic acid (Sigma/Aldrich 80615).
7. $^{2}H_9$-Pipecolic acid (CDN Isotopes D5087).
8. HCl 37% (Merck 100317).
9. MilliQ water (Millipore).
10. Eluent A: 1% acetic acid in water, mix 1 part acetic acid with 99 parts of MilliQ.
11. Eluent B: acetonitrile.
12. Standards: PA 500 µmol/l (6.5 mg in 100 ml water).
13. Make dilutions in a range of 0.5–100 µmol/l.
14. Internal standard $2H_9$-PA 100 µmol/l (1.4 mg in 100 ml water).
15. 12 M NaOH: dissolve 4.8 g NaOH in 10 ml water.
16. 6M HCl: add slowly one part HCl 37% to one part water.
17. NA_2HPO_4 buffer pH 11.0: dissolve 7.0 g Na_2HPO_4 in 100 ml water and adjust the pH to 11.0 with 12 M NaOH.

2.4.4.5 Instrumentation

1. TSQ Quantum AM tandem mass spectrometer (Thermo Finnigan).
2. Surveyor autosampler (Thermo Finnigan).
3. Surveyor liquid chromatography pump (Thermo Finnigan).
4. Hydrosphere C18 column (250 × 2.1 mm, 3 µm particles; YMC).
5. DB-3 sample concentrator (Techne).

2.4.4.6 Procedure

Pipette plasma, urine (both 50 µl), or CSF (200 µl) into an Eppendorf tube. Add 50 µl internal standard. Add twice 250 µl acetonitrile while vortexing. Spin down the protein at 12,000 rpm (12,000 × *g*) in the refrigerated microcentrifuge for 10 min. Transfer the supernatant to an evaporation vial and blow nitrogen at 37°C until dry. The residue is taken up in 200 µl buffer and vortexed. Check the pH (11). Transfer to another Eppendorf vial, add 20 µl methyl chloroformate, react at ambient temperature for 5 min (check pH >6). Stop the reaction with 20 µl 6 M HCl (check pH=1). Centrifuge again at 12,000 rpm (12,000 × *g*) and 4°C for 10 min (two layers will form). The upper layer is transferred to an autosampler vial.

Ten microliters are injected onto the HPLC column. Elution is performed at a flow rate of 200 µl/min with a gradient of 70% A/30% B to 1%A/ 99% B in 10 min. The total analysis time is 12 min. PA is monitored at the transition 188 → 142, the internal standard $2H_9$-PA disintegrates from 197 → 151. The tandem mass spectrometer is in the positive ion mode; the collision energy is 20 eV (see Fig. 2.4.3).

2.4.4.7 Quality Control

Plasma, urine, and CSF pool samples, both native physiological and spiked pathological, are implemented in each series. The results of these analyses are displayed

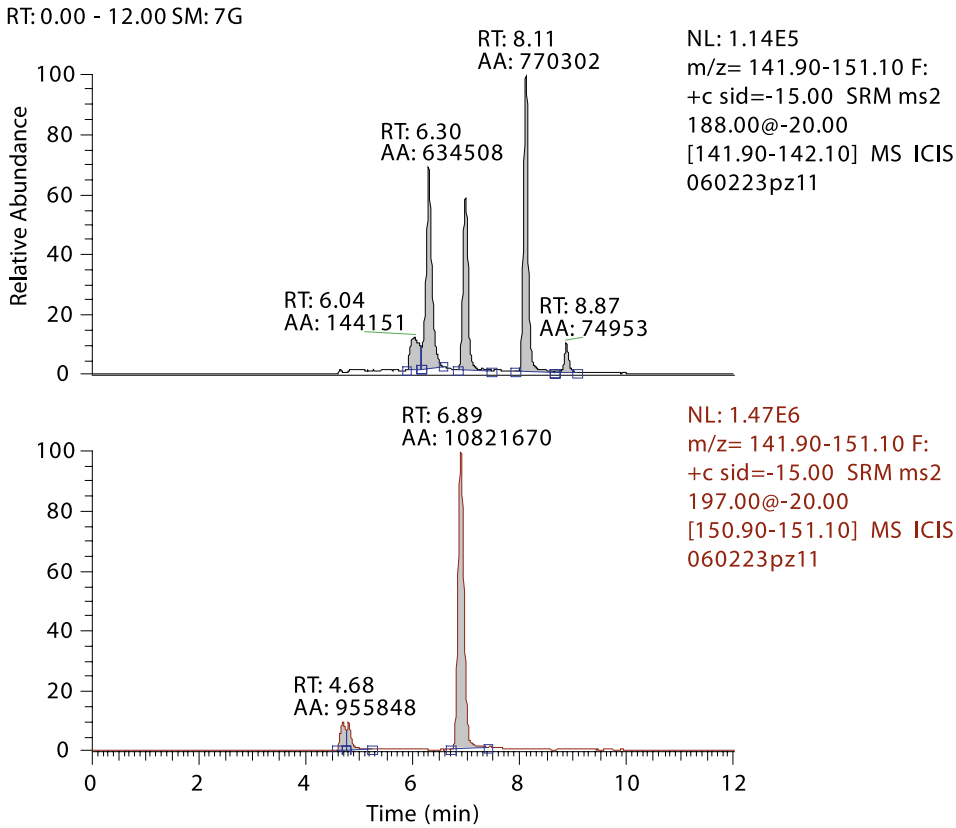

Fig. 2.4.3 Tandem mass spectrometry analysis of pipecolic acid in plasma and the internal standard $2H_9$-pipecolic acid. Both substances elute at approximately 6.9 min

in a Shewhart plot. External quality assurance is accomplished by participation in the quantitative European Research Network for evaluation and improvement of screening, Diagnosis and treatment of Inherited disorders of Metabolism (ERNDIM) schemes. Both special assays schemes for plasma and urine contain PA. Eight samples (four pairs at four concentration levels) are analyzed throughout the year.

Validation Data

All calculations were made on three concentration levels. The intra-assay coefficient of variation (CV) for plasma ranged from 3.8 to 7.6%, the latter at a level of 1.4 μmol/l. For urine, the CVs ranged from 4.4 to 18%, the latter at 0.7 μmol/l. CSF had CVs of 4.2–5.0%.

Inter-assay CVs range from 1.6 to 3.7% for plasma; the respective data for urine and CSF were 1.9–5.8% and 2.5–4.2%.

The recovery throughout the whole procedure was tested in standard addition experiments and averaged 92% for urine and plasma and 114% for CSF.

2.4.5 Gas Chromatography/Mass Spectrometry Assay

2.4.5.1 Introduction

In the absence of tandem mass spectrometry equipment, almost equally reliable estimations of the PA concentrations can be made using gas chromatography-mass spectrometry (GC-MS). A standard quadrupole instrument, such as the one used for organic acid analysis, will be sufficient. Depending on the derivative, a choice between positive and negative ionization will have to be made. In general, a more extensive prepurification of the biological samples, will have to be realized.

2.4.5.2 Principle of Assay

Urine, plasma, or CSF, to which a ^{2}H-labeled PA internal standard has been added, is deproteinized with sulfosalicylic acid (SSA). PA is subsequently isolated on a cation-exchange column, derivatized with N-methyl-N-(tert-butyldimethylsilyl) trifluoroacetamide (MTBSTFA) and analyzed by GC-MS using selected ion monitoring.

2.4.5.3 Sample

A 100-µl sample of urine or plasma, or alternatively 200 µl of CSF, is used for the assay.

2.4.5.4 Reagents and Chemicals

1. SSA (Merck M691).
2. AG50W-X8 cation-exchange resin 200–400 mesh (BioRad 142–1451).
3. Ammonia (Merck 5432).
4. HCl 37% (Merck 317).
5. Methanol (Merck 6007).
6. Acetonitrile (Merck 30).
7. MTBSTFA (Pierce 48920).
8. PA (Sigma P2519).
9. $^{2}H_{9}$-PA (CDN Isotopes D-5087).
10. MilliQ water (Millipore).
11. Standards: internal standard $^{2}H_{9}$-PA (100 µmol/l; 1.4 mg/100 ml water).
12. SSA 12% (12 g/100 ml water).
13. Ammonia 4 M: dilute the concentrated ammonia 3.3-fold.
14. HCl 0.1 M: dilute the concentrated HCl 76-fold.

2.4.5.5 Instrumentation

1. HP6890 Gas chromatograph (Agilent).
2. MSD5973 Mass selective detector (Agilent).

3. HP 7683 Autosamplet (Agilent).
4. HP Chemstation software (Agilent).
5. CPSil-5CB low-bleed capillary column (25 m×0.25 mm×0.25 µm; Chrompack).
6. All glassware standard laboratory equipment.

2.4.5.6 Procedure

Take 100 µl plasma or urine (or 200 µl CSF) and add 100 µl internal standard solution. While vortexing, add 400 µl of 12% SSA; subsequently add 1 ml of water and allow protein precipitation at 4°C for 30 min. Spin down at 1500×*g* for 10 min.

The ion-exchange columns (6 g resin for ten columns with 6 ml water) are conditioned by washing with 5 ml of 4 M NH_4OH and water until neutral, followed by 5 ml of 0.1 M HCl and water until neutral. The deproteinized supernatant is applied to the column and washed with 3 ml of 0.1 M HCl and 10 ml water. Elution of PA is achieved with 10 ml of 4 M NH_4OH. The solvent is evaporated on a rotary evaporator.

The residue is transferred to a reacti-vial with methanol, evaporated to dryness, and derivatized with 50 µl MTBSTFA in 50 µl acetonitrile under nitrogen at 110°C for 2 h.

Two microliters of the sample are injected by splitless injection (290°) and separated with a constant helium flow of 1.5 ml/min while programming the oven temperature from 80–290°C in approximately 10 min.

The mass spectrometer is set at m/z 198.2 (PA) and 207.2 ($^2H_9$-PA), both representing the [M-57] fragment of the derivatized molecule (loss of a tertiary butyl group).

A control plasma is analyzed in each series and serves as the internal quality control sample. Analysis of plasmas and urines of the ERNDIM special assays schemes (eight samples per year, four pairs at four concentration levels) serves as the external quality control program.

2.4.5.7 Validation Data

Plasma PA (mean value 9.3 µmol/l) was analyzed tenfold; the CV was 2.5%. Another plasma (PA level 25 µmol/l) was analyzed in ten different series; the interassay CV reached 7.6%.

2.4.6 Interpretation, Normal/Pathological Values, and Pitfalls

Increased PA may be encountered in several inherited conditions:
1. Generalized peroxisomal dysfunction (Zellweger syndrome and variants).
2. AASA dehydrogenase deficiency (pyridoxine-responsive convulsions).
3. Hyperlysinemia types 1 or 2.
4. Defects of proline metabolism.
5. Generalized aminoaciduria.

The presence of PA in patients with defective peroxisomal metabolism may be a diagnostic tool in distinguishing the peroxisome biogenesis defects from isolated enzyme

defects such as D-bifunctional protein deficiency. The latter condition has no PA involvement.

PA is secondarily increased in AASA dehydrogenase deficiency and may be an important diagnostic criterium. The primary accumulating AASA – the toxic substance inactivating pyridoxine – is still difficult to analyze.

The hyperlysinemias are characterized by a block in the saccharopine pathway. Subsequently, the PA pathway is overloaded. It is assumed that the capacity of the latter pathway is not sufficient to tackle all lysine molecules.

Because of the structural similarity between PA and proline, it can easily be understood that the two imino acids may share the same transport mechanism(s). Therefore it is not surprising to see increased PA in prolinemia type 2 patients.

Theoretically, patients with an isolated defect of PA oxidase will exist. No good description of this condition has appeared; there is one report on an adult with isolated hyperpipecolic acidemia. Unfortunately, no clinical symptoms appear to be associated with this condition.

Patients with severe hepatocellular dysfunction may have elevated PA levels. Thus far this is unexplained.

PA reference values for plasma, urine, and CSF are: 2.5±1.25 μmol/l, 0–6 mmol/mol creatinine, and <0.12 μmol/l, respectively. Pathological values may cover a very wide range; as an example, patients with the Zellweger syndrome may have plasma PA levels up to 170 μmol/l; the CSF of a AASA-dehydrogenase-deficient patient may show PA levels as high as 3 μmol/l.

References

1. Wanders RJA (1999) Peroxisomal disorders: clinical, biochemical and molecular aspects. Neurochem Res 24:565–580
2. Rashed MS, Al-Ahaidib LY, Aboul-Enein HY, Al-Amoudi M and Jacob M. (2001) Determination of L-pipecolic acid in plasma using chiral liquid chromatography-electrospray tandem mass spectrometry. Clin Chem 47:2124–2130
3. Kok RM, Kaster L, de Jong AP, Poll-The BT, Saudubray JM, Jakobs C (1987) Stable isotope dilution analysis of pipecolic acid in cerebrospinal fluid, plasma, urine and amniotic fluid using electron capture negative ion mass fragmentography. Clin Chim Acta 168:143–152
4. Mills PB, Struys E, Jakobs C, Plecko B, Baxter P, Baumgartner M, Willemsen MAAP, Omran H, Tacke U, Uhlenberg B, Weschke B, Clayton PT (2006) Mutations in antiquitin in individuals with pyridoxine-dependent seizures. Nat Med 12:307–309
5. Kerckaert I, Poll-The BT, Espeel M, Duran M, Roeleveld AB, Wanders RJA, Roels F (2000) Hepatic peroxisomes in isolated hyperpipecolic acidaemia: evidence supporting its classifications as a single peroxisomal enzyme deficiency. Virchows Arch 436:459–465

3.1 Organic Acids

Piero Rinaldo

This chapter is dedicated to the memory of Dr. Kay Tanaka (1929–2005)

3.1.1 Introduction

More than 40 years ago, Dr. Kay Tanaka began his journey to characterize the clinical, biochemical, and molecular basis of a distal disorder of leucine catabolism caused by a deficiency of the enzyme isovaleryl-coenzyme A (CoA) dehydrogenase [36]. He did so by first recognizing the diagnostic importance of organic acid profiling in urine, and by seeking one of the earliest applications of mass spectrometry to the study of an inborn error of metabolism. The impact of his seminal contributions was best illustrated by Chalmers and Lawson in their classic monograph of 26 years ago [9], in which a compelling figure (see page 3) showed the virtually linear expansion of the number of known disorders of organic acid metabolism for almost 20 years following the discovery of isovaleric acidemia. Dr. Tanaka passed away in the summer of 2005 [31], and this chapter is dedicated to his memory; a small tribute to one of the founding fathers and most distinguished scientists devoted to the study of inborn errors of metabolism.

Organic acidemias are a heterogeneous group of inborn errors of metabolism that are characterized biochemically by the accumulation of organic acids in urine and, to a lesser extent, in other body fluids. Some organic acids are essentially undetectable under physiological conditions, deriving from alternative pathways activated in response to the loss of a given enzyme function, for example 2-methylcitric acid in defects of propionate metabolism [9]. Several of the clinically significant organic acids are otherwise normal components of urine profiles that accumulate under pathologic conditions.

Table 3.1.1 shows a summary of known disorders of organic acid metabolism [32]. Available data on the rate of detection by clinical ascertainment and expanded newborn screening indicate a collective incidence of between 1:10,000 and 1:30,000 live births [16, 17, 36, 37]. These estimates are not inclusive of other inborn errors of metabolism (i.e., fatty acid oxidation disorders, primary lactic acidemias, primary amino acid disorders) in which there is also a significant accumulation and urinary excretion of specific organic acid species. Although not systematically addressed in this chapter, some of the figures herein use as examples findings related to fatty acid oxidation disorders such as medium-chain acyl-CoA dehydrogenase deficiency and long-chain L-3-hydroxy acyl-CoA dehydrogenase deficiency [32].

Table 3.1.1 *Disorders of organic acid metabolism (in alphabetical order). This table does not include disorders with primary accumulation of amino acids, disorders of mitochondrial fatty acid oxidation, or primary lactic acidemias.* CoA *Coenzyme A,* FAD *flavin adenine dinucleotide*

Disorder	Defective enzyme
2-Keto adipic aciduria	2-Keto adipic dehydrogenase
2-Keto glutaric aciduria	2-Keto glutaric dehydrogenase
2-Ketothiolase deficiency	2-Methylacetoacetyl-CoA thiolase
2-Methyl 3-hydroxy butyric aciduria	2-Methyl 3-hydroxy butyryl-CoA dehydrogenase
2-Methylbutyrylglycinuria	2-Methylbutyryl-CoA dehydrogenase
3-Hydroxy 3-methyl glutaric aciduria	3-Hydroxy 3-methyl glutaryl-CoA lyase
3-Methylcrotonylglycinuria	3-Methylcrotonyl-CoA carboxylase
3-Methylglutaconic aciduria	3-Methyl glutaconyl-CoA hydratase
4-Hydroxy butyric aciduria	Succinic semialdehyde dehydrogenase
Alkaptonuria	Homogentisic dioxygenase
Canavan disease	N-Aspartoacylase
D-2-Hydroxy glutaric aciduria	D-2-Hydroxyglutaric dehydrogenase
Ethylmalonic encephalopathy	Unknown (ETHE1 gene)
Fumaric aciduria	Fumarase
Glutaric aciduria type I	Glutaryl-CoA dehydrogenase
Glyceroluria (X-linked)	Glycerol kinase
Hawkinsinuria (autosomal dominant)	4-Hydroxy phenylpyruvic acid dioxygenase
Hyperoxaluria type I	Alanine:glyoxylate aminotransferase
Hyperoxaluria type II	D-Glyceric dehydrogenase
Isobutyrylglycinuria	Isobutyryl-CoA dehydrogenase
Isovaleric aciduria	Isovaleryl-CoA dehydrogenase
L-2-Hydroxy glutaric aciduria	L-2-Hydroxy dehydrogenase (Duranin)
Malonic aciduria	Malonyl-CoA decarboxylase
Methylmalonic acidurias	Methylmalonyl-CoA mutase, other defects
Mevalonic aciduria	Mevalonate kinase
Multiple carboxylase deficiency	Holocarboxylase synthase
Propionic aciduria	Propionyl-CoA carboxylase
Pyroglutamic aciduria	Glutathione synthase

3.1.2 Properties of Analytes

Organic acids are water-soluble compounds containing one or more carboxyl groups and other nonamino functional groups (Fig. 3.1.1). They originate from the intermediary metabolism of all major groups of organic cellular components. Primary precursors are amino acids, lipids, carbohydrates, nucleic acids, and steroids. Table 3.1.2 shows the basic nomenclature of common monocarboxylic and dicarboxylic acids with a chain length between C2 and C10. Familiarity with the basic information shown in Fig. 3.1.1 and Table 3.1.2 should be sufficient to visualize the chemical structure of the vast majority of organic acid species encountered in laboratory practice. Such knowledge is particularly helpful to individuals interested in developing interpretive skills based on identification of mass spectra and pattern recognition of organic acid profiles.

Also detected by organic acid analysis is a distinct group of compounds called acylglycines. The metabolites listed on Table 3.1.3 are formed by the conjugation of a diverse group of acyl-CoA species to glycine, a reaction catalyzed by the mitochondrial enzyme glycine N-acylase [5]. Although acylglycines are important biochemical markers of several metabolic disorders, they may not be readily recognized in a routine organic acid profile of trimethylsilyl derivatives because of low levels of excretion (often below 10 mmol/mol creatinine) and appearance of multiple peaks due to inconsistent derivatization of the amino group on the glycine molecule [29].

3.1.3 Methods

Because of their relatively low molecular weight, solubility, and other physical characteristics, most organic acids are readily excreted in urine, where their detection is

Table 3.1.2 *Nomenclature of most common C2–C10 organic acids*

Chain length	Monocarboxylic acid	Dicarboxylic acid
C2	Acetic acid	Oxalic acid
C3	Propionic acid	Malonic acid
C4	Butyric acid Isobutyric acid	Succinic acid
C5	Valeric acid Isovaleric acid 2-Methylbutyric acid	Glutaric acid
C6	Hexanoic (caproic) acid	Adipic acid
C7	Heptanoic (enanthic) acid	Pimelic acid
C8	Octanoic (caprylic) acid	Suberic acid
C9	Nonanoic (pelargonic) acid	Azelaic acid
C10	Decanoic (capric) acid	Sebacic acid

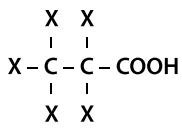

Functional Group	X
(hydrogen)	– H
(keto)	= O
(hydroxy)	– OH
(carboxyl)	– COOH
(side chain)	$-(CH_2)_n$

Side chain	Structure
Methyl	$CH_3 -$
Ethyl	$CH_3 - CH_2 -$
Propyl	$CH_3 - CH_2 - CH_2 -$
Butyl	$CH_3 - CH_2 - CH_2 - CH_2 -$

Fig. 3.1.1 Basic structure of organic acids. The symbol X could be any of the functional groups and side chains

almost universally achieved using gas chromatography-mass spectrometry (GC-MS) [12, 15, 23, 35]. Other methods for organic acid profiling, but of limited application in routine practice, include capillary electrophoresis [4, 10], high-resolution proton nuclear magnetic resonance [34], and electrospray ionization tandem mass spectrometry (MS/MS) [6, 27]. The latter is faster and to some extent less labor intensive, but is limited to the detection of analytes included in a pre-determined list of targets, the inability to separate some isomers, and a poor response of several compounds that are significant for the detection of specific disorders. On the other hand, MS/MS is clearly emerging as the platform of choice for the rapid and accurate determination of single analytes, including several organic acids and related compounds [1, 19, 24, 25, 28].

3.1.3.1 Principle

The GC-MS methods described here reflect the practice in the laboratory of the author. Organic acids are extracted from biological fluids by liquid-liquid extraction after mixing the specimen with an internal standard solution and a small amount of mineral acid (HCl) to bring the pH to ≤ 2. Oximation of 2-keto acids with hydroxylamine hydrochloride is not performed routinely, but only as a repeat analysis when the primary analysis reveals an abnormal excretion of 2-keto acids (e.g., lactic acidemia, ketonuria) and the potential presence of other compounds (e.g., glyoxylic acid, succinylacetone).

An equal volume of organic solvent (ethyl acetate, ether) is added and the tube is capped and vigorously mixed by shaking. Organic acids, which are in their neutral (protonated) state due to the acidification, will selectively favor the organic portion of the mixture. This liquid-liquid extraction is performed multiple times, each time removing the upper organic solvent layer to a clean test tube. The pooled layers are dried over sodium sulfate, and evaporated in a water bath under a gentle stream of nitrogen. After evaporation, organic acids are converted to their corresponding

Table 3.1.3 *Pathologic acylglycine species detected by organic acid analysis.* CoA *coenzyme A,* FAO *fatty acid oxidation,* ILE *isoleucine,* LEU *Leucine,* MCAD *medium-chain acyl-CoA dehydrogenase,* MET *methionine,* PHE *phenylalanine,* SCAD *short-chain acyl-CoA dehydrogenase,* THR *threonine,* VAL *valine*

Name	Chain length (acyl)	Precursors	Conditions with abnormal urinary excretion
Propionylglycine	C3	LEU MET THR VAL	Propionic acidemia Methylmalonic acidemias
Butyrylglycine	C4	Butyryl-CoA (FAO)	SCAD deficiency Glutaric acidemia type II
Isobutyrylglycine	C4	VAL	Isobutyryl-CoA dehydrogenase deficiency Glutaric acidemia type II Ethylmalonic encephalopathy
Tiglylglycine	C5:1	ILE	Propionic acidemia Methylmalonic acidemias Ketothiolase deficiency
3-Methyl crotonylglycine	C5:1	LEU	3-Methylcrotonyl-CoA carboxylase deficiency Multiple carboxylase deficiency
Isovalerylglycine	C5	LEU	Isovaleric acidemia
2-Methylbutyrylglycine	C5	ILE	2-Methylbutyryl-CoA dehydrogenase deficiency Glutaric acidemia type II Ethylmalonic encephalopathy
Hexanoylglycine	C6	Hexanoyl-CoA (FAO)	MCAD deficiency Glutaric acidemia type II
Octanoylglycine	C8	Octanoyl-CoA (FAO)	MCAD deficiency
Suberylglycine	C8	Suberyl-CoA	MCAD deficiency Glutaric acidemia type II
Phenylpropionylglycine	C9	PHE	MCAD deficiency
Trans-cinnamoylglycine	C9:1	PHE	No known defect

trimethylsilyl (TMS) ethers with N,O,-bis-(trimethylsilyl)trifluoroacetamide (BSTFA) containing 1% trimethylchlorosilane (TMCS). The derivatization imparts volatility to the organic acids, necessary for the GC-MS analysis. The organic acid-TMS ethers are separated in a capillary gas chromatography column containing an immobilized, nonpolar stationary phase. After chromatographic separation, organic

acids are routinely detected by electron impact mass spectrometry performed in the scan mode with a mass range between m/z 50 and 550. Identification is achieved by comparison to published spectra of bona fide compounds, or spectra generated by in-house analysis of pure standard compounds. Quantification is by comparison to calibration of pure standard compounds in ratio to an internal standard.

Alternative extraction methods [20, 35], oximation [9, 35], and derivatization agents [26] are available, but will not be discussed further in this chapter.

3.1.3.2 Pre-analytical

Listed below are specimen requirements, reagents, and the procedures used for sample preparation.

Specimen

The preferred specimen is a random urine collection (approximately 10 ml, minimum volume 2 ml) collected without addition of preservative. No particular patient preparation is required. Transport of a refrigerated (wet ice) specimen to a local laboratory is acceptable, but specimens should be frozen when sent to an outside laboratory. Alternatively, spotting and drying urine on filter paper is possible when shipment on dry ice is either problematic or too expensive. Urine spotted on filter paper has been used successfully for large-scale population screening programs for neuroblastoma [3]. Upon receipt, the filter paper could be soaked in reverse osmosis (RO) water for several hours with gentle shaking, and treated afterwards as a conventional urine specimen. Collection of urine at autopsy is often unsuccessful. However, minute amounts of urine could be obtained by use of cotton swabs applied to the posterior wall of the bladder during the postmortem examination [30].

Organic acid analysis could be performed in other biological specimens [14, 22] when targeting specific analyte(s) in previously diagnosed patients, or fetuses at risk for a specific condition. Plasma/serum profiling is not helpful in the laboratory evaluation of patients without a specific diagnosis, and should be avoided [2].

Recommended specimen information, in addition to mandatory patient identifiers, include age, date and time of collection, reason for the request (i.e., confirmatory testing following an abnormal newborn screening result), and clinical status. Knowledge of clinical status at the time of specimen collection is essential when a STAT analysis is requested (i.e., when results are required within 2–3 h), because specimens for metabolic investigations may not have been secured ahead of aggressive therapeutic intervention. Specimens collected even after a partial recovery may not reveal diagnostic abnormalities that are more readily detectable, under acute conditions.

Reagents and Chemicals

In this chapter, two separate methods are described, one for the standard analysis of organic acids by GC-MS in total ion current (TIC) mode (GC-MS TIC) and another

for the determination in selected ion monitoring (SIM) mode of a limited number of acylglycine and organic acid species (GC-MS SIM).

GC-MS TIC Analysis

1. Pentadecanoic acid (PDA; internal standard), stock solution 1 mg/ml in methanol. Dissolve 100 mg of PDA in 100 ml of methanol in a volumetric flask. Store refrigerated. Stable for 1 month.
2. Pure standards of organic acids are obtained from several commercial sources. Storage is according to manufacturer specifications (–20°C, refrigerated under desiccant, room temperature). Stock solutions are prepared in methanol 1 mg/ml solutions and are stored refrigerated.
3. BSTFA + TMCS (Pierce 38831 J; 10 × 1 ml ampules). BSTFA + TMCS (CAS-NO 25561-30-2 and 75-77-4) is a clear, colorless liquid that is highly sensitive to moisture. It is packaged under nitrogen in 1-ml ampules. Upon contact with water or water vapor, it hydrolyzes to form N-(trimethylsilyl)trifluoroacetamide, trifluoroacetamide, HCl, and hexamethyldisiloxane (reactivity rating: 1). BSTFA + TMCS is flammable (rating: 3) and harmful by inhalation (rating: 2), with danger of cumulative effects resulting in irritation of eyes, airways, and skin.
4. Sodium hydroxide (NaOH), aqueous, 6 mol/l: 48 g of NaOH is dissolved in RO water, the final volume made to 200 ml. Stable at room temperature.
5. HCl, concentrated: HCl, 6 mol/l. Mix 250 ml of RO water and 250 ml of HCl. Stable at room temperature.
6. Ethyl acetate, high-performance liquid chromatography (HPLC) grade.
7. Sodium sulfate, Na_2SO_4, anhydrous.
8. Methanol, HPLC grade.
9. Hydroxylamine hydrochloride, NH_2OH-HCl: 2.5% NH_2OH-HCl aqueous for oximation; 25 g of NH_2OH-HCl is diluted with 1 l RO water. Store at room temperature in a dark bottle. Stable at room temperature.
10. Nitrogen, compressed.
11. Helium, compressed, research grade.
12. Sodium chloride, NaCl.

GC-MS SIM Analysis (only if not mentioned above)

1. Stock standard solutions (labeled internal standards and unlabeled compounds) and working solution amounts are shown in Table 3.1.4. The internal standard working solution is a mixture of 11 stable-isotope-labeled compounds in methanol. Butyrylglycine, isobutyrylglycine, *n*-hexanoylglycine, 3-phenylpropionylglycine, *trans*-cinnamoylglycine, isovalerylglycine, *n*-octanoylglycine, 2-methylbutyrylglycine, suberylglycine, and all the labeled acylglycine internal standards have been synthesized in the author's laboratory. The synthesis principle is the Schottent-Baumann reaction involving the addition of an acyl chloride to an amine under cold, basic conditions to yield an amide (procedure available upon request). Labeled C12:0, C14:0, and C16:0 dicarboxylic acids were purchased after custom synthesis from Cambridge Isotope Laboratories. All other standards are commercially available.
2. 3.0 N HCl in *n*-butanol (Regis 201009).

Table 3.1.4 *Preparation of stock and working solutions for gas chromatography-mass spectrometry (GC-MS) selected ion monitoring (SIM) analysis.* 2MBG *2-methylbutyrylglycine,* BG *butyrylglycine,* DCA *dicarboxylic acid,* EMA *ethylmalonic acid,* GLUT *glutaric acid,* HG *hexanoylglycine,* IBG *isobutyrylglycine,* IVG *isovalerylglycine,* MW *Molecular weight,* MSA *methylsuccinic acid,* OG n-*octanoylglycine,* PPG *3-phenylpropionylglycine,* SG *suberylglycine,* tCG trans-*cinnamoylglycine*

Compound	MW	mg/10 ml	Stock	Working	nmol/100 µl	µg/100 µl
EMA	132	7.92	6.0	0.3	30	3.96
MSA	132	7.92	6.0	0.30	30	3.96
[D_3]EMA	135	8.10	6.0	0.30	30	4.05
GLUT	132	7.92	6.0	0.30	30	3.96
[D_4]GLUT	136	8.16	6.0	0.30	30	4.08
IBG	145	14.50	10.0	0.50	50	7.25
BG	145	14.50	10	0.50	50	7.25
[1,2-^{13}C]BG	147	14.70	10	0.50	50	7.35
2MBG	159	11.13	7.0	0.35	35	5.57
[1,2-^{13}C]2MBG	161	11.34	7.0	0.35	35	5.67
IVG	159	11.13	7.0	0.35	35	5.57
[1,2-^{13}C]IVG	161	11.34	7.0	0.35	35	5.67
HG	173	10.38	6.0	0.30	30	5.19
[1,2-^{13}C]HG	175	10.50	6.0	0.30	30	5.25
OG	201	16.08	8.0	0.40	40	8.04
[1,2-^{13}C]OG	203	16.24	8.0	0.40	40	8.12
PPG	207	16.56	8.0	0.40	40	8.28
[1,2-^{13}C]PPG	209	16.72	8.0	0.40	40	8.36
SG	231	57.75	25.0	1.25	125	28.88
[1,2-^{13}C]SG	233	58.25	25.0	1.25	125	29.13
tCG	205	20.50	10.0	0.50	50	10.25
[1,2-^{13}C]tCG	207	20.70	10.0	0.50	50	10.35
$C_{12:0}$ DCA	230	23.00	10.0	0.50	50	11.50
[D_{20}]$C_{12:0}$	250	25.00	10.0	0.50	50	11.60
$C_{14:0}$ DCA	258	25.80	10.0	0.50	50	12.90
[D_{24}]$C_{14:0}$	282	28.20	10.0	0.50	50	13.00
$C_{16:0}$ DCA	286	28.60	10.0	0.5	50	14.30
[D_{28}]$C_{16:0}$	314	31.40	10.0	0.5	50	14.40

Sample Preparation Procedure

GC-MS TIC Analysis

1. Obtain the creatinine concentration (mg/dl) on the specimen to be analyzed. Determine the amount of urine equivalent to 0.25 mg creatinine. If the creatinine value is <8 mg/dl, extract 3.0 ml of urine.
2. Transfer the urine sample to a clean standard glass tube. If necessary, add RO water to a final volume of 3.0 ml. Add 100 µl of internal standard solution. Cap the tube tightly and mix carefully. If oximation is not required, proceed to step 4.
3. If oximation is required (stabilization of 2-keto acids):
   a. Adjust the pH to 7.0 (dropwise addition of 6 mol/l HCl or 30% NaOH as needed; verify with pH paper).
   b. Add 0.5 ml of 2.5% aqueous NH_2OH-HCl. Allow to react in a 60°C water bath for 30 min. Cool the capped tubes at room temperature.
4. Add one scoop of NaCl (equal to about 1.0 g) and 250 µl of 6 mol/l HCl to each tube. Shake and mix carefully.
5. Liquid-liquid extraction: Add 3.0 ml of ethyl acetate using an automatic dispenser. Cap tightly, shake and mix vigorously. Centrifuge for 1 min at 2000 rpm ($470 \times g$).
6. Transfer the top solvent phase to a second appropriately labeled glass tube using a Pasteur pipette.
7. Repeat steps 5–6 three more times. Pool all four ethyl acetate phases in the same tube for each sample.
8. Add one scoop of Na_2SO_4 (equal to about 1.0 g) to each tube. Shake and mix carefully. Let tubes stand undisturbed for 5–10 min.
9. Centrifuge for 1 min at 2000 rpm ($470 \times g$). Pour the solvent phase to a clean appropriately labeled glass tube.
10. Evaporate each sample just to dryness under a gentle nitrogen flow.
11. Add 100 µl of BSTFA+TMCS to each tube. Open ampules fresh daily. Mix carefully, cap, and allow to react in a heating block for 30 min at 80°C. Discard any left-over reagent.
12. Remove tubes from the heating block and allow to cool to room temperature. Remove the caps and transfer the contents of each tube to a clean GC-MS autosampler vial. Cap the vials. Samples may be stored in the refrigerator until analysis for up to 24 h.

GC-MS SIM Analysis

1. Establish the creatinine concentration (mg/dl) on the specimen to be analyzed. Determine the amount of urine equivalent to 0.50 mg creatinine. If the creatinine value is <4 mg/dl, extract 3.0 ml of urine.
2. Transfer the urine sample to a clean standard glass tube. If necessary, add RO water to a final volume of 3.0 ml. Add 100 µl of internal standard solution. Cap the tube tightly and mix carefully.
3. Add one scoop of NaCl (equal to about 1.0 g) and 250 µl of 6 mol/l HCl to each tube. Shake and mix carefully.
4. Liquid-liquid extraction: Add 3.0 ml of ethyl acetate using an automatic dispenser. Cap tightly, shake, and mix vigorously. Centrifuge for 1 min at 2000 rpm ($470 \times g$).

5. Transfer the top solvent phase to a second appropriately labeled glass tube using a Pasteur pipette.
6. Repeat step 4–5 three more times. Pool all four ethyl acetate phases into the same tube for each sample.
7. Add one scoop of Na_2SO_4 (equal to about 1.0 g) to each tube. Shake and mix carefully. Let the tubes stand undisturbed for 5–10 min.
8. Centrifuge for 1 min at 2000 rpm ($470 \times g$). Pour the solvent phase to a clean appropriately labeled glass tube.
9. Evaporate each sample just to dryness under a gentle nitrogen flow.
10. Pipette 100 µl of 3.0 N HCl in *n*-butanol to each tube under hood. Cap, vortex, and place in 65°C heating block for 15 min.
11. Remove the tubes from the heating block and let them cool to room temperature.
12. Evaporate the 3 N HCl in *n*-butanol at 40°C until dry.
13. Add 100 µl of hexane to each tube and vortex to mix. Transfer to a glass gas chromatography vial and cap.

Calibration

The setup of a calibration curve is not always feasible because pure standards of many clinically significant organic acids are not available commercially. This limitation underscores the importance of qualitative profile interpretation as the primary means by which to report organic acid results in clinical practice, rather than generating extensive lists of quantitative measurements of individual analytes.

When a reference standard is available and is calibrated against an internal standard in the TIC mode, six-point calibration curves of either individual or closely related analytes (for example, the isomers ethylmalonic acid, 2-methylsuccinic, and glutaric acid) are run according to the standard/internal standard amount ratio shown in Table 3.1.5. Variations of this basic scheme may be indicated depending on the intensity of target ions ($[M\text{-}15]^+$ species), the level of excretion in normal and disease states, and the linearity limit.

A new calibration curve must be implemented every time a new stock of internal standard solution is prepared, and at least twice per year. New calibration curves are validated by the following criteria for acceptability: point-to-point comparison (<10% difference from the previous calibration curve), coefficient of linear regression (>0.99), intercept and slope (<10% difference from previous calibration curve). Normal and abnormal control samples are calculated against the new and the old curve and compared to the current quality control (QC) mean as the final step in the validation of the new curve. The new calibration curve is then used with subsequent runs if the curve validation is acceptable. Curves are unique to each instrument and therefore must be established for each instrument prior to clinical use.

Quality Control

Every sample is evaluated for the presence and intensity of the internal standard peak and abnormalities of the baseline. Any evidence of interference requires the extraction of that particular sample to be repeated. Every batch of clinical specimens includes a normal and abnormal control QC sample.

Table 3.1.5 *Analyte concentrations for the calibration curve used in the GC-MS SIM method.* ISTD *Internal standard*

Analyte	Calibration number/[Analyte]:[ISTD] ratio [a]					
	1/0.25	2/0.50	3/0.75	4/1.00	5/1.50	6/2.00
EMA	0.99	1.98	2.97	3.96	5.94	7.92
MSA	0.99	1.98	2.97	3.96	5.94	7.92
GLUT	0.99	1.98	2.97	3.96	5.94	7.92
IBG	1.81	3.63	5.44	7.25	10.87	14.50
BG	1.81	3.63	5.44	7.25	10.87	14.50
2MBG	1.39	2.78	4.18	5.57	8.34	11.14
IVG	1.39	2.78	4.18	5.57	8.34	11.14
HG	1.30	2.59	3.89	5.19	7.78	10.38
OG	2.01	4.02	6.30	8.04	12.60	16.08
PPG	2.07	4.14	6.21	8.28	12.42	16.56
SG	7.22	14.44	21.66	28.88	43.32	57.76
tCG	2.56	5.12	7.69	10.25	15.37	20.50
C_{12}DCA	2.87	5.75	8.62	11.50	17.25	23.00
C_{14}DCA	3.22	6.45	9.67	12.90	19.35	25.80
C_{16}DCA	3.57	7.15	10.72	14.30	21.45	28.60

[a] These ratios are used for all calibration curves (TIC or SIM; see text)

Normal Control

A volume equivalent to 0.25 mg of creatinine from 500 mL of urine of a healthy adult donor is analyzed to exclude unusual findings or presence of drugs and/or other interfering compounds in the organic acid profile. If the specimen is deemed free of interference and suitable to be used as a QC normal control, the collection is diluted with RO water so that 3 ml equals 0.25 mg creatinine equivalent, and aliquoted into screw-cap vials during continued mixing; then stored frozen.

Abnormal Control

A volume equivalent to 0.25 mg of creatinine from 500 mL of urine of a healthy adult donor is analyzed as described above. The collection is then spiked with up to ten organic acids (1 mg/ml stock solutions), selected from those with an active calibration curve by GC-MS TIC, to mimic a concentration of 100 µg acid/mg creatinine. The spiked collection is aliquoted into screw-cap vials during continued mixing, then stored frozen. For GC-MS SIM analysis, all compounds listed in Table 3.1.5 are included in the abnormal control, at a concentration matching the fourth point of the calibration curve (1:1 molar ratio to the labeled internal standard, see Table 3.1.5).

The means and standard deviations (SD) for the organic acids in the QC samples are calculated from ten interassay values for each control, and used for QC purposes

for the duration of the lot (approximately 3 months). Routine assay control values are entered into a spreadsheet that automatically plots the value in relation to the mean. Control values that fall within ± 2 SD of the mean are acceptable and require no further action. Shifts or trends in the control values as determined by control values that are >2 SD from the respective target value in more than three consecutive batches require corrective action. Any control values that are >3 SD require immediate corrective action.

3.1.3.3 Analytical

Most vendors of GC-MS systems provide software capable of autotuning. Although highly reliable, it is a requirement for accreditation by the American College of Pathologists (CAP) to maintain documentation of the specific criteria being met. For users of Agilent systems, tuning with perfluorotributylamine should be performed at least after any hardware manipulation, possibly daily, and meet the criteria illustrated in Table 3.1.6. A practical example of an unbalanced tuning is the failure to detect low-intensity $[M\text{-}15]^+$ ion species such as in the case of unsaturated C_{12}–C_{14} 3-hydroxy dicarboxylic acids.

Different capillary columns are available for organic acid separation and analysis. In our laboratory, the gas chromatography column in all GC-MS applications is crosslinked 5% phenyl (poly)methyl silicone, 25 m; internal diameter 0.20 mm; stationary phase film thickness 0.33 µm (Agilent HP-5, DB-5, or equivalent). Several instrument configurations are commercially available, which allow for positive identification of compounds by their mass spectra obtained in the electron impact ionization mode. A commercially available bench-top GC-MS system with autosampler (Agilent 6890/5973, or equivalent) is suitable. Software for data analysis is available and recommended. The use of a computer library of mass spectra for comparison and visualization of the printed spectra is required for definitive identification and interpretation of each patient specimen.

Instrumentation

GC-MS (TIC)

Agilent GC-MS ChemStation System equipped with capillary gas chromatograph HP 5972,5973, or 6890 series; Agilent 6890 series autosampler. The GC-MS system is operated in the positive-ion, electron-impact ionization mode. Chromatographic parameters of the acquisition method are listed in Table 3.1.7. TIC is recorded over the mass range m/z 50–550, and the total run time is 33 min.

GC-MS (SIM)

Agilent GC-MS ChemStation System equipped with capillary gas chromatograph HP 5972,5973, or 6890 series; Agilent 6890 series autosampler. The GC-MS system is operated in the positive-ion, chemical-ionization mode; the reagent gas is ammonia. The chromatographic parameters of the acquisition method, the sequence of SIM windows, and the ion species being monitored are listed in Tables 3.1.8 and 3.1.9. The total run time is 17.88 min.

Table 3.1.6 *Tuning criteria (Agilent Technologies systems, perfluorotributylamine)*

Parameter	Optimal value
Peak width at half height	
m/z 69, 219, 502	0.5 ± 0.15
Peak intensity ratios	
m/z 69	100%
m/z 219	> 40%
m/z 502	> 2%
m/z 614	Detected
Isotopic mass ratios	
m/z 70	0.5–2.0%
m/z 220	3.5–5.0%
m/z 503	9.0–11.0%
Air peaks	
m/z 28, 32	< 5%
Voltages	
Ion focus lens	< 100 V
Electron multiplier	< 2000 V

Table 3.1.7 *Acquisition parameters of the GC-MS TIC method.* GC *Gas chromatograph,* MS *mass spectrometer*

Parameter	Temperature	Time	Other
Carrier gas	–	–	Helium
Column head pressure	–	–	30 psi (207 Pa)
Injection volume	–	–	2 µl
Injection mode	–	–	Split (50:1 ratio)
Injector temperature	250°C	–	–
Initial GC temperature	80°C	4 min	–
GC ramp rate	8°C/min	26.25 min	–
Final GC temperature	290°C	2.75 min	–
Transfer line temperature	290°C	–	–
MS source temperature	230°C	–	–
Quadrupole temperature	150°C	–	–

Table 3.1.8 *Acquisition parameters of GC-MS SIM method*

Parameter	Temperature	Time	Other
Carrier gas	–	–	Helium
Column head pressure	–	–	30 psi (207 Pa)
Injection volume	–	–	1 µl
Injection mode	–	0.25 min	Splitless
Injector temperature	250°C	–	–
First GC temperature	130°C	0 min	–
GC Ramp rate 1	8°C/min	8.1 min	–
Second GC temperature	195°C	0 min	–
GC Ramp rate 2	20°C/min	4.8 min	–
Final GC temperature	290°C	5 min	–
Transfer line temperature	280°C	–	–
MS source temperature	250°C	–	–
Quadrupole temperature	116°C	–	–
Ammonia source pressure	–	–	1.0 torr (133.3 Pa)

Table 3.1.9 *Acquisition windows and ion species monitored by the GC-MS SIM method. The window start times may vary slightly and are column and instrument specific*

Analytes per window	Start time (min)	Ion species (m/z)	Dwell time (ms)
IBG, BG EMA, MSA	4.5	201.1, 204.1, 219.1, 221.1, 245.1, 248.2, 262.2, 265.2	50
2MBG, IVG	6.06	216.1, 218.1, 233.2, 235.2	100
GLUT	6.7	245.1, 262.2, 249.2, 266.2	100
HG	7.6	230.1, 232.1, 247.2, 249.2	100
OG	9.2	258.2, 260.2, 275.2, 277.2	100
PPG	10.7	264.1, 266.1, 281.1, 283.1	100
C_{12}DCA, tCG	11.8	262.1, 264.1, 279.2, 281.2, 343.3, 360.3, 363.4, 380.4	50
SG, C_{14}DCA	12.75	344.2, 346.2, 361.3, 363.3, 371.3, 388.3, 395.4, 412.5	50
C_{16}DCA	13.8	399.3, 416.4, 427.5, 444.6	100

Other Instrumentation

1. Water bath with nitrogen supply (Zymark Turbo Vap LV or equivalent).
2. Centrifuge (IEC Centra CL2 or equivalent).
3. Dry heating block (Pierce Reacti-Therm III or equivalent).

Calculations

A post-run custom analysis program generates a report listing organic acids and acylglycines in amounts expressed as μg/mg creatinine, flagged abnormal if outside the corresponding reference range. An example of a report generated using commercially available software is shown in Fig. 3.1.2.

3.1.3.4 Postanalytical

Organic acid analysis is one of the most challenging tests applied to the diagnosis of inborn errors of metabolism. Several hundreds of compounds are excreted in the urine of individuals free of apparent disease, and the excretion of informative markers could be marginal depending on clinical status. Therefore, pattern recognition and descriptive interpretation are essential for proper utilization of this test.

The conventional approach is to extract from the TIC profile the mass spectra of all peaks above a predetermined intensity and to perform either manual or computer-assisted [39] identification of each mass spectrum. Analysis of mass spectra should be carried out only by properly trained technologists, under the supervision of a qualified laboratory director. Libraries of mass spectra should be available for identification of peaks that are not readily recognized. This library should be user-created, indexed by retention time and molecular weight, and have the capacity to be expanded and edited.

Interpretation

As recommended in the standards and guidelines issued by the American College of Medical Genetics (ACMG) [2], the extent of interpretation that is necessary to make organic acid results meaningful to the ordering clinician is the defining characteristic of the high-complexity procedures provided by a biochemical genetics laboratory. When no significant abnormalities are detected, an organic acid analysis may be reported in qualitative terms only. However, if a specific reason for referral was provided, the interpretation should include a reference to what organic acid species were not detected or elevated, and an indication of what conditions(s) were not possible to confirm. This is particularly indicated when the test was ordered as part of the follow up of an abnormal newborn screening result. Similarly, it should be recorded in the report when a repeat analysis is being performed to follow up a previously inconclusive result.

When pathologic species or amounts are detected, the interpretation should include a list of positive and negative results (for example, ketotic vs nonketotic dicarboxylic aciduria) organized in a logical sequence, because interpretation is based on

URINE ACYLGLYCINE ANALYSIS

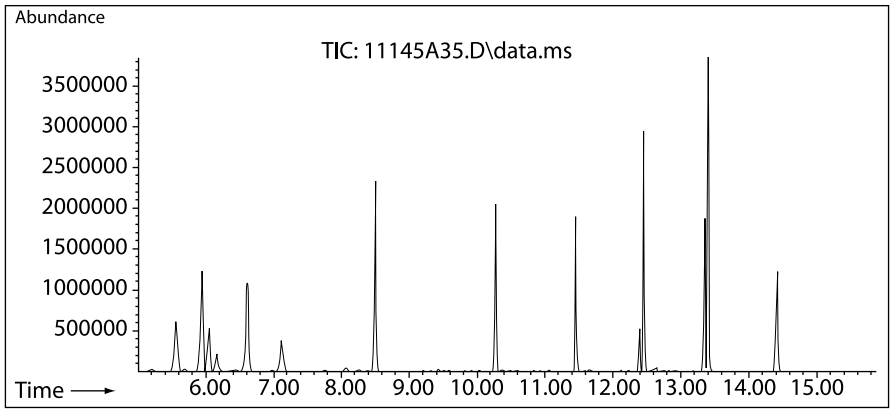

File Name		File Name	091605
File Path		File Path	
Name		Multipler	4.76

Compound	IS R.T.	R.T.	Amount µg/mg creatinine		Controls
EMA	5.56	5.58	**2.12**		0.50–20.20
MSA		6.16	**3.15**		0.40–13.80
GLUTARIC	7.11	7.15	**5.85**		0.60–15.20
IBG		5.43	**0.13**		0.01–11.00
BG	6.06	6.06	**1.26**		0.10–2.06
2MBG		6.44	**0.20**		0.30–7.50
IVG	6.61	6.60	**1.64**		0.30–14.30
HG	8.50	8.50	**32.69**	H	0.20–1.90
OG	10.28	10.28	**1.84**		0.10–2.10
PPG	11.46	11.46	**1.59**	H	0.01–1.10
SG	13.40	13.40	**34.48**	H	0.01–11.00
tCG	12.40	12.39	**1.28**		0.20–14.70
C12	12.45	12.52	**0.03**		0.01–1.10
C14	13.35	13.42	**0.01**		0.01–1.00
C16	14.42	14.57	**0.00**		0.01–1.00

Fig. 3.1.2 Example of customized report of gas chromatography-mass spectrometry (GC-MS) selected ion monitoring (SIM) method. The profile corresponds to a case with medium-chain acyl-CoA dehydrogenase (MCAD) deficiency. This report is generated automatically at the end of each acquisition using an Excel template. The file can be customized offline to meet virtually any requirement, including plots (total ion current – TIC – and/or extracted ion chromatograms), calculations, ratios, formulas, and flagging when values are not within a predetermined reference range. *2MBG* 2-methylbutyrylglycine, *BG* butyrylglycine, *C12* dodecanedioic acid, *C14* tetradecanedioic acid, *C16* hexadecanedioic acid, *EMA* ethylmalonic acid, *GLUTARIC* glutaric acid, *H* high value, *HG* hexanoylglycine, *IBG* isobutyrylglycine, *IS* internal standard, *IVG* isovalerylglycine, *MSA* methylsuccinic acid, *OG* octanoylglycine, *PPG* 3-phenylpropionylglycine, *R.T.* retention time, *SG* suberylglycine, *tCG trans*-cinnamoylglycine

pattern recognition and correlation of all relevant findings rather than on individual abnormal values. Other required components of an interpretive comment are a correlation to available clinical information, elements of differential diagnosis, and recommendations for additional biochemical testing and in vitro confirmatory studies (enzyme assay, molecular analysis). As in the case of virtually all biochemical tests, an abnormal organic acid analysis is not sufficient to establish a definite diagnosis of a particular metabolic disorder. Therefore, it should be recommended to seek confirmation by an independent method, typically by in-vitro enzyme assay (blood or cultured cells, tissue biopsy) or molecular analysis. Finally, a report should provide the location and contact information of laboratories that may provide these studies, and a phone number to reach the reporting laboratory in case the referring physician has additional questions.

3.1.4 Chromatograms

Figure 3.1.3a shows a normal urine organic acid profile. Panel B represents an expansion of the same profile (5% of original abundance) to emphasize the underlying complexity of the urine organic acid fraction and the need to appreciate how informative findings could be hidden within a background of comparable intensity (see section 2.1.8.3). For this reason, exclusive reliance on computer-driven identification is not a safe option because visual evaluation is required, for example in the case of the critical overlaps discussed later in this chapter.

On the other hand, the SIM analysis of a predefined set of analytes (Fig. 3.1.4a) require visual inspection, but only to exclude unexpected interferences in the signal of a target compound. For the purpose of detecting unexpected interferences, it is necessary, and is also a CAP accreditation requirement, to monitor at least two ion species per compound (Fig. 3.1.4b and c), so as to recognize artificial variations in the intensity ratios between two ion chromatograms. Figure 3.1.5 shows examples of characteristic organic acid profiles in patients with selected conditions [32].

3.1.5 Reference Values

Urine reference values of several organic acids are characteristically age-dependent, particularly in the newborn period. Reporting of quantitative results requires matching against a properly defined age group. Table 3.1.10 shows a summary of the reference ranges established in the author's laboratory [32]. More comprehensive lists have been published elsewhere [7, 13, 15]. As mentioned previously (see section 3.1.3.4, subheading "Interpretation"), pattern recognition cannot be replaced by a listing of analytes matched against reference ranges, even when properly defined. When dealing with complex profiles, the likelihood of coincidental, nonsignificant findings is high, and if they are not properly interpreted they could lead to labeling of patients with a questionable "diagnosis," resulting in unnecessary work up that may include invasive and/or expensive procedures.

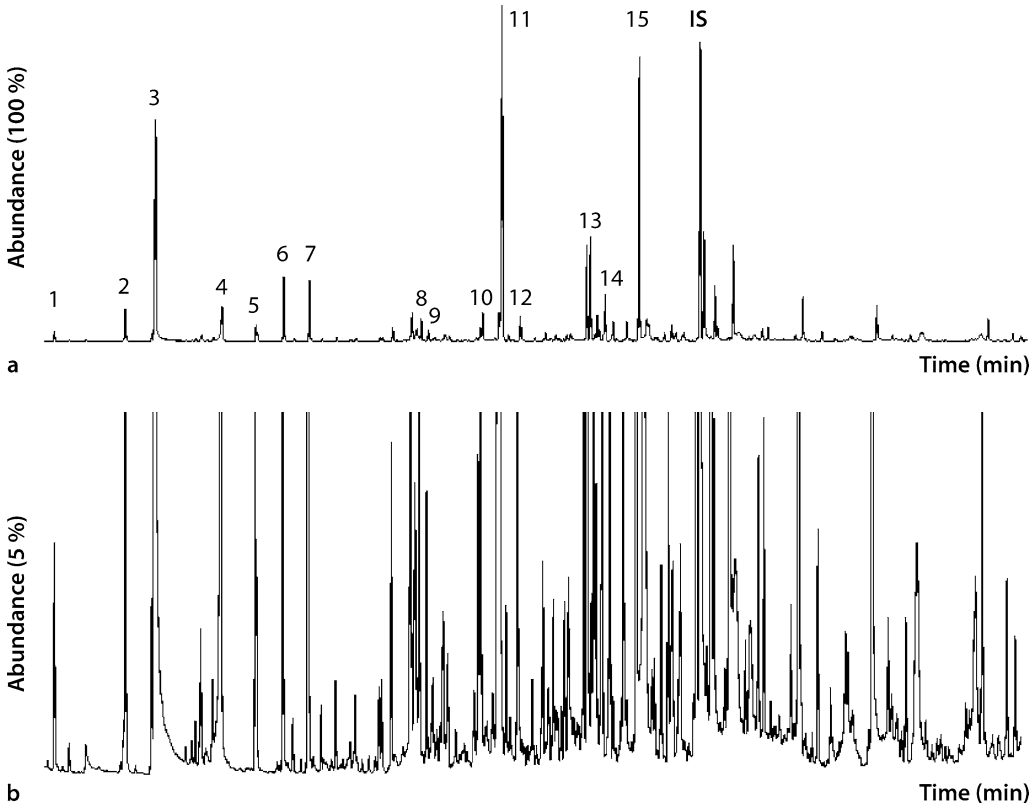

Fig. 3.1.3 **a** Normal urine organic acid profile of a healthy newborn, as assessed by GC-MS TIC analysis. The total run time is 33 min. **b** Same profile shown in panel A scaled to 5% of the original signal intensity. Peak legend as follows: 1 lactic acid; 2 oxalic acid; 3 sulfate; 4 urea; 5 phosphate (overlapping with ethylmalonic acid); 6 succinic acid; 7 fumaric acid; 8 malic acid; 9, adipic acid; 10 3-hydroxy-3-methylglutaric acid; 11 2-keto glutaric (not oximated); 12 4-hydroxy phenylacetic acid; 13 cis-aconitic acid; 14 homovanillic acid; 15 citric acid; IS pentadecanoic acid

3.1.6 Typical Pathological Values

The excretion of diagnostic markers in organic acidurias may vary from minimal (< 10 mmol/mol creatinine) to massive (> 10,000 mmol/mol creatinine) even in the same patient in response to diverse genetic and environmental factors, including the residual catalytic activity of the defective enzyme, the dietary load of precursors, and especially the clinical status at the time of specimen collection. For these reasons, ranges of pathologic values for urinary organic acids [15, 35] may have only limited utility in clinical practice, as they can span several orders of magnitude.

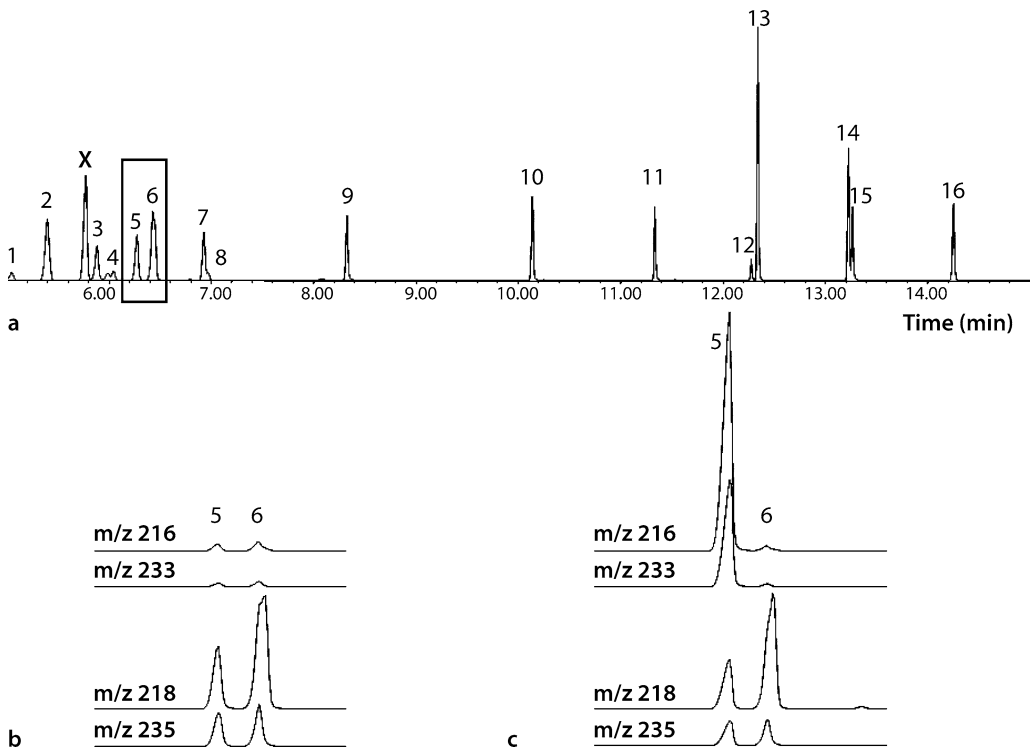

Fig. 3.1.4 **a** GC-MS SIM profile of a healthy patient; peak legend as follows (*indicates coelution with a stable-isotope-labeled IS): *1* IBG; *2*, EMA*; X interference; *3* BG*; *4* MSA; *5* 2MBG*; *6* IVG*; *7* d_4-glutaric acid; *8* glutaric acid; *9* HG*; *10* OG*; *11* PPG*; *12* tCG*; *13* C12*; *14* SG*; *15* C14*; *16* C16*. **b** Extracted ion chromatograms of $[M+H]^+$ and $[M+NH_4]^+$ species of 2MBG, IVG (m/z 216.1 and m/z 233.2), and their respective IS (m/z 218.1 and m/z 235.2) of the profile shown in **a**. Peaks are scaled on the most intense signal ($[M+H]^+$ of [1,2-^{13}C]IVG; **c** Extracted ion chromatograms of 2MBG, IVG, and their respective IS in a patient with 2-methylbutyryl-CoA dehydrogenase deficiency. In this sample, the excretion was 18 μg/mg creatinine

3.1.7 Pitfalls

Organic acid analysis is probably the most complex test performed in a biochemical genetics laboratory [2]. Errors and oversights may happen at all stages of the testing process and can be categorized as shown in Table 3.1.11.

3.1.7.1 Pre-analytical Pitfalls

Specimen contamination may not be immediately apparent on visual inspection. A large peak of glycerol, especially in a female newborn or infant, should be considered an artifact at first and verified by a repeat specimen before raising the possibility of glycerol kinase deficiency. Medium- and long-chain monocarboxylic fatty acids (C_{10}–C_{18}) could be very prominent peaks in a urine profile following contamination

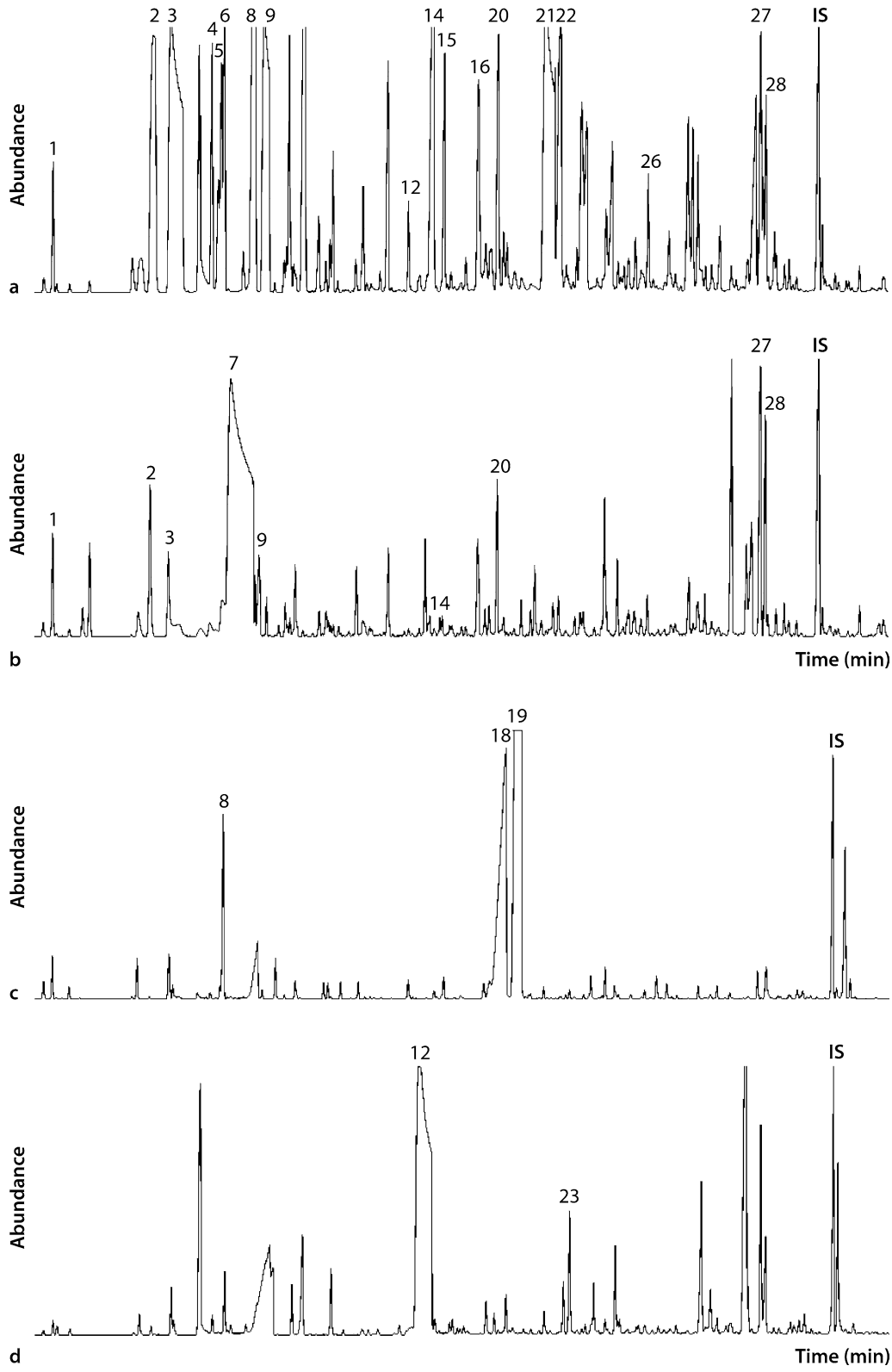
Abundance
a
1
2 3
4
5
6
8 9
12
14
15
16
20
21
22
26
27
28
IS
Abundance
b
1
2
3
7
9
14
20
27
28
IS
Time (min)
Abundance
c
8
18
19
IS
Abundance
d
12
23
IS
Time (min)

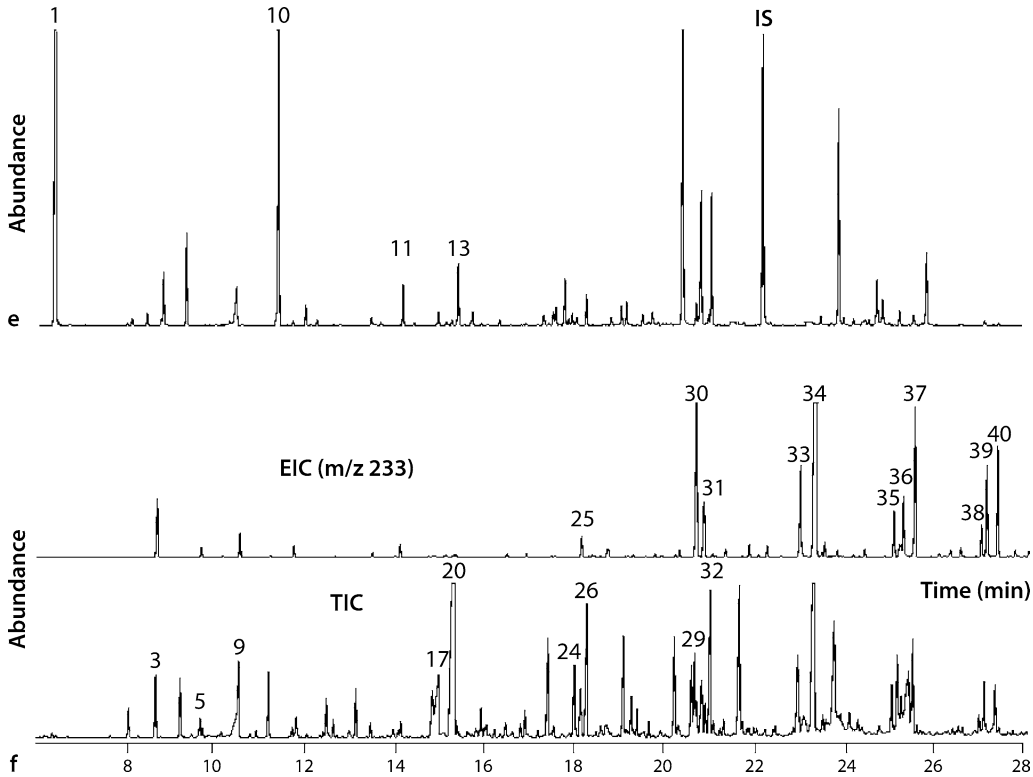

◄▲**Fig. 3.1.5a–f** Examples of GC-MS TIC organic acid profiles in patients with organic aciduria. **a**Propionic aciduria. **b** Methylmalonic aciduria. **c** Isovaleric aciduria. **d** Glutaric aciduria type I. **e** Ethylmalonic encephalopathy. **f** LCHAD deficiency (*EIC* extracted ion chromatogram). Peak labeling is common to all panels and is as follows: *1* Lactic acid, *2* 3-hydroxy propionic acid, *3* 3-hydroxy butyric acid, *4* 2-methyl 3-hydroxy butyric acid, *5* acetoacetic acid (peak I), *6* 3-hydroxy valeric acid, *7* methylmalonic acid, *8* 3-hydroxy valeric acid, *9* acetoacetic acid (peak II), *10* EMA, *11* IBG (di-TMS), *12* glutaric acid, *13* 2MBG (di-TMS), *14* propionylglycine (di-TMS), *15* 3-methylglutaconic acid (peak I), *16* 3-methylglutaconic acid (peak II), *17* 3-hydroxy adipic lactone, *18* IVG (di-TMS), *19* IVG (mono-TMS), *20* adipic acid, *21* tiglylglycine (di-TMS), *22* tiglylglycine (mono-TMS), *23* 3-hydroxy glutaric acid, *24* octenedioic acid, *25* 3-hydroxy adipic acid, *26* suberic acid, *27* methylcitric acid (peak I), *28* methylcitric acid (peak II), *29* decenedioic acid (multiple isomers), *30* 3-hydroxy octanedioic acid, *31* 3-hydroxy suberic acid, *32* sebacic acid, *33* 3-hydroxy decenedioic acid, *34* 3-hydroxy sebacic acid, *35* 3-hydroxy C12 (C12:2), *36* 3-hydroxy C12, *37* 3-hydroxy C12, *38* 3-hydroxy C14 (C14:2), *39* 3-hydroxy C14, *40* 3-hydroxy C14. The symbol * marks the IS (pentadecanoic acid), signal abundance is normalized to the intensity of the IS peak. Reproduced from [32], with permission

■ ***Table 3.1.10*** *Reference ranges of organic acids and acylglycines in urine in children of different ages. Values are presented as mmol/mol creatinine. TIC average detection limit: 0.1 mmol/mol creatinine; SIM average detection limit (with stable-isotope-labeled internal standard: 0.01 mmol/mol creatinine. Reproduced from reference [32], with permission.*
nd *Not detected*

Analyte	Age group			
	0–1 Month	1–6 Months	6 Months–5 years	>5 Years
Acetylaspartic acid	nd–13	nd–13	nd–13	nd–13
cis-Aconitic acid	5–31	10–97	10–97	3–44
Adipic acid	9–37	9–37	nd–15	nd–5
Azelaic acid	nd–1	nd–1	nd–1	nd–1
BG	0.1–2	0.1–2	0.1–2	0.1–2
tCG*	0.1–8	0.1–8	0.1–8	0.1–8
Citric acid	nd–1045	104–268	0–656	87–639
$C_{12}DCA_{12}$*	nd–0.05	nd–0.05	nd–0.05	nd–0.05
EMA*	0.4–17	0.4–17	0.4–17	0.4–17
Fumaric acid	10–45	4–45	1–27	2–4
Glutaric acid*	0.5–13	0.5–13	0.5–13	0.5–13
Glyceric acid*	nd–39	nd–184	nd–70	0–60
Glycolic acid*	nd–62	nd–104	3–121	nd–166
Glyoxylic acid*	nd–13	0–16	nd–7	nd–9
$C_{16}DCA_{16}$	nd–0.4	nd–0.4	nd–0.4	nd–0.4
HG*	0.1–1.2	0.1–1.2	0.1–1.2	0.1–1.2
Homogentisic acid	nd–10	nd–10	nd–10	nd–10
Homovanillic acid*	nd–22	nd–22	nd–8	nd–7
3-Hydroxy butyric acid	nd–5	nd–5	nd–5	nd–10
2-Hydroxy glutaric acid	nd–15	nd–15	nd–15	nd–15
5-Hydroxy indoleacetic acid*	nd–12	nd–12	nd–12	nd–9
4-Hydroxy phenyllactic acid	nd–50	nd–10	nd–10	nd–10
4-Hydroxy phenylpyruvic acid	nd–20	nd–5	nd–	nd–5
IBG*	nd–9	0–9	0–9	0–9
Isocitric acid	0–368	0–67	0–77	16–99
IVG*	0.2–10	0.2–10	0.2–10	0.2–10
2-Ketoglutaric acid	22–567	63–552	36–103	41–82
Lactic acid	46–348	57–346	21–38	20–101

Table 3.1.10 (continued) *Reference ranges of organic acids and acylglycines in urine in children of different ages. Values are presented as mmol/mol creatinine. TIC average detection limit: 0.1 mmol/mol creatinine; SIM average detection limit (with stable-isotope-labeled internal standard: 0.01 mmol/mol creatinine. Reproduced from reference [32], with permission.*
nd *Not detected*

Analyte	Age group			
	0–1 Month	1–6 Months	6 Months–5 years	> 5 Years
Malic acid	0–52	8–73	4–57	17–47
2MBG*	0.2–5	0.2–5	0.2–5	0.2–5
Methylmalonic acid*	nd–3.6	nd–3.6	nd–3.6	nd–3.6
MSA*	0–12	0–12	0–12	0–12
OG*	0.1–1.2	0.1–1.2	0.1–1.2	0.1–1.2
Orotic acid	1.4–5.3	1–3.2	0.5–3.3	0.4–1.2
Oxalic acid*	51–931	7–567	7–352	nd–187
PPG*	nd–0.6	nd–0.6	nd–0.6	nd–0.6
Pimelic acid	nd–1	nd–1	nd–1	nd–1
Pyroglutamic acid	nd–61	nd–61	nd–61	nd–61
Pyruvic acid	24–123	8–90	3–19	6–9
Sebacic acid	3–16	3–16	nd–8	nd–8
Suberic acid	4–20	4–20	nd–8	nd–8
SG*	nd–5.4	nd–5.4	nd–5.4	nd–5.4
Succinic acid	35–547	34–156	16–118	29–87
$C_{14}DCA_{14}$*	nd–0.40	nd–0.40	nd–0.40	nd–0.4
Uracil*	nd–32	nd–32	nd–21	nd–17
Uric acid*	359–2644	359–2644	185–1134	199–1034
Vannillylmandelic acid*	nd–15	nd–10	nd–7	nd–5

* Measured using a stable-isotope-labeled internal standard

Table 3.1.11 *Common pitfalls in organic acid analysis*

Pitfall	Underlying reason
Pre-analytical	
Specimen contamination	Fecal material Skin care products Plasticizers
Extraction	Skipped/inadequate acidification Cross-contamination of solvent pools
Derivatization	Residual moisture (incomplete evaporation to dryness)
Analytical	
Instrument out of tune	
Inadequate chromatographic separation	
Peak saturation	
Postanalytical	
Missed identification	Oversight (low excretion) Overlap
Misidentification	"Look-alike" compounds
Incomplete pattern recognition	
Handling of unknown compounds	
Inadequate interpretive report	

with skincare products; other species may also be detected (for example pimelic acid and azelaic acid). The presence of any of these compounds is not necessarily a reason to discard the specimen, as clinically significant findings could be detected independently, if present.

Avoidance of errors in sample preparation (extraction, derivatization) could be minimized by rigorous training of laboratory personnel, including appreciation of the patient behind each anonymous test tube. An environment free of noise and distractions is required to minimize the risk of serial solvent extractions being pooled in the wrong tube; redundant labeling of glassware and step-by-step checklists are also critical elements of error prevention and detection.

3.1.7.2 Analytical Pitfalls

The analytical parameters for GC-MS TIC analysis of organic acids listed in Table 3.1.7 represent a reasonable compromise between degree of separation and analytical time, resulting in the profile shown in Fig. 3.1.3. A faster run time, usually achieved by increasing the ramp rate (°C/min) of the chromatographic method, may

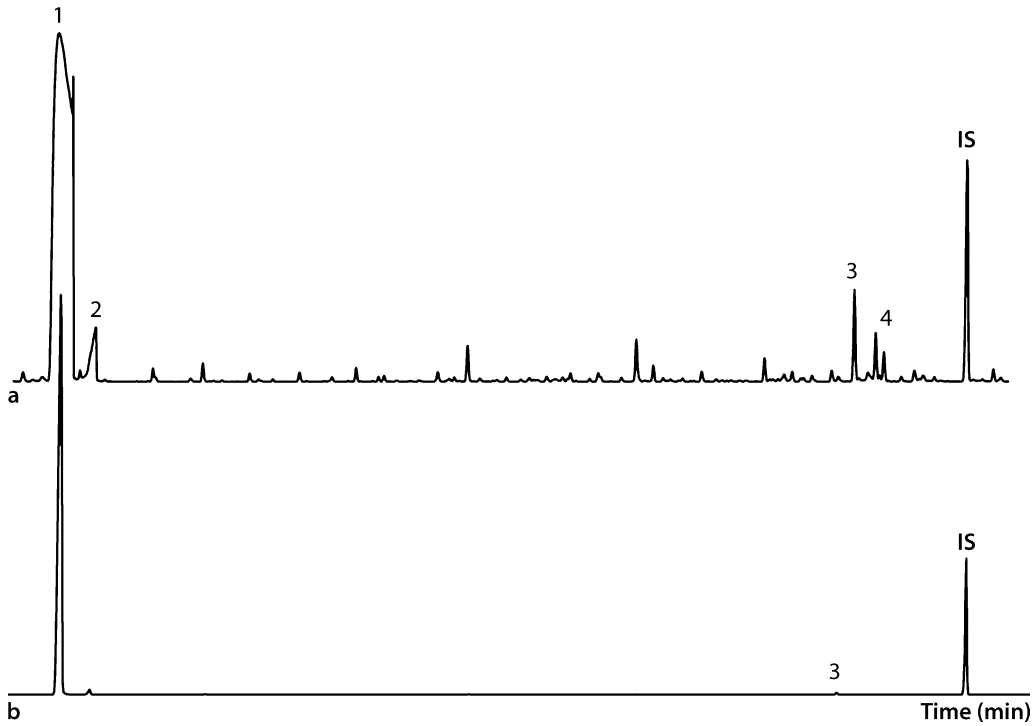

Fig. 3.1.6 GC-MS TIC organic acid profile of a patient with methylmalonic acidemia. **a** sample volume corresponding to 0.25 mg creatinine (standard procedure). **b** 10× dilution (0.025 mg creatinine). Peak legend: *1* methylmalonic acid (note the characteristic broad shape and spike, *2* urea, *3* citric acid, *4* 2-methylcitric acid (two peaks). There was a fourfold difference in the measurement of methylmalonic acid excretion between the two analyses, with a substantial underestimation in the undiluted specimen

lead to failure to detect critical findings because of either peak oversight or overlapping mass spectra (see below). Similarly, use of a larger than necessary sample size (determined by volume rather than a creatinine equivalent) and injection volume (for example, use of a splitless injection mode) may easily yield excessively complex, overlapping, and hence un-interpretable profiles.

Capillary columns are easily overloaded by the level of excretion detectable in acutely ill patients. Any profile with the characteristic appearance of oversaturated peaks (see Fig. 3.1.5a and b) should be repeated after proper dilution when quantitation has to be provided using a GC-MS TIC method (Fig. 3.1.6).

3.1.7.3 Postanalytical Pitfalls

Missed detection of informative organic acids is unfortunately a frequent problem, as reflected by the high rate of incorrect responses in proficiency testing programs like the one administered in the United States by the Biochemical and Molecular Genetics Resource Committee, formed jointly by CAP and the ACMG [8]. The root causes of missed identification are oversight of organic acids and acylglycines ex-

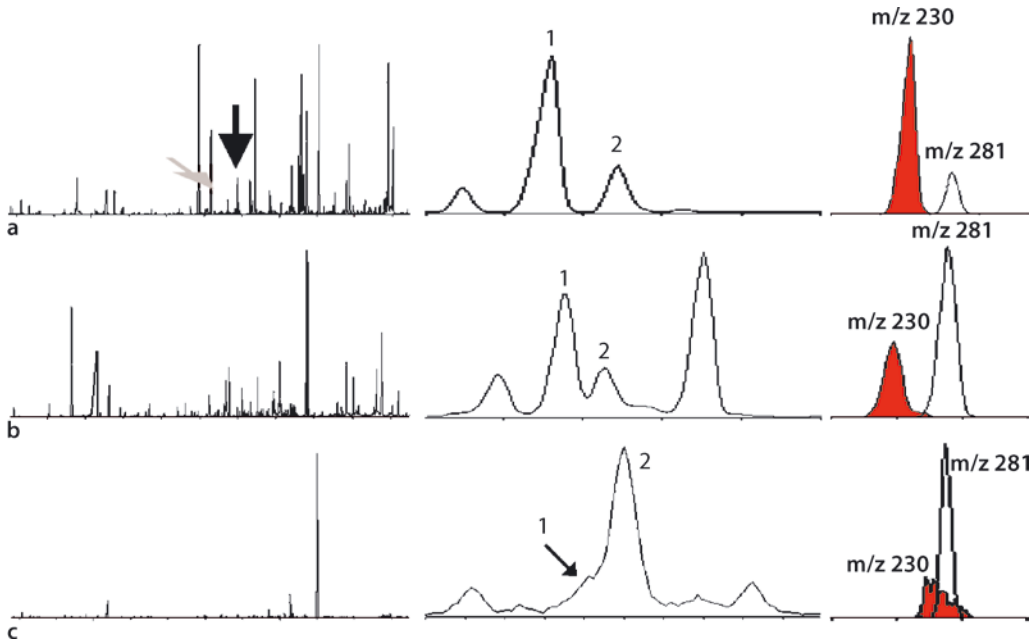

Fig. 3.1.7 Detection of HG by the GC-MS TIC method in the urine of patients with MCAD deficiency collected at different clinical statuses. **A,** left panel: Organic acid profile of an acutely ill patient. The *arrow* indicates the portion of the chromatogram shown in the middle panel. Peak labeling: *1* HG, *2* 4-hydroxyphenylacetic acid. Right panel: extracted ion chromatograms of the [M-15]+ ion of HG (m/z 230; *red*) and 4-hydroxyphenylacetic acid (m/z 281). **B** Patient recovering from an acute episode. **C** Asymptomatic patient. The latter profile represents a situation where there is a high probability that HG may not be detected by a GC-MS TIC method

creted in low amounts (Fig. 3.1.7), and failure to appreciate the presence of a diagnostic compound coeluting with a normal, often abundant component of the urine matrix. Coelution is clearly dependent on the choice of column and acquisition parameters, so the examples listed in Table 3.1.12 are specific to the method used in the author's laboratory. However, there is little doubt that similar situations may occur under any set of conditions applied in laboratory practice.

Misidentification is a potential risk when the library of mass spectra is relatively incomplete. Lacking the availability of a comprehensive, commercially available library, laboratories resort to make their own and it could take several years to develop a comprehensive tool, although hardly ever complete. Lack of reference spectra could lead to incorrect identification of isovalerylglycine (pivalic acid conjugates), 3-methylglutaconic acid (cyclohexanedioic acid) [33], and orotic acid (2-octenylsuccinic acid) [11, 18], just to name a few. The existence of at least six isomers of hydroxy butyric acid could represent a problem, especially when the presence of 3-hydroxy isobutyric acid is overlooked because of a coeluting peak of 3-hydroxy butyric acid (Fig. 3.1.8).

Incomplete pattern recognition is intimately related to the need to provide a complete and informative interpretation of all abnormal results (see section 2.1.4.4, subheading "Interpretation"). Not only critical information may not be reported (for ex-

Table 3.1.12 *Critical overlaps. on species included in this table correspond to the most informative ion chromatograms to be displayed for visual inspection and resolution of the overlapping compounds*

Informative marker	Ion species (m/z)		Overlapping compound	Ion species (m/z)	
3-Hydroxy isobutyric acid	177	233	3-Hydroxy butyric	191	233
4-Hydroxy butyric acid	204	233	Urea	189	204
Ethylmalonic acid	261	217	Phosphoric acid	299	314
3-Methylglutaconic acid (peak II)	273	198	3-Hydroxy adipic lactone	157	201
Hexanoylglycine	230	158	4-Hydroxy phenylacetic acid	281	296
Orotic acid	254	357	Cis-aconitic acid	229	375

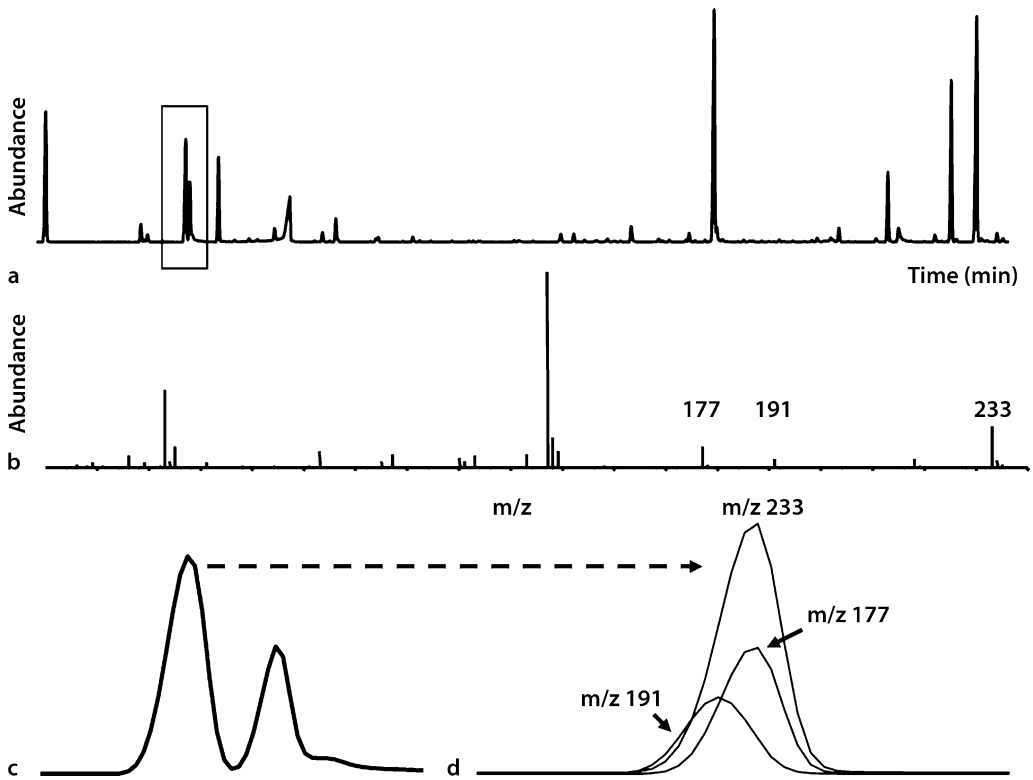

Fig. 3.1.8 Example of a postanalytical pitfall: GC-MS TIC profile showing coelution of 3-hydroxy isobutyric acid and 3-hydroxy butyric acid. **a** Complete organic acid profile; **b** Electron impact mass spectrum of coeluting peaks, showing the common [M-15]+ ion (m/z 233) and the unique fragments of 3-hydroxy isobutyric acid (m/z 177) and 3-hydroxybutyric acid (m/z 191); **c** magnification of the coeluting peaks (*boxed* in **a**) showing no distortion of peak shape, a finding that could lead to the assumption of no interference. **d** EIC showing partial but recognizable separation between the two isomers. Visual verification of the two ion chromatograms is recommended in all cases with an apparent increased excretion of 3-hydroxy butyric acid

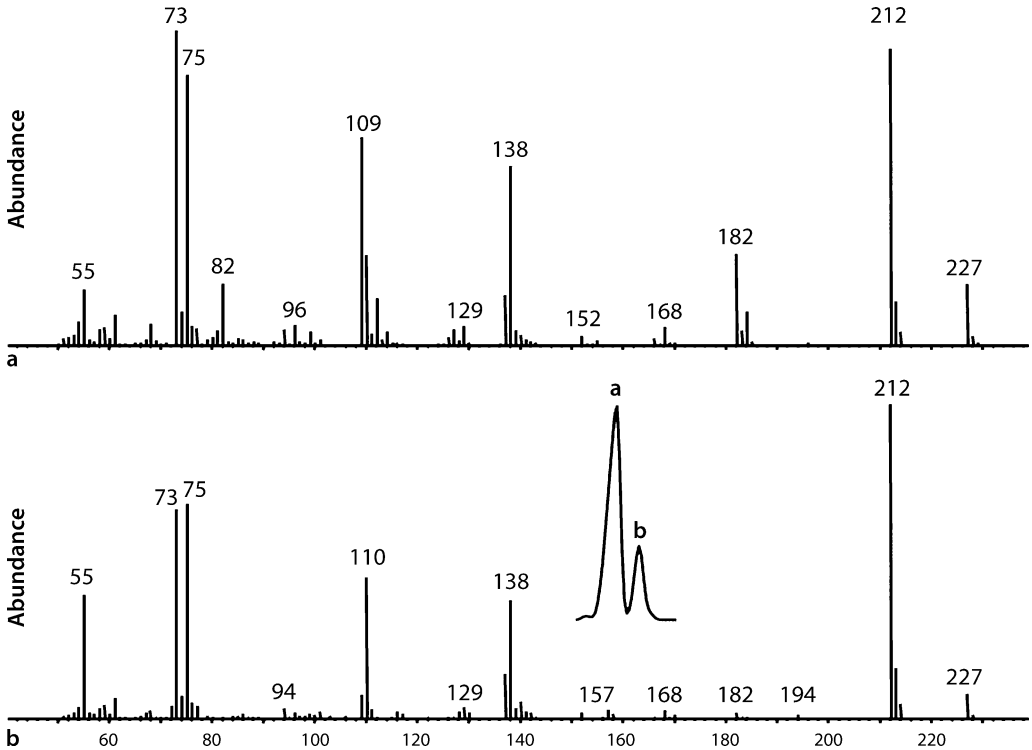

Fig. 3.1.9 Mass spectra of succinylacetone. **a,b** Peaks I and II, with oximation (reagent: hydroxylamine hydrochloride). The insert shows the characteristic appearance of the two chromatographic peaks [32]; **c–e** *see next page*

ample a report of dicarboxylic aciduria without mention of the presence or absence of concurrent ketonuria), but there is also the situation where all possible conditions are not included in the differential diagnosis because of a postanalytical oversight. For example, the presence of a large peak of ethylmalonic acid could be incorrectly attributed either to short-chain acyl-CoA dehydrogenase deficiency or to glutaric acidemia type II, an error that could be prevented by looking for small amounts of isobutyrylglycine and 2-methylbutyrylglycine, findings that suggest a diagnosis of ethylmalonic encephalopathy [32].

Unknown compounds are detected frequently, and laboratories eventually develop some level of comfort in recognizing them as artifacts that are not significant clinically, at least for the purpose of ruling out a possible inborn error of metabolism [21]. However, there are instances when an unknown compound is found in multiple specimens from the same patient and cannot be associated with ongoing drug and known dietary intake. This was the set of circumstances that led to the identification of 2-octenylsuccinic acid as the compound referred to by some laboratories as "pseudo-orotic acid" [11, 18]. On the other hand, the spectrum shown in Fig. 3.1.10, tentatively identified as 4-hydroxy 2-hexenoic acid by GC-MS/MS, belongs to a compound that appears in the urine of patients with disorders of propionate me-

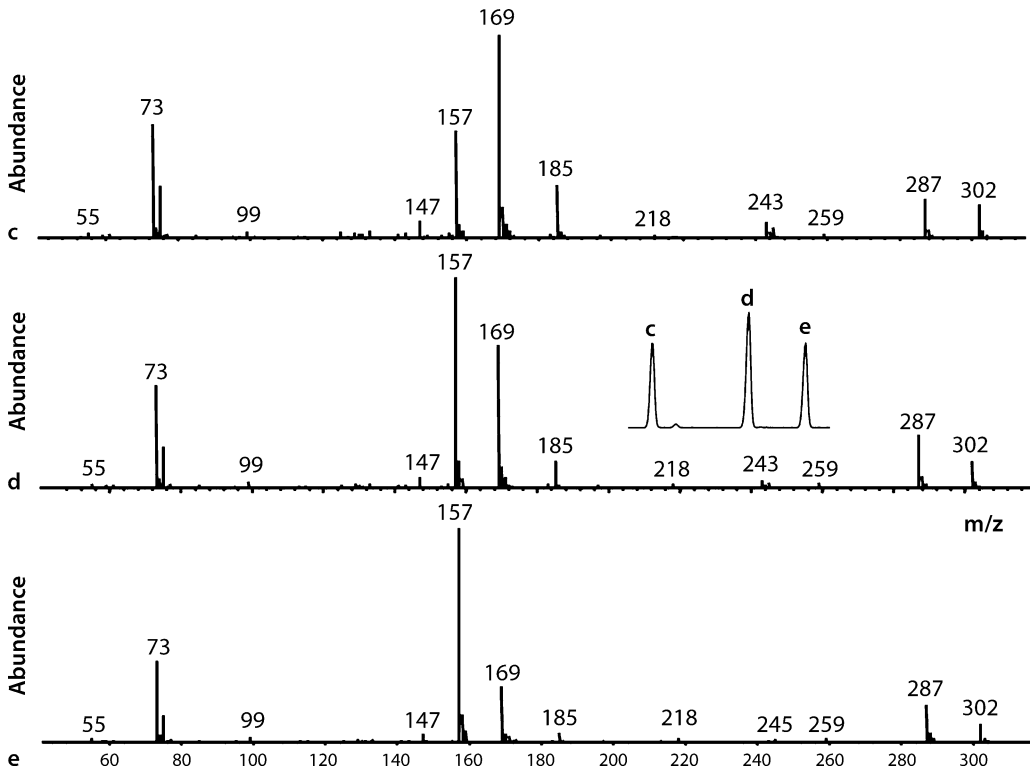

Fig. 3.1.9 (*continued*) **c–e,** peaks I–III without oximation; chromatographic separation shown in insert

tabolism when acutely ill. Likely to be a minor finding under those circumstances, this compound has been detected alone and in very large amounts in multiple urine specimens of a patient under evaluation for a possible, still unrecognized metabolic disorder (Ubaldo Caruso, Genova, Italy, personal communication).

Other pitfalls worth mentioning are the potential failure to recognize the multiple peaks of succinylacetone in a patient with tyrosyluria when oximation is not performed (Fig. 3.1.9) and the excretion of 2-cystein-S-yl-1,4-dihydroxycyclohex-5-en-1-yl) acetic acid (hawkinsin; Fig. 3.1.11), the biochemical marker of 4-hydroxyphenylpyruvate dioxygenase deficiency, a rare example of an autosomal dominant inborn error of metabolism [38]. This compound is another example of a past proficiency-testing challenge that resulted in a large number of incorrect responses. Therefore, it seems appropriate to include it in this chapter to facilitate its prospective recognition in clinical specimens.

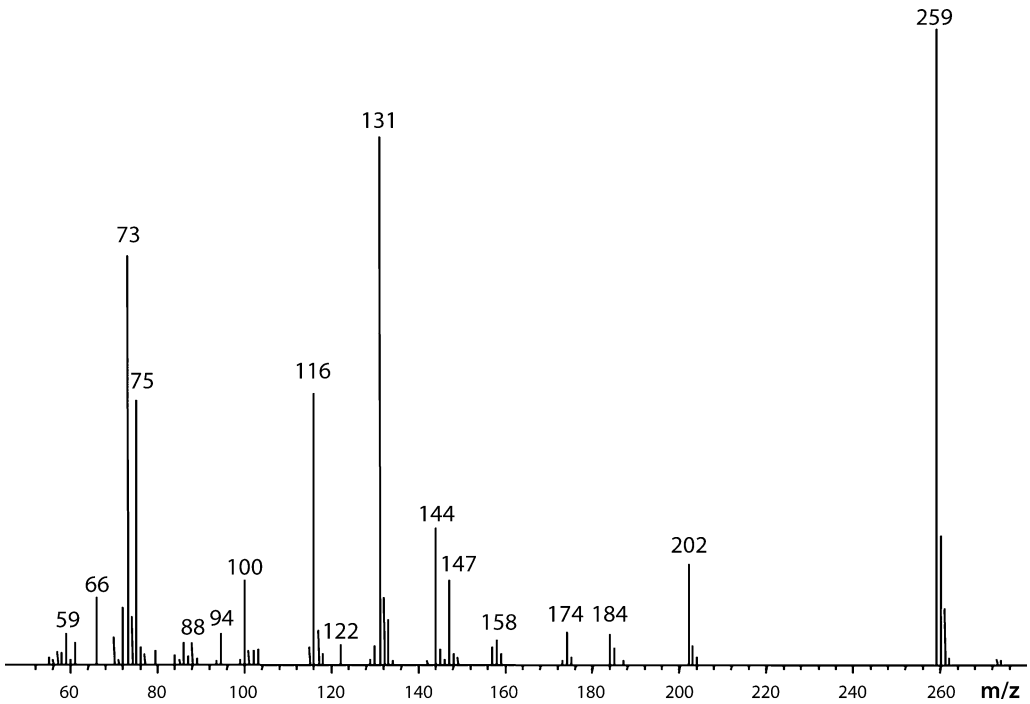

Fig. 3.1.10 Electron-impact mass spectrum of an unknown compound tentatively identified by GC-MS-MS as 4-hydroxy 2-hexenoic acid

References

1. Al-Dirbashi OY, Rashed MS, Brink HJ, Jakobs C, Filimban N, Al-Ahaidib LY, Jacob M, Al-Sayed MM, Al-Hassnan Z, Faqeih E (2006) Determination of succinylacetone in dried blood spots and liquid urine as a dansylhydrazone by liquid chromatography tandem mass spectrometry. J Chromatogr B 831:274–280
2. American College of Medical Genetics Standards and Guidelines for Clinical Genetics Laboratories: http://www.acmg.net/
3. Auray-Blais C, Giguere R, Lemieux B (2003) Newborn urine screening programme in the province of Quebec: an update of 30 years' experience. J Inherit Metab Dis 26:393–402
4. Baena B, Cifuentes A, Barbas C (2005) Analysis of carboxylic acids in biological fluids by capillary electrophoresis. Electrophoresis 26:2622–2636
5. Bartlett K, Gompertz D (1974) The specificity of glycine-N-acylase and acylglycine excretion in the organic acidaemias. Biochem Med 10:15–23
6. Bonafe L, Troxler H, Kuster T, Heizmann CW, Chamoles NA, Burlina AB, Blau N (2000) Evaluation of urinary acylglycines by electrospray tandem mass spectrometry in mitochondrial energy metabolism defects and organic acidurias. Mol Genet Metab 69:302–311
7. Boulat O, Gradwohl M, Matos V, Guignard JP, Bachmann C (2002) Organic acids in the second morning urine in a healthy Swiss paediatric population. Clin Chem Lab Med 41:1642–1658
8. CAP survey catalog web site: http://www.cap.org/apps/docs/proficiency_testing

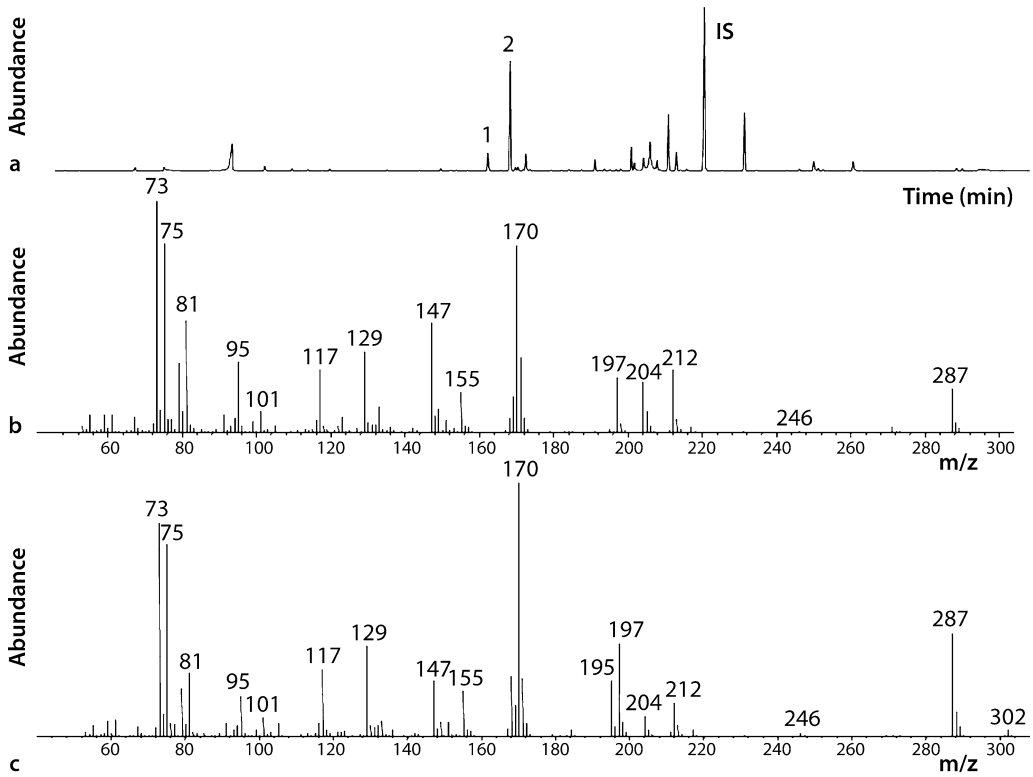

Fig. 3.1.11a GC-MS TIC organic acid profile of a patient with 4hydroxyphenylpyruvate dioxygenase deficiency (hawkinsinuria); **b,c** Electron impact mass spectra of two peaks of 2-cystein-S-yl-1,4-dihydroxycyclohex-5-en-1-yl) acetic acid

9. Chalmers RA, Lawson AM (1982) Organic Acids in Man: Analytical Chemistry, Biochemistry and Diagnosis of the Organic Acidurias. Chapman and Hall, London
10. Garcia A, Barbas C (2003) Capillary electrophoresis for the determination of organic acidurias in body fluids: a review. Clin Chem Lab Med 41:755–761
11. Giordano G, McMurray WJ, Previs SF, Welch RD, Rinaldo P (1990) Identification of 2-(2'-octenyl) succinic acid in urine. Rapid Commun Mass Spectrom 4:170–172
12. Goodman SI, Markey SP (1981) Diagnosis of Organic Acidemias by Gas Chromatography-Mass Spectrometry. Alan R. Liss, New York
13. Guneral F, Bachmann C (1994) Age-related reference values for urinary organic acids in a healthy Turkish pediatric population. Clin Chem 1994 40:862–866
14. Guth HJ, Zschiesche M, Panzig E, Rudolph PE, Jager B, Kraatz G (1999) Which organic acids does hemofiltrate contain in the presence of acute renal failure? Int J Artif Organs 22:805–810
15. Hoffman GF. Organic acid analysis. In: Blau N, Duran M, Blaskovics ME (eds) Physician's Guide to the Laboratory Diagnosis of Metabolic Diseases. Chapman Hall, London, pp 31–49
16. Hoffmann GF, von Kries R, Klose D, Lindner M, Schulze A, Muntau AC, Roschinger W, Liebl B, Mayatepek E, Roscher AA (2004) Frequencies of inherited organic acidurias and disorders of mitochondrial fatty acid transport and oxidation in Germany. Eur J Pediatr 163:76–80

17. Hori D, Hasegawa Y, Kimura M, Yang Y, Verma IC, Yamaguchi S (2005) Clinical onset and prognosis of Asian children with organic acidemias, as detected by analysis of urinary organic acids using GC/MS, instead of mass screening. Brain Dev 27:39–45
18. Kelley RI (1991) Octenylsuccinic aciduria in children fed protein-hydrolysate formulas containing modified cornstarch. Pediatr Res 30:564–569
19. Kroll CA, Magera MJ, Helgeson JK, Matern D, Rinaldo P (2002) A liquid chromatography-tandem mass spectrometry method for the determination of 5-hydroxyindole-3-acetic acid in urine. Clin Chem 48:2049–2051
20. Kuhara T (2002) Diagnosis and monitoring of inborn errors of metabolism using urease-pretreatment of urine, isotope dilution, and gas chromatography-mass spectrometry. J Chromatogr B 781:497–517
21. Kumps A, Duez P, Mardens Y (2002) Metabolic, nutritional, iatrogenic, and artifactual sources of urinary organic acids: a comprehensive table. Clin Chem 48:708–717
22. Kumps A, Vamos E, Mardens Y, Abramowicz M, Genin J, Duez P (2004) Assessment of an electron-impact GC-MS method for organic acids and glycine conjugates in amniotic fluid. J Inherit Metab Dis 27:567–579
23. Lehotay DC, Clarke JTR (1995) Organic acidurias and related abnormalities. Crit Rev Clin Lab Sci 32:377–429
24. Magera MJ, Helgeson JK, Matern D, Rinaldo P (2000) Methylmalonic acid measured in plasma and urine by stable-isotope dilution and electrospray tandem mass spectrometry. Clin Chem 46:1804–1810
25. Magera MJ, Thompson AL, Stoor AL, Helgeson JK, Matern D, Rinaldo P (2003) Determination of vanillylmandelic acid in urine by stable isotope dilution and electrospray tandem mass spectrometry. Clin Chem 49:825–826
26. Ohie T, Fu X, Iga M, Kimura M, Yamaguchi S (2000) Gas chromatography-mass spectrometry with tert.-butyldimethylsilyl derivation: use of the simplified sample preparations and the automated data system to screen for organic acidemias. J Chromatogr B Biomed Sci Appl 746:63–73
27. Pitt JJ, Eggington M, Kahler SG (2002) Comprehensive screening of urine samples for inborn errors of metabolism by electrospray tandem mass spectrometry. Clin Chem 48:1970–1980
28. Rashed MS, Aboul-Enein HY, Al-Amoudi M, Jakob M, Al-Ahaideb LY, Abbad A, Shabib S, Al-Jishi E (2002) Chiral liquid chromatography tandem mass spectrometry in the determination of the configuration of glyceric acid in urine of patients with D-glyceric and L-glyceric acidurias. Biomed Chromatogr 16:191–198
29. Rinaldo P, O'Shea JJ, Coates PM, Hale DE, Stanley CA, Tanaka K (1988) Medium-chain acyl-CoA dehydrogenase deficiency. Diagnosis by Stable-isotope dilution measurement of urinary *n*-hexanoylglycine and 3-phenylpropionylglycine. N Engl J Med 319:1308–1313
30. Rinaldo P, Yoon HR, Yu C, Raymond K, Tiozzo C, Giordano G (1999) Sudden and unexpected neonatal death: a protocol for the postmortem diagnosis of fatty acid oxidation disorders. Semin Perinatol 23:204–210
31. Rinaldo P, Coates PM, Vockley J (2005) In memoriam. Mol Genet Metab 86:335–336
32. Rinaldo P, Hahn SH, Matern D (2005) Inborn errors of amino acid, organic acid, and fatty acid metabolism. In: Burtis CA, Ashwood ER, Bruns DE (eds) Tietz Textbook of Clinical Chemistry and Molecular Diagnostics, 4th edn. Saunders, St. Louis, Missouri, pp 2207–2247
33. Sewell AC, Bohles HJ (1991) 4-Hydroxycyclohexanecarboxylic acid: a rare compound in urinary organic acid analysis. Clin Chem 37:1301–1302
34. Sims CJ, Fujito DT, Burholt DR, Dadok J, Giles HR, Wilkinson DA (1993) Quantification of human amniotic fluid constituents by high resolution proton nuclear magnetic resonance (NMR) spectroscopy. Prenat Diagn 13:473–480
35. Sweetman L (1991) Organic acid analysis. In: Hommes FA (ed) Techniques in Diagnostic Human Biochemical Genetics. Wiley-Liss, New York, pp 143–176
36. Tanaka K (1990) Isovaleric acidemia: personal history, clinical survey, and study of the molecular basis. Progr Clin Biol Res 321:273–290

37. Wajner M, Raymond K, Barschak A, Luft AP, Ferreira G, Domingues G, Chiochetta M, Sirtori L, Goulart L, Pulrolnik V, Pires R, Grillo E, Lohr A, Funayama C, Sanseverino MT, Longuercio-Leite JC, Coelho JC, Giugliani R, Regla-Vargas C (2002) Detection of organic acidemias in Brazil. Arch Med Res 33:581–585
38. Wilcken B, Hammond JW, Howard N, Bohane T, Hocart C, Halpern B (1981) Hawkinsinuria: a dominantly inherited defect of tyrosine metabolism with severe effects in infancy. N Engl J Med 305:865–868
39. Yamaguchi S, Kimura M, Iga M, Fu XW, Ohie T, Yamamoto T (1999) Automated, simplified GC/MS data processing system for organic acidemia screening and its application. Southeast Asian J Trop Med Publ Health 30:174–180

3.2 Acylcarnitines, Including In Vitro Loading Tests

Dietrich Matern

3.2.1 Introduction

Carnitine and its esters are physiologically present in all biological fluids, but carnitine is most abundant in tissues with high energy requirements, particularly skeletal and cardiac muscle [1]. Carnitine was discovered early in the last century by Gulewitsch and Krimberg when studying meat extracts [2]. Because its function was unknown, and considering the source of this compound, they suggested naming it "carnitine". The chemical structure was determined in 1927 [3] and in 1952 it was categorized as a B vitamin when studies in the meal worm *Tenebrio molitor* suggested a role of carnitine as a growth factor (Vitamin B_T) [4, 5].

In 1955, Fritz determined that carnitine plays an essential role in fatty acid β-oxidation (FAO), and in 1973 the first two clinically relevant disorders affecting this pathway were described: primary carnitine deficiency by Engel and Angelini, and carnitine palmitoyltransferase (CPT) type II (CPT-II) deficiency by DiMauro and DiMauro [6, 7]. To date, more than 20 different enzyme deficiency states affecting fatty acid transport and mitochondrial β-oxidation have been described [8] and additional enzymes involved in this pathway are still being discovered [9, 10].

Carnitine is not only involved in the metabolism of long-chain fatty acids, but also in branched-chain amino acid metabolism. Most of the classic organic acidurias resulting from defects in the latter metabolic pathway are associated with secondary carnitine deficiency. In fact, the clinical utility of acylcarnitine analysis was first identified for organoacidopathies such as propionic, methylmalonic, and isovaleric acidemias [11–16]. In these early studies, urine was the preferred specimen. However, plasma quickly became the specimen of choice because acylcarnitine profiles even in healthy probands are generally less complex in plasma than in urine, and because it was felt that the sensitivity of acylcarnitine analysis is higher when plasma is analyzed as opposed to urine, especially for the diagnosis of long-chain FAO disorders [17]. It is only recently that the analysis of urine has been revisited [18]. It now appears that urine acylcarnitine analysis can add diagnostic value to the metabolic work up of patients with organic acidemias but inconclusive or borderline abnormal urine organic acid and plasma acylcarnitine profiles [19–21].

Acylcarnitine analysis for the diagnosis of organic acidemias and particularly of FAO disorders plays an increasingly prominent role in all venues of clinical biochemical genetics: prenatal diagnosis, newborn screening, evaluation of symptomatic patients, and postmortem screening. Almost exclusively performed by tandem

mass spectrometry (MS/MS), plasma/serum is the primary specimen type in diagnostic settings. Blood dried on filter paper is analyzed for newborn screening and together with bile in the postmortem evaluation of cases of sudden and unexpected death [8, 22, 23]. Cell-free supernatant of amniotic fluid is used for the prenatal diagnosis of selected inborn errors of metabolism [24–27].

Cultured fibroblasts or amniocytes can be probed with FAO substrates and carnitine. Cell cultures deficient of an FAO enzyme will accumulate specific acylcarnitine species when incubated with substrates such as palmitate, allowing for the diagnosis of FAO disorders [28–37]. Modifications of this assay system have also been developed for the diagnosis of defects affecting the metabolism of branched-chain amino acids [20, 31, 34]. Recently, this approach was also adapted for the study of peripheral blood mononuclear cells [38].

Acylcarnitine analysis using stable-isotope-labeled internal standards provides quantitative data for acylcarnitine species [14]. However, to provide meaningful results to referring healthcare providers, it is critical to complement analytical proficiency with in-depth interpretation of results, as is true for many other examples of complex metabolic profiles [39].

3.2.2 Carnitine and Acylcarnitines

Carnitine, L-3-hydroxy-4-(trimethylammonium)butyrate, is a water-soluble, trimethylammonium derivative of γ-amino-β-hydroxybutyric acid, which is formed from trimethyllysine via γ-butyrobetaine [40]. About 75% of carnitine is obtained from dietary intake of meat, fish, and dairy products containing proteins with trimethyllysine residues. Under normal conditions, endogenous synthesis from lysine and methionine plays a minor role, but can be stimulated by a diet low in carnitine. Carnitine is not further metabolized and is excreted in urine and bile as free carnitine or as conjugated carnitine esters [1, 41, 42]. Adequate intracellular levels of carnitine are therefore maintained by mechanisms that modulate dietary intake, endogenous synthesis, reabsorption, and cellular uptake.

Under physiologic conditions, carnitine is primarily required to shuttle long-chain fatty acids across the inner mitochondrial membrane for FAO and products of peroxisomal β-oxidation to the mitochondria for further metabolism in the citric acid cycle [40, 43]. Acylcarnitines are formed by conjugating acyl-CoA moieties to carnitine, which in the case of activated long-chain fatty acids is accomplished by CPT type I (CPT-I) [8, 44]. The acyl-group of the activated fatty acid (fatty acyl-CoA) is transferred by CPT-I from the sulfur atom of CoA to the hydroxyl group of carnitine (Fig. 3.2.1). Carnitine acylcarnitine translocase (CACT) then transfers the long-chain acylcarnitines across the inner mitochondrial membrane, where CPT-II reverses the action of CPT-I by the formation of acyl-CoA and release of free unesterified carnitine.

In pathologic conditions, such as FAO disorders or organic acidemias due to acyl-CoA dehydrogenase deficiencies, the functions of carnitine as a regulator of substrate flux and energy balance across cell membranes and as a modulator of intracellular concentrations of free CoA become crucial. In such conditions, acyl-CoAs accumulate within the mitochondrial matrix and carnitine is utilized to shuttle these compounds out of the mitochondria as acylcarnitines, providing for free CoA at the same time.

Carnitine and its esters are present in all biological fluids, and depending on the enzyme defect, a particular acylcarnitine pattern becomes apparent where those acylcarnitine species serving as direct substrates for the defective enzyme accumulate disproportionately to the down- and upstream metabolites (Table 3.2.1).

3.2.3 Methods

Several techniques have been described to differentiate and eventually quantify specific carnitine esters. In 1977, Bieber and Choi demonstrated the presence of short-chain acylcarnitine species in several animal tissues by use of gas chromatography (GC) and mass spectrometry (MS) [45]. This approach was improved over time and as recently as 1997, new protocols for quantitative GC-MS analysis of acylcarnitines were published [46]. Additional methods described and which do not require volatile samples include thin-layer chromatography and radioisotopic exchange/high-performance liquid chromatography (HPLC) [47], as well as liquid-chromatography (LC)-MS. HPLC thermospray MS and fast atom bombardment-MS were first applied to acylcarnitine analysis by Alfred Yergey, David Millington, Charles Roe, and colleagues in the early 1980s [12, 48, 49]. This group later applied MS-MS to the analysis of selected amino acids [50], then to acylcarnitine analysis [51]. The advantage of MS-MS over other methods lies in its sensitivity, which allows for efficient preparation procedures of small sample volumes and fast analytical times, therefore providing for rapid throughput of even large numbers of samples. However, the significant cost and sophistication of MS-MS instruments delayed the adoption of this technology in other than highly specialized, often research laboratories. It was only in the late 1990s that instruments became commercially available that are affordable, robust, computer-driven, and increasingly user-friendly [52]. Today, acylcarnitines are analyzed by a large number of laboratories and for the most part by MS/MS. The

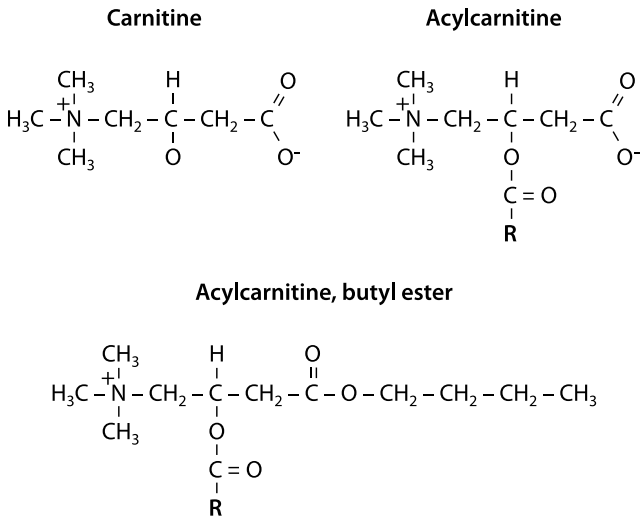

Fig. 3.2.1 Structures of carnitine, acylcarnitine and butylated acylcarnitine. The R represents the acylcarnitine species with up to 18 carbons, which are typically the aim of an acylcarnitine analysis

■ ***Table 3.2.1*** *Clinically relevant acylcarnitine species included in a typical acylcarnitine analysis and their relevance when abnormally elevated (unless otherwise noted).* BKT β-*ketothiolase,* CACT *carnitine-acylcarnitine translocase,* CPT *carnitine palmitoyltransferase,* DCR *24-dienoyl-CoA reductase,* EE *ethylmalonic encephalopathy,* FIGLU *formiminoglutamate,* GA-1 *glutaric acidemia type I (glutaryl-CoA dehydrogenase deficiency),* GA-2 *glutaric acidemia type II (multiple acyl-CoA dehydrogenase deficiency),* HMG *3-hydroxy 3-methylglutaryl-CoA lyase,* IBDH *isobutyryl-CoA dehydrogenase,* IVA *isovaleric acidemia (isovaleryl-CoA dehydrogenase deficiency),* LCHAD *long-chain 3-hydroxy acyl-CoA dehydrogenase,* MCAD *medium-chain acyl-CoA dehydrogenase,* MCC *3-methylcrotonyl-CoA carboxylase,* MCD *multiple carboxylase (holocarboxylase),* MGA *3-methylglutaconic aciduria type I (3-methylglutaconyl-CoA hydratase deficiency),* MKAT *medium-chain 3-ketoacyl-CoA thiolase,* MMA *methylmalonic acidemias,* MHBD *2-methyl 3-hydroxy butyryl-CoA dehydrogenase,* PA *propionic acidemia (propionyl-CoA carboxylase deficiency),* SBCAD *short-branched-chain acyl-CoA dehydrogenase,* SCAD *short-chain acyl-CoA dehydrogenase,* SCHAD *short-chain 3-hydroxy acyl-CoA dehydrogenase,* SUCLA2 *ATP-dependent-proteolysis-factor-forming succinyl-CoA synthetase,* TFP *mitochondrial trifunctional protein,* VLCAD *very long-chain acyl-CoA dehydrogenase*

Mass[a]	Acylcarnitine species		Disorder/ Condition
218	C0	Free carnitine	Carnitine supplementation (deficiency if low)
260	C2	Acetyl-	Carnitine supplementation or ketosis (deficiency if low)
274	C3	Propionyl-	PA, MMA, SUCLA2 deficiency [66], treatment with heptanoic acid [67]
287		FIGLU [64]	Glutamate formimino-transferase deficiency
288	C4	Butyryl-/ Isobutyryl-	SCAD deficiency, IBDH deficiency, GA-2, EE
300	C5:1	Tiglyl-	BKT deficiency, MCC deficiency, MHBD deficiency
302	C5	Isovaleryl-/ 2-Methylbutyryl-/ Pivaloyl-	IVA, SBCAD deficiency, GA-2, EE, antibiotics-derived artifact [60], treatment with heptanoic acid
304	C4-OH	3-Hydroxy butyryl-	SCHAD deficiency, ketosis
314	C6:1	3-Methylglutaconyl-	MGA
316	C6	Hexanoyl-	MCAD deficiency, MKAT deficiency, GA-2
318	C5-OH	3-Hydroxy isovaleryl-	Biotinidase deficiency, HMG deficiency, MCC deficiency, MCD deficiency, MGA deficiency
		2-Methyl 3-hydroxy butyryl-	BKT deficiency, MHBD deficiency
330	C7	Heptanoyl-	Treatment with heptanoic acid
342	C8	Octanoyl-	MCAD deficiency, M/SCHAD deficiency, MKAT deficiency, GA-2
360	C3-DC	Malonyl-	Malonic aciduria
	C8-OH	3-Hydroxy octanoyl-	MKAT deficiency
368	C10:2	Decadienoyl-	DCR deficiency
370	C10:1	Decenoyl-	MCAD deficiency
372	C10	Decanoyl-	MCAD deficiency, GA-2
374	C4-DC	Methylmalonyl-/succinyl	MMA[b], SUCLA2 deficiency [66]
388	C5-DC	Glutaryl-	GA-1
	C10-OH	3-Hydroxy decanoyl-	M/SCHAD deficiency, MKAT deficiency

■ ***Table 3.2.1*** (continued)

Mass[a]	Acylcarnitine species		Disorder
400	C12	Dodecanoyl-	GA-2
402	C6-DC	3-Methylglutaryl-	HMG deficiency
416	C12-OH	3-Hydroxy dodecanoyl-	LCHAD/TFP deficiency
424	C14:2	Tetradecadienoyl-	
426	C14:1	Tetradecenoyl-	CACT deficiency, CPT type II deficiency, GA-2, VLCAD deficiency, LCHAD/TFP deficiency
428	C14	Myristoyl-	CACT deficiency, CPT type II deficiency, GA-2, VLCAD deficiency, LCHAD/TFP deficiency
444	C14-OH	3-Hydroxy tetradecanoyl-	LCHAD/TFP deficiency
456	C16	Palmitoyl-	CACT deficiency, CPT type II deficiency, VL-CAD deficiency, LCHAD/TFP deficiency; CPT type I deficiency[c]
470	C16:1-OH	3-Hydroxy hexadecenoyl-	Antibiotics derived artifact [63]
472	C16-OH	3-Hydroxy hexadecanoyl-	LCHAD/TFP deficiency
480	C18:2	Linoleyl-	CACT deficiency, CPT type II deficiency, VLCAD deficiency, LCHAD/TFP deficiency
482	C18:1	Oleyl-	CACT deficiency, CPT type II deficiency, VLCAD deficiency, LCHAD/TFP deficiency; CPT type I deficiency[c]
484	C18	Stearoyl-	CACT deficiency, CPT type II deficiency, VLCAD deficiency, LCHAD/TFP deficiency
498	C18:1-OH	3-Hydroxy oleoyl-	LCHAD/TFP deficiency
500	C18-OH	3-Hydroxy stearoyl-	LCHAD/TFP deficiency

[a] Mass of the molecular ion of the butylated acylcarnitine esters
[b] Respective analyte is not consistently elevated in MMA
[c] CPT type I is suggested by low concentrations of long-chain acylcarnitine species and relatively high free carnitine

primarily used instruments are triple quadrupole analyzers combined with electrospray ionization (ESI) sources. With ESI-MS/MS, the liquid sample is introduced into the ion source through a capillary tube and exposed to a strong electric field and a counter flow of nitrogen gas, which in combination produce the electrospray (see Chap. 8.1). The solvent evaporates and eventually desorption of charged ions occurs into the mass analyzer. ESI occurs under atmospheric pressure, allowing efficient ionization, and the mass analyzers operate at very low pressure. The combination is possible by introducing the ions into the analyzers through a very small orifice (< 1 mm) and using powerful vacuum pumps.

This chapter focuses on acylcarnitine analysis in various sample types following derivatization to butyl- or methylesters and flow injection ESI-MS/MS. Capillary electrophoresis MS/MS and LC-MS/MS methods have also been described in recent years with the noted benefits of isomer separation and further simplification of the sample preparation steps, although at the cost of larger sample volume requirements and longer analytical times [53, 54].

3.2.4 Acylcarnitine Analysis of Plasma or Serum by MS/MS

3.2.4.1 Principle

Acylcarnitines are extracted from the sample by mixing with methanol or an acidified acetonitrile solution containing isotopically labeled acylcarnitines of various chain lengths at defined concentrations as internal standards. Following centrifugation, the supernatant is evaporated and the residue derivatized with either *n*-butanol HCl or *n*-methanol HCl, yielding the acylcarnitines for analysis by flow injection ESI/MS-MS. Following analysis, a graphical acylcarnitine profile is generated by the software provided by the MS-MS vendor, which can be interpreted qualitatively. Additional vendor-provided software allows semiquantitative calculation of the concentration of each individual acylcarnitine species based on the abundance of the assigned internal standard.

3.2.4.2 Pre-analytical

Specimen

A variety of body fluids can be used for acylcarnitine analysis. While initially the favored specimen, urine acylcarnitine analysis is the least appropriate when an FAO disorder is under diagnostic consideration. Heparinized plasma or whole blood spotted on filter paper are preferred in this context.

Most informative results are generally achieved when samples are obtained during acute illness. Because inborn errors of metabolism are traditionally not entered early into differential diagnostic considerations, sample collection should alternatively be timed before a meal, preferably after an overnight fast. A prolonged fasting challenge, however, should not routinely be undertaken, as these require close surveillance typically not possible in an outpatient setting.

All sample types, except for dried blood and bile spots (which can be sent at room temperature), should be kept frozen until analysis. Reliable results, particularly for short-chain acylcarnitine species, for any sample, liquid or dried on filter paper, can not be achieved following long-term storage at ambient temperatures [55].

Reagents and Chemicals

Standards

The following standards are used in our laboratory:

1. Acetylcarnitine (C_2).
2. Propionylcarnitine (C_3).
3. Butyrylcarnitine ($_{C4}$).
4. Isovalerylcarnitine (C_5).
5. Hexanoylcarnitine (C_6).
6. Octanoylcarnitine (C_8).
7. Decanoylcarnitine (C_{10}).
8. Dodecanoylcarnitine (C_{12}).
9. Tetradecanoylcarnitine (C_{14}).
10. Hexadecanoylcarnitine (C_{16}).
11. Octadecanoylcarnitine (C_{18}).

Isotopically labeled standards (internal standards) include:

1. Acetyl-d^3-carnitine (C_2).
2. Propionyl-d^3-carnitine (C_3).
3. Butyryl-d^3-carnitine (C_4).
4. Octanoyl-d^3-carnitine (C_8).
5. Dodecanoyl-d^3-carnitine (C_{12}).
6. Palmitoyl-d^3-carnitine (C_{16}).

The internal standards are dissolved in methanol. The final working internal standard solution is prepared in acetonitrile at the following concentrations:

1. 1.330 µmol/l acetyl-d^3-carnitine.
2. 0.266 µmol/l propionyl-d^3-carnitine.
3. 0.266 µmol/l butyryl-d^3-carnitine.
4. 0.266 µmol/l octanoyl-d^3-carnitine.
5. 0.266 µmol/l dodecanoyl- d^3-carnitine.
6. 0.543 µmol/l palmitoyl-d^3-carnitine.

Additional or different internal standards can be used. Labeled and unlabeled acylcarnitine standards are available from Dr. Herman J. ten Brink, VU University Medical Center, Amsterdam, The Netherlands (http://www.vumc.nl/metabool/index.html) or from Cambridge Isotope Laboratories, Andover, Massachusetts, USA (http://www.isotope.com).

1. 3N HCl in *n*-butanol (butanolic-HCl; # 201009, Regis Chemical, Morton Grove, IL, USA)
2. Methanol

3. 80% Acetonitrile:water [1].
4. Nitrogen gas, in-house, scrubbed with the Big Hydrocarbon Trap (BHT)-1 (Chrom Tech, Apple Valley, MN, USA).
5. Air, compressed.
6. Air, zero grade (filtered by a Balston filter unit).
7. Formic acid, 98–100%.

Equipment and Supplies

1. Pierce Reacti-Therm heating module.
2. Pierce Reacti-Vap evaporating unit.
3. Chrom Tech React vials, #402001.
4. 1-ml Screw-cap micro vial, Chrom Tech.
5. Thermolyne MaxiMix 2 Type 37600 vortex mixer.
6. Centrifuge, Abbott, #3531 X Systems.
7. 1.5-ml Micro tube, Sarstedt, 39 × 10 mm.
8. Autosampler vials, Fisher #0334064.
9. Autosampler caps, Fisher #0337749.
10. Applied Biosystems/MDS SCIEX API 3000 MS-MS system.
11. PE Series 200 isocratic LC pump.
12. PE Series 200 LC autosampler.
13. 0.5-U Peek filter end fitting, Chrom Tech A-428X.
14. 0.5-U filters, Chrom Tech A-431.
15. Back pressure column, BDS Hypersil C18, 3 µm, 50 × 1, Keystone Scientific, #053-46-1.

Calibration

Mass calibration of the quadrupole mass spectrometers, Q1 and Q3, is based on poly(propylene)glycol in methanol as supplied by the instrument manufacturer and following instructions on calibration and tuning provided in the instrument operating manual.

QC

Quality Control Samples

A quality control (QC) standard mixture, a normal control and an abnormal control are run with each batch. The normal control is made by aliquoting 100-µl portions of a normal range pooled plasma into screw-cap vials. The abnormal control is made by spiking 50 ml of normal pooled plasma with defined concentrations of unlabeled acylcarnitine standards spanning the mass range covered by the analysis (see Reagents and Chemicals). The concentration for each standard should be chosen based on the upper limit of the reference range for the respective acylcarnitine species. The

1 Use of reverse osmosis or HPLC grade water in every step requiring water is recommended.

100-µl portions are aliquotted into screw-cap vials and stored frozen. The mean and standard deviation for each QC sample is calculated with a minimum of 20 between-run values.

In our laboratory, control values that fall within ±2 standard deviations of the mean are considered acceptable and require no further action. Any control values that are either greater than 2 standard deviations or trends require review by a laboratory director. The laboratory director decides whether the analysis of the complete batch or of specific samples needs to be repeated and initiates troubleshooting.

3.2.4.3 Analytical

Sample Preparation

Formic acid is added to the working internal standard solution to achieve a concentration of 0.3% formic acid. Aliquots of 300 µl are then pipetted into labeled Eppendorf tubes before 20 µl of thawed plasma sample is added. After thorough vortexing and centrifugation for 2 min at 13,000 rpm (11,337 × *g*), the supernatant is transferred to clean Reacti-Vials and dried under a gentle stream of warm nitrogen. The samples are then derivatized to butylesters by the addition of 100 µl 3N butanol-HCl and heating at 65°C in a Reacti-Therm system for 15 min. The vials are allowed to cool before they are again dried down under warm nitrogen. The dried samples are redissolved in 100 µl of 80% acetonitrile:water and briefly vortexed. After transfer of the solution to LC autosampler vials, the samples are ready for MS-MS analysis, which should proceed promptly. If necessary, prepared samples can be stored refrigerated for up to 24 h prior to analysis.

Instrument Setup

LC system

Controlled by the MS-MS software, the PE Series 200-micro LC pump operates isocratically using 80% acetonitrile:water at 40 µl/min. A 50 × 1 mm C18 column (Keystone) is used between the pump and autosampler to provide back-pressure. The syringe/system flush solution is the 80% acetonitrile:water used as the mobile phase. The autosampler is connected directly to the MS-MS TurboIon Spray source. The injected sample volume is 20 µl.

A 0.5-U Peek filter is installed between the autosampler and TurboIon Spray APCI electrospray interface source. The filter end fitting is discarded and replaced after approximately 200 injections.

MS-MS system

Acylcarnitine analysis is performed as a precursor scan in positive ion mode. Q1 is set to scan a mass range from m/z 200 to 500, while Q3 is set to determine a precursor ion of m/z 85. The method is optimized for a mixture of butylesters containing d^3-C_2, d^3-C_3, d^3-C_4, d^3-C_8, d^3-C_{12}, and d^3-C_{16} acylcarnitine.

The sample queue is entered into the MS-MS instrument's software (Analyst for SCIEX instruments) according to the manufacturer's instructions. Samples can be

given specific designations that allow for the correct QC and reference range assignment. Prior to analysis, the method should be equilibrated and the system purged if necessary. The LC line should be attached to the sprayer after proper equilibration for approximately 30 min.

Calculation

A datafile is generated for each sample and presented as a mass profile. All ion species in a mass range from 200 to 500 Da that generate a product m/z of 85 Da are represented in this profile based on their detected abundance.

Calculation of the molecular weights of the *n*-butyl esters of acylcarnitines, expressed as $(M+H)^+$ molecular ions, allows the designation of each peak (Table 3.2.1). Quantitation software provided by the instrument vendor (i.e., Chemoview for SCIEX instruments) allows calculation of quantitative and semiquantitative concentrations for these acylcarnitines by comparison of the detected abundance of each acylcarnitine versus that of a designated internal standard with a known concentration. The results for each sample are further compared to age-appropriate reference ranges (Table 3.2.2).

3.2.4.4 Post-analytical: Interpretation and Reference Ranges

The laboratory director, typically a board-certified clinical biochemical geneticist, reviews all profiles and provides an interpretation based on pattern recognition and not simply on single abnormal values (Table 3.2.2). The laboratory director also determines the need for sample dilutions and carryover checks.

Simple reporting of numeric results is not appropriate because most physicians are not familiar with pattern recognition. A comprehensive interpretation takes into consideration any available clinical and dietary information and other laboratory results, provides possible differential diagnoses, recommendations for additional biochemical testing and confirmatory studies if indicated, as well as contact information for the laboratory director in case the referring physician has additional questions.

3.2.4.5 Pitfalls

Acylcarnitine profiles are dependent on the clinical status of the patient at the time of sample collection [56, 57]. It is therefore important to provide the biochemical genetics laboratory with information regarding the clinical context during which the sample was collected. The laboratory must be conscientious of the fact that carnitine deficiency states can be associated with acylcarnitine profiles that lack any acylcarnitine species that are elevated above the reference range. Therefore, it is essential that the complete profiles are reviewed and even borderline elevated acylcarnitines should prompt further follow up in the presence of abnormally low free acetylcarnitine (Fig. 3.2.2). If clinically indicated, a repeat sample should be collected at least 24 h after L-carnitine supplementation.

Table 3.2.2 *Reference ranges for plasma acylcarnitine species (µmol/l) in different age groups*

Acylcarnitine species	≤7 days (*n* = 36)	8 days–7 years (*n* = 139)	>7 years (*n* = 140)
C0	6.08–22.21	6.29–27.73	5.55–20.88
C2	2.14–15.89	2.00–27.57	2.00–17.83
C3	0.07–0.54	0.08–1.77	0.10–0.87
C4	0.06–0.45	0.06–1.05	0.04–0.82
C5:1	0.00–0.04	0.00–0.10	0.00–0.10
C5	0.06–0.37	0.05–0.62	0.06–0.50
C4-OH	0.01–0.12	0.01–0.50	0.01–0.17
C6	0.01–0.13	0.01–0.22	0.02–0.16
C5-OH	0.01–0.07	0.01–0.11	0.00–0.09
C7	0.00–0.04	0.00–0.04	0.00–0.05
C6-OH	0.00–0.07	0.00–0.18	0.00–0.08
C8:1	0.03–0.47	0.02–0.90	0.04–0.87
C8	0.03–0.18	0.01–0.44	0.02–0.77
C3-DC	0.01–0.08	0.00–0.13	0.00–0.25
C10:2	0.01–0.10	0.00–0.11	0.00–0.25
C10:1	0.03–0.24	0.01–0.45	0.03–0.46
C10	0.02–0.26	0.02–0.90	0.03–0.87
C4-DC	0.00–0.04	0.00–0.04	0.00–0.04
C10:1-OH	0.00–0.11	0.00–0.11	0.00–0.12
C5-DC	0.00–0.05	0.00–0.09	0.00–0.10
C12:1	0.01–0.18	0.00–0.36	0.00–0.34
C12	0.02–0.17	0.02–0.34	0.01–0.25
C12:1-OH	0.00–0.06	0.00–0.05	0.00–0.08
C12-OH	0.00–0.05	0.00–0.08	0.00–0.07
C14:2	0.01–0.08	0.01–0.12	0.01–0.17
C14:1	0.00–0.15	0.01–0.34	0.00–0.23
C14	0.01–0.10	0.01–0.14	0.00–0.11
C14:1-OH	0.01–0.05	0.00–0.17	0.00–0.12
C14-OH	0.00–0.03	0.00–0.04	0.00–0.07
C16:1	0.01–0.14	0.00–0.20	0.00–0.09
C16	0.06–0.35	0.04–0.51	0.03–0.22
C16:1-OH	0.00–0.77	0.00–0.35	0.00–0.05
C16-OH	0.00–0.09	0.00–0.06	0.00–0.05
C18:2	0.01–0.11	0.00–0.30	0.02–0.23

■ ***Table 3.2.2*** (continued) *Reference ranges for plasma acylcarnitine species (μmol/l) in different age groups*

Acylcarnitine species	≤ 7 days ($n = 36$)	8 days–7 years ($n = 139$)	> 7 years ($n = 140$)
C18:1	0.02–0.24	0.03–0.44	0.02–0.38
C18	0.01–0.09	0.01–0.11	0.01–0.13
C18:2-OH	0.00–0.03	0.00–0.05	0.00–0.05
C18:1-OH	0.00–0.02	0.00–0.03	0.00–0.05
C18-OH	0.00–0.02	0.00–0.04	0.00–0.02

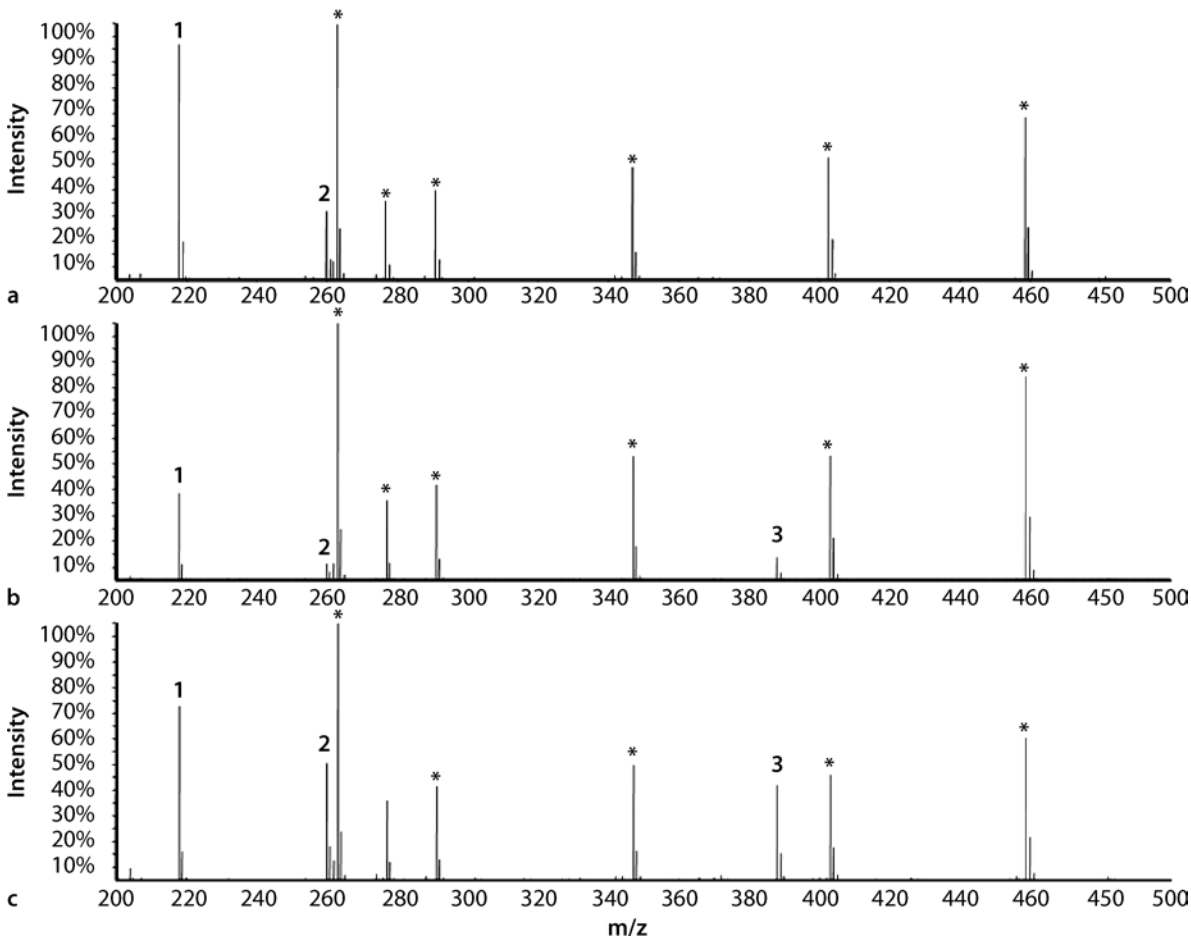

Fig. 3.2.2 Profiles of acylcarnitines as their butyl esters in plasma (precursor of m/z 85 scan) of a normal control (**a**), a patient with glutaric acidemia type I and low carnitine levels (**b**), and a patient with glutaric acidemia type I and normal carnitine status (**c**). *Peak 1* free carnitine (m/z 218), *peak 2* acetylcarnitine (C_2; m/z 260), *peak 3* glutarylcarnitine (C_5-DC; m/z 388). The *asterisks* represent the internal standards (from left to right): d^3-acetylcarnitine (C_2; m/z 263), d^3-propionylcarnitine (C_3; m/z 277), d^3-butyrylcarnitine (C_4; m/z 291), d^3-octanoylcarnitine (C_8; m/z 347), d^3-dodecanoylcarnitine (C_{12}; m/z 403), and d^3-palmitoylcarnitine (C_{16}; m/z 459)

While MS-MS allows for unequivocal identification of most metabolites, there are a few exceptions. In particular, the short-chain acylcarnitines of 4 and 5 carbons represent more than one analyte. C_4-Acylcarnitine is known to be a mixture of butyrylcarnitine derived from fatty acid metabolism and isobutyrylcarnitine derived from the metabolism of valine (Fig. 3.2.3) [21, 58]. C_5-Acylcarnitine is a mixture of isovalerylcarnitine and 2-methylbutyrylcarnitine derived from leucine and isoleucine degradation, respectively (Fig. 3.2.4) [20, 59]. Samples of patients treated with antibiotics containing pivalic acid may contain pivaloylcarnitine another C_5 species

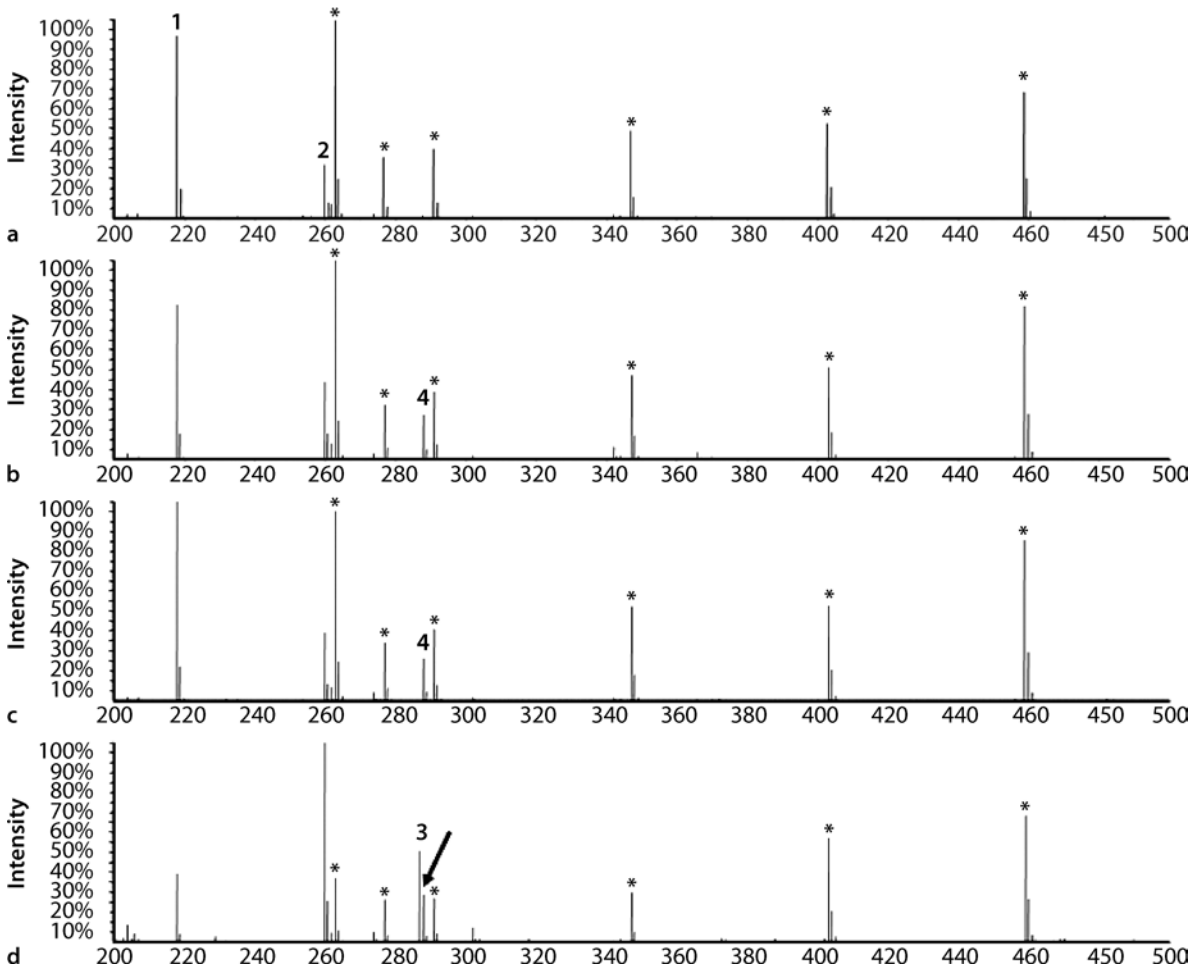

Fig. 3.2.3 Profiles of acylcarnitines as their butyl esters in plasma (precursor of m/z 85 scan) of a normal control (**a**) and three patients with elevated C_4-acylcarnitine (m/z 288; peak 4) that represents primarily butyrylcarnitine in a patient with short-chain acyl-CoA dehydrogenase (SCAD) deficiency (**b**), isobutyrylcarnitine in a patient with isobutyryl-CoA dehydrogenase (IBDH) deficiency (**c**), and a natural isotope of formiminoglutamate (FIGLU; m/z 287; peak 3) in a patient with glutamate formimino-transferase deficiency (**d**). *Peak 1* free carnitine (m/z 218), *peak 2* acetylcarnitine (C_2; m/z 260). The *asterisks* represent the internal standards (from left to right): d^3-acetylcarnitine (C_2; m/z 263), d^3-propionylcarnitine (C_3; m/z 277), d^3-butyrylcarnitine (C_4; m/z 291), d^3-octanoylcarnitine (C_8; m/z 347), d^3-dodecanoylcarnitine (C_{12}; m/z 403), and d^3-palmitoylcarnitine (C_{16}; m/z 459)

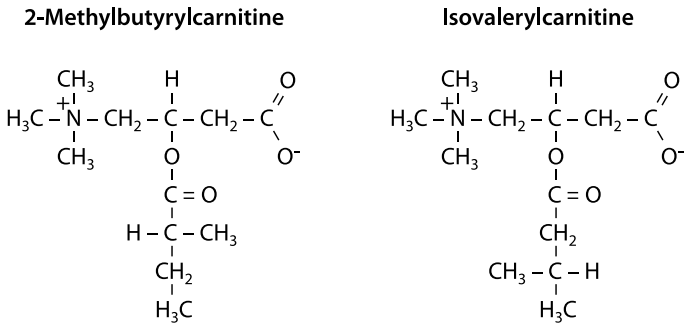

Fig. 3.2.4 Structures of the isomers 2-methylbutyryl- and isovalerylcarnitine. These isomers can not be differentiated by acylcarnitine analysis as described here because both appear as butylated C_5-acylcarnitine esters at m/z 302. Differentiation would require an additional chromatography step prior to tandem mass spectrometry analysis

[60]. Differentiation is of clinical importance and most efficiently achieved by urine acylglycine and organic acid analyses. Patients with short-chain acyl-CoA dehydrogenase (SCAD) deficiency, for example, will reveal an abnormal excretion of ethylmalonic acid, suggesting that an elevated C_4-acylcarnitine represents primarily butyrylcarnitine. Patients with isobutyryl-CoA dehydrogenase deficiency, on the other hand, will demonstrate an elevated C_4-acylcarnitine in plasma and urine and either normal acylglycines or an elevated excretion of isobutyrylglycine [21]. The detection of an overexcretion of either isovalerylglycine or 2-methylbutyrylglycine will determine the origin of a C_5-acylcarnitine elevation as either due to isovaleric acidemia or 2-methylbutyrylglycinuria as opposed to an antibiotics-derived artifact [59].

Several other metabolites are also nonspecific markers for several disorders. For example, C5-OH acylcarnitine, which represents 3-hydroxy isovalerylcarnitine and 2-methyl 3-hydroxybutyrylcarnitine, can be elevated in seven different organic acidemias (Table 3.2.1; Fig. 3.2.5). The interpretation of elevated C5-OH acylcarnitine in newborns or breast-fed infants is further complicated by the fact that it can indicate maternal 3-methylcrotonylglycinuria in an unaffected carrier infant [61].

The long-chain FAO disorders of CACT deficiency and CPT-II deficiency can not be differentiated because both cause accumulation of the same long-chain acylcarnitine species, which is explained by the fact that neither enzyme is involved in the chain-shortening action of FAO (Table 3.2.1; Fig. 3.2.6e and f). Isolated long-chain 3-hydroxy acyl-CoA dehydrogenase (LCHAD) deficiency and complete mitochondrial trifunctional protein (TFP) deficiency also can not be differentiated by routine acylcarnitine analysis [55, 57, 62]. When such profiles are encountered, delineation of the correct defect is only possible by either specific enzyme assay in cell cultures or molecular genetic analysis of the relevant genes, the latter of which is often only available in research laboratories. Isolated elevations of propionylcarnitine (C_3) are not specific for propionic acidemia, but are also observed in methylmalonic acidemias of various etiologies (Table 3.2.1; Fig. 3.2.5b and c). Because methylmalonylcarnitine (C_4-DC) is not consistently elevated in methylmalonic acidemias, elucidation of the correct diagnosis requires at a minimum, urine organic acid analysis.

Another antibiotic that may cause problems in the interpretation of butylated acylcarnitines is cefotaxime (Fig. 3.2.5d) [63]. This antibiotic, or metabolites thereof, reveals itself by acylcarnitine analysis at m/z 470, which is otherwise considered to represent the monounsaturated form of 3-hydroxy hexadecenoylcarnitine ($C_{16:1}$-OH). In poorly resolved scans this may be difficult to differentiate from m/z 472, which is a marker for LCHAD and TFP deficiencies. However, whereas m/z 472 (C_{16}-OH) is more abundant than $C_{16:1}$-OH in these FAO disorders, the profile of a patient treated with cefotaxime usually reveals an m/z 470 to m/z 472 ratio that is greater than 1. Furthermore, and in contrast to cefotaxime treatment, both LCHAD and TFP deficiencies are usually accompanied by elevations of other long-chain species (Table 3.2.1) [57].

Formiminoglutamate (FIGLU), a marker for glutamate formimino-transferase deficiency, was recently also shown to be detectable by acylcarnitine analysis; represented as a peak with m/z 287 (Fig. 3.2.3d) [64]. In poorly resolved acylcarnitine profiles, this peak may be confused with iso-/butyrylcarnitine (m/z 288). To avoid the incorrect interpretation of acylcarnitine profiles, we recommend performing the analysis in product scan mode as opposed to multiple reaction monitoring (MRM) mode. For example, the FIGLU peak at m/z 287 would not have been correctly identified in MRM mode because the transition of 287 to 85 is typically not selected. However, the 288/85 transition would reveal abnormal results, but in fact not represent either butyryl- or isobutyrylcarnitine, but another FIGLU related ion species.

3.2.5 Acylcarnitine Analysis in Urine by MS/MS

3.2.5.1 Principle

Acylcarnitine analysis was first performed in urine specimens in the evaluation of patients with organic acidemias. However, because it was found that acylcarnitine analysis of plasma is more informative for the diagnosis of FAO disorders than analysis of urine specimens, plasma has become the preferred specimen [17]. It is only recently that it was shown that urine acylcarnitine analysis still has a role in the diagnostic evaluation of patients with organic acidurias but uninformative or borderline abnormal results of plasma acylcarnitine and urine organic acid analysis [18–21]. In our laboratory, sample preparation and analysis is identical to that of plasma once a urine aliquot has been prepared that is based on the creatinine concentration.

3.2.5.2 Specimen

Urine is collected from patients suspected to have an organic acidemia preferably during an acute metabolic decompensation. As this is often not possible, an early morning specimen should be collected. The sample should be sent frozen and without preservatives.

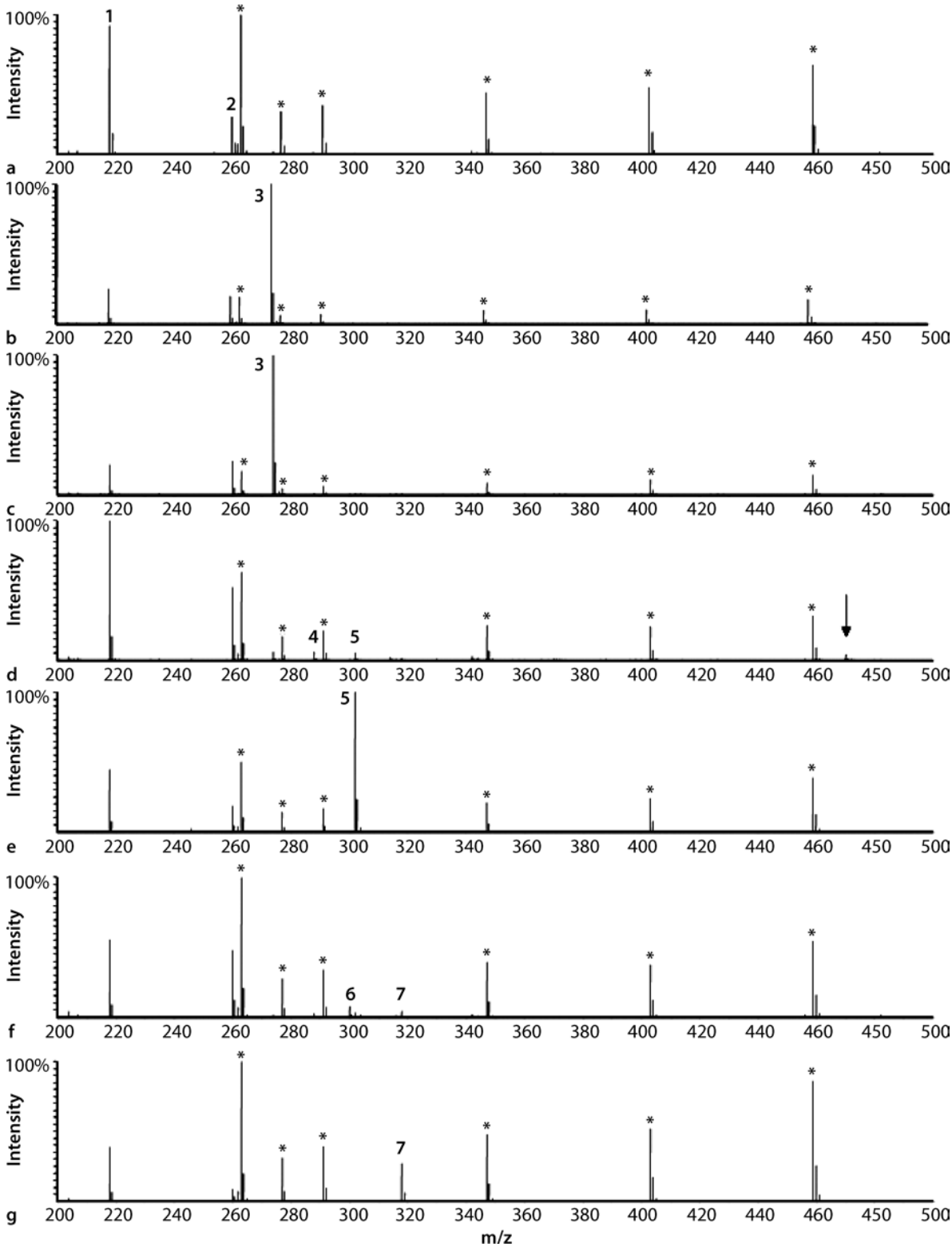
100%
Intensity
a
b
c
d
e
f
g
200 220 240 260 280 300 320 340 360 380 400 420 440 460 450 500
m/z

◄ **Fig. 3.2.5** Profiles of acylcarnitines as their butyl esters in plasma (precursor of m/z 85 scan) of a normal control (**a**) and patients with various organic acidemias. Propionylcarnitine (C_3; m/z 274; peak 3) is the primary marker for both propionic acidemia (**b**) and methylmalonic acidemias (**c**). Note that an elevation of methylmalonylcarnitine (C_4-DC; m/z 374) is not typically found in patients with methylmalonic acidemias. In the three cases of ethylmalonic encephalopathy (**d**) analyzed in our laboratory, elevations of C_4- (m/z 288; peak 4) and C_5-acylcarnitine (m/z 302; peak 5) species were noted. Isolated C_5-acylcarnitine elevations are encountered in patients with isovaleric acidemia (**e**), where it represents isovalerylcarnitine. C_5-Acylcarnitine is also elevated in patients with short/branched chain acyl-CoA dehydrogenase deficiency, where it represents 2-methylbutyrylcarnitine (see Fig. 3.2.4), and in patients treated with antibiotics that contain pivalic acid, where it represents pivaloylcarnitine [20, 59, 60]. Patients with β-ketothiolase deficiency (**f**) present with elevations of tiglylcarnitine ($C_{5:1}$; m/z 300; peak 6) and C_5-OH acylcarnitine (m/z 318; peak 7). In most cases of 3-methylcrotonyl-CoA carboxylase deficiency (**g**) C_5-OH acylcarnitine is the only abnormal acylcarnitine species present. The differential diagnosis of C_5-OH acylcarnitine elevations includes eight different conditions (Table 3.2.1). Also note that C_5-OH acylcarnitine represents 3-hydroxy isovalerylcarnitine in 3-methylcrotonyl-CoA carboxylase deficiency (**g**), and 2-methyl 3-hydroxy butyrylcarnitine in β-ketothiolase deficiency (**f**). The arrow in D represents an artifact at m/z 470 (the same mass as $C_{16:1}$-OH acylcarnitine) secondary to the patient being treated with cefotaxime [63]. The asterisks represent the internal standards (from left to right): d^3-acetylcarnitine (C_2; m/z 263), d^3-propionylcarnitine (C_3; m/z 277), d^3-butyrylcarnitine (C_4; m/z 291), d^3-octanoylcarnitine (C_8; m/z 347), d^3-dodecanoylcarnitine (C_{12}; m/z 403), and d^3-palmitoylcarnitine (C_{16}; m/z 459)

3.2.5.3 Procedure and Calculation

The creatinine concentration is measured in the sample using routine methods (i.e., the Jaffe reaction). A urine volume equivalent to 0.25 mg creatinine is diluted to 300 µl with deionized water (if the creatinine equivalent exceeds 300 µl, no dilution is made). A 20-µl aliquot of the diluted or undiluted urine is then analyzed following the procedure described above for plasma acylcarnitine analysis (section 3.2.4). The final result is expressed as mmol/mol creatinine.

3.2.5.4 Interpretation

As is true for plasma acylcarnitine analysis, the interpretation of urine acylcarnitine profiles is based on quantitative reference ranges and pattern recognition. The reference ranges used in our laboratory for urine are provided in Table 3.2.3.

3.2.5.5 Pitfalls

Aside from the aforementioned potential problems (see 3.2.4, subheading "Pitfalls"), such as the inability to discriminate isomers and interfering metabolites of antibiotics, the interpretation of urine acylcarnitine profiles is inherently more complex and overinterpretation must be avoided. Therefore, urine acylcarnitine analysis should not be included in the first-line screening investigations, but be targeted to specific diagnostic considerations, in particular organic acidemias. A role of urine acylcarnitine analysis for the diagnosis of FAO disorders has not been established to date.

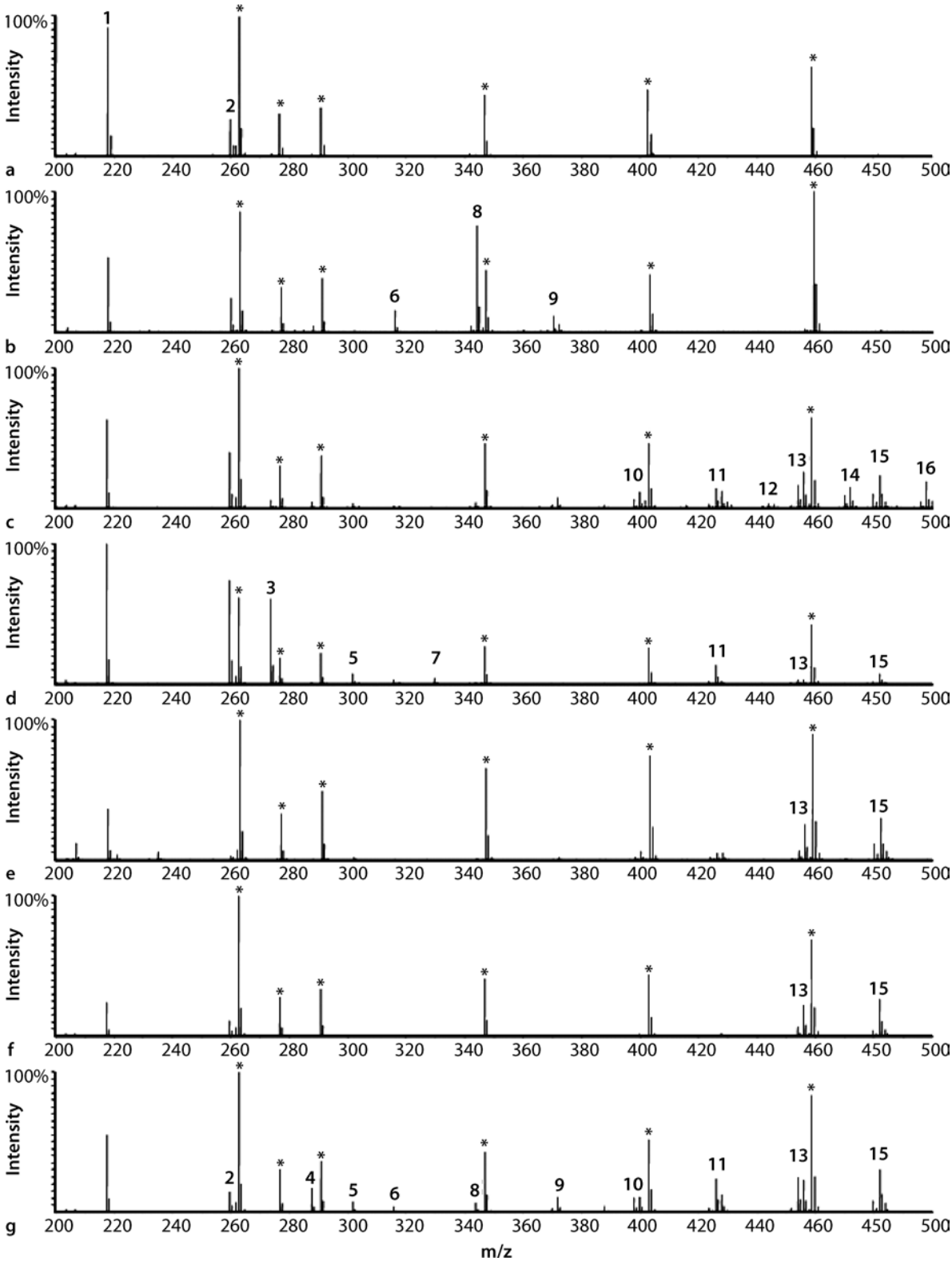
100%
Intensity
a
b
c
d
e
f
g
200 220 240 260 280 300 320 340 360 380 400 420 440 460 450 500
m/z

◄ **Fig. 3.2.6a–g** Profiles of acylcarnitines as their butyl esters in plasma (precursor of m/z 85 scan) of a normal control (**a**) and patients with various fatty acid *β*-oxidation disorders. A typical profile observed in patients with medium-chain acyl-CoA dehydrogenase deficiency is shown in **b**, where octanoylcarnitine (C_8; m/z 344; peak 8) is greater than both hexanoylcarnitine (C_6; m/z 316; peak 6) and decenoylcarnitine ($C_{10:1}$; m/z 370; peak 9). In long-chain 3-hydroxy acyl-CoA dehydrogenase (LCHAD; **c**) and very long-chain acyl-CoA dehydrogenase (VLCAD; **d**) deficiencies long-chain acylcarnitines (C_{12} [m/z 400; peak 10], $C_{14:1}$ [m/z 426; peak 11], C_{16} [m/z 456; peak 13], $C_{18:1}$ [m/z 482; peak 15]) are elevated including long-chain 3-hydroxy species (C_{14}-OH [m/z 444; peak 12], C_{16}-OH [m/z 472; peak 14], and $C_{18:1}$-OH [m/z 498; peak 16]) in LCHAD deficiency. Carnitine palmitoyltransferase type II (**e**) and carnitine-acylcarnitine translocase (**f**) deficiencies are indistinguishable by acylcarnitine analysis. Patients with severe glutaric acidemia type II (**g**) reveal elevations of most acylcarnitine species with chain-length of C_4 (m/z 288; peak 4) and longer. Note that the samples represented in panels e, f, and g have low levels of free carnitine (m/z 218; peak 1) and acetylcarnitine (C_2; m/z 260; peak 2) indicating relative carnitine deficiency. Also note that the patient with VLCAD deficiency (**d**) reveals only moderate elevations of long-chain acylcarnitine species while free carnitine (m/z 218) is relatively high, suggesting ongoing L-carnitine supplementation. Furthermore, the odd-chain species C_3- (m/z 374; peak 3), C_5- (m/z 302; peak 5), and C_7-acylcarnitine (m/z 330; peak 7) are elevated which represent dietary artifacts secondary to the patient being supplemented with triheptanoin [66]. The *asterisks* represent the internal standards (from left to right): d^3-acetylcarnitine (C_2; m/z 263), d^3-propionylcarnitine (C_3; m/z 277), d^3-butyrylcarnitine (C_4; m/z 291), d^3-octanoylcarnitine (C_8; m/z 347), d^3-dodecanoylcarnitine (C_{12}; m/z 403), and d^3-palmitoylcarnitine (C_{16}; m/z 459)

3.2.6 Acylcarnitine Analysis in Dried Blood and Bile Spots by MS/MS

3.2.6.1 Principle

Acylcarnitine analysis of dried blood or bile spots is very similar to the analysis of plasma. A small disk (diameter typically 5 mm or less) is punched out of the blood spot and the acylcarnitines extracted by the addition of methanol and known concentrations of isotopically labeled acylcarnitines, which function as internal standards. The extract is dried under a stream of nitrogen, and derivatized by the addition of either *n*-butanol HCl or *n*-methanol HCl. The acylcarnitines are measured as their butyl or methyl esters by MS-MS. The concentrations of the analytes are established by computerized comparison of ion intensities of these analytes to that of the internal standards.

3.2.6.2 Pre-analytical

Specimen

For postmortem analysis, blood and bile are collected at the latest at the time of autopsy. Otherwise, as is true for plasma samples, the most informative results are obtained when blood samples are collected during acute illness or at least prior to a meal (see 3.2.4, subheading “Specimen”). Blood should be obtained by capillary stick of well-perfused skin (heels in young infants or fingers) and free dripping of a few drops of blood directly on the filter paper card. Following complete drying at room temperature for at least 3 h, the sample can be sent ambient. Analysis should be

Table 3.2.3 *Reference ranges for urine acylcarnitines based on samples with normal organic acid results (n = 40)*

Acylcarnitine species	(µmol/l)	Acylcarnitine species	(µmol/l)
C0	0.35–31.60	**C12**	< 0.19
C2	< 16.46	**C6-DC**	< 0.81
C3	< 1.20	**C12:1-OH**	< 0.27
C4	< 2.74	**C12-OH**	< 0.16
C5:1	< 0.34	**C14:2**	< 0.02
C5	< 1.53	**C14:1**	< 0.21
C4-OH	< 0.26	**C14**	< 0.39
C6	< 0.16	**C14:1-OH**	< 0.14
C5-OH	< 0.52	**C14-OH**	< 0.09
C6-OH	< 0.32	**C16:1**	< 0.04
C8:1	< 4.30	**C16**	< 0.18
C8	< 0.61	**C16:1-OH**	< 0.02
C3-DC	< 0.50	**C16-OH**	< 0.05
C10:2	< 0.48	**C18:2**	< 0.02
C10:1	< 0.65	**C18:1**	< 0.02
C10	< 0.21	**C18**	< 0.05
C4-DC	< 0.57	**C18:2-OH**	< 0.01
C10:1-OH	< 0.26	**C18:1-OH**	< 0.03
C5-DC (C10-OH)	< 0.37	**C18-OH**	< 0.02
C12:1	< 0.07		

completed within a few days. While diagnostic results can be obtained in most cases of medium- and long-chain FAO defects even after prolonged storage time at room temperature, samples should be stored frozen because short-chain acylcarnitine species in particular are not reliably measurable several months after collection [55].

Materials

The reagents used for filter paper analysis are the same as for plasma acylcarnitine analysis except for the internal standard/extraction solution, which is prepared using methanol as opposed to acetonitrile.

The samples are typically collected on Whatman 903 Protein Saver paper (Florhman, NJ, USA) and punched using automatic (i.e., Wallac DBS Puncher, PerkinElmer Life And Analytical Sciences, Wellesley, MA, USA) or manual punchers (i.e., M.C. Mieth Manufacturing, Port Orange, FL, USA), depending on testing volume.

QC samples

A QC standard, normal blood, and normal bile spots are run with each assay. The controls are made by pooling normal blood or bile and spotting it onto filter paper.

3.2.6.3 Sample Preparation and Calculation

One 5-mm blood or bile spot is punched out and placed into a labeled Eppendorf tube, together with 300 µl internal standard/extraction solution. Following agitation for 30 min on a plate rotator, the liquid is transferred to clean Reacti-Vials and dried under a gentle stream of warm nitrogen. Butylesters are then formed and the analysis performed as described for plasma samples (see 3.2.4, subheading "Sample Preparation").

When large sample volumes need to be analyzed, automation of the sample preparation should be considered by using pipette robots and a 96-well plate format as opposed to single vials.

3.2.6.4 Interpretation

As noted for acylcarnitine analysis of other specimen types, the interpretation of results for blood and bile spots is based on quantitative reference ranges and ultimately pattern recognition by a trained biochemical geneticist. The reference ranges used in our laboratory for postmortem blood and bile spots represent prospectively updated percentile ranks (Table 3.2.4).

3.2.7 In vitro Probe Assay for the Diagnosis of FAO Disorders and Selected Organic Acidemias in Fibroblast Cultures Utilizing MS/MS

3.2.7.1 Principle

Most FAO disorders have a rather similar presentation and their biochemical diagnosis can at times be difficult. Commonly used metabolite screens, such as urine organic acids, plasma acylcarnitines and fatty acids are influenced by dietary factors and the clinical status of the patient [57]. This often leads to incomplete diagnostic information or even false negative results [56]. Enzyme assays are limited to one enzyme per assay, and molecular assays for common mutations are limited by the frequent occurrence of compound heterozygous patients with an uncommon, private mutation that must be distinguished from unaffected carriers. Furthermore, neither specific enzyme assays nor molecular genetic testing are available for each of the known defects. The purpose of the in vitro probe assay is to offer screening for several defects of FAO and organic acid metabolism under controlled laboratory conditions using fibroblast cultures (Table 3.2.5). This assay is not informative if the deficient enzyme is not expressed physiologically in skin fibroblasts.

As indicated in the introduction to this chapter (section 3.2.1), several different approaches to the in vitro probing of mitochondrial FAO have been published

■ ***Table 3.2.4*** *Percentile ranks of acylcarnitine species in postmortem dried blood and bile spots*

Acylcarnitine species	Blood spots ($n = 1480$)		Bile spots ($n = 1590$)	
	5^{th} percentile	95^{th} percentile	5^{th} percentile	95^{th} percentile
C0	36.71–268.8		25.04–263.8	
C2	25.87–236.8		23.59–313.5	
C3	–	9.11	–	11.00
C4	–	16.46	–	6.20
C5:1	–	0.25	–	0.54
C5	–	2.35	–	3.30
C4-OH	–	7.21	–	2.52
C6	–	1.62	–	2.78
C5-OH	–	0.73	–	0.71
C7	–	0.14	–	0.63
C6-OH	–	0.45	–	0.64
C8:1	–	0.56	–	34.37
C8	–	0.84	–	5.81
C3-DC	–	0.35	–	0.89
C10:2	–	0.10	–	3.56
C10:1	–	0.17	–	9.97
C10	–	0.46	–	6.55
C4-DC	–	0.79	–	0.81
C10:1-OH	–	0.13	–	1.54
C5-DC	–	0.20	–	1.14
C12:1	–	0.11	–	9.14
C12	–	0.48	–	6.77
C12:1-OH	–	0.13	–	2.96
C12-OH	–	0.15	–	1.46
C14:2	–	0.22	–	7.25
C14:1	–	0.24	–	10.64
C14	–	0.41	–	3.34
C14:1-OH	–	0.11	–	2.26
C14-OH	–	0.09	–	0.88
C16:1	–	0.29	–	2.41
C16	–	2.02	–	3.35
C16:1-OH	–	0.18	–	1.31

■ ***Table 3.2.4*** (continued) *Percentile ranks of acylcarnitine species in postmortem dried blood and bile spots*

Acylcarnitine species	Blood spots ($n = 1480$)		Bile spots ($n = 1590$)	
	5th percentile	95th percentile	5th percentile	95th percentile
C16-OH	< 0.12		< 1.27	
C18:2	< 0.66		< 2.70	
C18:1	< 1.95		< 3.68	
C18	< 1.39		< 2.25	
C18:2-OH	< 0.09		< 0.60	
C18:1-OH	< 0.13		< 0.93	
C18-OH	< 0.09		< 0.60	

■ ***Table 3.2.5*** *Disorders detectable by the in vitro probe assay.* ETF *Electron transfer flavoprotein,* MADD *multiple acyl-CoA dehydrogenase deficiency*

Disorder	Deficiency
Fatty acid β-oxidation disorders	SCAD
	MCAD
	LCHAD
	TFP
	VLCAD
	CPT-II
	CACT
Organoacidopathies	ETF
	ETF-dehydrogenase (MADD; glutaric acidemia type II)
	Isovaleric acidemia
	SBCAD (2-methylbutyrylglycinuria)
	IBDH

and are in use in an increasing number of biochemical genetic laboratories around the world [30–38]. The method described here is based on that published by Shen et al., [31] and was further modified to allow for the diagnosis of several defects of branched chain amino acid metabolism [20, 21].

The principle of this assay relies on the assumption that skin fibroblasts of patients affected with an FAO deficiency will accumulate certain species of acyl-CoA esters, reflecting the metabolic defect, when the cell medium is supplemented with

a long-chain fatty acid. This in turn leads to the accumulation of acylcarnitine species through the action of carnitine acyltransferases. The formation of acylcarnitines from acyl-CoA esters in an equilibrium process can be driven by the addition of excess L-carnitine in the medium. Metabolites of branched-chain amino acids can be differentiated by the addition of isotopically labeled branched-chain amino acids to the incubation medium (Fig. 3.2.7). Acylcarnitine profiles in the cell medium following incubation are easily obtained by MS-MS as for the other sample types described above.

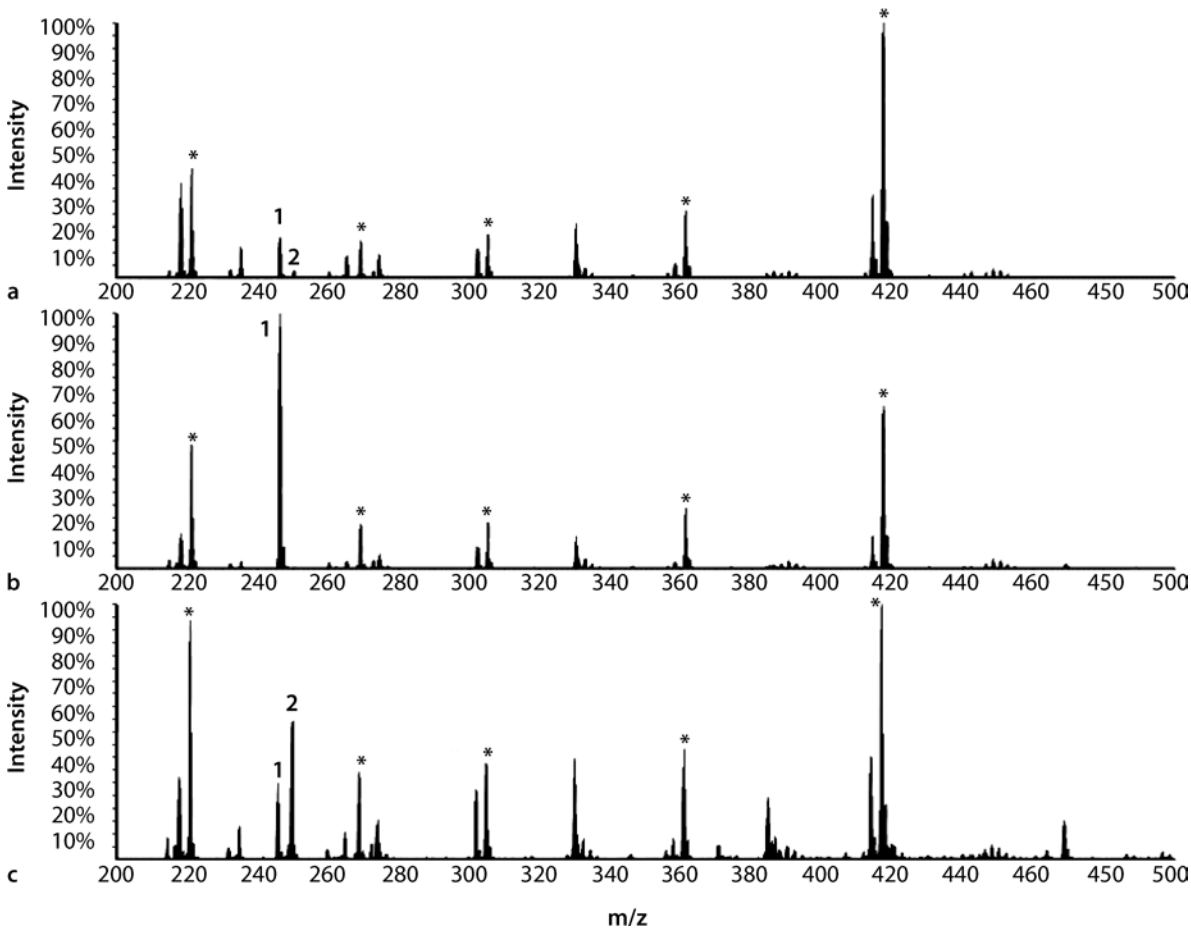

Fig. 3.2.7a–c Profiles of acylcarnitines as their methyl esters in cell culture medium (precursor of m/z 99 scan) following the in vitro probe assay in fibroblast cultures of a normal control (**a**) and a patient with SCAD deficiency (**b**) and isobutyryl-CoA dehydrogenase deficiency (**c**). *Peak 1*: unlabeled C_4-acylcarnitine (m/z 246), representing butyrylcarnitine accumulating due to SCAD deficiency causing a block in fatty acid β-oxidation of unlabeled palmitate. *Peak 2*: isotopically labeled (^{13}C) C_4-acylcarnitine (m/z 250), representing isobutyrylcarnitine accumulating in **c** due to IBDH deficiency causing a block in the degradation of isotopically labeled L-valine. The *asterisks* represent the internal standards (from left to right): d^3-acetylcarnitine (C_2; m/z 221), d^9-isovalerylcarnitine (C_5; m/z 269), d^3-octanoylcarnitine (C_8; m/z 305), d^3-dodecanoylcarnitine (C_{12}; m/z 361), and d^3-palmitoylcarnitine (C_{16}; m/z 419).

3.2.7.2 Pre-analytical

Specimen

Fibroblasts are typically grown from a small skin biopsy sample collected during an outpatient visit or as part of a planned surgical procedure following routine culturing techniques. Cell cultures may also be derived from umbilical cord or, for prenatal diagnostic purposes, from amniocytes obtained by amniocentesis. In our laboratory the analysis for each patient is performed in triplicate.

Reagents and Chemicals

Isotopically labeled standards (internal standards) include:
1. Acetyl-d^3-carnitine (d^3-C_2).
2. Isovaleryl-d^9-carnitine (d^9-C_5).
3. Octanoyl-d^3-carnitine (d^3-C_8).
4. Dodecanoyl-d^3-carnitine (d^3-C_{12}).
5. Palmitoyl-d^3-carntitine (d^3-C_{16}).

The internal standards are dissolved in methanol and a final working internal standard solution is prepared in methanol at the following concentrations:
1. 131.1 nmol/l acetyl-d^3-carnitine.
2. 25.3 nmol/l isovaleryl-d^9-carnitine.
3. 25.0 nmol/l octanoyl-d^3-carnitine.
4. 24.6 nmol/l dodecanoyl- d^3-carnitine.
5. 48.5 nmol/l palmitoyl-d^3-carnitine.

Standards (unlabeled) include:
1. Acetylcarnitine (C_2).
2. Isovalerylcarnitine (C_5).
3. Octanoylcarnitine (C_8).
4. Dodecanoylcarnitine (C_{12}).
5. Palmitoylcarntitine (C_{16}).

Standards are dissolved in methanol at the same concentrations as the internal standards (see above).

Additional or different labeled and unlabeled standards can be used. However, note that the incubation as described here includes isotopically labeled L-valine and L-isoleucine and that the metabolites of these branched chain amino acids can interfere with isotopically labeled internal standards for butyrylcarnitine or propionylcarnitine.
1. Methanol.
2. 80% Acetonitrile: water[2].
3. Nitrogen gas, in-house, scrubbed with BHT-1 hydrocarbon trap (Chrom Tech, Apple Valley, MN, USA).

2 Use of reverse osmosis or HPLC grade water in every step requiring water is recommended.

4. Minimal essential medium (MEM) with Earl's salts and L-glutamine (Sigma M4655). Note: complete MEM is used during fibroblast culturing, but the in vitro probe medium (IVPM; see below) is used during the 72-h incubation described in the procedure.
5. Palmitic acid (16:0) 200 mmol/l (molecular weight, MW = 256.4; Sigma P-5585).
6. Dissolve 104 mg of palmitic acid into 2 ml of absolute ethanol.
7. L-carnitine inner salt 400 mmol/l (MW = 161.2; Sigma C-0158).
8. Dissolve 128 mg L-carnitine into 2 ml water.
9. 18% Bovine serum albumin (BSA) solution essentially fatty acid free (MW = 66,200; Sigma A-6003): To make 5 ml BSA solution, 0.9 g BSA is added to a 50 ml conical tube containing 5 ml phosphate-buffered saline (PBS; Dulbecco's 1× PBS, Gibco Laboratories, 14190-144).
10. Antibiotic antimycotic solution 100× (Invitrogen 15240-062): 6 ml of gentamicin reagent solution (10 mg/ml; Sigma G1272) are added to a 100-ml bottle of antibiotic solution, which is then sterilized using a 0.2-μm Nalgene filtration flask.
11. L-Valine-U-$^{13}C_5$ (Cambridge Isotope Laboratories, CLM-2249): 48 mg is added to a 10-ml volumetric flask, which is then filled to 10 ml with water.
12. L-Isoleucine-U-$^{13}C_6$ (Cambridge Isotope Laboratories, CLM-2248): 54 mg is added to a 10-ml volumetric flask, which is then filled to 10 ml with water.
13. Unlabeled amino acid solution (10× stock): See Table 3.2.6. These amino acids, which are included in the natural L-amino acid kit (ICN Biomedical, #100586), except for the two alkaline amino acids (cystine and tyrosine), are mixed into a 100-ml volumetric flask. Then, 10 ml of L-glutamine (200 mM, Sigma G7513; must be in solution before use) and 50 ml water are added and the solution stirred until all components are dissolved. For L-cystine and L-tyrosine, the indicated amount is added to a 10-ml volumetric flask and the pH adjusted to > 8.0 by adding 2N NaOH drop by drop until the amino acids are dissolved. Then water is added to the 10-ml mark and the solution transferred to a 100-ml flask to complete the solution. Aliquots of 10 ml are prepared using 15-ml conical screw-top tubes and stored at –80°C.
14. IVPM (incomplete): For each 100 ml of medium needed, the following components are mixed and the pH adjusted to 7.0–7.2 using 1N NaOH or 1N HCl as needed. The medium is then filter sterilized using a 0.2-μm Nalgene filter flask, which causes an increase of the final pH by approximately 0.18:
    a. 70.8 ml water
    b. 10.0 ml Earle's balanced salt solution 10× (Sigma E-7510).
    c. 1.0 ml MEM vitamin solution 100× (Sigma M-6895).
    d. 2.9 ml Sodium bicarbonate solution 7.5% (w/v; Invitrogen 25080-094).
    e. 2.0 ml L-Valine-U-$^{13}C_5$ solution (see above).
    f. 2.0 ml L-Isoleucine-U-$^{13}C_6$ solution (see above).
    g. 10.0 ml Unlabeled amino acid solution (see above).
    h. 1.2 ml Complete antibiotic antimycotic solution 100x (see above).
    i. 0.1 ml L-carnitine (see above).
16. IVPM (complete; made fresh each time assay is performed): For 50 ml of medium, first 1.0 ml of BSA solution (see above) is added to a 15×85 mm glass test tube and prewarmed to 37°C. While vortexing, 50 μl palmitic acid (see above) is added and this solution is then, also under vortexing, added to the 50 ml of

incomplete IVPM (see above) that has been pre-warmed to 37°C. The complete IVPM is mixed well and sterilized via a 0.2-μm filtration flask.

Equipment and Supplies

1. Sonicator/cell disruptor (Misonics, Farmingdale, NY, USA).
2. SPE Dry-96, plate sample concentrator (Argonaut, Charlottesville, VA, USA).
3. Six-well cell culture plates (Corning Life Sciences, Acton, MA, USA).
4. Cluster Tubes 96 tubes per rack (Corning Life Sciences, Acton, MA, USA; #4410).
5. Cluster tubes, 8-Cap Strips-Costar 4418.
6. Filter paper – Schleicher and Schuell (UK) #900.
7. Micromat Clear 96-well, 7-mm preslit, plate cover mat (Sun International #300005).
8. Microtest lid for 96-well assay plate (Falcon #353071).
9. Assay plate, 96-well, U-bottom (Falcon #353918).
10. Nalgene 0.90-mm, 0.2-μm filter flask (500 ml).
11. Applied Biosystems/MDS SCIEX API 5000 MS-MS system.
12. PE Series 200 isocratic LC pump.
13. PE Series 200 LC autosampler with 96-well plate sample tray insert.
14. Back pressure column, BDS Hypersil C18 Low Pressure Column (Keystone Scientific, PA, USA; 053-46-1).

Calibration

Please refer to section 3.2.4, subheadings “Pre-analytical”, “Calibration”.

Table 3.2.6 *Unlabeled amino acid solution (10 × stock)*

Amino acid	Concentration of 10 × stock	Concentration in medium	
L-Arginine-HCl	0.126 g/100 ml	126 mg/l	
L-Cystine-2HCl	0.031 g/100 ml	31 mg/l	Alkaline pH
L-Histidine HCl-H_2O	0.042 g/100 ml	42 mg/l	
L-Leucine	0.052 g/100 ml	52 mg/l	
L-Lysine-HCl	0.073 g/100 ml	73 mg/l	
L-Methionine	0.015 g/100 ml	15 mg/l	
L-Phenylalanine	0.032 g/100 ml	32 mg/l	
L-Threonine	0.048 g/100 ml	48 mg/l	
L-Trytophan	0.010 g/100 ml	10 mg/l	
L-Tyr-2Na-$2H_2O$	0.052 g/100 ml	52 mg/l	Alkaline pH

QC

QC samples

Cell medium is pooled after incubation of several negative cell lines and added to the acylcarnitine analysis of each batch as controls. The mean and standard deviation is calculated with a minimum of ten between-run values. A standard solution made up of equimolar amounts of standard and internal standard solution will undergo acylcarnitine analysis with each batch (standard control). The expectation is that the standard and corresponding internal standard peaks are of equal abundance in the acylcarnitine profile and that no other acylcarnitine peaks are present.

In addition, at least one cell line from a proband not affected with an FAO disorder will be analyzed with each run as a normal control. At least two cell lines from patients with different, previously established FAO disorders are also analyzed simultaneously. The latter cell lines act as abnormal controls.

Control values for the pooled QC sample that fall within ±2 standard deviations of the mean are considered acceptable and require no further action. Any control values that are either greater than 2 standard deviations or trends require review by a laboratory director. The results for the normal and abnormal control cell lines and the control samples are reviewed by the laboratory director, who determines whether the analysis of the complete batch or of specific samples needs to be repeated.

3.2.7.3 Analytical

Cell Culture and Pre-incubation

Fibroblast cultures for each patient and control are grown to confluency in T-75 culture flasks. The assay is then performed in triplicate using six-well plates. First, 1 ml of 0.25% trypsin-ethylenediaminetetraacetic acid (EDTA) solution (Sigma T4049) is added to each T-75 flask. After the cells have lifted from the flask, they are resuspended in 6 ml complete MEM. A 1-ml aliquot of the cell suspension is transferred to a 50-ml conical tube containing 14 ml of MEM complete medium (see above). Following further resuspension, 4 mL is plated into each of three wells in a six-well culture plate and placed into an incubator. Once the cells have attached to the seeded plates and are approximately 90–100% confluent (3–4 days), complete MEM is replaced with 1.5 ml of complete IVPM (see above).

Incubation and Harvesting

After 72 h incubation at 37°C, 1.0 ml of medium is removed for acylcarnitine analysis. It can be spotted on filter paper immediately or stored frozen for later acylcarnitine analysis. The remaining medium is discarded. Then, 2.0 ml of 0.85% sterile saline solution is added to each well and each flask gently washed. The saline solution is then replaced by 0.2 ml of 0.25% Trypsin-EDTA solution. After 3–5 min the cells will lift off the plate bottom, which should be confirmed by light microscopy. To bring the cells back into suspension, 1.0 ml Dulbecco's 1× PBS (Gibco Labo-

ratories, 14190-144) is added to each trypsinized well, and cell clumps are broken up by careful pipetting. The cell suspension is then transferred to 1.5-ml microfuge tubes and centrifuged at 3000 rpm ($800 \times g$) for 10 min. Afterwards, the supernatant is carefully removed without disrupting the cell pellet, to which 75 µl of water is now added. Without further manipulation, the cell pellet and water are stored frozen at –20°C until protein analysis.

Protein Analysis of Cell Pellet

Cell pellets are thawed at room temperature. Then each tube is sonicated twice for at least 10 s, with cooling on ice between each 10-s burst. The protein concentration is determined by a routine method (i.e., the Lowry method) and the result recorded for each cell pellet.

Preparation of Cell Medium for Acylcarnitine Analysis

Into each well of a 96-well flat bottom plate, one 6-mm filter paper disc (Schleicher & Schuell #900) is placed using a paper puncher (i.e., M.C. Mieth Manufacturing). For each patient and control, 50 µl of collected cell culture medium is dripped onto a filter disc. In addition, 50 µl of complete IVPM is added to one disk as a blank. After the samples have dried over night, 300 µl labeled internal standard/extraction solution (see above) is added to each well and the plate agitated on an orbital mixer for 30 min. Then, 100 µl of the extract is transferred to a clean U-bottom 96-well plate and dried under nitrogen. To derivatize the acylcarnitines to methylesters, 100 µl of 3N methanolic-HCl (TCI America X0041) is added to each well and the covered plate heated at 50°C for 15 min before the samples are dried again under warm nitrogen. After reconstitution of the dried residue in 100 µl of 80:20 acetonitrile:water (mobile phase) the samples are ready for acylcarnitine analysis.

Instrument Setup

LC System

Controlled by the MS-MS software, the PE Series 200-micro LC pump operates isocratically using 80% acetonitrile:water at 40 µl/min. A 500×1 mm C18 column (Keystone) is used between the pump and autosampler to provide back pressure. The syringe/system flush solution is the 80% Acetonitrile:water used as the mobile phase. The autosampler is connected directly to the MS-MS TurboIon Spray source. The injected sample volume is 20 µl.

A 0.5-U Peek filter is installed between the autosampler and TurboIon Spray APCI electrospray interface source. The filter end fitting is discarded and replaced after approximately 200 injections.

MS-MS System

Acylcarnitine analysis is performed as precursor scan in positive ion mode. Q1 is set to scan a mass range from m/z 200 to 500 m/z, while Q3 is set to determine a precur-

sor ion of m/z 99. The method is optimized for a mixture of methylesters containing d^3-C_2, d^9-C_5, d^3-C_8, d^3-C_{12}, and d^3-C_{16} acylcarnitine.

The sample queue is entered into the MS-MS instrument's software (Analyst for SCIEX instruments) according to the manufacturer's instructions. Samples can be given specific designations that allow for correct QC and reference range assignment. Prior to analysis, the equipment should be equilibrated and the system purged if necessary. The LC line should be attached to the sprayer after proper equilibration for approximately 30 min.

Calculation

A datafile is generated for each sample and presented as a mass profile. All ion species in a mass range from 200 to 500 Da that generate a product m/z of 99 are represented in this profile based on their detected abundance. Calculation of the molecular weights of the *n*-methyl esters of acylcarnitines, expressed as $(M+H)^+$ molecular ions, allows the designation of each peak (Table 3.2.7). Quantitation software provided by the instrument vendor (i.e., Chemoview for SCIEX Instruments) allows the calculation of quantitative and semiquantitative concentrations for these acylcarnitines by comparison of the detected abundance of each acylcarnitine versus that of a designated internal standard with known concentration. The final results for each acylcarnitine species are normalized to the protein concentration determined in the cell pellet (see "Protein Analysis of Cell Pellet" above). The results for each sample and analyte are compared to previously established reference ranges (Table 3.2.7).

3.2.7.4 Post-analytical: Interpretation and Reference Ranges

As always, the interpretation of metabolite profiles is aided by the comparison of analytes to quantitative reference ranges established during implementation and validation of the assay. Ultimately, however, the interpretation is based on pattern recognition by a trained biochemical geneticist.

3.2.7.5 Pitfalls

The in vitro probe assay is performed under standardized conditions and is independent of the patient's status at the time the skin biopsy sample is obtained. The accumulation of acylcarnitines in this assay system appears to be dependent on potentially present residual enzyme activity and therefore provides information regarding the severity of an enzyme deficiency state for some disorders. This has been well documented for VLCAD deficiency (Fig. 3.2.8) [34]. In our experience, this also seems to hold true for the different SCAD genotypes. Cells lines homozygous or compound heterozygous for mutations that abolish SCAD activity accumulate larger amounts of butyrylcarnitine than those that are homozygous or compound heterozygous for only the SCAD variants, 625G>A and 511C>T. Furthermore, as is true for acylcarnitine analysis of other sample types, CPT-II and CACT deficiencies can not be differentiated using this assay system. However, recent work by Roe et al. suggests that there are specific metabolite ratios that may facilitate this differentiation [65]. Finally, the analysis of fibroblasts does not allow for the diagnosis of enzyme

Table 3.2.7 *Mass assignment and reference range for acylcarnitine species accumulating in fibroblast cultures following incubation with palmitate, $^{13}C_5$-valine, $^{13}C_6$-isoleucine, and L-carnitine*

Mass[a]	Acylcarnitine species		(μmol/g protein)
218	C_2	Acetyl-	< 1.850
221	d^3-C_2	*Internal standard*	
232	C_3	Propionyl-	< 0.074
235[b]	$^{13}C_3$	Propionyl-	< 0.532
246	C_4	Butyryl-	< 0.125
250[b]	$^{13}C_4$	Isobutyryl-	< 0.025
260	C_5	Isovaleryl-	< 0.035
265[b]	$^{13}C_5$	2-Methylbutyryl-	< 0.122
269	d^9-C_5	*Internal standard*	
274	C_6	Hexanoyl-	< 0.084
302	C_8	Octanoyl-	< 0.098
304	C_5-DC	Glutaryl-	< 0.026
305	d^3-C_8	*Internal Standard*	
326	$C_{10:2}$	Decadienoyl-	< 0.003
328	$C_{10:1}$	Decenoyl-	< 0.009
330	C_{10}	Decanoyl-	< 0.147
358	C_{12}	Dodecanoyl-	< 0.035
361	d^3-C_{12}	*Internal standard*	
374	C_{12}-OH	3-Hydroxy dodecanoyl-	< 0.006
384	$C_{14:1}$	Tetradecenoyl-	< 0.008
386	C_{14}	Myristoyl-	< 0.034
402	C_{14}-OH	3-Hydroxy tetradecanoyl-	< 0.005
456	C_{16}	Palmitoyl-	< 0.271
459	d^3-C_{16}	*Internal standard*	
430	C_{16}-OH	3-Hydroxy hexadecanoyl-	< 0.013
438	$C_{18:2}$	Linoleyl-	< 0.003
440	$C_{18:1}$	Oleyl-	< 0.018
442	C_{18}	Stearoyl-	< 0.020
458	C_{18}-OH	3-hydroxy stearoyl-	< 0.009

[a] Mass of the molecular ion of the methylated acylcarnitine esters

[b] Mass corresponds to analyte derived from incubation with isotope-labeled valine and isoleucine

deficiency states that are not expressed in this tissue (for example, the liver-specific short-chain 3-hydroxy acyl-CoA dehydrogenase deficiency). In conclusion, the ordering physician must be aware of the limitations of this assay system and should consider involving the biochemical genetics laboratory in discussions regarding the most appropriate diagnostic work up of patients.

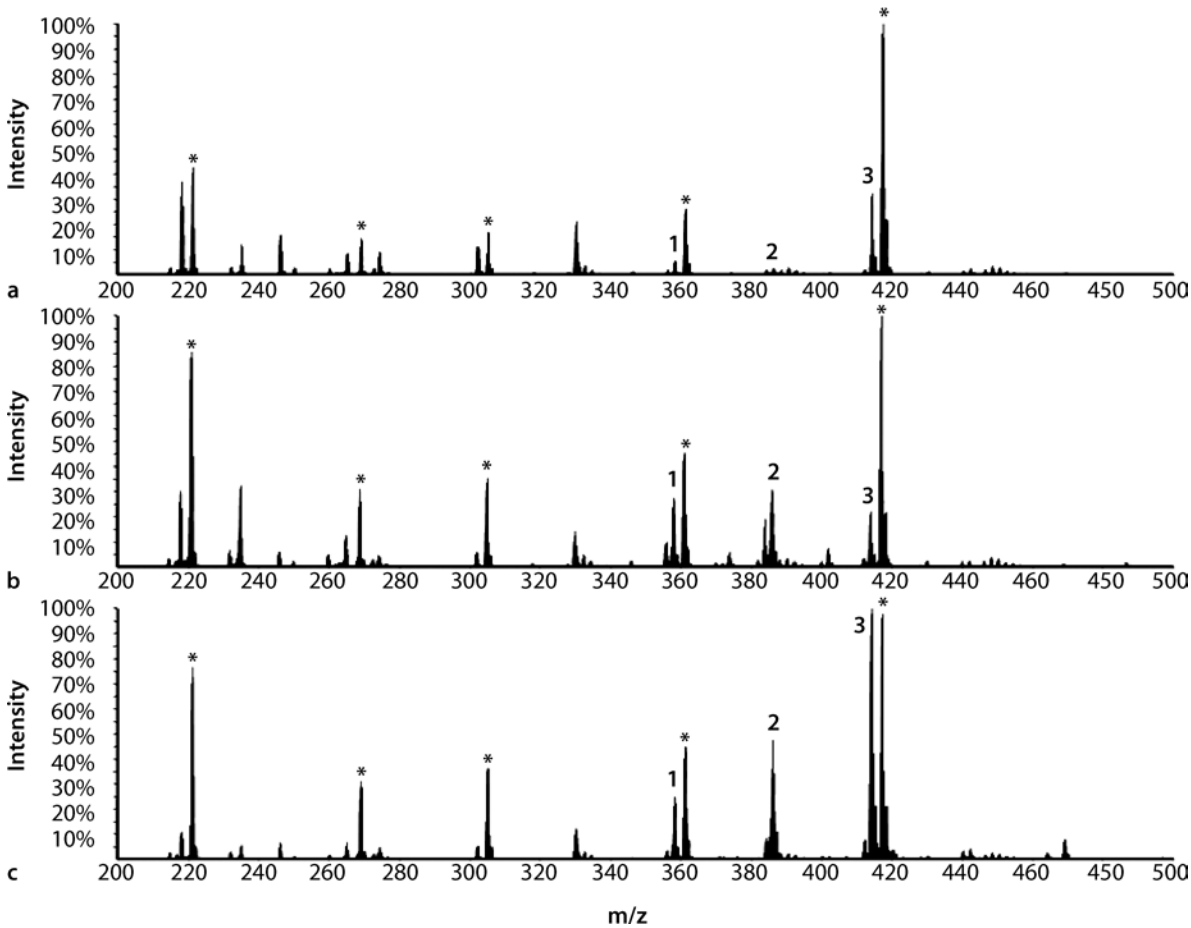

Fig. 3.2.8a–c Profiles of acylcarnitines as their methyl esters in cell culture medium (precursor of m/z 99 scan) following the in vitro probe assay in fibroblast cultures of a normal control (**a**) and a patient with the milder (**b**) and the more severe variant (**c**) of VLCAD deficiency. Note the more prominent elevation of dodecanoyl- (C_{12}; m/z 358; peak 1) and myristoylcarnitine (C_{14}; m/z 386; peak 2) compared to a relatively normal accumulation of palmitoylcarnitine (C_{16}; m/z 416; peak 3) in the milder VLCAD variant compared to the severe variant, where palmitoylcarnitine is markedly elevated. The *asterisks* represent the internal standards (from left to right): d^3-acetylcarnitine (C_2; m/z 221), d^9-isovalerylcarnitine (C_5; m/z 269), d^3-octanoylcarnitine (C_8; m/z 305), d^3-dodecanoylcarnitine (C_{12}; m/z 361), and d^3-palmitoylcarnitine (C_{16}; m/z 419)

References

1. Bremer J (1983) Carnitine – metabolism and functions. Physiol Rev 63:1420–1480
2. Gulewitsch WI, Krimberg R (1905) Zur Kenntnis der Extraktivstoffe der Muskeln. II. Mitteilung. Ueber das Carnitin. Hoppe Seylers Z Physiol Chem 45:326–330
3. Tomita M, Sendju Y (1927) Über die Oxyaminverbindungen, welche die Biuretreaktion zeigen. III. Spaltung der gamma-Amino-beta-oxy-buttersäure in die optisch-aktiven Komponenten. Hoppe Seylers Z Physiol Chem 169:263–277
4. Carter HE, Bhattacharyya PK, Weidman KR, Fraenkel G (1952) Chemical studies on vitamin BT isolation and characterization as carnitine. Arch Biochem Biophys 38:405–416
5. Bhattacharyya PK, Carter HE, Fraenkel G, Weidman KR (1952) The identity of vitamin BT with carnitine. Arch Biochem 35:241–242
6. Engel AG, Angelini C (1973) Carnitine deficiency of human skeletal muscle with associated lipid storage myopathy: a new syndrome. Science 179:899–902
7. DiMauro S, DiMauro PM (1973) Muscle carnitine palmityltransferase deficiency and myoglobinuria. Science 182:929–931
8. Rinaldo P, Matern D, Bennett MJ (2002) Fatty Acid oxidation disorders. Annu Rev Physiol 64:477–502
9. Zhang J, Zhang W, Zou D, et a (2002) Cloning and functional characterization of ACAD-9, a novel member of human acyl-CoA dehydrogenase family. Biochem Biophys Res Commun 297:1033–1042
10. Ensenauer R, He M, Willard JM, et al (2005) Human acyl-CoA dehydrogenase-9 plays a novel role in the mitochondrial beta-oxidation of unsaturated fatty acids. J Biol Chem 280:32309–32316
11. Roe CR, Bohan TP (1982) L-carnitine therapy in propionicacidaemia. Lancet 1:1411–1412
12. Roe CR, Hoppel CL, Stacey TE, Chalmers RA, Tracey BM, Millington DS (1983) Metabolic response to carnitine in methylmalonic aciduria. An effective strategy for elimination of propionyl groups. Arch Dis Child 58:916–920
13. Chalmers RA, Roe CR, Stacey TE, Hoppel CL (1988) Urinary excretion of L-carnitine and acylcarnitines by patients with disorders of organic acid metabolism: evidence for secondary insufficiency of L-carnitine. Pediatr Res 18:1325–1328
14. Millington DS, Roe CR, Maltby DA (1984) Application of high resolution fast atom bombardment and constant B/E ratio linked scanning to the identification and analysis of acylcarnitines in metabolic disease. Biomed Mass Spectrom 11:236–241
15. Roe CR, Millington DS, Maltby DA, Kahler SG, Bohan TP (1984) L-carnitine therapy in isovaleric acidemia. J Clin Invest 74:2290–2295
16. Roe CR, Millington DS, Maltby DA, Bohan TP, Hoppel CL (1984) L-carnitine enhances excretion of propionyl coenzyme A as propionylcarnitine in propionic acidemia. J Clin Invest 73:1785–1788
17. Millington DS, Terada N, Chace DH, et al (1992) The role of tandem mass spectrometry in the diagnosis of fatty acid oxidation disorders. Prog Clin Biol Res 375:339–354
18. Pitt JJ, Eggington M, Kahler SG (2002) Comprehensive screening of urine samples for inborn errors of metabolism by electrospray tandem mass spectrometry. Clin Chem 48:1970–1980
19. Tortorelli S, Hahn SH, Cowan TM, Brewster TG, Rinaldo P, Matern D (2005) The urinary excretion of glutarylcarnitine is an informative tool in the biochemical diagnosis of glutaric acidemia type I. Mol Genet Metab 84:137–143
20. Ensenauer R, Vockley J, Willard JM, et al (2004) A common mutation is associated with a mild, potentially asymptomatic phenotype in patients with isovaleric acidemia diagnosed by newborn screening. Am J Hum Genet 75:1136–1142
21. Oglesbee D, He M, Majumder N, et al (2007) Development of a newborn screening follow-up algorithm for the diagnosis of isobutyryl-CoA dehydrogenase deficiency. Genet Med 9:108–116

22. Millington DS, Kodo N, Norwood DL, Roe CR (1990) Tandem mass spectrometry: a new method for acylcarnitine profiling with potential for neonatal screening for inborn errors of metabolism. J Inherit Metab Dis 13:321–324
23. Rinaldo P, Hahn S, Matern D (2004) Clinical biochemical genetics in the twenty-first century. Acta Paediatr 93:22–26
24. Rinaldo P, Studinski AL, Matern D (2001) Prenatal diagnosis of disorders of fatty acid transport and mitochondrial oxidation. Prenat Diagn 21:52–54
25. Morel CF, Watkins D, Scott P, Rinaldo P, Rosenblatt DS (2005) Prenatal diagnosis for methylmalonic acidemia and inborn errors of vitamin B12 metabolism and transport. Mol Genet Metab 86:160–171
26. Braida L, Crovella S, Boniotto M, et al (2001) A rapid and quantitative mass spectrometry method for determining the concentration of acylcarnitines and amino acids in amniotic fluid. Prenat Diagn 21:543–546
27. Van Hove JL, Chace DH, Kahler SG, Millington DS (1993) Acylcarnitines in amniotic fluid: application to the prenatal diagnosis of propionic acidaemia. J Inherit Metab Dis 16:361–367
28. Nada MA, Rhead WJ, Sprecher H, Schulz H, Roe CR (1995) Evidence for intermediate channeling in mitochondrial beta-oxidation. J Biol Chem 270:530–535
29. Nada MA, Vianey-Saban C, Roe CR, et al (1996) Prenatal diagnosis of mitochondrial fatty acid oxidation defects. Prenat Diagn 16:117–124
30. Schmidt-Sommerfeld E, Bobrowski PJ, Penn D, Rhead WJ, Wanders RJA, Bennet MJ (1998) Analysis of carnitine esters by radio-high performance liquid chromatography in cultured skin fibroblasts from patients with mitochondrial fatty acid oxidation disorders. Pediatr Res 44:210–214
31. Roe CR, Roe DS (1999) Recent developments in the investigation of inherited metabolic disorders using cultured human cells. Mol Genet Metab 68:243–257
32. Ventura FV, Costa CG, Struys EA, et al (1999) Quantitative acylcarnitine profiling in fibroblasts using U-C-13 palmitic acid: an improved tool for the diagnosis of fatty acid oxidation defects. Clin Chim Acta281:1–17
33. Shen JJ, Matern D, Millington DS, et al (2000) Acylcarnitines in fibroblasts of patients with long-chain 3-hydroxyacyl-CoA dehydrogenase deficiency and other fatty acid oxidation disorders. J Inherit Metab Dis 23:27–44
34. Roe DS, Vianey-Saban C, Sharma S, Zabot MT, Roe CR (2001) Oxidation of unsaturated fatty acids by human fibroblasts with very-long-chain acyl-CoA dehydrogenase deficiency: aspects of substrate specificity and correlation with clinical phenotype. Clin Chim Acta 312:55–67
35. Giak Sim K, Carpenter K, Hammond J, Christodoulou J, Wilcken B (2002) Quantitative fibroblast acylcarnitine profiles in mitochondrial fatty acid beta-oxidation defects: phenotype/metabolite correlations. Mol Genet Metab 76:327–334
36. Okun JG, Kolker S, Schulze A, et al (2002) A method for quantitative acylcarnitine profiling in human skin fibroblasts using unlabelled palmitic acid: diagnosis of fatty acid oxidation disorders and differentiation between biochemical phenotypes of MCAD deficiency. Biochim Biophys Acta 1584:91–98
37. Young SP, Matern D, Gregersen N, et al (2003) A comparison of in vitro acylcarnitine profiling methods for the diagnosis of classical and variant short chain acyl-CoA dehydrogenase deficiency. Clin Chim Acta 337:103–113
38. Schulze-Bergkamen A, Okun JG, Spiekerkotter U, et al (2005) Quantitative acylcarnitine profiling in peripheral blood mononuclear cells using in vitro loading with palmitic and 2-oxoadipic acids: biochemical confirmation of fatty acid oxidation and organic acid disorders. Pediatr Res 58:873–880
39. American College of Medical Genetics. Standards and Guidelines for Clinical Genetics Laboratorie, 2005
40. Vaz FM, Wanders RJ (2002) Carnitine biosynthesis in mammals. Biochem J 361:417–429

41. Hamilton JJ, Hahn P (1987) Carnitine and carnitine esters in rat bile and human duodenal fluid. Can J Physiol Pharmacol 65:1816–1820
42. Rashed MS, Ozand PT, Bennett MJ, Barnard JJ, Govindaraju DR, Rinaldo P (1995) Inborn errors of metabolism diagnosed in sudden death cases by acylcarnitine analysis of postmortem bile. Clin Chem 41:1109–1114
43. Jakobs BS, Wanders RJ (1995) Fatty acid beta-oxidation in peroxisomes and mitochondria: the first, unequivocal evidence for the involvement of carnitine in shuttling propionyl-CoA from peroxisomes to mitochondria. Biochem Biophys Res Commun 213:1035–1041
44. Bonnefont JP, Djouadi F, Prip-Buus C, Gobin S, Munnich A, Bastin J (2004) Carnitine palmitoyltransferases 1 and 2: biochemical, molecular and medical aspects. Mol Aspects Med 25:495–520
45. Bieber LL, Choi YR (1977) Isolation and identification of aliphatic short-chain acylcarnitines from beef heart: possible role for carnitine in branched-chain amino acid metabolism. Proc Natl Acad Sci U S A 74:2795–2798
46. Costa CG, Struys EA, Bootsma A, et al (1997) Quantitative analysis of plasma acylcarnitines using gas chromatography chemical ionization mass fragmentography. J Lipid Res 38:173–182
47. Schmidt-Sommerfeld E, Penn D, Duran M, et al (1992) Detection and quantitation of acylcarnitines in plasma and blood spots from patients with inborn errors of fatty acid oxidation. Prog Clin Biol Res 375:355–362
48. Yergey AL, Liberato DJ, Millington DS (1984) Thermospray liquid chromatography/mass spectrometry for the analysis of L-carnitine and its short-chain acyl derivatives. Anal Biochem 139:278–283
49. Millington DS, Bohan TP, Roe CR, Yergey AL, Liberato DJ (1985) Valproylcarnitine: a novel drug metabolite identified by fast atom bombardment and thermospray liquid chromatography-mass spectrometry. Clin Chim Acta 145:69–76
50. Millington DS, Maltby DA, Roe CR (1986) Rapid detection of argininosuccinic aciduria and citrullinuria by fast atom bombardment and tandem mass spectrometry. Clin Chim Acta 155:173–178
51. Millington DS, Norwood DL, Kodo N, Roe CR, Inoue F (1989) Application of fast atom bombardment with tandem mass spectrometry and liquid chromatography/mass spectrometry to the analysis of acylcarnitines in human urine, blood, and tissue. Anal Biochem 180:331–339
52. Matern D, Magera MJ (2001) Mass spectrometry methods for metabolic and health assessment. J Nutr 131:1615S–1620S
53. Heinig K, Henion J (1999) Determination of carnitine and acylcarnitines in biological samples by capillary electrophoresis-mass spectrometry. J Chromatogr B Biomed Sci Appl 735:171–188
54. Ghoshal AK, Guo T, Soukhova N, Soldin SJ (2005) Rapid measurement of plasma acylcarnitines by liquid chromatography-tandem mass spectrometry without derivatization. Clin Chim Acta 358:104–112
55. Matern D, Strauss AW, Hillman SL, Mayatepek E, Millington DS, Trefz FK (1999) Diagnosis of mitochondrial trifunctional protein deficiency in a blood spot from the newborn screening card by tandem mass spectrometry and DNA analysis. Pediatr Res 46:45–49
56. Browning MF, Larson C, Strauss A, Marsden DL (2005) Normal acylcarnitine levels during confirmation of abnormal newborn screening in long-chain fatty acid oxidation defects. J Inherit Metab Dis 28:545–550
57. Van Hove JL, Kahler SG, Feezor MD, et al (2000) Acylcarnitines in plasma and blood spots of patients with long-chain 3-hydroxyacyl-coenzyme A dehydrogenase deficiency. J Inherit Metab Dis 23:571–582
58. Koeberl DD, Young SP, Gregersen NS, et al (2003) Rare disorders of metabolism with elevated butyryl- and isobutyryl-carnitine detected by tandem mass spectrometry newborn screening. Pediatr Res 54:219–223

59. Matern D, He M, Berry SA, et al (2003) Prospective diagnosis of 2-methylbutyryl-CoA dehydrogenase deficiency in the Hmong population by newborn screening using tandem mass spectrometry. Pediatrics 112:74–78
60. Abdenur JE, Chamoles NA, Guinle AE, Schenone AB, Fuertes AN (1998) Diagnosis of isovaleric acidaemia by tandem mass spectrometry: false positive result due to pivaloylcarnitine in a newborn screening programme. J Inherit Metab Dis 21:624–630
61. Gibson KM, Bennett MJ, Naylor EW, Morton DH (1998) 3-Methylcrotonyl-coenzyme a carboxylase deficiency in amish/mennonite adults identified by detection of increased acylcarnitines in blood spots of their children. J Pediatr 132:519–523
62. Hintz SR, Matern D, Strauss A, et al (2002) Early neonatal diagnosis of long-chain 3-hydroxyacyl coenzyme a dehydrogenase and mitochondrial trifunctional protein deficiencies. Mol Genet Metab 75:120–127
63. Vianey-Saban C, Boyer S, Levrat V, et al (2004) Interference of Cefotaxime in plasma acylcarnitine profile mimicking an increase of 3-hydroxypalmitoleylcarnitine (C16:1-OH) using butyl esters. J Inherit Metab Dis 27:94
64. Malvagia S, la Marca G, Casetta B, et al (2006) Falsely elevated C4-carnitine as expression of glutamate formiminotransferase deficiency in tandem mass spectrometry newborn screening. J Mass Spectrom 41:263–265
65. Roe DS, Yang BZ, Vianey-Saban C, Struys E, Sweetman L, Roe CR (2006) Differentiation of long-chain fatty acid oxidation disorders using alternative precursors and acylcarnitine profiling in fibroblasts. Mol Genet Metab 87:40–47
66. Carrozzo R, Dionisi-Vici C, Steuerwald U, et al. (2007) SUCLA2 mutations are associated with mild methylmalonic aciduria, Leigh-like encephalomyopathy, dystonia and deafness. Brain 130(Pt 3):862-74.
67. Roe CR, Sweetman L, Roe DS, David F, Brunengraber H (2002) Treatment of cardiomyopathy and rhabdomyolysis in long-chain fat oxidation disorders using an anaplerotic odd-chain triglyceride. J Clin Invest 110:259–269

3.3 Plasmalogens and Polyunsaturated Fatty Acids

Marinus Duran, Ronald J.A. Wanders

3.3.1 Introduction

Long-chain fatty acids constitute the major chemical content of various lipids such as triglycerides, cholesterol esters and phospholipids. These substances are the most important constituents of the cellular membranes, which are basically composed of lipid bilayers. The human organism is capable of synthesising saturated fatty acids from acetyl-CoA, but the (poly)unsaturated fatty acids, also called essential fatty acids, are derived from the diet. In this respect three series of fatty acids are distinguished, the ω-3, ω-6 and ω-9 series. The number attached to the omega denotes the number of carbon atoms removed from the tail end of the molecule in the position of the first double bond. Oleic acid belongs to the ω-9 series, linoleic acid to the ω-6 series and the trienoic acid linolenic acid to the ω-3 series. These three fatty acids form the basis of the synthesis of all other essential fatty acids through elongation and desaturation (see Fig. 3.3.1) [5].

The most important biologically active essential fatty acids are arachidonic acid (AA, 20:4ω6), eicosapentaenoic acid (EPA, 20:5ω3) and docosahexaenoic acid (DHA, 22:6ω3) [1]. These fatty acids play an important role in cell membrane composition, thereby influencing cell surface biochemical signalling. They may also serve as natural ligands for nuclear receptors affecting gene expression [12]. Furthermore, AA and EPA act as precursors of eicosanoids and prostanoids. The end products of AA transformation include leucotrienes and prostaglandins, their formation being catalysed by 5-lipoxygenase and cyclo-oxygenase enzymes. DHA also gives rise to the formation of protective metabolites, which are especially active in liver disease. In short, the ω-6 fatty acids exert a pro-inflammatory action whereas the ω-3 series gives rise to anti-inflammatory actions, the mechanisms underlying which are not yet completely understood [8].

To date there are no true inborn errors associated with essential fatty acid metabolism. However, we do know that the final step of DHA formation is the peroxisomal beta-oxidation of a homologous C24 fatty acid [7]. Consequently, patients with a generalised defect of peroxisomal function, such as Zellweger syndrome, are prone to develop deficiencies of essential fatty acids including DHA [9].

In addition, many different psychiatric conditions such as schizophrenia, depression and post-traumatic stress syndrome have been associated with changes in the essential fatty acid levels that can easily be measured in erythrocytes or plasma [2, 3].

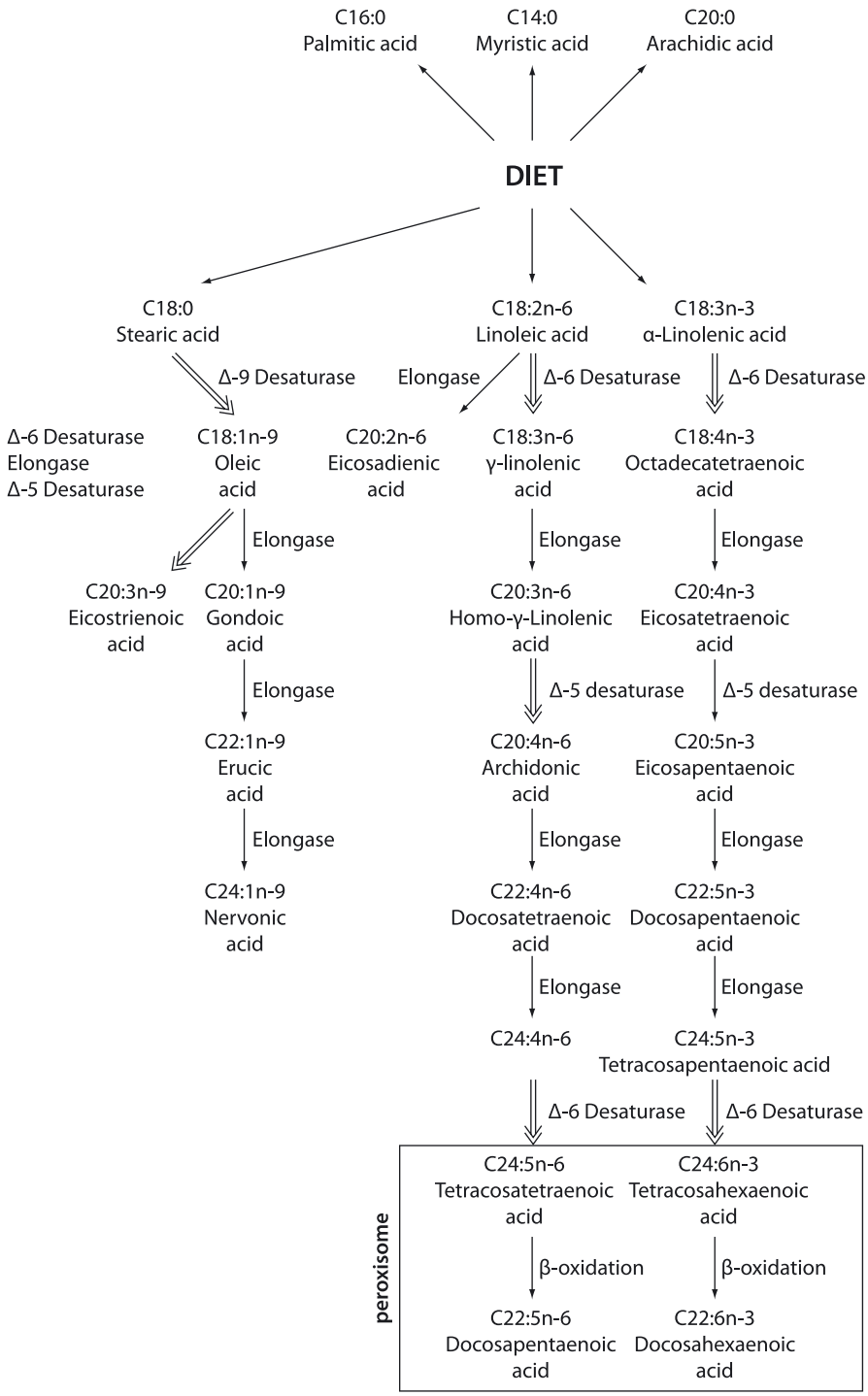

Fig. 3.3.1 Pathways of essential fatty acid formation from the dietary (poly)unsaturated fatty acids. The total set of elongases and desaturases has not been completely clarified. The notation (n-3) and (n-6) are alternatives for (ω-3) and (ω-6), respectively

Fish oil has been one of the hottest topics in general nutrition and health care over the past few years, mainly because it is primarily composed of ω-3 fatty acids. The benefits of fish oil have a strong foundation in well-documented scientific studies, the most important ones dealing with the treatment of heart disease. Treatment of any condition associated with essential fatty acid changes inevitably involves the use of fish oil or more specific mixtures of the primary important essential fatty acids [14].

While the fatty acids are present as esters of glycerol or phosphoglycerol, other glycerol derivatives are known, such as the glycerol ethers, which are known as plasmalogens. These substances are equally important as building blocks of all kinds of membranes and structures with a high fat content such as myelin. The plasmalogens have an unsaturated alkane as the functional group attached to the glycerol backbone. Plasmalogen synthesis takes place through a series of enzyme reactions, some of which are confined to the peroxisome. Consequently, patients with an inability to form peroxisomes (Zellweger spectrum) will end up with a deficiency of plasmalogens, most probably contributing to the complex of clinical signs and symptoms.

The analysis of essential fatty acids involves hydrolysis of the ester bonds and subsequent formation of the fatty acid methyl esters, which can be separated by gas chromatography (GC) [10]. By accident, the plasmalogens are hydrolysed in the same reaction and the methylation reaction transforms them into dimethylacetals, which appear in the GC run of the fatty acid methyl esters [4].

3.3.2 Properties of Analytes

Long-chain fatty acids are hydrophobic substances; in plasma they occur in the esterified state or bound to protein (mainly albumin). As a consequence, long-chain fatty acids are not excreted into the urine and are measured either in the plasma or in erythrocytes, where they are part of the membrane. Erythrocyte levels of polyunsaturated fatty acids (PUFA) are fairly constant and may reliably reflect the long-term availability or deficiency of the essential fatty acids. A list of fatty acids that can be separated and analysed by GC is shown in Table 3.3.1.

PUFA are prone to decomposition or modification through the action of oxygen. Various substances can be formed in this way, among which are the epoxy acids. In order to minimise these processes, it is advised to protect the acids by adding an anti-oxidant to the samples of interest such as 2,6-di-tert.butyl-4-hydroxytoluene (BHT).

3.3.3 Specimens for Analysis

The most logical material for the analysis of PUFA and plasmalogens are the erythrocytes. Fatty acids can also be quantitated in plasma. The plasmalogens are also easily detectable in homogenates of cultured fibroblasts and may add to the definitive diagnosis of patients with a generalised or isolated peroxisomal dysfunction.

A 1-ml ethylenediaminetetraacetic acid (EDTA)-treated blood sample is sufficient for both analyses. Blood is usually transported to the laboratory within a day, at which point the cells are separated from the plasma. The latter is stored at – 20°C, whereas the red cells are stored at 6°C for a maximum of 3 weeks. Should the red

Table 3.3.1 *The following fatty acids can be separated and quantitated using the gas chromatography method*

Chain length	Name
C14:0	Myristic acid
C15:0	Pentadecanoic acid
C16:0	Palmitic acid
C18:0	Stearic acid
C20:0	Arachidic acid
C22:0	Behenic acid
C24:0	Lignoceric acid
C18:3ω3	Linolenic acid
C18:4ω3	Octadecatetraenoic acid
C20:5ω3	Eicosapentaenoic acid
C22:5ω3	Docosapentaenoic acid
C22:6ω3	Docosahexaenoic acid
C14:1ω5	Myristoleic acid
C18:2ω6	Linoleic acid
C18:3ω6	Gamma-linolenic acid
C20:2ω6	Eicosadienoic acid
C20:3ω6	Homogamma-linolenic acid
C20:4ω6	Arachidonic acid
C22:2ω6	Docosadienoic acid
C22:4ω6	Docosatetraenoic acid
C22:5ω6	Docosapentaenoic acid
C16:1ω7	Palmitoleic acid
C18:1ω7	Vaccenic acid
C20:1ω7	13-Eicosenoic acid
C16:1ω9	Hypogeic acid
C18:1ω9	Oleic acid
C20:1ω9	Gondoic acid
C20:3ω9	Eicosatrienoic acid
C22:1ω9	Erucic acid
C24:1ω9	Nervonic acid

cells be stored for a longer period of time, then a cell count has to performed, after which the pellet can be stored at –80°C, which results in a complete haemolysis of the cells.

3.3.4 GC Assay

3.3.4.1 Introduction

An optimum separation of fatty acids is achieved by the GC analysis of the methyl esters on a suitable column. Authentic reference methyl esters are commercially available and the order of elution as well as the retention times can be kept constant [6]. There is no need for mass spectrometric verification of the structures and in general no major exogenous interfering compounds will be present. The flame ionisation detector of the GC instrument has an extremely wide linear range enabling the quantitative evaluation of the whole range of fatty acids, with thousand-fold differing concentrations, in one run. The fatty acid extract will contain less volatile substances such as cholesterol, thereby necessitating a careful cleaning procedure for the GC column after each injection.

3.3.4.2 Principle of Assay

The fatty acid glycerol esters and the plasmalogens are transmethylated by adding methanolic HCl to the sample and heating the mixture in a closed vial at 90°C for 4 h. After cooling the sample, the fatty acid methyl esters and the dimethylacetals are extracted with hexane. The concentrated hexane solution is ready for analysis by GC.

3.3.4.3 Sample

A minimum of 50 µl of plasma or red-cell haemolysate is needed. Usually approximately 1 ml of EDTA-blood will be drawn. The erythrocytes are separated from the plasma by centrifugation (3000 rpm, 1500 × *g*, for 10 min) and washed with an equal volume of saline. Following the removal of the saline, the cells are diluted 1:1 with saline and stored in a freshly-BHT-treated Eppendorf vial (see below). A small sample is taken from the cell suspension for counting of the erythrocytes.

Plasma is stored at –20°C, in which condition the fatty acids are stable for 1 year; in the authors' laboratory the red cell suspension will be stored at 6°C for a maximum of 3 weeks, after which they are kept at –80°C for a maximum of 1 year.

3.3.4.4 Reagents and Chemicals

The fatty acids are purchased in the form of methyl esters (see Table 3.3.2).

1. Internal standard stock solution: weigh 33 mg of the 18-methyl-C19:0 methylester and dissolve it in 50 ml of chloroform (approximately 2 mmol/l, store at 6°C).

Table 3.3.2 *Sources of the required reagents.* BHT *2,6-di-tert.Butyl-4-hydroxytoluene*

Reagent	Source
C14:0	Sigma M3378
C16:0	Sigma P5177
C18:0	Sigma S5376
C20:0	Sigma A3881
C22:0	Sigma B3271
C24:0	Sigma L6766
C18:3ω3	Sigma L2626
C18:4ω3	Sigma O5130
C20:5ω3	Sigma E2012
C22:5ω3	Sigma D5679
C22:6ω3	Sigma D2659
C14:1ω5	Sigma M8380
C18:2ω6	Sigma L1876
C18:3ω6	Sigma L6503
C20:2ω6	Sigma E7877
C20:3ω6	Sigma E3511
C20:4ω6	Sigma A9298
C22:2ω6	Sigma D4034
C22:4ω6	Sigma D3534
C22:5ω6	Larodan qualmix fish 89-5550
C16:1ω7	Sigma P6087
C18:1ω7	Sigma V1256
C20:1ω7	Sigma E3512
C16:1ω9	Sigma
C18:1ω9	Sigma O4754
C20:1ω9	Sigma E6885
C20:3ω9	Sigma E6013
C22:1ω9	Sigma E3510
C24:1ω9	Sigma N6767
C16 dimethylacetal	Sigma H7391
18-methyl-C19:0	Sigma M5906
Saline solution	NPBI 39-208/1
Methanolic HCl (3N)	Supelco 3-3050
Hexane	Merck 4391

Table 3.3.2 (continued) *Sources of the required reagents.* BHT *2,6-di-tert. Butyl-4-hydroxytoluene*

Reagent	Source
Chloroform	Merck 2444
BHT	Merck 822021
Ethanol	Merck

2. Internal standard working solution: dilute the stock solution 28-fold with chloroform. The final concentration is 72 µmol/l.
3. PUFA mix: accurately weigh each of the fatty acid methylesters and dissolve these in 50 ml chloroform, reaching a concentration level that is identical to that of the internal standard. Add 200 mg BHT to the solution in order to prevent oxidation of the fatty acids.
4. BHT solution: dissolve 1.0 g BHT in 100 ml ethanol. Store the solution in a dark bottle at 6°C. Stable for 1 year. Immediately prior to handling of the erythrocytes, 100 µl BHT is put into an Eppendorf tube and dried under a stream of nitrogen at 40°C.

3.3.4.5 Instrumentation

A gas chromatograph of the Hewlett-Packard 5890 series with a HP 7673A injector and a flame ionisation detector can be used. A capillary free fatty acid phase (Hewlett-Packard FFAP 19091F-105) column (50 m × 0.20 mm × 0.33 µm) is cut into two equal 25-m lengths, which are used for the separation, provided that a capillary pre-column (J&W Scientific Altech 93493) with a 50% phenyl silicone DB 17 coating (1.35 m of a 15 m × 0.25 mm × 0.25 µm column) is installed.

3.3.4.6 Procedure

Erythrocyte suspensions are frozen at –20°C overnight prior to analysis. Pipette 100 µl of the internal standard working solution in a 4-ml glass vial. Add 50 µl of plasma or erythrocyte suspension. Add 1 ml of 3N methanolic HCl, close the vial with a screw cap and Teflon insert and allow the transmethylation to proceed at 90°C for 4 h.

After cooling the vials to room temperature, add 2 ml hexane, close the vial again and vortex for 10 s. Transfer the upper (hexane) layer to a glass tube with a cone bottom and carefully evaporate the hexane with a gentle stream of nitrogen at room temperature. Finally, dissolve the residue in 100 µl (plasma) or 80 µl (erythrocytes) of hexane and transfer the sample to a GC injection vial with a crimp cap or a screw cap. Inject 1 µl into the GC.

Because of the sensitivity of the PUFA towards oxidation, the glass wool in the liner of the GC system should be replaced prior to each series of erythrocyte analy-

ses. The plasmalogen dimethylacetals are even more sensitive to decomposition in "active spots" in the injection system. Accordingly, the inertness of the injection system should be checked with every series by analysing a "plasmalogen extract" (see 3.3.4.7). Samples that are primarily to be analysed for plasmalogen levels are positioned in the first part of the sample queue in order to minimise the risk of "active spot" formation.

Injection of a blank hexane sample will show the presence of any high-boiling artefacts that have remained on the column since the previous series and emerge with the hexane.

Samples are injected (1 µl) using the splitless mode, and helium is used as a carrier gas with an inlet pressure of 2.5 Bar (250 kPa). The temperature programme starts at 50°C and is maintained for 1.5 min, followed by an increase to 190°C at a rate of 30°C/min. After holding the temperature at this level for 5 min, the gradient continues at a rate of 8°C/min until a final level of 230°C. This will be sufficiently maintained to allow all high-boiling substances (cholesterol!) to be eluted. The total analysis time will be approximately 45 min. An example of a chromatogram of control erythrocytes is shown in Fig. 3.3.2.

3.3.4.7 Quality Control

Three different internal quality control samples are used. These are:

1. A pool of erythrocyte samples. This is made up of erythrocytes from left-over EDTA-blood of a large number of different patients. Aliquots of 300 µl suspension are stored in BHT-treated Eppendorf vials at –20°C for a maximum period of 1 year. One of these samples is included in each weekly series of analyses. The results of ten selected fatty acids are plotted on an electronic Shewhart chart.
2. A mixture of EDTA-plasma samples of left-over blood of a large number of patients. Samples of 150 µl plasma are stored in Eppendorf vials at –20°C for a maximum of 1 year. Every series of analyses includes one pool plasma sample. Ten fatty acid results are plotted on an electronic Shewhart chart.
3. A so-called plasmalogen extract. This is a pool of extracted and derivatised erythrocyte samples. It is used solely to check for the detector response of the plasmalogens, thereby identifying "active spots" in the injection system.

No external quality control scheme is available for this analysis.

3.3.4.8 Validation Data

The best indicator of the reliability of the assay is the precision, expressed as the mean and coefficient of variation (CV), of a series of analyses carried out on consecutive days (the between-run variation). In the authors' laboratory the internal quality control samples were run in ten series of analyses over a 2-month period. The calculated mean, standard deviation and coefficient of variation are shown in Table 3.3.3.

It can readily be seen that most fatty acids have CV scores between 5 and 8%. Those acids that are present at much lower levels, such as some of the acids of the ω-9 series, have considerably higher CVs.

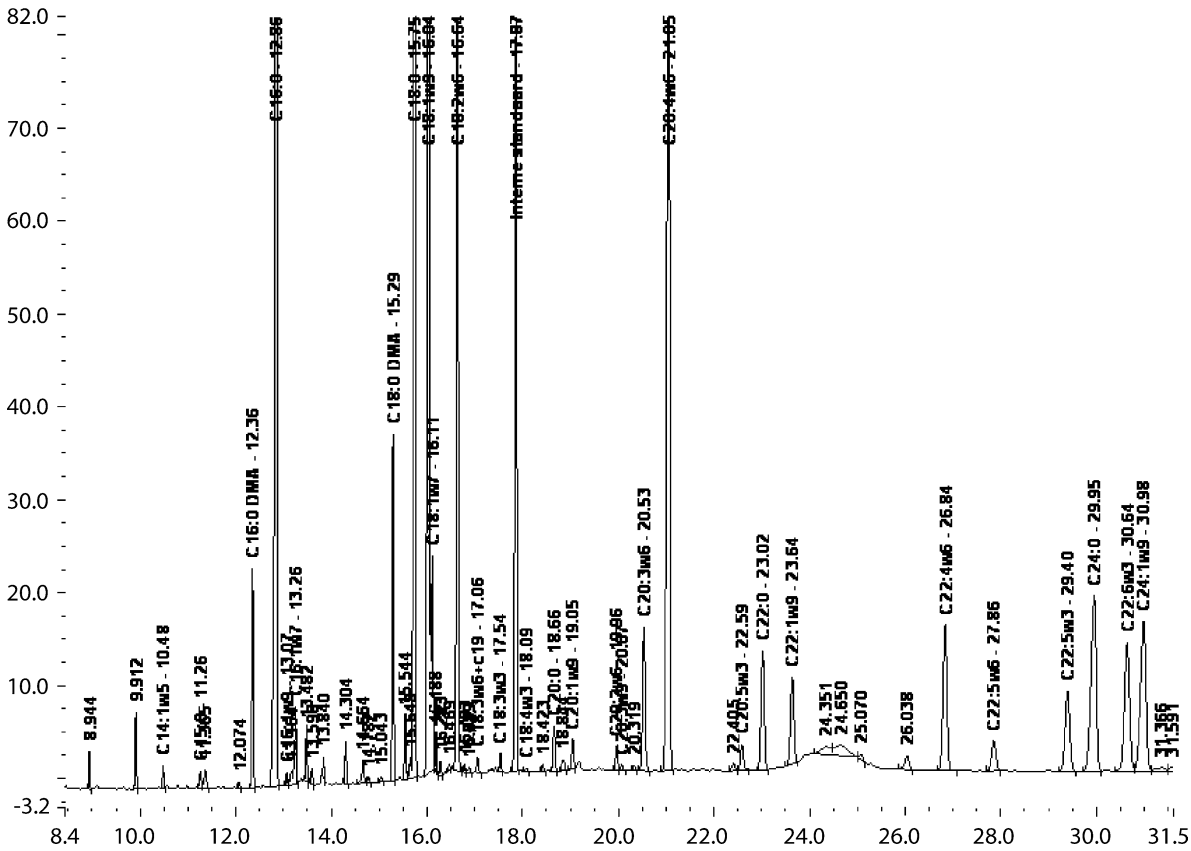

Fig. 3.3.2 Gas chromatography trace of essential fatty acid methyl esters and plasmalogen dimethylacetals in control erythrocytes. The plasmalogens are eluted adjacent to their corresponding fatty acid methyl esters

3.3.5 Interpretation: Normal/Pathological Values and Pitfalls

3.3.5.1 Reference Values for Plasmalogens and Pathological Values

The plasmalogen values are not expressed in absolute values, but as a percentage of the level of the corresponding fatty acid. Hence, the C16:0 dimethylacetal is compared with the C16:0 fatty acid methylester. The lower limit of reporting is 0.2%. Thirty random control erythrocyte samples were analysed. The lowest and highest percentages were chosen as cut-off values. For plasmalogen, this range for C16:0 and C18:0 is 6.8–11.9% and 10.6–24.9, respectively. The respective patient groups are characterised by the values listed in Table 3.3.4. Please note that this is the experience of the authors' laboratory; novel variants are currently being identified, and these may have somewhat different values.

The Zellweger spectrum is quite wide, ranging from the severe neonatal type, with characteristic dysmorphic signs and extreme hypotonia, to the milder types, with prolonged survival characterised by psychomotor retardation, hypotonia, and

Table 3.3.3 *Precision of the polyunsaturated fatty acid analysis assessed in control samples analysed over a 10-week-period.* AVG *Average,* SD *standard deviation,* CV *coefficient of variation*

Plasma (N = 10)				Erythrocytes (N = 10)			
Fatty acid	**AVG**	**SD**	**CV (%)**	**Fatty Acid**	**AVG**	**SD**	**CV (%)**
C14:0	165	12	7	**C14:0**	3.0	1.4	46.0
C15:0	32	2	6	**C15:0**	0.8	0.2	29.4
C16:0	2898	174	6	**C16:0**	126.3	9.2	7.3
C18:0	725	40	5	**C18:0**	84.9	5.1	6.0
C20:0	24	1	6	**C20:0**	2.0	0.1	4.6
C22:0	54	3	6	**C22:0**	7.0	0.3	4.6
C24:0	33	3	9	**C24:0**	15.1	1.0	6.4
C18:3w3	57	3	6	**C18:3w3**	0.7	0.1	10.6
C18:4w3	2	1	66	**C18:4w3**	0.3	0.0	14.2
C20:5w3	65	5	8	**C20:5w3**	2.0	0.2	8.3
C22:5w3	28	2	8	**C22:5w3**	6.8	0.6	8.8
C22:6w3	113	9	8	**C22:6w3**	11.8	1.1	9.0
C14:1w5	11	1	7	**C14:1w5**	0.4	0.1	35.4
C18:2w6	2885	214	7	**C18:2w6**	48.2	3.5	7.2
C18:3w6	49	3	6	**C18:3w6**	0.6	0.2	39.1
C20:2w6	19	1	7	**C20:2w6**	1.1	0.1	8.0
C20:3w6	146	10	7	**C20:3w6**	5.7	0.3	5.7
C20:4w6	546	36	7	**C20:4w6**	60.9	4.0	6.6
C22:4w6	14	1	6	**C22:4w6**	10.8	0.7	6.9
C22:5w6	10	1	14	**C22:5w6**	1.7	0.2	12.2
C16:1w7	284	20	7	**C16:1w7**	1.9	0.2	12.0
C18:1w7	173	12	7	**C18:1w7**	6.1	0.6	9.9
C20:1w7	9	7	74	**C20:1w7**	0.2	0.0	0.0
C16:1w9	52	4	7	**C16:1w9**	0.6	0.2	41.1
C18:1w9	2211	136	6	**C18:1w9**	61.8	4.3	6.9
C20:1w9	16	2	10	**C20:1w9**	1.0	0.1	9.8
C20:3w9	12	1	5	**C20:3w9**	0.4	0.1	27.2
C22:1w9	12	5	42	**C22:1w9**	1.5	0.5	35.4
C24:1w9	61	5	9	**C24:1w9**	14.5	1.1	7.4

Table 3.3.4 *Pathological plasmalogen levels: all figures represent the percentage of the corresponding fatty acid.* DHAPAT *Dihydroxyacetone phosphate acyltransferase,* RCDP *rhizomelic chondrodysplasia punctata*

Disorder	C16:0 Plasmalogen	C18:0 Plasmalogen
Classical Zellweger syndrome	2.2–4.6	3.6–7.1
Variant Zellweger syndrome	6.4–8.5	8.0–13.5
Classical RCDP (PEX 7)	0.2–0.6	0–0.2
Variant RCDP (PEX 7)	2.4–5.9	6.5–13.6
DHAPAT-deficiency	0.3	1.2

visual and hearing problems. Mildly affected patients with a proven defect of one of the peroxisome assembly genes may have entirely normal plasmalogen levels.

Classical rhizomelic chondrodysplasia punctata (RCDP) patients have a marked shortening of their proximal extremities, calcified stippling of the epiphyses and cataracts in addition to their absent psychomotor development. Patients with a variant form of RCDP have normal bones, but will have cataracts and some degree of mental retardation. Patients with a deficiency of dihydroxyacetone phosphate acyltransferase are clinically indistinguishable from the classical RCDP phenotype.

Increased plasmalogen levels have not been observed. Erroneously low red cell levels can be encountered when the transmethylation process has not been completed. Breaking the ether lipid bond of the plasmalogens requires more energy than hydrolysis of the fatty acid esters. Evaluation of the plasmalogen levels should not be done after a blood transfusion. Donor erythrocytes will be present for up to 120 days following a transfusion.

Attempts to raise the plasmalogen levels in RCDP patients involve the administration of shark liver extracts, which may contain appreciable amounts of batyl alcohol, a C16:0 precursor. By doing this, the balance between the C16:0 and C18:0 plasmalogens will be perturbed. It is still unknown whether there is clinical efficacy from such treatment.

3.3.5.2 Reference Values, Pathological Values and Pitfalls for PUFA

Levels of PUFA in plasma are subject to multiple different dietary influences. The plasma PUFA profile may be determined not only by the time elapsed between the ingestion of fat-containing foods, but also by the type of dietary lipid ingested. In this respect, the red cells are more stable, as it is generally believed that these cells keep their PUFA distribution throughout their life. Erythrocyte levels of PUFA may reflect the long-term essential fatty acid intake. Although humans are capable of synthesising all PUFA from oleic acid, linoleic acid and linolenic acid, a growing number of food constituents are currently fortified with the prime essential fatty acids AA, DHA and EPA.

Our normal values were obtained from a group of 20–30 volunteers. Blood samples were taken at mid-morning after a self-chosen simple breakfast. The individual values are listed in Table 3.3.5.

Pathological values invariably refer to decreased levels of the essential fatty acids, either in erythrocytes or in plasma. For a correct understanding of the mechanisms resulting in lowering of the fatty acid levels, one has to take note of the source of the fatty acids and their interconversion.

Dietary intake is of great importance. Linoleic acid (C18:2ω6) and α-linolenic acid (C18:3ω3) are the parent essential fatty acids for humans. Both fatty acids derive from vegetable oils. Higher fatty acids are then produced by chain elongation and desaturation. In addition, some of the prime essential fatty acids, AA (C20:4ω6), EPA (C20:5ω3) and DHA (C22:6ω3), can be obtained directly from the diet. Meat and eggs are rich in AA, whereas fish is a rich source of EPA and DHA [14].

As outlined herein, humans are unable to synthesise DHA from its precursor C22:5ω3. The latter is therefore first converted into its C24 analogue, followed by desaturation and subsequent chain-shortening by peroxisomal β-oxidation [7].

It has been shown that flux through the peroxisomal β-oxidation pathway is limited [5], mainly as a result of the relatively small oxidative capacity of peroxisomes. Subjects on a vegan diet have considerably lower DHA levels compared to omnivores.

Patients with a peroxisome biogenesis defect (Zellweger syndrome) are especially low in DHA for two reasons: (1) they have no peroxisomal fatty acid β-oxidation and (2) they do not produce the C_{24}-bile acids that are essential for the intestinal resorption of fatty acids. Patients with isolated defects of peroxisomal β-oxidation such as D-bifunctional protein deficiency may have similarly low levels of DHA and AA. There seems to be an adequate response to dietary supplementation of these fatty acids.

In contrast to the general peroxisome biogenesis defects, patients with X-linked adrenoleucodystrophy, whose very-long-chain fatty acid oxidation is impaired as a result of an uptake defect, show minimal abnormalities of their DHA levels.

Severe deficiency of all essential fatty acids can be observed in patients suffering from β-lipoproteinaemia and related defects affecting the handling of lipids. An equally impressive shortage of fatty acids occurs in patients who rely on a synthetic diet, such as an amino acid mixture replacing natural protein. This is exemplified by diets of patients with phenylketonuria, maple syrup urine disease and the organic acidaemias including glutaric aciduria type 1. In addition, numerous metabolic and non-metabolic conditions affecting the essential fatty acid changes have been described, including disorders such as hypothyroidism [13] and behavioural effects (e.g. smoking) [11].

The ω-3 fatty acids have numerous important functions, especially in the brain. Accordingly, a deficiency of DHA and EPA may cause dysfunction of the central nervous system and probably also the retina, thereby resulting in impaired vision. In addition, there is a variety of neurological and psychiatric disorders that have been associated with decreased levels of especially DHA and AA, such as, for example, schizophrenia and depression [3], post-traumatic stress syndrome, autism and attention deficit hyperactivity disorder. Since no primary inherited defect of essential fatty acid interconversion has yet been described, no specific explanations for the essential fatty acid concentration changes are readily available.

Table 3.3.5 *Reference values for total (= bound + free) fatty acids in plasma and erythrocytes. The plasma values are expressed as µmol/l, those for erythrocytes as pmol/10^6 cells*

Fatty acid	Plasma (N = 29) 5–90% Confidence interval	Erythrocytes (N = 20) Lowest–highest values
C14:0	50–145	0.7–6.9
C16:0	1465–2790	113–193
C18:0	465–755	81–141
C20:0	15–30	2–3.4
C22:0	40–100	6.3–13.7
C24:0	35–75	16.3–33.1
ω3-series		
C18:3ω3	30–70	0.1–1.8
C18:4ω3	0–10	0–0.9
C20:5ω3	15–95	1.1–7.7
C22:5ω3	20–50	7.6–23
C22:6ω3	75–180	15.2–37.6
ω5-series		
C14:1ω5	0–10	0–3
ω6-series		
C18:2ω6	1950–3500	52–89
C18:3ω6	15–50	0–0.4
C20:2ω6	10–40	0.2–2.4
C20:3ω6	70–190	6–19.6
C20:4ω6	300–650	67–107
C22:2ω6	0–5	0–4
C22:4ω6	10–25	9.5–26.6
C22:5ω6	5–20	1.4–6.2
ω7-series		
C16:1ω7	85–330	2.1–12.9
C18:1ω7	130–250	0.2–10
C20:1ω7	0–5	0–3
ω9-series		
C16:1ω9	15–90	0–7.2
C18:1ω9	1035–2025	58–115
C20:1ω9	10–25	0–3.5
C20:3ω9	10–20	1–4.1
C22:1ω9	0–8	0.2–8.3
C24:1ω9	55–85	15.5–35.8
Total fatty acids	5950–11600	535–840

References

1. Anderson GJ, Connor WE, Corliss JD (1990) Docosahexaenoic acid is the preferred dietary ω-3 fatty acid for the development of the brain and retina. Pediatr Res 27:89–97
2. Assies J, Lieverse R, Vreken P, Wanders RJA, Dingemans PMJA, Linszen DH (2001) Significantly reduced docosahexaenoic and docosapentaenoic acid concentrations in erythrocyte membranes form schizophrenic patients compared with a carefully matched control group. Biol Psychiatr 45:510–522
3. Assies J, Lok A, Bockting CL, Weverling GJ, Lieverse R, Visser I, Abeling NGGM, Duran M, Schene AH (2004) Fatty acids and homocysteine levels in patients with recurrent depression: an explorative pilot study. Prostaglandins Leukot Essent Fatty Acids 70:349–356
4. Björkhem I, Sisfontes L, Bostrom B, Kase BF, Blomstrand R (1986) Simple diagnosis of the Zellweger syndrome by gas-liquid chromatography of dimethylacetals. J Lipid Res 27:786–791
5. Burdge GC, Wootton SA (2002) Conversion of alpha-linolenic acid to eicosapentaenoic, docosapentaenoic and docosahexaenoic acids in young women. Br J Nutr 88:411–420
6. Dacremont G, Vincent G (1995) Assay of plasmalogens and polyunsaturated fatty acids (PUFA) in erythrocytes and fibroblasts. J Inherit Metab Dis 18:84–89
7. Ferdinandusse S, Denis SW, Mooijer PAW, Zhang Z, Reddy JK, Spector AA, Wanders RJA (2001) Identification of the peroxisomal beta-oxidation enzymes involved in the biosynthesis of docosahexaenoic acid. J Lipid Res 42:1987–1995
8. Lee S, Gura KM, Puder M (2007) Omega-3 fatty acids and liver disease. Hepatology 45:841–845
9. Martinez M (1990) Severe deficiency of docosahexaenoic acid in peroxisomal disorders: a defect of delta 4 desaturation? Neurology 40:1292–1298
10. Muskiet FAJ, van Doormaal JJ, Martini IA, Wolthers BG, W van der Slik (1983) Capillary gas chromatographic profiling of total long-chain fatty acids and cholesterol in biological materials. J Chromatogr 278:231–244
11. Pawlowski R, Hibbeln J, Wegher B, Sebring N, Salem N Jr (1999) The effects of cigarette smoking on the metabolism of essential fatty acids. Lipids 34:S287
12. Price PT, Nelson CM, Clarke SD (2000) Omega-3 polyunsaturated fatty acid regulation of gene expression. Curr Opin Lipidol 11:3–7
13. Raederstorff D, Meier CA, Moser U, Walter P (1991) Hypothyroidism and thyroxin substitution affect the ω-3 fatty acid composition of rat liver mitochondria. Lipids 26:781–787
14. Smit EN, Oelen EA, Seerat E, Boersma ER, Muskiet FAJ (2000) Fish oil supplementation improves docosahexaenoic acid status of malnourished infants. Arch Dis Child 82:366–369

3.4 Very-Long-Chain Fatty Acids and Phytanic Acid

Ronald J.A. Wanders, Marinus Duran

3.4.1 Introduction

Peroxisomes are subcellular organelles, just like, for example, mitochondria, lysosomes and endosomes. Recent evidence suggests that peroxisomes, which lack their own DNA, are semi-autonomous organelles that are able to grow and divide into daughter peroxisomes, but are originally derived from a special subdomain of the endoplasmic reticulum. It is well established now that peroxisomes catalyse several essential metabolic functions that cannot be carried out by other organelles. From the perspective of genetic diseases in humans, the following functions are of special interest: (1) fatty acid beta-oxidation, (2) etherphospholipid biosynthesis, (3) fatty acid alpha-oxidation and (4) glyoxylate detoxification. Although peroxisomes were originally thought to play a major role in the biosynthesis of isoprenoids, including cholesterol, recent data strongly suggest otherwise.

In order to carry out all of these different functions, peroxisomes are equipped with a unique set of enzyme proteins, catalysing the different reactions involved. In addition, the peroxisomal membrane contains specific transporters in order to take up substrates from the cytosol and release the end products of peroxisomal metabolism. Since peroxisomes lack a citric acid cycle as well as a respiratory chain, the end products of peroxisomal metabolism, such as acetyl-CoA, propionyl-CoA and a range of other acyl-CoA esters predominantly derived from fatty acid beta-oxidation, are exported from the peroxisomal interior and shuttled to mitochondria for full oxidation to CO_2 and H_2O. The same applies to the NADH produced during beta-oxidation, which is reoxidised via redox-shuttles so that the NADH generated in peroxisomes is ultimately reoxidised in the mitochondrial respiratory chain at the expense of molecular oxygen.

Both the integral membrane proteins of peroxisomes as well as the peroxisomal matrix proteins are synthesised on free polyribosomes and are specifically targeted to peroxisomes via dedicated peroxisomal targeting signals. The biogenesis of peroxisomes follows a sequential pattern, which involves first the insertion of peroxisomal membrane proteins into the membrane of the pre-peroxisomal structure, derived from the endoplasmic reticulum, followed by insertion of the various matrix proteins.

3.4.1.1 Peroxisomal Disorders

The peroxisomal disorders so far recognised are usually subdivided into two groups: (1) the peroxisome biogenesis disorders and (2) the single peroxisomal enzyme deficiencies. Group 1 contains two distinct subgroups including the Zellweger spectrum disorders (ZSDs), and rhizomelic chondrodysplasia punctata (RCDP) type 1. In the ZSDs with Zellweger syndrome, neonatal adrenoleukodystrophy (ALD) and infantile Refsum disease as main representatives [16], peroxisome biogenesis is fully impaired, although to variable extents, whereas in RCDP type 1, peroxisome biogenesis is only partially deficient. This explains why in ZSDs basically all peroxisomal functions are impaired, which leads to the accumulation of a whole series of peroxisomal metabolites in plasma, whereas in RCDP type 1 only etherphospholipid biosynthesis and phytanic acid alpha-oxidation are affected.

Group 2 contains the single peroxisomal enzyme deficiencies [14]. This group is also subdivided in different classes, including the peroxisomal beta-oxidation deficiencies (X-linked adrenoleucodystrophy, X-ALD), acyl-CoA oxidase 1 deficiency [4], D-bifunctional protein deficiency [5], 2-methyl acyl-CoA racemase (AMACR) deficiency [3] and sterol carrier protein (SCP-x) deficiency [6], the disorders of etherphospholipid biosynthesis (dihydroxyacetone phosphate acyltransferase and alkyl- dihydroxyacetone phosphate synthase deficiency) [2], the disorders of phytanic acid alpha-oxidation (Refsum disease) [15], and the disorders of glyoxylate detoxification with hyperoxaluria type 1 as caused by alanine glyoxylate aminotransferase deficiency as a sole representative.

Table 3.4.1 depicts the different peroxisomal disorders and the very-long-chain, pristanic and phytanic acid levels in each of these disorders. The results clearly show that very-long-chain fatty acids (VLCFA) are increased in the ZSDs as well as in X-ALD, acyl-CoA oxidase 1 deficiency, and D-bifunctional protein deficiency, but normal in all other disorders, including SCP-x deficiency, and AMACR deficiency. In the latter two disorders, however, pristanic acid accumulates as well as the bile acid intermediates di- and trihydroxycholestanoic acid. Phytanic acid is elevated in the ZSDs, in RCDP type 1, and also in Refsum disease. The data of Table 1 clearly show that combined analysis of VLCFA, pristanic acid and phytanic acid is a powerful method to diagnose patients affected by a peroxisomal disorder, although the disorders of etherphospholipid biosynthesis, notably RCDP type 2 and 3, as well as hyperoxaluria type 1 require testing of other metabolites, including plasmalogen levels in erythrocytes, and glyoxylate, glycolate and oxalate levels in urine, respectively.

3.4.2 Properties of Analytes

The VLCFA as well as the branched-chain fatty acids phytanic acid and pristanic acid are extremely hydrophobic and practically insoluble in water. Their intracellular presence is in the form of coenzyme A esters. These acids are usually stored in lipid-containing tissues such as adipose tissue, but they may also be constituents of various physiologically important lipids such as myelin. In this respect, the VLCFA and the branched-chain fatty acids are abundant in many tissues/organs.

Circulating VLCFA and branched-chain fatty acids are mainly present in an esterified form such as triglycerides, phospholipids, cholesterol esters and even car-

Table 3.4.1 *Levels of very-long-chain fatty acids (*VLCFA*), pristanic acid and phytanic acid in the different peroxisomal disorders.* AMACR *2-methyl acyl-CoA racemase,* N *normal,* RCDP *rhizomelic chondrodysplasia punctata,* SCP-x *sterol carrier protein,* ZSDs *Zellweger spectrum disorders,* ↑ *elevated*

Group 1	VLCFA	Pristanic acid	Phytanic acid
ZSDs	↑	**N-↑**[a]	**N-↑**[a]
RCDP type1	**N**	**↓-N**	**N-↑**[a]
Group 2			
Peroxisomal beta-oxidation deficiencies			
X-linked adrenoleucodystrophy	↑	**N**	**N**
Acyl-CoA oxidase deficiency	↑	**N**	**N**
D-bifunctional protein deficiency	↑	**N-↑**[a]	**N-↑**[a]
SCP-x deficiency	**N**	**N-↑**[a]	**N-↑**[a]
AMACR deficiency	**N**	**N-↑**[a]	**N-↑**[a]
Etherphospholipid biosynthesis deficiencies			
RCDP type 2	**N**	**N**	**N**
RCDP type 3	**N**	**N**	**N**
Phytanic acid alpha-oxidation deficiencies			
Refsum disease	**N**	**N**	**N-↑**[a]
Glyoxylate detoxification deficiencies			
Hyperoxaluria type 1	**N**	**N**	**N**

[a] Levels may vary from normal to (markedly) elevated, which depends on the diet and on age

nitine esters [9]. The free forms of the VLCFA are hardly detectable: if any, they will be bound to plasma proteins such as albumin. Consequently, the VLCFA are not filtered by the kidneys and do not appear in the urine.

The saturated VLCFA and branched-chain fatty acids are stable compounds: they are not likely to be destroyed by oxidative processes. In this respect, storage of samples does not require more precautions than freezing.

Various VLCFA may occur as constituents of industrial waxes or grease. In the light of the low level of especially the C26-fatty acid in plasma, one should clean all glassware used in the analytical procedure meticulously.

Although patients with impaired peroxisomal function will accumulate VLCFA with chain lengths in excess of 26 [7], the diagnostic process can be carried out safely using C22, C24 and C26 fatty acids and their ratios [8].

3.4.3 Specimens for Analysis

A 2- to 5-ml venous blood sample is taken, preferably using EDTA as anti-coagulant, centrifuged for 10 min at 1000 × *g*, preferably within 1 h of sample collection, and the plasma is collected by aspiration and stored at –20° C. If possible, samples should be collected before breakfast after an overnight fast. However, since at least the levels of VLCFA show only minimal diurnal variation upon consumption of a usual Western diet, postprandial samples are also acceptable. Although EDTA samples are preferred, heparinised samples give equivalent results. Importantly, since the levels of VLCFA, phytanic acid and pristanic acid are not affected by storage at room temperature for up to several days, samples may be sent at ambient temperature, although we recommend that samples be sent frozen, especially when transit times exceed 48 h. The levels of the analytes in frozen plasma are stable for 2 years.

3.4.4 Stable Isotope Dilution Gas Chromatography/Mass Spectrometry

3.4.4.1 Principle

Several techniques have been described in the past for the analysis of VLCFA, pristanic acid and phytanic acid [1, 10]. In our hands gas chromatography-mass spectrometry (GC-MS) analysis after derivatisation with N-methyl-N-(tert-butyldimethylsilyl) trifluoroacetamide (MTBSTFA), is a robust and reliable method for the quantitative analysis of VLCFA, pristanic acid and phytanic acid, especially when combined with stable isotopes for C26:0, C24:0, C22:0, phytanic acid and pristanic acid [13]. In order to allow measurement of the total pool of VLCFA, pristanic acid and phytanic acid, samples need to be subjected to both acidic and alkaline hydrolysis, followed by extraction into hexane. After the hexane phase is washed once more, the sample is dried under nitrogen followed by addition of pyridine and MTBSTFA and heating of the samples at 80°C. The sample is subsequently dried again under nitrogen and taken up in hexane, followed by GC-MS analysis.

In recent years, alternative methods for analysis of VLCFA have gone into development. These include the application of electrospray tandem mass spectrometry [12]. Although this method looks promising concerning the aspect of speed of analysis, it has not yet been applied diagnostically.

3.4.4.2 Standards and Chemicals

The following internal standards suitable:

1. C26:0-d_4 (3,3,5,5-$^2H_4$-hexacosanoic acid).
2. C24:0-d_4 (3,3,5,5-$^2H_4$-tetracosanoic acid).
3. C22:0-d_4 (3,3,5,5-$^2H_4$-docosanoic acid).
4. Pristanic acid-d_3 (2-methyl-$^2H_3$-6,10,14-trimethyl) pentadecanoic acid).
5. Phytanic acid-d_3 (3-methyl-$^2H_3$-7,11,15-trimethyl) hexadecanoic acid.

All labelled and unlabelled standards can be obtained from Dr. Herman ten Brink, VU Medical Centre, Amsterdam, The Netherlands (http://www.vumc.nl/metabool/index.html) or from other sources.

Other Materials/Chemicals

1. Acetonitrile (Merck).
2. HCl 37% (Merck).
3. HCl 25% (Merck).
4. Sodium hydroxide (NaOH; Merck).
5. Potassium hydroxide (KOH; Merck).
6. n-Hexane (Merck).
7. Pyridine (Merck).
8. Toluene analytical grade (Merck).
9. MTBSTFA (Aldrich).
10. Double-distilled water (Millipore).
11. Nitrogen gas.
12. Phosphate-buffered saline, produced in-house.
13. Acid hydrolysis reagent: Mix 1 part of 37% HCl with 23 parts of acetonitrile. Prepare freshly before each series of analyses.
14. Alkaline hydrolysis reagent: Dissolve 8.0 g of NaOH in approximately 10 ml water and dilute to 200 ml. The solution is stable for 1 year when stored at room temperature.
15. 1 M KOH: Dissolve 56 g of KOH in 1 l of water. Stored at room temperature. The solution will remain suitable for us for one year.

The internal standard solution is made up in toluene. All labelled fatty acids are carefully weighed in such a way that the following concentrations are reached:

1. $^{2}H_{3}$-pristanic acid: 1 μmol/l.
2. $^{2}H_{3}$-phytanic acid: 4 μmol/l.
3. $^{2}H_{4}$-C22:0: 50 μmol/l.
4. $^{2}H_{4}$-C24:0: 50 μmol/l.
5. $^{2}H_{4}$-C26:0: 1 μmol/l.

3.4.4.3 Instrumentation

Measurements are performed on a bench-top GC-MS (Hewlett Packard Gas Chromatograph type 6890N) operating in the electron impact mode, and the acquired data are processed by the accompanying GC-MS software (Chemstation). The GC is equipped with a CPSil19 capillary column (25 m×0.25 mm×0.20 μm; Varian); the injection system is used in the splitless mode and kept at 300°C. The interface to the mass selective detector is set at 290°C. GC separation of the analytes is achieved using the following column temperature program: initial temperature 60°C for 1 min; increase to 240°C at a rate of 30°C/min; further increase to 270°C at a rate of 10°C/min; final increase to 300°C at 4°C/min, and 5 min isothermal at the latter level. Figure 3.4.1 shows the mass fragmentogram of a control, a Refsum patient, and a patient with Zellweger syndrome.

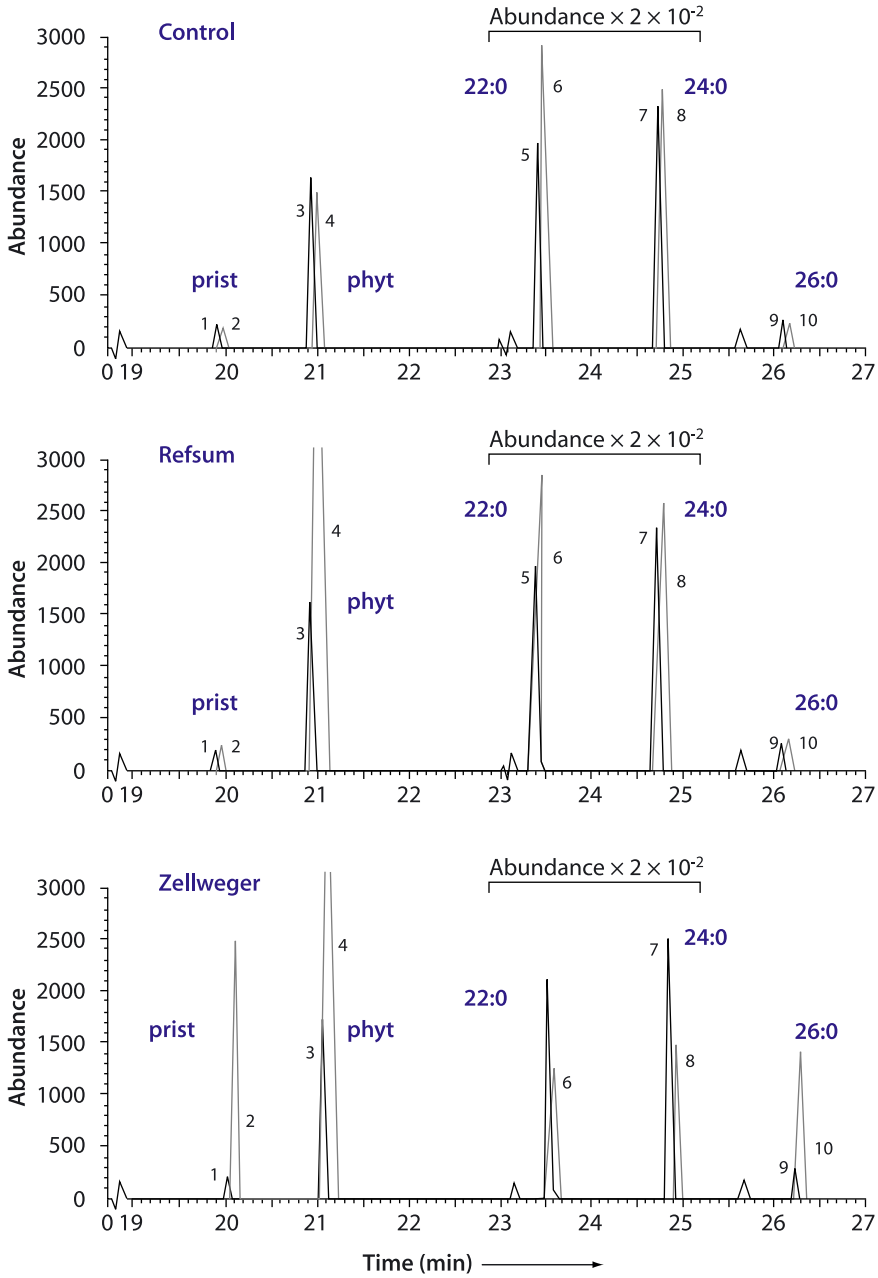

Fig. 3.4.1 Mass fragmentogram of the plasma very-long-chain fatty acids, phytanic acid and pristanic acid in a control, a patient with Refsum disease and a patient with a peroxisome biogenesis defect (Zellweger syndrome). Plots represent the (m-57)-fragments of the tertiarybutyl-dimethylsilyl derivatives. Numbered peaks represent: (1) $2H_3$-pristanic acid; (2) native pristanic acid; (3) $^2H_3$-phytanic acid (4) native phytanic acid; (5) $^2H_4$-$C_{22:0}$ fatty acid; (6) native $C_{22:0}$ fatty acid; (7) $^2H_4$-$C_{24:0}$ fatty acid; (8) native $C_{24:0}$ fatty acid; (9) $^2H_4$-$C_{26:0}$ fatty acid; (10) native $C_{26:0}$ fatty acid. *prist* Pristanic acid, *phyt* phytanic acid, *22:0* $C_{22:0}$ fatty acid, *24:0* $C_{24:0}$ fatty acid, *26:0* $C_{26:0}$ fatty acid

3.4.4.4 Procedure

1. Thaw plasma or serum and internal standard mixtures on ice.
2. Set heating block at 110°C.
3. Collect and label 4-ml standard glass tubes equipped with screw caps and Teflon liner (Alltech).
4. Transfer 100 µl plasma/serum into a 4-ml glass tube.
5. Add 100 µl internal standard solution plus 2 ml acid hydrolysis reagent. Cap the tubes tightly, mix carefully and put the tubes in the heating block for 45 min.
6. Remove the tubes from the heating block and allow to cool down to room temperature.
7. Remove the screw caps and add 2 ml of alkaline hydrolysis reagent.
8. Cap the tubes tightly, mix carefully and put the tubes in the heating block again for 45 min at 110°C.
9. Remove the tubes from the heating block and allow to cool down to room temperature.
10. Remove the screw caps and add 0.5 ml of 25% hydrochloric acid.
11. Add 4 ml hexane, screw the tubes tightly and mix for about 60 s by hand.
12. Allow phase separation, collect the upper hexane layer with the aid of a glass Pasteur pipette and transfer the sample into a glass 10-ml tube equipped with a screw cap.
13. Add 3.5 ml 1M KOH to the tubes, screw the tubes tightly and mix the samples by hand.
14. Remove the upper hexane phase with the aid of a glass pipette attached to a water pump.
15. Add 0.6 ml of 25% hydrochloric acid (HCl).
16. Add 4 ml hexane again and mix the samples by hand
17. Transfer the upper hexane layer in a glass 4-ml tube with the aid of a glass Pasteur pipette; dry the samples under nitrogen in a heating block set at 50°C.
18. Rinse the tubes with 50 µl pyridine and add 100 µl MTBSTFA reagent.
19. Cap the tubes tightly and allow derivatisation at 80°C for 30 min.
20. Dry the samples under nitrogen in a heating block set at 50°C.
21. Rinse the tubes with 200 µl hexane and transfer the contents into a 1-ml injection vial.
22. Samples are now ready for analysis by GC-MS

3.4.5 Quality Control

A pool of a large number of left-over plasma samples of patients is thoroughly mixed. Aliquots of 150 µl are put into Eppendorf vials and stored at –20°C. These samples are stable for 1 year. Each series of analyses has one pool plasma sample. The concentrations of the five analytes are introduced into an electronic Shewhart chart, which is renewed each year.

External quality control samples are provided by European Research Network for the evaluation and improvement of screening, Diagnosis and treatment of Inherited disorders of Metabolism in its Special Assays Serum scheme. Eight lyophilised samples are distributed each year, consisting of four pairs of samples with increasing

fatty acid levels, from physiological to pathological concentrations. This gives a good indication of the precision, linearity and recovery of the laboratory's analytical performance. Comparison of the results with the mean of all participating laboratories gives an indication of the accuracy.

3.4.6 Validation Data

The intra- and inter-assay variation is determined in tenfold analyses of a pool plasma sample. Table 3.4.2 shows the results of these measurements. The linearity of this method should be assessed for all analytes. Pristanic acid and the C26:0 fatty acid were linear up to 16 µmol/l, phytanic acid to 100 µmol/l and the C22:0 and C24:0 fatty acid to 200 µmol/l. The lower detection limit for all analytes was at a level of less than 0.01 µmol/l, for the lower reporting levels (LOQ), an analysis of a blank solution was taken into account. The blank levels of the analytes phytanic acid, pristanic acid, and fatty acids C22:0, C24:0 and C26:0 were 0.04, 0.01, 0.41, 0.68 and 0.18 µmol/l, respectively.
It was agreed to set the LOQ at twice the blank level. This may render occasional problems for the C26:0 fatty acid as the LOQ of 0.336 µmol/l is close to the lower end of the physiological concentration range. Glassware should be ultra-pure to reduce the blank values as much as possible.

3.4.7 Reference Values, Pathological Values and Pitfalls

The VLCFA are produced in the peroxisomes. These cellular organelles do not show an appreciable variation of enzyme activities over the day or with age. Consequently, reliable reference values are available and it is our experience that approximately the same values are used in most experienced laboratories.

Our reference values for the straight-chain fatty acids were established using 157 controls (see Table 3.4.3). The concentrations of VLCFA in controls were independent of age. Phytanic and pristanic acid – or their precursor phytol – are exclusively derived from the diet. Accordingly, the reference values for these substances are somewhat age-dependent, especially below the age of 2 years [11]. The upper refer-

■ ***Table 3.4.2*** *Validation data calculated from ten-fold analyses of a low-pool (left two data panels) and a high-pool (right two data panels); all concentrations are given in µmol/l.* CV *Coefficient of variation*

Compound	Intra-assay average	Intra-assay CV (%)	Inter-assay average	Inter-assay CV(%)
Pristanic acid	0.44	1.7	2.8	4.6
Phytanic acid	2.9	1.7	10	5.6
C22:0	61	3.0	40	3.8
C24:0	48	3.0	54	3.0
C26:0	0.52	8.0	3.1	6.4

Table 3.4.3 *Concentrations of VLCFA in the plasma of 157 controls. All values are presented in µmol/l*

Analyte	Median value	5–95% Confidence interval
C22:0	75	40–119
C24:0	56	33–84
C26:0	0.79	0.45–1.32
C24/C22	0.75	0.57–0.92
C26/C22	0.01	0.01–0.02

ence level for phytanic acid is 10 µmol/l, whereas that for pristanic acid is 3 µmol/l for subjects aged 2 years or more.

Pathological values may vary in the different inherited defects of peroxisomal function. It is important to correlate the findings of as many peroxisomal functions as possible. In our laboratory a selective screening for peroxisomal dysfunction may include the assay of VLCFA, phytanic acid, pristanic acid, bile acids and pipecolic acid in plasma as well as plasmalogens in erythrocytes. This does not only apply to the infant with hypotonia and the characteristic dysmorphic signs of the Zellweger syndrome, but also to the adult (both male and female) with an unexplained leucodystrophy. It seems attractive to limit oneself to VLCFA analysis for adult patients – aimed at X-ALD or adrenomyeloneuropathy (AMN) – but the recent descriptions of AMACR – and SCP-x-defects warrant a broader screening as other pathways are equally affected in these patients [6].

Concerning the pathological values of VLCFA, the C26:0 fatty acid is the most informative. Classical Zellweger patients have C26:0 values of 3–12 µmol/l, still only three- to ten-fold the upper reference range. In comparison, the male ALD or AMN patients generally have C26:0 values of 2–4 µmol/l. False negative male ALD/AMN results are extremely rare, in contrast to the values of C26:0 in female ALD carriers, which range from 1.1 to 2.9 µmol/l and thus may be entirely normal. The situation for the C24:0 fatty acid is slightly different: there is a considerable overlap between patient values and control values. However, the C24:C22 ratio, which is < 0.92 in controls, will be in excess of 1.06 in virtually all patients, with the exception again of female ALD carriers, who may have C24:C22 ratios as low as 0.8. Exclusion of the ALD carrier status cannot be achieved by VLCFA analysis alone; a normal result of this test will have to be followed up by DNA testing.

Patients with an inherited defect of peroxisomal function usually have both an increased C26:0 level and an increased C24:C22 ratio. An isolated moderate increase of C26:0 has only rarely led to a true diagnosis. Nevertheless, every persistent abnormality of VLCFA levels and/or ratios should be checked by studies in fibroblasts in order to arrive at an accurate diagnosis so that genetic counselling of the family can be arranged. Erroneously increased VLCFA levels are rare; a ketogenic diet is the only well-known example.

Phytanic and pristanic acid results should always be interpreted in conjunction with each other. In general, patients with a peroxisome biogenesis defect or a de-

fect in the peroxisomal beta-oxidation system will show increases of both branched-chain fatty acids in variable ratios. Exceptions are of course patients with ALD/AMN or acyl-CoA oxidase deficiency having normal branched-chain fatty acid levels.

Patients with Refsum disease may have extremely high phytanic acid levels, up to 1500 µmol/l, whereas pristanic acid is low (< 1 µmol/l) as a consequence of the phytanoyl-CoA hydroxylase deficiency. Less pronounced phytanic acid elevations will be observed in RCDP type 1 patients, which applies to both the classical form as well as the variant forms. Values may range from 200 to 900 µmol/l, somewhat depending on age. There is some discussion on the time of onset of phytanic acid accumulation in the classical neonatal RCDP-patients. Normal plasma phytanic acid levels (0.7–5.8 µmol/l) were recorded in the authors' laboratory in patients aged less than 1 week. Two- to three-week-old RCDP patients had increased phytanic acid levels of 9.1–13.2 µmol/l. Classical patients invariably had undetectable plasmalogen levels of the erythrocytes at any age.

Isolated mild increases of phytanic acid are occasionally observed, with levels of 15–25 µmol/l. So far no explanation has been found for this phenomenon despite extensive fibroblast studies in several patients.

The dietary origin of phytanic acid makes the conditions associated with phytanic acid accumulation accessible to dietary treatment. Refsum patients should be able to reach near-normal plasma phytanic acid levels with a strict diet, assisted by plasmapheresis, when needed.

Unfortunately, a minority of the patients with peroxisomal dysfunction cannot be diagnosed using plasma parameters. In the authors' laboratory, patients have been seen with peroxisome biogenesis defects, D-bifunctional protein deficiency, and acyl-CoA oxidase deficiency in whom no abnormalities of plasma VLCFA, phytanic acid, pristanic acid or bile acids could be established. Hence, a strong clinical suspicion of peroxisomal disease should always be verified by fibroblast investigation, regardless of the outcome of plasma analyses.

References

1. Aubourg P, Bougneres PF, Rocchiccioli F (1985) Capillary gas-liquid chromatographic-mass spectrometric measurement of very long chain (C22 to C26) fatty acids in microliter samples of plasma. J Lipid Res 26:263–267
2. Clayton PT, Eckhardt S, Wilson J, Hall CM, Yousuf Y, Wanders RJA, Schutgens RBH (1994) Isolated dihydroxyacetonephosphate acyltransferase deficiency presenting with developmental delay. J Inherit Metab Dis 17:533–540
3. Ferdinandusse S, Denis S, Clayton PT, Graham A, Rees JE, Allen JT, Mclean BN, Brown AY, Vreken P, Waterham HR, Wanders RJA (2000) Mutations in the gene encoding peroxisomal alpha-methylacyl-CoA racemase cause adult-onset sensory motor neuropathy. Nat Genet 24:188–191
4. Ferdinandusse S, Denis S, Hogenhout EM, Koster J, van Roermund CWT, IJlst L, Moser AB, Wanders RJA, Waterham HR (2007) Clinical, biochemical, and mutational spectrum of peroxisomal acyl-coenzyme A oxidase deficiency. Hum Mutat 28:904–912
5. Ferdinandusse S, Denis S, Mooyer PA, Dekker C, Duran M, Soorani-Lunsing RJ, Boltshauser E, Macaya A, Gartner J, Majoie CB, Barth PG, Wanders RJ, Poll-The BT (2006) Clinical and biochemical spectrum of D-bifunctional protein deficiency. Ann Neurol 59:92–104
6. Ferdinandusse S, Kostopoulos P, Denis S, Rusch H, Overmars H, Dillmann U, Reith W, Haas D, Wanders RJA, Duran M, Marziniak M (2006) Mutations in the gene encoding peroxisomal

sterol carrier protein X (SCPx) cause leukencephalopathy with dystonia and motor neuropathy. Am J Hum Genet 78:1046–1052

7. Kemp S, Valianpour F, Denis S, Ofman R, Sanders RJ, Mooyer P, Barth PG, Wanders RJ (2005) Elongation of very long-chain fatty acids is enhanced in X-linked adrenoleukodystrophy. Mol Genet Metab 84:144–151
8. Moser AB, Kreiter N, Bezman L, Lu S, Raymond GV, Naidu S, Moser HW (1999) Plasma very long chain fatty acids in 3,000 peroxisome disease patients and 29,000 controls. Ann Neurol 45:100–110
9. Rizzo C, Boenzi S, Wanders RJA, Duran M, Caruso U, Dionisi-Vici C (2003) Characteristic acylcarnitine profiles in inherited defects of peroxisome biogenesis: a novel tool for screening diagnosis using tandem-MS. Pediatr Res 53:1–6
10. Stellaard F, ten Brink HJ, Kok RM, van den Heuvel L, Jakobs C (1990) Stable isotope dilution analysis of very long chain fatty acids in plasma, urine and amniotic fluid by electron capture negative ion mass fragmentography. Clin Chim Acta 192:33–144
11. ten Brink HJ, Stellaard F, van den Heuvel CM, Kok RM, Schor DS, Wanders RJA, Jakobs C (1992) Pristanic acid and phytanic acid in plasma from patients with peroxisomal disorders: stable isotope dilution analysis with electron capture negative ion mass fragmentography. J Lipid Res 33:1–47
12. Valianpour F, Selhorst JJ, van Lint LE, Van Gennip AH, Wanders RJA, Kemp S (2003) Analysis of very long-chain fatty acids using electrospray ionization mass spectrometry. Mol Genet Metab 79:189–196
13. Vreken P, Van Lint AEM, Bootsma AH, Overmars H, Wanders RJA, Van Gennip AH (1998) Rapid stable isotope dilution analysis of very-long-chain fatty acids, pristanic acid and phytanic acid using gas chromatography-electron impact mass spectrometry. J Chromatogr 713:281–287
14. Wanders RJA, Barth PG, Heymans HSA (2001) Single peroxisomal enzyme deficiencies. In: Scriver CR, Beaudet AL, Sly WS, Valle D (eds) The Metabolic & Molecular Bases of Inherited Disease. McGraw-Hill, New York, pp 3219–3256
15. Wanders R.J.A, Jakobs C, and Skjeldal O.H (2001) Refsum disease. In: Scriver CR, Beaudet AL, Sly WS, Valle D (eds) The Metabolic & Molecular Bases of Inherited Disease. McGraw-Hill, New York, pp 3303–3321
16. Wilson GN, Holmes RD, Custer J, Lipowitz JL, Stover J, Datta N, Hajra A (1986) Zellweger syndrome: diagnostic assays, syndrome delineation and potential therapy. Am J Med Genet 24:69–82

3.5 Oxalate, Glycolate, Glycerate, Sulfate, and Citrate

Nenad Blau

3.5.1 Introduction

Measurement of oxalate in urine is important for the diagnosis of primary hyperoxaluria (McKusick 259900) and the secondary forms resulting from excessive intake or abnormal intestinal absorption of oxalate [1]. Determination of glycolic acid is essential for the diagnosis of primary hyperoxaluria type I (PH-I), caused by low or absent activity of the liver-specific peroxisomal alanine:glyoxylate aminotransferase. In addition, to estimate the risk of stone formation in calcium oxalate urolithiasis and nephrocalcinosis, simultaneous determination not only of calcium, but also of citrate (a potent inhibitor of calcium oxalate and calcium phosphate crystallization) and other constituents (electrolytes, phosphate, and sulfate) are required to calculate the urinary calcium saturation [2]. Primary hyperoxaluria type II (PH-II) is caused by low or absent activity of D-glycerate dehydrogenase and hydroxypyruvate reductase activity, leading to elevated urinary excretion of both oxalate and L-glyceric acid [1].

Ion chromatography high-performance liquid chromatography (HPLC) is the method of choice for the quantification of oxalate, glycolate, and glycerate [3, 4]. In addition, preservation and storage of the liquid samples may influence the stability of oxalate and glycolate. Use of urinary filter spots is a practical alternative approach for the collection and safe transport of samples to be analyzed for many metabolic disorders [5].

3.5.2 Properties of Oxalate, Glycolate, and Glycerate

Oxalic acid (or ethanedioic acid, $H_2C_2O_4$; molecular weight, MW = 90.03) is a dicarboxylic acid with structure HOOC-COOH (Fig. 3.5.1). Because of the joining of two carboxyl groups, this is one of the strongest organic acids. It is also a reducing agent. The anions of oxalic acid, as well as its salts, and esters are known as oxalates. The root and leaves of rhubarb contain dangerously high concentrations of oxalic acid. Foods that are edible, but still contain significant concentrations of oxalic acid include – in decreasing order – buckwheat, star fruit (carambola), black pepper, parsley, poppy seed, rhubarb stalks, amaranth, spinach, chard, beets, cocoa, chocolate, most nuts, most berries, and beans. Bodily oxalic acid may also be synthesized via the metabolism of either glyoxylic acid or unused ascorbic acid (vitamin C).

Glycolic acid (or hydroxyacetic acid; $C_2H_4O_3$, MW = 76.05) is the smallest α-hydroxy acid (Fig. 3.5.2). In its pure form, glycolic acid is a colorless, crystalline solid. It is very soluble in water (0.1 g/ml), alcohols, acetone, and ethyl acetate. Glycolic acid is isolated from sugarcane, sugar beets, and unripe grapes.

D-Glyceric acid (or D-2,3-dihydroxypropanoic acid; $C_3H_6O_4$, MW = 125.10) is a hydroxy acid derived from the oxidation of C1 of glycerol or glyceraldehyde to a carboxyl group; various phosphorylated derivatives of L-glycerate are important intermediates in glucose metabolism (Fig. 3.5.3).

3.5.3 Methods

All three analytes oxalate, glycolate, and glycerate are analyzed using ion-exchange chromatography (HPIC) with conductivity detection. Oxalate, sulfate, and citrate are measured in the same run and glycolate and glycerate are measured on the same system, but under different conditions. The background conductivity is minimized using an anion suppressor unit.

3.5.3.1 Pre-analytical

Specimen

Ascorbic acid is the main endogenous precursor of oxalic acid and in healthy persons up to 30% of urinary oxalate can originate from ascorbate. Ascorbate is extremely unstable in neutral and alkaline solutions and degrades to oxalate nonenzymatically [6]. Acidification to pH 1–2 is required to prevent deposition of insoluble Ca-oxalate.

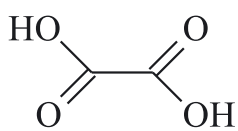

Oxalic acid

Fig. 3.5.1 Structure of oxalic acid

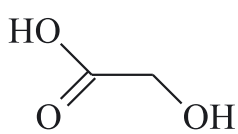

Glycolic acid

Fig. 3.5.2 Structure of glycolic acid

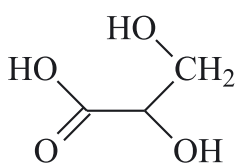

Glyceric acid

Fig. 3.5.3 Structure of glyceric acid

Urine

Twenty-four-hour or spot urine should be collected in the presence of HCl. Add 10 ml of 20% (v/v) HCl per liter of urine. Keep samples frozen at – 20°C. Before injection into the HPLC system, dilute the urine: (1) for oxalate 0.2 ml of centrifuged (3000 × *g* for 5 min) urine with 1.8 ml of 0.3 M boric acid (see below); (2) for glycolate and glycerate 0.2 ml of centrifuged (3000 × *g* for 5 min) urine with 1.8 ml of water.

Alternatively, acidified urine can be collected on a filter paper. The urine is preserved with 20% HCl as described above. Filter paper strips (3 × 5 cm filter paper backing, cat. No. 165-0921, Bio-Rad) are dipped into urine to 1 cm below the upper edge. Excess urine is wiped off, and the filter is left to dry at room temperature. Urinary filter paper spots are then cut into small pieces, shaken in 3 ml of water for 15 min at room temperature, and sonicated for 5 min at room temperature. The extracts are filtered through an Ultrafree-MC filter with 10-kDa cutoff (Millipore, USA) at 2000*g* for 10 min at room temperature. The clear supernatant is analyzed by HPIC.

Plasma

Place Li-heparinized blood (3–5 ml) directly on ice and immediately centrifuge at 1000 × *g* for 5 min at 4°C. This procedure should be completed within 10 min of vein puncture. Plasma is then ultrafiltered at 1500 × *g* for 30 min at 4°C using a Centrisart I ultrafiltration vial (Sartorius, NY, USA). Plasma is placed in the outer chamber and 40 ml of 1 M HCl per milliliter plasma is added in the inner chamber to ensure simultaneous acidification of the ultrafiltrate. Ultrafiltrate should be analyzed immediately or frozen at – 20°C. Before injection into the HPIC system, dilute the ultrafiltrate as follows:

1. For oxalate: 0.2 ml ultrafiltrate with 0.2 ml of 0.3 M boric acid; for patients with PH-I, dilute 0.1 ml ultrafiltrate with 0.4 or 0.9 ml of 0.3 M boric acid.
2. For sulfate and citrate: 0.1 ml of ultrafiltrate with 0.4 ml of 0.3 M boric acid.

Reagents and Chemicals

Oxalate, Sulfate, and Citrate

The chemicals required are:

1. Water, HPLC quality.
2. HCl, 37% (MW; 36.46).
3. NaOH, 50% (MW; 40.00).
4. Boric acid (H_3BO_3, MG; 61.83;v Merck, no. 165.1000).
5. Sodium sulfate, water free (Na_2SO_4, MW; 142.04; Merck no. 1.06649.1000).
6. Citric acid monohydrate ($C_6H_8O_7.H_2O$, MW; 210.14; Merck no. 242.1000).
7. Sodium oxalate ($C_2O_4Na_2$, MW; 134.0; Fluka no. 71800).

Stock solutions:

1. 20% (v/v) HCl: dilute 541 ml of 37% HCl with water to 1000 ml. Store at room temperature.
2. 1 M HCl: dilute 8.26 ml of 37% HCl with water to 100 ml. Store at room temperature.
3. 2 mM sulfate standard: dissolve 14.2 mg Na_2SO_4 in 10 ml of water and dilute 2 ml of the resulting solution with 8 ml of water. Store at – 20°C.

4. 2 mM oxalate standard: dissolve 13.4 mg sodium oxalate in 10 ml of water and dilute 2 ml of the resulting solution with 8 ml of water. Store at – 20°C.
5. 2 mM citrate standard: dissolve 21.0 mg citric acid monohydrate in 10 ml of water and dilute 2 ml of the resulting solution with 8 ml of water. Store at – 20°C.
6. 0.3 M boric acid: dissolve 18.56 g of boric acid in 1000 ml of water. Store at 4°C.

Standard mixtures:
1. Standard mixture I for urine: 50 µM oxalate, 100 µM glycolate, 100 µM sulfate, 100 µM citrate. Pipette the stock solutions (1.25 ml oxalate, 2.5 ml glycolate, 2.5 ml sulfate, and 2.5 ml citrate) into a 50-ml flask and add 0.3 M boric acid to the mark. Store in aliquots at – 20°C.
2. Standard mixture II for plasma: 10 µM oxalate, 20 µM glycolate, 20 µM sulfate, 20 µM citrate. Dilute 200 µl of the standard mixture I with 800 µl of 0.3 M boric acid. Prepare fresh before running the assay.

For the urine control sample, dilute 0.2 ml of control urine with 1.8 ml of 0.3 M boric acid.

Glycolate and Glycerate

The following chemicals are required:
1. Water, HPLC quality.
2. HCl, 37% (MW 36.46).
3. NaOH, 50% (MW 40.00).
4. Disodium tetraborate ($Na_2B_4O_7.10\ H_2O$; MW 381.37; Merck, no. 1.0037.1000).
5. Sodium carbonate, water free (Na_2CO_3; MW 105.99; Merck, no. 6392).
6. Glycolic acid ($C_2H_4O_3$, MW 76.05) (Sigma, no. G-1884).
7. Glyceric acid ($C_3H_5O_4$.1/2 Ca; MG, 125.1; Sigma, no. G-1144).

Stock solutions:
1. Water, twice distilled, 18.2 mΩ quality, degassed.
2. 20% (v/v) HCl: dilute 541 ml of 37% HCl with water to 1000 ml. Store at room temperature.
3. 0.1 M NaOH: dilute 10.4 ml of 50% NaOH with water to a final volume of 2000 ml. Store at room temperature.
4. 50 mM Sodium tetraborate: dissolve 38.1 g of sodium tetraborate in 2000 ml of water. Store at room temperature.
5. 50 mM Sodium carbonate: dissolve 10.6 g sodium carbonate in 2000 ml of water. Store at room temperature.
6. 2 mM Glycolate standard: dissolve 7.61 mg glycolic acid in 10 ml of water and dilute 2 ml of the resulting solution with 8 ml of water. Store at – 20°C.
7. 2 mM Glycerate standard: dissolve 12.5 mg glyceric acid in 10 ml of water and dilute 2 ml of the resulting solution with 8 ml of water. Store at – 20°C.

Standard mixtures (100 µM glycolate, 100 µM glycerate): pipette stock solutions (2.5 ml glycolate, 2.5 ml glycerate) into a 50-ml flask and add water to the mark. Store at aliquots at – 20°C.

Instrumentation (HPIC system)

Dionex Liquid Chromatograph DX-600 with a conductivity detector, suppressor ASRS Ultra II, and Waters Autosampler 717 +.

Oxalate, Sulfate, and Citrate

1. IonPac AG11 guard column (4 × 50 mm, Dionex).
2. IonPac AS 11 analytical column (4 × 250 mm, Dionex).
3. Eluent A: H_2O.
4. Eluent B: 100 mM NaOH.
5. LO LIMIT: 0 psi (0 Pa).
6. HI LIMIT: 2800 psi (19,305 kPa).
7. Flow: 2.0 ml/min.

See Table 3.5.1.

Glycolate and Glycerate

1. CarboPac PA1 guard column (4 × 50 mm, Dionex).
2. CarboPac PA1 analytical column (4 × 250 mm, Dionex).
3. Eluent A: H_2O.
4. Eluent B: 100 mM NaOH.
5. Eluent C: 50 mM sodium tetraborate.
6. Eluent D: 50 mM sodium carbonate.
7. LO LIMIT: 0 psi (0 Pa).
8. HI LIMIT: 2800 psi (19,305 kPa).
9. Flow: 2.2 ml/min.

See Table 3.5.2.

3.5.3.2 Analytical

Fill the autosampler vials with the corresponding standard mixtures, quality control sample, and patient samples. For plasma ultrafiltrates use low-volume inserts. Inject 50 µl of the sample.

Calculation

- For the external standard method, measure creatinine in the urine samples and calculate the results per mol of creatinine (oxalate, citrate, glycolate, and glycerate = mmol/mol creatinine; sulfate = mol/mol creatinine).

Performance

Linearity: 10–600 µmol/l. The detection limits for urine and plasma are 10 µmol/l and 1 µmol/l, respectively.

■ ***Table 3.5.1*** *Timetable for oxalate, sulfate, and citrate*

Time (min)	H_2O (%A)	NaOH (%B)
0	94	6
4	94	6
12	100	30
17	100	30
18	94	6
25	94	6

■ ***Table 3.5.2*** *Timetable for glycolate and glycerate*

Time (min)	H_2O (%A)	NaOH (%B)	Na_2CO_3 (%C) (Na-carbonate)	$Na_2B_4C_7$ (%D) (Na-tetraborate)
0	63	35	0	2
20.0	63	35	0	2
20.1	0	0	100	0
30.0	0	0	100	0
30.1	0	0	0	100
40.0	0	0	0	100
40.1	63	35	0	2
60.0	63	35	0	2

3.5.3.3 Post-analytical

Reference Values

The reference values for urine and plasma are given in Table 3.5.3.

Pathological Values

Figures 3.5.4 and 3.5.5 show chromatograms of healthy controls, and patients with PH-I and PH-II. Tables 3.5.4 and 3.5.5 summarize the laboratory findings for patients with PH-I and PH-II, respectively.

Table 3.5.3 *Reference values for urinary oxalate, glycolate, citrate, glycerate (given in mmol/mol creatinine), and sulfate (given in mol/mol creatinine), and plasma oxalate, citrate, and sulfate (given in μmol/l)*

Age	Oxalate	Glycolate	Citrate	Glycerate	Sulfate
Urine					
< 6 months	141–360	11–109	129–2222	trace	0.96–5.08
6 months–3 years	61–162	22–139	84–1436	trace	1.22–8.03
3–8 years	35–126	17–103	150–1007	trace	1.45–3.86
8–16 years	19–76	18–92	66–763	trace	0.70–4.97
>16 years	15–32	6–80	107–653	trace	0.63–4.78
Plasma					
<16 years	4.31–8.55		24.5–134.1		64.4–405.6

Table 3.5.4 *Laboratory findings for patients with primary hyperoxaluria type I (modified from Schnakenburg and Latta [1]).* N *Normal,* P *plasma,* U *urine*

	Renal failure (all ages)	Neonate	Infant	Children	Adolescent	Adult
Creatinine	++	N-↑	N-↑	N-↑	N-↑	N-↑
Urea	++	N-↑	N-↑	N-↑	N-↑	N-↑
Oxalate (U)	N-↑	↑-↑↑	↑-↑↑	↑-↑↑	↑-↑↑	↑-↑↑
Glycolate (U)	N-↑	N-↑	N-↑	N-↑	N-↑	N-↑
Oxalate (P)	↑↑↑	↑-↑↑	↑-↑↑	↑-↑↑	↑-↑↑	↑-↑↑
Glycolate (P)	↑-↑↑	N-↑	N-↑	N-↑	N-↑	N-↑

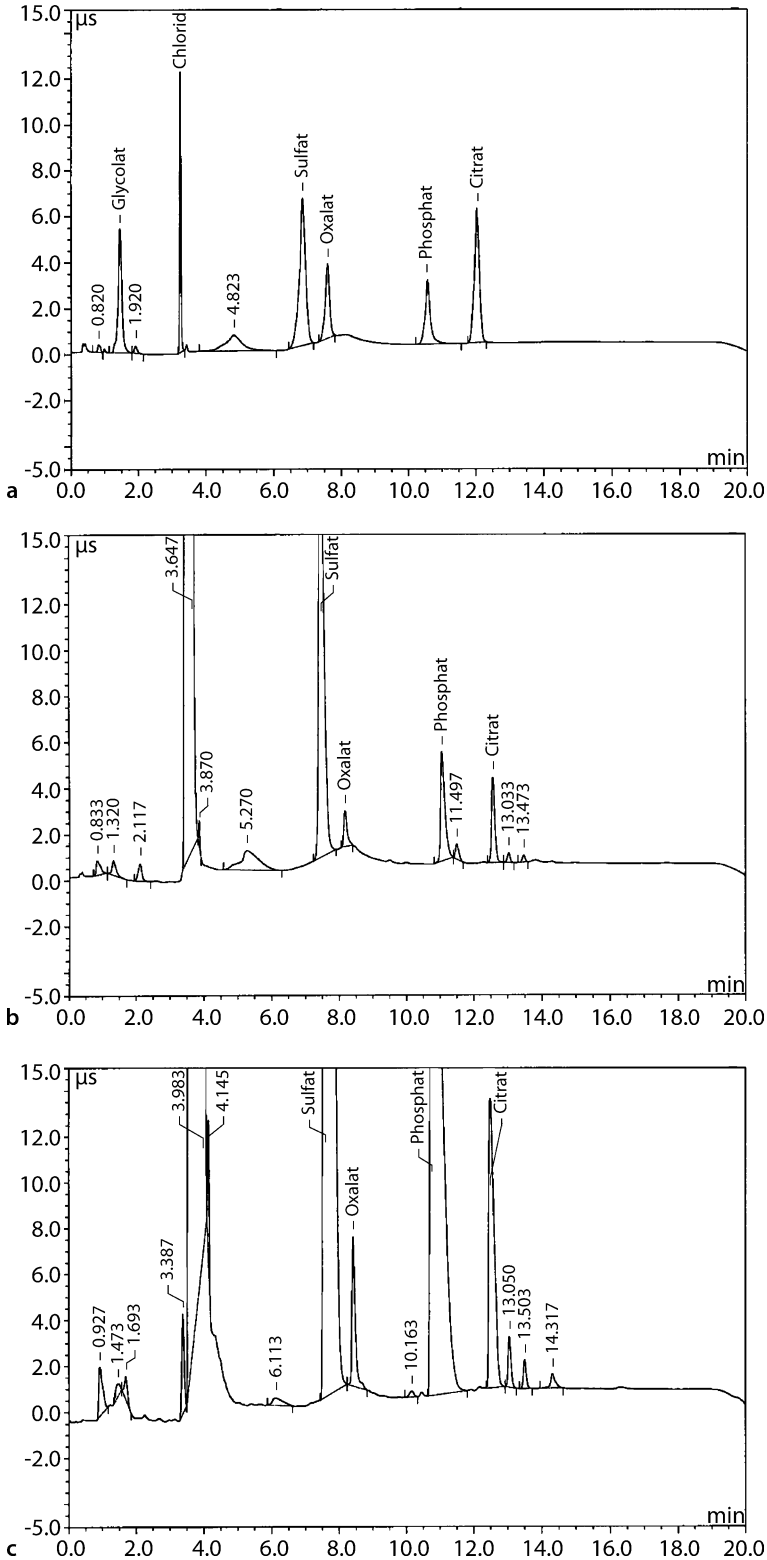

Fig. 3.5.4a–c Chromatographic separation of glycolate, chloride, sulfate, oxalate, phosphate, and citrate. **a** Standard mixture; **b** nondiseased urine; **C** urine from a patient with primary hyperoxaluria type I. In this system, glycolate coelutes with fluoride

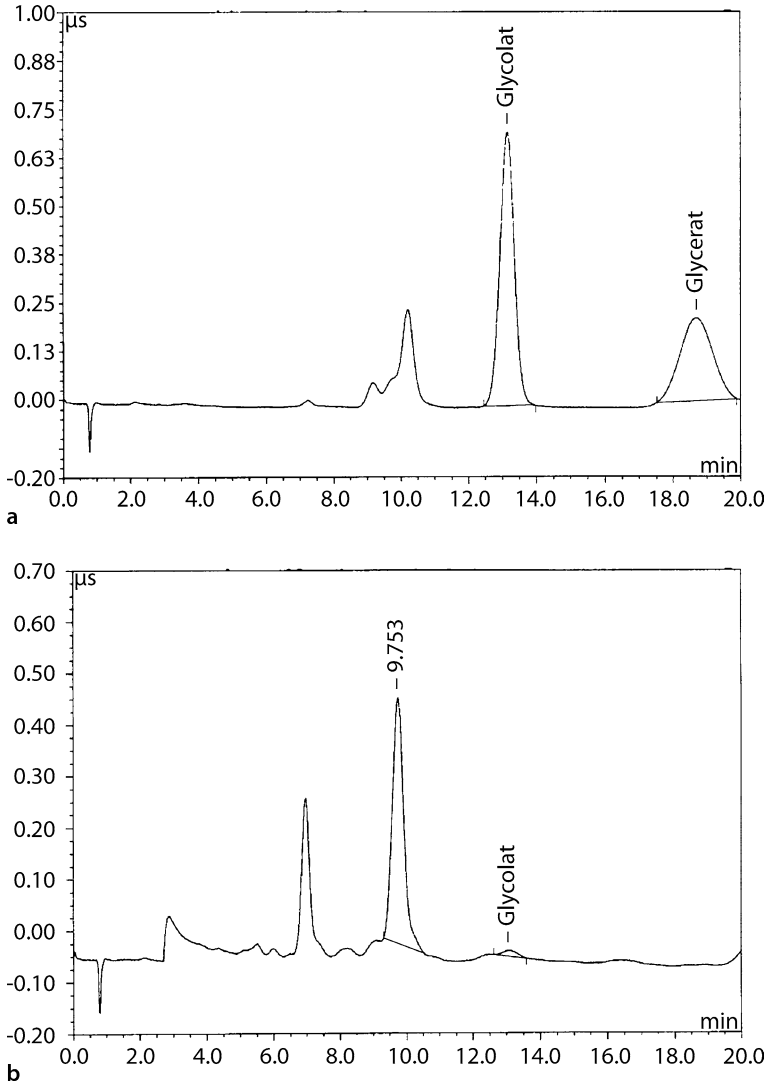

Fig. 3.5.5a–d Chromatographic separation of glycolate and glycerate. **a** Standard mixture; **b** nondiseased urine; **c,d** *see next page*

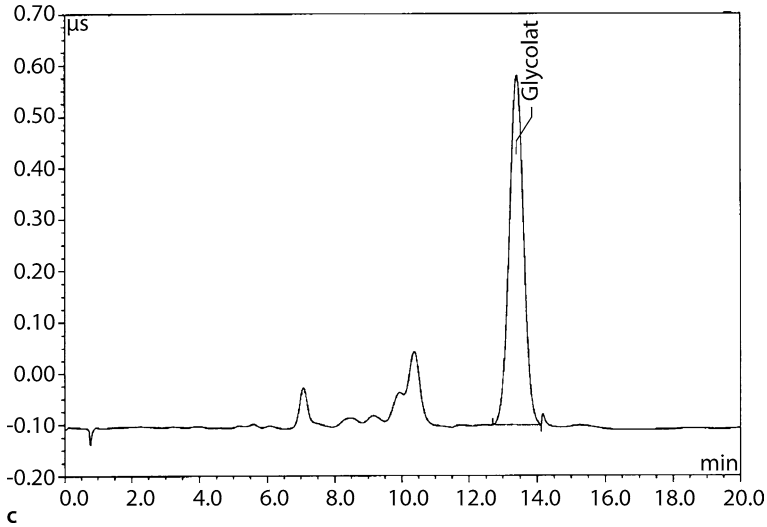

c

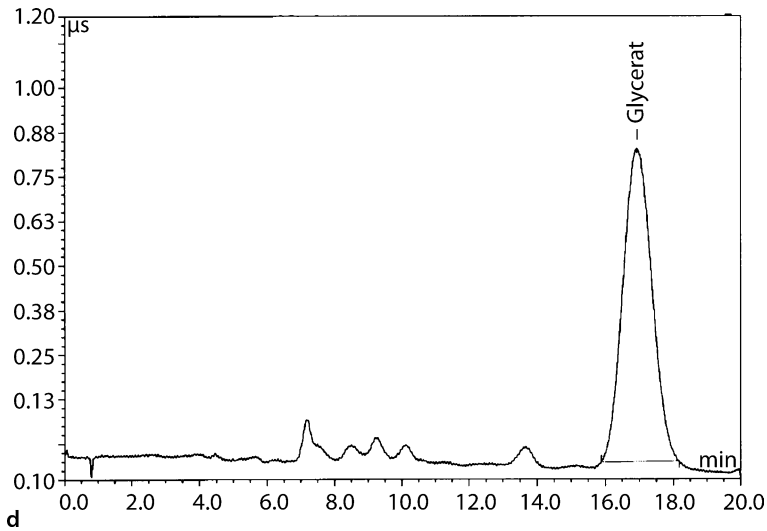

d

Fig. 3.5.5a–d (*continued*) **c** urine from a patient with primary hyperoxaluria type 1; **d** urine from a patient with primary hyperoxaluria type II

Table 3.5.5 *Laboratory findings in patients with primary hyperoxaluria type II (modified from Schnakenburg and Latta [1])*

	Renal failure (all ages)	Neonate	Infant	Child	Adolescent	Adult
Creatinine	++	N-↑	N-↑	N-↑	N-↑	N-↑
Urea	++	N-↑	N-↑	N-↑	N-↑	N-↑
Oxalate (U)	N-↑	↑-↑↑	↑-↑↑	↑-↑↑	↑-↑↑	↑-↑↑
Glycerate (U)	?	↑-↑↑	↑-↑↑	↑-↑↑	↑-↑↑	↑-↑↑
Oxalate (P)	↑↑↑	↑-↑↑	↑-↑↑	↑-↑↑	↑-↑↑	↑-↑↑

References

1. Von Schnakenburg C, Latta K (2005) Hyperoxaluria. In: Blau N, Duran M, Blaskovics M, Gibson KM (eds) Physician's Guide to the Laboratory Diagnosis of Metabolic Disease, 2nd edn. Springer, Heidelberg, pp 509–518
2. Leumann E, Hoppe B, Neuhaus T, Blau N (1995) Efficacy of oral citrate administration in primary hyperoxaluria. Nephrol Dial Transplant 10:14–16
3. Politi L, Chiaraluce R, Consalvi V, Cerulli N, Scandurra R (1989) Oxalate, phosphate and sulphate determination in serum and urine by ion chromatography. Clin Chim Acta 184:155–165
4. Hoppe B, Kemper MJ, Hvizd MG, Sailer DE, Langman CB. (1998) Simultaneous determination of oxalate, citrate and sulfate in children's plasma with ion chromatography. Kidney Int 53:1348–1352
5. Blau N, Matasovic A, Lukasiewicz-Weldechowicz A, Heizmann CW, Leumann E (1998) Simultaneous determination of oxalate, glycolate, citrate, and sulfate from dried urine filter paper spots in a pediatric population. Clin Chem 44:1554–1556
6. Williams HE (1978) Oxalic acid and the hyperoxaluric syndromes. Kidney Int 13:410–417

3.6 Glycerol and Glycerol Phosphates

Katrina M. Dipple, Edward R.B. McCabe

3.6.1 Introduction

Disorders of glycerol metabolism include glycerol kinase (GK) deficiency (GKD) and glycerol intolerance syndrome (GIS). Of these, only GKD is well characterized and has a defined biochemical defect [1].

GKD is due to mutations, insertions, or deletions within the GK gene on Xp21. There are two distinct forms of GKD [1, 5]. The complex form (cGKD) involves large deletions and other genes in this region including the adrenal hypoplasia congenita, and Duchenne muscular dystrophy loci. The isolated form (iGKD) can be either symptomatic or asymptomatic and is due only to mutations, insertions, or deletions within the GK gene on Xp21.

Patients with both forms of GKD have hyperglyceroluria and hyperglycerolemia [1, 5]. The glyceroluria is detected on routine gas chromatography-mass spectrometry (GC-MS) of urine done as part of the metabolic work-up (see Chap. 3.1). The hyperglycerolemia is detected by routine clinical laboratory testing either as pseudo-hypteriglyceridemia or elevated glycerol. In addition, glycerol can be quantified using isotope dilution methods or commercially available kits.

Glycerol kinase activity can be determined from leukocytes, fibroblasts, transformed lymphoblastoid cell lines, or liver tissue [11]. Individuals with GKD also have decreased GK activity in other tissues including kidney, small intestines, and adrenal glands [5]. The kinase activity can be assessed directly by measuring glycerol phosphorylation, or indirectly by incorporation or oxidation.

3.6.2 Properties of Analyte

Glycerol is a neutral, hygroscopic, colorless, clear liquid [5]. Its chemical name is 1,2,3-propanetriol and its chemical formula is $C_3H_8O_3$ (Fig. 3.6.1a). It has a molecular

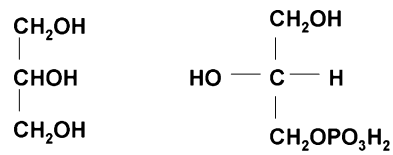

Glycerol
a

sn-Glycerol-3-phosphate
b

Fig. 3.6.1 Structure of glycerol (**a**) and sn-glycerol-3-phosphate (**b**)

mass of 92.0 grams per mole. It is a neutral compound; however, since it is often detected by GC-MS of urine done during the work-up of a metabolic crisis, GKD is often considered together with the organic acidemias [5].

Glycerol is phosphorylated to glycerol-3-phosphate (G-3-P) by glycerol kinase (ATP:glycerol-3-phosphotransferase, EC 2.7.1.30) [5]. G-3-P is also known as sn-glycerol 3-phosphate, glycerophosphoric acid, phosphatidyl glycerol, and sn-Gro-1-P (Fig. 3.6.1b). It has a chemical formula of $C_3H_9O_6P$ and a molecular mass of 172.07 grams per mole (http://pubchem.ncbi.nlm.nih.gov).

3.6.3 Methods

3.6.3.1 Glyceroluria

Principle

Because glycerol is a neutral compound, it can be detected by GC-MS of urine performed by the usual protocols (see Chap. 3.1) if a solvent extraction procedure is used [2, 5, 6]. If, however, the sample for urine organic acid analysis is treated by an ion-exchange procedure, then glycerol will be in the column wash fraction with other neutral compounds and not in the organic acid fraction. Glycerol is not well extracted by organic solvents, but it is so highly abundant in patients with GKD that it is therefore easily detected by GC-MS [2]. In addition, glycerol concentration can also be determined from commercially available kits such as the Sigma serum triglyceride determination kit (TR0100, Sigma, St. Louis MO, USA) or an isotope dilution protocol as detailed below for glycerolemia [9].

Glycerol is present in many medications, ointments, suppositories, and emollient solutions. Therefore, many cases of glyceroluria are due to contamination of the sample by exogenous sources [5].

Pre-analytical

Specimen

Urine is obtained using standard techniques including sterile midstream catch or catheterization. In infants, urine specimens obtained by placing a bag in the genitourinary region is undesirable due to contamination of glycerol from ointment and glycerin suppositories, unless the perineum is washed and rinsed well and no suppositories have been used recently [2, 5].

Reagents and Chemicals

These must be glycerol free. A solvent extraction procedure must be used prior to GC-MS [2, 5, 6]. If the sample is prepared with ion-exchange chromatography, the glycerol will remain in the neutral fraction and not be detected by GC-MS [2, 5]. Hydrochloric acid (5 N), pH paper, sodium sulfate (anhydrous), ethyl acetate (free of contaminants), diethyl ether (anhydrous, peroxide-free, and free of contaminants except 2,6-ditertbutylcresol, which is an antioxidant found in all ether), and malonic acid (26.25 mg/50 ml methanol).

Instrumentation

Standard GC-MS used for organic acid analysis (see Chap. 3.1). Data regarding calibration and quality control in this procedure can be found in Chap. 3.1 of this book.

Analytical

Procedure: the Solvent Extraction Method

This method is based on the protocol described by Goodman and Markey [2]. Determine urine creatinine using standard methods. Add malonic acid (26.25 mg/50ml) to 1 ml urine in a 12- to 13-ml round-bottom, glass-stoppered test tube as indicated in Table 3.6.1. Add two to three drops of 5 N HCI until the pH is 1, as determined by pH paper. Add 3 ml ethyl acetate, stopper, shake vigorously (1 min), and centrifuge briefly. Transfer the upper (ethyl acetate) phase to a clean tube. Re-extract the lower (urine, aqueous) phase with 3 ml diethyl ether, stopper, and shake (1 min). Take the upper (ether) phase and combine with the previous ethyl acetate extract. Repeat the diethyl ether extraction. Take the upper ether phase and pool the extracts. Discard the lower (aqueous) phase. To the extracts, add 2 g sodium sulfate, stopper, shake vigorously (1 min), then centrifuge (5 min). Transfer the anhydrous extract into a 12- to 13-ml conical, glass-stoppered tube and evaporate to dryness at 37°C under nitrogen. The sample is now ready for derivatization and injection into the GS-MS as described in Chap. 3.1 of this book.

Post-analytical

Interpretation/Chromatograms

The interpretation of results and chromatograms are described in Chap. 3.1 of this book.

Reference Values

In urine the normal values of glycerol are ≤ 0.2 mM; not detectable as mmole/mmole creatinine; or ≤1 mmole/24 h [5].

Table 3.6.1 *Malonic acid needed for solvent extraction of urine*

Creatine[a] (mg/100 ml) Urinary	**Malonic acid (26.25 mg/50 ml methanol) (μl)**
1–5	25
6–10	50
11–20	100
21–40	200
41–60	300
61–80	400
81–100	500

[a] If >100 mg/100 ml, use 0.5 ml of urine for solvent extraction and use the volume of malonic acid corresponding to one-half of the creatine concentration. Adapted from [2]

Typical Pathological Values

Typical pathological values in urine are 41–345 mM; 90– 193 mmole/mmole creatinine; or 11–360 mmole/24 h [5].

Pitfalls

Glycerol contamination from exogenous sources such as lotions, medications, and suppositories is quite common [5]. A solvent extraction procedure must be used to detect the glycerol [2, 5, 6]. If, however, the sample for urine organic acid analysis is treated by an ion-exchange procedure, then glycerol will be in the column wash fraction and therefore not detected. Overevaporation during the solvent extraction will lead to loss of organic acids [2].

3.6.3.2 Glycerolemia

Principle

In the blood, hyperglycerolemia is detected by routine clinical laboratory work up and is often misdiagnosed as pseudo-hypertriglyceridemia [3, 5] primarily because the clinical laboratory work ups do not perform a blank to account for the high levels of glycerol in the patient's blood secondary to the GKD. If the clinical laboratory measures triglycerides as the glycerol released after lipolysis, the individual with GKD will be identified secondary to the hypertriglyceridemia [5]. This is pseudo-hypertriglyceridemia [3]. However, if the clinical laboratory uses a solvent extraction and colorimetry method, there is no interference from the free glycerol secondary to GKD [5, 8]. Glycerol can be detected by many routine methods including oxidation, esterification, dehydration reactions, ether formation, enzymatic determination, and chromatographic methods [13]. Alternatives include determination of glycerol concentration using an enzymatic-based isotope-dilution method, as described here [10], or commercially available kits such as the Sigma serum triglyceride determination kit (TR0100, Sigma-Aldrich).

Pre-analytical

Specimen

Blood is drawn using standard techniques in a non-glycerol containing collection tube.

Reagents and Chemicals

These must be glycerol free. One potential source is the lubricant used between the stopper and tube of some Vacutainer collection devices. Glycerol standards (3–10mM), ethanol (100 % chilled), GK solution (0.2 ng/µl; made from dry *Escherichia coli* GK, G4509, Sigma-Aldrich, in 1 M Tris/10 mM ethylenediaminetetraacetic acid – EDTA – pH 7.4), ATP (100 mM), magnesium sulfate (40 mM), sodium fluoride (62.5 mM), 1 M Tris/10 mM EDTA pH 7.4, β-mercaptoethanol (200 mM made from 14.3 M standard solution), ^{14}C glycerol, diethylaminoethyl (DEAE) cellulose, water, glycerol (1 M), and scintillation vials.

Instrumentation

Standard scintillation counter and water baths.

Calibration

Standard curve using glycerol standards.

Analytical

Procedure

Prepare a cocktail containing 6 µl of 100 mM ATP, 10 µl of 40 mM $MgSO_4$, 10 µl of 62.5 mM NaF, 10 µl of 1 M Tris/10 mM EDTA pH 7.4, and 10 µl of 200 mM β-mercaptoethanol per sample needed (total volume of cocktail is 46 µl per sample). Prepare a 1.5-ml microfuge tube for each sample and four standards (0, 3, 8, and 10 mM glycerol) and put 4 6µl of cocktail into each tube. Add ^{14}C glycerol (to final concentration of 25 µM in a final total volume of 100 µl). Add water to make the volume of ^{14}C-glycerol 24 µl. Add 10 µl of sample or standard. Add 20 µl of GK solution, mix, and incubate at 37°C in a water bath for 20 min. Stop the reaction by adding 100 µl of chilled 100% ethanol and place on ice for at least 5 min. Centrifuge on maximum speed for 5 min. Spot 100 µl of sample onto DEAE cellulose. Allow the discs to dry fully then wash them in water for 5 min using very gentle agitation. Discard the water in radioactive waste and the wash filters with 1 M glycerol. Repeat and the discard waste in the radioactive waste. Repeat the water wash twice. Place the discs briefly on a paper towel and then put them into scintillation vials containing scintillation fluid. Vortex vigorously until the paper is dispersed. Quantify ^{14}C using a scintillation counter.

Calculation

Prepare a standard curve using the glycerol concentrations and the radioactivity on the filter paper.

Post-analytical

Interpretation

Use the standard curve to determine the concentration of the samples.

Reference Values

In serum and plasma, normal glycerol levels are 0.02–0.27 mM [5] or less than 1.6 mg/dl [2].

Typical Pathological Values

Typical pathological values range from 1.8 to 8.3 mM [5].

Pitfalls

If ^{3}H-labeled glycerol-3-phosphate is used, the radioactivity is self-absorbed by the DEAE cellulose, and must be acid-eluted for scintillation counting. DEAE cellulose breaks very easily so washes must be very gentle.

3.6.4 Follow-up Enzyme Assays

Glycerol kinase activity can be measured directly or indirectly; however, these assays are not available as a clinical test and are done exclusively on a research basis. The direct method is as has been described previously [4, 6] and is used in the isotope dilution method indicated above. The amount of protein and the incubation time vary between cell types and it is important to be within the linear range of the assay for the given cell type. The indirect methods involve incorporation of ^{14}C from glycerol into macromolecules and its subsequent oxidation to $^{14}C0_2$ [7, 11].

3.6.5 DNA Testing

Deletions causing cGKD can be detected using fluorescence in situ hybridization analysis or by genomic array hybridization, which are available as clinical tests (www.genetests.org). In addition, cGKD can be detected and the break points of the individual's deletion determined by single nucleotide polymorphism mapping arrays on a research basis [12]. For iGKD, the causative mutation can be determined by direct DNA sequencing; however, this remains available on a research basis only [14].

References

1. Dipple KM, McCabe ERB (2003) Disorders of glycerol metabolism. In: Blau N, Duran M, Blaskovics ME, Gibson KM, (eds) Physician's Guide to the Laboratory Diagnosis of Metabolic Diseases. Springer-Verlag, Berlin, pp 369–376
2. Goodman SI, Markey SP (1981) Diagnosis of Organic Acidemias by Gas Chromatography-Mass Spectrometry. Alan R. Liss, New York
3. Goussault Y, Turpin E, Neel D, Dreux C, Chanu B, Bakir R, Rouffy J (1982) "Pseudohypertriglyceridemia" caused by hyperglycerolemia due to congenital enzyme deficiency. Clin Chim Acta 123:269–274
4. Guggenheim MA, McCabe ER, Roig M, Goodman SI, Lum GM, Bullen WW, Ringel SP (1980) Glycerol kinase deficiency with neuromuscular, skeletal, and adrenal abnormalities. Ann Neurol 7:441–449
5. McCabe E (2001) Disorders of glycerol metabolism. In: Scriver C, Beaudet A, Sly W, Valle D, Childs B, Vogelstein B (eds) Metabolic and Molecular Bases of Inherited Diseases. McGraw-Hill, New York, pp 2217–2237
6. McCabe ER, Fennessey PV, Guggenheim MA, Miles BS, Bullen WW, Sceats DJ, Goodman SI (1977) Human glycerol kinase deficiency with hyperglycerolemia and glyceroluria. Biochem Biophys Res Commun 78:1327–1333
7. McCabe ER, Sadava D, Bullen WW, McKelvey HA, Seltzer WK, Rose CI (1982) Human glycerol kinase deficiency: enzyme kinetics and fibroblast hybridization. J Inherit Metab Dis 5:177–182
8. Rose CI, Haines DS (1978) Familial hyperglycerolemia. J Clin Invest 61:163–170

9. Seltzer WK, McCabe ER (1984) Human and rat adrenal glycerol kinase: subcellular distribution and bisubstrate kinetics. Mol Cell Biochem 62:43–50
10. Seltzer WK, McCabe ER (1984) Subcellular distribution and kinetic properties of soluble and particulate–associated bovine adrenal glycerol kinase. Mol Cell Biochem 64:51–61
11. Sjarif DR, Hellerud C, van Amstel JK, Kleijer WJ, Sperl W, Lacombe D, Sass JO, Beemer FA, Duran M, Poll-The BT (2004) Glycerol kinase deficiency: residual activity explained by reduced transcription and enzyme conformation. Eur J Hum Genet 12:424–432
12. Stanczak CM, Chen Z, Zhang YH, Nelson SF, McCabe ERB (2007) Deletion mapping in Xp21 for patients with complex glycerol kinase deficiency using SNP mapping arrays. Hum Mutat 28:235–242
13. Wu LC, Cheng CM (2005) Flow-injection enzymatic analysis for glycerol and triacylglycerol. Anal Biochem 346:234–240
14. Zhang Y, Dipple KM, Vilain E, Huang BL, Finlayson G, Therrell BL, Worley K, Deininger P, McCabe ER (2000) AluY insertion (ivs4-52ins316alu) in the glycerol kinase gene from an individual with benign glycerol kinase deficiency. Hum Mutat 15:316–323

3.7 Biotinidase

Terttu Suormala, Matthias R. Baumgartner, Brian Fowler

3.7.1 Introduction

Biotinidase (EC 3.5.1.12) is required for the recycling of biotin and for the utilization of protein bound biotin from the diet. Biotin (vitamin H) functions as a prosthetic group of four carboxylases in man: the mitochondrial propionyl-CoA carboxylase, 3-methylcrotonyl-CoA carboxylase and pyruvate carboxylases, and the cytosolic acetyl-CoA carboxylase, which are involved in central processes in protein, carbohydrate and fatty acid metabolism [2, 30]. Biotin is covalently bound by the enzyme holocarboxylase synthetase (HCS) to a conserved lysine residue of the carboxylases, and after proteolytic degradation during natural turnover of endogenous enzymes or during digestion of food, biotin remains bound to this lysine residue in the form of biocytin (biotinyl-ε-lysine) or short biotinyl-peptides. Biotinidase is the only enzyme that can release biotin from this linkage to make it available for use in the body.

Biotinidase deficiency is an autosomal recessively inherited disorder (MIM 253260). Patients are usually classified as having profound (residual activity 0–10 % of the mean normal value) or partial (residual activity 10–30%) biotinidase deficiency with incidences of about 1:112,000 and 1:129,000, respectively [30]. Heterozygous individuals show activities intermediate between the deficient and normal activity. Biotinidase-deficient patients lose biotin by excretion in urine, mainly in the form of biocytin [24]. They become progressively biotin deficient, which results in reduced activity of all biotin-dependent carboxylases and severe life-threatening illness [3, 4]. Typical symptoms are hypotonia, seizures, ataxia, developmental delay, skin rash and alopecia [2, 30]. Deficiency of the mitochondrial carboxylases due to either biotinidase deficiency or HCS deficiency is associated with typical organic aciduria including elevated excretion of 3-hydroxyisovaleric acid, 3-methylcrotonylglycine, methylcitrate and lactate, which can be an important clue for the diagnosis. However, in biotinidase deficiency the brain becomes biotin deficient earlier and more severely than, for example, the liver and kidney, and therefore patients may present with serious neurological disease without showing clear abnormalities of organic acid excretion [4].

Patients with complete biotinidase deficiency usually present between 3 and 6 months of age, but severe illness has already been noted at the 2nd and 3rd week of life [9]. On the contrary, patients defined as having profound biotinidase deficiency, who have levels of residual activity as low as 1–3%, may never develop obvious clinical symptoms [17, 33], but may suffer from moderate biotin deficiency when carefully evaluated [25]. Biotin deficiency can be effectively avoided by oral

administration of pharmacological doses of biotin. All patients with biotinidase deficiency have responded to biotin therapy. However, delayed treatment may result in irreversible damage, such as sensorineural hearing loss, optic atrophy and persisting ataxia. Therefore, biotinidase deficiency is detected optimally by neonatal screening followed by prompt introduction of biotin therapy.

The natural substrate of biotinidase is biocytin, but it also readily cleaves an amine bond between biotin and a variety of different compounds, allowing the use of artificial substrates for the quantitation of biotinidase activity. The most common method is the colorimetric assay described by Knappe and coworkers in 1963 [14, 32], which uses biotinyl-p-aminobenzoic acid (B-PABA) as substrate. The assay of plasma biotinidase activity by this method allows rapid detection of individuals with biotinidase deficiency.

The disadvantage of the colorimetric assay is its low sensitivity with a lower limit of reliable detection of residual plasma biotinidase activity of about 3% of the mean normal value [25]. Differentiation of patients with residual activity of less than 3% from those with complete deficiency, assay of activity in tissues, cells (cultured skin fibroblasts, white blood cells) and body fluids other than plasma as well as the determination of kinetic parameters require a more sensitive method. Thus, fluorometric assays have been described that use biotinyl-6-aminoquinoline as the substrate, and can be used also for kinetic studies [28]. This fluorometric as well as the colorimetric assay with B-PABA as the substrate have been adapted for testing of biotinidase activity in dried blood spots on filter paper (Guthrie card) for neonatal screening [5, 11]. Sensitive radioassays that employ ^{14}C-biocytin [27], ^{14}C-B-PABA [34] or a radioiodinated biotinylamide analogue [16] have been described, but none of these substrates is commercially available. Assays with the natural unlabelled substrate, biocytin, have also been described but they are all cumbersome. Bioassays have been described in which the liberated biotin is estimated by activation of apocarboxylases in fibroblasts [29] or by monitoring the growth of biotin-dependent bacteria or protozoa [1, 15, 35]. In our laboratory we have employed an assay in which liberated biotin is separated from biocytin by high-performance liquid chromatography (HPLC) and quantitated in collected fractions by a radioisotopic avidin-binding assay [25]. This method is time consuming but sensitive enough to allow the reliable differentiation of patients with complete deficiency of plasma biotinidase from those with 0.5% or more residual activity as well as determination of the Michaelis–Menten constant (K_m) for biocytin in plasma of patients or in homogenates of their cultured skin fibroblasts [25, 26].

Since the colorimetric assay is inexpensive, reproducible and easy to perform, and can be adapted to detect biotinidase K_m variants [26], we recommend the use of this assay for routine determination of biotinidase activity in plasma and describe here its use for diagnosis of patients with different forms of biotinidase deficiency.

3.7.2 Properties of Biotinidase

Human biotinidase is a monomeric glycoprotein with a molecular mass of 76 kDa when analysed by sodium dodecylsulphate-polyacrylamide gel electrophoresis [7]. The cDNA for human biotinidase was isolated and sequenced in 1994 by Cole and coworkers [6]. The deduced protein contains 502 amino acids, has a molecular mass of 57 kDa and contains 6 potential N-linked glycosylation sites. The biotinidase gene

is located on human chromosome 3p25 and is over 23 kb long [6]. Serum biotinidase originates from the liver [8], and at least nine different isoforms were detected by isoelectric focusing of human serum biotinidase [10].

In addition to its hydrolase activity with maximal velocity at acidic pH, biotinidase also possesses biotinyl-transferase activity at physiological pH, resulting in the biotinylation of nucleophilic compounds such as histones [13]. This activity may play an important role in the regulation of gene expression [30]. Both hydrolase and transferase activities are affected in patients with biotinidase deficiency [13].

Biotinidase has been detected in all tissues and body fluids investigated so far [6, 20] with highest specific activities measured in kidney, liver and adrenal gland, and also plasma, allowing the use of this easily available and minimally invasive material for diagnostic purposes.

3.7.3 Method

3.7.3.1 Principle

Biotinidase activity in plasma is quantitated by a simple colorimetric assay that uses the artificial substrate B-PABA. Biotinidase cleaves the amide bond of B-PABA forming free biotin and p-aminobenzoic acid (PABA). PABA is then converted to a purple azo dye and quantitated spectrophotometrically. No colour develops when biotinidase is inactive. Biotinidase with reduced affinity for the substrate (K_m variant) can be detected by simultaneous assay of the activity with two substrate concentrations, a saturating standard concentration of 0.15 mM and a ten-times higher concentration of 1.5 mM [26]. Greater than 1.2 times higher activity with the higher substrate concentration indicates a K_m defect.

3.7.3.2 Pre-analytical

Specimen

Quantitative assay of biotinidase activity including evaluation for the presence of a K_m defect requires 1 ml of plasma. Serum samples can be also used. Biotin therapy does not affect the assay [32]. The activity in plasma may decrease during storage (see "Pitfalls and Limitations", below). We recommend the use of ethylene-diaminetetraacetic acid (EDTA)-plasma separated from whole blood and assayed within 4–6 h, or if not processed within this time plasma can be stored at – 20°C for up to 2 months or at – 70°C. If samples are sent to a reference laboratory they can be transported as whole EDTA-blood at room temperature within 4 h, or as plasma that has been stored at – 70°C or at – 20°C for a maximum of 2 months, on dry ice.

Reagents and Chemicals

For the enzyme reaction:

1. Assay buffer (0.4 M K-phosphate buffer pH 6.0): Dissolve 13.93 g K_2HPO_4 (Cat. No. 5101, Merck, Dietikon, Switzerland) in 200 ml demineralised water. Dissolve

5.44 g KH_2PO_4 (Cat. No. 4873, Merck) in 100 ml demineralised water. Adjust the pH of the K_2HPO_4 solution to 6.0 with the KH_2PO_4 solution. Store at + 4°C.

2. Substrate N(+)-biotinyl-4-aminobenzoic acid (B-PABA) (Cat. No. 14408, Fluka, Buchs Switzerland); molecular weight 363.43. Prepare the following stock solutions and store at –20°C:
   a. 10 × substrate stock solution (10 × S), 15 mM B-PABA. Example for a batch with 98% purity: Dissolve 55.63 mg B-PABA in about 8 ml demineralised water by adjusting the pH to 7.8 with 1 N NaOH, then make up to a final volume of 10 ml.
   b. 1 × substrate stock solution (1 × S), 1.5 mM B-PABA: dilute from 10 × S with demineralised water.

   It is important to adjust the pH of the 15-mM stock solution carefully and check that all substrate is dissolved. Add NaOH drop by drop, mix using a magnetic stirrer and monitor the pH with a pH electrode. Stock-solutions with a lower pH than 7.8 may form a precipitate when added to the assay mixture at room temperature turning the reaction mixture turbid. However, during incubation at 30°C the substrate is re-dissolved and obtained activity is at the expected level.
3. Dithiothreitol (DTT) (Cat. No. 20710, Serva , Heidelberg, Germany); molecular weight 154.3: Prepare 10 mM solution fresh before use: dissolve 1.54 mg DTT in 10 ml demineralised water.
4. Standard: 4-aminobenzoic acid (PABA) (Cat. No. 06930, Fluka); molecular weight 137.14.
   a. 10 × PABA stock solution, 3.0 mM: dissolve 4.12 mg in 10 ml demineralised water; store at – 20°C (it is not necessary to neutralize the standard as with the substrate).
   b. PABA working-solution, 0.3 mM: dilute fresh from the 10 × PABA stock solution in demineralised water.
5. Bovine serum albumin (BSA) (Cat. No. A-2153, Sigma, Buchs, Switzerland): dissolve 60 mg BSA in 1 ml demineralised water; store at – 20°C.
6. Trichloroacetic acid (TCA) 30% (w/v); store at room temperature in a dark glass bottle.

For the colour reaction prepare fresh each day:

1. Sodium nitrite 0.1% (w/v; Cat. No. 106549, Merck): dissolve 10 mg in 10 ml demineralised water.
2. Ammonium sulphamate 0.5% (w/v; Cat. No. 09960, Fluka): dissolve 50 mg in 10 ml demineralised water.
3. N-(1-Naphtyl)ethylendiamine dihydrochloride monomethanolate (NEDD) 0.1% (w/v; Cat. No. 70720, Fluka): dissolve 10 mg in 10 ml demineralised water; if not immediately used, protect from light by storing in a vessel wrapped in aluminium foil.

Instrumentation

Routine laboratory equipment: Vortex mixer, 30°C shaking water bath, laboratory centrifuge, analytical balance and ultraviolet/visible spectrophotometer.

Calibration

1. Calibration is performed for each plasma sample by omitting the substrate and adding 15 nmol PABA/assay tube (Table 3.7.1; tubes 7 and 8).
2. Background tubes are prepared for each plasma sample separately by omitting the substrate (Table 3.7.1; tubes 1 and 2; also see "Pitfalls and Limitations" below).
3. Nonenzymatic hydrolysis of substrate is measured by replacing plasma with BSA (Table 3.7.1; tubes 9–12).

Assay of the PABA standard individually in the presence of each plasma sample is necessary (Table 3.7.1; tubes 7 and 8) since some heparin-based anticoagulating agents sometimes used to prepare plasma may diminish the colour development, thus reducing the intensity of the colour. Falsely low activities would be measured in such a sample if the standard factor required to convert the absorbance units to nanomoles (see "Calculation", below), is determined in the absence of the plasma.

Quality Control

Biotinidase has not been included in external quality control programs, and no control samples are commercially available. Assessment of quality is performed by including a plasma sample of an individual with normal biotinidase activity in each assay set. Such a sample is ideally stored at – 70°C in aliquots and thawed just once (see "Pitfalls and Limitations", below).

3.7.3.3 Analytical

Biotinidase activity is assayed at 30°C for 60 minutes in a final volume of 1 ml in an assay mixture containing 50 µl plasma, 0.1 M K-phosphate buffer pH 6.0, 0.5 mM

Table 3.7.1 *Colorimetric assay of plasma biotinidase activity: pipetting schedule and typical absorbance values obtained with normal plasma.* B-PABA *biotinyl-p-aminobenzoic acid,* BSA *bovine serum albumin,* DTT *dithiothreitol,* PABA *p-aminobenzoic acid,* S *substrate stock solution*

Tube No		Water µl	Buffer µl	DTT µl	PABA µl	B-PABA solution	µl	BSA µl	Plasma	Typical A_{546} [a]
1,2	Background	650	250	50	–	–	–	–	50	0.010
3,4	Reaction (1 × S)	550	250	50	–	1 × S	100	–	50	0.461
5,6	Reaction (10 × S)	550	250	50	–	10 × S	100	–	50	0.467
7,8	Standard	600	250	50	50	–	–	–	50	0.406
9,10	Blank (1 × S)	550	250	50	–	1 × S	100	50	–	0.011
11,12	Blank (10 × S)	550	250	50	–	10 × S	100	50	–	0.017

[a] Typical absorbance values obtained with a normal plasma sample after setting the absorbance to zero with demineralised water

DTT, and either 0.15 mM or 1.5 mM B-PABA (final concentrations in the assay mixture). The reaction is terminated by the addition of TCA, the precipitated proteins are removed by centrifugation, and liberated PABA in an aliquot of the supernatant is converted in a simple colour reaction to a purple compound, which is quantitated by measuring the absorbance at 546 nm.

This assay was developed using an incubation temperature of 30°C, although 37°C is used in other centres [32]. The assay at 30°C is linear with 50 µl plasma/assay tube for at least 60 min, and with a assay time of 60 min with at least 100 µl plasma/assay tube. When insufficient plasma is available, the assay can be performed with 25 µl plasma/assay tube (+ 25 µl demineralised water) for 120 min. If an assay temperature of 37°C is preferred, the assay time with 50 µl plasma/assay tube should be reduced to 30 min. Normal values measured at 37°C [31, 32] are higher (theoretically 1.7 times) than those measured at 30°C (Table 3.7.2).

Procedure

1. Prepare 5-ml plastic tubes in duplicate for each assay condition (background, reaction with 1 × S, reaction with 10 × S, standard), that is eight tubes for each plasma sample (include one control plasma as quality control for each assay set), and four additional tubes for each assay set as shown in Table 3.7.1.
2. Allow reagents to reach room temperature and prepare DTT and PABA working-solutions.
3. Thaw plasma samples if stored frozen, mix carefully and centrifuge to remove particulate material.
4. Pipette water, assay buffer, DTT solution, PABA working solution, BSA and the B-PABA substrate solutions (1 × S and 10 × S) into assay tubes according to the schedule in Table 3.7.1.
5. Start the reaction by adding 50 µl of plasma sample to the appropriate assay tubes, pulse mix by Vortex and place the tubes in a 30°C water bath.
6. Incubate for 60 min and stop the reaction by adding 100 µl of 30% TCA. Mix by Vortex then allow the tubes to stand at room temperature for about 15 min to precipitate the protein.
7. Centrifuge the tubes for 10 min at about 3000 rpm (1800 × g) in a routine laboratory centrifuge to sediment the precipitate.
8. Weigh and dissolve the reagents required for the colour reaction.
9. Prepare a new set of 5-ml plastic tubes and pipette 750 µl of clear supernatant and 250 µl demineralised water into each tube.
10. Perform the colour reaction as follows:
    a. Add 100 µl of 0.1% sodium nitrite, mix by Vortex.
    b. After exactly 3 min add 100 µl of 0.5% ammonium sulphamate, mix by Vortex.
    c. After exactly 3 further min add 100 µl of 0.1% NEDD, mix by Vortex.
    d. Allow the colour to develop for a further 6–10 min at room temperature.
    e. Measure the absorbance at 546 nm within 30 min.

Table 3.7.1 shows typical absorbance values obtained with a normal plasma sample after setting the absorbance zero with demineralised water.

Table 3.7.2 *Biotinidase activity in plasma from normal subjects, patients with different forms of biotinidase deficiency and in obligate heterozygotes (parents) measured at 30°C by colorimetric assay using two different substrate concentrations.* K_m *Michaelis–Menten constant,* n *number of individuals*

	Biotinidase activity in plasma (nmol/min/ml plasma) [a] Substrate concentration Activity ratio		
Phenotype	0.15 mM	1.5 mM	1.5/0.15 [b]
Normal individuals			
$n = 269$	5.97 ± 1.07	5.97 ± 1.09	1.00 ± 0.03
	(3.94–9.16)	(4.00–9.57)	(0.84–1.11)
Families with profound biotinidase deficiency			
Patients [c], $n = 59$	0.25 ± 0.15	0.23 ± 0.16	0.88 ± 0.22
	(0.08–0.57)	(0.02–0.65)	(0.20–1.16)
Parents, $n = 56$	2.93 ± 0.45	2.90 ± 0.45	0.99 ± 0.03
(28 mothers, 28 fathers)	(2.06–4.02)	(2.07–3.94)	(0.91–1.05)
Families with partial biotinidase deficiency			
Patients, $n = 85$	1.11 ± 0.25	1.10 ± 0.25	1.00 ± 0.06
	(0.62–1.77)	(0.60–1.75)	(0.85–1.11)
Parents, $n = 30$	3.53 ± 0.82	3.52 ± 0.81	1.00 ± 0.02
(17 mothers, 13 fathers)	(2.37–5.32)	(2.33–5.27)	(0.93–1.06)
Examples of patients with a biotinidase K_m defect [d]			
Patient 1	0.16	0.28	1.75
Patient 2	0.24	1.01	4.21
Patient 3	0.22	0.68	3.09
Patient 4	1.04	1.46	1.40
Patient 5	1.23	1.57	1.28

[a] Values are the mean ± SD and (range) of activities in different individuals, except for individual patients with a biotinidase K_m defect in whom the activities are the mean of parallel determinations in a single experiment

[b] The ratio of activity with 1.5 mM substrate divided by activity with 0.15 mM substrate

[c] Families with complete biotinidase deficiency, estimated by a sensitive high-performance liquid chromatography assay [25], were excluded

[d] For more details see reference[26]

Calculation

Biotinidase activity is expressed as nmol PABA liberated per minute and millilitre of plasma. Calculate as follows:

1. Background: the mean absorbance of the tubes in which substrate is omitted (Table 3.7.1; tubes 1 and 2). Calculated for each plasma sample separately.
2. Standard factor: subtract the background absorbance from the absorbance of the standard tubes (Table 3.7.1; tubes 7 and 8), divide by 15 (15 nmols PABA added in standard tubes) and calculate the mean value. The standard factor expresses how many absorbance units (AU) correspond to 1 nmol PABA. In the example in Table 3.7.1, a standard factor of 0.0264 AU is obtained.
3. Blank value for 1 × S and 10 × S (reagent controls):
   a. For 1 × S the mean absorbance of the tubes with 1 × S in which plasma is replaced by BSA (Table 3.7.1; tubes 9 and 10).
   b. For 10 × S the mean absorbance of the tubes with 10 × S in which plasma is replaced by BSA (Table 3.7.1; tubes 11 and 12).
4. Activity with 1 × S: subtract the corresponding blank value (or the individual background value if this is higher than the blank value) from the absorbance values of both reaction tubes with 1 × S (Table 3.7.1; tubes 3 and 4). Divide by the standard factor to obtain nmols/assay. Further divide by 60 min (assay time) to obtain nmol/min/assay. Multiply by 20 (1 ml/0.050 ml) to obtain nmol/min/ml plasma. Calculate the mean value of activity with 1 × S.
5. Activity with 10 × S: As for 1 × S, similarly calculate the activity with 10 × S by first subtracting the corresponding blank value (or the individual background value if this is higher).
6. Calculate the activity ratio by dividing the mean activity with 10 × S by the mean activity with 1 × S.

3.7.3.4 Post-analytical

Interpretation

Reference Values

Table 3.7.2. shows the mean ± SD and (range) of plasma biotinidase activities as well as the activity ratio with 1.5 mM and 0.15 mM substrate obtained in our laboratory. The values in normal individuals (age: 2 months to adult) are used as reference values, with the mean activity in the presence of 0.15 mM substrate used as the 100% value in calculations. These plasma samples were stored at – 20°C and assayed within 1 day to 2 months. Since mutation analyses were not performed, these controls may include individuals heterozygous for a mutation in the biotinidase gene.

Typical Pathological Values

Activities obtained in plasma of (1) patients with profound biotinidase deficiency (less than 10% residual activity), (2) subjects with partial biotinidase deficiency (10–30% residual activity), (3) some of their parents (obligate heterozygotes) and (4) individual patients with a biotinidase K_m defect are also shown in Table 3.7.2. Patients with complete biotinidase deficiency defined by assay with a sensitive HPLC method [25] were excluded due to large variation of the activity ratio.

Heterozygous individuals usually have intermediate enzyme activity, especially in families with a profound deficiency, with some overlap with the normal range. Thus, biotinidase activity with 0.15 mM substrate was within the normal range in 6 (5%) out of 117 parents from families with a profound deficiency, and in 15 (20%) out of 75 parents from families with a partial deficiency.

Individuals with a K_m defect show at least 1.2 times higher activity with the higher substrate concentration compared with the standard substrate concentration. These individuals include both those with a single elevated K_m (patients 1 and 2) and those with biphasic enzyme kinetics due to simultaneous presence of biotinidase with elevated K_m and with normal K_m (patients 3–5; for details see reference [26]).

Of interest is the observation that markedly elevated plasma biotinidase activity may indicate glycogen storage disease type 1a [31].

Differential Diagnosis

It is important to note that normal plasma biotinidase activity does not exclude that the patient has another cause of multiple carboxylase deficiency (i.e. HCS deficiency or acquired biotin deficiency) [2, 30].

Patients with HCS deficiency (MIM 253270) can show severe illness very early, within the first hours or days of life, but they can also present later with clinical findings similar to those seen in biotinidase deficiency. The majority of HCS-deficient patients show reduced affinity of HCS for biotin and respond well to oral biotin therapy, but usually require higher doses (20–100 mg/day) than are required for biotinidase deficiency. A few patients respond only partially to high-dose biotin therapy [2]. Diagnosis of HCS deficiency can be made by showing multiple carboxylase deficiency in skin fibroblasts cultured in low biotin medium but normal or clearly higher activities in high biotin medium [2, 30].

Acquired biotin deficiency is extremely rare but may occur in special conditions such as long-term parenteral nutrition without biotin supplementation, short bowel syndrome and after excessive intake of raw egg white, which contains the potent biotin-binding protein avidin. The main symptoms are alopecia and skin abnormalities which resolve after administration of biotin [2, 30].

Pitfalls and Limitations

Sensitivity

The sensitivity of the colorimetric assay is limited, allowing reliable determination of residual activities of 3% or more of the mean normal value. A more sensitive assay method is required to differentiate patients with complete deficiency from those with low residual activity [25].

Stability

Biotinidase activity in blood and plasma samples can decrease, often in an unpredictable manner, during storage at room temperature or at +4°C, but also during prolonged storage at –20°C, whereas no decrease has been observed at –70°C [5, 15, 32, 35]. However, storage at –70°C is not possible in many centres or practises that send samples for biotinidase assay. Addition of a sulphydryl compound to the assay mixture has been shown to restore activity in blood samples stored at room temperature [35]. Using our assay, which includes 0.5 mM DTT in the assay mix-

ture, biotinidase activity remained stable in plasma samples separated from whole blood within 6 h and stored at – 20°C for up to 2 months. Activity in 18 such samples assayed after storage at – 20°C was 99 ± 9% (mean ± SD; range: 88–118%) of the activity in a fresh sample.

Conditions that Can Cause Falsely Low Plasma Biotinidase Activity

1. Lower-than-normal activities are often obtained in newborns and in preterm and small-for-age infants [12, 23], especially if they have neonatal jaundice [22]. Plasma biotinidase activity increases with advancing age, reaching maximum values at between 20 and 40 days [23].
2. Biotinidase activities in the plasma of children and adults with chronic liver disease may be reduced to below 30% of the mean normal value [8, 18, 19].
3. Severe plasma turbidity due to hyperlipidaemia, as found in lipoprotein lipase deficiency, was shown to result in false-positive newborn screening results when dried blood spots on filter paper are used, but does not usually affect the quantitative colorimetric assay employing plasma samples (reference [21] and our own unpublished experience).

Conditions that Can Cause Falsely High Plasma Biotinidase Activity

1. Blood samples collected shortly after blood transfusions can contain significant levels of biotinidase activity in patients with biotinidase deficiency.
2. Plasma samples obtained during medication with drugs containing primary aromatic amides, such as sulphonamides, develop the purple colour in the absence of PABA [11]. The intensity of the colour can be higher than after a reaction with normal plasma. Therefore, it is essential to assay the background absorbance of each plasma sample (Table 3.7.1; tubes 1 and 2). In cases with clearly elevated background values, a repeat sample should be obtained after stopping medication.

3.7.4 Follow-up Enzyme Assays

Biotinidase activity in plasma of some newborns may be lower than that in adults (see "Pitfalls and Limitations") [12, 23]. Therefore when activities within the partially deficient or heterozygous range are obtained in newborns, this finding should be confirmed by repeating the assay at the age of about 6 months or later.

Family studies often reveal older siblings or parents with partial or profound biotinidase deficiency [17, 25, 33]. These individuals are usually asymptomatic but may suffer from moderate biotin deficiency [23] and might benefit from biotin therapy. Therefore, all family members should be investigated.

References

1. Baker H, DeAngelis B, Frank O (1989) Plasma biotinidase assay using the protozoan *Ochromonas danica*. Nutr Rep Int 39:243–251
2. Baumgartner ER, Suormala T (1997) Multiple carboxylase deficiency: inherited and acquired disorders of biotin metabolism. Int J Vitam Nutr Res 67:377–384

3. Baumgartner ER, Suormala T. Wick H, Bausch J, Bonjour JP (1985) Biotinidase deficiency associated with renal loss of biocytin and biotin. Ann N Y Acad Sci 447:272–287
4. Baumgartner ER, Suormala TM, Wick H, Probst A, Blauenstein U, Bachmann C, Vest M (1989) Biotinidase deficiency: a cause of subacute necrotizing encephalomyelopathy (Leigh Syndrome) Report of a case with lethal outcome. Pediatr Res 26:260–266
5. Broda E, Baumgartner ER, Scholl S, Stopsack M, Horn A, Rhode H (2001) Biotinidase determination in serum and dried blood spots – high sensitivity fluorometric ultramicro-assay. Clin Chim Acta 314:175–185
6. Cole H, Reynolds TR, Lockyer JM, Buck GA, Denson T, Spence JE, Hymes J, Wolf B (1994) Human serum biotinidase. cDNA cloning, sequence, and characterization. J Biol Chem 269:6566–6570
7. Craft DV, Goss NH, Chandramouli N, Wood HG (1985) Purification of biotinidase from human plasma and its activity on biotinyl peptides. Biochemistry 24:2471–2476
8. Grier RE, Heard GS, Watkins P, Wolf B (1989) Low biotinidase activities in the sera of patients with impaired liver function: evidence that the liver is the source of serum biotinidase. Clin Chim Acta 186:397–400
9. Haagerup A, Andersen JB, Blichfeldt S, Christensen MF (1997) Biotinidase deficiency: two cases of very early presentation. Dev Med Child Neurol 39:832–835
10. Hart PS, Hymes J, Wolf B (1991) Isoforms of human serum biotinidase. Clin Chim Acta 197:257–264
11. Heard GS, Secor McVoy JR, Wolf B (1984) A screening method for biotinidase deficiency in newborns. Clin Chem 30:125–127
12. Heard GS, Wolf B, Jefferson LG, Weissbecker KA, Nance WE, Secor McVoy JR, Napolitano A, Mitchell PL, Lambert FW, Linyear AS (1986) Neonatal screening for biotinidase deficiency: results of a 1-year pilot study. J Pediatr 108:40–46
13. Hymes J, Fleischhauer K, Wolf B (1995) Biotinylation of histones by human serum biotinidase: assessment of biotinyl-transferase activity in sera from normal individuals and children with biotinidase deficiency. Biochem Mol Med 56:76–83
14. Knappe J, Brümmer W, Biederbick K (1963) Reinigung und Eigenschaften der Biotinidase aus Schweinenieren und *Lactobacillus casei*. Biochem Z 338:599–613
15. Kumasaka K, Muratsuga M, Fukui T, Kimura M, Takagi Y, Hashizume N (2001) A new quantitative analytical method of serum biotinidase activity using biocytin as a substrate and its clinical significance in Japan. Clin Chim Acta 306:71–77
16. Livaniou E, Evangelatos GP, Ithakissios DS (1987) Biotin radioligand assay with an ^{125}I-labeled biotin derivative, avidin, and avidin double-antibody reagents. Clin Chem 33:1983–1988
17. Möslinger D, Stöckler-Ipsiroglu S, Scheibenreiter S, Tiefenthaler M, Mühl A, Seidl R, Strobl W, Plecko B, Suormala T, Baumgather ER (2001) Clinical and neuropsychological outcome in 33 patients with biotinidase deficiency ascertained by nationwide newborn screening and family studies in Austria. Eur J Pediatr 160:277–282
18. Nagamine T, Saito S, Yamada S, Arai T, Takehara K, Fukui T (1993) Biotinidase activity in patients with liver disease. Scand J Gastroenterol 28:899–906
19. Pabuccuoglu A, Aydogdu S, Bas M (2002) Serum biotinidase activity in children with chronic liver disease and its clinical significance. J Pediatr Gastroenterol Nutr 34:59–62
20. Pispa J (1965) Animal biotinidase. Ann Med Exp Biol Fenn 43:1–39
21. Santer R, Gokcay G, Demirkol M, Gal A, Lukacs Z (2005) Hyperchylomicronaemia due to lipoprotein lipase deficiency as a cause of false-positive newborn screening for biotinidase deficiency. J Inherit Metab Dis 28:137–140
22. Schulpis KH, Gavrili S, Tjamouranis J, Karikas GA, Kapiki A, Costalos C (2003) The effect of neonatal jaundice on biotinidase activity. Early Hum Dev 72:15–24
23. Suormala T, Wick H, Baumgartner ER (1988) Low biotinidase activity in plasma of some preterm infants: possible source of false-positive screening results. Eur J Pediatr 147:478–480

24. Suormala TM, Baumgartner ER, Bausch J, Holick W, Wick H (1988) Quantitative determination of biocytin in urine of patients with biotinidase deficiency using high-performance liquid chromatography (HPLC). Clin Chim Acta 177:253–270
25. Suormala TM, Baumgartner ER, Wick H, Scheibenreiter S, Schweitzer S (1990) Comparison of patients with complete and partial biotinidase deficiency: biochemical studies. J Inherit Metab Dis 13:76–92
26. Suormala T, Ramaekers VTH, Schweitzer S, Fowler B, Laub MC, Schwermer C, Bachmann J, Baumgartner ER (1995) Biotinidase K_m-variants: detection and detailed biochemical investigations. J Inherit Metab Dis 18:689–700
27. Thuy LP, Zielinska B, Sweetman L, Nyhan WL (1985) Determination of biotinidase activity in human plasma using (^{14}C)-biocytin as substrate. Ann N Y Acad Sci 447:434
28. Wastell H, Dale G, Bartlett K (1984) A sensitive rate assay for biotinidase using a new derivative of biotin, biotinyl-6-aminoquinoline. Anal Biochem 140:69–73
29. Weiner DL, Grier RE, Wolf B (1985) A bioassay for determining biotinidase activity and for discriminating biocytin from biotin using holocarboxylase synthetase-deficient cultured fibroblasts. J Inherit Metab Dis 8:101–102
30. Wolf B (2001) Disorders of biotin metabolism. In: Scriver CR, Beaudet AL, Sly VS, Valle D (eds) The Metabolic and Molecular Basis of Inherited Disease. McGraw-Hill, New York, pp 3935–3962
31. Wolf B, Freehaus CL, Thomas JA, Gordon PL, Greene CL, Ward JC (2003) Markedly elevated serum biotinidase activity may indicate glycogen storage disease type 1a. J Inherit Metab Dis 26:805–809
32. Wolf B, Grier RE, Allen RJ, Goodman SI, Kien CL (1983) Biotinidase deficiency: the enzymatic defect in late-onset multiple carboxylase deficiency. Clin Chim Acta 131:273–281
33. Wolf B, Norrgard KJ, Pomponio RJ, Mock DM, McVoy JRS, Fleischhauer K, Shapiro S, Blitzer MG, Hymes J (1997) Profound biotinidase deficiency in two asymptomatic adults. Am J Med Genet 73:5–9
34. Wolf B, Secor McVoy J (1983) A sensitive radioassay for biotinidase activity: deficient activity in tissues of serum biotinidase-deficient individuals. Clin Chim Acta 135:275–281
35. Wright LD, Driscoll CA, Boger WP (1954) Biocytinase, an enzyme concerned with hydrolytic cleavage of biocytin. Proc Soc Exp Biol Med 86:335–337

3.8 Mitochondrial Respiratory Chain

Pierre Rustin

3.8.1 Introduction

In the last decade, the number of human diseases recognized to originate from a dysfunction of the mitochondrial respiratory chain (MRC) has simply exploded [1, 2]. In addition to an increasing number of either pure neurological or neuromuscular diseases, several additional conditions have been ascribed to MRC dysfunction, specifically involving one or two organs, or widespread to the organism [3]. Although MRC dysfunction often results in cell loss, ultimately impairing organ function, an abnormal proliferation of cells leading to tumor formation has also been reported to originate from such defects, for example paraganglioma [4,5]. To this, one should add the observation that several drugs, because they readily accumulate into the charged mitochondria, producing dramatic side effects. This is exemplified by the electrically case of AIDS patients treated with nucleoside analogs [6]. Zidovudine, yet a precious and irreplaceable tool that is being used to counteract HIV-1 progression, has been proved to target the mitochondrion and its genome. Finally, the long-standing idea that MRC dysfunction could play an instrumental role in the aging process and possibly in several age-associated diseases has received strong support from animal model studies [7]. All of these findings make it worthwhile to be in a position to successfully assay MRC activity in a large number of conditions.

The striking variety of human diseases associated with MRC dysfunction reflects the many fundamental roles of mitochondria in mammal cells. In addition to the control exerted on countless metabolic pathways, mitochondria are recognized to play a central role in a subset of death pathways but, conversely, to also affect cell proliferation signaling [8]. These multiple roles are echoed by the genetic complexity of the processes ensuring the biogenesis and the functioning of the mitochondria (Fig. 3.8.1). Up to 3000 genes (not far from 10% of human genes) might be involved in this process. A subset of about 100 of these nuclear genes directly encodes components of the MRC (Fig. 3.8.1). This takes place in a concerted manner with the expression of the mitochondrial genomes. The number of mitochondrial genomes per cell varies from a few hundreds to several thousands, with the possibility of an intracellular genetic heterogeneity, with more than one mitochondrial DNA (mtDNA) type in the same cell (better known as heteroplasmy), but also functional heterogeneity, opening the way to an unimaginable complexity in the regulatory processes [9]. Finally, the plasticity of the mitochondrial compartment, in terms of both structure and function, implies careful consideration if one has to quantify any parameter that may be related to mitochondrial activity, as is, obviously, the MRC.

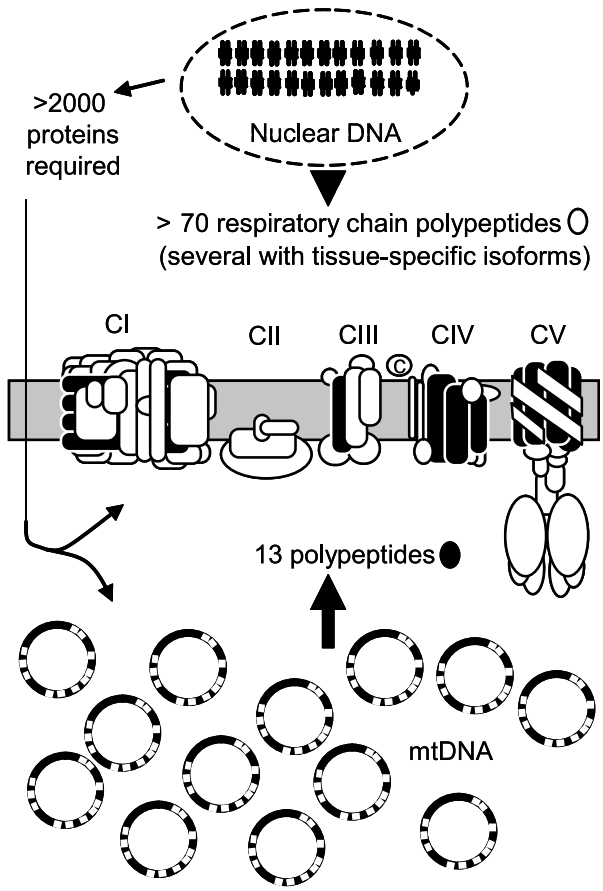

Fig. 3.8.1 The genetic complexity of the mitochondrial respiratory chain biogenesis. *CI–V* Respiratory chain complexes I–V, *mtDNA* mitochondrial DNA

Given the genetic and functional complexity and the fundamental role of mitochondria depicted above, it is not surprising that MRC disorders, or oxidative phosphorylation (OXPHOS) disorders, encompass a huge number of clinical presentations, possibly affecting any of the different body systems.

Central and/or peripheral nervous system involvement is one of the most frequent features, often resulting in the neonatal period in drowsiness, poor sucking, severe hypotonia, abnormal movements, seizures, respiratory distress, and fatal ketoacidotic coma with lactic acidosis [3]. To these severe conditions echo late-onset diseases now frequently attributed to or associated with mitochondrial OXPHOS defects, such as Alzheimer's or Parkinson's disease [10]. Major neurological symptoms, in variable combinations, involve trunk hypotonia, cranial nerve and brainstem involvement (with abnormal eye movements, ophthalmoplegia, recurrent apneas), cerebellar ataxia, myoclonia, seizures, pyramidal syndrome, peripheral neuropathy, poliodystrophy, and leukodystrophy infections [27, 28]. A diffuse impairment of the cerebral white matter (leukodystrophy) mostly results in motor disturbance with mental retardation and low incidence of seizures.

Muscle involvement varies from fatal infantile myopathy to progressive muscle weakness in childhood and adulthood [27]. While infantile myopathy can be fatal, spontaneous remissions have also been reported [29]. Myopathy may become associated with symptoms such as retinal dystrophies, ophthalmoplegia, or other organ involvement. Few cases have been reported, with recurrent attacks of trunk and limb hypotonia, myalgias, muscle stiffness, lethargy, and iterative episodes of myoglobinuria ascribed to MRC deficiency [30, 31]. OXPHOS disorders are responsible for a significant number of cases of cardiomyopathy in children [32, 33]. Most patients have concentric hypertrophic cardiomyopathy frequently followed by dilatation of the myocardium [34]. Endomyocardial biopsy sampling is a reliable diagnostic tool in cardiomyopathy [33]. Barth syndrome is an important subtype of syndromic mitochondrial cardiomyopathy with cyclic neutropenia and a rapidly fatal outcome [12, 35]. It is reasonable to consider heart transplantation in slowly progressive forms limited to the myocardium. OXPHOS disorders frequently involve the kidney. The most common manifestation is a proximal tubulopathy, with de Toni-Debré-Fanconi syndrome characterized by an impairment of proximal tubular reabsorption, leading to urinary loss of amino acids, glucose, proteins, ions, and water [36]; in MRC deficiency it is frequently limited to mild aminoaciduria, and is rarely responsible for metabolic acidosis.

While affected neonates are often small for gestational age [37], postnatal growth failure may occur at any age, after apparently normal development. Severe anorexia, recurrent vomiting, chronic diarrhea with villous atrophy, and/or exocrine pancreatic dysfunction occasionally occur [38]. In adulthood, chronic intestinal pseudoobstruction has been occasionally ascribed to MRC deficiency [21].

A neonatal form of hepatic failure has a rapidly fatal course and frequently includes severe hypotonia, myoclonus epilepsy, and psychomotor retardation [39]. Another type (found in children aged 2–18 months) has a milder clinical course with infrequent fatal outcome [11]. Abnormal histology (steatosis, micro and macronodular cirrhosis) and elevated plasma or cerebrospinal fluid (CSF) lactate are consistent features of the disease, regardless of the clinical subtype. The brain is often involved in these presentations, but other organs could also be involved. Dwarfism [40], diabetes mellitus [41], hypoparathyroidism [42], and rarely hypothyroidism and adrenocorticotropic hormone deficiency have been ascribed to the endocrine presentation of OXPHOS diseases. Diabetes mellitus (either insulin dependent or independent) can occur at very early stages of the disease. The main clinical feature of mitochondrial diabetes is its nearly constant association with other symptoms: e.g., deafness and heart and renal failure. In Japan, the prevalence of the $tRNA^{Leu}$ mutation is 6% in familial and 0% in sporadic-type I diabetes mellitus, respectively and 2% in familial-type II diabetes [43]. Myelodysplasia occasionally occurs as the initial symptom of an MRC deficiency [44]. Refractory anemia with ring sideroblasts and vacuolization of marrow precursors is usually associated with variable degrees of neutropenia and thrombopenia [45]. Nonsyndromic sensorineural hearing loss following aminoglycoside exposure has been described in individuals carrying specific mitochondrial mutations that presumably render the RNA more similar to the bacterial RNA involved in aminoglycoside-induced bactericidal activity. Yet, inbred pedigrees have been reported with family members being deaf without drug exposure [46]. A two-hit model of development has therefore been proposed. Heteroplasmic mtDNA mutation represents the first hit, the second hit consisting of either ami-

noglycoside exposure (nontoxic doses) or homozygosity for an autosomal recessive mutation, altering a putative cochlear-specific rRNA subunit [47].

The ophthalmologic manifestations of OXPHOS disorders involve the retina (pigmentary degeneration), optic nerve (optic atrophy), anterior chamber (cataract, corneal opacities), and the extraocular muscles (limitation of eye movements, ophthlamoplegia, diplopia, lid ptosis). Hair and skin anomalies include mottled pigmentation of photoexposed areas, acrocyanosis, hypertrichosis, alopecia, and abnormal hairs [48]. Palmoplantar keratoderma affecting the plantar surfaces has been reported in association with deafness in large pedigrees segregating with the mitochondrial A7445G mutation [49].

Mitochondrial disorders are not commonly regarded as causes of malformations. Facial features included round face, high forehead, small nose, and long flat philtrum, reminiscent of the fetal alcohol syndrome. Limb and trunk involvements included short hands, brachydactyly, hypoplasia of the distal and middle phalanges, hypoplastic nails, and the VACTERL [vertebral anomalies, anal atresia, cardiovascular anomalies, tracheoesophageal fistula, esophageal atresia, renal (kidney) and/or radial anomalies, and preaxial limb anomalies (in front of or above the central axis of the limb)] association [50].

Some specific clinical associations have been occasionally recognized as distinct syndromes (Table 3.8.1), although attempts to delineate tight boundaries between syndromes are questionable, especially as the nature, clinical course, and severity of recruited symptoms vary among affected individuals.

3.8.2 Methods

Except perhaps for few well-defined syndromes (see Table 3.8.1), no single method actually allows the unequivocal prediction or preclusion of an OXPHOS defect in a patient at risk. Clinical features, biochemical markers in body fluids, enzyme assays, histochemical or enzymological study, immunodetection study, or molecular study: all might be informative and necessary at the end to reach a definite conclusion. An additional difficulty arises from the fact that there is no general agreement on how to proceed. Direct molecular study targeting mtDNA or a given nuclear gene can be sometimes indicated by the clinical presentation. However, except for syndromic presentations, the whole set of approaches may be necessary, each with its particular drawback(s). However, enzyme studies, as detailed below, are probably still the most appropriate approach for the detection of an OXPHOS defect in between 20 and 30% of cases.

3.8.3 Screening of Patients at Risk

3.8.3.1 Clinical Indications

In view of the various clinical presentations possibly associated with OXPHOS diseases, it is becoming increasingly important for clinicians to recognize at least the syndromic presentations that are strongly suggestive of a mitochondrial disorder. In addition, however, any unexplained combination of neuromuscular and/or

Table 3.8.1 *The clinical presentation of the most important syndromes recognized so far in humans as resulting from mitochondrial oxidative phosphorylation defect. DIDMOAD Diabetes mellitus and insipidus with optic atrophy and deafness; FRDA Friedreich's ataxia; MELAS mitochondrial encephalomyopathy with lactic acidosis and stroke-like episodes; MERRF myoclonus epilepsy with ragged red fibers; MNGIE mitochondrial myopathy, peripheral neuropathy, encephalopathy and gastro intestinal disease; mtDNA mitochondrial DNA; NARP Neurogenic muscle weakness, ataxia, retinitis pigmentosa; PEO progressive external ophthalmoplegia; RC respiratory chain; SDHB, C, D succinate dehydrogenase complex subunits B, C and D, respectively;*

Alpers' progressive sclerosing poliodystrophy [11]	RC deficiency has been found in the liver of children meeting the criteria of Alpers' poliodystrophy. Children suffered myoclonus epilepsy related to the gradual involvement of the grey matter and developed delayed-onset hepatic involvement that was frequently triggered by valproate intake. Liver enlargement with mild cytolysis and steatosis were noted and patients frequently died shortly thereafter.
Barth syndrome [12]	An X-linked dilated cardiomyopathy with cyclic neutropenia, and skeletal myopathy and abnormal mitochondria. This condition has been ascribed to mutations of the tafazzin gene. This gene might also account for nonsyndromic forms of X-linked cardiomyopathy and isolated noncompaction of the left ventricle myocardium.
Dominant optic atrophy [13, 14]	The most prevalent hereditary optic atrophy resulting in a progressive loss of visual acuity, centrocecal scotoma and bilateral temporal atrophy of the optic nerve. It has been ascribed to mutations in the OPA1 gene encoding a dynamin-related protein localized to mitochondria. Anomalies of mitochondrial integrity and distribution are suspected to result from impairment of protein function.
FRDA [14]	The most frequent autosomal recessive degenerative disease, characterized by cerebellar ataxia with progressive gait and limb ataxia, dysarthria, lack of tendon reflexes, and pyramidal weakness of the inferior limbs and hypertrophic cardiomyopathy. FRDA is caused primarily by a GAA repeat expression in the first intron of the frataxin gene on chromosome 9q13. Loss of frataxin triggers iron-sulfur cluster-containing mitochondrial respiratory enzyme deficiency (complexes I, II, and III) and aconitase deficiency in the heart and brain of FRDA patients.
Hereditary paraganglioma [15]	Benign or malignant vascularized tumors in the head and neck, with the most common tumor site found in the carotid body, a chemoreceptive organ sensing blood oxygen level. Mutations in the SDHB, SDHC, and SDHD genes have been reported to cause hereditary paraganglioma.
Hereditary spastic paraplegia [16]	A progressive weakness and spasticity of the lower limbs due to degeneration of the corticospinal axons. An autosomal recessive form has been mapped to chromosome 16q24.3. The gene, SPG7, encodes paraplegin, a protein that localizes to mitochondria and is highly homologous to the yeast metalloproteases with proteolytic and chaperone-like activities at the inner mitochondrial membrane.
Kearns-Sayre syndrome [17]	A multisystem disorder characterized by the invariant triad: onset before age 20 years, PEO, pigmentary retinal degeneration plus at least one of the following: complete heart block, cerebrospinal fluid protein above 100 mg/dl, cerebellar ataxia. Large-scale heteroplasmic mitochondrial DNA deletions are frequently detected in skeletal muscle (rarely in other tissues).
Leber hereditary optic neuroretinopathy [18]	A rapid bilateral central vision loss due to optic nerve death. The disease has been associated with several missense mutations in the mtDNA that can act autonomously or in association with each other to cause the disease.
Leigh and Leigh-like [19]	A devastating subacute necrotizing encephalopathy characterized by recurrent attacks of psychomotor regression with pyramidal and extrapyramidal symptoms, leukodystrophy, and brainstem dysfunction The pathological hallmark consists of focal, symmetrical, and necrotic lesions in the thalamus, brainstem, and posterior columns of the spinal cord. Microscopically, these spongiform lesions show demyelination, vascular proliferation, and astrocytosis. Mutations in both mtDNA and nuclear genes encoding mitochondrial proteins have been shown to cause the disease.

Table 3.8.1 (continued) *The clinical presentation of the most important syndromes recognized so far in humans as resulting from mitochondrial oxidative phosphorylation defect. DIDMOAD Diabetes mellitus and insipidus with optic atrophy and deafness; FRDA Friedreich's ataxia; MELAS mitochondrial encephalomyopathy with lactic acidosis and stroke-like episodes; MERRF myoclonus epilepsy with ragged red fibers; MNGIE mitochondrial myopathy, peripheral neuropathy, encephalopathy and gastro intestinal disease; mtDNA mitochondrial DNA; NARP Neurogenic muscle weakness, ataxia, retinitis pigmentosa; PEO progressive external ophthalmoplegia; RC respiratory chain; SDHB, C, D succinate dehydrogenase complex subunits B, C and D, respectively;*

MELAS [20]	Early-onset disease with intermittent hemicranial headache, vomiting, proximal limb weakness, and recurrent neurological deficit resembling strokes (hemiparesis, cortical blindness, hemianopsia), lactic acidosis, and occasionally ragged red fibers in the muscle biopsy. Computed tomography brain scan shows low-density areas (usually posterior) that may affect both the white and grey matter. The disease is most frequently caused by a mutation in the $tRNA^{Leu}$ gene (A3243G).
MNGIE [21]	Intermittent diarrhea and intestinal pseudo-obstruction (myoneurogastrointestinal encephalopathy). Mutations in the thymidine-phosphorylase-encoding gene leads to multiple mtDNA deletion and anomalies in mtDNA synthesis.
MERRF [22]	An encephalomyopathy with myoclonus, ataxia, hearing loss, muscle weakness, and generalized seizures. A missense mutation in the mt $tRNA^{Lys}$ gene (A8344G) accounts for 80% of MERRF cases.
NARP [23]	Variable sensory neuropathy, seizures, and mental retardation due to an amino-acid change in the (T8993G).
Pearson syndrome [24]	A refractory sideroblastic anemia, with variable neutropenia and thrombocytopenia, vacuolization of marrow precursors, and exocrine pancreatic dysfunction. Severe transfusion-dependent macrocytic anemia begins in early infancy (before 1 year) and the disease is fatal before 3 years in 62% of cases. Large-scale heteroplasmic deletions/duplications of mtDNA are constantly observed in affected and nonaffected organs.
PEO [25]	A myopathy with progressive muscle weakness and external ophthalmoplegia. Ataxia, episodic ketoacidotic coma, and early death have been reported associated with single or multiple DNA deletions. Mutations in the gene encoding the muscle isoform of the adenylate carrier (ANT1) have been reported to cause PEO, presumably due to abnormal nucleotide availability for mtDNA synthesis.
Wolfram syndrome [26]	A syndrome of DIDMOAD. While most cases have been ascribed to an autosomal recessive gene mapping to chromosome 4p16, some cases of early-onset DIDMOAD might result from mtDNA mutations or deletions.

nonneuromuscular symptoms, a progressive course, and the involvement of seemingly unrelated organs or tissues, should also draw attention. The symptoms, isolated or in combination, may occur at any age, an increasing number of organs involved in the course of the disease being often observed [3]. Finally, the symptoms may infrequently improve as other organs become involved [51]. As a consequence, a mitochondrial disorder is often evoked after the elimination of other causes, resulting in extensive/expensive laboratory works on patients with poor indications.

3.8.3.2 Assay of Metabolites In Vivo

Among the recognized hallmarks for OXPHOS disorders is the determination of plasma lactate, pyruvate, ketone bodies and their molar ratios, as indexes of oxidation/reduction status in cytosol and mitochondria, respectively. In order to avoid artifactual elevations of lactic acid, blood samples should be taken from the patient at rest through a heparinized venous catheter and immediately deproteinized by perchloric acid [52]. Samples should be immediately processed or immediately frozen. Blood glucose and nonesterified fatty acids should also be monitored. Investigation of the redox status in plasma can help discriminate between the different forms of congenital lactic acidosis. A significant impairment of OXPHOS usually results in lactate:pyruvate ratios above 20 and ketone body ratios above 2, whereas a defect of the pyruvate dehydrogenase complex results in low lactate:pyruvate ratios (below 10). When basal screening tests are inconclusive, a glucose-loading test (2 g/kg, orally) can unmask latent hyperlactatemia and/or paradoxical hyperketonemia [53]. The urinary excretion of Krebs cycle intermediates and/or 3-methyl-glutaconic aciduria has a good diagnostic value but is nonspecific [54]. When the redox status of plasma is not altered, determination of the redox status in the CSF can be performed. Amino acid chromatography shows indirect evidence of hyperlactatemia (i.e., elevated plasma α-alanine and proline) and occasionally hypermethioninemia.

Pitfalls associated with metabolic screening are numerous. They can result from proximal tubulopathy, causing a reduction in blood lactate and an increase in urinary lactate; from diabetes mellitus, hampering entry of pyruvate into the citric acid cycle; from tissue-specific involvement or partial deficiency, which may barely alter the redox status in plasma. When metabolic tests are negative, respiratory chain deficiency may be misdiagnosed.

3.8.4 Tissue-Specific Investigation

Dealing with diseases ranging from tissue-specific to pluriorgan diseases, the question of what tissue to study should be paid particular attention. In principle, a relevant tissue is one that is clinically involved. When faced with a muscle weakness, the appropriate material to study is a skeletal muscle microbiopsy sample (e.g., deltoid). When the hematopoietic system expresses the disease (i.e., Pearson syndrome), tests should be carried out on circulating lymphocytes, polymorphonuclearcytes or bone marrow. In the case of liver disease, a needle biopsy of the liver, or in case of a cardiomyopathy an endomyocardial biopsy can be unavoidable [55]. When the disease is essentially expressed in a barely accessible organ (brain, retina, endocrine, smooth muscle), peripheral tissues should be tested extensively (including skeletal muscle, cultured skin fibroblasts, and circulating lymphocytes). Whatever the affected organ, it is mandatory to take a patient skin biopsy for subsequent investigations on cultured fibroblasts (even post mortem). Various culture media can be used for growing fibroblasts designated to investigate OXPHOS function, but one should be aware that the presence of uridine (200 μM) and pyruvate (2 mM) is a requisite to ensure optimal growth or even survival of some cells with OXPHOS defect [56]. Any cells endowed with mitochondria without functional quinone, or complex III, IV, or V,

will encounter difficulties in synthesizing uridine, the biosynthesis of which is linked to MRC function. Similarly, addition of pyruvate is required to ensure cell redox equilibrium in any severe case of OXPHOS defect.

It should be born in mind that normal MRC activity can be found in an organ or a tissue that does not clinically express the disease. One might deal with a tissue-specific organ deficiency, as observed in Friedreich's ataxia where iron-sulfur deficiency is barely detectable in skeletal muscle or skin fibroblasts [57]. Tissue specificity is far from being understood; it is often observed even in the case of patients harboring deleterious mutation in nuclear genes with widespread expression in the organism [9].

3.8.5 Assay of Mitochondrial OXPHOS Function

The activity of OXPHOS can be first assayed as an integrated ensemble either through oxygen consumption [55] or through ATP production [58]. A limitation of these somewhat irreplaceable approaches is that both require the use of intact mitochondria, thus requiring the study of fresh material only. Indeed, frozen tissues present variable and incontrollable loss of cellular/intracellular membrane integrity. For obvious reasons, the isolation of a pure mitochondrial fraction should be proscribed since it could readily result in the isolation of a subset of the mitochondrial population, defective mitochondria being possibly more fragile or could present significant differences in either charge or density.

3.8.5.1 Polarography

The polarographic method using a Clark oxygen electrode (Fig. 3.8.2) is a well-established method that dates back to the middle of the 20th century. This method can provide insights to numerous properties of cell respiration and mitochondrial substrate oxidation [59]. It is based on the recording of a current generated at the cathode of an amperometric oxygen sensor, that current being proportional to the oxygen reduced (consumed). This oxygen is in equilibrium through a Teflon membrane with the oxygen dissolved in a small volume of respiratory medium containing cells or mitochondria (Fig. 3.8.2).

In the Clark cell, the voltage of approximately 800 mV necessary to reduce the oxygen is provided externally by a battery source. The Clark electrode makes use of an Ag/AgCl half-cell and a cathode, best made of platinum. Using KCl as an electrolyte, the reaction catalyzed at the anode is: $2Ag + 2Cl^- \rightarrow 2AgCl + 2e^-$, while the reaction catalyzed at the cathode is: $2e^- + ½O_2 + H_2O \rightarrow 2\ OH^-$, the net result of the two reaction being: $2Ag + 2e^- + ½O_2 + H_2O + 2Cl^- \rightarrow 2AgCl + 2OH^- + 2e^-$. Noticeably, because the net result of the chemical reaction is AgCl, there will be a progressive build up of AgCl coating the anode. When the whole area of the anode is covered, the reaction stops because the oxygen probe has stopped working. This necessitates regular cleaning of the anode to remove the AgCl deposit, allowing reactivation of the probe. The OH^- ions produced at the cathode initially tend to alkalinize the KCl electrolyte at around the neutral pH value. This shifts the electrolyte potential into the negative range, causing a zero shift. This shift occurs consistently and, over time, the electro-

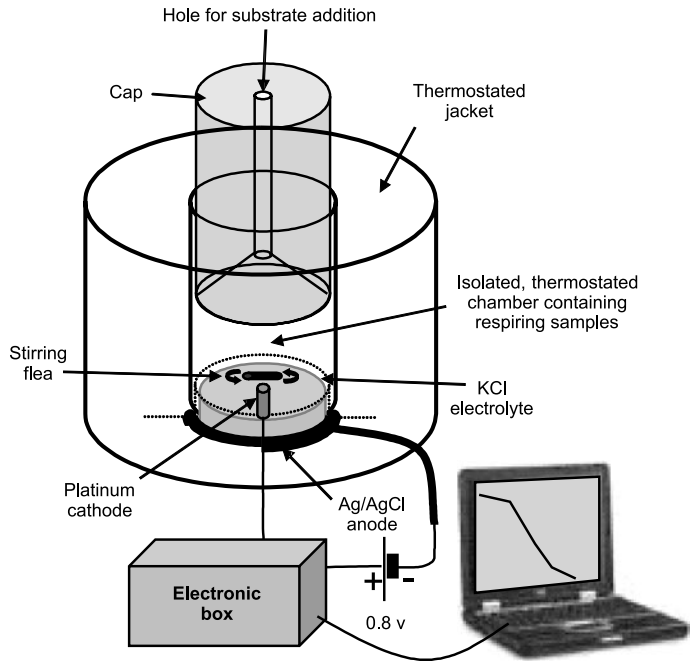

Fig. 3.8.2 Standard polarographic device with a Clark oxygen electrode

lyte needs to be changed. The electrolyte also needs to be changed because of progressive Cl^- consumption. The sensor is extremely sensitive to shifts in temperature, which therefore have to be tightly controlled. In particular, on connecting the probe, the user must wait for it to be polarized and its temperature stabilized. This warm up time may take as long as a few minutes (5–10 min). Measuring during this time results in falsely higher values displayed.

Although several parameters can be quantified using a polarographic device, we established that two traces (two recordings) are sufficient to gain most of the information on the OXPHOS capacities of the cells/mitochondria [55]. These two traces are depicted in detail in Fig. 3.8.3. In the context of screening procedures, we recommend the use of two polarographic cells, one devoted to studies requiring the use of rotenone (a specific inhibitor of complex I that tends to tightly bind to plastic parts of polarographic cells).

Studying cells (e.g., circulating lymphocytes, cultured skin fibroblasts, cultured myoblasts), the first trace consists of the initial recording of intact cell respiration for a few minutes (Fig. 3.8.3a), after which cells are made permeable by a tiny amount of digitonin (or saponin), which binds membrane cholesterol [60]. Because the cholesterol content of plasmalemma is much higher than that of mitochondrial membranes [61], this specifically destabilizes the plasmalemma, allowing small molecules of the cytosol such as respiratory substrates to leak out and be diluted in the medium. As a consequence, the respiration gradually stops. Then, any respiratory substrate can be added to these permeable cellular "ghosts" containing intact mitochondria. These latter can be studied further, as would be isolated mitochondria for most of their characteristics. Using digitonin-permeabilized cells or mitochondria-enriched

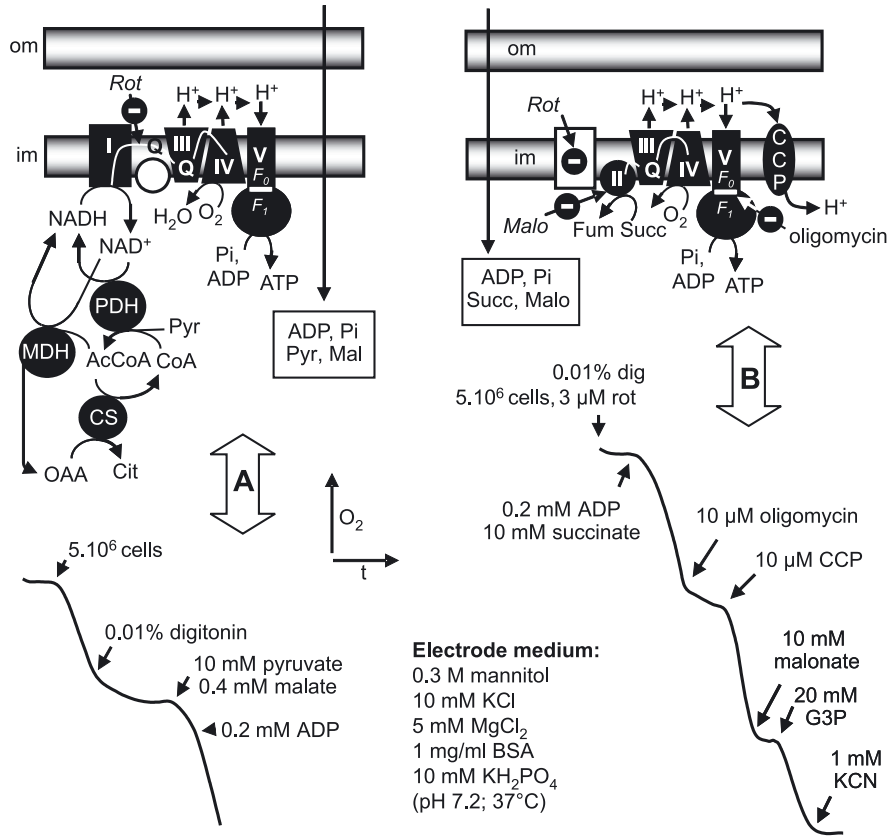

Fig.3.8.3 Oxygen uptake by intact (**a**) and digitonin-permeabilized (**b**) fibroblasts. *I–V* Respiratory chain complexes I–V, *AcCoA* acetylcoenzyme A, *BSA* bovine serum albumin, *CCP* carbonyl cyanide m-chlorophenylhydrazone, *Cit* citrate, *CoA* coenzyme A, *CS* citrate synthase, *Dig* digitonin, *Fo* & *F1* the ATPase components, *Fum* fumarase, *G3P* glycerol-3-phosphate, *im* inner membrane, *Mal* malate, *Malo* malonate, *MDH* malate dehydrogenase, *OAA* oxaloacetate, *om* outer membrane, *PDH* pyruvate dehydrogenase, *Pi* inorganic phosphate, *Pyr* pyruvate, *Q* ubiquinone, *Rot* rotenone, *Succ* succinate, *t* time

fractions, the addition of pyruvate plus a trace of malate triggers oxygen uptake through complex I–IV of the MRC. Pyruvate is oxidized by the coenzyme A (CoA)-dependent pyruvate dehydrogenase, generating acetylCoA and NADH. Malate is simultaneously oxidized by malate dehydrogenase, producing the small amount of oxaloacetate necessary to regenerate CoA by condensing with acetylCoA to form citrate. A subsequent addition of ADP triggers a maximal flux of electrons through the MRC, thanks to the dissipation of the proton gradient by the ATPase reaction. Noticeably, in most cell and nonpurified mitochondria preparations, the ATP formed is rapidly hydrolyzed by nonmitochondrial ATPases, prohibiting confident determination of the yield of the phosphorylation process, the so-called ADP:O ratio. This first trace may allow the detection of any significant defect in the activity of the components of the MRC, except complex II. In addition, it represents a quite sensitive assay for pyruvate dehydrogenase and import carriers (pyruvate, ADP).

The second trace is carried out in the presence of rotenone to avoid any functioning of complex I, which could result in the production of oxaloacetate by malate dehydrogenase during succinate oxidation (Fig. 3.8.3B). Oxaloacetate is a potent inhibitor of complex II and its production should be absolutely avoided to allow for sustained succinate oxidation [62]. After addition of cells plus digitonin or mitochondria, rotenone and succinate are added, triggering oxygen uptake, which is increased by the addition of ADP, allowing measurement of the maximal rate of succinate oxidation. Adding oligomycin, which inhibits the mitochondrial ATPase through binding to its oligomycin-sensitivity-conferring protein subunit [63], should significantly reduce oxygen uptake. A large decrease reflects a good quality of the coupling between the phosphorylation process and the electron flow. The addition of an uncoupler such as m-chlorophenylhydrazone carbonyl cyanide permits the protons to re-enter the mitochondrial matrix so that maximal electron flow through the MRC recommences. Succinate oxidation can then be fully stopped by malonate, a specific inhibitor of complex II. Addition of duroquinol in the presence of ethylenediaminetetraacetic acid (EDTA) allows the measurement of cyanide-sensitive complex III plus IV activities. Conversely, adding glycerol-3-phosphate permits measurement of electron flow capacity by the glycerol-3-phosphate dehydrogenase (limiting the rate), and complexes III plus IV.

Polarographic studies can also be used to screen for much more specific defects suspected in some patients, such as impaired mitochondrial glutamate transport in cultured skin fibroblasts from patients presenting with neonatal myoclonic epilepsy [64].

3.8.5.2 ATP Synthesis

Rather than measuring the oxygen consumed by cells/mitochondria oxidizing substrates, it is also possible to quantify ATP synthesis by the luciferin/luciferase luminescence-based assay in the presence of the substrate and ADP [58]. Firefly luciferase is an enzyme that catalyzes the two-step oxidation of luciferin, which yields light at 560 nm (Fig. 3.8.4). The first step involves activation of the protein by ATP to produce a reactive mixed anhydride intermediate. Then, the intermediate reacts with oxygen to yield dioxetane, which quickly breaks down to the oxidized product oxyluciferin and carbon dioxide along with a burst of light. When ATP is the limiting component, the intensity of light is proportional to the concentration of ATP. Thus, the measurement of the light intensity using a luminometer allows the quantitation of ATP. Using a combination of substrates similar to those described for polarography, this method also allows an overview of the integrated functioning of the MRC to be obtained, but as with polarographic studies, it requires preservation of an intact mitochondrial membrane, necessitating the use of fresh tissues/cells. The recent re-investigation of this rather tedious method has shown that inorganic phosphate concentration is critical to obtain a maximal rate for ATP measurement. It has been successfully applied to study ATP production by isolated mitochondria, but the method might be more difficult to use in the case of whole-cell studies (circulating lymphocytes, skin fibroblasts) where it has not been reported in the context of a screening procedure.

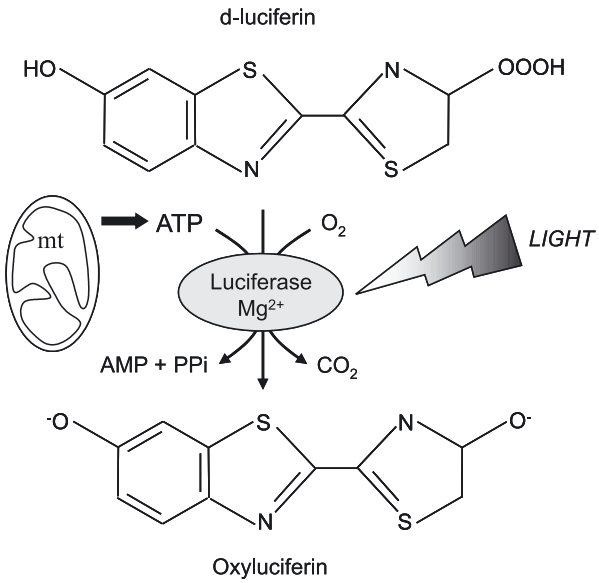

Fig. 3.8.4 The principle of luminometric measurement of mitochondrial (*mt*) ATP using the luciferin/luciferase assay. *PPi* Pyrophosphate

3.8.6 Determination of Enzyme Activity

3.8.6.1 General

The determination of OXPHOS activity is best made with the aid of spectrophotometric assays [55, 65]. Using a judicious set of electron donors and acceptors, it is possible to measure the activity of MRC complexes either isolated or in combination, as described below. Beside the residual activity of each complex, ratios of their respective activities are of fundamental importance. Indeed, the balance between complexes (the ratio between their activities) determines on the one hand the relative access of each dehydrogenase to the MRC, and on the other hand the amount of superoxides possibly escaping the chain [55]. It is therefore quite important to both analyze residual activities corrected for the variable amount of mitochondria using the citrate synthase as reference enzyme, and the various ratios inside the MRC [66,67]. It is also important to note that enzyme determination is (supposedly at least) done under maximal rate (V_{max}) conditions only, often leaving aside any discrete anomalies possibly affecting affinity and regulatory properties.

Several different experimental conditions are used, depending on the laboratory, without any consensus agreement on which of these should be used for screening. This in part renders difficult comparison of results between laboratories. However, whatever the recipes used, one has to fully understand the complex regulatory properties of each of these activities before proceeding. These are presented below for each MRC complex routinely measured in the context of screening procedures. It is preferable to use a (pseudo-)double-wavelength spectrophotometer, since such a machine can now be obtained at a reasonable price and results in better, more

specific signals by using a reference wavelength along with the measurements. This is done by selecting isosbestic points (wavelength values where the absorbance is not affected by the redox status of the probe) for each of the probe used.

3.8.6.2 Complex I (EC 1.6.5.3)

The activity of complex I is measured by following the oxidation of NADH at 340 nm (ε: 4870·M^{-1}·cm^{-1}; isosbestic point: 380 nm) in the presence of an exogenous short-chain quinone analog (e.g., decylubiquinone; Fig. 3.8.5). The activity is checked to be specifically catalyzed by MRC complex I by controlling its rotenone sensitivity. Several difficulties can be encountered in measuring this activity. First, it should be known that NADH is not perfectly stable, and that its degradation products (yielding to a more yellowish color of the solution) have a rather equivalent absorption at 340 nm as NADH. This depends on the batch and conservation procedure. High temperature and alkaline conditions have recently been shown to result in even more active degradation of NADH into an inhibitory compound [68]. Small aliquots of NADH can be prepared and kept deep frozen at – 80°C, but should be discarded after thawing. Decylubiquinone is readily soluble in dimethyl sulfoxide (DMSO) and can be kept frozen for months. Rotenone is not a very stable compound (it metabolizes to elliptone in vivo, and is an active complex I inhibitor); however, at the concentration recommended the low inhibitory constant (K_i) of complex I for rotenone, this does not lead to a problem in its laboratory utilization. Most of the difficulties estimating complex I activity arise (depending on the nature of the samples) from either the occurrence of unspecific activities (however reduced for NADH-quinone reductase as compared to NADH-cytochrome c reductase) or from the poor ability of the exogenous quinone to interact with the membranous complex, or finally the ability of NADH to enter the mitochondrial vesicles necessarily used to measure complex I (an intact endogenous membrane being totally impermeable to NADH) [69]. The conditions proposed here (see Fig. 3.8.5) are still not totally satisfying, since they yield rates just lower than the maximal rates of oxygen consumption calculated for NADH-generating substrates by intact mitochondria, as measured by polarographic method (see above).

3.8.6.3 Complex II (EC 1.3.5.1)

The activity of complex II (succinate dehydrogenase) is measured as the succinate-dependent reduction of decylubiquinone, which is in turn recorded spectrophotometrically through the reduction of dichlorophenol indophenol at 600 nm (ε: 19,100·M^{-1}·cm^{-1}; Fig. 3.8.5). In order to ensure a linear rate for the activity, the medium is added with rotenone, ATP, and a high concentration of succinate. As noticed previously for complex I, decylubiquinone is not a perfect acceptor for electrons from the membrane-inserted complex II [70]. Malonate, a competitive inhibitor of the enzyme, is used to inhibit it. Rather than decylubiquinone, phenazine methosulfate can be utilized, which diverts the electrons from the complex before they are conveyed through subunits C and D, therefore allowing measurement of the activity of subunits A and B.

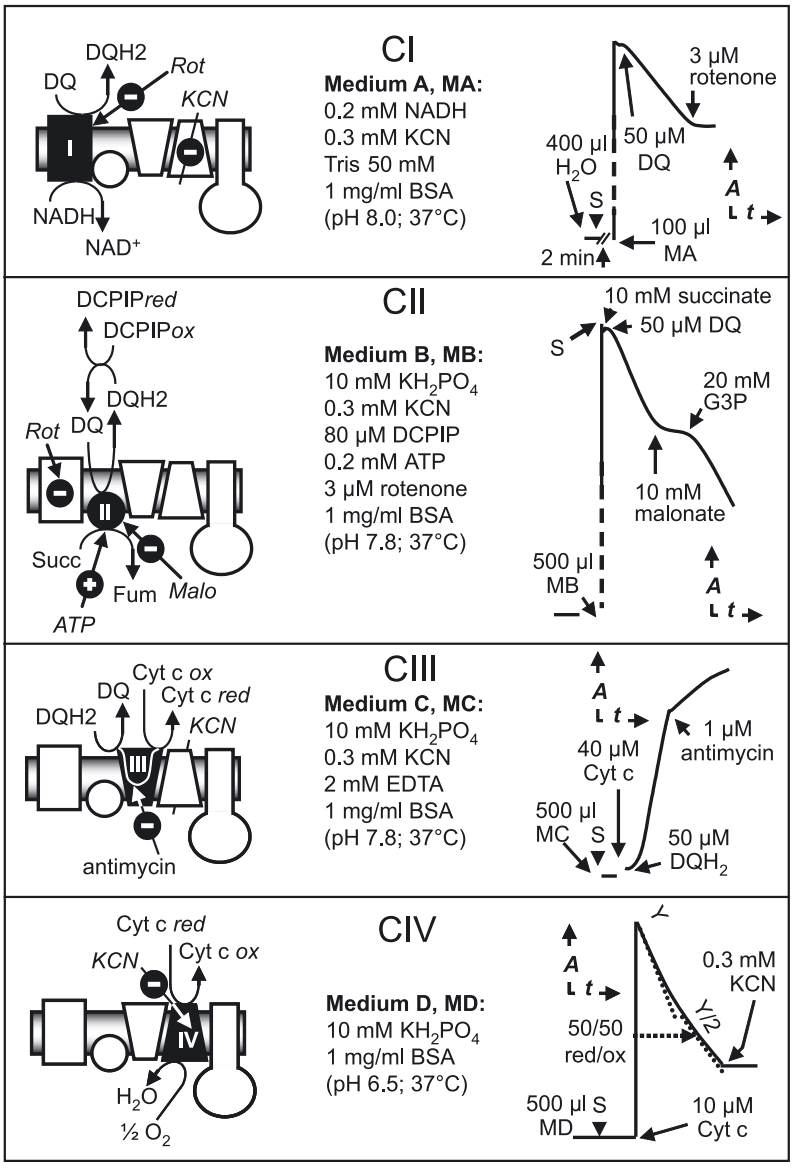

Fig. 3.8.5 Spectrophotometric assays of the activities of complexes I–IV. *CI* Complex I, *CII* complex II, *CIII* complex III, *CIV* complex IV, *Cyt* cytochrome, *DCPIP* di-chlorophenol-indophenol, *DQ* oxidized form of decylubiquinone, *DQH2* reduced form of decylubiquinone, *EDTA* ethylenediaminetetraacetic acid, *MA* medium A, *MB* medium B, *MC* medium C, *MD* medium D, *ox* oxidized, *red* reduced, *S* sample

3.8.6.4 Complex III (EC 1.10.2.2)

The activity of complex III is measured as quinol (decylubiquinol) cytochrome c reductase activity by recording cytochrome c reduction at 550 nm (ε: 19,100·M^{-1}·cm^{-1}; isosbestic point: 540 nm; Fig. 3.8.5). The activity is fully sensitive to antimycin. Cytochrome c is prepared daily, or alternatively kept as small aliquots deep frozen at – 80°C. The preparation of decylubiquinol is more delicate. First dilute 25 mg of decylubiquinone (oxidized powder commercially available) with 2.5 ml DMSO in a 10-ml Becher. While stirring the solution magnetically, add 450 µl of acidified water (400 µl H_2O + 50 µl HCl 1/10 N) and progressively about half a tea-spoon of dithionite (sodium hydrosulfite). This latter has to be in very large excess. The initially yellow solution/suspension should gradually turn to transparency in about 1 h depending on the temperature. When the solution is colorless/white, allow it sediment and dispatch the supernatant into 1.5-ml centrifugation tubes. After centrifugation for 5 min at 10,000 rpm (9300 × g), the supernatants are poured into a 10-ml Becher and stirred again for 10 min. All steps should be carried out using a chemical hood. Store small samples (less than 50 µl) at – 80°C and upon thawing carefully resuspend the crystal, which is generally present at the bottom of the tube. The various redox reactions between the components of the assay (Fig. 3.8.5) have been studied in great detail and largely determine the rate of the antimycin-insensitive decylubiquinol cytochrome c reduction [71]. Unfortunately, some batches of purified cytochrome c appear to contain traces of contaminants, possibly free iron, which may catalyze a high rate of decylubiquinol autooxidation, triggering antimycin-resistant cytochrome c reduction. Addition of a chelator such as EDTA reduces, but does not prevent, iron-induced decylubiquinol auto-oxidation.

3.8.6.5 Complex IV (EC 1.9.3.1)

Complex IV (cytochrome c oxidase) activity is measured by following at 550 nm (ε: 19,100·M^{-1}·cm^{-1}; isosbestic point: 540 nm) the oxidation of cytochrome c (Fig. 3.8.5). It could be calculated as a first-order rate constant, or by estimating the pseudolinear initial rate of the reaction. Noticeably as a check, this initial rate should represent about double the rate measurable when 50% of the added cytochrome c has been oxidized (Fig. 3.8.5). Indeed, the affinity constant (K_m) for reduced cytochrome c is about equivalent to the K_i for oxidized cytochrome c. Reduced cytochrome c is easily prepared by adding a few crystals of dithionite to a solution of oxidized cytochrome c. After the immediate color change (from deep red to light orange-red), the solution should be carefully stirred to eliminate any trace of dithionite and should be totally odorless.

3.8.6.6 Complex V (EC 3.6.1.34)

The activity of complex V (ATP synthase) can be conveniently measured in the reverse direction, ATP hydrolysis with a coupled assay thereafter described [72] (Fig. 3.8.6). The use of oligomycin, a specific inhibitor of the enzyme, allows discrimination of the mitochondrial enzyme from any nonmitochondrial ATPases.

The ADP produced by the hydrolysis of ATP is continuously used up by added purified pyruvate kinase, which in the presence of phosphoenol pyruvate produces pyruvate and ATP (Fig. 3.8.6). Pyruvate is then utilized by added lactate dehydrogenase, which in the presence of NADH produces lactate and NAD^+. Complex V activity is estimated from the rate of NADH oxidation at 340 nm (ε: 4870·M^{-1}·cm^{-1}; isosbestic point: 380 nm), after subtracting the oligomycin-resistant activity. It should be kept in mind that oligomicyn sensitivity requires the preserved attachment of the F_1 component of the enzyme to the membranous F_0 component. The attachment is readily lost upon freeze-thaw cycles. Consequently, it is reasonable to measure the activity on fresh material only.

3.8.6.7 Complexes I–III (EC 1.6.99.3)

The activity of this segment of the MRC, NADH-cytochrome c reductase, is often difficult to measure due to the presence of contaminating activity, which may represent as high as 90% of the activity depending on the type of tissues/cells studied [73]. Incubation for a few minutes of the biological samples in pure distillated water in the spectrophotometer cuvette just before commencing activity has been shown to destabilize part of the contaminating activity [73]. The activity is of cytochrome c reduction recorded at 550 nm (ε : 19,100·M^{-1}·cm^{-1}; isosbestic point: 540 nm) is linear and should be sensitive to rotenone for a part significant enough to have a confident estimation (Fig. 3.8.6). The rate-limiting factor when measuring this MRC segment is complex I.

3.8.6.8 Complexes II–III (EC 1.3.99.1)

Succinate-cytochrome c reductase has to be measured under conditions ensuring a maximal activity of the succinate dehydrogenase (see section 3.8.7.3; Fig. 3.8.6). The activity of cytochrome c reduction recorded at 550 nm (ε: 19,100·M^{-1}·cm^{-1}; isosbestic point: 540 nm) is linear for several minutes. Noticeably, as frequently observed when an oxidized redox compound is added to a biological extract, a part of the initial reducing activity can be triggered by reducing substances present in the tissues. This is particularly true in the case of tissues harboring defective mitochondria or that are maintained in a hypoxic condition. Adding malonate allows the determination of any activity not associated with succinate utilization by succinate dehydrogenase. The activity of this segment of the MRC is limited by complex II activity. It is only partially affected in the case of ubiquinone deficiency [74] and because adding exogenous oxidized quinone changes sensitivity to malonate, it is not very convenient to test for ubiquinone pool dysfunction.

3.8.6.9 Glycerol-3-Phosphate-Dehydrogenase-Associated Activities

Glycerol-3-phosphate may be used as a substrate for the MRC in a subset of tissues. It is conveniently added after malonate when measuring either complex II (allowing measurement of glycerol-3-phosphate dehydrogenase; EC 1.1.95.5) or complex II–III

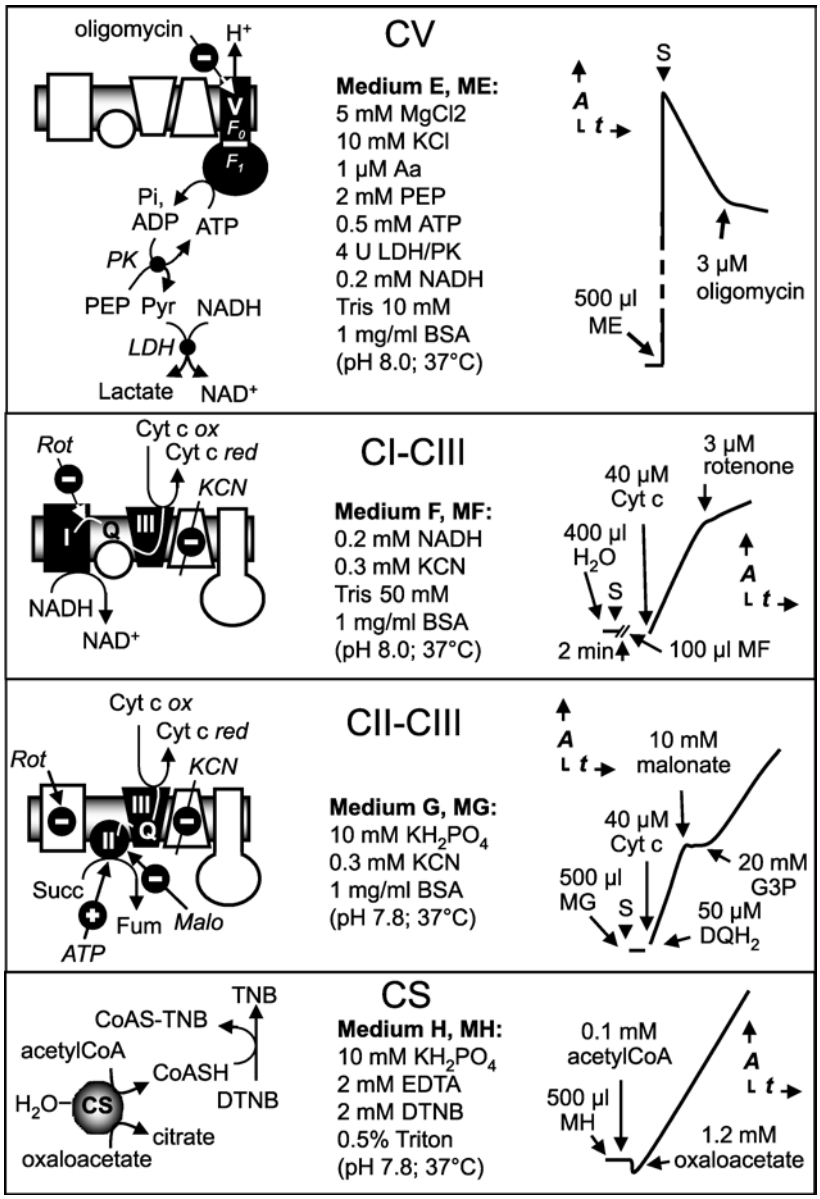

Fig. 3.8.6 Spectrophotometric assays of complexes V, I–III, II–III, and citrate synthase activity. *DTNB* Dithio-nitrobenzoic acid, *LDH* lactic dehydrogenase, *ME* medium E, *MF* medium F, *MG* medium G, *MH* medium H, *PEP* phosphoenol pyruvate, *PK* Pyruvate kinase, *TNB* thio-nitrobenzoic acid

(allowing measurement of glycerol-3-phosphate cytochrome c reductase). No potent inhibitors of the enzyme are available. The measurement of glycerol-3-phosphate is, however, a very sensitive tool for detecting ubiquinone deficiency [75]. Similarly to dehydro-orotate dehydrogenase, the link between this externally located dehydrogenase and the quinol oxidizing site of CIII appears to rely on the pool function of

ubiquinone, and is therefore extremely sensitive to any significant decrease of the ubiquinone content of the mitochondrial membrane.

3.8.6.10 Marker/Reference Enzymes

Because the number/ activity of the mitochondria in a given tissue readily varies under several conditions, particularly in the case of an OXPHOS deficiency, it is generally a good idea to quantify the activity of several marker enzymes. Krebs cycle enzymes have often been measured as reference enzymes to estimate variation in the number of mitochondria and it has been widely assumed that the activity of these enzymes are not affected in the case of an OXPHOS deficiency. Citrate synthase (EC 2.3.3.1) is conveniently measured by analyzing the CoA liberated during the condensation of acetylCoA and oxaloacetate (Fig. 3.8.6). Reduced thiol from CoA readily reduces the blue dithio-nitrobenzoic acid (ε: 13,600·M^{-1}·cm^{-1}) to the colorless thio-nitrobenzoic acid, which can be recorded spectrophotometrically at 412 nm. Oxaloacetate is very fragile, particularly at neutral pH or above, being decarboxylated into pyruvate. Fumarase (EC 4.2.1.2), with both a mitochondrial and a cytosolic form in most human tissues but the brain, is also easily measured spectrophotometrically in the far ultraviolet at 250 nM by analyzing fumarate (ε: 5090·M^{-1}·cm^{-1}) production from malate. Because its activity only requires using a minute amount of biological sample, lactic dehydrogenase (EC 1.1.1.27) can be measured by analyzing NADH oxidation in the presence of pyruvate.

It should be noticed, however, that the activity of all of the redox enzymes used as marker/reference enzymes can be affected by a disease condition and therefore more than one should be measured, if possible.

3.8.7 Alternative Methods

A very useful complement to enzyme assays as described above is histochemical study, which can provide additional information [76]. In particular, because it is possible to measure the activity cell per cell, histochemistry permits, in the case of a heteroplasmic population of mitochondria, the detection of even a small number of affected cells, which may have remained undetected by biochemical assays. Spectacular images showing, side-by-side, cells endowed with either high or absent enzyme activity can be obtained. The limitation of the method is in part due to the few activities possibly measured (essentially complex IV, succinic dehydrogenase, and less specifically, ATPase and NADH reductase) and to the fact that it is poorly quantitative. Histochemical investigations are performed under selected conditions (e.g., substrate concentrations, pH), which often differ from those used for enzyme assays, thus possibly introducing discrepancy between the two approaches.

Immunological studies are not yet widely used in the context of screening procedures, but they are becoming easier to perform [77]. Their use is rendered possible by the observation that at least a subset of the OXPHOS defects originates from, or results in, anomalies in complex assembly with increased protein degradation. As a result, a net decrease of the immunoreactive material can be used to trace some OXPHOS deficiencies. The large number of antibodies available makes this approach

a useful complement, despite the obvious drawback to only detect OXPHOS defects associated with protein loss.

3.8.8 Molecular Analyses

Because of the dual genetic origin of the OXPHOS system, of the number of genes involved, and also of the high number of cell processes that can result in secondary OXPHOS dysfunctions, establishing the molecular basis of OXPHOS defects has proved to be a very difficult task [78], yet of utmost importance for the affected families. Unfortunately, in most cases the enzyme assays or the immunological studies do not indicate which of the subunits of a given deficient complex is mutated. The first deleterious deletions causing an OXPHOS defect were identified in the mtDNA [22, 79]. Then, a series of mutations of the mtDNA were described as causing several defined syndromes, often with overlapping symptoms [78]. All of the information on mtDNA mutations can now be found through regularly updated specialized web sites (e.g., http://www.mitomap.org/). Nuclear gene mutations were thereafter reported, the very first in 1995 in the gene encoding the subunit A of complex II [80]. It is not easy to obtain figures for the respective proportions of mutations affecting either the mitochondrial component compared to the nuclear genome causing an OXPHOS defect. But, the former might represent up to 10–15% of the cases. Anyway, leaving aside well-defined syndromes known to originate from a given molecular event, because of the tedious work and the high cost/low yield of systematic sequencing of the mitochondrial genome, it appears reasonable to seek for a rational approach to better direct the molecular investigations. With this aim, it should be stressed that mitochondrial mutations being most frequently heteroplasmic, a histochemical picture showing a patchy distribution of mitochondrial activities between cells, or a normalization of mitochondrial activity along the culture of defective cells (skin fibroblasts) grown in a medium selective for a functional respiratory chain (i.e., grown in the absence of glucose, uridine, and pyruvate), are strongly suggestive of a mtDNA alteration. The available tools have also been recently enriched by the increasingly expanding remarkable panoply of both antibodies against MRC subunits, bound to various supports [77], and retroviruses endowed with specific genes encoding proteins of the MRC or required for its biogenesis/maintenance [81].

The recognized associations between a subset of nuclear genes and some clinical features have also to be known. A permanent update of these associations defining candidate genes for a subset of patients can now be easily found through web sites devoted to mitochondria/mitochondrial pathology related to the nuclear genome (e.g. http://www-lecb.ncifcrf.gov/mitoDat). The candidate gene approach is also facilitated by the knowledge of MRC biogenesis in other aerobic organisms, particularly yeast. Finally, the linkage analyses in large families (segregation of microsatellite markers with deleterious traits) can allow determination of genomic regions potentially harboring the mutant gene. This latter can be further identifird by a candidate gene approach or systematic sequencing of genes located in the selected region. Noticeably, an absolute prerequisite to these linkage analyses is to obtain samples (e.g., blood) from the maximal number of family members, affected or not.

References

1. Dimauro S, Davidzon G (2005) Ann Med 37:222–232
2. Zeviani M, Di Donato S (2004) Brain 127:2153–2172
3. Munnich A, Rustin P (2001) Am J Med Genet 106:4–17
4. Briere JJ, Favier J, Ghouzzi VE, Djouadi F, Benit P, Gimenez AP, Rustin P (2005) Cell Mol Life Sci 62:2317–2324
5. Favier J, Briere JJ, Strompf L, Amar L, Filali M, Jeunemaitre X, Rustin P, Gimenez-Roqueplo AP (2005) Horm Res 63:171–179
6. Moyle G (2004) J HIV Ther 9:45–47
7. Trifunovic A, Wredenberg A, Falkenberg M, Spelbrink JN, Rovio AT, Bruder CE, Bohlooly YM, Gidlof S, Oldfors A, Wibom R, Tornell J, Jacobs HT, Larsson NG (2004) Nature 429:417–423
8. Rustin P (2002) Nat Genet 30:352–353
9. Briere JJ, Chretien D, Benit P, Rustin P (2004) Biochim Biophys Acta 1659:172–177
10. Orth M Schapira AH (2001) Am J Med Genet 106:27–36
11. Cormier-Daire V, Chretien D, Rustin P, Rotig A, Dubuisson C, Jacquemin E, Hadchouel M, Bernard O, Munnich, A (1997) J Pediatr 130:817–822
12. Barth PG, Valianpou F, BoweM, La J, Dura M, Vaz FM, Wanders RJ (2004) Am J Med Genet A 126:349–354
13. Delettre C, Lenaers G, Griffoin JM, Gigarel N, Lorenzo C, Belenguer P, Pelloquin L, Grosgeorge J, Turc-Carel C, Perret E, Astarie-Dequeker C, Lasquellec L, Arnaud B, Ducommun B, Kaplan J, Hamel CP (2000) Nat Genet 26:207–210
14. Durr A, Cossee M, Agid Y, Campuzano V, Mignard C, Penet C, Mandel JL, Brice A, Koenig M (1996) N Engl J Med 335:1169–1175
15. Baysal BE (2003) Trends Endocrinol Metab 14:453–459
16. Casari G, De Fusco M, Ciarmatori S, Zeviani M, Mora M, Fernandez P, De Michele G, Filla A, Cocozza S, Marconi R, Durr A, Fontaine B, Ballabio A (1998) Cell 93:973–983
17. Lestienne P, Ponsot G (1988) Lancet 1:885
18. Johns DR, Neufeld MJ (1993) Am J Hum Genet 53:916–920
19. Valanne L, Ketonen L, Majander A, Suomalainen A, Pihko H (1998) AJNR Am J Neuroradiol 19:369–377
20. Goto Y, Nonaka I, Horai S (1990) Nature 348:651–653
21. Hirano M, Nishigaki Y, Marti, R (2004) Neurologist 10:8–17
22. Wallace DC, Zheng XX, Lott MT, Shoffner JM, Hodge JA, Kelley RI, Epstein CM, Hopkins LC (1988) Cell 55:601–610
23. Holt IJ, Harding AE, Petty RK, Morgan-Hughes JA (1990) Am J Hum Genet 46:428–433
24. Rotig A, Cormier V, Blanche S, Bonnefont JP, Ledeist F, Romero N, Schmitz J, Rustin P, Fischer A, Saudubray JM (1990) J Clin Invest 86:1601–1608
25. Kaukonen J, Juselius JK, Tiranti V, Kyttala A, Zeviani M, Comi GP, Keranen S, Peltonen L, Suomalainen A (2000) Science 289:782–785
26. Rotig A, Cormier V, Chatelain P, Francois R, Saudubray JM, Rustin P, Munnich A (1993) J Clin Invest 91:1095–1098
27. Shoffner JM, Wallace DC (1995) Oxidative phosphorylation diseases. In: Scriver CR, Beaudet AL, Sly WS, Valle D, Childs B, Kinzler KW, Vogelstein B (eds) The Metabolic and Molecular Bases of Inherited Disease. McGraw-Hill, New York pp 1535–1609
28. DiMauro SB (1993) Mitochondrial encephalomyopathies. In: Rosenberg RN, Prusiner SB, Barchi RL, DiMauro S (eds) The Molecular and Genetic Basis of Neurological Disease. Butterworth-Heinemann, Boston, pp 665–696
29. DiMauro S, Nicholson JF, Hays AP, Eastwood AB, Papadimitriou A, Koenigsberger R, DeVivo DC (1983) Ann Neurol 14:226–234
30. Saunier P, Chretien D, Wood C, Rotig A, Bonnefont JP, Saudubray JM, Rabier D, Munnich A, Rustin P (1995) Neuromuscul Disord 5:285–289

31. Keightley JA, Hoffbuhr KC, Burton MD, Salas VM, Johnston WS, Penn AM, Buist NR, Kennaway NG (1996) Nat Genet 12:410–416
32. Marin-Garcia J, Goldenthal MJ (1997) Pediatr Cardiol 18:251–260
33. Rustin P, Lebidois J, Chretien D, Bourgeron T, Piechaud JF, Rotig A, Munnich A, Sidi D (1994) J Pediatr 124:224–228
34. Fosslien E (2003) Ann Clin Lab Sci 33:371–395
35. Bione S, D'Adamo P, Maestrini E, Gedeon AK, Bolhuis PA, Toniolo D (1996) Nat Genet 12:385–389
36. Wendel U, Ruitenbeek W, Bentlage HA, Sengers RC, Trijbels JM (1995) Eur J Pediatr 154:915–918
37. von Kleist-Retzow JC, Cormier-Daire V, Viot G, Goldenberg A, Mardach B, Amiel J, Saada P, Dumez Y, Brunelle F, Saudubray JM, Chretien D, Rotig A, Rustin P, Munnich A, De Lonlay P (2003) J Pediatr 143:208–212
38. Cormier-Daire V, Bonnefont JP, Rustin P, Maurage C, Ogler H, Schmitz J, Ricour C, Saudubray JM, Munnich A, Rotig A (1994) J Pediatr 124:63–70
39. Bakker HD, Scholte HR, Dingemans KP, Spelbrink JN, Wijburg FA, Van den Bogert C (1996) J Pediatr 128:683–687
40. Tulinius MH, Oldfors A, Holme E, Larsson NG, Houshmand M, Fahleson P, Sigstrom L, Kristiansson B (1995) Eur J Pediatr 154:35–42
41. Gerbitz KD, van den Ouweland JM, Maassen JA, Jaksch M (1995) Biochim Biophys Acta 1271:253–260
42. Tengan CH, Kiyomoto BH, Rocha MS, Tavares VL, Gabbai AA, Moraes CT (1998) J Clin Endocrinol Metab 83:125–129
43. Kadowaki T, Kadowaki H, Mori Y, Tobe K, Sakuta R, Suzuki Y, Tanabe Y, Sakura H, Awata T, Goto Y, et al (1994) N Engl J Med 330:962–968
44. Bader-Meunier B, Rotig A, Mielot F, Lavergne JM, Croisille L, Rustin P, Landrieu P, Dommergues JP, Munnich A, Tchernia G (1994) Br J Haematol 87:381–385
45. Smith OP, Hann IM, Woodward CE, Brockington M (1995) Br J Haematol 90:469–472
46. Matthijs G, Claes S, Longo-Mbenza B, Cassiman JJ (1996) Eur J Hum Genet 4:46–51
47. Fischel-Ghodsian N (1998) Am J Hum Genet 62:15–19
48. Bodemer C, Rotig A, Rustin P, Cormier V, Niaudet P, Saudubray JM, Rabier D, Munnich A, de Prost Y (1999) Pediatrics 103:428–433
49. Sevior KB, Hatamochi A, Stewart IA, Bykhovskaya Y, Allen-Powell DR, Fischel-Ghodsian N, Maw MA (1998) Am J Med Genet 75:179–185
50. Damian MS, Seibel P, Schachenmayr W, Reichmann H, Dorndorf W (1996) Am J Med Genet 62:398–403
51. Akman CI, Sue CM, Shanske S, Tanji K, Bonilla E, Ojaimi J, Krishna S, Schubert R, DiMauro S (2004) J Child Neurol 19:258–261
52. Trijbels JM, Scholte HR, Ruitenbeek W, Sengers RC, Janssen AJ, Busch HF (1993) Eur J Pediatr 152:178–184
53. Touati G, Rigal O, Lombes A, Frachon P, Giraud M, Ogier de Baulny H (1997) Arch Dis Child 76:16–21
54. Gibson KM, Elpeleg ON, Jakobs C, Costeff H, Kelley RI (1993) Pediatr Neurol 9:120–123
55. Rustin P, Chretien D, Bourgeron T, Gerard B, Rotig A, Saudubray JM, Munnich A (1994) Clin Chim Acta 228:35–51
56. Bourgeron T, Chretien D, Rotig A, Munnich A, Rustin P (1993) J Biol Chem 268:19369–19376
57. Rotig A, de Lonlay P, Chretien D, Foury F, Koenig M, Sidi D, Munnich A, Rustin P (1997) Nat Genet 17:215–217
58. Wibom R, Hagenfeldt L, von Dobeln U (2002) Anal Biochem 311:139–151
59. Clark LC Jr, Clark EW (1964) Ala J Med Sci 18:142–148
60. Fruhling J, Penasse W, Sand G, Mrena E, Claude A (1970) Arch Int Physiol Biochim 78:997–998

61. Wesslen N (1985) Biomed Biochim Acta 44:95–98
62. Rustin P, Lance C (1991) Biochem J 274:249–255
63. Rubinstein J, Walker J (2002) J Mol Biol 321:613–619
64. Molinari F, Raas-Rothschild A, Rio M, Fiermonte G, Encha-Razavi F, Palmieri L, Palmieri F, Ben-Neriah Z, Kadhom N, Vekemans M, Attie-Bitach T, Munnich A, Rustin P, Colleaux L (2005) Am J Hum Genet 76:334–339
65. Taylor RW, Birch-Machin MA, Lowerson S, Sherratt HS, West IC, Bartlett K, Turnbull DM (1993) Biochem Soc Trans 21:804–807
66. Rustin P, Chretien D, Bourgeron T, Wucher A, Saudubray JM, Rotig A, Munnich A (1991) Lancet 338:60
67. Chretien D, Gallego J, Barrientos A, Casademont J, Cardellach F, Munnich A, Rotig A, Rustin P (1998) Biochem J 329:249–254
68. Kotlyar AB, Karliner JS, Cecchini G (2005) FEBS Lett 579:4861–4866
69. Chretien D, Benit P, Chol M, Lebon S, Rotig A, Munnich A, Rustin P (2003) Biochem Biophys Res Commun 301:222–224
70. Cecchini G (2003) Annu Rev Biochem 72:77–109
71. Chretien D, Slama A, Briere JJ, Munnich A, Rotig A, Rustin P (2004) Curr Med Chem 11:233–239
72. Penefsky HS (1979) Adv Enzymol Relat Areas Mol Biol 49:223–280
73. Chretien D, Bourgeron T, Rotig A, Munnich A, Rustin P (1990) Biochem Biophys Res Commun 173:26–33
74. Rustin P, Munnich A, Rotig A (2002) Eur J Hum Genet 10:289–291
75. Rotig A, Appelkvist EL, Geromel V, Chretien D, Kadhom N, Edery P, Lebideau M, Dallner G, Munnich A, Ernster L, Rustin P (2000) Lancet 356:391–395
76. Taylor RW, Schaefer AM, Barron MJ, McFarland R, Turnbull DM (2004) Neuromuscul Disord 14:237–245
77. Capaldi RA, Murray J, Byrne L, Janes MS, Marusich MF (2004) Mitochondrion 4:417–426
78. Larsson NG, Clayton DA (1995) Annu Rev Genet 29:151–178
79. Holt IJ, Harding AE, Morgan-Hughes JA (1988) Nature 331:717–719
80. Bourgeron T, Rustin P, Chretien D, Birch-Machin M, Bourgeois M, Viegas-Pequignot E, Munnich A, Rotig A (1995) Nat Genet 11:144–149
81. Oquendo CE, Antonicka H, Shoubridge EA, Reardon W, Brown GK (2004) J Med Genet 41:540–544

4.1 Mucopolysaccharides

Zoltan Lukacs

4.1.1 Introduction

"*Advance of knowledge in a field tends to cloud it for a time and an area which had seemed very simple becomes temporarily confused, and then again becomes simple when knowledge advances even further.*" – V.A. McKusick, 1969 [48]

The understanding of mucopolysaccharidoses (MPSs) as a group of disorders has greatly advanced since Brante first demonstrated storage of mucopolysaccharide in the liver of a patient with MPS type I (MPS I) [6]. Nowadays, the enzymatic and genetic causes of the disorders have been elucidated. In that process, MPS type V (MPS V, Scheie syndrome) has been recognized to be genetically identical to MPS I (Hurler syndrome), despite its different phenotype. Therefore, both, Hurler and Scheie syndromes are assigned to MPS I, and MPS V is no longer used.

Frantantoni et al. first recognized that MPSs are disorders of lysosomal degradation of glycosaminoglycans (GAGs), a group of polysaccharides derived from the hydrolytic cleavage of proteoglycans [22]. The undegraded material is stored in the lysosomes of mesenchymal and parenchymal tissues. The classification of the disorders is still based on historically derived names and numbers (Table 4.1.1). All MPSs represent chronic progressive disorders, which usually exhibit a wide variety in clinical manifestations. MPS I (Hurler/Scheie syndrome), a disorder characterized by missing α-L-iduronidase activity, stresses this point. The severe phenotype (Hurler syndrome) has an early onset and patients may show skeletal deformities (dysostosis multiplex), coarse facial features, hepatosplenomegaly, an enlarged tongue and head, cardiomyopathy, hearing loss, macroglossia, and respiratory tract infections. Developmental delay is usually apparent between 12 and 24 months of age. Death occurs usually before the age of ten years. In contrast, the phenotype designated as Scheie syndrome is characterized by normal intelligence and stature. However, joint involvement, visual impairment, and obstructive airway disease persist. The age of onset is commonly beyond 5 years. An intermediate phenotype (Hurler/Scheie) can also be found in the literature. MPS type II (MPS II, Hunter syndrome) is the only X-linked disorder among the MPSs, which are usually autosomal recessive traits. However, a few female patients who are affected by MPS II are also known [63]. Generally, the phenotype is similar to MPS I with a lack of corneal clouding and slower somatic and central nervous system involvement. Once again, less severe forms do not demonstrate intellectual impairment. Pebbly, ivory-colored skin lesions unique to Hunter syndrome are sometimes observed and may aid in its diagnosis. MPS type III (MPS III, Sanfilippo syndrome) constitutes a group of disorders with similar clinical

features. Four types are distinguished according to the underlying defect of heparan sulfate degradation. Diagnosis is often not straightforward as somatic features are frequently rather mild and hallmarks of the other MPS disorders, like coarse facial features and skeletal abnormalities may easily be missed. Clinical symptoms are usually noticed between the age of 2 and 6 years. At first, behavioral problems and delayed development may become apparent. Later, severe neurological degeneration leads to loss of intellectual and motor skills. Death most often occurs in the second decade of life. As Sanfilippo types A–D are clinically indistinguishable, enzyme activity measurements are required to elucidate the cause of the disorder. MPS type IV (MPS IV, Morquio syndrome) is a disorder of the degradation of keratan sulfate, found in cartilage and cornea, and thus explains the unique clinical features of the disease. Either N-acetylgalactosamine-6-sulfatase (Morquio A) or β-galactosidase (Morquio B) is deficient. Complete deficiency of the latter gives rise to GM1-gangliosidosis, while specific mutations that affect keratan sulfate metabolism are supposed to cause Morquio syndrome B. The predominant features of patients with that disorder are severe skeletal abnormalities and short-trunk dwarfism, in severe cases giving rise to neurological abnormalities. Mild corneal clouding and coarse facial features are also noted. Intellectual development is not usually impaired [52]. MPS type VI (MPS IV, Maroteaux-Lamy syndrome) is caused by deficiency of arylsulfatase B. It is characterized by dysostosis multiplex, corneal clouding, claw-hand deformities, and carpal tunnel syndrome. Growth, which is normal at first, virtually stops at the age of 6–8 years. Hepatosplenomegaly is also always present after that age. In general, symptoms are similar to Hurler syndrome, while normal intelligence is preserved. MPS type VII (MPS VII, Sly syndrome) occurs less frequently than the other MPSs. It is caused by a deficiency of β-glucuronidase and varies significantly in clinical severity among the patients described so far. Early onset of the disease is often accompanied by Hurler-like features, while later onset is characterized by normal intelligence and no corneal clouding [51, 71].

The recognition of increased GAG excretion in urine of patients with Hurler syndrome by Dorfman et al. facilitated its diagnosis and is still used as a diagnostic marker [21]. Generally, diagnosis should be based on firm clinical observations before biochemical tests are initiated. A four-step process is then recommended, with the first step being a rather unspecific screening test for urinary GAG excretion. The second step should be the differentiation of urinary GAGs, usually by electrophoresis or thin-layer chromatography (TLC). At this point, the disease type can already be suggested. Proceeding along these lines, the enzyme deficiency should be demonstrated in the third step. In conjunction with the clinical features, this can be regarded as a final confirmation of the diagnosis. However, for future genetic counseling, the identification of the distinct genetic mutations in both alleles should be considered.

In this chapter, the dimethylenblue method as a urinary screening assay, electrophoresis, and TLC for GAG differentiation and the enzyme assays will be introduced. Furthermore, pitfalls will be discussed and a short survey of alternative methods will be given.

Table 4.1.1 *Summary of the different types of mucopolysaccharidosis* (MPS)

MPS type	Eponym	McKusick No.	Enzyme	Incidence [a]
I	Hurler/Scheie	607014	α-L-Iduronidase	1:76,000–144,000
II	Hunter	309900	Iduronate-2-sulfatase	1:34,000–132,000
III	Sanfilippo			1:280,000 [b]
IIIA	Sanfilippo A	252900	Heparan-N-sulfatase	
IIIB	Sanfilippo B	252920	α-N-acetylglucosaminidase	
IIIC	Sanfilippo C	252930	Acetyltransferase [c]	
IIID	Sanfilippo D	252940	N-acetylglucosamine-6-sulfate	
IV	Morquio			
IVA	Morquio A	253000	N-acetylgalactosamine-6-sulfate	1:76,000–216,000 1:40,000–50,000 [d]
IVB	Morquio B	253010	β-D-galactosidase	
VI	Maroteaux-Lamy	253200	Arylsulfatase B [e]	1:840,000–1,300,000 1:248,000 [f]
VII	Sly	253220	β-D-glucuronidase	1:840,000–1,300,000

[a] Estimated incidence according to Neufeld [51] unless otherwise noted
[b] For Sanfilippo A and B in Northern Ireland (see [a])
[c] Acetyl CoA:α-glucosaminide-N-acetyltransferase
[d] Northover [52]
[e] N-acetyl-galactosamine-4-sulfatase
[f] Hein [30]

4.1.2 Glycosaminoglycans

GAGs (in older literature: mucopolysaccharides) are found in the extracellular matrix and are also associated with proteoglycans within the plasma membrane of most mammalian cells. Functionally, they are attached to proteins that channel the flow of water and nutrients through dense connective tissues. Furthermore, certain domains can bind to biologically active compounds like, for example, fibroblast growth factor-β or chemokines [8, 49, 57]. Initial cleavage of the protein-bound GAGs results in sulfated polysaccharide chains, which are subsequently degraded within the lysosomes starting from the nonreducing end of the molecule. They reach the lysosome via adsorptive pinocytosis and fusion of endocytic vessels with the organelle. There are also some endoglycosidases within certain tissues that can hydrolyze GAGs to oligosaccharide products. Contribution of the latter pathway to degradation of the polymer seems to be of minor importance, as diseases resulting from deficiency of one lysosomal enzyme cannot be counteracted by increased endoglycosidase activity.

In general GAGs are polysaccharides, which consist of repeating disaccharide units. However, a large degree of heterogeneity exists within the subunits regarding individual degrees of sulfatation, acetylation, and insertion of other monosaccharides. Therefore, the structures shown below will provide a general idea about the

most important GAGs. The complexity of the structures also complicates biochemical analysis and structure elucidation.

Quantitatively, the most important GAG is chondroitin sulfate, which comprises alternating units of glucuronic acid and N-acetylgalactosamine (Fig. 4.1.1). Cleavage sites for the enzymes, which are important for MPS disorders, are indicated in the figures. Dermatan sulfate consists of chains of iduronic acid and N-acetygalactosamine (Fig. 4.1.2). In addition, variable amounts of iduronic acid are epimerized to glucuronic acid, which may be sulfated at C-2. Heparan sulfate degradation is mainly affected in MPS III. The polymer contains iduronic acid, glucosamine, glucuronic acid, and N-acetylgalactosamine in varying amounts (Fig. 4.1.3). Interestingly, the amino group of the glucosamine may be sulfated, resulting in a sulfamate group. Cleavage by the respective enzyme yields the free amino group. However, this compound cannot be digested so that acetylation by an acetyltransferase is required before further degradation can occur. Finally, keratan sulfate is found mainly in cartilage and the cornea. It consists of alternating galactose and N-acetylglucosamine subunits (Fig. 4.1.4).

Failure to cleave certain monosaccharides or functional groups from the nonreducing end prevents further degradation. The resulting polymer will be stored within the lysosome and some excessive oligo- and polymers will also be found in urine [40]. Comparison of urinary GAGs and the polymers stored in the kidney has revealed significant differences, so that it seems most likely that the urinary GAGs reflect a mixture of the pattern found in all tissues of the body [8]. Storage of hepa-

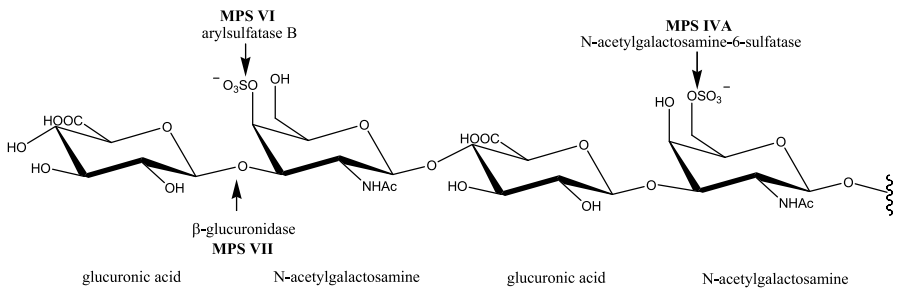

Fig. 4.1.1 Structure of chondroitin sulfate. Cleavage sites for lysosomal enzymes are also indicated (*arrows*). *MPS* Mucopolysaccharidosis

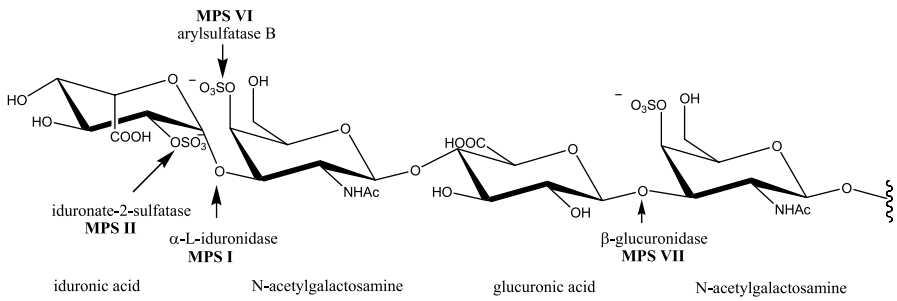

Fig. 4.1.2 Structure of dermatan sulfate. Cleavage sites for lysosomal enzymes are also indicated (*arrows*)

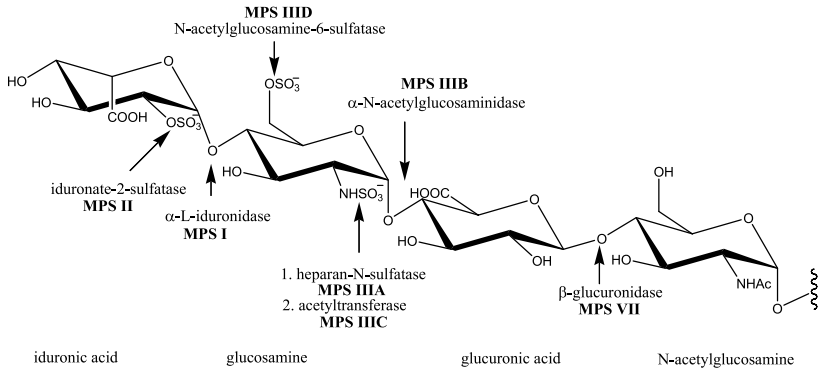

Fig. 4.1.3 Structure of heparan sulfate. Cleavage sites for lysosomal enzymes are also indicated (*arrows*)

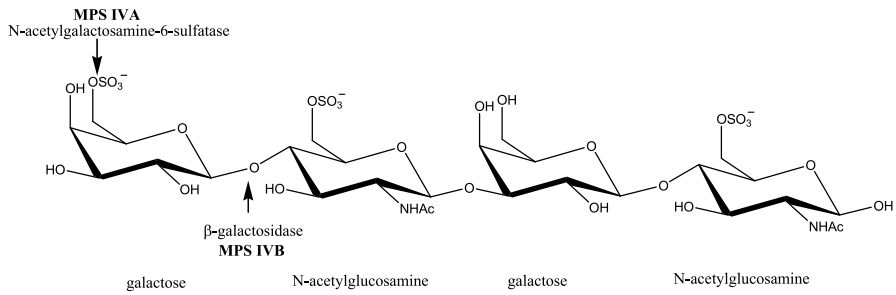

Fig. 4.1.4 Structure of keratan sulfate. Cleavage sites for lysosomal enzymes are also indicated (*arrows*)

ran sulfate seems to be related to neurodegeneration, while the other GAGs mainly contribute to skeletal or other physical problems [37].

4.1.3 Methods

4.1.3.1 Screening Assays for GAGs

Berry Spot Test

Principle

The Berry spot test provides a rapid qualitative evaluation of urine. GAGs react with toluidine blue, a cationic dye, to yield a pink-colored compound. Alternative spot tests have been published but suffer from the same drawbacks regarding false-negative and false-positive specimens [2, 10, 15, 34]. Nevertheless, this fast procedure may pick up patients who have been referred to a laboratory for other metabolic examinations. For specific, initial MPS testing, the 1,9-dimethylene blue (DMB) assay, described below, is recommended.

Pre-analytical

■ Specimen

Un-timed urine specimens are used for this assay. Early-morning urine should be discarded because GAG excretion referred to creatinine concentration is increased during the night. During the day, the GAG:creatinine ratio remains fairly constant [54]. It is not usually necessary to add preservative unless bacterial contamination is suspected (e.g., urinary tract infections). A few drops of chloroform do not negatively affect the assay and can be evaporated once the sample is received at the laboratory; however, tubes that withstand organic solvents should then be used. When the expected delay between receipt of the samples and measurement does not exceed 2–3 days, storage at 4°C is preferred over –20°C. Frozen urine should be thawed in a water bath at 37°C and carefully vortexed prior to analysis.

■ Reagents and Chemicals

1. Toluidine blue solution: a 0.4-mM solution is prepared by dissolving 1.22 g toluidine blue 0 in 800 ml acetone under continuous stirring. The solution is acidified with few drops of H_2SO_4 (1 M). The volume is adjusted to 1000 ml with demineralized water. The reagent is stable for 1 year at room temperature. As commercial dyes can be of varying quality, the mixture should be tested with known standards.
2. Standard solution/positive control: chondroitin sulfate (50 mg/l) in demineralized water.
3. Wash solution: 1.8 M acetic acid.

■ Instrumentation

None required.

■ Calibration

None required.

■ Quality Control

Chondroitin sulfate (10 µl) and a negative control (50 µl of urine from a healthy subject) are spotted on each filter paper strip according to the procedure below. The test can be accepted when the negative control remains blue after staining, while the positive control turns into a pink-colored spot.

Analytical

■ Procedure

Quality controls (10 µl) and patient urines (50 µl) are spotted onto filter paper strips (Whatman 903 paper, Whatman, Dassel Germany) in 5- to 10-µl increments using a gas chromatography syringe (10 or 25-µl volume). Allow each spot to dry before adding the next amount of material. Automatic spotters for TLC plates may also be used. The paper is then dipped into toluidine blue solution for 2 min. Discard used solution afterwards. Allow the paper to dry. Excessive dye is removed by washing the strip in 1.8 M acetic acid (3×) and demineralized water (1×), for 5 min each. Positive samples will be purple against a bluish background [3, 4].

- Calculation

None required.

Post-analytical

- Interpretation

The spots are rated according to the intensity of their color. The positive control should be taken as an orientation point. Blue specimens are rated as negative, distinctly colored samples are considered positive (Fig. 4.1.5), while intensely pink specimens are rated strongly positive. The latter are highly suspicious of MPSs and follow-up examinations are recommended. Positive specimens (rating 2) should be discussed with the patient's physician. Depending on the clinical symptoms, further evaluations may be indicated.

Pitfalls

The spot test may yield false-negative results for certain patients as it does not return quantitative results, despite the age-dependence of urinary GAG excretion. In addition, neonatal samples, especially in the first few weeks of life, may give positive results due to elevated normal GAG excretion during this period [3]. These samples should not be run with the Berry spot test because ambiguous results can be expected. The limit of detection for the Berry spot test is generally 0.1 mg/ml. The moderate excretion of GAGs in MPS III and MPS IV, particularly for patients who are several years of age, provides another challenge. It can be expected that about 50% of such patient samples will be negative [13].

4.1.3.2 Spectrophotometric Assay Using DMB

Principle

A first line-screening assay for MPSs is useful to evaluate the possibility of an MPS and to avoid tedious and expensive further laboratory testing of patients. The spot test described above can be used for a more general screening, for example when organic acids are requested from urine. However, GAG excretion is related to age, and

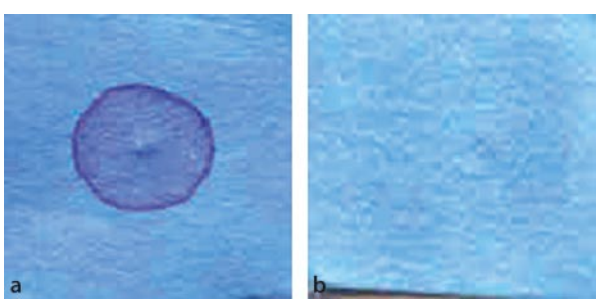

Fig. 4.1.5 Examples of a positive (**a**) and a negative (**b**) Berry spot test from urine. The filter paper will remain light blue after washing. The pink spot is typical for elevated glycosaminoglycan (GAG) excretion

therefore quantitative tests are superior to qualitative assays when MPS testing is specifically requested., Numerous methods have been developed for that purpose. The turbidity test exploits the interaction of GAGs with cationic detergents or albumin. Its sensitivity depends on the GAG type and may result in false-negative samples, especially in the case of MPS III and MPS IV patients. The uronic acid-carbazole test visualizes uronic acids that are a part of many GAGs [5]. It requires time-consuming precipitation of the GAGs from urine [20]. In addition, keratan sulfate, the main storage material in MPS IV, does not contain uronic acid residues. Consequently, another test has to be run to detect this compound. Thus, direct spectrophotometric assays have gained popularity and are nowadays used by many laboratories. Alcian blue was among the first dyes used in that manner [25, 26]. Today, DMB is more frequently applied due to its higher sensitivity (Fig. 4.1.6) [17]. It forms a complex with sulfated GAGs present in urine that can be measured at 520 nm [14, 16, 53, 70].

Pre-analytical

■ Specimen

The specimen requirements are the same as for the Berry spot test.

■ Reagents and Chemicals

Standard method:

1. Formiate buffer (55 nmol/l): 2.13 ml formic acid is dissolved in 1000 ml demineralized water. The pH is adjusted to 3.3 with 2 M NaOH.
2. DMB reagent: 3.2 mg DMB (pure substrate available from Aldrich, cat. no. 341088, Taufkirchen, Germany) is dissolved in 150 ml formiate buffer. The solution can be stored at 4°C for up to 3 weeks.
3. Standard solution: 0.5 mg heparan or chondroitin sulfate is dissolved in 10.0 ml demineralized water (final concentration: 50 µg/ml). Aliquots (500 µl) are kept at –20°C until required.

Alternative method:

1. Formiate buffer: see above.
2. DMB reagent (31 µMol): 10.7 mg DMB is dissolved in 1000 ml of formiate buffer.
3. Tris base: 2 mol/l Tris base in demineralized water.
4. Standard solution: see above.

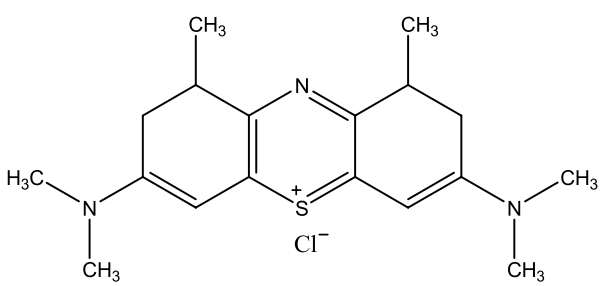

Fig. 4.1.6 Structure of 1,9-dimethylene blue

■ Instrumentation

Spectrophotometer for cuvettes, or microtiter plates that can measure wavelengths between 500 and 700 nm.

■ Calibration

A calibration curve is recorded for each batch of samples (e.g., 100 µl, 50 µl, 25 µl, and 0 µl standard solution). The curve is plotted and results are calculated. Urines with absorptions exceeding the highest standard are diluted and remeasured.

■ Quality Control

For internal quality control, urine from a known MPS patient and a solution containing chondroitin sulfate (50 µg/ml) are used. Results for urine and the artificial control should not exceed 3 standard deviations when plotted over time; if it does, the test has to be repeated. In addition, absolute absorption values, the slope of the calibration curve, and the coefficient of variance (CV) of duplicates have to be within certain limits defined by the laboratory.

For external quality control, laboratories running the DMB assay should regularly exchange samples and discuss problematic cases. Currently, there is no official quality control scheme/proficiency testing available.

Analytical

■ Procedure

Standard Method

Add 1 ml of DMB reagent to 100 µl of demineralized water (blank) or 100 µl of urine in a cuvette. In addition, 100 µl of each urine should be added to 1 ml of formiate buffer to assess the absorbance of the pure sample (sample blank). Each sample should be measured against pure formiate buffer (buffer blank, when measured separately). The color of the GAG-DMB complex is not stable over time, so that assay conditions have to be strictly standardized. Urine, standard, or water is added to all cuvettes first. The DMB reagent must then be added swiftly. All cuvettes are mixed with a spatula (10×) and after 3 min samples are measured at 520 nm. When the absorbance exceeds the linear range, the urine has to be diluted. It is also recommended to measure all samples in duplicate using 50 and 100 µl of urine. This allows an evaluation of the plausibility of results.

Alternative Method

According to de Jong et al. [16] and Piraud et al. [55] urinary protein suppresses DMB-GAG complex formation and results in lower total GAG concentrations. An alternative assay has been developed that avoids problems with GAG-protein interactions. The main difference is that measurements are carried out at basic pH.

In general, most procedures are like the ones described above. For the modified method, an alternative DMB reagent is used and ten parts of this reagent are added to one part of Tris buffer to yield a reagent with a pH of 8.7–8.8. The reagent – Tris mixture is not stable and has to be prepared just prior to analysis. First, 20 µl of urine (sample) or water (blank) is added to the cuvettes or microtiter plates. The volume of standards, samples, and blanks are adjusted to 50 µl with demineralized water. Then, 275 µl of DMB-Tris reagent is added to each cuvette/well. Either all samples

are measured against formiate-Tris buffer (10 + 1) or this buffer mixture is measured separately (buffer blank). Absorbance is read 70 s after mixing.

Within-run CVs of 2–6% were obtained, while between-run CVs range from 6 to 7%.

■ Calculation

The standard curves are plotted and results are calculated using the curve. Absorbance of the sample is corrected for background absorbance as follows:

1. Measurements against buffer:
   Sample absorbance = measured absorbance – (blank + sample blank)
2. Measurement against water or air:
   Sampleabsorbance = measuredabsorbance – [(blank + sampleblank) – bufferblank)]

To eliminate variations in urinary excretion of GAGs, the results are referred to creatinine content of the sample. As an alternative to measuring the increase of absorption at 520 nm, the assessment of decreased absorption at 596 nm may be advantageous [61].

Post-analytical

■ Interpretation

Excretion of urinary GAGs is related to the age of the patients. Each laboratory should assess its own reference range, as minor differences may already alter results. Therefore, the reference ranges given below can only offer some guidance. It is also useful to calculate the Z-score of the results (i.e., to assess the deviation of the result from the mean expressed in multiples of the standard deviation for that age group). Results exceeding two standard deviations are usually considered as potentially pathological and further clinical and biochemical work-up is recommended. Generally, due to the many pitfalls, reports should emphasize that a certain percentage of MPS patients excrete normal concentrations of urinary GAGs and if clinical symptoms are indicative of an MPS, further studies should be initiated regardless of the total GAG measurement.

Spectra

Pure DMB displays maxima at 596 nm and 648 nm (Fig. 4.1.7). GAG-DMB complexes show an increase in absorption at around 525 nm. As the purity of DMB is crucial for meaningful results, each new batch should be checked for a constant ratio of the peak at 648 nm to the peak at 596 nm. In its purest form, this ratio should be 1:1.5 and will be reduced with sulfate contaminations [61]. After addition of GAG-containing urine, the decrease in absorption at 596 nm will be more pronounced than that at 648 nm.

Reference Values

Reference values for the standard and alternative methods are given in Tables 4.1.2 and 4.1.3, respectively (the latter adapted from de Jong et al. 1992 [16]).

■ Typical pathological values

A list of typical pathological values is given in Table 4.1.4.

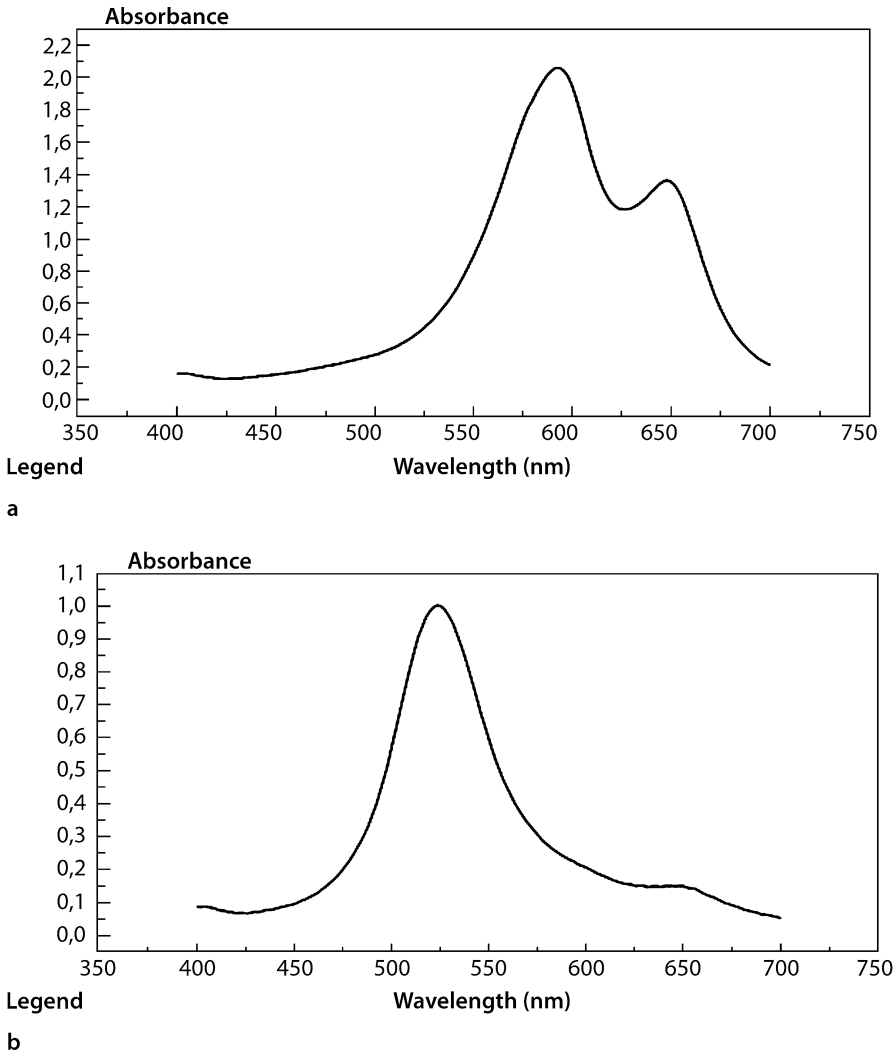

Fig. 4.1.7 Spectra of 1,9-dimethylene blue dissolved in formiate/tris buffer without (**a**) and with (**b**) the addition of chondroitin sulfate

Pitfalls

It is crucial to establish age-dependent reference ranges for this method. During the first few weeks/months of life in particular, rapid changes in urinary GAG excretion are observed. In the case of low creatinine, another sample should be requested. For this method, Mabe et al. reported a sensitivity of 100%, while 25% of samples came out as false positives [45]. In our experience, the false-positive rate is significantly lower. A pilot quality assurance study in the UK found a false-positive rate of 5.1% for the Alcian blue method, which should be comparable to the DMB assay [7]. Patients with excessive connective tissue destruction may give positive results [54]. Among these are patients with rickets, malabsorption syndrome with gross osteomalacia, malignant disorders with extensive secondary deposits (including leukemia), patients with disseminated lupus erythematosus, some patients with rheumatoid ar-

Table 4.1.2 *Age-dependent reference ranges for glycosaminoglycan (GAG) concentrations in urine (healthy controls) using the standard 1,9-dimethylene blue (DMB) method*

Age	Mean (mg/g creatinine)	Reference range (mg/g creatinine)
0–1 month	13.0	0–21.7
1–3 months	12.2	0–19.2
4–6 months	17.1	0–25.2
7–12 months	13.6	0–19.6
1–2 years	15.7	0–21.6
2–5 years	9.7	0–14.5
5–9 years	6.1	0–10.1
9–16 years	5.2	0–8.4
16–18 years	–	–
Above 18 years	2.0	0–2.8

Table 4.1.3 *Age-dependent reference values for GAG concentrations in urine (healthy controls) for the alternate DMB assay [16].* SD *Standard deviation*

Age	Mean (mg/mmol creatinine)	SD (mg/mmol creatinine)
0–5 months	33.6	9.2
6–12 months	23.3	4.1
1 year	19.5	5.2
2–3 years	14.4	3.4
4–5 years	11.0	1.7
6–7 years	9.3	1.8
8–9 years	8.4	1.6
10–14 years	7.0	1.8
15–19 years	4.1	1.3
Above 20 years	3.3	0.9

■ ***Table 4.1.4*** *Pathological values for urinary GAG concentrations using the alternate method described in 4.1.3.2 (values adapted from Chih-Kuang et al. [13])*

MPS type	Mean(mg/mmol creatinine)	SD(mg/mmol creatinine)
I	39.6	11.8
II	54.3	23.3
III	34.5	17.8
IV	33.4	11.0
VI	35.8	5.7

thritis, and some patients with Marfan syndrome. In addition, heparin and acrylic acid polymer used in paper diapers will interfere with the assay [36]. In all of these cases, follow-up analysis by TLC or electrophoresis will reveal a normal GAG pattern. Unfortunately, false-negative results are also inevitable, especially in cases of MPS III and MPS IV, and results should be communicated noting this fact [14].

4.1.3.3 Differentiation of GAGs

The pattern of urinary GAGs should be assessed in a case of a positive urinary MPS screening result or when clinical symptoms are suggestive of MPS despite normal GAG excretion. This also facilitates the choice of further enzymatic studies. In addition, approximately 5–6% of abnormal samples in the quantitative DMB method are false-positive results that can usually be identified as such by checking the distribution of GAG excretion [16].

Thin-Layer Chromatography

Principle

Urinary GAGs are precipitated before TLC is performed. Separation of the GAGs is achieved by exploiting the different solubility of their calcium salts in various concentrations of ethanol [18, 35, 42]. TLC can provide an inexpensive alternative to electrophoretic techniques, especially when such equipment is not available.

Pre-analytical

■ Specimen

The specimen requirements are the same as for the Berry spot test.

■ Reagents and Chemicals

1. Precipitation buffer: sodium citrate solution (0.2 M) in demineralized water. The pH is adjusted to pH 4.8 and 1 g/l cetylpyridinium chloride (CPC) is dissolved in this buffer.
2. Aqueous 2 M LiCl solution.

3. Solvents for TLC:
   1. 70% ethanol and 2.5% calcium acetate in 0.5 M acetic acid.
   2. 50% ethanol and 5.0% calcium acetate in 0.5 M acetic acid.
   3. 40% ethanol and 5.0% calcium acetate in 0.5 M acetic acid.
   4. 30% ethanol and 5.0% calcium acetate in 0.5 M acetic acid.
   5. 20% ethanol and 5.0% calcium acetate in 0.5 M acetic acid.
   6. 10% ethanol and 5.0% calcium acetate in 0.5 M acetic acid.
      All solutions have to be prepared on a daily basis.
   7. Staining solution: 1% Alcian blue in 70% ethanol/acetic acid (95:5 v/v).
   8. Acetic acid (10%).
   9. Standard mixtures of keratan sulfate, dermatan sulfate, heparan sulfate, and chondroitin sulfate (1.0 mg/ml) in 0.05 M NaOH.
   10. Ethanol p.a.

■ Instrumentation

1. Tanks for TLC.
2. Cellulose TLC plates (20 × 20 cm). Plates should be run with demineralized water and dried at –80°C overnight before using them for GAG analysis. This cleaning procedure improves the separation of urinary GAGs (Professor Paschke, personal communication).
3. If possible: automatic spotter, or a syringe for volumes between 10 and 25 µl.

■ Calibration

The standard mixture (5–10 µl) is spotted onto the TLC plate, approximately 4 cm from the lower edge and at least 3 cm from the side. The migration pattern is used as a reference to assess patient urines.

■ Quality Control

The standard mixture will also serve as a quality control for the separation of the GAGs. Exchange of positive patient samples as an external quality control and a means to gain experience concerning the interpretation of patterns is highly recommended.

Analytical

■ Procedure

The procedure was first described by Lippiello et al. [42] and applied to urinary GAGs by Humbel and Chamoles [35]. The slightly modified method by Pennock [54] is described here.

Precipitation of GAGs

Urine is centrifuged at 1500 × *g* (25°C/10 min). A volume of the supernatant that is equivalent to 10 µmol creatinine is mixed with an equal volume of 0.2 M precipitation buffer. This mixture is incubated for 30 min at 37°C in a water bath, once again centrifuged at 1500 × *g* (10 min) and the supernatant is discarded. In addition, the tube is drained for 30 min by inversion. The pellet is dissolved in 150 µl aqueous LiCl solution (2 M) and mixed with 800 µl ethanol. This solution is transferred to a centrifuge tube and spun at 1500 × *g* (10 min). The supernatant is aspirated and the

resulting pellet is dried in a stream of nitrogen at room temperature [32]. Urine from healthy individuals will provide a recovery of 10–40% of GAGs present [39].

TLC

Aqueous solutions (10 µl) of approximately 5–50 µg GAGs/5 µl are spotted onto a TLC plate 3–4 cm from its lower edge. To achieve good reproducibility, automatic spotters are recommended, but manual spotting with a syringe is also feasible. Starting with the origin every 2 cm, six lines are drawn with a soft pencil. These indicate the borders for each solvent system. The plate is subsequently placed into six different tanks that contain decreasing amounts of ethanol. After removal of the plate from one tank, the bottom is swiftly blotted with filter paper and placed into the next tank. Each solvent system is allowed to proceed to the line assigned to it (i.e., tank one is developed until the solvent reaches line 1, tank 2 until it reaches line 2, and so on). One complete run requires approximately 1 h. The plate is allowed to dry and then is placed into the Alcian blue staining solution for 3 min. Excess dye is removed by repeated washing with acetic acid.

■ Calculation

None required.

Post-analytical

■ Interpretation

Spot patterns should always be assessed relative to the standard mixture. In general, keratan sulfate will migrate with the leading front, while chondroitin-6-sulfate should be located between fronts 5 and 6, chondroitin-4-sulfate between fronts 4 and 5, heparan sulfate between fronts 3 and 4, hyaluronic acid between fronts 2 and 3, and dermatan sulfate between fronts 1 and 2.

Chromatogram

A typical chromatogram is shown in Fig. 4.1.8.

Typical Pathological Patterns

Typical patterns of GAG excretion can be found in the urine of MPS patients [37]. For MPS I and II an increased excretion of dermatan and heparan sulfate is found, with the first being especially pronounced on TLC. In case of MPS III, heparan sulfate will be increased, while a prominent keratan sulfate band characterizes MPS IV. MPS VI shows slightly increased dermatan sulfate excretion that can also be found for the MPS I Scheie variant.

Pitfalls

Dermatan sulfate may show two bands, one migrating between the first and second front, while another one remains at the origin. In addition, heparan sulfate from the urine of MPS III patients may show a greater retention factor value in comparison to the standard. Spiking of the original sample may help to identify the spot in ambiguous cases. Small modifications in the ethanol content of the solvent systems readily influence chromtographic behavior, so that exact volumes and short opening times of the tanks are crucial [18].

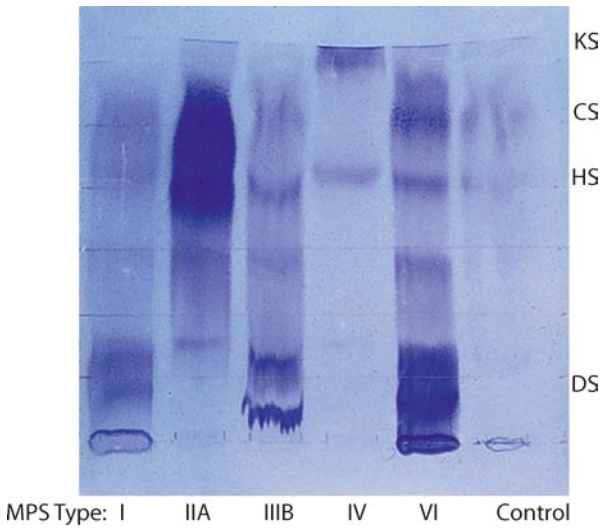

Fig. 4.1.8 Thin-layer chromatography of patient urines and a normal control. The MPS types are indicated beneath each band. The positions of dermatan sulfate (*DS*), heparan sulfate (*HS*), chondroitin sulfate (*CS*), and keratan sulfate (*KS*) are given on the right. The chromatogram was kindly provided by Professor E. Paschke, Laboratory of Metabolic Disease, Department of Pediatrics, University of Graz, Austria

Electrophoresis

Principle

GAGs are separated by electrophoresis to yield a distinct pattern for the different MPS types [32, 33]. It was found that electrophoresis in barium acetate depends largely on the structure of the GAGs, whereas the degree of sulfatation is of minor importance [69]. One-dimensional electrophoresis, as described here, offers lower resolution than two-dimensional techniques [28], but is simpler to evaluate and allows the assessment of several patients in one run.

Pre-analytical

■ Specimen

The specimen requirements are the same as for the Berry spot test.

■ Reagents and chemicals

1. Precipitation buffer: sodium citrate solution (0.2 M) in demineralized water. The pH is adjusted to 4.8 and 1 g/l CPC is dissolved in this buffer.
2. 2 M aqueous LiCl solution.
3. Ethanol p.a.
4. Barium acetate buffer (0.1 M) at pH 5.0.
5. Barium acetate buffer (1.0 M) at pH 5.0.
6. Aqueous solution of phenol red (0.5 g/l).
7. Alcian blue (0.25%) solution in demineralized water.

8. 0.18 M Acetic acid.
9. Cellulose acetate strips.

■ Instrumentation

An electrophoresis unit (e.g., Multiphor II with MultiTemp III and electrophoresis power supply EPS 3500 XL, Pharmacia Biotech, Freiburg, Germany) and a scanner with software for densitometry (e.g., AIDA, Raytest, Straubenhardt, Germany).

■ Calibration

None required.

■ Quality Control

A standard mixture of GAGs is applied to the cellulose acetate plate and treated like a patient sample. The quality of the separation/staining can be evaluated using this standard. Known patient samples should be taken through this procedure to evaluate the process. No external quality control is available at this time.

Analytical

■ Procedure

Precipitation of the GAGs from urine is carried out according to the procedure described for thin-layer chromatography. The pellet is dissolved in 20 µl demineralized water containing 0.5 g/l phenol red and a volume equivalent to 5 µg GAGs is loaded onto a cellulose acetate strip using a sample applicator. Phenol red facilitates the alignment of samples on the plate and high salt concentrations, which interfere with electrophoresis, will impede the migration of the dye [9]. Prior to loading, the strip was soaked in 0.1 M barium acetate buffer and lightly blotted with filter paper to remove any excess buffer. Electrophoresis is carried out in 1.0 M barium acetate buffer applying 200 V for 5 min while the cellulose acetate strip is placed on a plastic film-insulated cooling plate (15°C). In addition, the strip is covered with Parafilm (American Can, Greenwich, Conn., USA), further insulated with a sheet of foam plastic, and pressure is applied from the top with several layers of glass plates (approximately 950 g). After the first electrophoresis step, the strip is removed from the electrophoresis unit and immersed in 0.1 M barium acetate buffer (2 min), which contains 15% (v/v) ethanol. The cellulose acetate film is blotted again with filter paper and subjected to electrophoresis at 200 V for 30 min. Subsequently, the strip is soaked in 0.1 M barium acetate buffer containing 50% (v/v) ethanol for 2 min. The strip is blotted and a final electrophoresis at 200 V/10 min is performed. The length of time required to achieve a good separation depends on the efficiency of the cooling apparatus, and therefore has to be evaluated individually [19]. The strip is then stained with Alcian blue for 15 min and washed with 0.18 M acetic acid and demineralized water [32]. After drying at room temperature, the cellulose acetate film can be scanned and evaluated by densitometry. Staining with azure A-silver can be used alternatively when only small amounts of urine are available; this method is reported to be approximately 200 times more sensitive than Alcian blue staining [64].

■ Calculation

The sum of all GAG spots is considered 100% in densitometry and the distribution among the different GAGs is calculated and expressed in percent.

Post-analytical

■ Interpretation

The pattern of spots is evaluated in reference to the standard mixture. Dermatan sulfate yields two spots, one of which can overlap with hyaluronic acid. Abnormal presence of dermatan sulfate and heparan sulfate is an indication of MPS I or MPS II, while a prominent heparan sulfate spot points to MPS III. The subtypes of MPS III can only be differentiated by enzyme studies. Elevated excretion of keratan sulfate is indicative of MPS IV. In contrast, high dermatan sulfate excretion is most likely to be associated with MPS VI, while milder cases of MPS I may also show such a pattern (cf. Table 4.1.5) [56].

Chromatogram

A typical chromatogram is shown in Fig. 4.1.9.

Pitfalls

Excretion of heparan sulfate may also be slightly increased in cases of mucosulfatidoses. MPS VII is difficult to identify as variable patterns of GAG excretion are observed and it may frequently look similar to normal controls. Keratan sulfate excretion in the case of MPS IV patients may be only 5–16% of total urinary GAGs, so that identification of patients may require an overloading of the plate [19].

Some disorders may cause an abnormal excretion of GAGs in urine. Among those are various bone diseases, connective tissue diseases, hypothyroidism, urinary dysfunction, and aspartylglucosaminuria. Faint spots for keratan sulfate can also be found in spondyloepiphyseal dysplasia as well as in type II mucolipidoses, where traces of dermatan sulfate may additionally be visible. Furthermore, heparin and tris(hydroxymethyl)aminomethane (Trometamol) can interfere with electrophoretic patterns [56]. To provide a good interpretation of results the clinical features of the patient and the current therapy have to be known. Furthermore, a study of the urin-

■ **Table 4.1.5** *Approximate age of diagnosis and excretion products for the different MPS types [58]*

MPS Type	Age Range (years) [a]	Major excretion products
I	0.3–6.6	DS, HS
II	0.2–35.0	DS, HS
IIIA	1.0–18.4	HS, CS
IIIB	0.5–10.00	HS, CS
IIIC	0.2–14.1	HS, CS
IIID	–	HS, CS
IVA	0.6–15.0	KS, CS
VI	2.0–38.0	DS, C
VII	–	CS

[a] Age at diagnosis given for severe phenotype (MPS type I, Hurler syndrome)

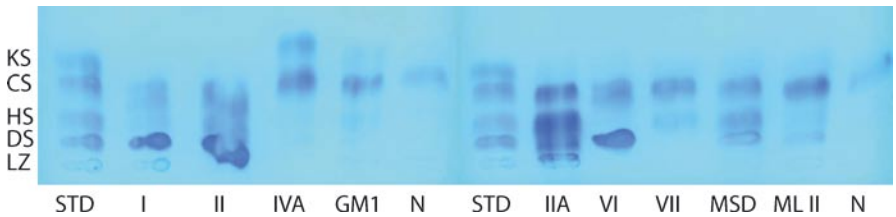

Fig. 4.1.9 Electrophoresis pattern of different types of MPS (indicated beneath the corresponding band). Standards (*STD*) and normal controls (*N*) were also run on each gel. GAGs are labeled on the left side of the figure. The picture was kindly provided by Dr. F. Buerger, Metabolic Center Heidelberg, Germany. *GM1* GM1-gangliosidosis, *MSD* multiple sulfatase deficiency *ML II* mucolipidosis II, *LZ* loading zone of the gel

ary oligosaccharide pattern seems to be useful. Generally, interpretation of patterns should be carried out by experienced laboratory staff only.

4.1.3.4 Determination of Enzyme Activity

General

Principle

The activity of lysosomal enzymes is usually measured at acidic pH in leukocyte or fibroblast homogenates. Serum or plasma samples may also be used when enzyme activity in those materials is sufficiently high. More recently, lysosomal enzymes have also been determined from dried blood spots, traditionally used in neonatal screening [11, 44]. We use dried blood for initial testing, wherever possible, as it facilitates shipping, and enzyme activity remains stable for a long period of time. Subsequently, ethylenediaminetetraacetic acid (EDTA)-blood or skin fibroblasts are requested for confirmation of positive or ambiguous results. In the past, radioactively labeled substrates have been common [27, 41], but these have been replaced by fluorogenic compounds for most enzymes. In this chapter, predominantly those methods using fluorogenic substrates for the determination of enzyme activities in leukocytes or dried blood (wherever applicable) will be described.

Pre-analytical

- Specimen

Dried blood specimens can easily be checked visually for their general quality. Discolored, overloaded, or insufficient material should be rejected and new samples should be requested. Dried blood on filter paper can be shipped by regular mail at room temperature.

EDTA-treated or heparinized blood (3–5 ml) can be used for the isolation of leukocytes. Blood should be sent by express mail to ensure rapid transport. During the summer months, cooling of the samples is required (e.g., frozen cooling packs

with Styrofoam insulation between samples and coolant to prevent freezing of the sample or ice-cold water in tightly sealed tubes wrapped around the samples).

Reagents and Chemicals

1. Dextran solution: 5 g dextran (relative molecular mass = 250,000; Sigma, Taufkirchen, Germany), 0.7 g NaCl, 50 mg heparin (Roth, Karlsruhe, Germany), and 10 mg sodium azide (Merck, Darmstadt, Germany) are dissolved in 100 ml demineralized water. The solution is stored at –20°C.
2. Stop solution/glycine-carbonate buffer (pH 9.6): dissolve 12.8 g ammonia-free glycine (ICN Biomedicals, Eschwege, Germany) and 18.0 g dry Na_2CO_3 (Merck) in 200 ml demineralized water. The solution can be stored at 4°C for up to 3 months.
3. 4-Methylumbelliferone (4-MU) standard: 4-MU (Sigma) is dissolved in glycine-carbonate buffer (diluted 1:5) to yield a 0.05-M solution. For practical purposes, 88.10 mg 4-MU is dissolved in 100 ml glycine-carbonate buffer (1:5 diluted). This stock solution is further diluted to 1:100 when needed. The standard and the stock solution are stored at –20°C and protected from light.
4. NaCl solution (1.8%).

Instrumentation

1. White, 96-well microtiter plates (PerkinElmer Life Sciences, Boston, MA, USA) for fluorescence measurements.
2. Clear, 96-well microtiter plates (VWR, Darmstadt, Germany) for ultraviolet/visible (UV/VIS) spectrophotometry measurements.
3. Microtiter plate shaker (e.g., Certomat MT, Braun Biotech, Mainz, Germany).
4. Enzyme-linked immunosorbent assay reader or UV/VIS spectrophotometer for microtiter plates (e.g., Dynatech, Chantilly, VA, USA).
5. Fluorometer for microtiter plates (e.g., Victor D, PerkinElmer Life Science).
6. Ultrasound homogenizer (e.g., Bandelin sonoplus GM 70, Bandelin, Berlin, Germany).

Calibration

A calibration curve is recorded for each plate (Fig. 4.1.10). 4-MU standards at absolute concentrations of 0.25 µmol (5 µl), 0.5 µmol (10 µl), 1.0 µmol (20 µl), 2.5 µmol (50 µl) and 5.0 µmol (100 µl) are measured in duplicates. The volume for each well is adjusted with demineralized water to the volume used in the assay. Before measurement, 200 µl stop solution are added and the plate is shaken for 5 min on a plate shaker. Fluorescence is read with an excitation wavelength of 355 nm and an emission wavelength of 460 nm. For leukocyte and dried blood measurements blanks that contain substrate and buffer solution without leukocyte homogenate or dried blood spots are prepared. After incubation and addition of the stop solution, the plate is read immediately for all assays based on leukocytes, while one dried blood spot from an arbitrary sample is added to each blank in case of dried blood assays. Hence, hemoglobin is eluted from blood spots for 30 min and these spots are removed again before measurement. It is crucial to match the age of these specimens to the age of the patient samples. If large variations (several weeks) are evident concerning the age of the samples on the same plate then a separate blank for each patient sample has to be prepared.

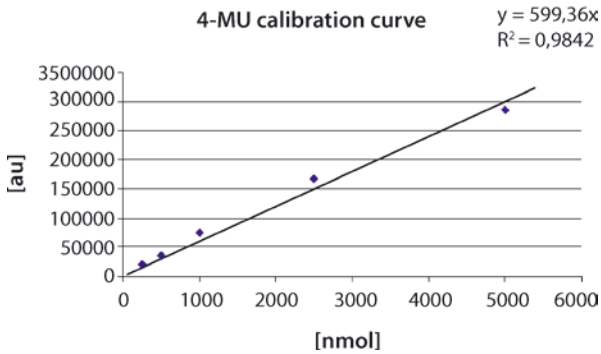

Fig. 4.1.10 Typical calibration curve for 4-methylumbelliferone (*4-MU*) in glycine/carbonate buffer. Fluorescence was read at an excitation wavelength of 355 nm and an emission wavelength of 460 nm. *au* Arbitrary units

Quality Control

Sample quality is generally assessed by the determination of β-galactosidase activity. For MPS type IVB, the α-mannosidase activity is chosen as an indicator enzyme. Leukocyte homogenates that are sufficient for at least 20 separate runs are prepared from one source and aliquots are kept frozen. These samples serve as quality controls for each run. Heat-inactivated leukocyte homogenates may serve as a positive control (patient-mimics).

The preparation of a large batch of dried blood spot samples (e.g., ten filter paper cards) from one source requires about 5 ml whole blood. These samples can serve as quality control for at least 150 separate runs. Positive controls from patients may also be prepared in that manner and patients are far more likely to consent to this use of their blood due to the small amount necessary.

Quality control samples are run in duplicate for each assay. Currently, there is no official external quality control program available.

Analytical

Procedure

Dried blood spots are prepared from native blood on standardized filter paper (Whatman 903, Whatman). The paper has to be fully soaked with blood and dried at room temperature. Blood has to be applied from one side only, to ensure even distribution throughout the filter paper. Do not use any plastic wrapping before the paper is completely dry. For further details, consult the guidelines from your closest newborn screening facility or metabolic laboratory processing dried blood specimens.

Leukocytes are prepared from EDTA-blood (approximately 3–5 ml) by the density gradient method. EDTA-blood is mixed by inversion and 5 ml is slowly added to 1 ml dextran solution. The blood and dextran solution are carefully mixed so that formation of foam is avoided. The mixture is allowed to stand for 1 h. If further time for sedimentation is required, it has to be noted as it may affect the resulting enzymatic activities. The time needed for proper sedimentation depends on sample quality and should not exceed 3 h. The upper phase including the white cells is transferred to another tube and spun at 600–1000 g for 10 min. The supernatant is

removed and 3 ml of demineralized water is added so that the pellet becomes solubilized again. Then 3 ml of a NaCl solution (1.8%) is added and the tube is centrifuged at 600–1000 × *g* for 10 min. After discarding the supernatant, the pellet should be of a yellowish color and thus free of erythrocytes. If apparent significant hemoglobin contamination persists, the procedure should be repeated once. The leukocyte pellet is stored at –20°C.

Before enzyme measurements, approximately 300–500 µl of demineralized water is added and the mixture is sonicated for 10 s on ice. Depending on the ultrasound homogenizer, the time required may vary slightly. Protein is determined according to Lowry et al. [43]. The final protein content for enzyme measurements is adjusted to approximately 5 mg/ml with demineralized water.

■ Calculation

Results are calculated from the calibration curve after adjusting for the blank. The protein content of the leukocyte homogenate is measured with the method described by Lowry et al. [43]. Results are usually expressed as nmol/min·mg protein for leukocyte homogenates and as nmol/spot·incubation time for dried blood specimens.

α-L-Iduronidase (E.C. 3.2.1.76)

■ Principle

See section 4.1.3.4, subheading "Principle."

Pre-analytical

■ Specimen

See section 4.1.3.4, subheading "Specimen."

■ Reagents and Chemicals

1. Citric acid solution (0.1 M): 21.0 g citric acid (Merck) dissolved in 1000 ml demineralized water.
2. Phosphate buffer (0.2 M): 28.4 g Na_2HPO_4 (dry; Merck) are dissolved in 1000 ml demineralized water.
3. Reaction buffer: 40 ml citric acid solution and 8 ml phosphate buffer are mixed and the pH is adjusted to 3.5 using one of either solution (only few additional drops required).
4. Inhibition buffer: 210.1 mg D-saccharic acid-1,4-lactone (10 mM; Sigma) is dissolved in 100 ml demineralized water.
5. Substrate buffer: 1.657 mg 4-methylumbelliferyl-*α*-L-(idopyranosid)-uronic acid-sodium salt (6.6 mM; Toronto Research Chemicals) is dissolved in 333 µl demineralized water. The same volume of reaction buffer is added and the solution is vortexed for 30 s. The substrate buffer is stored at –20°C and protected from light.
6. Stop solution/glycine-carbonate buffer (pH 9.6): dissolve 12.8 g ammonia-free glycine (ICN Biomedicals) and 18.0 g dry Na_2CO_3 (Merck) in 200 ml demineralized water. The solution can be stored at 4°C for up to 3 months.

Analytical

- Procedure

Leukocytes

The assay is based on the method described by Stirling et al. [59, 60]. Prepare a calibration curve and blanks according to section 4.1.3.4 "Calibration." For each patient sample, 5 and 10 µl of leukocyte homogenate is transferred to individual wells on the microtiter plate. Then 20 µl of inhibition buffer as well as 20 µl of substrate buffer are added and the volume is adjusted to 200 µl using the reaction buffer. The plate is sealed with tape and covered in aluminum wrapping. It is incubated at 37°C for 21 h. The reaction is stopped with 200 µl stop solution. The plate is shaken briefly and read with an excitation wavelength of 365 nm and an emission wavelength of 450 nm.

Dried Blood Spots

The method is a modification of that described by Chamoles et al. [12]. One 3-mm spot is punched from dried blood on filter paper and placed into one well of a microtiter plate. Then 20 µl of substrate buffer, 20 µl of inhibition buffer and 110 µl of incubation buffer are added to each sample. The plate is sealed with tape, covered with aluminum wrapping and incubated at 37°C for 45 h. After incubation, the assay is stopped with 200 µl stop solution, blanks are treated as described in section 4.1.3.4 "Calibration," and fluorescence is read with an excitation wavelength of 365 nm and an emission wavelength of 450 nm. All tests are performed in duplicate.

- Calculation

See section 4.1.3.4, subheading "Calculation." As iduronidase activity is rather low in leukocytes, results should be expressed as nmol/h·mg protein.

Reference Values/Typical Pathological Values

Activities from leukocytes range from 0.27 to 2.45 nmol/mg·h while patient samples have barely detectable activity. Leukocytes from patients after bone marrow transplantation yielded activities from 0.1 to 1.87 nmol/mg·h. Activity is variable within certain limits, but if a clear trend to lower activities is observed over time then usually chimerism will also be diminished and a recurrence of clinical symptoms may occur. Dried blood samples from healthy newborns show activities of between 0.04 and 0.40 nmol/spot·45 h.

Iduronate-2-Sulfatase (E.C. 3.1.6.13)

Principle

See section 4.1.3.4, subheading "Principle."

Pre-analytical

- Specimen

See section 4.1.3.4, subheading "Specimen."

Reagents and Chemicals

1. Acetate-buffer (0.1 M): 0.82 g sodium acetate (Aldrich) and 0.379 g lead acetate (10 mM, Aldrich) are dissolved in 100 ml demineralized water and the pH is adjusted to 5.0.
2. Substrate buffer: 0.60 mg 4-methylumbelliferyl-α-iduronate-2-sulfate (Moscerdam Substrates, Rotterdam, The Netherlands) is dissolved in 1.0 ml acetate buffer to yield a 1.25 mmol/l solution.
3. McIlvain's buffer: concentrated McIlvain's buffer is prepared by dissolving 6.558 g sodium phosphate and 5.162 g sodium citrate in 100 ml demineralized water. The pH is adjusted to pH 4.5.
4. Iduronidase solution: lyophilized lysosomal enzymes purified from bovine testis (Moscerdam Substrates) are reconstituted in 2.2 ml demineralized water and aliquots are stored at –80°C.
5. Stop-buffer: 53.0 g Na_2CO_3 and 42.0 g $NaHCO_3$ are dissolved in 1 l demineralized water. The pH is adjusted to 10.7.

Analytical

Procedure

Leukocytes

The assay is carried out according to the method published by Voznyi et al. [67]. Prepare a calibration curve and blanks according to section 4.1.3.4, subheading "Calibration." For each patient sample, 5 and 10 µl of leukocyte homogenate are transferred to individual wells on the microtiter plate. Then, 20 µl of substrate buffer is added and the plate is sealed with tape and covered in aluminum wrapping. Lead acetate present in the substrate buffer has been found to reduce inhibition by phosphates and sulfates present in the solution while having no adverse effect on iduronate-2-sulfatase activity. The plate is incubated at 37°C for 4 h. Afterwards, 40 µl of McIlvain's buffer and 10 µl of the iduronidase solution are added. The plate is briefly shaken, resealed, and incubated at 37°C for 24 h. This second incubation step is necessary to liberate 4-MU from the substrate. The reaction is stopped with 200 µl stop solution; the plate is shaken briefly and read with an excitation wavelength of 365 nm and an emission wavelength of 450 nm.

Calculation

See section 4.1.3.4, subheading "Calculation."

As iduronidase-2-sulfatase activity is rather low in leukocytes, results should be expressed as nmol/h·mg protein.

Reference Values/Typical Pathological Values

Leukocytes from normal controls show activities from 7.5 to 13.3 nmol/mg protein·h, while patient leukocytes have activities below 0.3 nmol/mg protein·h.

Pitfalls

Fibroblasts from patients with multiple sulfatase deficiency may show 6–15% of normal activity. Similarly, fibroblasts from patients with mucolipidoses II and III have about 15% of normal activity, while serum activity is approximately 20-fold increased.

Storage and pipetting of the concentrated lysosomal enzyme solution should be carried out separately to avoid contamination of microtiter plates and pipettes.

Heparan-N-sulfatase (E.C. 3.10.1.1)

Principle

See section 4.1.3.4, subheading "Principle."

Pre-analytical

- Specimen

See section 4.1.3.4, subheading "Specimen."

- Reagents and Chemicals

1. Piperazine-1,4-bis(2-ethanesulfonic acid) (PIPES) buffer: Dissolve 1.385 g PIPES (Sigma) and 0.235 g sodium acetate (Merck) in 20 ml demineralized water.
2. NaCl solution: Dissolve 8.5 g NaCl in 100 ml demineralized water.
3. Reaction buffer: Mix 20 ml PIPES buffer with 50 ml NaCl solution and add another 30 ml demineralized water in a 250-ml flask. The pH is adjusted to 6.5 with 0.1 M HCl. Fill to the 250-ml mark with demineralized water.
4. Substrate buffer: 9.10 mg 4-methylumbelliferyl-α-D-N-sulfoglucosamide (Moscerdam Substrates) is dissolved in 1 ml reaction buffer to yield a 20 mM solution.
5. Pefabloc solution: 0.45 mg Pefabloc SC (Roche, Mannheim, Germany) is dissolved in 1 ml reaction buffer. The solution must be prepared fresh.
6. Phosphate/citrate-buffer: 4.208 g citric acid (Merck) and 5.678 g disodiumhydrogenphosphate (Merck) are dissolved in 80 ml demineralized water; the pH is adjusted to 6.7 using 10 M NaOH. Adjust the volume to 100 ml with demineralized water.
7. α-Glucosidase-solution: dissolve 50 units of α-glucosidase from *Bacillus stearothermophilus* (Sigma) in 5 ml 0.2% bovine serum albumin (BSA) solution (20 mg BSA in 10 ml demineralized water). The solution is stable at –80°C for 1 year.
8. NaCl solution II (0.9% in demineralized water).
9. Stop solution/glycine-carbonate buffer (pH 9.6): dissolve 12.8 g ammonia-free glycine (ICN Biomedicals) and 18.0 g dry Na_2CO_3 (Merck) in 200 ml demineralized water. The solution can be stored at 4°C for up to 3 months.

Analytical

- Procedure

The assay is based on a method published by Karpova et al. [38]. Prepare a calibration curve and blanks according to section 4.1.3.4, subheading "Calibration." For each patient, 10- and 20-µl samples of leukocyte homogenate are transferred to individual wells on the microtiter plate. Subsequently, 10 µl of Pefabloc solution (a protease inhibitor) and 10 µl of substrate buffer are added. The volume is adjusted to 40 µl by adding NaCl solution II. The plate is briefly shaken, sealed with tape, and covered with aluminum wrapping. Incubation is carried out at 47°C for 21 h. The reaction is stopped with 6 µl of phosphate/citrate-buffer, and 10 µl of α-glucosidase-solution is added. After resealing, the plate is shaken for 1 min and incubated at 37°C for 24 h. During the second incubation, the enzyme cleaves the glucosamine moiety from

the 4-MU substrate. The enzymatic reaction is terminated by addition of 200 µl stop solution and the fluorescence is read with an excitation wavelength of 365 nm and an emission wavelength of 450 nm.

■ Calculation

See section 4.1.3.4, subheading "Calculation."

As heparan-N-sulfatase activity is fairly low in leukocytes, results should be expressed as nmol/h·mg protein.

Reference Values/Typical Pathological Values

Leukocytes from normal controls showed activities ranging from 0.6 to 3.0 nmol/mg protein·h, while patient leukocytes have activities between 0 and 0.14 nmol/mg protein·h.

Pitfalls

Storage and pipetting of α-glucosidase should be carried out separately from all other lysosomal enzymes to avoid contamination of microtiter plates and pipettes.

α-N-Acetylglucosaminidase (E.C. 3.2.1.50)

Principle

See section 4.1.3.4, subheading "Principle."

Pre-analytical

■ Specimen

See section 4.1.3.4, subheading "Specimen."

■ Reagents and Chemicals

1. Citrate-solution (2 M): 4.20 g citric acid (Merck) is dissolved in 10 ml demineralized water.
2. Citrate/phosphate-buffer: 1.78 g $Na_2HPO_4 \cdot 2H_2O$ (Merck) is dissolved in 50 ml demineralized water and the pH is adjusted to 5.0 with citrate solution. Subsequently, demineralized water is added until a total volume of 100 ml is obtained.
3. Substrate buffer: 3.79 mg 4-methylumbelliferyl-N-acetyl-α-D-glucosaminide (Moscerdam Substrates) is dissolved in 10 ml citrate/phosphate buffer. For faster dissolution, the mixture is sonicated (1 min). The substrate buffer is stored at –20°C and protected from light.
4. Stop solution/glycine-carbonate buffer (pH 9.6): dissolve 12.8 g ammonia-free glycine (ICN Biomedicals) and 18.0 g dry Na_2CO_3 (Merck) in 200 ml demineralized water. The solution can be stored at 4°C for up to 3 months.

Analytical

■ Procedure

Prepare a calibration curve and blanks according to section 4.1.3.4, subheading "Calibration". For each patient sample, 10 and 20 µl of leukocyte homogenate are transferred to individual wells on the microtiter plate. Then 50 µl of substrate buffer is added and the volume is adjusted to a total of 70 µl using citrate/phosphate buf-

fer. The mixture is incubated at 37°C for 4 h before 200 µl of stop solution is added. The fluorescence is read with an excitation wavelength of 365 nm and an emission wavelength of 450 nm.

■ Calculation

See section 4.1.3.4, subheading "Calculation". As α-N-acetylglucosaminidase activity is fairly low in leukocytes, results should be expressed as nmol/mg protein·h.

Reference Values/Typical Pathological Values

Leukocytes from normal controls showed activities ranging from 0.3 to 0.8 nmol/mg protein·h while the activity of a patient sample was 0.03 nmol/mg protein·h.

Acetyl CoA:α-Glucosaminide N-Acetyltransferase (E.C. 2.3.1.3)

Principle

See section 4.1.3.4, subheading "Principle."

Pre-analytical

■ Specimen

See section 4.1.3.4, subheading "Specimen."

■ Reagents and Chemicals

1. Triton X-100 solution: 0.25 ml Triton X-100 (Merck) is dissolved in 100 ml demineralized water.
2. Reaction buffer: 8.546 g citric acid (0.2 mol/l; Merck) and 5.678 g Na_2HPO_4 (0.2 mol/l; Merck) are initially dissolved in 150 ml Triton X-100 solution and the pH is adjusted to 5.5 using solid NaOH (Merck). When close to pH 5.3, a 1-M NaOH solution should be used for the final adjustment of the pH. Triton X-100 solution is added up to a total volume of 200 ml. The reaction buffer is stored at –20°C.
3. Substrate buffer: 1.01 mg 4-methylumbelliferyl-β-D-glucosaminide (Moscerdam Substrates) is dissolved in 1 ml reaction buffer to yield a 3-mM solution. The substrate buffer has to be stored at –20°C and protected from light.
4. AcetylCoA-solution: 5.0 mg acetylcoenzyme A (Sigma) is dissolved in 1.008 ml demineralized water to yield a 6-mM solution that should be prepared immediately before the assay is run.
5. NaCl solution (0.9%).
6. Stop solution/glycine-carbonate buffer (pH 9.6): dissolve 12.8 g ammonia-free glycine (ICN Biomedicals) and 18.0 g dry Na_2CO_3 (Merck) in 200 ml demineralized water. The solution can be stored at 4°C for up to 3 months.

Analytical

■ Procedure

The assay is based on a method described by Voznyi et al. [66]. Prepare a calibration curve and blanks according to section 4.1.3.4, subheading "Calibration". For each patient sample, 5 and 10 µl of leukocyte homogenate are transferred to individual wells on the microtiter plate. Then 10 µl of acetyl CoA solution and 10 µl of the substrate

buffer are added and the volume is adjusted to a total of 30 µl using the NaCl solution. The microtiter plate is sealed, protected from light by an aluminum cover, and shaken on a plate shaker (1 min). The mixture is incubated at 37°C for 21 h before 200 µl stop solution is added (use less for the standard curve when the total volume of 230 µl would be exceeded). The hexosaminidase activity present in the samples is sufficient to liberate the 4-MU moiety from the substrate after its initial acetylation. The fluorescence is read with an excitation wavelength of 365 nm and an emission wavelength of 450 nm.

■ Calculation

See section 4.1.3.4, subheading "Calculation." As acetyl CoA:*α*-glucosaminide N-acetyltransferase activity is fairly low in leukocytes, results should be expressed as nmol/mg protein·h.

Reference Values/Typical Pathological Values

Leukocytes from normal controls showed activities ranging from 0.2 to 0.65 nmol/mg protein·h, while patients with MPS IIIC display almost no detectable activity.

Pitfalls

In cases of missing *β*-hexosaminidase activity (Sandhoff disease), the detected acetyl CoA:*α*-glucosaminide N-acetyltransferase activity will be low because liberation of the fluorophore is the rate-limiting step. Therefore, low measured activity of acetyltransferase with normal *β*-galactosidase activity should always trigger an assessment of the *β*-hexosaminidase activity from the same material. In contrast, missing *β*-hexosamindase A activity (Tay-Sachs disease) does not impede the assay.

N-Acetylglucosamine-6-Sulfatase (E.C. 3.1.6.14)

Principle

See section 4.1.3.4, subheading "Principle."

Pre-analytical

■ Specimen

See section 4.1.3.4, subheading "Specimen."

■ Reagents and Chemicals

1. Reaction buffer: 1.15 ml acetic acid (99.7%; Sigma) and 758.68 mg $PbAc_2 \cdot 3H_2O$ (Aldrich) are dissolved in 60 ml demineralized water and 250 µl Triton X-100 (Merck) is added. The pH is adjusted to pH 5.6 using a 10 M NaOH solution. Demineralized water is added up to a total volume of 100 ml. The reaction buffer is stored at –20°C.
2. Substrate buffer: 4.81 mg of the sodium salt of 4-methylumbelliferyl-*α*-N-acetylglucosaminide-6-sulfate (Moscerdam Substrates) is dissolved in 1 ml of reaction buffer. The substrate buffer is stored at –80°C and protected from light.
3. Lysosomal enzyme solution: One vial of lyophilized lysosomal enzymes purified from bovine testis (Moscerdam Substrates) is reconstituted with 1 ml of demineralized water. Aliquots can be stored at –80°C. The enzyme solution can be frozen and thawed several times.

4. Phosphate-solution: 7.12 g $Na_2HPO_4 \cdot 2\ H_2O$ is dissolved in 100 ml demineralized water.
5. Citric acid solution: 4.203 g citric acid is dissolved in 100 ml demineralized water.
6. Phosphate/citrate-buffer: 50 ml citric acid solution is put into a 100 ml flask and the pH is adjusted to 4.7 with phosphate solution. The flask is filled up to the 100-ml mark with demineralized water. Store at –20°C.
7. Stop solution/glycine-carbonate buffer (pH 9.6): dissolve 12.8 g ammonia-free glycine (ICN Biomedicals) and 18.0 g dry Na_2CO_3 (Merck) in 200 ml demineralized water. The solution can be stored at 4°C for up to 3 months.

Analytical

Procedure

The assay is carried out according to the method published by He et al. [29]. Prepare a calibration curve and blanks according to section 4.1.3.4, subheading "Calibration." For each patient sample, 10 and 20 µl of leukocyte homogenate are transferred to individual wells on the microtiter plate. Then 10 µl of substrate buffer is added. The total volume is adjusted to 50 µl using the reaction buffer and the plate is sealed with tape and covered in aluminum wrapping. Lead acetate present in the substrate buffer has been found to reduce inhibition by phosphates and sulfates present in the solution, while having no adverse effect on the enzyme activity. The plate is incubated at 37°C for 21 h. Afterwards, 40 µl of phosphate/citrate buffer and 20 µl of the lysosomal enzyme solution are added. The plate is briefly shaken, resealed and incubated at 37°C for 6 h. This second incubation step is necessary to liberate 4-MU from the substrate. The reaction is stopped with 200 µl stop solution (use less for the standard curve when the total volume of 310 µl would be exceeded). The plate is shaken briefly and read with an excitation wavelength of 365 nm and an emission wavelength of 450 nm.

Calculation

See section 4.1.3.4, subheading "Calculation." As N-acetylglucosamine-6-sulfatase activity is fairly low in leukocytes, results should be expressed as nmol/ mg protein·h.

Reference Values/Typical Pathological Values

Leukocytes from normal controls showed activities ranging from 0.05 to 0.22 nmol/ mg protein·h, while patients with MPS IIID should display almost no detectable activity.

Pitfalls

Patients with multiple sulfatase deficiency also show low N-acetylglucosamine-6-sulfatase activity. Therefore, arylsulfatase A or another sulfatase should also be determined in case of low results for a single sulfatase, especially when β-galactosidase activity is in the normal range for that sample.

N-Acetylgalactosamine-6-Sulfatase (E.C. 3.1.6.4)

Principle

See section 4.1.3.4, subheading "Principle."

Pre-analytical

■ Specimen

See section 4.1.3.4, subheading "Specimen."

■ Reagents and Chemicals

1. Dialysis buffer: 0.8203 g $NaCH_3COO$ (10 mM, Aldrich) and 5.844 g NaCl (100 mM, Aldrich) are dissolved in 1000 ml demineralized water. The pH is adjusted to 6.0.
2. Reaction buffer: 5.844 g NaCl (100 mM, Aldrich) and 8.203 g NaCHCOO (100 mM, Aldrich) are dissolved in 1000 ml demineralized water. The pH is adjusted to 4.3. The reaction buffer is stored at –20°C.
3. Substrate buffer: 4-methylumbelliferyl-β-D-6-sulfo-N-acetylglucosaminide (Moscerdam Substrates) is dissolved in reaction buffer to yield a 1-mM solution. The substrate buffer is stored at –80°C and protected from light.
4. Phosphate buffer: 16.394 g Na_3PO_4 (100 mM, Aldrich) is dissolved in 1000 ml demineralized water. The buffer is stored at –20°C.
5. Stop solution/glycine-carbonate buffer (pH 9.6): dissolve 12.8 g ammonia-free glycine (ICN Biomedicals) and 18.0 g dry Na_2CO_3 (Merck) in 200 ml demineralized water. The solution can be stored at 4°C for up to 3 months.

Analytical

■ Procedure

The assay is carried out according to the method published by van Diggelen et al. [65]. Patient samples have to be dialyzed before the assay can be run. For that purpose, leukocyte homogenates (0.5–1 mg protein) are sonicated in 100 µl demineralized water. The tubes are centrifuged at 10,000 × *g* for 10 min (4°C) and the supernatant is dialyzed against the dialysis buffer for 17 h at 4°C.

Prepare a calibration curve according to section 4.1.3.4, subheading "Calibration." For each patient sample, 5 and 10 µl of dialyzed supernatant are transferred to individual wells on the microtiter plate. Then 20 µl of substrate buffer is added. The total volume is adjusted to 30 µl using the reaction buffer. Blanks are prepared by substitution of the sample with 10 µl phosphate buffer. The excess of phosphate will inhibit lysosomal sulfatases, while other unspecific phosphate-insensitive sulfatases are not impeded. The plate is sealed with tape, covered in aluminum wrapping and incubated at 37°C for 17 h. During this incubation, β-galactosidase liberates 4-MU from the substrate after the initial cleavage of the sulfate moiety. Usually, β-galactosidase activity present in the sample is sufficient for that purpose. The reaction is stopped with 200 µl stop solution (use less for the standard curve when the total volume of 230 µl would be exceeded). The plate is shaken briefly and read with an excitation wavelength of 365 nm and an emission wavelength of 450 nm.

■ Calculation

See section 4.1.3.4, subheading "Calculation." As N-acetylgalactosamine-6-sulfatase activity is fairly low in leukocytes, results should be expressed as nmol/mg protein·17 h.

Reference Values/Typical Pathological Values

Leukocytes from normal controls showed activities ranging from 18.6 to 61.8 nmol/mg protein·17 h, while activities from patients with MPS IVA were below 2.5 nmol/mg protein·17 h.

Pitfalls

For cells with β-galactosidase deficiency (GM1 gangliosidosis or Morquio type B as well as I-cell disease), the measured enzyme activity will be significantly lower than the true enzyme activity. In addition, cases of multiple sulfatase deficiency will also show low N-acetylgalactosamine-6-sulfatase activity. Therefore, arylsulfatase A or another sulfatase, as well as β-galactosidase activities should also be determined in case of suspicious results. To exclude poor sample quality, the determination of α-mannosidase is recommended.

β-D-Galactosidase (E.C. 3.2.1.23)

Principle

See section 4.1.3.4, subheading "Principle."

Pre-analytical

- Specimen

See section 4.1.3.4, subheading "Specimen."

- Reagents and Chemicals

1. Citrate buffer (0.1 M): 21.0 g citric acid (Merck) is dissolved in 1000 ml demineralized water. The pH is adjusted to 4.4 with NaOH. The citrate buffer is stored at –20°C.
2. Substrate buffer: 3.4 mg 4-methylumbelliferyl-β-D-galactoside (Sigma) is dissolved in 5.0 ml citrate buffer to yield a 2-mM solution. The substrate buffer is stored at –20°C and protected from light.
3. Stop solution/glycine-carbonate buffer (pH 9.6): dissolve 12.8 g ammonia-free glycine (ICN Biomedicals) and 18.0 g dry Na_2CO_3 (Merck) in 200 ml demineralized water. The solution can be stored at 4°C for up to 3 months.

Analytical

- Procedure

Prepare a calibration curve and blanks according to section 4.1.3.4, subheading "Calibration".

Leukocytes

For each patient sample, 10 and 20 µl of leukocyte homogenate are transferred to individual wells on the microtiter plate. Subsequently, 100 µl substrate buffer are added and the volume is adjusted to a total of 200 µl by adding demineralized water. The plate is briefly shaken, sealed with tape and covered with aluminum wrapping. Incubation is carried out at 37°C for 45 min. The reaction is stopped with 200 µl stop solution and the fluorescence is read with an excitation wavelength of 365 nm and an emission wavelength of 450 nm.

Dried Blood Spots

Dried blood spots (3 mm) are punched from filter paper cards (Whatman 903 paper, Whatman) and distributed in a microtiter plate. Each patient sample is run in duplicates. Subsequently, 100 µl of substrate buffer and 100 µl of citrate buffer are added to each specimen. The plate is shaken for 45 min, sealed with tape, covered with aluminum wrapping and incubated at 37°C for 21 h. The reaction is terminated by the addition of 200 µl stop solution and the fluorescence is read with an excitation wavelength of 365 nm and an emission wavelength of 450 nm.

■ Calculation

See section 4.1.3.4, subheading "Calculation."

Reference Values/Typical Pathological Values

Leukocytes from normal controls showed activities ranging from 0.1 to 1.38 nmol/mg protein·min. Dried blood spots from healthy subjects displayed activities between 0.3 and 2.6 nmol/spot·21 h. Patient samples are expected to exhibit barely detectable activities.

Pitfalls

In most cases, missing β-galactosidase activity will be associated with GM1-gangliosidosis. The differential diagnosis between GM1-gangliosidosis and Morquio type B disease must be based on the clinical evaluation of the patient because the enzymatic activity alone will not be helpful.

To exclude I-cell disease in cases of low β-galactosidase activity, this enzyme should also be assessed in serum. Furthermore, to evaluate the quality of the material it is recommended to determine the activity of α-mannosidase.

N-Acetyl-Galactosamine-4-Sulfatase (Arylsulfatase B; E.C. 3.1.6.1)

Principle

See section 4.1.3.4, subheading "Principle."

Pre-analytical

■ Specimen

See section 4.1.3.4, subheading "Specimen."

■ Reagents and Chemicals

1. Nitrocatechol solution (1.0 mM): 77.55 mg 4-nitrocatechol (Sigma) is dissolved in 500 ml glycine-carbonate buffer (0.25 M).
2. Sodium acetate buffer (0.5 M): 20.5 g sodium acetate (Aldrich) and 1.277 g barium acetate (0.01 M; Aldrich) are dissolved in 500 ml demineralized water. The pH is adjusted to 6.0 with NaOH. The acetate buffer is stored at –20°C.
3. Substrate buffer: 155.7 mg 4-nitrocatechol sulfate dipotassium salt (50 mM, Sigma) is dissolved in 10 ml sodium acetate buffer. The substrate buffer is stored at –20°C and protected from light.
4. Stop solution: 1 M NaOH.

Analytical

Procedure

The assay is carried out according to Baum et al. [1]. Each plate contains a calibration curve using the nitrocatechol solution at absolute concentrations of 5 nmol (5 µl), 10 nmol (10 µl), 20 nmol (20 µl), 50 nmol (50 µl), and 100 nmol (100 µl). All standards are run in duplicate and the volume for each well is adjusted to 150 µl with demineralized water. A substrate blank that does not contain leukocyte homogenate is included for both incubation times. In addition, a patient blank (no substrate buffer) and one plate blank (sodium acetate buffer only) is included in the assay.

For each patient sample, 10 and 20 µl of leukocyte homogenate are transferred to individual wells on the microtiter plate. As two different incubation times are necessary, the same volumes of all samples are also pipetted into the lower part of the plate. Subsequently, 100 µl of substrate buffer is added to each well and the volume is adjusted to a total of 150 µl by adding sodium acetate buffer containing barium acetate. Arylsulfatase A will be inhibited in the presence of barium ions. The plate is briefly shaken, sealed with tape, and covered with aluminum wrapping. Incubation is carried out at 37°C for 30 min (upper half including the standard curve) and 90 min (lower half). The reaction is stopped with 200 µl stop solution and the absorbance is read at 490 nm.

Calculation

The individual activity is calculated as follows:

$$\begin{aligned}\text{absorption (30 min)} = {} & \text{absorption (patient sample, 30 min)} \\ & - \{[\text{absorption (substrate blank)} \\ & + \text{absorption (patient blank)}] - \text{absorption (plate blank)}\}\end{aligned}$$

$$\begin{aligned}\text{absorption (90 min)} = {} & \text{absorption (patient sample, 90 min)} \\ & - \{[\text{absorption (substrate blank)} \\ & + \text{absorption (patient blank)}] - \text{absorption (plate blank)}\}\end{aligned}$$

$$\text{absorption (patient)} = \text{absorption (90 min)} - \text{absorption (30min)}$$

The activity is calculated using the standard curve and the result for the absorption (patient) because during the first 30 min of incubation some of the activity may be derived from arylsulfatase A instead of arylsulfatase B. Results are expressed in nmol/ mg protein·h.

Reference Values/Typical Pathological Values

Not available.

β-D-Glucuronidase (E.C. 3.2.1.31)

Principle

See section 4.1.3.4, subheading “Principle.”

Pre-analytical

■ Specimen

See section 4.1.3.4, subheading "Specimen."

■ Reagents and Chemicals

1. Acetate buffer (0.1 M):1.144 ml acetic acid (Sigma) is added to 150 ml demineralized water and the pH is adjusted to 4.05 with NaOH (1 M). Demineralized water is added up to a total volume of 200 ml. The acetate buffer is stored at –20°C.
2. Substrate buffer: 1.9 mg 4-methylumbelliferyl-*β*-D-glucuronide (Sigma) is dissolved in 5.0 ml acetate buffer. The substrate buffer is stored at –20°C and protected from light.
3. Stop solution/glycine-carbonate buffer (pH 9.6) : dissolve 12.8 g ammonia-free glycine (ICN Biomedicals) and 18.0 g dry Na_2CO_3 (Merck) in 200 ml demineralized water. The solution can be stored at 4°C for up to 3 months.

Analytical

■ Procedure

The method is based on that described by Glaser and Sly [24]. Prepare a calibration curve and blanks according to section 4.1.3.4, subheading "Procedure."

Leukocytes

For each patient sample, 5 and 10 µl of leukocyte homogenate are transferred to individual wells on the microtiter plate. Subsequently, 100 µl substrate buffer is added and the volume is adjusted to a total of 200 µl by adding demineralized water. The plate is briefly shaken, sealed with tape, and covered with aluminum wrapping. Incubation is carried out at 37°C for 45 min. The reaction is stopped with 200 µl stop solution and the fluorescence is read with an excitation wavelength of 365 nm and an emission wavelength of 450 nm.

Dried Blood Spots

Dried blood spots (3 mm) are punched from filter paper cards (Whatman 903 paper, Whatman) and distributed into microtiter plates. Each patient sample is run in duplicate. Subsequently, 100 µl of substrate buffer and 100 µl of acetate buffer are added to each specimen. The plate is shaken for 45 min, sealed with tape, covered with aluminum wrapping, and incubated at 37°C for 21 h. The reaction is terminated by the addition of 200 µl stop solution and the fluorescence is read with an excitation wavelength of 365 nm and an emission wavelength of 450 nm.

■ Calculation

See section 4.1.3.4, subheading "Calculation."

Reference Values/Typical Pathological Values

Leukocytes from normal controls show activities ranging from 0.45 to 3.0 nmol/mg protein·min. Dried blood spots from healthy subjects displayed activities between 0.9 and 1.8 nmol/spot·21 h. Patient samples are expected to exhibit barely detectable activities.

Pitfalls

In cases of low β-glucuronidase activity, the activity of this enzyme in serum should also be assessed to avoid missing I-cell disease.

4.1.4 Alternative Methods

There are some alternative methods for the quantitation of GAGs and the determination of enzymatic activities in patient samples. High-performance liquid chromatography was successfully employed, particularly for serum or plasma specimens. The sequential application of chondroitinases AC and ABC yielded disaccharides that were separated by isocratic HPLC. The method showed a linear range of 7–7000 μM and a low CV. Nevertheless, due to several incubation and separation steps it is rather time-consuming and labor-intensive [23]. Another research group described the analysis of fluoro-labeled GAGs on a hydroxyapatite column [50]. In addition, gel-permeation chromatography was employed for the separation of GAGs as copper (II) complexes. This method was also successfully applied to chemically derivatized GAGs that cannot be depolymerized by enzymes [62]. Similarly, capillary electrophoresis (CE) can be used for digested GAGs that are then detected by ultraviolet spectroscopy or mass spectrometry. Complexation of GAGs using copper (II) ions improved the sensitivity. However, complete separation of intact GAGs was not feasible by CE and most methods still rely on enzymatic or chemical depolymerization prior to analysis [46].

Alternatively, urinary GAGs were isolated by anion-exchange chromatography and subsequently analyzed by two-dimensional nuclear magnetic resonance. Typical patterns for the different MPS types were recognized and it was suggested that this method could be used for disease monitoring and elucidation of pathogenesis [31].

Recently, microchip electrophoresis was applied to GAG analysis using ethidium bromide as a fluorescent dye. In particular, separation times were reduced to 150 s, while sensitivity remained comparable to that of conventional electrophoretic methods that rely on cellulose acetate membranes [47].

For the measurement of α-iduronidase activity, a novel substrate was developed that was detected by mass spectrometry. It was possible to combine this method with similar assays for Niemann-Pick type A/B, Krabbe, Gaucher, Pompe, and Fabry disease. However, separate incubation is necessary, and some additional work-up procedures are usually required to purify the sample before mass spectrophotometric analysis [68].

References

1. Baum H, Dodgson KS, Spencer B (1959) The assay of arylsulphatase A and B in human urine. Clin Chim Acta 4:453–455
2. Berman ER, Vered J, Bach G (1971) A reliable spot test for mucopolysaccharidoses. Clin Chem 17:886–890
3. Berry HK, Berry MA, Spinanger J (1960) A paper spot test useful in study of Hurler's syndrome. J Lab Clin Med 55:136–138
4. Berry HK (1987) Screening for mucopolysaccharide disorders with the Berry spot test. Clin Biochem 20:365–371

5. Bitter T, Muir HM (1962) A modified uronic acid carbazole reaction. Anal Biochem 4:330–334
6. Brante G (1952) Gargoylism: a mucopolysaccharidosis. Scand J Clin Lab Invest 4:43–46
7. Brimble A, Pennock C, Stone J (1990) Results of a quality assurance exercise for urinary glycosaminoglycan excretion. Ann Clin Biochem 27:133–138
8. Byers S, Rozaklis T, Brumfield LK, Ranieri E, Hopwood JJ (1998) Glycosaminoglycan accumulation and excretion in the mucopolysaccharidoses: characterization and basis of a diagnostic test for MPS. Mol Genet Metab 65:282–290
9. Cappelletti R, del Rosso M, Chiarugi VP (1979) A New electrophoretic method for the complete separation of all known animal glycosaminoglycans in a monodimensional run. Anal Biochem 99:311–315
10. Carson NAJ, Neill DW (1962) Metabolic abnormalities detected in a survey of mentally backward individuals in Northern Ireland. Arch Dis Child 37:505–513
11. Chamoles NA, Blanco MB, Gaggioli D, Casentini C (2001) Hurler-like Phenotype: enzymatic diagnosis in dried blood spots on filter paper. Clin Chem 47:2098–2102
12. Chamoles NA, Blanco M, Gaggioli D (2001) Diagnosis of α-L-iduronidase deficiency in dried blood spots on filter paper: the possibility of newborn diagnosis. Clin Chem 47:780–781
13. Chih-Kuang C, Shuan-Pei L, Shyue-Jye L, Tuen-Jen W (2002) MPS screening methods, the Berry Spot and acid turbidity tests, cause a high incidence of false-negative results in Sanfilippo and Morquio syndromes. J Clin Lab Anal 16:253–258
14. De Jong JGN, Wevers RA, Laarakkers C, Poorthuis BJHM (1989) Dimethylene blue-based spectrophotometry of glycosaminoglycans in untreated urine: a rapid screening procedure for mucopolysaccharidoses. Clin Chem 35:1472–1477
15. De Jong JGN, Hasselman JJF, Landeghem AAJ, Vader HL, Wevers RA (1991) The spot test is not a reliable screening procedure for mucopolysaccharidoses. Clin Chem 37:572–575
16. De Jong JGN, Wevers RA, Liebrand-van Sambeek R (1992) Measuring urinary glycosaminoglycans in the presence of protein: an improved screening procedure for mucopolysaccharidoses based on dimethylene blue. Clin Chem 38:803–807
17. De Jong JGN, Heijs WM, Wevers RA (1994) Mucopolysaccharidoses screening: dimethylene blue versus Alcian blue. Ann Clin Biochem 31:267–271
18. Dembure PP, Drumheller JE, Barr SM, Elsas LJ (1990) Selective urinary screening for mucopolysaccharidoses. Clin Biochem 23:91–96
19. Dembure PP, Roesel RA (1991) Screening for mucopolysaccharidoses by analysis of urinary glycosaminoglycans. In: Hommes FA (ed) Techniques in Diagnostic Human Biochemical Genetics. Wiley-Liss, New York, pp 77–86
20. Di Ferrante NM (1967) The measurement of urinary mucopolysaccharides. Anal Biochem 21:98–106
21. Dorfman A, Lorincz AE (1957) Occurrence of urinary acid mucopolysaccharides in the Hurler syndrome. 43:443–446
22. Frantatoni JC, Hall CW, Neufeld EF (1968) The defect in Hurler's and Hunter's syndromes: faulty degradation of mucopolysaccharides. Proc Natl Acad Sci U S A 60:699–706
23. Gässler N, Reißner C, Janzen N, Kähnert H, Kleesiek K (1993) A high-performance liquid chromatography method for the determination of glycosaminoglycans in human blood. Eur J Clin Chem Clin Biochem 31:503–511
24. Glaser JH, Sly WS (1973) β-Glucuronidase deficiency mucopolysaccharidosis: methods for enzymatic diagnosis. J Lab Clin Med 82:969–977
25. Gold EW (1979) A simple spectrophotometric method for estimating glycosaminoglycan concentrations. Anal Biochem 99:183–188
26. Gold EW (1981) The quantitative spectrophotometric estimation of total sulfated glycosaminoglycan levels. Biochim Biophys Acta 673:40–415
27. Hall CW, Liebaers I, Di Natale P, Neufeld EF (1978) Enzymic diagnosis of the genetic mucopolysaccharide storage disorders. Methods Enzymol 50:439–456
28. Hata R, Nagai Y (1972) A rapid and micro method for separation of acidic glycosaminoglycans by two-dimensional electrophoresis. Anal Biochem 45:462–468

29. He W, Voznyi YV, Boer AM, Kleijer WJ, van Diggelen OP (1993) A fluorimetric enzyme assay for the diagnosis of Sanfilippo disease type D (MPS IIID). J Inherit Metab Dis 16:935–941
30. Hein LK, Meikle PJ, Dean CJ, Bockmann MR, Auclair D, Hopwood JJ, Brooks DA (2005) Development of an assay for the detection of mucopolysaccharidosis type VI patients using dried blood spots. Clin Chim Acta 353:67–74
31. Hochuli M, Wüthrich K, Steinmann B (2003) Two-dimensional NMR spectroscopy of urinary glycosaminoglycans from patients with different mucopolysaccharidoses. NMR Biomed 16:224–236
32. Hopwood JJ, Harrison JR (1982) High-resolution electrophoresis of urinary glycosaminoglycans: an improved screening test for the mucopolysaccharidoses. Anal Biochem 119:120–127
33. Hsu D, Hoffman P, Mashburn TA (1972) Micro colorimetric method of dye staining and its application to cellulose polyacetate strip electrophoresis for the determination of acid glycosaminoglycans. Anal Biochem 46:156–163
34. Huang K, Sukegawa K, Orii T (1985) Screening test for urinary glycosaminoglycans and differentiation of various mucopolysaccharidoses. Clin Chim Acta 151:147–156
35. Humbel R, Chamoles NA (1972) Sequential thin layer chromatography of urinary acid glycosaminoglycans. Clin Chim Acta 40:290–293
36. Iwata S, Sukegawa K, Sasaki T, Kokuryu M, Yamasita S, Noma A, Iwasa S, Kondo N, Orii T (1997) Mass screening test for mucopolysaccharidoses using the 1,9-dimethylene blue method: positive interference from paper diapers. Clin Chim Acta 264:245–250
37. Kaplan D (1969) Classification of the mucopolysaccharidoses based on the pattern of mucopolysaccharidiuria. Am J Med 47:721–729
38. Karpova EA, Voznyi YV, Keulemans JLM, Hoogeveen AT, Winchester B, Tsvetkova IV, van Diggelen OP (1996) A fluorimetric enzyme assay for the diagnosis of Sanfilippo disease type A (MPS IIIA). J Inherit Metab Dis 19:278–285
39. Kodama C (1988) Methods for analysis of urinary glycosaminoglycans. J Chromatogr 429:293–313
40. Kresse H, Cantz M, von Figura K, Glössl J, Paschke E (1981) The mucopolysaccharidoses: biochemistry and clinical symptoms. Klin Wochenschr 59:867–876
41. Kresse H, von Figura K, Klein U, Glössl J, Paschke E, Pohlmann R (1982) Enzymic diagnosis of genetic mucopolysaccharide storage disorders. Methods Enzymol 83:559–572
42. Lippiello L, Mankin HJ (1971) Thin-layer chromatographic separation of the isomeric chondroitin sulfates, dermatan sulfate and keratan sulfate. Anal Biochem 39:54–58
43. Lowry OH, Roseborough NJ, Farr AL, Randall RJ (1951) Protein measurements with Folin phenol reagent. J Biol Chem 193:265–275
44. Lukacs Z, Santavuori P, Keil A, Steinfeld R, Kohlschütter A (2003) Rapid and simple assay for the determination of tripeptidyl peptidase and palmitoyl protein thioesterase activities in dried blood spots. Clin Chem 49:509–511
45. Mabe P, Valiente A, Soto V, Cornejo V, Raimann E (2004) Evaluation of reliability for urine mucopolysaccharidosis screening by dimethylene blue and Berry spot tests. Clin Chim Acta 345:135–140
46. Mao W, Thanawiroon C, Linhardt RJ (2002) Capillary electrophoresis for the analysis of glycosaminoglycans and glycosaminoglycan-derived oligosaccharides. Biomed Chromatogr 16:77–94
47. Matsuno Y, Kinoshita M, Kakehi K (2005) Fast analysis of glycosaminoglycans by microchip electrophoresis with in situ fluorescent detection using ethidium bromide. J Pharm Biomed Anal 37:429–436
48. McKusick VA (1969) The nosology of the mucopolysaccharidoses. Am J Med 47:730–747
49. Miura RO, Yamagata S, Miura Y, Harada T, Yamagata T (1995) Analysis of glycosaminoglycan-degrading enzymes by substrate gel electrophoresis (zymography) Anal Biochem 225:333–340
50. Narita H, Takeda Y, Takagaki K, Nakamura T, Harata S, Endo M (1995) Identification of glycosaminoglycans using high-performance liquid chromatography on a hydroxyapatite column. Anal Biochem 232:133–136

51. Neufeld EF, Muenzer J (2001) The mucopolysaccharidoses. In: Scriver CR, Sly WS, Childs B, Beaudet AL, Valle D, Kinzler KW, Vogelstein B (eds) The Metabolic and Molecular Basis of Inherited Disease, 8th edn. McGraw-Hill, New York, pp 3421–3452
52. Northover H, Cowie RA, Wraith JE (1996) Mucopolysaccharidosis type IVA (Morquio syndrome): a clinical review. J Inherit Metab Dis 19:357–365
53. Panin G, Naia S, DallÂ´Amico R, Chiandetti L, Zachello F, Catassi C, Felici, L, Coppa GV (1986) Simple spectrophotometric quantification of urinary, excretion of glycosaminoglycan sulfates. Clin Chem 32:2073–2076
54. Pennock CA (1976) A review and selection of simple laboratory methods used for the study of glycosaminoglycan excretion and the diagnosis of the mucopolysaccharidoses. J Clin Pathol 29:111–123
55. Piraud M, Maire I, Mathieu M (1993) Pitfalls of screening for mucopolysaccharidoses by the dimethylene blue test. Clin Chem 39:163–164
56. Piraud M, Boyer M, Mathieu M, Maire I (1993) Diagnosis of mucopolysaccharidoses in a clinically selected population by urinary glycosaminoglycan analysis: a study of 2000 urine samples. Clin Chim Acta 221:171–181
57. Proudfoot AEI, Handel TM, Johnson Z, Lau EK, LiWang P, Clark-Lewis I, Borlat F, Wells TNC, Kosco-Villbois MH (2003) Glycosaminoglycan binding and oligomerization are essential for the in vivo activity of certain chemokines. Proc Natl Acad Sci U S A 100:1885–1890
58. Sewell AC (1988) Urinary screening for disorders of heteroglycan metabolism. Klin Wochenschr 66:48–53
59. Stirling JL, Robinson D, Fensom AH, Benson PF, Baker JE (1978) Fluorimetric assay for prenatal detection of Hurler and Scheie homozygotes or heterozygotes. Lancet 1:147
60. Stirling JL, Robinson D, Fensom AH, Benson PF, Baker JE, Button LR (1979) Prenatal diagnosis of two Hurler fetuses using an improved assay for methylumbelliferyl-α-L-iduronidase. Lancet 2:37
61. Stone JE, Akhtar N, Botchway S, Pennock CA (1994) Interaction of 1,9 dimethylene blue with glycosaminoglycans. Ann Clin Biochem 31:147–152
62. Toida T, Shima M, Azumaya S, Maruyama T, Toyoda H, Imanari T, Linhardt RJ (1997) Detection of glycosaminoglycans as copper (II) complex in high-performance liquid chromatography. J Chromatogr A 787:266–270
63. Tuschl K, Gal A, Paschke E, Kircher S, Bodamer O (2004) Mucopolysaccharidosis type ii in females: case report and review of literature. Pediatr Neurol 32:270–272
64. Van den Lest CHA, Versteeg EMM, Veerkamp JH, van Kuppevelt TH (1994) Quantification and characterization of glycosaminoglycans at nanogram level by a combined azure A-silver staining in agarose gels. Anal Biochem 221:356–361
65. Van Diggelen OP, Zhao H, Kleijer WJ, Janse HC, Poorthuis BJHM, van Pelt J, Kamerling JP, Galjaard H (1990) A fluorimetric enzyme assay for the diagnosis of Morquio disease type A (MPS IV A) Clin Chim Acta 187:131–140
66. Voznyi YV, Karpova EA, Dudukina TV, Tsvetkova IV, Boer AM, Janse HC, van Diggelen OP (1993) A fluorimetric enzyme assay for the diagnosis of Sanfilippo disease C (MPS III C) J Inherit Metab Dis 16:465–472
67. Voznyi YV, Keulemans JLM, van Diggelen OP (2001) A fluorimetric assay for the diagnosis of MPS II (Hunter's disease). J Inherit Metab Dis 24:675–680
68. Wang D, Eadala B, Sadilek M, Chamoles NA, Turecek F, Scott R, Gelb MH (2005) Tandem mass spectrometric analysis of dried blood spots for screening of mucopolysaccharidoses I in newborns. Clin Chem 51:898–900
69. Wessler E (1968) Analytical and preparative separation of acidic glycosaminoglycans by electrophoresis in barium acetate. Anal Biochem 26:439–444
70. Whitley CB, Ridnour MD, Draper KA, Dutton CM, Neglia JP (1989) Diagnostic test for mucopolysaccharidosis. I. Direct method for quantifying excessive urinary glycosaminoglycan excretion. Clin Chem 35:374–379
71. Wraith JE (1995) The mucopolysaccharidoses: a clinical review and guide to management. Arch Dis Child 72:263–267

4.2 Oligosaccharides

Adrian C. Sewell

4.2.1 Introduction

Oligosaccharides are low-molecular-weight carbohydrate chains composed of at least three monosaccharide subunits. When covalently bound to a protein backbone, they are termed glycoconjugates or glycoproteins. Glycoproteins are widely distributed macromolecules with a wide variety of functions. Glycoproteins are found in serum and urine, in almost all secretions, in intracellular and plasma membranes, on the surface of many lysosomal enzymes, in the extracellular space of connective tissue and in the blood group substances of erythrocyte membranes [3, 12]. Due to their diversity, the proteins are as different and complex as carbohydrate-free proteins in general [16], and the carbohydrate portion ranges from 1 to 80% of the total weight of the molecule [32]. The most commonly occurring monosaccharides are sialic acid (N-acetylneuraminic acid), L-fucose, D-galactose, D-mannose, D-glucose, N-acetyl-D-glucosamine and N-acetyl-D-galactosamine. Other sugars such as arabinose and xylose are rarely present.

Mammalian tissues contain two major groups of glycoproteins with distinct structural differences and separate synthetic pathways [3]. In the sugar nucleotide pathway, oligosaccharides are synthesised by the transfer of sugar moieties from sugar nucleotides to the growing oligosaccharide chain. They are then linked to the protein by the O-glycosidic linkage of N-acetylgalactosamine to threonine or serine. Such glycoproteins include blood group substances and mucins.

The second biosynthetic pathway, the dolichol pathway, involves lipid-linked intermediates [3]. The entire oligosaccharide chain is linked via the N-glycosidic linkage to asparagine. The oligosaccharide side chain then undergoes a series of trimming or elongation steps to form the "high mannose" or "complex" forms of glycoproteins [17].

4.2.1.1 Glycoprotein Degradation

The degradation of glycoproteins is predominantly lysosomal. Lysosomes contain an arsenal of enzymes required for the complete degradation of glycoproteins, including proteases for the protein core and glycosidases for the carbohydrate chains. The sugars are removed in an ordered fashion beginning at the non-reducing ends and, to a lesser extent, cleavage at the reducing end of the asparagine-linked oligosaccharides [1]. The commonly occurring glycosidases are α-neuraminidase (sialidase), α-L-fu-

cosidase, β-D-galactosidase, α-D-mannosidase, β-D-mannosidase, β-D-glucosidase, α-N-acetylhexosaminidase and β-N-acetylhexosaminidase. A partial degradation of the protein core by a variety of proteolytic enzymes appears to occur as the first step of glycoprotein degradation. The process leads to the formation of glycopeptides, which are attacked by N-aspartyl-β-glucosaminidase. This enzyme cleaves the aspartylglucosamine linkage between the polypeptide and the carbohydrate moiety of glycopeptides, liberating aspartic acid, ammonia and the oligosaccharide [31].

4.2.1.2 Normal Oligosaccharidiuria

Small amounts of 20–30 carbohydrates and several oligosaccharides are present in normal human urine [23], including a glucotetrasaccharide derived from glycogen [19] and a series of tri- to pentasacccharides, the presence of which depends upon the ABO blood group, secretor status and diet [20]. Increased oligosaccharidiuria is seen in the urine of pregnant women [18], breast-milk-fed neonates or preterm infants fed with milk fortified with glucose polymers [25].

4.2.1.3 Pathological Oligosaccharidiuria

In the late 1960s, patients with phenotypes resembling the genetic mucopolysaccharidoses but without mucopolysaccharidiuria were described. It quickly became apparent that these individuals belonged to a new group of disorders resulting from inherited defects in the lysosomal degradation of glycoproteins.

The discovery of these disorders presented the problem of differential diagnosis. Most patients in childhood appear phenotypically similar and therefore a simple screen for oligosaccharide storage diseases was warranted. A one-dimensional thin-layer chromatography (TLC) method on silica gel was first described by Palo and Savolainen [21] for oligosaccharide screening of native urine from patients with aspartylglucosaminuria. This method was extended by Humbel and Collart [14] to include fucosidosis, mannosidosis and GM1-gangliosidosis. Further modifications were introduced to enable a wider range of diseases to be detected [10, 27, 28, 35].

4.2.2 Clinical Significance

Genetic defects in the degradation of glycoproteins are representative of lysosomal storage disorders. Each disease is caused by a deficiency of a lysosomal hydrolase, accumulation and urinary excretion of substrates, a progressive clinical course and considerable phenotypic variation. These disorders also manifest the clinical symptoms normally associated with genetic mucopolysaccharidoses, namely coarse facies, dysostosis multiplex and/or ocular involvement.

Table 4.2.1 lists the disorders of glycoprotein degradation that are detected by urinary oligosaccharide screening. It is beyond the scope of this article to give clinical descriptions of all of the disorders listed; therefore the reader is referred to the references given in Table 4.2.1.

Table 4.2.1 *Genetic glycoprotein storage disorders*

α-Mannosidosis [34]
α-Fucosidosis [34]
Aspartylglucosaminuria [2]
β-Mannosidosis [34]
Galactosialidosis [5]
GM1-gangliosidosis [33]
GM2-gangliosidosis Sandhoff [13]
Sialidosis [34]

4.2.3 Method

4.2.3.1 Principle

One-dimensional TLC of native urine is done on silica gel plates with development in two solvent systems. Oligosaccharides are visualised by spraying with orcinol reagent followed by heating at 100°C and examination by transparency.

4.2.3.2 Specimen

If possible, 24-h urine collections should be obtained. This is usually not possible in small infants or those who are physically or mentally handicapped, therefore a random urine sample (10–15 ml) is sufficient. The sample may be stabilised with toluene or chloroform, but thymol and acidification should be avoided. Samples may be sent by normal mail or alternatively deep-frozen on dry ice, and are then stored deep-frozen at –20°C prior to analysis.

4.2.3.3 Materials

Pre-coated glass TLC plates (20×20 cm; Merck 5721, Germany); 100-µl glass syringe (Hamilton, Switzerland); TLC tank (Desaga, Germany), hotplate (Gerhardt, Germany), spray (Eco-spray, Labochimie, France).

N-Butanol (Analar, Merck 1.01990); glacial acetic acid (96%, Analar, Roth 3738.2); *n*-propanol (Analar, Merck 1.00997); nitromethane (Analar, Merck 820894); 3,5 dihydroxytoluolmonohydrate (orcinol, Analar, Merck 820933); concentrated sulphuric acid (Analar, Merck 1.00731).

All of these reagents are stable at room temperature.

4.2.3.4 Standards

Standard carbohydrates (lactose, raffinose and glucotetrasaccharide) were obtained from Sigma (Munich, Germany).

Mannose tri-, tetra- and pentasaccharide together with GM1 octasaccharide were a gift from Dr. M.A. Chester (Lund, Sweden). At the time of writing, these standards are no longer available. Pentasaccharides (from human urine) and sialylated tetrasaccharides (from human milk) are available from Sigma; however, they are cost-prohibitive for routine use.

All standards are prepared as 1 μg/μl solutions in distilled water and stored at –20°C.

4.2.3.5 Procedure

Urinary creatinine is determined on a Cobas Bio Analyser using a commercial modification of the Jaffé acid-picrate method (Wako, Neuss, Germany). Urine samples corresponding to 20 μg creatinine are applied directly as a thin streak in a stream of warm air, 1.5 cm from the lower edge of a 20×20 cm pre-coated silica gel TLC plate. Reference standards (10 μg) are used at a concentration of 1 μg/μl.

The plate is developed overnight (16 h) in a freshly prepared mixture of *n*-butanol: glacial acetic acid:distilled water (100:50:50, v/v/v), removed, quickly dried in warm air and placed in a mixture of nitromethane:n-propanol:distilled water (80:100:60, v/v/v). Development is continued for a further 4 h.

The plate is finally removed, dried and sprayed with a freshly prepared solution of orcinol (0.2 g/dl) in sulphuric acid (20 g/dl). The oligosaccharide bands are then visualised by heating on a hotplate at 100°C and examined by transparency.

4.2.3.6 Quality Control

Analytical quality is maintained by including at least one known pathological sample in each run. There is no universal quality control scheme for oligosaccharide analysis due to the lack of sufficient patient samples.

4.2.4 Interpretation and Limitations

Oligosaccharide standards are depicted in Fig. 4.2.1 and the respective R_f (distance travelled on the gel) values relative to raffinose are given in Table 4.2.2.

In normal urine, only faint bands are usually seen below the raffinose standard. In neonates, many violet bands are encountered below the raffinose standard (most likely milk oligosaccharides), in which case repeated testing is recommended at the age of 6 months to 1 year.

Figure 4.2.2 depicts the urinary oligosaccharide patterns of sialidosis (α-neuraminidase deficiency), GM1 gangliosidosis and mucopolysaccharidosis type IVB (β-galactosidase deficiency) compared to a normal urine and standards of raffinose, lactose and glucose. In patients with sialidosis, a densely staining band close to the

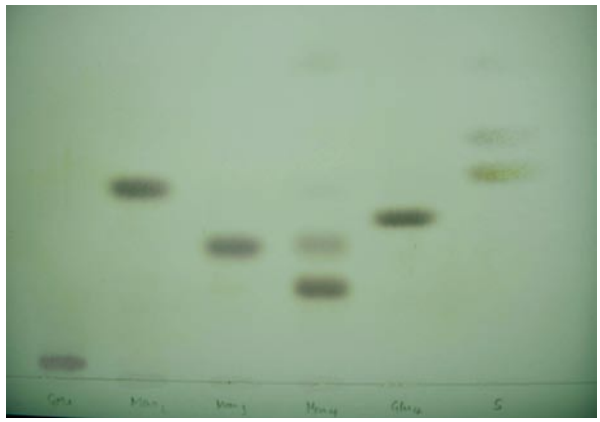

Fig. 4.2.1 Thin-layer chromatography (TLC) of oligosaccharide standards. Left to right: GM1 octasaccharide, mannotrisaccharide, mannotetrasaccharide, mannopentasaccharide, glucotetrasaccharide and standards of raffinose (lower) and lactose (upper)

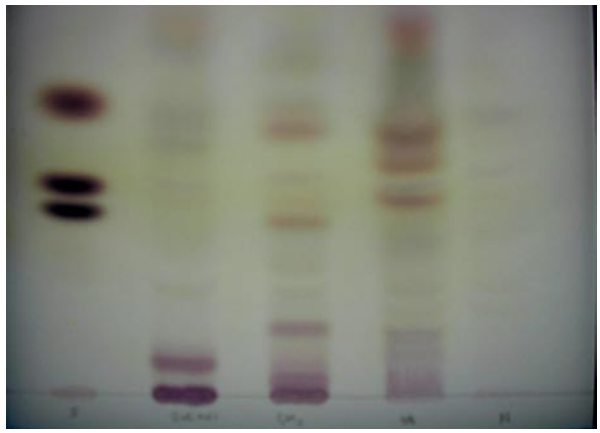

Fig. 4.2.2 TLC of urinary oligosaccharides. Left to right: standards of raffinose (lower), lactose (middle) and glucose (upper), sialidosis, GM1 gangliosidosis, mucopolysaccharidosis IVB and a control

Table 4.2.2 *R_f values (distance travelled by the substance on the plate) of oligosaccharide standards*

Standard	R_f (relative to raffinose)
Raffinose	1.00
Glucotetrasaccharide	0.78
Mannotrisaccharide	0.92
Mannotetrasaccharide	0.67
Mannopentasaccharide	0.47
GM1 octasaccharide	0.10

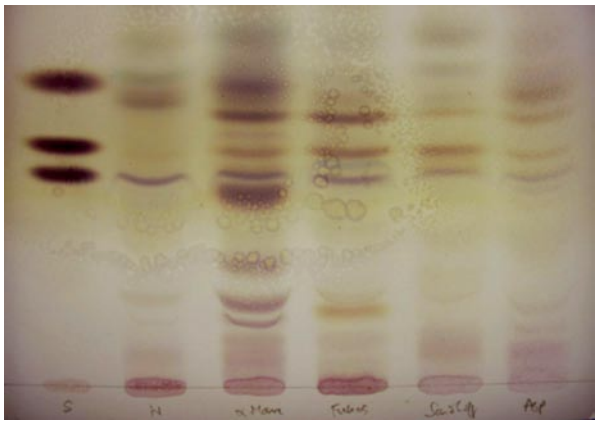

Fig. 4.2.3 TLC of urinary oligosaccharides. Left to right: standards (as in Fig. 4.2.2), a normal control, α-mannosidosis, fucosidosis, GM2 gangliosidosis type Sandhoff and aspartylglucosaminuria

origin (R_f 0.18) and a lighter band migrating further (R_f 0.56) are characteristic. Patients with infantile GM1 gangliosidosis show heavily staining bands close to the origin (R_f 0.08) corresponding to a possible octasaccharide. A further band (R_f 0.37) appears in the pentasaccharide region. The juvenile form of the disease shows a similar but less intense pattern. Adult forms and patients with mucopolysaccharidosis type IVB show only slight banding (R_f 0.37) with no octasaccharide.

Figure 4.2.3 depicts the urinary oligosaccharide excretion patterns of patients with α-mannosidosis, fucosidosis, GM2 gangliosidosis type Sandhoff and aspartylglucosaminuria together with a normal urine and standards. Patients with α-mannosidosis excrete a series of mannose-containing oligosaccharides (disaccharide to heptasaccharide). Urine from β-mannosidosis patients fails to show an abnormal oligosaccharideuria.

Patients with fucosidosis excrete a characteristic brown/pink band and densely staining bands at the origin. In Sandhoff disease, again dense staining is seen at the origin and urine from patients with aspartylglucosaminuria shows the presence of closely migrating bands near the origin.

All of the above-mentioned patterns are specific for the particular disease. The method is suitable as an initial screen to identify those patients in whom such a disorder must be excluded. The diagnosis must then be confirmed by enzyme analysis in serum, leucocytes or cultured skin fibroblasts or by way of mutation analysis.

The method does have limitations. Neonatal excretion patterns due to milk oligosaccharide excretion may be confused with that of α-mannosidosis; however, in neonatal urine samples, the bands stain lilac, whereas in α-mannosidosis, they are brown. The same "neonatal pattern" is observed in the urine of pregnant or lactating women [18]. Patients receiving dextran infusions or plasma expanders (e.g. HAES) excrete abnormal oligosaccharides, but are not disease-specific. In glycogen storage disease type II, an abnormal oligosaccharide pattern is seen [4], likewise in type III [11], and patients with type VI excrete a characteristic tetrasaccharide [29].

Some disorders may be missed; β-mannosidase deficiency is not detected in this system and perhaps a special method for β-manno-oligosaccharides [9] should be applied. Mucolipidosis types II and III are also not detected; however, the diagnosis can well be accomplished on clinical grounds. Caution must be exercised in cases of sialidosis. Patients with galactosialidosis show the same excretion pattern as patients with a primary α-neuraminidase deficiency [30]. The diagnosis can only be achieved by enzyme analysis. The oligosaccharide excretion pattern described in patients with N-acetylgalactosaminidase deficiency (Schindler/Kanzaki disease) [8] has not been seen with the described method. There again, perhaps the use of ninhydrin as a detection reagent may reveal the pattern [26]. Likewise, the reported oligosaccharide excretion pattern of patients with Gaucher disease [7] has not been confirmed by the author.

In all cases of abnormal oligosaccharidurias with patterns not characteristic of a known glycoprotein storage disease, a structural analysis of excreted oligosaccharides is required. High-performance liquid chromatographic methods have been used [6, 22], but do not give any more information than TLC methods. The advent of new technologies (time-of-flight mass spectrometry [15], tandem mass spectrometry) has paved the way towards a rapid and accurate oligosaccharide analysis. It is now possible to determine oligosaccharides and glycolipids in amniotic fluid as an aid to prenatal diagnosis [24] and to accurately monitor glucotetrasaccharide in Pompe disease by tandem mass spectrometry [36], a prerequisite for enzyme replacement therapy in this disorder.

References

1. Aronson NN Jr, Kuranda MJ (1989) Lysosomal degradation of Asn-linked glycoproteins. FASEB J 3:2615–2622
2. Aula P, Jalanko A, Peltonen L (2001) Aspartylglucosaminuria. In: Scriver CR, Beaudet AL, Sly WS, Valle D (eds) The Metabolic and Molecular Bases of Inherited Disease, vol III, 8th edn. McGraw-Hill, New York, pp 3535–3550
3. Berger EG, Buddecke E, Kamerling JP, Kobata A, Paulson JC, Vliegenthart JF (1982) Structure, biosynthesis and functions of glycoprotein glycans. Experientia 38:1129–1162
4. Blom W, Luteyn JC, Kelholt-Dijkman HH, Huijmans JG, Loonen MC (1983) Thin-layer chromatography of oligosaccharides in urine as a rapid indication for the diagnosis of lysosomal acid maltase deficiency (Pompe's disease). Clin Chim Acta 134:221–227
5. D'Azzo A, Andria G, Striscuiglio P, Galjaard H (2001) Galactosialidosis. In: Scriver CR, Beaudet AL, Sly WS, Valle D (eds) The Metabolic and Molecular Bases of Inherited Disease, vol III, 8th edn. McGraw-Hill, New York, pp 3811–3826
6. Daniel PF, De Feudis DF, Lott IT, McCluer RH (1981) Quantitative microanalysis of oligosaccharides by high performance liquid chromatography. Carbohydr Res 97:161–180
7. De Jong JG, Aerts JM, van Weely S, et al (1998) Oligosaccharide excretion in adult Gaucher disease. J Inherit Metab Dis 21:49–59
8. Desnick RJ, Schindler D (2001) α-N-Acetylgalactosaminidase deficiency: Schindler disease. In: Scriver CR, Beaudet AL, Sly WS, Valle D (eds) The Metabolic and Molecular Bases of Inherited Disease, vol III, 8th edn. McGraw-Hill, New York, pp 3483–3505
9. Dorland L, Duran M, Hoefnagels FET, Breg JN, Fabery de Jonge H, Cransberg K, van Sprang FJ, van Diggelen OP (1988) Beta-Mannosidosis in two brothers with hearing loss. J Inherit Metab Dis 11:255–258

10. Friedman RB, Williams MA, Moser HW, Kolodny EH (1978) Inproved thin-layer chromatographic method in the diagnosis of mannosidosis. Clin Chem 24:1576–1577
11. Galvin-Parton P, Hommes FA (1996) Abnormal oligosaccharide pattern in glycogen storage disease type III. J Inherit Metab Dis 19:383–384
12. Ginsberg V, Neufeld EH (1969) Complex heterosaccharides of animals. Annu Rev Biochem 38:371–386
13. Gravel RA, Kaback MM, Proia RL, Sandhoff K, Suzuki K, Suzuki K (2001) The GM2 gangliosidoses. In: Scriver CR, Beaudet AL, Sly WS, Valle D (eds) The Metabolic and Molecular Bases of Inherited Disease, vol III, 8th edn. McGraw-Hill, New York, pp 3827–3876
14. Humbel R, Collart M (1975) Oligosaccharides in the urine of patients with glycoprotein storage diseases. I. Rapid detection by thin-layer chromatography. Clin Chim Acta 60:143–145
15. Klein A, Lebreton A, Lemoine J, Perini J-M, Roussel P, Michalski J-C (1998) Identification of urinary oligosaccharides by matrix-assisted laser desorption ionisation time-of-flight mass spectrometry. Clin Chem 44:2422–2428
16. Kornfeld R, Kornfeld S (1976) Comparative aspects of glycoprotein structure. Annu Rev Biochem 45:217–237
17. Kornfeld R, Kornfeld S (1985) Assembly of asparagine-linked oligosaccharides. Annu Rev Biochem 54:631–634
18. Kuczynski TW, Kendzierski KS, Sewell AC (1993) Urinary oligosaccharides in pregnant or lactating women: a pitfall in screening. Clin Chem 39:2346–2347
19. Kumlien J, Chester MA, Lindberg BS, Pizzo P, Zopf D, Lundblad A (1988) Urinary excretion of a glucose containing tetrasaccharide. A parameter for increased degradation of glycogen. Clin Chim Acta 176:39–48
20. Lundblad A (1970) Blood group specific oligosaccharides in urine. In: Aminoff D (ed) Blood and Tissue Antigens. Academic, New York, pp 427–435
21. Palo J, Savolainen H (1972) Studies on serum and urinary glycopeptides and glycosaminoglycans in aspartylglucosaminuria. Clin Chim Acta 36:431–437
22. Peelen GO, de Jong JG, Wevers RA (1994) HPLC analysis of oligosaccharides in urine from oligosaccharidosis patients. Clin Chem 40:914–921
23. Pileggi V, Szustkiewicz CP (1974) Urinary carbohydrates. In: Henry RJ, Cannon DC, Winkelmann JW (eds) Clinical Chemistry, Principles and Techniques. Harper and Row, New York, pp1267–1268
24. Ramsay SL, Maire I, Bindloss C, Fuller M, Whitfield PD, Piraud M, Hopwood JJ, Meikle PJ (2004) Determination of oligosaccharides and glycolipids in amniotic fluid by electrospray ionisation tandem mass spectrometry: in utero indicators of lysosomal storage diseases. Mol Genet Metab 83:231–238
25. Rudloff S, Pohlentz G, Diekmann L, Egge H, Kunz C (1996) Urinary excretion of lactose and oligosaccharides in preterm infants fed human milk or infant formula. Acta Paediatr 85:598–603
26. Schindler D, Kanzaki T, Desnick RJ (1990) A method for the rapid detection of urinary glycopeptides in alpha-N-acetylgalactosaminidase deficiency and other lysosomal storage diseases. Clin Chim Acta 190:81–91
27. Sewell AC (1979) An improved thin-layer chromatographic method for urinary oligosaccharide screening. Clin Chim Acta 92:411–414
28. Sewell AC (1981) Simple laboratory determination of excess oligosaccharidurie. Clin Chem 27:243–245
29. Sewell AC (1986) Urinary oligosaccharide screening detects type VI glycogen storage disease. Clin Chem 32:392
30. Sewell AC, Pontz BF, Weitzel D, Humburg C (1987) Clinical heterogeneity in infantile galactosialidosis. Eur J Pediatr 146:528–531
31. Spik G (1977) Etude des proprietes des glycosidases impliques dans le catabolisme des glycoproteines. In: Farriaux JP (ed) Les Oligosaccharidoses. Crouant et Roques, Lille, pp 31–41
32. Spiro RG (1973) Glycoproteins. Adv Protein Chem 27:349–367

33. Suzuki Y, Oshima A, Nanba E (2001) β-Galactosidase deficiency (β-galactosidosis):GM1 gangliosidosis and Morquio B disease. In: Scriver CR, Beaudet AL, Sly WS, Valle D (eds) The Metabolic and Molecular Bases of Inherited Disease, vol III, 8th edn. McGraw-Hill, New York, pp 3775–3809
34. Thomas GH (2001) Disorders of glycoprotein degradation: α-mannosidosis, β-mannosidosis, fucosidosis and sialidosis. In: Scriver CR, Beaudet AL, Sly WS, Valle D (eds) The Metabolic and Molecular Bases of Inherited Disease, vol III, 8th edn. McGraw-Hill, New York, pp 3507–3533
35. Tsai MY, Marshall JG (1979) Screening for urinary oligosaccharides and simple sugars by thin-layer chromatography. Med Lab Sci 36:85–90
36. Young SP, Stevens RD, An Y, Chen YT, Millington DS (2003) Analysis of a glucose tetrasaccharide elevated in Pompe disease by stable isotope dilution-electrospray ionisation tandem mass spectrometry. Anal Biochem 316:175–180

4.3 Sialic Acid

Frans W. Verheijen

4.3.1 Introduction

The sialic acids comprise a family of about 40 derivatives of neuraminic acid. The major type of sialic acid in humans is N-acetylneuraminic acid (NeuAc; Fig. 4.3.1). In other mammalians, a variable but often minor percentage of the sialic acids is represented by N-glycolylneuraminic acid (NeuGc). These monocarboxylic N-substituted monosaccharides are essential components of oligosaccharides (OGSs) present in glycoproteins and gangliosides. Under normal circumstances only a small portion of total sialic acid is present in its free form in tissues and body fluids without a clear biological function. Sialic acid is present mainly in a bound form with an α-glycosidic linkage as the terminal sugar of the carbohydrate chains of macromolecules. Since the pK of the carboxyl group of sialic acid is low (around 2.6), it provides a strong negative charge to such sugar chains. OGS-bound sialic acid is involved in main metabolic functions like immunological processes, hormonal responses, signal transmission in neurons, tumor progression, cell adhesion, and protection mechanisms [17, 18].

The essential steps of intracellular sialic acid metabolism in humans are depicted schematically in Fig. 4.3.2. The synthesis starts with glucose, which is converted to uridine diphosphate (UDP)-N-acetyl-D-glucosamine (UDP-GlcNAc). The next step, the conversion to N-acetylmannosamine (ManNAc) by UDP-GlcNAc-2-epimerase, is subject to feedback regulation by cytidine-5'-monophosphate (CMP)-NeuAc, the end product of the pathway. NeuAc is produced after a phosphorylation step from ManNAc to ManNAc-6-phosphate, a phosphate synthase step to NeuAc-9-phosphate, and finally a specific phosphatase acting on NeuAc-9-phosphate. A variety of reactions can occur leading to modified and activated sialic acids. Modifications can be enzymatic conversion of the N-acetyl group to N-glycolyl and O-acetylation

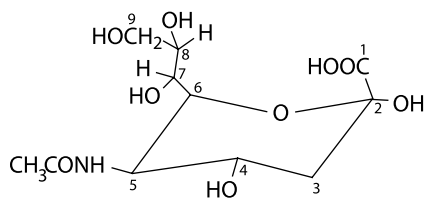

Fig. 4.3.1 Structure of N-acetylneuraminic acid (NeuAc)

at positions 4, 7, 8, and 9 of the neuraminic acid molecule. Following modification at the monosaccharide level, activation to CMP-NeuAc takes place. This reaction is catalyzed by CMP-NeuAc synthase in the nucleus. CMP-NeuAc is transported into the Golgi apparatus by a specific transporter and functions as a sialic acid donor for sialyltransferase reactions, leading to sialylated OGSs of glycoproteins and glycolipids. This concludes the synthesis part of the pathway. Most of the degradation starts from sialylated glycoconjugates in the lysosome. The OGS chains are sequentially degraded by several specific lysosomal enzymes. This starts with cleavage of the terminal sialic acid residue by a specific acid neuraminidase (sialidase). Free NeuAc is transported out of the lysosome by a specific transporter, acting as a proton symporter [11]. The free NeuAc can be reutilized or further degraded by acylneuraminate pyruvate-lyase to pyruvate.

Three different rare genetic metabolic defects in sialic acid metabolism are known, as indicated in Fig. 4.3.2 [3, 21]: (1) free sialic acid storage disease (SASD; Online Mendelian Inheritance in Man, OMIM 604369, 269920), a lysosomal membrane transporter defect; (2) sialuria (OMIM 269921), a feedback inhibition defect in sialic acid biosynthesis; (3) sialidosis (OMIM 256550), a breakdown defect of sialyloligosaccharides caused by a defect of lysosomal sialidase. In all these genetic defects, an increased amount of sialic acid can be found in tissues and or body fluids, either bound to OGSs as in (3), or in its free state as in (1) and (2).

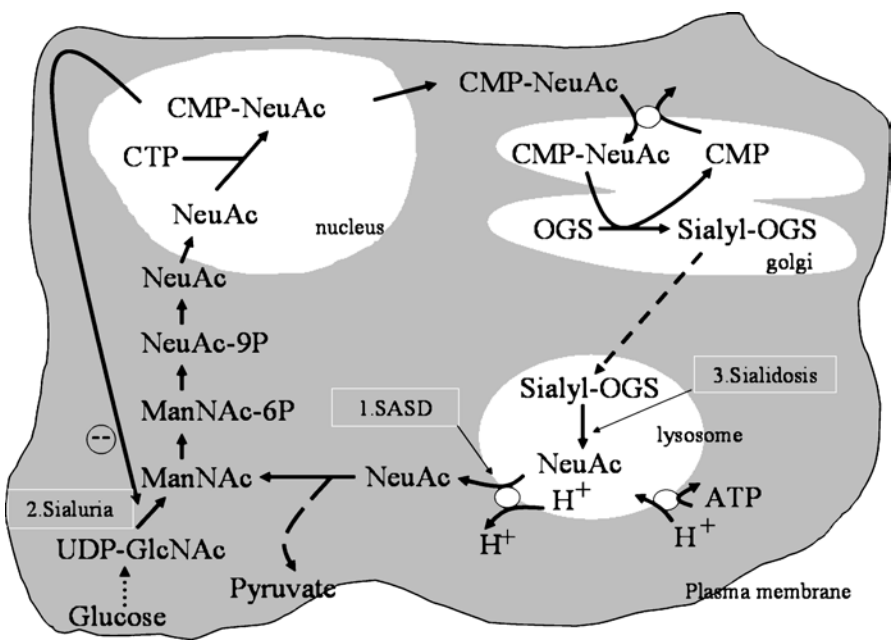

Fig. 4.3.2 Human sialic acid metabolism and genetic defects. *-6P* -6-Phosphate, *-9P* -9-phosphate, *CMP* cytidine 5'-monophosphate, *CTP* cytidine 5'-triphosphate, *UDP-GlcNAc* uridine diphosphate-N-acetyl-D-glucosamine, *ManNAc* N-acetylmannosamine, *NeuAc* N-acetylneuraminic acid, *OGS* oligosaccharides, *SASD* sialic acid storage disease

4.3.2 Clinical Manifestation of SASD

The lysosomal disorder SASD is characterized by accumulation of the free acid monosaccharide sialic acid in the lysosomal compartment of the cell. Diagnosis is based on the demonstration of abnormal excretion of free, not OGS-bound sialic acid in urine, coupled with accumulation of free sialic acid in cultured fibroblasts, and on microscopic evidence of vacuoles (increased and swollen lysosomes filled with light electron-lucent material in skin biopsy and peripheral blood lymphocytes). The inheritance is autosomal recessive. There are different clinical forms of this disorder: an adult form, called Salla disease (SD) or Finnish sialuria (OMIM 604369); infantile SASD (ISSD; OMIM 269920); and an intermediate form, severe Salla disease [3,16].

Salla disease, the milder adult form, was originally described in a group of patients originating from a circumscribed area in northern Finland, which lends the eponym [2]. Nystagmus, hypotonia, and ataxia by the end of the 1st year are typical signs of SD. Deep mental retardation, dementia, loss of deambulation, and loss of acquired speech characterize the latter stages of the disease, which spans several decades. Hypomyelination and dysmyelination can be observed on magnetic imaging brain scans. Although most patients with SD are of Finnish origin, the disease has also been described in Sweden and sporadically in The Netherlands (G.M.S. Mancini, unpublished observations). Patients with the intermediate form show moderate signs of neurodegeneration, marked growth retardation, and delayed puberty associated with endocrine failure [8].

The infantile form (ISSD) represents the most severe form of the disease, with failure to thrive, severe psychomotor retardation, visceromegaly with ascites, dysostosis multiplex. Onset is at birth or in utero and is followed by early death, usually within the 1st year [6].

All clinical forms of the disease are due to a defect in the lysosomal membrane transporter for sialic acid necessary for the export of sialic acid out of the lysosome [11]. The gene coding for this transporter, *SLC17A5*, contains 11 exons and encodes a 495-amino-acid transmembrane protein, sialin [20].

SASD must be discriminated from other disorders of sialic acid storage [3]: (1) sialidosis and galactosialidosis, defects respectively in lysosomal sialidase and both sialidase and β-galactosidase. (OMIM 256550 and 256540); (2) nonlysosomal sialuria (OMIM 269921).

Sialidosis (and also galactosialidosis) is characterized by the accumulation of OGS-bound sialic acid. Free sialic acid is normal. Diagnosis is confirmed by enzyme analysis of sialidase (sialidosis) or both sialidase and β-galactosidase (galactosialidosis) in fibroblasts. The clinical presentation of infantile sialidosis (type II), galactosialidosis, and ISSD may be very similar during the neonatal period, with hepatosplenomegaly, ascites, and dysmorphic features. Typical ocular findings for sialidosis and galactosialidosis, cherry red spots, are not yet detectable at an early age. Sialidosis type I, cherry red spot myoclonus syndrome, is milder and clinically very different from ISSD.

Nonlysosomal sialuria (also called French-type sialuria) is characterized by massive excretion of free sialic acid in urine. Only four patients have been described. The defect is caused by a defective feedback inhibition of UDP-GlcNAc-2-epimerase [15]. The accumulation is cytosolic and not lysosomal. The clinical presentation is

variable, but includes developmental delay, hepatosplenomegaly, and coarse facial features. Some individuals with this disorder are asymptomatic. The disorder shows autosomal dominant inheritance [10].

For an overview of clinical and biochemical discrimination of all disorders with accumulation of sialic acid see Table 4.3.1. For a diagnostic workflow see Table 4.3.2.

■ ***Table 4.3.1*** *Disorders of sialic acid metabolism with storage of sialic acid, clinical, and biochemical discrimination.* ISSD *Infantile sialic acid storage disease,* OGS *oligosaccharide,* SASD *free sialic acid storage disease*

Disease	Clinical severity	Biochemistry sialic acid (amount in urine, tissues)
Free sialic acid storage disorders, SASD		
ISSD	+++	+++
Intermediate	++	+ / ++
Salla	+	+
Other		
French-type Sialuria	– / +	++++
(Galacto)sialidosis	++	+ (OGS-bound)
Sialidosis type I	+	

■ ***Table 4.3.2*** *Diagnostic workflow of disorders with accumulation of free or oligosaccharide-bound sialic acid.* MRI *Magnetic resonance imaging,* TLC *thin-layer chromatography*

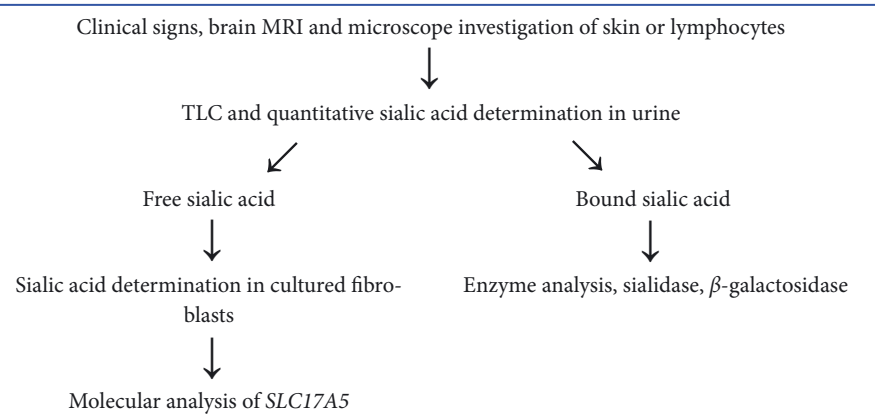

4.3.3 Methods

4.3.3.1 Thin-Layer Chromatography

Principle

Thin-layer chromatography (TLC; in one dimension) provides a rapid, easy, and economical separation method useful for the initial screening of large amounts of samples. Separation is achieved by the differences in solubility of the individual monosaccharides and OGSs. It can be easily applied to screen urine samples for free sialic acid and for sialyloligosaccharides. The technique is also used for the screening of several other lysosomal storage disorders in which OGSs accumulate. For sialic acid (free or bound to OGSs), a specific staining of the plates is essential.

Specimen

In general, untimed urine specimens can be used for this assay. However, preferably 24-h urine samples should be used. Samples should be frozen as soon as possible after collection.

Reagents and Chemicals

1. Solvent for TLC: 75 ml butanol with 37.5 ml acetic acid and 37.5 ml distilled water (prepared on weekly basis).
2. Staining solution (Bial's reagent), prepared freshly: 50 mg orcine monohydrate is dissolved in 12.5 ml distilled water, 20 ml HCl 37%, and 0.5 ml 1% ferric chloride hexahydrate ($FeCl_3.6H_2O$).
3. Reference sample: 1 mg/ml NeuAc.

Instrumentation

1. Small table centrifuge (for 1.5-ml volume reaction vials).
2. Tank for TLC.
3. Silica 60 TLC plates, 20 × 20 cm.
4. If possible, an automatic spotter, or else a pipette for volumes between 10 and 25 µl.
5. TLC spray apparatus.
6. Stove (100°C).

Procedure

A 1.0-ml sample of urine is placed in a 1.5-ml reaction vial and centrifuged for 5 min, at room temperature, and at 10,000 rpm (about 10,000 × *g*). The supernatant can be applied to the TLC plate. The amount to be applied is dependent on the age of the

patient and the creatinine concentration of the urine sample. We use the following formula:

$$\text{volume of urine (µl)} = \text{age factor} \times 1/\text{creatinine (mmol/l)},$$

whereby the age factor is 75, 100, 150, and 200 for the age groups 0–1 years, 1–2 years, 2–8 years, and > 8 years, respectively. For good reproducibility an automatic spotter is used, but manual spotting using a pipette is also possible. During manual spotting portions of (maximum) 10- to 20-µl sample are applied carefully to a 1.5-cm-wide horizontal pencil line, about 2 cm from the left border of the plate and about 1.5 cm from the bottom of the plate. If more is necessary, the first portion is dried using a hairdryer before the second portion is applied to it. The next sample is applied with a distance of 2.5 cm. As a reference standard, a 10-µl sample of free sialic acid (NeuAc, 1 mg/ml) is applied to the last lane of the TLC plate.

The chromatography tank is filled with TLC solvent solution to about 1 cm below the applied samples. Three strokes of filter paper saturated with solvent solution are placed at three sides of the tank. The tank is closed with a glass plate and sealed using grease. When the solvent level has reached the top of the plate (5–8 h), the plate is dried in a fume hood or on a stove heated to 100ºC. The plate is sprayed with staining solution using a spray apparatus. The plate is covered with a glass plate and placed in a 100ºC stove for about 15 min. After color development, the glass plated covering the tank is removed and the TLC plate is placed into the fume hood for further drying and interpretation.

Interpretation

The patterns are compared to the reference standard and to control samples. A picture of a typical pathological pattern is shown in Fig. 4.3.3. In case of an increased free sialic acid band, or increased sialyloligosaccharides, the next step is the quantita-

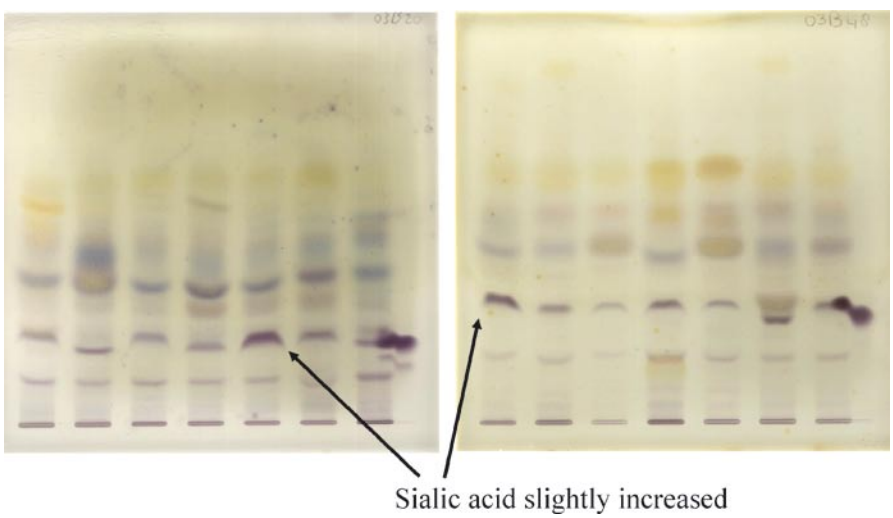

Fig. 4.3.3 Example of thin-layer chromatography of human urine samples

tive determination of free and bound sialic acid, respectively. It should be noted that the increase in sialic acid can be modest in some patients, and can vary from sample to sample. In these cases the assay should be repeated on a fresh sample, (if possible a 24-h sample).

4.3.3.2 Quantitative Analysis in Urine

Principle

Usually this analysis is done after the initial TLC screenings test. The test determines only free sialic acid. It should be noted that not all different sialic acids (see section 4.3.1) are detected by this test. In relation to human disorders, however, we are only interested in NeuAc. The analysis is performed to quantify the amount of NeuAc present as either free sialic acid, which is increased in SASD, or OGS-bound sialic acid, which is increased in sialidosis and galactosialidosis. In the case that determination of free sialic acid is required, the test can be performed directly. In the case of suspicion of OGS-bound sialic acid, the test is performed after an acid hydrolysis step to liberate sialic acid. The subsequent test determines the total amount of sialic acid, the initially free form plus the liberated bound form, via the widely used periodate-thiobarbituric acid (TBA) assay [4, 5, 22]. Treatment of sialic acid with periodate under acidic conditions produces β-formylpyruvate, which reacts with TBA to produce a red/purple chromophore with an absorption maximum at 549 nm. Extraction of the chromophore in an organic solvent, cyclohexanon, or acid butanol stabilizes and intensifies the color. Several compounds present in urine (e.g., deoxyribose) can form malonaldehyde, which condenses with TBA to form a chromophore with an absorption maximum at 532 nm. Since both absorption maxima are very close to each other, this can easily give rise to interference in the quantitation of sialic acid. Interference can be decreased by a neutral butanol extraction step for the interfering chromophore that precedes the final acid butanol extraction step in which the specific chromophore is extracted [14].

Specimen

See section 4.3.3.1, subheading “Specimen.”

Reagents and Chemicals

1. Butanol.
2. Periodate (0.025 M) in 0.25 M HCl (prepare fresh).
3. 5% Sodium thiosulfate (prepare fresh).
4. 0.1 M 2-TBA pH 5.5–7.0 (prepare fresh): 40 ml distilled water with 720 mg barbituric acid. Add 5 N NaOH to dissolve the salt and take the pH to 5.5–7.0. Add distilled water to a total volume of 50 ml.
5. Acid butanol (95 ml butanol with 5 ml HCl).
6. 0.1 M Sulfuric acid.

7. 5 N NaOH.
8. Stock solution of NeuAc acid 0.05% (500 mg/l): (prepare fresh dilutions from 200 µl volume: 25, 50,125, 250, and 375 mg/l.

Instrumentation

1. Table centrifuge.
2. Water bath (shaking) 37°C.
3. Water bath 80°C.
4. Spectrophotometer.
5. Vortex.

Procedure

All determinations are performed in duplicate. For total (free plus bound) sialic acid: take 50 µl sample (distilled water blank; or standard; or urine sample), add 50 µl H_2SO_4 and incubate for 60 min at 80°C in closed reaction tubes. For free sialic acid, pipette the same without incubation at 80°C.

Add 250 µl periodate to all tubes, close the tubes and then incubate for 30 min at 37°C in a shaking water bath. Add 5% sodium thiosulfate dropwise during mixing on vortex to all tubes. Add 1.25 ml TBA to each tube; mix, close the tubes and incubate for 15 min in a boiling water bath. Cool the tubes down in iced water then place at room temperature. Add 20 µl of 5 N NaOH and 2.2 ml butanol; mix carefully, centrifuge for 10 min at 3000 rpm about (about $2000 \times g$), and remove the upper butanol layer using a Pasteur pipette and vacuum aspiration. Add 2.2 ml acid butanol, mix carefully, centrifuge for 10 min at 3000 rpm about (about $2000 \times g$). Take about 2 ml from the upper butanol layer and put into small plastic tubes (5 ml volume); centrifuge for 3 min at 3000 rpm about (about $2000 \times g$). Pipette 800 µl of the supernatant into 1-ml cuvettes. Measure the absorbance at 549 nm against the blank sample (set at 0).

Interpretation

For each batch of samples, a calibration curve of six standard concentrations is calculated (25, 50, 125, 250, 375, and 500 mg/l). The curve is plotted and the sample concentrations are calculated. The correlation coefficient of the standard plot must be > 0.98. The concentration is determined in mmol/mol creatinine:

(concentration in mg/l × 1000)/(creatinine concentration in mmol/l × 309.28),

where 309.28 is the molecular mass of NeuAc. When the absorbance of the urine sample is higher, then the highest standard concentration the urine sample is diluted accordingly and remeasured. For reference values, which are age dependent, use can be made of the tables given in Waters et al. [23] (see a short overview in Table 4.3.3). Some typical pathological values are reported in Table 4.3.4. As mentioned earlier,

Table 4.3.3 *Normal reference values of free and bound N-acetylneuraminic acid (*NeuAc*) in human urine (adapted from Waters [23])*

Age (years)	Range (mmol/mol creatinine)	
	Free NeuAc	**Bound NeuAc**
	0–2 years: 20–130	15–260
	2–4 years: 20–75	25–150
	4–6 years: 20–60	30–100
	6–8 years: 20–50	20–60
	8–16 years: 10–30	15–50

Table 4.3.4 *Some typical pathological free NeuAc values in urine samples of different clinical forms of SASD (values from own experience and the literature)*

	NeuAc (mmol/mol creatinine)
Salla disease (age 12 years)	50
ISSD (from the literature)	121–1608
Intermediate forms (age 3 years)	125
French-type sialuria (from the literature)	14,680; 8950

increases in sialic acid can be modest in some patients, and can vary from sample to sample. In such cases the assay should be repeated on a fresh sample, if possible a 24-h sample. A positive test should always be followed by determination in cultured fibroblasts (see next topic). In cases where an increase in bound sialic acid is found (on TLC sialyloligosaccharides and quantitative increase after acid hydrolysis), neuraminidase (sialidase) enzyme determination should be performed.

4.3.3.3 Quantitative Analysis in Cultured Skin Fibroblasts

Principle

The test is performed for diagnosis of all clinical forms of SASD. This analysis is usually done after an initial TLC screening test that is positive for free sialic acid, and an increased free sialic acid value in the quantitative urine determination test. The test is like the quantitative urine test performed with the periodate-TBA assay [5, 22]. However, in this case interference is decreased by prepurification of the sample using ion-exchange chromatography [12]. Fibroblasts are cultured under standardized conditions. Cell lysates are prepared by tip sonification in distilled water and the cleared lysates are applied to small Dowex columns. NeuAc is eluted, freeze dried,

dissolved, and then used in the test. In this case, extraction of the formed chromophore is carried out directly with acid butanol.

Specimen

Cultured skin fibroblasts.

Reagents and Chemicals

1. Cell culture facility.
2. Acid butanol (95 ml butanol with 5 ml HCl).
3. 0.1 M 2-TBA pH 5.5–7.0: 40 ml distilled water with 720 mg barbituric acid, add 5 N NaOH to dissolve and take the pH to 5.5–7.0. Add distilled water to a total volume of 50 ml.
4. Dowex anion exchange resin, AG 1-X8, acetate form.
5. 0.25 M HCl.
6. 0.025 M Periodate in 0.25 M HCl (prepare fresh).
7. 0.2 M Sodium thiosulfate (prepare fresh).
8. 250 ml Ammonium acetate buffer pH 5.4 (prepare fresh).
9. 250 ml 0.2 M Ammonium formate buffer pH 5.4 (prepare fresh).
10. Stock solution of NeuAc-2, 33.4 μM (2 nmol/60 μl), kept frozen.
11. Stock solution of NeuAc-5, 83.5 μM (5 nmol/60 μl), kept frozen.
12. Stock solution of NeuAc-10, 167 μM (10 nmol/60 μl), kept frozen.

Instrumentation

1. Vortex.
2. Spectrophotometer with 100-μl cuvettes.
3. 5-ml Disposable columns.
4. Freeze dryer.
5. Sintered glass funnel.
6. Small table centrifuge (for 1.5-ml sample vials).
7. Incubator.
8. Water bath 100°C.

Procedure

Fibroblasts are cultured under standard conditions in $F10^{+}$ medium with 15% fetal calf serum. The level of free NeuAc is greatly influenced by culture conditions. Do not use Chang medium (leads to very high control values). The final culture is done in a 175-cm^2 culture flask for 7 days, the last 3 days with 5% fetal calf serum. Medium is removed, cells are washed with phosphate-buffered saline (PBS), trypsinized, centrifuged at $100 \times g$, and washed with PBS. The resultant pellets are frozen before use, in 1.5-ml sample vials at –80°C.

A sonic homogenate is prepared of a fibroblast cell pellet in 250-µl distilled water using a tip sonificator, followed by centrifugation for 10 min at 10,000 rpm (about 10,000 × *g*) and 4 °C. The supernatant is used for the purification procedure and for protein determination using the BCA kit of Pierce Chemicals.

Purification Procedure by Ion-Exchange Chromatography

Dowex (2.5 g per column) is prewashed in a sintered glass funnel with distilled water. Disposable columns (5 ml) are filled with 2 ml bed volume of prewashed Dowex. Columns are washed with 6 ml ice-cold distilled water. A 60-µl aliquot of each standard (NeuAc-2, NeuAc-5, and NeuAc-10) and a water blank are applied to the column. For diagnostic samples, patients and controls apply 200 µl to the column. Wash all columns three times with 2-ml ice-cold ammonium acetate buffer. Elute NeuAc by applying 3 × 2 ml and 1 × 1 ml ice-cold ammonium formate buffer. Close the collection tubes (50-ml volume) with a pierced cap and centrifuge fast to spin down droplets from the wall of the tube. Freeze the eluates in an upright position in liquid nitrogen.

Lyophilization

Place the frozen eluates in a freeze dryer for about 20 h. Carefully rinse the wall of the tubes three times with 500 µl distilled water and transfer the dissolved NeuAc to small 2-ml reaction vials with pierced caps. Freeze in liquid nitrogen and lyophilize again for about 13 h. Store residues at –20°C until determination of NeuAc.

NeuAc Determination

All determinations are performed in duplicate. Prepare samples by dissolving the lyophilized residue carefully in 60 µl of distilled water; keep on ice. Take a 20-µl sample and add 20 µl periodate; mix and incubate for 30 min at 37°C. Add 20 µl thiosulfate and vortex (a brown color will develop and disappear by vortexing).

Add 125 µl TBA, vortex, and place for 15 min into a boiling water bath. Cool down in ice water and centrifuge fast at room temperature. Add 125 µl acid butanol, vortex twice for about 5 s each. Centrifuge for 10 min at 3000 rpm (2000 × *g*).

Measurement

Transfer 100–110 µl of the butanol top layer in a 100-µl cuvette and read the absorbance at 549 nm (A_{549}) using a spectrophotometer. If the A_{549} is too high (> 2.5), take sample out of the cuvette and dilute four times in acid butanol and remeasure. Take care of air bubbles and check that the cuvette is filled appropriately. Avoid pipetting the bottom aqueous layer!

Interpretation

A standard curve is plotted from the standard samples that have been treated like the other samples (after purification and lyophilization); NeuAc concentrations in the samples are calculated from this plot. The concentration is reported in nmol NeuAc/mg protein in the original sample lysate. Normal reference values and pathological values as found in our laboratory are reported in Table 4.3.5.

Table 4.3.5 *Normal and pathological values of free NeuAc in cultured fibroblasts of controls and in patients with the different clinical forms of SASD*

	NeuAc in nmol/mg protein
Controls ($n = 40$)	0.1–2.3
Salla disease ($n = 5$)	5–12
ISSD ($n = 10$)	36–92
Intermediate forms ($n = 5$)	3–35

4.3.3.4 Molecular Diagnosis

The *SLC17A5* gene, responsible for lysosomal membrane sialic acid transport, is located on chromosome 6q14-15, contains 11 exons, and encodes a transmembrane protein of 495 amino acids, sialin [20]. Mutation analysis confirmed that SD, ISSD, and intermediate forms are allelic disorders. Mutation analysis in SD showed a "founder" missense mutation, 115 C > T, Arg39Cys in exon 2 in almost all of the affected Finnish patients. This mutation also seems to be associated with a milder course in either homozygous or heterozygous patients from other European countries. Many different mutations have been found throughout the gene in unrelated individuals. No particular mutation is associated with this phenotype [1, 6, 20].

Mutation analysis should be considered in those families with an affected child who are interested in prenatal diagnosis of a future pregnancy. Biochemical diagnosis has been reported to be difficult in amniotic fluid supernatant and cells, and chorionic villus cells, especially in SD. The increase in free sialic acid may be moderate even in cases with severe in utero presentation [3, 6]. It has been reported that prenatal diagnosis is reliable in trophoblast biopsy samples, using a high-performance liquid chromatography (HPLC), modified sialic acid test [6]. However, for a fast and reliable prenatal diagnosis, molecular diagnosis is now the preferred method.

4.3.3.5 Alternative Methods

Several alternative methods for the determination of sialic acid in body fluids and tissues have been described. Most of these methods make use of the classic periodate-TBA assay in combination with purification using HPLC [13]. Another method makes use of fluorometric HPLC of sialic acids after derivatization with a fluorogenic compound [9]. The most promising new method for the determination of free sialic acid in urine (and probably also other body fluids and tissues) is the HPLC-tandem mass spectrometry method [19]. This method is rapid, accurate, and sensitive, and is more robust than earlier methods. The only disadvantage is the expensive equipment that is required, which makes it only economical for specialized metabolic laboratories. Since this equipment is used for many different metabolic assays, the investment is certainly warranted, and nowadays almost essential for any metabolic laboratory.

This method may serve in the future as the reference method for free sialic acid in the diagnosis of SASD.

4.3.3.6 Enzyme Analysis in Cultured Fibroblasts

Principle

This test is performed when bound sialic acid is increased and when sialyloligosaccharides are found by TLC screening test. The lysosomal enzyme neuraminidase (sialidase) cleaves terminal sialic acid residues from the OGS chains in the lysosome (see section 4.3.1). The enzyme activity can be determined with an artificial substrate , 4-methylumbelliferone (4-MU) coupled to sialic acid. Upon incubation and enzymatic cleavage, free sialic acid and free 4-MU are formed; under alkaline conditions, the latter is a strongly fluorescent compound. The amount of 4-MU formed is indicative of the sialidase activity. This enzymatic assay can be used for the diagnosis of sialidosis (mucolipidosis 1) and galactosialidosis (combined sialidase and β-galactosidase deficiency). For discrimination of both disorders, a β-galactosidase assay is also performed. The principle is similar, but using galactose coupled to 4-MU as a substrate [7].

Specimen

Cultured skin fibroblasts.

Reagents and Chemicals

1. 4 mM 4-methylumbelliferyl-α-D-NeuAc sodium salt (MU-NeuAc), stock solution in distilled water, stored in 100-µl aliquots at –20°C.
2. 1 mM 4-methylumbelliferyl-β-d-galactopyranoside (MU-Gal) in 0.1 M sodium acetate buffer with 0.1 M NaCl pH 4.3.
3. 0.5 M Sodium carbonate buffer pH 10.7 with 0.025% Triton X-100.
4. Bovine serum albumin (BSA) 0.2% (pH and heat inactivated).
5. 30 µM 4-MU standard solution.

Instrumentation

Spectrophotometer (excitation 365 nm, emission 448 nm) and a heat block 37°C for 96-well plates.

Procedure and Interpretation

Prepare a fresh fibroblast homogenate in 130 µl distilled water (note: sialidase is highly labile upon sonification and freezing!), using a small (200-µl) Potter appara-

tus. Measure the protein concentration using the BCA method (Pierce Chemicals). Prepare fresh MU-NeuAc substrate, dilute 1:1 with 0.1 M sodium acetate buffer pH 4.3. Always keep fresh MU-NeuAc on ice to minimize hydrolysis, which leads to high blank values.

All determinations are performed in duplicate. The blank is 10 µl BSA solution + 10 µl MU-NeuAc substrate pH 4.3 in a well of a 96-well plate. The sample comprises 10 µl homogenate (diluted until the protein concentration is 3 mg/ml) + 10 µl of substrate. Incubate the samples for 1 h at 37°C on a heat block. Add 200 µl carbonate buffer and read the fluorescence. For calibration, 25 µl 4-MU standard solution (750 pmol) is mixed with 200 µl carbonate buffer and measured. For β-galactosidase, the homogenate is diluted until the protein concentration is 0.3 mg/ml. The incubation solution is as follows: 10 µl + 20 µl MU-Gal.

Activities are calculated and compared to internal control samples. Normal reference values and pathological values as found in our laboratory are reported in Table 4.3.6.

■ ***Table 4.3.6*** *Normal and pathological values of sialidase and β-galactosidase activity in cultured fibroblasts of controls and patients with sialidosis or galactosialidosis*

	Sialidase activity (nmol/mg protein/h)	**β-galactosidase activity (nmol/mg protein/h)**
Controls	20–120 (n = 124)	392–1600 (n = 1500)
Sialidosis	0–2.2 (n = 14)	Normal
Galactosialidosis	0–6.3 (n = 20)	32–186 (n = 20)

References

1. Aula N, Salomaki P, Timonen R, Verheijen F, Mancini G, Mansson JE, Aula P, Peltonen L (2000) The spectrum of SLC17A5-gene mutations resulting in free sialic acid-storage diseases indicates some genotype-phenotype correlation. Am J Hum Genet 67:832–840
2. Aula P, Autio S, Raivio KO, Rapola J, Thoden CJ, Koskela SL, Yamashina I (1979) "Salla disease": a new lysosomal storage disorder. Arch Neurol 36:88–94
3. Aula P, Gahl WA (2001) Disorders of free sialic acid storage. In: Scriver CR, Beaudet AL, Sly WS, Valle D (eds) The Metabolic and Molecular Bases of Inherited Disease. New York, McGraw Hill, pp 5109–5120
4. Cardo PP, Lombardo C, Gatti R (1985) A simple detection of sialic acid storage disorders by urinary 'free' and 'total' sialic acid determinations. Clin Chim Acta 150:129–135
5. Denny PC, Denny PA, Allerton SE (1983) Determination of sialic acid using 2-thiobarbituric acid in the absence of hazardous sodium arsenite. Clin Chim Acta 131:333–336

6. Froissart R, Cheillan D, Bouvier R, Tourret S, Bonnet V, Piraud M, Maire I (2005) Clinical, morphological, and molecular aspects of sialic acid storage disease manifesting in utero. J Med Genet 42:829–836
7. Galjaard H (1980) Genetic Metabolic Diseases. Elsevier/North-Holland Biomedical, Amsterdam
8. Grosso S, Berardi R, Farnetani MA, Margollicci M, Mancini MG, Morgese G, Balestri P (2001) Multiple neuroendocrine disorder in Salla disease. J Child Neurol 16:775–777
9. Ito M, Ikeda K, Suzuki Y, Tanaka K, Saito M (2002) An improved fluorometric high-performance liquid chromatography method for sialic acid determination: an internal standard method and its application to sialic acid analysis of human apolipoprotein E. Anal Biochem 300:260–266
10. Krasnewich DM, Tietze F, Krause W, Pretzlaff R, Wenger DA, Diwadkar V, Gahl WA (1993) Clinical and biochemical studies in an American child with sialuria. Biochem Med Metab Biol 49:90–96
11. Mancini GM, Beerens CE, Aula PP, Verheijen FW (1991) Sialic acid storage diseases. A multiple lysosomal transport defect for acidic monosaccharides. J Clin Invest 87:1329–1335
12. Mancini GM, Hu P, Verheijen FW, van Diggelen OP, Janse HC, Kleijer WJ, Beemer FA, Jennekens FG (1992) Salla disease variant in a Dutch patient. Potential value of polymorphonuclear leucocytes for heterozygote detection. Eur J Pediatr 151:590–595
13. Powell LD, Hart GW (1986) Quantitation of picomole levels of N-acetyl- and N-glycolylneuraminic acids by a HPLC-adaptation of the thiobarbituric acid assay. Anal Biochem 157:179–185
14. Roboz J, Suttajit M, Bekesi JG (1981) Elimination of 2-deoxyribose interference in the thiobarbituric acid determination of N-acetylneuraminic acid in tumor cells by pH-dependent extraction with cyclohexanone. Anal Biochem 110:380–388
15. Seppala R, Lehto VP, Gahl WA (1999) Mutations in the human UDP-N-acetylglucosamine 2-epimerase gene define the disease sialuria and the allosteric site of the enzyme. Am J Hum Genet 64:1563–1569
16. Sewell AC, Poets CF, Degen I, Stoss H, Pontz BF (1996) The spectrum of free neuraminic acid storage disease in childhood: clinical, morphological and biochemical observations in three non-Finnish patients. Am J Med Genet 63:203–208
17. Schauer R (2000) Achievements and challenges of sialic acid research. Glycoconj J 17:485–499
18. Traving C, Schauer R (1998) Structure, function and metabolism of sialic acids. Cell Mol Life Sci 54:1330–1349
19. Valianpour F, Abeling NG, Duran M, Huijmans JG, Kulik W (2004) Quantification of free sialic acid in urine by HPLC-electrospray tandem mass spectrometry: a tool for the diagnosis of sialic acid storage disease. Clin Chem 50:403–409
20. Verheijen FW, Verbeek E, Aula N, Beerens CE, Havelaar AC, Joosse M, Peltonen L, Aula P, Galjaard H, van der Spek PJ, Mancini GM (1999) A new gene, encoding an anion transporter, is mutated in sialic acid storage diseases. Nat Genet 23:462–465
21. Verheijen FW, Mancini GM (2003) Lysosomal sialic acid transporter sialin (SLC17A5):sialic acid storage disease (SASD). In: Broer S, Wagner CA (eds) Membrane Transporter Diseases. Kluwer Academic/Plenum, New York, pp 233–239
22. Warren L (1959) The thiobarbituric acid assay of sialic acids. J Biol Chem 234:1971–1975
23. Waters PJ, Lewry E, Pennock CA (1992) Measurement of sialic acid in serum and urine: clinical applications and limitations. Ann Clin Biochem 29:625–637

4.4 Glycosphingolipids

Ben J.H.M. Poorthuis, Johannes M.F.G. Aerts

4.4.1 Introduction

Sphingolipidoses are a group of genetic disorders caused by a deficiency in the lysosomal degradation or transport of sphingolipids (i.e., sphingomyelin, ceramide, neutral glycosphingolipids, and gangliosides). The enzymes involved in the stepwise degradation of sphingolipids are exohydrolases with optimal activity at acidic pH. A deficiency of one of these enzymes gives rise to a particular sphingolipid storage disorder (Table 4.4.1, Fig. 4.4.1). Since most of the enzymes involved in the degradation of sphingolipids require an activator protein for activity in vivo, a deficiency of an activator protein gives rise to a storage disease with clinical features similar to the disease caused by the enzyme deficiency (see Fig. 4.4.1) [25]. Niemann-Pick disease type C (NPC) is an exception in that this complex (glycosphingo-)lipid storage disease is not caused by an enzyme deficiency, but can be considered as a (glycosphingo-)lipid trafficking defect caused by a deficiency of one of two proteins NPC1 or NPC2 (Table 4.4.1) [57].

Sphingolipidoses are clinically and genetically heterogeneous and may present at any age, varying from a very severe presentation with hydrops fetalis [65], to late-onset diseases with mainly psychiatric symptoms. In general, a good correlation exists between the levels of residual enzyme activity and the clinical severity of the disease [27]). A classification of subtypes with infantile, juvenile, and adult presentation is useful, but it should be realized that in many diseases the presentation of each individual patient is part of a continuum of possible clinical presentations [15, 18, 41, 57]. All sphingolipidoses present with neurological disease with the exception of Fabry disease, Gaucher disease type 1, and Niemann-Pick disease type B. This stands to reason considering the important role of glycosphingolipids in neuronal cells and myelin. In addition to neurological symptoms, some sphingolipidoses present with visceral symptoms and skeletal problems. For example, patients with the early-onset form of GM1-gangliosidosis present with features resembling the mucopolysaccharidoses and the oligosaccharidoses in addition to neurological problems. This stems from the fact that the enzyme β-galactosidase also plays a role in the lysosomal degradation of mucopolysaccharides and oligosaccharides. A summary of the main presenting features of each disease is given by Wenger et al. [60] and Beck [3]. More detailed information can be obtained from authoritative reviews [50].

Lysosomal storage diseases are rare, with an estimated birth prevalence of about 1:5000 to 1:7000 newborns. The sphingolipidoses make up about one-half of the total number of patients with lysosomal storage diseases [35, 44, 45]. In some popu-

Table 4.4.1 *Enzyme and protein deficiencies and the associated sphingolipid storage disorders.* D *Dried blood spot,* F *fibroblasts,* L *leukocytes,* NPC1 *Niemann-Pick disease type C1,* NPC2 *Niemann-Pick disease type C2,* OMIM *Online Mendelian Inheritance in Man,* P *plasma,* U *urine*

Sphingolipidosis	OMIM numbers	Enzyme deficiency/defective protein	Source of enzyme for postnatal diagnosis	Main glycosphingolipid storage products	Sample for storage product analysis
GM1-gangliosidosis types I, II, and III	230500/230600/230650	Acid β-galactosidase (EC 3.2.1.23)	L, F, P, D	GM1-ganglioside	U (oligosaccharides)
GM2-gangliosidosis, B-variant, Tay-Sachs disease	272800	β-Hexosaminidase A (EC3.2.1.52)	L, F, P, D	GM2-ganglioside	
GM2-gangliosidosis, O-variant, Sandhoff disease	268800	β-Hexosaminidase A and B (EC 3.2.1.52)	L, F, P, D	GM2-ganglioside, GA2 (asialio-GM2)-ganglioside, globoside	U (oligosaccharides)
Gaucher disease types I, II, and S	230800/230900/231000	β-Glucocerebrosidase (EC 3.2.1.46)	L, F, P, D	Glucocerebroside	P
Farber disease	228000	Acid ceramidase (EC 3.5.1.23)	L, F	Ceramide	
Fabry disease	301500	α-Galactosidase A (EC 3.2.1.47)	L, F, P, D	Ceramide trihexoside, digalactosylceramide	U, P
Krabbe disease	245200	β-Galactocerebrosidase (EC 3.2.1.45)	L, F	Galactocerebroside	
Metachromatic leukodystrophy	250100	Arylsulfatase A (EC 3.1.6.8)	L, F	Sulfatide	U
Niemann-Pick disease types A and B	257200/607616	Acid sphingomyelinase (EC 3.1.4.12)	L, F, D	Sphingomyelin	
NPC1	257220	NPC1 protein	F	Complex (glyco-sphingo-)lipid storage disorder	
NPC2	607625	NPC2 protein	F	Complex (glyco-sphingo-)lipid storage disorder	

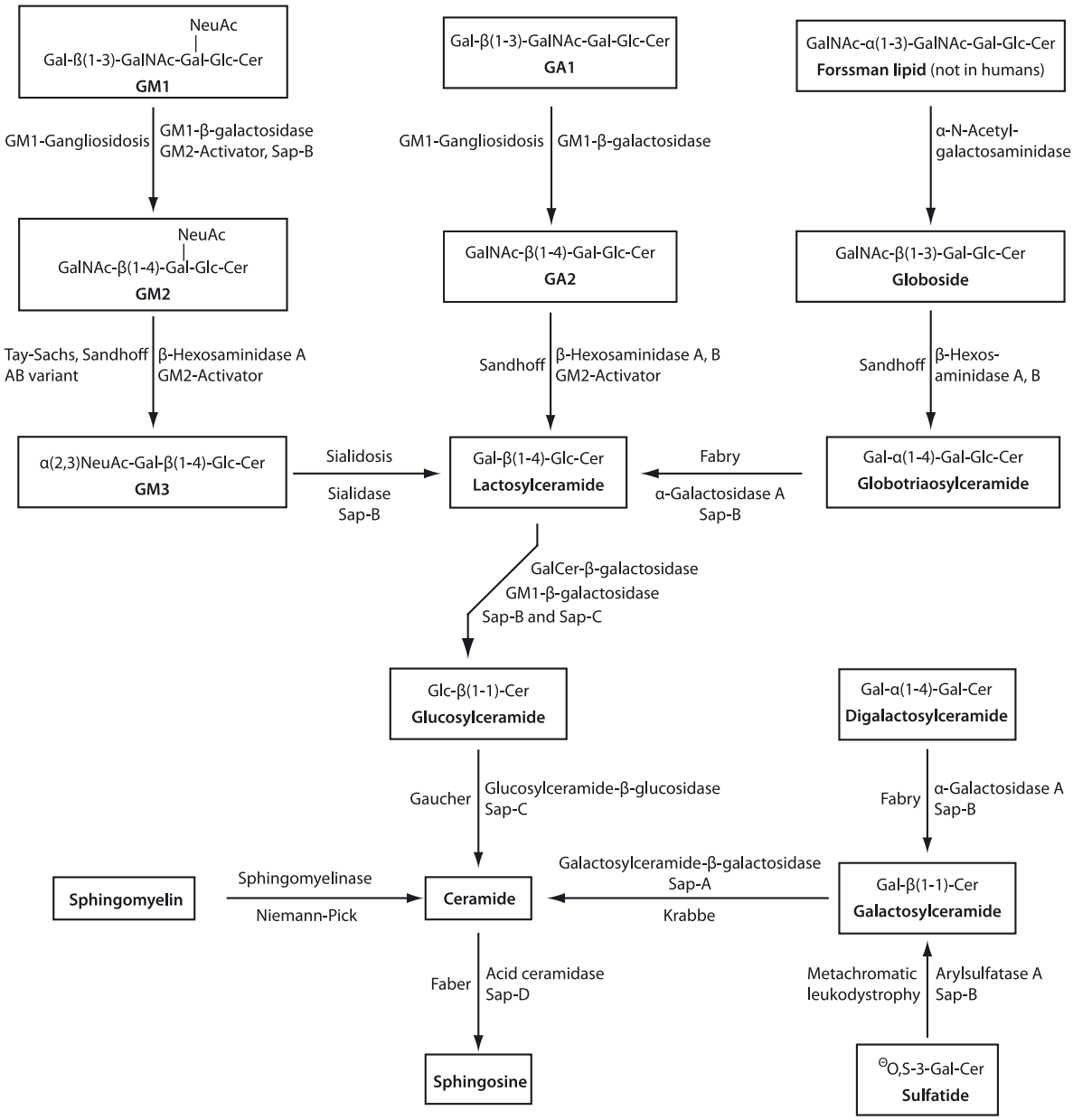

Fig. 4.4.1 Stepwise degradation of sphingolipids by lysosomal hydrolases and the activator proteins required for each step. The names of the sphingolipidoses corresponding to each hydrolase deficiency are indicated. Adapted from Kolter and Sandhoff [25]. *Cer* Ceramide, *GA1* asialo-GM1-ganglioside, *GA2* asialo-GM2-ganglioside, *Gal* galactose, *GalNAc* N-acetylgalactosamine, *Glc* glucose, *GM1* GM1-ganglioside, *GM2* GM2-ganglioside, *NeuAc* N-acetylneuraminic acid, *Sap* saposin

lations the birth prevalence is much higher. For example, Tay-Sachs disease, Niemann-Pick disease type A/B, and Gaucher disease are particularly prevalent among the Ashkenazi Jewish population in the United States and Israel, where prevention programs based on heterozygote detection have been implemented for these diseases [1, 24]. All sphingolipidoses are autosomal recessive diseases with the exception of Fabry's disease, which is X-linked.

While the genes for all of the sphingolipidoses are known and many mutations have been characterized [14], molecular analysis is rarely used for the initial diagnosis of a patient suspected of suffering from a sphingolipidosis. Rather, determination of the enzyme activity in easily obtainable cells like leukocytes and fibroblasts and in dried blood spots (in some instances supplemented by the identification of storage products in urine or plasma) are the methods of choice for diagnosing new patients (Table 4.4.1). For NPC, the diagnostic work-up involves showing the presence of a cholesterol-trafficking defect in fibroblasts [42, 58].

Since there is always some overlap between enzyme activities observed in carriers and normal individuals from the general population, enzyme analysis does not usually give a definitive answer with respect to carrier testing. Here, molecular analysis within an affected family can give the definitive answer provided the mutation is known. For carrier testing of members from the general population, screening for common mutations has been implemented for some diseases [1]. Mutation analysis can also be used for prenatal testing for all of the sphingolipidoses and is especially useful in those cases where a low enzyme activity can be expected, such as carrier status or pseudodeficiency in Krabbe disease or metachromatic leukodystrophy [46, 61]. A pseudodeficiency is defined as the in vitro measurement of low enzyme activity in a healthy person. In most cases the finding of a deficient enzyme activity could be considered as diagnostic for a certain lysosomal storage disorder, especially when the clinical symptoms are characteristic for the disease. However, the occurrence of a pseudodeficiency in patients with milder or atypical symptoms may lead to diagnostic confusion. The enzyme activity measured in vitro in pseudodeficiency states is usually less than 15% of the normal mean for controls and is difficult to distinguish from the enzyme deficiency measured in affected patients. Pseudodeficiencies have been reported for β-hexosaminidase A, β-hexosaminidase A and B, β-galactosidase A, β-galactocerebrosidase, and arylsulfatase A [53]. In the case of arylsulfatase A the pseudodeficiency mutation is particularly prevalent, with a carrier frequency of 15–20%. This implies that homozygotes and compound heterozygotes carrying a pseudodeficiency allele and a mutation causing metachromatic leukodystrophy are frequently found among individuals with low arylsulfatase A activity. These individuals have no clinical evidence of disease. This means that great care has to be taken in interpreting an arylsulfatase A deficiency. Additional test such as mutation analysis and the determination of sulfatide in urine (see below) are necessary to establish the diagnosis of metachromatic leukodystrophy with certainty, especially in cases with a mild or atypical clinical phenotype. It is important to note that mutations causing metachromatic leukodystrophy can also occur in *cis* with the common pseudodeficiency mutation [46].

Prenatal diagnosis is available for all the sphingolipidoses. This makes an early and reliable diagnosis of the utmost importance. For many of the sphingolipidoses, symptomatic treatment in the form of bone marrow transplantation, enzyme replacement therapy, substrate reduction therapy, or chemical chaperone therapy is

either available or under development [3]. In general it can be stated that therapy, when available, should start as early as possible or as early as indicated, again emphasizing the importance of an early diagnosis [34]. This has led some authors to consider the possibility of newborn screening for lysosomal storage disorders [33] and the development of methodology to diagnose asymptomatic patients through a newborn screening program [32]. Some biochemical markers have proved useful in monitoring the effect of therapy and will be discussed here.

The selection of biochemical tests is based on the patient's clinical history, the suggestions from the physician, and the experience of the laboratory. The clinical biochemical geneticist should be familiar with the clinical presentation of the different lysosomal storage disorders and their subtypes in order to be able to select the most appropriate tests and to interpret the test results. Therefore, it is strongly recommended that the diagnostic work-up of patients with sphingolipidoses be restricted to specialized laboratories with sufficient experience in diagnosing patients with these rare disorders.

4.4.2 Enzyme Activity Determinations

4.4.2.1 General Principle

All enzymes are measured at acidic pH with artificial fluorogenic substrates, except for arylsulfatase A, which is measured with a chromogenic substrate. The fluorogenic substrates are derivatives of 4-methylumbelliferone or 6-hexadecanoylamino-4-methylumbelliferone. The reactions with fluorogenic substrates are stopped with a basic buffer and the strong fluorescence of the liberated 4-methylumbelliferone is measured at excitation wavelength 366 nm and emission wavelength 442 nm with a fluorometer equipped with a flow cell and a sipper device; 6-hexadecanoylamino-4-methylumbelliferone is measured at an excitation wavelength of 372 nm and emission wavelength 442 nm with 4-methylumbelliferone as standard. 6-Hexadecanoylamino-4-methylumbelliferone has become available commercially only recently; its use as a standard instead of 4-methylumbelliferone will make possible more accurate measurements of the specific activities of β-galactocerebrosidase (see 4.4.10) and acid sphingomyelinase (see 4.4.13). In the procedures for the enzyme assays described below, the tests are usually performed in test tubes or Eppendorf vials using incubation volumes of 30–150 µl. The final volume after addition of stop buffer is 3 ml for test tubes and 1.5 ml for Eppendorf vials. Alternatively, these assays may be performed on 96-well plates using a fluorometer for microtiter plates (see also Chap. 4.1) by proportionally decreasing the incubation volume and adjusting the volume of stop buffer. Specific activities are usually expressed as nmol/mg protein·h or nmol/mg protein·incubation time for homogenates from leukocytes and fibroblasts, and as µmol/l·h for plasma and dried blood spots. As mentioned in the introduction (section 4.4.1), the use of artificial substrates precludes the detection of activator protein deficiencies. When a normal result for the enzyme assay is obtained despite a strong clinical suspicion for a particular sphingolipidosis, additional tests must be applied to confirm or exclude an activator protein deficiency. Some of these tests will be discussed below, while others are only performed in a few laboratories with a special interest in these lysosomal storage diseases. In general, the use of

artificial substrates instead of more natural radioactive substrates poses no problems in identifying patients with a lysosomal enzyme deficiency. However, in some cases, for example in Niemann-Pick disease type A/B, the use of artificial substrates has led to false-negative results [18]. In this case the use of the chromogenic substrate 2-N-(hexadecanoyl)amino-4-nitrophenylphosphorylcholine is not recommended and the assay with the fluorogenic substrate 6-hexadecanoylamino-4-methylumbelliferylphosphorylcholine should be used with caution [54]. Assay using natural radioactive substrate is probably still the most reliable and will be described below in addition to assay using a fluorogenic substrate.

4.4.2.2 Specimen

The activity of the lysosomal enzymes involved in glycosphingolipid degradation is measured at acidic pH with homogenates from leukocytes or fibroblast. Plasma samples may also be used for some enzymes (Table 4.4.1). Leukocytes isolated from ethylenediaminetetraacetic acid-treated blood (EDTA-blood) are the preferred material for first-line screening. Heparin is also acceptable as an anticoagulant. The isolation of leukocytes from whole blood is performed by standard procedures, either by the dextran sedimentation method [51] or the ammonium chloride lysis method [48]. Leukocytes pellets and plasma samples are stored at –80 C until use. Fibroblast cultures are started from skin biopsy samples using standard tissue-culture techniques. Fibroblasts are grown in Ham's F-10 medium until 1 week past confluency. Cells are harvested and cell pellets are stored at –80 C. Leukocyte and fibroblast pellets are taken up in 0.2 ml ice-cold distilled water and sonicated briefly (3–5 s) at low power with a Branson sonicator equipped with a microprobe. The protein content of the homogenates is measured with the Folin phenol reagent [29] or other (commercially) available methods. Homogenates are either used fresh or stored at –20 C until use.

Recently dried blood spots have been shown useful for the determination of several lysosomal enzymes involved in glycosphingolipid degradation [7–10]. Lysosomal enzymes are remarkably stable on the dried blood spots, allowing easy transportation over long distances by regular mail. Only small blood volumes are required and there is no need to isolate leukocytes prior to enzyme assay. In addition, dried blood spots are the material of choice for possible newborn screening of lysosomal storage diseases. Some, but not all, standard enzyme assays for the diagnosis of sphingolipidoses in leukocytes can be easily adapted for dried blood spots (Table 4.4.1). A disadvantage of dried blood spots is that the amount of enzyme is fixed and may not be optimal for each assay. In addition inhibitors of some enzymes may be present and hemoglobin may considerably quench the fluorescence of 4-methylumbelliferone when present at high concentrations. This should be taken into account when the assays described here are adapted for microtiter plates. Dried blood spots are prepared on newborn screening cards (Schleicher & Schull filter paper number 903) by pipetting exactly 65 µl EDTA-blood onto the center of each circle on the screening card. Blood spots are dried overnight at room temperature and subsequently stored at 4 C in a sealed plastic bag. Enzyme assays are performed with a 3-mmdiameter punch, which corresponds to approximately 3.4 µl blood. About ten punches can be taken from each bloodspot.

For the determination of glycosphingolipids in urine, a 24-h or a first-morning voiding urine is collected.

4.4.2.3 Quality Control and Validation

Both internal and external quality controls are necessary to be able to perform the enzymatic diagnostic work-up of patients with lysosomal storage disorders with confidence. There is currently no formal external quality control program, but these are now under development in Europe [30, 49]. Each laboratory should develop a system of internal quality control, which as minimal elements should contain a check for each assay on linearity with incubation time and protein concentration and the ability of each assay to detect a deficiency in patients. In other words: each laboratory should perform an analytical and clinical validation of each assay. In addition the intra- and interassay variability of each assay should be determined. Leukocyte pellets sufficient for at least 1 year are prepared from one single source and kept frozen at –80 C. A large batch of bloodspots is prepared from 5–10 ml blood from one single source. For each assay, a reference sample is run in duplicate as a quality control. The specific activity of the reference sample should fall between predetermined values, which depend on the interassay variability or reproducibility of a given assay. The value of the reference samples should generally lie between the mean ±2 standard deviations. If the control value is outside the acceptable range the test should be discarded. A control chart is kept on which the consecutive values are recorded to obtain a running average and standard deviation and to detect sudden changes or trends in the specific activity of the control sample, for example, when a new batch of substrate is used [28, 49]. Each new batch of substrate should be tested for purity by measuring the blank values and for its suitability to detect patients by measuring the residual activity in a known patient sample. In addition, the quality of each sample should be assessed by measuring a reference enzyme, for example, acid β-galactosidase activity, whose activity should fall within the reference range. All assays are performed in duplicate. Each laboratory should establish its own reference values for normal and pathological ranges for each assay.

4.4.3 Enzyme Assays

4.4.3.1 Stock Solutions for the Preparation of Reaction Buffers

Assays are performed at acidic pH either in 0.1 M citrate buffer/0.2 M phosphate buffer or in acetate buffers.

1. Citric acid stock solution (0.1 M): dissolve 21.0 g citric acid monohydrate in 1000 ml water.
2. Phosphate stock solution (0.2 M): dissolve 35.6 g $Na_2HPO_4 \cdot 2H_2O$ in 1000 ml water.
3. Sodium acetate trihydrate stock solution (0.1 M): dissolve 13.6 g in 1000 ml water.
4. Acetic acid (0.1 M): dilute 5.7 ml glacial acetic acid to 1 l with water.

4.4.3.2 Stop Buffers

The stop buffer comprises 0.2 M Na_2CO_3/glycine pH 10.5: Dissolve 21.2 g Na_2CO_3 in 400 ml water. Dissolve 3.75 g glycine in 100 ml water. Titrate 400 ml of the Na_2CO_3 solution with the glycine solution to pH 10.5. Add water to 1 L. This stop buffer is used in all assays unless indicated otherwise. When assays are adapted to microtiter plates, detergent (0.025% w/v Triton X-100) should be present in the stop buffers in order to minimize meniscus effects.

4.4.3.3 Standard 4-Methylumbelliferone Solution

Dissolve 17.6 mg 4-methylumbelliferone (molecular weight, MW, 176) in 10 ml stop buffer to a final concentration of 10 mM. Dilute stepwise to 10 µM.

4.4.4 Acid β-Galactosidase (EC 3.2.1.23)

This enzyme is deficient in GM1-gangliosidosis (Table 4.4.1, Fig. 4.4.1). The assay is based on the method described by Ho and O'Brien [19, 20].

4.4.4.1 Reagents and Chemicals

1. Reaction buffer: mix 57 ml 0.1 M citric acid with 43 ml 0.2 M phosphate solution and dissolve 1.17 g NaCl (0.2 M) in the buffer. Adjust the pH to 4.3 with either citric acid or phosphate solution.
2. Substrate/buffer solution: dissolve 1.70 mg 4-methylumbelliferyl-β-D-galactopyranoside (MW 338.3) in 10 ml of reaction buffer to a final concentration of 0.5 mM.

4.4.4.2 Assay Conditions

1. Incubate 10 µl homogenate (5 µg of leukocyte protein or 1–2 µg of fibroblast protein) with 100 µl substrate/buffer for 30 min at 37 C.
2. Incubate 10 µl plasma with 100 µl substrate/buffer for 60 min at 37 C.
3. Incubate one bloodspot with 100 µl substrate/buffer for 2 h at 37 C.
4. Blank incubation: incubate with water instead of protein.
5. Stop the reaction with 2.89 ml stop buffer for test tubes or 1.39 ml stop buffer for vials.
6. Read the fluorescence at excitation wavelength 366 nm and emission wavelength 442 nm. Include a two-point calibration curve of 500 and 1000 pmol 4-methylumbelliferone (50 and 100 µl of the 10 µM standard solution); this curve should be linear.

4.4.4.3 Reference Values/Pathological Values

1. Reference range for leukocytes: 80–240 nml/mg·h.
2. Pathological range for leukocytes: < 10 nmol/mg·h.
3. Reference range for fibroblasts: 350–800 nmol/mg·h.
4. Pathological value for fibroblasts: < 10 nmol/mg·h.
5. Reference range for dried blood spots: 40–150 µmol/l·h.
6. Pathological range for dried blood spots: < 5 µmol/l·h.

4.4.5 β-Hexosaminidase A (EC 3.2.1.52)

This enzyme is deficient in GM2-gangliosidosis, B-variant (Tay-Sachs disease; Table 4.4.1, Fig. 4.4.1). The assay is based on the method described by Inui and Wenger [23].

4.4.5.1 Reagents and Chemicals

1. Reaction buffer: mix 58.6 ml 0.1 M citric acid with 41.4 ml 0.2 M phosphate solution. Adjust the pH to 4.2 with either citric acid or phosphate solution.
2. Substrate/buffer solution. Dissolve 25 mg 4-methylumbelliferyl-6-sulfo-2-acetamido-2-deoxy-β-D-glucopyranoside (sodium salt, MW 483.5) in 2.58 ml of reaction buffer to a final concentration of 20 mM.

4.4.5.2 Assay Conditions

1. Incubate 20 µl homogenate (10 µg leukocyte protein or 10 µg of fibroblast protein) with 25 µl reaction buffer and 5 µl substrate/buffer for 20 min at 37 C.
2. Incubate 10 µl plasma with 35 µl reaction buffer and 5 µl substrate/buffer for 20 min at 37 C.
3. Incubate one bloodspot with 20 µl water, 25 µl reaction buffer, and 5 µl substrate/buffer for 2 h at 37 C.
4. Blank incubation: incubate with water instead of protein.
5. Stop the reaction with 2.95 ml stop buffer for reaction tubes and 1.45 ml stop buffer for vials.
6. Read the fluorescence at excitation wavelength 366 nm and emission wavelength 442 nm. Include a two-point calibration curve of 500 and 1000 pmol 4-methylumbelliferone (50 and 100 µl of the 10-µM standard solution); this curve should be linear.

4.4.5.3 Reference Values/Pathological Values

1. Reference range for leukocytes: 150–365 nmol/mg·h.
2. Pathological value for leukocytes: < 15 nmol/mg·h.
3. Reference range for fibroblasts: 500–1500 nmol/mg·h.

4. Pathological value for fibroblasts: < 60 nmol/mg·h.
5. Reference range for dried blood spots: 60–150 µmol/l·h.
6. Pathological range for dried blood spots: < 10 µmol/l·h.

4.4.5.4 Special Remarks/Pitfalls

β-Hexosaminidase A is also deficient in GM2-gangliosidosis, O-variant (Sandhoff disease), when measured with this assay, but to a lesser degree than in Tay-Sachs disease. When a normal activity of *β*-hexosaminidase A is found in a patient with characteristic symptoms of Tay-Sachs disease, the possibility of a GM2-activator protein deficiency should be considered (GM2-gangliosidosis AB variant; see Fig. 4.4.1). This activator protein deficiency can be diagnosed by decreased metabolism of GM2-ganglioside in living fibroblasts upon a ganglioside-loading test or by mutation analysis of the GM2-activator protein gene. These tests are available in a few specialized laboratories only.

4.4.6 *β*-Hexosaminidase A and B (EC 3.2.1.52)

These enzymes are deficient in GM2-gangliosidosis, O-variant (Sandhoff disease; Table 4.4.1, Fig. 4.4.1). The assay is based on the method described by O'Brien et al. [40].

4.4.6.1 Reagents and Chemicals

1. Reaction buffer: mix 55.9 ml 0.1 M citric acid with 44.1 ml 0.2 M phosphate solution. Adjust the pH to 4.4 with either citric acid or phosphate solution.
2. Substrate/buffer solution: dissolve 20 mg 4-methylumbelliferyl-2-acetamido-2-deoxy-*β*-D-glucopyranoside (MW 379.4) in 10.5 ml of reaction buffer to a final concentration of 5 mM.
3. 1% (w/v) bovine serum albumin (BSA) solution: dissolve 10 mg BSA in 1 ml of water and heat inactivate for 2 h at 56 C.

4.4.6.2 Assay Conditions

1. Incubate 45 µl homogenate (4 µg leukocyte protein or 1 µg of fibroblast protein) with 5 µl 1% BSA and 50 µl substrate/buffer for 30 min at 37 C.
2. Incubate 5 µl plasma and 45 µl water with 100 µl substrate/buffer for 30 min at 37 C.
3. Incubate one blood spot with 50 µl water and 50 µl substrate/buffer for 30 min at 37 C.
4. Blank incubation: incubate with water instead of protein.
5. Stop the reaction with either 2.90 or 2.85 ml stop buffer for test tubes or 1.4 or 1.35 ml of stop buffer for vials.

6. Read the fluorescence at excitation wavelength 366 nm and emission wavelength 442 nm. Include a two-point calibration curve of 500 and 1000 pmol 4-methylumbelliferone (50 and 100 µl of the 10-µM standard solution); this curve should be linear.

4.4.6.3 Reference Values/Pathological Values

1. Reference range for leukocytes: 600–3500 nml/mg.h.
2. Pathological value for leukocytes: < 125 nmol/mg·h.
3. Reference range for fibroblasts: 3000–20000 nmol/mg·h.
4. Pathological value fibroblasts: < 250 nmol/mg·h.
5. Reference range for dried blood spots: 560–1200 µmol/l·h.
6. Pathological value for dried blood spots: < 50 µmol/l·h.

4.4.7 β-Glucocerebrosidase (EC 3.2.1.45)

This enzyme is deficient in Gaucher disease (Table 4.4.1, Fig. 4.4.1). The assay is based on the method described by Peters et al. [43] and Daniels et al. [11].

4.4.7.1 Reagents and Chemicals

1. Reaction buffer: mix 43 ml 0.1 M citric acid with 57 ml 0.2 M phosphate solution. Adjust the pH to 5.5 with either citric acid or phosphate solution.
2. 15% (w/v) Taurocholate: dissolve 30 mg taurocholate in 2 ml reaction buffer.
3. Substrate/buffer solution. Dissolve 6.8 mg 4-methylumbelliferyl-β-D-glucopyranoside (MW 338.3) in 3.6 ml of reaction buffer to a final concentration of 5.6 mM. Add 0.4 ml of taurocholate in reaction buffer and mix. The final substrate concentration is 5 mM.

4.4.7.2 Assay Conditions

1. Incubate 50 µl homogenate (40 µg of leukocyte protein or 1–2 µg of fibroblast protein; preferably freshly prepared) with 100 µl substrate/buffer for 1 h at 37 C.
2. Incubate one blood spot with 50 µl water and 100 µl substrate/buffer for 17 h at 37 C.
3. Blank incubation: incubate with water instead of protein.
4. Stop the reaction with 2.85 ml stop buffer for test tubes and 1.35 ml for vials.
5. Read the fluorescence at excitation wavelength 366 nm and emission wavelength 442 nm. Include a two-point calibration curve of 500 and 1000 pmol 4-methylumbelliferone (50 and 100 µl of the 10-µM standard solution); this curve should be linear.

4.4.7.3 Reference Values/Pathological Values

1. Reference range for leukocytes: 10–25 nmol/mg·h.
2. Pathological value for leukocytes: < 3 nmol/mg·h.
3. Reference range for fibroblasts: 160–580 nmol/mg·h.
4. Pathological value for fibroblasts: < 30 nmol/mg·h.
5. Reference range for dried blood spots: 1.3–6.2 µmol/l·h.
6. Pathological value for dried blood spots: < 0.7 µmol/l·h.

4.4.8 Chitotriosidase (EC 3.2.1.14)

This enzyme is increased in Gaucher disease and may also be increased, but to a lesser extent, in other sphingolipidoses such as Niemann-Pick disease type A/B and NPC, Krabbe disease, and GM1-gangliosidosis. The assay is based on the method described by Hollak et al. [22] and Guo et al. [17].

4.4.8.1 Reagents and Chemicals

1. Reaction buffer: mix 46.4 ml 0.1 M citric acid with 53.6 ml 0.2 M phosphate solution. Adjust the pH to 5.2 with either citric acid or phosphate solution. Dissolve 10 mg BSA in 10 ml reaction buffer and heat inactivate at 50 C for 2 h.
2. Substrate/buffer solution: dissolve 1 mg 4-methylumbelliferyl-β-N-N,N",-triacetylchitotriose (MW 786) in 578 µl reaction buffer to a final concentration of 2.22 mM. Store at –20 C. Dilute 100 µl of this solution with 9.90 ml reaction buffer to a final concentration of 4-methylumbelliferyl- β-N-N,N",-triacetylchitotriose of 0.22 mM.

4.4.8.2 Assay Conditions

1. Incubate 5 µl plasma (1:50 diluted with water in the case of Gaucher disease) with 100 µl substrate/buffer for 30 min at 37 C.
2. Incubate one blood spot with 100 µl substrate/buffer for 1 h at 37 C.
3. Stop the reaction with 2.895 ml stop buffer for test tubes and 1.395 ml for vials and with 1.4 ml in the case of blood spots.
4. Read the fluorescence at excitation wavelength 366 nm and emission wavelength 442 nm. Include a two-point calibration curve of 500 and 1000 pmol 4-methylumbelliferone (50 and 100 µl of the 10 µM standard solution); this curve should be linear.

4.4.8.3 Reference Values/Pathological Values

1. Reference range for plasma: 0–200 µmol/l·h.
2. Pathological value for plasma >200 µmol/l·h.
3. Reference range for dried blood spots: 15–290 µmol/l·h.
4. Pathological value for dried blood spots: >300 µmol/l·h.

4.4.8.4 Special Remarks/Pitfalls

When a strongly increased value of chitotriosidase activity is obtained with plasma, such as in Gaucher disease, the assay should be repeated with a 1:50 diluted plasma sample. When chitotriosidase is measured in blood spots from Gaucher patients the incubation time should be reduced to 10 min in order to accurately measure the strongly increased activity.

Chitotriosidase is deficient in about 6% of the general population. This is an autosomal recessive trait and the high carrier frequency has to be taken into account when comparing patient values [5]. Chitotriosidase measurements are also extremely useful for monitoring the effect of enzyme therapy or substrate reduction therapy in patients with Gaucher disease [21]. In case of a deficiency of chitotriosidase, the determination of the chemokine CCL 18/PARC is a good alternative [6, 12]. Chitotriosidase should also be measured when a normal β-glucocerebrosidase activity is found in a patient with symptoms characteristic of Gaucher disease. Increased chitotriosidase is indicative of an activator protein/saposin C deficiency in such cases (Fig. 4.4.1). In addition the measurement of glucocerebroside in plasma could be useful [16]. As stated above, chitotriosidase may be moderately increased in other sphingolipidoses, but the sensitivity to detect patients is less than 100% [17, 47].

4.4.9 α-Galactosidase A (EC 3.2.1.47)

This enzyme is deficient in Fabry disease (Table 4.4.1, Fig. 4.4.1). The assay is based on the methods described by Desnick et al. [13] and Mayes et al. [31].

4.4.9.1 Reagents and Chemicals

1. Reaction buffer 0.1 M acetate buffer pH 4.5: mix 43 ml 0.1 M sodium acetate stock solution with 57 ml 0.1 M acetic acid. Adjust the pH to 4.5 with either acetate or acetic acid.
2. Substrate/buffer: dissolve 8.5 mg of 4-methylumbelliferyl-α-d-galactopyranoside (MW 338.3) in 5 ml reaction buffer to a final concentration of 5 mM.
3. 1.0 M N-acetylgalactosamine (MW 221): dissolve 2.21 g N-acetylgalactosamine in water and bring the final volume to 10 ml.

4.4.9.2 Assay Conditions

1. Incubate 35 µl homogenate (10 µg of leukocyte protein or 15 µg of fibroblast protein) with 15 µl 1.0 M N-acetylgalactosamine and 100 µl substrate/buffer for 30 min at 37 C.
2. Incubate 25 µl plasma with 25 µl H_2O and 100 µl substrate/buffer for 30 min at 37 C.
3. Incubate one blood spot with 35 µl water, 15 µl 1.0 M N-acetylgalactosamine, and 100 µl substrate/buffer for 17 h at 37 C.
4. Blank incubation: incubate with water instead of protein.
5. Stop the reaction with 2.85 ml stop buffer for test tubes and 1.35 ml for vials.

6. Read the fluorescence at excitation wavelength 366 nm and emission wavelength 442 nm. Include a two-point calibration curve of 500 and 1000 pmol 4-methylumbelliferone (50 and 100 µl of the 10 µM standard solution); this curve should be linear.

4.4.9.3 Reference Values/Pathological Values

1. Reference range for leukocytes: 32–60 nmol/mg·h.
2. Pathological value for leukocytes hemizygotes: < 3 nmol/mg·h.
3. Pathological value for leukocytes heterozygotes: < 30 nmol/mg·h (see also 4.4.9.4).
4. Reference range for fibroblasts: 15–50 nmol/mg·h.
5. Pathological value for fibroblasts: < 3 nmol/mg·h.
6. Reference range for dried blood spots: 3.3–21.4 µmol/l·h.
7. Pathological value for dried blood spots: < 0.6 µmol/l·h.

4.4.9.4 Special Remarks/Pitfalls

Fabry disease is an X-linked disorder and accurate carrier detection is important for genetic counseling and because enzyme therapy is available for clinically affected hemizygote and heterozygote patients. Because of random X-inactivation, not all heterozygotes can be reliably identified by enzyme assay, and mutation analysis is strongly recommended.

4.4.10 β-Galactocerebrosidase (EC 3.2.1.46)

This enzyme is deficient in Krabbe disease (Table 4.4.1, Fig. 4.4.1). The assay is based on the method described Wiederschain et al. [64] as modified by van Diggelen (unpublished data).

4.4.10.1 Reagents and Chemicals

1. Oleic acid stock solution: dissolve 6 mg oleic acid (MW 282) in 1 ml of hexane (prepare fresh).
2. Taurocholate stock solution: dissolve 30 mg sodium taurocholate (MW 538) in 1 ml chloroform/methanol (2/1 v/v).
3. Stock solution 6-hexadecanoylamino-4-methylumbelliferyl- β-D-galactopyranoside (MW 591): dissolve 2.66 mg in 5 ml chloroform/methanol (2/1 v/v) to a final concentration of 0.9 mM.
4. Reaction buffer: mix 46.4 ml citric acid with 53.6 ml phosphate solution. Adjust the pH to 5.2 with either citric acid or phosphate solution.
5. Substrate/buffer solution (prepare fresh): Mix 75 µl oleic acid, 50 µl taurocholate and 250 µl 6-hexadecanoylamino-4-methylumbelliferyl- β-d-galactopyranoside stock solution in a 1.5-ml Eppendorf vial and take the mixture to dryness under a gentle stream of nitrogen. Add 500 µl of reaction buffer at room temperature,

mix vigorously on a Vortex mixer. Sonicate the solution for 10 s using a Branson sonicator with a microprobe. The final concentrations of oleic acid, taurocholate, and 6-hexadecanoylamino-4-methylumbelliferyl- β-D-galactopyranoside are 0.9 mg/ml, 3 mg/ml, and 0.45 mM, respectively.
6. Stop buffer 0.2 M glycine/NaOH buffer pH 10.7, 0.2% (w/v) sodiumdodecyl sulfate, 0.2% (w/v) Triton X-100.

4.4.10.2 Assay Conditions

1. Incubate 10 µl homogenate (20 µg of leukocyte protein or 20 µg of fibroblast protein) with 20 µl substrate/buffer for 17 h at 37 C in Eppendorf vials.
2. Blank incubation: incubate with water instead of protein.
3. Stop the reaction with 1.47 ml stop buffer.
4. Read the fluorescence at excitation wavelength 372 nm and emission wavelength 442 nm. Include a two-point calibration curve of 500 and 1000 pmol 4-methylumbelliferone (50 and 100 µl of the 10 µM standard solution in stop buffer); this curve should be linear.

4.4.10.3 Reference Values/Pathological Values

1. Reference range for leukocytes: 25–105 nmol/mg·17 h.
2. Pathological value for leukocytes: < 4 nmol/mg·17 h.
3. Reference range for fibroblasts: 12–40 nmol/mg·17 h.
4. Pathological value for fibroblasts: < 2.5 nmol/mg·17 h.

4.4.10.4 Special Remarks

A normal low activity allele for galactocerebrosidase due to polymorphic mutations in the GALC (galactocerebrosidase) gene may be present. When polymorphic mutations are present in both GALC alleles or when a low-activity GALC allele is present in the compound heterozygous state with a Krabbe allele, this may pose diagnostic difficulties, especially in patients with nonspecific neurological problems or in the case of a prenatal diagnosis. Therefore, it is very important to measure galactocerebrosidase in the parents of a (suspected) Krabbe patient [62]. In such cases, and also for carrier testing, mutation analysis can be useful.

4.4.11 Arylsulfatase A (EC 3.1.6.8)

This enzyme is deficient in metachromatic leukodystrophy (Table 4.4.1, Fig. 4.4.1). The assay is based on the method described by Baum et al. [2] as modified by Lee-Vaupel et al. [26].

4.4.11.1 Reagents and Chemicals

1. Reaction buffer 0.5 M acetate buffer pH 4.5: mix 43 ml 0.5 M sodium acetate stock solution with 57 ml 0.5 M acetic acid. Adjust the pH to 4.5 with either acetate or acetic acid. Dissolve 9.93 g NaCl (MW 58.4) and 13.3 mg $Na_4P_2O_7$ (MW 265.9) in the acetate buffer and bring the volume to 100 ml. The final concentrations of NaCl and $Na_4P_2O_7$ are 1.7 M and 0.5 mM, respectively.
2. Substrate/buffer: dissolve 31.1 mg p-nitrocatecholsulfate (MW 311) in 10 ml of reaction buffer to a final concentration of 10 mM.
3. 1 M NaOH: dissolve 4 g NaOH in 100 ml water.

4.4.11.2 Assay Conditions

1. Incubate 50 µl homogenate (100 µg of leukocyte protein or 30 µg of fibroblast protein) with 200 µl substrate/buffer for 17 h at 0 C in Eppendorf vials on melting ice in the cold room or refrigerator.
2. Blank incubation: incubate with water instead of protein.
3. Protein blank: incubate protein with water instead of substrate/buffer.
4. Stop the reaction with 250 µl 1 N NaOH. Read the extinction in a spectrophotometer in microcuvettes at 515 nm. The molar extinction coefficient of p-nitrocatechol at 515 nm is 12,400/Mol/cm.

4.4.11.3 Reference Values/Pathological Values

1. Reference range for leukocytes: 45–260 nmol/mg·17 h.
2. Pathological value for leukocytes: < 15 nmol/mg·17 h.
3. Reference range for fibroblasts: 550–1100 nmol/mg·17 h.
4. Pathological value for fibroblasts: < 60 nmol/mg·17 h.

4.4.11.4 Special Remarks/Pitfalls

In case of a deficiency of arylsulfatase A, at least one other sulfatase should be measured to exclude multiple sulfatase deficiency (see Chap. 4.1 for the assays of arylsulfatase B and other sulfatases). Sulfatide excretion in urine should be measured (see assay below) and/or mutation analysis should to performed to confirm the diagnosis, especially if the clinical symptoms are atypical and in order to exclude a pseudodeficiency of arylsulfatase A. The enzyme should always be measured in the parents to check for the presence of compound heterozygosity of a metachromatic leukodystrophy and a pseudodeficiency allele. This is very important for the interpretation of the results of arylsulfatase A assays, especially when performed in asymptomatic or presymptomatic siblings or in the context of a prenatal diagnosis. Sulfatide should also be measured in case a normal arylsulfatase A activity is found in a patient with symptoms characteristic of (juvenile) metachromatic leukodystrophy. Increased urinary sulfatide excretion is indicative of an activator protein/saposin B deficiency (Fig. 4.4.1).

4.4.12 Sulfatide in Urine

Sulfatide in urine can be quantified by high-performance liquid chromatography (HPLC) [39] and tandem mass spectrometry techniques [63]. Here, a simple semi-quantitative thin-layer chromatography (TLC) method is described, as modified from Rafi et al. [46].

4.4.12.1 Reagents and Chemicals

1. Orcinol spray: dissolve 60 mg orcinol in 26 ml ethanol. Carefully add 4 ml concentrated sulfuric acid (95–97%) in the fume hood. Allow to cool before use and prepare fresh.
2. 0.6 M NaOH in methanol: dissolve 2.4 g NaOH in 100 ml methanol.
3. 0.5 M HCl in methanol: mix 4.13 ml HCl with methanol to a final volume of 100 ml.
4. 0.73% NaCl solution: dissolve 0.73 g NaCl in 100 ml distilled water.
5. Sulfatide standard solution: dissolve 0.9 mg sulfatides in 1 ml chloroform/methanol 2/1 (v/v)

4.4.12.2 Assay Conditions

Adjust the pH of 10 ml first morning voiding or 24-h collection of urine to pH 5.0 with a few drops of glacial acetic acid and leave at 4 C overnight. Centrifuge the urine at 1500 × *g* for 10 min. Resuspend the precipitate in 1 ml distilled water by brief sonication. Add 5 ml of chloroform/methanol 2/1 (v/v) and vortex for 1 min. Centrifuge for 5 min at 1500 × *g*. Remove the upper phase and dry the lower phase under a stream of nitrogen. Add 1 ml 0.6 M NaOH in methanol (prepare fresh). Vortex and leave for 1 h at room temperature. Neutralize with 1.2 ml 0.5 M HCl in methanol. Add 1.7 ml distilled water and 3.4 ml chloroform. Vortex and centrifuge for 5 min at 1500 × *g*. Remove the lower phase and dry with nitrogen. Add 50 µl chloroform/methanol 2/1 (v/v) and apply 25 µl to a silica gel 60 high-performance TLC plate together with 2.5, 5, 10, 15, and 20 nmol sulfatide standard. Develop the plate with chloroform/methanol/water 72/28/3.5 (v/v/v). Dry the plate and spray with orcinol spray. Heat at 100 C for approximately 10 minor until the pink color is fully developed. The excretion of sulfatide is estimated by either visual inspection of the plate or by densitometry.

4.4.12.3 Reference Values/Pathological Values

The method is semiquantitative. Pathological sulfatide levels are in the micromolar range and give clearly visible bands on orcinol spraying, while normal levels of sulfatide give barely visible or nonvisible bands.

4.4.13 Acid Sphingomyelinase (EC 3.1.4.12)

This enzyme is deficient in Niemann-Pick disease type A/B (Table 4.4.1, Fig. 4.4.1). The assay with radioactive natural substrate is based on the method described by Wenger [59]. The assay with fluorescent substrate is based on the method described by van Diggelen et al. [54]. These assays have not yet been validated in the authors' laboratory for use with dried blood spots. For this application the reader is referred to Chamoles et al. [9].

4.4.13.1 Reagents and Chemicals (Assay with Radioactive Natural Substrate)

1. Sodium acetate trihydrate stock solution (1.0 M): dissolve 13.6 g in 100 ml water.
2. Acetic acid (approximately 1.0 M): dilute 5.7 ml glacial acetic acid to 100 ml with water.
3. Reaction buffer: mix 70 ml sodium acetate with 30 ml acetic acid and adjust the pH to 5.0 with either sodium acetate or acetic acid solution.
4. 10% Triton X-100 (w/v) in chloroform/methanol 2/1 (v/v). Dissolve 1gr Triton X-100 in final volume of 10 ml chloroform/methanol 2/1.
5. ^{14}C-sphingomyelin (specific activity 50 mCi/mmol, concentration 0.02 mCi/ml, where 1 Ci = 3.7×10^{10} Bq).
6. Sphingomyelin 5 µmol/ml in chloroform/methanol 2/1.
7. Mix 150 µl ^{14}C-sphingomyelin (3 µCi, 60 nmol) with 488 µl (2440 nmol) cold sphingomyelin and add 1 ml 10% Triton X-100. Add chloroform/methanol to a final volume of 2.5 ml. The final concentration of sphingomyelin is 1 mM (specific activity 1.2 µCi/µmol).
8. 5% (w/v) BSA in H_2O (heat inactivated at 56 C for 30 min).

4.4.13.2 Assay Conditions (Assay with Radioactive Natural Substrate)

1. Pipette 50 µl substrate in glass tubes and evaporate the substrate solution under nitrogen.
2. Add 100 µl reaction buffer and vortex vigorously.
3. Add 100 µl homogenate (350 µg of leukocyte protein or 10 µg of fibroblast protein). Vortex vigorously.
4. Blank incubation: add 70 µl 5% BSA and 30 µl water instead of homogenate.
5. Incubate for 1.5 h at 37 C.
6. Stop the reaction by adding 100 µl ice-cold water and put the tubes on ice. Add 1.5 ml chloroform/methanol 2/1. Vortex and centrifuge for 5 min at 1000 × *g*.
7. Remove the lower (chloroform phase) and add 1 ml chloroform to the upper phase. Vortex and centrifuge for 5 min at 1000 × *g*.
8. Pipette carefully 400 µl from the upper phase (total volume 675 µl) in scintillation vials and add counting fluid suitable for counting water containing samples (Ultima Gold); measure the radioactivity in a scintillation counter.

4.4.13.3 Reagents and Chemicals (Assay with Fluorogenic Substrate)

1. Reaction buffer 0.1 M sodium acetate buffer pH 5.2: mix 79 ml 0.1 M acetate with 21 ml 0.1 M acetic acid and bring the pH to 5.2 with either acetate or acetic acid solution. Dissolve 20 mg sodium taurocholate in 10 ml of buffer to a final concentration of 0.2% (w/v).
2. Substrate/buffer: make a solution of 4 mg 6-hexadecanoylamino-4-methylumbelliferyl-phosphorylcholine (MW 610) in 5 ml reaction buffer to a final concentration of 1.32 mM. Briefly heat at 60 C until the solution becomes clear. Store in aliquots at –80 C until use.
3. Lysosphingomyelin 12 mmol/l (MW 464.6): dissolve 5.6 mg lysosphingomyelin/ml reaction buffer at room temperature.
4. Stop buffer: 0.2 M glycine/NaOH buffer pH 10.7, 0.2% (w/v) sodiumdodecyl sulfate, 0.2% (w/v) Triton X-100.

4.4.13.4 Assay Conditions (Assay with Fluorogenic Substrate)

1. Incubate 10 µl homogenate (30 µg of leukocyte protein or 5–10 µg of fibroblast protein) with 10 µl substrate/buffer and 10 µl reaction buffer or 10 µl lysosphingomyelin in reaction buffer for 17 h at 37 C in Eppendorf vials in the case of leukocytes, and 1 h at 37 C in the case of fibroblasts.
2. Blank incubation: incubate with water instead of protein.
3. Stop the reaction by adding 1.47 ml stop buffer.
4. Read the fluorescence at excitation wavelength 372 nm and emission wavelength 442 nm. Include a two-point calibration curve of 500 and 1000 pmol 4-methylumbelliferone (50 and 100 µl of the 10 µM standard solution in a total volume of 1.5 ml stop buffer; this curve should be linear.

4.4.13.5 Reference Values/Pathological Values for the Radioactive Natural Substrate

1. Reference range for leukocytes: 1.2–5.2 nmol/mg·h.
2. Pathological value for leukocytes: < 0.5 nmol/mg·h.
3. Reference range for fibroblasts: 200–500 nmol/mg·h.
4. Pathological value for fibroblasts: < 15 nmol/mg·h.

4.4.13.6 Reference Values/Pathological Values for the Fluorogenic Substrate

1. Reference range for leukocytes: 10–53 nmol/mg·17 h.
2. Pathological value for leukocytes: < 4 nmol/mg·17 h.
3. Reference range for fibroblasts: 100–420 nmol/mg·h.
4. Pathological value for fibroblasts: < 15 nmol/mg·h.

4.4.13.7 Special Remarks/Pitfalls

The specific activity of acid sphingomyelinase in leukocytes is relatively low, while the apparent residual activities with the fluorogenic substrate may be considerable, especially in Niemann-Pick disease type B patients. Special care is required in the lipid extraction step of the assay with radioactive natural substrate to ensure low blank values, especially when using leukocytes as the enzyme source. A serious drawback of the fluorogenic assay is that it does not detect a deficiency of acid sphingomyelinase in patients, who are homozygous or compound heterozygous for the Q292K mutation [18]. However, the presence of this mutation gives rise to an apparent lack of inhibition of acid sphingomyelinase in the fluorogenic assay by lysosphingomyelin in those patients as compared to controls [54].

4.4.14 Filipin Staining for Cholesterol Storage

Cholesterol storage in lysosomes/endosomes is a hallmark of Niemann-Pick type C disease. The assay is based on the procedure described by Vanier et al. [58].

4.4.14.1 Reagents and Chemicals

1. Hanks balanced salt solution.
2. Phosphate buffered saline (PBS).
3. Formalin (acid free); filter before use.
4. Fixative: mix 1 part of filtered formalin with 9 parts of PBS and add sucrose to a final concentration of 0.1 M. Adjust the pH to 7.4.
5. Filipin stock solution: dissolve 12.5 mg filipin in 5 ml dimethylformamide. Store at –20 C. Filipin assay solution: dissolve 20 µl filipin stock solution in 1 ml PBS.
6. 1,4-Diazabicyclo(2,2,2)octane (DABCO) stock solution: dissolve 1.25 g DABCO in 50 ml glycerol.
7. DABCO mounting solution: mix 3 ml PBS pH 7.4 with 27 ml DABCO stock solution. Store at 4 C.
8. Triton X-100 solution: dissolve 50 mg Triton X-100 in 100 ml PBS.

4.4.14.2 Assay

Grow the fibroblasts in Ham F-10 medium with 10% fetal calf serum (FCS). Harvest the cells, seed at a density of 30,000 cells and grow to near confluency on cover slips in 6-well plates in Ham F-10 medium with 10% FCS. Remove the medium and wash the cells three times with 2 ml Hanks balanced salt solution. Fix the cells with 3 ml fixative. Seal the plate with tape and store in the refrigerator at 4 C until staining.

Let the plates come to room temperature and rinse the cover slips twice with PBS. Incubate the cover slips for 5 min with 2 ml Triton X-100 solution, remove, and rinse twice with 2 ml PBS. Remove the PBS and incubate the cover slips for 30 min with 2 ml of filipin assay solution. Remove the filipin assay solution and rinse the cover slips twice with PBS. Remove the PBS and let the cover slips dry at ambient temperature. Mount the cover slips on a microscope slide with one drop of DABCO solution

and seal with nail polish. Store at 4 C. View the cells with a fluorescence microscope with a G365 band-pass excitation filter and either a 470-nm long-path emission filter with a 460 nm dichroic mirror or a 515-nm long-pass filter with a 500 nm dichroic mirror.

4.4.14.3 Reference Values/Pathological Values

In the so-called "classical" biochemical phenotype, which represents more than 80% of the cases of NPC, more than 90% of the cells show a characteristic perinuclear punctate fluorescence.

4.4.14.4 Special Remarks/Pitfalls

The assay described above has a limited sensitivity (80–85%) to detect patients, especially patients with the so-called "variant" biochemical phenotype, and should be considered as an initial screening test [52, 55]. For increased sensitivity the cells should be cultured in medium with 10% lipoprotein-deficient medium (LPDS) for 2 days and subsequently with medium supplemented with 10% fresh human serum as described below for low-density lipoprotein (LDL)-stimulated cholesteryl ester formation.

4.4.15 LDL-Stimulated Cholesteryl Ester Formation

Lack of stimulation of cholesteryl ester formation by exogenously added LDL is a hallmark of NPC. The assay is based on the procedure described by Vanier et al. [58]. The test is only performed after a positive filipin staining test is obtained.

4.4.15.1 Reagents and Chemicals

1. [9,10-^{3}H(N)]-Oleic acid (specific activity 22.7 Ci/mmol, 5 mCi/ml).
2. Oleic acid (MW 282.5) stock solution 12.5 mmol/l in ethanol (3.52 mg/ml).
3. Fatty-acid-free BSA (14% w/v) in Ham F10 medium.
4. Preparation of ^{3}H-oleic acid working solution in medium sufficient to assay six cell lines when the cholesterol esterification is measured at three different time points (or nine cell lines at two different time points): pipette 62 µl of ^{3}H-oleic acid and 456 µl cold oleic acid stock solution and dry with nitrogen. Take up in 90 µl ethanol, mix on a Vortex mixer, and keep at 56 C. Drop by drop and very slowly add 456 µl of 14% BSA kept at 56 C while mixing on a Vortex mixer. The final solution should be clear with a yellowish color. Allow to cool to room temperature. Add Ham F-10 medium to a final volume of 5 ml. Divide into two portions of 2.5 ml in a 50-ml tube and add to the first tube 2.9 ml human LPDS and to the second tube 2.9 ml fresh human serum. Mix. Bring the final volume of each tube to 29 ml with Ham F-10 medium. Sterilize by filtering through a 0.45-µm filter. The final concentration of ^{3}H-oleic acid is 100 µM (specific activity 54 µCi/µmol) in medium containing either 10% LPDS or 10% human serum.

4.4.15.2 Assay

Fibroblasts are grown under standard conditions in Ham F10 medium supplemented with 10% FCS. Cells are harvested by trypsinization, taken up in medium, counted, and reseeded in 6-well plates at a density of 200,000 cells per well (2.5 ml cell suspension, 80,000 cells per milliliter). A total of six wells on three different plates is needed per cell line (two wells per plate for duplicate assays). For each assay, one control and one NPC cell line with "classical" biochemical phenotype is included. Incubate for 3 days in Ham F-10 with 10% FCS, remove the culture medium and grow the cells in 1.5 ml medium with 10% LPDS for 2 days. Remove the medium and start the esterification test by incubating the cholesterol-deprived fibroblasts with either 1.5 ml medium containing 10% LPDS (esterification in the absence of LDL) and ^{3}H-oleic acid, or 1.5 ml medium containing 10% fresh human serum (esterification in the presence of LDL) and ^{3}H-oleic acid. Incubate for 4.5, 7, and 24 h. Stop the reaction by removing the medium and wash the cells three times with PBS. Trypsinize the cells, take the cells up in 1 ml of PBS in Eppendorf vials and centrifuge for 2 min at 14,000 × *g*. Remove the PBS. The cell pellets can be stored at –20 C until analysis.

Add 200 µl water to the cell pellet and sonicate briefly at low power. Use 50 µl homogenate for a protein determination and 100 µl for lipid extraction. To 100 µl homogenate add 4 ml chloroform/methanol 2/1 (v/v). Leave for 1 h at room temperature and add 0.8 ml of 0.73% NaCl. Vortex and centrifuge for 5 min at 1000 × *g* to separate the phases. Remove the lower chloroform phase and add 10 nmol cholesteryl oleate and 10 nmol triolein as a cold carrier. Dry the sample under nitrogen. Take the sample up in 25 µl chloroform/methanol 2/1 (v/v) and spot the sample on a silica gel plate (0.5 cm streak). Rinse the tube with 25 µl chloroform/methanol 2/1 (v/v) and spot the sample on a silica gel plate. Develop the plate with hexane/diethylether/acetic acid, 70/30/1 (v/v/v). Remove the plate from the tank when the solvent front almost reaches the top, dry the plate, and expose briefly to iodine vapor to localize the cholesteryl oleate. Scrape the spots into scintillation vials, mix thoroughly, and count in a scintillation counter.

4.4.15.3 Reference Values/Pathological Values

LDL stimulated cholesteryl ester formation in fibroblasts reference values:
1. 4.5 h time point: 0.7–2.5 nmol/mg·4.5 h.
2. 7 h time point: 2.4–7.8 nmol/mg·7 h.
3. 24 h time point: 7.2–20 nmol/mg·24 h.

LDL stimulated cholesteryl ester formation in fibroblasts pathological values for the "classical" biochemical phenotype:
1. 4.5 h time point: < 0.25 nmol/mg·4.5 h.
2. 7 h time point: < 0.4 nmol/mg·7 h.
3. 24 h time point: < 2.0 nmol/mg·24 h.

Intermediate values between the pathological and reference range or (near) normal values may be found in patients with a "variant" biochemical phenotype.

4.4.15.4 Special Remarks/Pitfalls

The filipin staining and cholesterol esterification tests do not distinguish between NPC caused by mutations in NPC1 and NPC2. Although 95% of the patients have mutations in NPC1, to establish the diagnosis with certainty at the molecular level mutation analysis should be performed [37]. While the prenatal diagnosis of Niemann-Pick disease is possible by biochemical tests in cases in which a clear biochemical abnormality has been established in the index case, mutation analysis is preferred when the mutations are known [56], especially in "variant" cases.

4.4.16 Acid Ceramidase (EC 3.5.1.23)

This enzyme is deficient in Farber disease (Table 4.4.1, Fig. 4.4.1). Assays of acid ceramidase are not easy to perform. This is due to the complexity of the substrate/detergent mixtures used and the instability of the enzyme. The acid ceramidase assay is infrequently requested in the general practice of the lysosomal diseases laboratory. The authors have experience with two different assays, one with radioactive natural substrate based on the method described by Ben-Yoseph et al. [4] and another assay based on the formation of sphingosine from endogenous ceramide, glycosphingolipids, and sphingomyelin, which is monitored by HPLC [38]. The former method requires the preparation of radioactive N-laurylsphingosine and a complex substrate mixture containing substrate and detergents. The latter assay does not require any substrate preparations and is described below.

4.4.16.1 Reagents and Chemicals

1. 0.25 M sucrose 1 mM EDTA pH 7.4; weigh 80.9 mg dipotassium-EDTA and 17.1 g sucrose and dissolve in 150 ml distilled water; adjust the pH to 7.4 with KOH and adjust the final volume to 200 ml.
2. Sodium cholate in methanol: dissolve 20 mg sodium cholate in 1 ml methanol.
3. Reaction buffer: mix 54.6 ml 0.1 M citric acid (see above) with 45.4 ml 0.2 M Na_2HPO_4. Adjust to pH 4.5 with either citric acid or phosphate solution.
4. 0.6 M NaOH in methanol: dissolve 2.4 g NaOH in 100 ml methanol.
5. 0.5 M HCl in methanol: mix 4.13 ml HCl with methanol to a final volume of 100 ml.
6. 0.73% NaCl solution: dissolve 0.73 g NaCl in 100 ml distilled water.
7. 25 µM D-erythro-C20-sphinganine (MW 329.6). Dissolve 1 mg C20-sphinganine in 1 ml methanol (stock solution). Dilute 100 µl of this stock solution with methanol to 1 ml (stock solution 1:10). Dilute 100 µl of the stock solution 1:10 with 1100 µl methanol. The final concentration of C20-sphinganine is 25 µM.

4.4.16.2 Specimen

Culture fibroblasts in medium with 10% FCS until 1 week past confluency. Harvest the cells by trypsinization and wash them twice with PBS. Homogenize the cell pellet

in 425 µl sucrose/EDTA pH 7.4 with a Potter-Elvehjem homogenizer. Determine the protein concentration, which should be between 1 and 2 mg/ml. Freshly prepared homogenates should be used in this assay.

4.4.16.3 Assay Conditions

1. Pipette 25 µl sodium cholate in methanol in a Pyrex tube and dry with nitrogen. For each patient a duplicate sample and a duplicate blank (t=0) is measured. Add 0.1 ml reaction buffer, vortex, and sonicate briefly (about 3 s) at low power (Branson sonicator with a microprobe). Start the incubation by adding 0.1 ml homogenate or 0.1 ml sucrose EDTA and incubate for 3 h in a shaking incubator at 37 C. Stop the reaction by adding 5 ml chloroform/methanol 2/1 (v/v).
2. Prepare a blank (t=0) by adding the homogenate to the buffer and immediately stopping the reaction by adding 5 ml chloroform/methanol 2/1 (v/v).
3. Add to each tube 5 µl internal standard (25 µM D-erythro-C20-sphinganine).
4. After 1 h add 1.0 ml 0.73% NaCl to the chloroform/methanol extracts. Vortex and centrifuge for 5 min at 1000 × g to separate the phases. Pipette the lower chloroform phase into a Pyrex tube. Extract the upper phase twice with 1 ml chloroform and add these chloroform lower phases to the first chloroform phase; take the combined chloroform phases to dryness with nitrogen.
5. Dissolve the residue in 1 ml chloroform. Add 1.0 ml methanolic NaOH and vortex. Leave at room temperature for 1 h. Neutralize with 1.2 ml methanolic HCl. Add 1.7 ml water and 3.4 ml chloroform. Vortex and centrifuge for 5 min at 1000 × g. Remove the chloroform (lower) phase and dry under nitrogen. The sphingoid bases are derivatized with o-phtaldialdehyde (OPA) for 30 min with 25 µl OPA reagent (5 mg OPA, 0.1 ml ethanol, 5 µl 2-mercaptoethanol, and 10 ml 3% w/v boric acid adjusted to pH 10.5 with KOH) essentially as described by Merrill [36]. OPA-derivatized sphingoid bases are separated using an HPLC system (Waters Associates, Milford, MA, USA) with an Altima BDS C_{18} 3 µ, 150 × 4.6 mm reverse-phase column. The eluent used is methanol:water; 88:12 (w/w). The OPA-derivatized sphingoid bases are quantified by fluorescence detection at excitation wavelength 340 nm and emission wavelength 435 nm. Peak identification is based on comparison of the retention times of the peaks with those of authentic standards for sphingosine and sphinganine.

4.4.16.4 Reference Values/Pathological Values

1. Reference range for fibroblasts: 400–2100 pmol/mg·3 h.
2. Pathological value for fibroblasts: < 40 nmol/mg·3 h.

4.4.16.5 Special Remarks/Pitfalls

Other sphingolipidoses like Niemann-Pick type A/B (sphingomyelinase deficiency) that could lead to impaired ceramide formation should be excluded.

References

1. Bach G, Zeigler M, Zlotogora J (2007) Prevention of lysosomal storage diseases in Israel. Mol Genet Metab 90:353–357
2. Baum H, Dodgson KS, Spencer B (1959) The assay of arylsulfatases A and B in human urine. Clin Chim Acta 4:453–455
3. Beck M (2007) New therapeutic options for lysosomal storage disorders: enzyme replacement, small molecules and gene therapy. Hum Genet 121:1–22
4. Ben-Yoseph Y, Gagne R, Parvathy MR, Mitchell DA, Momoi T (1989) Leukocyte and plasma N-laurylsphingosine deacylase (ceramidase) in Farber disease. Clin Genet 36:38–42
5. Boot RG, Renkema GH, Verhoek M, Strijland A, Bliek J, de Meulemeester TM, Mannens MM, Aerts JM (1998) The human chitotriosidase gene. Nature of inherited enzyme deficiency. J Biol Chem 273:25680–25685
6. Boot RG, Verhoek M, de Fost M, Hollak CEM, Maas M, Bleijlevens B, van Breemen MJ, van Meurs M, Boven LA, Laman JD, Moran MT, Cox TM, Aerts JMFG (2004) Marked elevation of the chemokine CCL 18/PARC in Gaucher disease: a novel surrogate marker for assessing therapeutic intervention. Blood 103:33–39
7. Chamoles NA, Blanco M, Gaggioli D (2001) Fabry disease: enzymatic diagnosis in dried blood spots on filter paper. Clin Chim Acta 308:195–196
8. Chamoles NA, Blanco M, Gaggioli D, Casentini C (2002) Tay-Sachs and Sandhoff diseases: enzymatic diagnosis in dried blood spots on filter paper: retrospective diagnoses in newborn-screening cards. Clin Chim Acta 318:133–137
9. Chamoles NA, Blanco M, Gaggiolo D, Casentini C (2002) Gaucher and Niemann-Pick diseases – enzymatic diagnosis in dried blood spots on filter paper: retrospective diagnoses in newborn-screening cards. Clin Chim Acta 317:191–197
10. Chamoles NA, Blanco MB, Iocansky S, Gaggioli D, Specola N, Casentini C (2001) Retrospective diagnosis of GM1 gangliosidosis by use of a newborn-screening card. Clin Chem 47:2068
11. Daniels LB, Glew RH, Diven WF, Lee RE, Radin NS (1981) An improved fluorometric leukocyte beta-glucosidase assay for Gaucher's disease. Clin Chim Acta 115:369–375
12. Deegan PD, Moran MT, McFarlane I, Schofield JP, Boot RG, Aerts JMFG, Cox TM (2005) Clinical evaluation of chemokine and enzymatic biomarkers of Gaucher disease. Blood Cells Mol Dis 35:259–267
13. Desnick RJ, Allen KY, Desnick SJ, Raman MK, Bernlohr RW, Krivit W (1973) Fabry's disease: enzymatic diagnosis of hemizygotes and heterozygotes. J Lab Clin Med 81:157–171
14. Gieselmann V (1995) Lysosomal storage disorders. Biochim Biophys Acta 1270:103–136
15. Goker-Alpan O.R, Park JK, Stubblefield K, Tayebi N, Sidransky E (2006) Divergent phenotypes in Gaucher disease implicate the role of modifiers J Med Genet 42:37–44
16. Groener JE, Poorthuis BJ, Kuijper S, Helmond MTJ, Hollak CE, Aerts JM (2007) HPLC for simultaneous quantification of total ceramide, glucosylceramide, and ceramide trihexoside concentrations in plasma. Clin Chem 53:742–747
17. Guo Y, He W, Boer AM, Wevers RA, de Bruijn AM, Groener JEM, Hollak CEM, Aerts JMFG, Galjaard H, van Diggelen OP (1995) Elevated plasma chitotriosidase activity in various lysosomal storage disorders. J Inherit Metab Dis 18:717–722
18. Harzer K, Rolfs A, Bauer P, Zschiesche M, Mengel E, Backes J, Kustermann-Kuhn B, Bruchelt G, van Diggelen OP, Mayrhofer H, Krägeloh-Mann I (2003) Niemann-Pick disease type A and B are clinically but also enzymatically heterogeneous: pitfalls in the laboratory diagnosis of sphingomyelinase deficiency associated with the mutation Q292K. Neuropediatrics 34:301–306
19. Ho MW, O'Brien JS (1970) Stimulation of acid beta-galactosidase activity by chloride ions. Clin Chim Acta 30:531–534
20. Ho MW, O'Brien JS (1971) Differential effect of chloride ions on beta-galactosidase isoenzymes: a method for separate assay. Clin Chim Acta 32:443–450

21. Hollak CEM, Maas M, Aerts JM (2001) Clinically relevant therapeutic endpoints in type I Gaucher disease. J Inherit Metab Dis 24:97–105
22. Hollak CEM, van Weely S, van Oers MHJ, Aerts JMFG (1994) Marked elevations of plasma chitotriosidase activity. A novel hallmark of Gaucher disease. J Clin Invest 93:1288–129
23. Inui K, Wenger DA (1984) Usefulness of 4-methylumbelliferyl-6-sulfo-2-acetamido-2-deoxy-beta-D-glucopyranoside for the diagnosis of GM2 gangliosidoses in leukocytes. Clin Genet 26:318–321
24. Kaback MM (2001) Screening and prevention in Tay Sachs disease: origins, update and impact. Adv Genet 44:253–265
25. Kolter T, Sandhoff K (2005) Principles of lysosomal membrane digestion: stimulation of sphingolipid degradation by sphingolipid activator proteins and anionic lysosomal lipids. Annu Rev Cell Dev Biol 21:81–103
26. Lee-Vaupel M, Conzelmann E (1987) A simple chromogenic assay for arylsulfatase A. Clin Chim Acta 164:171–180
27. Leinekugel P, Michel S, Conzelmann E, Sandhoff K (1992) Quantitative correlation between the residual activity of beta-hexosaminidase A and arylsulfatase A and the severity of the resulting lysosomal storage disease. Hum Genet 88:513–523
28. Levey S, Jennings ER (1950) The use of control charts in the clinical laboratory. Am J Clin Pathol 20:1059–1066
29. Lowry OH, Rosebrough AL, Farr AL, Randall RJ (1951) Protein measurement with the Folin phenol reagent. J Biol Chem 193:265–275
30. Lukacs Z, Keil A, Peters V, Kohlschütter A, Hoffmann GF, Cantz M, Kopitz J (2003) Towards quality assurance in the determination of lysosomal enzymes: a two-centre study. J Inherit Metab Dis 26:571–581
31. Mayes JS, Scheerer JB, Sifers RN, Donaldson ML (1981) Differential assay for lysosomal alpha-galactosidases in human tissues and its application to Fabry's disease. Clin Chim Acta 112:247–251
32. Meikle PJ, Dallas JG, Dean CJ, Lang DL, Bockmann M, Whittle AM, Fietz MJ, Simonsen H, Fuller M, Brooks DA, Hopwood JJ (2006) Newborn screening for lysosomal storage disorders. Mol Genet Metab 88:307–314
33. Meikle PJ, Fietz MJ, Hopwood JJ (2004) Diagnosis of lysosomal storage disorders: current techniques and future directions. Expert Rev Mol Diagn 4:677–691
34. Meikle PJ, Hopwood J (2003) Lysosomal storage disorders: emerging therapeutic options require early diagnosis. Eur J Pediatr 162:S34–S37
35. Meikle PJ, Hopwood JJ, Clague AE, Carey WF (1999) Prevalence of lysosomal storage disorders. JAMA 281:249–254
36. Merrill AH Jr, Wang E, Mullins RE, Jamison WCL, Nimkar S, Liotta DC (1988) Quantitation of free sphingosine in liver by high-performance liquid chromatography. Anal Biochem 171:373–381
37. Millat G, Baïlo N, Molinero S, Rodriguez C, Chikh K, Vanier MT (2005) Niemann-Pick C disease: use of denaturing high performance liquid chromatography for the detection of NPC1 and NPC2 genetic variations and impact on management of patients and families. Mol Genet Metab 86:220–232
38. Mitsuo K, Kobayashi T, Shinnoh N, Goto I (1988) A high-performance liquid chromatographic assay for acid ceramidase activity in cultured fibroblasts from patients with Farber's disease and from controls. Clin Chim Acta 173:281–288
39. Natowicz MR, Prence EM, Chaturvedi P, Newburg DS (1996) Urinary sulfatides and the diagnosis of metachromatic leukodystrophy. Clin Chem 42:232–238
40. O'Brien JS, Okada S, Chen A, Fillerup DL (1970) Tay-Sachs disease. Detection of heterozygotes and homozygotes by serum hexosaminidase assay. N Engl J Med 283:15–20
41. Pavlu-Pereira H, Asfaw B, Poupetova H, Ledvinova J, Sikora J, Vanier MT, Sandhoff K, Zeman J, Novaotna Z, Chudoba D, Elleder M (2005) Acid sphingomyelinase deficiency. Phenotype variability with prevalence of intermediate phenotype in a series of twenty-five Czech and Slovak patients. A multi-approach study. J Inherit Metab Dis 28:203–227

42. Pentchev PG, Comly ME, Kruth HS, Vanier MT, Wenger DA, Patel S, Brady RO (1985) A defect in cholesterol esterification in Niemann-Pick disease (type C) patients. Proc Natl Acad Sci U S A 82:8247–8251
43. Peters SP, Glew RH, Lee RE (1977) Gaucher disease In: Glew RH, Peters SP (eds) Practical Enzymology of the Sphingolipidoses. AR Liss, New York, pp 71–100
44. Pinto R, Caseiro C, Lemos M, Lopes L, Fontes A, Ribeiro H, Pinto E, Silva E, Rocha S, Marcao A, Ribeiro I, Lacerda L, Ribeiro G, Amaral O, Sa Miranda MC (2004) Prevalence of lysosomal storage disorders in Portugal. Eur J Hum Genet 12:87–92
45. Poorthuis BJHM, Wevers RA, Kleijer WJ, Groener JEM, de Jong JGN, van Weely S, Niezen-Koning KE, van Diggelen OP (1999) The frequency of lysosomal storage diseases in The Netherlands. Hum Genet 105:151–156
46. Rafi MA, Coppola S, Liu SL, Rao HZ, Wenger DA (2003) Disease-causing mutations in cis with the common arylsulfatase A pseudodeficiency allele compound the difficulties in accurately identifying patients and carriers of metachromatic leukodystrophy. Mol Genet Metab 79:83–90
47. Ries M, Schaefer E, Lührs T, Mani L, Kuhn J, Vanier MT, Krummenauer F, Gal A, Beck M, Mengel E (2006) Critical assessment of chitotriosidase analysis in the rational laboratory diagnosis of children with Gaucher disease and Niemann-Pick disease type A/B and C. J Inherit Metab Dis 29:647–652
48. Roos D, Loos JA (1970) Changes in the carbohydrate metabolism of mitogenically stimulated human peripheral lymphocytes. I. Stimulation by phytohaemagglutinin. Biochim Biophys Acta 222:565–582
49. Ruijter GJG, Boer M, Weykamp CW, de Vries R, van den Berg I, Janssens-Puister J, Niezen-Koning K, Wevers RA, Poorthuis BJHM, van Diggelen OP (2005) External quality assurance programme for enzymatic analysis of lysosomal storage diseases: a pilot study. J Inherit Metab Dis 28:979–990
50. Scriver CR, Beaudet AL, Sly WS, Valle D, Childs B, Kinzler KW, Vogelstein B (2001) The metabolic molecular bases of inherited disease. Vol III Lysosomal storage disorders McGraw-Hill, New York, Chapters 134, 143, 144–148, 150, 151, and 153
51. Skoog WA, Beck WS (1956) Studies on the fibrinogen, dextran and phytohemagglutinin methods of isolating leukocytes. Blood 11:436–454
52. Sun X, Marks DL, Park WD, Wheatley CL, Puri V, O'Brien JF, Kraft L, Lundquist PA, Patterson MC, Pagano RE, Snow K (2001) Niemann-Pick C variant detection by altered sphingolipid trafficking and correlation with mutations within a specific domain of NPC1. Am J Hum Genet 68:1361–1372
53. Thomas GH (1994) "Pseudodeficiencies" of lysosomal hydrolases. Am J Hum Genet 54:934–940
54. Van Diggelen OP, Voznyi YV, Keulemans JLM, Schoonderwoerd K, Ledvinova J, Mengel E, Zschiesche M, Santer R, Harzer K (2005) A new fluorimetric assay for the diagnosis of Niemann-Pick A/B, with specificity of natural sphingomyelinase substrate. J Inherit Metab Dis 28:733–741
55. Vanier MT (1997) Phenotypic and genetic heterogeneity in Niemann-Pick type C: current knowledge and practical implications. Wien Klin Wochenschr 109:68–73
56. Vanier MT (2002) Prenatal diagnosis of Niemann-Pick types A, B and C. Prenat Diagn 22:630–632
57. Vanier M, Millat G (2003) Niemann-Pick disease type C. Clin Genet 64:269–281
58. Vanier MT, Rodriguez-Lafrasse C, Rousson R, Gazzah N, Juge M-C, Pentchev PG, Revol A, Louisot P (1991) Type C Niemann-Pick disease: spectrum of phenotypic variation in disruption of intracellular LDL-derived cholesterol processing. Biochim Biophys Acta 1096:328–337
59. Wenger DA (1977) Niemann-Pick disease. In: Glew RH, Peters SP (eds) Practical Enzymology of the Sphingolipidose . AR Liss, New York, pp 39–70
60. Wenger DA, Coppola S, Liu SL (2003) Insight in the diagnosis and treatment of lysosomal storage diseases. Arch Neurol 60:322–328

61. Wenger DA, Louie E (1991) Pseudodeficiencies of arylsulfatase A and galactocerebrosidase activities. Dev Neurosci 13:216–221
62. Wenger DA, Rafi MA, Luzi P, Datto J, Constantino-Cerrarini E (2000) Krabbe disease: genetic aspects and progress toward therapy. Mol Genet Metab 70:1–9
63. Whitfield PD, Sharp PC, Johnson DW, Nelson P, Meikle PJ (2001) Characterization of urinary sulfatides in metachromatic leukodystrophy using electrospray ionization-tandem mass spectrometry. Mol Genet Metab 73:30–37
64. Wiederschain G, Raghavan S, Kolodny E (1992) Characterization of 6-hexadecanoylamino-4-methylumbelliferyl-beta-D-galactopyranoside as fluorogenic substrate of galactocerebrosidase for the diagnosis of Krabbe disease. Clin Chim Acta 205:87–96
65. Wraith JE (2002) Lysosomal storage disorders. Semin Neonatol 7:75–83

4.5 Congenital Disorders of Glycosylation

Christian Körner, Jürgen Lübbehusen, Christian Thiel

4.5.1 Introduction

4.5.1.1 Biosynthesis of Glycoproteins

The term "protein glycosylation" describes the co-translational linkage of oligosaccharide moieties onto newly synthesised proteins. This complex metabolic process, which has been found in nearly all forms of life from bacteria to man, comprises one of the most widespread and variable forms of protein modifications. The sugar moieties, which are also termed "oligosaccharides" or "glycans", are necessary for protein quality control, directed transport and biological activity. Glycosylation affects a variety of physicochemical properties of proteins on behalf of their stability, solubility, and polarity. Glycoproteins play an important role in many complex biological processes such as growth, differentiation, organ development, signal transduction and immunologic defence, but are also concerned with pathologic processes like tumour progression. Due to their structural variability, glycans are carriers of a code that is much more complex compared to nucleic acids and proteins [12]. In man, the glycosylation apparatus comprises more than 300 proteins, such as glycosyltransferases, glycosidases, and sugar-nucleotide transporters, which are located in different cellular compartments such as the cytosol, endoplasmic reticulum and Golgi apparatus (Fig. 4.5.1).

4.5.1.2 Congenital Disorders of Glycosylation

"Congenital disorders of glycosylation" (CDG), formerly termed "carbohydrate-deficient glycoprotein syndrome" [1], comprise a rapidly expanding group of autosomal recessive inherited metabolic diseases that affect the de novo biosynthesis of glycoproteins. The multisystemic disorders are mostly combined with severe neurological impairment. Thus far, 20 different types of CDG have been identified [7, 9, 16] (see also Table 4.5.1). Although investigations on new types of CDG have proceeded rapidly in recent years, the complexity of the affected metabolic pathway indicates that they number considerably more than 100.

So far, CDG nomenclature is based on the cellular localisation of the molecular defects in the different subtypes. The disorders are divided into two subgroups.

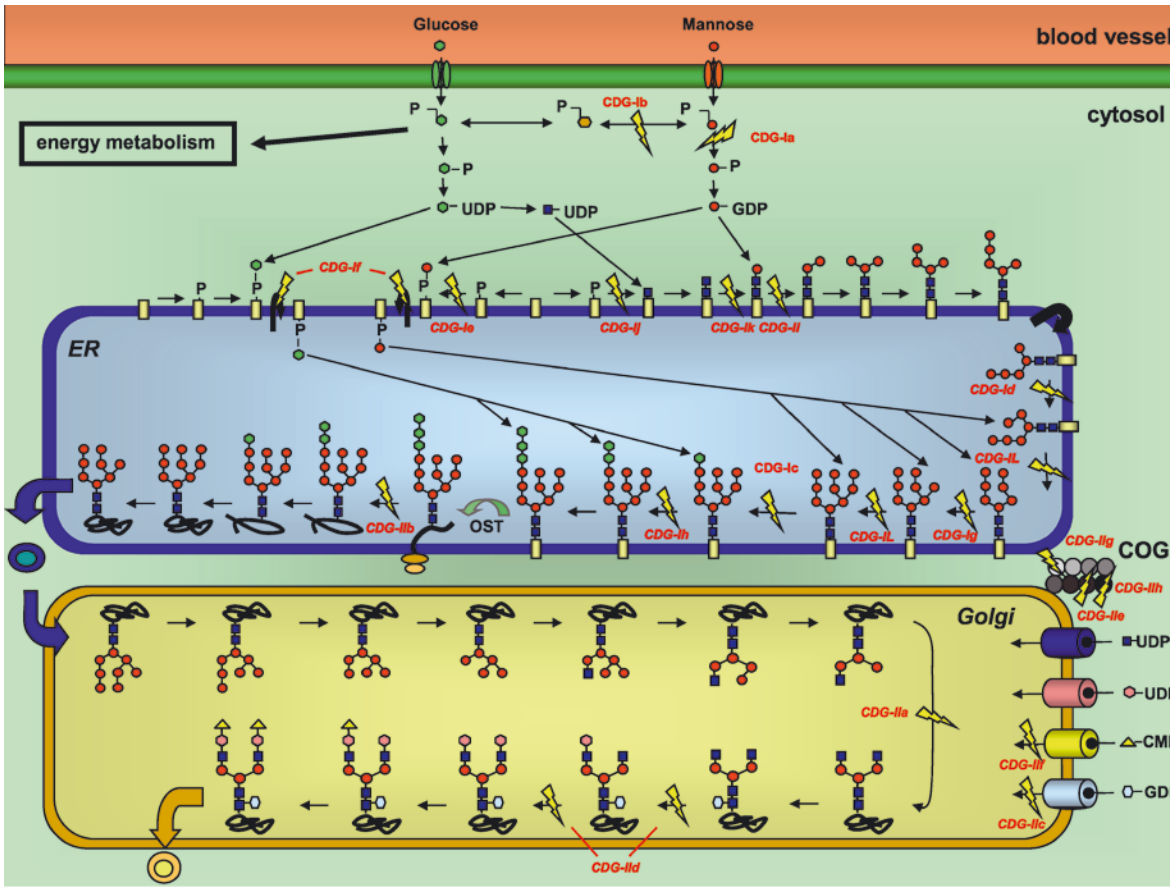

dolichol; N-acetylglucosamine; mannose; glucose; fucose; galactose; sialic acid; fructose; GDP = guanosine diphosphate; UDP = uridine diphosphate; CMP = cytidine monophosphate; P = phosphate; = CDG-defect; COG = conserved oligomeric Golgi complex

Fig. 4.5.1 Overview on glycoprotein biosynthesis and known types of congenital disorders of glycosylation (CDG). Initial steps in the biosynthesis of N-glycans are catalysed by glycosyltransferases, which transfer nucleotide-activated N-acetylglucosamine and mannose residues onto the lipid carrier dolichol-phosphate. At the cytosolic side of the endoplasmic reticulum (*ER*) membrane, the oligosaccharide intermediate dolichol-PP-$GlcNAc_2Man_5$ is synthesised and is subsequently transferred into the lumen of the ER, where it is further elongated by a subset of mannosyl- and glucosyltransferases, which utilise dolichol-phosphate-mannose and -glucose as donor substrates, to dolichol-PP-$GlcNAc_2Man_9Glc_3$. This oligosaccharide is subsequently transferred to nascent glycoproteins by the oligosaccharyltransferase complex. In the subsequent reactions, $GlcNAc_2Man_9Glc_3$ moieties undergo trimming of the three glucose residues and one mannose residue in the ER, which is crucial for quality control in protein folding. Newly synthesised glycoproteins are transferred to the Golgi apparatus by vesicular transport, where further processing by different mannosidases takes place. Shortened oligosaccharides are elongated by N-acetylglucosaminetransferases, galactosyltransferases, sialic acid transferases and fucosyltransferases, followed by transfer of mature glycoproteins to their destination point. All CDG defects identified so far are indicated by yellow flashes. *CMP* Cytidine monophosphate, *COG* conserved oligomeric Golgi complex, *GDP* guanosine diphosphate, *OST* oligosaccharyltransferase complex, *P* phosphate, *UDP* uridine diphosphate

CDG-I comprises deficiencies that affect either the biosynthesis of lipid-linked oligosaccharides (LLO) or the transfer of oligosaccharides onto newly synthesised proteins by the oligosaccharyltransferase complex in the endoplasmic reticulum. CDG-II disorders affect subsequent trimming and elongation of N-glycans in the endoplasmic reticulum and the Golgi apparatus. The CDG are assigned to one of the two groups and are numbered by small letters in chronological order of the identification of the defective gene (Fig. 4.5.1 and Table 4.5.1).

The knowledge of the genetic and biochemical background of CDG has not only improved diagnostic strategies for defects in glycoprotein biosynthesis, but has also led in the case of two of the CDG to simple and effective therapies [19, 22].

4.5.1.3 Diagnostic, Analytic, and Therapeutic Approaches to CDG

The clinical phenotype of CDG is highly heterogeneous. In all known types it affects several organ systems and is mostly combined with neurological impairment. Typical clinical features present with growth retardation either due to disturbed nutrition uptake and recurrent vomiting or hormone disturbance. Microcephaly often leads to ataxia, and nerve conduction velocity was shown to be reduced. At birth, many CDG-patients show inverted nipples and fat pads at the bottom and the upper arms. Moreover, strabismus, retinitis pigmentosa, optic atrophy, coloboma of the iris and cataracts have been described. Some CDG patients suffer from hypogonadism and hyperinsulinism. Orthopaedic problems present in some cases with osteopenia, exostosis and contractures of the joints. Coagulation abnormalities appear quite frequently with thrombosis, haemophilia, and phlebitis. During the first months after birth, life-threatening cardiac problems may appear that are caused by cardiomyopathy, pericarditis, and pericardial effusion. Gastrointestinal defects in CDG often present with chronic diarrhoea, hepatomegaly and protein-losing enteropathy. In some cases, renal complications with proteinuria, microcysts, and proximal tubulopathy have been observed.

Primary diagnostics on CDG commonly start with investigations on the glycosylation state of serum transferrin by isoelectric focusing (IEF¸ Fig. 4.5.2). Patients who present with a type I CDG pattern in IEF (Fig. 4.5.3) are routinely analysed for enzymatic activity of phosphomannomutase (PMM) and phosphomannose isomerase (PMI) to exclude CDG-Ia and CDG-Ib. Further studies on other CDG types are carried out by metabolic labelling of LLO in skin fibroblasts or immortalised lymphoblasts followed by high-performance liquid chromatography (HPLC) analysis and subsequent genetic analysis of the presumably affected genes (Fig. 4.5.2, left). In the case of a CDG-II pattern, further analysis is initiated by investigations on transferrin-linked oligosaccharides by HPLC and mass spectrometry, followed by determination of specific glycosyltransferase- and nucleotide-activated monosaccharide transporter activities, immunocytochemistry and mutational analysis. In two types of CDG, CDG-IIb and CDG-IIc, the IEF pattern is not affected. Since these diseases are very rare, further investigations should be performed in specialised laboratories (Fig. 4.5.2, right).

A novel approach in initial CDG diagnostics has currently been described by analysing the glycosylation state of serum transferrin using electrospray ionisation-tandem mass spectrometry (ESI-MS/MS). This method requires expensive technical

■ ***Table 4.5.1*** *Summary of known molecular defects in congenital disorders of glycosylation* (CDG). OMIM *Online Mendelian Inheritanc in Man*

CDG-type	Affected protein	Gene	Chromosome	OMIM
CDG-Ia	Phosphomannomutase II	*PMM2*	16p13	212065
				601785
CDG-Ib	Phosphomannose isomerase	*MPI*	15q22	154550
				602579
CDG-Ic	Dol-P-Glc:$Man_9GlcNAc_2$-PP-dolichol glucosyltransferase	*hALG6*	1p22	604566
				604655
CDG-Id	Dol-P-Man:$Man_5GlcNAc_2$-PP-dolichol mannosyltransferase	*hALG3*	3q27	601110
CDG-Ie	Dolicholphosphate-mannose synthase 1	*DPM1*	20q13	608789
CDG-If	Mannose-P-dolichol utilisation defect 1 protein	*MPDU1*	17p13	604041
CDG-Ig	Dol-P-Man:$Man_7GlcNAc_2$-PP-dolichol mannosyltransferase	*hALG12*	22q13	607143
CDG-Ih	Dol-P-Glc:$Glc_1Man_9GlcNAc_2$-PP-dolichol-α1,3-glucosyltransferase	*hALG8*	11p15	608104
CDG-Ii	GDP-Man:$Man_1GlcNAc_2$-PP-dolichol mannosyltransferase	*hALG2*	9q22	607906
CDG-Ij	UDP-GlcNAc:dolichol phosphate N-acetylglucosaminephosphotransferase 1	*DPAGT1*	11q23	608093
CDG-Ik	GDP-Man:$GlcNAc_2$-PP-dolichol mannosyltransferase	*hALG1*	16p13	608540
CDG-IL	Dolichol-P-mannose:α-1,2-mannosyltransferase	*hALG9*	11q23	608776
CDG-IIa	Golgi N-acetylglucosaminyltransferase II	*MGAT2*	14q21	212066
CDG-IIb	ER glucosidase I	*GCS1*	2p13	606056
CDG-IIc	Golgi GDP-fucose transporter	*FUCT1*	11p11	605881
				266265
CDG-IId	Golgi UDP-galactose:N-acetylglucosamine β-1,4-galactosyltransferase	*ß4GALT1*	9p13	607091
CDG-IIe	Subunit 7 of COG-complex	*COG7*	16p12	608779
				606978
CDG-IIf	CMP-NANA transporter	*CMP-NANA transporter*	6q15	605634
CDG-IIg	Subunit 1 of COG-complex	*COG1*	17q25	606973
CDG-IIh	Subunit 8 of COG-complex	*COG8*	16q22	606979

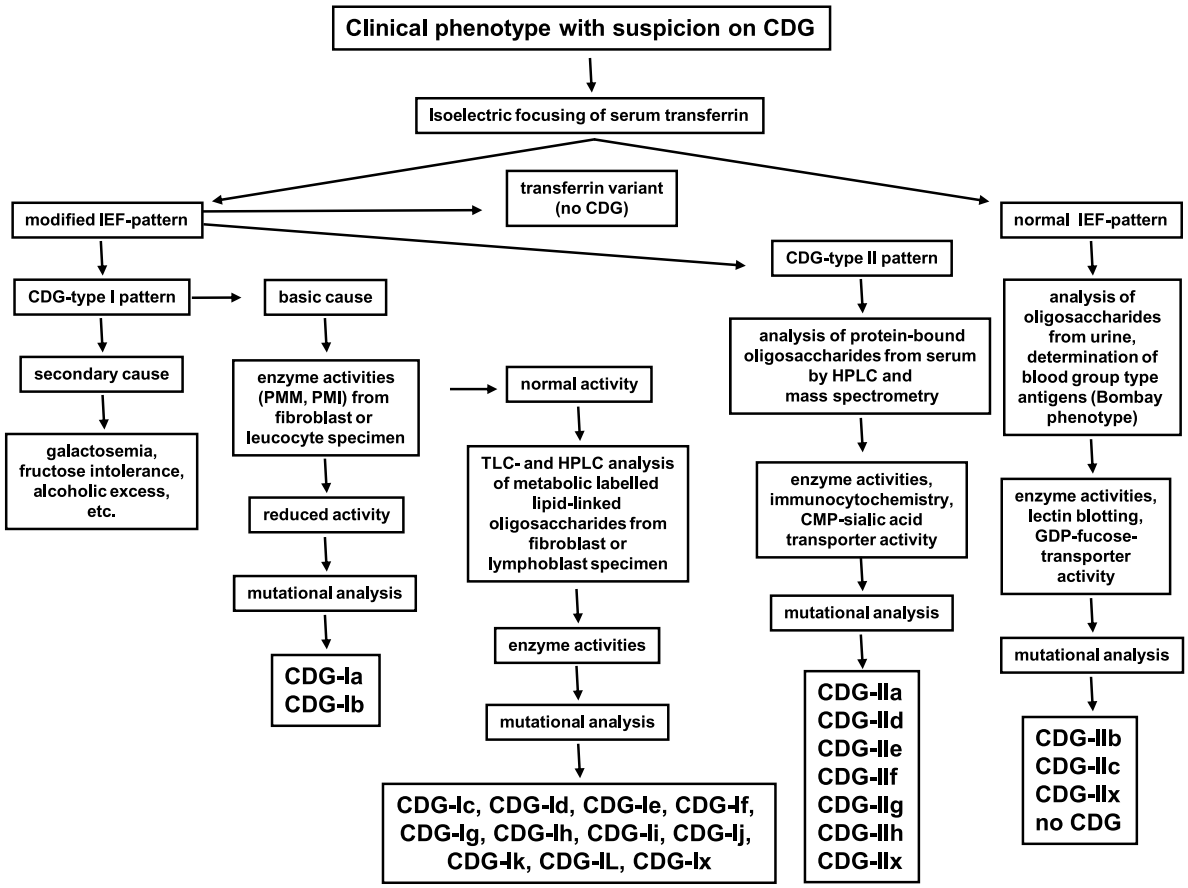

Fig. 4.5.2 Actual strategies for CDG diagnosis. Initial investigations on CDG patients are routinely carried out by isoelectric focusing (*IEF*) of serum transferrin. With a CDG type I pattern, subsequent analysis should imply determination of phosphomannomutase (*PMM*) and phosphomannose isomerase (*PMI*) activities. Further studies, like analysis of the lipid-linked- and protein-bound-oligosaccharides, determination of enzyme or sugar transporter activities and molecular biology studies often have to be performed in more specialised laboratories. *HPLC* High-performance liquid chromatography, *TLC* thin-layer chromatography

equipment and is not very widespread so far. It is comparable to IEF of serum transferrin, but it is faster, more precise and allows the determination of loss of distinct monosaccharide residues or complete oligosaccharide chains [16, 29].

Although IEF of serum transferrin is relatively easy to perform, it is assumed that many CDG patients are still missed. Due to the complex clinical presentation of CDG, all patients suffering from unclear multi-organ diseases, especially in combination with mental and psychomotor retardation, strabismus, cerebellar atrophy and blood-clotting problems, should be investigated for CDG.

4.5.2 Methods

4.5.2.1 IEF of Serum Transferrin

Principle

In most types of CDG, loss or shortening of oligosaccharide moieties linked to glycoproteins have been observed. Due to the fact that the iron-binding glycoprotein, transferrin, is highly abundant in serum (about 5% of all plasma proteins) and the structure of its N-linked oligosaccharide moieties is highly uniform, it is predominantly used for initial CDG diagnostics by IEF, thereby analysing the charge of the protein in an electric field. In healthy persons, transferrin is found mainly in the tetrasialo form due to the linkage of the protein to two biantennary complex-type oligosaccharide chains carrying four negatively charged terminal sialic acid residues (Fig. 4.5.3).

In all known types of CDG-I it has been observed that due to the loss of sialic acid residues, in addition to tetrasialo-transferrin, more or less pronounced di- and asialotransferrin bands appear, which are evoked by the loss of either one or both complete oligosaccharide chains (Fig. 4.5.3, lanes 2–4). In contrast to CDG-I, changes in the charge of serum transferrin of most known CDG-II types are due to shortening of the oligosaccharide moieties (Fig. 4.5.3, lanes 5–7).

Pre-analytical

Specimen

Serum, 0.1 ml.

Reagents and Chemicals

1. 200 μM Fe(III)-citrate p.a. (Merck, Darmstadt, Germany).
2. 150 mM NaCl p.a. (Roth, Karlsruhe, Germany).
3. Formaldehyde (36.5–38%; Sigma-Aldrich, Taufkirchen, Germany).
4. Glutardialdehyde 25% Microscopy (Merck).
5. Acetic acid 100% p.a. (Roth).
6. Ethanol 99.8% p.a. (Roth).
7. Silver nitrate p.a. (Merck).
8. Trichloroacetic acid (TCA) Sigma Ultra 99% (Sigma-Aldrich).
9. Sodium carbonate p.a. (Merck).
10. Antibody: rabbit anti-human transferrin (DakoCytomation, Hamburg, Germany).
11. Fixation: 20% TCA (Sigma-Aldrich).
12. Wash solution 1: 50% ethanol (Roth)/10% acetic acid (Roth).
13. Wash solution 2: 10% ethanol (Roth)/5% acetic acid (Roth).
14. Developer: 2.5% (w/v) sodium carbonate (Merck)/0.015% formaldehyde (v/v; Sigma-Aldrich).
15. Stop solution: 50 mM ethylenediaminetetraacetic acid (EDTA; Titriplex III, Roth).

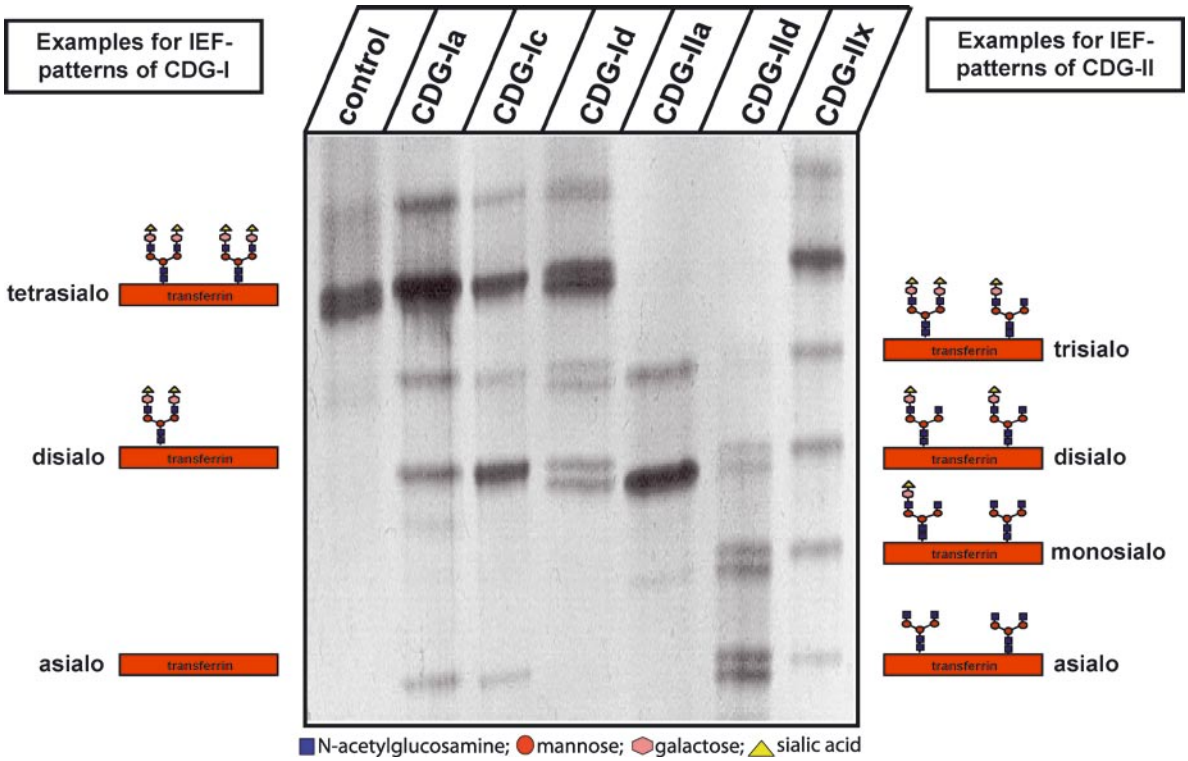

Fig. 4.5.3 IEF patterns of serum transferrin. Sera from a control (lane 1), three CDG-I (CDG-Ia, CDG-Ic and CDG-Id; lanes 2–4) and three CDG-II patients (CDG-IIa, CDG-IId and CDG-IIx; lanes 5–7) were analysed by IEF. In case of a control person, the main form of the protein carries four negatively charged sialic acid residues, even though small amounts of penta- and trisialotransferrin are detectable. Additional disialo- and asialotransferrin forms indicate CDG-type I (left side). In some cases of CDG type II, additional trisialo- and monosialotransferrin forms may occur, which are due to the loss of either one or three sialic acid residues (right side). Isoforms of transferrin that are independent of a pathological phenotype and that cause double bands in IEF are visible in lanes 4 and 6. CDG-IIx indicates a transferrin pattern that is caused by a so far unknown molecular defect from the CDG-II type

Instrumentation

1. PhastSystem (Amersham Biosciences, Freiburg, Germany)
2. PhastGel pH 4–6.5 (Amersham Biosciences)
3. PhastGel sample appplicator 8/1 (Amersham Biosciences)

Calibration

Calibration of IEF is performed with sera from healthy control persons as well as sera derived from patients with defined CDG types.

Running Conditions

- Isoelectric Focusing

Please refer to Table 4.5.2

1. Sample applicator down at 1.2, 0 Vh.
2. Sample applicator up at 1.3, 0 Vh.
3. Extra alarm to sound at 1.1, 73 Vh.

■ Silver Staining

Please refer to Table 4.5.3.

Analytical

Procedure

To saturate serum transferrin with iron, 10 µl of serum and 10 µl 200 µM Fe(III)-citrate are added to 30 µl of double-distilled water. After incubation for 10 min at room temperature the mixture is diluted 1:50 with double-distilled water. A 1-µl aliquot is loaded onto the PhastGel sample applicator 8/1 and IEF is performed as described above. After separation, gels are incubated with rabbit anti-human transferrin antibody (dilution 1:3 in 150 mM NaCl) for 40 min followed by washing in

■ ***Table 4.5.2*** *Set up for isoelectric focusing of serum transferrin*

Sep 1.1	2000 V	2.5 mA	3.5 W	15°C	75 Vh
Sep 1.2	200 V	2.5 mA	3.5 W	15°C	15 Vh
Sep 1.3	2000 V	5 mA	3.5 W	15°C	185 Vh

■ ***Table 4.5.3*** *Conditions for silver staining.* DD *double-distilled*

Dev 1.1	Fixation	5 min	20°C
Dev 1.2	Wash solution 1	2 min	50°C
Dev 1.3	wash solution 2	2 min	50°C
Dev 1.4	wash solution 2	4 min	50°C
Dev 1.5	8.3% glutardialdehyde	6 min	50°C
Dev 1.6	wash solution 2	3 min	50°C
Dev 1.7	wash solution 2	5 min	50°C
Dev 1.8	DD water	2 min	50°C
Dev 1.9	DD water	2 min	50°C
Dev 1.10	0.5% silver nitrate	10 min	50°C
Dev 1.11	DD water	0.5 min	50°C
Dev 1.12	DD water	0.5 min	50°C
Dev 1.13	developer	0.5 min	50°C
Dev 1.14	developer	12 min	50°C
Dev 1.15	stop solution	5 min	50°C
Dev 1.16	DD water	5 min	50°C

150 mM NaCl overnight. Automated silver staining of gels is performed as described above using the PhastSystem [10, 23].

Post Analytical

Interpretation

Data analysis is carried out by comparing IEF patterns of controls and defined CDG types with patients in suspicion of CDG. IEF of transferrin from controls show predominantly the tetrasialo form of the protein, whereas in case of CDG-I patients additional di- and asialo bands appear (Fig. 4.5.3).

Pitfalls

IEF of serum transferrin can detect nearly all known CDG-I types as well as most CDG-II types and many CDG-X cases. Nevertheless, deficiencies of ER-glucosidase I (CDG-IIb) and Golgi GDP-fucose transporter (CDG-IIc) are missed. In the known cases of CDG, prenatal diagnostics by IEF analysis from foetal blood is not reliable [4, 28]. Moreover, IEF of serum from children aged less than 2 weeks may result in false-positive results [15]. Heavy alcohol consumption can also result in serum transferrin deficiency in carbohydrate moieties, leading to an abnormal IEF-pattern [27]. Mutations in the protein backbone of transferrin, which lead to either loss or addition of charged amino acid residues, might produce IEF patterns that resemble those of CDG. To avoid false-positive results, desialylation of transferrin by neuraminidase treatment (see section 4.5.2.3) or IEF of an alternative glycoprotein like α-1-antitrypsin (see section 4.5.2.4) should be performed.

4.5.2.2 IEF of Transferrin Derived from Guthrie Cards

Procedure

A punched out piece of the Guthrie card is incubated in 50 µl of distilled water for 10 min at room temperature. A 10-µl aliquot of Fe(III)-citrate (200 µM) and 50 µl of distilled water are added to the sample and incubation is performed for 10 min at room temperature. One microlitre of the dissolved material is subsequently investigated by PhastGel electrophoresis as described above.

Pitfalls

In the case of unclear transferrin patterns obtained from IEF analysis of blood samples derived from Guthrie cards, the analysis should be repeated with serum.

4.5.2.3 Desialylation of Transferrin-Linked Oligosaccharides by Neuraminidase Treatment

Principle

Mutations that lead to amino acid changes in transferrin may alter the charge of the protein, thereby leading to shifts in the IEF pattern, which mostly resemble to either

tri- or pentasialo transferrin. To avoid false-positive results, desialylation of transferrin by neuraminidase treatment or IEF of an alternative glycoprotein like α-1-antitrypsin (see section 4.5.2.4) should be performed (Figs. 4.5.4 and 4.5.5).

Pre-analytical

Specimen

Serum, 6 µl.

Reagents and Chemicals

1. Neuraminidase (1 U/100 µl; Roche, Mannheim, Germany).
2. 1 M Sodium acetate (pH 5.0; Merck).
3. 10 mM Tris (pH 7.0; p.a., Roth)/0.9% NaCl (p.a., Roth).
4. Dialysis membrane (cut-off: 12–14 kDa; Neolab, Heidelberg, Germany).

Instrumentation

1. Heating block (Eppendorf, Hamburg, Germany).
2. Speed-vac (Bachofer, Weilheim, Germany).
3. Magnetic stirrer (Heidolph, Kehlheim, Germany).

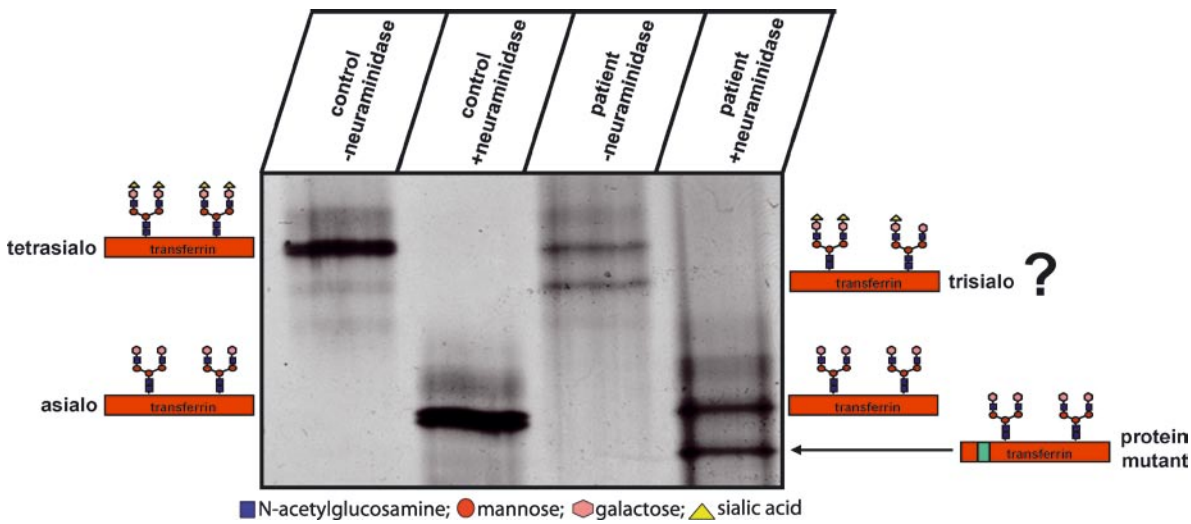

Fig. 4.5.4 Identification of mutations in the transferrin protein by neuraminidase treatment. Unusual patterns in the IEF of serum transferrin might lead to pitfalls in CDG diagnostics. These varying patterns are often due to mutations of charged amino acids in the protein backbone of the transferrin molecule, which might lead, for example, to an accumulation of trisialo transferrin bands (lane 3, indicated by a *question mark*). Further investigations are carried out by cleaving off charged sialic acid monosaccharide moieties from transferrin-linked oligosaccharides by neuraminidase treatment, followed by IEF and transferrin antibody staining. In the case of protein mutations, additional bands below (lane 4) or above (not shown) the desialylated transferrin form appear

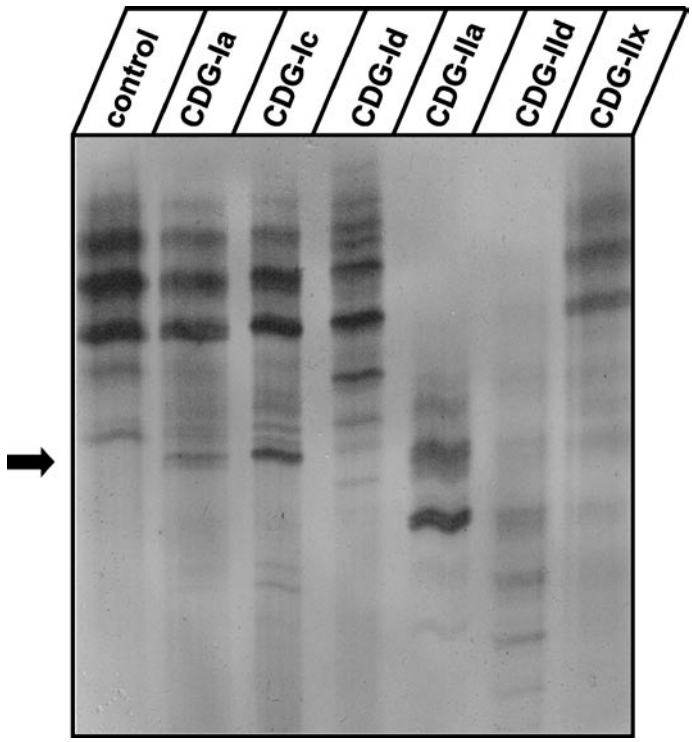

Fig. 4.5.5 IEF pattern of α-1-antitrypsin. Sera from a control (lane 1), three CDG-I patients (CDG-Ia, CDG-Ic and CDG-Id; lanes 2-4) and three CDG-II patients (CDG-IIa, CDG-IId and CDG-IIx; lanes 5-7) were analysed by IEF. The normal pattern (lane 1, left) reveals seven bands. In abnormal patterns (lanes 2–7, left to right), the position of the first additional abnormal cathodal band is indicated by an *arrow*. This band and also all bands below are abnormal and indicate a glycosylation deficiency

Calibration

To compare sera from patients suffering from unclear CDG types, sera of healthy persons and patients with already defined CDG are used as controls for neuraminidase treatment studies.

Analytical

Procedure

Neuraminidase digestion of transferrin is performed from 6 µl of serum, 2.5 µl 1 M sodium acetate (pH 5.0), 15.5 µl double-distilled water and 1 µl neuraminidase (0.01 U). Incubation is carried out overnight at 37°C followed by dialysis against double-distilled water at 4°C for 12 h and subsequent drying by lyophilisation. Dried samples are resuspended in 1.5 ml 10 mM Tris (pH 7.0)/0.9% NaCl and analysed by IEF, followed by silver staining as described above.

Post analytical

Interpretation

Data analysis is carried out by comparing IEF patterns from patients suspected of having a CDG with healthy controls and already defined CDG types. Following neuraminidase treatment, controls and CDG patients will predominantly present with the asialo form of transferrin. In the case of mutations that affect the protein backbone of transferrin, additional bands appear (Fig. 4.5.4).

4.5.2.4 IEF of α-1-Antitrypsin

Principle

Standard initial investigations on CDG are based on the identification of hyposialylated serum transferrin by IEF. Since mutations in the protein backbone of transferrin might lead to false-positive results, neuraminidase treatment of serum-transferrin is performed (see above; Fig. 4.5.4). Alternatively, other serum glycoproteins like α-1-antitrypsin might be used to confirm CDG [6]. Human plasma α-1-antitrypsin is normally fully glycosylated at amino acid residues 46, 83 and 247 [20]. Due to combinations of tri- and diantennary-complex-type oligosaccharides and shortened isoforms of the protein, a pattern of seven bands in IEF analysis of α-1-antitrypsin in healthy controls is detectable. In the case of CDG it has been shown that additional bands with a cathodal shift appear, the number and size of which depend on the corresponding type of CDG (Fig. 4.5.5) [6].

Pre-analytical

Specimen

Serum, 1–3 µl.

Reagents and Chemicals

1. Pharmalyte pH 4.2–4.9 (Amersham Biosciences).
2. Antibody: rabbit anti-human α-1-antitrypsin (DakoCytomation).

Also, see 4.5.2.1, subheading "Reagents and Chemicals", above.

Instrumentation

1. PhastSystem (Amersham Biosciences).
2. PhastGel dry gel (Amersham Biosciences).
3. PhastGel sample applicator 8/1 (Amersham Biosciences).
4. PhastGel cassette (Amersham Biosciences).

Calibration

Calibration of IEF is carried out with sera from healthy controls as well as sera derived from patients with defined types of CDG.

Running Conditions

- Isoelectric Focusing

Please refer to Table 4.5.4

1. Sample applicator: down at 1.2, 0 Vh.
2. Sample applicator: up at 1.3, 100 Vh.
3. Extra alarm: to sound at 1.1, 73 Vh.

- Silver Staining

Please refer to Table 4.5.5.

Table 4.5.4 *Set up for isoelectric focusing of α-1-antitrypsin*

Sep 1.1	2000 V	2.5 mA	3.5 W	15°C	75 Vh
Sep 1.2	200 V	2.5 mA	3.5 W	15°C	15 Vh
Sep 1.3	2000 V	2.5 mA	3.5 W	15°C	100 Vh
Sep 1.4	1000 V	2.5 mA	3.5 W	15°C	280 Vh

Table 4.5.5 *Conditions for silver staining*

Dev 1.1	fixation	5 min	20°C
Dev 1.2	wash solution 1	2 min	50°C
Dev 1.3	wash solution 2	2 min	50°C
Dev 1.4	wash solution 2	4 min	50°C
Dev 1.5	8.3% glutardialdehyde	6 min	50°C
Dev 1.6	wash solution 2	3 min	50°C
Dev 1.7	wash solution 2	5 min	50°C
Dev 1.8	DD water	2 min	50°C
Dev 1.9	DD water	2 min	50°C
Dev 1.10	0.5% silver nitrate	10 min	50°C
Dev 1.11	DD water	0.5 min	50°C
Dev 1.12	DD water	0.5 min	50°C
Dev 1.13	developer	0.5 min	50°C
Dev 1.14	developer	12 min	50°C
Dev 1.15	stop solution	5 min	50°C
Dev 1.16	DD water	5 min	50°C

Analytical

Procedure

IEF PhastGels are rehydrated for 30 min at room temperature in a solution containing double-distilled water and 60 ml/l Pharmalyte (4.2–4.9) in a PhastGel cassette. The sera are diluted to 1:150 and 0.85 µl of the samples are loaded on the PhastGel sample appplicator 8/1 for IEF. After separation, the gels are incubated with a rabbit anti-human α-1-antitrypsin antibody for 40 min followed by washing in 150 mM NaCl overnight. Automated silver staining of gels by the PhastSystem is performed as described above [10, 23].

Post-analytical

Interpretation

Data are analysed by comparing the α-1-antitrypsin IEF patterns of patients suspected of having an altered transferrin protein backbone to healthy controls and patients with an already defined CDG. A normal pattern of α-1-antitrypsin in questionable patients indicates changes in the protein moiety of transferrin instead of a glycosylation deficiency.

4.5.2.5 Screening for CDG-I: Analysis of Phosphomannomutase Activity

Principle

In case of CDG-I IEF pattern, further investigations are initiated by the determination of PMM activity. PMM2 is the defective enzyme in the most widespread form of CDG known so far: CDG-Ia (about 80% of all known CDG-cases). It is caused by mutations in the gene, which result in a severe decrease in PMM2 activity, catalysing the conversion of mannose-6-phosphate to mannose-1-phosphate in the cytosol (Fig. 4.5.1). Determination of enzyme activity may be carried out by incubation of protein extracts from patient-derived fibroblasts or leukocytes with [2-^{3}H]mannose-6-phosphate and subsequent high-voltage paper electrophoresis. This technique is highly sensitive and needs only a very small amount of material (10 µg of protein). Another approach is based on the determination of PMM activity by a coupled optical enzyme assay (100 µg of protein is needed). This technique is described elsewhere [26].

Pre-analytical

Specimen

Leukocytes from 2.5–5 ml EDTA-treated blood or 1×10^6 primary skin fibroblasts.

Reagents and Chemicals

For preparation of [2-^{3}H]mannose-6-phosphate:

1. [2-^{3}H]mannose (15.0 Ci/ mMol, where 1 Ci = 3.7×10^{10}Bq), Amersham Biosciences).
2. 1 M Tris-HCl (pH 7.4; Roth).
3. 1 M $MgCl_2$ (Merck, Darmstadt, Germany).
4. 100 mM ATP (Sigma, Steinheim, Germany).
5. Hexokinase (1500 U/ml; Sigma).
6. Whatman 3MM paper (Schleicher & Schuell, Einbeck, Germany).
7. 80 mM Pyridine (Merck).
8. Acetic acid (Merck).
9. Water (HPLC grade; Merck).
10. Argon/methane (90%/10%) for thin-layer chromatography (TLC) analyser.
11. Orange G (5% in water; Sigma).

For PMM activity (reagents in addition to the preparation of [2-^{3}H]mannose-6-phosphate):
1. 50,000 dpm [2-^{3}H]mannose-6-phosphate (see below for preparation).
2. 100 mM Tris-HCl (pH 7.5)/4 mM $MgCl_2$ (Roth).
3. 1 mM Glucose-1,6-bisphosphate (Boehringer, Mannheim, Germany).

Instrumentation

1. Power supply EC4000P (Thermo, Dreieich, Germany).
2. Electrophoresis chamber (CAMAG, Muttenz, Switzerland).
3. Thermomixer (Eppendorf).
4. Lyophiliser (Schrader, Nentershausen, Germany).
5. Automatic TLC-scanner (Tracemaster 20, Berthold, Bad Wildbach, Germany).

Calibration

For calibration, cell extracts from a CDG-Ia patient and a healthy control are used.

Analytical

Procedure

■ Preparation of [2-^{3}H]mannose-6-phosphate

A 100-µl aliquot of [2-^{3}H]mannose (15.0 Ci/mMol) is evaporated under a flow of nitrogen. For the reaction mixture, 10 µl of 1 M Tris-HCl (pH 7.4), 1 µl of 1 M $MgCl_2$, 10 µl of 100 mM ATP and 0.67 µl hexokinase (1,500 U/ml) are filled up with water to 100 µl and added to the dried [2-^{3}H]mannose. Incubation is performed for 4 h at 37°C and stopped by heating for 2 min at 95°C. Orange G (4 µl) is added and the samples are subjected to high-voltage electrophoresis at 33 V/cm for 2 h on Whatman 3MM paper in a buffer containing 80 mM pyridine (pH 5.5, adjusted with acetic acid) to separate [2-^{3}H]mannose and [2-^{3}H]mannose-6-phosphate. Evaluation is carried out on a TLC scanner. [2-^{3}H]mannose-6-phosphate spots are cut out and eluted overnight at 4°C in 20 ml of water in a 50-ml vial. Samples are centrifuged for 10 min at $5000 \times g$. The supernatant containing [2-^{3}H]mannose-6-phosphate is removed, quantified by liquid scintillation counting, lyophilised and adjusted to 50,000 dpm/µl with water.

■ Analysis of PMM Activity

PMM activity is determined by following the conversion of mannose-6-phosphate to mannose-1,6-bisphosphate in the presence of an excess of glucose-1,6-bisphosphate. The assay mixture contains 12.5 µl 100 mM Tris-HCl (pH 7.5)/4 mM $mgCl_2$, 50,000 dpm [2-^{3}H]mannose-6-phosphate, 1 mM glucose-1,6-bisphosphate and 10 µg of protein of cell extracts in a total volume of 25 µl. After incubation for 30 min at 37°C the supernatants are collected by centrifugation and [2-^{3}H]mannose-6-phosphate is separated from [2-^{3}H]mannose-1,6-bisphosphate by high-voltage paper electrophoresis as described above.

Calculation

The conversion of [2-^{3}H]mannose-6-phosphate to [2-^{3}H]mannose-1,6-bisphosphate in extracts from skin fibroblasts or leukocytes derived from patients is compared to controls. Calculation is performed by the TLC-analyser software "Chromas 1.1".

Post-analytical

Interpretation

In most CDG-Ia patients PMM activity is reduced to less than 10% compared to controls. Follow-up investigations are carried out by mutational analysis of the *PMM2* gene.

4.5.2.6 Screening for CDG-I: Analysis of PMI Activity

Principle

CDG-Ib is caused by PMI deficiency. This enzyme catalyses the conversion of fructose-6-phosphate to mannose-6-phosphate in the cytosol (Fig. 4.5.1). The IEF pattern of serum transferrin in CDG-Ib is comparable to that of CDG-Ia, although the clinical phenotype is completely different, with gastrointestinal bleedings and hepatopathy. Determination of PMI activity is performed by a coupled optical test.

Pre-analytical

Specimen

Protein, 30 µg, isolated from fibroblasts or leukocytes.

Reagents and Chemicals

1. 1 M 4-(2-Hydroxyethyl)-1-piperazineethanesulphonic acid (Hepes; pH 7.1; Roth).
2. 1 M KCl (Roth).
3. 0.2 M Dithiothreitol (Sigma-Aldrich).
4. 10 mg/ml Leupeptin (Sigma-Aldrich).
5. 10 mg/ml Antipain (Sigma-Aldrich).
6. 1 M $MgCl_2$ (Merck).

7. 0.1 mM NADP (Sigma-Aldrich).
8. Phosphoglucose isomerase (2 mg/ml; 350 U/mg) (Boehringer).
9. Glucose-6-phosphate dehydrogenase (5 mg/ml) (Boehringer).
10. 0.1 M Mannose-6-phosphate (Sigma-Aldrich).
11. Double-distilled water.

Instrumentation

1. Branson sonicator (Heinemann, Schwäbisch Gmünd, Germany).
2. Spectrophotometer (U-2000, Hitachi, Hamburg, Germany).

Calibration

PMI activities from fibroblasts or leukocytes of healthy controls are compared to the cellular material of the patient.

Analytical

Procedure

Trypsinised cells are collected by centrifugation, resuspended in 200 µl of lysis buffer containing 20 mM Hepes (pH 7.1), 25 mM KCl, 1 mM dithiothreitol, 10 µg/ml leupeptin and 10 µg/ml antipain. After a freeze-thaw cycle at –80°C, cells are disrupted by passing 20 times through a 22-guage syringe followed by centrifugation for 15 min at 100,000 × *g*. The supernatant is transferred to new vials, protein concentration is determined and adjusted to a concentration of 600 µg/ml with lysis buffer. PMI activity is determined from 30 µg (in 50 µl lysis buffer) of total cellular protein by addition of 50 µl reaction buffer (100 mM Hepes, pH 7.1, 10 mM $MgCl_2$, 0.5 mM NADP, 1 µg phosphoglucose isomerase and 1 µg glucose-6-phosphate dehydrogenase). The enzymatic reaction is started by the addition of mannose-6-phosphate (1 mM final concentration). Incubation of samples is carried out at room temperature and enzymatic activity is followed in a double-beam spectrophotometer at $OD_{340\,nm}$ (i.e. the decreasing rate per minute of absorption at 340 nm) over 30 min.

Calculation

Enzyme activity is investigated in a double-beam spectrophotometer in the presence or absence of substrate. PMI activity is determined according to the relative formation of $NADPH + H^+$ in the sample containing the substrate compared to that of the substrate-free sample over 30 min of continuous measurement.

Post-analytical

Interpretation

A reduction of PMI activity to less than 20% of that of controls indicates the presence of CDG-Ib and indicates mutational analysis of the corresponding *PMI* gene.

4.5.2.7 Screening for CDG-I: Analysis of LLO by [2-^{3}H]Mannose Labelling

Principle

Metabolic labelling studies on LLO with [2-^{3}H]mannose are carried out in fibroblasts of patients who present with a characteristic CDG-type I IEF transferrin pattern but normal PMM and PMI activities, thereby excluding CDG-Ia and CDG-Ib. Investigations require the extraction and analysis of LLO by HPLC and TLC.

Pre-analytical

Specimen

Metabolic labelling studies require primary skin fibroblasts from patients and healthy controls. It is also helpful to have an internal control from CDG-type I patients, who accumulate shortened LLO, like $Man_5GlcNAc_2$ (CDG-Id, CDG-Ie) or $Man_7GlcNAc_2$ (CDG-Ig; Fig. 4.5.6).

■ Cell Culture

Primary fibroblasts from skin biopsy samples are grown at 37°C in the presence of 5% CO_2 in Dulbecco's modified Eagle's medium (DMEM) supplemented with 10% foetal calf serum (FCS) and 1% penicillin/streptomycin. For passaging, confluent cells are washed with phosphate-buffered saline (PBS) and incubated for 5–10 min at 37°C in the presence of trypsin.

■ Reagents, Chemicals and Instrumentation for Cell Culture

1. DMEM (PAA, Pasching, Austria).
2. FCS (PAA).
3. PBS (PAA).
4. Trypsin (PAA).
5. Penicillin/streptomycin (PAA).
6. Cell culture flasks of different sizes (Sarstedt, Nuembrecht, Germany).
7. Cell incubator (Sanyo, Wiesloch, Germany).

Reagents and Chemicals for LLO Analysis

1. Minimum essential medium (MEM) with glucose reduced to 0.5 mM (Gibco/Invitrogen, Karlruhe, Germany).
2. [2-^{3}H]mannose (15 Ci/mmol) (Amersham Biosciences).
3. PBS (PAA).
4. Triton X-100 (Sigma-Aldrich).
5. Methanol (Roth).
6. Chloroform (Merck).
7. 1 M $MgCl_2$ (Sigma-Aldrich).
8. 1-Propanol Rotipuran (Roth).
9. 0.02 N HCl (Merck).
10. 1 M Tris-HCl (pH 8.0; Roth).
11. Acetonitrile Licrosolv (Merck).
12. Water (HPLC grade, Neolab).

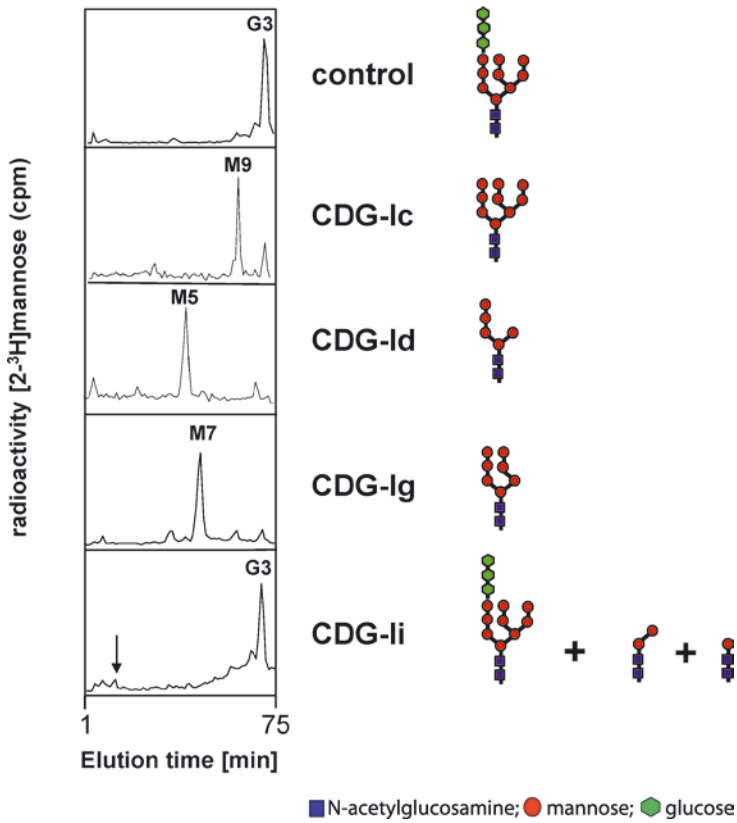

Fig. 4.5.6 Lipid-linked oligosaccharides (LLO) isolated from different CDG-I patients. Fibroblasts from a control and different CDG-I patients (CDG-Ic, CDG-Id, CDG-Ig, CDG-Ii) were metabolically labelled with 2-[^{3}H]mannose for 30 min. [^{3}H]oligosaccharides were released from LLO by mild acid hydrolysis and size-fractionated by HPLC. M5, M7, M9 and G3 refer to the positions of $GlcNAc_2Man_5$, $GlcNAc_2Man_7$, $GlcNAc_2Man_9$ and $GlcNAc_2Man_9Glc_3$, respectively. The *arrow* marks shortened [2-^{3}H]mannose-labelled oligosaccharides accumulating in the case of very early CDG-I types like CDG-Ii, which are often hard to detect by standard LLO-HPLC analysis

13. Ultima Gold (Perkin-Elmer, Germany).
14. Argon/methane (90%/ 10%) for the TLC scanner.

Instrumentation

1. TLC Silica gel 60 aluminium sheets (Merck).
2. TLC-Chamber (Sigma-Aldrich).
3. Supelcosil LC-NH_2 column (25 cm × 4.6 mM; 5 µm; Supelco; Sigma-Aldrich).
4. LC-NH_2 (2 cm × 4.6 mm) precolumn (Sigma-Aldrich).
5. HPLC-pump 1525 (Waters).
6. In-line degasser (Waters).
7. Waters Fraction Collector III (Waters).

8. Scintillation counter (Beckmann).
9. Branson sonicator (Heinemann).
10. TLC scanner (Tracemaster 20, Berthold).

Calibration

Analysis of LLO from controls reveals predominantly an LLO structure consisting of 14 monosaccharide residues ($Glc_3Man_9GlcNAc_2$), whereas CDG-patients with defined type-I deficiencies show shortened LLO profiles, which help to identify defects in patients with unknown CDG-I types.

Analytical

Procedure

Fibroblasts ($6.6 \times 10^4/cm^2$) are plated onto 6-cm culture dishes and grown for 60 h in DMEM. Cells are metabolically labelled for 30 min in MEM with a reduced glucose concentration of 0.5 mM, which is supplemented by 125 µCi [2-^{3}H]mannose. Cells are washed three times with ice-cold 10 mM PBS (pH 7.4), scraped into 2 ml of ice-cold methanol, and lysed by sonication. After addition of 4 ml chloroform, the material is again sonicated, followed by centrifugation for 10 min at $5000 \times g$ at 4°C. Supernatants are collected and the pellets are extracted two more times with chloroform/methanol (3:2). Combined supernatants containing LLO of small size are dried under a stream of nitrogen, dissolved in 3 ml chloroform/methanol (3:2), washed two times with 2 ml of a solution containing 96 ml methanol, 94 ml water, 6 ml chloroform and 200 µl 1 M $MgCl_2$. The upper phase is discarded and the lower phase is washed another two times with 2 ml of a solution containing 96 ml methanol, 98 ml water and 6 ml chloroform. The lower phase is dried under nitrogen, solved in 500 µl chloroform/ methanol (3:2), and analysed by TLC on Silica gel 60 coated aluminium sheets in a running buffer containing chloroform/ methanol/ water (65:25:4). The silica gel sheets are air dried and evaluated on a TLC scanner (Fig. 4.5.7).

The remaining pellet, which contains large sized LLO, is washed two times with 2 ml of a solution containing 96 ml methanol, 94 ml water, 6 ml chloroform and 200 µl 1 M $MgCl_2$. The supernatants are discarded and the pellet is washed another two times with 2 ml of a solution containing 96 ml methanol, 98 ml water and 6 ml chloroform. The pellet is washed once with 1 ml methanol. Large-sized LLO are extracted with 2 ml chloroform/methanol/water (10:10:3) three times. The supernatants are combined, evaporated under a nitrogen flow and dissolved in 500 µl chloroform/methanol/water (10:10:3). Corresponding aliquots of the chloroform/ methanol and chloroform/ methanol/water extracts are combined and dried under nitrogen and resuspended in 50 µl 1-propanol. Oligosaccharide moieties are released by mild acid hydrolysis in 500 µl 0.02 N HCl for 30 min at 95°C. The hydrolysed material is dried under a stream of nitrogen, solved by sonication in 200 µl H_2O and cleared by centrifugation. Supernatants that contain the released oligosaccharides are used for HPLC analysis. Separation of LLO is performed on a Supelcosil LC-NH_2 column. A linear gradient of acetonitrile from 70–50% in water (total volume 75 ml) is applied at a flow rate of 1 ml/min. Eluate fractions are analysed by liquid scintillation counting.

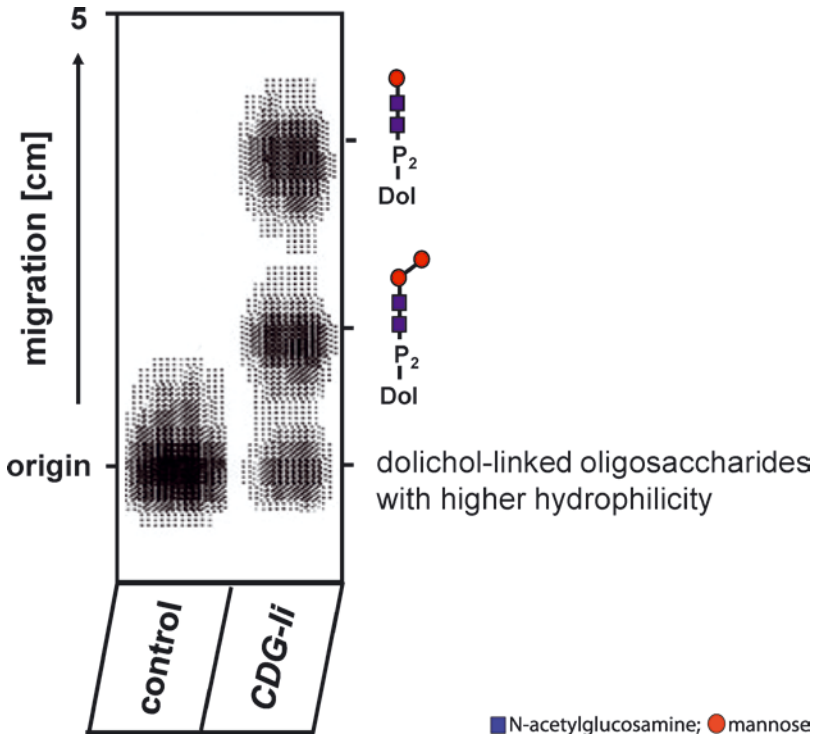

Fig. 4.5.7 TLC analysis of short LLO. Fibroblasts derived from a control (lane 1, left) and a CDG-Ii patient (lane 2, right) were metabolically labelled for 30 min with [2-^{3}H]mannose. Short LLO were extracted with chloroform/methanol (3:2) and further analysis carried out by TLC in a running buffer containing chloroform/methanol/H_2O (65:25:4). The position of the origin, and the positions of [^{3}H]$Man_1GlcNAc_2$-PP-dolichol and [^{3}H]$Man_2GlcNAc_2$-PP-dolichol are indicated

Calculation

The incorporated radioactivity is plotted against the fractions and compared to the HPLC profile of radioactive labelled oligosaccharide standards.

Post analytical

Interpretation

Comparison of the main peak fractions derived from controls ($Glc_3Man_9GlcNAc_2$) and internal standards ($Man_5GlcNAc_2$, $Man_7GlcNAc_2$) give a hint to the underlying defect in patients with a suspected CDG-I (Fig. 4.5.6), which allows subsequent analysis of the putative affected gene.

Pitfalls

Metabolic labelling of cells with [2-^{3}H]mannose fails to detect deficiencies in the very early onset of LLO biosynthesis as in CDG-Ij and CDG-Ik (Fig. 4.5.1). In this case,

labelling of patient-derived fibroblasts should be performed with [6-^{3}H]glucosamine instead of [2-^{3}H]mannose (see below).

A defect in the human orthologue of the yeast ALG10 protein (CDG-Ih), which catalyses the transfer of the second glucose residue to the LLO intermediate $Glc_1Man_9GlcNAc_2$, will lead to accumulation of $Man_9GlcNAc_2$, because of the high affinity of $Glc_1Man_9GlcNAc_2$ for ER-glucosidase 2. In the case of accumulation of $Man_9GlcNAc_2$, therefore, a defect in ALG6 (CDG-Ic) or ALG10 (Fig. 4.5.1) should always be considered.

4.5.2.8 Screening for CDG-I: Analysis of LLO by [6-^{3}H]Glucosamine Labelling

Principle

Defects in the early steps of LLO biosynthesis (Fig. 4.5.1) lead to an accumulation of shortened LLO that escape the extraction procedure described above (e.g. CDG-Ik). Moreover, defects in the initiating steps of LLO biosynthesis, such as the addition of the two glucosamine residues and the first mannose residue, are missed by metabolic labelling with [2-^{3}H]mannose. In this case it is necessary to label fibroblasts with [6-^{3}H]glucosamine.

Pre-analytical

Specimen

Metabolic labelling is carried out in primary skin fibroblasts. It is helpful to have an internal control from a CDG-type I patient with an early N-glycosylation deficiency like CDG-Ii or CDG-Ik.

Reagents and Chemicals in Addition to LLO Analysis

1. 1 mCi [6-^{3}H]glucosamine (33.0 Ci/mmol, Amersham Biosciences).
2. DMEM (Gibco/Invitrogen).
3. 2% Dialysed FCS.
4. 0.5 mM Glucose (Sigma).
5. 0.5 mM mannose (Sigma).

Calibration

Metabolically labelled fibroblasts from CDG-patients with defined deficiencies in the very early steps of LLO biosynthesis are compared to LLO profiles of patients with a suspected CDG.

Analytical

Procedure

Prior to the experiment (60 h), 3.6×10^6 control- and patient-derived fibroblasts are plated onto 100 mM cell-culture dishes. Cells are labelled for 60 min in the presence of 1 mCi [6-^{3}H]glucosamine in DMEM containing 2% dialysed FCS, 0.5 mM glucose

and 0.5 mM mannose. Fibroblasts are scraped into methanol, and the short LLO are extracted and analysed by TLC as described above.

Calculation

The LLO profile of the patient under investigation is compared to profiles of controls and patients with known CDG types.

Post-analytical

Interpretation

Peak fractions that appear in addition to the control give a clear indication of an accumulation of shortened LLO and accordingly to an early CDG defect in the patient. Mutational analysis of the corresponding gene would follow.

4.5.2.9 Screening for CDG-II: Analysis of Transferrin-Linked Oligosaccharides

Principle

Processing of oligosaccharides linked to newly synthesised glycoproteins comprise several trimming and elongation steps in the endoplasmic reticulum and the Golgi apparatus (Fig. 4.5.1). Defects in these steps result in truncated forms of glycans due to the partial loss of monosaccharide residues, thereby leading to the appearance of mono- and trisialo transferrin in addition to di- and asialo transferrin forms in IEF. Analysis of the glycan composition involves purification of transferrin from human serum, release of oligosaccharide moieties from isolated transferrin by N-glycosidase F digestion, 2-AB labelling of the extracted oligosaccharides and HPLC analysis. Since HPLC analysis by GlycoSepN columns separates oligosaccharides only by size compared to defined standards, further investigations on fractionated peaks can be achieved by mass spectrometry (matrix-assisted laser desorption ionisation – time of flight, MALDI-ToF) to determine the molecular weights of the oligosaccharides, thereby providing data regarding their molecular composition.

Purification of Serum Transferrin

Pre-analytical

- Specimen

Serum, 250 µl, from a control and the patient.

- Reagents and Chemicals

1. 6,9-Di-amino-2-ethoxyacridine lactate (Sigma-Aldrich).
2. NaCl p.a. (Roth).
3. Saturated ammonium sulphate solution p.a. (J.T. Baker, Phillipsburg, USA).
4. 10 mM Tris-HCl (pH 7.4) p.a. (Roth).
5. Dialysis membrane (cut-off: 12–14 kDa; Neolab).

■ Instrumentation

1. Microcentrifuge (Eppendorf).
2. Magnetic stirrer (Heidolph).
3. Speed-vac (Bachofer).

Analytical

■ Procedure

Purification of transferrin from 250 µl of total serum is initiated by the addition of 175 µl double-distilled water and 175 µl of 3% 6,9-di-amino-2-ethoxyacridine lactate in a 1.5-ml reaction device. After gently mixing, centrifugation is carried out at 10,000 × *g* for 10 min. The supernatant is transferred into a new 1.5-ml sample device containing 25 mg NaCl, mixed and centrifuged again. An equal amount of saturated ammonium sulphate solution is added to the supernatant. Incubation is carried out at room temperature for 10 min, followed by the next centrifugation step. The supernatant is dialysed against 1 l of 10 mM Tris-HCl (pH 7.4), dried under vacuum and resolved in double-distilled. water (see "Procedure" for "Release of Oligosaccharides from Purified Transferrin by N-Glycosidase F Digestion" below).

Release of Oligosaccharides from Purified Transferrin by N-Glycosidase F Digestion

Pre-analytical

■ Reagents and Chemicals

1. *β*-Mercaptoethanol for synthesis (Merck).
2. Sodium dodecylsulphate (SDS p.a.; Serva, Heidelberg, Germany).
3. 0.5 M Tris-HCl (pH 8.0) p.a. (Roth).
4. 0.2 M 1,10-Phenanthrolin (Sigma-Aldrich).
5. 10% Triton X-100 (Sigma-Aldrich).
6. N-Glycosidase F (PNGase; Roche).
7. Butanol 99.5% p.a. (Roth).
8. Ethanol 99.8% p.a. (Roth).

■ Instrumentation

1. Heating block (Eppendorf).
2. Speed-vac (Bachofer).
3. Paper for chromatography, Whatman (BG002; Schleicher & Schuell).
4. Filtropur S 0.2 (Sarstedt).

Analytical

■ Procedure

After determination of the protein concentration in the sample, a mixture of 0.1 M *β*-mercaptoethanol/0.5% SDS is added. The amount of SDS should be in a 1.2- to 1.5-fold (w/w) excess to the amount of sample protein. The sample is denatured for 5 min at 95°C, chilled on ice and subsequently incubated at 37°C for 12 h in the presence of 2.5 U N-glycosidase F in a buffer containing the final concentrations of 0.12 M Tris-HCl (pH 8.0), 0.01 M 1,10-phenanthrolin and 1% Triton X-100. Samples are dried by lyophilisation, dissolved in 20 µl double-distilled water and oligosaccharide

moieties are separated from other components by descending paper chromatography on Whatman GB002 in butanol:ethanol:water (4:1:1) for 20 h [24]. Under these conditions, oligosaccharides remain at the origin and are cut out of the chromatography paper at the end of the run. Glycans are dissolved by sonication in 3 × 750 µl double-distilled water, followed by filtration (0.2 µm) and lyophilisation.

2-Aminobenzamide Labelling of Oligosaccharides

Pre-analytical

Reagents and Chemicals

1. Dimethylsulphoxide (DMSO) Seccosolv (Merck).
2. Acetic acid 100% (Merck).
3. Sodium sulphate p.a. (Roth).
4. Anthranilamide (2-aminobenzamide, 2-AB, 98%; Sigma-Aldrich).
5. Sodium cyanoborohydride purum (>95%; Fluka, Seelze, Germany).
6. Ethyl acetate p.a. (Fluka).

Instrumentation

1. Speed-vac (Bachofer).
2. Paper for chromatography (Whatman BG002, Schleicher & Schuell).
3. Filtropur S 0.2 (Sarstedt).
4. Incubator (Memmert, Schwabach, Germany).
5. Screw vials N8-1 brown (Machery-Nagel, Dueren, Germany).
6. Sealing disks N8 (Machery-Nagel).
7. Screw caps N8 (Machery-Nagel).
8. Microinsert standards (Machery-Nagel).

Analytical

Procedure

DMSO and acetic acid are dehydrated overnight in the presence of sodium sulphate at 120°C. 4.5 mg 2-AB and 6.3 mg sodium cyanoborohydride are dissolved in 100 µl DMSO:acetic acid (7:3) and pre-incubated at 65°C for 10 min. Labelling is initiated by the addition of 10 µl of the mixture to the dried oligosaccharides inside the microinserts. Incubation is carried out at 65°C for 2 h under vacuum. Free labelling is removed by ascending paper chromatography on Whatman GB002 in ethylacetate for 30–45 min. Under these running conditions, oligosaccharides remain at the origin. They are cut out of the chromatography paper, dissolved by sonication in 3 × 750 µl double-distilled water, purified by filtration (0.2 µm) and freeze dried [3, 13].

HPLC Analysis of 2-AB-Labelled Oligosaccharides

Pre-analytical

Reagents and Chemicals

1. Acetonitrile, Licrosolv for liquid chromatography (Merck).
2. Ammoniac 25% p.a. (Merck).

3. Formic acid 98–100% Suprapur (Merck).
4. HPLC-water (Neolab).
5. Glucose homopolymer standard (Oxford Glycoscience, Oxford, UK).
6. Buffer: add 6 ml ammoniac (25%, Merck) to 900 ml HPLC-water, titrate with formic acid 98–100% Suprapur (Merck) to pH 4.4 and fill up to 1 l to obtain 80 mM ammonium formate (pH 4.4).

Instrumentation

1. HPLC pump 1525 (Waters).
2. Fluorescence detector 2475 (Waters).
3. In-line degasser (Waters).
4. Column oven (Waters).
5. Waters Fraction Collector III (Waters).
6. HPLC column (GlycoSepN: 4.6 × 250 mM, normal Phase, Oxford Glycoscience).

Calibration

The HPLC system is calibrated with a glucose homopolymer standard that separates oligosaccharides consisting of 3 to at least 20 monosaccharide residues.

Running conditions

Please refer to Table 4.5.6.

Analytical

Procedure

2-AB-labelled oligosaccharides are resolved in 50 µl 65% acetonitrile/35% 80 mM ammonium formate (pH 4.4). Aliquots (50 µl) of 1:10 diluted samples are injected onto the HPLC column. Analysis of the eluate is carried out by fluorescence detection (excitation at 330 nm, emission at 420 nm). Peak fractions are further investigated by mass spectrometry.

Table 4.5.6 *Running conditions for high-performance liquid chromatography analysis of 2-aminobenzamide-labelled oligosaccharides*

Time (min)	100% Acetonitrile	80 mM Ammonium formate (pH 4.4)	Flow (ml/min)
0	65%	35%	0.4
72	47%	53%	0.4
75	0%	100%	0.4
77	0%	100%	1
92	0%	100%	1
95	65%	35%	1
100	65%	35%	0.4

Mass Spectrometric Analysis of 2-AB-Labelled Oligosaccharides by MALDI-ToF

Pre-analytical

Reagents and Chemicals

1. 2,5-Dihydroxybenzoic acid (Sigma-Aldrich).
2. Acetone (Merck).
3. Acetonitrile Licrosolv for liquid chromatography (Merck).
4. 5% Perfluorinated Nafion (Sigma-Aldrich).
5. Trifluoroacetic acid (TFA; Merck).
6. 2,5-Dihydroxybenzoic acid (DHB) solution 1: dissolve 10 mg DHB in 500 µl acetone.
7. DHB solution 2: dissolve 10 mg DHB in 333 µl acetonitrile, 167 µl water, 10 µl 5% perfluorinated Nafion and 0.5 µl TFA.

Instrumentation

Bruker REFLEX III (Bruker Daltonik GmbH, Bremen, Germany).

Analytical

Procedure

Mass spectrometric analysis is performed on a Bruker REFLEX III mass spectrometer with a matrix consisting of DHB. DHB solution 1 (10.5 µl) is applied to the slide and dried to a thin layer. 2-AB-labelled glycans are dissolved in water, applied (0.5–1.0 µl) to the target and dried under a slight air stream. DHB solution 2 (0.5 µl) is added to the glycans and dried again by a slight air stream. The effective path length is 145 cm. The samples are ionised with a nitrogen laser at 337.1 nm. Charged oligosaccharides are analysed in the linear, negative mode [25]. Uncharged oligosaccharides are analysed in the linear, positive mode [21].

Calculation

Determination of oligosaccharide size is calculated from the mass of monosaccharide residues and the 2-AB label (Fig. 4.5.8). An example of the biantennary complex-type oligosaccharide is:

(2-AB)-$GlcNAc_2$-Man_3-$GlcNAc_2$-Gal_2-Sia_2 (2342.92 Da)

$136.15 + (203.08 \times 2) + (162.05 \times 3) + (203.08 \times 2) + (162.05 \times 2) + (292.10 \times 2) = 2342.92$ Da

Post analytical

Interpretation

For oligosaccharide size, the detected masses are compared to calculated molecular masses of variable oligosaccharide moieties to determine the monosaccharide residues that are lacking in each patient (Fig. 4.5.9).

Pitfalls

Determination of oligosaccharides in the positive mode leads to the separation of sialic acid from the glycans, therefore the results reveal the masses of desialylated oligosaccharides.

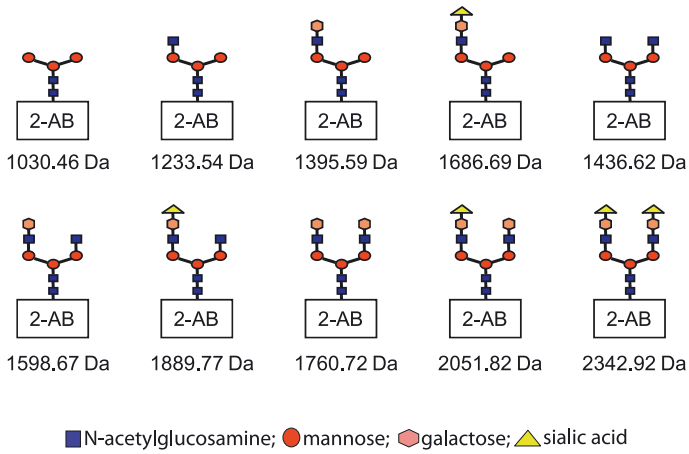

Fig. 4.5.8 Examples for structures and molecular masses of 2-aminobenzamide (2-AB)-labelled oligosaccharide moieties derived from serum transferrin. Values below the oligosaccharide structures indicate the expected masses (in Da) by matrix-assisted laser desorption ionisation – time of flight analysis.

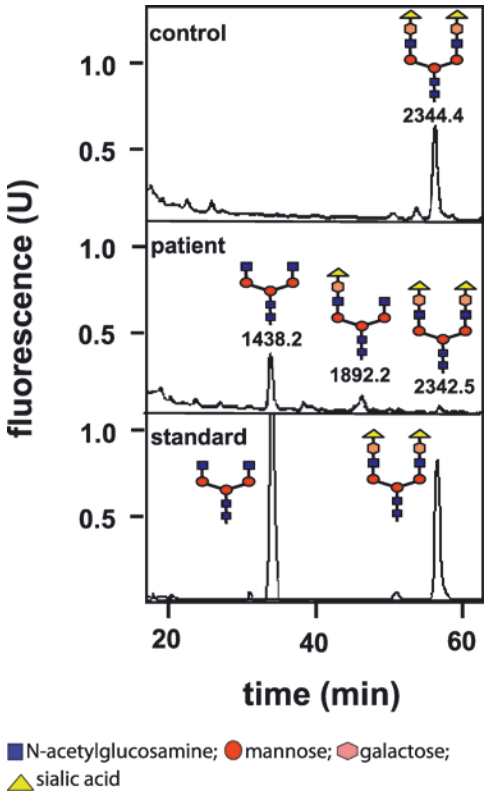

Fig. 4.5.9 HPLC and mass-spectrometric analysis of transferrin-linked oligosaccharides. Transferrin is purified from sera of a control and the index CDG-IId patient. Oligosaccharides are released by N-glycosidase F digestion and subsequently analysed by HPLC. Peak fractions of the control and the patient are further investigated by mass spectrometry and are compared to oligosaccharide standards. Values above the HPLC peaks indicate the detected masses

4.5.2.10 Apolipoprotein C-III as a Marker for Core-1 O-Glycosylation Deficiencies

Principles

IEF of apolipoprotein C-III (ApoC-III) is a simple and rapid technique that allows the quantitative determination of the three ApoC-III isoforms derived from serum or plasma, thereby serving as marker for defects in the biosynthesis of core 1 mucin type O-glycans (Fig. 4.5.10). By far the most common type of O-glycosylation, the core 1 mucin type is widely distributed in all human organs, with particularly high abundance in the nervous system. Core 2 mucin type O-glycans are synthesised from non-substituted core 1 mucin type O-glycans. Therefore, a defect in the biosynthesis of non-substituted core 1 O-glycans will also affect the synthesis of core 2 mucin type O-glycans. Recently, evidence for the existence of inborn errors in the biosynthesis of core 1 mucin type O-glycans have been described [30].

Other human O-glycosylation deficiencies that are not detectable by IEF of ApoC-III affect oligosaccharides in O-mannosidic linkage to α-dystroglycan in Walker-Warburg syndrome and muscle-eye-brain disease [2, 32], and fucosylated N- and O-glycans in CDG-IIc [17, 19].

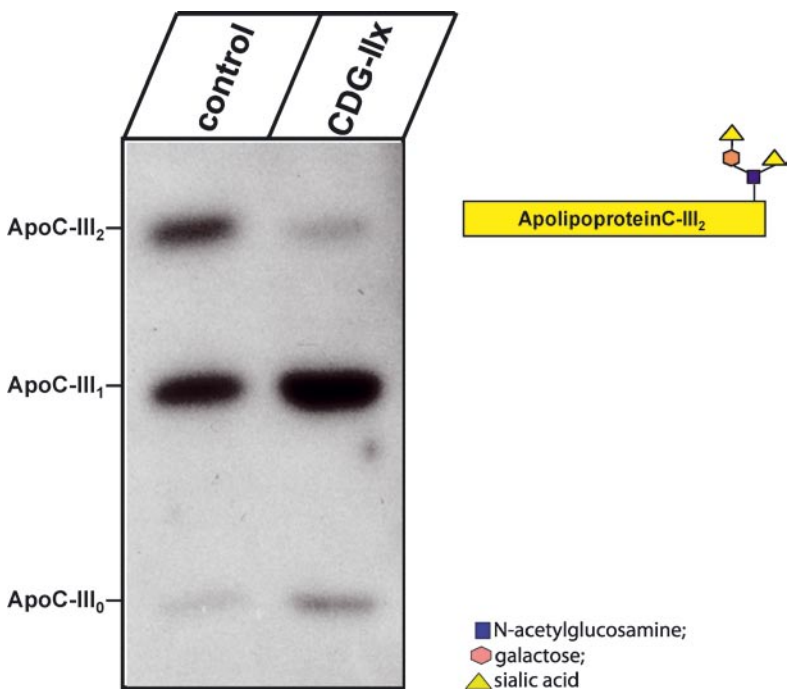

Fig. 4.5.10 Analysis of core-1 mucin type O-linked glycans derived from apolipoprotein C-III (ApoC-III). Serum-derived ApoC-III from a control (lane 1, left) and a CDG-IIx patient (lane 2, right) was investigated by IEF followed by antibody staining with a polyclonal rabbit-α-human ApoC-III antibody. ApoC-III$_2$, ApoC-III$_1$ and ApoC-III$_0$ indicate the variability in the amount of sialic acid residues linked to ApoC-III

Pre-analytical

Specimen

Serum, 1–3 µl.

Reagents and Chemicals

1. Urea p.a. (Roth).
2. Pharmalyte (pH 4.2–4.9; Amersham Biosciences).
3. Servalyte pH 3–5 (Serva).
4. Nitrocellulose membrane enhanced chemiluminescence (ECL; Amersham Biosciences).
5. Rabbit anti-human ApoC-III antibody (Biotrend, Cologne, Germany).
6. Goat anti-rabbit horseradish-peroxidase-conjugated antibody (Dianova, Hamburg, Germany).
7. Tween-20 (Roth).
8. Super Signal West Pico Chemiluminescence Substrate (ECL; Perbio, Bonn, Germany).
9. PBS: 10 mM Na_2HPO_4 (pH 7.4), 150 mM NaCl, 2.5 mM KCl, 1.5 mM KH_2PO_4 (Roth).

Instrumentation

1. PhastSystem (Amersham Biosciences).
2. PhastGel Dry Gel (Amersham Biosciences).
3. PhastGel sample Appplicator 8/1 (Amersham Biosciences).
4. PhastGel cassette (Amersham Biosciences).
5. Hyperfilm ECL (Amersham Biosciences).
6. Kodak RP X-Omat 2000 Processor (Kodak, Stuttgart, Germany).

Calibration

The IEF pattern of a healthy person is used as a control.

Running Conditions for IEF

Please refer to Table 4.5.7.

1. Sample applicator down at 1.2, 0 Vh.
2. Sample applicator up at 1.3, 100 Vh.
3. Extra alarm to sound at 1.1, 73 Vh.

Analytical

Procedure for IEF

Rehydration of dried IEF gels is carried out for 1.5 h at room temperature in a solution of 8 mol/l urea and 60 ml/l ampholytes, which contains Pharmalyte (pH 4.2–4.9) and Servalyt (pH 3.0–5.0) in a ratio of 2:1. Serum (0.5 µl) is applied to the gel and IEF is performed as described above.

Western Blot Analysis

Proteins are blotted onto a nitrocellulose membrane by diffusion for 1 h at 60°C. Non-specific sites on the nitrocellulose membrane are blocked with 50 g/l powdered milk dissolved in PBS/0.1% Tween-20. The membrane is washed in PBS/0.1%

Table 4.5.7 *Running conditions for isoelectric focusing of apolipoprotein C-III*

Sep 1.1	2000 V	2.5 mA	3.5 W	15°C	75 Vh
Sep 1.2	200 V	2.5 mA	3.5 W	15°C	15 Vh
Sep 1.3	1000 V	2.5 mA	3.5 W	15°C	100 Vh
Sep 1.4	2000 V	2.5 mA	3.5 W	15°C	495 Vh

Tween-20. The primary rabbit anti-human ApoC-III antibody is diluted to 1:1000 in PBS/0.1% Tween-20. The secondary goat anti-rabbit horseradish-peroxidase-conjugated antibody is diluted to 1:10000 in the same buffer solution. ECL detection reagent (0.1 ml/cm² of membrane) is added. A chemiluminescence reaction occurs between the horseradish peroxidase and the luminol in the ECL reagents, producing light emission. The blot is placed against an autoradiography film and exposed for different times. The film is developed on a Kodak RP X-Omat 2000 Processor.

Post-analytical

Interpretation

Evaluation of patient-derived data is performed by comparative densitometric analysis of ApoC-III IEF patterns from healthy controls (Fig. 4.5.10).

Appendix

A.1 Enzyme Assays for CDG-IIa, CDG-IIb, CDG-IIc, CDG-IId, CDG-IIe, CDG-IIg and CDG-IIh

To complete actual CDG diagnostics, the following protocols for biochemical determinations in CDG-IIa, CDG-IIb, CDG-IIc, CDG-IId, CDG-IIe, CDG-IIg and CDG-IIh are added. Nevertheless, due to either restricted availability of the substrates or time-consuming, expensive and complicated technical approaches, these assays should be performed in specialised laboratories.

A.1.1 Enzyme Assay for CDG-IIa (Golgi N-Acetylglucosaminyl-Transferase II Deficiency, [14])

A.1.1.1 Specimen

Protein extract from skin fibroblasts (0.1-0.3 mg).

A.1.1.2 Procedure

The reaction mixture in the enzyme assay contained, in a total volume of 0.02 ml, 0.25 mM M3-octyl (Manα1,6Manα1,3Manβ-octyl, synthesised in the laboratory of Prof. H. Paulsen, Hamburg, Germany), 0.1 M MES, pH 6.5, 0.1 M NaCl, 20 mM

manganese chloride, 0.5 mM uridine diphosphate (UDP)-[^{3}H]GlcNAc (10,000 dpm/min), 0.25% Triton X-100, 10 mM AMP, 0.2 M GlcNAc, 0.02% sodium acid, and enzyme extract (0.1-0.3 mg). After incubation at 37°C for 30-60 minutes, the reaction was stopped with 0.5 ml water and frozen at -70°C. Product formation was assayed by adsorption to Sep-Pak C18 reverse phase cartridges (Waters), elution with 3.0 ml methanol and scintillation counting. Values were corrected for radioactivity obtained in control incubations lacking the acceptor substrate.

A.1.2 Enzyme Assay for CDG-IIb (ER Glucosidase I Deficiency [5])

A.1.2.1 Specimen

Liver specimen or skin fibroblasts.

A.1.2.2 Procedure

One volume of liver specimen or fibroblast cells is suspended in nine volumes of either buffer A (10 mM sodium phosphate, pH 6.8, containing 0.2% polyoxyethylene-20-cetyl ether, 50 µM phenylmethanesulphonylfluoride and 1 µg/ml leupeptin) or buffer B (50 mM sodium phosphate, pH 6.5, containing 1% Thesit, 50 µM phenylmethanesulphonylfluoride and 1 µg/ml leupeptin), and then is disrupted by means of a motor-driven glass/Teflon homogeniser. The homogenates are centrifuged at $5600 \times g$ for 1 min and the supernatants assayed for glucosidase I, glucosidase II, Man_9-mannosidase and endo-α-1,2-mannosidase activity. Hydrolysis by glucosidase I and glucosidase II of fluorescent tetramethylrhodamine (TMR)-labelled trisaccharide Glc(α1-2)Glc(α1-3)Glc(α1-O)-$(CH_2)_8COOCH_3$ and TMR-labelled disaccharide Glc(α1-3)Glc(α1-O)-$(CH_2)_8COOCH_3$, respectively, is measured by incubation of 15 µl of the homogenates (containing 50–250 µg total protein) in buffer A with 5 µl of a 2-mM solution of the corresponding synthetic substrate in a total volume of 20 µl at 37°C. At various time intervals, 0.5 µl samples are removed and analysed on silica gel 60 F_{254} plates, which are developed in 2-propanol:water:NH_4OH (7:2:1 v/v/v). Cleavage products are quantified directly on TLC plates by means of a Biometra Biodoc II system (Westburg) and a LumiAnalyst 3.0 programme (Boehringer).

To determine glucosidase I and II activities with the radiolabelled oligosaccharide intermediates, 25-µl aliquots of liver or fibroblast cell homogenates prepared in buffer B (100–200 µg protein) are incubated at 37°C with 5 µl of an aqueous stock solution containing 200 cpm/µl of [^{14}C]$Glc_3Man_9GlcNAc_2$ or [^{14}C]$Glc_2Man_9GlcNAc_2$. At predetermined times, the reaction is stopped by the addition of 30 µl acetic acid and the cleavage products subjected to paper chromatography by means of 2-propanol:acetic acid:water (29:4:9 v/v/v). Substrate hydrolysis is determined as described. The activity of Man_9-mannosidase is assayed under identical conditions with the use of 1000 cpm of either [^{14}C]-labelled $Man_9GlcNAc_2$ or $Man_5GlcNAc_2$ as the substrate. For the determination of endo-α-1,2-mannosidase activity, 25 µl of the homogenates is incubated with 1000 cpm of [^{14}C]$Glc_3Man_9GlcNAc_2$ at 37°C, for 24 h and for 48 h, in the presence of 1 mM EDTA and 2 mM of the glucosidase I/II inhibitor 1-deoxynojirimycin, in order to prevent non-specific substrate degradation. Samples are subjected to chromatography with the more polar solvent (2-propanol:

acetic acid:water; 29:8:15 v/v/v), to separate [^{14}C]Glc_3Man from uncleaved substrate. [^{14}C]$Glc_{3\text{-}1}Man_9GlcNAc_2$, [^{14}C]$Man_9GlcNAc_2$ and [^{14}C]$Man_5GlcNAc_2$ are synthesised as described elsewhere. Radioactivity was determined with Bray's solution as scintillation fluid.

A.1.3 Enzyme Assay for CDG-IIc (Golgi GDP-Fucose Transporter Deficiency [18])

A.1.3.1 Specimen

Primary skin fibroblasts.

A.1.3.2 Procedure

■ Preparation of Golgi-Enriched Membrane Fractions

For each experiment, two 150-cm^2 cell culture dishes are seeded with 3×10^6 fibroblasts each. After culturing for 10 days, the cells are washed three times with ice-cold Hanks buffer. Cells were scraped into 0.25 M sucrose, 3 mM imidazole, 1 mM EDTA, pH 7.4 and centrifuged for 5 min at $1000 \times g$ and 4°C. Pellets are redissolved in 2 ml of 0.25 M sucrose, 3 mM imidazole, pH 7.4, disrupted in a tight-fitting Dounce homogeniser and centrifuged at $1000 \times g$ for 10 min at 4°C. Homogenisation of the pellet in sucrose/imidazole and centrifugation are repeated. The supernatants are combined and overlaid onto a cushion of 1.3 M sucrose in 3 mM imidazole, pH 7.4, for density gradient centrifugation in an SW 40-rotor (Beckman Instruments) at $10^5 \times g$ for 70 min at 4°C. Golgi-enriched membranes are collected at the 0.25–1.3 M sucrose interphase and quantified by galactosyltransferase activity.

A.1.3.3 DP-[^{14}C]Fucose and UDP-[^{3}H]Galactose Import

Import of nucleotide sugars into Golgi-enriched vesicles is determined by the addition of Golgi-enriched vesicles (60–100 µg) to buffer A (10 mM Tris-HCl, pH 7.5, 150 mM KCl, 1 mM $MgCl_2$, 0.25 M sucrose) containing GDP-[^{14}C]fucose or UDP-[^{3}H]galactose in a final volume of 0.47 ml. Unless otherwise stated, the assays contained 3 µM GDP-[^{14}C]fucose (~885,000 dpm) or 0.5 µM UDP-[^{3}H]galactose ($\sim 4.3 \times 10^6$ dpm). After incubation for 10 min at 37°C the reaction is stopped by the addition of 0.8 ml of ice-cold buffer A, followed by centrifugation at $10^5 \times g$ for 30 min at 4°C in a TLA-45 rotor (Beckman Instruments). The supernatant is removed and used for the calculation of radioactivity in the incubation medium. The pellet is washed three times with ice-cold buffer A, redissolved in 0.5 ml of 50 mM Tris-HCl, pH 8.8, containing 5 mM EDTA and 2% SDS by sonication for 2 min (Branson), and incubated for 30 min at 23°C. To differentiate in the vesicles between nucleotide sugar- and glycoprotein-associated radioactivity, 0.05 ml of 0.5 N HCl, containing 20% TCA and 1% phosphotungstic acid are added to the solubilised pellet. After overnight precipitation and centrifugation, the pellet is solubilised in 2.5 N NaOH, and the radioactivity determined.

A.1.3.4 Calculation

The value for imported nucleotide sugar is obtained by correcting the radioactivity associated with the pellet for the radioactivity trapped in the extravesicular space.

A.1.3.5 Post-analytical

■ Interpretation

The amount of radioactivity associated with the pellet represents the nucleotide sugars imported into vesicles, including the sugars transferred to glycoconjugates and the radioactivity trapped in the extravesicular space of the pellet. Under standard conditions using membranes from control fibroblasts, the trapped radioactivity represents 17 ± 5% of the [^{14}C]fucose or 12 ± 2% of the [^{3}H]galactose radioactivity associated with the pellet. Under standard conditions, 25% of the imported [^{14}C]fucose and 14% of the imported [^{3}H]galactose are transferred to glycoproteins.

A.1.4 Enzyme Assay for CDG-IId (Golgi UDP-Galactose: N-Acetylglucosamine β-1,4-Galactosyltransferase I Deficiency [11])

A.1.4.1 Specimen

Primary skin fibroblasts.

A.1.4.2 Procedure

To determine β-1,4-galactosyltransferase I activity, 20 µl buffer A (10 mM Tris-HCl. pH 7.7, 250 mM sucrose, 0.5% Triton X-100, 1 mM EDTA) containing 1 µg of fibroblast homogenate is used. The reaction is initiated by the addition of 30 µl buffer B (5.2 µl 0.5 M Tris-HCl, pH 7.4, 5% Triton X-100, 4.4 µl 0.2 M $MnCl_2$, 19.85 µl H_2O, 0.35 mg ovalbumin, 0.44 µl 0.2 M ATP, and 0.44 µCi UDP-[^{3}H]galactose [16 Ci/mmol; Amersham Biosciences]). Incubation is carried out for 1 h at 37°C and stopped by adding 500 µl of a 10% TCA solution. Precipitation is carried out at 4°C for 1 h. Samples are centrifuged at 13,600 × *g* for 10 min at 4°C, and the supernatants are removed. The pellets are washed three times with ice-cold 5% TCA and subsequently dissolved in 200 µl 2.5 N NaOH and incubated at 95°C for 10 min, followed by the addition of 600 µl H_2O and 200 µl 100% acetic acid. Incorporated radioactivity is determined by liquid scintillation counting.

A.1.5 Analysis of Conserved Oligomeric Golgi Complex Subunits in CDG-IIe (COG 7 Deficiency [31]), CDG-IIg (COG 1 Deficiency [8]) and CDG-IIh (COG 8 Deficiency [7, 16])

A.1.5.1 Specimen

Primary skin fibroblasts.

A.1.5.2 Procedure

Initial investigations on all conserved oligomeric Golgi complex subunit deficiencies known so far, are carried out by Western blot analysis. The defects evoke disruption of the complex, thereby leading to reduced amounts of defined subunits, which are further analysed by genetic studies.

A.2 Specimen Collection: Material for Standard Assays for CDG-Diagnosis

Test	Material needed
Isoelectric focusin of serum transferrin	Serum
CDG-Ia (PMM activity)	White blood cells, fibroblasts
CDG-Ib (PMI activity)	White blood cells, fibroblasts
Other enzyme assays (need expert experience)	White blood cells, fibroblasts
Lipid-linked oligosaccharides	Fibroblasts
Protein-linked oligosaccharides	Serum
Mutational analysis	White blood cells, fibroblasts
Prenatal analysis	Chorionic villus sampling or cultured amniotic fluid cells

A.3 Summary of Known Molecular Defects in CDG

CDG-type	Affected protein	Gene	Chromosome	OMIM
CDG-Ia	Phosphomannomutase II	*PMM2*	16p13	212065 601785
CDG-Ib	Phosphomannose isomerase	*MPI*	15q22	154550 602579
CDG-Ic	Dol-P-Glc:$Man_9GlcNAc_2$-PP-dolichol glucosyltransferase	h*ALG6*	1p22	604566 604655
CDG-Id	Dol-P-Man:$Man_5GlcNAc_2$-PP-dolichol mannosyltransferase	h*ALG3*	3q27	601110
CDG-Ie	Dolicholphosphate-mannose synthase 1	*DPM1*	20q13	608789
CDG-If	Mannose-P-dolichol utilisation defect 1 protein	*MPDU1*	17p13	604041
CDG-Ig	Dol-P-Man:$Man_7GlcNAc_2$-PP-dolichol mannosyltransferase	h*ALG12*	22q13	607143
CDG-Ih	Dol-P-Glc:$Glc_1Man_9GlcNAc_2$-PP-dolichol-α1,3-glucosyltransferase	h*ALG8*	11p15	608104
CDG-Ii	GDP-Man:$Man_1GlcNAc_2$-PP-dolichol mannosyltransferase	h*ALG2*	9q22	607906
CDG-Ij	UDP-GlcNAc:dolichol phosphate N-acetylglucosaminephosphotransferase 1	*DPAGT1*	11q23	608093
CDG-Ik	GDP-Man:$GlcNAc_2$-PP-dolichol mannosyltransferase	h*ALG1*	16p13	608540
CDG-IL	Dolichol-P-mannose:α-1,2-mannosyltransferase	h*ALG9*	11q23	608776
CDG-IIa	Golgi N-acetylglucosaminyltransferase II	*MGAT2*	14q21	212066
CDG-IIb	ER glucosidase I	*GCS1*	2p13	606056

A.3 Summary of Known Molecular Defects in CDG

CDG-type	Affected protein	Gene	Chromosome	OMIM
CDG-IIc	Golgi GDP-fucose transporter	*FUCT1*	11p11	605881 266265
CDG-IId	Golgi UDP-galactose:N-acetylglucosamine β-1,4-galactosyltransferase	*ß4GALT1*	9p13	607091
CDG-IIe	Subunit 7 of COG-complex	*COG7*	16p12	608779 606978
CDG-IIf	CMP-NANA transporter	*CMP-NANA transporter*	6q15	605634
CDG-IIg	Subunit 1 of COG-complex	*COG1*	17q25	606973
CDG-IIh	Subunit 8 of COG-complex	*COG8*	16q22	606979

References

1. Aebi M, Helenius A, Schenk B, Barone R, Fiumara A, Berger EG, Hennet T, Imbach T, Stutz A, Bjursell C, Uller A, Wahlstrom JG, Briones P, Cardo E, Clayton P, Winchester B, Cormier-Dalre V, de Lonlay P, Cuer M, Dupre T, Seta N, de Koning T, Dorland L, de Loos F, Kupers L, et al (1999) Carbohydrate-deficient glycoprotein syndromes become congenital disorders of glycosylation: an updated nomenclature for CDG. First International Workshop on CDGS. Glycoconj J 16:669–671
2. Beltran-Valero de Bernabe D, Currier S, Steinbrecher A, Celli J, van Beusekom E, van der Zwaag B, Kayserili H, Merlini L, Chitayat D, Dobyns WB, Cormand B, Lehesjoki AE, Cruces J, Voit T, Walsh CA, van Bokhoven H, Brunner HG (2002) Mutations in the O-mannosyltransferase gene POMT1 give rise to the severe neuronal migration disorder Walker-Warburg syndrome. Am J Hum Genet 71:1033–1043
3. Bigge JC, Patel TP, Bruce JA, Goulding PN, Charles SM, Parekh RB (1995) Nonselective and efficient fluorescent labelling of glycans using 2-amino benzamide and anthranilic acid. Anal Biochem 230:229–238
4. Clayton P, Winchester B, Di Tamaso E, Young E, Keir G, Rodeck C (1993) Carbohydrate-deficient glycoprotein syndrome: normal glycosylation in the fetus. Lancet 341:956
5. De Praeter CM, Gerwig GJ, Bause E, Nuytinck LK, Vliegenthart JF, Breuer W, Kamerling JP, Espeel MF, Martin JJ, De Paepe AM, Chan NW, Dacremont GA, Van Coster RN (2000) A novel disorder caused by defective biosynthesis of N-linked oligosaccharides due to glucosidase I deficiency. Am J Hum Genet 66:1744–1756
6. Fang J, Peters V, Körner C and Hoffmann GF (2004) Improvement of CDG diagnosis by combined examination of several glycoproteins. J Inherit Metab Dis 27:581–590
7. Foulquier F, Ungar D, Reynders E, Zeevaert R, Mills P, Garcia-Silva MT, Briones P, Winchester B, Morelle W, Krieger M, Annaert W, Matthijs G (2007) A new inborn error of glycosylation due to a Cog8 deficiency reveals a critical role for the Cog1-Cog8 interaction in COG complex formation. Hum Mol Genet 16:717–730
8. Foulquier F, Vasile E, Schollen E, Callewaert N, Raemaekers T, Quelhas D, Jaeken J, Mills P, Winchester B, Krieger M, Annaert W and Matthijs G (2006) Conserved oligomeric Golgi complex subunit 1 deficiency reveals a previously uncharacterized congenital disorder of glycosylation type II. Proc Natl Acad Sci U S A 103:3764–3769

9. Freeze HH (2006) Genetic defects in the human glycome. Nat Rev Genet 7:537–551
10. Hackler R, Arndt T, Peters V, Assmann B, Hoffmann GF, Steinmetz A (1998) Automated isoelectric focusing of serum isotransferrins for laboratory diagnosis of carbohydrate deficient glycoprotein syndrome using the PhastSystem™. Scand J Clin Lab Invest 58:66–67
11. Hansske B, Thiel C, Lübke T, Hasilik M, Höning S, Peters V, Heidemann PH, Hoffmann GF, Berger EG, von Figura K, Körner C (2002) Deficiency of UDP-galactose:N-acetylglucosamine β-1,4-galactosyltransferase I causes the congenital disorder of glycosylation type IId. J Clin Invest 109: 725–733
12. Helenius A, Aebi M (2001) Intracellular functions of N-linked glycans. Science 23:2364–2369
13. Iourin O, Mattu TS, Mian N, Keir G, Winchester B, Dwek RA, Rudd PM (1996) The identification of abnormal glycoforms of serum transferrin in carbohydrate deficient glycoprotein syndrome type I by capillary zone electrophoresis. Glycoconj J 13:1031–1042
14. Jaeken J, Schachter H, Carchon, H, De Cock P, Coddeville B, Spik G (1994) Carbohydrate deficient glycoprotein syndrome type II: a deficiency in Golgi localised N-acetyl-glucosaminyltransferase II. Arch Dis Child 71:123–127
15. Jaeken J, Stibler H, Hagberg B (1991) The carbohydrate-deficient glycoprotein syndrome. A new inherited multisystemic disease with severe nervous system involvement. Acta Paediatr Scand Suppl 375:1–71
16. Kranz C, Ng BG, Sun L, Sharma V, Eklund EA, Miura Y, Ungar D, Lupashin V, Winkel DR, Cipollo JF, Costello CE, Loh E, Hong W, Freeze HH (2007) COG8 deficiency causes new congenital disorder of glycosylation type IIh. Hum Mol Genet 16:731–741
17. Lübke T, Marquardt T, Etzioni A, Hartmann E, von Figura K, Körner C (2001) Complementation cloning identifies CDG-IIc, a new type of congenital disorders of glycosylation, as a GDP-fucose transporter deficiency. Nat Genet 28:73–76
18. Lübke T, Marquardt T, von Figura K, Körner C (1999) A new type of carbohydrate-deficient glycoprotein syndrome due to a decreased import of GDP-fucose into the Golgi. J Biol Chem 274:25986–25989
19. Marquardt T, Luhn K, Srikrishna G, Freeze HH, Harms E, Vestweber D (1999) Correction of leukocyte adhesion deficiency type II with oral fucose. Blood 94:3976–3985
20. Mills K, Mills PB, Clayton PT, Mian N, Johnson AW, Winchester BG (2003) The underglycosylation of plasma alpha 1-antitrypsin in congenital disorders of glycosylation type I is not random. Glycobiology 13:73–85
21. Mock KK, Davey M, Cottrell JS (1991) The analysis of underivatised oligosaccharides by matrix-assisted laser desorption mass spectrometry. Biochem Biophys Res Commun 177:644–651
22. Niehues R, Hasilik M, Alton G, Körner C, Schiebe-Sukumar M, Koch HG, Zimmer KP, Wu R, Harms E, Reiter K, von Figura K, Freeze HH, Harms HK, Marquardt T (1998) Carbohydrate-deficient glycoprotein syndrome type Ib. Phosphomannose isomerase deficiency and mannose therapy. J Clin Invest 101:1414–1420
23. Noll B, Hackler R, Pelzer M, Pelzer S, Nusser P, Maisch B, Schaefer JR, Steinmetz A (1999) Semi-automated rapid isoelectric focusing of apolipoproteins C from human plasma using PhastSystem and immunofixation. Clin Chem Lab Med 37:643–648
24. Patel T, Bruce J, Merry A, Bigge C, Wormald M, Jaques A, Parekh R (1993) Use of hydrazine to release in intact and unreduced form both N- and O-linked oligosaccharides from glycoproteins. Biochemistry 32:679–693
25. Powell AK, Harvey DJ (1996) Stabilization of sialic acids in N-linked oligosaccharides and gangliosides for analysis by positive ion matrix-assisted laser desorption/ionization mass spectrometry. Rapid Commun Mass Spectrom 10:1027–1032
26. Schaftingen E van, Jaeken J (1995) Phosphomannomutase deficiency is a cause of carbohydrate-deficient glycoprotein syndrome type I. FEBS Lett 377:318–320
27. Stibler H, Borg S, Allgulander C (1979) Clinical significance of abnormal heterogeneity of transferrin in relation to alcohol consumption. Acta Med Scand 206:275–281

28. Stibler H, Skovby F (1994) Failure to diagnose carbohydrate-deficient glycoprotein syndrome prenatally. Pediatr Neurol 11:71
29. Wada Y (2006) Mass spectrometry for congenital disorder of glycosylation, CDG. J Chromatogr B Analyt Technol Biomed Life Sci 838:3–8
30. Wopereis S, Grünewald S, Morava E, Penzien JM, Briones P, García-Silva MT, Demacker PMN, Huijben KMLC, Wevers RA (2003) Apolipoprotein C-III isofocusing in the diagnosis of genetic defects in O-glycan biosynthesis. Clin Chem 49:1839–1845
31. Wu X, Steet RA, Bohorov O, Bakker J, Newell J, Krieger M, Spaapen L, Kornfeld S, Freeze HH (2004) Mutation of the COG complex subunit gene COG7 causes a lethal congenital disorder. Nat Med 10:518–523
32. Yoshida A, Kobayashi K, Manya H, Taniguchi K, Kano H, Mizuno M, Inazu T, Mitsuhashi H, Takahashi S, Takeuchi M, Herrmann R, Straub V, Talim B, Voit T, Topaloglu H, Toda T, Endo T (2001) Muscular dystrophy and neuronal migration disorder caused by mutations in a glycosyltransferase, POMGnT1. Dev Cell 1:717–724

4.6 Enzymes and Metabolites of Carbohydrate Metabolism

Nils U. Bosshard, Beat Steinmann

4.6.1 Introduction

This chapter deals with the assays used for the diagnosis of three groups of inborn errors of metabolism of carbohydrates, i.e.:

1. Classical galactosemia and the related diseases galactokinase and uridine diphosphate (UDP) galactose-4-epimerase deficiencies, a consequence of disturbances in the pathway galactose → galactose-1-phosphate → UDP-galactose → UDP-glucose.
2. Hereditary fructose intolerance (HFI), caused by the deficiency of fructaldolase, and fructose-1,6-bisphosphatase deficiency.
3. Glycogenoses, or glycogen storage diseases (GSD)
   a. Type Ia, deficiency of glucose-6-phosphatase
   b. Type II, deficiency of α-glucosidase (acid maltase)
   c. Type III, deficiency of amylo-1,6-glucosidase (debranching enzyme)
   d. Type IV, deficiency of 1,4-glucan branching enzyme
   e. Type V, deficiency of myophosphorylase
   f. Type VI, deficiency of liver phosphorylase
   g. Type VII, deficiency of phosphofructokinase
   h. Type IX, deficiency of phosphorylase b-kinase
   i. Type 0, deficiency of glycogen synthase.

Readers interested in more details about these disorders are referred to [11, 21, 34, 36].

4.6.2 Galactose

4.6.2.1 Principle

$$\text{D-Galactose} + \text{NAD}^+ \xrightarrow{\textit{Galactose dehydrogenase}} \text{D-galactolactone} + \text{NADH} + \text{H}^+ .$$

NADH is determined ultraviolet (UV)-photometrically as a measure of the amount of the substrate D-galactose present in the reaction [26].

4.6.2.2 Solutions

1. Tris-HCl-buffer, 0.1 M, pH 8.6: Trizma base (molecular weight, MW 121.1) (3.0 g/250 ml H_2O). Adjust the pH to 8.6 with HCl. Store at 4°C.
2. Nicotinamide adenine dinucleotide (NAD), 13 mM: NAD (formula weight, FW, variable) (approximately 10 mg/ml H_2O).
3. Galactose dehydrogenase (Gal-DH) suspension: 50 U/0.33 ml. Store at 4°C.
4. Perchloric acid, 0.33 M: $HClO_4$ (60% = 9.1 M), (36.1 ml, fill to 1000 ml with H_2O). Store at 4°C.

4.6.2.3 Samples

1. Blood from heparin/fluoride tubes: in a centrifuge tube on ice/H_2O add 0.5 ml 0.33 M perchloric acid to 0.1 ml blood sample. Mix on ice, centrifuge for 10 min at $2000 \times g$. Use the supernatant as the assay sample.
2. Urine: Centrifuge for 5 min at $1000 \times g$. Use the supernatant undiluted or, if necessary, dilute 10–100 times with H_2O. *Caveat*: with highly diluted samples, also measure a blank (i.e., H_2O instead of urine) in the assay to correct for possible turbidity.

4.6.2.4 Assay

Pipette into a cuvette (1 cm), thermostatted at 25°C, 3.0 ml Tris-HCl buffer, 0.1 ml NAD, and 0.2 ml of the sample supernatant. Read off the optical density (OD) at 340 nm when constant ($= E_1$). Add Gal-DH (approximately 1 U). Read off the OD at 340 nm when it has leveled off (i.e., after 30–50 min; $= E_2$).

4.6.2.5 Calculation

$$\text{mM} = \frac{\Delta E \times V}{\varepsilon \times d \times v} = \frac{\Delta E \times 3.3}{6.22 \times 1 \times 0.2} = \Delta E \times 2.653 \,.$$

where $\Delta E = E_2 - E_1$, V = total assay volume, v = sample volume in the assay, ε = extinction coefficient NADH (mM), d = light path length of the cuvette (cm).
mg galactose/100 ml = concentration (mM) × 18 = $\Delta E \times 47.75$
where galactose MW = 180.

1. For blood:
   mg/100 ml = $\Delta E \times 47.75 \times \frac{0.6}{0.1}$ (dilution before assay)
   mg/100 ml = $\Delta E \times 286.5$
2. For urine:
   mg/100 ml = $\Delta E \times 47.75 \times$ dilution before assay.

4.6.2.6 Control Values

Blood: 0.0–3.0 mg/100 ml = 0.0–0.16 mM, depending on fasting state or lactose consumption.

4.6.2.7 Pathological Values

Elevated in deficiencies of galactokinase, galactose-1-phosphate uridyltransferase (classical galactosemia), UDP galactose-4-epimerase, and Fanconi-Bickel-syndrome, portocaval shunt, and cirrhosis, depending on time after lactose consumption.

4.6.2.8 Notes

Galactose is stable for 48 h only if kept in fluorinated syringe tubes. A sufficient amount of Gal-DH is crucial for the assay to ensure that it is not limiting for the reaction. A galactose-loading test can be used as a functional test [15].

4.6.3 Galactose-1-Phosphate

4.6.3.1 Principle

1. $\text{Galactose-1-phosphate} + H_2O \xrightarrow{\textit{Alkaline phosphatase}} \text{galactose} + P_i$
2. $\text{D-Galactose} + NAD^+ \xrightarrow{\textit{Galactose dehydrogenase}} \text{D-galactone} + NADH + H^+ .$

NADH is determined UV-photometrically as a measure of the amount of the substrate galactose-1-phosphate present in the reaction [14].

4.6.3.2 Solutions

1. Tris-HCl-buffer, 0.1 M, pH 8.6: Trizma base (MW 121.1) (3.0 g/250 ml H_2O). Adjust the pH to 8.6 with HCl. Store at 4°C.
2. NAD, 13 mM: NAD (FW variable) (Approximately 10 mg/ml H_2O).
3. Gal-DH: Gal-DH, suspension (50 U/0.33 ml). Store at 4°C.
4. Alkaline phosphatase: alkaline phosphatase (1500 U/100 µl). Store at 4°C.

4.6.3.3 Samples

Washed red blood cells (RBC). Store packed cells at –20°C.

4.6.3.4 Assay

Add to centrifuge tube 1.6 ml Tris-HCl buffer and 0.4 ml RBC sample. Boil for 3 min while stirring with glass rod, cool on ice, then centrifuge for 10 min at 2000 × *g*. Decant the supernatant in a new tube and centrifuge again for 5 min at 2000 × *g*. Pipette 0.6 ml from the top of the supernatant, stir with a glass rod or on vortex, and use for the assay:

1. Pipette in two cuvettes (1 cm), each 3.0 ml Tris-HCl buffer, 0.1 ml NAD and 0.2 ml of the sample supernatant.

2. Warm the cuvettes to 25°C in a photometer and read off the OD at 340 nm when it has become constant (= E_1).
3. Add 2 µl Gal-DH to the first cuvette and 2 µl Gal-DH plus 2 µl alkaline phosphatase to the second cuvette.
4. Read off the OD at 340 nm when it has leveled off (after 30–50 min; = E_2).

4.6.3.5 Calculation

$\Delta E\,(+\mathrm{AP}) = E_2\,(+\mathrm{AP}) - E_1\,(+\mathrm{AP})$

$\Delta E\,(-\mathrm{AP}) = E_2\,(-\mathrm{AP}) - \mathrm{E}_1\,(-\mathrm{AP})$,

where AP = alkaline phosphatase.

For the calculation:
$\Delta E = \Delta E\,(+\mathrm{AP}) - \Delta E\,(-\mathrm{AP})$

$$\text{concentration [mM]} = \frac{\Delta E \times V}{\varepsilon \times d \times v} = \frac{\Delta E \times 3.22}{6.22 \times 1 \times 0.2} = \Delta E \times 2.669\ ,$$

where V = total assay volume, v = sample (RBC lysate) volume in the assay, ε = extinction coefficient NADH (mM), and d = light path length of cuvette (cm).

mg galactose-1-phosphate /ml = concentration [mM] × 0.2601 = $\Delta E \times 0.6942$
(galactose-1-phosphate MW = 260.1).

Assuming a hematocrit value of 92% for "packed RBC", a 0.4-ml "RBC sample" diluted with 1.6 ml Tris buffer, actually contains only 0.368 ml of RBC; thus, the dilution before the assay is:

$$\frac{2.0}{0.368} = 5.435$$

→ mg galactose-1-phosphate/ml RBC = $\Delta E \times 0.6942 \times 5.435 = \Delta E \times 3.773$
and mg/100 ml RBC = $\Delta E \times 377.3$
or:
mmol/l RBC = $\Delta E \times 377.3 \times 1/26$ (galactose-1-phosphate MW = 260.1).

4.6.3.6 Control Values

No galactose-1-phosphate can be detected in RBC of controls.

4.6.3.7 Pathological Values

Levels of galactose-1-phosphate are elevated to above 100 mg/100 ml RBC in untreated galactose-1-phosphate uridyltransferase deficiency (classical galactosemia) and, to a lesser degree, in UDP galactose-4-epimerase deficiency.

4.6.4 Galactokinase (EC 2.7.1.6)

4.6.4.1 Enzyme Deficiency

Galactokinase is the enzyme deficient in galactokinase deficiency (MIM 230 200). This disorder is caused by impairment of the pathway step from galactose to galactose-1-phosphate.

4.6.4.2 Principle

$$^{14}\text{C-Galactose} \xrightarrow[\text{ATP} \rightarrow \text{ADP}]{\textbf{Galactokinase}} {}^{14}\text{C-galactose-1-phosphate}\,.$$

Separation of radioactively labeled substrate and product on diethylaminoethyl (DEAE) cellulose: ^{14}C-galactose is eluted by H_2O, ^{14}C-galactose-1-phosphate is retained; ^{14}C-galactose-1-phosphate is subsequently eluted by 100 mM HCl. Determination of eluted radioactivity in a liquid scintillation counter (β-counter) [5, 13, 30].

4.6.4.3 Solutions

1. Galactose (nonradioactive), 6.67 mM: galactose (MW 180.16) (120 mg/100 ml H_2O). Prepare fresh for preparation of substrate mix (see 3. below).
2. Galactose (radioactive): ^{14}C-galactose (20 µCi/ml H_2O, where 1 Ci = 3.7×10^{10} Bq).
3. Substrate mix: 4.5 ml nonradioactive galactose solution (see 1. above), 1.0 ml ^{14}C-galactose (see 2. above), and 2.0 ml H_2O. Store at –20°C; stable for months.
4. Magnesium sulfate 60 mM: $MgSO_4 \cdot 7H_2O$ (MW 246.48) (14.8 mg/ml H_2O). Store at –20 C.
5. Sodium fluoride 60 mM: NaF (MW 41.99) (2.5 mg/ml H_2O). Store at –20 C.
6. 1.0 M Tris-HCl buffer, pH 8.0: Trizma base (MW 121.1) (12.1 g/100 ml H_2O).
7. Tris-2-mercaptoethanol (BME) buffer 60 mM: BME (14.3 M) (10 µl/2.32 ml of Tris-HCl buffer – see 6. above).
8. Digitonin 50 % saturated: digitonin 50 mg/10 ml H_2O, boil, cool to room temperature and filter. Dilute 1:1 with H_2O and store aliquots at –20 C.
9. Reagent mix: prepare fresh before use! See Table 4.6.1

Preparation of DEAE Cellulose

Stock preparation: wash DEAE cellulose three times with H_2O on a magnetic stirrer for some minutes. Allow the cellulose to sediment and pour off the supernatant with fine particles. Leave the cellulose for 30 min in 1 M NaOH, then wash with H_2O until the pH of the supernatant is neutral: DEAE cellulose (OH^- form). Leave cellulose for 30 min in 1 M HCl, then wash until the pH of supernatant is neutral: DEAE cellulose (Cl^- form). Store at 4°C. This solution is stable for 1 year without preservative.

Test of the Separation Efficiency of DEAE Cellulose

Every new charge of DEAE cellulose (Cl^- form) should be tested. Dry 10 µl each of ^{14}C-galactose and ^{14}C-galactose-1-phosphate with nitrogen and dissolve in 300 µl H_2O, each. Put 100 µl of each into a counter vial containing 15 ml of OptiPhase (= 100%), 100 µl of each onto columns with 1 ml DEAE cellulose, and 100 µl of both onto a third column (mix).

1. Elution with H_2O: five times 2 ml, collect in five counter tubes containing 15 ml scintillation liquid. ^{14}C-galactose is eluted.
2. Elution with 20 mM HCl: five times 2 ml, collect in five counter tubes containing 15 ml scintillation liquid. ^{14}C-Galactose-1-phosphate is eluted. ^{14}C-Galactose and ^{14}C-galactose-1-phosphate should be separated completely by this procedure.

Purification of ^{14}C-Galactose by Hexokinase

Dry 50 µCi of ^{14}C-galactose with nitrogen, dissolve in a solution containing 1.0 ml Tris-HCl (pH 8, 2 mM), 5 µl $MgCl_2$ (100 mM), 10 µl ATP (60 mM) and 100 µl hexokinase (2 U/ml) to a total of 1.115 ml). Incubate at 37°C for 60 min. Put 1 ml of DEAE-cellulose into a column, rinse with H_2O, add a few drops of galactose 3.8 mM, then rinse with H_2O again. Apply the incubated reaction mix, elute with H_2O, discard the first 0.5 ml, and check later eluate fractions for radioactivity. Dry in a vacuum and dissolve in H_2O according to the desired concentration for the assay mix.

Table 4.6.1 *Reagent mix for detection of galactokinase deficiency.* BME *(2-Mercaptoethanol)*

Reagent mix	Initial concentration	Amount in aliquot	Concentration	
			In mix	In assay
ATP (formula weight varies)	7.5 mM	≈4.7 mg	7.5 mM	5.0 mM
Substrate mix		188 µl	0.75 mM	0.5 mM
$MgSO_4 \cdot 7H_2O$	60 mM	125 µl	7.5 mM	5.0 mM
NaF	60 mM	125 µl	7.5 mM	5.0 mM
Tris-BME buffer		250 µl		
H_2O		313 µl		
Total		*1.0 ml*		

4.6.4.4 Samples

1. Heparinized blood: 300 µl blood+300 µl digitonin 50%; determine hemoglobin (Hb) concentration in the mix.

2. RBC lysate (use only if heparinized blood is not available as the enzyme in RBC is not stable): 150 µl RBC lysate + 450 µl digitonin 50%; determine the Hb concentration.
3. Liver: 1% homogenate in 10 mM Tris-HCl (pH 8.0)/10 mM BME. Centrifuge for 10 min at 27,000 × *g*. Use the supernatant for protein determination and for the assay at a protein concentration of 1.0–1.6 mg/ml.
4. Fibroblasts: homogenate in glycine-NaOH buffer, 10 mM, pH 8.7. Centrifuge for 5 min at 20,000 × *g*. Use the supernatant for protein determination and for the assay at a protein concentration of 0.5–1.0 mg/ml.

4.6.4.5 Assay

Heparinized Blood or RBC

Use 100 µl of heparinized blood or RBC. Incubate for 10 min at 37°C, then add 200 µl of reagent mix. Incubate for 15 min at 37°C, boil for 2 min, put on ice, and stir with a glass rod. Centrifuge for 10 min at 2,000 × *g*. Apply 100 µl of supernatant to the DEAE column (see below).

Blank

Boil 150 µl of either sample (heparinized blood or RBC) for 2 min, put on ice, then add 300 µl of reagent mix. Stir with a glass rod. Centrifuge for 10 min at 2,000 × *g*. Apply 100 µl of the supernatant to the DEAE column (= blank, see below) and put 100 µl of the supernatant and 2.4 ml of 100 mM HCl into the β-counter vial (= 100% value, see below).

Liver or Fibroblasts

Add together 50 µl of either the liver or fibroblast sample (prepared as described above) and 100 µl reagent mix. Incubate and continue as with blood samples.

Blank

Boil 100 µl of either sample (liver or fibroblast) for 2 min, put on ice, then add 200 µl of reagent mix. Continue as for the blood sample blanks.

Separation of Substrate and Reaction Product by Chromatography

1. Preparation of columns: put 1 ml of DEAE cellulose into a 2-ml column (with a nylon mesh, 40 µm, to retain the cellulose). Equilibrate the column three times with 2 ml of H_2O.
2. Separation: apply 100 µl from the assay and blank supernatants onto one column each. Wash the columns five times with 2 ml of H_2O (discard the eluate, containing ^{14}C-galactose). Elute ^{14}C-galactose-1-phosphate with 2.5 ml of 100 mM HCl into a counter vial containing 15 ml of scintillation liquid. Repeat the elution with 2.5 ml 100 mM HCl into a second vial.

4.6.4.6 Measurement

Liquid scintillation counter, ^{14}C, dpm, against background (see below).

4.6.4.7 Calculation

1. Background: 15 ml scintillation liquid + 2.5 ml 0.1 M HCl.
2. 100% value (dpm): 15 ml scintillation liquid + 100 µl supernatant of blank (for blood or liver/fibroblasts.
3. Sample value (dpm): total counts of the two vials of ^{14}C-galactose-1-phosphate elution.
4. Blank value (dpm): total counts of the two vials of ^{14}C-galactose-1-phosphate elution of the blank column.

   Δ dpm (sample) = dpm (sample value) – dpm (blank value) .

5. Blood samples:

$$\mu\text{mol/h/g Hb} = \underset{(1)}{\frac{\Delta\text{dpm (sample)}}{\text{dpm (100\%)}}} \times \underset{(2)}{500} \times \underset{(3)}{\frac{300}{1000}} \times \underset{(4)}{\frac{1}{t\,(\text{h})}} \times \underset{(5)}{\frac{1000}{100}} \times \underset{(6)}{\frac{1}{\text{Hb (g/l)}}}$$

   where term (1) is the turnover, term (2) is the substrate concentration (nmol/ml), term (3) is the substrate dilution (300 µl→1 ml), term (4) is the incubation time (h), term (5) is the sample dilution (100 µl→1 ml), and term (6) is Hb.

$$\mu\text{mol/h/g Hb} = \frac{\Delta\text{dpm (sample)}}{\text{dpm (100\%)}} \times \frac{1}{\text{Hb (g/l)}} \times 6000 .$$

   Normal values: hematocrit 45%, Hb 150 g/l
   → 1 ml erythrocytes (Ec) = 1/3 g Hb.

$$\text{Thus, } \mu\text{mol/h/ml Ec} = \frac{\Delta\text{dpm (sample)}}{\text{dpm (100\%)}} \times \frac{1}{\text{Hb (g/l)}} \times 2000 .$$

6. Tissue samples: mU/mg protein = nmol/min/mg =

$$\underset{(1)}{\frac{\Delta\text{dpm (sample)}}{\text{dpm (100\%)}}} \times \underset{(2)}{500} \times \underset{(3)}{\frac{150}{1000}} \times \underset{(4)}{\frac{1}{t\,(\text{min})}} \times \underset{(5)}{\frac{1000}{50}} \times \underset{(6)}{\text{dil.}} \times \underset{(7)}{\frac{1}{\text{mg/ml}}} ,$$

   where term (1) is the turnover, term (2) is the substrate concentration (nmol/ml), term (3) is the substrate dil. (150 µl→1.0 ml), term (4) is the incubation time (min), term (5) is the enzyme dilution (50 µl→1.0 ml), term (6) is the dilution before the assay, and term (7) is the protein concentration.

$$\text{Thus: mU/mg protein} = \frac{\Delta\text{dpm (sample)}}{\text{dpm (100\%)}} \times \frac{1}{\text{mg/ml}} \times 1500 \times \frac{1}{t} \times \text{dilution} .$$

4.6.4.8 Enzyme Activities

■ ***Table 4.6.2*** *Enzyme activities.* Ec *Erythrocytes,* RBC *red blood cells*

Condition	Mean	Range	*n*
RBC			
Controls			
Age 2 weeks – 9 months	1.29 mmol/h/ml Ec	0.69–2.57	10
Age > 9 months	0.64 mmol/h/ml Ec	0.42–0.99	22
Heterozygotes	0.35 mmol/h/ml Ec	0.24–0.47	13
Kinase deficiency	0.03 mmol/h/ml Ec	0.00–0.05	9
Fibroblasts [30]			
Controls	0.29; 0.45 U/g soluble protein [a]		2
Heterozygote	0.12 U/g soluble protein		1

[a] The two individual values are given for both subjects

4.6.4.9 Notes

Stability of Galactokinase

The enzyme in heparinized blood is stable for 8 days at 4°C. There is a rapid loss of enzyme activity in RBC stored at 4°C or –20°C, but no loss of enzyme activity in fibroblast pellets stored for 45 days at –20°C.

4.6.5 Galactose-1-Phosphate Uridyltransferase (EC 2.7.7.12)

4.6.5.1 Enzyme Deficiency

Galactose-1-phosphate uridyltransferase is the enzyme deficient in classical galactosaemia (MIM 230 400). This disorder is caused by an impairment in the pathway step from galactose-1-phosphate to UDP-galactose.

4.6.5.2 Principle

$$\frac{^{14}\text{C-Galactose-1-phosphate}}{\text{UDP-glucose}} \xrightarrow{\textbf{Transferase}} \frac{\text{Glucose-1-phosphate}}{\text{UDP-}^{14}\text{C-galactose}} .$$

Separation of the radioactively labeled product from the labeled substrate on a DEAE cellulose column; with 20 mM HCl, ^{14}C-galactose-1-phosphate is eluted and UDP-^{14}C-galactose is retained. The latter is eluted with 100 mM HCl. Radioactivity is determined with the aid of a scintillation counter (β-counter) [unpublished].

4.6.5.3 Solutions

1. Galactose-1-phosphate, 28.8 mM: galactose-1-phosphate dipotassium salt (FW variable, calculate the concentration for each batch). Dissolve in H_2O.
2. ^{14}C-Galactose-1-phosphate: ^{14}C-galactose-1-phosphate disodium salt. Dry 20 µCi of the solution under nitrogen and dissolve in 1 ml H_2O.
3. Galactose-1-phosphate substrate mix: 2 ml galactose-1-phosphate (see 1. above) and 1 ml ^{14}C-galactose-1-phosphate (see 2. above). Mix and store at –20°C.
4. UDP-glucose, 21.6 mM: UDP-glucose disodium salt (FW variable; calculate the concentration for each batch). Dissolve in H_2O.
5. Glycine-NaOH buffer, 1 M, pH 8.5: 7.5 g glycine (MW 75.07) in 100 ml H_2O. Adjust the pH to 8.5 with NaOH and store at 4°C.
6. Glycine-BME buffer: 200 mM BME (14.3 M; 10 µl in 0.7 ml glycine-NaOH buffer).
7. Digitonin 50% saturated: digitonin 50 mg/10 ml H_2O. Boil, cool to room temperature, and filter. Dilute 1:1 with H_2O. Store aliquots at –20°C.
8. Reagents mix (prepare fresh before use): The reagent mix contains 150 µl galactose-1-phosphate substrate mix (see 3. above) (4.8 mM in the mixture, 3.2 mM in the assay), 100 µl UDP-glucose (see 4. above) (3.63 mM in the mixture, 2.4 mM in the assay), 150 µl glycine-BME buffer (see 6. above) and 200 µl H_2O (giving a total reagent mix of 600 µl).
9. Preparation of DEAE cellulose stock: wash DEAE cellulose three times with H_2O on a magnetic stirrer for some minutes. Allow the cellulose to sediment and pour off the supernatant with fine particles. Leave the cellulose for 30 min in 1 M NaOH and then wash with H_2O until the pH of the supernatant is neutral. This is the DEAE cellulose (OH^- form). Leave the cellulose for 30 min in 1 M HCl, then wash until the pH of the supernatant is neutral: This is the DEAE cellulose (Cl^- form). Store both preparations at 4°C. They are stable for 1 year without preservative.
10. Test of the separation efficiency of the DEAE cellulose: every new charge of DEAE cellulose (Cl^- form) should be tested. Dry 10 µl each of ^{14}C-galactose-1-phosphate and UDP-^{14}C-galactose with nitrogen and dissolve in 300 µl H_2O, each. Put 100 µl of each in a counter vial containing 15 ml scintillation liquid (= 100%), 100 µl of each on columns with 1 ml DEAE cellulose, and 100 µl of both substances on a third column (mix).
    a) Elution with 20 mM HCl: 5 × 2 ml, collect in five counter tubes containing 15 ml scintillation liquid. ^{14}C-galactose-1-phosphate is eluted.
    b) Elution with 100 mM HCl: 5 × 2 ml, collect in five counter tubes containing 15 ml scintillation liquid. UDP-^{14}C-galactose is eluted. ^{14}C-Galactose-1-phosphate and UDP-^{14}C-galactose should be separated completely by this procedure.
11. Purity test of ^{14}C-galactose-1-phosphate: dry 10 µl of ^{14}C-galactose-1-phosphate with nitrogen, dissolve in 200 µl of H_2O. Put 100 µl in a counter vial with 15 ml scintillation liquid (= 100%) and apply 100 µl on a DEAE column. Elute stepwise as described in a) and b) above. Contamination, eluted with 100 mM HCl, should not exceed 0.1–0.2% of the total radioactivity eluted.

4.6.5.4 Samples

1. Heparinized blood: 1 part (e.g., 300 µl) blood + 1 part digitonin 50%. Incubate for 10 min at 37°C. Determine the Hb concentration.
2. RBC lysate: use if heparinized blood is not available: 1 part (e.g., 150 µl) RBC + 3 parts digitonin 50%. Incubate for 10 min at 37°C. Determine the Hb concentration.
3. Liver: 1% homogenate in 10 mM glycine-NaOH-buffer (solution 5, above, diluted 1:100). Centrifuge for 10 min at 27,000 × *g*. Determine the protein concentration in the supernatant and use it for assay (diluted to approximately 1 mg protein/ml supernatant).
4. Fibroblasts: homogenate in 10 mM glycine-NaOH-buffer (solution 5, above, diluted 1:100). Centrifuge for 10 min at 27,000 × *g*. Determine the protein concentration in the supernatant and use it for assay (diluted to approximately 1 mg protein/ml supernatant).

4.6.5.5 Assay

Heparinized blood or RBC

Incubate 100 µl of either heparinized blood or RBC (prepared as described in section 4.6.5.4) for 10 min at 37°C, then add 200 µl of the reagents mix. Incubate for 10 min at 37 °C, boil for 2 min, put on ice and stir. Centrifuge for 10 min at 2000 × *g*. Apply 100 µl of supernatant to the DEAE column (see below).

Blank

Boil 150 µl of either heparinized blood or RBC (prepared as described above in section 4.6.5.4) for 2 min. Put the solution on ice then add 300 µl of the reagents mix and stir. Centrifuge for 10 min at 2000 × *g*. Apply 100 µl of the supernatant to the DEAE column (= blank; see below) and put 100 µl of the supernatant and 2.4 ml of 0.1 M HCl into the β-counter vial (= 100% value; see below).

Liver or Fibroblasts

Incubate 50 µl of samples of either liver or fibroblasts (prepared as described above in section 4.6.5.4) at 37°C for 10 min (liver) or 60 min (fibroblasts). Continue as with blood samples.

Blank

Boil 100 µl of either liver or fibroblasts (prepared as described above in section 4.6.5.4) for 2 min then put on ice. Add 200 µl of the reagents mix then continue as with blood samples.

Separation of Substrate and Reaction Product by Chromatography

1. Preparation of columns: put 1 ml of DEAE cellulose into a 2-ml column (with a nylon mesh. 40 µm, to retain the cellulose). Equilibrate column with 3 × 2 ml of 0.02 M HCl.
2. Separation: apply 100 µl from the assay and blank supernatants onto one column each. Wash the columns with 5 × 2 ml of 20 mM HCl (discard the eluate, which contains ^{14}C-galactose-1-phosphate), elute UDP-^{14}C-galactose with 2.5 ml of 100 mM HCl into a counter vial containing 15 ml of scintillation liquid. Repeat the elution with 2.5 ml of 100 mM HCl into a second vial.

4.6.5.6 Measurement

Liquid scintillation counter, ^{14}C, dpm, against background (see below).

4.6.5.7 Calculation

1. Background: 15 ml scintillation liquid + 2.5 ml 100 mM HCl.
2. 100% value (dpm): 15 ml scintillation liquid + 100 µl supernatant of blank (for blood or liver fibroblasts).
3. Sample value (dpm): total counts of the two vials of UDP-^{14}C-galactose elution.
4. Blank value (dpm): total counts of the two vials of UDP-^{14}C-galactose elution of the blank column.
5. Δdpm (sample) = dpm (sample) – dpm (blank).
6. Blood samples

$$\mu\text{mol/h/g Hb} = \underset{(1)}{\frac{\Delta\text{dpm (sample)}}{\text{dpm (100\%)}}} \times \underset{(2)}{\frac{3.2 \times 300}{1000}} \times \underset{(3)}{\frac{60}{10}} \times \underset{(4)}{\frac{1000}{100}} \times \underset{(5)}{\frac{1000}{\text{Hb (g/l)}}} ,$$

where term (1) is the turnover, term (2) is the substrate concentration (µmol/ml), term (3) is the incubation time (h), term (4) is the sample dilution (100 µl→1 ml), and term (5) is the amount of Hb (g) per milliliter.

$$\mu\text{mol/h/g Hb} = \frac{\Delta\text{dpm (sample)}}{\text{dpm (100\%)}} \times \frac{1}{\text{Hb (g/l)}} \times 57600 .$$

7. Tissue samples: mU/mg protein = nmol/min/mg =

$$\underset{(1)}{\frac{\Delta\text{dpm (sample)}}{\text{dpm (100\%)}}} \times \underset{(2)}{\frac{3.2 \times 300 \times 1000}{1000}} \times \underset{(3)}{\frac{1}{t\,(\text{min})}} \times \underset{(4)}{\frac{1000}{100}} \times \underset{(5)}{\frac{1}{\text{mg/ml}}} ,$$

where term (1) is the turnover, term (2) is the substrate concentration (nmol/ml), term (3) is the incubation time (min), term (4) is the enzyme dilution (100 µl→1 ml), and term (5) is the protein concentration. Thus:

$$\text{mU/mg protein} = \frac{\Delta\text{dpm (sample)}}{\text{dpm (100 \%)}} \times \frac{1}{\text{mg/ml}} \times 9600 .$$

4.6.5.8 Control Values

Table 4.6.3 *Control values for galactose-1-phosphate uridyltransferase*

Sample	Control value	Range
RBC ($n = 24$; mean value)	26.6 (μmol/h/g Hb)	18.9–37.9 (μmol/h/g Hb)
Liver ($n = 1$)	8.77 U/g soluble protein	
Fibroblasts ($n = 2$)	1.75; 2.29 U/g soluble protein	

4.6.5.9 Pathological Values

1. Classical galactosemia: below 5% of normal.
2. Compound heterozygotes for galactosemia and Duarte variant: ≈25% of normal, not pathogenic.
3. Heterozygote galactosemia: ≈50% of normal, not pathogenic.
4. Homozygote Duarte variant: ≈50% of normal, not pathogenic.
5. Heterozygote Duarte variant: ≈75% of normal, not pathogenic.

4.6.5.10 Notes

Enzyme activity is stable in blood at room temperature for at least 2 days; samples can be shipped without cooling. At 4°C, samples can be stored for 2 weeks.

4.6.6 UDP-Galactose-4-Epimerase (EC 5.1.3.2)

4.6.6.1 Enzyme Deficiency

UDP-galactose-4-epimerase is deficient in epimerase deficiency (MIM 230 350). This disorder is caused by the impaired pathway step from UDP-galactose to UDP-glucose.

4.6.6.2 Principle

1. $\text{UDP-galactose} \xrightarrow{\textbf{Epimerase} + \text{NAD}} \text{UDP-glucose}$.
2. $\text{UDP-glucose} + \text{H}_2\text{O} + 2\ \text{NAD}^+ \xrightarrow{\textit{UDPG-DH}} \text{UDP-glucuronate} + \text{NADH} + 2\text{H}^+$,

   where UDPG-DH is uridyldiphosphate-galactose-dehydrogenase. NADH is determined UV-photometrically as a measure of the substrate UDP-galactose turnover (i.e., of the epimerase activity) [2, 31, 32].

4.6.6.3 Solutions

1. Glycine-NaOH buffer 1 M, pH 9.0 : 1 M glycine (MW 75.07 ; 7.5 g/100 ml) adjusted to pH 9.0 with NaOH.
2. Glycine-NaOH buffer 250 mM, pH 8.7 : 250 mM glycine (MW 75.07; 1.88 g/100 ml) adjusted to pH 8.7 with NaOH.
3. NAD 50 mM, pH 8–9 : 50 mM NAD^+ (FW variable; approximately 36 mg/ml H_2O). Adjust to pH 8–9 with 0.1 M NaOH (1 to 2 drops/ml). Prepare fresh before use.
4. NAD 10 mM : Dilute 50 mM NAD solution five times with H_2O.
5. UDP-galactose 4 mM : 4 mM UDP-galactose (FW variable; approximately 2.5 mg/ml H_2O). Solid UDP-galactose is not stable when stored at –20°C; after 2 years 20% is decomposed!).
6. UDP-glucose dehydrogenase: UDP-glucose dehydrogenase (5 mg/ml H_2O).
7. Sodium chloride 4.5% : NaCl (4.5 g/100 ml H_2O).

4.6.6.4 Samples

Washed and packed RBC.

4.6.6.5 Assay

1. Add 0.2 ml of NaCl solution to each of four tubes marked 2, 4, 6, and 8 min and put them into boiling H_2O 30 s before the respective incubation time is due. Make up a mixture containing 0.4 ml glycine-NaOH, 0.2 ml 50 mM NAD^+, 0.3 ml RBC sample, 0.7 ml H_2O, and 0.4 ml UDP-galactose. Incubate at 37°C for 2, 4, 6, and 8 min. Take out 0.4-ml aliquots at the given time point and add them to the prepared tubes containing NaCl, boil for 2 min while stirring the sample with a glass rod. Cool on ice, centrifuge for 10 min at 1500 × *g*; use the supernatant for measurement.
2. Determine the OD in a photometer at 340 nm: Make up a mixture containing 0.6 ml glycine-NaOH (pH 8.7), 0.1 ml 10 mM NAD^+, and 0.2 ml of the supernatant. Put this mixture into a 1 ml photometer cuvette. Mix and let the cuvette in the photometer until the extinction is constant. Read off the OD: E_1. Add 0.1 ml UDPG-DH, mix and put back into the photometer. Read of the OD when the maximum value is constant: E_2.

4.6.6.6 Calculation

Calculate the increase in OD for each time point (i.e. E_2–E_1) and determine ΔOD for 10 min:

$$\mu\text{mol/h/ml RBC} = \Delta\text{OD}/10\ \text{min} \times \underset{(1)}{\frac{1}{12.44}} \times \underset{(2)}{\frac{2.0}{0.3}} \times \underset{(3)}{\frac{0.6}{0.4}} \times \underset{(4)}{\frac{1.0}{0.2}} \times \underset{(5)}{6}\ ,$$

where term (1) is α_{mM} NAD × 2, term (2) is the dilution in the incubation mix, terms (3) and (4) are the dilution of the incubated aliquot before and after centrifugation, and term (5) is the incubation time 10 min, result expressed per h.

$$\mu mol/h/ml = \Delta OD/10\ min \times 24.115\ .$$

4.6.6.7 Enzyme Activities

■ ***Table 4.6.4*** *Enzyme activities for UDP-galactose-4-epimerase*

Condition	Mean (mmol/h/ml)	Range (mmol/h/ml)	*n*
Controls	4.90	2.72–7.91	36
Heterozygotes	1.38	0.29–2.80	14
Epimerase deficiency	0.36	0.00–0.98	14

4.6.6.8 Notes

Enzyme activity in blood samples is stable at room temperature for about 2 days; samples can be shipped without cooling. Washed and packed RBC should be kept at –20°C and used on the next day for assay. If stored for a longer time, activity is lost.

4.6.7 Fructose

4.6.7.1 Principle

1. D-Fructose + ATP $\xrightarrow{Hexokinase}$ Fructose-6-phosphate + ADP .
2. Fructose-6-phosphate $\xrightarrow{Phosphoglucoisomerase}$ Glucose-6-phosphate .
3. Glucose-6-phosphate + $NADP^+$ $\xrightarrow{G6P-DH}$ Gluconate-6-phosphate + $NADPH+H^+$

where G6P-DH is glucose-6-phosphate dehydrogenase and NADPH is nicotinamide adenine dinucleotide phosphate. NADPH is determined UV-photometrically as a measure of the amount of the substrate D-fructose present in the reaction [6, 36].

4.6.7.2 Solutions

1. Perchloric acid 0.6 M: add 5.2 ml of 70% $HClO_4$ ad 100 ml H_2O.
2. Potassium carbonate 0.75 M: 2,58 g K_2CO_3 (MW 138.21) in 25 ml H_2O.

3. Triethanolamine (TEA) 0.75 M/$MgSO_4$ buffer (pH 7.6): dissolve 14.0 g TEA HCl (MW 185.65) and 0.25 g $MgSO_4 \cdot 7H_2O$ (MW 246.5; final conc. 10 mM) in 80 ml H_2O. Adjust the pH to 7.6 with NaOH and make up to 100 ml with H_2O.
4. NADPH 11.5 mM: 60 mg disodium NADP (MW 765.39) in 6 ml H_2O.
5. ATP 81 mM: dissolve 300 mg ATP-$Na_2H_2 \cdot 3$ H_2O (MW 551.14) and 300 mg $NaHCO_3$ (MW 84.01) in 6 ml H_2O.
6. Hexokinase 280 kU/l/glucose-6-phosphate dehydrogenase 140 kU/l: hexokinase and glucose-6-phosphate dehydrogenase from yeast, suspended in 3.2 M ammonium sulfate solution. Dilute stock solutions with 3.2 M ammonium sulfate solution according to specified activity to 280 kU/l and 140 kU/l, respectively.
7. Glucose-phosphate isomerase (phosphoglucose isomerase, PGI); 700 kU/l: PGI suspension in ammonium sulfate solution. Dilute with 3.2 M ammonium sulfate to 700 kU/l if required.

4.6.7.3 Samples

1. Blood: Blood is taken from the vein without stasis. Additions of oxalate, fluoride, heparin, or ethylenediaminetetraacetic acid (EDTA) are without effect. Add 3 ml blood to 6 ml ice-cold perchloric acid, mix thoroughly and centrifuge for 15 min at 1000 × *g*. To 3 ml of the supernatant add 1 ml of potassium carbonate solution. After 15 min in an ice-bath, filter off the precipitate. Use the resultant solution for assay at room temperature. The content of fructose in blood is stable for 24 h when stored at 4°C.
2. Urine: treat the same as blood.

Table 4.6.5 *Mixtures required for blank and sample assay for fructose. The preparation of these solutions is described in the text in section 4.6.7.2. Pipette these successively into 1-cm cuvettes. The absorbance of the mixtures is read twice (at 340 nm): before (OD_1) and after (OD_2) the addition of glucose-phosphate isomerase.* G6P-DH *glucose-6-phosphate dehydrogenase,* HK *hexokinase,* NADP *nicotinamide adenine dinucleotide,* PGI *glucose phosphate isomerase,* TEA *triethanolamine*

Solution	Blank (ml)	Sample (ml)	Concentration in assay mix
Buffer	1.00	1.00	TEA: 0.23 M
NADP solution	0.10	0.10	NADP: 0.36 mM
ATP solution	0.10	0.10	
Sample		0.10	
H_2O	2.00	1.90	
HK/G6P-DH	0.02	0.02	HK: 1.7 kU/l G6P-DH: 0.9 kU/l
PGI[a]	0.02	0.02	PGI: 4.3 kU/l

[a] Read the absorbance before (OD_1) and after the addition of PGI (OD_2)

4.6.7.4 Assay

Photometer at wavelength 340 nm, at room temperature, against air. The amounts of the various solutions required for the blank and sample for this assay are given in Table 4.6.5. Place the stated amounts of the solutions (prepared as described in section 4.6.7.2) successively into 1-cm cuvettes – without PGI (see Table 4.6.5). Mix thoroughly and monitor the absorbance until it is constant. Read the absorbance (OD_1). Add 0.02 ml PGI, mix, and read the absorbance after 10–15 min (OD_2).

4.6.7.5 Calculation

$$\Delta OD = (OD_2 - OD_1)_{\mathbf{sample}} - (OD_2 - OD_1)_{\mathbf{blank}}$$

$$c = \Delta OD \times \frac{V \times MW}{\varepsilon \times d \times v \times 1000} \times \frac{9 \times 4^*}{3 \times 3},$$

where c is the concentration of fructose (g/l), V is the final volume (i.e., 3.24 ml), v is the sample volume in the assay (i.e., 0.10 ml), MW is the molecular weight (i.e., 180.14 g/mol), d is the length of the light path (i.e., 1 cm), and ε is the extinction coefficient (mM) of NADPH at 340 nm (i.e., 6.3). *Note that when using blood, the specific weight (about 1.06) and fluid content (about 90%) must be taken into consideration, and thus the factor 3.8 applies instead of 4.

$$\text{Thus, } c = \Delta OD \times \frac{3.24 \times 180.16}{6.3 \times 1 \times 0.1 \times 1000} \times 3.8$$

$$c = \Delta OD \times 3.521 \text{ g/l}$$

or $\Delta OD \times 1.954$ mM.

4.6.7.6 Control Values

Depending on fructose, sucrose, or sorbitol intake, mean (± SD) blood and urine levels of fructose are normally 31 ± 3 µmol/l (range 19–47 µmol/l) [29] and 1.44 ± 0.79 µmol/d/kg [28], respectively.

4.6.7.7 Pathological Values

For values during an intravenous fructose tolerance test in controls and individuals with deficiencies of fructokinase, fructaldolase, and fructose-1,6-bisphosphatase, see Steinmann et al. [36].

4.6.8 Fructose-Bisphosphate Aldolase (Aldolase, EC 4.1.2.13)

4.6.8.1 Enzyme Deficiency

Fructose-bisphosphate aldolase, which also acts on fructose-1-phosphate, is the enzyme deficient in hereditary fructose intolerance (HFI, MIM 229 600).

4.6.8.2 Principle

1. F-1-P $\xleftrightarrow{\textbf{Aldolase}}$ DHA-P + D-glyceraldehyde
2. DHA-P + NADH + H^+ $\xleftrightarrow{GDH}$ α-glycerophosphate + 1 NAD^+

where F-1-P is fructose-1-phosphate, or:

1. F-1,6-P $\xleftrightarrow{\textbf{Aldolase}}$ DHA-P + D-glyceraldehyde-3-phosphate
2. D-glyceraldehyde-3-phosphate $\xleftrightarrow{TIM}$ DHA-P
3. 2 DHA-P + 2 NADH + H^+ $\xleftrightarrow{GDH}$ 2 α-glycerophosphate + 2 NAD^+,

where F-1,6-P is fructose-1,6-bisphosphate, DHA-P is dihydroxyacetone phosphate, GDH is α-glycerophosphate dehydrogenase, and TIM is triosephosphate isomerase. The decrease in OD of NADH + H^+ at 340 nm, in other words the increase of NAD^+, is a measure of aldolase activity [18, 36].

4.6.8.3 Solutions

1. Tris-HCl buffer 0.1 M, pH 7.6: 12.1 g Trizma base (MW 121.1) in 1000 ml H_2O. Adjust the pH to 7.6 with 1 M HCl.
2. F-1,6-P substrate mix 2 mM: dissolve approximately 9.2 mg (depending on FW; e.g. 917) D-F-1,6-P trisodium salt and 1.0 mg (final conc. 0.3 mM) disodium NADH (MW 709.4) in 5 ml of Tris-HCl buffer. Always prepare fresh before use.
3. F-1-P substrate mix 40 mM: dissolve approximately 36.5 mg (depending on FW; e.g. 304) D-F-1-P sodium salt and 0.6 mg (final conc. 0.3 mM) disodium NADH (MW 709.4) in 3 ml Tris-HCl buffer. Always prepare fresh before use.

4.6.8.4 Samples

Liver (1% homogenate): place 1–3 mg tissue into a plastic tube and add 100 µl of Tris-HCl buffer. homogenize, and then dilute to 1% with the same buffer. Centrifuge for 10 min at 27,000 × *g*. Use the resulting supernatant for the assay.

4.6.8.5 Assay

Photometer at 340 nm, thermostatted at 25°C. Pipette directly into four 1-ml cuvettes 630 µl substrate mix (F-1-P and F-1,6-P, two each) and 10 µl GDH/TIM suspension (total 640 µl). Place the cuvettes into the photometer and wait until the OD is constant. Then add 20 µl sample into one each of the cuvettes containing F-1-P and F-1,6-P, and 20 µl of Tris-HCl buffer into the two remaining reference cuvettes. Read off the OD at given time intervals and determine ΔOD/min when the increase in OD versus time is linear.

4.6.8.6 Calculation

Molecular extinction of NAD^+: α_{mM} (µmol/ml) = 6.22

U/g soluble liver extract = µmol/min/g =

$$\Delta OD/min \times \underset{(1)}{\frac{1}{6.22}} \times 0.66 \times \underset{(2)}{\frac{1000}{20}} \times \underset{(3)}{100} \times \underset{(4)}{\frac{1^*}{2}}, \quad (5)^*$$

where term (1) is the extinction coefficient of NAD^+ (i.e. α_{mM}), term (2) is the assay volume, term (3) is the dilution of the sample in the assay [20µl → lg], term (4) is the dilution of the homogenate, and term (5)* is required only for F-1,6-P.

Thus: for substrate F-1,6-P, U/g = ΔOD/min × 265.3
for substrate F-1-P, U/g = ΔOD/min × 531.5.

4.6.8.7 Control Values

Table 4.6.6 *Control values for fructose-1-phosphate and fructose-1,6-bisphosphate aldolases [36]*

Enzyme (substrate)	Mean ± SD	Range	*n*
Fructose-1,6-bisphosphate aldolase (F-1,6-P)	2.61 ± 0.46 U/g	2.07–3.79 U/g	10
Fructose-1-phosphate aldolase (F-1-P)	2.40 ± 0.49 U/g	1.82–3.40 U/g	10
F-1,6-P : F-1-P	1.10 ± 0.10	1.00–1.20	10

4.6.8.8 Pathological Values

■ ***Table 4.6.7*** *Pathological values of fructose-1-phosphate and fructose-1,6-bisphosphate in patients with hereditary fructose intolerance* (HFI) *[36]*

Enzyme (substrate)	Mean ± SD	Range	*n*
Fructose-1,6-bisphosphate aldolase (F-1,6-P)	0.46 ± 0.16 U/g	0.13–0.82 U/g	35
Fructose-1-phosphate aldolase (F-1-P)	0.11 ± 0.09 U/g	0.00–0.36 U/g	35
F-1,6-P : F-1-P	3.9	1.7– ∞	35

4.6.8.9 Note

Enzyme stored at –20°C is stable for at least 12 months.

4.6.9 Fructose-1,6-Bisphosphatase (EC 3.1.3.11)

4.6.9.1 Enzyme Deficiency

Fructose-1,6-bisphosphatase is the enzyme deficient in fructose-1,6-bisphosphatase deficiency (MIM 229 700).

4.6.9.2 Principle

1. $\text{F-1,6-P} + \text{H}_2\text{O} \xleftarrow{\textbf{Fructose-1,6-bisphosphatase}\ (\text{Mg}^{2+})} \text{F-6-P} + \text{P}_i$
2. $\text{F-6-P} \xleftrightarrow{PGI} \text{G-6-P}$
3. $\text{G-6-P} + \text{NADP}^+ \xleftrightarrow{G6P\text{-}DH} \text{6-PG} + \text{NADPH} + \text{H}^+$
4. $\text{6-PG} + \text{NADP}^+ \xleftrightarrow{6\text{-}PGDH} \text{Rib-5'-P} + \text{NADPH} + \text{H}^+ + \text{CO}_2$

Σ: $\text{F-1,6-P} + \text{H}_2\text{O} + 2\ \text{NADP}^+ \rightarrow \text{Rib-5'-P} + \text{P}_i + \text{CO}_2 + 2\ \text{NADPH}$,

where F-6-P is fructose-6-phosphate, P_i is inorganic phosphorus, PGI is phosphoglucose isomerase, G-6-P is glucose-6-phosphate, G6P-DH is glucose-6-phosphate dehydrogenase, 6-PG is gluconolactone-6-phosphate, 6-PGDH is gluconolactone-6-phosphate dehydrogenase, and Rib-5'-P is ribulose-5-phosphate. Photometric determination of $\text{NADPH} + \text{H}^+$ is achieved by measuring the increase in OD at 340 nm as a measure of enzyme activity [1, 36].

4.6.9.3 Solutions

1. Potassium chloride 0.15 M: 1.12 g KCl (MW 74.56) in 100 ml H_2O. Store at 4°C.
2. Tris-HCl-buffer 0.2 M, pH 8.5: 2.4 g Trizma base (MW 121.1) in 100 ml H_2O. Adjust the pH to 8.5 with 1 N HCl. Store at 4°C.
3. Magnesium chloride 30 mM: 2.03 g $MgCl_2 \cdot 6H_2O$ (MW 203.31) in 100 ml H_2O (i. e. final conc. 0.1 M). Keep at 4°C. Dilute immediately before use by adding 30 ml stock solution to 70 ml H_2O.
4. EDTA solution 2 mM: 74.5 mg EDTA-Na_2 (MW 372.24) in 100 ml H_2O. Store at 4°C.
5. NADP solution 4 mM: 3.1 mg NADP (MW 787.4) in ml H_2O. Prepare fresh before use.
6. F-1,6-P 2 mM: 3.7 mg F-1,6-P (MW 917.0) in 2 ml H_2O. Prepare fresh before use.

4.6.9.4 Samples

Liver (1% homogenate): homogenize 1–3 mg of liver in 100 µl of 0.15 M KCl. Further dilute the solution to 1% with more 0.15 M KCl. Centrifuge for 10 min at 27,000 × *g*. Use the supernatant for the assay. The stability of the enzyme in liver tissue at –20°C is 100% for 2 months and 50–75% for 12 months.

4.6.9.5 Assay

Photometer at 340 nm, thermostatted at 25°C. Pipette directly into four 1-ml cuvettes: 250 µl Tris-HCL (50 mM in the assay mix), 50 µl $MgCL_2$ (1.5 mM in the assay mix), 50 µl EDTA (0.1 mM in the assay mix), 50 µl NADP (0.2 mM in the assay mix), 5 µl PGI (suspension), 5 µl 6-PGDH (suspension), 2 µl G6P-DH (suspension), 20 µl sample (supernatant), and 530 µl H_2O. Mix well and keep in the photometer to stabilize OD and temperature. Then add 50 µl F-1,6-P into two of the cuvettes and 50 µl H_2O into the remaining cuvettes (as blanks). Read off the OD at given time intervals and determine ΔOD/min when the increase in OD versus time is linear.

4.6.9.6 Calculation

Molecular extinction of NADPH: α_{mM} (µmol/ml) = 6.3

$$\text{U/g soluble liver extract} = \mu\text{mol/min/g} = \Delta\text{OD/min} \times \underset{(1)}{\frac{1}{6.3}} \times \underset{(2)}{\frac{1000}{20}} \times \underset{(3)}{100} \times \underset{(4)}{\frac{1}{2}},$$

where term (1) is the molecular extinction of NADPH (i.e. α_{mM}), term (2) is the dilution in the assay, term (3) is the dilution of the homogenate, and term (4) represents 2 NADPH generated per reaction. Thus:

$$\text{U/g liver} = \Delta\text{OD/min} \times 396.82.$$

4.6.9.7 Enzyme Activities

■ ***Table 4.6.8*** *Normal liver fructose-1,6-bisphosphatase activities [36]*

Liver	Mean (U/g)	Range (U/g)	*n*
Controls	3.34	1.78–4.98	16
Heterozygotes	0.80; 1.37[a]		2
F-1,6-P deficiency	0.23	0.09–0.53	11

[a] The two individual values are given for both parents

4.6.10 Glucose

4.6.10.1 Principle

1. D-Glucose + ATP $\xleftarrow{Hexokinase}$ G-6-P + ADP

   G-6-P + $NADP^+$ $\xleftarrow{G\text{-}6\text{-}PDH}$ D-glucono-δ-lactone + NADPH + H^+,

   where G-6-P is glucose-6-phosphate and G-6-PDH is glucose-6-phosphate dehydrogenase. The amount of NADPH formed in the reaction, which is proportional to the amount of glucose, is determined UV-photometrically [25].

4.6.10.2 Solutions

1. Phosphate buffer/ATP/NADP: Dissolve in 40 ml H_2O 546 mg (final conc. 70 mM) $NaH_2PO_4 \cdot 2H_2O$ (MW 156.01), 49.3 mg (final conc. 4 mM) $MgSO_4 \cdot 7H_2O$ (MW 246.48), approximately 48.4 mg (final conc. 1.6 mM) ATP-Na_2 (FW 620, variable), and 63.0 mg (final conc. 1.6 mM) NADP-Na_2 (MW 787.4). Adjust the pH to 7.7 with 1 M NaOH and make up to 50 ml with H_2O. This solution is stable for 2 weeks at 4°C.
2. Enzyme mix: Add together 100 mM $MgSO_4 \cdot 7H_2O$ (MW 246.48; 14.8 mg in 450 µl H_2O), 70 U hexokinase (50 µl of suspension, 1500 U/ml) and 70 U G-6-PDH (100 µl of suspension, 140 U/ml, 5 mg/ml). This mixture is stable for 1 month at 4°C.
3. Glucose standard 1 mM: 18 mg glucose (MW 180.16) in 100 ml H_2O.

4.6.10.3 Assay

1. Put directly in cuvettes: 200 µl sample (or glucose standard, see below) and 2 ml phosphate buffer/ATP/NADP (see above 1.).
   a. Glucose standard: 10 µl standard + 190 µl H_2O = 10 nmol glucose
      20 µl standard + 180 µl H_2O = 20 nmol glucose
      50 µl standard + 150 µl H_2O = 50 nmol glucose.

2. Put the cuvettes into the photometer at 25°C and read off the OD at 340 nm for time 0 min.
3. Add 20 µl enzyme mixture and mix.
4. Determine OD values at 5-min intervals until the increase in absorption levels off (end-point determination).

4.6.10.4 Calculation

Determine nmol glucose in the 200-µl sample by linear regression calculation of standard values. Calculate glucose concentration of the sample in mmol/l.

4.6.11 Glycogen, Quantitative Determination in Liver and Muscle

4.6.11.1 Principle

Digestion of the tissue to make glycogen accessible to the anthrone reaction [19, 35].

4.6.11.2 Solutions

1. KOH, 33%.
2. Anthrone reagent: 0.2% anthrone (2 mg/ml 95% H_2SO_4).
3. Glycogen standard, 0.1%: bovine liver glycogen (1 mg/ml H_2O).

4.6.11.3 Samples

1. Liver: 1% homogenate in H_2O.
2. Muscle: 2% homogenate in H_2O.

4.6.11.4 Assay

1. Add 50 µl sample (homogenate) and 200 µl 33% KOH to a test tube. Use high test tubes because of concentrated sulfuric acid. Boil for 20 min with the tubes covered with a glass marble. After cooling on ice-H_2O add 1.75 ml H_2O.
2. Standard: 0, 10, 30, 50 µl of glycogen standard, each brought to a volume of 2.0 ml with H_2O.
3. At room temperature, add 4 ml of anthrone reagent, each to sample and standards. Vortex and let stand for 10 min, vortex again and leave for another 10 min before measuring the OD.

4.6.11.5 Measurement

Measure the OD in a photometer at 620 nm.

4.6.11.6 Calculation

Calculate from linear regression of the standard values the glycogen content of the sample (µg glycogen in 50 µl of homogenate).

1. Liver: g glycogen/100 g tissue (%) = $\underset{(1)}{\mu g/50\mu l} \times \underset{(2)}{20 \times 100} \times \underset{(3)}{\frac{1}{10^4}}$,

   where term (1) is the dilution factor (i.e. 50 µl→1.0 ml), term (2) is the dilution of the homogenate, and (3) represents the conversion of µg/ml→g/100 g. Thus: g glycogen/100 g tissue (%) = µg/50 µl × 0.2.

2. Muscle: g glycogen/100 g tissue (%) = $\underset{(1)}{\mu g/50\mu l} \times \underset{(2)}{20 \times 50} \times \underset{(3)}{\frac{1}{10^4}}$,

   where term (1) is the dilution factor (i.e. 50 µl→1.0 ml), term (2) is the dilution of the homogenate, and (3) represents the conversion of µg/ml→g/100 g. Thus: g glycogen/100 g tissue (%) = µg/50 µl × 0.1.

4.6.11.7 Control Values

1. Liver: 4.6 mean and range 2.4–6.4 g/100 g liver.
2. Muscle: 0.7–2.0 g/100 g muscle.

4.6.11.8 Pathological Values

In glycogen storage diseases GSD I, II, III, IV, VI, and IX, glycogen content in the liver is above the normal range, up to above 20 g/100 g. Elevated values are also found in Fanconi-Bickel syndrome and Mauriac syndrome. In glycogen synthase deficiency, liver glycogen content is usually below the normal range: mean value 2.1 g/100 g (range 0.7–3.4; $n = 10$). In glycogen storage diseases GSD II, V, VII, and variants of GSD III and IX, glycogen content in muscle is elevated.

4.6.12 Glycogen Structure (Iodine Spectrum)

4.6.12.1 Application

In glycogenosis type III, the outer chain length of glycogen is reduced; in glycogenosis type IV, it is increased.

4.6.12.2 Principle

A spectrum of the color reaction of glycogen with iodine is recorded. The wavelength of the absorption maximum is positively correlated with the outer chain length of glycogen (i.e., the chain length distal of the branching points) [24].

4.6.12.3 Reagents

1. Glycogen (bovine liver; Sigma G-0885).
2. Glycogen, long- and short-chain preparation see below.
3. β-Amylase (sweet potato; Sigma A-7005).
4. Starch (from potato) for electrophoresis (Sigma S-5651).

4.6.12.4 Solutions

1. KOH, 33%.
2. Ethanol, 96%.
3. $CaCl_2$, saturated: saturated solution in H_2O at room temperature (about 5.5 M).
4. NH_4Cl, saturated: saturated solution in H_2O at room temperature (about 5.2 M).
5. Iodine reagent: 260 mg J_2 + 2.6 g KJ. Dissolve in 10 ml H_2O.
6. Glycogen standards:
   a. Glycogen (bovine liver): 1 mg/ml H_2O.
   b. Glycogen, short-chain: 2 mg/ml H_2O.
   c. Glycogen, long-chain: 1 mg/ml H_2O.
7. Preparation of short-chain glycogen: Mix together 1 g glycogen (bovine liver), 100 ml 0.2 mM sodium acetate buffer (pH 5.0), 1000 U β-amylase (750–1000 U/mg). Incubate at 37°C for 2 h. Stop the reaction with 680 ml ethanol (96%). Centrifuge for 10 min at 1000 × *g* in 40-ml tubes, decant the supernatants and wash sediments in 20 ml ethanol (66%) per tube, centrifuge, decant supernatant, and wash sediments in 10 ml acetone each. Centrifuge, decant supernatant, and dry the sediment (vacuum or nitrogen). One gram of glycogen yields about 600–700 mg of short-chain glycogen.
8. Preparation of long-chain glycogen: dissolve 10 mg starch (potato) in 3 ml H_2O and boil for 15 min. Allow the solution to cool to room temperature and filter through a Swinnex 0.45-µm filter. Put into a centrifugation tube 2 ml dissolved starch (filtrate) and 2.6 ml ethanol (96%). Add 0.9% NaCl until a flaky precipitate appears. Centrifuge for 10 min at 1000 × g, discard the supernatant and dissolve the sediment in 2 ml H_2O. Add ethanol and NaCl solution as above, then centrifuge for 10 min at 1000 × g. Discard the supernatant and allow the sediment to dry. Wash the sediment in 2 ml acetone, centrifuge for 10 min at 1000 × g, discard the supernatant, and let the sediment dry. The sediment is long-chain glycogen.

4.6.12.5 Samples

1. Liver: 1% homogenate in H_2O.
2. Muscle: 10% homogenate in H_2O.

4.6.12.6 Assay

1. Mix 0.4 ml of sample (homogenate) and 1.6 ml 33% KOH 33% in a centrifuge tube and boil for 30 min (with the tube covered with a glass marble). Cool on

ice/H_2O, centrifuge for 10 min at 1000 × *g*, and decant the supernatant into a new tube. Add 2.6 ml ethanol (96%) to the supernatant (approximately 2 ml), heat to boiling, and then cool on ice/H_2O. Centrifuge for 5 min at 1000 × *g*, discard the supernatant and allow the precipitated glycogen to dry in the tube.
2. For muscle glycogen dissolve the sediment again in 1 ml H_2O, add 1.3 ml ethanol (96%), mix, heat to boiling, add 10 µl of HCl (0.05 N), and allow the glycogen to precipitate for 15 min on ice/H_2O. Centrifuge for 5 min at 1000 × g, discard the supernatant, and allow the precipitate to dry in the tube.
3. For both muscle and liver, dissolve the sediment in 0.3 ml saturated NH_4Cl, boil for 5 min and cool on ice/H_2O.
4. Add 0.3 ml H_2O and 1.95 ml $CaCl_2$ (saturated) and mix – "solution A".
5. Add 50 µl iodine reagent and 6.5 ml $CaCl_2$ (saturated) and mix – "solution B".
6. Standards: Add 0.30 ml NH_4Cl (saturated) and 1.95 ml $CaCl_2$ (saturated) to 0.3 ml of each of the standards (see 4.6.12.4.6, above) and mix to make "standard solutions A".

4.6.12.7 Measurement

Run spectrum in photometer from 380 nm to 600 nm, using "tandem cuvettes". Put 1 ml of solution "A" into one chamber and 1 ml of solution "B" into the other chamber of each of two tandem cuvettes:
1. "A"/"B": reference cuvette (do not mix "A" and "B").
2. "A"/"B": sample or standard cuvettes (mix "A" and "B").

Determine the absorption maximum (nm) of the spectrum.

4.6.12.8 Normal Values

Table 4.6.9 *Normal absorption maxima for glycogen*

Control livers	454–478 nm ($n = 8$)
Glycogen (bovine liver)	459 nm
Glycogen, short-chain	409 nm
Glycogen, long-chain	530 nm

4.6.12.9 Pathological Values

In glycogenosis type III (debranching enzyme deficiency) the absorption maximum is around 410 nm in muscle; in liver the maximum remains around 460 nm, but there is a pronounced shoulder at 410 nm. In glycogenosis type IV (branching enzyme deficiency) the absorption maximum is around 530 nm.

4.6.13 Glucose-6-Phosphatase (EC 3.1.3.9)

4.6.13.1 Enzyme Deficiency

Glucose-6-phosphatase is the enzyme deficient in glycogenosis type Ia (GSD Ia, MIM 232 200).

4.6.13.2 Principle

$$\text{Glucose-6-phosphate} \xleftarrow{\textbf{Glucose-6-phosphatase}} \text{glucose} + P_i\,.$$

Colorimetric determination of P_i as a measure of the enzyme activity [19].

4.6.13.3 Solutions

1. Sodium acetate buffer 0.1 M, pH 5.0: Dilute 1 M sodium acetate stock solution (81.04 g/l) with H_2O and adjust to pH 5.0 with acetic acid. Make up to ten times the original volume with H_2O.
2. Substrate: 0.1 M glucose-6-phosphate (FW 288; 28.8 mg/ml H_2O). Adjust to pH 6.5 with 1 N NaOH.
3. Stop solution: 36 mM H_2SO_4 concentrated (36 N = 18 M; 200 µl/100 ml H_2O).
4. Ammonium molybdate/$FeSO_4$ 8 mM/144 mM: add together 2.5 g ammonium molybdate · H_2O (MW 1235.86) and 6.9 ml (final conc. 0.5 M) H_2SO_4 concentrated (18 M). Fill up to 250 ml with H_2O and store in a dark bottle at room temperature. Directly before use add 40 mg $FeSO_4 \times 7H_2O$ (MW 278.02) to 1 ml of this solution.
5. P_i standard solution 80 µg P_i/ml: put together 351.5 mg (final conc. 2.58 mM) KH_2PO_4 (MW 136.01), [2.58 mM P_i (MW 30.98) = 80 mg P_i/l], and 10 ml concentrated H_2SO_4 (18 M). Make up to 1000 ml with H_2O.

4.6.13.4 Samples

Liver: 1% homogenate (w/v) in H_2O. The enzyme is stable at –20°C for at least 8 weeks.

4.6.13.5 Assay

1. Blank: put together 50 µl sample (homogenate) and 5 µl sodium acetate buffer (total aliquot volume of 55 µl), incubate for 5 min at 37°C (glucose-6-phosphatase activity is destroyed while unspecific phosphatase activity is retained).
2. Sample (homogenate): add together 50 µl sample and 5 µl H_2O (total aliquot volume of 55 µl).
3. Add to both sample and blank 50 µl glucose-6-phosphate (pH 6.5) – giving a total aliquot volume of 105 µl.

4. Incubate at 37°C for 0 and 20 min, then add 1 ml stop solution and 1 ml ammonium molybdate/$FeSO_4$. Mix and centrifuge for 5 min at 1000 × g and use the supernatant for OD measurement.
5. Standards: add to each of the following 1 ml stop solution and 1 ml ammonium molybdate/$FeSO_4$
   a) 0 µg P_i: 100 µl H_2O
   b) 4 µg P_i: 50 µl H_2O + 50 µl P_i standard
   c) 8 µg P_i: 100 µl P_i standard.
6. Mix and use for OD measurement.

4.6.13.6 Measurement

Photometer at 700 nm.

4.6.13.7 Calculation

1. ΔOD (sample) = OD (20 min) – OD (0 min) without preincubation.
2. ΔOD (blank) = OD (20 min) – OD (0 min) with preincubation.
3. ΔOD = ΔOD (sample) – ΔOD (blank).

$$\text{U/g liver} = \text{µmol } P_i/\text{min/g} = \Delta\text{OD} \times \underbrace{\frac{\text{µg (std)}}{\text{OD (std)}}}_{(1)} \times \underbrace{\frac{1}{t\,(\text{min})}}_{(2)} \times \underbrace{\frac{1}{31}}_{(3)} \times \underbrace{100}_{(4)} \times 20\,,$$

where "std" is standard, term (1) is the incubation time, term (2) is the MW of P_i, term (3) is the dilution factor of the homogenate, and term (4) is the dilution factor of the homogenate in the assay sample. Thus:

$$\text{U/g} = \Delta\text{OD} \times \frac{\text{µg (std)}}{\text{OD (std)}} \times \frac{1}{t\,(\text{min})} \times 64.5\,.$$

4.6.13.8 Control Values

Normal liver: 6.3 U/g (range 3.7–9.6 U/g; $n = 17$).

4.6.13.9 Pathological Values

In glycogenosis Ia the enzyme activity is 0 to 10 % of normal.

4.6.13.10 Notes

In glycogenosis type Ib (GSD I "non-a"), glucose-6-phosphatase activity is normal or even elevated when measured in liver homogenates, but it is low when measured in a fraction of intact liver microsomes [10].

4.6.14 α-Glucosidase (Acid Maltase, EC 3.2.1.20)

4.6.14.1 Enzyme Deficiency

α-Glucosidase is the enzyme deficient in glycogenosis type II (GSD II, M. Pompe, MIM 232 300).

4.6.14.2 Principle

$$\text{Maltose} + H_2O \xleftrightarrow{\alpha\text{ - Glucosidase}} 2\ \alpha\text{-D-glucose}\ .$$

Colorimetric determination of the produced α-D-glucose [19].

4.6.14.3 Solutions

1. Sodium acetate-buffer 0.1 M pH 4.0 and 4.5: dilute 1 M sodium acetate stock solution (81.04 g/l) with H_2O and adjust to pH 4.0 or 4.5 with acetic acid. Make up to ten times the original volume with H_2O.
2. Potassium phosphate buffer 0.1 M pH 6.5 and 7.0: Make up 0.1 M KH_2PO_4 (MW 136.09; 13.61 g/l H_2O: Solution A) and 0.1 M K_2HPO_4 (MW 228.23; 22.82 g/l H_2O: Solution B). For potassium phosphate buffer pH 6.5 mix 20 ml solution A and approximately 11 ml solution B. For potassium phosphate buffer pH 7.0 mix 20 ml solution A with approximately 40 ml solution B.
3. Maltose substrate: 14 mM (0.5%) Maltose (MW 360.3; 25 mg/5 ml H_2O). Store at –20°C.
4. Tris-HCl-buffer 1.0 M pH 7.0: 1 M Trizma base (MW 121.1). Dissolve in approximately 800 ml H_2O and adjust the pH to 7.0 (at room temperature) with HCl. Make up to 1000 ml with H_2O.
5. Glucose reagent: dissolve 13 mg glucose oxidase and 2 mg peroxidase in 100 ml Tris-HCl buffer. Add 0.5 ml o-dianisidine (1% w/v in ethanol, prepare fresh). This reagent is stable for 1 week at 4°C stored in the dark.
6. Hydrochloric acid 6 M: 48 ml 12.5 M HCl in 100 ml H_2O.
7. Glucose standard solution 1 mM: 180 mg D-glucose (MW 180.16) in 1 l H_2O.

4.6.14.4 Samples

1. Liver: 1% homogenate in H_2O.
2. Muscle: 2% homogenate in H_2O.
3. Chorionic villi: 1% homogenate in 0.2% Triton X-100, centrifuge 5 min at 12,000 × *g*. Use the supernatant for assay. Do not freeze the sample before assay.
4. Fibroblasts: homogenate in H_2O (approximately 1 mg protein/ml).

4.6.14.5 Assay

1. Add 25 µl substrate (maltose), 25 µl buffer for each pH (i.e. sodium acetate buffer pH 4.0 and 4.5, and potassium phosphate buffer pH 6.5 and 7.0), and 50 µl sample (giving a total aliquot volume of 100 µl).
2. Incubation:
   a) Liver, chorionic villi: 60 min and 0 min (blank) at 37°C.
   b) Muscle, fibroblasts: 120 min and 0 min (blank) at 37°C.
3. Stop: add 100 µl H_2O, boil for 2 min, put on ice. Centrifuge for 10 min at 3000 × *g*. Use the supernatant for assay.
4. Assay: Add 100 µl supernatant, or 100 µl standard 0 µmol (i.e. 100 µl Tris-HCl buffer pH 7.0), standard 0.05 µmol (i.e. 50 µl Tris buffer + 50 µl 1 mM glucose standard solution), or 100 µl standard 0.1 µmol (i. e., 100 µl glucose standard solution), each to 1.0 ml of glucose reagent. Incubate at 37°C for 60 min. Stop the reaction with 1 drop of 6 M HCl.

4.6.14.6 Measurement

Photometer at 420 nm.

4.6.14.7 Calculation

1. Liver:

$$\text{U/g liver} = \mu\text{mol/min/g} = \Delta\text{OD}\,(60'\text{–}0') \times \frac{\mu\text{mol (std)}}{\text{OD (std)}} \times 20 \times \frac{1}{t\,(\text{min})} \times \frac{200}{100} \times 100 \times \frac{1}{2}$$

(1) (2) (3) (4) (5)

where "std" is standard, term (1) is the dilution factor (50 µl → 1 ml), term (2) is the incubation time, term (3) is the dilution after centrifugation, term (4) is the dilution factor of the homogenate, and term (5) represents "two glucose" from the reaction. Thus:

$$\text{U/g} = \Delta\text{OD} \times \frac{\mu\text{mol (std)}}{\text{OD (std)}} \times \frac{1}{t\,(\text{min})} \times 2000\,.$$

2. Muscle:

$$\text{mU/g muscle} = \text{nmol/min/g} = \Delta\text{OD}\,(60'\text{–}0') \times \frac{\mu\text{mol (std)}}{\text{OD (std)}} \times 1000 \times 20 \times \frac{1}{t\,(\text{min})} \times \frac{200}{100} \times 50 \times \frac{1}{2}\,,$$

(1) (2) (3) (4) (5) (6)

where term (1) is the conversion factor (U → mU), term (2) is the dilution factor (50 µl→1 ml), term (3) is the incubation time, term (4) is the dilution after

centrifugation, term (5) is the dilution factor of the homogenate, and term (6) represents "two glucose" from the reaction. Thus:

$$\text{mU/g} = \Delta\text{OD} \times \frac{\mu\text{mol (std)}}{\text{OD (std)}} \times \frac{1}{t\,(\text{min})} \times 1000 \times 1000\,.$$

3. Fibroblasts, Chorionic villi:

$$\text{mU/mg protein} = \text{nmol/min/mg} =$$

$$\Delta\text{OD}\,(60'\text{–}0') \times \frac{\mu\text{mol (std)}}{\text{OD (std)}} \times 1000 \times 20 \times \frac{1}{t\,(\text{min})} \times \frac{200}{100} \times \frac{1}{\text{mg/ml}} \times \frac{1}{2}\,,$$

(1) (2) (3) (4) (5) (6)

where term (1) is the conversion (U→ mU), term (2) is the dilution factor (50 µl→ 1 ml), term (3) is the incubation time, term (4) is the dilution after centrifugation, term (5) is the protein concentration of the homogenate, and term (6) represents "two glucose" from the reaction. Thus:

$$\text{mU/mg} = \Delta\text{OD} \times \frac{\mu\text{mol (std)}}{\text{OD (std)}} \times \frac{1}{t\,(\text{min})} \times 20{,}000 \times \frac{1}{\text{mg prot./ml}}\,.$$

4.6.14.8 Enzyme Activities

■ ***Table 4.6.10*** *Activities of α-glucosidase in controls and in patients with glycogen storage disease type II (GSD II)*

Tissue	Controls			GSD II Homozygotes		
	Mean	Range	*n*	Mean	Range	*n*
Muscle (U/g muscle)	52	24–85	7	3.0	0.0–6.9	4
Liver (U/g liver)	0.8	0.5–1.1	16	0.005	0.0–0.02	8
Fibroblasts (U/g protein)	5.80	4.65–6.55	3	0.14	0.0–0.48	10
Chorionic villi (mU/ml soluble protein)	16.6	10.2–19.0	6	0.0, 1.02[a]	–	2

[a] The two individual values are given for both subjects

4.6.14.9 Notes

1. If not enough sample material is available, only measure at pH 4.0 and 6.5.
2. Leukocytes contain other α-glucosidases in the neutral pH range, interfering with the assay; they can be suppressed by acarbose (see section 4.6.15).

4.6.15 α-Glucosidase in Leukocytes (Acid Maltase, EC 3.2.1.20)

4.6.15.1 Enzyme Deficiency

α-Glucosidase is the enzyme deficient in glycogenosis type II (GSD II, M. Pompe, MIM 232 300).

4.6.15.2 Principle

$$\text{Glycogen}_{(n)} \xrightarrow[\text{Acarbose}]{\textbf{α-Glucosidase}} \text{glycogen}_{(n-1)} + \alpha\text{-D-glucose}\ .$$

Colorimetric determination of the produced α-D-glucose. Acarbose is added to inhibit unspecific α-glucosidases present in leukocytes [33].

4.6.15.3 Solutions

1. 0.1 M Sodium acetate buffer, pH 3.8: dilute 1 M sodium acetate stock solution (81.04 g/l) with H_2O and adjust to pH 3.8 with acetic acid. Add H_2O to make up to ten times the original volume.
2. Acarbose stock solution 1mM: acarbose (Glucobay, Bayer, MW 645.6). Dissolve one tablet (containing 50 mg acarbose) in 10 ml H_2O (7.74 mM). Transfer 130 µl of 7.74 mM acarbose into an Eppendorf tube and add 870 µl H_2O (1 mM). Store at –20°C.
3. Glycogen substrate (without acarbose): dissolve 250 mg glycogen in 5 ml sodium acetate buffer (5% glycogen solution). Store at –20°C.
4. Glycogen substrate with 6 µM acarbose: dissolve 250 mg glycogen in 5 ml sodium acetate buffer (5% glycogen solution). Add 30 µl of 1 mM acarbose stock solution. Store at –20°C.
5. 1 M Tris-HCl buffer, pH 7.0: Dissolve 121.1 g Trizma base (MW 121.1) in approximately 800 ml H_2O. Adjust the pH to 7.0 (at room temperature) with HCl. Make up to 1000 ml with H_2O.
6. Glucose reagent: dissolve 13.0 mg glucose oxidase and 2.0 mg peroxidase in 100 ml Tris-HCl buffer. Add 0.5 ml o-dianisidine (1% w/v in ethanol, prepare fresh). Stable for 1 week at 4°C in the dark.
7. Hydrochloric acid, 6 M: add 48 ml 12.5 M HCl to 100 ml H_2O.
8. Glucose standard solution, 1 mM: 180 mg D-glucose (MW 180.16) in 1 ml H_2O.

4.6.15.4 Sample

Leukocytes: homogenate in 0.2% Triton X-100. Dilute with 0.2% Triton X-100 to 0.5–1 mg protein/ml.

4.6.15.5 Assay

Add 50 µl substrate (glycogen either with or without acarbose) to 50 µl sample and incubate for 120 min and 0 min (blank) at 37°C. To stop the reaction: add 100 µl H_2O, boil for 2 min and then put on ice. Centrifuge for 10 min at 3000 × g; use 100 µl supernatant for glucose determination.

4.6.15.6 Glucose Determination

Sample: 100 µl supernatant + 1 ml glucose reagent
Glucose standards:

1. 0 µmol: 100 µl 1 M Tris-HCl buffer (pH 7.0) + 1 ml glucose reagent.
2. 0.01 µmol: 90 µl 1 M Tris-HCl buffer (pH 7.0) + 10 µl glucose standard solution (1 mM) + 1 ml glucose reagent.
3. 0.03 µmol: 70 µl 1 M Tris-HCl buffer (pH 7.0) + 30 µl glucose standard solution (1 mM) + 1 ml glucose reagent.
4. 0.05 µmol: 50 µl 1 M Tris-HCl buffer (pH 7.0) + 50 µl glucose standard solution (1 mM) + 1 ml glucose reagent.

Incubate the mixtures at 37°C for 60 min. Stop the reaction by adding 10 µl 6 M HCl.

4.6.15.7 Measurement

Photometer at 420 nm.

4.6.15.8 Calculation

mU/mg protein = nmol/min/mg =

$$\Delta OD(120'-0') \times \frac{\mu mol\ (std)}{OD\ (std)} \times \underset{(1)}{1000} \times \underset{(2)}{20} \times \underset{(3)}{\frac{1}{t\ (min)}} \times \underset{(4)}{\frac{200}{100}} \times \underset{(5)}{\frac{1}{mg/ml}},$$

where "std" is standard, term (1) is the conversion (U→mU), term (2) is the dilution factor (50 µl→1 ml), term (3) is the incubation time, term (4) is the dilution after centrifugation, and term (5) is the protein concentration. Thus:

$$mU/mg = \Delta OD \times \frac{\mu mol\ (std)}{OD\ (std)} \times \frac{1}{t\ (min)} \times \frac{1}{mg/ml} \times 40{,}000\ .$$

4.6.15.9 Enzyme Activities

For controls, the mean α-glucosidase level is 0.81 mU/mg protein (range 0.60–1.50; $n = 14$). For patients with GSD II, these figures are 0.05 mU/mg protein (range 0.00–0.10; $n = 4$). Note that obligate heterozygotes are not detectable reliably.

4.6.16 Amylo-1,6-Glucosidase (Debranching Enzyme, EC 3.2.1.33), Assay with [^{14}C]-Glucose

4.6.16.1 Enzyme Deficiency

Amylo-1,6-glucosidase is the enzyme deficient in glycogenosis type III (GSD III, MIM 232 400). Hydrolysis of glycogen by phosphorylase stops four glucose units before a 1,6-branching site in the glycogen 1,4-chain, yielding "phosphorylase limit dextrin". Amylo-1,6-glucosidase (debranching enzyme) has a dual enzyme function in the debranching action of glycogen: (1) glucan transferase: 3 glucose units from the 1,6-branch of the limit dextrin are transferred to the 1,4-branch, and (2) amylo-1,6-glucosidase: the 1,6- bond of the remaining glucose unit is hydrolyzed, yielding glucose and a 1,4-chain of glycogen, which can be further degraded by phosphorylase, yielding glucose-1-phosphate.

4.6.16.2 Principle

Incorporation of [^{14}C]-glucose into glycogen by the reverse reaction of the hydrolase amylo-1,6-glucosidase. Measurement of the incorporated radioactivity in the precipitated glycogen [20, 39]. This assay can only test the enzymes function of the hydrolysis of the 1-6 bond (see section 4.6.16.1).

4.6.16.3 Solutions

1. Histidine-HCl, pH 6.5: 50 mM L-Histidine-HCl (MW 209.63; 52 mg/5 ml H_2O). Adjust to pH 6.5 with 1 M NaOH. After storage check the pH before use.
2. Substrate for liver and muscle tissue: [^{14}C]-glucose, 3 µCi in 30 µmol glucose/ml: the specific activity for each batch of [^{14}C]-glucose differs (e.g., 0.05 mCi/0.026 mg in 5 ml ethanol/H_2O 9:1 = 348.2 mCi/mmol). The desired activity is 3 µCi in 30 µmol glucose/ml = 50 µCi in 500 µmol/16.7 ml. Dry 0.5 ml of [^{14}C]-glucose solution with nitrogen, add 16.7 ml of nonlabeled glucose solution (see below), mix well, and store in aliquots of 2.5 ml at –20°C.
   a. Nonlabeled glucose solution:

30 mM glucose (MW 180.16). 30 mM = 30 µmol/ml	= 5.406 mg/ml
	= 90.280 mg/16.7 ml
[^{14}C]-glucose (s. above) contains	= 0.026 mg
Difference, for non labeled glucose	= 90.254 mg/16.7 ml
Prepare: glucose solution (e.g.)	100 mg/18.5 ml H_2O

3. Substrate for RBC: [^{14}C]-glucose, 15 µCi in 30 µmol glucose/ml: the specific activity for each batch of [^{14}C]-glucose differs (e.g., 0.25 mCi/0.059 mg in 2.5 ml ethanol/H_2O 9:1 = 304.7 mCi/mmol). The desired activity is 15 µCi in 30 µmol glucose/ml = 250 µCi in 500 µmol/16.7 ml. Dry 2.5 ml of [^{14}C]-glucose solution with nitrogen, add 16.7ml of nonlabeled glucose solution (see below), mix well, and store in aliquots of 2.5 ml at –20°C.

a. Non labeled glucose solution:
   30 mM Glucose (MW 180.16). 30 mM = 30 µmol/ml = 5.406 mg/ml
   = 90.280 mg/16.7 ml
   [^{14}C]-glucose (s. above) contains = 0.059 mg
   Difference, for non labeled glucose = 90.221 mg/16.7 ml
   Prepare: glucose solution (e.g.) 100 mg/18.5 ml H_2O

4. Trichloroacetic acid stop solution: 1.5 M trichloroacetic acid (MW 163.4; 24.5 g/100 ml H_2O).
5. Ethanol 95%.
6. KOH 20%.

4.6.16.4 Samples

1. Liver, muscle: 10% (w/v) homogenate in H_2O.
2. RBC: For determination of Hb dilute three times. The enzyme is stable in heparinized blood at room temperature or 4°C for 24–72 h without inactivation, and in isolated RBC at –20°C for 6 weeks without inactivation.

4.6.16.5 Assay

1. Incubate 40 mg glycogen (oyster), 0.2 ml histidine/HCl, 0.1 ml sample or H_2O (blank), and 0.1 ml substrate (giving a total aliquot volume of 0.4 ml) at 37°C for 60 min (liver, muscle) or 3 h (RBC). Then add 0.5 ml stop solution and place on ice. Then:
   a. Add 2.0 ml H_2O and 5.0 ml 95% ethanol. Mix, centrifuge for 10 min at 1000 × *g*. Discard the supernatant.
   b. Dissolve the remaining pellet in 2.0 ml H_2O, then add 5.0 ml 95% ethanol, repeat the procedure described in a) above.
   c. Dissolve the remaining pellet in 2.0 ml 20% KOH and boil for 30 min. Put on ice and add 5.0 ml 95% ethanol.
   d. Wash three times as described in a) above. If the precipitation of glycogen is too fine, add five drops of 1 M HCl to the H_2O/ethanol mixture.
   e. Dissolve the last pellet in 0.5 ml H_2O (results in an end volume of approximately 0.7 ml). Determine "vol (end)" in milliliters. Use 0.5 ml for counting of radioactivity.
2. The assay solutions required for counting for liver and muscle and for RBC are shown in Table 4.6.11.

4.6.16.6 Measurement

In a liquid scintillation counter.

■ ***Table 4.6.11*** *Mixtures for liquid scintillation counting of amylo-1,6-glucosidase (debranching enzyme; assay with [^{14}C]-glucose) for liver and muscle, and for RBC*

	H_2O (ml)	From assay (ml)	^{14}C-glucose (ml)	Scintillation liquid (ml)
Liver/muscle				
Background	0.5	–	–	10.0
Standard	0.47	–	0.03 (= 0.09 µCi)	10.0
Blank	–	0.5	–	10.0
Sample	–	0.5	–	10.0
RBC				
Background	0.5	–	–	10.0
Standard	0.49	–	0.01 (= 0.15 µCi)	10.0
Blank	–	0.5	–	10.0
Sample	–	0.5	–	10.0

4.6.16.7 Calculation

1. Standard: 10 µl substrate containing 0.09 µCi ^{14}C.
2. Expected dpm = 0.09 µCi × 2.22 × 10^6 dpm/µCi = 199,800 dpm.
3. Efficiency factor f = dpm (expected)/Δdpm (standard).
4. Δdpm (standard) = dpm (standard) – dpm (background).
5. Δdpm (sample) = dpm (sample) – dpm (blank).

For liver and muscle:

'U'/g tissue = ‰ substrate incorporated/h/g tissue =

$$\underset{(1)}{\frac{\Delta\text{dpm (sample)}}{\Delta\text{dpm (standard)}}} \times 1000 \times \underset{(2)}{\frac{30}{100}} \times \underset{(3)}{\frac{1}{t\,(\text{h})}} \times \underset{(4)}{10} \times \underset{(5)}{10} \times \underset{(6)}{\frac{\text{vol (end)}}{0.5\text{ ml}}} \times \underset{(7)}{f}\,,$$

where term (1) is ‰, term (2) is the dilution factor of the standard (30 µl → 100 µl), term (3) is the incubation time, term (4) is the dilution factor 100 µl → 1 ml, term (5) is the dilution of the homogenate, term (6) is the dilution of the sample before counting, and term (7) is the efficiency factor. Thus:

$$\text{'U'/g} = \frac{\Delta\text{dpm (sample)}}{\Delta\text{dpm (standard)}} \times \frac{1}{t\,(\text{h})} \times 60{,}000 \times \text{vol (end; ml)} \times f\,.$$

For RBC:

'U'/g tissue = ‰ substrate incorporated/h/g Hb =

$$\frac{\Delta\text{dpm (sample)}}{\Delta\text{dpm (standard)}} \times 1000 \times \frac{10}{100} \times \frac{1}{t\,(\text{h})} \times 10 \times \frac{\text{vol (end)}}{0.5\text{ ml}} \times \frac{1}{\text{g/ml}} \times f\,,$$

(1) (2) (3) (4) (5) (6) (7)

where term (1) is ‰, term (2) is the dilution factor of the standard (10 µl → 100 µl), term (3) is the incubation time, term (4) is the dilution factor 100 µl → 1 ml, term (5) is the dilution of the sample before counting, term (6) is the concentration of Hb, and term (7) is the efficiency factor. Thus:

$$\text{'U'/g} = \frac{\Delta\text{dpm (sample)}}{\Delta\text{dpm (standard)}} \times \frac{1}{t\,(\text{h})} \times 2000 \times \text{vol (end)} \times f\,.$$

4.6.16.8 Enzyme Activities

■ ***Table 4.6.12*** *Amylo-1,6-glucosidase activities in liver and RBC*

		Mean	Range	*n*
Liver ('U'/g liver)				
	Controls	214	157–280	16
	Homozygotes GSD III	11.2	0.0–49.4	18
RBC ('U'/g Hb)				
	Controls	2.3	0.9–4.2	33
	Heterozygotes	1.3	0.4–2.4	15
	Homozygotes GSD III	0.2	0.0–0.6	22

4.6.16.9 Note

In GSD IX (phosphorylase b-kinase deficiency), amylo-1,6-glucosidase activity in RBC is usually elevated.

4.6.17 Amylo-1,6-Glucosidase (Debranching Enzyme, EC 3.2.1.33), Assay with Limit Dextrin

4.6.17.1 Enzyme Deficiency

Amylo-1,6-glucosidase is the enzyme deficient in glycogenosis type III (GSD III, MIM 232 400).

4.6.17.2 Note

Hydrolysis of glycogen by phosphorylase stops four glucose units before a 1,6-branching site in the glycogen 1,4-chain, yielding "phosphorylase limit dextrin". Amylo-1,6-glucosidase (debranching enzyme) has a dual enzyme function in the debranching action of glycogen: (1) glucan transferase; 3 glucose units from the 1,6-branch of the limit dextrin are transferred to the 1,4-branch, and (2) amylo-1,6-glucosidase; the 1,6- bond of the remaining glucose unit is hydrolyzed, yielding glucose and a 1,4-chain of glycogen, which can be further degraded by phosphorylase, yielding glucose-1-phosphate.

4.6.17.3 Principle

The produced glucose from "phosphorylase limit dextrin" is determined as a measure of the debranching enzyme activity. This assay method is used for the detection of GSD IIId, a subtype in which only the translocase activity of the enzyme (see section 4.6.17.2) is affected [9, 12, 20].

4.6.17.4 Solutions

1. Citrate-phosphate/BME buffer 0.01 M, pH 6.0: mix 10 mM citric acid monohydrate (MW 210.14; 2.1 g/l) and 20 mM $Na_2PO_4 \cdot 2H_2O$ (3.6 g/l H_2O) at a ratio of approximately 37:63 so that pH 6.0 is reached. Add 5 mM BME (MW 78.13; 3.9 mg/10 ml buffer).
2. Citrate-phosphate /BME buffer 0.1 M, pH 6.0: mix 100 mM citric acid monohydrate (MW 210.14; 21.0 g/1 H_2O) and 200 mM $Na_2PO_4 \cdot 2H_2O$ (35.6 g/l H_2O) at a ratio of approximately 37:63 so that pH 6.0 is reached. Add 50 mM BME (39.1 mg/10 ml buffer).
3. Phosphorylase limit dextrin substrate (PLD): 5% (w/v) in H_2O (see 5. below).
4. Glycogen substrate: glycogen (oyster) 5% (w/v) in H_2O.
5. Production of phosphorylase limit dextrin (PLD).
   a. Solutions:
      I. Phosphate buffer, pH 7.4: mix 0.1 M KH_2PO_4 (MW 136.0; 13.6g/l H_2O) and 0.1 M $Na_2PO_4 \cdot 12\ H_2O$ (MW 358.14; 35.8 g/l H_2O) at a ratio of approximately 20:80 until pH 7.0 is reached.
      II. Dialysis buffer: dissolve 1.94 g (final conc. 4 mM) cystein (MW 121.16), approximately 1.69 g (final conc. 1 mM) adenosine 5'-monophosphate (AMP; FW approximately 423), 2.4 g (final conc. 106 U/l) penicillin G (1662 U/mg),

and 4.0 g (final conc. 0.1%) streptomycin sulfate in 4 l of phosphate buffer (see I above).

b. Procedure: dissolve 500 mg glycogen (oyster) and 10 mg phosphorylase b in 10 ml phosphate buffer (see I above). Dialyze for 48 h four times in 1 l of dialysis buffer (see II above) at room temperature, then dialyze for 16–24 h twice in 1 l phosphate buffer at room temperature. Add to the dialysate (approximately 10 ml) 2 ml of 33% KOH, boil for 20 min, put on ice, centrifuge at $1000 \times g$ for 10 min and collect the supernatant. Add 15.6 ml of 96% ethanol; put on ice for 10 min, centrifuge for 5 min at $1000 \times g$, discard the supernatant. Wash the pellet twice by dissolving in 10 ml H_2O, adding 13 ml of 96% ethanol, and centrifuging for 5 min at $1000 \times g$. Wash the final sediment (limit dextrin) in ethanol and acetone. Dry and store at –20°C. The yield of limit dextrin is about 50% of glycogen).

4.6.17.5 Samples

1. RBC: erythrocytes, undiluted; determine Hb concentration.
2. Tissues: 1% (w/v) homogenate in 0.01 M citrate-phosphate/BME buffer (pH 6.0).

4.6.17.6 Assay

Incubate 100 µl PLD substrate or glycogen substrate, 100 µl 0.1 M citrate-phosphate/BME buffer (pH 6.0), 700 µl H_2O, and 100 µl sample at 37 °C for 6 h. To stop the reaction boil for 1 min, put on ice, and then centrifuge for 10 min at $1000 \times g$. Use 0.5 ml of the resultant supernatant for the glucose assay (with hexokinase – see Chap. 4.6.10).

4.6.17.7 Calculation

1. For RBC:

$$\text{mU/g Hb} = \text{nmol glucose produced per min per g Hb} =$$

$$\underset{}{\text{nmol glucose}} \times \underset{(1)}{\frac{1}{t\,(\text{min})}} \times \underset{(2)}{10} \times \underset{(3)}{\frac{1000}{200}} \times \underset{(4)}{\frac{1000}{\text{Hb (g/l)}}} ,$$

where term (1) is the incubation time, term (2) is the dilution factor of the RBC (100 µl →1 ml), term (3) is the dilution factor in the glucose assay, and term (4) is the conversion for milliliters RBC→grams Hb. Thus:

$$\text{mU/g Hb} = \text{nmol (glucose)} \times \frac{1}{t\,(\text{min})} \times \frac{1}{\text{Hb (g/l)}} \times 50{,}000 .$$

2. For tissues (1% homogenates):

$$\text{mU/g tissue} = \text{nmol (glucose)} \times \frac{1}{t\,(\text{min})} \times 5{,}000 .$$

4.6.17.8 Enzyme Activities

Table 4.6.13 gives the PLD/glycogen values in the RBC of controls, heterozygotes and GSD III patients. With glycogen as substrate, glucose is produced by phosphorylase activity (via glucose-1-phosphate→glucose-6-phosphate→glucose), even if amylo-1,6-glucosidase is not active.

■ ***Table 4.6.13*** *Enzyme activities (amylo-1,6-glucosidase – as assessed by levels of phosphorylase limit dextrin,* PLD*, and glycogen) in RBC*

RBC	PLD substrate (mU/g Hb)	Glycogen substrate (mU/g Hb)	PLD/ Glycogen
Controls	46.6; 6.6	11.0; 13.3	0.42; 0.50
Heterozygotes	7.5; 2.4	15.1; 6.7	0.50; 0.39
GSD III patients[a]	0.0–4.1	12.1–24.4	0.0–0.25

[a] Values are for four regular GSD III patients, non-GSD III d types

4.6.18 1,4-α-Glucan Branching Enzyme (Amylo-(1,4→1,6)-Transglucosylase; EC 2.4.1.18)

4.6.18.1 Enzyme Deficiency

Branching enzyme is deficient in glycogenosis type IV (GSD IV, MIM 232 500).

4.6.18.2 Principle

Branching enzyme is responsible for the α-1,6-branching of the α-1,4-chain in the synthesis of glycogen. Branching enzyme enhances the rate of polysaccharide (endogenous glycogen) synthesis from glucose-1-phosphate by phosphorylase.

$$(\text{Glycogen})_n + \text{x glucose-1-phosphate} \xleftrightarrow[\textbf{Branching enzyme}]{\textit{Phosphorylase}} (\text{glycogen})_{n+x} + \text{x}\,P_i\,.$$

The inorganic phosphorus (P_i) produced in the reaction serves as an indirect measure of the branching enzyme activity [7].

4.6.18.3 Solutions

1. Glycylglycine-BME buffer 50 mM, pH 6.2: dissolve 661 mg glycylglycine (MW 132.12) and 70 µl BME in H_2O. Adjust the pH to 6.2 with NaOH and fill up to 100 ml with H_2O.
2. G-1-P-substrate: 0.4 M α-D-glucose-1-phosphate-K_2 (FW 380; 76 mg/0.5 ml H_2O). Adjust to pH 6.2 with HCl.

3. AMP 10 mM: AMP (FW 423; 4.2 mg/ml H_2O).
4. Phosphorylase a, 30 U/ml: 30 U/ml phosphorylase a (3 mg*/ml glycylglycine-BME buffer; *depending on product).
5. Stop solution: 36 mM H_2SO_4 conc. (18 M; 200 µl/100 ml H_2O).
6. Ammonium molybdate/$FeSO_4$, 8 mM/144 mM: Mix 25 g ammonium molybdate · $4H_2O$ (MW 1235.86) and 6.93 ml H_2SO_4 (18 M). Make up to 250 ml with H_2O. Store at room temperature in a dark bottle. Before use add 400 mg $FeSO_4$ heptahydrate (MW 278.02) to 10 ml of this solution.
7. P_i standard solution 80 µg P_i/ml: put together 351.5 mg (final conc. 2.58 mM) KH_2PO_4 (MW 136.01), [2.58 mM P_i (MW 30.98) = 80 mg P_i/l], and 10 ml concentrated H_2SO_4 (18 M). Make up to 1000 ml with H_2O.

4.6.18.4 Samples

Liver: 1% (w/v) homogenate in glycylglycine-BME buffer.

4.6.18.5 Assay

1. Assay sample: 100 µl glucose 1-phosphate, 50 µl AMP, 100 µl phosphorylase a (see above, 4), and 150 µl H_2O. Warm to 30°C, then start the reaction by adding 100 µl of sample (or glycylglycine-BME buffer = blank).
2. Incubation: at 30°C, remove at 15-min intervals 50-µl aliquots for P_i determination. Stop the reaction with 1 ml stop solution (H_2SO_4) + 1.0 ml ammonium molybdate/$FeSO_4$. Centrifuge at 1000 × *g* for 5 min and use the supernatant for OD measurement.
3. Measurement: photometer at 700 nm

4.6.18.6 Calculation

Calculate $\Delta OD/\Delta t$ from the linear region of the OD measurements.

U/g liver = µmol/min/g =

$$\Delta OD\ \text{sample} \times \underset{(1)}{\frac{\mu g\ (std)}{OD\ (std)}} \times \underset{(2)}{\frac{1}{31}} \times \frac{1}{\Delta t} \times \underset{(3)}{\frac{500}{100}} \times \underset{(4)}{\frac{500}{50}} \times \underset{(5)}{100},$$

where "std" is standard, term (1) is the conversion of P_i from µg→µmol, term (2) is the time interval for ΔOD, term (3) is the dilution factor in the assay before incubation, term (4) is the dilution in the assay after incubation, and term (5) is the dilution of the homogenate. Thus:

$$U/g = \Delta OD\ (\text{sample}) \times \frac{\mu g\ (\text{standard})}{OD\ (\text{standard})} \times \frac{1}{\Delta t} \times 161.3.$$

4.6.18.7 Enzyme Activities

Table 4.6.14 shows the enzyme activities in liver, muscle, and fibroblasts.

■ ***Table 4.6.14*** *Enzyme activities (1,4-α-glucan branching enzyme) in liver, muscle, and fibroblasts*

Sample assayed	Patient group	Activity (mean ± SD)	*n*
Liver (μmol/min/g tissue) [17]	Controls	170 ± 62	31
	GSD IV homozygotes	0.0; 1.1 [a]	2
Muscle (μmol/min/g tissue) [17]	Controls	7.2 ± 41	10
	GSD IV homozygotes	0.9; 1.4 [a]	2
Fibroblasts (μmol/min/mg protein) [8]	Controls	1.52 ± 0.47	82
	GSD IV heterozygotes	0.62 ± 0.18	20
	GSD IV homozygotes	0.07 ± 0.03	25

[a] The two individual values are given for both subjects

4.6.19 Phosphorylase (EC 2.4.1.1)

4.6.19.1 Enzyme Deficiency

Different phosphorylases are deficient in muscle in glycogenosis type V (GSD V, M. McArdle, MIM 232 600), and in liver in glycogenosis type VI (GSD VI, MIM 232 700), respectively.

4.6.19.2 Principle

$$(\text{Glycogen})_n + \text{glucose-1-phosphate} \xleftarrow[\text{AMP}]{\textbf{Phosphorylase}} (\text{glycogen})_{n+1} + P_i\,.$$

Photometric determination of P_i as a measure for substrate turnover. In vivo, the reaction is from right to left, in the assay, the reaction is from left to right (i.e., backwards) [19, 38].

4.6.19.3 Solutions

1. Substrate-mix: dissolve 192 mg glucose-1-phosphate (final conc. 0.1 M), 100 mg glycogen (final conc. 2%), 42 mg sodium fluoride (final conc. 0.2 M), and 6.3 mg AMP (FW 423; final conc. 3 mM) in 5 ml H_2O. Adjust pH to 6.1 (4–5 drops of 1 M HCl). This mix is stable at –20°C for 3 months.

2. H_2SO_4 stop solution, 36 mM: 200 µl H_2SO_4 conc. (36 N = 18 M) in 100 ml H_2O.
3. Ammonium molybdate/$FeSO_4$ 8 mM/144 mM: add together 2.5 g ammonium molybdate · H_2O (MW 1235.86) and 6.9 ml (final conc. 0.5 M) H_2SO_4 concentrated (18 M). Fill up to 250 ml with H_2O and store in a dark bottle at room temperature. Directly before use add 40 mg $FeSO_4 \times 7H_2O$ (MW 278.02) to 1 ml of this solution.
4. P_i standard solution 80 µg P_i/ml: put together 351.5 mg (final conc. 2.58 mM) KH_2PO_4 (MW 136.01), [2.58 mM P_i (MW 30.98) = 80 mg P_i/l], and 10 ml concentrated H_2SO_4 (18 M). Make up to 1000 ml with H_2O.

4.6.19.4 Samples

Liver, muscle: homogenate 1% w/v in H_2O. The enzyme is stable in liver at –20°C for 6–8 weeks, possibly longer.

4.6.19.5 Assay

1. Assay mix: add together 50 µl substrate mix and 50 µl sample (homogenate; giving a total of 100 µl).
2. Blank and standards:
   a) 0 µg P_i: 100 µl H_2O
   b) 4 µg P_i: 50 µl H_2O + 50 µl P_i standard (2.58 mM) = 100 µl
   c) 8 µg P_i: 100 µl P_i standard (2.58 mM) = 100 µl.
3. Incubation: 37°C for 0 and 20 min. Stop with 1.0 ml 36 mM H_2SO_4 + 1.0 ml ammonium molybdate/$FeSO_4$ (8 mM/144 mM). Centrifuge for 5 min at 1000 × *g*. Use the supernatant for OD measurement.
4. Measurement: photometer, OD at 700 nm.

4.6.19.6 Calculation

ΔOD (sample) = OD at 20 min – OD at 0 min

U/g liver or muscle = µmol/min/g =

$$\Delta\text{OD (sample)} \times \underset{(1)}{\frac{\mu\text{g (std)}}{\text{OD (std)}}} \times \underset{(2)}{\frac{1}{31}} \times \underset{(3)}{\frac{1}{t\,(\text{min})}} \times \underset{(4)}{\frac{1000}{50}} \times 100\,,$$

where "std" is standard, term (1) is the conversion of P_i from µg→µmol, term (2) is the incubation time (20 min), term (3) is the dilution factor in the assay, and term (4) is the dilution of the homogenate. Thus:

$$\text{U/g} = \Delta\text{OD (sample)} \times \frac{\mu\text{g (standard)}}{\text{OD (standard)}} \times 3.225.$$

4.6.19.7 Enzyme Activities

■ ***Table 4.6.15*** *Liver and muscle phosphorylase enzyme activities*

		Mean	Range	*n*
Liver (U/g)	Controls	22.3	11.3–31.3	16
	GSD VI patients	2.6	0.4–5.3	6
Muscle (U/g)	Controls	89.3	69.0–121.5	4
	GSD V patient	1.4[a]	–	1

[a] The individual value is given; not a mean

4.6.20 6-Phosphofructokinase (EC 2.7.1.11)

4.6.20.1 Enzyme Deficiency

6-Phosphofructokinase is the enzyme deficient in glycolysis leading to glycogenosis type VII (GSD VII, M. Tarui, MIM 232 800). The enzyme in its active form is a tetramer, composed of three different subunits: M (muscle), L (liver), and P or F (platelets, fibroblasts). The enzyme is found in different compositions in different tissues, as shown in Table 4.6.16. In glycogenosis type VII the enzyme deficiency can only be determined in muscle, because only the deficiency of the M form leads to GSD VII.

■ ***Table 4.6.16*** *Composition of 6-Phosphofructokinase in different tissues*

Tissue	Subunits
Muscle	M_4
Liver	L_4
Leukocytes	P_4, P_3L, P_2L_2, PL_3, and L_4 (the last form predominates)
Kidney	Mostly L_4
Thrombocytes	P_4, P_3L, P_2L_2
Erythrocytes	M_4, M_3L, M_2L_2, ML_3 (M and L normally in equal amounts)
Fibroblasts	P_4 (F_4) and some L (?)

4.6.20.2 Principle

1. $F6P + ATP \xleftrightarrow[Mg^{2+}]{\textbf{6-Phosphofructokinase}} FDP + ADP.$
2. $FDP \xleftrightarrow{Adolase} DHA\text{-}P + glyceraldehyde\text{-}3\text{-}phosphate.$
3. $glyceraldehyde\text{-}3\text{-}phosphate \xleftrightarrow{TIM} DHA\text{-}P.$
4. $2\ DHA\text{-}P + 2\ NADH + H^+ \xleftrightarrow{GDH} 2\ glycerol\text{-}3\text{-}phosphate + 2\ NAD^+.$

Σ: $F6P + ATP + 2\ NADH + H^+ \leftrightarrow 2\ glycerol\text{-}3\text{-}phosphate + ADP + 2\ NAD^+$
where F6P is fructose-6-phosphate, FDP is fructose-1,6-diphosphate, DHA-P is dihydroxyacetone phosphate, TIM is triosephosphate isomerase, and GDH is glycerol-3-phosphate dehydrogenase. The oxidation of NADH is a measure of the 6-PFK activity and is determined photometrically (decrease of OD per minute) [4].

4.6.20.3 Solutions

1. Tris-HCl 1 M, pH 8.0: 6.05 g Tris (MW 121.1) in 50 ml H_2O. Adjust to pH 8.0 with HCl.
2. Homogenization buffer, pH 8.2: add 18.6 mg (final conc. 1 mM) EDTA (MW 372.24), 61.6 mg (final conc. 5 mM) $MgSO_4$ (MW 246.48) to 40 ml of 50 mM Tris-HCl (dilute 1:20 from solution described above). Adjust pH to 8.2 with HCl. Fill up to 50 ml with 50 mM Tris.
3. $MgCl_2$ (MW 203.3): 100 mM (1.02 g/50 ml H_2O).
4. ATP (FW ≅ 620): 20 mM (≅ 12.4 mg/ml H_2O).
5. NADH-Na_2 (MW 709.4): 4 mM (2.8 mg/ml H_2O).
6. KCl (MW 74.56): 2 M (1.5 g/10 ml H_2O).
7. KCN (MW 65.12): 20 mM (13 mg/10 ml H_2O).
8. AMP (FW ≅ 405): 40 mM (≅ 16.2 mg/ml H_2O).
9. Fructose-6-phosphate substrate: 60 mM fructose-6-phosphate (MW 304.1; 18.2 mg/ml H_2O).
10. Enzyme mix: mix together 550 µl (→ 50 U) aldolase (suspension, 90 U/ml), 5 µl (→ 50 U) TIM (suspension, 10,000 U/ml), 145 µl (→ 50 U) GDH (suspension, 340 U/ml), and 300 µl $(NH_4)SO_4$ (saturated solution), giving a total aliquot volume of 1000 µl. Store at 4°C. Before use dilute 1:15 with 0.1 M Tris-HCl pH 8.0.

4.6.20.4 Samples

Muscle: homogenate 1:400 in homogenization buffer. Because of the fast inactivation of the enzyme in the homogenate, assay the enzyme at four different concentrations immediately after homogenization and determine the protein concentration later on. The enzyme is stable in muscle at –20°C for about 7 days, and at –70°C for about 1–4 months [23].

■ ***Table 4.6.17*** *Assay mixture for assessment of 6-phosphofructokinase activity. Pipette these solutions into 1-ml quartz cuvettes. Instructions for the preparation of these solutions are given in section 4.6.20.3*

Solution	Volume	Concentration in assay
0.1 M Tris-HCl buffer, pH 8.0	50 µl	
$MgCl_2$	50 µl	5.0 mM
ATP	50 µl	1.0 mM
NADH	50 µl	0.2 mM
KCl	50 µl	0.1 M
KCN	50 µl	1.0 mM
AMP	50 µl	2.0 mM
Enzyme mix 1:15	100 µl	
Sample (homogenate)*	10 µl or 20 µl, 30 µl, 50 µl	
H_2O	490 µl or 480 µl, 470 µl, 450 µl	
Start: fructose-6-phosphate substrate	50 µl	3.0 mM
or H_2O (blank) **	(50 µl)	
Total	1000 µl	

* 4 different volumes in 4 different cuvettes, accordingly 4 different volumes of H_2O.
** Switch blank and sample cuvettes in the photometer because OD is decreasing.

4.6.20.5 Assay

The constituents of the assay solution in the cuvettes is given in Table 4.6.17.

4.6.20.6 Measurement

In a photometer at 340 nm, thermostatted at 25°C. Determine ΔOD/min when good linearity is reached (i.e., when the correlation coefficient is near 1).

4.6.20.7 Calculation

For the calculation use the measurement with a protein concentration of the sample of 10–25 µg/ml.
Molar extinction of NADH = 6.22×10^3
α_{mM} (µmol/ml) = 6.22

$$\text{U/g muscle} = \mu\text{mol/min/g} = \Delta\text{OD/min} \times \underset{(1)}{\frac{1}{6.22}} \times \underset{(2)}{\frac{1000}{\times\,\mu\text{l}}} \times \underset{(3)}{400} \times \underset{(4)}{\frac{1}{2}},$$

where term (1) is the millimolar extinction of NADH, term (2) is the dilution factor in the assay (× µl is the sample volume with the desired protein concentration), term (3) is the dilution factor before the assay, and term (4) represents 2 NADH per reaction. Thus:

U/g muscle = ΔOD/min × dilution in assay* × 32.15

* Dilution in assay: 10 µl → 100×
20 µl → 50×
30 µl → 33×
50 µl → 20× .

4.6.20.8 Enzyme Activities

Mean enzyme activity in controls is 17.4 U/g muscle (14.0–22.6 U/g muscle; $n = 8$). That in a GSD VII patient was 0.13 U/g muscle [40].

4.6.21 Phosphorylase b-Kinase (EC 2.7.1.38)

4.6.21.1 Enzyme Deficiency

Phosphorylase b-kinase is the enzyme deficient in glycogenosis type IX (GSD IX, formerly GSD VIII, MIM 306 000).

4.6.21.2 Principle

Phosphorylase b-kinase converts the enzyme phosphorylase from its low activity form (phosphorylase b) to the high activity form (phosphorylase a) by phosphorylation. The enzyme activity of phosphorylase b-kinase is correlated with the increase of phosphorylase activity in the probands sample and is measured by determining the amount of P_i produced by phosphorylase activity.

1. Activation of phosphorylase b (first incubation at 30°C):

$$2\ \text{Phosphorylase b} + 4\ \text{ATP} \xleftarrow[Mg^{2+}]{\textbf{Phosphorylase b-kinase}} \text{phosphorylase a} + 4\ \text{ADP}$$

2. Measurement of phosphorylase a activity (second incubation at 37°C):

$$\text{Glycogen}_{(n)} + \text{G-1-P} \xleftarrow{\textit{Phosphorylase a}} \text{Glycogen}_{(n+1)} + P_i$$

(Addition of caffeine to inhibit phosphorylase b activity.)

3. Photometric determination of P_i production. One "colorimetric unit" of phosphorylase a is the amount of enzyme that produces 1 µmol P_i/min under assay conditions [3, 22].

4.6.21.3 Solutions

1. Magnesium acetate 330 mM: 708 mg magnesium acetate (MW 214.48) in 10 ml H_2O.
2. ATP 36 mM: 22.3 mg ATP (FW 627) in 1 ml H_2O. Prepare fresh before use!
3. β-Glycerophosphate 330 mM: 1.0 g β-glycerophosphate (MW 306.11) in 10 ml H_2O + 400 mg Tris (MW 121.1) in 10 ml H_2O (final conc. 330 mM). Adjust to pH 6.8 with 0.1 N HCl.
4. Phosphorylase b: According to the specification on the product, 150 U/ml H_2O. Prepare only the amount needed, fresh before use.
5. Substrate mix for kinase reaction (30°C): 2 parts 330 mM magnesium acetate + 10 parts ATP + 10 parts 330 mM β-glycerophosphate. Mix amount used for assay before use.
6. Stop-solution for kinase reaction: mix 420 mg NaF (MW 41.99 → 100 mM) and 186 mg EDTA (MW 372.24 → 5 mM). Fill to 100 ml with H_2O. Adjust the pH to 6.8 with 0.1 N NaOH.
7. Substrate mix for phosphorylase a reaction (37°C): Refer to Table 4.6.18 for the constituents of this substrate mix. Adjust to pH 6.1 with 1 N HCl and fill to 10 ml with H_2O. Store at –20 C. Check pH before use and adjust with HCl if necessary.
8. Sulfuric acid stop-solution, 36 mM: 200 µl H_2SO_4 conc. (36 N = 18 M) in 100 ml H_2O.
9. Ammonium molybdate/$FeSO_4$ 8 mM/144 mM: add together 2.5 g ammonium molybdate · H_2O (MW 1235.86) and 6.9 ml (final conc. 0.5 M) H_2SO_4 concentrated (18 M). Fill up to 250 ml with H_2O and store in a dark bottle at room temperature. Directly before use add 40 mg $FeSO_4 \times 7H_2O$ (MW 278.02) to 1 ml of this solution.
10. P_i standard solution 80 µg P_i/ml: put together 351.5 mg (final conc. 2.58 mM) KH_2PO_4 (MW 136.01), [2.58 mM P_i (MW 30.98) = 80 mg P_i/l], and 10 ml concentrated H_2SO_4 (18 M). Make up to 1000 ml with H_2O.

Table 4.6.18 *Substrate mixture for the phosphorylase reaction. Instructions for the preparation of these solutions are given in section 4.6.21.3*

Solution	Volume	End concentration in mix
Glucose-1-phosphate (MW 380), 0.5 M, 380 mg/2 ml H_2O	2.0 ml	100 mM
Glycogen, 200 mg/1.66 ml H_2O	1.66 ml	2%
Caffeine (MW 194.2), 60 mM, 11.65 mg/ml H_2O	0.2 ml	1.2 mM
NaF (MW 41.99), 1.25 M. 210 mg/4 ml H_2O	4.0 ml	0.5 mM
Total	7.86 ml	

4.6.21.4 Samples

1. RBS: dilute 200 µl hemolysate of RBC with 400 µl H_2O, centrifuge for 10 min at 30,000 × *g*, pipette 300 µl supernatant from the top and use this for the assay and measurement of Hb concentration. Heparin blood is stable at 4°C or room temperature for 48 h; RBC are stable at –70°C for 1 week.
2. Liver and muscle: 1% homogenate in H_2O.

4.6.21.5 Assay

Activation of Phosphorylase (First Incubation)

1. Incubate 50 µl phosphorylase b, 50 µl substrate mix, and 50 µl sample (hemolysate or homogenate) at 30°C for 0, 5, 10, 15, 20, and 25 min. After each of these incubation times, transfer 10 µl to a new vial and stop the reaction (see below).
2. Blanks (if sample material is sufficient):
   a. Without phosphorylase b, with enzyme (sample): incubate 50 µl substrate mix, 50 µl H_2O, and 50 µl sample. Incubate as described above. Remove 10 µl after the above incubation times and stop the reaction (see below).
   b. With phosphorylase b, without enzyme (sample): incubate 50 µl phosphorylase b, 50 µl substrate mix, and 50 µl H_2O. Remove 10 µl after the above incubation times and stop the reaction (see below).
3. Aliquots from the first incubation or blanks (10 µl) + stop-solution NaF/EDTA (200 µl) = 210 µl.

Determination of Phosphorylase Activity (Second Incubation)

Take 50 µl of the 210-µl sample from the first incubation and add 50 µl of substrate mix (phosphorylase a + caffeine). Incubate at 37°C for 30 min. Stop the reaction with 1.0 ml 36 mM H_2SO_4 + 1.0 ml ammonium molybdate/$FeSO_4$ (total volume now 2.1 ml). Centrifuge for 5 min at 1000 × *g* and use the supernatant for OD measurement.

Standard:	0 µg P_i	100 µl H_2O
	4 µg P_i:	50 µl P_i standard + 50 µl H_2O
	8 µg P_i	100 µl P_i standard
add to each 36 mM H_2SO_4		1.0 ml
Ammoniummolybdate/$FeSO_4$		1.0 ml

Total volume: 2.1 ml, each.

4.6.21.6 Measurement

Photometer, OD at 700 nm.

4.6.21.7 Calculation

Determine values for 0 min and 20 min by linear regression calculation from values of the six time points from 0 min to 25 min →
ΔOD (20') = OD (20' calculated) – OD (0' calculated)

1. For RBC:

U/g Hb = µmol/min/g =

$$\Delta OD\,(20') \times \frac{\mu g\,(std)}{OD\,(std)} \times \underset{(1)}{\frac{1}{31}} \times \underset{(2)}{\frac{1000}{50}} \times \underset{(3)}{\frac{150}{10}} \times \underset{(4)}{\frac{210}{50}} \times \underset{(5)}{\frac{1}{t1 \times t2}} \times \underset{(6)}{\frac{1000}{Hb\,(g/l)}},$$

where "std" is standard, term (1) is the conversion factor for µg→µmol P_i, term (2) is the dilution factor 50 µl→1.0 ml, terms (3) and (4) are the dilution in the assay, and term (5) represents the incubation times (min; *t*1: time of first incubation; *t*2: time of second incubation), and term (6) is g/ml Hb → g/l. Thus:

$$U/g\ Hb = \Delta OD\,(sample) \times \frac{\mu g\,(std)}{OD\,(std)} \times \frac{1}{t1} \times \frac{1}{t2} \times \frac{1}{Hb\,(g/l)} \times 40{,}645\,.$$

2. For liver and muscle tissue:

U/g tissue = µmol/min/g =

$$\Delta OD\,(20') \times \frac{\mu g\,(std)}{OD\,(std)} \times \underset{(1)}{\frac{1}{31}} \times \underset{(2)}{\frac{1000}{50}} \times \underset{(3)}{\frac{150}{10}} \times \underset{(4)}{\frac{210}{50}} \times \underset{(5)}{\frac{1}{t1 \times t2}} \times \underset{(6)}{100},$$

where term (1) is the conversion factor for µg→µmol P_i, term (2) is the dilution factor 50 µl→1.0 ml, terms (3) and (4) are the dilution in the assay, and term (5) represents the incubation times (min; first and second incubation), and term (6) is the dilution of the tissue sample. Thus:

$$U/g\ tissue = \Delta OD\,(sample) \times \frac{\mu g\,(std)}{OD\,(std)} \times \frac{1}{t1 \times t2} \times 4064.5\,.$$

3. For fibroblasts:

mU/mg protein = nmol/min/mg =

$$\Delta OD\,(20') \times \frac{\mu g\,(std)}{OD\,(std)} \times \underset{(1)}{\frac{1}{31}} \times \underset{(2)}{\frac{1000}{50}} \times \underset{(3)}{\frac{150}{10}} \times \underset{(4)}{\frac{210}{50}} \times \underset{(5)}{\frac{1}{t1 \times t2}} \times \underset{(6)}{1000} \times \underset{(7)}{\frac{1}{mg/ml}}$$

where term (1) is the conversion factor for µg→µmol P_i, term (2) is the dilution factor 50 µl→1.0 ml, terms (3) and (4) are the dilution in the assay, and term (5) represents the incubation times (min), term (6) is the conversion U→mU, and term (7) is the protein concentration in the homogenate. Thus:

$$mU/mg/protein = \Delta OD\,(sample) \times \frac{\mu g\,(std)}{OD\,(std)} \times \frac{1}{t1} \times \frac{1}{t2} \times \frac{1}{mg/ml} \times 40645\,.$$

4.6.21.8 Enzyme Activities

■ ***Table 4.6.19*** *Enzyme activities for phosphorylase b-kinase assay*

Sample	Cohort	Mean	Range	*n*
RBC (U/g Hb)	Controls	13.5	10.8–17.2	6
	GSD IX patients	2.0	0.6–4.8	7
Liver (U/g tissue)	Controls	83.5	55.5–112.8	7
	GSD IX patients	11.0	0.0–32.3	14
Muscle (U/g tissue)	Controls [27]	–	30.0–100.0	?

4.6.22 Glycogen Synthase (EC 2.4.1.11)

4.6.22.1 Enzyme Deficiency

Glycogen synthase is the enzyme deficient in glycogen synthase deficiency, also called glycogenosis type 0 (GSD 0, MIM 240 600).

4.6.22.2 Principle

$$\text{Glycogen}_{(n)} + \text{UDPG}^{2-} \xleftarrow{\textbf{Glycogen synthase}} \text{Glycogen}_{(n+1)} + \text{UDP}^{3-} + \text{H}^{+}\,.$$

Radioactively labeled glucose from UDPG-^{14}C is incorporated into glycogen. The remaining UDPG-^{14}C is removed by washing the glycogen. Glycogen is precipitated by ethanol and incorporated ^{14}C-glucose is determined in a scintillation counter [16, 37].

4.6.22.3 Solutions

1. Tris-HCl/EDTA buffer, pH 7.8: Add 605.5 mg Tris (MW 121.1 → 50 mM), 186.1 mg EDTA (MW 372.24 → 5 mM) to 100 ml H_2O. Adjust the pH 7.8 with HCl.
2. Homogenate buffer: sucrose 171 mg/2 ml Tris-HCl/EDTA buffer (MW 342.30 → 250 mM). Prepare fresh!
3. Substrate mix with glucose-6-phosphate (G-6-P): dissolve 7 µl UDPG-^{14}C (approximately 0.1 µCi/µmol unlabeled UDPG; dried with nitrogen gas), 4.3 mg UDP-glucose (FW 643, varies → 6.7 mM), 10 mg glycogen (bovine liver), and 2.9 mg G-6-P (FW 288, varies → 10 mM) in 1 ml of Tris-HCl/EDTA buffer. Prepare fresh!
4. Substrate mix without G-6-P: as for substrate mix with G-6-P but without G-6-P.

4.6.22.4 Samples

Liver: 5% (w/v) homogenate in homogenate buffer.

4.6.22.5 Assay

1. Make up two assay samples, one containing substrate mix with G-6-P [100 µl substrate mix + 25 µl sample (homogenate) + 25 µl homogenate buffer = 150 µl] and one containing substrate mix without G-6-P [100 µl substrate mix + 50 µl sample (homogenate) = 150 µl].
2. Incubate for 15 min at 30°C. Stop the reaction with 3.0 ml 66% ethanol.
3. Blank: 100 µl substrate mix (± G-6-P), 50 µl homogenate buffer, or, when available, sample homogenate (not incubated), and 3.0 ml 66% ethanol.
4. Allow the samples and blanks to precipitate for about 15 min at room temperature and centrifuge for 5-10 min at 2000 × *g*. Decant the supernatant carefully and resuspend the pellet in 3 ml ethanol (66%), then centrifuge for 5-10 min at 2000 × *g*. Resuspend the pellet in 2.5 ml acetone then centrifuge for 10 min at 2000 × *g*. Decant the supernatant carefully and dry the pellet in a vacuum or under gaseous nitrogen. Dissolve the pellet in 0.5 ml H_2O and add it to 10 ml scintillation liquid in counter vials. Rinse the centrifugation tube twice with 0.5 ml H_2O each and add to the sample in the scintillation liquid.
5. Standard = 100% value. Put 100 µl substrate mix (± G-6-P) into 10 ml scintillation liquid, add 1.4 ml H_2O.

4.6.22.6 Measurement

In a liquid scintillation counter: ^{14}C.

4.6.22.7 Calculation

Δdpm (sample) = dpm (sample) – dpm (blank)
U/g liver = µmol (incorp)/min/g =

$$\Delta\text{dpm (sample)} \times \frac{\mu\text{mol (std)}}{\text{dpm (std)}} \times \underbrace{\frac{1}{t(\text{min})}}_{(1)} \times \underbrace{\frac{1000}{50}}_{(2)} \times \text{dilution of homogenate}^{*},$$

where "std" is standard, term (1) is the incubation time, and term (2) is the dilution factor 50 µl→1.0 ml.

$$\Delta\text{dpm (sample)} \times \frac{0.67}{\text{dpm (std)}} \times \frac{1}{15} \times 20 \times \text{dilution of homogenate}^{*}$$

$$\text{U/g liver} = \frac{\Delta\text{dpm (sample)}}{\text{dpm (standard)}} \times \text{dilution of homogenate}^{*} \times 0.893.$$

* Dilution with substrate with G-6-P = 40 × (5% homogenate, dilution in assay 2×). Dilution with substrate without G-6-P = 20 × (5% homogenate). Thus

The difference between blanks with substrate and with homogenate (not incubated) are minimal and can be neglected (e.g., in mouse liver, the substrate blank was 0.6% of the sample and the homogenate blank was 1.2% of the sample value).

The enzyme is stable for 3 months at –20°C; after 6–12 months, a slight decrease of activity has been noted.

4.6.22.8 Control and Pathological Values

■ ***Table 4.6.20*** *Control and pathological values (U/g) for glycogen synthase assay*

Cohort	Assay sample	Mean	Range	n
Controls	With glucose-6-phosphate	2.5	1.1–5.5	13
	Without glucose-6-phosphate	0.17	0.03–0.6	13
GSD 0 patients	With glucose-6-phosphate	0.11	0.0–0.43	10
	Without glucose-6-phosphate	0.02	0.0–0.04	9

References

1. Baker L, Winegrad AI (1970) Fasting hypoglycaemia and metabolic acidosis associated with deficiency of hepatic fructose-1,6-diphosphatase activity. Lancet ii:13–16
2. Bergren WR, Ng WG, Donnel GN (1973) Uridine diphosphate galactose-4-epimerase in human and other mammalian haemolysates. Biochim Biophys Acta 313:464–472
3. Besley GTN (1987) Phosphorylase b kinase deficiency in glycogenosis type VIII: differentiation of different phenotypes and heterozygotes by erythrocyte enzyme assay. J Inherit Metab Dis 10:115–118
4. Beutler E (1971) Red Cell Metabolism, 2nd edn. Grune Stratton, New York, London, p 42
5. Beutler E, Paniker NV, Trinidad F (1971) The assay of red cell galactokinase. Biochem Med 5:325–332
6. Beutler HO (1984) D-Fructose. In: Bergmeyer HU, Bergmeyer J, Grassl M (eds) Methods of Enzymatic Analysis, 3rd edn, Vol VI. Verlag Chemie, Weinheim, Deerfield Beach/Florida, Basel, pp 321–327
7. Brown BI, Brown DH (1966) α-1,4-Glucan 6-glycosyltransferase from mammalian muscle. Methods Enzymol 8:395–403
8. Brown BI, Brown DH (1989) Branching enzyme activity of cultured amniocytes and chorionic villi: prenatal testing for type IV glycogen storage disease. Am J Hum Genet 44:378–381
9. Brown DH, Brown BI (1966) Enzymes of glycogen debranching: amylo-1,6-glucosidase and oligo-1,4->1,4-glucantransferase. Methods Enzymol 8:515–524
10. Burchell A, Gibb L (1991) Diagnosis of type 1 B and 1 C glycogen storage disease. J Inherit Metab Dis 14:305–307
11. Chen YT (2001) Glycogen storage diseases. In: Scriver CR, Beaudet AL, Sly WS, Valle D (eds) The Metabolic and Molecular Bases of Inherited Disease, 8th edn. McGraw-Hill, New York, pp 1521–1551
12. Chen YT, He JK, Ding JH, Brown BI (1987) Glycogen debranching enzyme: purification, antibody characterization, and immunoblot analysis of type III glycogen storage disease. Am J Hum Genet 41:1002–1015

13. Gitzelmann R (1967) Hereditary galactokinase deficiency, a newly recognized cause of juvenile cataracts. Pediatr Res 1:14–23
14. Gitzelmann R (1969) Estimation of galactose-1-phosphate in erythrocytes: a rapid and simple enzymatic method. Clin Chim Acta 26:313–316
15. Gitzelmann R, Steinmann B, Mitchell B, Haigis E (1976) Uridine diphosphate galactose 4'-epimerase deficiency. IV. Report of eight cases in three families. Helv Paediatr Acta 31:441–452
16. Gitzelmann R, Spycher MA, Feil G, Müller J, Seilnacht B, Stahl M, Bosshard, NU (1996) Liver glycogen synthase deficiency: a rarely diagnosed entity. Eur J Pediatr 155:561–567
17. Green HL, Ghishan FK, Brown B (1988) Hypoglycemia in type IV glycogenosis: hepatic improvement in two patients with nutritional management. J Pediatr 112:55–58
18. Gürtler B, Bally C, Leuthardt F (1971) Purification and properties of human liver aldolase. Hoppe Seylers Z Physiol Chem 352:1455–1462
19. Hers HG (1964) Glycogen storage disease. In: Levine R, Luft R (eds) Advances in Metabolic Disorders, Vol. 1. Academic Press, New York, London, pp 1–44
20. Hers HG, Verhue W, Van Hoof F (1967) The determination of amylo-1,6-glucosidase. Eur J Biochem 2:257–264
21. Holton JB, Walter JH, Tyfield LA (2001) Galactosemia. In: Scriver CR, Beaudet AL, Sly WS, Valle D (eds) The Metabolic and Molecular Bases of Inherited Disease, 8th edn. McGraw-Hill, New York, pp 1553–1587
22. Huijing F (1974) Glycogen and enzymes of glycogen metabolism. In: Curtius HCH, Roth M (eds) Clinical Biochemistry, Vol. II. W de Gruyter, Berlin/New York, pp 1208–1235
23. King RF, Macfie J, Hill G (1981) Activities of hexokinase, phosphofructokinase, fructose bisphosphatase and 2-oxoglutarate dehydrogenase in muscle of normal subjects and very ill surgical patients. Clin Sci 60:451–456
24. Krisman CR (1962) A method for the colorimetric estimation of glycogen with iodine. Anal Biochem 4:17–23
25. Kunst A, Draeger B, Ziegenhorn J (1984) UV-methods with hexokinase and glucose6-phosphate dehydrogenase. In: Bergmeyer HU, Bergmeyer J, Grassl M (eds) Methods of Enzymatic Analysis, Vol. VI. Verlag Chemie, Weinheim, Germany, pp 163–172
26. Kurz G, Wallenfels K (1970) D-Galactose. UV-Test mit Galactose-Dehydrogenase. In: Bergmeyer HU (ed) Methods of Enzymatic Analysis, Vol. 2. Verlag Chemie, Weinheim, Germany, pp 1241–1249
27. Lederer B, Van Hoof F, Van den Berghe G, Hers HG (1975) Glycogen phosphorylase and its converter enzymes in haemolysates of normal human subjects and of patients with type VI glycogen storage disease. A study of phosphorylase kinase deficiency. Biochem J 147:23–35
28. Lentner C (ed) (1977) Geigy Wissenschaftliche Tabellen, 8th edn, Vol 1. Ciba-Geigy, Basel/Switzerland
29. Lentner C (ed) (1979) Geigy Wissenschaftliche Tabellen, 8th edn, Vol 2. Ciba-Geigy, Basel/Switzerland
30. Mayes JS, Guthrie R (1968) Detection of heterozygotes for galactokinase deficiency in a human population. Biochem Genet 2:219–230
31. Mitchell B, Haigis E, Steinmann B, Gitzelmann R (1975) Reversal of UDP-galactose 4-epimerase deficiency of human leukocytes in culture. Proc Natl Acad Sci U S A 72:5026–5030
32. Ng WG, Donnel GN, Hodgman JE, Bergren WR (1967) Differences in uridine diphosphate galactose-4-epimerase between haemolysates of newborns and of adults. Nature 214:283–284
33. Okumiya T, Keulemans JLM, Kroos MA, Van der Beek NME, Boer MA, Takeuchi H, Van Diggelen OP, Reuser AJJ (2006) A new diagnostic assay for glycogen storage disease type II in mixed leukocytes. Mol Genet Metab 88:22–28
34. Online Mendelian Inheritance in Man, OMIM (TM) McKusick-Nathans Institute for Genetic Medicine, Johns Hopkins University (Baltimore, MD) and National Center for Biotechnology Information, National Library of Medicine (Bethesda, MD) World Wide Web URL: http://www.ncbi.nlm.nih.gov/omim/

35. Seifter S, Dayton S, Novic B, Muntwyler E (1950) The estimation of glycogen with the anthrone reagent. Arch Biochem 25:191–200
36. Steinmann B, Gitzelmann R, Van den Berghe G (2001) Disorders of fructose metabolism. In: Scriver CR, Beaudet AL, Sly WS, Valle D (eds) The Metabolic and Molecular Bases of Inherited Disease, 8th edn. McGraw-Hill, New York, pp 1489–1520
37. Thomas JA, Schlender KK, Larner J (1968) A rapid filter paper assay for UDP-glucose-glycogen glucosyltransferase, including an improved biosynthesis of UDP-^{14}C-glucose. Anal Biochem 25:486–499
38. Uyttenhove K, Bollen M, Stalmans W (1991) An optimized assay of phosphorylase kinase in crude liver preparations. Biochem J 278:899–904
39. Van Hoof F (1967) Amylo-1,6-glucosidase activity and normal glycogen content of the erythrocytes of normal subjects, patients with glycogen storage disease and heterozygotes. Eur J Biochem 2:271–274
40. Vora S, Corash L, Engel WK, Durham S, Seaman C, Piomelli S (1980) The molecular mechanism of the inherited phosphofructokinase deficiency associated with hemolysis and myopathy. Blood 55:629–635

4.7 Polyols

Nanda M. Verhoeven, Mirjam M.C. Wamelink, Cornelis Jakobs

4.7.1 Introduction

Polyols, or sugar alcohols, are formed by the reduction of simple sugars. They are classified based on the number of C-atoms: erythritol and threitol (C4-polyols, tetritols), ribitol, arabitol and xylitol (C5-polyols, pentitols), galactitol, sorbitol and mannitol (C6-polyols, hexitols) and sedoheptitol and perseitol (C7-polyols, heptitols). Knowledge of the metabolism and functions of most of the polyols is very limited. Galactitol is a metabolic end product that is derived from galactose. Highly elevated concentrations are found in urine and plasma from patients affected with galactose-1-phosphate uridyltransferase (GALT) deficiency (Online Mendelian Inheritance in Man, OMIM, 230400) and galactokinase deficiency (OMIM 230200) [1]. Sorbitol is derived from glucose, and can be converted into fructose. Elevated concentrations of sorbitol have been described in diabetes mellitus and in sorbitol dehydrogenase deficiency (OMIM 182500), and have been implicated in the pathophysiology of these metabolic disorders [6]. The pentitol xylitol is known to be an intermediate in the conversion of L-xylulose into D-xylulose. L-Arabitol is derived from L-xylulose and is elevated in essential pentosuria (OMIM 260800), a benign inborn error of xylitol metabolism that results from a partial deficiency of L-xylulose reductase [5]. L-Arabinosuria, which has been described in one patient with elevated excretion of L-arabinose and L-arabitol, is presumed to result from deficiency of L-arabitol dehydrogenase [7].

In recent years, two new inherited defects affecting polyol concentrations have been discovered [2, 8]. The first defect is deficiency of transaldolase (TALDO, OMIM 606003) [8]. This defect is associated with liver symptoms, whereas other organs are affected to various degrees. In urine, erythritol, arabitol, ribitol and a C7 sugar or polyol are elevated [8, 9]. Furthermore, sedoheptulose-7-phosphate was found to be elevated in blood spots, fibroblasts and lymphoblasts from the patients [11]. Currently, six patients have been identified with TALDO deficiency. The other defect, ribose-5-phosphate isomerase (RPI) deficiency (OMIM 608611) has been diagnosed in one patient, who presented with a slowly progressive leucoencephalopathy. Arabitol and ribitol concentrations are strongly elevated in urine, plasma and CSF, whereas xylitol was mildly elevated [2]. Both defects can be diagnosed by assessment of urinary concentrations of polyols.

4.7.2 Properties of Polyols

Polyols are neutral compounds that do not have functional groups enabling their direct selective isolation from biological materials (Fig. 4.7.1).

4.7.3 Methods

4.7.3.1 Principle

Twenty years ago, a gas chromatographic separation of urinary, plasma and erythrocyte sugars and polyols was published [3]. This method can be used for the diagnosis of the aforementioned defects.

We have recently developed two tandem mass spectrometry methods for the investigation of inborn errors affecting polyol metabolism [10]. In both methods, urine samples together with internal standards ($^{13}C_4$-erythritol, $^{13}C_2$-arabitol and D_3-sorbitol) are desalted by a mixed-bed ion-exchange resin. Separation is achieved by two different columns. Using a prevail carbohydrates ES 54 column, the isomers are not separated (method 1), whereas with the other column (Aminex HPX-87C), separation of the isomers is achieved (method 2). Multiple reaction monitoring (MRM) detection of the polyols is carried out by tandem mass spectrometry with an electron-spray source operating in the negative mode.

4.7.3.2 Pre-analytical

Specimen

A random urine sample can be used for the analysis of polyols. TALDO and RPI deficiencies, as well as galactosaemia and presumably sorbitol dehydrogenase deficiency, can be diagnosed using urine. The samples are stored frozen. Repeated freeze-thawing does not influence the concentrations of the polyols.

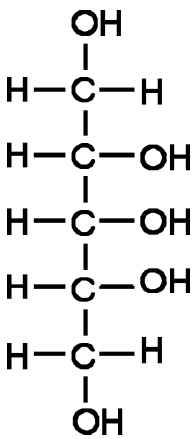

Fig. 4.7.1 Structure of pentitol

Reagents and Chemicals

1. Arabitol, erythritol, threitol, ribitol, xylitol, perseitol, sedoheptitol and sorbitol (Sigma-Aldrich, St. Louis, MO, USA); Mannitol (Merck, Darmstadt, Germany) and Galactitol (Calbiochem, Darmstadt, Germany).
2. Mixed-bed ion-exchange resin amberlite MB3 (100 g; Merck) is pretreated with 500 ml 10% acetic acid for 4 h, washed with distilled water and dried over 3 days.
3. D-[U-$^{13}C_4$]-Erythritol and D-$^{13}C_2$- [4,5]-arabitol (Omicron biochemicals, South Bend, IN, USA).
4. The internal standard (IS) [5,6,6-D_3]-sorbitol can be prepared by reduction of [5,6,6-D_3]-glucose following a described procedure [4].

Instrumentation

Detection of the polyols is carried out on a Quattro Micro tandem mass spectrometer (Micromass) equipped with an electron ion spray source operating in the negative mode. The mass spectrometer parameters are as follows: source temperature, 350°C; cone voltage, 30 V; collision energy, 10 eV. Detection of the polyols is performed by MRM. The MRM transition (Q1/Q3) settings for the different polyols are:

1. Erythritol and threitol: m/z 121/89.
2. $^{13}C_4$-Erythritol: m/z 125/92.
3. Ribitol, arabitol and xylitol: m/z 151/89.
4. $^{13}C_2$-Arabitol: m/z 153/91.
5. Galactitol, sorbitol, and mannitol: m/z 181/89.
6. D_3-Sorbitol: m/z 184/89.
7. Sedoheptitol and perseitol: m/z 211/89.

Data are acquired and processed using Masslynx software (version 4.0 sp1).

Calibration

Calibration curves for all polyols are prepared from a standard solution and are included in all series. The concentration ranges of the calibration curves are (based upon the concentrations found in urines): 0–4 nmol for ribitol, sedoheptitol and perseitol, 0–8 nmol for xylitol and sorbitol, 0–12 nmol for galactitol, 0–20 nmol for threitol, 0–32 nmol for mannitol, 0–40 nmol for erythritol and 0–48 nmol for arabitol.

Quality Control

For quality control, 100 µl pooled urine spiked with 8 µmol/l sedoheptitol and 8 µmol/l perseitol is included in each series. In addition, a 4× dilution of this sample and a pooled urine spiked with 180 µmol/l erythritol, 90 µmol/l threitol, 218 µmol/l arabitol, 36 µmol/l xylitol, 18 µmol/l ribitol, 36 µmol/l sorbitol, 145 µmol/l mannitol, 55 µmol/l galactitol, 16 µmol/l sedoheptitol and 16 µmol/l perseitol are included in each series. These three urine samples were chosen to obtain concentrations in the low, middle and high part of the calibration curves.

4.7.3.3 Analytical

Procedure

Different amounts of urine are used depending on the creatinine concentration. We use 200 µl urine when creatinine < 1.0 mmol/l; 100 µl urine when creatinine lies between 1.0 and 10.0 mmol/l; 50 µl urine when creatinine >10.0 mmol/l. Distilled water is added to obtain a total volume of 200 µl. $^{13}C_4$-Erythritol (2.5 nmol), $^{13}C_2$-arabitol (50 nmol) and D_3-sorbitol (10 nmol) are added as the IS. Pre-treated amberlite MB3 (20 µg) is added, mixed and centrifuged for 5 minutes at 410 × *g*. The supernatant is stored at –20°C until injection.

Method 1

Liquid chromatography (Waters, Alliance 2695 pump, Milford, MA, USA) is performed using a prevail carbohydrates ES 54 column (250 × 4.6 mm, bead size 5 µm, Alltech). An isocratic eluent of 50% acetonitrile/water is used, with the column kept at room temperature. The flow rate is set to 1 ml/min and is split after the analytical column in a ratio of 1:5, resulting in an inlet flow into the tandem mass spectrometer of 200 µl/min; 10 µl of sample is injected onto the column and the total run time is 6 min.

Method 2

Liquid chromatography (Waters, Alliance 2695 pump) is performed using an Aminex HPX-87C column (250 × 4.0 mm, bead size 9 µm, Bio-Rad Laboratories, Veenendaal, The Netherlands). An isocratic eluent of 40% acetonitrile/water is used, with the column kept at 65°C. The flow rate is set to 0.4 ml/min and is split after the analytical column in a ratio of 1:2, resulting in an inlet flow into the tandem mass spectrometer of 200 µl/min; 20 µl of sample is injected onto the column and the total run time is 24 min.

Calculation

Quantification of urinary polyols is performed using the corresponding calibration curves. $^{13}C_4$-erythritol is used as an IS for the tetritols, $^{13}C_2$-arabitol for the pentitols and D_3-sorbitol for the hexitols and heptitols. Concentrations are expressed in mmol/mol creatinine.

4.7.3.4 Post-analytical

Interpretation

The findings of combined elevation of C4, C5 and C7 polyols (method 1) and/or erythritol, arabitol, ribitol, sedoheptitol and perseitol (method 2) indicate a deficiency of the enzyme TALDO.

The patient affected with RPI deficiency exhibits high concentrations of arabitol and ribitol (method 2) and total pentitols (method 1).

Elevated total C6 may point to galactosaemia, or alternatively sorbitol dehydrogenase deficiency. Galactitol was found to be increased in both treated and untreated galactosaemia patients.

Chromatograms

See Figs. 4.7.2 and 4.7.3.

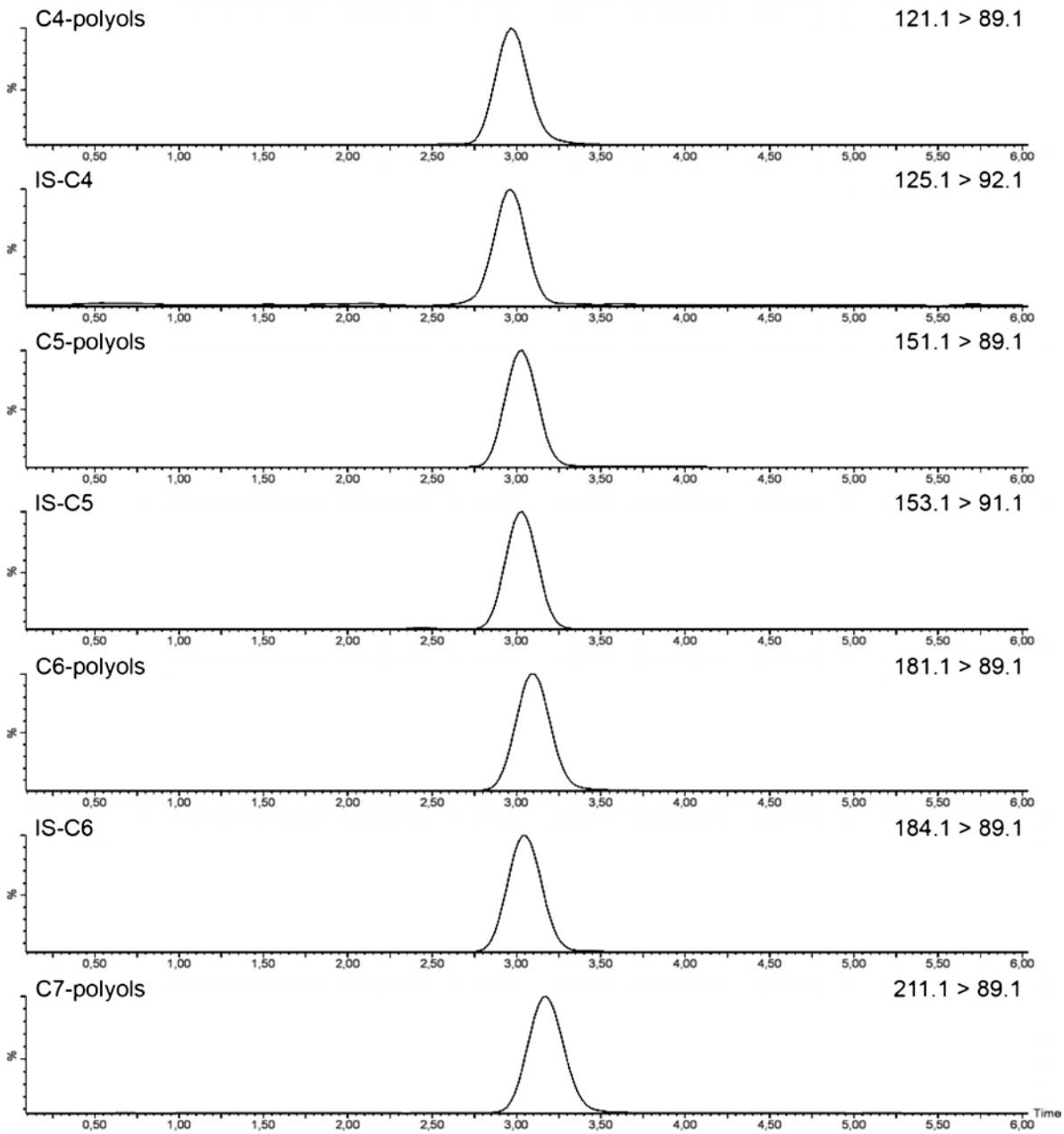

Fig. 4.7.2 Multiple reaction monitoring (MRM) chromatogram of pooled urine spiked with C7-polyols produced by method 1 (without separation of polyol isomers). MRM transitions are given for each mass transition. *IS* Internal standard

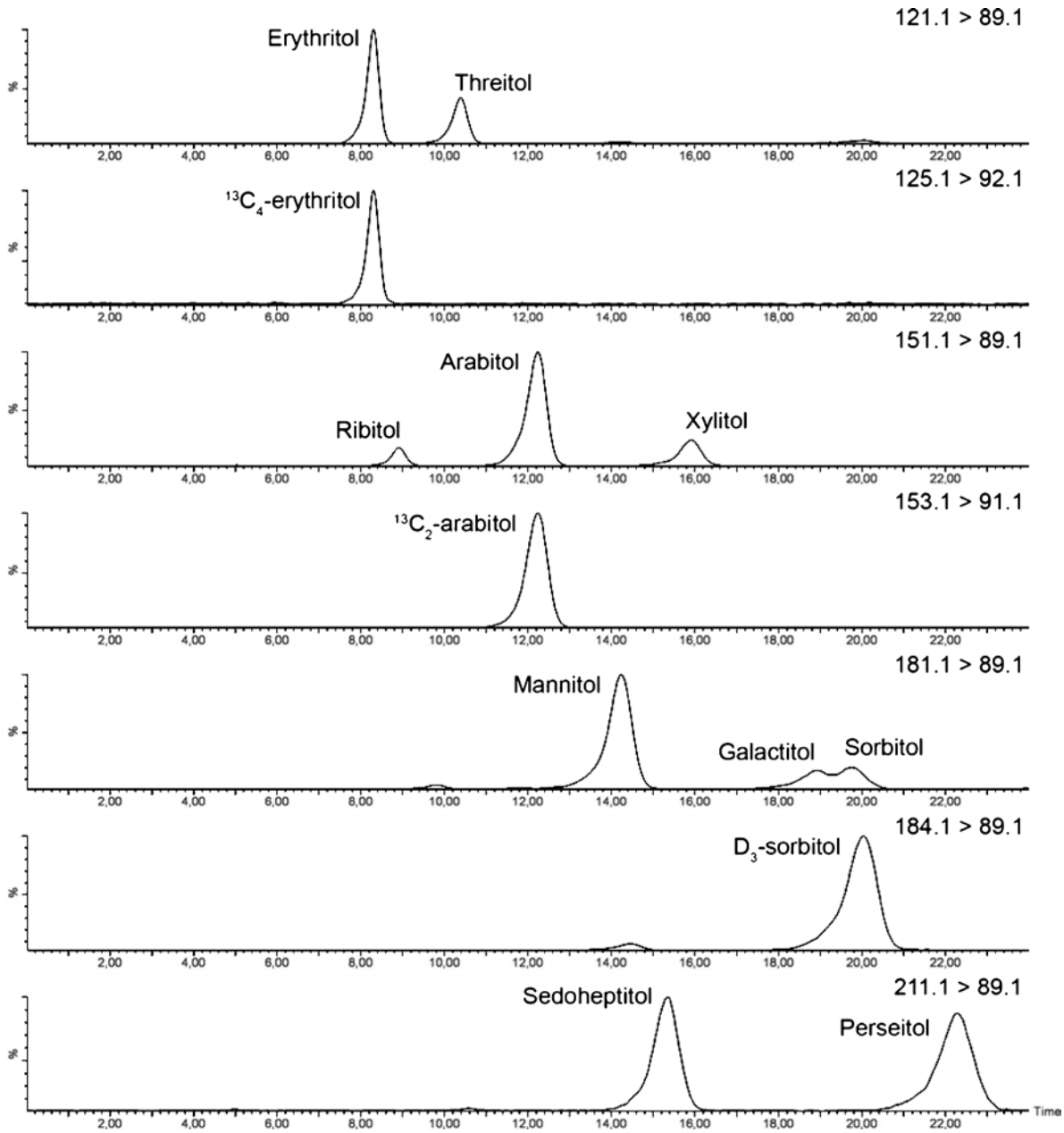

Fig. 4.7.3 MRM chromatogram of pooled urine spiked with C7-polyols produced by method 2 (with separation of polyol isomers). MRM transitions are given for each mass transition

Reference values

Urinary concentrations of polyols are age-dependent, as summarised in Tabes 4.7.1 and 4.7.2.

Typical Pathological Values

Tables 4.7.3 and 4.7.4 give an overview of pathological values found in patients affected with TALDO deficiency, RPI deficiency and in classical galactosaemia. In TALDO deficiency, polyol elevations are pronounced early and appear to decrease with age.

Pitfalls

Strongly elevated C6-polyol concentrations (above 200 nmol) interfere with the quantification of the C4-polyols in method 1, due to a co-eluting fragment in the chromatogram of MRM transition 121/89.

4.7.4 Follow-Up Enzyme Assays and Molecular Investigations

TALDO deficiency can be confirmed in lymphoblasts, fibroblasts and in erythrocytes. These cells are incubated with ribose-5-phosphate, after which formation of transketolase and TALDO products are analysed by gas chromatography with nitrogen phosphorous detection by liquid chromatography tandem mass spectrometry [8, 11]. A similar enzyme assay is available for RPI [2]. Confirmation of the gene defect can be performed by sequence analysis. Disease-causing mutations have been detected in all TALDO-deficient patients and in the RPI-deficient patient.

Table 4.7.1 *Reference values of polyols in urine determined by method 1. Concentrations are expressed in mmol/mol creatinine as mean (SD) and [± 2 SD]*

Polyol	Age	Concentration
C4	0–5 years ($n = 33$)	124 (39) [46–203]
	5–18 years ($n = 17$)	70 (23) [24–116]
	18–80 years ($n = 21$)	51 (20) [12–90]
C5	0–4 months ($n = 10$)	120 (43) [33–207]
	4 months–5 years ($n = 25$)	81 (24) [32–130]
	5–18 years ($n = 19$)	48 (13) [23–73]
	18–80 years ($n = 24$)	36 (13) [11–61]
C6	0–10 years ($n = 46$)	64 (26) [12–116]
	10–40 years ($n = 21$)	107 (117) [0–340]
	40–80 years ($n = 11$)	34 (15) [5–63]
C7	0–80 years ($n = 74$)	0 (0) [< 1]

Table 4.7.2 *Reference values of polyols in urine determined by method 2. Concentrations are given as the mean (SD) and [± 2 SD]*

Polyol	Age	Concentration
Erythritol	0–4 months ($n = 9$)	149 (30) [89–209])
	4 months–5 years ($n = 24$	93 (28) [38–148]
	5–80 years ($n = 38$)	51 (18) [14–88]
Threitol	0–5 years ($n = 33$)	36 (17) [2–70]
	5–80 years ($n = 37$)	17 (9) [0–35]
Ribitol	0–4 months ($n = 10$)	13 (6) [0–25]
	4 months–5 years ($n = 25$)	8 (3) [1–14]
	5–80 years ($n = 44$)	4 (2) [0–7]
Arabitol	0–4 months ($n = 10$)	90 (30) [30–151
	4 months–5 years ($n = 25$)]	63 (20) [22–103]
	5–80 years ($n = 44$)	33 (13) [6–60]
Xylitol	0–5 years ($n = 34$)	8 (2) [3–13]
	5–80 years ($n = 45$)	6 (3) [0–12]
Galactitol	0–2 years ($n = 23$)	55 (35) [0–125]
	2–5 years ($n = 14$)	14 (7) [0–28]
	5–80 years ($n = 44$)	7 (4) [0–15]
Mannitol	0–2 years ($n = 20$)	11 (7) [0–26]
	2–10 years ($n = 26$)	30 (19) [0–68]
	10–45 years ($n = 25$)	64 (70) [0–203]
	45–80 years ($n = 8$)	15 (6) [2–28]
Sorbitol	0–4 month ($n = 9$)	7 (3) [2–12
	4 month–5 years ($n = 25$)]	14 (7) [0–28]
	5–80 years ($n = 45$)	7 (4) [0–15]
Sedoheptitol	0–80 years ($n = 79$)	0 (0) [< 1]
Perseitol	0–80 years ($n = 78$)	0 (0) [< 1]

Table 4.7.3 *Concentrations of polyols in urines of patients with metabolic disorders, as determined by method 1. Concentrations are in mmol/mol creatinine (age-controlled reference range). Bold values are above the reference range.* Dist. *Disturbed peak, not quantifiable due to interference from a co-eluting fragment of C6-polyols,* GALT *galactose-1-phosphate uridyltransferase,* n.d. *not detectable,* RPI *ribose-5-phosphate isomerase,* TALDO *transaldolase*

Polyol	TALDO deficiency 1-month-old	TALDO deficiency 12-year-old	RPI deficiency, 14-year-old	GALT deficiency newborn	GALT deficiency on diet 9-year-old
C4	**349** (46–203)	**138** (24–116)	48 (24–116)	Dist. (46–203)	90 (24–116)
C5	**468** (33–207)	**148** (23–73)	**1090** (23–73)	167 (33–207)	55 (23–73)
C6	54 (12–116)	23 (0–340)	32 (0–340)	**19673** (12–116)	**169** (12–116)
C7	**10** (< 1)	**5** (< 1)	n.d. (< 1)	n.d. (< 1)	n.d. (< 1)

Table 4.7.4 *Concentrations of polyols in urines of patients with metabolic disorders, as determined by method 2. Concentrations are in mmol/mol creatinine (age-controlled reference range). Bold values are above the reference range.* Dist. *Disturbed peak, not quantifiable due to galactitol interference*

Polyol	TALDO deficiency (1-month-old)	TALDO deficiency (12-year-old)	RPI deficiency 1(4-year-old)	GALT deficiency (newborn)	GALT deficiency on diet (9-year-old)
Eythritol	**306** (89–209)	**110** (14–88)	23 (14–88)	147 (89–209)	55 (14–88)
Threitol	69 (2–70)	23 (0–35)	38 (0–35)	71 (2–70)	47 (0–35)
Ribitol	**131** (0–25)	**35** (0–7)	**137** (0–7)	25 (0–25)	3 (0–7)
Arabitol	**306** (30–151)	**106** (6–60)	**956** (6–60)	99 (30–151)	40 (6–60)
Xylitol	11 (3–13)	2 (0–12)	**19** (0–12)	**20** (3–13)	2 (0–12)
Galactitol	59 (0–125)	2 (0–15)	3 (0–15)	**22403** (0–125)	**163** (0–15)
Mannitol	8 (0–26)	13 (0–203)	21 (0–203)	Dist. (0–26)	16 (0–68)
Sorbitol	7 (2–12)	3 (0–15)	7 (0–15)	Dist. (2–12)	8 (0–15)
Sedoheptitol	**5** (< 1)	**2** (< 1)	n.d. (< 1)	n.d. (< 1)	n.d. (< 1)
Perseitol	**8** (< 1)	**3** (< 1)	n.d. (< 1)	n.d. (< 1)	n.d. (< 1)

Note added in proof:

Recently, a new diagnostic marker was confirmed for transaldolase deficiency. The seven carbon sugars sedoheptulose and mannoheptulose are highly elevated in urine and are specific biomarkers for transaldolase deficiency [12].

References

1. Endres W, Shin YS (1985) Cataract and metabolic disease. J Inherit Metab Dis 13:509–516
2. Huck HJ, Verhoeven NM, Struys EA, Salomons GS, Jakobs C, van der Knaap MS (2004) Ribose-5-phosphate isomerase deficiency: new inborn error in the pentose phosphate pathway associated with a slowly progressive leukoencephalopathy. Am J Hum Genet 74:745–751
3. Jansen G, Muskiet FA, Schierbeek H, Berger R, van der Slik SW (1986) Capillary gas chromatographic profiling of urinary, plasma and erythrocyte sugars and polyols as their trimethylsilyl derivatives, preceded by a simple and rapid prepurification method. Clin Chim Acta 157: 277–293
4. Karabinos JV, Ballun AT (1953) Direct reduction of aldoses and ketoses by Raney nickel. J Am Chem Soc 75:4501–4502
5. Lane AB (1985) On the nature of L-xylulose reductase deficiency in essential pentosuria. Biochem Genet 23:61–72
6. Lee AY, Chung SS (1999) Contributions of polyol pathway to oxidative stress in diabetic cataract. FASEB J 13:23–30
7. Onkenhout W, Groener JE, Verhoeven NM, Yin C, Laan LA (2002) L-Arabinosuria: a new defect in human pentose metabolism. Mol Genet Metab 77:80–85
8. Verhoeven NM, Huck JH, Roos B, Struys EA, Salomons GS, Douwes AC, van der Knaap MS, Jakobs C (2001) Transaldolase deficiency: liver cirrhosis associated with a new inborn error in the pentose phosphate pathway. Am J Hum Genet 68:1086–1092
9. Verhoeven NM, Wallot M, Huck JH, Dirsch O, Ballauf A, Neudorf U, Salomons GS, van der Knaap MS, Voit T, Jakobs C (2005) A newborn with severe liver failure, cardiomyopathy and transaldolase deficiency. J Inherit Metab Dis 2:169–179
10. Wamelink MM, Smith DE, Jakobs C, Verhoeven NM (2005) Analysis of polyols in urine by liquid chromatography-tandem mass spectrometry: a useful tool for recognition of inborn errors affecting polyol metabolism. J Inherit Metab Dis 28:951–963
11. Wamelink MM, Struys EA, Huck JH, Roos B, van der Knaap MS, Jakobs C, Verhoeven NM (2005) Quantification of sugar phosphate intermediates of the pentose phosphate pathway by LC-MS/MS: application to two new inherited defects of metabolism. J Chromatogr B Analyt Technol Biomed Life Sci 823:18–25
12. Wamelink MM, Smith DEC, Jansen EEW, Verhoeven NM, Struys EA, Jakobs C (2007) Detection of Transaldolase Deficiency by Quantitation of Novel Seven-Carbon Chain Carbohydrate Biomarkers in Urine. J Inherit Metab Dis 30: 735-742

5.1 Diagnosis of Inherited Defects of Cholesterol Biosynthesis

Hans R. Waterham, Marinus Duran

5.1.1 Introduction

Cholesterol is an important structural component of cellular membranes, where it plays a role in modulating membrane fluidity and phase transitions, and, together with sphingomyelin, forms lipid rafts or caveolae, which are sites where proteins involved in diverse signaling pathways become concentrated. Furthermore, cholesterol is a precursor of oxysterols, steroid hormones, and bile acids.

Mammalian cells may acquire cholesterol via receptor-mediated uptake as well as through endogenous biosynthesis via the isoprenoid/cholesterol biosynthetic pathway [1]. The recent identification and characterization of several inherited disorders due to a defect in cholesterol biosynthesis have shown that in addition to high cholesterol ((hypercholesterolemia), also low cholesterol levels (hypocholesterolemia) may have severe consequences for human health and development. Currently, eight distinct inherited disorders have been linked to different enzyme defects in the cholesterol/isoprenoid biosynthetic pathway [7, 9, 10]. Patients afflicted with these disorders are characterized by multiple morphogenic and congenital anomalies including internal organ, skeletal/or skin abnormalities, underlining the pivotal role of cholesterol in human embryogenesis and development [7, 9, 10].

Based on the clinical suspicion of a cholesterol biosynthesis defect, the first line of diagnosis for these various defects often involves sterol analysis in patient material where detection of a specific sterol intermediate is indicative for the respective defect. Confirmative diagnostic procedures involve enzymatic assays and/or molecular testing.

5.1.2 Cholesterol Biosynthesis and Defects Thereof

Mammalian cells acquire cholesterol either by de novo synthesis from acetyl-coenzyme A (CoA) or via the low-density lipoprotein (LDL)-receptor-mediated uptake of LDL particles that contain cholesterol esterified with long-chain fatty acids. These LDL cholesterol esters are subsequently hydrolyzed in lysosomes, after which free cholesterol molecules become available for synthesis of membranes, steroid hormones, bile acids, or oxysterols [1].

De novo synthesis of cholesterol is catalyzed by the isoprenoid biosynthesis pathway. This pathway produces a variety of sterol and nonsterol isoprenoids with

important cellular functions in such diverse processes as cell growth and differentiation, protein glycosylation, signal transduction pathways, and mitochondrial electron transport (Fig. 5.1.1).

The synthesis of all isoprenoids starts with acetyl-CoA, which in a series of six different enzyme reactions is converted into isopentenyl-diphosphate (-PP), the basic C-5 isoprene unit that is used for the synthesis of all subsequent isoprenoids (Fig. 5.1.1). At the level of farnesyl-PP the pathway divides into several branches that are involved in the production of the various isoprenoid end products. One of the major branches involves the cholesterol biosynthetic part of the pathway, of which squalene is the first committed intermediate in the production of sterols. Following cyclization of squalene, lanosterol is produced. To eventually produce cholesterol from la-

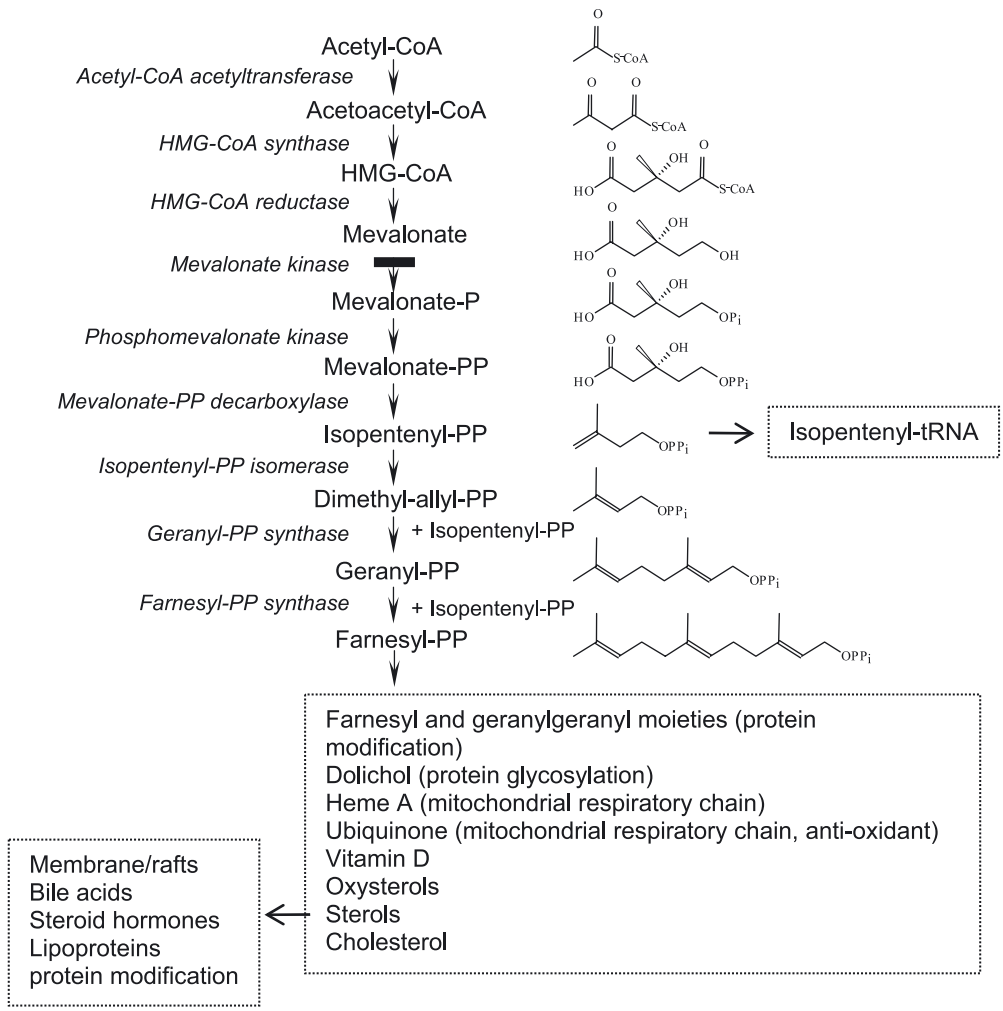

Fig. 5.1.1 Isoprenoid biosynthetic pathway. The enzyme mevalonate kinase (*black solid bar*) is deficient in patients affected with mevalonic aciduria and hyperimmunoglobulinemia D and periodic fever syndrome. *-CoA* -Coenzyme A, *HMG-CoA* 3-hydroxy-3-methyl-glutaryl-coenzyme A, *-PP* -pyrophosphate

nosterol, a series of at least eight different enzyme reactions is required, including one demethylation at C-14, two demethylations at C-4, one isomerization of $\Delta^{8(9)}$ to Δ^{7}, three reductions of the Δ^{24}, Δ^{14}, and Δ^{7} double bonds, and one desaturation between C-5 and C-6 (Fig. 5.1.2). Because the sequence of enzyme reactions required for the conversion of lanosterol to cholesterol may vary, two major routes involving the same enzymes have been proposed which, depending on the timing of reduction of the Δ^{24} double bond, postulate either 7-dehydrocholesterol or desmosterol as the ultimate precursor of cholesterol.

In the past decade, eight inherited disorders have been linked to specific enzyme defects in the isoprenoid/cholesterol biosynthetic pathway after the finding of abnormally increased levels of intermediate metabolites in tissues and/or body fluids of patients (Table 5.1.1) [7, 9, 10]. Two of these disorders are due to a defect of the enzyme mevalonate kinase, and in principle affect the synthesis of all isoprenoids (Fig. 5.1.1) [5]. The hallmark of these two disorders is the accumulation of mevalonic acid in body fluids and tissues, which can be detected by organic acid analysis, or preferably, by stable-isotope dilution gas chromatography (GC)-mass spectrometry (GC-MS) [2]. Confirmative diagnostic possibilities include direct measurement of mevalonate kinase activities in white blood cells or primary skin fibroblasts [3] from patients, and/or molecular analysis of the *MVK* gene [8].

The remaining six disorders are due to defects of enzymes involved specifically in the synthesis of cholesterol (Fig. 5.1.2). The detection of specific intermediate sterol species in cells, tissues, and/or body fluids of patients suspected to suffer from a defect in cholesterol biosynthesis based on their clinical presentation is often the first line of diagnosis, which can then be followed by enzyme and/or molecular diagnostic testing [9].

5.1.3 Methods

5.1.3.1 Principle

Sterols are separated by GC and detected using a flame ionization detector (FID). Sterol quantification is based on the detection of added internal standards. The identity of the detected sterols is verified using GC-MS of the trimethylsilylated derivatives of the sterols.

5.1.3.2 Pre-analytical

Specimen

Sterol analysis and quantification can be performed using plasma, serum, and cerebrospinal fluid (CSF) samples. Analysis of sterols from tissues and cells requires a pre-extraction work-up. The requirements for the different specimens are as follows:

1. Plasma: isolated from blood samples obtained by venipuncture and collected in standard heparin or ethylenediaminetetraacetic-acid-treated glass tubes; prepared

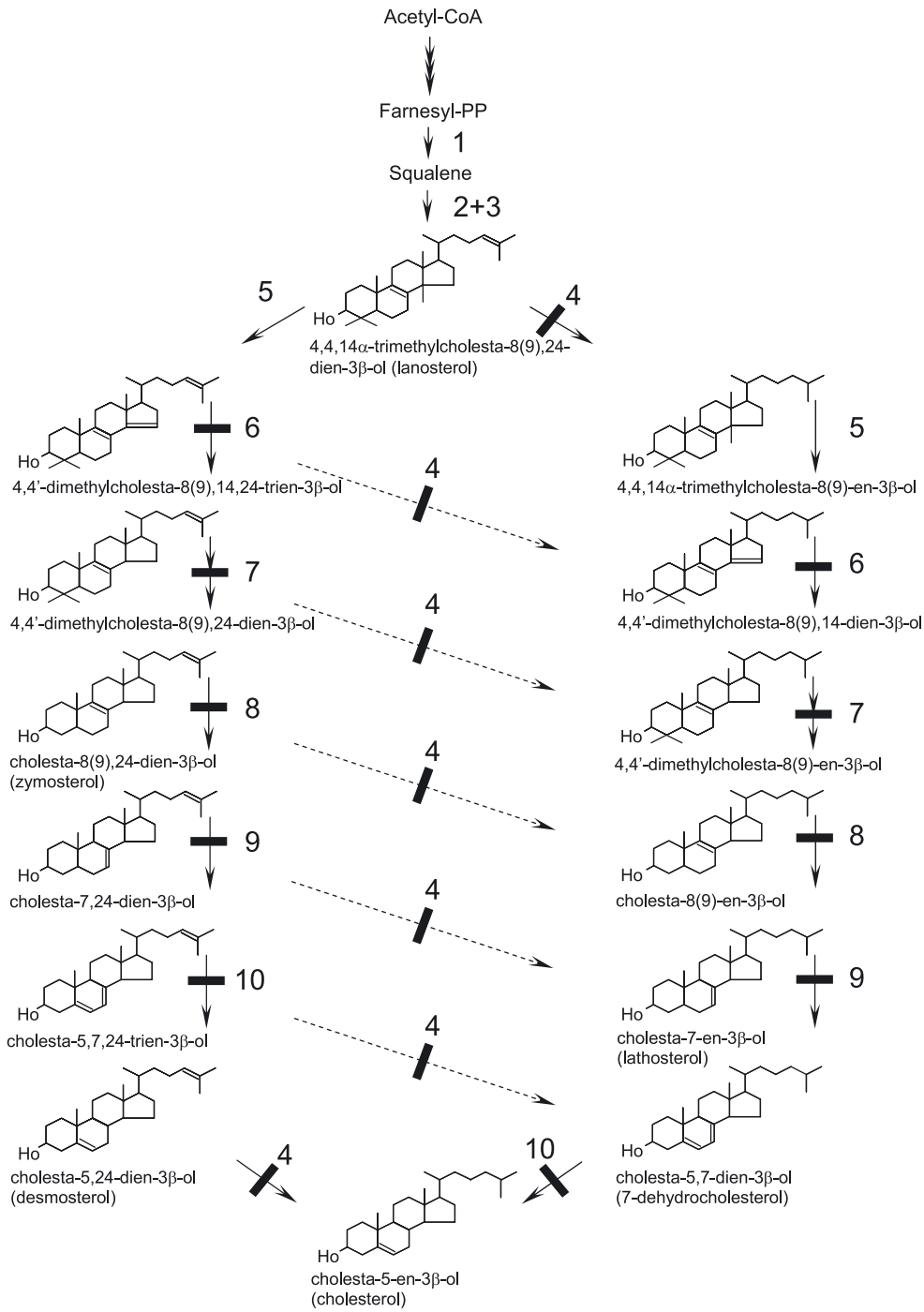
Acetyl-CoA
Farnesyl-PP
1
Squalene
2+3
5
4
Ho
4,4,14α-trimethylcholesta-8(9),24-dien-3β-ol (lanosterol)
6
4,4'-dimethylcholesta-8(9),14,24-trien-3β-ol
5
4,4,14α-trimethylcholesta-8(9)-en-3β-ol
7
4,4'-dimethylcholesta-8(9),24-dien-3β-ol
6
4,4'-dimethylcholesta-8(9),14-dien-3β-ol
8
cholesta-8(9),24-dien-3β-ol (zymosterol)
7
4,4'-dimethylcholesta-8(9)-en-3β-ol
9
cholesta-7,24-dien-3β-ol
8
cholesta-8(9)-en-3β-ol
10
cholesta-5,7,24-trien-3β-ol
9
cholesta-7-en-3β-ol (lathosterol)
cholesta-5,24-dien-3β-ol (desmosterol)
cholesta-5,7-dien-3β-ol (7-dehydrocholesterol)
cholesta-5-en-3β-ol (cholesterol)

◄**Fig. 5.1.2** Cholesterol biosynthesis branch of the isoprenoid biosynthetic pathway. Enzymes are numbered as follows: *1* squalene synthase; *2* squalene epoxidase; *3* 2,3-oxidosqualene sterol cyclase; *4* sterol Δ^{24}-reductase (desmosterolosis); *5* sterol C-14 demethylase; *6* sterol Δ^{14}-reductase (hydrops-ectopic calcification-moth-eaten, HEM, dysplasia); *7* sterol C-4 demethylase complex (including a 3β-hydroxysteroid dehydrogenase defective in congenital hemidysplasia with ichthyosiform nevus and limb defects, CHILD, syndrome); *8* sterol Δ^{8}-Δ^{7} isomerase (Conradi-Hunermann syndrome CDPX2); *9* sterol Δ^{5}-desaturase (lathosterolosis); *10* sterol Δ^{7}-reductase (Smith–Lemli–Opitz syndrome). Enzyme deficiencies are indicated by *solid bars* across the *arrows*

by centrifugation (10 min, 1600 × *g*) at room temperature; storage at – 18ºC or lower (stable for >1 year). The minimum amount required for analysis is 150 µl.

2. Serum: isolated from blood samples obtained by venipuncture and collected in glass tubes; prepared by centrifugation (10 min, 1600 × *g*) at room temperature following a clotting period for at least 1 h at room temperature; storage at – 18ºC or lower (stable for > 1 year). The minimum amount required for analysis is 150 µl.
3. CSF: No pretreatment is necessary; storage at – 18ºC or lower (stable for > 1 year). The minimum amount required for analysis is 150 µl.
4. Tissues: Small pieces of tissue from patients, stored at – 80ºC. The minimum amount required for analysis is 10 mg.
5. Cells: Lymphoblasts or primary skin fibroblasts cultured for 4–7 days in lipoprotein-depleted medium, harvested by centrifugation and used fresh or after storage as pellets at – 18ºC or lower. The minimum amount required for analysis is ≈ 1.10^6 cells.

Chemicals

1. Analytical/reagent grade *n*-hexane, heptane, KOH, NaOH, 2-propanol, and ethanol (Merck).
2. Epicoprostanol (5β-cholestan-3α-ol), cholestanol (5α-cholestan-3β-ol), cholesterol (cholesta-5-en-3β-ol), lathosterol (cholesta-7-en-3β-ol), desmosterol (cholesta-5,24-dien-3β-ol), and 7-dehydrocholesterol (cholesta-5,7-dien-3β-ol) (Sigma).
3. Coprostanol (5β-cholestan-3β-ol) (Steraolid).
4. MilliQ water: obtained by passing deionized water through a MilliQ Labo system (Millipore).
5. N,N-(Bis-trimethylsilyl)-trifluoroacetamide (BSTFA) with 1% trimethylchlorosilane (TMCS) (Pierce).

Reagents and Standards

1. Internal standard: prepare a stock solution of 6 mM epicoprostanol in ethanol. For use in the analysis, a portion of this stock solution will be diluted with ethanol to ≈ 0.6 µM.

Table 5.1.1 *Inherited disorders of isoprenoid/cholesterol biosynthesis.* CDPX2 *Conradi-Hunermann syndrome,* CHILD *congenital hemidysplasia with ichthyosiform nevus and limb defects,* HEM *hydrops-ectopic calcification-moth-eaten,* MA/HIDS *mevalonic aciduria/hyperimmunoglobulinemia D and periodic fever syndrome,* MIM *Mendelian Inheritance in Man*

Syndrome	Mevalonate kinase deficiency (MA/HIDS)	CHILD syndrome	CDPX2	HEM skeletal dysplasia	Lathosterolosis	Desmosterolosis	Smith–Lemli–Opitz syndrome
MIM number	251170/260920	308050	302960	215140	607330	602938	270400
Enzyme defect	Mevalonate kinase	3β-Hydroxy-steroid de-hydrogenase	3β-Hydroxy-sterol Δ^8-Δ^7-isomerase	3β-Hydroxysterol Δ^{14}-reductase	3β-Hydroxysterol Δ^5-desaturase	3β-Hydroxysterol Δ^{24}-reductase	3β-Hydroxysterol Δ^7-reductase
Accumulating metabolites	Mevalonic acid	Not detectable	Cholesta-8(9)-en-3β-ol	Cholesta-8,14-dien-3β-ol	Lathosterol	Desmosterol	7-Dehydrocholesterol 8-Dehydrocholesterol
Gene	*MVK*	*NSDHL*	*EBP*	*LBR*	*SC5D*	*DHCR24*	*DHCR7*
Chromosomal localization	12q24	Xq28	Xp11.22-23	1q42	11q23.3	1p31.1-p33	11q13

2. Saponification reagent: dissolve 1 g KOH in 5 ml MilliQ water and add 45 ml ethanol to make a 0.3 N KOH/ethyl alcohol solution.
3. 0.1 N NaOH: dissolve 0.4 g NaOH in 100 ml MilliQ water.
4. Sterol mixture: dissolve 2–3 mg epicoprostanol, coprostanol, cholestanol, cholesterol, lathosterol, desmosterol, and 7-dehydrocholesterol in heptane.
5. BSTFA with 1% TMCS is used as supplied.

Instrumentation

Gas chromatography

1. Hewlett Packard gas chromatograph type 5890 with an FID plus injector (or similar instrument) connected to a PC with Chromeleon integration software.
2. Hydrogen generator.
3. Chrompack capillary column CP WAX 52B [12.5 m × 0.25 mm inner diameter) × 0.20 μm(f)].
4. Temperature-controlled incubator.
5. Sonicator.

Gas Chromatography-Mass Spectrometry

1. Hewlett Packard gas chromatograph type 5890 coupled to a Hewlett Packard 5973 mass selective detector, with ChemStation software.
2. Chrompack column CP SIL5-CB [25 m × 0.25 mm inner diameter × 0.25 μm (f)].

GC and GC-MS Settings

The GC and GC-MS settings are listed in Table 5.1.2.

Quality Control

As internal control for sterol analysis in plasma, serum, and liquor, each series of samples includes a 150 μl aliquot of a large batch of control plasma samples in which cholestanol and cholesterol concentrations are determined and compared with previously determined concentrations. The values for these should fall within ± 2 standard deviations. The control plasma sample is composed of pooled plasma samples of different individuals stored as 150-μl aliquots at – 18°C.

5.1.3.3 Analytical

Procedures

Extraction of sterols from plasma and serum

1. Thaw plasma, serum, and internal standard on ice.
2. Set temperature-controlled incubator at 80°C.

■ ***Table 5.1.2*** *Gas chromatography (GC) and GC-mass spectrometry (MS) settings.* FID *Flame ionization detector,* MSD *mass selective detector,* NA *not applicable*

	GC settings			**GC/MS settings**		
Column	CP Wax 52B			CP SIL5-CB		
Injection	Splitless			Splitless		
Carrier	Helium			Helium (1 ml/min)		
Pressure	140 kPa			Constant flow		
Detection	FID			MSD		
H_2	Flow: 30 ± 5 ml/min Pressure 130 kPa			NA		
N_2	Flow: 30 ± 5 ml/min Pressure 190 kPa			NA		
Air	Flow: 300 ± 50 ml/min Pressure 260 kPa			NA		
Detector temperature	275 C			290 C		
Injector temperature	290 C			290 C		
Injection volume	1 µl			2 µl		
Purge	**Off**			**Off**		
Temperature progression	Temperature C	Time min	Rate C/min	Temperature C	Time min	Rate C/min
	85	1.2	20	85	2.0	20
	270	15		300	20	

3. Collect and label clean 4-ml glass vials including screw caps and Teflon liner (Alltech).
4. Transfer 100 µl plasma or serum into a 4-ml glass vial.
5. Add 100 µl internal standard using a glass pipette.
6. Add 1 ml saponification reagent and close the vial tightly with the screw cap and insert.
7. Mix the contents carefully and incubate for at least 2 h at 80 ± 5°C.
8. Cool the sample to room temperature.
9. Add 500 µl MilliQ water.
10. Add 2 ml *n*-hexane and mix for 10 s by vortex.
11. Transfer in duplicate 200 µl from the upper hexane layer into 1-ml glass vials.
12. Evaporate the samples to dryness under N_2 at 40 ± 10°C.
13. Dissolve the dried contents of one vial in 85 µl heptane.
14. Transfer the sample into a crimp-top vial and close the vial with cap and insert (Alltech). This sample is ready for GC analysis.
15. Dissolve the dried contents of the second, duplicate vial in 50 µl BSTFA + 1% TMCS.
16. Incubate the sample for 30 min at 80 ± 5°C.
17. Transfer the sample after cooling down into a crimp-cap vial and close the vial with a cap and insert (Alltech). This sample is ready for GC-MS analysis.

Extraction of Sterols From CSF

The procedure is the same as for plasma and serum.

Extraction of Sterols From Tissues

1. Thaw a small piece of tissue on ice.
2. Set the temperature-controlled incubator at 80°C.
3. Collect and label clean 4-ml glass vials including screw caps and Teflon liners (Alltech).
4. Homogenize tissue in 1 ml saponification reagent containing 10 µM internal standard. Transfer the suspension into a 4-ml glass vial and close the vial tightly with a screw cap and insert.
5. Mix the contents carefully and incubate for at least 2 h at 80 ± 5°C.
6. Cool the sample to room temperature.
7. Add 500 µl MilliQ water.
8. Add 2 ml *n*-hexane and mix for 10 s by vortex.
9. Transfer in 500 µl from the upper hexane layer into a 1-ml glass vial.
10. Evaporate the samples to dryness under N_2 at 40 ± 10°C.
11. Dissolve the dried contents of the vial in 100 µl BSTFA + 1% TMCS.
12. Incubate the sample for 30 min at 80 ± 5 C.
13. Transfer the sample after cooling down into a crimp-cap vial and close the vial with a cap and insert (Alltech). This sample is ready for GC-MS analysis.

Extraction of Sterols From Cells

1. Thaw cell pellets on ice.
2. Set the temperature-controlled incubator at 80°C.
3. Collect and label clean 4-ml glass vials including screw caps and Teflon liners (Alltech).
4. Resuspend cells in 1 ml saponification reagent containing 10 µM internal standard. Transfer the suspension into a 4-ml glass vial and close the vial tightly with a screw cap and insert.
5. Mix the contents carefully and incubate for at least 2 h at 80 ± 5°C.
6. Cool the sample to room temperature.
7. Add 500 µl MilliQ water.
8. Add 2 ml *n*-hexane and mix for 10 s by vortex.
9. Transfer in 500 µl from the upper hexane layer into a 1-ml glass vial.
10. Evaporate the samples to dryness under N_2 at 40 ± 10°C.
11. Dissolve the dried contents of the vial in 100 µl BSTFA + 1% TMCS.
12. Incubate the sample for 30 min at 80 ± 5°C.
13. Transfer the sample after cooling down into a crimp-cap vial and close the vial with a cap and insert (Alltech). This sample is ready for GC-MS analysis.

GC Analysis of Extracted Sterols

1. Use the GC settings outlined in Table 5.1.2.
2. Bring H_2, N_2 and air to pressure (Table 5.1.2).
3. Ignite the FID.
4. Re-inject 1 µl heptane without sterols until the baseline in the chromatogram is stable.

5. Inject standard sterol mixture (see "Reagents and Standards") to confirm the retention times of the various sterols.
6. Inject a reference Smith–Lemli–Opitz patient sample (7-dehydrocholesterol).
7. Inject the samples to be analyzed.

GC-MS Analysis of Extracted and Derivatized Sterols

1. Inject standard sterol mixture (see "Reagents and Standards").
2. Inject reference Smith–Lemli–Opitz and Conradi-Hunermann patient samples.
3. Inject the samples to be analyzed.

Calculation

The concentration of each sterol in plasma, serum, or liquor is calculated through integration of the corresponding peak area multiplied by the amount of internal standard added (in nmol) multiplied with 1000, divided by the peak area of the internal standard multiplied by the number of microliters of the sample.

5.1.3.4 Postanalytical

Interpretation

The detection of specific and often isolated intermediate sterols that are not observed in control samples or in higher concentrations than the reference range (see section 5.1.5) may be indicative for a specific enzyme defect in cholesterol biosynthesis (Table 5.1.1). Such elevated levels of intermediate sterols often, but not necessarily, coincide with decreased levels of cholesterol. The finding of elevated levels of intermediate sterols warrants further diagnostic investigations, including sterol profiling in cultured cells and/or molecular testing.

5.1.4 Chromatograms

Please refer to Fig. 5.1.3.

5.1.5 Reference Values in Plasma

Please refer to Table 5.1.3.

5.1.6 Typical Pathological Values

Intermediate sterol levels higher than observed (if observed at all) in control samples in conjunction with specific clinical symptoms may point to a defect in cholesterol biosynthesis and should be followed up by additional studies as outlined under section 5.1.8. Although cholesterol levels are often reduced, they may be (low) normal.

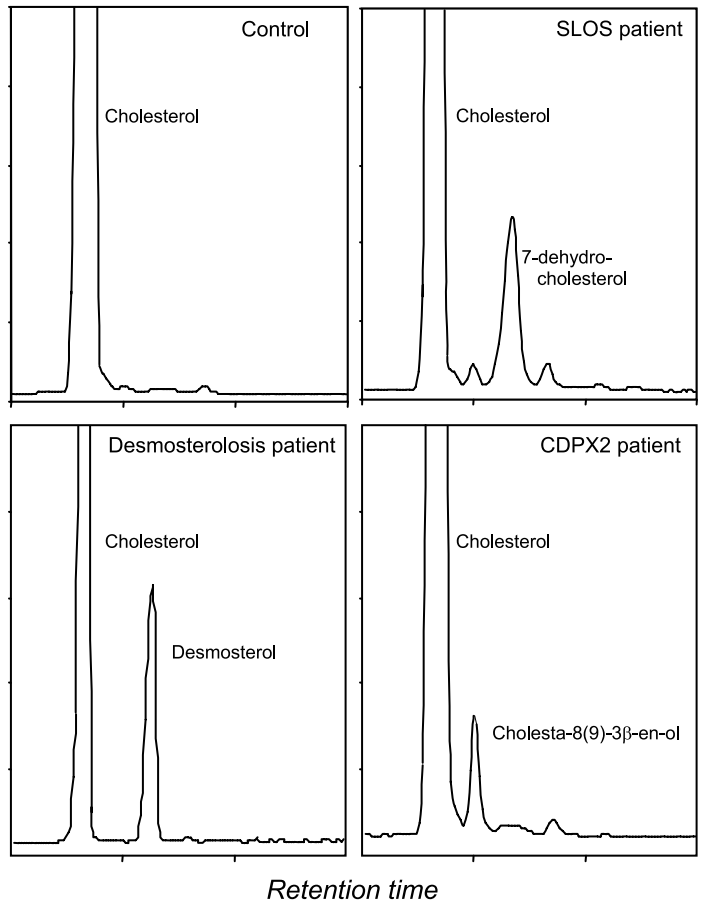

Fig. 5.1.3 Sterol analysis in patients with defective cholesterol biosynthesis. Gas chromatography-mass spectrometry analysis of trimethylsilyl derivatives of sterols extracted from primary skin fibroblasts of a control subject, a Smith–Lemli–Opitz syndrome (*SLOS*) patient, and a Conradi-Hunermann syndrome (*CDPX2*) patient, and lymphoblasts of a desmosterolosis patient cultured in lipoprotein-deficient medium reveals the accumulation of sterol intermediates indicative of a defect in cholesterol biosynthesis. Similar spectra can be obtained by sterol analysis of the plasma of such patients

5.1.7 Pitfalls

Some medications may exert some effect on cholesterol biosynthesis and result in elevated concentrations of intermediate sterol levels. A known example is ingestion of haloperidol, which may result in elevated levels of 7-dehydrocholesterol [6].

5.1.8 Follow-Up Assays

Assays to determine the activities of enzymes defective in any one of the six known disorders of cholesterol biosynthesis have only been described for sterol-delta7-reductase

■ ***Table 5.1.3*** *Reference values of sterols in plasma*

Sterol	Plasma concentration
7-Dehydrocholesterol	0.05–0.8 µmol/l
8-Dehydrocholesterol	< 0.26 µmol/l
Cholestanol	4.2–16 µmol/l
8-Lathosterol	< 2 µmol/l
Sitosterol	< 0.5 µmol/l

(defective in Smith–Lemli–Opitz syndrome) [4] and sterol-Δ^{24}-reductase (defective in desmosterolosis) [11], but are not useful for diagnostic purposes.

As an alternative, primary skin fibroblasts or lymphoblasts of patients suspected to be affected with a cholesterol biosynthesis defect can be cultured for 3–7 days in medium supplemented with fetal calf serum depleted of lipoproteins to induce cholesterol biosynthesis, whereupon the specific defect can be determined by sterol analysis using GC-MS as described above. This procedure will readily identify patients affected with Smith–Lemli–Opitz syndrome, desmosterolosis, lathosterolosis, hydrops-ectopic calcification-motheaten (HEM) skeletal dysplasia and most patients with Conradi-Hunermann syndrome (CDPX2). Patients with congenital hemidysplasia with ichthyosiform nevus and limb defects (CHILD) syndrome may not be identified with this assay, but they can be readily diagnosed on the basis of their typical clinical presentation.

For all defects, molecular testing through sequencing of the respective genes is available. Molecular testing is also the primary choice for prenatal testing [9].

References

1. Goldstein JL, Brown MS (1990) Regulation of the mevalonate pathway. Nature 343:425–430
2. Hoffmann GF, Sweetman L, et al. (1991) Facts and artefacts in mevalonic aciduria: development of a stable isotope dilution GCMS assay for mevalonic acid and its application to physiological fluids, tissue samples, prenatal diagnosis and carrier detection. Clin Chim Acta 198:209–227
3. Hoffmann GF, Brendel SU, et al. (1992) Mevalonate kinase assay using DEAE-cellulose column chromatography for first-trimester prenatal diagnosis and complementation analysis in mevalonic aciduria. J Inherit Metab Dis 15:738–746
4. Honda M, Tint GS, et al (1996) Measurement of 3β-hydroxysteroid Δ7-reductase activity in cultured skin fibroblasts utilizing ergosterol as a substrate: a new method for the diagnosis of the Smith–Lemli–Opitz syndrome. J. Lipid Res 37:2433–2438
5. Houten SM, Frenkel J, Waterham HR (2003) Isoprenoid biosynthesis in hereditary periodic fever syndromes and inflammation. Cell Mol Life Sci 60:1118–1134
6. Kelley RI, Hennekam RCM (2000) The Smith–Lemli–Opitz syndrome. J Med Genet 37:321–335
7. Kelley RI, Herman GE (2001) Inborn errors of sterol biosynthesis. Annu Rev Genomics Hum Genet 2:299–341

8. Mandey SH, Schneiders MS, et al. (2006) Mutational spectrum and genotype-phenotype correlations in mevalonate kinase deficiency. Hum Mutat 27:796–802
9. Waterham HR (2002) Inherited disorders of cholesterol biosynthesis. Clin Genet 61:393–403
10. Waterham HR (2006) Defects of cholesterol biosynthesis. FEBS Lett 580:5442–5449
11. Waterham HR, Koster J, et al. (2001) Mutations in the 3β-hydroxysteroid Δ^{24}-reductase gene cause desmosterolosis, an autosomal recessive disorder of cholesterol biosynthesis. Am J Hum Genet 69:685–694

5.2 Lipoproteins

Martin Hersberger, Lucia Rohrer, Arnold von Eckardstein

5.2.1 Function of Lipoproteins

Lipoproteins function as vehicles to transport the non-water-soluble lipids in blood as complexes of lipids and proteins. The lipid moiety consists mainly of triglycerides, cholesterol, and phospholipids. The protein moiety consists mainly of apolipoproteins, which act as detergents and are given letter designations ranging from A to M. The vast majority of lipoproteins are spherical particles with a core of hydrophobic triglycerides and cholesteryl-esters and a surrounding surface layer of more hydrophilic constituents including the apolipoproteins, cholesterol, and phospholipids.

Plasma lipoproteins can be divided into six major classes (see Fig. 5.2.1). Four of these classes derive from the liver and are present in the plasma of fasted subjects: very-low-density lipoproteins (VLDL), intermediate-density lipoproteins (IDL), low-density lipoproteins (LDL), and high-density lipoproteins (HDL). The other two classes of lipoproteins derive from the intestine and are found in the plasma of normolipidemic individuals only after a fatty meal (postprandially): chylomicrons and chylomicron remnants.

After absorption, dietary fat and vitamin E are assembled by intestinal brush border cells into triglyceride-rich chylomicrons. Nascent chylomicrons contain one molecule of apolipoprotein B48 as their structural apolipoprotein as well as apolipoprotein A-I (apoA-I) and apoA-IV, but receive additional apolipoproteins including apolipoprotein CII (apoCII) and apolipoprotein E (apoE) as well as cholesterol esters from HDL in the circulation. The triglycerides of the chylomicrons are hydrolyzed by lipoprotein lipase (LPL) on endothelial cells when its cofactor apoCII is present on the surface of the chylomicrons. Deficiency in either LPL or apoCII causes severe hyperchylomicronemia and predisposes to acute pancreatitis. When sufficient triglycerides are hydrolyzed, the resulting chylomicron remnants are removed from the blood by the liver via receptor-mediated uptake. This uptake depends on the interaction of apoE on the chylomicron remnants with the LDL receptor (LDLR) and other receptors of the liver [60]. Deficiency of apoE, or mutations that affect the receptor binding of apoE cause a defect in the clearance of chylomicron remnants.

The liver synthesizes VLDL to transport triglycerides, vitamin E and, to a lesser extent, cholesterol from the hepatocytes to various tissues of the body. Initially, VLDL contain apolipoprotein B-100 (apoB-100), apoE, and the C-apolipoproteins, but receive additional apolipoproteins and cholesterol esters from HDL in the circulation. Following triglyceride hydrolysis by LPL, VLDL remnants, termed IDL, are formed

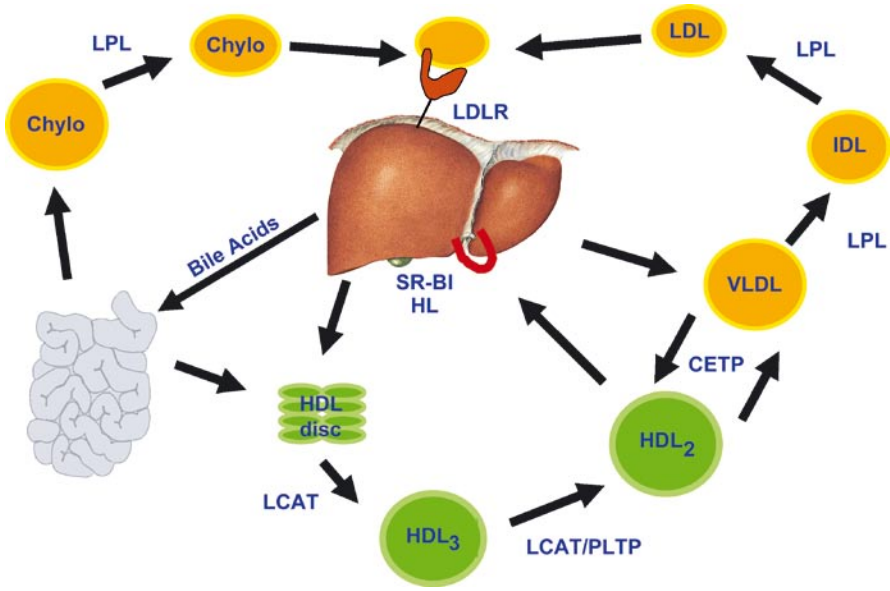

Fig. 5.2.1 The major metabolic pathways of the lipoprotein metabolism are shown. Chylomicrons (*Chylo*) are secreted from the intestine and are metabolized by lipoprotein lipase (*LPL*) before the remnants are taken up by the liver. The liver secretes very-low-density lipoproteins (*VLDL*) to distribute lipids to the periphery. These VLDL are hydrolyzed by LPL and hepatic lipase (*HL*) to result in intermediate-density lipoproteins (*IDL*) and low-density lipoproteins (*LDL*), respectively, which then is cleared from the blood by the LDL receptor (*LDLR*). The liver and the intestine secrete apolipoprotein AI, which forms pre-*β*-high-density lipoproteins (*pre-β-HDL*) in blood. These pre-*β*-HDL accept phospholipids and cholesterol from hepatic and peripheral cells through the activity of the ATP binding cassette transporter A1. Subsequent cholesterol esterification by lecithin:cholesterol acyltransferase (*LCAT*) and transfer of phospholipids by phospholipid transfer protein (*PLTP*) transform the nascent discoidal high-density lipoproteins (*HDL disc*) into a spherical particle and increase the size to HDL_2. For the elimination of cholesterol from HDL, two possible pathways exist: (1) direct hepatic uptake of lipids through scavenger receptor B1 (*SR-BI*) and HL, and (2) cholesteryl ester transfer protein (*CETP*)-mediated transfer of cholesterol-esters from HDL_2 to chylomicrons, and VLDL and hepatic uptake of the lipids via the LDLR pathway

and some of these are removed from the circulation by the same mechanisms as the chylomicron remnants. The major part is further metabolized to LDL by ongoing triglyceride hydrolysis through hepatic lipase (HL) and cholesterol ester acquisition from HDL through the cholesteryl ester transfer protein (CETP). Deficiency of HL is also associated with increased levels of remnant lipoproteins.

The LDL particles contain one apoB-100 as the structural protein and are the major cholesterol-transporting lipoproteins in human blood. Clearance of LDL from blood is mediated by the interaction of apoB-100 with the LDLR. Genetic defects either in the receptor binding region of apoB-100 or in the LDLR lead to decreased clearance of LDL and hence to their accumulation in the blood. The major metabolic pathways of the lipoprotein metabolism are shown in Fig. 5.2.1.

The liver and the intestinal mucosa secrete apoA-I, which accumulates lipids and forms lipid poor pre-*β*-HDL-precursors. These lipid poor particles acquire phospho-

lipids and unesterified cholesterol from hepatic and nonhepatic cells [42]. This initial step of HDL formation is interrupted in patients with Tangier disease, who lack the ATP-binding cassette transporter A1 (ABCA1). In patients with Tangier disease, cellular lipid efflux is drastically reduced, which causes the absence of lipid-rich HDL from the plasma [42]. HDL precursors generated by ABCA1-mediated lipid efflux become mature, lipid-rich, and spherical HDL_3 by acquisition of additional phospholipids and unesterified cholesterol either from cells or apoB-containing lipoproteins (at least partially mediated by phospholipid transfer protein, PLTP) and by the lecithin:cholesterol acyltransferase (LCAT)-mediated esterification of cholesterol. Ongoing LCAT-mediated cholesterol esterification and PLTP-mediated fusion with other HDL_3 further increases the size to the larger HDL_2 [42]. Genetic defects in apoA-I, ABCA1, and LCAT lead to hypoalphalipoproteinemia with low levels of HDL.

The HDL lipids are removed from the circulation by a selective uptake and by an indirect pathway. The selective uptake of cholesterol esters from HDL into hepatocytes and steroidogenic cells is mediated by the binding of HDL to scavenger receptor B1 (SR-BI). This selective uptake by SR-BI may depend on the presence of cofactors such as HL, which hydrolyses phospholipids on the surface of both HDL and plasma membranes and thereby enables the flux of cholesteryl esters from the lipoprotein core into the plasma membrane [42]. The indirect pathway involves the enzyme CETP, which exchanges cholesteryl esters of α-HDL with triglycerides of chylomicrons, VLDL, IDL, and LDL. The α-HDL derived cholesteryl esters are therefore removed via the LDL-receptor pathway. The removal of excess cholesterol from the periphery and the delivery to the liver for excretion in the bile is termed reverse cholesterol transport.

5.2.2 Clinical Consequences and Classification of Dyslipoproteinemias

Substantial evidence indicates that high plasma levels of lipoprotein remnants and LDL are atherogenic, while high levels of HDL are atheroprotective. Therefore, the class of lipoproteins that is increased or decreased will determine the clinical feature of a patient. Besides the influence on atherosclerosis, high levels of chylomicrons lead to acute pancreatitis, while markedly decreased levels of VLDL and LDL lead to retinal and neurologic disease, probably due to vitamin E deficiency.

Monogenic dyslipoproteinemias can generally be grouped into five categories: (1) hypertriglyceridemia with an increase in chylomicrons and the clinical sign of pancreatitis, (2) mixed hyperlipidemia with an increase in chylomicron and VLDL remnants and an increased risk of premature atherosclerosis, (3) hypercholesterolemia with an increase in LDL and an increased risk for premature atherosclerosis, (4) hypoalphalipoproteinemia with low HLD and an increased risk for premature atherosclerosis, and (5) hypolipoproteinemia with a decrease in VLDL and LDL, which may lead to neurological disease.

5.2.3 Hypertriglyceridemia

Hypertriglyceridemia suggests the presence of chylomicronemia, which may be caused by deficiency of LPL or its co-factors apoCII and apoAV. Blood triglyceride

levels are usually > 10 mmol/l, total cholesterol > 6.5 mmol/l, and HDL cholesterol is < 1.0 mmol/l. To verify chylomicronemia, the turbid serum can be stored overnight at 4°C. Chylomicrons will form a creamy layer on top of the serum, while other lipoproteins will not do so. To distinguish between LPL deficiency and apoCII deficiency, the following assays can be applied.

5.2.3.1 LPL Deficiency

Familial LPL deficiency (Online Mendelian Inheritance in Man number, OMIM, 238600) is a recessive disorder that is characterized by the massive accumulation of chylomicrons in plasma, which results from the inability to metabolize triglycerides in the core of the lipoproteins. Diagnosis is usually achieved by measuring LPL mass and/or activity in postheparin plasma. The mass of the LPL can easily be measured by commercially available enzyme-linked immunosorbent assay (ELISA), but this will only detect LPL deficiency caused by the absence of LPL and not by inactivating mutations leading to reduced LPL activity. In contrast, the LPL activity assay detects both the absence of LPL and mutant LPL with reduced activity [6]. An alternative method that also detects all sorts of mutations is the genetic approach. Screening of the entire coding region of the LPL gene is a reasonable approach to detect mutations [63].

LPL Activity

The hydrophobic nature of lipid molecules necessitates intravascular transport in the form of lipoproteins. Two enzymes, LPL and HL catalyze the triglyceride and phospholipids hydrolysis of lipoproteins. Both enzymes are located on the capillary endothelium, but only LPL is located on most if not on all of the peripheral capillary beds. LPL mainly hydrolyzes triglycerides and phospholipids on chylomicrons and VLDL and is involved in the synthesis of nascent HDL [42]. Consistent with these findings, LPL deficiency results in fasting chylomicronemia and hypertriglyceridemia , which is prone to cause acute pancreatitis when triglyceride levels exceed 23 mmol/l (2000 mg/dl). The enzyme binds to the endothelium through heparan sulfate proteoglycans and is released upon heparin administration because of its higher affinity for heparin than for the endogenous heparan sulfate proteoglycans. Intravenous injection of a heparin bolus displaces the LPL enzyme into postheparin plasma, where its activity can be quantified.

Principle

The LPL catalytic assay measures the hydrolysis of a [^{14}C]- or [^{3}H]-triolein emulsion producing the ^{14}C- or ^{3}H -labeled free oleic acid [6]. The ^{14}C- or ^{3}H-labeled oleic acid is isolated by a selective extraction procedure and its radioactivity is determined by liquid scintillation counting [40]. Lipase activity is calculated as nanomoles of oleic acid released per minute per milliliter of postheparin plasma [41].

Preanalytical

Specimen

Blood samples are drawn after an overnight fast of at least 12 h. Preheparin and postheparin plasma samples are collected to analyze the LPL activity. In general 50–100 IU/kg heparin is injected intravenously and the postheparin plasma sample is collected 15 min later [41]. Samples should be immediately centrifuged and the plasma should be directly analyzed or frozen at – 70°C.

Reagents and Chemicals

1. Scintillation vials.
2. Methanol:chloroform:heptane (56:50:4 by volume).
3. Toluene.
4. Glacial acetic acid.
5. Sodium dodecylsulfate (SDS).
6. 0.1 mM Carbonate-bicarbonate buffer, pH 10.5.
7. Intralipid 10%.
8. 0.2 mM Tris buffer, pH 8.2.
9. Bovine serum albumin (BSA).
10. NaCl.
11. Ferric acid.
12. [^{14}C]- or [^{3}H]-labeled triolein.
13. Heat-inactivated pooled human serum [41].

Instrumentation

1. Liquid scintillation counter for either ^{14}C or ^{3}H.
2. Sonicator.
3. Water bath or incubator.

Calibration

Calibrators can be obtained by pooling postheparin plasma from fasted volunteers, which is stored at – 70°C as aliquots [41].

Quality Control

Controls can be obtained by pooling postheparin plasma from another set of fasted volunteers, which is stored at – 70°C as aliquots [41].

Analytical

Procedure

The Intralipid emulsion containing [^{14}C]-triolein is produced by sonication. In detail, 1 ml of Intralipid, 5 µCi (where 1 Ci = 3.7×10^{10} Bq) of [^{14}C] triolein and 4.68 ml of 0.2 mM Tris buffer, pH 8.2 are mixed and sonicated at amplitude 10, with 24 cycles of 20 s on, 10 s off, and mixing the emulsion by inversion after every fourth cycle (Fisons Scientific Instruments, Crawley, UK). After sonication, 2.75 ml of 200 g/l BSA and 0.8 ml of 1.42 M NaCl (both in 0.2 mM Tris buffer, pH 8.2) will be added and the emulsion will be mixed by inversion [40].

Aliquots (420 µl) of the emulsion will be preincubated for 90 min at 37°C with 80 µl of heat-inactivated pooled human serum as a source of apoCII [40].

To inactivate the HL activity, samples (250 µl) are preincubated for 30 min with an equal volume of 70 mM SDS in 0.2 mM Tris buffer, pH 8.2 at room temperature [5]. As a blank, an aliquot of 0.9% physiological NaCl solution is treated identically to the samples.

On completion of the two pre-incubation steps, 10 µl of the preincubated sample will be added to 500 µl of the preincubated emulsion in triplicate, and the LPL-catalyzed triglyceride hydrolysis will be allowed to proceed for 1 h at 28°C. The reaction is stopped by adding 5.33 ml of methanol:chloroform:heptane (56:50:4 by volume) and vigorous shaking.

To extract the liberated fatty acids, 1.5 ml of 0.1 mM carbonate-bicarbonate buffer, pH 10.5 is added and the mixture is shaken for 10 s. Centrifugation for 45 min at 1500 × *g* in a swing-out rotor will separate the water from the lower organic phase. In a scintillation vial, 2 ml of the upper water phase are mixed with 50 µl of glacial acetic acid containing 500 µg ferric acid before the scintillation liquid is added (16 ml of Ecoscint:toluene (7:1 volume). Liquid scintillation counting is done for 5 min and the LPL activity is calculated from the difference in counts between the blank and the sample vials [40].

Calculation

Enzyme activity (µmol/ml/h) = (counts in probe – counts in blank) × 200/counts in blank × 2.4.

Postanalytical

■ Interpretation

Homozygous mutant and compound heterozygous mutant patients have reduced or absent LPL activity, while heterozygous carriers usually have normal LPL activity.

Chromatograms

None.

Reference Values

Since there is no standardization of the LPL activity assays, the reference values depend on the assay used [40]. LPL activity in women lies in the range 107–390 mmol/min/ml, while that for men is in the range 55–407 mmol/min/ml.

Typical Pathological Values

Inactivating LPL mutations lead to a > 60% reduction in LPL activity in postheparin plasma from homozygous individuals [49]. Mutations that result in only reduced LPL enzyme activity usually show less reduction in the activity assay, even in homozygous patients [64]. Heterozygous carriers of a mutation have no reduction in LPL activity and show no clinical signs.

Pitfalls

Low LPL activity can also be found secondary to metabolic dysregulation, notably in insulin resistance and type 2 diabetes mellitus. In fact, diabetic hypertriglyceridemia is caused in part by decreased LPL secretion in response to reduced insulin action. Another preanalytical pitfall results from the high affinity of LPL for triglyceride-rich lipoproteins. When extremely hypertriglyceridemic plasma is prepared by cen-

trifugation of blood, chylomicrons may stick to the wall of the plastic tube, and with them LPL. To recover LPL almost completely and to avoid falsely low LPL activity, it is important to remove all chylomicrons with plasma.

5.2.3.2 ApoCII Deficiency (OMIM 207750)

ApoCII deficiency is a recessive disorder that is characterized by the massive accumulation of chylomicrons in plasma. ApoCII deficiency is clinically indistinguishable from LPL deficiency, a finding that is explained by its function as the obligate cofactor for LPL to hydrolyze triglycerides in the core of the lipoproteins. This cofactor function is used commonly for the diagnosis of the disease in functional assays [27]. In these LPL assays, the capacity of apoCII to restore LPL activity to normal is measured. Comparing the LPL activity in normal postheparin plasma complemented with the heat-inactivated serum from the patient of interest to a normal source of apoCII from a heat-inactivated pooled human serum (see section 5.2.3.1 for "LPL Activity") will allow the diagnosis of apoCII deficiency. Several other methods of detecting apoCII deficiency have been successfully applied, including isoelectric focusing of plasma or triglyceride-rich lipoprotein preparations followed by Western blotting with an apoCII antibody [37] and immunochemical and chromatographic methods [13]. However, none of these assays will detect heterozygous carriers of apoCII null mutations.

The gene for apoCII is approximately 3.5 kb in size and has four exons that code for the 79-amino-acid protein. So far only point mutations and no major rearrangements of the apoCII gene have been reported. This allows screening of the promoter and the coding region by denaturing grading gel electrophoresis (DGGE) [71], single-stranded conformational polymorphism (SSCP) [80], denaturing high-pressure liquid chromatography (DHPLC), or by direct sequencing [59]. Considering the small size of the gene and the limited number of exons, direct sequencing of the four polymerase chain reaction (PCR) products ranging between 273 and 379 nt is feasible nowadays [71]. To date, 14 mutations have been detected in the apoCII gene.

Sequencing of the ApoCII Gene

Principle

The promoter region and all four exons of the apoCII gene are amplified in four separate PCR reactions. These PCR products are then purified from the amplification primers and the template is used for direct sequencing analysis using the method of Sanger et al. [83].

Preanalytical

- Specimen

EDTA-blood for DNA extraction. The samples are stable at room temperature for 2 days and can be shipped by overnight mail.

Reagents and Chemicals

1. DNA extraction kit for blood samples.
2. Oligonucleotides [59, 71].
3. Big Dye Terminator reaction mix (Applied Biosystems).
4. POP6 matrix for capillary sequencer (ABI 310, Applied Biosystems).
5. Template suppression reagent (ABI 310, Applied Biosystems).
6. MicroSpin S-300 columns (Pharmacia).
7. Autoseq G-50 columns (Pharmacia).

Instrumentation

DNA sequencer like ABI Prism 310, or others.

Calibration

None.

Quality Control

None.

Analytical

Procedure

Each amplicon is amplified by PCR using the appropriate thermal cycling conditions [59, 71]. The amplicons are then purified from the dNTPs and the oligonucleotides using the microspin S-300 spin columns.

Five microliters of these purified amplicons is then mixed with 1 µl of primer (10 µM) and 4 µl of the Big Dye Terminator reaction mix and the mixture is cycled for the sequencing reaction with the following conditions: initial denaturation at 94°C for 45 s, followed by 25 cycles of 96°C for 10 s, 50°C for 5 s, and 60°C for 90 s. The sequencing reaction is then stored at 4°C until clean up with Autoseq G-50 columns to eliminate the labeled ddNTP and the dNTPs from the reaction mixture. Ten microliters of this purified sequencing reaction is then mixed with 12 µl of the template suppression reagent, heated to 95°C for 7 min, and then cooled on ice.

Analysis of the sequencing reaction on the ABI 310 is achieved using POP6 polymer with 30 s injection at 5 kV, and the sample is run at 50°C with 15 kV for about 30 min.

Calculation

None.

Postanalytical

Interpretation

The raw data are analyzed by sequence analysis software and the sequence is displayed as an electropherogram for visual inspection. Each homozygous position in the DNA shows a single peak for a certain nucleotide and each heterozygous position shows two overlapping peaks for the presence of the two different nucleotides at this position (Fig. 5.2.2). The verified and edited sequence is then compared to the human apoCII sequence in the National Center for Biotechnology Information (NCBI)

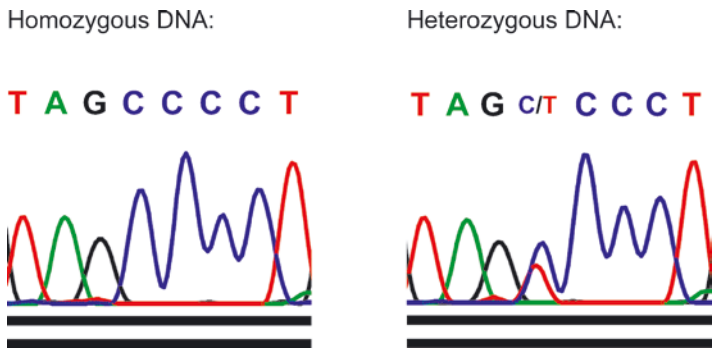

Fig. 5.2.2 Electropherograms for the same genetic region of a homozygous DNA and heterozygous DNA is shown. The sequence of the gene is read from left to right. Up to nucleotide number 4 the sequences are identical. At position number 4, the homozygous DNA has a cytidine on both chromosomes, while the heterozygous DNA has a cytidine only on one chromosome and a thymidine on the other chromosome

database (accession number M10612.1 at http://www.ncbi.nlm.nih.gov/entrez/query.fcgi?db = Nucleotide) for homozygous or for compound heterozygous mutations.

Chromatograms

Please refer to Fig. 5.2.2.

Reference Values

Please refer to the human apoCII sequence in the NCBI database (accession number M10612.1 at http://www.ncbi.nlm.nih.gov/entrez/query.fcgi?db = Nucleotide).

Typical Pathological Values

Mutations in the promoter region, in regions essential for correct splicing, and mutations in the coding region leading to amino acid changes are mainly responsible for inactivating mutations.

Pitfalls

Most recently mutations in apoAV have also been identified as the molecular basis of chylomicronemia. Their identification needs sequencing of the apoAV gene.

5.2.4 Mixed Hyperlipidemia

Mixed hyperlipidemia is one of the most common lipid disorders, but only a minor fraction of the affected patients has a monogenic inherited disease. Most patients with mixed hyperlipidemia have a familial combined hyperlipidemia, a multifactorial disease for which the causative factors are not known. Patients have elevated remnant lipoproteins with elevated triglycerides > 3.0 mmol/l and total cholesterol > 5.0 mmol/l. Two rare monogenic disorders lead to such a lipoprotein pattern,

familial dysbetalipoproteinemia, and HL deficiency. The following investigations can be applied to diagnose and distinguish the two disorders.

5.2.4.1 Familial Dysbetalipoproteinemia (OMIM + 107741)

Familial dysbetalipoproteinemia (type III) is characterized by the accumulation of chylomicron and VLDL remnants, which are enriched in cholesterol compared to their precursors. The primary molecular cause of familial dysbetalipoproteinemia (type III) is the homozygous presence of the apolipoprotein E2 (apoE2) isoform, which is associated with recessive inheritance of the disorder [62]. However, only 1 in 50 homozygotes for apoE2 will develop type III hyperlipoproteinemia, which is clinically characterized by palmar and tuberous xanthomas, arcus lipoides, and premature atherosclerosis of coronary, peripheral, and cerebral arteries. Precipitating factors include diabetes mellitus, renal disease, hemochromatosis, but also familial hypercholesterolemia. In addition, some rare mutations in the apoE gene have been found to cause dominant and more penetrant forms of type III hyperlipoproteinemia.

Lipoprotein Electrophoresis

Several methods have been developed to separate the plasma lipoproteins including ultracentrifugation, thin-layer chromatography, fast protein liquid chromatography analysis, immunological techniques, and electrophoresis. While ultracentrifugation is the gold standard for quantification of the different lipoprotein classes, it is too time consuming to be applied for clinical routine analysis and is used mainly for research purposes. In clinical routine analysis, agarose gel and cellulose acetate electrophoresis is most often used to separate the five major lipoprotein fractions present in serum [74]. Several commercial electrophoresis systems are available for the semiquantitative analysis of the lipoproteins. With these commercial systems, quantification of the lipoproteins is not possible without modification [45]; however, semiquantitative analysis is all that is necessary for phenotyping of the lipoprotein pattern [31]. Phenotyping is usually done according to the classification of Fredrickson and Lees [31], which distinguishes five different phenotypes. Type I is defined as hyperchylomicronemia, type II as hyperbetalipoproteinemia, type III as abnormal broad-β or dysbetalipoproteinemia, type IV as endogenous hypertriglyceridemia, and type V as mixed hypertriglyceridemia. However, the use of this classification in patient care has been displaced by the direct measurement of cholesterol in HDL and LDL and by the use of the Framingham or the Prospective Cardiovascular Münster (PROCAM) score to predict coronary risk. Lipoprotein electrophoresis is nowadays only indicated to support diagnosis of the rare familial dysbetalipoproteinemia (type III) or hyperchylomicronemia (types I or V).

Principle

Serum is separated by agarose gel electrophoresis and the gel is stained for lipids [45, 74]. Agarose electrophoresis separates four major lipoproteins (i.e., chylomicrons,

LDL, VLDL, and HDL). While the chylomicrons remain at the application point, the other lipoproteins migrate toward the anode in the electric field. LDL have the lowest mobility (β-mobility), followed by VLDL (pre-β-mobility), and HDL have the fastest migration (α-mobility). Sometimes, if present at high concentrations, lipoprotein(a) can be identified as a discrete band with fast pre-β-mobility. Staining of the lipids on the agarose gel allows identification of the different lipoproteins and densitometric scanning of the stained gels, including automatic integration of the optical density of the peaks allows a semiquantitative analysis.

Preanalytical

Specimen

The blood samples should be drawn after an overnight fast of at least 12 h. Fresh serum samples are recommended for the analysis. The samples can be stored at 2–8°C for up to 3 days but should not be frozen.

Reagents and Chemicals

1. Agarose gels (8 g/l).
2. Barbital buffer, 0.05 M, pH 8.6.
3. Fixing solution consisting of 5% glacial acetic acid in 75% ethanol.
4. Lipoprotein stain (Sudan Black B or Fat Red 7B).
5. Destaining solution (45% ethanol).

Instrumentation

1. Power supply with a minimum of 250 V and 100 mA output.
2. Electrophoretic cell [74] or commercial electrophoresis system.
3. Tanks and gel holders for staining and destaining.
4. Drying oven at 60–80°C.
5. Densitometer capable of scanning gels at a 570 nm for Sudan Black B or 525 nm for Fat Red 7B.

Calibration

Not necessary. Relative distribution between the five lipoprotein fractions of an individual is analyzed.

Quality Control

Commercial serum is available with relative values for LDL, VLDL, and HDL fractions.

Analytical

Procedure

Aliquots (2–5 µl) of serum are applied to an agarose gel using a sample application template. Incubation for 5–10 min allows diffusion of the sample into the gel before the gel is transferred to the electrophoresis unit. Depending on the gel size and commercial application, electrophoresis is performed at 50–80 V for 45–90 minutes in barbital buffer. The gel is then dried in an oven at 60–80°C for 10–20 min.

For staining, the gel is immersed in staining solution for 2–15 min. The superfluous stain is removed in destaining solution for 15 s to 15 min depending on the

lipoprotein stain used. The lipoprotein fractions are now clearly visible on the agarose gel and the gel is prepared for densitometric analysis by drying in an oven at 60–80°C for 5–10 min.

Densitometric scanning of the dried gels with integration of the optical density of the peaks allows then the semi-quantitative analysis of the different lipoproteins.

Calculation

The entire area under the curve for each lane is calculated and the area of each peak is calculated as the percentage of the total area under the curve.

Postanalytical

- Interpretation

Interpretation of the lipoprotein pattern is done according to Fredrickson and Lees [31]. Familial dysbetalipoproteinemia (type III) will result in one intense band, the so-called broad-β-band, encompassing bands with β- and pre-β-mobility (Fig. 5.2.3) and consisting mainly of chylomicron and VLDL remnants. This broad-β-band is

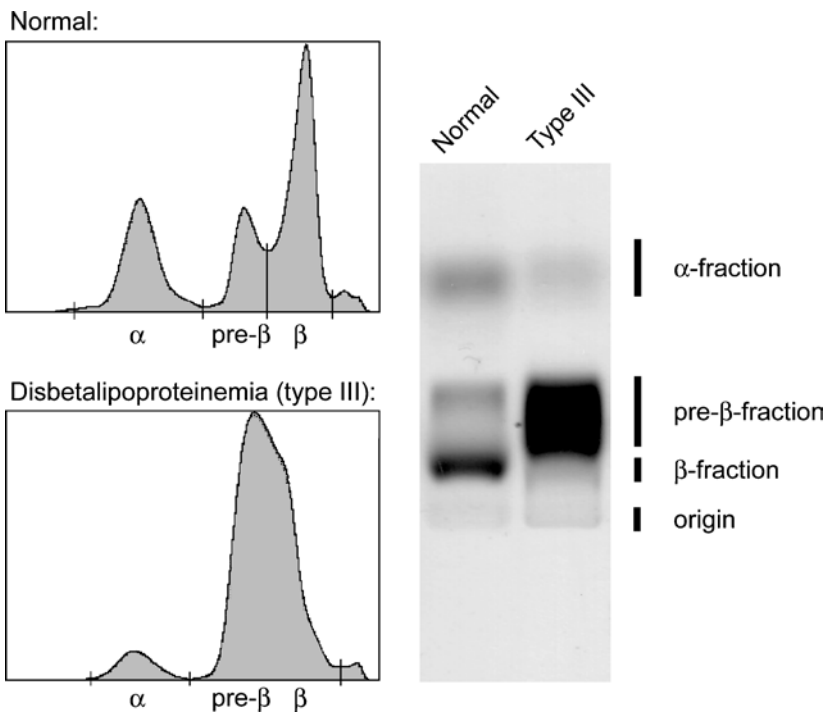

Fig. 5.2.3 Agarose gel electrophoresis of a normal serum (top) and a serum from a type III dyslipidemic patient (bottom), including the densitometric analysis of the two lanes (left and right, respectively). The normal serum sample shows an α-fraction, which is clearly separated from the pre-β- and the predominant β-fraction. In the serum sample from a type III dyslipidemic patient, the pre-β- and the β-fraction are highly elevated and cannot be separated (therefore termed broad-β-band), while the α-fraction is reduced

Table 5.2.1 *Reference values for lipoproteins stained with Sudan Black B.* HDL *High-density lipoprotein,* LDL *low-density lipoprotein,* VLDL *very-low-density lipoprotein*

Lipoproteins	Sudan Black B
α-Fraction (HDL)	0.22 – 0.53
Pre-β-fraction (VLDL)	0.04 – 0.23
β-Fraction (LDL)	0.39 – 0.69

very prominent, while the α-fraction (HDL) is reduced and chylomicrons are absent. The presence of chylomicrons in a serum sample is detected by the presence of a fraction at or near the application point (Fig. 5.2.3). For interpretation of the other phenotypes, see Fredrickson and Lees [31].

Chromatograms

Please refer to Fig. 5.2.4

Reference Values

Reference values depend on the stain used. Please refer to Table 5.2.1.

Typical Pathological Values

Familial dysbetalipoproteinemia (type III) will result in a highly elevated single fraction in the β-mobility to the pre-β-mobility region, and a reduced α-fraction (HDL).

Pitfalls

The results of the lipoprotein electrophoresis have to be interpreted in the context of other lipid parameters, like plasma total cholesterol and triglyceride levels. Patients with normal cholesterol and triglyceride values may sometimes show electrophoresis patterns that resemble pathologic patterns but should not be classified as such. For untreated type III patients, plasma total cholesterol levels should range from 7.5 to 13.0 mmol/l and triglycerides from 3.5 to 10.5 mmol/l. The presence of a broad-β-band in the absence of hyperlipidemia excludes familial dysbetalipoproteinemia (type III).

Cholestasis can lead to a similar occurrence of a broad-β-band. This results from the presence of lipoprotein X [Lp(X)], which migrates slightly closer to the application point than LDL but cannot be separated from it. Lp(X) is derived from bile lipids including free cholesterol and phospholipids that acquired apolipoproteins after they were released into the blood. However, this Lp(X)-derived broad-β-band migrates closer to the application point than LDL and can be distinguished from the broad-β-band of familial dysbetalipoproteinemia (type III).

Inappropriate storage of the serum will alter the mobility of the lipoproteins. When a hypertriglyceridemic serum is inappropriately stored, the pre-β-band and the β-band will merge and simulate the presence of a broad-β-band. This broad-β-band

migrates faster than in familial dysbetalipoproteinemia (type III) but may be difficult to distinguish. Concomitant to the merging of the pre-β-band and the β-band, the α-fraction will change its shape from a single peak to a misshaped double peak, which allows distinction from familial dysbetalipoproteinemia (type III).

VLDL-Cholesterol

Familial dysbetalipoproteinemia (type III) is characterized by the accumulation of chylomicron and VLDL remnants that are enriched in cholesterol compared to their native lipoproteins. Hazard et al. [38] observed that the VLDL cholesterol:plasma triglyceride ratio was increased in patients with familial dysbetalipoproteinemia (type III) compared to patients with other hypertriglyceridemas and first suggested this ratio to be useful in the diagnosis of familial dysbetalipoproteinemia (type III). Further research [32] in larger cohorts of hyperlipidemic patients confirmed these findings and revealed that a molar ratio of VLDL cholesterol to plasma triglyceride of > 0.69 (> 0.3 in mg/dl) was diagnostic for familial dysbetalipoproteinemia (type III) [17].

Principle

Ultracentrifugation of fasted serum leads to the separation of the VLDL lipoproteins from the LDL and the HDL lipoproteins. The cholesterol concentration is then measured in the VLDL fraction.

Preanalytical

- Specimen

The blood samples should be drawn after an overnight fast of at least 12 h. Fresh serum is recommended but the samples can be stored for several weeks at – 20°C. Plasma cannot be used.

- Reagents and Chemicals

Physiological NaCl solution (0.9%).

- Instrumentation

1. Ultracentrifuge and rotors.
2. Clinical chemistry analyzer or ELISA reader for the cholesterol analysis.

- Calibration

The cholesterol assays are commercial assays including cholesterol calibrations.

- QC

Serum from an individual with high VLDL cholesterol that has previously been analyzed and was stored at –20°C.

Analytical

- Procedure

Since untreated type III patients have plasma total cholesterol > 7.5 mmol/l and triglyceride levels > 3.5 mmol/l, only patients with cholesterol and triglyceride levels above these will usually be recruited for VLDL cholesterol determination. Therefore,

total cholesterol and triglyceride levels are measured before the VLDL cholesterol determination is performed.

Depending on the triglyceride concentration, the serum is diluted with 0.9% physiological NaCl solution to result in two different dilutions for each serum according to Table 5.2.2. Then 800 µl of each prediluted samples are mixed with 1200 µl 0.9% physiological NaCl solution and is transferred to an ultracentrifuge tube. Separation of cholesterol in the VLDL from the other lipoprotein fractions is done in a Beckmann TL100 ultracentrifuge using a TLA 100.3 rotor at 92,000 rpm (349,800 × *g*) for 2 h at 20°C.

Following ultracentrifugation, the bottom 800 µl (LDL and HDL) are collected (bottom layer) and the cholesterol concentration is determined. As a control, the top 800 µl including the creamy layer (VLDL) are also collected (top layer) and the cholesterol concentration is determined.

Calculation

The VLDL cholesterol is calculated as the difference from total cholesterol minus the bottom-layer cholesterol (LDL and HDL) and directly from the top-layer cholesterol (VLDL).

VLDL cholesterol from top layer = top layer cholesterol (VLDL) × dilution factor of the sample.

VLDL cholesterol from bottom layer = total cholesterol – (bottom cholesterol × dilution factor of the sample × 1.5).

The median VLDL cholesterol level is then calculated for the top layer and the bottom layer from the two dilutions for each sample. The difference between the VLDL cholesterol from the top and from the bottom layer should not exceed 30%.

Postanalytical

- Interpretation

The ratio of VLDL cholesterol to plasma triglycerides is calculated and compared to the cut-off.

Chromatograms

None.

Table 5.2.2 *Predilution of patients' serum samples according to total triglycerides*

Triglycerides	< 2.28 mmol/l (< 200 mg/dl)	Native and 1 + 1
Triglycerides	< 5.70 mmol/l (< 500 mg/dl)	1 + 1 and 1 + 3
Triglycerides	< 9.12 mmol/l (< 800 mg/dl)	1 + 3 and 1 + 5
Triglycerides	< 13.68 mmol/ (< 1200 mg/dl)	1 + 5 and 1 + 9
Triglycerides	> 13.68 mmol/l (> 1200 mg/dl)	1 + 9 and 1 + 19

Reference Values

1. VLDL cholesterol: < 1.1 mmol/l.
2. Ratio of VLDL cholesterol to plasma triglycerides: < 0.69 (in mmol/l) or 0.3 (in mg/dl).

Typical Pathological Values

Familial dysbetalipoproteinemia (Type III):

1. VLDL cholesterol: 1.8–8.4 mmol/l.
2. Ratio of VLDL cholesterol to plasma triglycerides: 0.72–1.12 (in mmol/l).

Pitfalls

Fasted blood samples have to be analyzed for this analysis. When non-fasting samples are analyzed, the triglyceride-rich chylomicrons will be included in the VLDL fraction during this procedure, which will lead to false results.

ApoE Genotype

Principle

In addition to several rare apoE alleles, three major isoforms have been identified in the population, termed E2, E3, and E4. The most common isoform is apoE3 with cystein at position 112 and arginine at position 158. The E2 and E4 isoforms differ from apoE3 by a cystein at position 158 and an arginine at position 112, respectively. The most frequent molecular cause of familial dysbetalipoproteinemia (type III) is the homozygous presence of the apoE2 isoform, which is associated with recessive inheritance of the disorder [62]. Several assays have been described to determine the apoE genotype using restriction fragment length polymorphism analysis and recently also melting curve analysis using fluorescence resonance energy transfer (FRET) on a LightCycler [2].

For the LightCycler assay, two fluorescently labeled oligonucleotides are designed that are complementary to the region encompassing cystein 112 and that allow FRET. One of the oligonucleotides is labeled with fluorescein at its 3' end and the other oligonucleotide, located within five nucleotides of the first oligonucleotide, is labeled with LC-red640 as fluorophore at its 5' end. When both oligonucleotides anneal to the PCR amplicon, fluorescence energy transfer between fluorescein and LC-red640 will occur, which can be detected as fluorescence at 640 nm. A second set of oligonucleotides is labeled with LC-red705 and fluorescein and is complementary to the region encompassing arginine 158. Hybridization of these two oligonucleotides will result in fluorescence at 705 nm. Fluorescence at both wavelengths is measured following PCR amplification, when the mixture is denatured and cooled to 40°C. Rising the temperature during the melting procedure will result in a rapid decrease in the fluorescence, when the oligonucleotide reaches its melting temperature. A mismatch under the oligonucleotide will lead to a reduction of the melting temperature and to an earlier decrease of the fluorescence. Since the melting temperatures for two alleles differ but are each highly reproducible, interpretation of the melting temperatures allows identification of the nature of the mutation.

Preanalytical

Specimen

EDTA-blood for DNA extraction. The samples are stable at room temperature for 2 days and can be shipped by overnight mail.

Reagents and Chemicals

1. DNA extraction kit for blood samples.
2. Oligonucleotides [2].
3. DNA master hybridization probes (Roche Molecular Biochemicals).

Instrumentation

LightCycler real-time PCR thermocycler.

Calibration

None.

Quality Control

Genomic DNA with at least two different apoE genotypes (E2, E4).

Analytical

Procedure

Genomic DNA (50 ng) is added to 1.2 µl $MgCl_2$ (25 mM), 1 µl of each amplification primer (10 µM), 0.4 µl of each fluorescently labeled oligonucleotide (10 µM), 2 µl dimethylsulfoxide, 2 µl DNA master hybridization probes (10 ×), and water to result in a final volume of 20 µl [2]. PCR is then performed in a LightCycler real-time PCR thermocycler using the following cycling conditions: denaturing at 94°C for 2 min, followed by 40 cycles of denaturation at 94°C for 0 s, annealing at 60°C for 10 s, and extension at 72°C for 15 s, with a ramping rate of 20°C/s.

The melting curves are generated by denaturing the sample at 94°C for 0 s, holding the sample at 40°C for 5 s, and then slowly heating the sample to 80°C with a ramp rate of 0.2°C/s, simultaneously monitoring the decline in fluorescence at 640 nm and 705 nm.

Calculation

None.

Postanalytical

Interpretation

Visual interpretation of the melting curves allows the assignment of the genotype. In this assay, the alleles with cystein 112 show a melting point of 55°C and alleles with arginine 112 of 63°C, when the fluorescence at 640 nm is measured. At 705 nm, the alleles with cystein 158 show a melting point of 59°C and alleles with arginine 158 of 67°C (Table 5.2.3).

Chromatograms

Please refer to Fig. 5.2.4.

Table 5.2.3 *Apolipoprotein E genotyping with melting curve analysis [2].* T_m *Melting point temperature*

Genotype	C112R (640 nm)		R158C (705 nm)	
	T_m 55 C	T_m 63 C	T_m 59 C	T_m 67 C
E2/E2	1	0	1	0
E3/E3	1	0	0	1
E4/E4	0	1	0	1
E2/E3	1	0	1	1
E2/E4	1	1	1	1
E3/E4	1	1	0	1

Reference Values

None.

Typical Pathological Values

None.

Pitfalls

Other mutations that are located under the fluorescently labeled oligonucleotides will result in reduced melting temperatures of the oligonucleotide and could allow misinterpretation of the genotype. However, each mutation has a characteristic melting temperature that is reproducible and strict adherence to this temperature will omit misinterpretation. It is noteworthy that the temperature of the melting peak depends on the ratio of PCR product to Mg^{2+} and oligonucleotide concentration. Hence

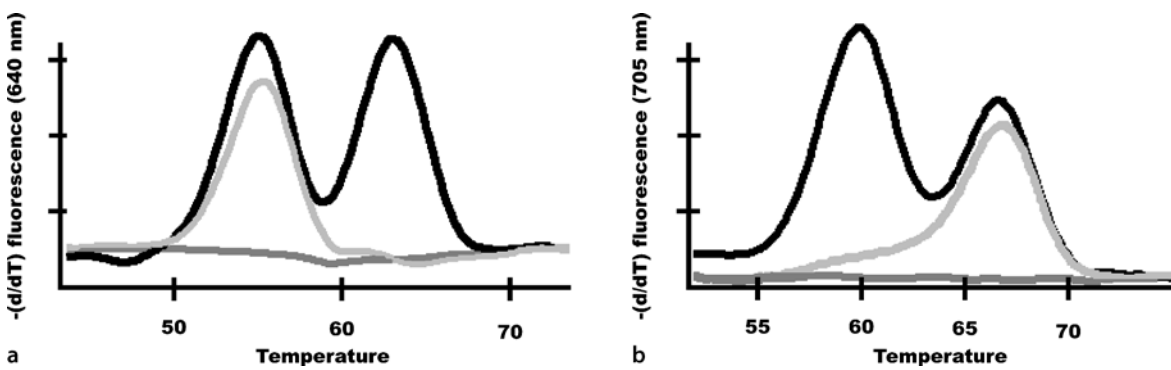

Figure 5.2.4 LightCycler assay to genotype the apolipoprotein E (apoE) isoforms. The cystein to arginine exchange at amino acid position 112 is identified at 640 nm and the arginine to cystein exchange at amino acid 158 in apoE is identified at 705 nm. LightCycler amplification with melting-curve analysis discriminates between the three major apoE alleles. Interpretation of the melting curves is done according to Table 5.2.3. The *dark line* represents a heterozygous E2/E4 genotype and the *light line* a homozygous E3/E3 genotype. The *light straight line* is the negative control (water)

the melting peak may vary according to the quantity of PCR product. In practice, the melting temperature for a given allele varies by < 1°C between different DNAs.

With this genetic approach only the common three apoE isoforms, E2, E3, and E4 are detected. Other rare mutations also leading to familial dysbetalipoproteinemia would be missed by this approach [88]. However, these rare variants are estimated to account for less than 1% of the apoE isoforms and they show a dominant inheritance of familial dysbetalipoproteinemia.

5.2.4.2 HL Deficiency (OMIM +151670)

Patients with HL deficiency present with hypercholesterolemia and hypertriglyceridemia, and accumulate VLDL remnants, triglyceride-rich LDL, and HDL [84]. These remnants mainly derive from a reduced catabolism of apoB-containing lipoproteins [82]. The disorder appears to be inherited in an autosomal recessive trait and is associated with an increased risk for coronary artery disease [8].

HL Activity

Whereas LPL predominantly hydrolyzes triglycerides in chylomicrons and VLDL, it has been shown that HL primarily hydrolyzes triglycerides and phospholipids from small VLDL, IDL, and HDL [82]. Like LPL, HL binds to the endothelium through heparan sulfate proteoglycans and is released upon heparin administration because of its higher affinity for heparin than for the endogenous heparan sulfate proteoglycans. Intravenous injection of a heparin bolus displaces the HL enzyme into postheparin plasma, where its activity can be quantified.

Principle

The HL catalytic assay measures the hydrolysis of a [^{14}C]- or [^{3}H]-triolein emulsion producing the [^{14}C]- or [^{3}H]-labeled free oleic acid. The labeled oleic acid is isolated by a selective extraction procedure and its mass is determined by liquid scintillation counting [40]. HL activity is calculated as nanomoles of oleic acid released per minute per milliliter of postheparin plasma. In addition to the described laboratory-made test, a commercial fluorimetric test for the measurement of HL activity is available (WAK-Chemie Medical, Bad Soden, Germany) [94].

Preanalytical

- Specimen

Blood samples are drawn after an overnight fast of at least 12 h. Preheparin and postheparin plasma samples are collected to analyze the HL activity. In general, 50–100 IU/kg heparin are injected intravenously and the postheparin plasma sample is collected 15 min later [41]. Samples should be immediately centrifuged and the plasma should be directly analyzed or frozen at – 70°C.

- Reagents and Chemicals

1. Scintillation vials.
2. Methanol:chloroform:heptane (56:50:4 by volume).
3. Toluene.

4. Glacial acetic acid.
5. Intralipid 10%.
6. 0.1 mM carbonate-bicarbonate buffer, pH 10.5.
7. 0.2 mM Tris buffer, pH 8.8.
8. BSA.
9. NaCl.
10. Ferric acid.
11. [^{14}C]- or [^{3}H]-labeled triolein.
12. Heat-inactivated pooled human serum [41].

Instrumentation

1. Liquid scintillation counter for either [^{14}C] or [^{3}H].
2. Sonicator (Fisons Scientific Instruments).
3. Water bath or incubator.

Calibration

None.

Quality Control

Controls can be obtained by pooling postheparin plasma from another set of fasted volunteers, which is stored at – 70°C as aliquots [41].

Analytical

Procedure

The Intralipid emulsion containing [^{14}C]-triolein is produced by sonication. Therefore, 1 ml of Intralipid, 5 µCi of [^{14}C] triolein, 2.75 ml of 200 g/l BSA, and 4.68 ml of 0.2 mM Tris buffer, pH 8.8 are mixed and sonicated at amplitude 10, with 24 cycles of 20 s on, 10 s off, and mixing the emulsion by inversion after every fourth cycle. After sonication, 2.58 ml of 3.24 M NaCl (in 0.2 mM Tris buffer, pH 8.8) will be added and the emulsion will be mixed by inversion [40]. This results in the inactivation of the LPL activity also present in the postheparin sample.

Ten microliters of each sample will be added to 500 µl of the triolein emulsion in triplicate and the HL-catalyzed triglyceride hydrolysis will be allowed to proceed for 1 h at 28°C. The reaction is stopped by adding 5.33 ml of methanol:chloroform: heptane (56:50:4 by volume) and vigorous shaking.

To extract the liberated fatty acids, 1.5 ml of 0.1 mM carbonate-bicarbonate buffer, pH 10.5 is added and the mixture is shaken for 10 s. Centrifugation for 45 min at 1500 × *g* in a swing-out rotor will separate the water from the lower organic phase. In a scintillation vial, 2 ml of the upper water phase is mixed with 50 µl of glacial acetic acid containing 500 µg of ferric acid before the scintillation liquid is added [16 ml of Ecoscint:toluene (7:1 volume)]. Liquid scintillation counting is done for 5 min and the HL activity is calculated from the difference in counts between the blank and the sample vials [40].

Calculation

Enzyme activity (µmol/ml/h)
= (counts in probe – counts in blank) × 100/counts in blank × 2.4.

Postanalytical

- Interpretation

Homozygous mutant and compound heterozygous mutant patients have reduced or absent HL activity, while heterozygous carriers usually have normal HL activity.

Chromatograms

None.

Reference Values

Since there is no standardization of the HL activity assays, the reference values depend on the assay used [40]. HL activity in women lies in the range 85–282 nmol/ml/min, while that for men is 141–648 nmol/ml/min.

Typical Pathological Values

Inactivating HL mutations lead to basically absent HL activity in postheparin plasma from homozygous individuals [81, 82]. Heterozygous carriers of a HL mutation have intermediate HL activity, which is lower than in normal controls. However, this lower HL activity does not translate into changes in lipoprotein metabolism, leaving these patients with similar lipoprotein profiles to normal controls [81, 82].

Pitfalls

The inhibition of LPL by sodium chloride may be incomplete. Specific inhibition is achieved by the addition of neutralizing anti-LPL antibodies.

5.2.5 Hypercholesterolemia

Most of the monogenic hypercholesterolemias are codominantly inherited disorders with elevated LDL levels. Heterozygous carriers usually have total cholesterol levels of > 6.5 mmol/l and homozygous or compound heterozygous patients usually have total cholesterol levels of > 13 mmol/l. The triglyceride levels are usually < 2.0 mmol/l and the HDL cholesterol levels are normal or reduced. Two forms of codominantly inherited hypercholesterolemia can be distinguished, familial hypercholesterolemia caused by defects in the LDLR gene and familial defective apoB-100 caused by point mutations in the apoB gene. More recently, the molecular basis of a recessive form of hypercholesterolemia has been unraveled, namely mutations in the gene of autosomal recessive hypercholesterolemia.

5.2.5.1 Familial Hypercholesterolemia (OMIM 143890)

Familial hypercholesterolemia (FH) is one of the most common genetic disorders in lipoprotein metabolism, and causes elevated cholesterol levels. This autosomal dominant disorder with a prevalence of about 1/500 in Western countries is caused by mutations in the LDLR gene. The LDLR defect impairs the catabolism of LDL and results in elevation of plasma LDL-cholesterol. Untreated heterozygous FH patients have 2–3 times elevated cholesterol levels and have a 100-fold increased risk to die

from coronary artery disease before the age of 40 years, while a 5-fold increased risk is still observed for patients over 40 years [86].

Worldwide, more than 900 mutations have been detected in the LDLR gene, and these are distributed over the entire coding region of the gene. Hence, the entire coding region of the LDLR including the exon-intron boundaries has to be screened for mutations. Most of the mutations have been found in two functional domains, the binding domain (42%) and the epidermal growth factor (EGF) precursor homology domain (47%). However, 3.4% of the mutations have been detected in the cytoplasmic domain, and 1.7% in the transmembrane domain and in the promoter region [39]. The nature of the mutations is diverse, with 58.9% missense mutations, 21.1% minor rearrangements (1–24 bp), 13.5% large rearrangements (>25 bp), and 6.6% splice site mutations. These mutations have been collected in two registers and can be accessed online (www.ucl.ac.uk/fh/ and www.umd.necker.fr/LDLR/research.html). Despite of the numerous mutations detected in the LDLR gene, an estimated 15–30% of the cases with clinically documented FH lack mutations in the LDLR and have no mutation in the apoB gene. Recently, mutations in the proprotein convertase subtilisin/kexin type 9 (PCSK9) have been associated with FH in a small number of cases [1], but subsequent studies revealed that mutations in PCSK9 will only explain a minor part of the FH patients without a mutation in the LDLR [14].

To diagnose FH, LDL-binding assays of fibroblasts or a genetic screening of the LDLR gene can be performed. For genetic screening, two complementary methods have to be applied to detect small mutations like single-nucleotide mutations and to detect large insertions or deletions. To screen for small mutations SSCP, DHPLC [7, 9], and direct sequencing [29] have been applied successfully, while Southern blot and long-range PCR [56, 72] have been used to detect larger deletions and insertions. Recently, a multiplex ligation-dependent probe assay was also developed to detect large deletions and insertions [93].

LDLR Binding Assay

Principle

Many cells, including skin fibroblasts, bind and internalize LDL through the LDLR. This opens the possibility of testing the binding capacity of the LDL receptor in cultivated skin fibroblasts of FH patients. The fibroblasts are incubated with radiolabeled LDL and the internalization of the labeled LDL is measured and compared to the internalization of fibroblasts from a normolipidemic donor.

Pre-Analytical

- Specimen

Fibroblasts cultivated from skin biopsy samples.

- Reagents and Chemicals

1. Dulbecco's modified Eagle's medium (DMEM), supplemented with L-glutamine (Sigma).
2. Sterile dishes or multiwell plates.
3. Antibiotic-antimycotic (100×; Gibco).
4. Fetal calf serum (FCS).
5. LDL (Biomedical Technologies), or isolated from plasma.

6. ^{125}I-LDL (Biomedical Technologies).
7. Lipoprotein-deficient serum (LPDS; Biomedical Technologies).
8. Sodium hydroxide (NaOH) 0.2 mol/l.
9. Protein assay (DC Bio-Rad).

Instrumentation

1. Sterile cell-culture facility.
2. Permit to work with ^{125}I-isotope.
3. Gamma-counter.

Calibration

None.

Quality Control

Parallel analysis of control skin fibroblasts from normolipidemic donors and, ideally, from patients with established diagnosis of FH is necessary.

Analytical

Procedure

Human skin fibroblasts are cultured from skin biopsy samples. The dermis is cut into small pieces (0.5 mm on each side) and placed in a dish containing DMEM, 10% (v/v) FCS, and 1% (v/v) antibiotic-antimycotic solution. When these primary cultures are confluent they are split into novel dishes. Cells between passages three and six are used for experiments.

For the ^{125}I-LDL binding assay, cells cultured in 24-well plates are incubated in DMEM containing 10% LPDS overnight [48]. Cells are washed with DMEM and incubated for 4 h at 37°C with DMEM containing LPDS (10%, v/v) and 10 µg/ml ^{125}I-LDL in the presence or absence of 400 µg cold LDL. After extensive washing of the cells with DMEM, the cells are solubilized with 0.1 mol/l NaOH and the amount of cell-associated radioactivity is determined using a gamma-counter. The protein content of each well is analyzed in parallel with a protein assay.

Calculation

Total LDL binding is calculated as (radioactivity in the cell lysate)/(total lysate protein concentration). The results obtained in the presence of excess cold LDL reveal the nonspecific binding. Specific binding is calculated by subtraction of nonspecific binding from total binding.

Postanalytical

Interpretation

LDL-binding of the patients' fibroblasts is compared to the binding of control fibroblasts from normolipidemic donors.

Chromatograms

None.

Reference Values

None.

Typical Pathological Values

In homozygous FH patients, specific LDL binding to fibroblasts is reduced by more than 90% compared to that for control fibroblasts from normolipidemic individuals. Heterozygous carriers of a FH mutation have significantly reduced LDL binding compared to normolipidemic individuals like unaffected family members.

Pitfalls

Basal LDL receptor activity in fibroblasts is relatively low in cells cultured in DMEM containing 10% FCS. To upregulate the LDLR and to increase the read-out of the assay it is crucial to preincubate the cells in lipoprotein-deficient medium prior to performing the assay.

Denaturing High-Pressure Liquid Chromatography

Principle

This method separates heteroduplex and homoduplex DNA based on their different electrophoretic mobilities under partially denaturing conditions [61]. A specific PCR product is first denatured by heat before cooling down to result in complementary homoduplexes for homozygous DNAs. In contrast, heterozygous DNAs also form heterodulexes that are not fully complementary but have a mismatch at the site of the mutation. These heteroduplexes have a lower melting temperature than the corresponding homoduplexes. Separation of the different complexes is done by high-performance liquid chromatograph (HPLC) analysis run at different temperatures ranging from nondenaturing to denaturing conditions to include the partially denaturing temperature of the heteroduplex. At this temperature the partially denatured heteroduplex elutes faster from the DNASep column than the nondenatured homoduplex. This method preferentially detects heteroduplexes as new chromatographic peaks and is less well suited to detect homozygous mutations [9].

Preanalytical

- Specimen

EDTA-blood for DNA extraction. The samples are stable at room temperature for 2 days and can be shipped by overnight mail.

- Reagents and Chemicals

1. DNA extraction kit for blood samples.
2. *Taq* polymerase, dNTPs and a PCR buffer.
3. Buffer A: 0.1 M triethylammonium acetate, 0.025% acetonitrile, pH 7.0.
4. Buffer B: 0.1 M triethylammonium acetate, 25% acetonitrile, pH 7.0.

- Instrumentation

HPLC system with an ultraviolet detector (254 nm) and a nonporous poly-(styrene-divinylbenzene) particle based C_{18} reversed-phase column, DNASep (Transgenomic, Omaha, NE, USA).

- Calibration

None.

■ Quality Control

Genomic DNA with and without a known mutation in the amplified region.

Analytical

■ Procedure

Nineteen different PCRs are performed to amplify the promoter region and the 18 exons of the LDLR [7]. Heating the PCR products to 94°C for 2 min and slowly cooling to 60°C within 30 min results in homoduplexes and heteroduplexes, which are separated on the DHPLC system. The DNA duplexes are eluted with a linear acetonitrile gradient prepared with buffer A and buffer B at a flow rate of 0.9 ml/min. The usual gradient increases the initial percentage of buffer B (40–50%) in two steps, with a small increase within the first 1–4 min to 50–70% buffer B and a larger increase within the next 7–10 min to 100% buffer B. The optimal melting temperature and the gradient composition can be calculated with the freely available software "DHPLC Melt Program" for each PCR product (http://insertion.Stanford.edu/melt.html) [51].

■ Calculation

None.

Postanalytical

■ Interpretation

DHPLC chromatograms are inspected for abnormal elution of PCR products in comparison to PCR products from genomic DNA with a known genotype. While homoduplexes elute mainly as a single peak at a certain temperature (Fig. 5.2.5), heteroduplexes show two and more elution peaks.

Chromatograms

Please refer to Fig. 5.2.5.

Reference Values

None.

Typical Pathological Values

None.

Pitfalls

Homozygous mutations will often be missed with this method. However, this can be overcome by supplementing the sample to be investigated with equal amounts of a sequenced sample lacking mutations. This will result in heteroduplexes formed between a mutant and the supplemented wild-type allele following the initial heat treatment and slow cooling of the PCR products. These heteroduplexes will be detected as abnormal patterns on the DHPLC.

Polymorphisms in the LDLR gene will also result in heteroduplexes and an abnormal migration pattern, when a DNA is heterozygous for the polymorphism. These polymorphisms are not causing FH but will interfere with the DHPLC analysis. Several of these polymorphisms are located in the region amplified for the DHPLC

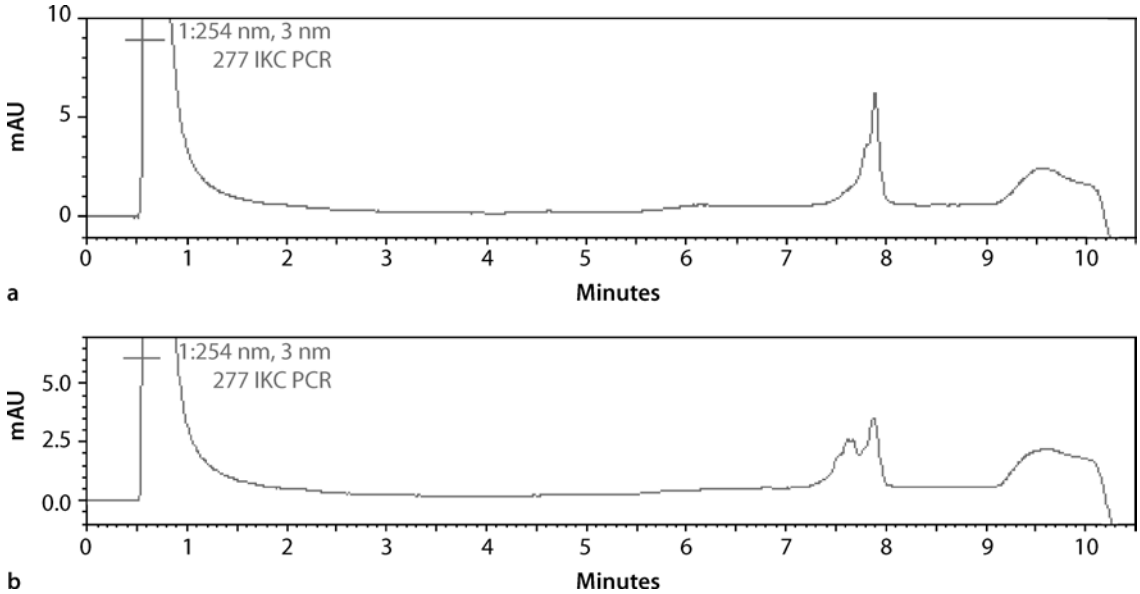

Fig. 5.2.5 a,b Denaturing high-pressure liquid chromatography chromatograms of two patient samples run at the recommended temperature (60°C) to detect mutations. **a** Sample without a mutation. The elution peak at 7.8 min represents homoduplexes. **b** Sample with a heterozygous mutation. In addition to the elution peak at 7.8 min for the homoduplexes an additional peak for heteroduplexes is visible at 7.6 min

analysis including seven in the coding region. However, the abnormal DHPLC pattern for each polymorphism is characteristic and can be distinguished from a novel mutation resulting in another pattern. Nevertheless, DHPLC analysis of exon 12 may be hampered because exon 12 contains two exonic polymorphisms that result in several abnormal DHPLC patterns.

Follow-up Investigation

All abnormal patterns have to be investigated by sequencing analysis to determine the nature of the mutation (for sequencing analysis see section 5.2.3.2 on apoCII deficiency). Comparison of the mutation to known mutations will help to evaluate whether a mutation causes FH or whether the mutation is silent or has no influence on LDLR activity.

Long-Distance PCR

Principle

Long-distance PCR is less labor-intensive compared to the previously used Southern blot analysis and relatively quick to detect large deletions and insertions in the LDLR. The method is based on the amplification of the entire coding region of the LDLR gene by five overlapping PCR reactions (Fig. 5.2.6) [56, 72]. Any large deletion and insertion will result in a reduction or in an increase of the size of one or two

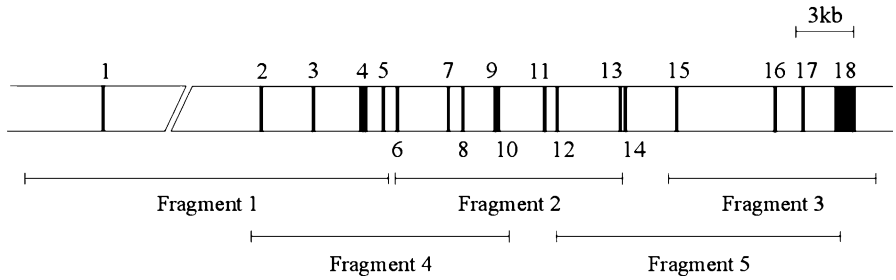

Fig. 5.2.6 Long-distance polymerase chain reaction (PCR) to detect large deletions and insertions in the low-density lipoprotein receptor (LDLR). The structure of the LDLR gene is shown from exon 1 through 18. The five fragments produced by the five long-distance PCRs are outlined. PCR1 covers exons 1 – 5, PCR2 exons 6 – 13, PCR3 exons 15 – 18, PCR 4 exons 2 – 10, and PCR5 exons 12 – 18

neighboring PCR products. These PCR products will be visualized following separation by agarose gel electrophoresis.

Preanalytical

Specimen

EDTA-blood for DNA extraction. The samples are stable at room temperature for 2 days and can be shipped by overnight mail.

Reagents and Chemicals

1. DNA extraction kit for blood samples.
2. Expand Long Template PCR System (Roche Molecular Biochemicals).
3. 1 × Tris-borate EDTA (TBE) buffer, pH 8.0: 89 mM Tris base, 89 mM boric acid, 2 mM EDTA.
4. Agarose: Seakem Gold (Cambrex).
5. DNA size standard: molecular weight marker XV (Roche Molecular Biochemicals).
6. Ethidium bromide: 2.5 μM ethidium bromide in 1 × TBE.

Instrumentation

1. Thermocycler.
2. Submarine gel chamber with an external circulation through heat exchangers to cool the electrophoresis buffer.
3. Power supply for electrophoresis, eventually a pulsing instrument.
4. Ultraviolet documentation system.

Calibration

None.

Quality Control

Genomic DNA without a deletion or an insertion in the LDLR.

Analytical

■ Procedure

Genomic DNA is amplified in five independent 50 µl PCR reactions with the following concentrations: 400 nM primer, 500 µM dNTPs, 2.6 U Expand Long Template enzyme, and 400 ng genomic DNA in 1 × Expand Long Template PCR buffer 3. The reaction is covered with 30 µl mineral oil and the PCR amplification is performed on a thermocycler [56, 72]. The PCR products are separated by 0.6% agarose gel electrophoresis in 1 × TBE. Large agarose gels (20 cm) are necessary to separate a difference in size of ≤ 1 kb between two PCR amplifications of 10–15 kb. The PCR products are visualized on the agarose gel by staining for 15 min with ethidium bromide in1 × TBE.

Calculation

None.

Postanalytical

■ Interpretation

The presence of an additional PCR amplification indicates the presence of an allele with either an insertion or a deletion (Fig. 5.2.7).

Chromatograms

Please refer to Fig. 5.2.7.

Reference Values

None.

Typical Pathological Values

None.

Pitfalls

Long-distance PCR can result in several unspecific amplicons that interfere with the analysis. Applying more stringent condition to the PCR, like increasing the annealing temperature or reducing the Mg^{2+} concentration will help to obtain a single fragment amplified. Regular agarose gel electrophoresis will identify deletions and insertions ≥ 1 kb but may miss smaller changes [72]. To improve the sensitivity for smaller changes ≤ 1 kb, field-inversion gel electrophoresis may be applied for a better separation of these large PCR amplicons [56].

Follow-up Investigation

To define the break points of the deletion or the insertion, further long-PCR amplifications have to be applied. For this, a set of primers is chosen that dissect the 3–8 kb of the region of interest into 1-kb pieces (Fig. 5.2.8). PCR on a heterozygous DNA will result in two amplicons, as long as the region with the deletion is contained in the amplified region. When the deletion or insertion is not part of the amplified region, only one amplicon will occur on the agarose gel. From these experiments the approximate size and location of the deletion or insertion can be determined. Sequencing of the remaining 1–2 kb will allow detection of the break points of the deletion or insertion (for sequencing analysis see section 5.2.3.2).

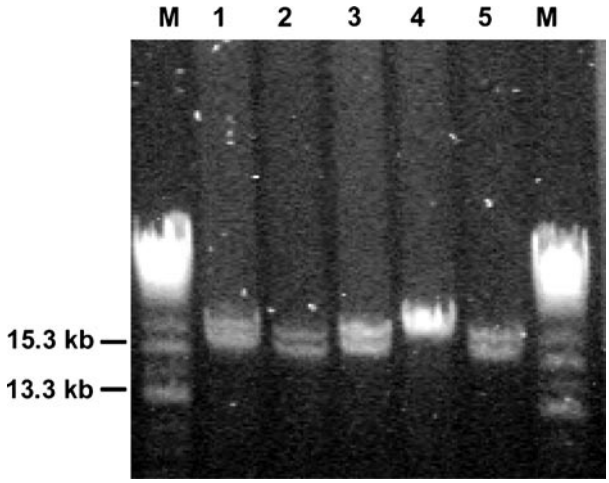

Fig. 5.2.7 Long-distance PCR for the ≈17-kb fragment 1 is shown. The result of five members (*1 – 5*) of a familial hypercholesterolemia (FH) family is shown. Member number 4 is not affected and shows only one amplicon. Members 1, 2, 3, and 5 have heterozygous FH and show a second amplicon carrying a 1.3-kb deletion of exon 4

5.2.5.2 Familial Defective ApoB-100 (OMIM 144010)

Familial Defective apoB-100 (FDB) is characterized by hypercholesterolemia, xanthomas and premature atherosclerosis. Hence, FDB is clinically not distinguishable from FH. FDB is an autosomal dominant disease with a prevalence of 1:1000 in Caucasians. However, the prevalence varies widely among Caucasians depending on the regional location. The highest prevalence is found in Switzerland, with 1:209 persons of the population carrying the mutation. In contrast, no FDB has been detected thus far in Finland [67]. Other mutations in the apoB gene have been associated with FDB, like R3500W, R3480W, and R3531C. However, these mutations are rare and their clinical significance is not yet clear [36, 79, 90].

Detection of ApoB R3500Q

Principle

Several commercial assays are available to detect the R3500Q mutation in the apoB gene. The assays depend on the amplification of the apoB gene region encompassing the G9775A mutation, leading to the R3500Q exchange. Detection of the mutation can be done by techniques like sequencing, 5' nuclease assays, allele-specific amplification, or by melting-curve analysis using fluorescence resonance energy transfer (FRET) on a LightCycler [70].

The LightCycler assay (Roche Diagnostics) is based on a melting-curve analysis to detect the mutation. Two fluorescently labeled oligonucleotides are designed that allow FRET. One of the oligonucleotides is labeled with fluorescein at its 3' end and the other oligonucleotide located within five nucleotides of the first oligonucleotide is labeled at its 5' end with the fluorophore LC-red640. When both oligonucleotides

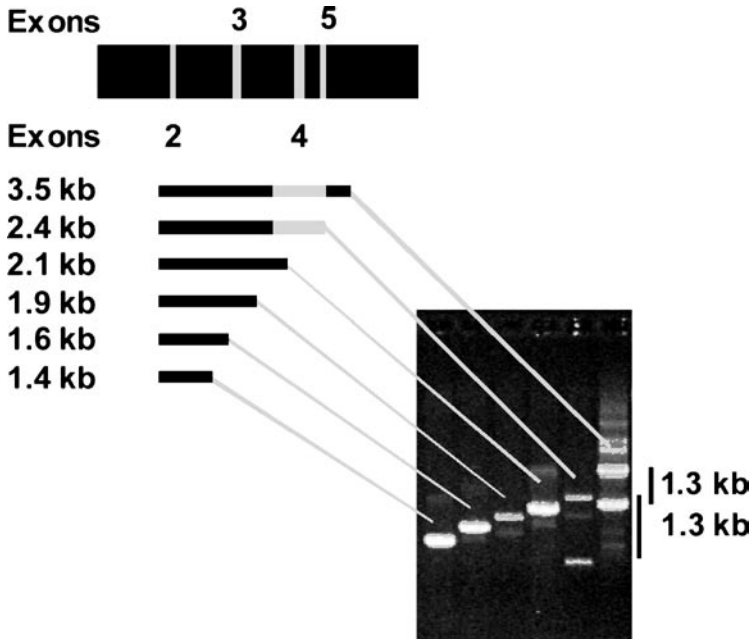

Fig. 5.2.8 Determining the deletion break-points in a heterozygous FH patient. Long-distance PCR amplification located the deletion between exons 2 and 5 (3.5 kb). A forward primer and a set of reverse primers have been designed to amplify this region (3.5 kb) and smaller regions lacking consecutive 3' sequences (2.4 – 1.4 kb). PCR over the largest two regions resulted in two amplicons with a size difference of 1.3 kb, while PCR over the smaller regions resulted in only one amplicon. This experiment locates the 1.3-kb deletion (*light gray*) to a region including exons 4 and 5

anneal to the PCR amplicon, fluorescence energy transfer between fluorescein and LC-red640 will occur, which can be detected as fluorescence at 640 nm. Such fluorescence is detected when the mixture is denatured and cooled to 40°C following PCR amplification. Raising the temperature during the melting procedure will result in a rapid decrease in the fluorescence, when the oligonucleotide reaches its melting temperature. A mismatch under the oligonucleotide will lead to a reduction of the melting temperature and to an earlier decrease in the fluorescence. Since the melting temperatures for two alleles differ but are each very reproducible, interpretation of the melting temperatures allows identification of the nature of the mutation.

Preanalytical

■ Specimen

EDTA-blood for DNA extraction. The samples are stable at room temperature for 2 days and can be shipped by overnight mail.

■ Reagents and Chemicals

1. DNA extraction kit for blood samples.
2. Commercial LightCycler-apoB mutation detection kit (Roche Molecular Biochemicals).

■ Instrumentation

LightCycler real-time PCR thermocycler.

■ Calibration

None.

■ Quality Control

Genomic DNA with at least two different apoB genotypes at position 9775 (G/G, G/A, and ev. A/A).

Analytical

■ Procedure

According to the manufacturers instructions.

■ Calculation

None.

Postanalytical

■ Interpretation

Visual interpretation of the melting curves allows the assignment of the genotype. In this assay, the G-allele has a melting point of 63°C and the A-allele of 54°C. The presence of only one melting peak at 63°C identifies a homozygous G/G DNA and a sole peak at 54°C a homozygous A/A DNA. The presence of two peaks in a DNA identifies a heterozygous DNA G/A [70].

Chromatograms

Please refer to Fig. 5.2.9.

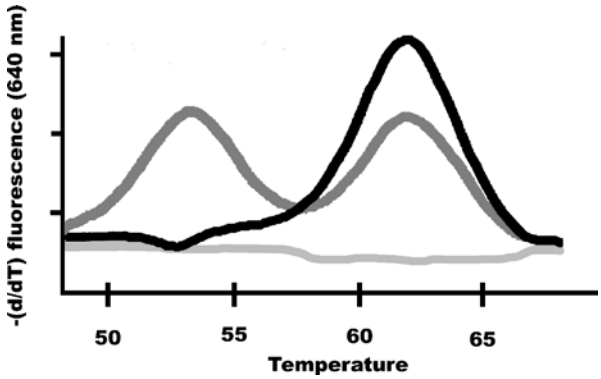

Fig. 5.2.9 LightCycler assay to detect the apolipoprotein B (apoB) R3500Q mutation. Identification of the adenine to guanine exchange in exon 26 of the apoB gene, which results in the exchange of arginine for glutamine at position 3500. A LightCycler analysis with melting-curve analysis discriminates between the two alleles. The G-allele has a melting point of 63°C and the A-allele a melting point of 54°C. The *black* melting curve shows one peak at 63°C representing the GG-genotype (wild type). The *grey* melting curve shows two peaks representing a heterozygous DNA (G/A). The flat light gray line is the negative control (water)

Reference Values

None.

Typical Pathological Values

None.

Pitfalls

Other mutations that are located under the fluorescently labeled oligonucleotides will result in reduced melting temperatures of the oligonucleotide and could allow misinterpretation of the genotype. However, each mutation has a characteristic melting temperature that is reproducible, and strict adherence to this temperature will omit misinterpretation. It is noteworthy that the temperature of the melting peak depends on the ratio of PCR product to Mg^{2+} and oligonucleotide concentration. Hence, the melting peak may vary according to the quantity of PCR product. In practice, the melting temperature for a given allele varies < 1°C between different DNAs.

5.2.6 HDL Deficiency

Numerous clinical and epidemiological studies have demonstrated the inverse and independent association between HDL cholesterol and the risk of fatal and nonfatal coronary heart disease events. As a consequence, many national and international guidelines endorse the screening for low HDL cholesterol and define 1.05 mmol/l (40 mg/dl) as the cardiovascular risk threshold value [18].

To date, the genetic origin of low HDL cholesterol has been unraveled only to a minor degree. Family studies in humans have identified at least 30 quantitative trait loci that cover almost all chromosomes. Most known mutations underlying monogenic forms of HDL deficiency have been found in genes that encode proteins involved in the formation, maturation, and catabolism of HDL.

However, very low plasma levels of HDL cholesterol are also found in patients with genetically disturbed metabolic pathways that are indirectly linked to HDL metabolism. For example, many patients with lipid storage diseases like Gaucher's disease (glucocerobrosidase deficiency, OMIM 230800–231000), Nieman-Pick disease types A or B (sphingomyelinase deficiency, OMIM 257200 and 607616, respectively), Niemann-Pick disease type C (OMIM 257220), hypertriglyceridemia, or diabetes mellitus present with low HDL cholesterol [22].

Here we focus on monogenic low HDL cholesterol disorders, which result from mutations in three pivotal genes for HDL metabolism, namely apoA-I, ATP binding cassette transporter A1 (ABCA1). and lecithin:cholesterol acyltransferase (LCAT). Mutations in these three genes were found in about 16% of men and women with HDL cholesterol levels below the fifth percentile [12]. Such heterozygous carriers of mutations usually have HDL-C levels < 0.9 mmol/l, while homozygous or compound heterozygous carriers have been identified by complete HDL deficiency. In the following, we will use the term HDL deficiency to describe the real or virtual absence of HDL as measured by routine clinical chemistry tests for HDL cholesterol, which have a lower detection limit of about 0.1 mmol/l (3–4 mg/dl) [69].

Although of much less clinical relevance, it must be emphasized that certain disturbances of HDL metabolism cause familial aggregation of elevated HDL cholesterol

concentration (i.e., familial hyperalphalipoproteinemia). CETP deficiency is the as yet only example of familial hyperalphalipoproteinemia for which the metabolic and molecular basis is resolved.

5.2.6.1 ApoA-I Deficiency (OMIM 107680)

As the quantitatively predominant HDL component, apoA-I is crucial for HDL formation. It is also needed to activate LCAT and to mediate the interaction between HDL and cell surface receptors, such as scavenger receptor B1 or plasma membrane transporters such as ABCA1 [42]. Numerous non-sense and missense mutations in the apoA-I gene have been found to interfere with the formation of HDL, and to cause gene-dose-dependent decreases in HDL cholesterol, with a virtual absence of HDL in homozygotes and half-normal levels of HDL cholesterol in heterozygotes [22, 89, 92].

Patients carrying two functionally relevant mutations – being either homozygous or compound heterozygous – present with HDL deficiency and with two different clinical hallmarks, namely xanthomas and corneal opacities. Xanthelasmas and planar xanthomas have also been described in adult patients and frequently these patients are affected with premature manifest coronary heart disease (below 50 or even 40 years of age). Patients who are homozygous or hemizygous for missense mutations, which lead to trace amounts of a structural apoA-I variant in plasma (typical apoA-I level 0.01–0.05 g/l), present without xanthomas but often with corneal opacities. Above the age of 40 years, the corneal cloudings are usually detectable by physical inspection and are indistinguishable from those found in patients with LCAT deficiency or fish-eye disease. At a younger age, slit-lamp examination is usually needed to detect the cloudings [22, 92].

Heterozygous carriers of functionally relevant mutations usually present with HDL cholesterol levels that are frequently below the fifth percentile. As would be expected, apoA-I levels are also frequently below the fifth percentile (i.e., < 1.05 g/l and < 1.1 g/l in Caucasian men and women, respectively). In most cases, heterozygous carriers of apoA-I variants do not present with specific clinical symptoms. An important exception are some structural apoA-I variants with amino acid substitutions in the amino terminus, which have been detected in patients with familial amyloidosis of the liver, the intestine, the kidney, the heart, peripheral nerves, and in the skin. In addition, some apoA-I variants like apoA-I L178P or L159P have been associated with increased risk of premature coronary heart disease or enhanced progression of carotid intima media thickness, whereas others did not show this association, or were even claimed to have reduced cardiovascular risk and advocated as possible agents for the treatment or prevention of atherosclerosis (notably apoA-I $R173C_{Milano}$) [22, 43, 53].

Sequencing of the ApoA-I Gene

The diagnosis of apoA-I deficiency requires sequencing of the apoA-I gene and the demonstration of a functionally relevant mutation. All known apoA-I mutations are sporadic. The apoA-I gene consists of 4 exons encoding the 267-amino-acid-long

pre-pro-apoA-I. This size allows direct genetic analysis including sequencing analysis. Several amplification primers for the apoA-I gene have been published that can be used for sequencing analysis [44, 73]. For technical details on sequencing analysis see section 5.2.3.2.

5.2.6.2 ABCA1 Deficiency and Tangier Disease (OMIM 205400)

The ABCA1 gene resides on chromosome 9q22-q31, contains 50 exons, and codes for a 2261-amino-acid-long membrane protein. As a member of the ATP binding cassette transporter gene family, ABCA1 consists of two transmembrane domains, each formed by six transmembrane alpha helices, and two intracellular nucleotide-binding domains. ABCA1 mediates the efflux of cellular cholesterol and phospholipids onto apoA-I and thereby plays a central role in both regulating cellular cholesterol homeostasis, and in the formation of HDL [76].

At present, more than 100 different mutations in the human ABCA1 gene have been described [78]. Heterozygous carriers of non-sense mutations, or functionally relevant missense mutations in the ABCA1 gene, present with HDL cholesterol concentrations typically below the fifth percentile but without specific clinical hallmarks. In large population studies, functionally relevant mutations in the ABCA1 gene were found to account for up to 10% of the cases with HDL cholesterol levels below the first percentile [33]. Heterozygosity for mutations in ABCA1 was associated with increased carotid intimal thickening and coronary event rates [43].

Patients with two defective ABCA1 alleles (i.e., Tangier disease) have very low or undetectable levels of HDL cholesterol (< 0.25 mmol/l). Frequently, serum levels of total and LDL cholesterol are also low, whereas serum levels of triglycerides are mildly elevated (> 2.3 mmol/l). The clinical presentation of Tangier disease varies considerably. Enlarged orange tonsils are found predominantly in children or adolescents, but can be undetectable or overlooked in adults because the tonsils have either been removed or are scarred. Adult patients are brought to medical attention mostly because of hepatomegaly, splenomegaly, or premature coronary heart disease. These symptoms result from lipid storage in cells of the reticuloendothelial system (i.e., macrophages, Kupfer cells, or histiocytes). Another limiting symptom for quality of life is peripheral neuropathy, which in Tangier disease has a highly variable expression. Clinically symptomatic patients present with two different forms. The multifocal demyelinating form is either mononeuropathic or asymmetric polyneuropathic, and affects motor and sensory nerves of the limbs or the head. The resulting symptoms (i.e., muscle weakness and sensory loss) are frequently transient and the course is benign. In contrast, the second form of Tangier neuropathy, which is a syringomyelia-like syndrome, is progressive and frequently debilitating. It starts with loss of pain and thermal sensation, atrophy, and paresis, especially in the face and the distal parts of the upper limbs. Sensory loss can progress to the trunk and the lower limbs. If present, clinical symptoms can be isolated or combined. With the widespread screening of HDL cholesterol in general populations, more and more Tangier disease patients have been identified who do not present with clinical symptoms [3].

The findings of virtual HDL deficiency and low levels of apoA-I are not sufficient for the diagnosis of Tangier disease, which ultimately requires ABCA1 gene sequence

analysis. Due to the large size of the ABCA1 gene, molecular diagnostics is extensive and therefore expensive. The following two tests can help to increase the likelihood for the diagnosis of Tangier disease in HDL-deficient patients:

1. The more widely accepted test is the cholesterol efflux assay on cultivated skin fibroblasts. After equilibration with radiolabeled cholesterol, fibroblasts are incubated with albumin in the presence or absence of lipid-free apoA-I. ApoA-I substantially increases cholesterol efflux from normal cells but not from Tangier cells [11, 30].
2. Nondenaturing two-dimensional electrophoresis and subsequent anti-apoA-I immunoblotting of normal plasma helps to discriminate a bulk of HDL, which has electrophoretic alpha mobility (α-HDL), from a quantitatively minor proportion, which has electrophoretic pre-β-mobility (preβ_1-HDL). In plasma from Tangier patients the latter particle is the only apoA-I containing lipoprotein [4, 26].

Cholesterol Efflux Assay

Principle

In the presence of lipid-free apoA-I, ABCA1 mediates cholesterol efflux from many cells including skin fibroblasts. This opens the possibility to test the activity of ABCA1 in cultivated skin fibroblasts of patients who are suspected to suffer from Tangier disease.

Preanalytical

Specimen

Fibroblasts cultivated from skin biopsy samples.

Reagents and Chemicals

1. DMEM supplemented with L-glutamine.
2. Sterile dishes or multiwell plates.
3. Antibiotic-antimycotic (100×; Gibco).
4. FCS.
5. BSA, fatty acid free.
6. ApoA-I (Biodesign or isolated from HDL).
7. Sodium hydroxide (NaOH) 0.2 mol/l.
8. [1,2-^{3}H]-cholesterol (40–60 µCi/mmol).
9. Free cholesterol solubilized in ethanol 30 mg/ml.

Instrumentation

1. Sterile cell culture facility.
2. Permit to work with ^{3}H-isotope.
3. *B*eta-scintillation counter.

Calibration

None.

Quality Control

Parallel analysis of control skin fibroblasts from normolipidemic donors and, ideally from patients with established diagnosis of Tangier disease, is needed. In addition,

both patient and control cells must be incubated with and without apoA-I to stimulate ABCA1-dependent cholesterol efflux.

Analytical

■ Procedure

Human skin fibroblasts are cultured from skin biopsy samples. The dermis is cut into small pieces (0.5 mm on each side) and placed into a dish in DMEM containing 10% (v/v) FCS and 1% (v/v) antibiotic-antimycotic solution. When these primary cultures are confluent they are split and cells between passage three and six are used for experiments. For the cholesterol efflux assay, cells are grown in 24-well plates to 60–80% confluence and are labeled with [1,2-^{3}H]-cholesterol (1 µCi/well) for 24 h. Cells are then washed with DMEM and incubated for 4 h at 37°C with DMEM containing BSA (0.2%, v/v) and either 0 (negative control) or 5–30 µg/ml apoA-I. The efflux medium is collected and centrifuged to remove cell debris. Cells are solubilized in 0.1 mol/l NaOH and the radioactivity in the efflux media and in the cell lysates is determined by scintillation counting [11, 30, 75].

Calculation

Fractional cholesterol efflux is calculated as radioactivity in the medium/(radioactivity in the medium + cellular radioactivity).

Postanalytical

■ Interpretation

Frequently results are reported as the percentage of efflux occurring in the presence of apoA-I relative to the efflux occurring in the absence of apoA-I. Data from patient fibroblasts are compared to those from control fibroblasts of normolipidemic donors.

Chromatograms

None.

Reference Values

None.

Typical Pathological Values

ApoA-I-mediated cholesterol efflux from fibroblasts of homozygous Tangier patients is reduced by more than 90% compared to normal control fibroblasts. Heterozygous carriers show significantly reduced cholesterol efflux from fibroblasts compared to unaffected family members.

Pitfalls

Partial cholesterol efflux defects may also occur secondary to other diseases (e.g., Niemann-Pick type C). Hence, this test is not that helpful in the diagnosis of single individuals with low HDL cholesterol and suspicion of heterozygous Tangier disease. Furthermore, basal ABCA1 activity in fibroblasts is low, leading to slow cholesterol efflux even in the presence of lipid-free apoA-I. Expression of ABCA1 can be enhanced by the incubation of fibroblasts with agonists of the transcription factor LXR (e.g., oxysterols or synthetic LXR agonists like T0901317; Sigma). This helps to pronounce the efflux defect of Tangier patients relative to normal controls.

HDL Subclass Identification

Principle

HDL consists of several subclasses that can be separated by two-dimensional non-denaturing gradient gel electrophoresis with the first-order agarose gel electrophoresis and the second order gradient polyacrylamide gel electrophoresis (PAGE). The proteins in the polyacrylamide gels are then blotted onto membranes, which can be probed with various antibodies against apolipoproteins. This allows the differentiation of HDL subclasses by electrophoretic mobility and antigenicity [24].

Preanalytical

Specimen

EDTA-blood samples are collected after overnight fasting and cooled immediately on ice. EDTA plasmas are obtained by centrifugation at 4°C for 15 min at 800 × *g*, aliquoted, and can be stored at −70°C.

Reagents and Chemicals

1. Gelbond sheets.
2. Agarose.
3. Tris base.
4. Barbital buffer (Sigma; 50 mM, pH 8.6), which contains (per liter) 44.3 g Tris and 0.53 g calcium lactate.
5. Calcium lactate.
6. Bromophenol blue.
7. Precast polyacrylamide gradient gels 4–20% (SERVA).
8. Tris glycine buffer (Sigma).
9. Tris HCl buffer pH 8.08.
10. Polyvinylidene fluoride (PVDF) membrane.
11. Anti-apoA-I antibody.
12. Horseradish peroxidase (HRP)-coupled secondary anti-IgG antibodies (species depending on primary antibody) enhanced chemiluminescence substrate (GE-Healthcare, Amersham).
13. BIOMAX film (Kodak).

Instrumentation

1. Power supplies with a minimum of 500 V and 100 mA outputs.
2. Horizontal (agarose gel) electrophoresis.
3. Vertical (polyacrylamide gradient) gel electrophoresis.
4. Electrotransfer chamber for Western blotting.

Calibration

None.

Quality Control

Control plasma of normolipidemic controls and, ideally, from patients with established diagnosis of Tangier disease are analyzed in parallel.

Analytical

■ Procedure

In the first dimension, 20 µl plasma is separated by electrophoresis at 4°C in a 0.75% agarose gel using a 1:2:16 dilution of a barbital buffer. Bromophenol blue is added to a standard sample to visualize albumin in the native gel. The electrophoresis is stopped when the albumin/bromophenol blue marker has migrated 6 cm. Agarose gel strips containing the preseparated lipoproteins are then transferred to a 4–20% polyacrylamide gradient gel. Separation in the second dimension is performed at 40 mA for 4–5 h at 10°C. The proteins separated in the PAGE gel are then electroblotted onto a PVDF membrane, and the apoA-I-containing lipoproteins are immunocomplexed by antibodies against human apoA-I. An HRP-labeled secondary antibody is used to visualize the immunocomplex [4, 26].

■ Calculation

None.

Postanalytical

■ Interpretation

Interpretation of the HDL subclass pattern is achieved according to von Eckardstein and colleagues [25, 26]. In normolipidemic plasma, the majority of apoA-I HDL is found in particles with electrophoretic α-mobility (α-LpA-I) and a minor part (about 5%) in a particle with pre-β-mobility (preβ_1-LpA-I). In Tangier disease, plasma α-LpA-I is absent and residual amounts of apoA-I reside in preβ_1-LpA-I (Fig. 5.2.10).

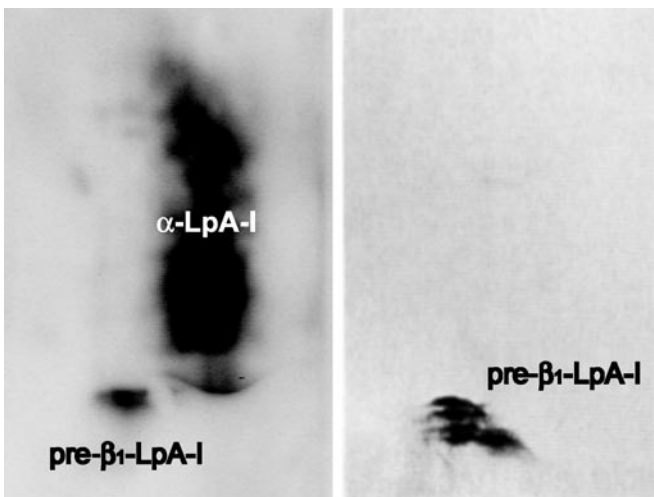

Fig. 5.2.10 Nondenaturing two-dimensional electrophoresis with agarose gel electrophoresis in the first dimension and gradient polyacrylamide gel electrophoresis in the second dimension combined with anti-apolipoprotein AI (apoA-I) immunoblotting differentiates apoA-I-containing lipoproteins by charge (pre-β1-LpA-I versus α-LpA-I) and size (HDL2 versus HDL3). In normal plasma the major part of the HDL pool is formed by α-LpA-I, a smaller by pre-β1-LpA-I (left picture). In the plasma from Tangier patients only some pre-β1-LpA-I particles are present (right picture)

Chromatograms

Please refer to Fig. 5.2.10.

Reference Values

None.

Typical Pathological Values

Residual amounts of apoA-I are exclusively present in pre-β_1-LpA-I, which in normolipidemic plasma accounts for less than 5% of total apoA-I. The α-migrating α-LpA-I, which in normolipidemic plasma represents the bulk of HDL, is absent from Tangier disease plasma.

Pitfalls

The method can only be used for the analysis of plasmas from homozygous or compound heterozygous patients. A similar pattern of HDL subclasses with a lack of α-LpA-I in the presence of pre β_1-LpA-I can be found in homozygous carriers of structural apoA-I variants [66].

5.2.6.3 LCAT Deficiency (OMIM 245900) and Fish-eye Disease (OMIM 136120)

LCAT catalyzes the transfer of a preferentially unesterified fatty acid from the sn-2 position of phosphatidylcholine to the 3β-hydroxy group of cholesterol, and thereby produces lysophosphatidylcholine and a cholesteryl ester [50]. Depending on the mutation in the LCAT gene, homozygous or compound heterozygous patients present with one of two clinical phenotypes, classical LCAT deficiency or fish-eye disease [58, 85]. Classical LCAT deficiency is caused by a broad spectrum of missense and non-sense mutations that interfere with the synthesis or secretion or affect the catalytic activity of LCAT [10]. Fish-eye disease is caused by a limited number of missense point mutations that alter the surface polarity, and thereby interfere with the binding of the enzyme to apoA-I containing lipoproteins [77]).

Homozygotes or compound heterozygotes are characterized by the occurrence of corneal cloudings, which after the third decade become apparent upon physical examination. In addition, patients with classical LCAT deficiency develop renal disease with proteinuria and hematuria, which progresses to terminal renal insufficiency and hemolytic anemia [58, 85].

Heterozygous carriers of LCAT mutations are clinically normal. Frequently, but not always, they present with low HDL cholesterol. Large family studies in the Netherlands indicated that heterozygous carriers of LCAT defects may have an increased risk for atherosclerotic vascular disease [43].

Homozygous or compound heterozygous patients with classical LCAT deficiency or fish-eye disease can be diagnosed by measuring LCAT activity [58, 85]). However, heterozygous carriers need genetic testing because LCAT activity can be reduced secondary to HDL deficiency due to other causes than defects in the LCAT gene. This is even true in families with known LCAT deficiency [35].

Biochemically, both patients with classical LCAT deficiency and fish-eye disease present with very low levels of HDL cholesterol (< 0.3 mmol/l), although some pa-

tients were reported to have higher values, including individuals with HDL cholesterol levels >0.5 mmol/l. Serum levels of apoA-I usually are below 0.5 g/l but not as low as in patients with apoA-I deficiency or Tangier disease. In addition, apoB-containing lipoproteins are highly abnormal in patients with LCAT deficiency. They are rich in phospholipids, unesterified cholesterol, and apoC, and thereby resemble LpX, which is otherwise found in cholestatic liver disease. Routine lipid and lipoprotein analyses do not help to distinguish patients with classical LCAT deficiency and fish-eye disease from one another and from other HDL deficiency syndromes. This is only possible by measuring unesterified cholesterol and determining LCAT activity and/or by sequence analysis of the LCAT gene [10, 58, 85].

LCAT Activity

Principle

LCAT acts preferentially on lipids transported by HDL (so-called α-LCAT activity), but also on lipids transported by apoB-containing lipoproteins (so-called β-LCAT activity) [58, 85]. In practice, LCAT activity is measured either as the activity required to esterify radioactive cholesterol that has been exogenously incorporated into native HDL or into artificial HDL-like particles (α-LCAT activity) or which has been equilibrated with endogenous lipoproteins of the plasma sample (cholesterol esterification rate, CER) [21, 58, 85]. Several variations of these assays have been reported, some of which are available as commercial test kits (e.g., Roar Biomedical, New York, USA). In addition, LCAT concentration can be determined by either laboratory-made tests or by a commercial ELISA kits [57]. However, the decrease in LCAT concentration is difficult to judge since it also decreases secondary to HDL deficiency due to causes other than LCAT deficiency. Plasma from patients with LCAT deficiency fails to esterify radioactive cholesterol provided by any substrate. By contrast, plasmas of patients with fish-eye disease show a near-normal cholesterol esterification rate but have a selective inability to esterify radioactive cholesterol provided to plasma with native HDL or reconstituted HDL (α-LCAT activity) [58, 85].

Preanalytical

Specimen

EDTA-blood samples are collected after overnight fasting and cooled immediately on ice. EDTA-plasmas are obtained by centrifugation at 4°C for 15 min at $800 \times g$, aliquoted, and then stored at −70°C.

Reagents and Chemicals

For the CER:

1. [1,2-^{3}H]-cholesterol.
2. Ethanol.
3. Paper filter disks of 5 mm diameter.
4. Thin layer chromatography (TLC) plates.
5. Unesterified cholesterol.
6. Cholesteryl oleate.
7. Chloroform.
8. Methanol.

9. Diethylether.
10. *n*-Hexane.
11. Iodine.

For α-LCAT activity:
1. Egg yolk phosphatidylcholine. [7-$_3$H(N)]-cholesterol. ApoA-I. NaCl. Ethanol.
2. BSA.
3. EDTA.
4. Tris HCl.
5. Analysis buffer (0.15 M NaCl, 5 mM EDTA, 10 mM Tris-HCl, pH 7.4).
6. 2-Mercaptoethanol.
7. Unesterified cholesterol.
8. Cholesteryl oleate.
9. TLC plates.
10. Chloroform.
11. Methanol.
12. Diethylether.
13. *n*-Hexane.
14. Iodine.

Instrumentation

1. Centrifuge.
2. TLC chamber.
3. Beta counter.

Calibration

None.

Quality Control

Frozen pool plasma for precision testing.

Analytical

Procedure

For the CER: 3 µl of 21 Ci/mmol [7-^{3}H(N)]-cholesterol are dissolved in 100 µl of pure ethanol; 3 µl of this solution are spotted and dried onto filter plates of 5 mm diameter. These plates are incubated overnight with 200 µl plasma in an ice bath at 4°C. The next day, 50 µl of the radiolabeled plasma is removed and kept on ice, whereas the remainder is incubated for 30 min at 37°C. The 50 µl aliquots obtained before and after incubation are transferred into glass tubes and incubated with 1 ml pure ethanol. After 2 h of incubation with repeated shaking the tubes with the samples are centrifuged for 15 min at 3000 rpm ($2000 \times g$). The lipid-containing supernatant is removed for subsequent evaporation of the alcohol. Radiolabeled unesterified and esterified cholesterol are separated by TLC using diethylether/hexane in a ratio of 3:2 as the mobile phase. Standards with cholesterol and cholesteryl esters are run in parallel to identify their bands with iodine staining. The two bands containing unesterified and esterified cholesterol are cut out of the TLC gel and transferred into separate scintillation vials. Radioactivity is determined with beta counting [20, 34].

For α-LCAT activity: the apoA-I proteoliposome emulsion is prepared by evaporating 260 µl of 5 mg/ml egg yolk phosphatidylcholine, 150 µl of 1 mg/ml unesterified cholesterol, and 3 µl of 21 Ci/mmol [7-^{3}H(N)]-cholesterol. The dried lipids are dissolved in 125 µl pure ethanol and injected into 10 ml of analysis buffer and vortexed. The emulsion is concentrated by ultrafiltration to less than 2.5 ml and then filled up to 2.5 ml. A 300-µL aliquot of this emulsion is incubated with 75–150 mg of apoA-I and 1.1 ml analysis buffer. The optimal amount of apoA-I varies from lot to lot and has to be optimized using normal plasma samples.

For the analysis, 140 µl of the apoA-I proteoliposomes is supplemented with 50µl of 8% BSA in analysis buffer, 10 µl of 0.1 M 2-mercaptoethanol, and 15 µl plasma. The mixture is incubated by shaking for 30 min at 37°C. The LCAT reaction is stopped by adding 4 ml of chloroform: methanol (2:1, v/v). Lipids are extracted by incubation at room temperature for 2 h. Hydrophilic and lipophilic phases are separated by adding 1.5 ml of 0.15 M NaCl, shaking and centrifugation for 10 minutes at 4°C at 3000 rpm ($2000 \times g$). (Radioactive) cholesterol and cholesteryl esters in the lipophilic upper phase are then separated by TLC as described for the CER [34].

Calculation

CER: The fractional esterification rate (FER) is calculated as [cpm [^{3}H] cholesteryl esters/(cpm [^{3}H]cholesteryl esters + cpm unesterified [^{3}H] cholesterol)].

α-LCAT activity: $\text{FER} \times 2 \times 4.66 \times 1000/15$ (in nmol esterified cholesterol/ml/h).

Postanalytical

■ Interpretation

Patients with classical LCAT deficiency fail to esterify cholesterol in any substrate and hence have both an undetectable or very low cholesterol esterification rate and α-LCAT activity. Patients with fish-eye disease usually have a normal cholesterol esterification rate and a selective α-LCAT deficiency.

Chromatograms

None.

Reference Values

CER (95% interval): 3.7–8.2% cholesteryl esters/h [23]. Variations among laboratories are possible so that every laboratory should determine its own reference intervals).

α-LCAT activity: 15–25 nmol/ml/h [23]. Variations among laboratories are possible so that every laboratory should determine its own reference intervals.

Typical Pathological Values

Plasmas from patients with classical LCAT deficiency fail to esterify cholesterol in any substrate and hence have both an undetectable or very low cholesterol esterification rate and α-LCAT activity. By contrast, plasmas of patients with fish-eye disease have a normal or significantly residual cholesterol esterification rate and a selective α-LCAT deficiency. LCAT mass concentrations are reduced or not detectable in patients with either LCAT deficiency or fish-eye disease [10, 34].

Pitfalls

Considerable amounts of LCAT are carried by HDL; therefore α-LCAT activity is also secondarily reduced in other forms of familial HDL deficiency. Notably, this partial LCAT deficiency has been repeatedly documented in forms of apoA-I deficiency due to structural defects in apoA-I. However, despite secondary LCAT deficiency these patients have a normal unesterified cholesterol:total cholesterol ratio [35].

Unesterified Cholesterol

Principle

Assays for the determination of cholesterol in routine clinical laboratories include cholesterol esterase and thus quantify total cholesterol (i.e., unesterified and esterified cholesterol). However, specific assays are also available that lack cholesterol esterase and hence allow the determination of unesterified or free cholesterol. The difference between total and unesterified cholesterol gives the concentration of cholesterol esters.

Preanalytical

- Specimen

Blood samples are collected after overnight fasting and cooled immediately on ice. Serum is obtained by centrifugation at 4°C for 15 min at $800 \times g$, aliquoted, and stored at −70°C.

- Reagents and Chemicals

1. Free cholesterol assay (WAKO Chemicals, Richmond, CA, USA).
2. Total cholesterol assay.

- Instrumentation

Photometer that measures absorption at 505 nm, or a clinical chemistry analyzer.

- Calibration

Commercial calibration available.

- Quality Control

Commercial controls for precision and accuracy testing available

Analytical

- Procedure

According to the manufacturers' protocols for both, the total cholesterol assay and for the unesterified cholesterol assay.

- Calculation

None.

Postanalytical

- Interpretation

From the measurement of the total cholesterol and the unesterified cholesterol in the sample, the ratio of the unesterified to total cholesterol is calculated.

Chromatograms

None.

Reference Values

In normolipidemic controls the unesterified cholesterol is < 30% of the total cholesterol.

Typical Pathological Values

Patients with classical LCAT deficiency show an increased proportion of unesterified cholesterol in plasma (80–100%). By contrast, the plasma from patients with fish-eye disease has a slightly elevated proportion of unesterified cholesterol (up to 70%).

Pitfalls

None.

5.2.6.4 CETP Deficiency (OMIM 607322)

CETP exchanges cholesteryl esters of HDL with triglycerides of VLDL, IDL, and LDL. The HDL-derived cholesteryl esters are subsequently removed from the circulation via the LDL receptor pathway [28, 91]. Absence of functional CETP results in pronounced elevations of plasma concentrations of HDL cholesterol (2.5–8 mmol/l) and apoA-I. In parallel, plasma concentrations of LDL cholesterol and apoB are relatively low. Heterozygous CETP deficiency is associated with a milder elevation of HDL cholesterol. Most patients with CETP deficiency do not present with specific clinical symptoms. Some were reported to exhibit corneal opacities. CETP deficiency has been claimed to reduce the risk of atherosclerotic vascular disease and to prolong life expectancy. However, in some situations (e.g., in hypertriglyceridemia or in the absence of high HDL cholesterol), CETP deficiency may also increase cardiovascular risk [15, 28, 91].

CETP deficiency was originally found in Japan. There, heterozygosity for the two most frequent mutations has a prevalence of 1–2%. In Japan, these two frequent mutations together with some rare variants of CETP explain 20% of the variance in HDL cholesterol and 50% of cases with hyperalphalipoproteinemia. Among Caucasians, CETP deficiency is much rarer [15].

CETP Activity

Principle

CETP can be measured both as activity and mass concentration. For the latter, laboratory-made and commercial immunoassays have been described [16, 65]. Various assays have been described for the measurement of CETP activity. Most of them

use either native or reconstituted HDL as donors of either radioactive or fluorescent cholesteryl esters [16]. We used and describe here the assay that is employed by in Japanese laboratories for the characterization of CETP deficiency [23, 55, 68].

Preanalytical

Specimen

EDTA-plasma.

Reagents and Chemicals

1. LDL isolated from plasma (density = 1.1019–1.063 kg/l).
2. Egg yolk phosphatidylcholine. Cholesterol. Cholesteryl oleate. [$_3$H]-cholesteryl oleate. Chloroform. Ethanol. Sodium phosphate. EDTA. NaN_3. Sodium cholate. NaCl.
3. Dithiobis-(2-nitorobenzoic) acid (DTNB) as an LCAT inhibitor.
4. Magnesium dichloride.
5. Dextran sulfate.
6. NaOH.
7. Scintillation vials.

Instrumentation

1. Ultracentrifuge.
2. Beta counter.
3. Centrifuge.

Calibration

None.

Quality Control

Pool plasma for assessing precision.

Analytical

Procedure

To prepare proteoliposomes, 7 mg egg yolk phosphatidylcholine, 1.16 µg cholesterol, 77.5 µg cholesteryl oleate and 10 µCi [^{3}H]-cholesteryl oleate, all dissolved in chloroform are mixed. After evaporation of chloroform with nitrogen, the lipids are resolved in 400 µl ethanol. The ethanolic solution is injected into 5 ml of a vortexing buffer with 39 mmol/l sodium phosphate, 0.01% EDTA, 2 mmol/l NaN_3, and 12 mmol/l sodium cholate (pH 7.4); 3 mg apoA-I is added. The solution is subsequently dialyzed against a buffer with 39 mmol/l sodium phosphate, 0.01% EDTA, 2 mmol/l NaN_3, and 12 mmol/l sodium cholate (pH 7.4) at 4°C. At the end the solution is filled up with analysis buffer containing 39 mmol/l sodium phosphate, 0.02% EDTA, and 60 mmol/l NaCl (pH 7.4). The proteoliposome solution can be maintained at 4°C. Thereafter, 100 µl of this proteoliposome solution, 200 µg LDL (by protein), 0.42 µmol DTNB (final concentration), and 5 µl of plasma are taken up to 300 µl with analysis buffer (39 mmol/l sodium phosphate, 0.02% EDTA, and 60 mmol/l NaCl (pH 7.4)). The mixture is incubated for 20 min at 37°C while shaking. The reaction is terminated by placing the tube on ice. For the separation of LDL and proteoliposomes, 30 µl of 60 mmol/l $MgCl_2$ and 30 ml of 1% dextran sulfate are

added. After incubation for 20 min on ice, the apoB-containing lipoproteins are precipitated by centrifugation at 3000 rpm (2000 × *g*). The supernatant is then carefully removed without leaving any fluid on the precipitate. The precipitate is dissolved in 100 µl 0.1 mol/l NaOH; 80 µl of the dissolved precipitate is transferred into a scintillation vial for radioactivity counting. In every series blank samples without plasma are analyzed, where radioactivity is measured in both the supernatant and the precipitate [23, 55, 68].

■ Calculation

Counts per minute $(CPM)_{total}$ = CPM in blank sample
(or $CPM_{total} \times 10$ in ml proteoliposomes)

Concentration of cholesteryl esters in 1 ml proteoliposome = 775 ng/651 × 10
= 12 nmol/l

Specific radioactivity (S) = $CPM_{total} \times 10/12$

Net transfer $CPM_{net} = CPM_{precipitate\ sample} - CPM_{precipitate\ blank}$

CETP activity (in nmol/ml/h) = $CPM_{net} \times 200 \times 3/S/10/12$

Postanalytical

■ Interpretation

The CETP activity is compared to the reference values.

Chromatograms

None.

Reference Values

CETP activity: 45–120 nmol/ml/h [23]. Variations among laboratories are possible so that every laboratory should determine its own reference intervals.

Typical Pathological Values

Homozygous CETP deficient patients have very low or undetectable own plasma CETP activity.

Pitfalls

None.

5.2.7 Abeta- and Hypobetalipoproteinemia (OMIM 200100 and 605019)

Defects in the assembly or secretion of apoB-containing lipoproteins lead to the occurrence of familial hypobetalipoproteinemia (FHBL), abetalipoproteinemia (ABL), and Anderson's disease.

FHBL (OMIM 107730) is a codominant disorder characterized by plasma levels of total cholesterol, LDL-cholesterol, triglycerides, and apoB below the fifth percentile of the distribution in the general population. FHBL is genetically heterogeneous; it may be linked to the apoB gene. The best-characterized FHBL cases are those due

to the non-sense or frameshift mutations of the apoB gene, which prevent the complete translation of apoB mRNA, leading to the production of truncated forms of apoB of various sizes. Frameshift mutations that encode for truncated peptides with less than 29% of the amino terminal portion of apoB prevent the formation of apoB isoforms, which are detectable in plasma. The longer the truncated apoB peptide, the more buoyant the apoB particles formed thereof. The smallest particles have the size of HDL. Truncated isoforms containing more than 89% of the normal apoB sequence form VLDL. Most FHBL subjects are heterozygotes for defects in the apoB gene and asymptomatic or mildly symptomatic. Homozygotes and compound heterozygotes for apoB gene defects present with the near absence of apoB-containing lipoproteins and with clinical symptoms that are also found in abetalipoproteinemia [54, 87].

ABL (OMIM 200100) is a rare recessive disorder that is caused by the deficiency of microsomal triglyceride transfer protein (MTP). To date, more than 20 mutations have been identified in the MTP gene of ABL patients. Most of them are frameshift, non-sense, and splice site mutations that are predicted to encode truncated forms of MTP that are completely devoid of function. In the absence of MTP, apoB cannot be properly lipidated and is rapidly degraded in liver and intestinal cells. As the result, plasma concentrations of cholesterol, triglycerides, and apoB are extremely low. Clinically, ABL patients present with steatorrhea because of fat malabsorption, hepatomegaly because of fatty liver, and neurological disorders including Friedreich ataxia, retinitis pigmentosa, and peripheral neuropathy. The blood smear shows acanthocytosis [47, 54].

In chylomicron retention disease (Anderson's disease) the secretory defect is restricted to intestinal apoB-containing lipoproteins (i.e., chylomicrons). This very rare recessively inherited disorder results from defects in a GTPase, Sar1b, which plays a critical role in the intracellular assembly and trafficking of chylomicrons. The affected patients present with fat malabsorption resulting in steatorrhea and deficiency of fat-soluble vitamins [46, 52, 54].

Since hypobetalipoproteinemia and abetalipoproteinemia are genetically variable and in a considerable proportion caused by defects in as yet unknown genes, the diagnosis is frequently phenomenological because of the finding of very low concentrations of cholesterol, triglycerides, and apoB. Family studies to unravel the mode of inheritance (codominant or recessive) are important to discriminate the candidate gene apoB from the candidate genes *MTP* and *SAR1B*. In the case of FHBL it may be advisable to investigate plasma samples of patients by SDS-PAGE and subsequent Western blotting for the presence of truncated apoB isoforms. However, notably very small ones can be overlooked. Therefore, genetic diagnostics is ultimately needed. The underlying mutations in *apoB*, *MTP*, or *SAR1B* are sporadic so that screening for mutations by DHPLC or DGGE and subsequent gene sequencing is the method of choice. Primers have been described in the literature (for example see [19, 52]). For DHPLC and sequencing analysis see section 5.2.5.1 (Familial Hypercholesterolemia) and 5.2.3.2 (ApoCII Deficiency), respectively.

References

1. Abifadel M, Varret M, Rabes JP, Allard D, Ouguerram K, Devillers M, Cruaud C, Benjannet S, Wickham L, Erlich D, Derre A, Villeger L, Farnier M, Beucler I, Bruckert E, Chambaz J, Chanu B, Lecerf JM, Luc G, Moulin P, Weissenbach J, Prat A, Krempf M, Junien C, Seidah

NG, Boileau C (2003) Mutations in PCSK9 cause autosomal dominant hypercholesterolemia. Nat Genet 34:154–156
2. Aslanidis C, Schmitz G (1999) High-speed apolipoprotein E genotyping and apolipoprotein B3500 mutation detection using real-time fluorescence PCR and melting curves. Clin Chem 45:1094–1097
3. Assmann G, von Eckardstein A, Brewer HJ (2000) Familial analphalipoproteinemia: tangier Disease. In: Scriver C, Beaudet A, Sly E, Valle D (eds) The Metabolic and Molecular Bases of Inherited Disease, 8th edn. New York, McGraw-Hill, pp 2937–2960
4. Asztalos BF, Brousseau ME, McNamara JR, Horvath KV, Roheim PS, Schaefer EJ (2001) Subpopulations of high density lipoproteins in homozygous and heterozygous Tangier disease. Atherosclerosis 156:217–225
5. Baginsky ML, Brown WV (1979) A new method for the measurement of lipoprotein lipase in postheparin plasma using sodium dodecyl sulfate for the inactivation of hepatic triglyceride lipase. J Lipid Res 20:548–556
6. Blache D, Bouthillier D, Davignon J (1983) Simple, reproducible procedure for selective measurement of lipoprotein lipase and hepatic lipase. Clin Chem 29:154–158
7. Bodamer OA, Bercovich D, Schlabach M, Ballantyne C, Zoch D, Beaudet AL (2002) Use of denaturing HPLC to provide efficient detection of mutations causing familial hypercholesterolemia. Clin Chem 48:1913–1918
8. Breckenridge WC, Little JA, Alaupovic P, Wang CS, Kuksis A, Kakis G, Lindgren F, Gardiner G (1982) Lipoprotein abnormalities associated with a familial deficiency of hepatic lipase. Atherosclerosis 45:161–179
9. Bunn CF, Lintott CJ, Scott RS, George PM (2002) Comparison of SSCP and DHPLC for the detection of LDLR mutations in a New Zealand cohort. Hum Mutat 19:311
10. Calabresi L, Pisciotta L, Costantin A, Frigerio I, Eberini I, Alessandrini P, Arca M, Bon GB, Boscutti G, Busnach G, Frasca G, Gesualdo L, Gigante M, Lupattelli G, Montali A, Pizzolitto S, Rabbone I, Rolleri M, Ruotolo G, Sampietro T, Sessa A, Vaudo G, Cantafora A, Veglia F, Calandra S, Bertolini S, Franceschini G (2005) The molecular basis of lecithin: cholesterol acyltransferase deficiency syndromes: a comprehensive study of molecular and biochemical findings in 13 unrelated Italian families. Arterioscler Thromb Vasc Biol 25:1972–1978
11. Clee SM, Kastelein JJ, van Dam M, Marcil M, Roomp K, Zwarts KY, Collins JA, Roelants R, Tamasawa N, Stulc T, Suda T, Ceska R, Boucher B, Rondeau C, DeSouich C, Brooks-Wilson A, Molhuizen HO, Frohlich J, Genest J, Jr., Hayden MR (2000) Age and residual cholesterol efflux affect HDL cholesterol levels and coronary artery disease in ABCA1 heterozygotes. J Clin Invest 106:1263–1270
12. Cohen JC, Kiss RS, Pertsemlidis A, Marcel YL, McPherson R, Hobbs HH (2004) Multiple rare alleles contribute to low plasma levels of HDL cholesterol. Science 305:869–872
13. Connelly PW, Vezina C, Maguire GF (1996) Quantification of apolipoprotein C-II by immunochemical and chromatographic methods. Methods Enzymol 263:188–208
14. Damgaard D, Jensen JM, Larsen ML, Soerensen VR, Jensen HK, Gregersen N, Jensen LG, Faergeman O (2004) No genetic linkage or molecular evidence for involvement of the PCSK9, ARH or CYP7A1 genes in the Familial Hypercholesterolemia phenotype in a sample of Danish families without pathogenic mutations in the LDL receptor and apoB genes. Atherosclerosis 177:415–422
15. de Grooth GJ, Klerkx AH, Stroes ES, Stalenhoef AF, Kastelein JJ, Kuivenhoven JA (2004) A review of CETP and its relation to atherosclerosis. J Lipid Res 45:1967–1974
16. Dedecjus M, Masson D, Gautier T, de Barros JP, Gambert P, Lewinski A, Adamczewski Z, Moulin P, Lagrost L (2003) Low cholesteryl ester transfer protein (CETP) concentration but normal CETP activity in serum from patients with short-term hypothyroidism Lack of relationship to lipoprotein abnormalities. Clin Endocrinol (Oxf) 58:581–588
17. Devaraj S, Hirany S, Jialal I (2000) Ratio of remnant-like particle cholesterol to serum total triglycerides is a reliable screening test for type III dyslipidaemia. Ann Clin Biochem 37:790–791

18. Devroey D, Vantomme K, Betz W, Vandevoorde J, Kartounian J (2004) A review of the treatment guidelines on the management of low levels of high-density lipoprotein cholesterol. Cardiology 102:61–66
19. Di Leo E, Lancellotti S, Penacchioni JY, Cefalu AB, Averna M, Pisciotta L, Bertolini S, Calandra S, Gabelli C, Tarugi P (2005) Mutations in MTP gene in abeta- and hypobeta-lipoproteinemia. Atherosclerosis 180:311–318
20. Dobiasova M, Frohlich J (1996) Measurement of fractional esterification rate of cholesterol in plasma depleted of apoprotein B containing lipoprotein: methods and normal values. Physiol Res 45:65–73
21. Dobiasova M, Frohlich JJ (1998) Assays of lecithin cholesterol acyltransferase (LCAT) Methods Mol Biol 110:217–230
22. Eckardstein A von (2005) Differential diagnosis of familial high density lipoprotein deficiency syndromes. Atherosclerosis 186:231–239
23. Eckardstein A von, Funke H, Chirazi A, Chen-Haudenschild C, Schulte H, Schonfeld R, Kohler E, Schwarz S, Steinmetz A, Assmann G (1994) Sex-specific effects of the glutamine/histidine polymorphism in apo A-IV on HDL metabolism. Arterioscler Thromb 14:1114–1120
24. Eckardstein A von, Huang Y, Assmann G (1994) Physiological role and clinical relevance of high-density lipoprotein subclasses. Curr Opin Lipidol 5:404–416
25. Eckardstein A von, Huang Y, Kastelein JJ, Geisel J, Real JT, Kuivenhoven JA, Miccoli R, Noseda G, Assmann G (1998) Lipid-free apolipoprotein (apo) A-I is converted into alpha-migrating high density lipoproteins by lipoprotein-depleted plasma of normolipidemic donors and apo A-I-deficient patients but not of Tangier disease patients. Atherosclerosis 138:25–34
26. Eckardstein A von, Huang Y, Wu S, Funke H, Noseda G, Assmann G (1995) Reverse cholesterol transport in plasma of patients with different forms of familial HDL deficiency. Arterioscler Thromb Vasc Biol 15:691–703
27. Fojo SS, Brewer HB (1992) Hypertriglyceridaemia due to genetic defects in lipoprotein lipase and apolipoprotein C-II. J Intern Med 231:669–677
28. Forrester JS, Makkar R, Shah PK (2005) Increasing high-density lipoprotein cholesterol in dyslipidemia by cholesteryl ester transfer protein inhibition: an update for clinicians. Circulation 111:1847–1854
29. Fouchier SW, Kastelein JJ, Defesche JC (2005) Update of the molecular basis of familial hypercholesterolemia in The Netherlands. Hum Mutat 26:550–556
30. Francis GA, Knopp RH, Oram JF (1995) Defective removal of cellular cholesterol and phospholipids by apolipoprotein A-I in Tangier disease. J Clin Invest 96:78–87
31. Fredrickson DS, Lees RS (1965) A system for phenotyping hyperlipoproteinemia. Circulation 31:321–327
32. Fredrickson DS, Morganroth J, Levy RI (1975) Type III hyperlipoproteinemia: an analysis of two contemporary definitions. Ann Intern Med 82:150–157
33. Frikke-Schmidt R, Nordestgaard BG, Jensen GB, Tybjaerg-Hansen A (2004) Genetic variation in ABC transporter A1 contributes to HDL cholesterol in the general population. J Clin Invest 114:1343–1353
34. Funke H, Eckardstein A von, Pritchard PH, Albers JJ, Kastelein JJ, Droste C, Assmann G (1991) A molecular defect causing fish eye disease: an amino acid exchange in lecithin-cholesterol acyltransferase (LCAT) leads to the selective loss of alpha-LCAT activity. Proc Natl Acad Sci U S A 88:4855–4859
35. Funke H, Eckardstein A von, Pritchard PH, Karas M, Albers JJ, Assmann G (1991) A frameshift mutation in the human apolipoprotein A-I gene causes high density lipoprotein deficiency, partial lecithin: cholesterol-acyltransferase deficiency, and corneal opacities. J Clin Invest 87:371–376
36. Gaffney D, Reid JM, Cameron IM, Vass K, Caslake MJ, Shepherd J, Packard CJ (1995) Independent mutations at codon 3500 of the apolipoprotein B gene are associated with hyperlipidemia. Arterioscler Thromb Vasc Biol 15:1025–1029
37. Haase R, Menke-Mollers I, Oette K (1988) Analysis of human apolipoproteins C by isoelectric focusing in immobilized pH gradients. Electrophoresis 9:569–575

38. Hazzard WR, Porte D Jr., Bierman EL (1972) Abnormal lipid composition of very low density lipoproteins in diagnosis of broad-beta disease (type 3 hyperlipoproteinemia). Metabolism 21:1009–1019
39. Heath KE, Gahan M, Whittall RA, Humphries SE (2001) Low-density lipoprotein receptor gene (LDLR) world-wide website in familial hypercholesterolaemia:update, new features and mutation analysis. Atherosclerosis 154:243–246
40. Henderson AD, Richmond W, Elkeles RS (1993) Hepatic and lipoprotein lipases selectively assayed in postheparin plasma. Clin Chem 39:218–223
41. Henriksen FL, Petersen PH, Beck-Nielsen H, Horder M (2001) Calibration, specificity and trueness of a postheparin plasma lipoprotein lipase assay. Clin Chem Lab Med 39:263–269
42. Hersberger M, Eckardstein A von (2003) Low high-density lipoprotein cholesterol: physiological background, clinical importance and drug treatment. Drugs 63:1907–1945
43. Hovingh GK, de Groot E, van der Steeg W, Boekholdt SM, Hutten BA, Kuivenhoven JA, Kastelein JJ (2005) Inherited disorders of HDL metabolism and atherosclerosis. Curr Opin Lipidol 16:139–145
44. Huang W, Sasaki J, Matsunaga A, Nanimatsu H, Moriyama K, Han H, Kugi M, Koga T, Yamaguchi K, Arakawa K (1998) A novel homozygous missense mutation in the apo A-I gene with apo A-I deficiency. Arterioscler Thromb Vasc Biol 18:389–396
45. Hulley SB, Cook SG, Wilson WS, Nichaman MZ, Hatch FT, Lindgren FT (1971) Quantitation of serum lipoproteins by electrophoresis on agarose gel: standardization in lipoprotein concentration units (mg-100 ml) by comparison with analytical ultracentrifugation. J Lipid Res 12:420–433
46. Hussain MM, Fatma S, Pan X, Iqbal J (2005) Intestinal lipoprotein assembly. Curr Opin Lipidol 16:281–285
47. Hussain MM, Shi J, Dreizen P (2003) Microsomal triglyceride transfer protein and its role in apoB-lipoprotein assembly. J Lipid Res 44:22–32
48. Innerarity TL, Pitas RE, Mahley RW (1986) Lipoprotein-receptor interactions. Methods Enzymol 129:542–565
49. Jap TS, Jenq SF, Wu YC, Chiu CY, Cheng HM (2003) Mutations in the lipoprotein lipase gene as a cause of hypertriglyceridemia and pancreatitis in Taiwan. Pancreas 27:122–126
50. Jonas A (2000) Lecithin cholesterol acyltransferase. Biochim Biophys Acta 1529:245–256
51. Jones AC, Austin J, Hansen N, Hoogendoorn B, Oefner PJ, Cheadle JP, O'Donovan MC (1999) Optimal temperature selection for mutation detection by denaturing HPLC and comparison to single-stranded conformation polymorphism and heteroduplex analysis. Clin Chem 45:1133–1140
52. Jones B, Jones EL, Bonney SA, Patel HN, Mensenkamp AR, Eichenbaum-Voline S, Rudling M, Myrdal U, Annesi G, Naik S, Meadows N, Quattrone A, Islam SA, Naoumova RP, Angelin B, Infante R, Levy E, Roy CC, Freemont PS, Scott J, Shoulders CC (2003) Mutations in a Sar1 GTPase of COPII vesicles are associated with lipid absorption disorders. Nat Genet 34:29–31
53. Joy T, Wang J, Hahn A, Hegele RA (2003) APOA1 related amyloidosis: a case report and literature review. Clin Biochem 36:641–645
54. Kane JP, Havel RJ (2001) Disorders of the biogenesis and secretion of lipoproteins containing the B apolipoproteins. In: Scriver C, Beaudet A, Sly E, Valle D (eds) The Metabolic and Molecular Bases of Inherited Disease, 8th edn. McGraw-Hill, New York, pp 2717–2752
55. Kato H, Nakanishi T, Arai H, Nishida HI, Nishida T (1989) Purification, microheterogeneity, and stability of human lipid transfer protein. J Biol Chem 264:4082–4087
56. Kim SH, Bae JH, Chae JJ, Kim UK, Choe SJ, Namkoong Y, Kim HS, Park YB, Lee CC (1999) Long-distance PCR-based screening for large rearrangements of the LDL receptor gene in Korean patients with familial hypercholesterolemia. Clin Chem 45:1424–1430
57. Kobori K, Saito K, Ito S, Kotani K, Manabe M, Kanno T (2002) A new enzyme-linked immunosorbent assay with two monoclonal antibodies to specific epitopes measures human lecithin-cholesterol acyltransferase. J Lipid Res 43:325–334

58. Kuivenhoven JA, Pritchard H, Hill J, Frohlich J, Assmann G, Kastelein J (1997) The molecular pathology of lecith in cholesterol acyltransferase (LCAT) deficiency syndromes. J Lipid Res 38:191–205
59. Lam CW, Yuen YP, Cheng WF, Chan YW, Tong SF (2006) Missense mutation Leu72Pro located on the carboxyl terminal amphipathic helix of apolipoprotein C-II causes familial chylomicronemia syndrome. Clin Chim Acta 364:256–259
60. Lee SJ, Grosskopf I, Choi SY, Cooper AD (2004) Chylomicron remnant uptake in the livers of mice expressing human apolipoproteins E3, E2 (Arg158→Cys), and E3-Leiden. J Lipid Res 45:2199–2210
61. Liu W, Smith DI, Rechtzigel KJ, Thibodeau SN, James CD (1998) Denaturing high performance liquid chromatography (DHPLC) used in the detection of germline and somatic mutations. Nucleic Acids Res 26:1396–1400
62. Mahley RW, Huang Y, Rall SC Jr (1999) Pathogenesis of type III hyperlipoproteinemia (dysbetalipoproteinemia). Questions, quandaries, and paradoxes. J Lipid Res 40:1933–1949
63. Mailly F, Palmen J, Muller DP, Gibbs T, Lloyd J, Brunzell J, Durrington P, Mitropoulos K, Betteridge J, Watts G, Lithell H, Angelico F, Humphries SE, Talmud PJ (1997) Familial lipoprotein lipase (LPL) deficiency: a catalogue of LPL gene mutations identified in 20 patients from the UK, Sweden, and Italy. Hum Mutat 10:465–473
64. Merkel M, Eckel RH, Goldberg IJ (2002) Lipoprotein lipase:genetics, lipid uptake, and regulation. J Lipid Res 43:1997–2006
65. Mezdour H, Kora I, Parra HJ, Tartar A, Marcel YL, Fruchart JC (1994) Two-site enzyme immunoassay of cholesteryl ester transfer protein with monoclonal and oligoclonal antibodies. Clin Chem 40:593–597
66. Miccoli R, Zhu Y, Daum U, Wessling J, Huang Y, Navalesi R, Assmann G, Eckardstein A von (1997) A natural apolipoprotein A-I variant, apoA-I (L141R)Pisa, interferes with the formation of alpha-high density lipoproteins (HDL) but not with the formation of pre beta 1-HDL and influences efflux of cholesterol into plasma. J Lipid Res 38:1242–1253
67. Miserez AR, Laager R, Chiodetti N, Keller U (1994) High prevalence of familial defective apolipoprotein B-100 in Switzerland. J Lipid Res 35:574–583
68. Nakanishi T, Tahara D, Akazawa S, Miyake S, Nagataki S (1990) Plasma lipid transfer activities in hyper-high-density lipoprotein cholesterolemic and healthy control subjects. Metabolism 39:225–230
69. Nauck M, Marz W, Jarausch J, Cobbaert C, Sagers A, Bernard D, Delanghe J, Honauer G, Lehmann P, Oestrich E, Eckardstein A von, Walch S, Wieland H, Assmann G (1997) Multicenter evaluation of a homogeneous assay for HDL-cholesterol without sample pretreatment. Clin Chem 43:1622–1629
70. Nauck M, Wieland H, Marz W (2000) Evaluation of the Roche Diagnostics LightCycler-Apo B 3500 Mutation Detection Kit. Clin Chem Lab Med 38:667–671
71. Nauck MS, Nissen H, Hoffmann MM, Herwig J, Pullinger CR, Averna M, Geisel J, Wieland H, Marz W (1998) Detection of mutations in the apolipoprotein CII gene by denaturing gradient gel electrophoresis. Identification of the splice site variant apolipoprotein CII-Hamburg in a patient with severe hypertriglyceridemia. Clin Chem 44:1388–1396
72. Neff D, Ruschitzka F, Hersberger M, Enseleit F, Hurlimann D, Noll G, Luscher T, Hanseler E (2003) Detection of a novel exon 4 low-density lipoprotein receptor gene deletion in a swiss family with severe familial hypercholesterolemia. Clin Chem Lab Med 41:266–271
73. Ng DS, Leiter LA, Vezina C, Connelly PW, Hegele RA (1994) Apolipoprotein A-I Q[-2]X causing isolated apolipoprotein A-I deficiency in a family with analphalipoproteinemia. J Clin Invest 93:223–229
74. Noble RP (1968) Electrophoretic separation of plasma lipoproteins in agarose gel. J Lipid Res 9:693–700
75. Nofer JR, Remaley AT, Feuerborn R, Wolinska I, Engel T, von Eckardstein A, Assmann G (2006) Apolipoprotein A-I (APO A-I) activates CDC42 signaling through ABCA1 transporter. J Lipid Res 47:794–803

76. Oram JF, Heinecke JW (2005) ATP-binding cassette transporter A1: a cell cholesterol exporter that protects against cardiovascular disease. Physiol Rev 85:1343–1372
77. Peelman F, Vandekerckhove J, Rosseneu M (2000) Structure and function of lecithin cholesterol acyl transferase: new insights from structural predictions and animal models. Curr Opin Lipidol 11:155–160
78. Probst MC, Thumann H, Aslanidis C, Langmann T, Buechler C, Patsch W, Baralle FE, Dallinga-Thie GM, Geisel J, Keller C, Menys VC, Schmitz G (2004) Screening for functional sequence variations and mutations in ABCA1. Atherosclerosis 175:269–279
79. Rabes JP, Varret M, Devillers M, Aegerter P, Villeger L, Krempf M, Junien C, Boileau C (2000) R3531C mutation in the apolipoprotein B gene is not sufficient to cause hypercholesterolemia. Arterioscler Thromb Vasc Biol 20:E76–82
80. Reina M, Brunzell JD, Deeb SS (1992) Molecular basis of familial chylomicronemia:mutations in the lipoprotein lipase and apolipoprotein C-II genes. J Lipid Res 33:1823–1832
81. Ruel IL, Couture P, Cohn JS, Bensadoun A, Marcil M, Lamarche B (2004) Evidence that hepatic lipase deficiency in humans is not associated with proatherogenic changes in HDL composition and metabolism. J Lipid Res 45:1528–1537
82. Ruel IL, Couture P, Cohn JS, Lamarche B (2005) Plasma metabolism of apoB-containing lipoproteins in patients with hepatic lipase deficiency. Atherosclerosis 180:355–366
83. Sanger F, Nicklen S, Coulson AR (1977) DNA sequencing with chain-terminating inhibitors. Proc Natl Acad Sci U S A 74:5463–5467
84. Santamarina-Fojo S, Haudenschild C, Amar M (1998) The role of hepatic lipase in lipoprotein metabolism and atherosclerosis. Curr Opin Lipidol 9:211–219
85. Santamarina-Fojo S, Hoeg J, Assmann G, Brewer HJ (2000) Lecithin: cholesterol acyltransferase deficiency and fish-eye disease. In: Scirver C, Beaudet A, Sly E, Valle D (eds) The Metabolic and Molecular Bases of Inherited Disease, 8th edn. McGraw-Hill, New York, pp 2817–2833
86. Scientific Steering Committee on behalf of the Simon Broome Register Group (1991) Risk of fatal coronary heart disease in familial hypercholesterolaemia. Scientific Steering Committee on behalf of the Simon Broome Register Group. BMJ 303:893–896
87. Schonfeld G (2003) Familial hypobetalipoproteinemia: a review. J Lipid Res 44:878–883
88. Smelt AH, de Beer F (2004) Apolipoprotein E and familial dysbetalipoproteinemia:clinical, biochemical, and genetic aspects. Semin Vasc Med 4:249–257
89. Sorci-Thomas MG, Thomas MJ (2002) The effects of altered apolipoprotein A-I structure on plasma HDL concentration. Trends Cardiovasc Med 12:121–128
90. Soufi M, Sattler AM, Maerz W, Starke A, Herzum M, Maisch B, Schaefer JR (2004) A new but frequent mutation of apoB-100-apoB His3543Tyr. Atherosclerosis 174:11–16
91. Stein O, Stein Y (2005) Lipid transfer proteins (LTP) and atherosclerosis. Atherosclerosis 178:217–230
92. Tall A, Breslow J, Rubin E (2000) Genetic disorders affecting high density lipoproteins. In: Scriver C, Beaudet A, Sly E, Valle D (eds) The Metabolic and Molecular Bases of Inherited Disease, 8th edn. McGraw-Hill, New York, pp 2915–2936
93. Wang J, Ban MR, Hegele RA (2005) Multiplex ligation-dependent probe amplification of LDLR enhances molecular diagnosis of familial hypercholesterolemia. J Lipid Res 46:366–372
94. Zandonella G, Haalck L, Spener F, Faber K, Paltauf F, Hermetter A (1995) Inversion of lipase stereospecificity for fluorogenic alkyldiacyl glycerols. Effect of substrate solubilization. Eur J Biochem 231:50–55

5.3 Genetic Disorders of Steroid Metabolism Diagnosed by Mass Spectrometry

Cedric Shackleton

5.3.1 Introduction

It is 70 years since Guy Marrian identified pregnanetriol (5β-pregnane-3α,17α,20α-triol) as a key diagnostic analyte for the form of the adrenogenital syndrome (congenital adrenal hyperplasia, CAH) known as 21-hydroxylase deficiency [9]. Four years ago saw the description of the latest form of CAH, P450 oxidoreductase deficiency [1, 2, 17], and interestingly pregnanetriol remains a key urinary analyte in the diagnosis of this new disorder [91]. In the long period between these findings there has been a steady uncovering of new genetic disorders of steroid synthesis and metabolism.

For 40 years genetic disorders of steroid metabolism have been studied in individual patients primarily through the quantification of select blood analytes by immunoassay and related techniques. The primary analytes are steroids secreted by the adrenal glands and gonads, and most of clinical significance are listed in Table 5.3.1. The similarity of steroid structures has meant that immunoassay techniques can be compromised by crossreactivity and the College of American Pathologists Proficiency testing program demonstrated this to be an almost universal problem in commercial testing, and a particular problem when low levels of hormones are being quantified, such as in pediatrics or postmenopausal women. Within the last few years there has been a push by clinicians investigating patients with potential hormonal disorders to have more accurate data than they have previously accepted, and at quantitative levels much lower.

With the maturation of tandem mass spectrometry (MS/MS) instruments and methodologies, many commercial laboratories are switching to this technique, and high-sensitivity measurements on high volumes of samples are becoming routinely achieved. Since the future of steroid hormone analysis is MS/MS, only MS techniques will be described in this chapter. Immunoassay procedures have been well described and reviewed over the years and will cease to be mainstream methodologies within the next decade.

While the clinical use of MS/MS of hormonal steroids is new, metabolite analysis by gas chromatography (GC)-mass spectrometry (MS) has been available for 40 years, since few immunoassays were developed for urinary analytes. Profile analysis is a very powerful technique and it must be recognized that with few exceptions, all disorders of steroid synthesis and metabolism first had their metabolome defined

Table 5.3.1 *Unconjugated steroids and steroid sulfates of diagnostic importance: Reference ranges (ng/ml, classical techniques or mass spectrometry, MS), MS monitored ions and positive ion MRM transitions, except as noted*

Steroid	Parent ions and MRM transitions	Adult range and/or mean	Child (age, gender, median value, range)	Males (range)	Females (range)	Reference
Pregnenolone	332→86[e] 332→300	**0.12–2.29**	**0.12–2.35**	**0.28–1.65**	**0.17–1.3**	[45]
Labeled d_4	336→90 336→304					
Progesterone	315→109	**0.1–31**	≤0.2	**≤0.3**[b]	**<0.14 fol**	[24, 25]
Labeled d_9	324→100				**<0.31 lut**	Quest Diagnostics (pers. comm.)
17-OH-progesterone	331→97	0.32–2.85	<1 years, 0.11–1.7	**0.32–3.07**	**<1.85 fol**	Quest Diagnostics (pers. comm.)
Labeled d_8	339→100		1–10 years, **0.04–1.15**		**<2.85 lut**	
			10–17 years, **0.16–2.83**			
Analyte	331→109		<0.5 years, MF, **0.32, <2.74**			
	331→97		1–6 years, MF, **0.04,<0.94**			[70]
Labeled d_8	339→113		7–12 years, MF, **0.24, <1.1**			
			13–15 years, MF, **0.34, <2.3**			
			15–18 years, MF, **0.64, <1.64**			
Analyte[e]	361→124	**0.1–1.98**	**10–17 years, M, <1.93**	**0.25–1.39**	**0.1–1.98**	[45]
	361→112		**10–17 years, F, <2.08**			
Labeled d_8	369→128					
	369→115					
Analyte	331→109	**0.47 ± 0.53**				[24, 25, 30]
	331→97					
Labeled d_8	339→113					
17-OH-pregnenolone[e]	348→330	**<1.87–4.09**	**<2.08–4.78**	**0.36–4.09**	**<2.08**	[44]
	348→312					
Labeled d_3	351→333					
	351→333					
21-Deoxycortisol	347→311					[13]
	347→293					

DOC	(331)		0.01–0.1	0.035–0.11	0.015–0.08 fol 0.035–0.13 lut	
Corticosterone Labeled d_8	347→121 355→125	**0.6–12.9**[b]	**0.8–20.3**			[24, 25, 30]
	NA	**0.59–12.93** (am) ≤ **3.86** (pm)	< 1 years, **0.8–17.5** ≤ 10 years, ≤ **12.9** 10–17 years ≤ **14.2**			Quest Diagnostics (pers. comm.)
Aldosterone	361→325 361→315	**0.03–0.28**	**5–9 years, < 0.09** **1–17 years, < 0.35**			Quest diagnostics (pers. comm.)
Analyte	359→331[c]	**0.03–0.16**				[18]
Analyte Labeled d_6	359→331[c] 365→337	**0.046 ± 0.036** (n = **21**)				[25, 30]
11-Deoxycortisol Labeled d_2	347→97 349→97	**0.2–1.3** **0.79 ± 113** (n = **21**)	**0.1–2.0**			[24, 25, 30]
Analyte Labeled d_2	NA	**≤ 1.35**	**< 1 years, 0.1–2.0** **< 10 years, ≤ 1.22** **10–17 years, ≤ 2.45**	**≤ 1.35**	**≤ 1.07**	Quest Diagnostics (pers. comm.)
Analyte[e] Labeled d_2	377→124 377→112 379→124 379→112	**< 0.5**	**< 10 years, < 1.18** **10–15 < 1.34**	**< 0.5**	**< 0.41**	[44]

[a] Bracketed number would be the molecular cation if mass spectrometry is used for quantification
[b] Numbers in bold were obtained by tandem mass spectrometry; others by immunoassay techniques (from Quest Diagnostics manual)
[c] Negative ion
[d] Dansyl derivative
[e] Oxime derivative
[f] If gender not given, values apply to both boys and girls
DHEA Dehydroepiandrosterone, *DHT* dihydrotestosterone, *DOC* deoxycorticosterone, *F* female, *fol* follicular, *lut* luteal, *M* male, *mid* mid-cycle, *MRM* multiple reaction monitoring, *NA* information proprietary, *OH-F* hydroxycortisol, *PM* postmenopausal

■ ***Table 5.3.1*** (continued) *Unconjugated steroids and steroid sulfates of diagnostic importance: Reference ranges (ng/ml, classical techniques or mass spectrometry, MS), MS monitored ions and positive ion MRM transitions, except as noted.*

Steroid	Parent ions and MRM transitions	Adult range and/or mean	Child (age, gender, median value, range)	Males (range)	Females (range)	Reference
Cortisone (E)	361→161 361→105	**6–27**	**2.3–17.7**			[43]
Cortisone (urine, µg/24 h)	361→105	**23–195**		**17–141**	**15–122**	Quest Diagnostics (pers. comm.) [62, 98][f]
Cortisol (F) d_4 labeled	363→97 363→121 367→121	**20–240** **115 ± 54** (n = **21**)	**20–230**			[24, 25, 30, 43]
Analyte[c] Labeled d_2	361→331 363→333	**50–210** (8–10 am) **20–140** (4–6 pm)	1–17 years, **20–170**			Quest Diagnostics (pers. comm.)
Cortisol (urine,µg/24h) d_4 labeled	363→121 363→97 367→121	**4.0–50**	1–4 years, **0.9–8.2** 5–14 years, **1.0–45** 14–17 years, **3.0–55**	**4.2–60**	**3.0–43**	Quest Diagnostics (pers. comm.) [62, 98][f]
18-OH-cortisol (urine, µg/24h)	379→121	**43–515**		**51–515**	**43–295**	Quest Diagnostics (pers. comm.) [62][f]
DHEA Labeled d_2	271→213 273→213	**1.3–12.5** **3.29 ± 4.0** (n = **21**)		**1.8–12.5**	**1.3–9.8**	[24, 25, 30]
DHEA sulfate Labeled d_2	365[c] 367	**1000–2850**	< 5 days[e], 100–2540 < 5 years, 10–400 10–17 years, 150–5550	**1800–3450**	**670–3700**	[86]
Analyte Labeled d_2	271→213 273→213	**2400 ± 1800**				[25, 30]
Testosterone (total) Labeled d_5	289→109 289→97 294→112 294→99		< 10 years, F ≤ **0.35** < 0 years, M, ≤ **0.4** > 10 years, F, ≤ **0.40** > 10 years, M, **0.21–10.0**	**1.2–11.1**	**0.03–0.46**	Quest Diagnostics (pers. comm.)

Analyte	289→109		<0.5 years, M, **0.39, <4.2**			[96]
	289→97		<0.5 years, F, **0.11, <0.85**			
Labeled d_5	294→113		1–6 years, M, **0.06, <0.4**			
			1–6 years, F, **0.05, <0.16**			
			7–12 years, M, **0.10,<2.63**			
			7–12 years, F, **0.13, <0.96**			
			13–15 years, M, **0.82, 0.05–15.5**			
			13–15 years, F, **0.55, 0.19–0.74**			
Analyte[e]	304→112	**0.11–7.8**	<10 years, F, **<0.15**	**2.0–7.8**	**0.11–0.59**	[45]
	304→124		<10 years, M, **<0.09**			
Labeled d_3	307→112		>10 years, F, **0.02–0.63**			
	307→124		>10 years, M, **0.02–8.9**			
DHT (total)	291→255	0.05–0.75		0.25–0.75	0.05–0.3	[107]
Androstenedione	287→97	**0.2–2.85**		**0.4–2.2**	**0.2–0.75**	[24, 25, 30]
Labeled d_7	294→100	**0.43 ± 0.41**			**0.6–2.85**	Quest Diagnostics (pers. comm.)
Analyte	287→97		<0.5 years, M, **0.59, <1.8**			
Labeled d_7	294→113		<0.5 years, F, **0.45, <1.65**			
			1–6 years, M, **0.18, <0.45**			
			1–6 years, F, **0.19, <0.66**			
			7–12 years, M, **0.39, 0.07–1.5**			
			7–12 years, F, **0.58, 0.12–3.3**			
			13–15 years, M, **0.53, 0.08–1.7**			
			13–15 years, F, **1.79, 0.56–4.0**			
Estriol	287→171	≤0.1		≤0.1	≤0.1	[24]
Estriol d_2	289→147					

[a]Bracketed number would be the molecular cation if mass spectrometry is used for quantification

[b]Numbers in bold were obtained by tandem mass spectrometry; others by immunoassay techniques (from Quest Diagnostics manual)

[c]Negative ion

[d]Dansyl derivative

[e]Oxime derivative

[f]If gender not given, values apply to both boys and girls

DHEA Dehydroepiandrosterone, *DHT* dihydrotestosterone, *DOC* deoxycorticosterone, *F* female, *fol* follicular, *lut* luteal, *M* male, *mid* mid-cycle, *MRM* multiple reaction monitoring, *NA* information proprietary, *OH-F* hydroxycortisol, *PM* postmenopausal

■ ***Table 5.3.1*** (continued) *Unconjugated steroids and steroid sulfates of diagnostic importance: Reference ranges (ng/ml, classical techniques or mass spectrometry, MS), MS monitored ions and positive ion MRM transitions, except as noted.*

Steroid	Parent ions and MRM transitions	Adult range and/or mean	Child (age, gender, median value, range)	Males (range)	Females (range)	Reference
Estrone	504→171[d]			**0.01–0.06**	**0.017–0.20** **PM[e] <0.05**	[60]
	NA		< 10 years, F, ≤ **0.03** 10–14 years, F, ≤ **0.07** 15–15, F, ≤ **0.19**	≤ **0.07**	**0.01–0.14 fol** **0.05–0.27mid** **0.02–0.17 lut** ≤ **0.07**	Quest Diagnostics (pers. comm.)
Estradiol	506→171[d]			**0.01–0.04**	**0.015–0.35**	[60]
Analyte Labeled d_4	**255→159** **259→161**					
	NA	**0.03–0.76**	<10 years, 0.005–0.06 10–17 years, F, 0.005–0.4 10–17 years, M, 0.005–0.04	**<0.03**	**0.04–0.37 fol** **0.09–0.76 mid** **0.05–0.44 lut** **≤0.01 PM**	Quest Diagnostics (pers. comm.)
Cholesterol sulfate $^{13}C_2$ labeled	465[c] 467[c]	**50–300**				[79]

[a]Bracketed number would be the molecular cation if mass spectrometry is used for quantification
[b]Numbers in bold were obtained by tandem mass spectrometry; others by immunoassay techniques (from Quest Diagnostics manual)
[c]Negative ion
[d]Dansyl derivative
[e]Oxime derivative
[f]If gender not given, values apply to both boys and girls
DHEA Dehydroepiandrosterone, *DHT* dihydrotestosterone, *DOC* deoxycorticosterone, *F* female, *fol* follicular, *lut* luteal, *M* male, *mid* mid-cycle, *MRM* multiple reaction monitoring, *NA* information proprietary, *OH-F* hydroxycortisol, *PM* postmenopausal
References:
1) Guo et al. 2004, 2) Guo et al, 2006; 3) Quest diagnostics application notes or personal communication of Dr Nigel Clarke; 4) Minutti et al 2004; 5) Cristoni et al. 2004; 6) Fredline et al 1998; 7) Kushnir et al 2003; 8) Taylor et al 2004; 9) Palermo et al 1996; 10) Kletke et al 1991; 11) Starkevic et al 2003; 12) Zhao et al 2003; 13) Nelson et al. 2004; 14) Shackleton and Reid 1989. 15) Holst et al. 2007, 16) Rauh et al. 2006; 17) Kushnir et al. 2006a; 18) Kushnir et al. 2006b;19) Rauh et al. 2006

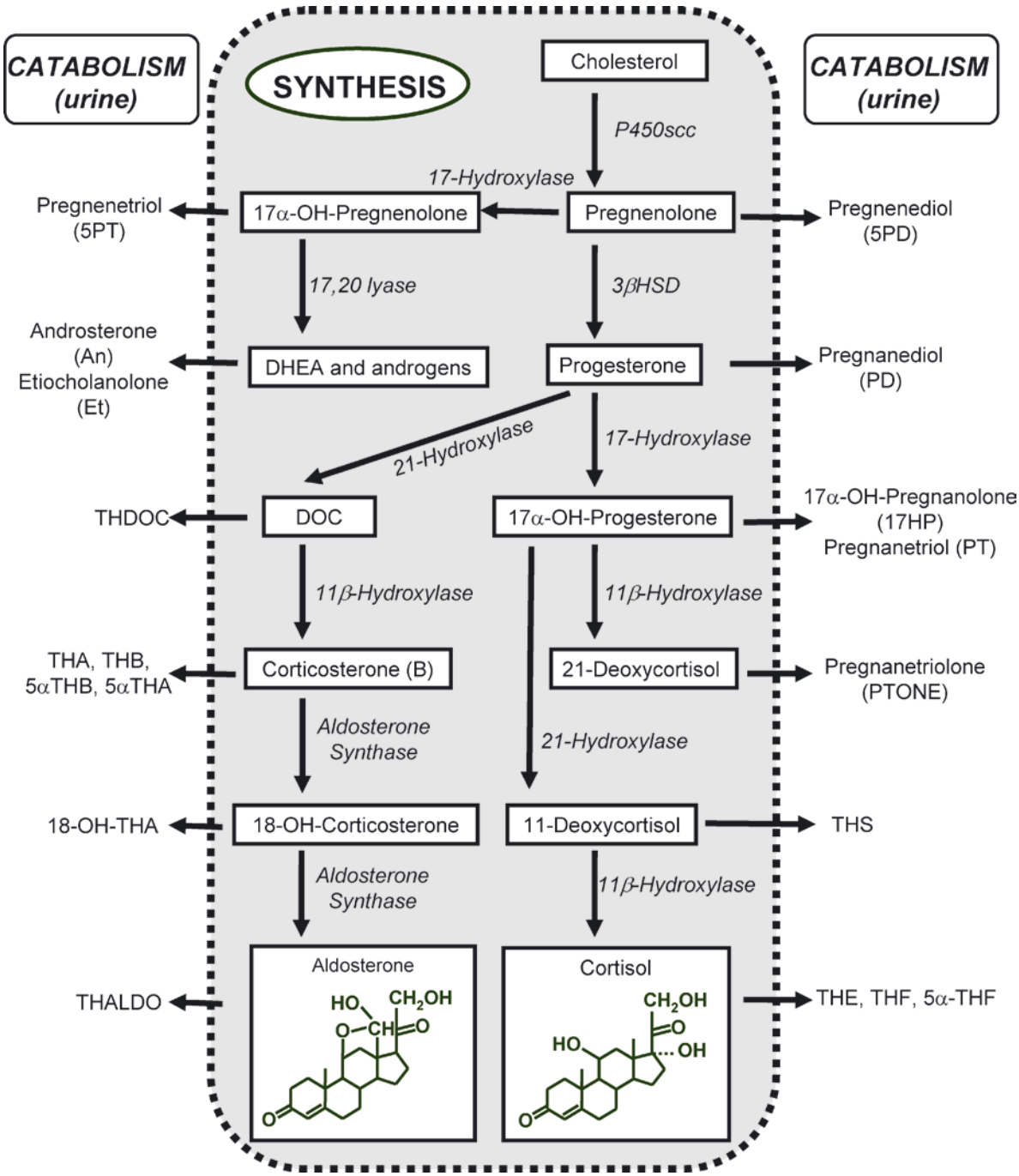

Fig. 5.3.1 Adrenal steroid synthesis and catabolism in man.
3βHSD 3β-Hydroxysteroid dehydrogenase, *DOC* deoxycorticosterone, *THA* tetrahydro-11-dehydrocorticosterone, *THALDO* tetrahydroaldosterone, *THB* tetrahydrocorticosterone, *THDOC* tetrahydrodeoxycorticosterone, *THE* tetrahydrocortisone, *THF* tetrahydrocortisol, *THS* tetrahydro-11-deoxycortisol

using urine analysis, even up to the present day. The greater part of this chapter will detail clinical use of GC-MS profile analysis because this field has been the specialty of the author. The methodology description in this chapter will be divided into two sections, "hormones and precursors [analysis by high-performance liquid chromatography (HPLC)-MS]", and "steroid metabolites (analysis by GC-MS)". The reason behind this division relates to the relatively poor resolution of HPLC compared to GC, which has delayed the use of the former technique in steroid metabolomics, although it is ideal for discrete compound analysis. However, the recent commercialization of instrumentation utilizing small-particle-size liquid chromatography (LC) packings (< 2 μm) may change this as these columns allow separations competitive with GC. Both the Agilent and Waters companies offer such systems, termed rapid resolution LC and ultraperformance LC, respectively [68, 106].

5.3.2 Methods

5.3.2.1 Hormones and Precursors (HPLC-MS)

The Analytes

The synthesis of adrenal steroids is illustrated in Fig. 5.3.1. Cortisol, corticosterone, and aldosterone are formed by sequential hydroxylations and oxidoreductions from pregnenolone and progesterone. 17α-Hydroxypregnenolone (17HP) is a branch-point constituent because it can be converted to cortisol or adrenal androgens. All of the components of this pathway can be quantified by MS/MS. The steroids around the periphery are urinary metabolites and these are measured by GC-MS following hydrolysis of conjugates and derivatization.

HPLC-MS Instrumentation

All major mass spectrometer manufacturers produce suitable instruments for steroid analyses. Typical instruments used in steroid assays are the Applied Biosystems API 2000-5000 series (www.appliedbiosytems.com), the Finnigan TSQ quantum (www.thermo.com), Agilent QQQ or QTof instruments (www.Agilent.com), and Micromass Quattro instruments (www.waters.com).

There are three major ionization sources now used for steroid LC-MS: electrospray ionization MS (ESI), atmospheric pressure chemical ionization (APCI), and atmospheric pressure photoionization (APPI). Under optimal conditions, all ionization methods have similar absolute sensitivities. ESI is preferred for polar and charged (steroid conjugates) molecules, but derivatization or chemical modification of less-polar molecules may be necessary for this technique to match the sensitivity of APPI or APCI.

APCI and APPI are probably the ionization methods of choice for unconjugated, underivatized steroids. They are related techniques; in APCI a corona discharge initiates the ionization process, while this is initiated by ultraviolet light in APPI. There are probably no absolute rules regarding sensitivity, it being very much dependent on the instrument design. A particular source on a particular instrument may be

the most sensitive, but the opposite may be true with a different source/instrument pairing. Kushnir et al. [44, 45] extol the value of oxime derivatization for improving sensitivity, their paper on testosterone quantification containing a figure illustrating the relative sensitivities of APPI, APCI, and ESI sources with and without steroid oximation.

Positive-ion MS is used in the majority of published works and is preferable for most hormonal steroids, with the possible exception of aldosterone. Estrogens and steroid conjugates have greater sensitivity in negative-ion mode.

Standards

Authentic Compounds

Most nonlabeled reference steroids can be obtained from Sigma Aldrich (www.sigmaaldrich.com), Steraloids (www.steraloids.com), and Research Plus (www.researchplus.com). 3β,5β-Tetrahydroaldosterone was kindly supplied by Dr. Bernhard Dick and 3α,5β-tetrahydroaldosterone by Quest Diagnostics. Dr. Liwei Guo and Dr. William Wilson synthesized the Δ^7 and Δ^8 steroids used in the studies.

Internal Standards

The choice of an internal standard is fundamental to accuracy in mass spectrometric procedures. Ideally, the internal standard should not differ in basic structure from the analyte so stable labeled analogs are preferred, with mass differences preferably of more than 4 Da. However, full availability of labeled internal standards for steroid quantification has still not been achieved and non-biological steroids of similar structures may have to be used. This must change soon as too many published methods are compromised by the use of "nonidentical" internal standards.

The following companies supply most of the labeled internal standards used in these studies and potential investigators should review their online catalogues: CIL (Cambridge Isotope Laboratories, www.isotope.com); CDN Isotopes (www.cdnisotopes.com); Medical Isotopes (www.medicalisotopes.com), and Isotec (www.sigmaaldrich.com). These manufacturers will undertake custom syntheses.

Derivatization or Modification for HPLC-MS

In contrast to GC-MS analysis, derivatization is not a prerequisite for steroid analysis by HPLC, but can allow for improvement in sensitivity.

Girard Hydrazones

Preparation of Girard hydrazone increases the ESI sensitivity of steroids with a carbonyl function. Shackleton and co-workers [87] utilized the Girard T hydrazone, a quaternary ammonium cation, and Johnson [41] report ketosteroid profiling using Girard reagents T and P. In the latter method for mono-Girard derivatives, 140 µl Girard reagent T (10 mmol/l in methanol containing 1% acetic acid) is added to the sample. After 15 min at ambient temperature the solvent is removed under nitrogen and 150 µl acetonitrile/water/formic acid (50:50:0.025, v/v/v) added. The aqueous layer is infused into the mass spectrometer. For making di-Girard T derivatives,

Johnson substitutes trifluoroacetic acid (TFA) for acetic acid and conducts the derivatization at 75 C. Griffiths et al. [22] also report extensively on Girard hydrazone derivatives applied to LC-MS analysis of oxosteroids.

Dansyl Derivatization

Nelson et al. [60] published a method for estrone and estradiol measurement using the dansyl derivatives with analysis by APCI. After adding d_4-estrone and d_5-estradiol to 0.5 ml serum, the steroids are extracted with 6 ml methylene chloride. After drying the solvent, 50 µl of sodium bicarbonate and (100 mmol/l, pH 10.5) 50 µl of dansyl chloride (1 g/l) are added. The samples can be injected after heating at 60 C for 1 min.

2-Hydrazino-1-Methylpyridine Derivatization

Higashi and coworkers [28] used 2-hydrazino-1-methylpyridine (HMP) derivatization to introduce a positively charged moiety in testosterone and dihydrotestosterone (DHT) to achieve a sensitivity improvement of 70- to 1600-fold compared to underivatized molecules in ESI. However, they found the derivative was unsuitable for di-keto steroids such as androstenedione and progesterone, so this form of derivatization is unlikely to be widely accepted. Separable syn- and anti- (E and Z) stereoisomers are formed using this derivative. Preparation is as follows: a solution of 10 µg HMP in 50 µl ethanol containing 25 µg TFA was added to the steroid dissolved in 30 µl ethanol. After heating for 1 h at 60 C, the solvents can be removed and sample injected.

Hydroximation

In their studies, Kushnir and co-workers [44, 45] found an increase in sensitivity of ESI detection of testosterone and adrenal steroids when they convert carbonyl groups to oximes. The steroid mixture is dissolved in 300 µl of an aqueous hydroxylamine solution (1.5 mol, pH 10), and following heating for 30 min at 90 C the derivatives are extracted with methyl t-butyl ether (2 ml).

Enzymatic oxidation

Griffiths et al. [23] studied the ESI MS of sterols, and while they are not hormonal steroids, similar derivatization methods can be used. He converts 3β-hydroxy-Δ^5 sterols to 3-oxo-4-ene sterols using cholesterol oxidase and follows this by preparation of Girard P hydrazones. This increases the sensitivity by 1000 in ESI. This technique would also be applicable to pregnenolone, dehydroepiandrosterone (DHEA) and similar Δ^5 steroids, which can also be oxidized by cholesterol oxidase.

Sample Preparation, Sample Introduction, and Automation

The remaining major bottleneck in clinical steroid analysis by MS/MS is sample extraction, and so the development of automated extraction techniques is vital. Quest Diagnostics in California (www.questdiagnostics.com) are leaders in the use of an on-line extraction system based on turbulent flow principles, and through this have overcome the rate-limiting step impeding high-throughput LC-MS/MS analysis. They use a Cohesive Technologies (www.cohesivetech.com) TX4 multiplexing turbulent flow system (high-turbulence liquid chromatography, HTLC) for on-line ex-

traction of steroids from 150 µl serum previously treated with 1% TCA (Dr. Nigel Clark, personal communication). The HTLC system is divided into two functions: solid-phase extraction (SPE) using a large-particle-size (50 µm) column and high flow rate. The high flow rate causes turbulence inside the column, which ensures optimized binding of steroid to the large particles and the passage of residual protein and debris to waste. Following a loading step from 96-well plates, the flow is reversed and the sample is eluted off the loading column and onto the analytical column. Typically, sequential sample injections can be made every 1–2 min.

There is also a current revolution in HPLC with the introduction of small-particle-size (< 0.2 µm) columns and associated instrumentation, which dramatically improves speed and component resolution [68, 106]. This may finally allow the use of LC-MS for steroid metabolomics (i.e., comprehensive analysis of the steroids in human urine or serum).

Recently Published Methods

There are a finite number of analytes that have been measured commercially for many years for the diagnosis of steroid synthetic and metabolic disorders. The discussion of analytes and methodologies below is restricted to these analytes, as listed in Table 5.3.1. This table summarizes the best quantitative normative values available at the time of writing. Accurate values of most steroids listed have been obtained by MS/MS quantitation using isotope-labeled internal standards.

17-Hydroxyprogesterone

Measurement of 17-hydroxyprogesterone has universally been the initial focus of analysts wanting to improve the accuracy of clinical steroid methods through introduction of HPLC-MS/MS and there have been multiple recent publications on this topic. The impetus for this has been the introduction of state-mandated newborn screening for 21-hydroxylase deficiency in the USA. The diagnosis of this disorder in the newborn period is extremely problematic because of major fetal steroid components interfering with the 17-hydroxyprogesterone radioimmunoassay (RIA) [105] and accurate assay procedures for confirming CAH in the newborn period were needed.

Investigators at the Mayo Clinic measured a panel of three steroids (17-hydroxyprogesterone, cortisol, and androstenedione) in blood spots as a follow-up test for newborn screening [46, 58]. The MS was carried out on an API 3000 instrument with a Turboionspray source operating in positive-ion mode. LC was conducted on a microbore C_{18} column with a methanol:water solvent system operating in gradient mode. The internal standard for the three steroids analyzed was $^{2}H_{8}$-17-hydroxyprogesterone. Steroids were analyzed by multiple reaction monitoring (MRM). The transitions utilized are as follows: for analyte 331→109 and 97, and for d_8 internal standard 339→113. The reproducibility of the assay was good, with inter- and intra-assay coefficients of variation of (CVs) about 20% at the lowest level of 1.9 µg/l improving to a mean of about 5% at 50 µg/l. The run times are 4 min for serum steroids and 14 min for paper extracts. In two other works, investigators have chosen to use derivatives in order to improve sensitivity. Chien-Chen Lai and co-workers [47] use the Girard P reagent with 6α-methylprednisolone as an internal standard. They have partially automated the extraction and derivatization by employing 96-well technol-

ogy. They used an ABI 2000 instrument with a Turboionspray source and separation on a C_{18} column. Each analysis took 3 min and 300 could be carried out before instrument cleaning. Intra- and interassay CVs were < 12%. The maximum number of samples analyzed daily was 192 for one technician and one instrument, an equivalent workload to the RIA assay employed in their laboratory. Johnson [41] describes LC-MS/MS of a serum 17-hydroxyprogesterone, cortisol, and androstenedione panel using made with the Girard reagent T hydrazones. He maintains that preparation of the derivative results in a tenfold improvement in sensitivity compared to analysis of the steroids with underivatized ketones. Sample size was 100 µl and the linearity of response was over a 1–1000 ng range. He wisely used three labeled internal standards: $^2H_8$ 17-hydroxyprogesterone, $^2H_3$ androstenedione, and $^2H_3$ cortisol.

Kushnir et al. [44, 45] also measured 17-hydroxyprogesterone within a profile of four adrenal steroids (detailed in "Hormonal Steroid Profiles" below). They utilized an oxime derivative to improve ESI sensitivity and carried out analyses on an ABI 4000 instrument. Rauh and co-workers [70] published a method for 17-hydroxyprogesterone with ancillary measurement of androstenedione and testosterone. The mass spectrometer was an ABI 4000 instrument with an APCI source, operated in positive-ion mode and with on-line cartridge sample extraction and column switching. The MRM transitions were as used by other workers (Table 5.3.1)

21-Deoxycortisol

It has surprised this reviewer that in the effort to lower the rate of false-positive findings in neonatal screening and in young infants there has not been much attention paid to measurement of 21-deoxycortisol, another key analyte overproduced in CAH.

Cristoni and co-workers [13] report the analysis of 21-deoxycortisol by electrospray (ES)-MS and APCI using a Thermofinnigan LCQ ion-trap instrument operated in positive-ion mode. They found that ES afforded greater sensitivity. They addressed the problem of the possible interference of the 21-deoxycortisol isomer 11-deoxycortisol, itself the analyte for diagnosis of 11β-hydroxylase deficiency. While the steroids share many fragmentations. some are specific for each and can be used for MRM MS/MS. In addition, the two compounds are chromatographically separated. Cristoni and co-workers maintain that 21-deoxycortisol is a good analyte for identifying heterozygous individuals for 21-hydroxylase deficiency, and certainly their measurement of 11-deoxycortisol will in the future allow the diagnosis of 11β-hydroxylase deficiency. Good normative data are not available.

Cortisol and Related Compounds

The measurement of these compounds in urine is essential for the study of Cushing's disease, glucocorticoid remediable aldosteronism (GRA), apparent mineralocorticoid excess syndrome (AME), and related conditions. While RIA has been generally satisfactory for serum cortisol assay, urine contains many crossreacting steroids, rendering RIA unreliable.

In an early study Turpeinen and Stenman [99] published a negative-ion MRM ES-MS/MS method for urinary cortisol. The internal standard used was 6α-methylprednisolone and manual extraction was employed. Both steroids eluted within 6 min from the microbore column, but the total run and equilibration time was not reported. The transitions monitored were m/z 361→331 for cortisol and m/z 373→343 for internal standard. The sample size was 1 ml.

Table 5.3.2 *The gas chromatography (GC)-MS urinary free cortisol (*UFF*) and metabolite panel: internal standards, monitored ions, and normal excretions*

Steroid	Ions monitored	Amount of IS added (μg)	Excretion (μg/24 h) adult males, mean and range ($n = 17$)	Excretion (μg/24 h) adult females, mean and range ($n = 17$)
Cortisol (UFF)	605		35, 10–57	23, 8–61
F-d_4	609	0.18		
Cortisone (UFE)	531		58, 13–104	50, 21–107
E-d_2	533	0.12		
6β-OH-F	513		164, 70–261	108, 36–250
6β-OH-F-d_2	515	0.8		
18-OH F	385		148, 53–274	71, 28–133
18-OH-F-d_2	387	0.4		

Taylor and colleagues [98] at the Mayo Clinic published a method for the simultaneous analysis of urinary cortisol and cortisone. They used $^2H_4$ cortisol as an internal standard and took a 0.5-ml urine sample. An API 2000 with Turboionspray source was used in the positive-ion mode. Chromatography was conducted on a standard-bore C_{18} column with C_{18} precolumn filter. MRM was conducted in the positive-ion mode monitoring *m/z* 363→121 for cortisol, 367→121 for $^2H_4$ cortisol, and 361→121 for cortisone. Cortisol and cortisone were separated and both were eluted within 2 min. Inter- and intra-assay variation for both compounds was <9% for amounts above 2 μg/dl. The values obtained agree well with those of other studies, such as ours (Table 5.3.2) [62]. They found a range for cortisol for adult males of 4.2–60 μg/24 h and for adult females 3.0–43 μg/24 h. In summary, the 3-min run time of their method has allowed the Mayo group to completely transfer their cortisol and cortisone workload from RIA and HPLC to MS/MS.

Quest Diagnostics use an LC-MS/MS panel for diagnosing cortisol-related disorders by urine analysis. This panel was designed to diagnose Cushing's syndrome and the hypertensive conditions AME and GRA. The panel quantifies cortisone, cortisol, 6β-hydroxycortisol and 18-hydroxycortisol (18-OHF). The Quest analysis uses $^2H_4$ cortisol as an internal standard and HTLC for on-line extraction. This panel has replaced the RIA and HPLC methods previously used by this commercial laboratory. Another recent publication describes MS/MS of cortisone and cortisol in serum using APPI and similar conditions and MRM transformations to those listed above [43].

The usefulness of cortisol and cortisone measurements in evaluating 11β-hydroxysteroid dehydrogenase (11βHSD) activity has spurned interest in the HPLC-MS analysis of their tetrahydrometabolites, an assay until now conducted by GC-MS as part of metabolic profiling. Turpeinen et al. [100] report on the measurement of unconjugated tetrahydrocortisol, 5α-tetrahydrocortisol, and tetrahydrocortisone and Raffaelli and co-workers [69] present data on developing a method for the

free and conjugated metabolites. These were preliminary studies and the HPLC-MS/MS technique is not yet mature enough to replace GC-MS methods.

Corticosterone and Deoxycorticosterone

Corticosterone is a component of the steroid profile (see "Hormonal Steroid Profiles", below) developed by Guo et al. [25]. The analysis uses positive APPI and a d_8 corticosterone internal standard. MRM was conducted with the *m/z* 347→121, and 355→125 transitions, respectively. The lower detection limit (LOD) was 2 pg/ml. Quest Diagnostics offer MS/MS analysis of this steroid commercially and have published normative values, as listed in Table 5.3.1. Marwah et al. [56] have published a method for the quantitation of corticosterone in rat plasma using electrospray MS. MS/MS methods for deoxycorticosterone (DOC) have not been published.

11-Deoxycortisol

CAH caused by 11β-hydroxylase deficiency is diagnosed by finding elevated 11-deoxycortisol. This steroid is included in the profiles of Guo et al. [24, 25] and Kushnir et al. [44] described below in "Hormonal Steroid Profiles". Guo et al. monitored the transitions *m/z* 347→97 for the analyte and 349→97 for the dideutero internal standard. Kushnir et al., utilizing the oxime derivative monitored transitions 371→24 and 112 for the analyte and 379→124 and 112 for the dideutero standard. Quest diagnostics offer this MS/MS method and provide most of the quantitative values listed in Table 5.3.1.

Aldosterone

Fredline et al. [18] report an MRM negative-ion ESI method for aldosterone using flumethasone as an internal standard. The MRM transition used was 359→331. The assay was linear over a 15- to 5000-pg/ml range and the limit of quantitation was 15 pg/ml. A manual extraction was used and recovery and accuracy were excellent.

This steroid is included in the panel of steroids profiled by Guo et al. [25]. They also use negative-ion detection (APPI) monitoring the transitions 359→331 and 365→337 for the analyte and d_6 internal standard, respectively. The LOD was 10 pg/ml. Quantitative data on circulating levels obtained using this methodology are given in Holst et al. [30]. Quest Diagnostics use APCI in positive-ion mode monitoring the transitions 361→325 and 361→315 (Table 5.3.1).

Pregnenolone and 17HP

These steroids are components of the profile of Kushnir et al. [44, 45] and are discussed below in "Hormonal Steroid Profiles". They were analyzed as the oxime derivatives by ESI on an API 4000 instrument. The MRM transitions for pregnenolone oxime were 332→86 and 300, and for the d_4 internal standard 336→90 and 334. Transitions for 17HP were 348→330 and 312, and for the d_3 internal standard 351→333 and 315. The publication gives quantitative data for Tanner stage 1–5 male and female children and for several age groups up to 52 years.

Testosterone and DHT

Testosterone assays have been notoriously inaccurate, particularly at the low levels found in women and children. Excess testosterone in women is often a cause of infertility, hirsutism, amenorrhea, and obesity, and accurate measurement is essential

for evaluating the causes of these disorders. Accurate measurement in small sample volumes is essential in pediatrics. Starcevic and coworkers [96] report the LC-MS/MS of serum testosterone using an ABI triple-quadrupole mass spectrometer in the positive-ion mode. Trideutero-testosterone was the internal standard. The run time is 1.25 min. They monitored the transition *m/z* 289→97 for the analyte and 292→97 for the internal standard. These investigators achieve excellent reproducibility and linearity. Sensitivity down to 10 pg/ml allows them to readily measure the hormone in samples from females and children. Data produced using this new method correlates perfectly with data produced by classical methodology. Higashi and co-workers [27] use an ESI MS/MS method for measuring testosterone and DHT with HMP derivatization to improve the sensitivity.

Oxime derivatization was utilized by Kushnir et al. [44] to improve ESI sensitivity for testosterone measurement. Using a C_{18} column for separation (3-min run times) and an API 4000 they monitored MRM transitions 304→124 and 112 for testosterone oxime and 307→14 and 112 for the d_3 internal standard. Within-run and between-run irreproducibility was < 12%. The LOD was 10 pg/ml, allowing accurate measurement of testosterone in women and children. Reference intervals for the steroid in children of different ages and different Tanner stages are given in the publication as well as values for both free and total testosterone.

Quest Diagnostics have established a routine system for testosterone, which has now replaced their other methods of analysis (Goldman et al., poster, US Endocrine Society meeting, San Diego, 2005). The analysis is carried out on a Thermofinnigan TSQ Quantum Ultra operated with an APCI source in the positive-ion mode. They use two transitions, 289→109 and 289→97, for the analyte and 294→112 and 294→99 for the $^2H_5$-labeled internal standard. On-line extraction and short retention times allow them to assay several thousand samples per month per instrument, making it cost-effective in spite of the high cost of instrumentation.

Androstenedione

Measured as part of a CAH panel by Minutti et al. [58], using the transition 287→97, see above ("17-Hydroxyprogesterone"). They stress the added specificity of CAH detection in second-tier analysis for CAH when androstenedione is measured as well as 17-hydroxyprogesterone. This is also measured commercially by Quest Diagnostics and included in the Guo et al. hormonal profile [24, 25] (see "Hormonal Steroid Profiles" below).

Estrone and Estradiol

The routine measurement of estrone and estradiol by immunoassay techniques has also given rise to the familiar problems of poor sensitivity, cross-reactivity, and poor intermethod reproducibility. Most automated methods cannot measure these steroids in sera of children and men. Development of LC-MS/MS methods has also proven challenging as most investigators have found that estrone and estradiol are poor ionizers and the desired sensitivity has not been achieved. The Mayo group [60] published the LC-MS/MS quantification of estradiol and estrone using dansyl chloride derivatives (described above) and $^2H_5$ estradiol and $^2H_4$ estrone internal standards.

Using the best of modern instrumentation, derivatization may not be necessary to reach sensitivity requirements for estradiol measurement. Estradiol is an analyte

within the Guo et al. [24, 25] panels (see "Hormonal Steroid Profiles" below). Using API 3000 and 5000 instruments with APPI sources in positive-ion mode they measure the *m/z* 255→159 transition for estradiol and *m/z* 259→161 for d_4 estradiol. The LOD was 10 pg/ml.

Quest diagnostics also provide commercial estrone and estradiol measurement by MS/MS and their normative data are listed in Table 5.3.1.

The Applied Biosystems Company have demonstrated outstanding estradiol measurement sensitivity at levels down to 0.1 pg "on-column" on their API 5000 instrument with an APCI source. The linearity was excellent over the range 0.001–10 ng/ml (company demonstration data). Thus, this analyte should not require derivatization if the latest equipment is available.

Estriol

This steroid is part of the Guo et al. [24] profile, monitoring negative-ion transitions *m/z* 287→171 for estriol and *m/z* 289→147 for dideuteroestriol.

DHEA and DHEA Sulfate

Guo et al. [24, 25] analyzed these in positive-ion mode APPI with transitions *m/z* 271→213 for DHEA and 273→213 for the dideutero internal standard. Quantitative data from these studies are reported by Holst et al. [30].

DHEA sulfate is more suited to measurement by negative-ion ES-MS, as demonstrated in an early study by Shackleton et al. [86].

Hormonal Steroid Profiles

I consider hormonal steroid profiles to be those analyses that encompass a panel of steroids that can diagnose different endocrine abnormalities. A panel of multiple steroids used to diagnose a single condition, for example 21-hydroxylase deficiency, would not be a steroid profile under this definition.

Guo and co-workers [24, 25] have spearheaded the development of MS/MS serum steroid profiles. Their most recent report describes profiling in 11 min of 12 steroids in 200 µl serum with minimal work-up, comprising acetonitrile protein precipitation. The steroids analyzed were as follows: DHEA sulfate, DHEA, aldosterone, cortisol, corticosterone, 11-deoxycortisol, androstenedione, estradiol, testosterone, 17-hydroxyprogesterone, progesterone, and 25-hydroxyvitamin D_3. Stable-isotope-labeled internal standards were incorporated for each steroid. An API-5000 instrument was used with the APPI source in positive-ion mode, with the exception of aldosterone, which had greater sensitivity in negative-ion mode. Separation was carried out on a C_8 column, which allowed more rapid separation than the more commonly utilized C_{18}. The MRM transitions utilized are shown in Table 5.3.1. The lower level of sensitivity was between 1.5 and 10 pg/ml, dependent on the steroid. The authors were exhaustive in addressing issues of accuracy, recovery (90–110%) and reproducibility (< 12.2% for same-day and between-day).

Kushnir et al. [45] report the HPLC-MS/MS analysis of four adrenal steroids, 17-hydroxyprogesterone, pregnenolone, 11-deoxycortisol, and 17HP designed to diagnose 21-, 17-, and 11β-hydroxylase deficiencies, and 3β-hydroxysteroid dehydrogenase (3βHSD) deficiency, respectively. These four compounds were measured in 200 µl serum following SPE, oxime formation, and re-extraction with methyl tert-butyl ether. Oxime formation was included because it gave rise to a great improvement in ESI

ionization efficiency and collision-induced dissociation fragmentation. The analysis was conducted on an API 4000 instrument operated in positive ESI mode following separation on a C_{18} column. Samples were injected every 7.5 min. Within-run and between-run imprecision was < 11%. The LODs were < 100 pg/ml.

Summary of MS/MS Quantitation

Clearly, there are basic successful practices evolving with regard to MS/MS steroid quantitation, which can be summarized as follows:

1. The use of positive-ion MS except for steroid conjugates, and possibly aldosterone and estrogens.
2. The use of APPI or APCI for unconjugated steroids; ESI for steroid conjugates or when derivatives are analyzed.
3. If possible use labeled internal standards for all analyses.
4. Utilize on-line extraction and separation techniques to minimize work-up procedures and increase throughput.

5.3.2.2 Metabolites of Hormones and Hormone Precursors by GC-MS

The Analytes

The synthesis of adrenal steroids and major excreted metabolites is illustrated in Fig. 5.3.1. Little secreted steroid product is excreted unchanged and most of the catabolism takes place in the liver, although cortisol metabolism by the kidney is clinically important and microbial metabolism in the gut can be quantitatively significant. The major metabolic transformations of hormonal steroids and precursors are detailed by Makin [54] and summarized in Fig. 5.3.2. GC-MS steroid profiling is the technique of choice for measurement of important urinary constituents.

Androgens such as DHEA and testosterone are largely excreted as 17-ketosteroids. The 17-oxo-:17β-hydroxy ratio in metabolites is about 10:1. Hormonal steroids with a 3-oxo-4-ene group are metabolized primarily to ring-A 3α-hydroxy-5βH (3α5β) and 3α5α metabolites. For 11-deoxy androgens the 5α:5β ratio is about 1:1, but for 11β-hydroxylated androgens, α-reduction dominates (5α:5β ratio about 3:1). For 21-deoxypregnanes and cortisol metabolites, 5β-reduction predominates for all but the first months of life, and for corticosterone metabolites, 5α-reduction is greater. The ring-A reduced metabolites of corticosteroids are frequently referred to as "tetrahydro-" metabolites. Reduction of the 20 carbonyl is predominately "α" for 21-deoxy steroids, but equally α- and β- for cortisol and its derivatives.

Typically, the ratio of 11-carbonyl to 11β-hydroxy metabolites of cortisol is about 1:1. Cortisol or its metabolites can be additionally metabolized by side-chain cleavage, giving 11-oxygenated C_{19} steroids (about 15%), and an average of 12% of cortisol is converted to cortoic acids by oxidation of the C-21 hydroxyl [59, 82]. 17-Deoxy corticosteroids have high biliary excretion and are subject to intestinal microbial 21-dehydroxylation prior to reabsorption and further hepatic metabolism. Minor amounts of steroids are subject to further hydroxylation. 6β- is typical for 3-oxo-4-ene steroids and 6α- and 1β- for ring-A saturated steroids. 3β-Hydroxy-5-ene steroids (e.g., DHEA) are largely metabolized by 16α-hydroxylation (and 16β to a lesser degree), particularly in fetal and neonatal life. Hydroxylation at 15 (α- and β-)- and

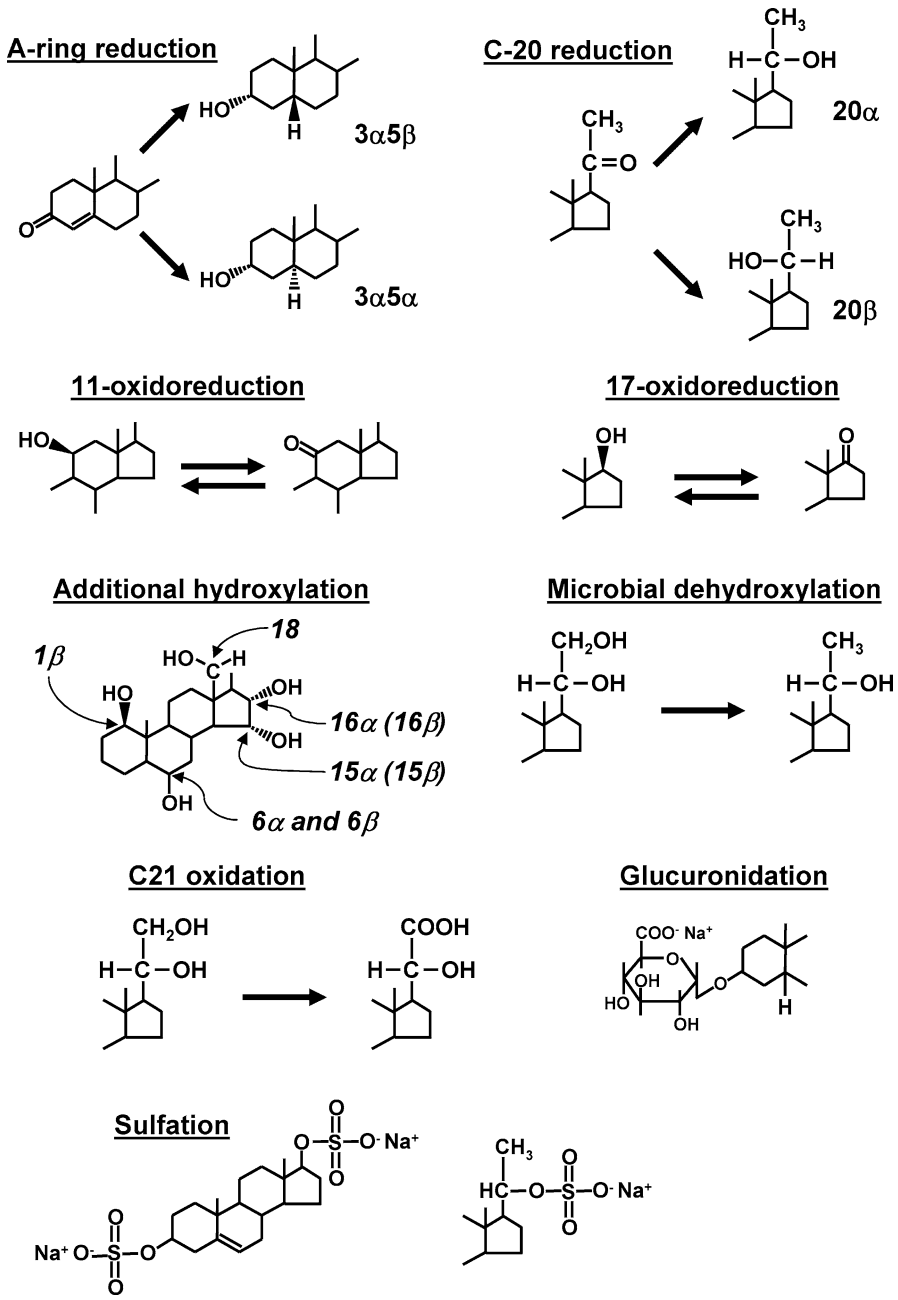

Fig. 5.3.2 Principal catabolic reactions undergone by steroid hormones and precursors

18 are also important in perinatal life [80]. In pregnancy, estriol (16α-hydroxy estradiol) is the major metabolite of fetal DHEA. Pregnenolone and 17HP are almost exclusively 20α-reduced prior to excretion. 3β-Hydroxy-5-ene steroids are also converted to 3β5α metabolites.

About 5–10% of steroids are excreted as free compounds. 3β-Hydroxy-5-ene steroids are almost exclusively excreted as sulfate esters, ring-A reduced steroids are excreted as glucuronides.

GC-MS Instrumentation

We use single-stage quadrupole (typically Agilent bench-top 5971 or 5973MSD) instruments for most applications. The current model offered is the Agilent 5975 (www.agilent.com).

Recent developments have made ion-trap mass spectrometers excellent tools for profile analysis. One of the biggest advantages of this kind of instrumentation lies in the ability to perform multiple stages of MS/MS (MS^n), unlike conventional quadrupole instruments. This capability increases the amount of structural information obtainable and reduces the background signal, allowing an improvement in the limit of detection. We use electron-impact ionization as it gives a greater ion choice for selected ion monitoring (SIM) than chemical ionization.

The Sample for Analysis

Should a 24-h sample be collected or does a random (spot) sample suffice? Our methodologies generally utilize a form of precursor:product ratio for the diagnosis of most conditions so we are satisfied with random collections. However, it is important that for certain analytes accurate quantification is achieved, which requires 24-h sample collection. Cases in point would be the excretion of unconjugated cortisol and related compounds, and the measurement of tetrahydroaldosterone (THAldo) required for the diagnosis of mineralocorticoid-related conditions.

We generally request that the aliquot be collected without preservatives, although if local conditions necessitate it, we suggest adding a Stabilur tablet (www.cargille.com). The sample should be frozen after collection and shipped overnight with an ice pack or dry ice. Samples can be shipped dry after extraction on a SPE C_{18} cartridge (detailed in " Work-Up Procedures" below). If random samples are analyzed then it may be desirable to also measure urinary creatinine so that excretions can be reported per gram of creatinine.

Sample Work-up Procedures

The methodology is detailed by Shackleton [76, 77]. For the comprehensive profile, 1–2 ml urine (or serum) is extracted by C_{18} solid SPE cartridge (Sep-Pak from Waters Corporation used in our studies, www.waters.com, but there are multiple vendors) by first passing 4 ml of methanol through, followed by 4 ml water, and then the urine sample. This is followed by 4 ml of water; finally the steroids are recovered with 4 ml

methanol. For free plus conjugate analysis, the methanolic extract is dried and 3 ml of 0.1 M acetate buffer (pH 4.5) is added, prepared by mixing three parts of 0.2 M sodium acetate with two parts 0.2 M acetic acid. After adding 10 mg sulfatase (type H1 from Sigma, www.sigmaaldrich.com) and 12 µl β-glucuronidase/aryl sulfatase (Roche Diagnostics, www.roche-diagnostics.com), hydrolysis is allowed to proceed for 3 h at 55 C. The Sep-Pak cartridge extraction is repeated.

Internal standards

We prepare a methanolic solution of up to five compounds. The principal three are 5α-androstan-3β-ol (androstanol), stigmasterol, and cholesteryl butyrate, although only the stigmasterol is used for quantification. The other two standards are used for monitoring column performance and temperature-dependent discrimination. The androstanol and cholesteryl butyrate bracket the steroids of interest, the former eluting first and latter last. Three steroids are not quantified against stigmasterol. Reference 18-hydroxy-tetrahydro-11-dehydrocorticosterone (18-OH-THA) is unavailable and cannot be included in the calibration mixture. It is quantified against the calibrated tetrahydrocortisone (THE) as the compounds are isomers (*m/z* 578, M-31 monitored). THAldo produces multiple derivatives through having a hemiacetal structure, and consistent derivatization is challenging. Thus, we provide it with its own standard, the nonhuman 3β,5β-epimer, which forms the same derivatives but is chromatographically resolved. We quantify the mono-oxime, bis-trimethylsilyl (TMS) derivative, which gives a strong M-103 ion at *m/z* 506.

18-Oxo-tetrahydrocortisol (18-oxo-THF) is an analyte that is useful for diagnosis of GRA, and if GC-MS is being used for the diagnosis of this condition the following method is suggested. The reference standard is unavailable so cannot be included in calibration mixture. This compound has two distinctive ions at *m/z* 420 and *m/z* 594. We quantify the 594 ion against the M + 1 ion of 5-pregnene-3β,17α,21-ol-20-one included in the internal standard mixture.

Derivatization

Methoxyamine hydrochloride (100 µl, 2% in pyridine) is added and derivatization allowed to proceed for 60 min at 55 C. The pyridine is blown off with nitrogen and 50 µl trimethylsilylimidazole (TMSI) added. The silylation proceeds for 16 h at 100 C. This silylation time can be reduced to 4 h by increasing the temperature to 120 C. TMSI is an involatile reagent and must be removed prior to GC-MS analysis, as follows: add 1 ml of cyclohexane while reaction tube is still hot. The TMSI is removed by adding 500 µl of water, vortexing, centrifugation, and discarding the bottom layer with a glass Pasteur pipette. The tube is vortexed with a further 500 µl of water and the top layer is transferred to injection vial, taking care not to transfer any of the water layer (Dr. Norman Taylor, personal communication).

GC-MS Analysis Conditions

Scanning or SIM?

True profile analysis requires scanning over the whole mass range for the acquisition of all data on excreted compounds. Quantitation has been more challenging on a quadrupole instrument because total ion current peaks are seldom a single component and extracted-ion chromatograms (EICs) when recovered from scanned data are of poor quality due to the lower sensitivity of scanning GC-MS. Thus, we developed profile analysis based on SIM of selected analytes but tried to ensure the components of every steroid class of interest were included. For ion traps the fundamental form of data collection (in non-MS/MS mode must be full –scans). Thus, the quantitative data produced are EICs obtained from scanned data. The EICs are of the same ions used for SIM in quadrupole instruments and the calibration external standards are the same.

Quadrupole MS

In our laboratory, GC-MS routine applications are carried out on a 5890 gas chromatograph coupled with a 5971 MSD (Hewlett-Packard, Palo Alto, CA, USA; now Agilent; www.agilent.com). The steroids are separated on a non-polarDB-1 crosslinked methyl-silicone column, 15 m × 0.25 mm inner diameter (i.d.), film thickness 0.25 μm (Agilent). Helium is used as the carrier gas at a constant pressure of 5 psi (34.47 kPa). A 2-μl aliquot of the final derivatized extract is injected into the system operated in splitless mode (valve opened at 2 min). The GC temperature is ramped as follows: initial 50°C, held for 3 min, increased to 230°C at 30°C/min, thereafter increased to 285°C at 2°C/min. The injector and transfer line are kept at 260°C and 280°C, respectively. When scanning, the mass range scanned is 90–650. The latest version of the Agilent instrument (MSD5975) has a mass range of 1000 and allows simultaneous scanning and SIM. Other useful new features are deconvolution software for background subtraction and automatic retention time adjustment so that the retention times of individual components remain constant.

Ion-Trap MS/MS

We use a GC Top 8000 gas chromatograph coupled with a PolarisQ ion-trap mass spectrometer and equipped with an AI3000S autosampler (Thermofinnigan; www.thermo.com). The steroids are separated on a DB-1 crosslinked methyl-silicone column, 15 m × 0.25 mm i.d., film thickness 0.25 μm (J&W Scientific; marketed by Agilent). Helium is used as a carrier gas at a constant pressure of about 35 kPa. A 1-μl aliquot of the final derivatized extract is injected into the system operated in splitless mode (valve opened at 2 min). The GC temperature program is the same described before for the quadrupole GC-MS system. The injector and transfer lines are kept at 260°C and 280°C, respectively. The ion source temperature is 225°C. A damping gas flow of helium is applied to the ion trap.

SIM Quantification (Selected Ion Chromatography for Ion Trap)

Mass spectra of methoxime (MO)-TMS derivatives of steroids typically give the following fragments: M-31 (loss of oxime), sequential "90" losses (trimethylsilanol), loss of the primary TMS group (M-103), and combinations thereof. Often the ion chosen for monitoring is one formed by the above fragmentations. A detailed de-

■ ***Table 5.3.3*** *The comprehensive urine steroid GC-MS profile*

Component	Retention time (min)	Specific ion monitored	Calibration mixture amount (µg)	Excretion Males µg/24 h ($n = 17$)	Excretion Females µg/24 h ($n = 17$)
5α-Androstan-3β-ol (IS)	11.28	333	2.5	–	–
3β5βTHAldo (IS)	21.34	506	0	–	–
5P-3β,17,21-ol-20-one (IS)	21.03	594	0.5	–	–
Stigmasterol (IS)	25.27	394	2.5	–	–
Sigmasterol underivatized	24.50	412	0		
Cholesteryl butyrate (IS)	28.77	368	2.5	–	–
Androsterone (An)	13.09	270	2.5	798–4705	373–3414
Etiocholanolone (Et)	13.23	270	2.5	689–3252	450–2900
11-Oxo-Et	14.28	269	2.5	79–1026	57–916
11β-OH-An	15.21	268	2.5	500–1733	191–854
11β-OH-Et	15.38	268	2.5	18–1034	14–687
5α-Androstan-3α,17β-diol	13.20	331	0.5	48–578	15–147
DHEA	13.83	268	2.5	5–1476	20–1139
5-androstene-3β,17β-diol (5AD)	14.03	239	2.5	45–954	28–201
16α-OH-DHEA	15.68[a]	266	2.5	40–796	35–655
5-androstene-3β,16α,17β-triol (5AT)	17.31	432	2.5	42–710	40–540
5,17-Pregnadien-3β-ol (5PD)	12.91[b]	372	0.5	10–50	10–50
5-Pregnene-3β,20α-diol (5PD)	17.17	372	0.5	10–150	10–150
5-Pregnene-3β,17α,20α-triol (5PT)	19.49	433	0.5	28–1062	44–342
Estriol	17.90	504	0.5	1–16	2–32
17-OH-pregnanolone (17HP)	15.19	476	2.5	41–728	32–657
Pregnanetriol (PT)	16.63	435	2.5	186–1505	87–1311
Pregnanetriolone (PTONE)	18.48	449	0.5	4–37	1–77
THS	17.54	564	0.5	10–109	17–117
THDOC	17.19	476	0.5	2–38	1–157

■ ***Table 5.3.3*** (continued) *The comprehensive urine steroid GC-MS profile*

Component	Retention time (min)	Specific ion monitored	Calibration mixture amount (μg)	Excretion Males μg/24 h ($n = 17$)	Excretion Females μg/24 h ($n = 17$)
THA	19.70	490	2.5	104–554	76–596
5αTHA	20.33	490	2.5	52–277	38–298
THB	19.96	564	2.5	32–238	26–262
5αTHB	20.27	564	2.5	135–588	49–447
(18-OH-THA)	21.37	457,578	0	45–184	25–207
THAldo	21.12	506	0.2	10–58	6–63
Cortisone (E)	24.39[a]	531	0.5	92–366	49–215
Cortisol (F)	25.73[a]	605	0.5	35–168	25–115
THE	19.38	578	2.5	1365–5788	727–3815
THF	20.39	562	2.5	942–2800	458–1907
5αTHF	20.61	562	2.5	796–2456	142–1589
(18-Oxo-THF)	20.40	594,420	0	1–10	1–10
α-Cortolone	20.99	449	2.5	449–2044	457–1564
β-Cortolone	21.60	449	2.5	231–1534	216–814
β-Cortol	21.46	343	2.5	196–880	124–690
α-Cortol	22.38	343	2.5	96–509	122–365
6β-OH-F	26.53	513	0.5	122–487	53–416

[a]These steroids give two peaks, both of which are integrated
[b]This steroid is an artifact of 5-pregnene-3β,20α-diol disulfate
5α*THA* 3α,21-Dihydroxy-5α-pregnane-11,20-dione, 5α*THB* 5α-tetrahydrocorticosterone (3α,11β,21-trihydroxy-5α-pregnane-20-one), 5α*THF* 3α,11β,17α,21-tetrahydroxy-5α-pregnane-20-one, IS internal standard, *THA* tetrahydro-11-dehydrocorticosterone (3α,21-dihydroxy-5β-pregnane-11,20-dione), *THAldo* tetrahydroaldosterone, *THB* tetrahydrocorticosterone (3α,11β,21-trihydroxy-5β-pregnane-20-one), *THDOC* tetrahydrodeoxycorticosterone (3α,21-dihydroxy-5β-pregnane-20-one), *THE* tetrahydrocortisone (3α,17α,21-trihydroxy-5β-pregnane-11,20-dione), *THF* tetrahydrocortisol (3α,11β,17α,21-tetrahydroxy-5β-pregnane-20-one), *THS* tetrahydrosubstance S (3α,17α,21-trihydroxy-5β-pregnane-20-one)

scription of fragmentations of steroid TMS and MO-TMS derivatives is given in Griffiths et al. [23] (2005).

Two features about steroid oximes should be mentioned since they impact quantification; firstly, an 11-carbonyl group is sterically hindered and not derivatized, so steroids containing this moiety have a mass 29 units less than expected. Secondly, each carbonyl can be derivatized two stereospecific ways, termed "syn-" and "anti-". These may or may not be resolved by GC. If they are resolved it is preferable to determine the area of both peaks since the relative amount of "syn-" and "anti-" forms may vary between different derivatizations.

Table 3.5.1 shows the list of steroids in our regular "adult" profile (termed comprehensive profile) with ions monitored, amount of steroid in the calibration mixture prepared, and excretion ranges.

External (Calibration) Standard

Table 5.3.3 gives the steroids included in the external calibration standard, with amounts derivatized. This table also lists the steroids we routinely measure in the urine of children and adults, the ions chosen for monitoring, and our excretion ranges for adults. The calibration mixture, or external standard, is prepared about every 3 months and the stock solution (in cyclohexane) stored in a freezer.

The quantitative steroid excretion ranges given in Table 5.3.3 are for guidance only, each analyst needs to establish his or her own normative values. Typical retention times are given in Table 5.3.3, which rarely change, but of course will be different from those of other investigators. The relative retention times should remain constant between investigators using columns with the same stationary phase and similar oven programs.

For space considerations we are not including here details regarding an SIM program used for profile analysis in the first days and weeks of life when steroid excretion is most different from that of older individuals [10, 80].

High-Sensitivity/High-Specificity Analysis by MS/MS

Our involvement in follow-up analysis to prenatal screening has required steroid profiling in midterm maternal serum. GC-MS profiling of steroids in small blood sample volumes using a single-stage quadrupole instrument has been a challenge because of the relatively poor sensitivity and high background.

Using the Thermofinnigan PolarisQ ion-trap, we developed a sensitive and specific MS/MS method for the prenatal diagnosis of "low-estriol" disorders. The method takes advantage of the resolving power of MS/MS to eliminate background interferences, thus increasing the overall sensitivity. Moreover, the high specificity achieved allowed a reduction in the overall run time (from 30 min to 15 min), by modifying the temperature program on the GC. For each of the 18 steroids in the profile (see "Summary" below), different fragmentation reactions were studied and their collision energies optimized.

Optimization of conditions was effected following a two-step process. In the first step, a full-scan spectrum was obtained for each of the steroids. Product-ion spectra at five different collision energies (0.5, 1, 1.5, 2, and 2.5 V) were then obtained for the main precursor ions of the full-scan spectra. Through these studies, candidates were chosen for both precursor and product ions in the MS/MS mode. Once all transitions had been chosen for the MS/MS mode, the final tuning process was carried out

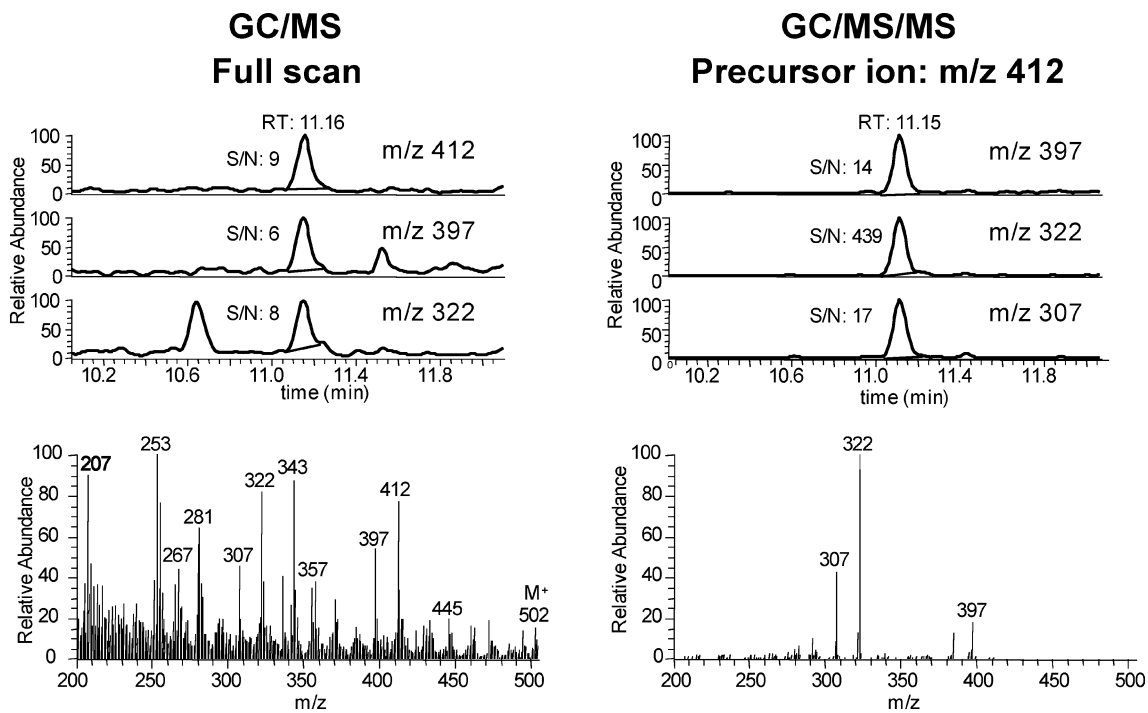

Fig. 5.3.3 Utilizing ion-trap tandem mass spectrometry (MS/MS) for improving the specificity and sensitivity of serum dehydroestriol quantification

by analyzing serum steroid derivatives. Each possible precursor ion was fragmented using ten different collision energies (in 0.1-V steps), bracketing the best value obtained from the previous experiment.

As an example of specificity improvement, Fig. 5.3.3 shows the full scan and product-ion MS/MS spectrum for 8-dehydroestriol, a prenatal hallmark of a fetus affected by Smith–Lemli–Opitz syndrome (SLOS), usually found in low concentrations. When using full scan mode, the detection of the most abundant ions (*m/z* 412, 397, 322, and visual appearance of the full spectrum) was compromised by the high background (Fig. 5.3.3, left). In contrast, acquisition in MS/MS mode (precursor ion *m/z* 412) provides a cleaner mass spectrum and a superior signal to noise ratio, especially for the transition product ion *m/z* 322 (Fig. 5.3.3, right).

Quantification

Quantification of all compounds is by relating the intensity of specified ions to that of the internal standard stigmasterol [*m/z* 394 (M-90)]. Instrument calibration was achieved by running the external standard daily.

Evaluation of Analysis Quality

Several factors can influence data quality. The relative instability of TMS ethers is a potential pitfall of profile analysis. Derivatives are readily hydrolyzed to the free

steroid under adverse conditions. We quantify this by quantifying underivatized stigmasterol (*m/z* 412) as well as the TMS ether. The underivatized component has a shorter retention time; if its peak area is > 3% of the derivatized, we resilylate the mixture (Fig. 5.3.4).

Capillary gas chromatography has classically shown discrimination against components of higher mass and with longer retention times. The degree of "discrimination" of individual components throughout a run is most easily determined by including internal standards before and after the steroids of interest (bracketing). Almost all normal urine steroids elute in a window defined by 5*α*-androstane-3*β*-ol and cholesteryl butyrate internal standards. Cholesteryl butyrate is useful in that it is subject to tailing when the column is failing and indicates that it should be replaced. Although we quantify against stigmasterol, in an acceptable run we expect the other two standards to give almost the same quantitative values. If this is not the case, then calibration using the external standard should be repeated.

Typical corrective measures for poor performance are resilylation, replacing injector glass insert, breaking off a few centimeters at the front end of the column, and replacing column. Serious loss of sensitivity may require cleaning the source, replacing the filaments, or cleaning the quadrupole rods.

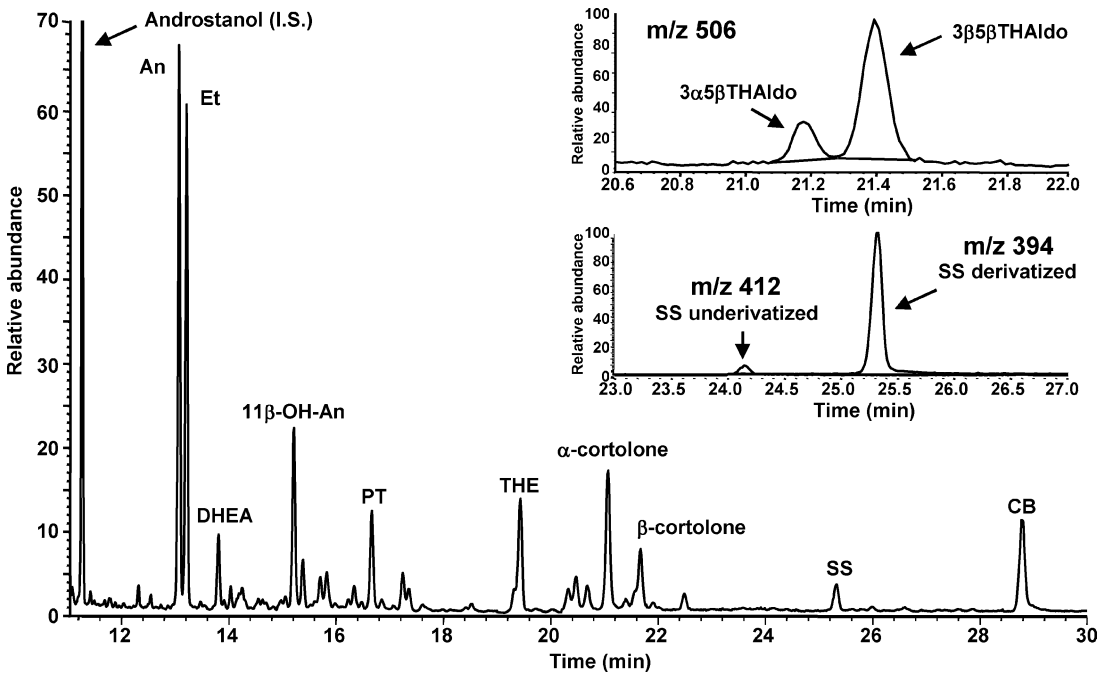

Fig. 5.3.4 The total monitored ion current (TMIC) chromatogram of a urine sample. One inset shows the quantification of THAldo against its 3*β*5*β*-tetrahydroaldosterone (*THAldo*) internal standard, and the second inset monitoring derivatized stigmasterol (*SS*) and its hydrolyzed counterpart, an indicator of derivative stability. Abbreviation: *An* androsterone, *CB* cholesteryl butyrate, *DHEA* dehydroepiandrosterone, *Et* etiocholanolone, *PT* pregnanetriol

Quality Assurance

A quality assurance sample is run with every batch of samples and results should not differ daily by more than 15%. Profile analysis licensed for commercial clinical diagnostic use may have to meet special requirements. For example, quantification against a five-point standard curve was required for each compound. We prepare a series of calibrants with identical amounts of internal standard, but increasing amounts of reference analyte, typically covering 100-fold dynamic range.

The quality assurance sample used is an aliquot of a urine pool prepared by mixing equal proportions of 24-h samples from 20 men and women. Thus, the values obtained on GC-MS analysis should approximate true average steroid excretions. We use these values to adjust the calibration of steroids without authentic materials in the external standard. We have determined that the excretion of 18-OH-THA in the quality assurance sample should be 90 μg/24 h; THAldo, 30 μg/24 h, and 18-oxo-THF, 5 μg/24 h. The amount of these steroids in clinical samples is thus calibrated against a "normal" excretion.

Diagnostic Ratios

Many disorders of steroid synthesis and metabolism are caused by disabling mutations in a particular enzyme, and characterization can usually be achieved by determining precursor/product ratios, or more precisely precursor metabolite:product metabolite ratios. For most adrenal disorders, cortisol is the "product" and the chosen denominators are cortisol metabolites; we usually choose the sum of three prominent ones, tetrahydrocortisone THE, tetrahydrocortisol (THF), and 5α-tetrahydrocortisol (5αTHF), which are together referred to as "Fs" and account for 50% of urinary metabolites. Neonates do not excrete significant amounts of the THFs and as a denominator we use THE plus α- and β-cortolone (also referred to as "Fs", which account for about 40% of cortisol metabolites). The cumulative excretions of the corticosterone metabolites tetrahydrocorticosterone (THB), 5α-tetrahydrocorticosterone (5αTHB), tetrahydro-11-dehydrocorticosterone (THA), and 5α-tetrahydro-11-dehydrocorticosterone (5αTHA) are referred to as "Bs". Another ratio is designed to quantify 17,20-lyase activity (i.e., androstenedione metabolites) is androsterone + etiocholanolone:17-OH-progesterone metabolites (17α-hydroxypregnanolone, 17HP + pregnanetriol, PT). Each disorder has its own panel of diagnostic ratios and while we suggest examples, other investigators may wish to designate their own.

Unconjugated Cortisol Metabolite Panel

The method measures cortisone (urinary free cortisone, UFE), cortisol (urinary free cortisol, UFF), 6β-hydroxycortisol, and 18-OHF using deuterated internal standards [62]. Commercial tetradeuterocortisol was used as an internal standard for cortisol, and the remaining dideutero homologs prepared in the laboratory by deuteration of Δ^1 analogues. UFF and UFE are considered better indicators of hormone availability and hypersecretion than the F and E (free plus conjugated) quantified in the comprehensive profile. Typically the values of total F and E are about three times that of

UFF and UFE [62]. 18-OHF is also better analyzed in the free fraction, since we find that the enzyme hydrolysis has a deleterious effect on the steroid. Derivatization is carried out after Sep-Pak extraction of 5 ml of urine without hydrolysis. Two or four peaks were given for each steroid on account of syn- and anti- forms of the oxime derivative; all were integrated. Dideutero internal standards are not ideal as there is significant contribution of analyte to the internal standard, and vice-versa. It is therefore important to utilize standard curves or a correction formula based on the measured contributions. Results obtained for normal males and females using this methodology are given in Table 5.3.2.

5.3.3 Diagnosis of Genetic Disorders From Infancy to Adulthood

Table 5.3.4 lists the information about the disorders amenable to diagnosis by profile analysis. In later tabulated data for each disorder, significant diagnostic ratio values are highlighted.

5.3.3.1 Congenital Adrenal Hyperplasia

21-Hydroxylase Deficiency

Disorders of 21-hydroxylation account for over 95% of patients with CAH and affect about 1 in 13,000 people. 21-Hydroxylation is catalyzed by P450c21 encoded by a gene *CYP21B* [95]. The disorder ranges from severe (salt-wasting), when even aldosterone synthesis is prevented, through "simple-virilizing," to mild forms, where adequate cortisol is produced.

Serum or Blood-Spot Analysis (HPLC-MS)

MS/MS is making an important contribution in confirmation (second-tier) testing following newborn screening. Neonatal blood-spot screening for CAH by measurement of 17-hydroxyprogesterone is routinely conducted in 40 states in the USA and in several other countries. Due to a high false-positive detection rate, follow-up confirmatory analysis is required. In neonatal life, many blood constituents crossreact with the RIA antigen and give rise to falsely high results with consequent screen-positive results. In an early HPLC/ESI-MS study we identified some of these materials as steroid sulfates [105]. The deficiencies in follow-up for newborn screening in CAH have been the subject of two recent editorials in endocrine journals [55, 94]. In the most ambitious study so far, researchers at the Mayo Clinic measured a panel of three steroids, 17-hydroxyprogesterone, cortisol, and androstenedione, in 1222 blood spots collected from neonates between the 2nd and 5th day of life [46, 58], 221 of which screened positive for CAH. Thirty-one were from patients diagnosed with CAH subsequent to neonatal screening, 190 were from patients who initially screened positive for CAH but who were subsequently found not to have the disorder, and the remaining 1001 were from newborns with negative screening results. The vast majority of false-positive cases had low17-hydroxyprogesterone levels measured by MS/MS accompanied by a substantial cortisol peak. Samples from confirmed cases characteristically lacked cortisol but had increased 17-hydroxyprogesterone

Table 5.3.4 *Genetic disorders of steroid synthesis and metabolism*

Disorder trivial name	Gene/enzyme mutation	Gene location	OMIM number
Congenital adrenal hyperplasia			
21-Hydroxylase deficiency	CYP 21A2	6p21.3	201190
11β-Hydroxylase deficiency	CYP11B1	8q21	202010
17α-Hydroxylase deficiency	CYP17A1	10q24.3	202110
3β-HSD deficiency type II	HSD3B2	1p.13.1	201810
P450 Oxidoreductase deficiency, Antley-Bixler syndrome	POR	7q11.2	124015 (207410)
Lipoid adrenal hyperplasia (LAH) Star protein defect	STARD1	8p11.2	600617 (201710)
LAH, P450scc deficiency	CYP11A1	15q23-q24	118485
Mineralocorticoid/Glucocorticoid			
Apparent mineralocorticoid excess syndrome (AME). 11βHSD 2 deficiency	HSD11B2	16q22	218030 (207765)
Glucocorticoid remediable aldosteronism (GRA)	CYP 11 B1, CYP11B2	8q21	124080, 202010
Pseudoaldosteronism (Liddle's syndrome) Na^+ channel defect	SCNN1B SCNN1G	16p13-p12 16p13-p12	600760 600761 (177200)
Aldosterone synthase deficiency (ASD)	CYP11B2	8q21	202010 (124080)
Pseudohypoaldosteronism, PHA-I Sodium channel defect or MR mutation	SCNN1A SCNN1B MR	12p13 16p13-p12	600228 600760
Pseudohypoaldosteronism, PHA-II	Cl^- shunt	4q31.1	600983
Adrenal hypoplasia	DAX-1 (NROB1)	Xp21.3-p21.2	300200, 300473
Cortisone reductase deficiency a) Cortisone reductase deficiency (CRD) b) Apparent cortisone reductase deficiency (ACRD)	HSD11B1 H6PD or G6PT1(GSD1b)	1q32-q41; 1pter-p36.13 11q23	604931, 600713, 138090 602671
Androgen oxidoreduction			
5α-Reductase deficiency type 2	SRD5A2	2p23	607306
5β-Reductase deficiency	AKR1D1 (SRD5B1)	7q32-q33	604741
17βHSD deficiency type III	HSD17B3	9q22	605573 (264300)

HSD Hydroxysteroid dehydrogenase, *OMIM* Online Mendelian Inheritance in Man

Table 5.3.4 (continued) *Genetic disorders of steroid synthesis and metabolism*

Disorder trivial name	Gene/enzyme mutation	Gene location	OMIM number
Miscellaneous			
Aromatase deficiency	CYP19A1	15q21.1	107910
Recessive X-linked ichthyosis (RXLI) steroid sulfatase deficiency	STS	Xp22.32	308100
Smith–Lemli–Opitz syndrome (SLOS)	DHCR7	11q12-q13	602858 (270400)

HSD Hydroxysteroid dehydrogenase, *OMIM* Online Mendelian Inheritance in Man

and androstenedione. The employment of the LC-MS/MS method has resulted in an 89% reduction in false positives.

The use of HPLC-MS for the diagnosis of 21-hydroxylase deficiency in older infants and children should be straightforward, with 17-hydroxyprogesterone being the primary analyte. However, caution must be exercised as other forms of CAH give rise to 17-hydroxyprogesterone (17-OHP) elevation (e.g., 3βHSD deficiency) and oxidoreductase deficiency (ORD). It is important that other confirmatory steroids should also analyzed to distinguish the conditions.

Urine Metabolite Analysis (GC-MS)

Diagnosis of this disorder by GC-MS is straightforward, and being the most common form of CAH, it was the subject of early studies [75]. Because of screening and the common availability of 17-OHP measurements with and without adrenocorticotrophic hormone (ACTH) stimulation, profile analysis is rarely utilized for diagnosis after the newborn period. With regard to urine analysis in adults and children, the classic disorder manifests itself in the almost absent excretion of cortisol metabolites and highly elevated excretions of 17-OHP and 21-dihydrocortisol metabolites (e.g., 17HP, PT, and pregnanetriolone, PTONE). For classic 21-hydroxylase deficiency, the 17HP + PT:Fs ratio should be greater than 10 and the PTONE:Fs ratio greater than 5.

Profile analysis is very useful for diagnosing patients with the mild, nonclassical, "late-onset" form of the disorder. They can have normal cortisol metabolite excretion, but ratios of 17-OHP and 21-dihydrocortisol metabolite to cortisol metabolite excretions are elevated. Typically, if the PT + 17HP:Fs ratio is > 0.34 and the PTONE:Fs ratio is greater than 0.05, nonclassical 21-hydroxylase disorder should be considered [85].

Neonatal Diagnosis

It is in the neonatal period that steroid profile analysis is most useful for CAH diagnosis because serum 17-OHP assays can give elevated results, even for nonaffected babies, due to lack of specificity of the RIAs used [105]. This is becoming less of a problem with the increasing use of HPLC-MS/MS for 17-OHP measurement as

detailed in the section above. In our earliest studies we found that the most noticeable feature of CAH profiles in the 1st week of life was the disproportionate amount of 16α-hydroxypregnenolone relative to 16α-hydroxyDHEA [53, 75]. Normally, the ratio is 1:1, but for CAH newborns it was typically > 3:1. Unlike adults, pregnanetriol appeared not to be the major diagnostic analyte in neonates, and 17-α-hydroxypregnanolone (17HP) and PTONE are quantitatively more important among the classical markers. Joannou [40] showed that CAH babies excrete large amounts of 3β,15β,17α-trihydroxy-5β-pregnan-20-one (15β-triolone and its 20α-dihydro companion), and this steroid was included in recent profile methods [10, 53]. We measure the ratios of 17-HP, PT, PTONE, and 15β-triolone to three cortisol metabolites (Fs; THE + α- and β-cortolone) and have shown that diagnosis is straightforward on the 1st day of life [10].

3β-HSD Δ5,4 Isomerase (3βHSD) Deficiency

The formation of 3-oxo-4-ene steroids from 3β-hydroxy-5-ene steroids is catalyzed by 3β-HSD. There are two main forms of the enzyme: 3βHSD I is found in the liver and placenta, and 3βHSD II is found in human gonads and adrenals; mutations in the latter result in CAH. 3βHSD deficiency causes salt loss and masculinization of female fetuses; male patients may show genital ambiguity due to reduced testosterone synthesis. In excess of 24 mutations of the gene have been described. It is a rare form of the disorder, probably comprising < 1% of CAH cases.

Serum Analysis (HPLC-MS)

There have been no reports yet of diagnosis of this disorder by LC-MS. Diagnosis should be straightforward: low serum cortisol and high serum levels of Δ^5 steroids such as DHEA, pregnenolone, and 17HP. Serum 17-OHP may also be elevated, potentially allowing misdiagnosis of the condition unless the Δ^5 steroids are included. The analysis of DHEA sulfate would be particularly useful and should give elevated results.

Urine Metabolite Analysis (GC-MS)

Bongiovanni and co-workers first reported 3βHSD deficiency disorder and described the characteristic urinary metabolites [5]. Urinary steroids from children and adults show dominance of 5-pregnene-3β,17α,20α-triol (5PT, the major metabolite of 17HP), and DHEA. 3βHSD deficiency could be confused with 21-hydroxylase deficiency because of the high excretion of PT and 17HP; however, it is distinguished by having low excretion of PTONE and high 5PT:PTONE ratio. Table 5.3.5 shows the results for five patients, four of who had mutation analysis carried out. One mutation (A82T) still allows some activity, as illustrated in the significant excretion of cortisol metabolites [57], but the Y245D mutation almost completely prevents activity [72, 74]. 3βHSD deficiency is more difficult to detect neonatally by steroid analysis because all infants have excessive 3β-hydroxy-5-ene steroid synthesis. However, 5PT is a minor urinary steroid component and its presence in the 1st weeks of life must indicate 3βHSD deficiency. Neonatal diagnostic ratios are listed in our recent paper [10]. The key for distinguishing 3βHSD from CAH is the 5PT:PTONE ratio, which is > 35 for 3βHSD, < 1.5 for 21-hydroxylase deficiency, and < 28 for normals.

■ ***Table 5.3.5*** *Steroid excretions (μg/24 h) and diagnostic ratios in patients with 3β-hydroxysteroid dehydrogenase type II (3βHSD II) deficiency*

Steroids	Pat 1	Pat 2	Pat 3	Normal	Pat 4	Normal	Pat 5	Normal	Pat 6	Normal	21HD
Age	15 d	3 m	3 m	2 m–2 yrs ($n=12$)	3 yrs	2–4 yrs ($n=12$)	9 yrs	8–10 yrs ($n=16$)	17 yrs	Adult ($n=34$)	
17HP+PT	223	303	28	13	2074	21	1306	121	33000	781	>10000
PTONE	3.0	27	10	0.9	56	5.4	7.4	6.1	630	17.5	>5000
5PT	102	426	987	10	3063	13	715	17	55500	237	<200
DHEA		158	100	0.6	58	3.0	122	15	22300	300	<200
16OHD-HEA	5683	2576	4870	19	239	5.0	1095	21	32600	245	<10
Fs	67	104	157	281	1981	1112	749	2881	3000	5073	<100
5PT:Fs	**1.5**	**4.1**	**6.3**	0.035	**1.55**	0.01	**0.95**	0.006	**18.5**	0.05	<0.1
DHEA:Fs		1.52	0.64	0.002	0.03	0.002	0.16	0.007	7.4	0.065	<0.1
5PT: PTONE	**34.0**	**15.8**	**98.7**	11.0	**546**	2.4	**96.6**	3.05	**88.1**	26.2	**<0.001**
17HP+PT: Fs	3.3	2.9	0.18	0.05	1.05	0.02	1.74	0.05	11.0	0.16	>10
PTONE:Fs	0.04	0.26	0.06	0.003	0.03	0.005	0.01	0.002	0.21	0.003	>1.0
Mutation			Y254 D		A82 T		A82 T		Y254 D		

Figures in bold are ratios most notably distinctive of the disorder.
21HD 21-Hydroxylase deficiency, *5PT* 5-pregnene-3*β*,17*α*,20*α*-triol, *16OHDHEA* 16*α*-hydroxyDHEA, *17HP* 17*α*-hydroxy-pregnanolone, *d* days, *Fs* cortisol metabolites, *m* months, *yrs* years, *Pat* patient, *PTONE* pregnanetriolone

Lipoid Adrenal Hyperplasia

Lipoid adrenal hyperplasia (LAH) is a potentially fatal disorder resulting in severely attenuated steroidogenesis in the gonads and adrenals, resulting in salt wasting and lack of virilization [19]. It is caused by deficiency in the conversion of cholesterol to pregnenolone. The adrenals in newborns with LAH are enlarged and contain excessive amounts of cholesterol and cholesterol esters. It was assumed that the disorder was due to deficiency of the cholesterol side-chain cleavage enzyme P450scc, but for many years no enzyme mutations were found. The cause in most patients was finally found to be mutations in the steroidogenic acute regulatory (StAR) protein, the entity responsible for transporting cholesterol from the outer to inner mitochondrial membrane where P450scc resides. More than 34 mutations have been identified [19]. More recently, three cases of LAH have been attributed to P450scc mutations [29].

Serum Analysis (HPLC-MS)

The disorder has not been studied by LC-MS, but low excretion of all hormonal steroids are predictive.

Urinary Metabolite Analysis (GC-MS)

Steroids have been measured by GC-MS in umbilical cord blood, amniotic fluid, and infancy urine of affected infants, and almost no steroids are found [73]. Only traces of progesterone metabolites were detected. Serum samples from women carrying an LAH fetus have normal concentrations of progesterone metabolites, formed placentally, since this organ produces the hormone independently of the StAR protein mechanism.

17*α*-Hydroxylase Deficiency

17-Hydroxylase is a branch-point enzyme in steroid biosynthesis. It adds the first additional hydroxyl in the pathway to cortisol in the adrenals, and through its 17,20-lyase activity is also the first step in the pathway to androgens and estrogens in both the adrenals and gonads. 17-Hydroxylase deficiency was first described by Biglieri and co-workers [4], and about 200 patients have been reported. Frequently, the condition is first diagnosed when phenotypic girls fail to enter puberty and display hypertension caused by excess DOC. More than 20 mutations have been described that abolish both activities. In addition, certain specific mutations only seriously affect side-chain cleavage, possibly because they are in a redox partner binding site, resulting in a disorder referred to as isolated 17,20-lyase deficiency.

Serum Steroid Analysis (HPLC-MS)

There are no reports on steroid quantitation by LC-MS, but cortisol, DHEA, and testosterone are very low when measured by RIA, and DOC and corticosterone are elevated. With the exception of DOC, all of these analyte assays are available by MS/MS, as are progesterone and pregnenolone, which should also be elevated in the condition.

Urinary Metabolite Analysis (GC-MS)

GC-MS profile analysis was employed early for the study of the disorder [32]. In children and adults, 17-hydroxylase deficiency is easily diagnosed because of lack of cortisol metabolites (e.g., THE, THF, and 5αTHF) and high excretions of corticosterone metabolites (THA, 5αTHA, THB, and 5αTHB). It has been determined that corticosterone synthesis is about 50–100 times normal. On occasion, confusion can arise because of the presence in urine of large amounts of 17-deoxy and 21-deoxy steroids instead of the conventional THA and THBs. Corticosterone (unlike cortisol) is significantly excreted in bile, resulting in it being susceptible to microbial 21-dehydroxylation prior to reabsorption [32]. In addition to high corticosterone metabolite excretion, affected patients typically have negligible urinary androsterone and etiocholanolone, the major C19 metabolites. In thirty Brazilian patients confirmed by mutation analysis, the mean Bs:Fs ratio was 143 (range 32–718) compared to 0.14 (range 0.06–0.29) for normal adults.

Neonatal

Neonates are rarely diagnosed with 17-hydroxylase deficiency as they have normal female genitalia and produce sufficient mineralocorticoid (DOC) and glucocorticoid (B) to avoid adrenal crisis. However, infants with a family history of the disorder have been diagnosed. The major corticosterone metabolite in neonates and young infants is 6α-hydroxyTHA [80], but accurate quantification of this analyte is not possible because of the lack of a reference standard. The steroid has a distinctive spectrum and known retention time. We quantify it against its isomer THE, present in the calibrant mixture. Diagnostic ratios for neonates are given by Caulfield and co-workers [10], one important ratio being 16α-hydroxypregnenolone/16α-hydroxyDHEA, which is typically > 10 for affected babies.

P450 ORD, "Combined 17- and 21-Hydroxylase Deficiency" and the Antley-Bixler Syndrome

A form of CAH only recently characterized is P450 oxidoreductase deficiency (P450 ORD). The history of this disorder goes back 30 years to the first descriptions of patients with ambiguous genitalia with a steroid metabolome indicative of combined 17- and 21-hydroxylase defects [65, 84]. Our early analysis of such patients showed high excretions of 17HP, PT, and PTONE, indicative of 21-hydroxylase deficiency together with high corticosterone metabolite excretions, indicative of 17-hydroxylase deficiency. Metabolites of upstream precursors such as progesterone and pregnenolone were particularly elevated. Cortisol metabolite excretions tended to be normal. Independently, clinicians studying the skeletal and craniofacial dysmorphology condition Antley-Bixler syndrome noted that many of such patients seemed to have steroid synthetic abnormalities similar to those associated with 17- or 21-hydroxylase deficiencies. Many papers published in the last 20 years included steroid data that did not fit well with the clinical symptoms and seemed to point to a new disorder. These were reviewed by Shackleton and Malunowicz [78].

In 2004, three groups demonstrated that the condition was caused by mutations in cytochrome P450 oxidoreductase, the essential redox partner for microsomal hydroxylases. Flück and co-workers [17] were the first to publish, followed soon after

by Arlt et al. [2] and Adachi et al. [1]. To date more than ten mutations in this enzyme have now been identified.

Serum Analysis (HPLC-MS)

Reports on serum steroids in affected patients (not analyzed by LC-MS) show elevated 17-OHP and low testosterone concentrations. In order to prevent confusion of this condition with 21- or 17-hydroxylase deficiency, the following panel of steroids should be analyzed: 17-OHP, 21-deoxycortisol, corticosterone, progesterone, and pregnenolone; all of which should be elevated. Cortisol should be normal and testosterone and DHEA (including sulfate) low for age. Patients show a blunted cortisol response to ACTH stimulation.

Urine Metabolite Analysis (GC-MS)

The urinary steroid metabolome in nine patients with the condition was published indicating the preferred steroid ratios for diagnosing the condition (Fig. 5.3.5) [92]. The following metabolites should be measured: pregnenediol (5-pregnene-3β,20α-diol, 5PD), pregnanediol, the tetrahydrometabolites of corticosterone and cortisol, androsterone and etiocholanolone, and pregnanetriol and 17HP. In profiles, one of the above analytes, pregnenediol is found in two forms, the bis-TMS derivative and

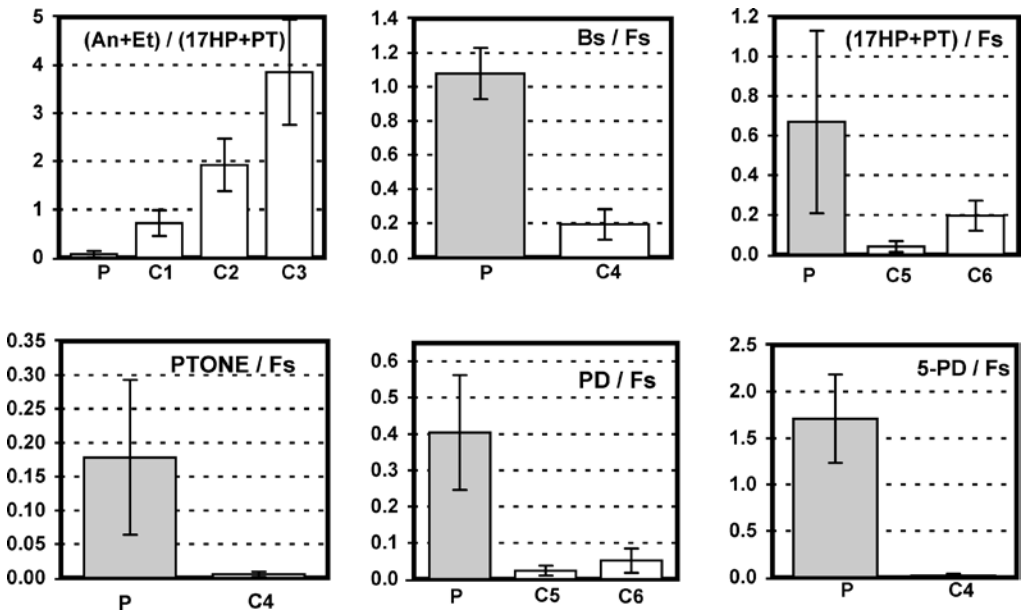

Fig. 5.3.5 Diagnostic ratios for oxidoreductase deficiency.
"*P*" represents mean values for nine patients, "*C*" are normal values for different age groups, as follows: C1 2 months—5 years; C2 5–10 years; C3 11–16 years; C4 2 months—16 years; C5 2 months—10 years, C6 2 months–16 years. The first ratio focuses on 17,20-lyase activity (androgens/C21-precursors), which is suppressed in the condition compared to normal controls. The remaining ratios illustrate precursor metabolites increased by attenuated 17- and 21-hydroxylation, relative to metabolites of the product cortisol.
Abbreviations: *Bs* corticosterone metabolites, *Fs* cortisol metabolites, *17HP* 17α-Hydroxypregnenolone, *5-PD* pregnenediol, *PTONE* pregnanetriolone

an artifact pregnadienol TMS formed from 5PD-20-sulfate during derivatization [23]. Both forms are quantified and the external calibration mixture contains standards for each. The 5PD quantity reported is the sum of both forms.

11β-Hydroxylase Deficiency

Patients with 11β-hydroxylase deficiency present with features of androgen excess, including masculinization of female newborns and precocious puberty in male children. There are two human isozymes that are responsible for cortisol and aldosterone synthesis, respectively. The CYP11B1 enzyme (p45011B) converts DOC to corticosterone (B) and 11-deoxycortisol (S or 11-dihydrocortisol) to cortisol (F). It is also capable of 18-hydroxylating DOC but cannot convert B to aldosterone. The latter transformation is carried out by CYP11B2 (also known as aldosterone synthase), which encompasses activity for 18-hydroxylation and subsequent 18-oxidation. When CAH is associated with hypertension, deficient 11β-hydroxylase (CYP11B1) is suspected; at this time more than ten mutations have been defined in affected individuals [103].

Serum Steroid Analysis (HPLC-MS)

Patients have undetectable cortisol. DOC, 11-deoxycortisol, testosterone, and androstenedione should be extremely elevated.

Urinary Metabolite Analysis (GC-MS)

Patients with a complete block have almost undetectable excretions of cortisol metabolites. The major urinary steroids are androsterone, etiocholanolone, tetrahydro-11-deoxycortisol (THS) and hexahydrosubstance S. Tetrahydrodeoxycorticosterone is also increased. Diagnosis is trivial through measurement of the THS:Fs and androsterone + etiocholanolone:Fs ratio.

Neonatal Diagnosis

One neonate was studied by us, and THS could not be detected until the 12th day of life, but this could be due to inadequacies of the older instrumentation [31]. A steroid identified as 6α-hydroxy-THS was also identified, and by the 27th day it was excreted at a rate more than 50% of THS. The diagnostic ratios for neonates are THS:THE + α- and β-cortolone (Fs), and 6α-hydroxyTHS:Fs [10].

5.3.3.2 Male Pseudohermaphroditism

5α-Reductase Deficiency

Deficiency of 5α-reductase-2 (5α-RD-2) is an important cause of male pseudohermaphroditism (MPH). It is occasionally found in large isolated kindreds, such as one studied in the Dominican Republic where the disorder was first detected [35]; more recently, extended families from Turkey and New Guinea have been studied.

Serum Analysis (HPLC-MS)

The disorder has not been studied by HPLC-MS, and will require development of a method for DHT. Diagnosis is by finding elevated testosterone and an increased testosterone:DHT ratio.

Urinary Metabolite Analysis (GC-MS)

Profile analysis is the best technique for diagnosing the condition in children and adults, although neonates present a greater challenge. Interestingly, although the impact of the deficiency is on the conversion of testosterone to 5*α*-DHT, by far the most diagnostic urinary steroid ratios are 5*β*:5*α* ratios of cortisol and corticosterone metabolites (THB:5*α*THB; THF:5*α*THF). Frequently, the 5*α*-reduced corticosteroids are almost undetectable. Paradoxically, the androsterone:etiocholanolone and 11*β*-hydroxyeiocholanolone/11*β*-hydroxyandrosterone ratios, although reduced, are less definitive even though the disorder is primarily of androgen biosynthetic importance. Mean values of diagnostic 5*β*:5*α* steroid ratios for affected patients, heterozygotes, and unaffected family members are given in Table 5.3.6. This is a condition in which heterozygotes within a kindred can be detected with relative ease [34].

Neonatal Period

Diagnosis in early infancy presents distinct challenges in terms of both plasma and urine assays. Plasma testosterone levels may not be markedly above the normal range, and testosterone:DHT ratios, while low on average, can also be close to normal. This is probably caused by the activity in fetal life of 5*α*-reductase-1, which no doubt can compensate for attenuated 5*α*-RD-2, and is responsible for some 5*α*THF synthesis, even in 5*α*RD-deficient patients. The urinary THF:5*α*THF ratio, which is the most discriminatory ratio in adults, is also the best for use in infants. However, neonates and young infants (< 4 months) excrete very little THF and 5*α*THF compared to THE (< 10%), which presents an analytical challenge. In three 2- to 4-month infants we studied with 5*α*-RD-2 deficiency, the THF:5*α*THF values were 2.5–4.7 (normal 0.2–0.5). Contrast this to the ratio of typically > 10 for children and adults with the disorder.

Table 5.3.6 *Diagnostic urinary steroid ratios for 5α-reductase deficiency (homozygous and heterozygous), and a patient with 5β-reductase deficiency.*

Steroid ratio	5*α*Reductase (homozygous, *n* = 48)	5*α*Reductase (heterozygous, *n* = 10)	Normal adults (*n* = 26)	5*β*-Reductase patient[a]
Et/An[c]	4.86 ± 2.98	2.35 ± 1.18	0.92 ± 0.34	0.15
11*β*OHEt/11*β*OHAn	2.49 ± 1.43	0.82 ± 0.53	0.48 ± 0.54	**0.04**
THB/5*α*THB	**3.01 ± 1.88**[b]	0.84 ± 0.34	0.51 ± 0.19	**< 0.01**
THF/5*α*THF	**23.3 ± 11.7**	4.56 ± 1.61	1.28 ± 0.54	**0.013**

[a] This patient was 13 years old at the time of collection. Results discussed in Palermo et al. [63]

[b] Figures in bold are ratios most notably distinctive of the disorders.

[c] Abbreviations: *An* Androsterone, *Et* etiocholanolone, *11β-OH-An* 11β-hydroxyandrosterone, *11β-OH-Et* 11β-hydroxyetiocholanolone, *THB* tetrahydrocorticosterone, *5αTHB* 5α-tetrahydrocorticosterone, *THF* tetrahydrocortisol, *5αTHF* 5α-tetrahydrocortisol

5β-Reductase Deficiency

Rationally, 5β-reductase deficiency would not be a cause of MPH, but it seems appropriate to place this disorder adjacent to its 5α-counterpart. 5β-Reductase (AKR1D1) is an essential bile-acid biosynthetic enzyme and patients with disabling mutations in this enzyme have a clinical phenotype associated with cholestasis and liver failure. In addition to its importance in bile-acid synthesis, this aldoketo-reductase is responsible for reducing approximately two-thirds of the mass of synthesized androgens, corticosteroids, and aldosterone prior to their excretion, so has a vital role in steroid metabolism.

We studied by GC-MS the urinary excretion of a single patient with a documented mutation [49] and have found that the 5β-reduced androgen metabolite excretion relative to 5α is decreased by about 80%, and 5β-corticosteroid metabolite excretion is essentially absent [63]. To date there has no report of an adverse endocrine phenotype related to corticosteroid, mineralocorticoid, or androgen metabolism.

17β-Hydroxysteroid Dehydrogenase Deficiency

Autosomal recessive mutations in the 17β-hydroxysteroid dehydrogenase (17βHSD) 3 gene impair the formation of testosterone in the fetal testis and give rise to genetic males with female external genitalia. Such individuals are usually raised as females, but virilize at the time of expected puberty as the result of increases in serum testosterone. More than 14 mutations have now been identified [20].

Serum Steroid Analysis (HPLC-MS)

Elevated concentrations of androstenedione and low concentration of testosterone would be expected, leading to a markedly elevated androstenedione:testosterone ratio.

Urine Metabolite Analysis (GC-MS)

The most noticeable feature in GC-MS profiles is the elevated excretion of the androstenedione metabolites androsterone and etiocholanolone, represented by increased androsterone + etiocholanolone:Fs ratio (Table 5.3.7), being greater than twice the upper limit of aged-matched controls. Two adult Turkish patients were studied by us who gave androsterone + etiocholanolone:Fs values of 2.9 and 4.3 compared to a normal mean of 0.65 (range 0.3–1.3). Disabling 17βHSD 3 mutations were found in these patients. The ratio of 17β-hydroxy:17-keto steroids (e.g., 5-androstene-3β,17β-diol:DHEA and 5α-androstane-3α,17β-diol:androsterone) was within the normal range in all patients we studied, reflecting compensatory activity of the multiple 17βHSD isozymes present in many tissues. This probably also explains the pubertal virilization seen in the disorder, the mechanism for testosterone formation in postpubertal subjects being the conversion of circulating androstenedione to testosterone by one or more of the unaffected 17β isoenzymes.

Table 5.3.7 *Steroid excretion in three patients with 17βHSD deficiency*

Steroid µg/24 h	Pat 1 (5 years)	Control (5–8 years, range)	Pat 2 (11 years)	Control (11–16 years, range)	Pat 3 (14 years)
An	417	5.1–210	5451	98–1402	33636
Et	109	7.1–135	2093	101–1552	8000
THE	1564	402–2451	3501	645–2386	2800
THF	327	152–1061	834	203–1169	976
5αTHF	696	215–1056	1371	156–1219	1021
An + Et:Fs	**0.20**	0.002–0.07	**1.32**	0.18–0.3	**9.3**

Figures in bold represent the ratios most elevated in the condition

5.3.3.3 Disorders of Cortisol 11-Oxidoreduction

AME, 11*β*HSD-II Defect

Studies 25 years ago described children with hypertension and low renin, hallmarks of mineralocorticoid excess, but no known mineralocorticoids were produced in excess [83, 101]. The urinary steroid profile of these patients showed a much reduced excretion of 11-carbonyl steroids (e.g., THE) relative to their 11*β*-hydroxylated counterparts, pointing to a diminished activity of 11*β*HSD. However, no mutations were found in the hepatic 11*β*HSD enzyme known at the time [61]. A kidney isozyme was identified by Stewart et al. [97] and others, and this was found to be responsible for the increased ratio of THF + 5*α*THF: THE seen in the disorder This enzyme termed 11*β*HSD2 was a renal tubule dehydrogenase responsible for deactivating cortisol, a steroid with equal mineralocorticoid receptor affinity to aldosterone but present in much greater quantities. Attenuated 11*β*HSD-II activity in AME permits binding of cortisol to the mineralocorticoid receptor binding, resulting in hypertension and other symptoms of the disorder.

Serum and Urine Analysis (HPLC-MS)

Serum analysis has not been utilized in AME diagnosis, probably because the F:E ratio is already high in normal individuals. HPLC-MS is useful in measuring urinary F (UFF) and E (UFE). and a high F:E ratio would be diagnostic for the disorder, although other conditions, such as Cushing's syndrome, can also give rise to a high F:E ratio.

Urine Metabolite Analysis (GC-MS)

Attenuated conversion of cortisol to cortisone in AME causes inhibition of cortisol synthesis (negative feedback), and excretion of total cortisol metabolites is typically 50% lower than normal. The condition is most commonly diagnosis by determining

the ratio of THF + 5αTHF:THE, although the ratios of all saturated 11β-hydroxy-containing metabolites to 11-oxo-metabolites are increased, for example, cortols: cortolones, THBs:THAs, and C_{19} steroids. While the THF + 5αTHF:THE ratio can be greater than 50, very mild cases have also been seen with ratios in the normal range (Table 5.3.8). These cases were formerly called AME type II, but mutations are still within 11βHSD-II. More than 25 individual mutations have now been detected [14, 50]. Diagnosis of "type II" or "mild" cases is helped by the measurement of the UFF: UFE ratio as well as the THF + 5αTHF:THE ratio [50].

Apparent Cortisone Reductase Deficiency

This condition was first noted in two markedly hirsute sisters who had elevated production of cortisol but were not Cushingoid [66]. It was found that these patients had elevated excretion of THE and related 11-oxo-steroids relative to 11β-hydroxylated compounds, and so the disorder was named apparent cortisone reductase deficiency (ACRD). Subsequently, the disorder has been documented in other patients (Table 5.3.8) [3, 15, 38, 54]. Presumably, the rapid and irreversible conversion of cortisol to cortisone protects against some of the negative manifestations of hypercortisolism. Hyperandrogenism secondary to increased cortisol clearance is the most serious clinical manifestation of the condition.

While defective 11βHSD I seemed the most likely cause of the disorder, no loss-of-function mutations were found in 11βHSD I in the first patients investigated [61]. The cause of the disorder in these cases proved to be mutations in hexose-6-phosphate dehydrogenase (H6PDH), the enzyme that supplies electrons to the NADPH utilized in oxidoreduction [15]. Later studies have found 11βHSD I mutations in some affected individuals. Thus, there are two monogenic disorders giving rise to a similar phenotype; cortisone reductase deficiency caused by 11βHSD I mutations,

Table 5.3.8 *Diagnosis of apparent mineralocorticoid excess syndrome (AME) by urine steroid analysis*

Excretion and ratios (mean and range)	AME "type1" [a] $n = 40$	AME "type II" [b] $n = 4$	AME "mild" [a] $n = 1$	Control ($n = 34$)
THAldo (μg/24 h)	< 5	< 5	< 5	31 (6–63)
THF + 5αTHF: THE	**32** (7–134) [c]	2.5 (1.9–4.53)	3.0	1.0 (0.55–2.44)
UFF:UFE	**10.3** (6–50)	**2.7** (1.4–7.5)		0.55 (0.19–0.98)
Mutation		R279C	P227L	

[a] From Li et al. [50]

[b] From Dave-Sharma et al. [14]

[c] Figures in bold represent ratios most elevated in the condition

and ACRD, which is attributed to H6PDH mutations. Most recently enzyme activities even more distal to 11βHSD I have been shown to affect its activity. The H6PDH enzyme utilizes glucose-6-phosphate and its activity is dependent on the availability of the latter, which is in turn controlled by the activity of glucose-6-phosphatase-α and the glucose-6-phosphate transporter. Patients with mutations in these enzymes have GSD1a or GSD1b deficiency, respectively; the former resulting in increased apparent 11βHSD I activity and the latter decreased activity, as determined by GC-MS of cortisol metabolites [48].

Serum and Urine Steroid Analysis (HPLC-MS)

Measurements of urinary unconjugated F and E (UFF and UFE) are not useful for accurate diagnosis of ACRD as the ratio between them is typically normal. Patients with ACRD will have elevated levels of androgens, DHEA, testosterone and androstenedione.

Urine metabolite analysis (GC-MS)

The THE:THF + 5αTHF ratio is commonly greater than 15 in these disorders, the opposite to AME syndrome. While the ratio of "saturated" steroids demonstrates a high 11-oxo:11β-hydroxy ratio, this is not the case for steroids retaining a 3-oxo-4-ene structure. The F:E ratio is normal or elevated (i.e., > 1; Table 5.3.9). Steroid profile analysis also typically reveals an elevated excretion of DHEA and other androgen metabolites. Clearly the excessive ACTH production resultant from an apparent cortisol deficiency is responsible for the elevated adrenal androgen production, which in turn is responsible for female virilization and other manifestations of polycystic ovary syndrome.

Table 5.3.9 *Steroid excretions and diagnostic ratios in five patients with ACRD*

Steroid	Pat 1 [a]	Pat 2 [a]	Pat 3 [b]	Pat 4 [c]	Pat 5 [d]	Normal [e]
THE (μg/24 h)	3560	10230	26603	36290	8412	2593
THE:THF + 5αTHF	**21.9** [g]	**25.8**	**15.1**	**25.0**	**47.6**	1.0
Cortolones:cortols	**13.9**	**14.5**	**17.0**	NR [f]	**12.5**	2.6
Cortisol (UFF; μg/24 h	36	18.1	134	70	NR	25.2
Cortisone (UFE; μg/24 h)	16	13.8	86	56	NR	53.9
UFF:UFE	2.25	1.31	1.6	1.25	NR	0.47

[a] Phillipov et al. [66]
[b] Biason-Lauber et al. [3]
[c] Draper et al. [15]
[d] Malunowicz et al. [54]
[e] Mean of 17 adult men and 17 women
[f] Not reported
[g] Values in bold represent ratio values that are particularly elevated

5.3.3.4 Mineralocorticoid Disorders

Mineralocorticoid disorders can have high or low aldosterone production. Even in hyperaldosteronism disorders, circulating aldosterone and aldosterone metabolite excretion can be in the upper normal range. For this reason it is important to determine the aldosterone:renin ratio.

GRA and Adrenal Adenoma

These conditions are associated with high renin and high aldosterone production. The hybrid corticosteroids 18-OHF, 18-oxo-F and 18-oxo-THF were isolated from the urine of a patient with adrenal adenoma by Ulick and coworkers [11]. These steroids were subsequently also shown to be dominant in GRA. Their formation in the latter condition was explained by Lifton and co-workers [51] with the discovery of a chimeric gene formed crossover of the 11β-hydroxylase (*CYP11β1*) and aldosterone synthase (*CYP11B2*) genes.

Serum and Urine Steroids (HPLC-MS)

18-OHF is almost exclusively excreted without undergoing A-ring reduction and conjugation and can be measured in urine by HPLC-MS. A useful diagnostic ratio is that of 18-OHF:UFF, which is normally about 5:1 and rises to 50:1 in GRA. Serum analysis is used to measure aldosterone (elevated in the disorder) and cortisol, but not typically for 18-OHF.

Urine Metabolite Analysis (GC-MS)

We measure unconjugated 18-OHF by GC-MS [62]. Values for 18-OHF (measured in the free steroid fraction) are typically < 150 μg/24 h for normals and > 500 μg/24 h for patients with GRA or adenoma [39]. Another important diagnostic analyte in the hydrolyzed extract is 18-oxo-THF; patients with GRA have values > 15 μg/24 h compared to the normal value of < 5 μg/24 h. Selected ratios are reported for GRA, including a cortisol 18-oxygenation quotient, which is the 18-OHF:cortisol ratio, giving a value about 4 for normals and > 25 for patients with GRA (Table 5.3.10) and 18-oxo-THF(×100):THF + 5αTHF, which is < 0.2 for normals and > 1.0 for those with GRA.

Overall, with the exception of 18-oxygenated cortisol metabolites, the patients with GRA we've studied have normal excretions of all cortisol metabolites. THAldo excretion is almost always elevated (> 50 μg/24 h), as expected.

Pseudohyperaldosteronism (Liddle's Syndrome)

Liddle's syndrome is an autosomal dominant form of hypertension. It is a disorder of the renal epithelial sodium channel, which has three subunits, α, β, and γ, and mutations within the first two are associated with increased sodium channel activity [7, 36]. This causes excessive sodium absorption in the distal nephron of the kidney. It gives rise to hypoglycemia, low –renin, and low aldosterone.

Table 5.3.10 *Corticosteroid excretion (μg/24 h) and diagnostic ratios in glucocorticoid remediable aldosteronism (GRA)*

Steroid	Patient no.						Normal [a]
	1	2	3	4	5	6	
UFF	53	32	55	31	31	39	29
UFE	107	70	207	106	NM	107	54
18-OHF	1640	1515	1493	803	1131	2349	110
18-OHF/UFF	**31**	**41**	**27**	**73**	**36**	**60**	4.1
18-Oxo-THF	NM	116	46	36	42	89	5.0
THAldo	147	182	55	32	47	242	31
18-Oxo-THF (×100):Fs	NM	**0.92**	**0.67**	**0.91**	**0.85**	**0.85**	0.12

[a] Mean of 34 adult men and women
Values in bold represent ratio values that are particularly elevated. *18-OHF* 18-hydroxycortisol, *NM* not measured

Serum Steroid Analysis (HPLC-MS)

Aldosterone values < 50 pg/ml are typical.

Urinary Metabolite Analysis (GC-MS)

This disorder must be suspected if THAldo is low (< 5 μg/24 h) without manifestations of disordered cortisol metabolism, such as AME syndrome. A useful ratio is THAldo(×100):Fs, which is typically < 2.

Pseudohypoaldosteronism

A form of salt loss in infancy was long considered to be due to renal tubules that were refractory to aldosterone. Recent studies have described variant roots of the condition, either mutations in the mineralocorticoid receptor, the genes coding the epithelial sodium channel (*ENaC*), or other causes [6]. Many infant patients recover spontaneously, probably due to maturation of proximal tubular function.

Serum Steroid Analysis (HPLC-MS)

In affected patients, plasma renin and aldosterone levels are high.

Urine Metabolite Analysis (GC-MS)

Table 5.3.11 gives values we obtained for cortisol metabolites and THAldo in eight patients [33]. A mean excretion of THAldo of 450 μg/24 h was obtained, a value about 40 times normal. This is reflected in the THAldo(×100):Fs ratio of 114 compared to a normal value of 1–3 for normal individuals. High THAldo and 18-OH-THA excretions were also found in hyponatremic preterm infants born between the

26th and 34th week of gestation, suggestive of a transient pseudohypoaldosteronism. While the values were normal (10–40 μg/24 h) in the first days of life, typically the values reached 100–300 μg/24 h by the 3rd week. Once again it is likely that the higher aldosterone production is a reflection of lower response of renal tubules to the hormone.

Hypoaldosteronism: Aldosterone Synthase Deficiency

Aldosterone synthesis involves the 11β- and 18-hydroxylation of DOC, forming 18-hydroxycorticosterone, followed by 18-oxidation. Classically, the corticosterone-to-aldosterone conversion was considered to be carried out by two enzymes corticosterone methyloxidase (CMO) I and CMO II. Recent findings show that a single enzyme, P450 aldosterone synthase (CYP11B2), is responsible for both functions and several deleterious mutations have been defined [104]. This enzyme has a 95% homology with 11β-hydroxylase. While no longer accurate, the CMO I, CMO II categorization was useful as it explained the steroid phenotype of plasma and urine.

Serum Steroid Analysis (HPLC-MS)

Two clinical forms are seen, one (so-called CMO I), which has low plasma aldosterone, elevated corticosterone, and normal 18-hydroxy B; the second (CMO II) has highly elevated 18-hydroxy B and normal B. Only MS/MS methods for aldosterone and corticosterone are currently available.

Table 5.3.11 *Steroid excretion and diagnostic ratios in infants with pseudohypoaldosteronism (PHA) and aldosterone synthase deficiency (ASD)*

Steroids (μg/24 h)	ASD		ASD	Normals	PHA	
	"CMO1" Mean ($n = 5$)	Range	"CMO2"	Mean ($n = 20$)	Mean ($n = 8$)	Range
Age (months)		0.5–50	48	2–60		2–70
THAldo	< 1.0	0–4	0.1	8.6	450	94–2257
18-OH-THA	283	30–650	1824	23.9	190	96–883
Bs	1007	140–2083	813	126	297	10–882
Fs	669	247–3132	377	696	659	212–1409
Bs:Fs	**1.50**	0.53–2.16	**2.15**	0.18	0.35	0.04–0.62
THAldo:18-OH-THA	< 0.02	< 0.02	< 0.01	0.36	1.08	0.22–1.39
THAldo × 100:Fs	< 0.1	< 0.1	< 0.02	1.2	**114**	11.0–656
18-OH-THA:Bs	0.24	0.1–0.31	**2.28**	0.19	3.0	0.5–10.9

Figures in bold represent excretory values and ratios diagnostic for the respective conditions.
CMO I Corticosterone methyloxidase I, *CMO II* corticosterone methyloxidase II, *18-OH-THA* 18-hydroxytetrahydro-11-dehydrocorticosterone, *Bs* the sum of tetrahydrometabolites of corticosterone, *Fs* the sum of the tetrahydrometabolites of cortisol

Urine Metabolite Analysis (GC-MS)

In profile analysis, "CMO I" shows low THAldo and 18-hydroxyTHA (the major 18-hydroxycorticosterone metabolite), but high excretions of THAs and THBs [26, 33]. In "CMO II," THAldo is low, the THAs and THBs normal, but 18-OH-THA is often grossly elevated. Representative excretions of several patients with both forms of the disorder are shown in Table 5.3.11. However, it must be emphasized that even if the steroid phenotype appears to have two forms, a single enzyme is responsible for aldosterone synthesis.

Adrenal Hypoplasia Congenita

Infants with salt-losing crisis and adrenal insufficiency in infancy may have adrenal hypoplasia congenita. This can be of two types: recessive, for which the cause has not been defined and which affects mostly the fetal zone, and X-linked, which is caused by mutations in the DAX-1 gene, which (with steroidogenic factor-1) controls definitive zone development and steroidogenesis [71]. GC-MS analysis of patients with the disorder show variant patterns from absence of neonatal Δ^5 steroids, appropriate for the recessive form [81], to extremely low cortisol production and transient 11β-hydroxylase deficiency, as evidenced through increased THS excretion (Malunowicz, personal communication).

5.3.3.5 Miscellaneous Conditions

Recessive X-Linked Ichthyosis

Recessive X-linked ichthyosis (RXLI) is a dermatological condition that is caused by steroid sulfatase deficiency (STSD), although the mechanism by which the deficiency causes the characteristic scaly skin has not been adequately explained. RXLI is the most common genetic disorder of steroid metabolism, affecting about 1:2000 males. Epstein and co workers [16] first demonstrated that serum cholesterol sulfate was elevated in the condition, and this compound has become the preferred analyte for diagnosis. The serum level is more than tenfold greater than normal in the condition.

An LC-MS method for quantification has been available for many years [79] using $^{13}C_2$ cholesterol sulfate as an internal standard. The deuterated material is now commercially available (CDN or ISOTEC). Negative-ion ESI-MS is used for quantitation and m/z 365 ($M\text{-}H^-$, analyte) and 367 ($M\text{-}H^-$, internal standard) are monitored. The mean cholesterol sulfate level in 166 cases of RXLI was 4859 ± 1589 µg/dl and for normal individuals 186 ± 112 µg/dl ($n = 109$).

7-Dehydrocholesterol Reductase Deficiency, Smith–Lemli–Opitz syndrome (SLOS)

This is one of the few disorders identified that affect enzymes upstream of cholesterol [37]. 7-Dehydrocholesterol reductase (DHCR7) catalyzes probably the last step in cholesterol synthesis, its formation from 7-dehydrocholesterol (7DHC). Reduced

activity manifests itself in cholesterol deficiency and a build-up of 7DHC and 8DHC, the latter because of the existence of an active Δ^{7-8} isomerase. Patients with this syndrome have SLOS, an autosomally recessive malformation, genital ambiguity, and mental retardation condition. Multiple mutations (>90) have been identified in patients with SLOS. Diagnosis of the condition has until this time been carried out by measurement of serum cholesterol, 7DHC, and 8DHC [42]. Patients can present symptoms of steroid hormone deficiency, not surprising since all steroids have cholesterol as precursor.

Serum Sterol Analysis (GC-MS)

GC or GC-MS analysis of cholesterol, 7DHC and 8DHC are generally used for diagnosis of the condition [42]. A DHC:cholesterol ratio of >0.03 is considered positive.

Urine Metabolite Analysis (GC-MS)

We found normal levels of conventional urinary steroids in this disorder, but these patients can show blunted response to ACTH, and adrenal hyperplasia is often noted post-mortem in nonsurviving newborns. Many distinctive metabolites have been found in urine from patients with the disorder, major examples being 5β-pregn-7-ene-3α,17α,20α-triol (7DHPT) and its 8-dehydroepimer (8DHPT) [90] and the presence of these steroids is diagnostic for the condition. These steroids are most easily quantified by selecting *m/z* 435 (M-117) for PT and *m/z* 343 (M-117-90) for the 7DHPT and 8DHPT. For these ions the mass response is approximately equal, so that both DHPT isomers can be quantified using PT as the external standard callibrant.

Diagnosis in Children

The DHPT:PT ratio is proportional to the DHC:cholesterol ratio and profile analysis can therefore be used diagnostically as an alternate to serum analysis (Fig. 5.3.6). The enzyme deficiency is never complete and the severity of the condition can be ascertained by determining the DHPT:PT ratio.

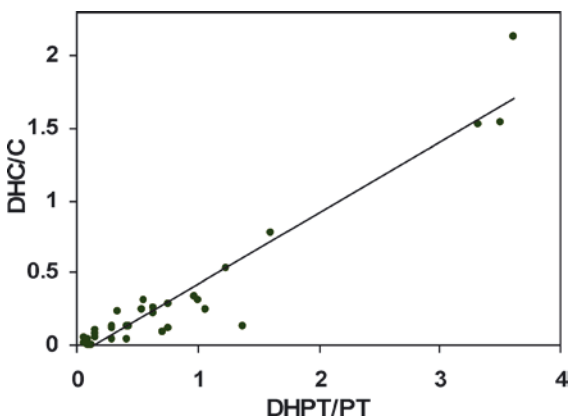

Fig. 5.3.6 Diagnose of Smith–Lemli–Opitz syndromesyndrome (SLOS). Urinary dehydropregnanetriols (*DHPT;* 5β-pregn-7-ene-3α,17α,20α-triol and 5β-pregn-8-ene-3α,17α,20α-triol) partially replace PT in 7-dehydrocholesterol reductase deficiency and can be used to diagnose SLOS. The ratio of DHPT/PT correlates with dehydrocholesterol (*DHC*)/cholesterol (*C*) in affected patients ($n=34$) and also correlates with clinical severity

Neonatal Diagnosis

In the neonatal period, additionally unsaturated forms of the conventional 3β-hydroxy-5-ene steroid sulfates can be the principal urinary components (e.g., 3β,16α-dihydroxy-5,7-pregnadien-20-one and related steroids) [88]. It is during early pregnancy that profile analysis is most used for SLOS diagnosis, and this will be discussed in the final section of the chapter.

MS Screening for SLOS

Pitt [67] published methodology for screening for SLOS based on direct infusion of urinary steroid conjugate extracts into a triple-quadrupole mass spectrometer. Through finding high levels of presumed dehydropregnenetriol sulfate in three SLOS patient urines compared to levels in 1700 controls, the SLOS patients were correctly identified. This method should be readily transferable to the analysis of blood spots as part of newborn screening, and may also be efficacious in prenatal testing.

5.3.4 Prenatal Diagnosis of Steroid Genetic Disorders

5.3.4.1 Congenital Adrenal Hyperplasia

Only 21-hydroxylase deficiency is routinely diagnosed prenatally, and then only in patients considered at risk for the condition. Although elevated levels of 17-OHP are found in amniotic fluid, molecular techniques are generally used for diagnosis.

5.3.4.2 Prenatal Diagnosis of Low-Estriol Conditions

The finding that mothers-to-be carrying an SLOS-affected fetus have low unconjugated serum estriol (uE_3) has necessitated methodology for diagnosing such conditions [8]. Serum estriol is measured as part of "triple (or quad) marker screening" for trisomies and neural-tube defects [102]. In the USA, more than half of pregnant women undertake this test, more than 2 million per year. Estriol concentration is reported as multiples of the median (MoM), and low values are a cause for concern as they can be indicative of serious fetal steroidogenic defects. The disorders shown in Fig. 5.3.7 attenuate estriol production and we have attempted to develop noninvasive methods of maternal urine or serum analysis to distinguish them. The most challenging diagnostically are fetal adrenal hypoplasia and LAH (StAR protein or P450scc deficiencies), as a mere reduction in concentration of conventional steroids is difficult to prove. In contrast, we found unique Δ^7 and/or Δ^8 steroids (dehydropregnanetriol and dehydroestriol) in maternal urine and serum of SLOS pregnancies, which can be used for prenatal diagnosis of this condition [89]. STSD is also readily diagnosed because the absence of placental sulfatase results in the fetal precursor (16α-OH-DHEA sulfate) being excreted in urine unchanged [21]. We have studied three ORD pregnancies and have found elevated excretions of epiallopregnanediol (epialloPD, 5α-pregnane-3β,20α-diol). This steroid is likely a metabolite of fetal pregnenolone overproduced as a result of attenuated 17-hydroxylase/17-20-lyase secondary to the ORD [92]. We believe this steroid would also be elevated in 17-hydroxylase deficiency. Although we have not encountered aromatase deficiency,

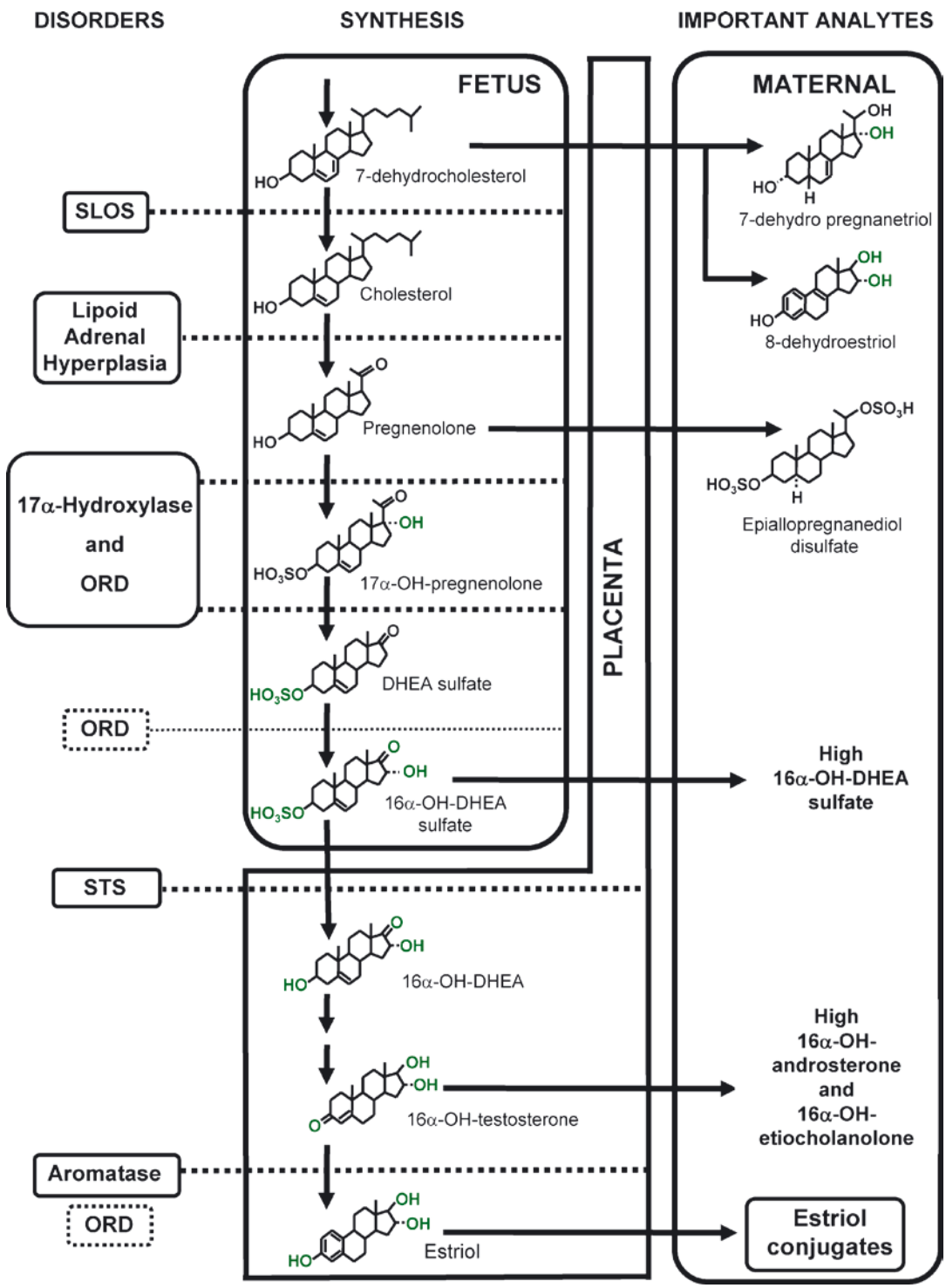

Fig. 5.3.7 Disorders that affect the placental/maternal synthesis of estriol and diagnostic analytes for serum and urine. *ORD* Oxidoreductase deficiency, *STS* steroid sulfatase deficiency

diagnosis should be straightforward since maternal excretion of 16α-hydroxyandrostenedione metabolites) should be elevated.

At what uE_3 level should follow-up analysis be conducted for diagnosis of disorders of estriol synthesis? It was the possibility of SLOS diagnosis that prompted this question, so this disorder has been used for targeting an estriol level where the majority of cases would be diagnosed without an unacceptably high false-positive rate. An algorithm was developed that was predicted to diagnose 60% of affected pregnancies; a constituent parameter of this algorithm was an estriol value of about < 0.3 MoM [64].

Urine and Serum Metabolite Analysis (GC-MS)

GC-MS SIM analysis for prenatal diagnosis requires a different calibration standard from that used for urine from children and adults. Table 5.3.12 shows the steroids present in our external standard and the monitored ions. For serum analysis we employ the highly sensitive ion-trap MS/MS technique described at the beginning of this chapter. Many steroid ratios have been calculated that can be used to distinguish causes of low-estriol, a few that we consider useful are given below, values considered positive for particular disorders are in parenthesis.

Diagnostic Ratios

1. For SLOS: DdehydroE$_3$:E$_3$; 7DHPT:PT and 8DHPT:PT.
2. For STSD: The most important ratio is 16α-OH-DHEA:estriol, although we frequently plot this with the 16α-OH-DHEA:PD ratio.
3. For ORD: EpialloPD:estriol; 16α-OH-androsterone:estriol; 16α-OH-androsterone:16α-OH-DHEA; androsterone:etiocholanolone.

Figure 5.3.8 illustrates results obtained for selected ratios for diagnosis of the above conditions. In the left-hand panel are illustrated ratios for all individuals we have studied with SLOS-affected fetuses compared to values obtained for low-estriol pregnancies that resulted in birth of apparently normal babies. We find significant elevation of the diagnostic ratios as early as the 11th gestational week. The affected pregnancies from our study of 737 low-estriol pregnancies are included; these pregnancies were all above 14 gestational weeks when samples for analysis were collected. Confirmation of the presence of SLOS fetuses was obtained by DHC measurement in the amniotic fluid or fetal tissue. From the data illustrated in Fig. 5.3.8, we determined that the cut-off for a "positive" DHPT:PT ratio was 0.02 after the 14th gestational week, and the corresponding value for the dehydroE$_3$:E$_3$ ratio was 0.03. From our study we determined the detection rate to be 100% and the false-positive rate to be 0% [12, 93].

The results for STSD diagnosis for the 737 low-estriol pregnancies are illustrated in the middle panel of Fig. 5.3.8. This shows results of the 16α-OH-DHEA:E$_3$ ratio for "apparently normal" but low-estriol pregnancies carrying male and female fetuses, pregnancies carrying STSD-affected fetuses (confirmed by family history or fluorescence in-situ hybridization testing for steroid sulfatase deletions). From this data we set a cut-off ratio value of 4.3 for positive STSD. With this value we determined that the detection rate was 100% and the false-positive rate was 3.2%. We determined the incidence of STSD to be 1:2000 males, a figure that agrees well with previous estimates.

■ ***Table 5.3.12*** *Prenatal testing of urine*

Component	Retention time	Specific ion monitored	Calibration mixture amount (μg)	Approximate range of excretions (μg/24 h)
Androstanol (IS)	11.29	333	2.5	
Stigmasterol (IS)	25.45	394	2.5	
Cholesteryl butyrate (IS)	28.91	368	2.5	
An	13.02	270	2.5	500–3000
Et	13.16	270	2.5	500–3000
16α-OH-An	14.25[a]	268	1.0	10–200
16α-OH-Et	13.81[a]	268	-	10–200
11β-OH-An	15.28	268	2.5	100–300
PD	16.32	269	10.0	3000–15000
PT	16.75	435	2.5	300–1500
7DHPT	16.83	343	1.0	0
8DHPT	16.32[b]	343	-	0
Estriol	18.03	504	1.0	1000–5000
DHE_3	18.86	412	1.0	0
DHEA	13.86	268	2.5	100–1000
16α-OH-DHEA	15.91	266	2.5	100–3000
EpialloPD[c]	13.05	374	1.0	10–50
EpialloPD	17.45	269	1.0	10–50
Pregnadienol	12.96	372	1.0	5–20

[a]These steroids give two peaks, both of which are quantified, the retention times are of the first peak. 16α-OH-Et is not an available reference compound so quantification is against the 16α-OH-An calibrant

[b]This steroid is quantified against the 7DHPT calibrant

[c]The first epialloPD is epiallopregnenol, an artifact of epioalloPD disulfate produced during derivatization

Steroid monitored ions, amount in calibration mixture and approximate normal range of excretions. *7DHPT* 5β-Pregn-7-ene-3α,17α,20α-triol, *8DHPT* 5β-pregn-8-ene-3α,17α,20α-triol, *DHE_3* dehydroestriol, *epialloPD* epiallopregnanediol

The right-hand panel of Fig. 5.3.8 shows ratios for the diagnosis of ORD. Pregnancies diagnosed with ORD-affected fetuses were not part of our study of 737 low-estriol pregnancies. The presence of ORD in the affected pregnancies was confirmed by gene sequencing (Dr. Wiebke Arlt). The cut-off values for ORD were determined to be 8.0 for the epialloPD:E_3 ratio and 0.8 for the 16α-OH-androsterone:E_3 ratio, if STSD-affected pregnancies were excluded. STSD-affected pregnancies give ratios between the "normals" and ORD-affected pregnancies. These ratios are predicted to also diagnose 17-hydroxylase and aromatase deficiencies.

If prenatal testing for steroid disorders remains important, and screening is increasingly adopted, the GC-MS methods described here will have to be supplanted by rapid, less labor-intensive LC-MS methods. We are actively pursuing this goal.

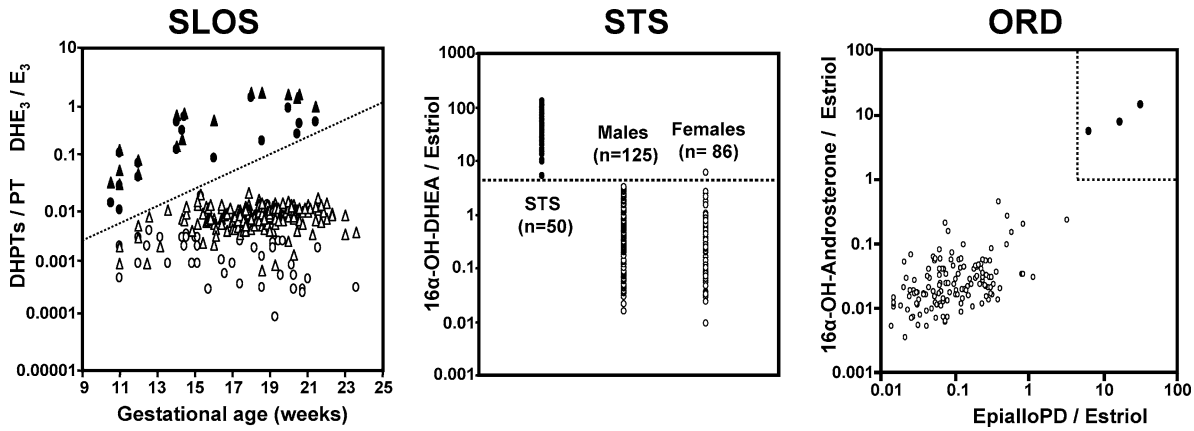

Fig. 5.3.8 Prenatal diagnosis of SLOS, STS, and ORD by determining the ratios of excreted steroids in maternal urine.
Solid symbols represent positive cases and *open symbols*, negative. The negative samples had serum unconjugated estriol (uE_3) < 0.3 multiples of the median, but resulted in normal births without apparent abnormalities. *DHE*$_3$ dehydroestriol, *E*$_3$ Estriol, *EpialloPD* epiallopregnanediol

5.3.5 Summary: The Future of Steroid Analysis

This chapter has described MS methods, some mature, some in an active stage of development, for the pre- and postnatal diagnosis of genetic disorders of steroid synthesis and metabolism. Broadly, the future will see an increasing use of MS/MS in this field, particularly for the more common disorders and well-known analytes, although GC-MS profiling will continue to play an active role in the study of individual patients with rare conditions. Until recently, advocates of molecular diagnosis were predicting the death knell of biochemical analysis, but the reverse has turned out to be true, with the reinvention of profiling as metabolomics. Further advances in LC-MS/MS technology will be forthcoming, and through automation and short analysis times biochemical analysis will attain a cost-effective role in the diagnosis of steroid genetic disorders.

Acknowledgements

The support of the NIH (recently grants 1S10 RR017854, R03 HD045302, R03 HD39707, R01HD38940) is acknowledged. The author wishes particularly to thank laboratory colleagues such as Dr. Norman Taylor, Dr. John Honour, Dr. Josep Marcos and Ms. Esther Roitman. The prenatal diagnosis studies have been conducted with many colleagues including Dr. Wendy Craig, Dr. James Haddow, Dr. Glenn Palomaki, Dr. Richard Kelley, Dr. Berthold Hauffa, Dr. Wiebke Arlt, and others. The author is grateful to Drs. Nigel Clarke and Mike Caulfield of Quest Diagnostics for describing their progress in developing MS/MS methods for routine commercial hormone measurement.

References

1. Adachi M, Tachibana K, Asakura Y, Yamamoto T, Hanaki K, Oka A (2004) Compound heterozygous mutations of cytochrome P450 oxidoreductase gene (POR) in two patients with Antley-Bixler syndrome. Am J Med Genet A 128:333–339
2. Arlt W, Walker EA, Draper N, Ivison HE, Ride JP, Hammer F, Chalder SM, Borucka-Ankiewicz M, Hauffa BP, Malunowicz EM, Stewart PM, Shackleton CH (2004) Congenital adrenal hyperplasia caused by mutant P450 oxidoreductase and human androgen synthesis: analytical study. Lancet 363:2128–2135
3. Biason-Lauber A, Suter SL, Shackleton CH, Zachmann M (2000) Apparent cortisone reductase deficiency: a rare cause of hyperandrogenemia and hypercortisolism. Horm Res 53:260–266
4. Biglieri EG, Herron MA, Brust M (1966) 17-Hydroxylation deficiency in man. J Clin Invest 45:1946–1954
5. Bongiovanni AM (1962) The adrenogenital syndrome with deficiency of 3β-hydroxysteroid dehydrogenase. J Clin Invest 41:2086–2092
6. Bonny O, Rossier BC (2002) Disturbances of Na/K balance: pseudohypoaldosteronism revisited. J Am Soc Nephrol 13:2399–2414
7. Botero-Velez M, Curtis JJ, Warnock DG (1994) Liddle's syndrome revisited – a disorder of sodium reabsorption in the distal tubule. N Engl J Med 330:178–181
8. Bradley LA, Palomaki GE, Knight GJ, Haddow JE, Opitz JM, Irons M, Kelley RI, Tint GS (1999) Levels of unconjugated estriol and other maternal serum markers in pregnancies with Smith–Lemli–Opitz syndrome(RSH) syndrome fetuses. Am J Med Genet 82:355–358
9. Butler GC, Marrian GF (1937) The isolation of pregnane-3,17,20-triol from the urine of women showing the adrenogenital syndrome. J Biol Chem 119:565–570
10. Caulfield MP, Lynn T, Gottschalk ME, Jones KL, Taylor NF, Malunowicz EM, Shackleton CH, Reitz RE, Fisher DA (2002) The diagnosis of congenital adrenal hyperplasia in the newborn by gas chromatography/mass spectrometry analysis of random urine specimens. J Clin Endocrinol Metab 87:3682–3690
11. Chu MD, Ulick S (1982) Isolation and identification of 18-hydroxycortisol from the urine of patients with primary aldosteronism. J Biol Chem 257:2218–2224
12. Craig WY, Haddow JE, Palomaki GE, Kelley RI, Kratz LE, Shackleton CH, Marcos J, Steven Tint G, MacRae AR, Nowaczyk MJ, Kloza EM, Irons MB, Roberson M, (2006) Identifying Smith–Lemli–Opitz syndrome in conjunction with prenatal screening for Down syndrome. Prenat Diagn 26:842–849
13. Cristoni S, Cuccato D, Sciannamblo M, Bernardi LR, Biunno I, Gerthoux P, Russo G, Weber G, Mora S (2004) Analysis of 21 deoxycortisol, a marker of congenital adrenal hyperplasia, in blood by atmospheric pressure chemical ionization and electrospray ionization using multiple reaction monitoring. Rapid Commun Mass Spectrom 18:77–82
14. Dave-Sharma S, Wilson RC, Harbison MD, Newfield R, Azar MR, Krozowski ZS, Funder JW, Shackleton CH, Bradlow HL, Wei JQ, Hertecant J, Moran A, Neiberger RE, Balfe JW, Fattah A, Daneman D, Akkurt HI, De Santis C, New MI (1998) Examination of genotype and phenotype relationships in 14 patients with apparent mineralocorticoid excess. J Clin Endocrinol Metab 83:2244–2254
15. Draper N, Walker EA, Bujalska IJ, Tomlinson JW, Chalder SM, Arlt, W, Lavery GG, Bedendo O, Ray DW, Laing I, Malunowicz E, White PC, Hewison M, Mason PJ, Connell JM, Shackleton CH, Stewart PM (2003) Mutations in the genes encoding 11 β-hydroxysteroid dehydrogenase type 1 and hexose-6-phosphate dehydrogenase interact to cause cortisone reductase deficiency. Nat Genet 34:434–439
16. Epstein EH Jr, Krauss RM, Shackleton CH (1981) X-linked ichthyosis: increased blood cholesterol sulfate and electrophoretic mobility of low-density lipoprotein. Science 214:659–660
17. Flück CE, Tajima T, Pandey AV, Arlt W, Okuhara K, Verge CF, Jabs EW, Mendonca BB, Fujieda K, Miller WL (2004) Mutant P450 oxidoreductase causes disordered steroidogenesis with and without Antley-Bixler syndrome. Nat Genet 36:228–230

18. Fredline VF, Taylor PJ, Dodds HM, Johnson AG (1997) A reference method for the analysis of aldosterone in blood by high-performance liquid chromatography-atmospheric pressure chemical ionization-tandem mass spectrometry. Anal Biochem 252:308–313
19. Fujieda K, Okuhara K, Abe S, Tajima T, Mukai T, Nakae J (2003) Molecular pathogenesis of lipoid adrenal hyperplasia and adrenal hypoplasia congenita. J Steroid Biochem Mol Biol 85:483–489
20. Geissler WM, Davis DL, Wu L, Bradshaw KD, Patel S, Mendonca BB, Elliston KO, Wilson JD, Russell DW, Andersson S (1994) Male pseudohermaphroditism caused by mutations of testicular 17β-hydroxysteroid dehydrogenase 3. Nat Genet 7:34–39
21. Glass IA, Lam RC, Chang T, Roitman E, Shapiro LJ, Shackleton CH (1998) Steroid sulphatase deficiency is the major cause of extremely low oestriol production at mid-pregnancy: a urinary steroid assay for the discrimination of steroid sulphatase deficiency from other causes. Prenat Diagn 18:789–800
22. Griffiths WJ, Alvelius G, Liu S, Sjovall J (2004) High-energy collision-induced dissociation of oxosteroids derivatised to Girard hydrazones. Eur J Mass Spectrom (Chichester, Eng) 10:63–88
23. Griffiths W, Shackleton CHL, Sjövall J (2005) Mass spectrometry of steroids. In: Caprioli R (ed) The Encyclopedia of Mass Spectrometry, Vol 7. Elsevier, Amsterdam, pp 447–473
24. Guo T, Chan M, Soldin SJ (2004) Steroid profiles using liquid chromatography-tandem mass spectrometry with atmospheric pressure photoionization source. Arch Path Lab Med 128:469–475
25. Guo T, Taylor RL, Singh RJ, Soldin SJ (2006) Simultaneous determination of 12 steroids by isotope dilution liquid chromatography-photospray ionization tandem mass spectrometry. Clin Chim Acta 372:76–82
26. Hauffa BP, Solyom J, Glaz E, Shackleton CH, Wambach G, Vecsei P, Stolecke H, Homoki J (1991) Severe hypoaldosteronism due to corticosterone methyl oxidase type II deficiency in two boys: metabolic and gas chromatography-mass spectrometry studies. Eur J Pediatr 150:149–153
27. Higashi T, Uamauchi A, Shimada K, Koh E, Mizokami A, Namiki M (2005a) Determination of prostatic androgens in 10 mg of tissue using liquid chromatography-tandem mass spectrometry with charged derivatization. Anal Bioanal Chem 382:1035–1043
28. Higashi T, Yamauchi A, Shimada K (2005b) 2-Hydrazino-1-methylpyridine: a highly sensitive derivatization reagent for oxosteroids in liquid chromatography-electrospray ionization-mass spectrometry. J Chromatogr B 825:214–222
29. Hiort O, Holterhus PM, Werner R, Marschke C, Hoppe U, Partsch CJ, Riepe FG, Achermann JC, Struve D (2005) Homozygous disruption of P450 side-chain cleavage (CYP11A1) is associated with prematurity, complete 46,XY sex reversal, and severe adrenal failure. J Clin Endocrinol Metab 90:538–541
30. Holst JP, Soldin SJ, Tractenberg RE, Guo T, Kundra P, Verbalis JG, Jonklaas J (2007) Use of steroid profiles in determining the cause of adrenal insufficiency. Steroids 72:71–84
31. Honour JW, Anderson, JM, Shackleton, CH (1983) Difficulties in the diagnosis of congenital adrenal hyperplasia in early infancy: the 11β-hydroxylase defect. Acta Endocrinol (Copenh) 103:101–109
32. Honour JW, Tourniaire J, Biglieri EG, Shackleton CHL (1978) Urinary steroid excretion in 17α-hydroxylase deficiency. J Steroid Biochem 9:495–505
33. Honour JW, Dillon MJ, Shackleton CH (1982) Analysis of steroids in urine for differentiation of pseudohypoaldosteronism and aldosterone biosynthetic defect. J Clin Endocrinol Metab 54:325–331
34. Imperato-McGinley J, Peterson RE, Gautier T, Arthur A, Shackleton C (1985) Decreased urinary C19 and C21 steroid 5α-metabolites in parents of male pseudohermaphrodites with 5α-reductase deficiency: detection of carriers. J Clin Endocrinol Metab 60:553–558
35. Imperato-McGinley J, Gautier T, Peterson RE, Shackleton C (1986) The prevalence of 5α-reductase deficiency in children with ambiguous genitalia in the Dominican Republic. J Urol 136:867–873

36. Inoue T, Okauchi Y, Matsuzaki Y, Kuwajima K, Kondo H, Horiuchi N, Nakao K, Iwata M, Yokogoshi Y, Shintani Y, Bando H, Saito S (1998) Identification of a single cytosine base insertion mutation at Arg-597 of the β subunit of the human epithelial sodium channel in a family with Liddle's disease. Eur J Endocrinol 138:691–697
37. Irons M, Elias ER, Salen G, Tint GS, Batta AK (1993) Defective cholesterol biosynthesis in Smith–Lemli–Opitz syndrome. Lancet 341:1414
38. Jamieson A, Wallace AM, Andrew R, Nunez BS, Walker BR, Fraser R White PC, Connell JMC (1999) Apparent cortisone reductase deficiency: a functional defect in 11β-hydroxysteroid dehydrogenase type 1. J Clin Endocrinol Metab 84:3570–3574
39. Jeunemaitre X, Charru A, Pascoe L, Guyene TT, Aupetit-Faisant B, Shackleton CH, Schambelan M, Plouin PF, Corvol P (1995) [Hyperaldosteronism sensitive to dexamethasone with adrenal adenoma. Clinical, biological and genetic study]. Presse Med 24:1243–1248
40. Joannou GE (1981) Identification of 15β-hydroxylated C21 Steroids in the neo-natal period: the role of 3α,15β,17α-trihydroxy-5β-pregnan-20-one in the perinatal diagnosis of congenital adrenal hyperplasia (CAH) due to a 21-hydroxylase deficiency. J Steroid Biochem 14:901–912
41. Johnson DW (2005) Ketosteroid profiling using Girard T derivatives and electrospray ionization tandem mass spectrometry: direct plasma analysis of androstenedione, 17-hydroxyprogesterone and cortisol. Rapid Commun Mass Spectrom 19:193–200
42. Kelley RI (1995) Diagnosis of Smith–Lemli–Opitz syndrome by gas chromatography/mass spectrometry of 7-dehydrocholesterol in plasma, amniotic fluid and cultured skin fibroblasts. Clin Chim Acta 236:45–58
43. Kushnir MM, Neilson R, Roberts WL, Rockwood AL (2004) Cortisol and cortisone analysis in serum and plasma by atmospheric pressure photoionization tandem mass spectrometry. Clin Biochem 37:357–362
44. Kushnir MM, Rockwood AL, Roberts WL, Pattison EG, Bunker AM, Fitzgerald RL, Meikle AW (2006) Performance characteristics of a novel tandem mass spectrometry assay for serum testosterone. Clin Chem 52:120–128
45. Kushnir MM, Rockwood AL, Roberts WL, Pattison EG, Owen WE, Bunker AM, Meikle AW (2006) Development and performance evaluation of a tandem mass spectrometry assay for 4 adrenal steroids. Clin Chem 52:1559–1567
46. Lacey JM, Minutti CZ, Magera MJ, Tauscher AL, Casetta B, McCann M, Lymp J, Hahn SH, Rinaldo P, Matern D (2004) Improved specificity of newborn screening for congenital adrenal hyperplasia by second-tier steroid profiling using tandem mass spectrometry. Clin Chem 50:621–625
47. Lai CC, Tsai CH, Tsai FJ, Wu JY, Lin WD, Lee CC (2002) Rapid screening assay of congenital adrenal hyperplasia by measuring 17 alpha-hydroxyprogesterone with high-performance liquid chromatography/electrospray ionization tandem mass spectrometry from dried blood spots. J Clin Lab Anal 16:20–25
48. Lavery GG, Walker EA, Slabbert A, Ride JP, Shackleton CHL, Tomlinson JW, Arlt W, Stewart PM (2008) Monogenic forms of hyperandrogenism due to defects in cortisol metabolism. New Engl J Med (in press)
49. Lemonde HA, Custard EJ, Bouquet J, Duran M, Overmars H, Scambler PJ, Clayton PT (2003) Mutations in SRD5B1 (AKR1D1), the gene encoding delta(4)-3-oxosteroid 5β-reductase, in hepatitis and liver failure in infancy. Gut 52:1494–1499
50. Li A, Tedde R, Krozowski ZS, Pala A, Li KX, Shackleton CH, Mantero F, Palermo M, Stewart PM (1998) Molecular basis for hypertension in the "type II variant" of apparent mineralocorticoid excess. Am J Hum Genet 63:370–379
51. Lifton RP, Dluhy RG, Powers M, Rich GM, Gutkin M, Fallo F, Gill JR Jr, Feld L, Ganguly A, Laidlaw JC, Murnaghan DJ, Kaufman C, Stockigt JR, Ulick S, Lalouel J (1992) Hereditary hypertension caused by chimaeric gene duplications and ectopic expression of aldosterone synthase. Nat Genet 2:66–74
52. Makin HLJ (ed) (1984) Biochemistry of Steroid Hormones, 2nd edn. Blackwell Scientific, Oxford, UK

53. Malunowicz EM, Mitkowska Z, Bal K, Nizankowska-Blaz T, Moszczynska E, Iwanicka Z, Romer TE (1997) Definitive diagnosis of enzymatic deficiencies of steroidogenesis in at-risk newborns and infants by urinary marker analysis using GC/MS-SIM. Horm Res 48:243–251
54. Malunowicz EM, Romer TE, Urban M, Bossowski A (2003) 11-β-Hydroxysteroid dehydrogenase type 1 deficiency ('Apparent Cortisone Reductase Deficiency') in a 6-year-old boy. Horm Res 59:205–210
55. Marsden D, Larson CA (2004) Emerging role for tandem mass spectrometry in detecting congenital adrenal hyperplasia. Clin Chem 50:467–468
56. Marwah A, Marwah P, Lardy H (2001) Liquid chromatography-electrospray ionization mass spectrometric analysis of corticosterone in rat plasma using selected ion monitoring. J Chromatogr B 757:333–342
57. Mendonca BB, Russell AJ, Vasconcelos-Leite M, Arnhold IJ, Bloise W, Wajchenberg BL, Nicolau W, Sutcliffe RG, Wallace AM (1994) Mutation in 3β-hydroxysteroid dehydrogenase type II associated with pseudohermaphroditism in males and premature pubarche or cryptic expression in females. J Mol Endocrinol 12:119–122
58. Minutti CZ, Lacey JM, Magera MJ, Hahn, SH, McCann M, Schulze A, Cheillan D, Dorche C, Chace DH, Lymp JF, Zimmerman D, Rinaldo P, Matern D (2004) Steroid profiling by tandem mass spectrometry improves the positive predictive value of newborn screening for congenital adrenal hyperplasia. J Clin Endocrinol Metab 89:3687–3693
59. Monder C, Bradlow HL (1980) Cortoic acids: explorations at the frontier of corticosteroid metabolism. Recent Prog Horm Res 36:345–400
60. Nelson RE, Grebe SK, O'Kane DJ, Singh RJ (2004) Liquid chromatography-tandem mass spectrometry assay for simultaneous measurement of estradiol and estrone in human plasma. Clin Chem 50:373–384
61. Nikkila H, Tannin GM, New MI, Taylor NF, Kalaitzoglou G, Monder C, White PC (1993) Defects in the HSD11 gene encoding 11β-hydroxysteroid dehydrogenase are not found in patients with apparent mineralocorticoid excess or 11-oxoreductase deficiency. J Clin Endocrinol Metab 77:687–691
62. Palermo M, Gomez-Sanchez C, Roitman E, Shackleton CH (1996) Quantitation of cortisol and related 3-oxo-4-ene steroids in urine using gas chromatography/mass spectrometry with stable isotope-labeled internal standards. Steroids 61:583–589
63. Palermo M, Marazzi MS, Hughes BA, Stewart PM, Shackleton CHL (2008) Human Δ^4-3-oxosteroid 5β-reductase (AKR1D1) deficiency and steroid metabolism. Steroids 2008; 73:417–23
64. Palomaki GE, Bradley LA, Knight GJ, Craig WY, Haddow JE (2002) Assigning risk for Smith–Lemli–Opitz syndrome as part of 2nd trimester screening for Down's syndrome J Med Screen 9:43–44
65. Peterson RE, Imperato-McGinley, J, Gautier T, Shackleton C (1985) Male pseudohermaphroditism due to multiple defects in steroid-biosynthetic microsomal mixed-function oxidases. A new variant of congenital adrenal hyperplasia. N Engl J Med 313:1182–1191
66. Phillipov G, Palermo M, Shackleton CH (1996) Apparent cortisone reductase deficiency: a unique form of hypercortisolism. J Clin Endocrinol Metab 81:3855–3860
67. Pitt JJ (2007) High-throughput urine screening for Smith–Lemli–Opitz syndrome and cerebrotendinous xanthomatosis using negative electrospray tandem mass spectrometry. Clin Chim Acta 380:81–88
68. Plumb R, Castro-Perez J, Granger J, Beattie I, Joncour K, Wright A (2004) Ultra-performance liquid chromatography coupled to quadrupole-orthogonal time-of-flight mass spectrometry. Rapid Commun Mass Spectrom 18:2331–2337
69. Raffaelli A, Saba A, Vignali E, Marcocci C, Salvadori P (2006) Direct determination of the ratio of tetrahydrocortisol + allo-tetrahydrocortisol to tetrahydrocortisone in urine by LC-MS/MS. J Chromatogr B Analyt Technol Biomed Life Sci 830:278–285
70. Rauh M, Groschl M, Rascher W, Dorr HG (2006) Automated, fast and sensitive quantification of 17 alpha-hydroxy-progesterone, androstenedione and testosterone by tandem mass spectrometry with on-line extraction. Steroids 71:450–458

71. Reutens AT, Achermann JC, Ito M, Ito M, Gu W-X, Habiby RL, Donohoue PA, Pang S, Hindmarsh PC, Jameson JL (1999) Clinical and functional effects of mutations in the DAX-1 gene in patients with adrenal hypoplasia congenita. J Clin Endocrinol Metab 84:504–511
72. Rosenfield RL, Rich BH, Wolfsdorf JI, Cassorla F, Parks JS, Bongiovanni AM, Wu CH, Shackleton CH (1980) Pubertal presentation of congenital Δ^5-3β-hydroxysteroid dehydrogenase deficiency. J Clin Endocrinol Metab 51:345–353
73. Saenger P, Klonari Z, Black SM, Compagnone N, Mellon SH, Fleischer A, Abrams CAL, Shackleton CHL, Miller WL (1995) Prenatal diagnosis of congenital lipoid adrenal hyperplasia. J Clin Endocrinol Metab 80:200–205
74. Sanchez R, Rheaume E, Laflamme N, Rosenfield RL, Labrie F, Simard J (1994) Detection and functional characterization of the novel missense mutation Y254D in type II 3 β-hydroxysteroid dehydrogenase (3βHSD) gene of a female patient with non salt-losing 3βHSD deficiency. J Clin Endocrinol Metab 78:561–567
75. Shackleton CH (1976) Congenital adrenal hyperplasia caused by defect in steroid 21-hydroxylase. Establishment of definitive urinary steroid excretion pattern during first weeks of life. Clin Chim Acta 67:287–298
76. Shackleton CH (1986) Profiling steroid hormones and urinary steroids. J Chromatogr 379:91–156
77. Shackleton CH (1993) Mass spectrometry in the diagnosis of steroid–related disorders and in hypertension research. J Steroid Biochem Mol Biol 45:127–140
78. Shackleton C, Malunowicz E (2003) Apparent pregnene hydroxylation deficiency (APHD): seeking the parentage of an orphan metabolome. Steroids 68:707–717
79. Shackleton CH, Reid S (1989) Diagnosis of recessive X-linked ichthyosis: quantitative HPLC/mass spectrometric analysis of plasma for cholesterol sulfate. Clin Chem 35:1906–1910
80. Shackleton CH, Honour JW, Taylor NF (1979a) Metabolism of fetal and neonatal adrenal steroids. J Steroid Biochem 11:523–529
81. Shackleton CH, Swift PG, Savage DC, Honour JW (1979b) Deficient 3β-hydroxy-5-ene steroid secretion by newborn infants. J Clin Endocrinol Metab 49:247–251
82. Shackleton CH, Roitman E, Monder C, Bradlow HL (1980a) Gas chromatographic and mass spectrometric analysis of urinary acidic metabolites of cortisol. Steroids 36:289–298
83. Shackleton CH, Honour JW, Dillon MJ, Chantler C, Jones RW (1980c) Hypertension in a four-year-old child: gas chromatographic and mass spectrometric evidence for deficient hepatic metabolism of steroids. J Clin Endocrinol Metab 50:786–802
84. Shackleton CH, Taylor NF, Honour JW (1980b) An Atlas of Gas Chromatographic Profiles of Neutral Urinary Steroids in Health in Disease. Packard-Becker, Delft
85. Shackleton CH, Irias J, McDonald C, Imperato-McGinley J (1986) Late-onset 21-hydroxylase deficiency: reliable diagnosis by steroid analysis of random urine collections. Steroids 48:239–250
86. Shackleton CHL, Kletke C, Wudy S, Pratt JH (1990) Dehydroepiandrosterone sulfate quantification in serum using high-performance liquid chromatography/mass spectrometry and a deuterated internal standard: a technique suitable for routine use or as a reference method. Steroids 55:472–478
87. Shackleton CH, Chuang H, Kim J, de la Torre X, Segura J (1997) Electrospray mass spectrometry of testosterone esters: potential for use in doping control. Steroids 62:523–529
88. Shackleton CH, Roitman E, Kelley R (1999) Neonatal urinary steroids in Smith–Lemli–Opitz syndrome associated with 7-dehydrocholesterol reductase deficiency. Steroids 64:481–490
89. Shackleton CH, Roitman E, Kratz L, Kelley R (2001) Dehydro-oestriol and dehydropregnanetriol are candidate analytes for prenatal diagnosis of Smith–Lemli–Opitz syndrome. Prenat Diagn 21:207–212
90. Shackleton C, Roitman E, Guo LW, Wilson WK, Porter FD (2002) Identification of 7(8) and 8(9) unsaturated adrenal steroid metabolites produced by patients with 7-dehydrosterol-Δ^7-reductase deficiency (Smith–Lemli–Opitz syndrome). J Steroid Biochem Mol Biol 82:225–232

91. Shackleton C, Marcos J, Malunowicz E, Szarras-Czapnik M, Jira P, Taylor NF, Murphy N, Crushell E, Gottschalk M, Hauffa BP, Cragun DL, Hopkin RJ, Adachi M, Arlt W (2004a) Biochemical diagnosis of Antley-Bixler syndrome by steroid analysis. Am J Med Genet 128:223–231
92. Shackleton C, Marcos J, Arlt W, Hauffa BP (2004b) Prenatal diagnosis of P450 oxidoreductase deficiency (ORD): a disorder causing low pregnancy estriol, maternal and fetal virilization, and the Antley-Bixler syndrome phenotype. Am J Med Genet A 129:105–112
93. Shackleton CHL, Marcos J, Palomaki GE, Craig WY, Kelley RE , Kratz LE , Haddow JE (2007) Dehydrosteroid measurements in maternal urine or serum for the prenatal diagnosis of Smith–Lemli–Opitz syndrome (SLOS). Am J Med Genet A 143:2129–2136
94. Speiser PW (2004) Improving neonatal screening for congenital adrenal hyperplasia. J Clin Endocrinol Metab 89:3685–3686
95. Speiser PW, White PC (2003) Congenital adrenal hyperplasia. N Engl J Med 349:776–788
96. Starcevic B, DiStefano E, Wang C, Catlin DH (2003) Liquid chromatography-tandem mass spectrometry assay for human serum testosterone and trideuterated testosterone. J Chromatogr B 792:197–204
97. Stewart PM, Murray BA, Mason JI (1994) Human kidney 11β-hydroxysteroid dehydrogenase is a high affinity nicotinamide adenine dinucleotide-dependent enzyme and differs from the cloned type I isoform. J Clin Endocrinol Metab 79:480–484
98. Taylor RL, Machacek D, Singh RJ (2002) Validation of a high-throughput liquid chromatography-tandem mass spectrometry method for urinary cortisol and cortisone. Clin Chem 48:1511–1519
99. Turpeinen U, Stenman U-H (2003) Determination of urinary free cortisol by liquid chromatography-tandem mass spectrometry. Scand J Clin Lab Invest 63:143–150
100. Turpeinen U, Markkanen H, Sane T, Hamalainen E (2006) Determination of free tetrahydrocortisol and tetrahydrocortisone ratio in urine by liquid chromatography-tandem mass spectrometry. Scand J Clin Lab Invest 66:147–159
101. Ulick S, Levine LS, Gunczler P, Zanconato G, Ramirez LC, Rauh W, Rosler A, Bradlow HL, New MI (1979) A syndrome of apparent mineralocorticoid excess associated with defects in the peripheral metabolism of cortisol. J Clin Endocrinol Metab 49:757–764
102. Wald NJ, Rodeck C, Hackshaw AK, Walters J, Chitty L, Mackinson AM (2003) First and second trimester antenatal screening for Down's syndrome: the results of the Serum, Urine and Ultrasound Screening Study (SURUSS) J Med Screen 10:56–104
103. White PC (2001) Steroid 11β-hydroxylase deficiency and related disorders. Endocrinol Metab Clin North Am 30:61–79
104. White PC (2004) Aldosterone synthase deficiency and related disorders. Mol Cell Endocrinol 217:81–87
105. Wong T, Shackleton CH, Covey TR, Ellis G (1992) Identification of the steroids in neonatal plasma that interfere with 17 α-hydroxyprogesterone radioimmunoassays. Clin Chem 38:1830–1837
106. Yoshida T, Majors RE (2006) High-speed analyses using rapid resolution liquid chromatography on 1.8-micron porous particles. J Sep Sci 29:2421–2432
107. Zhao M, Baker SD, Yan X, Zhao Y, Wright WW, Zirkin BR, Jarow JP (2004) Simultaneous determination of steroid composition of human testicular fluid using liquid chromatography tandem mass spectrometry. Steroids 69:721–726

5.4 Bile Acids

Giorgio Federici

5.4.1 Introduction

The liver is involved in a variety of both synthetic and catabolic functions, including metabolism of amino acids, lipids, carbohydrates, protein synthesis and detoxification [1]. These metabolic functions are performed mainly by hepatocytes, although the liver is made of three major cell types (hepatocytes, biliary epithelial cells and Kupffer cells). Exerting many different metabolic functions, the liver contains several different and specific enzymes, leakage of which into the bloodstream occurs in hepatic diseases.

Among the different roles previously described, the liver exerts an excretory function, being involved in the formation of bile, which drains into the small intestine. Bile salts in the bile play an important role as emulsifying agents for the reabsorption of lipids and fatty acids from the intestine. Hepatic and obstructive biliary diseases lead to abnormal metabolism of bile acids (BAs).

5.4.2 BA Structure

BAs are a group of acids with a steroidal ring structure and a terminal carboxylic group located in the side chain (Fig. 5.4.1), and represent the major end products of cholesterol catabolism [2].

Primary BAs, cholic acid (CA), and chenodeoxycholic acid (CDCA), are synthesised via the 5β-saturation of the cholesterol double bond by enzymes of the hepatocyte microsomal fraction, epimerisation of the 3β-hydroxyl group to the 3α-configuration, and further insertion of a 7α-hydroxyl group, with or without a further 12α-hydroxyl group. After shortening of the side chain by three carbons, oxidation of the terminal carbon of the side chain occurs to form the carboxylic group [3]. Alternative metabolic sequences add to the complexity of this metabolic pathway (Fig. 5.4.2).

After their synthesis, primary BAs are conjugated with glycine or taurine to form bile salts (glycocholate, taurocholate, glycochenodeoxycholate and taurochenodeoxycholate), which are excreted into the bile and collected in the gall bladder. This synthetic pathway is regulated by feedback inhibition, as BAs passing through the liver in the enterohepatic circulation inhibit cholesterol 7α-hydroxylase, which catalyses the first limiting step of their synthesis.

Secondary BAs, deoxycholic acid (DCA) and lithocholic acid (LCA), are formed in the intestinal lumen by bacterial dehydroxylation of primary BAs, after hydrolysis

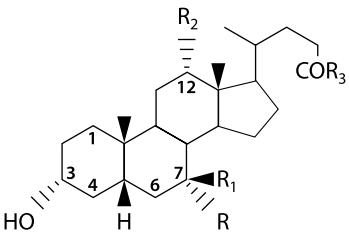

	R	R_1	R_2	R_3
CA	OH	H	OH	
CDCA	OH	H	H	
UDCA	H	OH	H	
DCA	H	H	OH	
LCA	H	H	H	
Free bile acids			OH	
Glycine conjugates			$NHCH_2CO_2H$	
Taurine conjugates			$NHCH_2CH_2SO_3H$	

Fig. 5.4.1 Chemical structures of bile acids (BAs) (reprinted from [2]). *CA* Cholic acid, *CDCA* chenodeoxycholic acid, *DCA* deoxycholic acid, *LCA* lithocholic acid, *UDCA* ursodeoxycholic acid

of taurine and glycine conjugates. CDCA is converted in the intestinal lumen by bacteria to 7-ketolithocholic acid, which is then metabolised to ursodeoxycholic acid (UDCA) in the liver.

In addition to these BAs, a wide range of minor components has been identified, including C_1, C_4 or C_6 hydroxylated derivatives as well as their epimers, C_{27} bile acids, oxo bile acids and conjugates on any of the hydroxyl groups with sulphuric acid, glucuronic acid, glucose or N-acetylglucosamine.

BAs are present in unconjugated and/or conjugated form in biological samples. They range from 1–2 μg/ml in serum and urine to significant amounts in the intestinal content and as much as 10 mg/ml in the gallbladder bile. BAs are present mainly as glycine and taurine conjugates in plasma and bile, unconjugated in faeces, and unconjugated as well as conjugated with glycine, taurine, glucuronic acid, and sulphuric acid in the urine. BAs are usually present in association with protein, sterols and their esters, free or esterified fatty acids, bile pigments and water-soluble small molecules. The faecal BA pattern is highly complex due to the extensive bacterial metabolism of BAs during intestinal transit. Thus, intestinal bacteria deconjugate BA conjugates, cleaving the glycine and taurine complexes, as well as glucuronides and sulphate esters.

5.4.3 BA Metabolism

BAs facilitate the excretion of bile lipids, including cholesterol, and the absorption of dietary lipids, including fat-soluble vitamins, in the intestines. These detergent properties result from their amphipathic structure, with the polar groups hydrated with water molecules, and a non-polar steroid skeleton attracting lipids; their detergent properties are further increased by conjugation with glycine and taurine. Compared

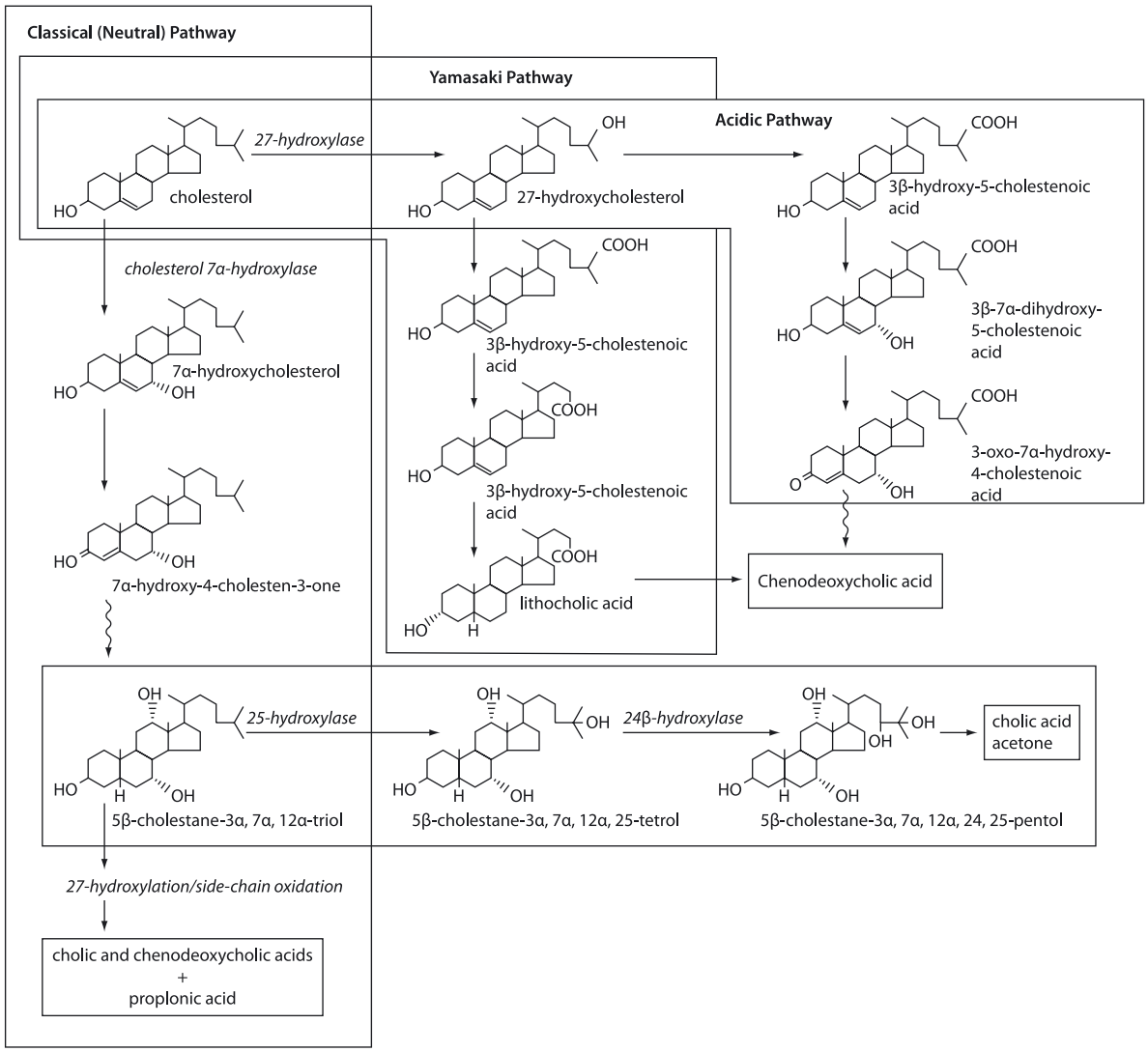

Fig. 5.4.2 The neutral BA synthetic pathway and alternative pathways, the acidic pathway and the Yamasaki pathway. (Reprinted from [4])

with BAs, bile salts are more soluble at an acid pH, form better micelles in bile, and, after passing through the small intestine, exert their role as emulsifying agents to efficiently reabsorb lipids and fatty acids from the ileum-proximal colon. A major fraction of reabsorbed bile salts then returns to the liver via the portal vein [5].

The circulation of bile components between the liver and intestine is known as enterohepatic circulation (Fig. 5.4.3). The total amount of conjugated and unconjugated BAs secreted per day by the liver is 20–30 g for an adult. However, the body maintains only a very small pool of 3–5 g, for they are toxic as detergents at higher concentrations. BAs are actively reabsorbed in the lower ileum, recirculated to the liver, and resecreted 4–10 times per day. Only about 0.8 g of BAs is secreted daily with the faeces.

Analysis of BAs in urine, serum, bile and stool is crucial for the diagnosis of inborn errors of BA metabolism. It is also helpful for understanding their pathophysiological role in acquired hepatic diseases and for monitoring the effects of therapy on metabolism. Several different inborn defects affecting BA synthetic pathway, have been described over last 20 years [7].

The initial steps in BA synthesis are characterised by the introduction of a hydroxylic group in the 7α position, or in position 27, followed by another in the 7α position into the cholesterol nucleus. Both synthetic pathways (the neutral and the acidic pathways) possess a distinct microsomal 7-oxysterol hydroxylase, which is regulated by different genes. The most recently described disorder of BA synthesis is cholesterol 7α-hydroxylase deficiency, in which their decreased production through the classical pathway is partially balanced by activation of the alternative pathway. Cholesterol levels increase in the liver, with a consequent low-density lipoprotein hypercholesterolemia, and cholesterol gallstones may result, although there is no liver disease. In contrast, a defect in the conversion of 27-hydroxy-cholesterol to 7α,27-dihydroxy-cholesterol due to deficiency of the oxysterol 7α-hydroxylase specific for the alternate pathway, causes severe neonatal liver disease [8].

In 3β-hydroxysteroid-Δ^5-oxidoreductase deficiency, 7α-hydroxycholesterol undergoes side-chain oxidation, producing 3β,7α-dihydroxy-5-cholenoic acid and 3β,7α,12α-trihydroxy-5-cholenoic acid: these two alternative end products are markedly excreted into the urine of affected patients.

In 3-oxosteroid Δ^4-steroid 5β-reductase deficiency, key intermediates for cholic and chenodeoxycholic synthesis, 7α-hydroxy-4-cholesten-3-one and 7α,12α-dihydroxy-4-cholesten-3-one undergo side-chain oxidation and conjugation to produce

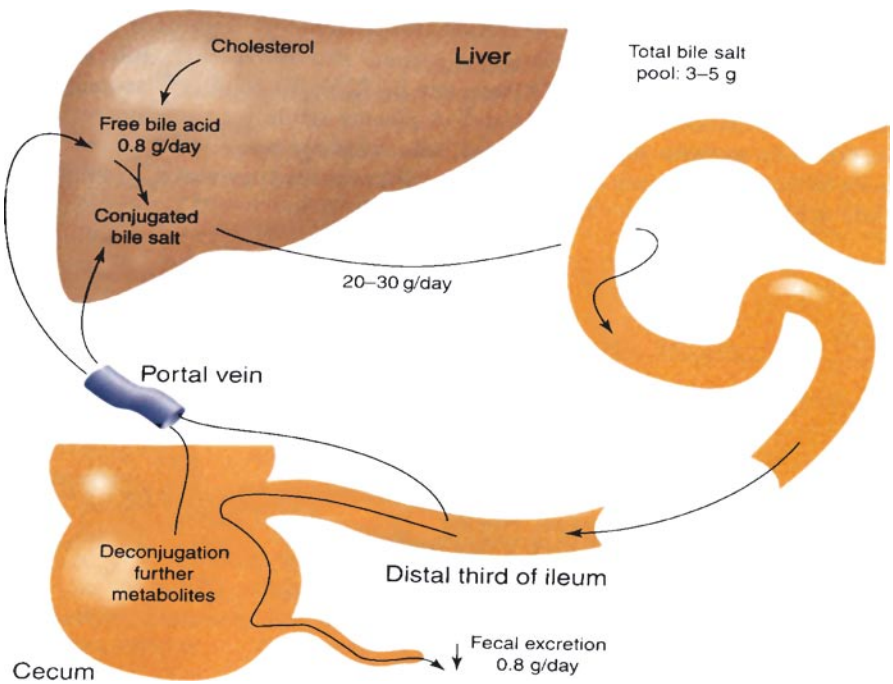

Fig. 5.4.3 Enterohepatic circulation of BAs. (Reprinted from [6])

taurine and glycine conjugates of 7α-hydroxy-3-keto-4-cholenoic acid and 7α,12α-dihydroxy-3-keto-4-cholenoic acid, which are excreted into the urine in large amounts.

Defective side-chain oxidation is found in patients affected by cerebrotendinous xanthomatosis (CTX), an autosomal recessive defect characterised by deficit of mitochondrial 27-hydroxylase. The CTX defect leads to an accumulation of cholestanol and cholesterol in most tissues, while serum concentrations of CA, as well as other BAs, are sensibly low.

Peroxisomal disorders (Zellweger syndrome, Refsum's disease, neonatal adrenoleukodystrophy) are characterised by defective peroxisome biogenesis, or, being present, peroxisomes lacking β-oxidative enzymes. In the BA biosynthetic pathway, dihydroxycoprostanic acid (DHCA) and trihydroxycoprostanic acid (THCA) are β-oxidised in peroxisomes to produce CA and CDCA, respectively, whereas peroxisomal disorders cause a defective oxidation of the BA precursor side chain, which leads to an accumulation of C_{27} bile acids, notably 3α,7α-dihydroxy-5β-cholestanoic acid (DHCA) and 3α,7α,12α-trihydroxy-5β-cholestanoic acid (THCA), in the plasma and urine of affected patients.

Determination of serum total BAs is useful for the screening, diagnosis, and prognostic evaluation of hepatobiliary diseases. Serum concentration changes markedly in patients with acquired hepatobiliary diseases. In healthy fasting subjects, the serum concentration of total BAs is usually lower than 2 μg/ml, while it increases to 40 μg/ml in liver cirrhosis, 90 μg/ml in hextrahepatic obstructive jaundice, and between 30 and 160 μg/ml in viral hepatitis. Acquired hepatobiliary diseases are often associated with disorders affecting BA metabolism, resulting in the accumulation of a variety of isomers as well as glucuronidated and sulphated conjugates.

Since hepatobiliary and intestinal dysfunctions are marked by variation in the concentration and relative proportions of major BAs and by increased levels of their minor forms, individual identification and accurate quantification of these compounds in biological samples are very important prognostic, diagnostic, and therapeutic monitoring indicators of liver and gastrointestinal tract diseases in humans.

5.4.4 BA Analysis

BAs are a heterogeneous class of compounds found in biological samples at very low concentration. They exhibit a great variety of isomeric forms, with different polarity and acidity, and low volatility; for these reasons their simultaneous determination is often difficult to achieve. Many different analytical techniques have been published over last 20 years to perform identification and accurate quantification of BAs [1, 2, 9–12]. Among these should be mentioned high-performance liquid chromatography (HPLC), gas chromatography with flame ionisation detection (GC/FID), gas chromatography coupled with mass spectrometry (GC-MS), liquid chromatography (LC) coupled with mass spectrometry (LC-MS), capillary electrophoresis (CE), radioimmunoassay (RIA), and enzymatic colorimetric assay.

From the available analytical techniques, the most commonly employed is HPLC coupled with an ultraviolet (UV) detector, which provides a rapid, relatively cheap and easy routine analysis of conjugated BAs from serum samples. HPLC with UV detection determination does not require sample derivatisation, but the sensitivity of

the UV detector is low and is affected by matrix interference [13]. For this reason, use of derivatisation allows us to obtain compounds with a higher extinction coefficient or that are detectable by fluorescence spectroscopy [14]. Evaporative light scattering detector (ELSD) measurements do not require derivatisation, pre- or post-column, because they are not based on the optical properties of analytes, but it is known that the ELSD detector is sensitive to solvent composition.

GC/FID and GC-MS have been widely used for years for qualitative and quantitative analysis in biological samples, since these technique are characterised by high sensitivity and specificity, but they are generally time consuming and require sample handling. In fact samples are always subjected to extraction, purification, conjugate hydrolysis, and derivatisation to obtain stable and volatile compounds. One of the main advantages exhibited by mass spectrometric detection is the identification of unknown compounds, even though the instrumentation and its maintenance are quite expensive.

Recently, more rapid LC-MS methods have been developed to simultaneously detect free BAs and their conjugates. LC-MS has proven to be a reliable technique for the diagnosis of inborn errors of BA metabolism, even with very little sample amounts available. The specificity, sensitivity, reproducibility, speed and the ability to perform simultaneous measurements characterise routine analysis of free BAs and their conjugates in LC-MS.

Below we report methodological studies based upon HPLC, GC/FID, GC-MS, LC-MS, matrix-assisted laser desorption ionisation coupled with time-of-flight mass spectrometry (MALDI-ToF/MS), CE, proton nuclear magnetic resonance (^{1}H NMR), RIA and enzymatic colorimetric techniques.

5.4.5 Gas Chromatography with Flame Ionisation Detector

5.4.5.1 Principle

The choice of an appropriate derivatisation of BAs is a crucial point for a good GC analysis [15]. Unconjugated BAs are commonly analysed as methyl ester-trimethylsilyl (TMS) ether derivatives, although interference from plasma sterols may occur at the LCA retention time. Use of *n*-butyl ester-TMS ether derivatives allows a better chromatographic separation between BAs, which elute later, and sterols. The advantage of this derivative procedure is the simplification of plasma pre-treatment.

5.4.5.2 Pre-analytical

Specimen

Plasma is separated from whole blood and stored at –20°C until analysis.

Reagents and Chemicals

All reagents are of analytical grade:

1. Anhydrous methanolic hydrocloridric acid.
2. *n*-Butanol.

3. Hydrogen chloride.
4. Dioxane.
5. Hexamethyldisilazane-trimethylchlorosilane-pyridine.
6. CA.
7. CDCA.
8. DCA.
9. LCA.
10. UDCA.
11. Ursocholic acid (UCA).
12. Nor-DCA.
13. Nor-CA.

Instrumentation

1. Gas chromatograph with a flame ionisation detection system, equipped with a capillary column (25 m, 0.22 mm inner diameter, i.d., 0.25 μm; stationary phase, 100% dimethyl siloxane).
2. C_{18} reversed-phase cartridges.

Calibration

Two synthetic internal standards are used (nor-DCA and nor-CA) to perform an external standardisation method. Calibration curves for each compound are built, starting from known amounts of standards ranging from 0.02 μg to 0.2 μg. BA standards are prepared and analysed as described in below in section 5.4.5.3 Analytical, "Procedure".

Quality Control

None.

5.4.5.3 Analytical

Procedure

BA standards methyl esters are prepared by adding 100 μl of 3% anhydrous methanolic hydrochloric acid, to 5–20 μg of each BA and storing them at room temperature for 2 h, followed by solvent evaporation at 55°C under nitrogen. The *n*-butyl esters are prepared by addition of 100 μl of *n*-butanol to 5–20 μg of each BA, followed by addition of 20 μl of a 40% solution of hydrogen chloride in dioxane. The reaction mixtures are heated at 60°C for 4 h, followed by overnight incubation at room temperature, and then evaporated at 60°C under nitrogen. Sil-Prep [hexamethyldisilazane-trimethylchlorosilane-pyridine (3:1:9)] is used for the preparation of TMS ether derivatives of BA esters. The esterified BAs (5–10 μg) are reacted

with 100 µl of Sil-Prep for 30 min at 55°C. Solvent is evaporated at 55°C under nitrogen and each TMS ether derivative formed is suspended in 100 µl of hexane, of which 1 µl is injected into the gas chromatograph (GC) column. Plasma samples (1 ml) are prepared by adding internal standard (nor-CA, 10 µg in 100 µl of methanol), acetate buffer pH 5.6 (2 ml), 1.86% ethylenediaminetetraacetic acid (EDTA; 1 ml), 0.87% mercaptoethanol (1 ml), and a solution containing 0.1 mg of cholylglycine hydrolase and 0.1 mg of β-glucuronidase (1 ml in acetate buffer, pH 5.6). The resulting suspension is then incubated at 37°C for 18 h. The reaction mixture is then passed through a prewashed C_{18} reversed-phase cartridge and then liberated BAs are eluted with 5 ml of acetone. After evaporation of the acetone, 100 µl of *n*-butanol and 20 µl of 40% solution of hydrogen chloride in dioxane are added and the contents are heated at 60°C for 4 h and then kept overnight at room temperature. After evaporation of solvent at 60°C, each sample is subjected to trimethylsilylation, taken in 100 µl of hexane, and 5 µl is injected in splitless mode into the GC column.

The GC operating conditions are as follows: split/splitless injector and detector are held fixed at 260°C and 290°C, respectively. After injection, the oven temperature is kept at 100°C for 2 min, and then programmed at a rate of 35°C/min to a final temperature of 278°C. Helium is used as a carrier gas.

5.4.5.4 Post-analytical

Interpretation

This specific derivatisation procedure allows a better separation between *n*-butyl ester-TMS ether of LCA and TMS ether of cholesterol and β-sitosterol (Fig. 5.4.4). Therefore, even if samples are not completely purified in the pre-analytic phase, sterols do not interfere in the quantitative analysis of plasma BAs, being well resolved on GC. Besides, the *n*-butyl ester-TMS ether of nor-CA is eluted later than the sterols and can be used safely as internal recovery standard.

The retention times of all BA derivatives are highly reproducible, and their detection limits are similar (0.01 µg).

Chromatogram

Please refer to Fig. 5.4.4.

Reference Values

None.

Typical Pathological Values

None.

Pitfalls

None.

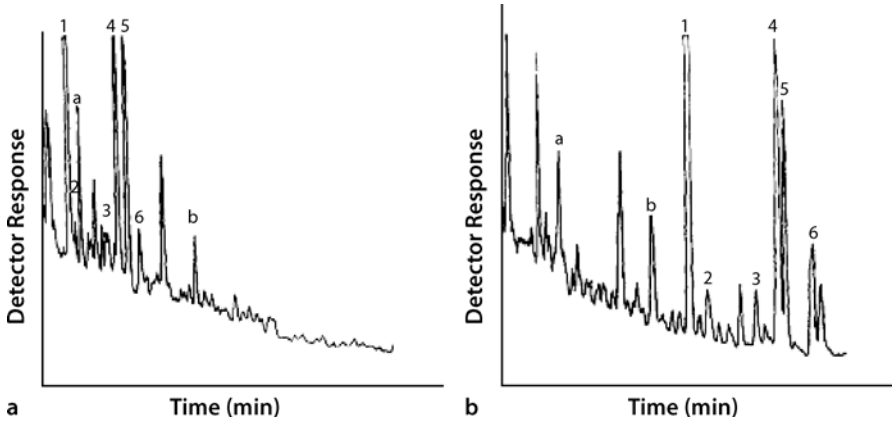

Fig. 5.4.4a Methyl ester-trimethylsilyl (TMS) ethers of BAs from a plasma sample. **b**: *n*-Butyl ester-TMS ethers of BAs from a plasma sample (adapted from [15]). *1* Nor-cholic acid, *2* litho-cholic acid, *3* deoxycholic acid, *4* chenodeoxycholic acid, *5* cholic acid, *6* ursodeoxycholic acid, *a* cholesterol, *b* sitosterol)

5.4.6 Gas Chromatography Coupled with Electron Impact Ionisation Mass Spectrometry

5.4.6.1 Principle

Gas chromatography coupled with electron impact (EI) ionisation mass spectrometry (GC-EI-MS) allows a very good qualitative and quantitative analysis of total faecal BAs, with moderate sample preparation [16]. Combining chromatographic separation and mass spectrometric detection adds up to a potential system with high specificity and sensitivity, making it useful in analysing complex biological matrices like faeces.

5.4.6.2 Pre-analytical

Specimen

Faeces samples were obtained from 86 healthy subjects (34 male, 52 female, age: 30 ± 8 years) to acquire a wide inter-individual range. All individual stools were collected in their entirety during a period of 5 days in plastic containers. They were weighed and, at the end, homogenised and pooled. Aliquots of stools are lyophilised and then stored frozen at –20°C until analysis.

Reagents and Chemicals

All reagents are of analytical grade:

1. LCA.
2. DCA.

3. CDCA.
4. CA.
5. Hyodeoxycholic acid (HDCA).
6. Hyocholic acid (HCA).
7. UDCA.
8. Iso-LCA.
9. Iso-DCA.
10. 12-Oxo-DCA.
11. methanolic hydrochloric acid (3 M).
12. Sylon HTP (hexamethyl disilazane/chlorotrimethyl silane/pyridine = 3:1:9).

Instrumentation

Gas chromatograph equipped with a split/splitless injector, a capillary column (30 m, 0.25 mm i.d., 0.25 μm) and an EI mass spectrometric detector.

Calibration

Unconjugated LCA, iso-LCA, DCA, iso-DCA, CDCA, CA, 12-oxo-DCA, and internal standard (HDCA) are weighed into a vessel and dissolved in ethyl acetate as stock solutions. A stock solution with standard specific concentrations (0.05–2 mg/ml) is prepared. Each of the six calibration standards is obtained by diluting the stock solution, whereas the concentrations of the analytes are one-half, one-quarter, one-eighth, etc. Aliquots of each solution are methylated, silylated, and resolved in decane, as described in sample preparation. The concentration of the internal standard HDCA ($m/z = 81.2$) is 0.5 mg/ml in each of the calibration standards.

Because of a consistent graduation in the analyte concentration within the calibrated range, a single calibration with three replicates per concentration is applied. The limits of detection are calculated from the calibration curves (Table 5.4.1).

Quality Control

None.

5.4.6.3 Analytical

Procedure

The procedure of sample preparation for faecal BA analysis and derivatisation is an adaptation of the method of Czubayko et al. [17]. The internal standard (125 μg HDCA) is added to the aqueous phase of extraction. The sample is saponified with 200 μl 10 mol/l sodium hydroxide at 120°C for 120 min and then acidified to pH 1 with hydrochloric acid. After extraction of BAs with diethyl ether (4 × 1 ml), the solvent phases are pooled and evaporated under a stream of nitrogen. The residue is

■ ***Table 5.4.1*** *Calibration statistics of faecal bile acids (Bas; reprinted from [16]).* CA *Cholic acid,* CDCA *chenodeoxycholic acid,* DCA *deoxycholic acid,* LCA *lithocholic acid*

Substance	Fragment (amu)	Range of linear calibration (mg/mL)	$y = mx + n$	r^2 ($n = 7$)	Rel. S.D.$_y$ (%)	S. D.$_{ro}$	V_{xo} (%)	Limit of detection (µg/mL)
iso-LCA	215.3(31)	0.005–0.500	*m*: 1.9069 *n*: 0.0001	0.9997	3.0	0.003	3.0	0.45
LCA	215.3(58)	0.010–1.000	*m*: 2.5449 *n*: –0.0007	0.9999	1.7	0.004	1.7	0.31
iso-DCA	75.1(91)	0.005–0.500	*m*: 3.2289 *n*: –0.0095	0.9998	2.1	0.003	2.0	0.86
DCA	255.3(93)	0.020–2.000	*m*: 7.7257 *n*: 0.0079	0.9998	3.2	0.013	3.2	0.16
CDCA	73.1(100)	0.005–0.500	*m*: 3.8610 *n*: –0.0046	0.9999	1.1	0.001	1.1	0.68
CA	253.2(44)	0.010–1.000	*m*: 3.6655 *n*: –0.0023	0.9999	0.3	0.001	0.3	0.64
12-oxo-DCA	231.3(52)	0.005–0.500	*m*: 1.9047 *n*: –0.0028	0.9999	1.0	0.001	1.0	0.61

$y = mx + n$ Linear regression line, r^2 correlation coefficient, S.D.$_y$ relative residual standard deviation, S. D.$_{ro}$ standard deviation of procedure, V_{xo} relative standard deviation of procedure; confidence intervall, 95%; data in parenthesis give size as percentage of base peak.

methylated with 650 µl dimethoxy propane, 950 µl methanol, and 50 µl methanolic hydrochloric acid (3 mol/l) for 45 min at 50°C. The solution is evaporated to dryness and the residue is dissolved in 150 µl Sylon HTP (see "Reagents and Chemicals", above). The silylation is carried out at 90°C for 60 min. After evaporation under a nitrogen stream, the residue is dissolved in 250 µl decane. The solution is shaken for 10 min and then centrifuged for 10 min at 1500 × *g*. The clear solution is transferred into a vial and 1 µl is injected for GC analysis.

The GC operating conditions are as follows: injection is performed in split mode (1:50) at 280°C. Helium is used as the mobile phase with a constant linear velocity of 32 cm/s and the interface temperature is kept at 300°C. The oven temperature is raised from 150 to 290°C [5 min at 150°C; 240°C (40°C/min); 255°C (1°C/min); 270°C (4°C/min); 278°C (1°C/min); 9 min at 278°C; 290°C (40°C/min); 4.7 min at 290°C]. The mass spectrometric detection is realised in total ion current (TIC), multi-ion current (MIC) and single-ion monitoring (SIM) mode for BA analysis with electron beam energy of 70 eV. The sampling rate is 5/s and the detector gain is turned to 1.5 kV. The sensitivity adjustment is performed in SIM as part of automatic tuning (perfluoro-tributyl amine, $m/z = 264.00$).

Calculation

The precision of this method was evaluated by repeated analysis of the main human faecal BAs (iso-LCA, LCA, iso-DCA, DCA, CDCA, CA, and 12-oxo-DCA). Within-run precision of ten samples amounted to 4–7% for all BAs. The between-run precision was approximately 5–10% of five time-shifted measurements over 1 month of faeces samples. A standard solution of DCA acetate methyl ester with a DCA concentration of 0.875 mg/ml was added to ten faecal samples of the same origin also used for within-run precision. The mean of concentrations amounted to 1.672 mg/ml, corresponding to a recovery of 94.6%.

Quantification of faecal BAs is carried out in SIM mode by using the internal standard method, and peak areas are obtained from the chromatograms generated by data handling. Component identification is based on fragmentation and comparison of the retention times with those of standards.

5.4.6.4 Post-analytical

Interpretation

The mass spectrometric detection is realised in TIC, MIC and SIM mode for BA analysis in order to obtain a specific analysis: the fragment ions used for BA determination are: $m/z = 44$ for CA, $m/z = 100$ for CDCA, $m/z = 93$ for DCA, $m/z = 91$ for iso-DCA, $m/z = 58$ for LCA, $m/z = 31$ for iso-LCA and $m/z = 81.2$ for HDCA. The specific fragments $m/z = 75.1$ for iso-DCA and $m/z = 255.3$ for DCA are chosen to exclude any possible over-estimation in iso-DCA and DCA quantification, due to the presence of artefacts.

Chromatogram

The chromatogram of a mixed standard (iso-LCA, LCA, iso-DCA, DCA, CDCA, CA, HDCA, UDCA, HCA, 12-oxo-DCA) by detection in TIC shows a good separation of all BA trimethylsilyl ether methyl esters (Fig. 5.4.5).

Reference Values

Please refer to Table 5.4.2.

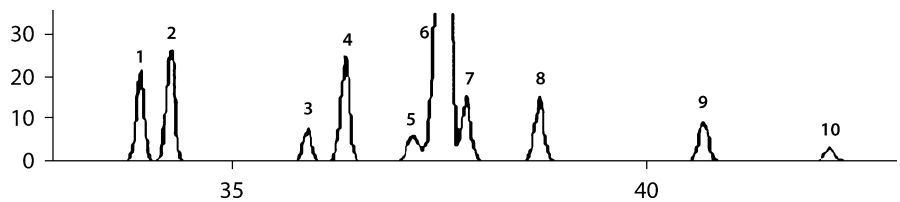

Fig. 5.4.5 Total ion current TIC of BA standard derivatives (reprinted from [16]): *1* iso-LCA (1 mg/ml), *2* LCA (1 mg/ml), *3* iso-DCA (0.25 mg/ml), *4* DCA (1 mg/ml), *5* CDCA (0.25 mg/ml), *6* CA (2 mg/ml); *7* HDCA (0.5 mg/ml), *8* UDCA (0.5 mg/ml), *9* HCA (0.5 mg/ml), *10* 12-oxo-DCA (0.5 mg/ml)

■ ***Table 5.4.2*** *Comparison of BA contents (dry weight, mg/g) in faecal matter of healthy subjects (reprinted from [16])*

	Dry weight (mg/g)
	86 Subjects
iso-LCA	1.48 ± 0.74
LCA	2.20 ± 0.92
iso-DCA	1.44 ± 0.96
DCA	4.60 ± 1.83
12-oxo-DCA	0.37 ± 0.35
CDCA	0.27 ± 0.32
CA	0.26 ± 0.48
Total BA	10.6 ± 3.5
Secondary BA	10.1 ± 3.6
Primary BA	0.5 ± 0.8

Data are presented as mean ± standard deviation of mean.

Typical Pathological Values

None.

■ Pitfalls

None.

5.4.7 Gas Chromatography Coupled with Chemical Ionisation Mass Spectrometry

5.4.7.1 Principle

Combined chromatographic separation and mass spectrometric detection adds up to a potential system with high specificity and sensitivity [18]. If EI-MS remains the method of choice for structural analysis, the negative chemical ionisation (NCI) technique is extremely sensitive, as the high ionisation efficiency initiated by electron-capture negative ionisation is combined with a low degree of fragmentation: only negative-ion-producing compounds are detected, and specific ions for pentafluorobenzyl bromide (PFB)-trimethylsilylimidazole (TMSi) derivatives are very high (*m/z* 445–665). This technique is also selective, as BAs are separated by mass according to the number of TMSi groups, oxo-groups, double bonds and the length of the side chain (C_{24} and C_{27}).

5.4.7.2 Pre-analytical

Specimen

Plasma was obtained from ten healthy fasting adults (44–70 years) who do not have any hepatobiliary or gastrointestinal disease, and then stored frozen at –20°C until analysis.

Reagents and Chemicals

All reagents are of analytical grade:
1. CA.
2. CDCA.
3. DCA.
4. LCA.
5. HDCA.
6. UDCA.
7. HCA.
8. UCA.
9. 3β-Hydroxychol-5-enic acid (3β-OHΔ^5).
10. THCA.
11. [2,2,4,4-d_4] Cholic acid (d_4CA, isotopic purity 98%).
12. [11,12-d_2] CDCA (d_2CDCA, isotopic purity 95%).
13. Cholyl-glycine hydrolase, PFB.

Instrumentation

Gas chromatograph equipped with a split/splitless injector, OV-1701 coated fused silica column (25 m, 0.25 mm i.d.) and chemical ionisation mass spectrometric detector.

Calibration

Calibration curves for CA, CDCA, DCA, LCA, HCA, UDCA, 3 β-hydroxychol- 5-enic acid and THCA are established for starting amounts ranging from 5 to 200 pmoles. The areas obtained for unlabelled CDCA, DCA, UDCA, LCA and 3 β-hydroxychol-5-enic acid are related to the area obtained for [11,12-d_2] CDCA, whereas the areas for unlabelled CA, HCA and THCA are related to the area of [2,2,4,4-d_4] CA.

Calibration curves for all BAs subjected to the sample work-up procedure were linear in the range 5–200 pmoles. The linear regression correlation coefficients varied from 0.991 to 0.999 and the slopes varied from 0.83 to 1.32, when the measured isotope ratios were plotted against the calculated ratios. Detection limits for all BAs investigated were 1 pg (2.5 fmol) injected onto the column.

Quality Control

None.

5.4.7.3 Analytical

Procedure

Plasma (200 µl) from fasting adults or 100 µl plasma from children are added to 0.25 nmol of [2,2,4,4-d_4] CA and 0.25 nmol of [11,12-d_2] CDCA as internal standards. BA conjugates are hydrolysed enzymatically as follows. The plasma is diluted with 500 µl of distilled water and 200 µl of acetate buffer (pH 5.6). The pH is adjusted to 5.6–6.0 with 0.2 M acetic acid. Then, 100 µl of 0.2 M EDTA, 100 µl of 0.2 M mercaptoethanol and 20 U of cholylglycine hydrolase are added, and the mixture is incubated at 37°C overnight in a water bath. After adjustment of the pH to above 10 with 200 µl of 1 N NaOH, the mixture is incubated at 64°C for 30 min to disrupt bile-acid – protein binding. After cooling to room temperature, 400 µl of 1 N HCl is added and free BAs are extracted two times with 6 ml diethylether, after saturating the aqueous phase with sodium chloride. After evaporation of the combined diethylether layers, the sample is treated with 100 µl of a 10% PFB solution in acetonitrile for 20 min at 30°C after addition of 20 µl of triethylamine. The PFB esters are extracted into 4 ml ethyl acetate after addition of 0.5 ml of 1 N HCl. The ethyl acetate is evaporated and the residue is treated with 100 µl of bis-trimethylsilyl-trifluoro acetamide-pyridine 1:1 (v/v) for 1 h at 80°C to form the TMSi ether derivatives, as described by Goto et al. [19]. Immediately prior to the analysis, the sample is evaporated and taken up into 25 µl of hexane: 1–2 µl are analysed by GC-MS.

The PFB ester-TMSi ether derivatives of BAs are separated in GC-NCI-MS using an OV-1701 coated fused silica column (25 m × 0.25 mm i.d.). The column is connected to an uncoated fused silica capillary inserted into the ion source of a quadrupole mass spectrometer. Helium is used as carrier gas at a flow rate of 1.5 ml/min. The sample is introduced by splitless injection at 320°C and the compounds of interest are trapped at the beginning of the column at an oven temperature of 150°C. After 1 min the oven temperature is raised to 320°C at 30°/min and kept at 320°C for 10 min. Under these conditions, BA PFB-TMSi derivatives elute at between 11 and 15 min. The capillary interface to the ion source and the ion source itself are maintained at 320°C. Electron capture NCI is achieved using methane as moderating gas at a source pressure of 10^{-4} mbar (where 1 mbar = 100 Pa). Mass spectra of authentic standards are obtained by scanning over the mass range *m/z* 50–800 with a 1-s scan time. The biological samples are analysed in the SIM mode using a 50-ms acquisition time at the base peak of each mass spectrum $[M\text{-}PFB]^-$.

Calculation

The reproducibility of this method was evaluated by eight repetitive analyses of single fasting plasma (Table 5.4.3). At the highest concentration studied (CDCA, mean 0.71 µmol/l) the coefficient of variation was 2.5%, whereas this value increased to 21.1% at the lowest concentration level (THCA, mean 0.004 µmol/l).

5.4.7.4 Post-analytical

Interpretation

The mass spectra of PFB-ester TMSi-ether derivatives of BAs consist mainly of the $[M-181]^-$ ion as a result of loss of the PFB group yielding the very stable carboxylate anion. The $[M-181]^-$ ion represents 50–60% of the total ion current. This lack of fragmentation creates a set of specific ions, determined by the length of the side chain and the number of TMSi groups, oxo groups and double bonds (Table 5.4.4). The fragment ions used for BA determination are: $m/z = 623$ for CA, UCA, HCA; $m/z = 535$ for DCA, CDCA, HDCA, UDCA; $m/z = 445$ for (3β-OHΔ^5), $m/z = 447$ for LCA, $m/z = 537$ for [11,12-d_2] CDCA, $m/z = 627$ for [2,2,4,4-d_4] CA and $m/z = 665$ for THCA.

Chromatogram

The chromatograms show a good separation of PFB-TMSi derivatives of BA standards (3β-OH Δ^5, LCA, DCA, CDCA, HDCA, UDCA, [11,12-d_2] CDCA, CA, UCA, HCA, [2,2,4,4 d_4] CA, THCA; Fig. 5.4.6). All primary (CA, CDCA), secondary (DCA, LCA, UDCA) and atypical BAs (3 β-hydroxychol-5-enic acid, HCA, THCA, DHCA) are consistently found. THCA and DHCA represented 0.9 and 1.6%, respectively, of their corresponding C_{24} metabolites CA and CDCA.

Reference Values

Concentrations of the various BAs analysed from adult fasting plasma are shown in Table 5.4.5.

Typical pathological Values

None.

Pitfalls

None.

Table 5.4.3 *Reproducibility of total analysis determined with 200-µl aliquots of fasting adult plasma* (n = 8; *reprinted from [18]).* DHCA *Dihydroxycoprostanic acid, THCA trihydroxycoprostanic acid*

	Mean Concentration	Coefficient of Variation
	µmol/l	%
CDCA	0.71	2.5
CA	0.29	2.3
DCA	0.41	3.2
DHCA	0.01	18.4
THCA	0.004	21.1

Table 5.4.4 *Characteristic negative chemical ionisation mass fragments for pentafluorobenzyl bromide-trimethylsilylimidazole (TMSi)derivatives of known BAs (reprinted from [18])*

Number of C-atoms	Number of TMSi-Groups	Number of Oxo-Groups	Number of Double Bonds	m/z
24	1	0	0	447
24	2	0	0	535
24	3	0	0	623
24	4	0	0	711
24	0	1	0	373
24	0	2	0	387
24	0	3	0	401
24	1	1	0	461
24	1	2	0	475
24	2	1	0	549
24	1	0	1	445
27	2	0	0	577
27	3	0	0	665
27	4	0	0	753
27	2	1	0	591
27	3	1	0	679
27	2	0	1	575
27	3	0	1	663

5.4.8 HPLC - Fluorescence

5.4.8.1 Principle

A method consisting in the HPLC analysis with fluorescence detection has been validated and applied in the management of primary biliary cirrhosis (PBC), a chronic cholestatic disease [20]. The rationale for this type of study is that increase of the BA concentrations in biological fluids reflects the dysfunction of hepatocytes and cholestasis. Pre-column derivatisation with 2-bromoacetyl-6-methoxynaphthalene (Br-AMN) as fluorogenic reagent of unconjugated and glycine-conjugated UDCA, CA, CDCA and DCA is performed to produce the corresponding naphthacyl esters [21]. Taurine conjugates are hydrolysed and analysed as free BAs. BAs are identified in the serum of healthy persons and patients. This method is also applied to the study of a patient affected by PBC and treated with an antibiotic (ampicillin), to assess the method feasibility in the clinical practice, in particular in diagnosis and therapy monitoring of hepatobiliary diseases.

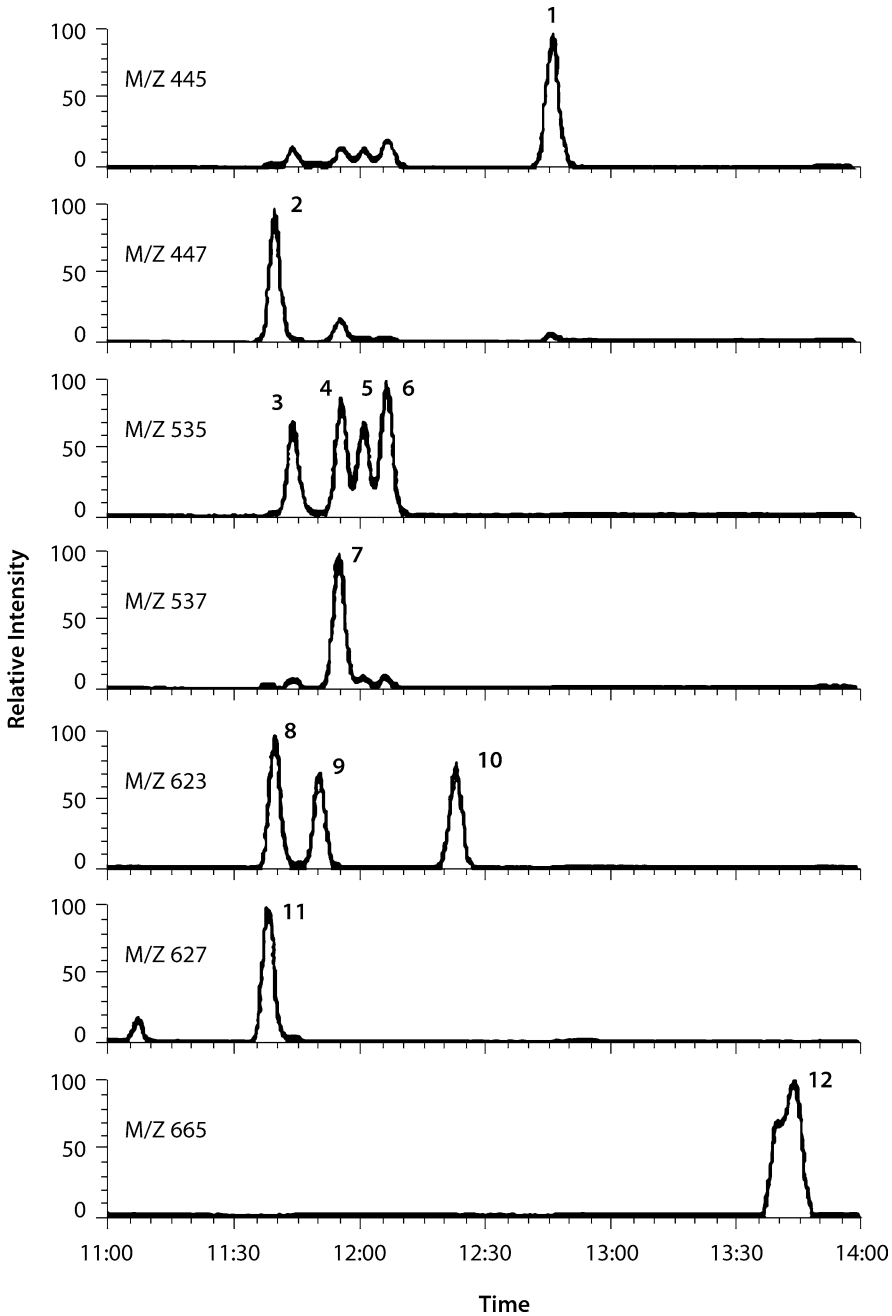

Fig. 5.4.6 Mass chromatograms of pentafluorobenzyl bromide-trimethylsilylimidazole derivatives of BA standards (reprinted from [18]). *1* 3β-hydroxychol-5-enic acid, *2* LCA, *3* DCA, *4* CDCA, *5* hyodeoxycholic acid (HDCA), *6* ursodeoxycholic acid (UDCA), *7* [11,12-d2] CDCA, *8* CA, *9* ursocholic acid (UCA), *10* hyocholic acid (HCA), *11* [2,2,4,4 d4] CA, *12* trihydroxycoprostanic acid (THCA)

Table 5.4.5 *Concentrations of BAs and the ratios THCA/CA and DHCA/CDCA in adult fasting plasma* (n = *10; reprinted from [18]).* 3βOHΔ^5 *3β-Hydroxychol-5-enic acid,* HCA *dihydroxycoprostanic acid,* UDCA *ursodeoxycholic acid*

Bile Acid	Concentration
	μmol/l ± SD
CDCA	0.90 ± 0.46
CA	0.23 ± 0.12
DCA	0.43 ± 0.37
LCA	0.071 ± 0.045
UDCA	0.053 ± 0.010
3βOH Δ^5	0.014 ± 0.002
HCA	0.015 ± 0.0.11
THCA	0.002 ± 0.001
DHCA	0.013 ± 0.002
Total	1.68 ± 0.71
	Ratio
THCA/CA	0.009 ± 0.009
DHCA/CDCA	0.016 ± 0.0007

5.4.8.2 Pre-analytical

Specimen

Human serum sample.

Reagents and Chemicals

1. Tetrakis (decyl) ammonium bromide (TDeABr).
2. Pelargonic (nonanoic) acid.
3. Lauric (dodecanoic) acid.
4. Br-AMN, prepared as described previously [22].
5. 2-Naphthacyl ester of pelargonic acid, prepared as described previously [22].
6. 2-Naphthacyl ester of lauric acid [22].
7. Bond-Elut (BE) C_{18} and SAX cartridges (500 mg).
8. Cholylglycine hydrolase.
9. Br-AMN solution: 2.1 mg/ml in acetone, stable for 2 weeks at 4°C.
10. TDeABr solution: 10 mM in aqueous 100 mM phosphate buffer, pH 7.0.
11. Stock solutions of free, and glycine- and taurine-conjugated BA in methanol.
12. Stock solutions of free, and glycine and taurine conjugated BA sodium in water.

13. Standard solutions in water:methanol (9:1, v/v) obtained from relative stock solutions.
14. Internal standards solution: 5.1×10^{16} M in acetonitrile.
15. 6-Methoxynaphthacylesters of lauric acid and of pelargonic acid solution in acetonitrile.

Instrumentation

1. HPLC: injector with a 50-µl sample loop; fluorescence spectrophotometer, operating at an emission wavelength of 460 nm with an excitation wavelength of 300 nm.
2. 250 × 4.6 mm i.d. column packed with 5 octadecyl silane (ODS).
3. Ultrasonicator with thermostatically controlled heating (30–80°C).

Calibration

Standard solutions of free BAs and of glycine-conjugated Bas are employed for the calibration. In the cited work the following concentration ranges were used: 0.47–9.53 nmol/ml for free BAs, 0.47–6.36 nmol/ml for glycine-conjugated BAs. Each standard solution (0.2 ml) is derivatised; 0.3 ml of the internal standard solution (lauric acid naphthacyl ester for free BA analysis and pelargonic acid naphthacyl ester for glycine-conjugated BA analysis) is added to each derivatised standard. The peak:height ratio of BA esters to internal standard is plotted versus the respective concentration to obtain the calibration curves. Linear calibration graphs should be obtained for each BA.

Quality Control

None.

5.4.8.3 Analytical

Procedure

Human serum sample (0.5 ml), diluted with 2.5 ml of 0.1 N NaOH is incubated at 65°C for 15 min. The free, and glycine- and taurine-conjugated fractions are isolated by means of solid-phase extraction, using BE C_{18} and BE SAX cartridges in succession [23]. The taurine fraction is enzymatically hydrolysed according to a previously described method [24]. The final residue is treated with 1 ml volume of 0.01% (w/v) KOH methanolic solution (methanol:water 1:9, v/v) at 40°C by ultrasonication for 3 min. Then, 0.2 ml of the obtained suspension is derivatised as described below. BA content is determined in each sample by comparison with an appropriate standard solution.

Derivatisation Procedure

Br-AMN (0.05 ml), 0.2 ml BA solution (or serum) and 0.3 ml TDeABr solution (10 mM in phosphate buffer, pH 7.0) are incubated for 10 min at 40°C under ultrasonication. The reaction mixture is spiked with 0.3 ml of the respective internal standard solution and ultrasonicated at room temperature for 1 min. Then, 50-µl aliquots of the BA naphthacyl ester mixture are injected into the HPLC.

Chromatographic Conditions

Separation of BAs in serum samples is carried out under gradient elution at a flow rate of 1.2 ml/min. The mobile phase is composed of a mixture of two solutions: A is water and B is a mixture of acetonitrile:methanol 60:40 (v/v). The elution gradient for free BA analysis is: (t) = 0 min 45% B; t = 20 min 45% B; t = 30 min 70% B; t = 55 min 70% B; t = 60 min 45% B. The elution gradient for glycine-conjugated BA analysis is: t = 0 min 25% B; t = 20 min 25% B; t = 30 min 50% B; t = 35 min 50% B; t = 40 min 25% B. In the fluorescence spectrophotometer the following parameters should be selected: λ_{exc} = 300 nm, λ_{em} = 460 nm, attenuation 2 (where λ_{exc} is the excitation wavelength and λ_{em} is the emission wavelength.

Calculation

The within-run precision of derivatisation and chromatography procedures was assessed in the reported work: a single standard solution was analysed in eight replicates. The relative standard deviation values of the peak-height ratios ranged from 2.0 to 3.6%. Method accuracy was verified by analysing serum samples spiked with known amounts of BA; quantitative recoveries were achieved in each experiment.

5.4.8.4 Post-analytical

Interpretation

BAs are identified by comparison of retention times with those relative to the standards added to the sample.

Chromatograms

The chromatogram of free BA standard mixture is reported in Fig. 5.4.7. The Br-AMN degradation products are eluted at lower retention times than derivatised BA, close to the solvent front, so they do not impair BA separation. Free BA fraction also encloses taurine conjugates, previously enzymatically hydrolysed. The separation of glycine conjugated BA is illustrated in Fig. 5.4.8. In both chromatograms, the peaks of BA naphthacyl esters are fully resolved and separated from the reagent peaks.

The possibility of defining serum BA composition was also assessed in the reported study. Analysis of the free fraction before and after treatment with ampicillin of a patient with PBC was performed (Fig. 5.4.9). The antibiotics are used in the therapy of cholestatic syndrome, but some studies have been carried out to define their use. This kind of therapy inhibits the production of secondary BAs (DCA and LCA) and the deconjugation of taurine and glycine conjugates. Consequently, an

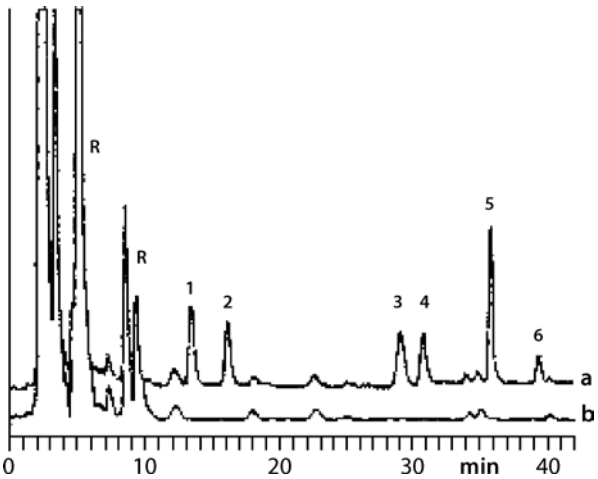

Fig. 5.4.7 HPLC resolution at 35°C of a standard mixture of free BA naphthacyl esters (3.18×10^{-6} M). Chromatogram (**a**): *1* UDCA, *2* CA, *3* CDCA, *4* DCA, *5* lauric acid (the internal standard), *6* LCA. Chromatogram (**b**): blank, consisting of reagent kept at reaction conditions. *R* is the reagent peak in both chromatograms (reprinted from [20])

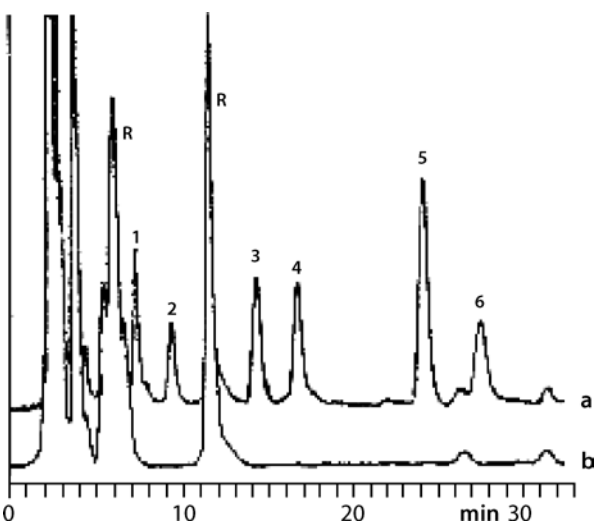

Fig. 5.4.8 HPLC resolution at 35°C of a standard mixture of glycine conjugated BA naphthacyl esters (3.18×10^{-6} M). Chromatogram (**a**): *1* glycoursodeoxycholic acid (GUDCA), *2* glycocholic acid (GCA), *3* glycochenodeoxycholic acid (GCDCA), *4* glycodeoxycholic acid (GDCA), *5* pelargonic acid (internal standard), *6* glycolithocholic acid (GLCA). Chromatogram (**b**): Blank, consisting of reagent kept at reaction conditions. *R* is the reagent peak in both chromatograms (reprinted from [20])

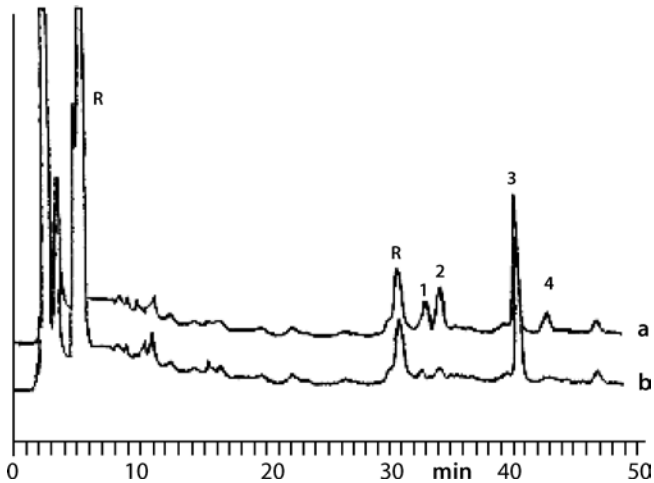

Fig. 5.4.9 HPLC chromatogram of the derivatised free BA fraction obtained from a human serum sample from a patient with primary biliary cirrhosis (PBC) before (**a**) and after (**b**) treatment with ampicillin. *1* CDCA, *2* DCA, *3* lauric acid (internal standard), *4* LCA. *R* peak represents the reagent peak. (Reprinted from [20])

increase of primary BA levels was found in serum after therapy; this last serum BA composition was considered less detergent and toxic. For the examined patient, the chromatogram before therapy showed the presence of CDCA, DCA and LCA peaks, whereas after treatment the LCA peak disappeared and the DCA peak intensity significantly decreased. In this case, therapy with antibiotic was useful.

Reference Values and Typical Pathological Values

Table 5.4.6 summarises reference values and pathological values measured in volunteers without hepatic disease and in patients, respectively. Very low levels were obtained for taurine-conjugated BA, in accordance with the literature [25]. The glycine-:taurine-conjugated molar ratio was about 2:1 in healthy persons and increased to 10:1 or 20:1 in hepatic diseases. The pathological conditions were confirmed by levels of the biological markers of cholestasis, such as serum alkaline phosphatase and γ-glutamyltranspeptidase. Serum BA composition was evaluated in patients before therapy, after therapy with ampicillin, and with UDCA, to assess the efficacy of drug therapy. The efficacy of treatment with UDCA in PBC patients was demonstrated by many clinical trials. It was hypothesised that this drug could replace toxic Bas, like DCA, in the BA serum pool [26]. After therapy, DCA and glycodeoxycholic acid (GDCA) values decreased, while UDCA, its hepatic metabolites glycoursodeoxycholic acid (GUDCA) and tauroursodeoxycholic acid (TUDCA) levels increased. Therapy did not influence LCA level.

Pitfalls

No pitfall was found in method development.

Table 5.4.6 *Serum BA composition in healthy subjects (1,2), in a patient (3) with primary biliary cirrhosis (PBC) before (A) and after (B) treatment with ampicillin and in a patient (4) with PBC before (A) and after (B) treatment with UDCA. Results are expressed in nmol/ml. RDS% of three measurements was in the range 3.1–7.5%. – Means non-detectable value (adapted from [20]).* GCA *glycocholic acid,* GDCA *glycodeoxycholic acid,* GCDCA *glycochenodeoxycholic acid,* GLCA *glycolithocholic acid,* GUDCA *glycoursodeoxycholic acid,* TCA *taurocholic acid,* TDCA *taurodeoxycholic acid,* TCDCA *taurochenodeoxycholic acid,* TLCA *taurolithocholic acid,* TUDCA *tauroursodeoxycholic acid*

Bile Acid	1	2	3		4	
			A	B	A	B
CA	0.88	–	–	–	3.57	0.58
CDCA	–	–	1.05	0.95	–	–
DCA	0.12	0.31	3.06	1.16	0.89	0.17
LCA	0.10	0.15	2.35	–	5.92	5.48
UDCA	–	–	–	–	–	12.42
GCA	0.50	0.55	0.98	1.21	4.47	2.27
GCDCA	0.67	1.50	1.22	0.66	5.49	3.00
GDCA	0.22	0.38	0.20	–	0.89	0.31
GLCA	–	–	0.10	–	–	–
GUDCA	–	–	–	–	–	13.46
TCA	0.19	0.45	0.07	0.38	0.58	1.00
TCDCA	0.33	0.65	0.13	0.25	0.37	0.54
TDCA	0.16	0.23	0.04	–	–	–
TLCA	0.10	0.12	–	–	–	–
TUDCA	–	–	–	–	–	2.04

5.4.9 HPLC-Evaporative Light-Scattering Detector

5.4.9.1 Principle

The method proposed by Torchia et al. [27] is based on HPLC in combination with an evaporative light scattering detector (ELSD) for analysis of the following compounds: β-muricholic acid (MCA), CA, CDCA, DCA, UDCA, LCA, nor-CA, nor-DCA, taurocholic acid (TCA), tauromuricholic acid (TMCA), taurochenodeoxycholic acid (TCDCA), taurodeoxycholic acid (TDCA), tauroursodeoxycholic acid (TUDCA), taurolithocholic acid (TLCA), glycocholic acid (GCA), glycochenodeoxycholic acid (GCDCA), glycodeoxycholic acid (GDCA), glycoursodeoxycholic acid (GUDCA) and glycolithocholic acid (GLCA). Both unconjugated and conjugated molecules can be resolved simultaneously. This method can be applied to BA measurement in human and rodent bile. This method also allows detection of TCDCA and CDCA

bound by the ileal lipid-binding protein (ILBP), a known BA binder. ELSD measurement does not require either pre- or post-column derivatisation because it is not dependent on the optical properties of the analytes; it is also known that the ELSD is sensitive to solvent composition. Chromatographic behaviour is due to the different hydroxylation grades of the steroid nucleus [28].

5.4.9.2 Pre-analytical

Specimen

Bile samples.

Reagents and Chemicals

1. HPLC grade water.
2. Methanol.
3. acetic acid.
4. Acetonitrile.
5. Aqueous ammonia.
6. BA standards (MCA, CA, CDCA, DCA, UDCA, LCA, nor-CA, nor-DCA, TCA, TMCA, TCDCA, TDCA, TUDCA, TLCA, GCA, GCDCA, GDCA, GUDCA, GLCA) are diluted in methanol; their final concentration is determined by means of a commercially available diagnostic kit based on 3α-steroid dehydrogenase colorimetric assay.
7. The mobile phase is a solution of methanol:acetonitrile:water (53:23:24) containing 30 mM ammonium acetate adjusted to pH 5.6 with acetic acid; this solution is filtered through polytetrafluoroethylene 0.45-μm filters.
8. Delipidated recombinant murine ILBP.
9. Sephadex G25 column.
10. $C_{18}/_{14}$ solid-phase extraction (SPE).
11. 0.22-μm filter.

Instrumentation

HPLC system, equipped with a C_{18} analytical column (5-μm particle size, 25 cm × 4.6 mm i.d.) fitted with a C_{18} guard column (4 mm × 3.0 mm i.d.), and coupled to an ELSD.

Calibration

An external standardisation method is employed to perform quantitative analysis. In the cited study, calibration curves for each compound are obtained by injecting amounts ranging from 0.08 to 10 nmol. The amount of injected standards is logarithmically proportional to the peak area.

Quality Control

In-vitro BA binding assay is performed to verify the association of TCDCA and CDCA with delipidated recombinant murine ILBP. A mixture of 400 µl of BA 117.0 nmol and ILBP 23.4 nmol are incubated at 37°C for 1 h. The mixture is pulled through a Sephadex G25 column to remove the unbound BA, instead other fractions collected and pooled are applied to $C_{18/14}$ SPE cartridges to extract the complex ILBP-BA. The cartridges are washed with 8 ml of distilled water and eluted with 4 ml of methanol. Then the complex is filtered through a 0.22-µm filter, dried under nitrogen, dissolved in 100 µl of methanol and analysed in HPLC.

5.4.9.3 Analytical

Procedure

Bile samples are treated with methanol (dilution 1:6) to precipitate proteins, and centrifuged at 20,000 × *g* for 10 min at room temperature. Six microlitres of the supernatant, diluted 1:20 in methanol, is injected into the HPLC. Nor-DCA 146 µM is used as an internal standard. The column has to be conditioned for a minimum of 3 h to assure good reproducibility. Since the ELSD is sensitive to mobile-phase composition [9], an isocratic elution at flow rate of 0.7 ml/min is performed on the reversed-phase column. In fact, a gradient would change the detector sensitivity for each BA and increases the baseline drift. Choice of the mobile phase (methanol: acetonitrile:water 53:23:24 containing 30 mM ammonium acetate adjusted to pH 5.6 with acetic acid) is critical to obtain an adequate separation. Acetonitrile decreases the retention time of unconjugated BAs and avoids tailing of late-eluting peaks. Ammonium acetate, by increasing the ionic strength of the mobile phase, allows a better resolution of hydrophilic BAs, such as TMCA. ELSD gas flow is fixed at 1.3 l/min, the temperature at 93°C. Table 5.4.7 shows retention times, capacity ratios and separation ratios, calculated according to Gilbert [29] for human and mouse BA standards. Retention times are highly reproducible between different runs and after long periods of column inactivity. The column should be purged with 100% methanol for 1 h before storage.

Calculation

The amounts of injected compounds are logarithmically proportional to the peak area. Calibration curves in the range from 0.08 to 10 nmol showed a regression coefficient from 0.991 to 0.998. Sensitivity was in the subnanomolar range. This method results in a versatile and cost-effective procedure for the detection and quantification of BAs.

Table 5.4.7 *Retention times, capacity ratios (*k*') and separation ratios (*α*) of the studied BAs (adapted from [27]).* MW *molecular weight,* MCA β-*muricholic acid,* Nor-CA *nor-cholic acid,* Nor-DCA *nor-deoxycholic acid,* TMCA *tauromuricholic acid,* UDCA *ursodeoxycholic acid*

Peak N°	BA	MW	Retention time (min)	*k'*	*α*
Unconjugated BA					
1	MCA	408.6	9.18	1.59	0.35
2	CA	408.6	15.43	3.37	0.75
3	CDCA	392.6	27.40	6.75	1.49
4	DCA	392.6	29.99	7.48	1.66
5	UDCA	392.6	11.53	2.26	0.50
6	Nor-CA	394.6	10.03	1.84	0.41
7	Nor-DCA	378.6	19.50	4.52	1.00
8	LCA	376.6	55.23	14.63	3.24
2-Aminoethanesulfonic acid (taurine) conjugates					
9	TMCA	515.7	5.00	0.42	0.09
10	TCA	515.7	7.63	1.16	0.26
11	TCDCA	499.7	10.80	2.06	0.46
12	TDCA	499.7	12.20	2.45	0.54
13	TUDCA	499.7	5.97	0.69	0.15
14	TLCA	499.7	18.23	4.16	0.92
Aminoacetic acid (glycine) conjugates					
15	GCA	465.6	8.75	1.48	0.33
16	GCDCA	449.6	12.85	2.64	0.58
17	GDCA	449.6	14.63	3.14	0.70
18	GUDCA	449.6	6.62	0.87	0.19
19	GLCA	433.6	22.58	5.39	1.19

5.4.9.4 Post-analytical

Interpretation

Qualitative analysis of bile samples is performed using retention time of nor-DCA (internal standard) as relative reference time.

Chromatograms

The chromatogram relative to the injection of a mixture of conjugated BAs is reported in Fig. 5.4.10a. Conjugated BAs are separated in 30 min. A solution of unconjugated

BAs is resolved in 55 min (Fig. 5.4.10b). A solution of 14 both conjugated and unconjugated BAs is resolved in 35 min, except LCA, which elutes in 55 min due to its high hydrophobicity (Fig. 5.4.10c). Figure 5.4.11 depicts calibration curves for selected Bas; coefficients of the regression lines ranged from 0.991 to 0.998.

Reference Values

None.

Typical Pathological Values

None.

Pitfalls

No pitfall was found in method development.

5.4.10 Capillary Electrophoresis

5.4.10.1 Principle

So far, not many CE methods for BA analysis have been published due to the poor reproducibility of this technique and to difficulties arising from the complexity of the matrix. However, in this study the method is optimised by means of investigation of the effect of sodium dodecyl sulfate (SDS) as a surfactant, the adjustment of pH of the buffer solution, the use of β-cyclodextrins (CD), which enable the enhancement of the competing partitioning mechanism, and the use of acetonitrile as an organic modifier. This technique has the benefit of minimising the problems associated with solvent disposal and provides a good and fast separation for conjugated Bas, becoming a fast clinical screening method. CE manages to separate nine BAs: TUDCA, TCA, TCDCA, TDCA, TLCA, GCA, GCDCA, GDCA and GLCA [30].

5.4.10.2 Pre-analytical

Specimen

In this study, serum specimens were collected from patients suffering from different types of hepatic disease.

Reagents and Chemicals

1. Surfactants: 8 mM β-CD and 20 mM SDS.
2. 5 mM Potassium dihydrogenphosphate (pH 4.5).
3. 10 mM Potassium dihydrogenphosphate (pH 7).
4. Methanol HPLC grade.
5. Acetonitrile HPLC grade.
6. Distilled and ionised water.
7. 0.1 M Sodium hydroxide.

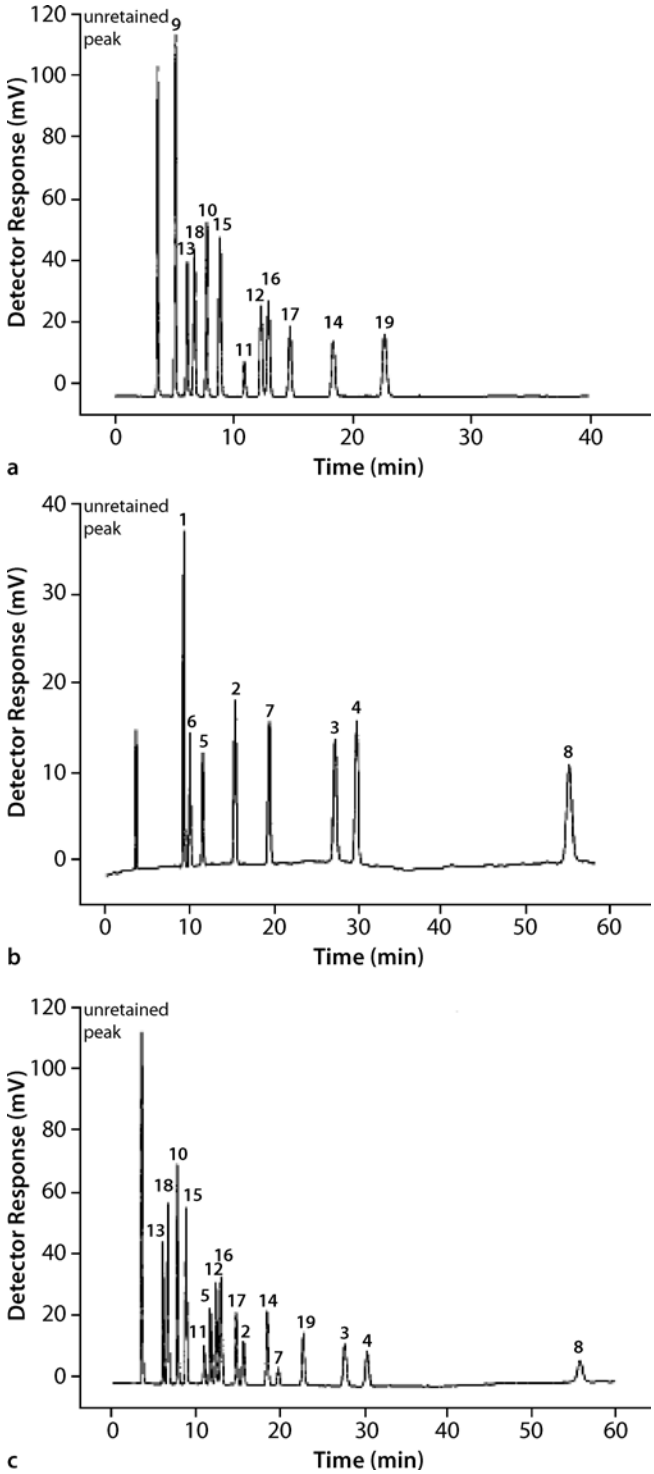

Fig. 5.4.10 **a** Chromatogram of conjugate BAs: tauromuricholic acid (TMCA; *peak 9*), tauroursodeoxycholic acid (TUDCA; *peak 13*), GUDCA (*peak 18*), TCA (*peak 10*), GCA (*peak 15*), taurochenodeoxycholic acid (TCDCA; *peak 11*), taurodeoxycholic acid (TDCA; *peak 12*), GCDCA (*peak 16*), GDCA (*peak 17*), taurolithocholic acid (TLCA; *peak 14*), GLCA (*peak 19*). **b** β-muricholic (MCA; *peak 1*), nor-CA (*peak 6*), UDCA (*peak 5*), CA (*peak 2*), nor-DCA (*peak 7*), CDCA (*peak 3*), DCA (*peak 4*), LCA (*peak 8*). **c** Chromatogram of a mixture of 14 BAs (reprinted from [27])

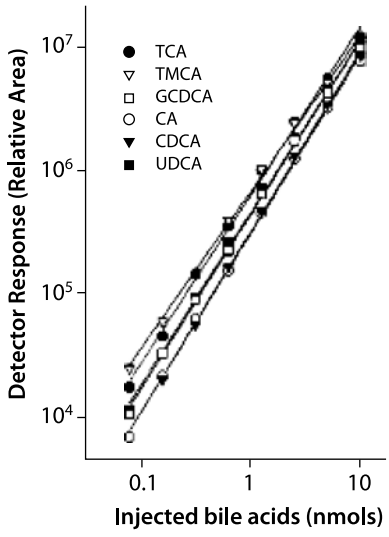

Fig. 5.4.11 Calibration curves for TCA, TMCA, GCDCA, CA, CDCA and UDCA (reprinted from [27])

8. 4% Phosphoric acid containing 20% acetonitrile.
9. 20% Acetonitrile in water.
10. Standards described in section 5.4.9.1 Principle, "Reagents and Chemicals".

Instrumentation

1. SPE vacuum manifold.
2. CE system equipped with a UV photodiode array detector set at 195 nm.

Calibration

Calibration is carried out using the external standard method. The calibration curve was linear for each of nine BAs in the range of 5–100 nmol/ml. The resulting concentrations were extrapolated by the plotted curve.

Quality Control

None.

5.4.10.3 Analytical

Procedure

Serum (200 µl) is deproteinised by means of methanol (200 µl) and vortexed for 1 min; the sample is then kept at room temperature for 10 min. Three volumes of 5 mM potassium dihydrogenphosphate (pH 4.5) are added, the mixture is mixed and centrifuged at 15,000 × *g* for 2 min, the supernatant is applied on the SPE column.

The column, filled with 100 mg of octadecyl silane (ODS-3, 10.5% carbon load, end capped), is preconditioned with 1 ml of methanol and 2 ml of water. The SPE column is washed with 500 µl of a solution of 5 mM potassium dihydrogenphosphate, 10% (v/v) of methanol. Analytes are eluted with 300 µl of methanol and centrifuged at 15,000 × *g* for 2 min prior to CE analysis.

Electrophoresis is carried out with a capillary cartridge containing an extended light path capillary (40 cm x 50 µm i.d.). A buffer solution for column conditioning and electrophoresis should be prepared with the following composition: 10 mM potassium dihydrogenphosphate, pH 7, 20 mM SDS, 8 mM CD and 20% acetonitrile (v/v). An aliquot of 50 µl of this solution, diluted ten times with distilled and deionised water, should be added to the sample.

The capillary column has to be pre-conditioned with buffer solution for 6 min. The sample introduction is carried out by pressurised injection of water, sample and buffer in the capillary column; each at 5 kPa for 5 s subsequently. Electrophoresis is performed for 8 min at 500 V/cm at 35°C in the running buffer solution. UV detector is set to 195 nm for analysis. Then the column is washed subsequently for 3 min with 0.1 M sodium hydroxide, 4% phosphoric acid containing 20% acetonitrile and 20% acetonitrile in water.

Calculation

None.

5.4.10.4 Post-analytical

Interpretation

This CE method provides an efficient approach for rapid and effective separation of serum conjugated BAs with an analysis time of 8 min. It is important to mention that each micellar solution plays an important role in the analysis: use of 20 mM SDS is to modify the electro-osmotic flow, whereas solubility of glycine-conjugated BAs and the peak shape of all BAs are maintained with 20% acetonitrile and the neutral pH of the phosphate buffer. The optimum condition for baseline separation is achieved with the addition of 8 mM CD.

Chromatogram

Please refer to Fig. 5.4.12.

Reference Values

Reference values are given in Table 5.4.8.

Typical Pathological Values

Typical pathological values are given in Table 5.4.9.

Pitfalls

Serum conjugated BAs are well resolved in an 8-min run. Nevertheless, it is known that a change in composition and concentration of the components of micellar solu-

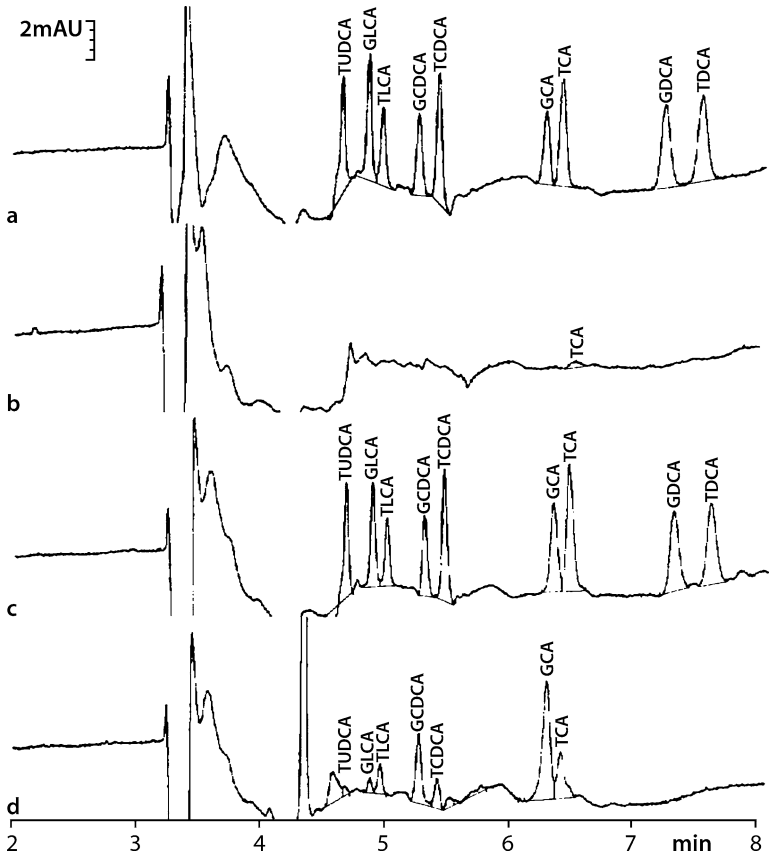

Fig. 5.4.12a–d Electropherograms of pure standards containing nine BA conjugates at a concentration of 50 nmol/ml (**a**), a blank serum sample from a healthy subject (**b**), the same serum sample spiked with 50 nmol/ml of nine different BAs (**c**) and serum sample from a patient with chronic hepatitis infection (**d**) analyzed by the capillary electrophoresis technique. Ultraviolet absorbance detection at 195 nm (reprinted from [30])

Table 5.4.8 *Values of serum bile acids from healthy subjects (adapted from [30])*

	GCA	GCDCA	GDCA	GLCA	TCA	TCDCA	TDCA	TLCA	TUDCA
Range (nmol/ml)	2–6	3–6	4–13	3–9	4–11	2–6	2–5	3–12	2

Table 5.4.9 *Values of serum bile acids from patients (adapted from [30])*

	GCA	GCDCA	GDCA	GLCA	TCA	TCDCA	TDCA	TLCA	TUDCA
Range (nmol/ml)	9–139	23–84	5–6	5–15	12–169	3–93	2–15	3–58	3–10

tion could affect the reproducibility and efficiency. Consequently, it is necessary to empty and refill vials with micellar solution by using the automatic replenishment system for each determination.

5.4.11 LC-MS (Method A)

5.4.11.1 Principle

This is a simple "one-step" method, developed in LC-MS/MS to achieve the reliability in mass screening of 14 BAs in plasma: CA, CDCA, LCA, DCA, UDCA, TCA, TCDCA, TDCA, TUDCA, TLCA, GCA, GCDCA, GDCA and GLCA [31]. Analytes are subjected to chromatographic separation using a reversed-phase C_{18} column with a methanol gradient. The eluate is routed into a triple-quadrupole mass spectrometer operating in the ion evaporation mode with an ion-spray ionisation probe. Spectra are acquired in negative ion mode, in the multiple reaction monitoring (MRM) mode: for each analyte a pseudomolecular ion in the first quadrupole is selected. The product ions arising from the fragmentation in the second quadrupole are then scanned by the third quadruple. The most intense transitions of each BA are chosen for quantitative analysis.

5.4.11.2 Pre-analytical

Specimen

This method requires 250 μl of plasma.

Reagents and Chemicals

All chemicals and solvents should be of the highest purity available.

1. Acetonitrile is used for protein precipitation.
2. Water, methanol, formic acid and ammonium acetate are used for chromatographic separation.
3. The following BA standards are used: CA, UDC, CDC, DC, LCA, TCA, TUDCA, TCDCA, TDCA, TLCA), GCA, GCDCA, GDCA and GLCA.

Instrumentation

1. Triple-quadrupole mass spectrometer coupled with an electrospray ionisation (ESI) source.
2. Data are acquired and processed using a software for chromatographic and spectral interpretation, and for quantitative processing.
3. Binary HPLC pump equipped with a reverse-phase C_{18} column (3 μm, 100 × 4.6 mm i.d.), coupled with an autosampler.

Calibration

BA standard solutions were prepared at five different concentrations and analysed for 4 days to test the linearity of the response. Calibration curves were linear over the range 0.1–100 µmol/l. Coefficients of linear regression were calculated using a "linear through zero" correlation.

Analytical sensitivity can be estimates from the slope of the calibration curves. The sensitivity of the proposed method is higher for unconjugated BAs than for the conjugated ones.

The detection limit (signal:noise ratio of 3:1) is evaluated on a plasma sample with low concentration of each of the BAs studied. The detection limit and linear regression (mean slope, standard deviation and correlation coefficient) data are shown in Table 5.4.10.

Quality Control

None.

Table 5.4.10 *Detection limit and linear regression parameters of the proposed method (adapted from [31]). TC*

BA	Detection limit (µmol/l)	Linear regression parameters	
		slope (SD)	*r*
TUDCA	0.004	7.2×10^4 (3×10^3)	0.99986
TCA	0.006	4.7×10^4 (9×10^2)	0.99965
GCA	0.008	4.6×10^4 (3×10^3)	0.99915
TCDCA	0.006	5.7×10^4 (1×10^3)	0.99962
TDCA	0.005	6.3×10^4 (7×10^2)	0.99958
GCDCA	0.006	6.9×10^4 (5×10^3)	0.99986
GDCA	0.006	7.0×10^4 (4×10^3)	0.99944
UDCA	0.004	8.5×10^4 (3×10^3)	0.99995
TLCA	0.004	1.6×10^5 (1×10^4)	0.99943
CA	0.002	7.6×10^4 (4×10^3)	0.99984
GLCA	0.005	2.3×10^5 (1×10^4)	0.99990
CDCA	0.003	1.7×10^5 (2×10^4)	0.99995
DCA	0.002	3.1×10^5 (2×10^4)	0.99985
LCA	0.001	1.6×10^5 (2×10^4)	0.99969

5.4.11.3 Analytical

Procedure

For protein precipitation 250 µl of plasma sample is mixed with 800 µl of acetonitrile and mixed for 1 min. After 15 min centrifugation at 13,000 × *g*, 900 µl of the supernatant are transferred to an autosampler vial and blown to dryness with nitrogen. The residue is dissolved with 125 µl of methanol and 125 µl of water (final dilution factor = 1.17). Forty microlitres of this solution (corresponding to 34.2 µl of the original plasma) is injected into the HPLC system using an autosampler. Chromatography is achieved using a reverse-phase C_{18} column (3 µm, 100 × 4.6 mm i.d.). Column flow is 1 ml/min and a 1:20 split is arranged upstream of the ion-spray probe. The elution gradient is optimised for the simultaneous separation of either unconjugated, or glycine- or taurine- conjugated BA within a single run. The binary gradient consists of three steps, as reported in Table 5.4.11, where solvent A is a water solution containing 0.012% formic acid and 5 mM ammonium acetate, and solvent B is methanol containing 0.012% formic acid and 5 mM ammonium acetate. BAs eluted from the column are analysed with a triple-quadrupole mass spectrometer with an ESI source. All experiments are performed in negative ion mode, with the orifice voltage set at a range between –61 and –74 V as automatically optimised for each single compound. The data are acquired in the MRM mode, setting specific precursor to product ion parameters for each analyte. To improve the overall performance, the chromatogram is split in two periods, the former ending at 10.5 min, and the latter starting there and continuing up to the end of the run. By doing so, the number of cycled MRM readings is split in two parts, resulting in a better signal:noise ratio for each analyte. Since the unchanged duty-cycle involved in the reading is shared by a smaller number of analytes within a single period, consequently dwell time becomes much longer than for unsplit period analysis. In the present experiment, LCA gets a significant benefit since in the second period it is the unique analyte encompassing the duty-cycle. In Table 5.4.12 are shown instrument parameters for all BA detection.

The resulting protocol of the coupling of HPLC with an MS/MS system, using an ion-spray interface, provides a means for sensitive and specific analysis of several BAs. Chromatographic separation allows the differentiation of isomeric forms. The MRM mode provides the necessary specificity even in the case of co-eluting components, thanks to the different transitions monitored: this is evidenced by extracting the specific reconstructed ion chromatogram (RIC). The RIC traces of a BA standard mixture are shown in Fig. 5.4.13.

Table 5.4.11 *High-performance liquid chromatography (*HPLC*) mobile phase gradient composition (adapted from [31])*

Step	Time (min)	Solvent A (%)	Solvent B (%)
0	0	30	70
1	10	5	95
2	2	5	95
3	8	30	70

Table 5.4.12 *The optimum HPLC-tandem mass spectrometry (*MS/MS*) parameters for each BA (adapted from [31]).* CAD *Collision-activated dissociation,* MRM *multiple reaction monitoring*

BA	CAD energy (eV)	MRM channel (Q1/Q3 *m/z*)	Retention time (min)
Period 1			
TUDCA	75	498/80	1.96
TCA	71	514/80	2.78
GCA	41	464/74	3.40
TCDCA	75	498/80	4.26
TDCA	75	498/80	4.74
GCDCA	41	448/74	5.17
GDCA	41	448/74	5.71
UDCA	21	391/391	5.81
TLCA	65	482/80	6.40
CA	18	407/407	7.16
GLCA	44	432/74	7.33
CDCA	21	391/391	9.17
DCA	21	391/391	9.40
Period 2			
LCA	27	375/375	10.99

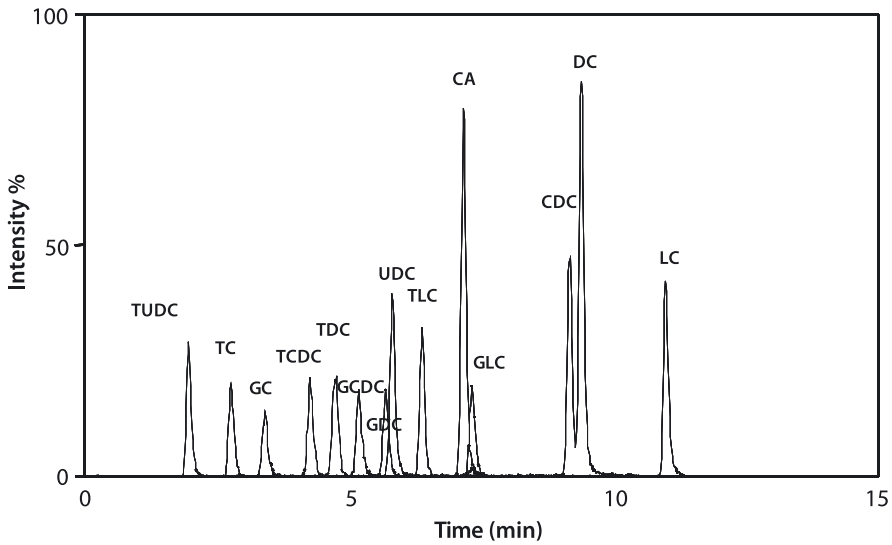

Fig. 5.4.13 HPLC-MS/MS separation of a mixture of 14 BA standards at a level of 0.5 mM per component. This experiment has been recorded in a single acquisition period for graphical display purpose (reprinted from [31])

Calculation

Amounts of injected compounds are proportional to the peak area. BA concentrations are calculated by comparison to standard calibration curves. This method does not need an internal standard for quantitative analysis.

5.4.11.4 Post-analytical

Interpretation

Peaks in patient chromatograms are identified by comparison to those of standard BA chromatograms. Signals of each BA are identified by retention time and mass transition.

Chromatograms

The RIC traces of BA standard mixture are shown in Fig. 5.4.13.

Reference Values

None.

Typical Pathological Values

None.

Pitfalls

No pitfall was found in method development.

5.4.12 LC-MS (Method B)

5.4.12.1 Principle

This is a simple, sensitive, and specific LC electrospray MS/MS (LC-MS/MS) method for the determination of conjugated BAs in human bile. BAs are directly measured without hydrolysis and derivatisation, and useful information regarding the state of conjugation is obtained [32].

BAs are extracted with a C_{18} reversed-phase column, identified and quantified by simultaneous monitoring of their parent and daughter ions, using the MRM mode. Identification and quantification of conjugated BAs in bile is achieved in 5 min. The detection limit is 1 ng, and the response is linear for concentrations up to 100 ng.

5.4.12.2 Pre-analytical

Specimen

Bile sample (20 μl) of bile sample are necessary to perform the analysis.

Reagents and Chemicals

1. Used BA standards, CA, CDCA, DCA, UDCA, LCA, and their glycine- and taurine-conjugated forms are dissolved in methanol at a concentration of 1 mg/ml.
2. Two internal standards are used (5 β-cholanic acid, 3,12-diol-7-one-5β-cholanic acid) and dissolved in methanol at a concentration of 1 mg/ml.
3. C_{18} extraction columns are used for BA extraction from biological fluids.
4. All used solvents and chemicals are of HPLC grade or of known analytical purity.
5. Solvents are methanol, water, chloroform, *n*-hexane and acetonitrile.

Instrumentation

1. HPLC system equipped with an automatic sample injector.
2. Electrospray tandem mass spectrometer.

Calibration

The detection limit for individual conjugated BA is 1 ng and the assay is linear over the range of analysis. In Table 5.4.13 are shown equations of calibration curves for all analysed BAs.

Quality Control

None.

Table 5.4.13 *Molecular weight, ion pseudo-molecular, correlation coefficient and calibration curves of BAs analysed (reprinted from [32])*

Bile Acid	Molecular Weight	$[M\text{-}H]^-$ Ion	Correlation Coefficient (r)	Calibration Curve Equation
Taurocholic acid	515	514	0.99	$y = 11.39x + 0.61$
Taurochenodeoxycholic acid	499	498	0.97	$y = 9.7x + 4.8$
Taurolithocholic acid	483	482	0.98	$y = 9.3x + 1.14$
Glycocholic acid	465	464	0.99	$y = 16.64x + 5.76$
Glycochenodeoxycholic acid	449	448	0.99	$y = 19.91x + 0.87$
Glycolithocholic acid	433	432	0.99	$y = 22.02x + 3.04$

5.4.12.3 Analytical

Procedure

A 20-µl sample of bile is diluted ten-fold in water, and then 20 µl from each diluted bile sample is transferred to a glass tube to which 1 µg of internal standard (3,12-diol-7-one-5β-cholanic acid) is added. The sample is dried under nitrogen, dissolved in 1 ml of water, and then subjected to SPE using a C_{18} cartridge. The C_{18} cartridge should have been preconditioned prior to loading the sample with successive elutions of 2 ml of chloroform/methanol 2:1 (v/v), 2 ml of methanol and 2 ml of water solutions. After sample loading, the column is washed with 2 ml water and 2 ml of *n*-hexane. The column is left for 10 min to completely dry. BAs are eluted from the cartridge with 5 ml of methanol. The solvent is then evaporated under nitrogen and the residue is dissolved in 1 ml of acetonitrile/water 1:1 (v/v). Sample (10 µl) is injected into the HPLC system by the automatic autosampler injector. The HPLC system is kept at room temperature, and the isocratic mobile phase is acetonitrile/water 1:1. The flow rate is 10 µl/min. The system works in flow injection analysis without a chromatographic column, and the sample is injected directly into the mass spectrometer, after elution from the LC system. The mass spectrometer works in negative mode and the sample spectrum is recorded using the MRM mode, which allows a higher sensitivity compared to scan-mode analysis. The molecular and daughter ions, selected for MRM analysis for each glycine-conjugate (tri-, di- and mono-hydroxylated BAs), are as follows: *m/z* 464.6/74, 448.6/74 and 432.6/74, respectively. For taurine-conjugates (tri-, di- and mono-hydroxylated BAs) the used fragment is the *m/z* 124 and the transitions are *m/z* 514.6/124, 498.6/124 and 482.6/124, respectively. For the internal standard (3,12-diol-7-one-5 β-cholanic acid) the transition is *m/z* 405.6/123.

Calculation

None.

5.4.12.4 Post-analytical

Interpretation

BAs in patient spectra are identified by comparison to the spectra of their standard. Signals of each BA are identified by their MRM mass transition.

Chromatograms

None.

Reference Values

None.

Typical Pathological Values

None.

Pitfalls

No pitfall was found in method development.

5.4.13 LC-MS (Method C)

5.4.13.1 Principle

This method allows a quantitative analysis of BAs present in biological fluids (free, and glycine- and taurine-conjugated forms) in a single chromatographic run, performed with an HPLC mass spectrometric system equipped with an electrospray interface [33].

5.4.13.2 Pre-analytical

Specimen

This method is applicable to urine, serum and bile. Analysis is performed with 200 µl of sample.

Reagents and Chemicals

All chemicals and solvents should be of analytical or HPLC grade. The following BA standards are used: TUDCA, GUDCA, UDCA, TCA, GCA, CA, TCDCA, GCDCA, CDCA, TDCA, GDCA, DCA, GLCA, TLCA and LCA. The internal standard is ^{13}C glycoursodeoxycholic acid.

Instrumentation

1. BAs are analysed with an HPLC-MS system equipped with an electrospray interface.
2. The HPLC system is equipped with an autosampler, and a C_{18} column (3 µm particle size, 70 × 4.6 mm i.d.).

Calibration

None.

Quality Control

None.

5.4.13.3 Analytical

Procedure

A 200-µl sample is diluted (1:4 v/v) with 0.1 M NaOH and loaded in a C_{18} column, which is previously activated with methanol and water. The column is washed with water and the sample eluted with methanol. The eluate is dried under nitrogen flow and the residue dissolved with a suitable quantity of mobile phase. For serum samples an additional pre-treatment is required: the sample is diluted with 3.5 ml of 0.1 M NaOH and incubated in a water bath for 30 min at 64°C. The sample is injected by an autosampler into a HPLC system equipped with a C_{18}, 70 × 4.6 mm i.d., 3-µm particle size. Flow rate is 0.3 ml/min and the gradient for simultaneous separation of all BAs is reported in Table 5.4.14. It consists in a six-step ternary gradient employing solvent A (66:34 v/v, methanol:ammonium acetate 15 mM, pH 5.38), solvent B (75:25 v/v, methanol:ammonium acetate 15 mM, pH 6.0) and solvent C (100% methanol).

At the end of the column the eluent is split, and the sample is introduced into the electrospray source of the mass spectrometer at a rate of about 20 µl/min. Spectrometer voltages are optimised to obtain the maximum signal for each BA. Spectra are acquired in negative ion mode.

Calculation

Quantitative analysis is performed making use of the linearity of the detector response. In fact, peak areas of standards and samples are well correlated with the injected amount, and it is possible to build a calibration curve without the use of an internal standard.

Table 5.4.14 *Mobile phase gradient composition used for simultaneous separation of free, and glycine- and taurine-conjugated BA within a single run (adapted from [33])*

Time (min)	Solvent A (%)	Solvent B (%)	Solvent C (%)
initial	90	–	10
15	90	–	10
23	100	–	–
40	–	80	20
50	–	100	–
60	–	65	35
70	90	–	10

5.4.13.4 Post-analytical

Interpretation

The amounts of injected compounds are proportional to the peak area. The BA concentrations are calculated in comparison with the calibration curve. This method does not need an internal standard.

Chromatograms

None.

Reference Values

None.

Typical Pathological Values

None.

Pitfalls

No pitfall was found in method development.

5.4.14 MALDI-ToF/MS

5.4.14.1 Principle

Recently, a method using MALDI-ToF/MS for the analysis of six CA derivatives in plasma was published [34]. BA derivatives investigated in this study are TCA, TCDCA, TLCA, GCA, GCDCA and GLCA. The matrix selected for this technique must ensure an efficient ionisation of the analytes: in this case, 9-aminoacridine removes protons from the carboxylic acid and sulphonyl acid groups of the BA conjugates, producing negative-ion spectra. Previous studies demonstrated the applicability of MALDI-ToF/MS to quantitative analysis in general [35–37]. To perform quantitative analysis, the internal standard *N*-1-naphthylphthalamic acid (NPA) is employed. This method is also employed for quantification of the same BAs in urine samples [38].

5.4.14.2 Pre-analytical

Specimen

Plasma samples.

Reagent and Chemicals

1. Matrix: 9-aminoacridine solution 20 mg/ml dissolved in 50:50 acetone:methanol.
2. Internal standard: NPA.

3. Standards: TCA, TCDCA, TLCA, GCA, GCDCA, GLCA.
4. Plasma samples commercially available.
5. Water HPLC grade.
6. Methanol HPLC grade.
7. Ethanol HPLC grade.
8. Acetone HPLC grade.

Instrumentation

Time of flight laser mass spectrometer equipped with a nitrogen laser emitting at 337 nm.

Calibration

Calibration curves for glycine and taurine conjugates are obtained plotting peak area (R_A) against conjugate concentrations. Each point of the curve represents the average over a 3-day period. Calibration curves for glycine conjugates were linear in the range 0–60 mg/ml. Calibration curves for taurine conjugates were linear in the range 0–4 mg/ml.

Quality Control

None.

5.4.14.3 Analytical

Procedure

Known concentrations of BA standards previously dissolved in ethanol are added to commercially available plasma samples. Spiked samples (2 ml) are diluted with 4 ml of water. SPE is used for sample clean up and analyte preconcentration. Each SPE C_{18} cartridge is preconditioned with 3 ml of methanol and then with 3 ml of water. The sample is loaded into the cartridge, washed with 2 ml of water, and then eluted with 1.5 ml of methanol. The final solution is composed of one volume of methanol eluent, two volumes of matrix and one volume of internal standard. Final mixture (2.0 μl) is spotted on a 64-well gold plate. Sample spectra are acquired in negative-ion mode ionisation and in reflector mode to increase the resolution. Sample acquisition can be performed in the automatic mode: the autosampler is used with three different raster search patterns. Eight scans at each position in a pattern are collected and a total of 128 scans are averaged, accepting only those ranging from 10,000 to 65,000 counts.

Calculation

An analytical data software is employed for mass calibration, data acquisition and peak area values calculation. Calibration curves are built using peak area values. To obtain the limit of integration, a tangent algorithm is adopted, and the peak separation parameter is set at 50%. Integration limits for unspiked samples (blank) are calculated as the average limits of integration for the rest of the calibration curve. The stated peak area (R_A) is calculated according the following formulae:

$$\text{peak area ratio} = (\text{BA peak area})/(\text{NPA peak area})$$
$$R_A = \text{peak area ratio (sample)} - \text{peak area ratio (blank)}.$$

The peak area ratio of the blank is due to the endogenous BA concentration in plasma samples. In the reported paper the 95% confidence limits of the calculated average concentrations were calculated as $x_0 \pm ts_{x0}$, where s_{x0}, the standard error for both the sample and the calibration curve, was determined using equation 5.10 from Miller and Miller [39]. This calculated average concentration was then compared to the actual concentration using a *t*-test.

The correlation coefficients for calibration curves were greater than 0.988 for all the analytes. The limit of detection (LOD) of the analytes ranged between 0.180 and 4.57 μg/ml. The increased slope of calibration curves and lower LOD observed in the taurine conjugates was the result of the easier ionisation of the relative sulphonate group compared to the carboxylic group of the glycine conjugates. The further increase of the calibration curve slope was due to a higher hydroxylation grade of the ring system. The reproducibility was verified by comparing average peak areas measured on 2 days by means of a standard *t*-test. An analysis of variance with *F*-test was also performed to compare between-day and within-day variances. The accuracy of calibration curves was assessed using the *t*-test to compare the calculated concentration with the spiked concentration of a blind sample of the mixture of all six BAs. The reliability of MALDI-ToF/MS in the quantitative analysis of BAs was so demonstrated.

5.4.14.4 Post-analytical

Interpretation

Compound identification was based on comparison with standards. The magnitude of BA peaks in the blank of the studied samples was above the limit of detection, at a signal:noise ratio of approximately 5.

Spectra

Figure 5.4.14 illustrates a MALDI spectrum of a plasma sample spiked with glycine conjugate (47.62 mg/ml) and taurine conjugate (3.175 mg/ml).

Reference Values

None.

Typical Pathological Values

None.

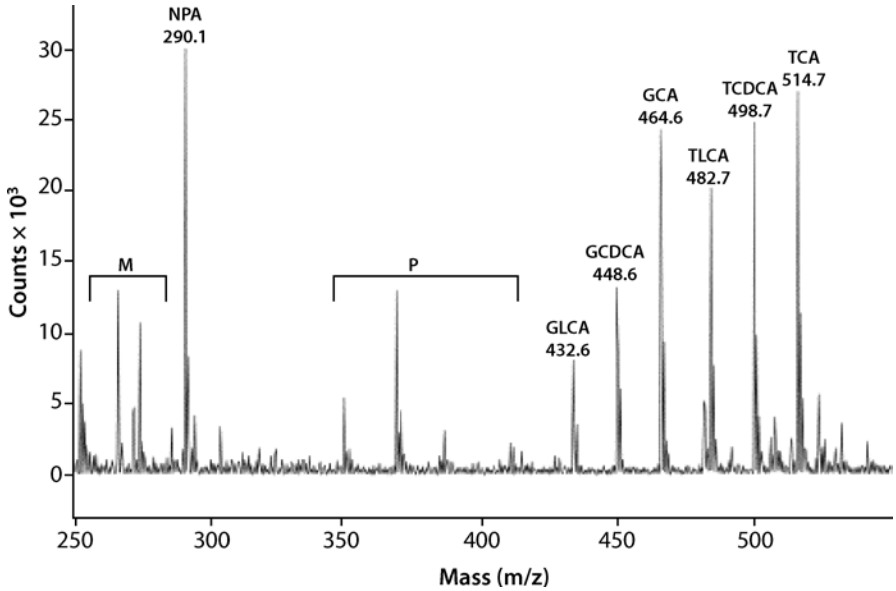

Fig. 5.4.14 Spectrum of a plasma sample spiked with glycine conjugate and taurine conjugate (reprinted from [34]). *M* Matrix peak, *P* peaks from other plasma components

Pitfalls

None.

5.4.15 Proton Nuclear Magnetic Resonance

5.4.15.1 Principle

This is a simple method for the quantification of total glycine and taurine conjugates in human bile using ^{1}H NMR spectroscopy [40]. This method analyses the amide NH signals of resonance of conjugated BAs, which is well separated from the rest of signals in the ^{1}H NMR bile spectrum. Under physiologic conditions, the signal intensities of human bile amides are attenuated by the chemical exchange, so the signal integrated area does not represent the real BA concentration. To quantify total glycine and taurine conjugates it is necessary to suppress the amide exchange by reducing the pH to a slightly lower than physiological value. The optimal value is 6.0 ± 0.5, because at this pH value there is no amide exchange and there is no precipitation of bile salts, due to acidic conditions. It is possible to determine the concentration of taurine and glycine conjugates. In fact, taurine H-26 signals, which appear at 3.08 ppm, usually do not overlap with other signals, so the integral of H-26 signals can be used to calculate the total quantity of taurine conjugates. The quantity of total glycine-conjugated BAs can be subsequently determined simply subtracting the quantity of taurine conjugates (integral of H-26) from the total conjugated BAs (integral of amide signal).

5.4.15.2 Pre-analytical

Specimen

Bile should be collected from the gall bladder of patients undergoing cholecystectomy for symptomatic gallstone disease. Samples should be stored in sterile dark conditions at –80°C until analysis is performed.

Reagent and Chemicals

1. Used standards are sodium salts of: GCA, GDCA, GCDA, TCA, TDCA, TCDA.
2. Cholesterol, deuterium oxide (D_2O), and trimethylsilylpropionic acid sodium salt-d_4.

Instrumentation

NMR experiments are performed on an NMR spectrometer using a 5-mm broadband inverse probe.

Calibration

For assigning the amide proton resonances in glycine- and taurine-conjugated bile salts, ^{1}H-^{1}H two-dimensional (2D) double quantum filtered correlated spectroscopy and ^{1}H-^{1}H 2D total correlated spectroscopy (TOCSY) experiments are performed on human bile. A mixture of standard BAs is dissolved in water (5 mg of each GCA, GDCA, TCA and TDCA). Suppression of intense water signal in all the 2D experiments is done with presaturation. The parameters used are as follows: spectral width, 4800 Hz in both dimensions; time domain data points, 2048; number of FIDs with t_1 incrementation, 512; relaxation delay, 2.5 s; number of transients, 24. A spin lock time of 80 ms is used for TOCSY experiment. Phase-sensitive data are obtained by the time-proportional phase increment (TPPI) method. Resulting data are zero filled to 1024 points in the t_1 dimension and Fourier transformed along both dimensions after multiplying the data by a squared sine-bell window function shifted by $\pi/2$. Figure 5.4.15a shows part of a TOCSY spectrum of human bile, highlighting the connectivity of amide protons with the H-25 and H-26 protons of glycine or taurine conjugated BAs, respectively. The corresponding TOCSY spectrum of a mixture of standard BAs (GCA, GDCA, TCA and TDCA) is also shown for comparison (Fig. 5.4.15b). It is also clear from the spectra that all the amide signals in the bile arise only from glycine and taurine conjugates.

Quality Control

None.

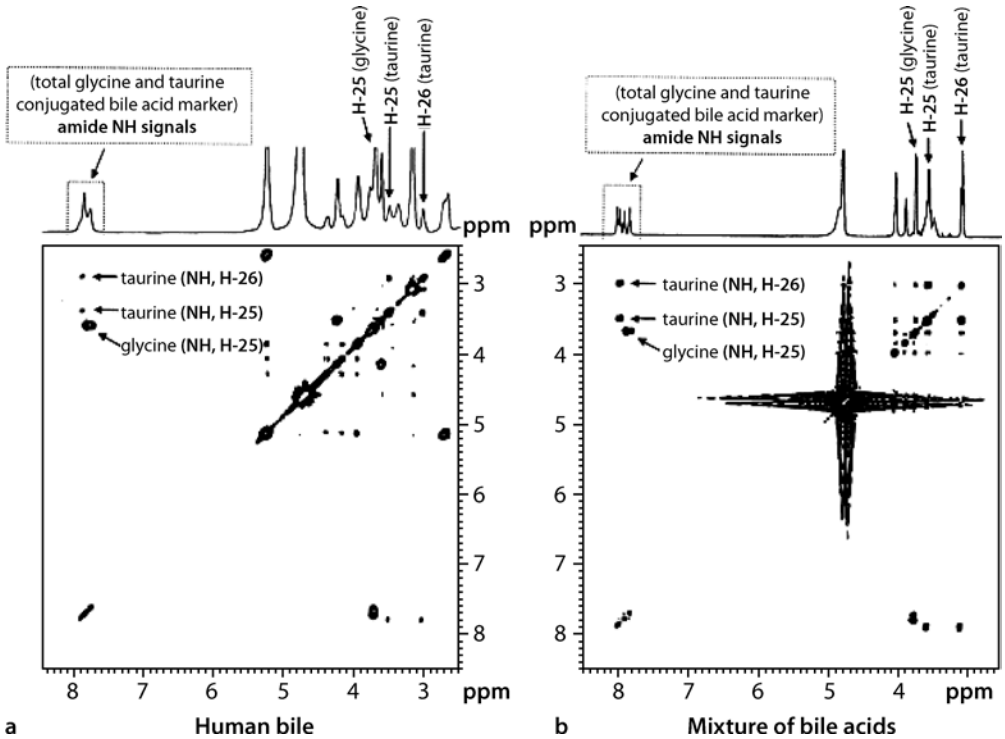

Fig. 5.4.15a,b Parts of two-dimensional total correlated spectroscopy spectra of human bile (**a**) and a mixture of standard solutions of GCA, GDCA, TCA and TDCA (**b**). These spectra show the connectivity of amide proton signals to H-25 and/or H-26 protons of glycine and/or taurine conjugated bile acids (reprinted from [40])

5.4.15.3 Analytical

Procedure

Human bile sample (500 µl) is placed into a 5-mm nuclear magnetic resonance (NMR) tube. The pH of the solution is adjusted at 6 ± 0.5 using HCl. This range of pH is the optimal value to avoid lowering of the amide integral due to the chemical exchange (alkaline pH) or to precipitation of bile salts (acidic pH).

For quantitative estimation, a sealed reusable capillary tube, with a known quantity of sodium salt of trimethylsilyl propionic acid (TSP) dissolved in 35 µl of D_2O, is inserted into the NMR tube while obtaining NMR spectra. The internal standard TSP is used as a chemical shift reference as well as a quantitative standard for the estimation of metabolites, and D_2O is used as the "field-frequency-lock". Spectra are acquired at room temperature. Typical spectra acquired at room temperature of human bile and standard glycine- and taurine-conjugated BAs are shown in Fig. 5.4.16.

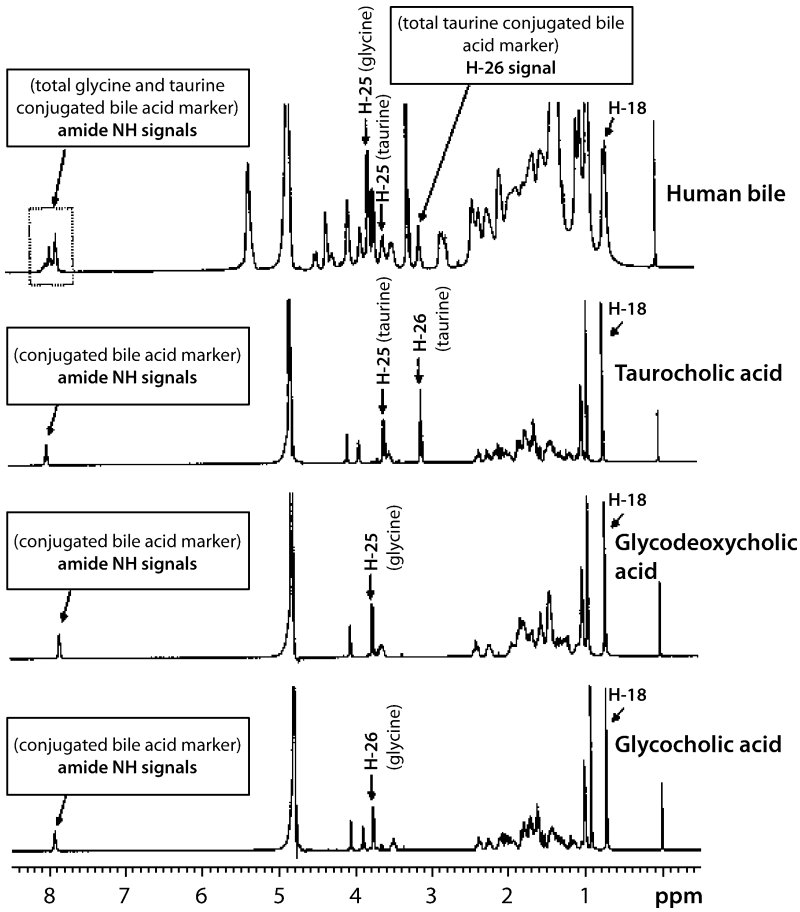

Fig. 5.4.16 Typical room temperature ^{1}H nuclear magnetic resonance spectra of human BA and standards of glycine- and taurine-conjugated bile acid. (reprinted from [40])

Calculation

For quantitative analysis of total glycine- and taurine-conjugated BAs the amide proton signal of the ^{1}H NMR spectra (7.8–8.1 ppm) is integrated and compared with the integral of internal standard TPS signal. The integral of H-26 signal is used for quantification of taurine conjugates. The quantity of glycine-conjugated BAs is determined by subtracting the quantity of taurine conjugates from total conjugated BAs.

5.4.15.4 Post-analytical

Interpretation

Identification of taurine- and glycine-conjugated BAs is based on the integral of the corresponding peak of total conjugated BAs at 7.8–8.1 ppm (signal of amide). Total

taurine conjugate determination is based on the integral of H-26 signal and total glycine conjugate concentration is calculated by subtracting the quantity of taurine conjugates from total conjugated BAs. The magnitude of BA peaks in the blank of the studied samples was above the limit of detection, at a signal:noise ratio of approximately 5.

Spectra

Please refer to Figs. 5.15 and 5.16.

Reference Values

None.

Typical Pathological Values

None.

Pitfalls

None.

5.4.16 Radioimmunoassay

5.4.16.1 Principle

The potential role of the RIA technique in the analysis of BAs was investigated some time ago in a study about the development of a method for the detection of 3β-hydroxy-5-cholenoic acid [41]. This technique was considered by the authors to be important in the evaluation of oxidation of the cholesterol side chain, a minor pathway of BA biosynthesis. 3β-Hydroxy-5-cholenoic acid was found in human meconium [42] and in amniotic fluid [43], suggesting an important role in foetal life. In healthy subjects this compound was found in urine [44] but not in serum [45]. The kidney probably excretes it and its serum concentration is too low to be detected. The aim of this report was to provide a new method for the investigation of the role of 3β-hydroxy-5-cholenoic acid in cholestatic disease.

5.4.16.2 Pre-analytical

Specimen

Serum from patients with liver diseases.

Reagents and Chemicals

1. All reagents are of analytical grade.
2. Thyroglobulin (type II: porcine).
3. ^{125}Iodine.

Instrumentation

A gamma spectrometer system is used for radioactivity counting.

Calibration

The standard curve can be obtained plotting the logit B/B_o versus the logarithm of standard concentration. In this study, each points is calculated from 12 measurements performed in different days over a period of 3 months. Standard deviation for all points is also evaluated.

Quality Control

None.

5.4.16.3 Analytical

Procedure

Female guinea pigs are immunised by injection of 200 µg of 3β-hydroxy-5-cholenoyl-thyroglobulin conjugate. Serum extraction, solvolysis and alkaline hydrolysis of BAs are performed according to the method of Ali and Javitt [46]: 3.5 ml of 2,2-dimethoxypropane and 0.4 ml of 1 M hydrochloric acid in methanol are added to 0.5 ml of serum or diluted serum (1:5 in water). This mixture is allowed to stand at –20°C for 0.5 h, at room temperature for 3 h and is then centrifuged. The supernatant is collected and the pellet is washed once with 0.5 ml acetone. The mixed supernatant and washing solution are neutralised with 1 M sodium hydroxide in methanol and dried at 40°C under nitrogen. The residue is dissolved in 2 ml of 1.25 M sodium hydroxide containing EDTA (13 mM) and boiled for 3 h at 1 atm (i.e., 101/3 kPa). Then, at room temperature, the mixture is adjusted to pH 1 with 6 M hydrochloric acid. Free BAs are extracted with 7 ml of chloroform and brought to dryness at 40°C under nitrogen. The residue is dissolved in about 100 µl of chloroform and cholesterol is separated from BAs by thin-layer chromatography (TLC) on silica gel using a solution isopropanol-ethyl acetate-ammonia-water 20:25:6:4 [47]. 3β-hydroxy-5-cholenoic acid is identified by a reference chromatogram; it is eluted from silica gel with boiling methanol and the solution is brought to dryness. The residue is dissolved in phosphate buffer and aliquots ranging from 20 to 100 µl are analysed by RIA. The 3β-hydroxy-5-cholenoylglycyl-^{125}I-histamine is employed as radioactive ligand. The association constant is 6.3×10^8 l/mol. Diluted serum (1 ml) is mixed with 0.1 ml of serum extract and 0.05 ml of tracer solution (8000–10,000 cpm). Samples are then incubated for 1 h at 37°C and 0.5 h at 4°C. Free antigen is adsorbed on dextran-coated charcoal, which is separated by centrifugation [48]. The supernatant is counted in a spectrometer system.

Calculation

Standard curves and serum samples are prepared in duplicate. In this study, standard curves were linear for values of B/B_o ranging from 0.1 to 0.9. The lower limit of sensitivity ($B/B_o = 0.9$) was 0.6 pmol, the upper limit ($B/B_o = 0.1$) was 37 pmol. A Scatchard plot revealed a linear relationship between the quotient bound to free antigen versus bound antigen, the binding capacity being 0.52 µmol/l of serum. The coefficient of variation ranged between 12 and 20% and recovery from 100 to 111%.

5.4.16.4 Post-analytical

Interpretation

None.

Chromatograms

None.

Reference Values

Healthy subjects showed serum concentration of 3β-hydroxy-5-cholenoic acid ranging from 0.08 to 0.45 µmol/l.

Typical Pathological Values

In this work, serum concentrations of 3β-hydroxy-5-cholenoic acid ranged from 0.9 to 6.8 µmol/l in patients with PBC; from 0.01 to 0.71 µmol/l in patients with chronic active hepatitis and from 0.03 to 1.20 µmol/l in subjects with alcoholic liver cirrhosis.

Pitfalls

Cross-reaction with other BAs was undetectable; However, cholesterol exhibited a cross-reactivity of 5.6%, and for this reason the separation step by TLC was introduced.

5.4.17 Enzymatic Colorimetric Method

5.4.17.1 Principle

Enzymatic colorimetric methods employing 3α-hydroxysteroid dehydrogenase and diaphorase for BAs analysis are reported in literature [49, 50]. The high costs of enzyme impair the suitability of these methods for routine use; despite this, they are considered simple, sensitive and specific. The cost of this assay can be reduced by enzyme immobilisation on solid support, which allows enzyme recycle. The choice of the support must take into account various problems. It is known that the enzyme immobilised onto organic supports, such as cellulose beads, are generally less stable and susceptible to fungal attack [51]. On the contrary, the enzyme bound covalently to inorganic supports, such as alkylamine glass beads, are more stable over a large pH range and in various solvents, and are resistant to microbial attack, but unfortunately the enzyme reaction at low pH is reversible because of Schiff base formation [49, 52].

The use of arylamine glass beads does not seem to exhibit this drawback [53]. In the method reported here [54], 3α-hydroxysteroid dehydrogenase from *Pseudomonas testosteroni* and diaphorase from *Clostridium* spp. are immobilised through diazotisation onto arylamine glass beads. A mixture in a 1:2 ratio of those beads is used for the assay. The NADH concentration produced by the reaction between BAs and 3α-hydroxysteroid dehydrogenase is measured by employing a colorimetric reaction with nitro blue tetrazolium (NBT) chloride salt, NAD^+ and diaphorase. The immobilisation produces a variation in enzyme kinetic properties, owing to steric and diffusional effects and change in the microenvironment [53].

5.4.17.2 Pre-analytical

Specimen

In the reported study, serum samples were withdrawn from healthy people and gallstone patients after cholecystectomy, and stored at –20°C. Bile samples were obtained from gallstone patients during laparoscopic cholecystectomy. Bile samples should be sterilised and stored at 4°C.

Reagent and Chemicals

1. Zirconia-coated arylamine glass beads (pore diameter 55 nm).
2. 3α-Hydroxysteroid dehydrogenase from *Pseudomonas testosterone*.
3. Diaphorase from *Clostridium* spp.
4. Taurodeoxycholic acid.
5. Nitro blue tetrazolium (NBT) chloride salt.
6. NAD^+.
7. NADH.

Instrumentation

Spectrophotometer.

Calibration

Standard curves should be built for serum and bile assays. All data are mean ± SD of six observations. All samples are read against controls comprising all reagents and beads without the enzymes. The zero is obtained by subtracting the value from the blank solution composed of all reagents except glass beads. Figure 5.4.17 illustrates a standard curve for TDCA.

Quality Control

None.

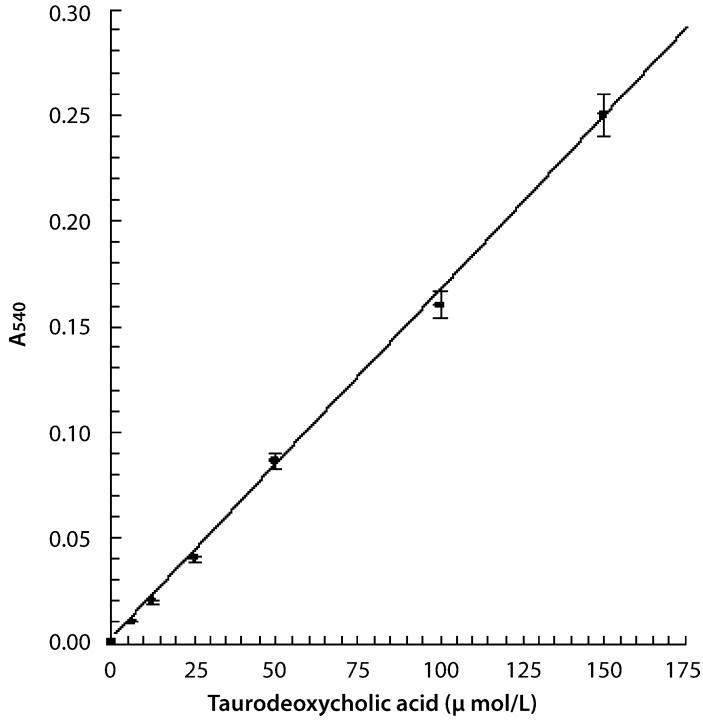

Fig. 5.4.17 Standard curve for TDCA (reprinted from [54])

5.4.17.3 Analytical

Procedure

Assay of Native 3*α*-Hydroxysteroid Dehydrogenase

Assay of native 3*α*-hydroxysteroid dehydrogenase has been previously described by Qureshi et al. [50]. 3*α*-Hydroxysteroid dehydrogenase (5 U) is dissolved in 2 ml sodium carbonate-bicarbonate buffer 0.1 M, pH 9.0. The colour reagent is composed of 0.075 g NAD^+, 0.025 g NBT chloride salt, 10 U diaphorase in 20 ml of 0.065 M sodium phosphate buffer, diluted in 45 ml of distilled water at pH 7.0. The colour reagent is stored at 4°C in an amber-coloured bottle and prepared fresh every day. Enzyme (0.1 ml), 0.5 ml of colour reagent and 0.2 ml of TDCA (200 µmol/l bovine serum) are kept in a 15 ml conical flask, at 25°C for 15 min in the dark. Stop solution (0.5 ml; 75 g/l Triton X-100, 38% HCl) are then added. The absorbance at 540 nm (A_{540}) of the reaction mixture is read against the control in Spectronic-20. A standard curve is constructed between NADH concentration (in 0.065 M sodium phosphate buffer, pH 7.0) and A_{540} using the lipoyl dehydrogenase reaction.

Immobilisation of 3*α*-Hydroxysteroid Dehydrogenase onto Arylamine Glass Beads

Glass beads are activated by diazotisation [55]. Glass beads (100 mg) glass beads, 2 ml chilled HCl 2 N are mixed in a 15-ml conical flask kept in on ice. Diazotisation is carried out by adding 50 mg solid $NaNO_2$ and incubating for 30 min with

occasional stirring; then, excess HNO_2 is decanted. The beads are washed repeatedly with sodium phosphate buffer (0.1 M, pH 7.0) until the pH of washing is 7.0. 3α-Hydroxysteroid dehydrogenase solution (1.0 ml) is incubated with the beads for 48 h at 4°C with occasional stirring. The unbound enzyme is removed and tested for activity and protein. The beads are washed with sodium carbonate-bicarbonate buffer (0.1 M, pH 9.5), until no activity is detected in washing. The enzyme bound to the beads is estimated by subtracting the protein in the supernatant from enzyme solution.

Assay of Immobilised 3α-Hydroxysteroid Dehydrogenase

The assay of arylamine-glass-bound 3α-hydroxysteroid dehydrogenase (100 mg) is carried out as described for its free form with only one exception: the reaction mixture is kept under continuous stirring.

Assay of Native Diaphorase

The same procedure described for 3α-hydroxysteroid dehydrogenase assay can be applied with a few differences [50]. Diaphorase (33 U/ml) is dissolved in 2 ml sodium carbonate-bicarbonate buffer (0.1 M, pH 9.0). Colour reagent is deprived of diaphorase; NAD^+ is replaced by NADH. The reaction is started by adding 0.1 ml diaphorase.

Immobilisation of Diaphorase onto Arylamine Glass Beads

Dissolved diaphorase (2 ml) is immobilised onto arylamine glass beads (100 mg) through the same method reported for 3α-hydroxysteroid dehydrogenase. The immobilised enzyme is stored in 0.065 M sodium phosphate buffer, pH 7.0, at 4°C.

Assay of Immobilised Diaphorase

The assay of 100 mg arylamine glass beads coupled to diaphorase is carried out as described for the enzyme free form, but the reaction mixture is kept under continuous stirring during incubation.

Determination of Bile Acid in Serum and Bile

Serum or bile samples (0.2 ml) are incubated with 100 mg arylamine glass bound to 3α-hydroxysteroid dehydrogenase, 200 mg arylamine-glass-bound diaphorase and 0.5 ml colour reagent in a 15 ml conical flask, in the dark at 30°C for 15 min (standard assay conditions for mixture of immobilised enzyme) under continuous stirring. The A_{540} of the reaction mixture is read.

Recycle and Storage of Immobilised Enzymes

Both enzyme-coated glass beads can be recycled. Beads have to be washed five times with 1 ml reaction buffer. Washed beads can be stored in reaction buffer at 4°C.

Calculation

One unit of immobilised enzyme is defined as "the amount of enzyme bound to glass beads that generates 1 μmol NADH/min under standard assay conditions". BA concentration in the serum and bile is extrapolated from the standard curve be-

tween A_{540} versus concentration of TDCA, in the reported study, concentrations in the range from 6.25 to 800 μmol/l are used.

The method was linear in the concentration range 6.25–150 μmol/l. The recovery values of spiked bile and serum samples ranged between 85.5 and 97.6%. The precision of the method was also evaluated: within- and between-assay coefficients of variation in serum and bile samples were < 0.2, < 0.2, > 0.1 and < 0.1, respectively. The accuracy was assessed comparing this method with standard chemical method [56]; the correlation coefficients were 0.92 for serum and 0.97 for bile. The immobilised enzymes, stored in reaction buffer at 4°C, lost 50% of their initial activity after 300 dosages in 6 months, during 100 uses they lost only 30% of their initial activity. Conversely, the free forms were stable for only 1 week under similar conditions. The cost of this type of assay is lower than the cost of the assay performed using a commercial kit.

5.4.17.4 Post-analytical

Interpretation

This method is able to detect BA total concentration in the serum and bile of healthy persons and patients; however, total BA dosage has also been applied in various studies and in routine analysis.

Chromatogram

None.

Reference Values and Pathological Values

Table 5.4.15 shows serum BA values of healthy and gallstone individuals of different age and gender.

Table 5.4.15 *Serum bile acid levels of healthy subjects and gallstone patients (adapted from [54]).* F *female,* M *male*

Age group ($n = 20$)	Gender	Serum bile acid, μmol/l (mean ± SD)		*t* test
		Healthy persons	Diseased persons	
Children (below 20 years)	F	4.21 ± 1.96	–	
	M	6.61 ± 2.43	–	
Adult (21–50 years)	F	4.34 ± 2.43	84.2 ± 73.2	$p < 0.001$
	M	6.74 ± 3.31	67.4 ± 27.0	$p < 0.001$
Old aged (above 50 years)	F	10.46 ± 4.31	84.9 ± 34.6	$p < 0.001$
	M	8.87 ± 3.87	376 ± 218	$p < 0.001$
Range	F	2.6–15.9	31.8–159	
	M	2.6–15.9	47.7–690	

Pitfalls

To evaluate the presence of possible interferences, the following metabolites were tested at their physiological concentration: bilirubin, sucrose, cholesterol, triglycerides, acetone, urea, uric acid, citric acid, L-ascorbic acid, citrate, pyruvate, haemoglobin, γ-globulin, sodium pyruvate, NaCl, KCl, Ca^{2+} and EDTA. Urea, uric acid, L-ascorbic acid, NaCl, KCl and Ca^{2+} generated a slight interference.

References

1. Niwa T (1995) Mass spectrometry in hepatic diseases. Clin Chim Acta 241–242:253–289
2. Scalia S (1995) Bile acid separation. J Chromatogr B Biomed Appl 671:299–317
3. Batta AK, Salen G (1999) Gas chromatography of bile acids. J Chromatogr B Biomed Sci Appl 723:1–16
4. Bove KE, Daugherty CC, Tyson W, Mierau G, Heubi JE, Balistreri WF, Setchell KDR (2000) Bile acids synthetic defect and liver disease. Pediatr Dev Pathol 3:1–16
5. Hopfer U (2002) Digestion and absorption of basic nutritional constituents. In: Devlin T (ed) Textbook of Biochemistry with Clinical Correlations. Wiley-Liss, New York, pp 1110–1113
6. Clark ML and Harries JT (1975) In: McColl I, Sladen GE (eds) Intestinal Absorption in Man. Academic Press, New York, p. 195
7. Björkhem I, Boberg KM, Leitersdorf E (2001) Inborn Errors in bile acid biosynthesis and storage of sterols other than cholesterol. In: Scriver C, Beaudet A, Sly W, Valle D (eds) The Metabolic Molecular Bases of Inherited Disease. McGraw-Hill, New York, pp 2961–2964 and 2967–2978
8. Bove K, Heubi J, Balistreri W, Setchell K (2004) Bile acid synthetic defects and liver disease: a comprehensive review. Pediatr Dev Pathol 7:315–334
9. Roda A, Piazza F, Baraldini M (1998) Separation techniques for bile salts analysis. J Chromatogr B Biomed Sci Appl 717:263–278
10. Setchell KDR, Lawson AM, Tanida N, Sjövall J (1983) General methods for the analysis of metabolic profiles of bile acids and related compounds in faeces. J Lipid Res 24:1085–1100
11. Setchell KDR, Street JM, Sjövall J (1988) Methods and applications. In: Setchell KDR, Kritchevsky D, Nair PP (eds) The Bile Acids: Chemistry, Physiology and Metabolism. Plenum, London, p 441
12. Shimada K, Mitamura K, Higashi T (2001) Gas chromatography and high-performance liquid chromatography of natural steroids. J Chromatogr A 935:141–172
13. Scalia S, Pazzi P (1994) HPLC assay of conjugated bile acids in human fluids using on-line sample pretreatment on a standard isocratic chromatograph. Clin Chim Acta 224:181–190
14. Wang GF, Stacey NH, Earl J (1990) Determination of individual bile acids in serum by high performance liquid chromatography. Biomed Chromatogr 4:136–140
15. Batta AK, Salen G, Rapole KR, Batta M, Earnest D, Alberts D (1998) Capillary gas chromatographic analysis of serum bile acids as the *n*-butyl ester-trimethylsilyl ether derivatives. J Chromatogr B Biomed Sci Appl 706:337–341
16. Keller S, Jahreis G (2004) Determination of underivatised sterols and bile acid trimethyl silyl ether methyl esters by gas chromatography-mass spectrometry-single ion monitoring in faeces. J Chromatogr B Analyt Technol Biomed Life Sci 813:199–207
17. Czubayko F, Beumers B, Lammsfuss S, Lutjohann D, von Bergmann K (1991) A simplified micro-method for quantification of fecal excretion of neutral and acidic sterols for outpatient studies in humans. J Lipid Res 32:1861–1867
18. Stellaard F, Langelaar SA, Kok RM, Jakobs C (1989) Determination of plasma bile acids by capillary gas-liquid chromatography-electron capture negative chemical ionization mass fragmentography. J Lipid Res 30:1647–1652

19. Goto J, Watanabe K, Miura H, Nambara T, Iida T (1987) Trace analysis of bile acids by gas chromatography-mass spectrometry with negative ion chemical ionization detection. J Chromatogr 388:379–387
20. Gatti R, Roda A, Cerre C, Bonazzi D, Cavrini V (1997) HPLC-fluorescence determination of bile acids. Biomed Chromatog 11:11–15
21. Cavrini V, Gatti R, Roda A, Cerrè C, Roveri P (1993) HPLC-fluorescence determination of bile acids in pharmaceuticals and bile after derivatization with 2-bromoacetyl-6-methoxynaphthalene. J Pharm Biomed Anal 11:761–770
22. Roda A, Gatti R, Cavrini V, Cerrè C, Simoni P (1993) HPLC study of the impurities present in different ursodeoxycholic acid preparations: comparative evaluation of four detectors. J Pharm Biomed Anal 11:751–760
23. Scalia S (1990) Group separation of free and conjugated bile acids by pre-packed anion-exchange cartridges. J Pharm Biomed Anal 8:235–241
24. Nair PP, Garcia C (1969) A modified gas-liquid chromatographic procedure for the rapid determination of bile acids in biological fluids. Anal Biochem 29:164–166
25. Matoba N, Une M, Hoshita T (1986) Identification of unconjugated bile acids in human bile. J Lipid Res 27:1154–1162
26. Poupon RE, Chretien Y, Poupon R, Paumgartner G (1993) Serum bile acids in primary biliary cirrhosis: effect of ursodeoxycholic acid therapy. Hepatology 17:599–604
27. Torchia EC, Labonte ED, Agellon LB (2001) Separation and quantitation of bile acids using an isocratic solvent system for high performance liquid chromatography coupled to an evaporative light scattering detector. Anal Biochem 298:293–298
28. Goto T, Shibata A, Sasaki D, Suzuki N, Hishinuma T, Kakiyama G, Iida T, Mano N, Goto J (2005) Identification of a novel conjugate in human urine: bile acid acyl galactosides. Steroids 70:185–192
29. Gilbert MT (1987) High Performance Liquid Chromatography, IOP Publishing, Bristol
30. Lee BL, New AL, Ong CN (1997) Comparative analysis of conjugated bile acids in human serum using high-performance liquid chromatography and capillary electrophoresis. J Chromatogr B Biomed Sci Appl 704:35–42
31. Tagliacozzi D, Mozzi AF, Casetta B, Bertucci P, Bernardini S, Di Ilio C, Urbani A, Federici G (2003) Quantitative analysis of bile acids in human plasma by liquid chromatography-electrospray tandem mass spectrometry: a simple and rapid one-step method. Clin Chem Lab Med 41:1633–1641
32. Perwaiz S, Tuchweber B, Mignault D, Gilat T, Yousef IM (2001) Determination of bile acids in biological fluids by liquid chromatography-electrospray tandem mass spectrometry. J Lipid Res 42:114–119
33. Roda A, Gioacchini AM, Cerre C, Baraldini M (1995) High-performance liquid chromatographic-electrospray mass spectrometric analysis of bile acids in biological fluids. J Chromatogr B Biomed Appl 665:281–294
34. Mims D, Hercules D (2004) Quantification of bile acids directly from plasma by MALDI-TOF/MS. Anal Bioanal Chem 378:1322–1326
35. Duncan MW, Matanovic G, Cerpa-Poljak A (1993) Quantitative analysis of low molecular weight compounds of biological interest by matrix-assisted laser desorption ionization. Rapid Commun Mass Spectrom 7:1090–1094
36. Ling YC, Lin L, Chen YT (1998) Quantitative analysis of antibiotics by matrix-assisted laser desorption/ionization time-of-flight mass spectrometry. Rapid Commun Mass Spectrom 12:317–327
37. Biroccio A, Urbani A, Massoud R, di Ilio C, Sacchetta P, Bernardini S, Cortese C, Federici G (2005) A quantitative method for the analysis of glycated and glutathionylated hemoglobin by matrix-assisted laser desorption ionization-time of flight mass spectrometry. Anal Biochem Jan 336:279–288
38. Mims D, Hercules D (2003) Quantification of bile acids directly from urine by MALDI-TOF-MS. Anal Bioanal Chem 375:609–316

39. Miller JN, Miller JC 2000 (eds) Statistics and Chemometrics for Analytical Chemistry. Prentice Hall, New York
40. Ijare OB, Somashekar BS, Gowda GA, Sharma A, Kapoor VK, Khetrapal CL (2005) Quantification of glycine and taurine conjugated bile acids in human bile using ^{1}H NMR spectroscopy. Magn Reson Med 53:1441–1446
41. Minder EI, Karlaganis G, Paumgartner G (1979) Radioimmunological determination of serum 3β-hydroxy-5-cholenoic acid in normal subjects and patients with liver disease. J Lipid Res 20:986–993
42. Back P, Ross K (1973) Identification of 3β-hydroxy-5-cholenoic acid in human meconium. Hoppe Seylers Z Physiol Chem 354:83–89
43. Délèze G, Paumgartner G, Karlaganis G, Giger W, Reinhard M, Sidiropoulos D (1978) Bile acid pattern in human amniotic fluid. Eur J Clin Invest 8:41–45
44. Almé B, Bremmelgaard A, Siövall J, Thomassen P (1977) Analysis of metabolic profiles of bile acids in urine using a lipophilic anion exchanger and computerized gas-liquid chromatography-mass spectrometry. J Lipid Res 18:339–362
45. Back P, Siövall J, Siövall K (1974) Monohydroxy bile acids in plasma in intrahepatic cholestasis of pregnancy. Identification by computerized gas chromatography-mass spectrometry. Med Biol 52:31–38
46. Ali SS, Javitt NB (1970) Quantitative estimation of bile salts in serum. Can J Biochem 48:1054–1057
47. Goswami SK, Frey CF (1974) Separation of bile acids from neutral lipids on thin layer chromatograms. J Chromatogr 100:200–201
48. Minder E, Karlaganis G, Schmied U, Vitins P, Paumgartner G (1979) A highly specific ^{125}I-radioimmunoassay for cholic acid conjugates. Clin Chim Acta 92:177–185
49. Porter JL, Fordtran JS, Santa Ana CA, Emmett M, Hagey LR, Macdonald EA, Hofmann AF (2003) Accurate enzymatic measurement of fecal bile acids in patients with malabsorption. J Lab Clin Med 141:411–418
50. Qureshi MY, Smith SM, Murphy GM (1984) Colorimetric enzymatic measurement of serum total 3α-hydroxy bile acid concentrations without extraction. Clin Pathol 37:317–320
51. Bovara R, Carrea G, Cremonesi P, Mazzola G (1981) Continuous-flow analysis of 3α-hydroxysteroids using immobilized 3α-hydroxysteroid dehydrogenase. Anal Biochem 112:239–243
52. Kawasaki T, Maeda M, Tsuji A (1983) Immobilized 3α-hydroxysteroid dehydrogenase and dansyl hydrazine as a pre-labeling reagent for high-performance liquid chromatography with fluorescence detection of bile acids. J Chromatogr 272:261–268
53. Kennedy JF (1975) Data on techniques of enzyme immobilization and bioaffinity procedure. In: Wiseman A (ed) Handbook of Enzyme Biotechnology. Wiley, New York, pp 147–201
54. Rani K, Garg P, Pundir CS (2004) Measurement of bile acid in serum and bile with arylamine-glass-bound 3α-hydroxysteroid dehydrogenase and diaphorase. Anal Biochem 332:32–37
55. Lynn M (1975) In: Weetall HH (ed) Immobilized Enzyme Antigen Antibodies and Peptide, Marcel Dekker, New York, pp 1–17
56. Carey JB (1958) The serum trihydroxy/dihydroxy bile acid ratio in liver and biliary tract disease. J Clin Lab Invest 17:1494–1497

6.1 Pterins and Related Enzymes

Nenad Blau, Beat Thöny

6.1.1 Introduction

Tetrahydrobiopterin (BH_4) cofactor is essential for various enzyme activities, including phenylalanine-4-hydroxylase (PAH), tyrosine-3-hydroxylase (TH), tryptophan-5-hydroxylase (TPH), nitric oxide synthase (NOS), and glyceryl-ether monooxygenase (GEMO). The de novo biosynthesis pathway of BH_4 from guanosine triphosphate (GTP) involves GTP cyclohydrolase I (GTPCH), 6-pyruvoyl-tetrahydropterin synthase (PTPS), and sepiapterin reductase (SR). Three additional enzymes catalyze the last two steps of reduction: aldose reductase (AR), carbonyl reductase (CR), and 3α-hydroxysteroid dehydrogenase type 2 (HSDH2). Cofactor regeneration requires pterin-4a-carbinolamine dehydratase (PCD) and dihydropteridine reductase (DHPR)[1].

The pteridines, a group to which BH_4 also belongs, constitute naturally occurring compounds with a base structure of pyrazino [2,3d] pyrimidine (Fig. 6.1.1). Pteridines with the structure 2-amino-4-oxo are designated by the term "pterins," and those with the structure 2,4-dioxo by the term "lumazines" (Fig. 6.1.1). Two groups of pterins can be distinguished: the first have p-aminobenzoate and glutamate attached to the pterin. These pteridines are designated as conjugated pterins (e.g., folic acid). The second group consists of unconjugated pterins, which contain neither of these two substitutions; instead, substitutions occur at the 6-position of the pterin ring nucleus by the aliphatic side chain. The most important blue-fluorescing unconjugated pterins are neopterin, monapterin, biopterin, isoxanthopterin, primapterin, and pterin (Fig. 6.1.1). Several other pterins, like xanthopterin, sepiapterin, and 3'-hydroxy-sepiepterin, are yellow-fluorescing species (Fig. 6.1.2). Pterins can exist in different oxidation stages, but only fully reduced forms are biologically active. Biopterin is present in biological samples as biopterin, 7,8-dihydrobiopterin (BH_2), and 5,6,7,8-tetrahydrobiopterin (BH_4) (Fig. 6.1.3).

In man, BH_4 is degraded either nonenzymatically by side-chain cleavage to pterin or is enzymatically metabolized in the gastrointestinal tract to become a lumazine [2]. Pterin and dihydropterin are converted by xanthine dehydrogenase to isoxanthopterin and xanthopterin, respectively [3,4]. It is assumed, however, that most of the ingested BH_4 is used as a cofactor (mainly for PAH in the liver) and is catabolized to nonfluorescing compounds; it may even be degraded to CO_2 and ammonia.

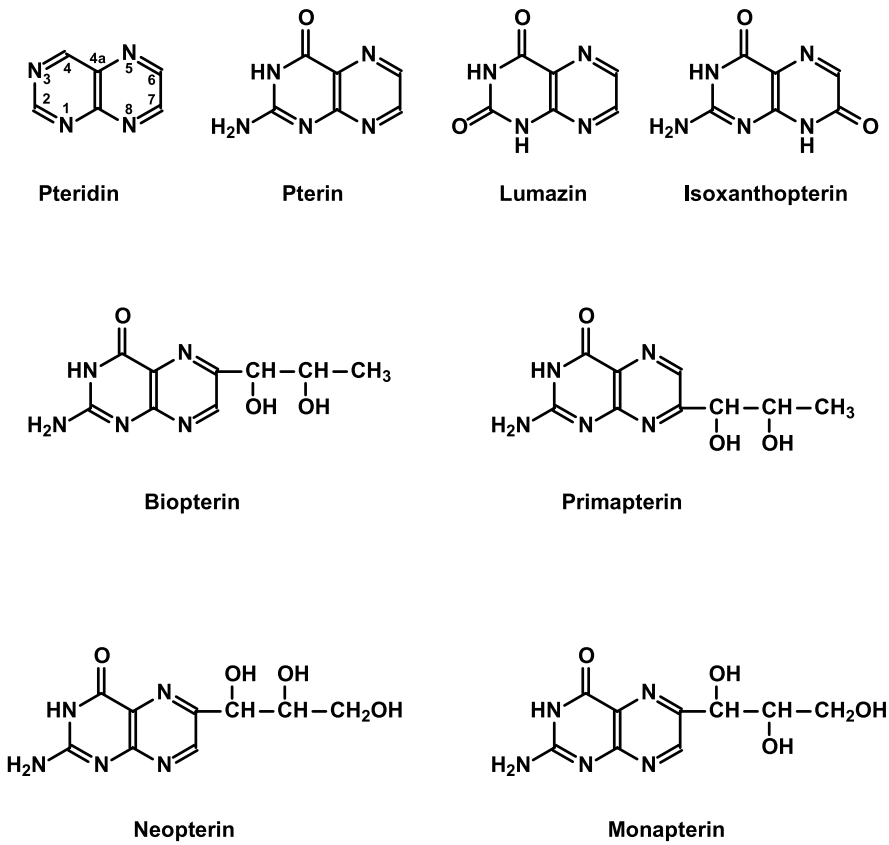

Fig. 6.1.1 The chemical structure of the most common blue-fluorescing pterins, including lumazin

6.1.1.1 Clinical Significance

Measurement of pterins in different biological fluids is the most common method for the screening and diagnosis of inborn errors of BH_4 metabolism. In addition, neopterin is widely used as a marker of T-helper-cell-1-derived cellular immune activation [5]. Under physiological conditions, intracellular BH_4 level plays a pivotal role in the regulation of tyrosine and tryptophan hydroxylase, the initial and rate-limiting steps in the biosynthesis of the catecholamines and serotonin; disturbance of biogenic amine metabolism has been implicated as an etiological factor in a variety of neurological disorders, such as Parkinson's disease, familial dystonia, Alzheimer's disease, and endogenous depression.

BH_4 deficiency can be caused by mutations in genes encoding the enzymes involved in its biosynthesis (GTPCH, PTPS, and SR) or regeneration (PCD/DCoH and DHPR). BH_4 deficiency due to autosomal recessive mutations in BH_4-metabolizing enzymes (except SR) has been described as a cause of hyperphenylalaninemia (HPA) [6]. Biochemical, clinical, and DNA data of patients with BH_4 deficiencies are tabulated in the BIODEF and BIOMDB databases and are available on the Internet (www.bh4.org) [7]. Depending on the enzyme defect and the mode of inheritance,

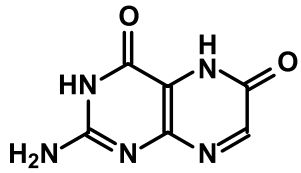

Xanthopterin

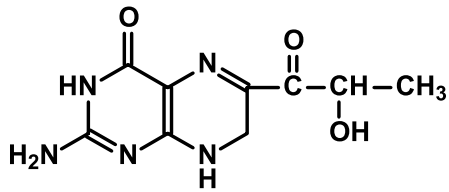

Sepiapterin

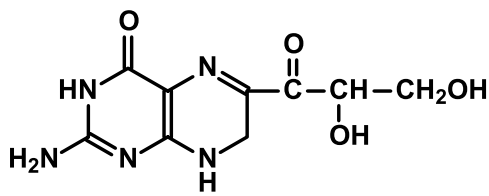

3'-Hydroxysepiapterin

Fig. 6.1.2 The chemical structure of yellow-fluorescing pterins

patients are diagnosed by different analytical and biochemical approaches. Early diagnosis and immediate treatment is essential for a good outcome. Two forms of BH_4 deficiency may occur without HPA. The autosomal dominantly inherited form of GTPCH deficiency (dopa-responsive dystonia, DRD, initially described as Segawa disease) [8], and SR deficiency [9]. Patients presenting with HPA are usually detected through the neonatal screening programs for phenylketonuria (PKU), while those presenting without HPA are recognized either by their typical clinical signs and symptoms or by analysis of neurotransmitter metabolites and pterins in their cerebrospinal fluid (CSF).

Screening for a BH_4 deficiency should be done in all newborns with plasma phenylalanine levels higher than 120 µmol/l, as well as in older children with neurologic signs and symptoms [10]. The following tests are recommended: (1) analysis of pterins in urine, (2) measurement of DHPR activity in blood from a Guthrie card, (3) loading test with BH_4, (4) analysis of pterins, folates, and neurotransmitter metabolites in CSF, and (5) measurement of enzyme activity. The first two tests are essential and enable all BH_4 defects presenting with HPA to be differentiated. With some limitations, the BH_4-loading test is an additional, useful diagnostic tool for the rapid differentiation between classic PKU and BH_4 variants. This test alone can not

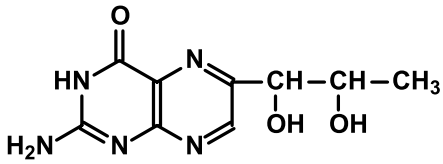

Biopterin

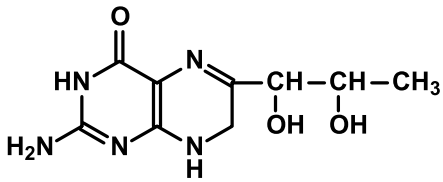

7,8-Dihydrobiopterin

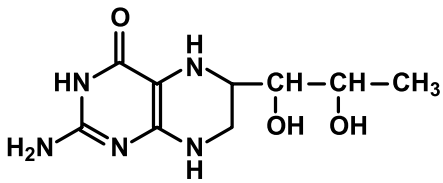

5,6,7,8-Tetrahydrobiopterin

Fig. 6.1.3 The chemical structure of the three oxidation stages of biopterin

differentiate between some patients with a mild form of PKU/HPA and BH_4 variants. Analysis of neopterin, biopterin, 5-methyl-tetrahydrofolic acid, and the neurotransmitter metabolites, 5-hydroxyindoleacetic acid, and homovanillic acid, enables differentiation between severe and mild forms of BH_4 deficiencies.

Major diagnostic applications of neopterin measurements are, for example, monitoring of allograft recipients to recognize immunological complications early. Neopterin production provides prognostic information in patients with malignant tumor diseases and in HIV-infected individuals, high levels being associated with poorer survival expectations. Neopterin measurements are also useful to monitor therapy in patients with autoimmune disorders and in individuals with HIV infection. Screening of neopterin concentrations in blood donations allows the detection of acute infections in a nonspecific way and improves the safety of blood transfusions. As high neopterin production is associated with increased production of reactive oxy-

gen species and with low serum concentrations of antioxidants like tocopherol, neopterin can also be regarded as a marker of reactive oxygen species formed by the activated cellular immune system. Therefore, measurement of neopterin not only allows estimation of the extent of cellular immune activation, but also the extent of oxidative stress [5].

6.1.2 Properties of Pterins

Pterins are well known for their poor solubility in water and in most organic solvents. It has been postulated that this poor solubility in water results from possible hydrogen bonding of the 2-amino and 4-oxo groups between pterin molecules, and that this bonding is preferred to hydration. The nature of the substituents and their position of attachment to the pterin ring influence dramatically the specific solubility. The solubilities of xanthopterin and isoxanthopterin (Fig. 6.1.1) in water are one part in 40,000 and in 200,000, respectively. Fully oxidized pterins are either blue- or yellow-fluorescent compounds (Table 6.1.1), while the fluorescence of reduced derivatives is much weaker. Reduced pterins (e.g., BH_4) are extremely light and oxygen sensitive, and decompose rapidly to breakdown products like pterin, pterin-6-caboxylic acid, xanthopterin, and isoxanthopterin.

6.1.3 Methods

Most naturally occurring pterins are present in body fluids in reduced forms and need to be oxidized to highly fluorescent species prior to high-performance liquid chromatography (HPLC). Neopterin, monapterin, biopterin, primapterin, isoxanthopterin, and pterin are blue-fluorescing compounds. Sepiapterin and 3-hydroxysepiapterin are yellow-fluorescing compounds and are detected in a separate system.

6.1.3.1 Analysis of Pterins in Urine, Plasma, Blood Spots, Amniotic Fluid, and CSF with HPLC and Fluorescence Detection

Preanalytical

Urine

Native urine should be protected from light and stored at –20°C until processed. Oxidized urine sample can be stored at room temperature, but light protection is still recommended. Two procedures for the oxidation of urine (and other samples) are used: (1) oxidation with manganese dioxide (MnO_2) under acidic conditions, and (2) oxidation with iodine (iodine/potassium iodide, I_2/KI) under acidic and basic conditions. The MnO_2 oxidation method is a routine method used to quantify total pterins (fully oxidized neopterin, monapterin, biopterin, primapterin, isoxanthopterin, and pterin); the I_2/KI method is used according to Fukushima and Nixon [11] for the differential oxidation of pterins and quantification of BH_4. Total biopterin represents the sum of BH_4, BH_2, and fully oxidized biopterin. Under acidic conditions BH_4 and BH_2 are oxidized to biopterin, while under basic conditions only BH_2 is oxidized to

■ ***Table 6.1.1*** *Chemical and physical properties of the most common pterins. MW Molecular weight, λ_{ex} excitation wavelength, λ_{em} emission wavelength*

Compound	MW	Side chain	Formula	Fluorescence λ_{ex}	Fluorescence λ_{em}
Pterin	163.1	–	$C_6H_5N_5O$	350	450
Xanthopterin	179.1	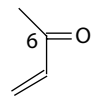	$C_6H_5N_5O_2$	425	530
Isoxanthopterin	179.1	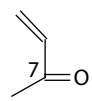	$C_6H_5N_5O_2$	365	480
Neopterin	253.2	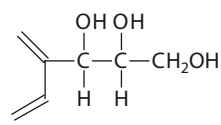	$C_9H_{11}N_5O_4$	350	450
7,8-Dihydroneopterin	255.2	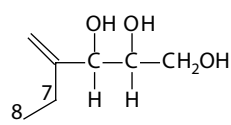	$C_9H_{13}N_5O_4$	–	–
Monapterin	253.2	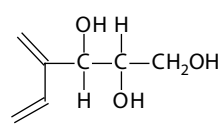	$C_9H_{11}N_5O_4$	350	450
Biopterin	237.2	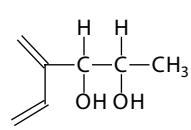	$C_9H_{11}N_5O_3$	350	450
7,8-Dihydrobiopterin	239.2	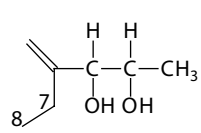	$C_9H_{13}N_5O_3$	–	–
5,6,7,8-Tetrahydrobiopterin	241.2	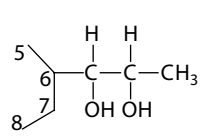	$C_9H_{15}N_5O_3$	–	–
Primapterin	237.2	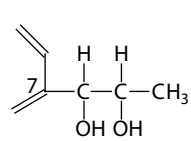	$C_9H_{11}N_5O_3$	350	450
Sepiapterin	237.2	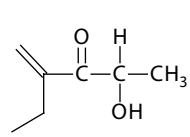	$C_9H_{11}N_5O_3$	425	530
3'-Hydroxysepiapterin	253.2	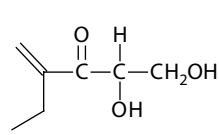	$C_9H_{11}N_5O_4$	425	530

biopterin and BH_4 undergoes side-chain cleavage to form pterin. The difference in biopterin content between the two oxidations represents the actual BH_4 levels.

■ Oxidation with MnO_2

Pipette 5 ml of fresh random urine into a centrifugation vial and adjust the pH to 1.0–1.5 with 200 µl of 6 M HCl. Add 100 mg of MnO_2 (No. 5957, Merck, Darmstadt, Germany) and shake for 5 min at room temperature. Centrifuge for 5 min at 3000 × *g*. Immediately transfer 1 ml of the clear supernatant into a vial. Wrap the vial in aluminum foil to protect from light.

For collection of dried urine specimens, fresh random urine is processed as described for the liquid specimen (see above). Filter paper strips (3 × 5 cm, filter paper backing 165-0921, BioRad, Richmond, USA) are dipped into the clear supernatant of the oxidized urine up to 1 cm below the upper edge. Excess urine is wiped off and the filter paper is left to completely dry at room temperature in dim light. The filter strip is then sent to the laboratory in an envelope by express mail.

■ Oxidation with Iodine

1. Acidic pH oxidation: 100 µl of urine is acidified by addition of 150 µl of 0.2 M hydrochloric acid, and 50 µl iodine solution (1% w/v I_2 in 2% w/v KI) is added. Samples are mixed and incubated for 1 h in the dark at room temperature. The reaction is stopped by adding 50 µl of 2% (w/v) ascorbic acid and 650 µl water.
2. Basic pH oxidation: to the same volume of urine (i.e., 100 µl) is added 100 µl of 0.2 M sodium hydroxide, and the oxidation is performed as described above. Samples are mixed and incubated for 1 h in the dark at room temperature. The reaction is stopped by adding 200 µl of 2 M hydrochloric acid, 50 µl of 2% (w/v) ascorbic acid, and 500 µl water.

The clear filtrate is injected into the HPLC system (see below).

Plasma

Blood is collected in 2.7 ml ethylenediaminetetraacetic acid (EDTA) tubes (Sarstedt, Switzerland) containing 0.1% (w/v) dithioerythritol (DTE), immediately centrifuged at 2000 × *g* for 10 min, and stored at –80°C. Keep fresh or thawed plasma samples on ice during the oxidation procedure.

■ Oxidation with MnO_2

Pipette 0.2 ml of plasma in an Ultrafree 10000 Filter Unit (Millipore, Bedford, MA, USA), add 40 µl of water, 30 µl of 30% (w/v) trichloracetic acid (TCA), and 1 mg of MnO_2 (see above) and shake for 5 min at room temperature. Centrifuge for 30 min at 2000 × *g*. Immediately transfer the clear supernatant into a vial.

■ Oxidation with Iodine

1. Acidic pH oxidation: 100 µl of plasma is acidified by addition of 20 µl of 1 M hydrochloric acid, and 50 µl of iodine solution (1% w/v I_2 in 2% w/v KI) is added. Samples are mixed and incubated for 1 h in the dark at room temperature. The reaction is stopped by adding 10 µl of 5% (w/v) ascorbic acid and 20 µl water.
2. Basic pH oxidation: to the same volume of plasma (i.e., 100 µl) add 20 µl of 1 M sodium hydroxide; oxidation is performed as described above. Samples are mixed

and incubated for 1 h in the dark at room temperature. The reaction is stopped by adding 10 µl of 5% (w/v) ascorbic acid and 20 µl of 2 M hydrochloric acid.

Oxidized samples are filtered in Millipore Ultrafilter with a 10,000-MW cut-off (Millipore) by centrifugation at 5000 × *g* for 30 min. The clear filtrate is injected into the HPLC system (see below).

Dried Blood Spots

Pterins are eluted from dried blood spots on filter paper (Guthrie cards). For every single measurement, 4–6 blood spots (6 mm diameter) are cut out and pterins are extracted with 500 µl of 20 mmol/l HCl and placed into an ultrasonic bath (Sonorex RK31, Bandelin, Germany) for 30 s. Extraction is continued for 10 min by mixing the filter spots solution five times for 5 s at room temperature. The extract is centrifuged at 6000 × *g* for 25 min at room temperature. A 60-µl aliquot of the clear supernatant is used for analysis of hemoglobin (Hb) on the hematology analyzer Sysmex KX-21N (Sysmex, Japan). The remaining supernatant is ultrafiltered on an Ultrafree system (NMWL 10000; Millipore) at 5000 × *g* for 5 min. Pterins are analyzed in clear filtrate by HPLC and fluorescence detection without prior oxidation.

CSF and Amniotic Fluid

Pipette 0.2 ml of CSF or amniotic fluid into an Ultrafree 10000 Filter Unit (Millipore), add 40 µl of water, 30 µl of 30% (w/v) TCA, and 1 mg of MnO_2 (see above); shake for 5 min at room temperature. Centrifuge for 30 min at 2000 × *g*. Immediately transfer the clear supernatant into a vial. For sepiapterin determination, samples should be analyzed without oxidation.

Reagents and Chemicals

Chemicals

1. Water, HPLC quality.
2. HCl, 37% (MW 36.46).
3. NaOH (MW 40.00).
4. Methanol (MW 32.00; Sigma).
5. Isopropanol (MW46.00; Sigma).
6. TCA (Cl_3CCOOH, MW 163.39; Merck No.1.00807).
7. Potassium phosphate monobasic (KH_2PO_4, MW 136.09; Merck No.4873.1000).
8. MnO_2 activated (MnO_2, MW 86.94; Merck No.8.05958.0100).
9. I_2 (MW 253.81).
10. KI (MW 166.00).
11. Ascorbic acid ($C_6H_8O_6$, MW 176.12).
12. DTE ($HSCH_2CH(OH)CH(OH)CH_2SH$, MW 154.25; Sigma-Aldrich No.D8255).
13. Neopterin ($C_9H_{11}N_5O_4$, MW 253.20; Schircks Laboratories, Switzerland).
14. Monapterin ($C_9H_{11}N_5O_4$, MW 253.20; Schircks Laboratories).
15. Biopterin ($C_9H_{11}N_5O_3$, MW 237.20; Schircks Laboratories).
16. Primapterin ($C_9H_{11}N_5O_3$, MW 237.20; Schircks Laboratories).
17. Isoxanthopterin ($C_6H_5N_5O_2$, MW 179.10; Schircks Laboratories).
18. Pterin ($C_6H_5N_5O$, MW 163.10; Schircks Laboratories).
19. Sepiapterin ($C_9H_{11}N_5O_3$, MW 237.2; Schircks Laboratories).

Reagents/Solutions

1. 1 M KH_2PO_4: dissolve 68 g KH_2PO_4 in 500 ml of water. Store at 4°C.
2. 30% (w/v) TCA: dissolve 30.0 g TCA in 100 ml of water. Store at RT.
3. 1% I_2/2% KI: dissolve 1 g I_2 in 1 ml of water in a 100-ml flask; add 2 g KI, and fill with water to the mark. Store at room temperature.
4. HPLC solvent A (1 mM KH_2PO_4 in 6% methanol): dilute 1 ml of 1 M KH_2PO_4 solution in a 1-l flask with 900 ml of water; add 60 ml methanol and fill with water to the mark.
5. HPLC solvent B (60% methanol): dilute 600 ml methanol with water to a final volume of 1 l.
6. HPLC solvent C (20% methanol): Dilute 200 ml methanol with water to a final volume of 1l.
7. HPLC solvent D (50% methanol): Dilute 500 ml methanol with water to a final volume of 1 l.
8. HPLC solvent E (10 mM KH_2PO_4, 3% methanol): Dilute 10 ml of 1M KH_2PO_4 with water; add 30 ml of methanol and fill with water to a final volume of 1 l. Adjust to pH 4.5 with HCl.
9. HPLC solvent F (0.5% methanol, 0.5% isopropanol, 0.05% acetic acid): mix 5 ml of methanol, 5 ml isopropanol, and 0.5 ml of acetic acid and fill with water to 1 l. Degas with nitrogen.
10. HPLC solvent G (49% methanol, 49% isopropanol, 2% acetic acid): mix 490 ml of methanol, 490 ml isopropanol, and 20 ml of acetic acid; fill with water to 1 l. Degas with nitrogen.

Stock Solutions and Standards

1. 0.01% (w/v) Pterin stock solution: dissolve separately 1 mg of neopterin, monapterin, biopterin, isoxanthopterin, or pterin in 1 ml 0.1 M NaOH. Keep for 30 s in an ultrasound bath; add 9 ml 0.1 M HCl, and keep for another 30 s in an ultrasound bath. Store at –20°C.
2. 0.001% (w/v) Pterins working solution: dilute 1 ml of each 0.01% pterin stock solution with 9 ml 0.05 M HCl. Store at –20°C.
3. Urine standard mixture: pipette the volumes given in Table 6.1.2 of 0.001% pterin working solutions in a 20-ml flask and fill with 0.05 M HCl to the mark. Store aliquots at –20°C.

Table 6.1.2 *Volumes of 0.001% pterins working solutions required to make up urine standard mixtures*

Pterin	Concentration µM	Volume 0.001% Stock solution (µl)
Neopterin	2.0	1012
Monapterin	0.2	101
Biopterin	2.0	948
Isoxanthopterin	1.0	358
Pterin	0.5	162

4. Plasma, CSF, and amniotic fluid standard mixture (40 nM neopterin; 40 nM biopterin): dilute 1 ml of the urine standard mixture with 59 ml of 0.05 M HCl. Store aliquots at –20°C.
5. Sepiapterin stock solution (100 µM): dissolve 2.36 mg sepiapterin in 100 ml degassed and nitrogen-washed double-distilled water. Store aliquots at –20°C.
6. Sepiapterin working solution (200 nM): Dilute 1 ml of 100 µM stock solution with water (degassed and nitrogen-washed double-distilled water) and mix 1 ml of this solution (1µM) with 4 ml of water (degassed and nitrogen-washed double-distilled water). Store aliquots at –20°C.

Instrumentation

HPLC Gradient System with Column Switching for Blue-Fluorescing Pterins

An automatic system with the facility of column switching, which allows the omission of sample pretreatment for analysis of total pterins in urine, serum, CSF, and amniotic fluid, is described. The system is essentially the one described by Niederwieser et al. [12]. It consists of a WISP 717+ auto-sampler (Waters, USA), three SunFlow 100 pumps with a pulse-damping device (SunChrom, Germany), a gradient mixer, three six-port type DC6W valves for column switching (Valco, USA), a three-way valve RE5302 (Rheodine, USA), a fluorescence spectrometer Model FP-1520 (Jasco, Japan), an analytical column Spherisorb ODS1 (250 × 4.6 mm i.d.), 5 µm (Waters), a precolumn Spherisorb C8 (40 × 4.6 mm i..d.), 10 µm (Stagroma, Switzerland), and a PC including the chromatography software ChromStar 4.0 (SCPA, Germany). The gradient program that is used to control the system is given in Table 6.1.3 (see also Figs. 6.1.4 and 6.1.5).

Pumps 1 and 2 deliver solvents A and B into a mixing chamber. The sample is injected through valve 1 to the precolumn, which is connected in series through valve 2 with the analytical column (Fig. 6.1.5 position a). The effluent flows through valve 3 into the fluorimeter. Both columns are equilibrated with solvent A. The faster-moving compounds including pterin are chromatographed with solvent A into the analytical column (Fig. 6.1.5, position b). After 2 min, before any of the components are able to elute from the analytical column, the precolumn is disconnected and stopped temporarily by switching valves 2 and 3. The slow-moving compounds are then eluted from the precolumn (Fig. 6.1.5, position c) into the detector using a solvent gradient (5–20% solvent b within 5 min). The slow-moving compounds appear on the chromatogram before the fast-moving compounds. The precolumn is disconnected and rinsed twice with solvents b and c, delivered through valve 4 by pump 3. During this time the compounds, temporarily trapped within the analytical column, are eluted with solvents a and b. After elution of pterin, both columns are connected in series and equilibrated. Fluorimeter settings: excitation wavelength (λ_{Ex}) = 350 nm; emission wavelength (λ_{Em})=450 nm

Isocratic HPLC System for Blue-Fluorescing Pterins

This simple HPLC system needs only a pump (e.g., Model 515, Wates), an injector (e.g., Model 7725i, Rheodyne), a precolumn (e.g., Spherisorb C8; 40 × 4.6 mm i.d.; 10 µm, Stagroma, Switzerland), an analytical column (e.g., Spherisorb ODS1; 250 × 4.6 mm i.d.; 5 µm Waters), and a fluorimeter (e.g., Model FP-1520, Jasco). Fluorimeter settings: λ_{Ex}=350 nm; λ_{Em}=450 nm.

Table 6.1.3 *Gradient program used to control the HPLC gradient system with column switching for blue-fluorescing pterins*

Time (min)	Function	Duration (min)	Remarks
0	0% Solvent B Flow 1.3 ml/min		Solvent A is running
2.0	Aux 2	30	Disconnect analytical column
	Aux 3	10	Precolumn connected with detector for 10 min
2.1	5% Solvent B		
4.0	20% Solvent B	5	Gradient 5–20% B within 5 min
9.0	0% Solvent B Flow 2.0 ml/min		
12.0	Aux 1	20	Analytical column connected with detector for 20 min
	Aux 4	20	Starts pump 3 for 20 min (1 ml/min)
	Aux 5	5	Pre-column rinsed with solvent C for 5 min
	Flow 1.2 ml/min		
19.0	20% Solvent B	10	Gradient 0–20% B within 10 min
22.0	Aux 5	5	Precolumn rinsed with solvent C for 5 min
29.0	100% Solvent B		
32.0	0% Solvent B		Column equilibration with solvent A
53.0	Aux 1	1	Capillaries equilibration with solvent A
55.0	Flow 1.3 ml/min		Next sample injection

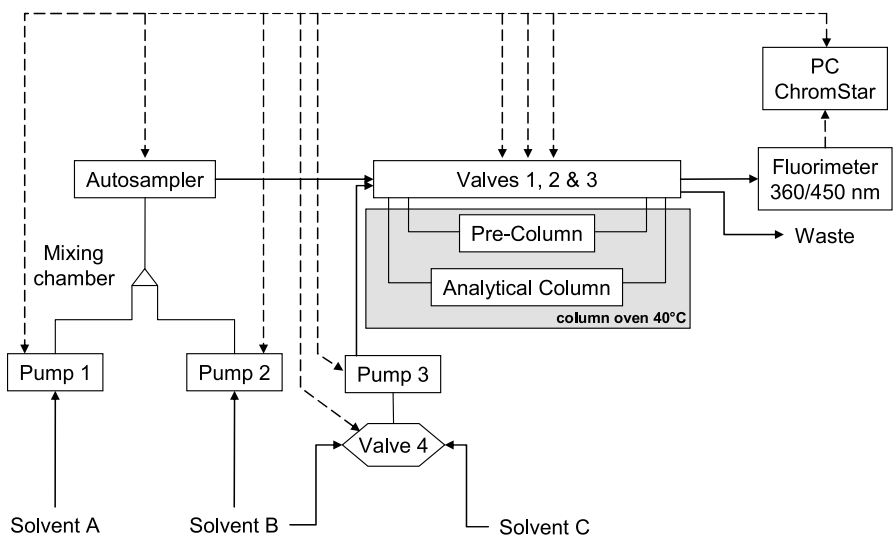

Fig. 6.1.4 Components of the high-performance liquid chromatography (HPLC) system for oxidized pterins with column switching. The autosampler starts the chromatography software, which controls valves and pumps. Pump 3 is used only for rinsing the precolumn. Details of the three valves and their different positions are explained in Fig. 6.1.5

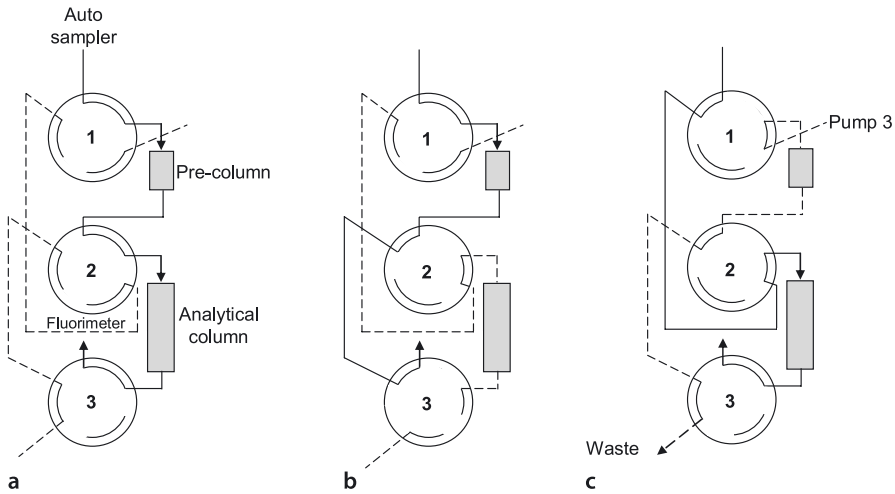

Fig. 6.1.5a–c Connections and positions of the three high-pressure valves used for column-switching HPLC of oxidized pterins. Position a: 0–2 min, injection of sample with precolumn and analytical column in series. Position b: 2–12 min, gradient elution of fast-moving compounds from the precolumn into the detector. Position c: 12–32 min, elution of slower-moving compounds from the analytical column into the detector, with simultaneous cleaning of precolumn

Table 6.1.4 *Gradient program used to maintain the flow rate of the HPLC system for yellow-fluorescing pterins at 1 ml/min*

0 min	100% Solvent F
2 min	0–2% Solvent G in 5 min
7 min	2% Solvent G
9 min	2–20% Solvent G in 10 min
19 min	20% Solvent G
20 min	40% Solvent G
25 min	100% Solvent F
35 min	Stop

Oxidized pterins are eluted isocratically with solvent E (see above) at a flow of 1 ml/min. After 20 min, when pterin is eluted, the next sample can be injected. After 10–20 injection of biological samples, the columns need to be rinsed with solvent D followed by solvent E, to condition them for the next series of samples.

HPLC System for Yellow-Fluorescing Pterins

A gradient HPLC system is used: System Gold (Beckman Instruments, USA) with a fluorescence detector (Model FP-1520, Jasco), LiChrosorb RP8, 5 µm, 40 × 4.6 mm precolumn in connection with LiChrosorb RP8, 5 µm, 125 × 4.6 mm analytical column (both Stagroma). Fluorimeter settings: λ_{Ex}=425 nm; λ_{Em}=530 nm. The flow rate was maintained at 1 ml/min using the gradient program given in Table 6.1.4.

Analytical

Fill the autosampler with corresponding standard mixtures, quality control samples, and analytical samples. Prepare a working list using the ChromStar software and start the program by running the autosampler (autosampler starts ChromStar). Dilute oxidized urine 1:5 with water. All other samples are analyzed undiluted. Inject 10–20 µl of the sample.

Calculation

External standard procedure using ChromStar software or manual calculation using an integrator. Measure the creatinine in urine and calculate the results as mmol/mol creatinine. Measure Hb in dried blood extracts and calculate results as nmol/g Hb.

■ Differential Oxidation

Under acidic conditions BH_4 and BH_2 are oxidized to biopterin, while under basic conditions only BH_2 is oxidized to biopterin and BH_4 undergoes side-chain cleavage to form pterin. The difference in biopterin ("Bio" in the equation below) content between the two oxidation procedures represents the actual BH_4 levels [11]:

$$\frac{Bio(acid) - Bio(basic)}{Bio(acid)} \times 100 = \%BH4$$

Chromatograms of a standard mixture of blue-fluorescing pterins are shown in Figs. 6.1.6 (isocratic) and 6.1.7a (column-switching). Figure 6.1.8 shows yellow-fluorescing pterins.

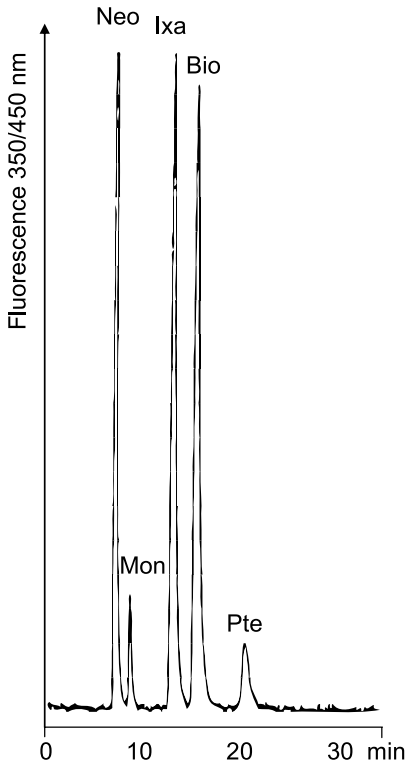

Fig. 6.1.6 HPLC of the pterins standard mixture using an isocratic system. *Bio* biopterin, *Ixa* isoxanthopterin, *Mon* monapterin, *Neo* neopterin, *Pte* pterin

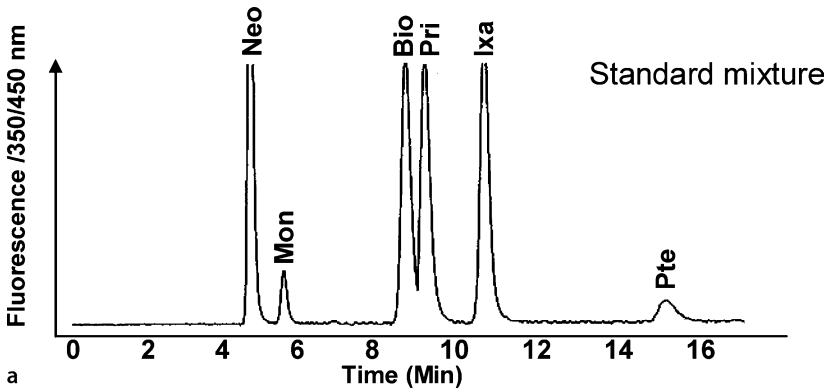
Standard mixture
Neo
Mon
Bio
Pri
Ixa
Pte
Fluorescence /350/450 nm
0 2 4 6 8 10 12 14 16
Time (Min)

a

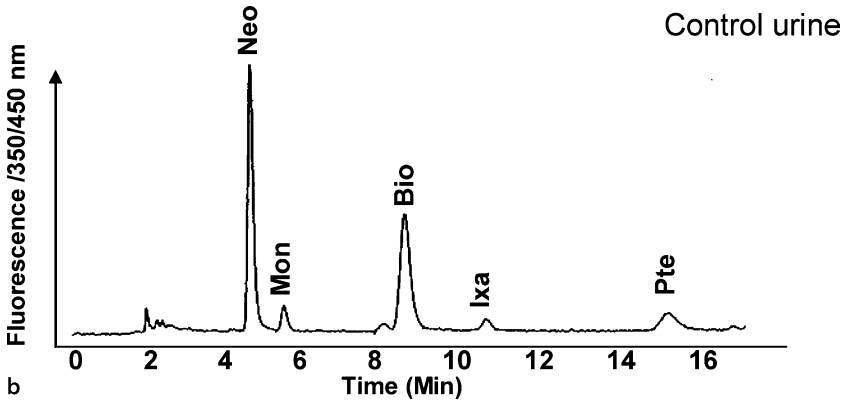
Control urine
Neo
Mon
Bio
Ixa
Pte
Fluorescence /350/450 nm
0 2 4 6 8 10 12 14 16
Time (Min)

b

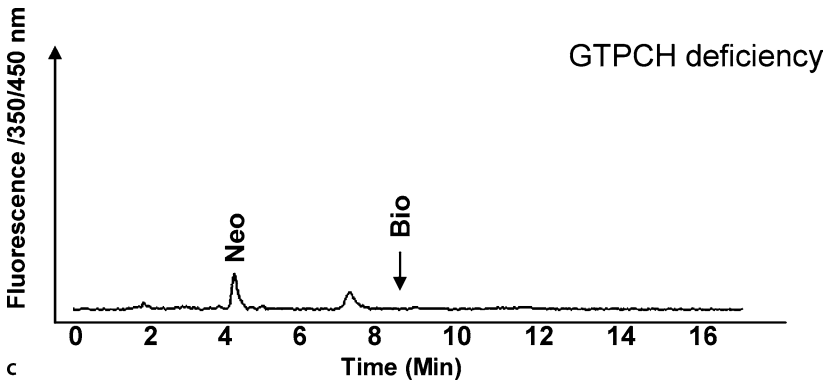
GTPCH deficiency
Neo
Bio
Fluorescence /350/450 nm
0 2 4 6 8 10 12 14 16
Time (Min)

c

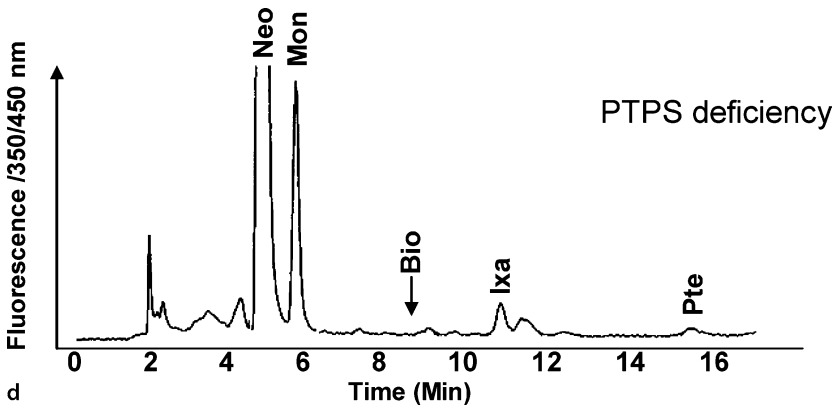
PTPS deficiency
Neo
Mon
Bio
Ixa
Pte
Fluorescence /350/450 nm
0 2 4 6 8 10 12 14 16
Time (Min)

d

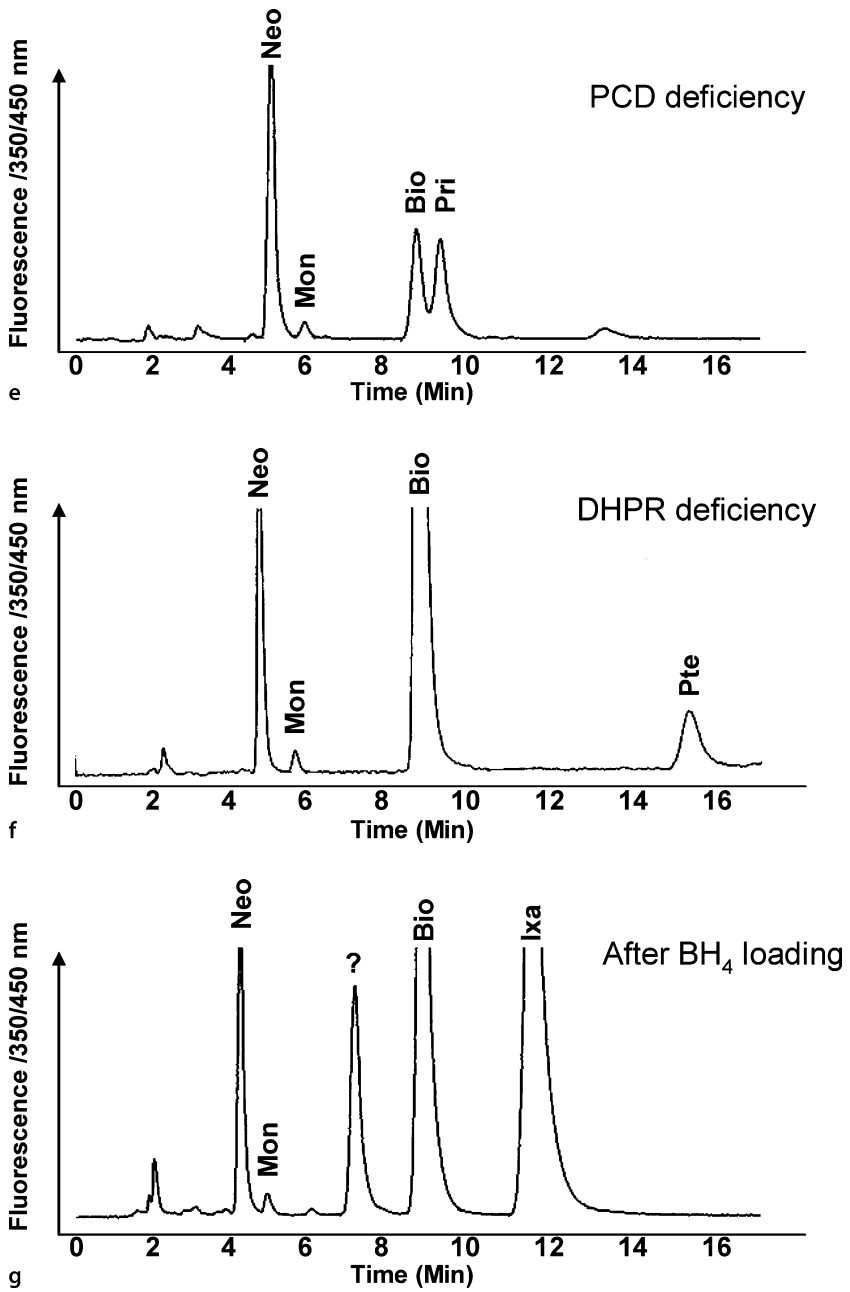

◄▲ **Fig. 6.1.7a–k** HPLC of pterins using a column-switching system: **a** standard mixture; **b** control urine; **c** urine guanosine triphosphate cyclohydrolase I (*GTPCH*) deficiency; **d** urine 6-pyruvoyl-tetrahydropterin synthase (*PTPS*) deficiency; **e** urine pterin-4a-carbinolamine dehydratase (*PCD*) deficiency; **f** urine dihydropteridine reductase (*DHPR*) deficiency; **g** urine phenylketonuria 4–8 h after tetrahydrobiopterin (BH_4) administration; **h–k** *see next page*

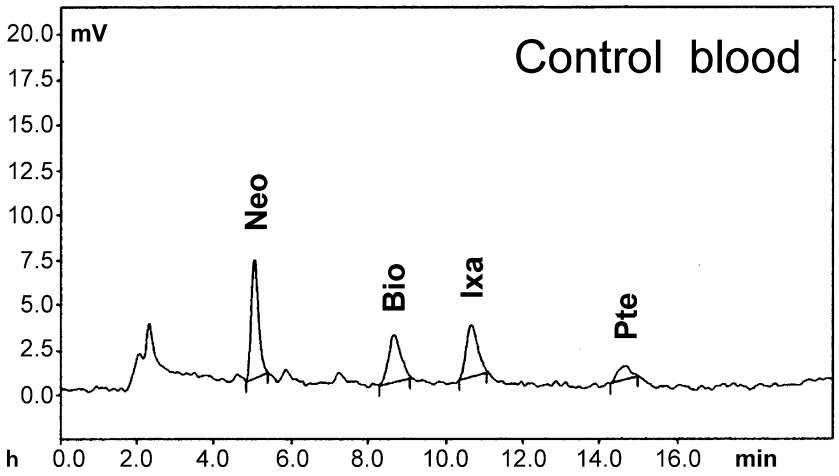
mV
Control blood
Neo
Bio
Ixa
Pte
20.0
17.5
15.0
12.5
10.0
7.5
5.0
2.5
0.0
h
0.0 2.0 4.0 6.0 8.0 10.0 12.0 14.0 16.0 min

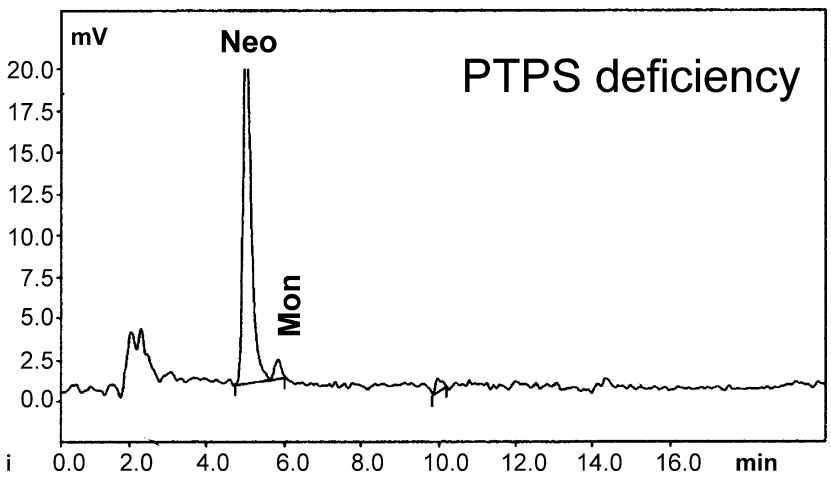
mV
Neo
PTPS deficiency
Mon
20.0
17.5
15.0
12.5
10.0
7.5
5.0
2.5
0.0
i
0.0 2.0 4.0 6.0 8.0 10.0 12.0 14.0 16.0 min

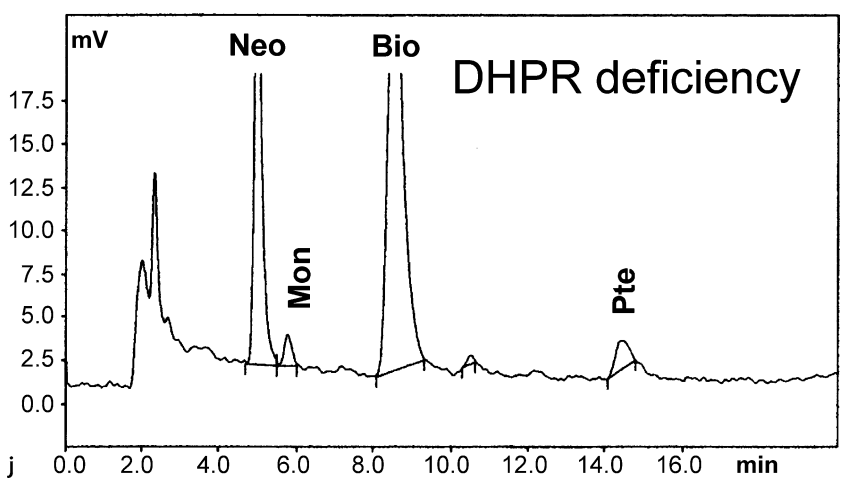
mV
Neo
Bio
DHPR deficiency
Mon
Pte
17.5
15.0
12.5
10.0
7.5
5.0
2.5
0.0
j
0.0 2.0 4.0 6.0 8.0 10.0 12.0 14.0 16.0 min

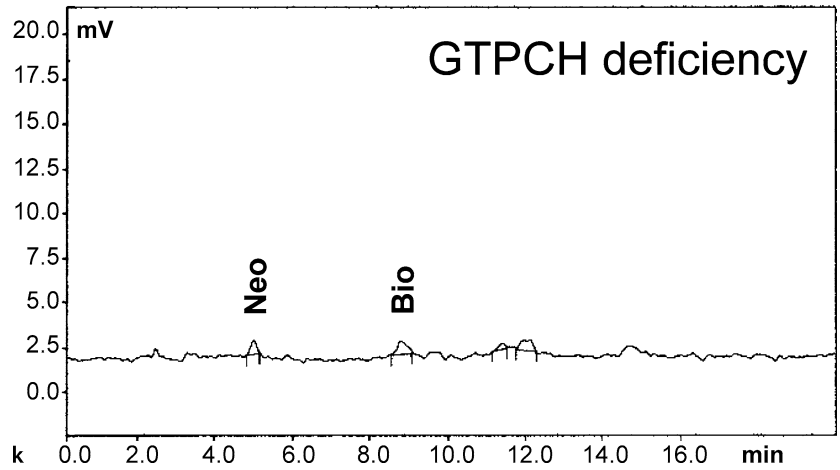

◄▲ **Fig. 6.1.7a–k** *(continued)* **h** control blood; **i** blood PTPS deficiency; **j** blood DHPR deficiency; **k** blood GTPCH deficiency. *Neo* Neopterin, *Pri* primapterin

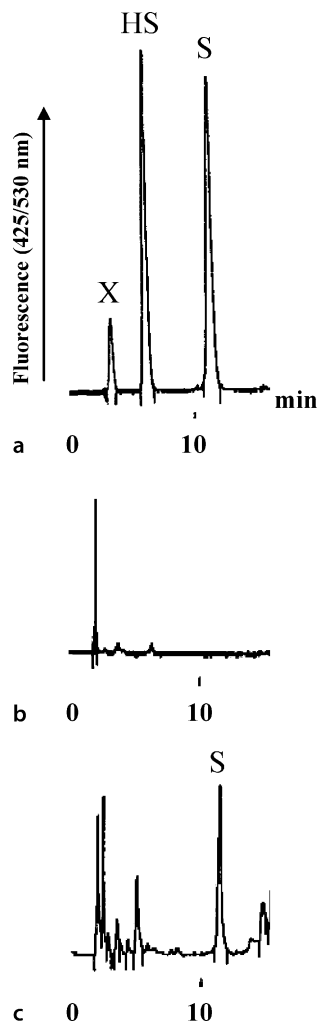

Fig. 6.1.8a–c HPLC of the yellow-fluorescing pterins. **a** Standard mixture; **b** control cerebrospinal fluid (CSF); **c** CSF sepiapterin reductase deficiency. *HS* 3'-Hydroxysepiapterin, *S* sepiapterin, *X* xanthopterin

Post-Analytical

Figure 6.1.7 b–f shows chromatograms of pterins in urine from patients with different enzyme defects of BH_4 metabolism, and Fig. 6.1.7 h–k chromatograms of pterins in dried blood. The pattern of pterins in plasma, dried blood, and CSF is similar to that in urine in patients with BH_4 deficiency. Only urine and dried blood spots are suitable for screening. For more details see Blau et al. [13].

6.1.3.2 Analysis of Reduced Pterins in CSF with Electrochemical Detection

Preanalytical

BH_4 in CSF is sensitive to auto-oxidation, and correct sample collection and storage are essential for the performance of the method. CSF (1 ml) should be collected in tubes containing 1 mg DTE and 1 mg diethylenetriaminepentaacetic acid (DTPA). Samples should be immediately stored at –70°C [14].

Reagents and Chemicals

Chemicals

1. Water, HPLC quality.
2. Citric acid ($C_6H_8O_7$, MW 192.13; Merck 100247).
3. Sodium acetate ($C_2H_3NaO_2$, MW 82.03; Merck 106281).
4. DTE ($HSCH_2CH(OH)CH(OH)CH_2SH$, MW 154.25; Sigma-Aldrich No.D8255).
5. EDTA ($C_{10}H_{16}N_2O_8$, MW 292.25;)(Merck 108417).
6. DTPA ($C_{14}H_{23}N_3O_{10}$; MW 393.34; Merck 108426).
7. Tetrahydrobiopterin dichloride ($C_9H_{15}N_5O_3$, MW 314.2; Schircks Laboratories 11.212).
8. BH_2 ($C_9H_{13}N_5O_3$, MW 239.2; Schircks Laboratories 11.206).

Regents/Solutions

HPLC mobile phase (50 mM sodium acetate/5 mM citric acid/48 µM EDTA/160 µM DTE, pH 5.2): Dissolve 6.8 g sodium acetate, 1.05 g citric acid, 18 mg EDTA, and 25 mg DTE in 1 l of water. The mobile phase is degassed with helium during the chromatographic run.

Stock and Standard Solutions

1. BH_4 stock solution (0.5 mM): dissolve 15.7 mg BH_4 and 100 mg DTE in 100 ml of 0.1 M HCl. Store 1 ml aliquots at –70°C.
2. BH_2 stock solution (0.5 mM): dissolve 12 mg BH_2 and 100 mg DTE in 100 ml of 0.1 M HCl. Store 1 ml aliquots at –70°C.
3. Neopterin stock solution (0.5 mM): dissolve 12.7 mg neopterin and 100 mg DTE in water. Add 10 µl of 10 M NaOH and add water to 100 ml. Store 1-ml aliquots at 70°C.
4. Pterins (BH_4, BH_2, neopterin) working standard solutions (100 nM): dilute 200 µl of each BH_4 and BH_2 stock solution to 100 ml with 1% (w/v) DTE. Keep in the dark and on ice (4°C) for no more than 6 h.

Instrumentation

Separation was achieved using a Merck LiChrosphere RP-18 5 µm (40 × 4 mm) guard column and a Merck Supelcosil RP-18 (250 × 4 mm) analytical column at a flow rate of 1.3 ml/min. BH_4 was measured with an ESA Coulochem 5100A electrochemical detector with a model ESA 5011 electrode in the redox mode. Electrodes 1 and 2 were set to –0.2 V and –0.5 V, respectively. Dihydropterins were electrochemically oxidized to neopterin and biopterin using an ESA model 5021 conditioning cell (+ 1.0 V). The fully oxidized pterins were detected by a Jasco FP-920 fluorescence detector at 350/450 nm.

Note that the actual voltages applied can vary between runs. Apply a voltage that gives a background current at electrode 1 of 0.5 µA and at electrode 2 of 0.05 µA. Get the system up and running, apply approximate voltages, then drop the flow rate to 0.3 ml/min and leave to run overnight. The next day, increase the flow rate to 1.3 ml/min and start changing the volatages to get the required background currents. Run the mobile phase to waste.

Analytical

Run the standard mixture, quality control samples, and analytical samples using either an autosampler or with manual injection.

Calculation

External standard procedure.

Post-analytical

Figure 6.1.9b,c shows chromatograms of reduced (electrochemical detection) and oxidized (fluorescence detection) pterins in the CSF of a 2-year-old control subject and a patient with DHPR deficiency. Elevated BH_2 is characteristic for CSF from patients with DHPR and SR deficiency. In both groups BH_4 concentrations are subnormal and oxidized biopterin is elevated.

6.1.3.3 Reference Values

Reference pterin values for urine, serum, and CSF are given in Table 6.1.5. Those for amniotic fluid and dried blood are given in Table 6.1.6.

6.1.3.4 Pathological Values

Pathological pterin values for plasma are given in Table 6.1.7, and those for urine and CSF are given in Table 6.1.8.

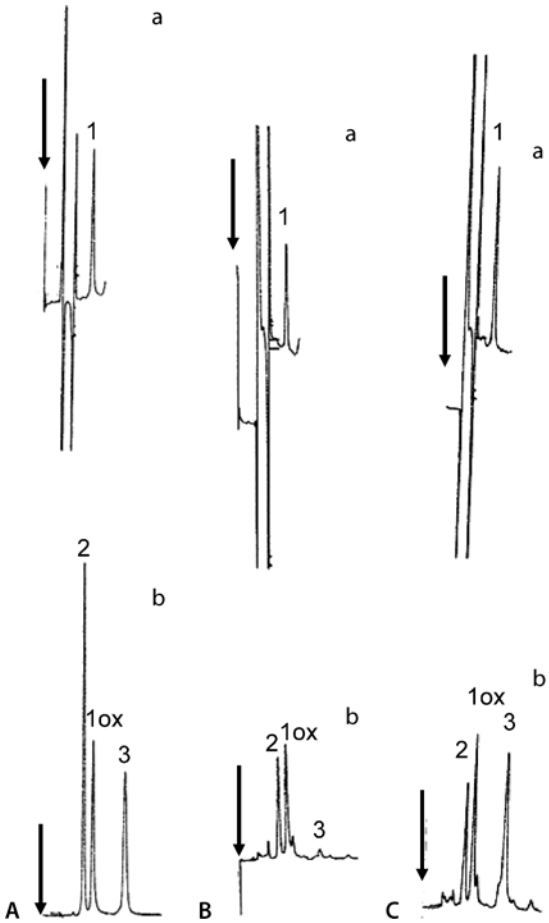

Fig. 6.1.9A–C Electrochemical detector (**a**) and florescence chromatograms (**b**), the latter generated following post-column oxidation. **A** Standards – 50 nM. *1* BH_4 (retention time = 5.12 min); *2* dihydroneopterin (retention time = 4.17 min), *1ox* "oxidized BH_4" generated by electrochemical detector oxidation. N.B. This peak is variable in height/area and is not used for quantification; *3* dihydrobiopterin (BH_2; retention time = 8.52 min). **B** Control CSF from a 2-year-old male. **C** DHPR-deficient CSF in a 6-month-old male. Note the elevated BH_2. The shoulder on the peak is biopterin. Also note that BH_4 concentration can be within the appropriate reference range in DHPR deficiency states [39]. The *arrow* denotes the injection point. Figure courtesy of Dr. Simon Heales, London

■ ***Table 6.1.5*** *Reference values for pterins in urine, serum, and cerebrospinal fluid.* Bio *biopterin,* CSF *cerebrospinal fluid,* Neo *neopterin,* S *serum,* Sep *sepiapterin,* U *urine*

Age (years)	Neo (U) mmol/mol creatinine	Bio (U) mmol/mol creatinine	Neo (S) nmol/l	Bio (S) nmol/l	Neo (CSF) nmol/l	Bio (CSF) nmol/l	Sep (CSF) nmol/l
Newborns	1.1–4.0	0.5–3.0	3–11	4–18	15–35	20–70	< 1
0–1	1.1–4.0	0.5–3.0	3–11	4–18	12–30	15–40	< 1
2–4y	1.1–4.0	0.5–3.0	3–11	4–18	9–20	10–30	< 1
5–10	1.1–4.0	0.5–3.0	3–11	4–18	9–20	10–30	< 1
11–16	0.2–1.7	0.5–2.7	3–11	4–18	9–20	10–30	< 1
> 16	0.2–1.7	0.5–2.7	3–11	4–18	9–20	10–30	< 1

■ ***Table 6.1.6*** *Reference values for pterins in amniotic fluid and dried blood (from a Guthrie card).* A *amniotic fluid,* B *blood,* Hb *hemoglobin,* Pte *pterin*

Neo (A) nmol/l	Bio (A) nmol/l	Neo (B) nmol/g Hb	Bio + Pte (B) nmol/g Hb	%Bio + Pte (B)
16–40	6–21	0.31–4.45	0.15–2.91	13.9–78.3

■ ***Table 6.1.7*** *Pathological pterin values in plasma.* Phe *Phenylalanine*

Actual Phe[a] (µmol/l)	Neo (S) nmol/l	Bio (S) nmol/l
200–600	2–32	12–46
600–1200	9–27	24–39

[a] Plasma neopterin and biopterin values depend strongly upon the actual hyperphenylalaninemia.

■ ***Table 6.1.8*** *Pathological pterin values in urine and CSF.* DHPR *Dihydropteridine reductase,* DRD *dopa-responsive dystonia,* GTPCH *GTP cyclohydrolase I,* n *normal,* PCD *pterin-4a-carbinolamine dehydratase,* PTPS *6-pyruvoyltetrahydrobiopterin synthase,* SR *sepiapterin reductase*

Variant	Neo (U)	Bio (U)	Neo (CSF)	Bio (CSF)	Sep (CSF)
	mmol/mol creatinine		nmol/l		
1.2 GTPCH deficiency	< 0.2	< 0.2	0.05–3.0	1.5–7.5	*n*
1.3 PTPS deficiency (severe)	5.0–51.2	< 0.5	47–402	1.0–16.0	*n*
1.3 PTPS deficiency (mild)	5.0–51.2	< 0.5	25–230	13–56	*n*
1.4 DHPR deficiency (severe)	0.5–23.2	3.8–25.6	11–70	43–117	*n*
1.4 DHPR deficiency (mild)	0.5–23.2	3.8–25.6	11–70	43–117	*n*
1.5 PCD deficiency (benign)	4.1–22.5	0.7–1.5[a]	43–117	16–96	*n*
1.6 DRD	*n*	*n*	1.1–6.2	3.1–7.6	*n*
1.7 SR deficiency	*n*	*n*	14–51	72–102[b]	7–23

[a] Primapterin (7-Bio) ↑
[b] 7,8-dihydrobiopterin ↑

6.1.4 Follow-Up Enzyme Assays

6.1.4.1 GTP Cyclohydrolase I

Principle

GTPCH (EC 3.5.4.16) converts the substrate GTP to 7,8-dihydroneopterin triphosphate (H_2NTP) and formate. GTPCH activity is determined by measuring neopterin, the completely oxidized and dephosphorylated H_2NTP-product of the enzyme reaction. Conversion of H_2NTP to neopterin is carried out after the enzymatic reaction in presence of iodine at pH 1.0, followed by dephosphorylation with alkaline phosphatase at pH 8.5–9.0. Neopterin is detected fluorimetrically at 350/440 nm upon HPLC separation. The assay is based with some modifications on the methods published by Viveros et al. and Hatakeyama and Yoneyama [15,16].

Preanalytical

Specimen

GTPCH activity may be determined from cultivated primary dermal fibroblasts or from lysates of tissue samples (e.g., liver, brain, and chorionic villi). Fibroblasts do not express GTPCH unless they are stimulated with cytokines. For standard analysis of GTPCH activity, confluent fibroblast cells are stimulated for 24 h in 5 ml of fresh Dulbecco's modified Eagle's medium (DMEM) incubated at 37°C (5% CO_2) with a cytokine cocktail containing 1250 U interferon-γ (IFN-γ) and 500 U tumor necrosis factor α (TNF-α; see also below). After cytokine stimulation, cells are analyzed immediately by washing first twice with phosphate-buffered saline (PBS). Beyond this point, all manipulations are carried out at 4°C. Fibroblasts from one confluent 78-cm² plate are lysed in 0.2 ml of freshly prepared homogenization buffer by six cycles of freeze-thawing and subsequent centrifugation at 13,000 × *g* for 5 min. An aliquot of 0.15 ml of supernatant is desalted on a Sephadex G-25 column that has been pre-equilibrated with homogenization buffer. Lysates are centrifuged for 2 min at 800 × *g* (e.g., in a Heraeus Biofuge A at 3000 rpm) and used directly for enzymatic assays.

Tissues samples should be shock-frozen in liquid nitrogen and stored at –80°C. For tissue lysate preparation, grind a frozen piece of tissue to powder in the presence of liquid nitrogen, following the addition of ten volumes of homogenization buffer (see below); ideally prepare 50 mg to a maximum of 100 mg of wet tissue weight and add 0.5–1.0 ml of ice-chilled homogenization buffer. All of the following steps are carried out at 4°C. Tissue samples are homogenized in an electric blender two times for 30 s and then centrifuged at 15,000 × *g* for 20 min to harvest the supernatant for enzymatic assays.

Additional freeze-thawing of tissue or fibroblast lysates may result in reduced GTPCH activity, and it is thus recommended to assay activity always from freshly lysed material. Alternatively, lysates may be kept for 1–2 days at –80°C (this may not be the case for PTPS, SR, and DHPR assays, as extracts can be kept at –80°C for a longer period without loosing activity).

Reagents and Chemicals

1. PBS buffer (Gibco, Cat No 70011-036): 137 mM NaCl, 8 mM Na_2HPO_4, 1.5 mM KH_2PO_4, 2.7 mM KCl, pH 7.4.
2. IFN-γ (Sigma, Cat No I-3265): dissolve 10^6 U in 2 ml PBS; store at –20°C.
3. TNF-α (Sigma, Cat No T-0157): dissolve 2×10^5 U in 1 ml PBS; store at –20°C.
4. DMEM for fibroblast culturing (Gibco BRL, Cat No 31600-075): add fresh 10% fetal calf serum (Gibco BRL, Cat No 10106-078), 5 kU/l penicillin plus 5 g/l streptomycin (Gibco BRL, Cat No 15070-022); store at – 20°C. For a 10-cm (78-cm^2) confluent dish, 2.5 µl of each cytokine is dissolved in 5 ml of DMEM.
5. Reaction buffer: 5 ml of 1 M Tris-HCl pH 7.4, 750 mg KCl, 0.2 ml 0.5 M EDTA; add water to a final volume of 10 ml. Store at room temperature.
6. Dithiothreitol (DTT) 1 M (Fluka, Cat No 43815; MW154.25): dissolve 15.4 mg in 0.1 ml water; store at –20°C.
7. Phenylmethylsulfonyl fluoride (PMSF) 200 mM (Fluka Cat No 78830; MW 174.2): dissolve 34 mg in 1 ml of 2-propanol; store at –20°C.
8. Leupeptin 2 mM (Roche, Cat No 11017101; MW 426.6): dissolve 1.0 mg in 1 ml water; store at –20°C.
9. Pepstatin 2 mM (Fluka, Cat No 77170; MW 685.91): dissolve 1.37 mg in 1 ml methanol; store at –20°C.
10. Homogenization buffer: 50 mM Tris-HCl pH 7.4, 100 mM KCl, 1 mM EDTA, 1 mM DTT, 0.2 mM PMSF, 1 µM leupeptin, 1 µM pepstatin. Mix the buffer fresh before use as follows: 2 ml of reaction buffer, 2 µl of 200 mM PMSF, 1 µl of 2 mM leupeptin, 1 µl of 2 mM pepstatin, 2 µl of 1 M DTT.
11. Sephadex G-25 column "MicroSpin" (Amersham Bioscience, Cat No 275325).
12. Alkaline phosphatase B solution (Roche, Cat No 10108162001): mix freshly, 0.22 ml alkaline phosphatase B, 0.01 ml 1 M $MgCl_2$, 0.01 ml 100 mM $ZnCl_2$, 0.76 ml 0.1 M Tris-HCl pH 8.
13. GTP 100 mM Li-salt (Roche Diagnostics, Cat No 1140957); store 10 µl aliquots at –20°C.
14. Oxidizing solution (0.5% I_2, 1% KI in 1 M HCl): dissolve 0.5 g KI and 0.25 g I_2 in 50 ml of 1 M HCl; store at room temperature in the dark.
15. Ascorbic acid 2% (Fluka, Cat No 95209; MW 176): dissolve freshly, 0.2 g in 10 ml water.
16. Micron 10,000 Filter (Millipore, Ultracel YM-10, Cat No 42408).
17. Protein assay solution (BioRad, Cat No 500-0006): determine the protein concentration according to the user manual.

Instrumentation

Routine laboratory equipment: vortex mixer, laboratory centrifuge, analytical balance, water bath, pH meter, HPLC system with fluorescence detection at 350/440 nm (for neopterin; see 6.1.3.1, subheading "Instrumentation").

Quality Control

GTPCH activity measurements are not available in external control programs and can only be compared by exchanging results from other laboratories (for examples see www.bh4.org). Control biopterin and neopterin samples are commercially available from Dr. Schircks Laboratories, Jona, Switzerland (www.schircks.com). We recommend using internal controls (e.g., normal control fibroblasts in each enzyme

assay and standard biopterin for HPLC analysis; see 6.1.3.1, subheading "Instrumentation").

Analytical

Procedure

Besides the enzymatic incubation in the "reaction mixture," all procedures are carried out at 4°C. GTPCH activity is assayed by measuring the neopterin produced upon enzymatic incubation at 37°C for 60 min in a final volume of 0.1 ml in the dark (due to light sensitivity of pterins), followed by chemical oxidation and dephosphorylation. Two separate blanks are prepared, a blank reaction with cell lysate that is immediately oxidized to detect the neopterin that was present in the lysate, and a blank reaction without cell lysate to detect the neopterin that is generated from the incubation (substrate) buffer. The sum of both blanks is later subtracted from the value of the incubation reaction to determine the enzymatically produced neopterin.

1. Reaction mixture: 74 µl of reaction buffer, 1 µl of 100 mM GTP and 25 µl of filtered cell or tissue lysate. Incubate for 1 h at 37°C in the dark, followed by chilling the reaction on ice and addition of 10 µl of oxidizing solution. Incubate for 1 h at room temperature in the dark, followed by adding 10 µl of ascorbic acid (2%), 14 µl of 1 M NaOH pH 8.5–9, and 20 µl of alkaline phosphatase B solution. After further incubation for 1 h at 37°C in the dark, add 5 µl of 2 M HCl and centrifuge for 15 min at 5000 × *g* through a Millipore Ultrafree-MC 10,000 filter at 4°C. The final volume is 159 µl with 25 µl of lysate analyzed, resulting in a ratio of 159/25 = 6.36. Analyze filtrate samples of approximately 10 µl in a HPLC CSF system.
2. Blank reaction with cell lysate: 74 µl of reaction buffer, 1 µl of 100 mM GTP and 25 µl of filtered cell or tissue lysate. Add immediately 10 µl of oxidizing solution and proceed as for the reaction mixture.
3. Blank reaction without cell lysate: mix 25 µl of homogenization buffer, 74 µl of reaction buffer and 1 µl of 100 mM GTP and proceed by starting the incubation for 1 h at 37°C in the dark, as described for the reaction mixture.

To determine the protein concentration, use filtrates from Sephadex G-25 (Micro-Spin) columns and proceed according to the protein assay method (BioRad). The results are given in mg protein/ml.

Calculation

GTPCH activity is determined as µU/mg protein. One unit of GTPCH produces 1 µmol neopterin/min at 37°C. The results from the neopterin (N) determination by HPLC are given in nmol/l.

Calculate as follows:

1. Background: subtract the sum of blanks from the reaction mixture:

$$N\ [\text{nmol/l}] = N_{\text{reaction mixture}} - (N_{\text{blank reaction with cell lysate}} + N_{\text{blank reaction without cell lysate}})$$

2. Correction factor: the ratio of 6.36 divided by 60 min results in nmol/ l (factor of 0.106):

$$N\ [\text{nmol/l}] \times 0.106 = \mu\text{U GTPCH/ml}$$

3. Activity per milligram of protein: divide the activity per milliliter by the amount of protein per ml:

   μU GTPCH/ml divided by mg protein/ml = μU GTPCH/mg protein

Postanalytical

Interpretation

1. Chromatograms: chromatogram standards involve neopterin, biopterin, monapterin, pterin, and isoxanthopterin.
2. Reference and pathological values (GTPCH): reference values for cytokine-stimulated fibroblasts for GTPCH are for control cells 2.6 μU/mg (50th percentile; 1.4 μU/mg for the 5th percentile, and 6.5 μU/mg for the 95th percentile), for autosomal recessive GTPCH deficiency 0.8 μU/mg (range 0.7–1.0 μU/mg), and for DRD 0.4 μU/mg (range 0.1–0.6 μU/mg). Nonstimulated fibroblasts have no detectable activity (<0.05 μU/mg). The reference values for amniocytes are 0.2 μU/mg (for the 50th percentile; 0.04 μU/mg for the 5th percentile, and 1.8 μU/mg for the 95th percentile). For the mouse, liver tissue values range from 1.1 to 4.9 μU/mg for adults and from 0.2 to 0.3 μU/mg for newborns, whereas whole brain tissue contains activity between 0.06 and 0.15 μU/mg (adults). For references see [17,18].

Pitfalls

1. Sensitivity: not known. The threshold value for detection of enzyme activity is < 0.04 μU/mg.
2. Stability: as mentioned before, freeze-thawing of tissue or fibroblast lysates may result in reduced GTPCH activity, and it is thus recommended that activity always be assayed from freshly lysed material. However, lysates may be kept for 1–2 days at –80°C.

6.1.4.2 PTPS (Red Blood Cells, Fibroblasts, Amniocytes, Tissue)

Principle

PTPS (EC 4.6.1.10) converts the substrate 7,8-dihydroneopterin triphosphate (H_2NTP) in a manganese-dependent reaction to the highly unstable intermediate 6-pyruvoyltetrahydropterin (PTP) and triphosphate. The reaction mixture contains also excess of SR to convert the PTP (in an NADPH-dependent reaction) to (6*R*)-L-*erythro*-5,6,7,8-tetrahydrobiopterin (BH_4), and NADH-dependent DHPR (to stabilize the formation of BH_4). PTPS activity is determined by measuring the biopterin, the completely oxidized form of BH_4. Oxidation is carried out in the presence of iodine at pH 1.0, and the generated biopterin is detected fluorimetrically at 350/440 nm upon HPLC separation. The assay was originally established by Shintaku et al. [19].

Preanalytical

Specimen

PTPS activity may be determined from red blood cells (RBC), cultivated primary dermal fibroblasts, or from lysates of tissue samples (e.g., liver or brain).

To prepare lysates from (nonstimulated) fibroblasts, cells from one confluent 78-cm^2 plate are suspended in 0.15 ml lysis buffer (see below) and lysed by freezing and thawing six times and subsequent centrifugation at 13,000 × *g* for 5 min. An aliquot of 0.05 ml of the supernatant is directly used for the enzyme assay. The preparation of tissue homogenate is described in section 6.1.4.1. GTP cyclohydrolase I, subheading "Specimen".

To assay PTPS from RBC, heparinized blood is the preferred sample. In case only EDTA-treated blood is available, manganese has to be added in excess to ensure that the manganese-dependent PTPS is fully operable (i.e., $MgCl_2$ is added to a final concentration of 14 mM). Furthermore, in order to avoid potential oxidation of the BH_4 product from the assay by the presence of oxygen bound to Hb (oxy-Hb), molecular oxygen has to be displaced by pretreatment of the blood with the gas carbon monoxide. A 2-ml aliquot of (heparin) blood is centrifuged for 10 min at 800 × *g*, the plasma discarded, and the approximately 0.2 ml of cells (RBC) are stored at –20°C. RBC are diluted with one volume (0.2 ml) of 0.2 M Tris-HCl buffer pH 7.4. Cells are lysed by freeze-thawing once with dry ice, treated with carbon monoxide for 1 min, and centrifuged at 15,000 × *g* for 2 min at 4°C. Supernatants of are kept at 4°C, or can be shock frozen and stored at –80°C.

Reagents and Chemicals (see also section 6.1.4.1, subheading "Reagents and Chemicals")

1. Lysis buffer: 10 mM Tris-HCl pH 7.4 containing 1% Triton X-100.
2. TCA solution 30% (Merck Cat No 1.00807.0100; MW 163.39): dissolve 30 g TCA in 100 ml of water; store at room temperature.
3. Iodine solution 1% (1% I_2; 2% KI): dissolve 0.1 g of I_2 and 0.2 g of KI in 10 ml of 1 M HCl; store in the dark.
4. Carbon monoxide gas: mix 2 ml of sulfuric acid (95–97%, Merck, Cat No 1.00731) and a few drops of formic acid (98–100%, Merck, Cat No 1.00263) in a glass container with a volume of 10–20 ml covered with a lid, and a syringe opening (gage 22). Carbon monoxide gas is produced spontaneously and exits through the syringe.
5. NADPH 20 mM (Boehringer, Mannheim, Cat No 107824; MW 833.4, tetrasodium salt): dissolve 16.7 mg in 1 ml of 0.1 M Tris-HCl pH 7.4; store at 4°C for 1 day. Prepare fresh.
6. NADH 20 mM (Boehringer, Mannheim, Cat No 107735; MW 709.4, disodium salt): dissolve 14.2 mg in 1 ml of 0.1 M Tris-HCl pH 7.4; store at 4°C for 1 day. Prepare fresh.
7. SR: the enzyme can be purified from erythrocytes [20] or as recombinant enzyme from bacteria [9,21,22]. Preferentially, we expressed the rat SR-cDNA as N-terminally poly histidine (His_6)-tagged protein in bacteria and purified it upon applying a commercially available nickel-nitrilotriacetic acid affinity column (Neuheiser, Blau and Thöny, unpublished). The noncleaved, highly active fusion protein is stored in liquid nitrogen at a concentration of 1 mg/ml and an activity of approximately 1 U/ml.

8. DHPR from sheep liver (Sigma, Cat No D-688): 96.15 U/ml; store at –20°C.
9. Dihydroneopterin triphosphate, NH_2P_3 (MW 492): NH_2P_3 is produced under nitrogen gas with immobilized recombinant rat GTPCH from the substrate GTP; store in liquid nitrogen or at –80°C. A concentration of approximately 0.5 mM of NH_2P_3 is used. A detailed description for the production of NH_2P_3 is in preparation elsewhere (Blau et al., unpublished). Alternatively, the substrate NH_2P_3 may be generated in situ by the presence of purified GTPCH in the reaction mixture. For more details see the method described by Ernst R. Werner and colleagues [23].
10. Reaction buffer is premixed immediately before use and contains 25 µl of 100mM Tris-HCL pH 7.4 (final concentration approximately 70 mM), 5.5 µl of 200 mM $MgCl_2$ (final concentration 10 mM), 5.5 µl of 20 mM NADPH (final concentration 1 mM), 5.5 µl of 20 mM NADH (final concentration 1 mM), 13.2 µl of 0.5 mM NH_2P_3 (final concentration 70–80 µM), 2.3 µl of 96 U/ml DHPR (final concentration 220 mU), and 3 µl of 1 U/ml SR (final concentration 3 mU).
11. Ascorbic acid 1% (Fluka, Cat No 95209; MW 176): dissolve freshly 0.1 g in 10 ml water.
12. Micron 10,000 filter (Millipore, Ultracel YM-10, Cat No 42408)
13. Protein assay solution (BioRad, Cat No 500-0006): determine the protein concentration according to the user manual.

Instrumentation

Besides routine laboratory equipment (see section 6.1.4.1, subheading "Instrumentation" under GTPCH), an HPLC system with fluorescent detection at 350/440 nm for biopterin determination is required (see section 6.1.3.1, subheading "Instrumentation").

Quality Control

PTPS activity measurements are not available in external control programs and can only be compared by exchanging results from other laboratories (for examples see www.bh4.org). Control biopterin (and neopterin) samples are commercially available from Dr. Schircks Laboratories, Jona, Switzerland (www.schircks.com). We recommend using internal controls (e.g., normal control fibroblasts in each enzyme assay and standard biopterin for HPLC analysis; see section 6.1.3.1, subheading "Instrumentation").

Analytical

Procedure

Besides the enzymatic incubation in the "reaction mixture," all procedures are carried out at 4°C. PTPS activity is assayed by measuring the biopterin produced upon enzymatic incubation at 37°C for 120 min in a final volume of 110 µl in the dark (due to the light sensitivity of pterins), followed by chemical oxidation. To stabilize the produced BH_4, DHPR and NADH are present in the enzyme assay. Two separate blanks are prepared, a blank reaction with cell lysate that is immediately oxidized to detect the biopterin that was present in the lysate, and a blank reaction without cell lysate to detect the biopterin that is generated from the incubation (substrate) buffer.

The sum of both blanks is later subtracted from the value of the incubation reaction to determine the enzymatic production of biopterin.

1. Reaction mixture: 60 µl of freshly prepared reaction buffer and 50 µl of filtered cell or tissue lysate (total volume of 110 µl). The reaction mixture is incubated for 2 h at 37°C in the dark, followed by adding 33 µl of 30% TCA solution, mixing, chilling on ice for 10 min, and centrifuged for 2 min at 13000 × *g*. A 100-µl aliquot of the supernatant is oxidized by adding 20 µl of 1% iodine solution. After incubation for 1 h in the dark at room temperature, 30 µl of 1% ascorbic acid is added, mixed, and centrifuged for 10 min at 13000 × *g* through a Millipore Ultrafree-MC 1000 filter. The filtrate is analyzed by HPLC (ideally only 10 µl of a 1:4 dilution with water is injected). The starting lysate of 50 µl was diluted twice, 2.86-fold and 1.5-fold, resulting in a final 4.29-fold dilution.
2. Blank reaction with cell lysate: 50 µl of filtered lysate plus 60 µl of 0.1 mM Tris-HCl buffer pH 7.4. Incubate at 4°C for 2 h in the dark, followed by the same oxidation procedure as for the reaction mixture (starting from adding the TCA solution).
3. Blank reaction without cell lysate: 60 µl of the reaction buffer plus 50 µl of 0.1 mM Tris-HCl pH 7.4 buffer. Incubate at 4°C for 2 h in the dark, followed by the same oxidation procedure as for the reaction mixture (starting from adding the TCA solution).

In RBC, the activity for PTPS is calculated in µU/g Hb. The Hb concentration is determined in g Hb/ volume (ml) by standard laboratory methods for Hb. The results for tissues or other cells like fibroblasts or amniocytes are given in mg protein/ml. To determine the protein concentration, use filtrates from Sephadex G-25 (MicroSpin) columns and proceed according to the protein assay method (BioRad).

Calculation

PTPS activity is determined as µU/g Hb or as µU/mg protein. One unit of PTPS produces 1 µmol of biopterin/min at 37°C. The results from the biopterin (B) determination by HPLC are given in nmol/l.

Calculate as follows:

1. Background: subtract the sum of blanks from the reaction mixture

$$B\ [\text{nmol/l}] = B_{\text{reaction mixture}} - (B_{\text{blank reaction with cell lysate}} + B_{\text{blank reaction without cell lysate}})$$

2. Correction factor:
   the ratio of 4.29 divided by 120 min results in nmol/l (factor of 0.03575):

$$B\ [\text{nmol/l}] \times 0.03575 = \mu\text{U PTPS/ml}$$

3. Activity per mg of protein: divide the activity per ml by the amount of Hb (in g) or total protein (in mg) per ml:

   µU PTPS/ml divided by g Hb/ml = µU PTPS/g Hb

   or

   µU PTPS/ml divided by mg protein/ml = µU PTPS/mg protein

Postanalytical

Interpretation

1. Chromatograms: chromatogram standards involve neopterin, biopterin, monapterin, pterin, and isoxanthopterin.
2. Reference and pathological values: reference values for PTPS of normal human RBC are 35–77 μU/g Hb for a fetus, 34–64 μU/g Hb for newborns (up to 1 month), and 11–29 μU/g Hb for children and adults. For dermal (nonstimulated) fibroblasts control values are 0.7 μU/mg (50th percentile; 0.4 μU/mg for the 5th percentile, and 1.6 μU/mg for the 95th percentile), and for autosomal recessive PTPS deficiency <0.05 μU/mg. The reference values for amniocytes are 3.0 μU/mg (50th percentile; 1.0 μU/mg for the 5th percentile, and 3.4 μU/mg for the 95th percentile). For the mouse, liver tissue values range from 13.0 to 25.8 μU/mg for adults and from 3.6 to 14.8 μU/mg for newborns, whereas whole brain tissue values are roughly threefold higher when given in μU/mg. For references see [13,24,25] and unpublished results from our laboratory.

Pitfalls

1. Sensitivity: not known. The threshold value for detection of enzyme activity is < 0.05 μU/mg.
2. Stability: freeze-thawing of tissue or fibroblast lysates may result in reduced PTPS activity, and it is thus recommended to assay activity always from freshly lysed material. However, lysates may be kept for 1–2 days at –80°C.
3. Check blood for the presence of reticulocytes (highest PTPS activity among all cells)!

6.1.4.3 SR (Fibroblasts, Amniocytes, Tissue)

Principle

The natural substrate for SR (EC 1.1.1.153) is the PTP that is converted in an NADPH-dependent reaction into BH_4. However, the activity of SR is assayed by measuring the conversion of the artificial substrate sepipaterin to BH_2 in the presence of NADPH in the dark. BH_2 is then oxidized in the presence of iodine at pH 1.0 to biopterin, which is detected fluorimetrically at 350/440 nm upon HPLC separation. The assay is based, with some modifications, on the method by Ferre and Naylor [24].

Preanalytical

Specimen

SR activity may be determined from cultivated primary dermal fibroblasts, or from lysates of tissue samples (e.g., liver or brain). To prepare lysates from (nonstimulated) fibroblasts, cells from one confluent 78-cm^2 plate are suspended in 1 ml of

lysis buffer (see below) and lysed by freezing and thawing six times and subsequent centrifugation at 13,000 × *g* for 5 min at 4°C. An aliquot of 0.05 ml of the supernatant is directly used for the enzyme assay. The preparation of tissue homogenate is described in section 6.1.4.1, subheading "Specimen". Supernatants are kept at 4°C, or can be shock frozen and stored at –80°C.

Reagents and Chemicals

1. Lysis buffer (0.1 M potassium phosphate pH 6.4, 0.15 mM KCl, 0.68 M glycerol, 2.5 mM EDTA): mix 20 ml of 1 M potassium phosphate pH 6.4, 2.2 g of KCl, 12.5 g glycerol, 1 ml of 0.5 M EDTA in a total volume of 200 ml water.
2. NADPH 2.5 mM (Boehringer, Cat No 107824; MW 833.4, tetrasodium salt): dissolve freshly 2.1 mg in 1 ml of 0.1 M potassium phosphate pH 6.4; store at 4°C for 1 day.
3. Sepiapterin 1.25 mM ($C_9H_{11}N_5O_3$, MW 237.2; aliquots of 0.1 ml are stored at –80°C): 3 mg are dissolved in 10 ml water. Upon opening, the tube is flushed with N_2. Verify concentration by measuring absorbance at 420 nm ($\varepsilon_{mM,420nm}$=10.4; i.e., for a 1:10 diluted solution, the absorbance is 1.3).
4. Reaction buffer (2 ×): the buffer is premixed immediately before use and contains 100 µl of 1 M KPO_4 pH 6.4 (final concentration 100 mM), 100 µl of 1.25 mM sepiapterin (final concentration 125 mM), 100 µl of 2.5 mM NADPH and 200 µl of water.
5. Oxidation solution (0.5% I_2, 1% KI in 1 M HCl): dissolve 0.25g I_2 and 0.5 g KI in 50 ml 1 M HCL; store at room temperature in the dark.
6. Ascorbic acid 1% (Fluka, Cat No 95209; MW 176): prepare freshly 1 mg in 0.1 ml water.
7. Micron 10,000 Filter (Millipore, Ultracel YM-10, Cat No 42408)
8. Protein Assay Solution (BioRad, Cat No 500-0006): determine the protein concentration according to the user manual.

Instrumentation

Besides routine laboratory equipment (see section 6.1.4.1, subheading "Instrumentation"), an HPLC system with fluorescent detection at 350/440 nm for biopterin determination is required (see section 6.1.3.1, subheading "Instrumentation").

Quality Control

SR activity measurements are not available in external control programs and can only be compared by exchanging results from other laboratories (for examples see www.bh4.org). Control biopterin (and neopterin) samples are commercially available from Dr. Schircks Laboratories, Jona, Switzerland (www.schircks.com). We recommend using internal controls (e.g., normal control fibroblasts in each enzyme assay and standard biopterin for HPLC analysis; see section 6.1.3.1, subheading "Instrumentation").

Analytical

Procedure

Besides the enzymatic incubation in the "reaction mixture," all procedures are carried out at 4°C. SR activity is assayed by measuring the BH_2 produced upon enzymatic incubation at 37°C for 30 min in a final volume of 50 µl in the dark (due to light sensitivity of pterins), followed by chemical oxidation to biopterin. Two separate blanks are prepared, a blank reaction with cell lysate that is immediately oxidized to detect the biopterin that was present in the lysate, and a blank reaction without cell lysate to detect the biopterin that is generated from the incubation (substrate) buffer. The sum of both blanks is later subtracted from the value of the incubation reaction to determine the enzymatic production of biopterin.

1. Reaction mixture: 25 µl of freshly prepared 2 × reaction buffer, 15 µl of water, and 10 µl of filtered cell or tissue lysate (total volume of 50 µl). The reaction mixture is incubated for 30 min at 37°C in the dark, followed by adding 10 µl of oxidation solution. After oxidation for 30 min in the dark at room temperature, 10 µl of 1% ascorbic acid is added, mixed, and centrifuged for 20 min at 14,000 × *g* through a Micron 10,000 filter (Millipore, Ultracel YM-10). The filtrate is analyzed by HPLC (ideally only 20 µl of a 1:2 dilution with water are injected into the HPLC system). The starting lysate of 10 µl was diluted sevenfold.
2. Blank reaction with cell lysate: 10 µl of lysis buffer, 25 µl of freshly prepared "2 ×" reaction buffer, and 15 µl of water. Incubate at room temperature for 30 min in the dark, followed by the same oxidation procedure as for the reaction mixture.
3. Blank reaction without cell lysate: contains 10 µl of filtered lysate, 25 µl of freshly prepared "2 ×" reaction buffer, and 15 µl of water. Incubate at room temperature for 30 min in the dark, followed by the same oxidation procedure as for the reaction mixture.

Calculation

SR activity is determined as µU/mg protein. One unit of SR produces biopterin at 1 µmol/min at 37°C. The results from the biopterin (B) determination by HPLC are given in nmol/l.

Calculate as follows:

1. Background: subtract the sum of blanks from the reaction mixture

$$B\ [\text{nmol/l}] = B_{\text{reaction mixture}} - (B_{\text{blank reaction with cell lysate}} + B_{\text{blank reaction without cell lysate}})$$

2. Correction factor: the ratio of 7 divided by 30 min results in nmol/l (factor of 0.233):

$$B\ [\text{nmol/l}] \times 0.233 = \mu\text{U SR/ml}$$

3. Activity per mg of protein: divide the activity per milliliter by the amount of total protein (in mg) per milliliter:

µU SR/ml divided by mg protein/ml = µU SR/mg protein

Postanalytical

Interpretation

1. Chromatograms: chromatogram standards involve neopterin, biopterin, monapterin, pterin, and isoxanthopterin.
2. Reference and pathological values: reference values for SR in (nonstimulated) dermal fibroblasts are for control cells 138 μU/mg (50th percentile; 99 μU/mg for the 5th percentile, and 185 μU/mg for the 95th percentile), and for autosomal recessive SR deficiency <10 μU/mg. The reference values for amniocytes are 143 μU/mg (50th percentile; 89 μU/mg for the 5th percentile, and 313 μU/mg for the 95th percentile). Mouse liver has an activity of around 150 μU/mg. For references see [26–29] and unpublished results from our laboratory.

Pitfalls

Not known.

6.1.4.4 DHPR (RBC, Fibroblasts, Amniocytes, Tissue)

Principle

DHPR (EC 1.6.99.7) converts (or recycles) under in vivo conditions the quinonoid BH_2 in an NADH-dependent reaction to BH_4. However, the activity of DHPR is assayed in fibroblasts by monitoring the oxidation of NADH at 340 nm during the reduction of 6,7-dimethyldihydropterin (quinonoid isomer) to 6,7-dimethyltetrahydropterin [30,31]. This method has high sensitivity but is not recommended for erythrocytes, due to interference with Hb. An alternative method for assaying DHPR from any source, including erythrocytes from whole blood or dried blood on Guthrie filter cards, is by nonenzymatic coupling of the oxidation of 6-methyltetrahydropterin (6-MPH_4) to quinonoid 6-methyldihydropterin to the reduction of ferricytochrome c to ferrocytochrome c. This nonenzymatic formation of ferrocytochrome c following an initial burst proceeds proportionally to the formation of 6-MPH_4 that is reduced back from quinonoid 6-methyldihydropterin by DHPR. Formation of ferrocytochrome c can be monitored at 550 nm. This assay is based on the method by Arai et al. [32,33].

Preanalytical

Specimen

DHPR activity may be determined from whole blood, RBC, dried blood from Guthrie cards, cultivated primary dermal fibroblasts, or from lysates of tissue samples (e.g., liver or brain).

To prepare hemolysate dilute 50 μl of whole blood or resuspend 25 μl of RBC in 1 ml of 0.15 M KCl and incubate for 30–40 min at room temperature for lysis. To prepare hemolysate from Guthrie cards, 4–6 circles with a diameter of 5 mm are cut

out from the filter paper and incubated for lysis in 1 ml of 0.15 M KCl for 30–40 min at room temperature. Centrifuge lysed erythrocytes cells from whole blood or from filter paper for 2 min at 12,000 × *g* and save supernatant for enzyme assay.

To prepare lysates from (nonstimulated) fibroblasts, cells from one confluent 78-cm² plate are suspended in 0.15 ml of lysis buffer (see below) and lysed by freezing and thawing six times and subsequent centrifugation at 13,000 × *g* for 5 min. An aliquot of 0.05 ml of the supernatant is directly used for the enzyme assay. The preparation of tissue homogenate is described in section 6.1.4.1, subheading "Specimen".

In RBC, the activity for DHPR is calculated in U/g Hb. The Hb concentration is determined in g Hb/ml by standard laboratory methods. The results for tissues or other cells like fibroblasts or amniocytes are given in mg protein/ml. To determine the protein concentration, use filtrates from Sephadex G-25 (MicroSpin) columns and proceed according to the protein assay method (BioRad). Supernatants are kept at 4°C, or can be shock frozen and stored at –80°C.

Reagents and Chemicals

1. Lysis buffer: 10 mM Tris-HCl buffer pH 7.4 containing 1% Triton X-100.
2. Ferricytochrome c 1 mM (Sigma, Typ VI No C 7752 ; MW 12'384): dissolve 99.2 mg in 8 ml of 5 mM Tris-HCl pH 7.4 containing 0.1 M KCl. Store at – 20°C for 1 month.
3. NADH 2 mM (Roche, Cat. No. 10107735001; MW 709.4, disodium salt): dissolve freshly 1.4 mg in 1 ml of 0.01 M KOH; store at 4°C for 1 day.
4. 6-MPH_4 20 mM (Schircks No 11.483, 6-MPH_4 × 2 HCl, MW 254): dissolve 5.1 mg of 6-MPH_4 ×2 HCl in 0.1 M HCl. The HCl solution should be freshly degassed. Freeze 0.1 ml aliquots at –20°C. Before use, an aliquot is thawed and diluted to 1 mM with 1.9 ml of 0.01 M HCl. This solution can be kept at 4°C for maximally 2 days.
5. DHPR as positive control (Sigma Sheep liver D-6888; 250 U in 2.6 ml; i.e., 96.15 U/ml): for dilution I (952 mU/ml) add 10 µl of the 96.15 U/ml DHPR to 1 ml of 0.15 M KCl; for dilution II (18.7 mU/ml) add 20 µl of the 952 mU/ml DHPR (dilution I) to 1 ml of 0.15 M KCl. Store dilutions at 4°C for 1 day. As a positive control, use 40 µl of dilution II for the assay (0.75 mU).

Instrumentation

Besides routine laboratory equipment (see section 6.1.4.1, subheading "Instrumentation"), a VIS photospectrometer for quantitative detection at 550 nm of ferrocytochrome c is required.

Quality Control

DHPR activity measurements are not available in external control programs and can only be compared by exchanging results from other laboratories (for examples see www.bh4.org). For internal control, we recommend using dilution II (40 µl, with an activity of 0.75 mU/ml; see below), and blood from normal control subjects.

Analytical

Procedure

DHPR activity is assayed by measuring the linear increase of ferrocytochrome c at 550 nm (ΔE_{550nm}; $\varepsilon_{mM,550nm} = 21$) upon enzymatic incubation at 25°C for 5 min in a volume of 1 ml. The incubation mixture contains 40 µl lysate, 875 µl of 50 mM Tris-HCl pH 7.6, 50 µl of the 1 mM ferricytochrome c solution, and 25 µl of the 2 mM NADH solution. The blank control contains 40 µl of Tris-HCl pH 7.6 instead of the lysate. These mixtures are preincubated for 5 min at 25°C, before the reaction is started by addition of 10 µl of the 1 mM 6-MPH_4 substrate. The reaction is monitored by measuring the ΔE_{550nm}/min over a period of 5 min. The starting lysate of 40 µl was diluted 25-fold.

Calculation

To calculate the DHPR activity in milliunits in the 1-ml assay, the observed ΔE_{550nm} is divided by 21 ($\varepsilon_{mM,550nm}$ for the ferrocytochrome c) and by 5 (per min), and multiplied by 25 for the dilution. One unit of DHPR produces 1 µmol of ferrocytochrome c per minute at 25°C.

Calculate as follows:

1. Background: for a single-beam ultraviolet instrument, subtract the ΔE_{550nm} from the reaction mixture from the ΔE_{550nm} for the blank control:

$$\Delta E_{550nm} = \Delta E_{550nm,\ reaction\ mixture} - \Delta E_{550nm,\ blank\ control}$$

2. Correction factor: the ratio of 25 divided by 5 (min) and by 21 (ε_{mM}) results in nmol/min [factor $238 = (1000 \times 25)/(21 \times 5)$]:

$$\Delta E_{550nm} \times 238 = \text{mU DHPR/ml}$$

Activity per mg of protein: divide the activity per milliliter by the amount of Hb (in mg) or total protein (in mg) per milliliter:

$$\text{mU DHPR/ml divided by mg Hb/ml} = \text{mU DHPR/mg Hb}$$

or

$$\text{mU DHPR/ml divided by mg protein/ml} = \text{mU DHPR/mg protein}$$

Postanalytical

Interpretation

1. Chromatograms: chromatogram standards involve neopterin, biopterin, monapterin, pterin, and isoxanthopterin.
2. Reference and pathological values: reference values for DHPR in (nonstimulated) dermal fibroblasts are for control cells 6.7 mU/mg (50th percentile; 4.5 mU/mg for the 5th percentile, and 8.3 mU/mg for the 95th percentile), and for autosomal recessive DHPR deficiency < 0.3 mU/mg. The reference values for amniocytes are 7.5 mU/mg (50th percentile; 5.6 mU/mg for the 5th percentile, and 9.6 mU/mg for the 95th percentile). References in dried blood from Guthrie cards are 1.8–3.8 mU/mg Hb). A decrease in activity was observed after 1 year of age (0–1 year, 5.4–8.9 mU/mg; >1 year, 4.2–7.0 mU/mg). No differences were

observed in other age groups over 1 year. For references see [34–37] and unpublished results from our laboratory.

Pitfalls

DHPR activity decreases with increasing Hb concentrations (unpublished observation).

6.1.4.5 Cytokine Stimulation (for GTPCH Assay and Pterin Production)

Principle

GTPCH activity may be regulated at the transcriptional and post-translational levels, and in many cells types, including dermal fibroblasts, expression is inducible by various immune stimuli like the cytokines INF-γ and TNF-α, but also phytohemagglutinins and endotoxins [30,38]. Primary dermal fibroblasts do not express GTPCH at all without prior immuostimulation, but contain all other BH_4-metabolizing enzymes. It thus became a standard diagnostic procedure to indirectly measure pterin metabolism and/or GTPCH deficiency by inducing GTPCH gene expression in primary dermal fibroblasts with a cocktail of INF-γ and TNF-α [31,34].

Preanalytical

Specimen

A confluent fibroblast cell monolayer in 78-cm² plates, cultured in fresh DMEM (see section 6.1.4.1, subheading "Specimen"), is incubated with recombinant human INF-γ (2.5 µl per 5 ml DMEM; 1250 U) and TNF-α (2.5 µl per 5 ml DMEM; 500 U). After stimulation for 24 h, cells are harvested by trypsinization, washed with PBS, and immediately lysed for neopterin and biopterin measurements and for GTPCH activity assay.

Reagents and Chemicals

See section 6.1.4.1, subheading "Reagents and Chemicals"

Instrumentation and Analytical Procedure

See above.

Acknowledgments

Lucja Kierat, Thomas Polanski, Konrad Gärtner, Marcel Zurflüh, Tanja Scherer, Ernst R. Werner

References

1. Thöny B, Auerbach G, Blau N (2000) Tetrahydrobiopterin biosynthesis, regeneration, and functions. Biochem J 347:1–26
2. Kuster T, Matasovic A, Niederwieser A (1984) Application of gas chromatography-mass spectrometry to the study of biopterin metabolism in man. Detection of biolumazine and 2'-deoxysepialumazine. J Chromatogr 290:303–310
3. Rembold H (1983) Pteridine catabolism. In: Curtius HC, Pfleidere W, Wachter H (eds) Biochemical and Clinical Aspects of Pteridines. Walter de Gruyter, Berlin, pp 107–122
4. Blau N, de Klerk JBC, Thöny B, Heizmann CW, Kierat L, Smeitink JAM, Duran M (1996) Tetrahydrobiopterin loading test in xanthine dehydrogenase and molybdenum cofactor deficiencies. Biochem Mol Med 58:199–203
5. Murr C, Widner B, Wirleitner B, Fuchs D (2002) Neopterin as a marker for immune system activation. Curr Drug Metab 3:175–187
6. Blau N, Thöny B, Cotton RGH, Hyland K (2001) Disorders of tetrahydrobiopterin and related biogenic amines. In: Scriver CR, Beaudet AL, Sly WS, Valle D, Childs B, Vogelstein B (eds)The Metabolic and Molecular Bases of Inherited Disease. McGraw-Hill, New York, pp 1725–1776
7. Blau N, Barnes I, Dhondt JL (1996) International database of tetrahydrobiopterin deficiencies. J Inherit Metab Dis 19:8–14
8. Ichinose H, Ohye T, Takahashi E, Seki N, Hori T, Segawa M, Nomura Y, Endo K, Tanaka H, Tsuji S, Fujita K, Nagatsu T (1994) Hereditary progressive dystonia with marked diurnal fluctuation caused by mutation in the GTP cyclohydrolase I gene. Nature Genet 8:236–241
9. Bonafé L, Thöny B, Penzien JM, Czarnecki B, Blau N (2001) Mutations in the sepiapterin reductase gene cause a novel tetrahydrobiopterin-dependent monoamine neurotransmitter deficiency without hyperphenylalaninemia. Am J Hum Genet 69:269–277
10. Blau N, Thöny B, Spada M, Ponzone A (1996) Tetrahydrobiopterin and inherited hyperphenylalaninemias. Turk J Pediatr 38:19–35
11. Fukushima T, Nixon JC (1980) Analysis of reduced forms of biopterin in biological tissues and fluids. Anal Biochem 102:176–188
12. Niederwieser A, Staudenmann W, Wetzel E (1984) High-performance liquid chromatography with column switching for the analysis of biogenic amine metabolites and pterins. J Chromatogr 290:237–246
13. Blau N, Bonafé L, Blaskovics M (2005) Disorders of phenylalanine and tetrahydrobiopterin metabolism. In: Blau N, Duran M, Blaskovics M, Gibson KM (eds) Physician's Guide to the Laboratory Diagnosis of Metabolic Disease. Springer, Heidelberg, pp 89–106
14. Howells DW, Hyland K (1987) Direct analysis of tetrahydrobiopterin in cerebrospinal fluid by high-performance liquid chromatography with redox electrochemistry: prevention of autoxidation during storage and analysis. Clin Chim Acta 167:23–30
15. Viveros OH, Lee CL, Abou-Donia MM, Nixon JC, Nichol CA (1981) Biopterin cofactor biosynthesis: independent regulation of GTP cyclohydrolase in adrenal medulla and cortex. Science 213:349–350
16. Hatakeyama K, Yoneyama T (1998) A sensitive assay for the enzymatic activity of GTP cyclohydrolase I. Methods Mol Biol 100: 265–272
17. Bonafé L, Thöny B, Leimbacher W, Kierat L, Blau N (2001) Diagnosis of Dopa-responsive dystonia and other tetrahydrobiopterin disorders by the study of biopterin metabolism in fibroblasts. Clin Chem 47:477–485
18. Elzaouk L, Leimbacher W, Turri M, Ledermann B, Bürki K, Blau N, Thöny B (2003) Dwarfism and low IGF-1 due to dopamine depletion in Pts–/– mice rescued by feeding neurotransmitter precursors and H4-biopterin. J Biol Chem 278:28303–28311
19. Shintaku H, Niederwieser A, Leimbacher W, Curtius HC (1988) Tetrahydrobiopterin deficiency: assay for 6-pyruvoyl-tetrahydropterin synthase activity in erythrocytes, and detection of patients and heterozygous carriers. Eur J Pediatr 147:15–19
20. Sueoka T, Katoh S (1982) Purification and characterization of sepiapterin reductase from rat erythrocytes. Biochim Biophys Acta 717:265–271

21. Citron BA, Milstien S, Gutierrez JC, Levine RA, Yanak BL, Kaufman S (1990) Isolation and expression of rat liver sepiapterin reductase cDNA. Proc Natl Acad Sci U S A 87:6436–6440
22. Ichinose H, Katoh S, Sueoka T, Titani K, Fujita K, Nagatsu T (1991) Cloning and sequencing of cDNA encoding human sepiapterin reductase – an enzyme involved in tetrahydrobiopterin biosynthesis. Biochem Biophys Res Commun 179:183–189
23. Werner ER, Wachter H, Werner Felmayer G (1997) Determination of tetrahydrobiopterin biosynthetic activities by high-performance liquid chromatography with fluorescence detection. In: McCormick DB, Suttie JW, Wagner C (eds) Methods in Enzymology: Vitamins and Coenzymes. Academic Press, San Diego, pp 53–61
24. Ferre J, Naylor EW (1988) Sepiapterin reductase in human amniotic and skin fibroblasts, chorionic villi, and various blood fractions. Clin Chim Acta 174:271–282
25. Blau N, Bonafé L, Thöny B (2001) Tetrahydrobiopterin deficiencies without hyperphenylalaninemia: diagnosis and genetics of Dopa-responsive dystonia and sepiapterin reductase deficiency. Mol Genet Metab 74:172–185
26. Milstien S, Holtzman NA, O Flynn ME, Thomas GH, Butler IJ, Kaufman S (1976) Hyperphenylalaninemia due to dihydropteridine reductase deficiency. Assay of the enzyme in fibroblasts from affected infants, heterozygotes, and in normal amniotic fluid cells. J Pediatr 89:763–766
27. Arai N, Narisawa K, Hayakawa H, Tada K (1982) Hyperphenylalaninemia due to dihydropteridine reductase deficiency: diagnosis by enzyme assays on dried blood spots. Pediatrics 70:426–430
28. Narisawa K, Arai N, Hayakawa H, Tada K (1981) Diagnosis of dihydropteridine reductase deficiency by erythrocyte enzyme assay. Pediatrics 68:591–592
29. Werner-Felmayer G, Golderer G, Werner ER (2002) Tetrahydrobiopterin biosynthesis, utilization and pharmacological effects. Curr Drug Metab 3:159–173
30. Thöny B (2006) Tetrahydrobiopterin and its function. In: Blau N (ed) PKU and BH4: Advances in Phenylketonuria and Tetrahydrobiopterin Research. SPS Publications, Heilbronn pp 503–554
31. Werner ER, Werner-Felmayer G, Fuchs D, Hausen A, Reibnegger G, Wachter H (1989) Parallel induction of tetrahydrobiopterin biosynthesis and indoleamine 2,3-dioxygenase activity in human cells and cell lines by interferon-gamma. Biochem J 262:861–866
32. Arai N, Narisawa K, Hayakawa H, Tada K (1982) Hyperphenylalaninemia due to dihydropteridine reductase deficiency: diagnosis by enzyme assays on dried blood spots. Pediatrics 70:426–430
33. Narisawa K, Arai N, Hayakawa H, Tada K (1981) Diagnosis of dihydropteridine reductase deficiency by erythrocyte enzyme assay. Pediatrics 68:591–592
34. Bonafe L, Thöny B, Leimbacher W, Kierat L, Blau N (2001) Diagnosis of dopa-responsive dystonia and other tetrahydrobiopterin disorders by the study of biopterin metabolism in fibroblasts. Clin Chem 47:477–485
35. Elzaouk L, Leimbacher W, Turri M, Ledermann B, Bürki K, Blau N, Thöny B (2003) Dwarfism and low insulin-like growth factor-1 due to dopamine depletion in Pts–/– mice rescued by feeding neurotransmitter precursors and H4-biopterin. J Biol Chem 278:28303–28311
36. Blau N, Duran M, Blaskovics ME, Gibson KM (eds) (2003) Physician's Guide to the Laboratory Diagnosis of Metabolic Diseases, 2nd edn. Springer Verlag, Berlin Heidelberg
37. Blau N, Bonafe L, Thöny B (2001) Tetrahydrobiopterin deficiencies without hyperphenylalaninemia: diagnosis and genetics of dopa-responsive dystonia and sepiapterin reductase deficiency. Mol Genet Metab 74:172–185
38. Werner-Felmayer G, Golderer G, Werner ER (2002) Tetrahydrobiopterin biosynthesis, utilization and pharmacological effects. Curr Drug Metab 3:159–173
39. Hyland K, Heales SJ. (1993) Tetrahydrobiopterin and quinonoid dihydrobiopterin concentrations in CSF from patients with dihydropteridine reductase deficiency. J Inherit Metab Dis 16:608–610

6.2 Biogenic Amines

Simon J.R. Heales

6.2.1 Introduction

Whilst the term "biogenic amine" strictly encompasses all amines of biological origin, for the purpose of this article it will be employed to refer to the catecholamine (dopamine, noradrenaline) and serotonin group of neurotransmitters. These neurotransmitters are generated from the amino acid precursors tyrosine and tryptophan, respectively, via the action of the tetrahydrobiopterin (BH_4)-dependent tyrosine and tryptophan hydroxylases. Hydroxylation of the amino acid substrates leads to formation of 3,4-dihydroxy-l-phenylalanine (l-dopa) and 5-hydroxytryptophan, which are then decarboxylated via the pyridoxalphosphate-dependent aromatic amino acid decarboxylase (AADC) to yield dopamine and serotonin [4]. In noradrenergic neurones, dopamine is further metabolised to noradrenaline through the action of dopamine-β-hydroxylase [1].

Within the central nervous system (CNS), dopamine, noradrenaline and serotonin have a diverse range of actions that include control of psychomotor function, regulation of motor coordination, processing of sensory input, arousal, emotional stability, temperature regulation, memory, appetite, mood and sleep. The biogenic amines considered here, in common with other neurotransmitter groups, exert their biological action as result of being released, in response to an action potential, from the presynaptic nerve terminal and binding to postsynaptic receptors where they elicit a biological response (e.g. excitation or inhibition of the target cell). The neurotransmitters are removed from the synaptic cleft and may be sequestered into vesicles and used again as neurotransmitters, or are metabolised further. With regard to the latter, dopamine is acted upon by catechol-O-methyltransferase (COMT) and the monoamine oxidase (MAO)/aldehyde dehydrogenase (ALD; MAO + ALD) system to form homovanillic acid (HVA). In similar manner, MAO + aldehyde reductase and COMT form 3-methoxy-4-hydroxy-phenylglycol (MHPG) from noradrenaline. With regard to serotonin, MAO + ALD activity results in the generation of 5-hydroxyindoleacetic acid (5HIAA). Determination of the concentration of these metabolites, particularly in cerebrospinal fluid (CSF), is considered to accurately reflect the integrity of catecholamine and serotonin metabolism within the CNS and has been instrumental in the identification and subsequent treatment of the disorders of biogenic amine metabolism (e.g. the inborn errors of BH_4 metabolism), tyrosine hydroxylase deficiency, AADC deficiency and disorders of pyridoxal phosphate metabolism [1, 3, 7].

6.2.2 Properties of Analytes

As a result of a high index of clinical suspicion and, on occasion, supporting biochemical data from other investigations, one of the first specialist investigations to ascertain whether a patient has an inborn error of biogenic amine metabolism is, as mentioned above, analysis of the CSF concentrations of HVA and 5HIAA. This is often performed in conjunction with the measurement of 3-methyldopa (3-MD), also known as 3-methoxytyrosine. 3-MD is formed from L-dopa via COMT activity and accumulates in conditions where aromatic amino acid decarboxylase activity is impaired. The chemical structures of HVA, 5HIAA and 3-MD are shown in Fig. 6.2.1.

The chemical properties of HVA, 5HIAA and 3-MD make them amenable to reverse-phase high-performance liquid chromatography (HPLC) with electrochemical detection. Furthermore, the composition of CSF means that little, if any, sample preparation is required prior to analysis. However, the susceptibility of these metabolites to oxidation means that careful sample collection and storage is required in order to minimise analyte degradation.

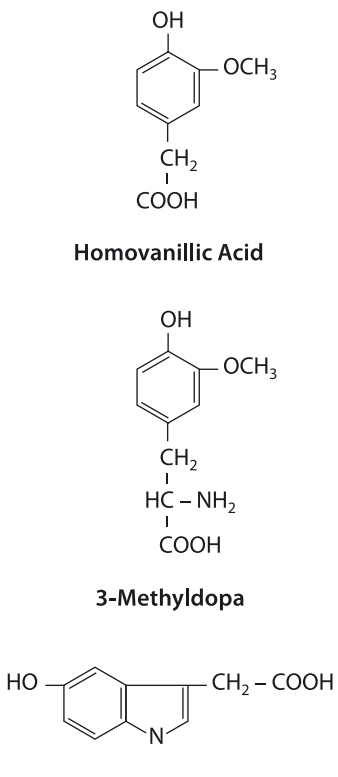

Fig. 6.2.1 The chemical structures of homovanillic acid (HVA), 5-hydroxyindoleacetic acid (5HIAA), and 3-methyldopa (3-MD)

6.2.3 Methods

6.2.3.1 Specimen – CSF

Lumbar CSF is required for this assay. As there is a rostrocaudal gradient for both HVA and 5HIAA, it is essential that the first 0.5 ml of fluid from the spinal tap is collected to allow accurate evaluation and interpretation of results in comparison to the age-dependent reference range. The sample must be collected into a properly labelled screw-top microcentrifuge tube and frozen at the bedside in liquid nitrogen or dry ice. Samples should then be transported to the laboratory on dry ice and stored at –70°C until analysis. Blood contamination will affect the results, as iron released from red blood cells will degrade both HVA and 5HIAA. If the CSF is contaminated with blood it should be placed on ice immediately and centrifuged within 5 min. The clear supernatant should then be frozen immediately and stored at –70°C.

6.2.3.2 HPLC of Biogenic Amine Metabolites

Principle

HVA, 5HIAA and 3-MD are amenable to separation by reverse-phase HPLC utilising an octadecylsilyl (ODS) column and detection by electrochemistry. The elution order of analytes on a reverse-phase HPLC column is in order of increasing hydrophobicity (i.e. 5HIAA elutes prior to HVA). The mobile phase is at an acidic pH to help suppress ionisation of the analytes. However, molecules with a catechol ring will remain positively charged even at pH 2. Consequently, an ion pairing agent, sodium octane sulphonic acid (OSS) is also added to the mobile phase to fully suppress the charge and hence optimise interaction with the stationary phase of the column. Methanol is also added in order to decrease the retention time of the analysis.

Chemicals

1. Potassium dihydrogen orthophosphate (KH_2PO_4).
2. OSS.
3. Ethylenediaminetetraacetic acid (EDTA).
4. Methanol (HPLC electrochemical detector grade).
5. Hydrochloric acid (HCl).
6. HVA.
7. 5HIAA.
8. 3-MD.

Instrumentation

1. Isocratic HPLC system with electrochemical detection (5010 Electrode, ESA, Chelmsford, USA). Upstream Electrode, 50 mV, downstream electrode, 450 mV.
2. Column: C18, 5 μm, 25 cm × 4.6 mm. Injection volume 50 μl.

3. Mobile phase: 50 mM potassium dihydrogen phosphate (pH 2.6, adjust with concentrated HCL), 1 mM OSS, 50 μM EDTA and 17% methanol. Ultrapure Milli-Q water (18 MΩ) must be employed throughout.
4. Flow rate 1.3 ml/min. The column is maintained at 35°C by surrounding the column with a heating block.

Calibration

Standards

Stock Solutions

The stock standards of HVA and 5HIAA and 3-MD are made to a final concentration of 500 μM as follows:

1. HVA and 5HIAA: using a 100 ml volumetric, dissolve 9.11 mg of HVA and 9.56 mg of 5HIAA in 80 ml of ultra pure H_2O. Make up to 100 ml using Milli-Q H_2O and sonicate for 1 min. Mix thoroughly and aliquot immediately the solid has dissolved. Aliquots of 0.5 ml should then be transferred into labelled Eppendorf tubes, frozen rapidly in liquid nitrogen, and stored at –70°C.
2. 3-MD: Using a 100 ml volumetric flask, dissolve 10.56 mg 3-MD in 80 ml of ultra pure H_2O. Make up to 100 ml using Milli-Q H_2O. Mix thoroughly and aliquot 0.5 ml into labelled Eppendorf tubes. Freeze rapidly in liquid nitrogen and store at –70°C.

Working Standard

The working standard solutions of HVA and 5HIAA, and 3-MD are stable for 1 day if stored at 2–8°C, and are made to a final concentration of 500 nM as follows. Remove the stock solution from the –70°C freezer, thaw, and mix thoroughly. Add three drops of concentrated HCl to approximately 80 ml of Milli-Q H_2O and mix. Add 100 μl of HVA, 5HIAA and 3-MD stock standards and make up to 100 ml. Mix well and store at 2–8°C.

Quality Control

An established external quality control (QC) scheme is not currently available. Pooled "disease control" CSF retained from other analyses is used. Aliquots of the pooled CSF are made and stored at –70ºC. This CSF is analysed on five separate occasions and the mean and standard deviation determined. For an analytical/diagnostic run to proceed, analysis of QC material must provide concentration values that are within two standard deviations (plus and minus) of the calculated mean for that particular QC. Construction of Levy-Jennings type control charts provide historical information of overall performance and highlight potential deterioration in the performance of the system.

Procedure

Fifty-microlitre aliquots of standards, QC material or neat CSF are injected directly onto the HPLC system. Blood-contaminated CSF should be filtered using a 10,000-molecular-weight (MW) centrifugal filtration system (e.g. Millipore Ultrafree-MC centrifugal filters) prior to injection.

Calculation

The concentrations of each analyte can be calculated by relating the peak area in the sample chromatogram to the peak area in the standard chromatogram as follows:

$$[\text{analyte}] = \frac{\text{peak area in sample}}{\text{peak area in standard}} \times 500 \text{ nM peak area in standard}$$

6.2.3.3 Interpretation

Chromatograms

Under normal conditions, a relatively clear chromatogram is generated following injection of calibration standards or CSF sample (Fig. 6.2.2). Peak identification and quantification of HVA, 5HIAA and 3-MD (when present) is straightforward. The authenticity of a particular assigned peak can be checked further by spiking CSF samples with standards of HVA, 5HIAA and 3-MD.

6.2.3.4 Reference Values

The data in Table 6.2.1 report reference ranges for HVA and 5HIAA when the first 0.5 ml of CSF is collected for analysis [6]. With regard to 3-MD, <300 nmol/l is considered as acceptable for children up to 6 months of age. Between 6 months and 1 year this declines to <100 nmol/l. For individuals 1 year and over, the acceptable upper limit is 50 nmol/l.

6.2.3.5 Diagnostic Profiles

Assignment of exact pathological values for the CSF biogenic amine metabolites encountered in the different known inborn errors of biogenic amine metabolism is not possible. Current experience suggests that the magnitude of the deficiency for a specific metabolite varies considerably. However, deviation of individual metabolite concentrations from established reference intervals provides profiles indicative of particular disorders. Table 6.2.2 provides a summary of such changes. However, these should be considered in conjunction with other investigations (see below) and the clinical picture before a suggested diagnosis is made and treatment regimes instigated.

Inspection of Table 6.2.2 shows that for tyrosine hydroxylase deficiency, only the concentration of HVA is decreased [2]. However, in cases of AADC deficiency, in

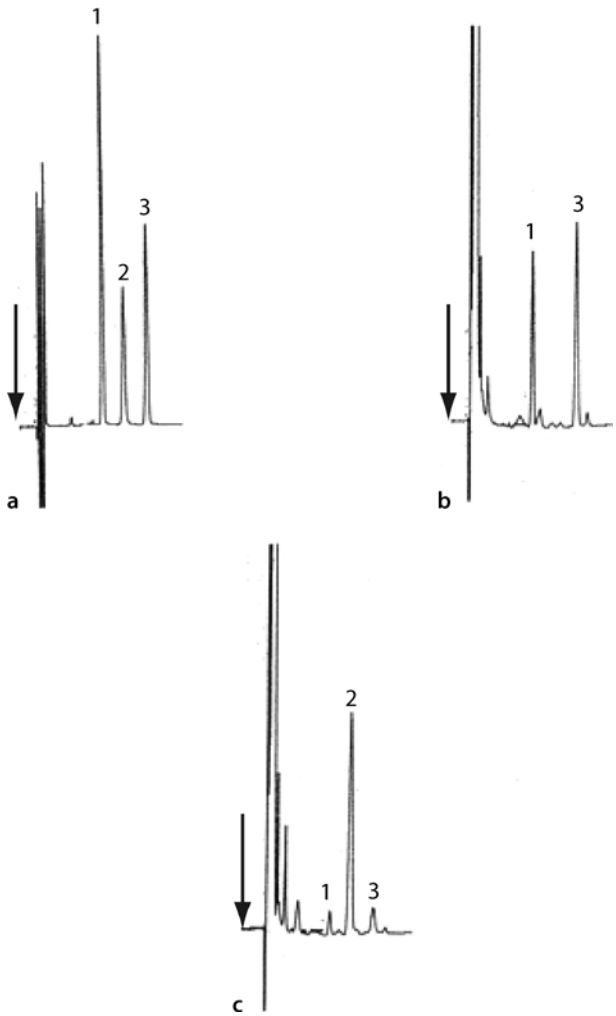

Fig. 6.2.2a–bc High-performance liquid chromatography (HPLC) with electrochemical (EC) detection of neurotransmitter metabolites. **a** standard mixture; **b** cerebrospinal fluid (CSF) sample – control; c CSF sample – aromatic amino acid decarboxylase (AADC) deficiency. Peak identification: 1 = 5HIAA (7.7 min), 2 = 3-MD (9.6 min), 3 = HVA (11.7 min)

view of the duel role this enzyme plays in dopamine and serotonin synthesis, both the HVA and 5HIAA concentration are decreased. Furthermore, deficiency of AADC will result in an accumulation of L-dopa, which, as described above, is metabolised to 3-MD. Hence in AADC deficiency there is an accumulation of 3-MD within the CSF (Fig. 6.2.2c) [5]. AADC is an enzyme that has a requirement for the co-factor, pyridoxal phosphate. Consequently, decreased availability of pyridoxal phosphate (PLP), as occurs in pyridox(am)ine-5'-phosphate oxidase (PNPO) deficiency, will impair AADC activity and result in a CSF biogenic amine metabolite profile that mimics AADC deficiency [7]. With regards to dopamine-β-hydroxylase deficiency, an increase in HVA concentration can occur due to dopamine accumulation.

Table 6.2.1 *Age-related reference ranges for homovanillic acid (*HVA*) and 5-hydroxindoleacetic acid (*5HIAA*). Values are expressed as nmol/l. These reference ranges were established in the author's laboratory using the first 0.5 ml of lumbar cerebrospinal fluid (*CSF*)*

	Age (years)	Minimum	Maximum
HVA (nmol/l)	0–0.33	324	1098
	0.34–0.66	362	955
	0.67–1.0	176	851
	1.1–5.0	154	867
	5.1–Adult	71	565
5HIAA (nmol/l)	0–0.33	199	608
	0.34–0.66	63	503
	0.67–1.0	68	451
	1.1–5.0	89	367
	5.1–Adult	58	220

Table 6.2.2 *Typical CSF profiles of HVA, 5HIAA and 3-methyldopa (*3-MD*) for the inborn errors of metabolism associated with a disruption of biogenic amine metabolism. A* downward-pointing arrow *indicates that a particular metabolite is below the established reference range. An* upward pointing arrow *is indicative that a metabolite is above the established reference range.* WR *indicates that the concentration of the metabolite is likely to be within the reference range.* AADC *Aromatic amino acid decarboxylase,* PNPO *pyridox(am)ine-5'-phosphate oxidase*

Deficiency	HVA	5HIAA	3-MD
Tyrosine hydroxylase	↓	WR	WR
AADC	↓	↓	↑
PNPO	↑	↑	↑
Dopamine β hydroxylase	↑	WR	WR
Pterin (recessive)	↓	↓	WR
Pterin (dominant)	WR - ↓	WR - ↓	WR
"Tryptophan hydroxylase"	WR	↓	WR

BH_4 is an obligatory cofactor for both tyrosine and tryptophan hydroxylase. Consequently, the inborn errors of BH_4 metabolism are associated with impaired dopamine and serotonin turnover, which is reflected by decreased concentrations of HVA and 5HIAA in the CSF. Whilst such a pattern is particularly true for the autosomal recessive disorders of BH_4 metabolism, an autosomal dominant disorder of BH_4 metabolism, (autosomal dominant GTP cyclohydrolase deficiency) is not always associated with marked decreases in the CSF concentration of HVA and 5HIAA [1].

To date, a fully documented case of tryptophan hydroxylase deficiency has not been described. However, such a deficiency would be predicted to have a characteristic CSF profile (i.e. an isolated decrease in CSF 5HIAA concentration).

In addition to the aforementioned inborn errors of metabolism, deficiencies in the catabolism of dopamine and serotonin would also be expected to result in decreased concentrations of HVA and 5HIAA (e.g. MAO deficiency and COMT deficiency).

Marked elevations in the CSF concentration of HVA have been reported in a group of children with infantile parkinsonism-dystonia. However, despite this unique metabolite profile, the underlying biochemical/molecular mechanism remains to be elucidated.

6.2.3.6 Pitfalls

Apparent perturbations of monoamine metabolism may arise as a consequence of an ongoing neurodegenerative process that results in the loss of dopamine- and/or serotonin-containing neurones. Such loss could therefore produce a CSF metabolite profile characteristic of one of the inborn errors of metabolism documented above.

The effects of any medication a patient is receiving close to the time of lumbar puncture should also be considered. Ideally, these should be documented on the sample request form. Thus, patients receiving L-dopa will have an elevated concentration of 3-MD in their CSF, which could, if the laboratory is not aware that the patient is receiving this drug, raise the possibility of AADC or PNPO deficiency. However, the 5-hydroxytryptophan concentration would be normal. Patients receiving ionotropic support in the form of dopamine will have markedly elevated levels of HVA, which could, if the laboratory is ignorant of the dopamine administration, suggest a disruption of dopamine metabolism (i.e. a profile would be generated that would be comparable to that described above for children with parkinsonism-dystonia).

Other medications that could theoretically lead to the erroneous suggestion that a patient has an inborn error of biogenic amine metabolism include serotonin reuptake inhibitors, MAO and COMT inhibitors.

In addition to the factors considered above, an apparent decrease in biogenic amine metabolite concentrations can arise as a result of poor sample handling or contamination of the CSF sample with blood. With regard to the former, a prolonged delay between obtaining a sample and freezing it can lead to a degradation of the metabolites to be analysed. This degradation is accelerated if the CSF is contaminated with blood. If blood contamination occurs, the sample should, if possible, be immediately centrifuged and the resulting clear supernatant stored frozen until analysis. If centrifugation is not possible, the CSF can be frozen. Upon thawing and prior to injection onto the HPLC system, the CSF can be centrifuged through a 10,000-MW cut-off filter. The clear filtrate can then be analysed. Whilst this procedure will eventually remove the blood contamination, it is likely that some metabolite degradation will have occurred prior to filtration. Consequently, reports generated from samples processed this way should clearly make this point.

6.2.4 Follow-up and Supporting Assays

Whenever a CSF profile is suggestive of a disruption of dopamine and/or serotonin metabolism, analysis of the pterin profile is extremely important in order to ascertain whether disruption of biogenic amine metabolism is directly related to alteration in BH_4 availability.

Defects affecting dopamine and serotonin metabolism can not be diagnosed with any confidence by metabolite profiling of peripheral fluids such as urine. Whilst urinary profiles of neurotransmitter metabolites can support a proposed diagnosis, it is clear that such metabolites can be within normal reference ranges in disorders such as tyrosine hydroxylase deficiency. With regard to tyrosine hydroxylase, the enzyme is expressed predominantly in the brain and adrenal medulla, which means that diagnostic enzymatic analysis is not an option. However, mutation analysis is now available in order to confirm or refute a finding from CSF analysis.

Analysis of dopamine-β-hydroxylase activity in plasma can not be used to make a definitive diagnosis, as approximately 4% of the population have very low plasma activities. Support for such a diagnosis can come from examining the noradrenaline: dopamine ratio in plasma. This is markedly reduced in this condition. Deficiencies of the MAO isoforms have been confirmed from enzymatic analysis of fibroblasts (MAO-A) or platelets (MAO-B).

With regard to AADC, vanillactic acid (a metabolite of 3-MD) appears in the urine and can be detected by organic acid analysis. As predicted, an increase in urinary vanillactic acid has also been reported in PNPO deficiency. The PLP concentration in CSF, which can be determined by HPLC, is also reported to be decreased in PNPO deficiency. Mutation analysis can also now confirm or refute a suggestion of PNPO deficiency.

As AADC is expressed in plasma, enzymatic analysis to elucidate further upon a suggestive CSF profile can be performed.

6.2.4.1 AADC Activity

Principle

This procedure is based on the formation of dopamine from L-dopa catalysed by AADC in plasma. The dopamine formed is detected by HPLC and electrochemical detection [4]:

$$\text{L-Dopa} \xrightarrow[\text{PLP}]{\text{AADC}} \text{dopamine}$$

Specimen

Plasma separated from heparin- or EDTA-treated blood. The required minimal volume is 1 ml. Store immediately at –80°C.

Pitfall

L-Dopa medication may interfere with the assay. Stop L-dopa at least 3 days before blood collection.

Chemicals

1. 1,4-Dithioerythritol (DTE).
2. L-Dopa.
3. Ascorbic acid.
4. Dopamine.
5. EDTA.
6. 6 M HCl.
7. Perchloric acid (PCA) 70% ($HC1O_4$).
8. Phosphoric acid 85% (H_3PO_4).
9. PLP.
10. Sodium phosphate dibasic (Na_2HPO_4).
11. Sodium phosphate monobasic (NaH_2PO_4).

Working Solutions

1. 0.4 M Sodium phosphate buffer pH 7.0. When performing the assay mix 10 ml of buffer with 10 mg DTE.
2. L-Dopa 10 mmol/l: dissolve 19.7 mg L-dopa and 10 µl of 6 M HCl in 4 ml H_2O; add Milli-Q H_2O to 5 ml. Store at room temperature until used (within 8 h).
3. PLP 0.7 mmol/l: dissolve 1.7 mg of PLP in 10 ml Milli-Q H_2O. Store at 5°C until used (within 8 h).
4. PCA 0.8 M: dilute 12.1 ml of 70% $HClO_4$ with Milli-Q H_2O to 250 ml.
5. Dopamine stock solution: dissolve 100 mg ascorbic acid and 9.5 mg dopamine in approximately 80 ml Milli-Q H_2O in a 100-ml flask. Add Milli-Q H_2O. Mix for 10 min on ice. Store 0.5-ml aliquots at –20°C.
6. Dopamine standard 1 µmol/l: add 0.5 ml of 6 M HC1 to approximately 40 ml of Milli-Q H_2O in a 50-ml flask. Add 100 µl of dopamine stock solution. Mix for 10 min on ice. Add Milli-Q H_2O to the mark. Prepare fresh every day. Store in a refrigerator at 4°C during the day of use (stable for at least 24 h).

Enzyme Assay

Set the water bath to 37°C, 30 min before incubating the samples. The setup for tubes and incubations is shown in Table 6.2.3.

Calculation

AADC activity is reported as dopamine formed as pmol/min/ml of plasma.

Table 6.2.3 *Enzyme assay to assess AADC activity: set-up and incubations.* CEN *Centrifuge,* INC *incubation,* PCA *perchloric acid,* PLP *pyridoxal phosphate*

	Assay buffer (µl)	PLP (µl)	Sample (µl)	INC A [a]	L-Dopa (µl)	INC B [b]	PCA (µl)	CEN [c]	Total volume (µl)
Blank minus substrate	350	50	100	↓		↓	500	↓	1000
Blank minus sample	400	50		↓	50	↓	500	↓	1000
Sample	300	50	100	↓	50	↓	500	↓	1000

[a] 120 min at 37 C

[b] 90 min at 37 C

[c] Place on ice for 10 min followed by bench centrifuge (12,000–14,000g) for 5 min at 4°C. Transfer the clear supernatants to new, appropriately labelled tubes and store at −70°C until used for dopamine measurement. Dilution factor = 10.

Reference Values

In newborns and children, normal values lie in the range 36–129 pmol/min/ml. For adults the normal range is 24–43 pmol/min/ml.

Instrumentation for HPLC

Determination of dopamine is by HPLC and electrochemical detection and is very similar to that described previously for the CSF determination of biogenic amines.

1. Isocratic HPLC system with 5011 ESA electrode, downstream electrode 450 mV.
2. Column: C18, 5 µM, 25 cm × 4.6 mm. Injection volume 50 µl.
3. Mobile phase: 40 mM sodium dihydrogen phosphate, 5 mM OSS, 60 µM EDTA, 2.8ml 85% phosphoric acid and 23% methanol (pH 2.9–3.1) at 1.2 ml/min.
4. Flow rate: 1.2 ml/min. The column is maintained at 37°C.

Standards and Calibration for HPLC

1. Dopamine stock solution (0.5 mmol/l): dissolve, in a 100-ml volumetric flask, 100 mg ascorbic acid and 9.5 mg dopamine. Bring to a final volume of 100 ml with H_2O and mix on ice for 10 min. Store 0.5-ml aliquots at −80°C.
2. Dopamine calibration standard (1000 nmol/l): add 0.5 ml of 6 M HCl to 40 ml H_2O in a 5-ml volumetric flask. Add 100 µl of 0.5 mM dopamine stock solution and mix for 10 min on ice. Stable for 8 h on ice.

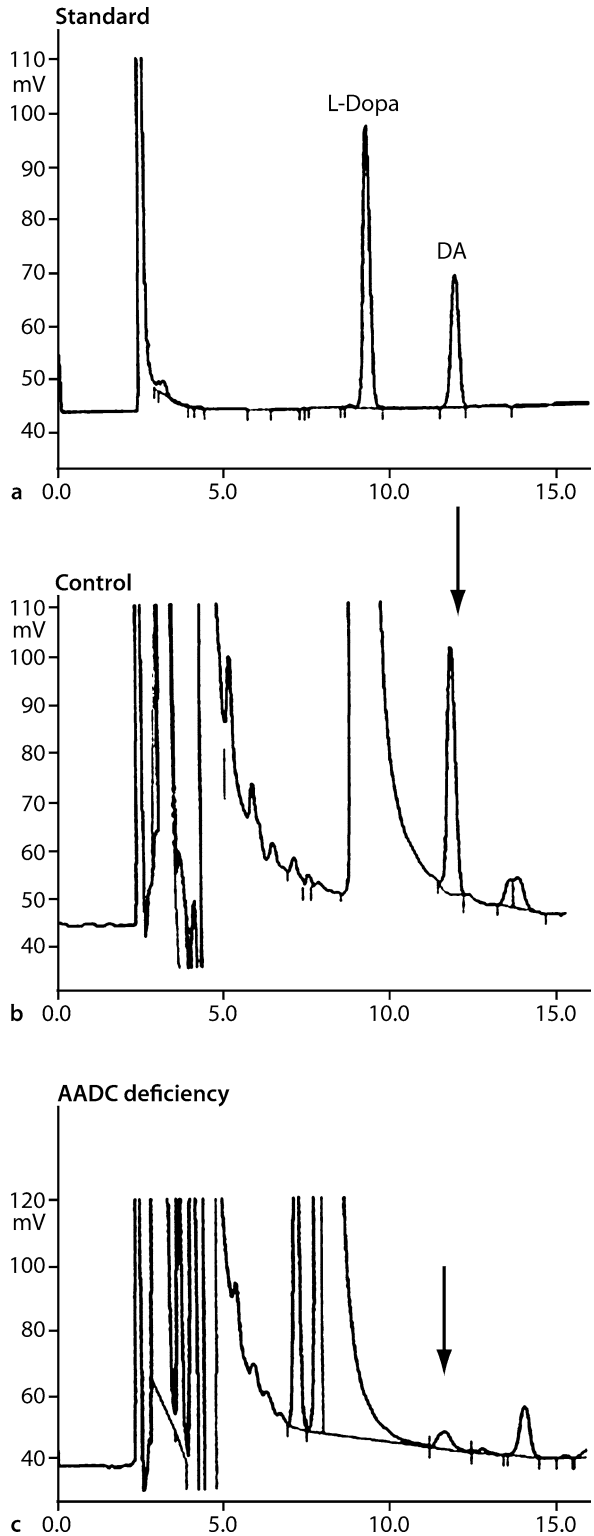

Fig. 6.2.3a–c AADC assay using HPLC and EC detection of dopamine. **a** Standard mixture; **b** serum control sample; **c** serum AADC deficiency. *DA* Dopamine, *L-Dopa* 3,4-dihydroxy-L-phenylalanine

References

1. Blau N, Thony B, Cotton RGH, Hyland K (2001) Disorders of tetrahydrobiopterin and related biogenic amine. In: Scriver CR, Sly WS, Childs B, Beaudet AL, Valle D, Kinzler W, Vogelstein B (eds) The Metabolic and Molecular Bases of Inherited Disease (8th edn). McGraw-Hill, New York, pp 1725–1776
2. Brautigam C, Wevers RA, Jansen RJT, Smeitink JAM, et al (1998) Biochemical hallmarks of tyrosine hydroxylase deficiency. Clin Chem 44:1897–1904
3. Hyland K (2003) The lumbar puncture for diagnosis of pediatric neurotransmitter diseases. Ann Neurol 54:S13–17
4. Hyland K, Clayton P (1992) Aromatic amino acid decarboxylase deficiency: diagnostic methodology. Clin Chem 38:2405–2410
5. Hyland K, Surtees RAH, Rodeck C, Clayton PT (1992) Aromatic l amino acid decarboxylase deficiency: clinical features, diagnosis and treatment of a new inborn error of neurotransmitter amine synthesis. Neurology 42:1980–1988
6. Hyland K, Surtees RAH, Heales SJR, Bowron A, et al (1993) Cerebrospinal fluid concentrations of pterins and metabolites of serotonin and dopamine in a pediatric reference population. Pediatr Res 34:10–14
7. Mills PB, Surtees RAH, Champion MP, Beesley CE, et al (2005) Neonatal epileptic encephalopathy caused by mutations in the PNPO gene encoding pyridox(am)ine 5'-phosphate oxidase. Hum Mol Genet 14:1077–1086

6.3 Folates

Nenad Blau, Thomas Opladen

6.3.1 Introduction

This chapter will deal with analytical procedures for 5-methyltetrahydrofolic acid (5MTHF) in cerebrospinal fluid (CSF) and serum. Folic acid is a water-soluble vitamin that functions as a one-carbon donor in various metabolic cycles. It is involved in the biosynthesis of thymidylates and purines, methionine synthesis via homocysteine remethylation, the methylation of phospholipids, the interconversion of serine and glycine, and the metabolism of histidine and formate. It is therefore essential for growth, reproduction, and maintenance of normal body function. The natural form is referred to as folate; it consists mainly of 5MTHF and 10-formyltetrahydrofolate in their polyglutamate derivatives [1]. 5MTHF is the active one-carbon donor. It is transported through the blood–brain barrier to serve for a number of reactions in the central nervous system

Serum folate deficiency is known to be associated with megaloblastic anemia, high blood levels of homocysteine, and neural tube defect in newborns as a result of folate shortage of the mother [2, 3]. Cerebral folate deficiency (CFD) is a recently recognized neurological disorder found in several children with psychomotor retardation, spastic paraplegia, cerebellar ataxia, and dyskinesia. These patients have very low 5MTHF in their CSF, normal blood folates [4, 5], and some patients display a high titer of folate receptor-blocking autoantibodies [6].

CFD is further associated with the following inherited metabolic disorders: 5,10-methylen-tetrahydrofolate reductase (MTHFR) deficiency [7], 3-phosphoglycerate dehydrogenase (PGDH) deficiency [8], dihydropteridine reductase (DHPR) deficiency [9], as well as with Rett syndrome [10], and Aicardi-Goutières Syndrome [11]. Furthermore, folate deficiency may be associated with congenital folate malabsorption, severe malnutrition, and formiminotransferase deficiency.

5MTHF was initially measured by microbiological and radioisotope dilution assay [12, 13], and later by high-pressure liquid chromatography (HPLC) using electrochemical (EC), ultraviolet, or fluorescence detection [14-16]. Compared to other methods, EC detection is more sensitive.

6.3.2 Properties of 5MTHF

5MTHF (Fig. 6.3.1) is synthesized biologically from 5,10-methylene-tetrahydrofolic acid through the action of MTHFR. Commercially, it is available as a calcium salt. The 5MTHF calcium salt is soluble as 500 mg in 100 ml water. A 1 mM solution

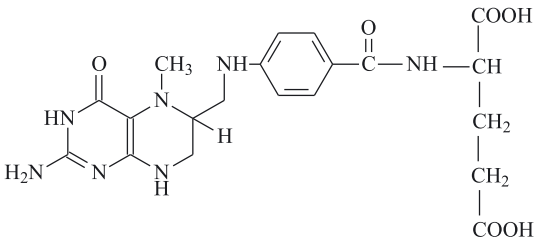

Fig. 6.3.1 Structure of 5-methyl-tetrahydrofolic acid (5MTHF)

in water has a pH of 5.9. Solutions are less stable than the solid form and should be made immediately before use. A 1 mM solution in water at room temperature for 2.5 h degrades by approximately 4%, and within 4 h 10% has degraded. The dry powder, open at room temperature for 3 months, is relatively stable, degrading by 0.5% over this time. The powder is hygroscopic, absorbing 10% of its weight in water within 4 h (www.eprova.ch).

6.3.3 Methods

5MTHF is separated from other folates by reverse-phase HPLC and quantified with EC detection [17]. Prior to HPLC, serum is extracted with Sep-Pak C18 cartridges, while CSF is injected without pretreatment [18]. The two HPLC systems described are very similar, and both can be used for CSF or serum.

6.3.3.1 Preanalytical

Specimen

Both CSF and serum samples should be immediately stored at –80°C. CSF contaminated with blood should be immediately centrifuged (20–30% lower values).

Serum Concentration

Serum (400 µl) is thawed immediately before measurement and mixed with 600 µl ice-cold 28 µmol/l ascorbic acid solution to protect against oxidation. After activation of the Sep-Pak C18 cartridge (Waters Chromatography) with 2 ml methanol and 10 ml of 14 µmol/l ascorbic acid solution, the mixture is applied. The cartridge is washed with 3 ml of 14 µmol/l ascorbic acid solution, and 5MTHF is eluted with 1.5 ml methanol in a light-protected tube. The eluates are evacuated under vacuum (Speed Vac, SVC 100, Savant) and dried samples are redissolved in 100 µl of 14 µmol/l ascorbic acid solution.

Regents and Chemicals

Chemicals

1. Water, HPLC quality.
2. Sodium acetate (CH_3COONa, MW 82.03; Merck no. 6268).

3. Acetic acid, anhydrous (CH_3COOH, MW 60.05; Sigma no. 338826).
4. Ascorbic acid ($C_6H_8O_6$, MW 176.12; Fluka no. 95210).
5. EDTA [$(HO_2CCH_2)_2NCH_2CH_2N(CH_2CO_2H)_2$; MW 292.24].
6. Methanol, HPLC quality (Fluka no. 65541).
7. 5MTHF-Ca ($C_{20}H_{23}N_7O_6$, MW 459.50; Schircks Laboratories).
8. Freon (Fridore).

Stock Solutions

1. 0.05% (w/v) Ascorbic acid: dissolve 500 mg ascorbic acid in 500 ml water. Store at 4°C.
2. 10% (w/v) EDTA: dissolve 10 g EDTA in 100 ml water. Store at room temperature.
3. 50 mM Sodium acetate (eluent): dissolve 4.1 g sodium acetate in 400 ml water and add 0.25 ml of 10% EDTA, 5 ml acetic acid, and 225 ml methanol. The pH is adjusted to 4.4–4.6 with 100% anhydrous acetic acid. Add water to the 1000-ml mark. Degas in a vacuum. Store at room temperature.
4. Ascorbic acid solutions, 28 µmol/l and 14 µmol/l: dissolve 5 mg of ascorbic acid in 1 ml of water. Dissolve 1:1000 for 28 µmol/l ascorbic acid solution and 1:2000 for 14 µmol/l ascorbic acid solution store on ice.

Standard Mixture

1. 200 µM 5MTHF: dissolve 10.0 mg 5MTHF-Ca in 100 ml of 0.05% ascorbic acid. Store 1 ml aliquots covered with Freon at –20°C. Stable for at least 1 year.
2. 100 nM 5MTHF (CSF): dilute 100 µl of 200 µM 5MTHF solution with 200 ml of 50 mM sodium acetate. Store 1 ml aliquots covered with Freon at –20°C. Stable for at least 1 year.
3. 6.25–1600 nM 5MTHF (serum): use 200 µM 5MTHF standard to prepare calibration standards (6.25, 12.5, 25, 50, 400, 800, 1600 nmol) by diluting with 50 mM sodium acetate store on ice.

Instrumentation (HPLC)

CSF system

Modular isocratic HPLC with ED detection: HPLC pump 515 (Waters), Injector 7725i (Rheodyne), Pulsation Reduced (Portman Instruments), Coulochem Detector Model 5100A (ESA), Analytical Cell 5011 (ESA), and PC with chromatography software (SCPA).

1. Analytical column: ODS1, 250 × 4.6 mm, 5 µm (Stagroma).
2. Eluent: 5 mM sodium acetate.
3. Flow: 1 ml/min.
4. Detector 1 settings:

Potential (V)	0.20
Polarity	–
Gain	0 × 0
Response time	2 s
Autozero	off
Digital display	–

5. Detector 2 settings:	Potential (V)	0.00
	Polarity	+
	Gain	10 × 10
	Response time	2 s
	Autozero	OUT
	Digital display	CH 2 OUT

Serum System

HPLC system Gold 128 (Beckman-Coulter) with autosampler (Midas, Spark) and EC detection CLC-100 (Chromsystems, Munich, Germany) is used. Sample results are analyzed by 32 Karat Software (Beckman Coulter).

1. Analytical column: Spherisorb ODS-1, 5 µm, 250 mm × 4.6 mm (Stagroma).
2. Precolumn: Spherisorb C8, 5 µm, 40 mm × 4.6 mm (Stagroma).
3. Eluent: 50 mM sodium acetate.
4. Flow: 1 ml/min.
5. EC detector settings: oxidation mode, potential of + 300 mV.

6.3.3.2 Analytical

Run CSF system for 2–4 h before the first injection. Keep samples on ice. Inject 10 µl of CSF.

Calculation

External standard method.

Performance

- Linearity: 3–300 nmol/l (CSF) or 5–1600 nmol/l (serum).
- Detection limit: 3 nmol/l (CSF) or 4.5 nmol/l (serum).

6.3.3.3 Postanalytical

Reference Values – CSF

Reference CSF values can be found in Table 6.3.1.

Reference Values – Serum

Reference serum values can be found in Table 6.3.2.

Table 6.3.1 *Reference cerebrospinal fluid 5-methyltetrahydrofolic acid (5MTHF) values*

Age (years)	5MTHF (nmol/l)
0–0.49	64–182
0.5–1.99	64–182
2–4 .99	63–111
5–10 .99	41–117
11–15.99	41–117
>16	41–90

Table 6.3.2 *Reference serum fluid values for 5MTHF*

Age (years)	5MTHF (nmol/l)
0–0.49	38–90
0.5–1.99	36–96
2–4.99	22–71
5–10.99	14–77
11–15.99	12–63
>16	10–39

Pathological Values

Figures 6.3.2 and 6.3.3 show chromatogram samples for CSF and serum. Low 5MTHF in CSF is associated with the following conditions:

1. CFD.
2. DHPR deficiency.
3. MTHFR deficiency.
4. PGDH deficiency.
5. Rett syndrome.
6. Aicardi-Goutières Syndrome.
7. Kearns-Sayre Syndrome.
8. High-dosage L-dopa/carbidopa therapy.

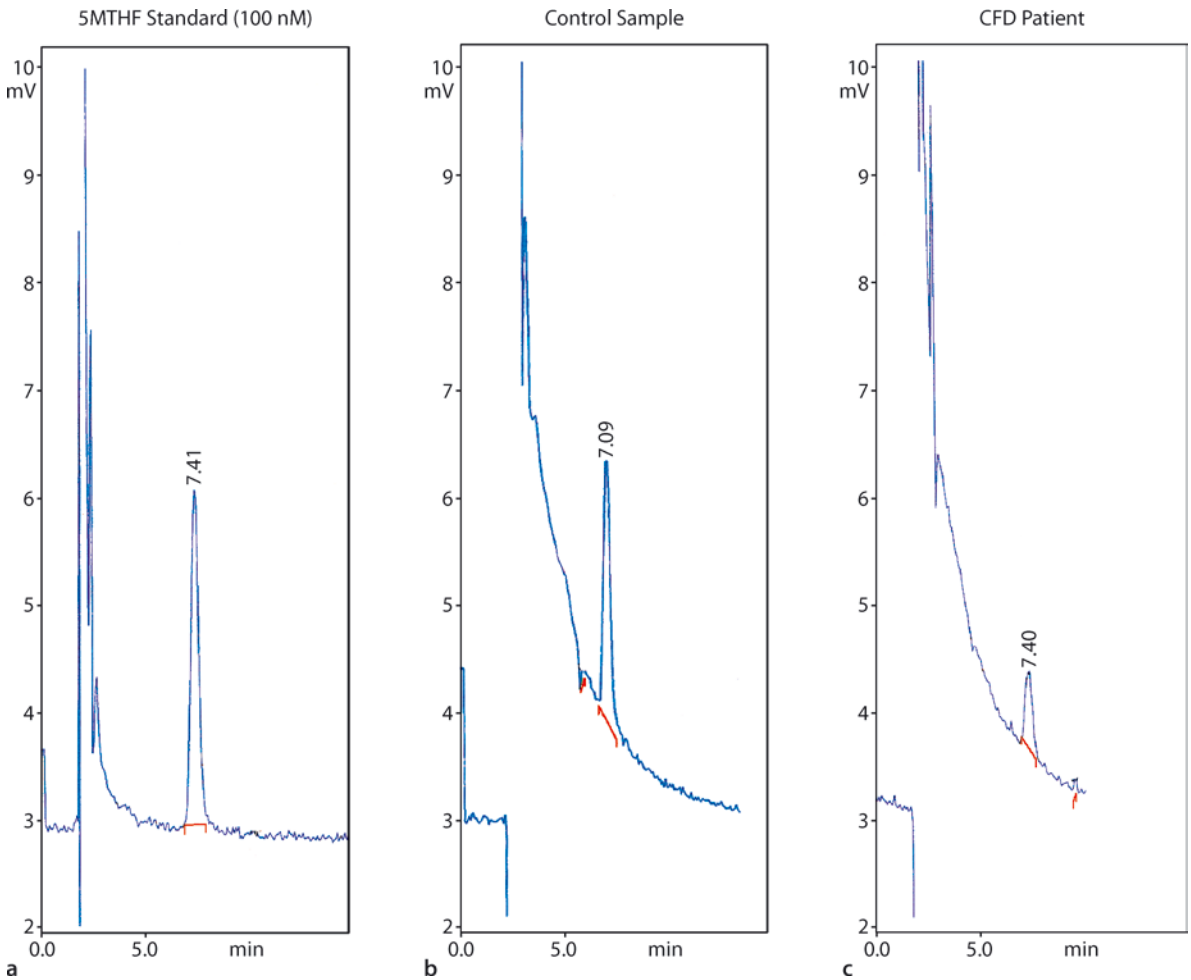

Fig. 6.3.2a–c Chromatogram of 5MTHF using electrochemical detection. **a** Standard, 100 nM; **b** control cerebrospinal fluid (CSF); **c** CSF from a patient with cerebral folate deficiency (*CFD*)

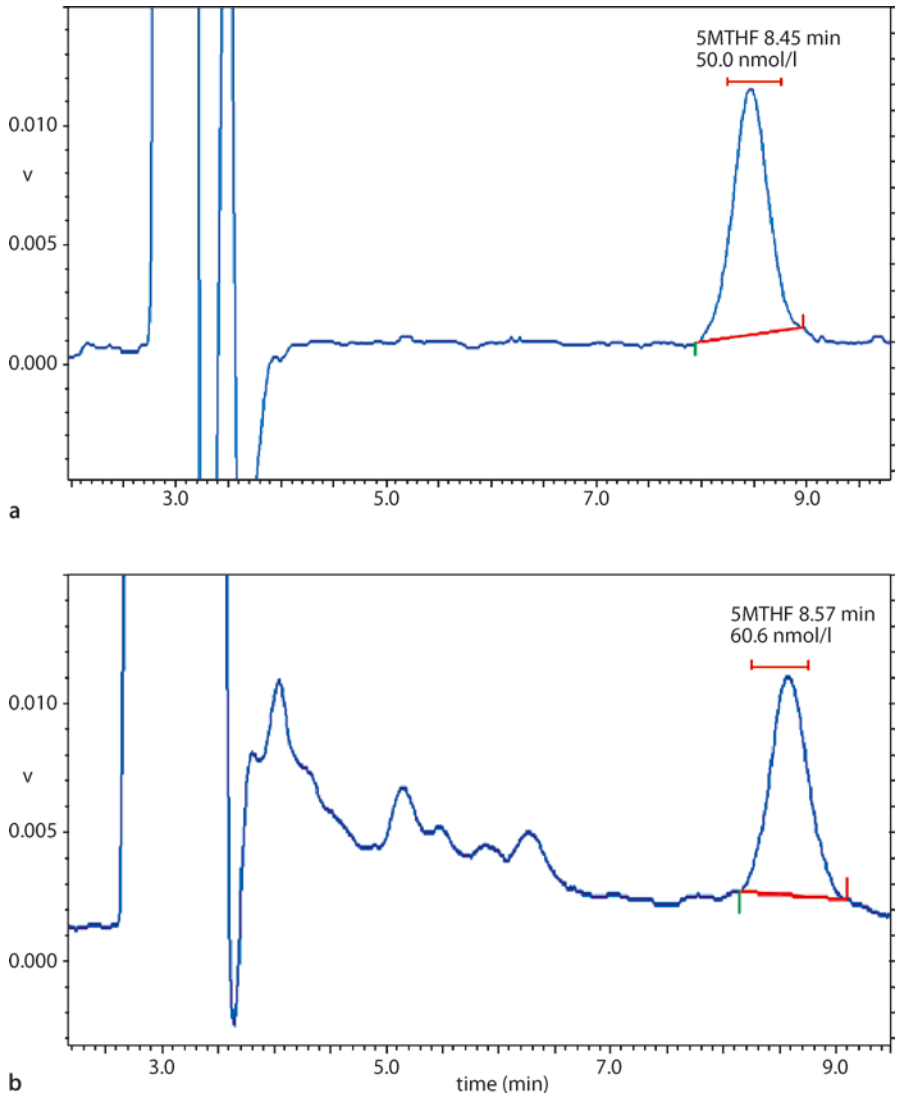

Fig. 6.3.3a,b Chromatogram of 5MTHF using electrochemical detection. **a** Standard, 50 nM; **b** Control serum

References

1. van der Put NMJ, van Straaten HWM, Trijbels FJM, Blom HJ (2001) Folate, homocysteine and neural tube defects: an overview. Exp Biol Med 226:243–270
2. Yerby MS (2003) Clinical care of pregnant women with epilepsy: neural tube defects and folic acid supplementation. Epilepsia 44:33–40
3. Moat SJ, Lang D, McDowell IF, Clarke ZL, Madhavan AK, Lewis MJ, Goodfellow J (2004) Folate, homocysteine, endothelial function and cardiovascular disease. J Nutr Biochem 15:64–79

4. Ramaekers VT, Blau N (2004) Cerebral folate deficiency. Dev Med Child Neurol 46:843–851
5. Ramaekers VT, Hausler M, Opladen T, Heimann G, Blau N (2002) Psychomotor retardation, spastic paraplegia, cerebellar ataxia and dyskinesia associated with low 5-methyltetrahydrofolate in cerebrospinal fluid: a novel neurometabolic condition responding to folinic acid substitution. Neuropediatrics 33:301–308
6. Ramaekers VT, Rothenberg SP, Sequeira J, Opladen T, Blau N, Quadros EV, Selhub J (2005) Autoantibodies to folate receptors in the cerebral folate deficiency syndrome.. Ns Engl J Med 352:1985–1991
7. Skovby F (2005) Disorders of sulfur amino acids. In: Blau N, Duran M, Blaskovics M, Gibson KM (eds) Physician's Guide to the Laboratory Diagnosis of Metabolic Disease. Springer, Heidelberg, pp 243–260
8. de Koning TJ, Duran M, Dorland L, Goosken R, Van Schaftingen E, Jaeken J, Blau N, Berger R, Poll-The BT (1998) Beneficial effect of L-serine and glycine in the management of seizures in 3-phosphoglycerate dehydrogenase deficiency. Ann Neurol 44:261–265
9. Ponzone A, Spada M, Ferraris S, Dianzani I, De Sanctis L (2004) Dihydropteridine reductase deficiency in man: from biology to treatment. Med Res Rev 24:127–150
10. Ramaekers VT, Steen-Ingemann H, Holm J, Opladen T, Senderek J, Häusler M, Heimann G, Fowler B, Maiwald R, Blau N (2003) Reduced folate transport to the brain in Rett syndrome. Neurology 61:506–514
11. Blau N, Bonafé L, Krägeloh-Mann I, Thöny B, Kierat L, Häusler M, Ramaekers VT (2003) Cerebrospinal fluid pterins and folates in Aicardi-Goutières syndrome: a new phenotype. Neurology 61:642–648
12. Dunnette J, Weinshilbourn RM (1977) Inheritance of low immunoreactive human plasma dopamine hydroxylase. Radioimmunoassay studies. J Clin Invest 609:1080
13. Thien KR, Blair JA, Leeming RJ, Cooke WT, Melikian V (1977) Serum folates in man. J Clin Pathol 30:438–448
14. Ghandour H, Bagley PJ, Shemin D, Hsu N, Jacques PF, Dworkin L, Bostom AG, Selhub J (2002) Distribution of plasma folate forms in hemodialysis patients receiving high daily doses of L-folinic or folic acid. Kidney Int 62:2246–2249
15. Burke PA, Luo ML, Zhu JW, Yaffe MB, Forse RA (1996) Injury induces rapid changes in hepatocyte nuclear factor-1-DNA binding. Surgery 120:374–381
16. Belz S, Frickel C, Wolfrom C, Nau H, Henze G (1994) High-performance liquid chromatographic determination of methotrexate, 7-hydroxymethotrexate, 5-methyltetrahydrofolic acid and folinic acid in serum and cerebrospinal fluid. J Chromatogr B Biomed Appl 661:109–118
17. Hyland K, Surtees R (1992) Measurement of 5-methyltetrahydrofolate in cerebrospinal fluid using HPLC with coulometric electrochemical detection. Pteridines 3:149–150
18. Opladen T, Ramaekers VT, Heimann G, Blau N (2006) Analysis of 5-methyltetrahydrofolate in serum of healthy children. Mol Genet Metab 87:61–65

7.1 Screening for Disorders of Purine and Pyrimidine Metabolism Using HPLC-Electrospray Tandem Mass Spectrometry

André B.P. van Kuilenburg,
Arno van Cruchten, Nico G.G.M. Abeling

7.1.1 Introduction

Inherited disorders of purine and pyrimidine metabolism have a wide variety of clinical presentations, which include, among others, anemia, immunodeficiency, kidney stones, convulsions, mental retardation, autism, and growth retardation. In contrast to the well-known defects of purine metabolism, most of the seven defects of pyrimidine metabolism have only recently been discovered. Genetic enzyme defects are not only biological curiosities, but they can have serious clinical consequences in more frequently occurring situations such as adverse reactions to medication. Defects in the degradation of pyrimidines have been associated with a variable clinical phenotype, whereas the same defects can lead to severe life-threatening toxicities when (partially) deficient individuals are treated with the pyrimidine analogue 5-fluorouracil [7, 8].

Because of this broad clinical spectrum, rapid and specific screening methods are desired for the diagnosis of these disorders in patients at risk to enable appropriate treatment, genetic counseling, and prenatal diagnosis. For these reasons, we have developed a general screening method for purine and pyrimidines and two specific methods to analyze the metabolites of the pyrimidine degradation pathway and the pyrimidine *de novo* pathway, using high-performance liquid chromatography (HPLC)-electrospray tandem mass spectrometry (MS/MS) of liquid urine or urine-soaked filter paper strips [2, 15, 16]. The availability of these methods provides powerful tools to (pre)screen patients at risk.

7.1.2 Purines and Pyrimidines

Purine and pyrimidine nucleotides are essential for a vast number of biological processes such as the synthesis of RNA, DNA, phospholipids, glycogen, and the sialylation and glycosylation of proteins. Both purines and pyrimidines can be synthesized *de novo* in mammalian cells through multistep processes. In addition to the *de novo* synthesis, purine nucleotides can also be synthesized via the salvage of

the purine bases adenosine, guanosine, and hypoxanthine. In contrast, the salvage pathway for pyrimidine nucleotides occurs at the level of the nucleosides uridine and cytidine. Patients with a deficiency of purine or pyrimidine metabolism usually present with altered levels of the nucleoside bases and/or (deoxy)ribonucleosides. The structures of the naturally occurring purine and pyrimidine nucleoside bases and (deoxy)ribonucleosides are shown in Figs. 7.1.1 and 7.1.2.

7.1.3. Methods

7.1.3.1 Principle

The metabolites of interest in urine are separated using reverse-phase HPLC combined with electrospray ionization (ESI)-MS/MS, and detection is performed using multiple-reaction monitoring. Stable-isotope-labeled reference compounds are used as internal standards.

7.1.3.2 Preanalytical

Specimen

Urine samples or urine-soaked filter paper strips (12 × 40 mm; type 2992; Schleicher & Schuell). Fresh urine samples are stored at 4°C and analyzed within 1 week. Otherwise, urine samples are stored at –20°C, until analysis. Prior to analysis, the liquid urine samples are centrifuged for 10 min at 10,000 × *g*.

Dip filter-paper strips completely into the urine and remove the excess urine by wiping it off along the wall of the test tube. Dry the strips at room temperature.

Chemicals

Thymine, hypoxanthine, xanthine, uridine, thymidine, adenine, inosine, adenosine, and guanosine are purchased from Calbiochem. Orotic acid, pseudouridine, 5-hydroxymethyluracil (5-OH-Me-ura), deoxyinosine, deoxyguanosine, deoxyuridine, and ammonium formate are purchased from Sigma. Deoxyadenosine is purchased from P-L Biochemicals. Uracil is purchased from Fluka. Dihydrothymine, dihydrouracil, and N-carbamyl-*β*-alanine are obtained from Sigma. 1,3-$^{15}N_2$-uracil; *α*,*α*,*α*,6-$^{2}H_4$-thymine; 1,3-$^{15}N_2$-orotic acid; ribose-1-^{13}C-uridine; methyl-^{13}C-thymidine; 8-^{13}C-adenine; ribose-1-^{13}C-adenosine; 5,6,6-$^{2}H_3$-Me-$^{2}H_3$-dihydrothymine; $^{13}C_4$,$^{15}N_2$-dihydrouracil; 5,6,6-$^{2}H_3$-Me-$^{2}H_3$-dihydrothymine; $^{13}C_4$,$^{15}N_2$-dihydrouracil, 5-hydroxymethyl-$^{13}C_2$,$^{2}H_2$-uracil are purchased from Cambridge Isotope Laboratories (Andover, Massachusetts, USA). Analytical/reagent-grade methanol and formic acid are purchased from Merck. Deionized water is passed through a MilliQ Labo system (Millipore).

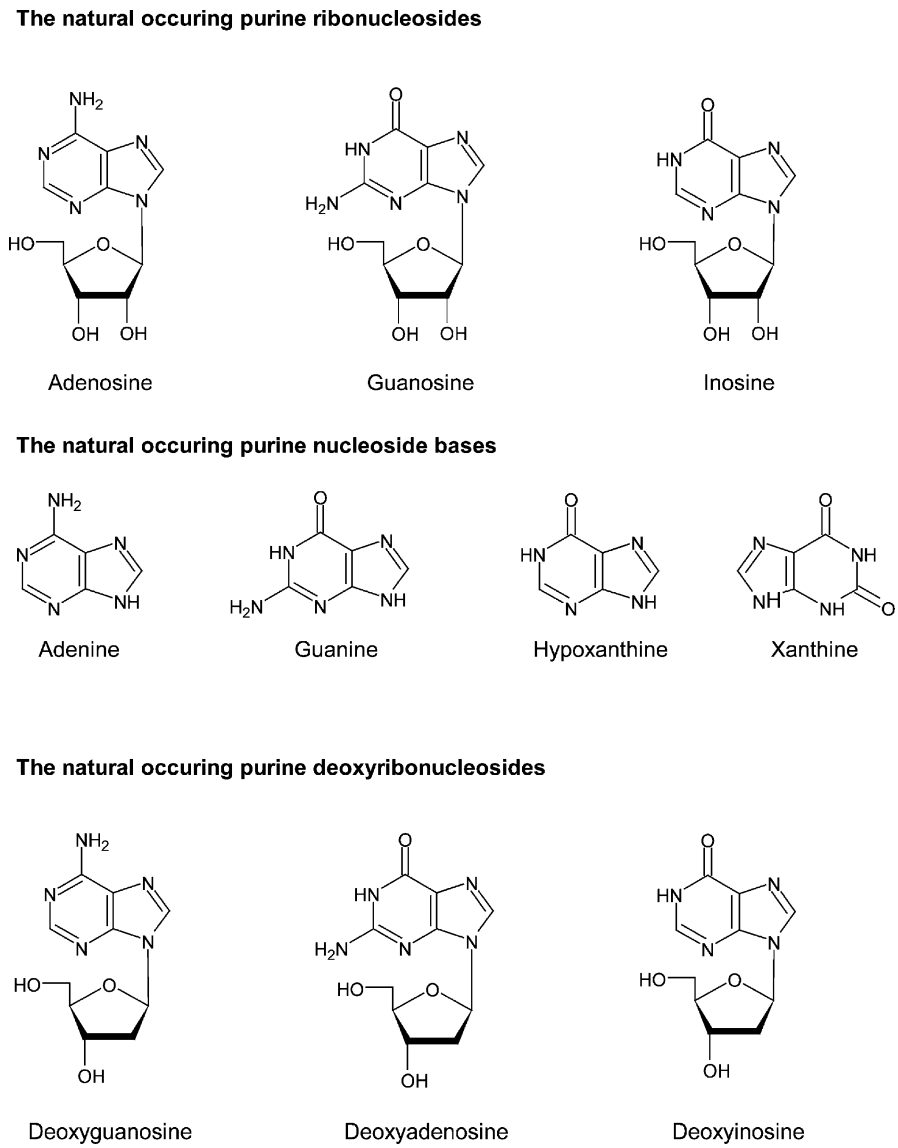

Fig. 7.1.1 Structure of the naturally occurring purine (deoxy)ribonucleosides and nucleoside bases

Reagents and Standards

1. Succinyladenosine is prepared essentially according to the method of Jaeken and Van den Berghe [4]. In short, 0.5 ml of a solution of 785.8 µM adenylosuccinate and 5 U of *Crotalus adamanteus* venom 5'-nucleotidase, both obtained from Sigma, are mixed in 40 mM Tris-HCl buffer, pH 8.0, containing 4 mM Mg^{2+} and incubated at 37°C for 2 h.
2. Reverse-phase HPLC is used to check hydrolysis efficiency and to calculate the amount of succinyladenosine formed during hydrolysis [6].

The natural occuring pyrimidine ribonucleosides

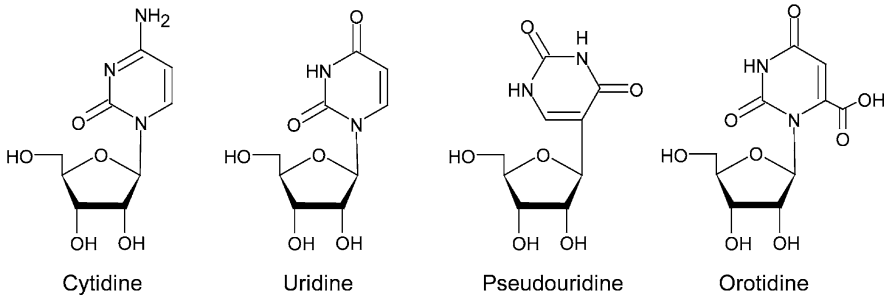

The natural occuring pyrimidine nucleoside bases

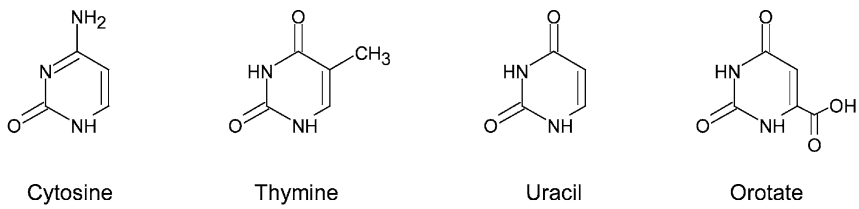

The natural occuring pyrimidine deoxyribonucleosides

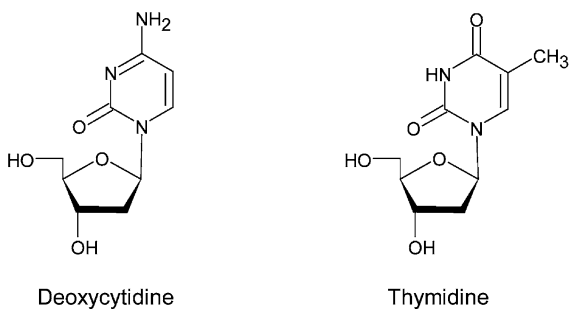

Fig. 7.1.2 Structure of the naturally occurring pyrimidine (deoxy)ribonucleosides and nucleoside bases

3. N-carbamyl-β-aminoisobutyric acid is prepared by the alkaline hydrolysis of dihydrothymine [10]. Dissolve dihydrothymine in 0.1 M NaOH and hydrolyze at 37°C for 1 h. Neutralize the solution with HCl. The stable-isotope-labeled $^{2}H_6$-N-carbamyl-β-aminoisobutyric acid and $^{15}N_2$,$^{13}C_4$-N-carbamyl-β-alanine are prepared by alkaline hydrolysis of the corresponding stable-isotope-labeled dihydropyrimidines.
4. Internal standard mixture IS(1) containing 500 µM of 1,3-$^{15}N_2$-uracil; α,α,α,6-$^{2}H_4$-thymine; 1,3-$^{15}N_2$-orotic acid; ribose-1-^{13}C-uridine; methyl-^{13}C-thymidine; 8-^{13}C-adenine; and ribose-1-^{13}C-adenosine is prepared in 100 mM NH_4OH adjusted to pH 7.15 with 10 M formic acid.

5. Internal standard mixture IS(2) containing 150 µM 1,3-$^{15}N_2$-uracil, 200 µM $\alpha,\alpha,\alpha,6$-$^{2}H_4$-thymine, 2 mM $^{13}C_4$,$^{15}N_2$-dihydrouracil, 1 mM 5,6,6-$^{2}H_3$-Me-$^{2}H_3$-dihydrothymine, 1 mM $^{15}N_2$,$^{13}C_4$-N-carbamyl-β-alanine, 1 mM $^{2}H_6$-N-carbamyl-β-aminoisobutyric acid, 1 mM 5-hydroxymethyl-$^{13}C_2$,$^{2}H_2$-uracil, and 15 µM methyl-^{13}C-thymidine.

Instrumentation

1. The HPLC system consist of an HP 1100 series binary gradient pump, a vacuum degasser, and a column temperature controller (all from Hewlett Packard), connected to a Gilson 231 XL autosampler (Gilson).
2. A Phenomenex Aqua analytical column (250 × 4.6 mm; particle size, 5 µm; Phenomenex) and a guard column (SecurityGuard C_{18} ODS; 4 × 3.0 mm; Phenomenex).
3. A Quattro II tandem mass spectrometer (Micromass).

Mass Spectrometry Settings and Chromatographic Conditions

The general purine and pyrimidine screening and the screening for pyrimidine bases and their degradation products are performed by separation of the compounds on a Phenomenex Aqua analytical column at ambient temperature. The mobile phases are as follows: 50 mM acetic acid, adjusted to pH 4.0 with 13 M NH_4OH (eluant A) and 50 mM acetic acid (pH 4):methanol (1:1 by volume; eluant B). The elution gradient is as follows (flow rate, 1 ml/min): 0–10 min, 100% A to 100% B; 10.0–10.1 min, 100% B to 100% A; 10.1–16 min, equilibration with 100% A. All gradient steps are linear and the total analysis time, including equilibration, is 16 min. A splitter between the HPLC column and the mass spectrometer is used and 50 µl/min of eluant is introduced into the mass spectrometer. An electrically operated valve is used so that only the eluant from 3.5 to 12.5 min is introduced into the mass spectrometer (preventing early-eluting salts and late-eluting peaks from contaminating the mass spectrometer).

A Quattro II tandem mass spectrometer I (Micromass) is used in the positive ESI mode for the general purine and pyrimidine screening application. Only orotic acid, the first eluting component, is measured in the negative ESI mode. The positive ESI mode is also used for screening of metabolites of the pyrimidine degradation pathway. Nitrogen is used as the nebulizing gas. The collision gas is argon and the cell pressure is 0.25 Pa. The source temperature is set at 80°C and the capillary voltage is maintained at 3.5 kV. The detector is used in the MS/MS mode using multiple-reaction monitoring to detect a specific transition of precursor ion to fragment for each analyte. The transition, cone voltage, and collision energy established for each compound are listed in Tables 7.1.1 and 7.1.2.

Calibration

Calibration curves are obtained for each analyte by least-squares regression for the analyte:internal standard peak-area ratio versus the concentration of the analyte in

Table 7.1.1 *Mass spectrometry (MS) settings for purine and pyrimidine screening in the positive electrospray ionization (ESI) mode, orotic acid in the negative ESI mode*

Compound	Mass	Parent ion (m/z)	Daughter ion (m/z)	Cone voltage (V)	Collision energy (eV)	Internal standard
Uracil	112	113	70	35	18	1,3-$^{15}N_2$-Uracil
Thymine	126	127	110	35	15	$^{2}H_4$-Thymine
Adenine	135	136	119	40	20	8-^{13}C-Adenine
Hypoxanthine	136	137	110	40	20	Ribose-1-^{13}C-uridine
Guanine	151	152	135	40	20	Ribose-1-^{13}C-uridine
5-hydroxymethyluracil	142	143	82	27	15	1,3-$^{15}N_2$-Uracil
Xanthine	152	153	110	35	20	Ribose-1-^{13}C-uridine
Orotic acid	156	155	111	20	10	1,3-$^{15}N_2$-Orotic acid
Thymidine	242	243	127	30	10	Me-^{13}C-thymidine
Uridine	244	245	113	25	10	Ribose-1-^{13}C-uridine
Pseudouridine	244	245	209	20	30	Ribose-1-^{13}C-uridine
Deoxyadenosine	251	252	136	25	15	Ribose-1-^{13}C-adenosine
Deoxyinosine	252	253	137	15	15	8-^{13}C-Adenine
Deoxyguanosine	267	268	152	20	10	8-^{13}C-Adenine
Inosine	268	269	137	20	20	8-^{13}C-Adenine
Guanosine	283	284	152	20	20	8-^{13}C-Adenine
Adenosine	267	268	136	30	15	Ribose-1-^{13}C-adenosine
Succinyladenosine	383	384	252	50	25	8-^{13}C-Adenine
Deoxyuridine	228	229	113	20	10	Ribose-1-^{13}C-uridine

the calibration mixture. The calibration curves are linear for all compounds up to 1 mM. Above this concentration, a deviation from linearity occurs for most compounds.

Parameters such as sensitivity of the HPLC-MS/MS system are checked by analyzing a standard containing 2.5 µM of each analyte.

Quality Control

1. A pool urine and a pool urine spiked with all relevant metabolites are analyzed and the concentrations of the metabolites are compared to previous analyses of these two control samples.

Table 7.1.2 *MS settings for pyrimidine degradation screening in the positive ESI mode*

Compound	Mass	Parent ion (*m/z*)	Daughter ion (*m/z*)	Cone voltage (V)	Collision energy (eV)	Internal standard
5-hydroxymethyluracil	142	143	82	27	15	5-Hydroxymethyl-$^{13}C_2$,$^{2}H_2$-uracil
Thymidine	242	243	127	30	10	Me-^{13}C-thymidine
Uracil	112	113	70	35	18	$^{15}N_2$-Uracil
Thymine	126	127	110	35	15	$^{2}H_4$-Thymine
Dihydrothymine	128	129	69	35	18	$^{2}H_6$-Dihydrothymine
Dihydrouracil	114	132	115	5	20	$^{13}C_4$,$^{15}N_2$-dihydrouracil
N-Carbamyl-β-alanine	132	133	90	30	8	$^{15}N_2$,$^{13}C_4$-N-carbamyl-β-alanine
N-Carbamyl-β-aminoisobutyric acid	146	147	129	20	8	$^{2}H_6$-N-carbamyl-β-aminoisobutyric acid

2. The response of the internal standards is monitored during a series and should be constant. In case of strong deviations in the response of an internal standard, there might be quenching of the signal and the sample should be reanalyzed after dilution.
3. In case the concentration of a metabolite is higher than the highest concentration of the calibration curve, the sample will be analyzed again after dilution.
4. In case the thymidine concentration is higher than 5 µM, a significant contribution of the natural isotope to the signal of the internal standard of thymidine occurs. In that case, the sample will be analyzed again either after dilution of the sample or after increasing the concentration of methyl-^{13}C-thymidine to 1 mM.
5. Parameters such as sensitivity of the HPLC-MS/MS system are checked by analyzing a standard containing 2.5 µM of each analyte.

7.1.3.3 Analytical

Procedure

Liquid Urine

1. Centrifuge 200 µl of urine at 10,000 × *g* for 10 min.
2. Transfer 100 µl of the clear urine, calibration standard or control into an autosampler vial (Gilson).
3. Add 10 µl of IS(1) or IS(2) and mix thoroughly.
4. Prior to analysis by HPLC-MS/MS, briefly centrifuge the sample at 10,000 × *g* for 2 min.

Urine-Soaked Filter Paper

1. Add 20 µl of IS(1) or IS(2) to the urine-soaked filter paper strip (see above).
2. After drying, transfer the filter paper strip to a 2-ml Eppendorf tube.
3. Add 1.5 ml of 75% (v/v) methanol and sonicate for 10 min.
4. Transfer the extract to a glass tube.
5. Evaporate the extract at 40°C under a constant stream of nitrogen.
6. Dissolve the dried extract in 200 µl of 50 mM acetic acid (pH 4.0) and sonicate for 5 min.
7. Centrifuge the sample at 1600 × *g* for 5 min.
8. Transfer the supernatant to an autosampler vial.
9. Save 100 µl of the supernatant for determination of the creatinine concentration.
10. Prior to analysis by HPLC-MS/MS, briefly centrifuge the sample at 10,000*g* for 2 min.
11. Inject 20 µl into the HPLC-MS/MS system.

Calculation

The concentration of each analyte was determined by use of the slope and intercept of the calibration curve that is obtained by least-squares regression for the analyte: internal standard peak-area ratio versus the concentration of the analyte in the calibration mixture.

The calibration curves are linear for all compounds up to 1 mM. Above this concentration, deviations from linearity occur for most compounds. Thus, in case the concentration of a sample proves to be above the linear part of the calibration curve, the sample will be diluted and measured again. In case the sample amount is limited, the concentrations are calculated by interpolation on a quadric curve for concentrations up to 5 mM.

7.1.3.4 Postanalytical

Interpretation

Concentrations of metabolites outside the reference ranges may constitute a typical pattern indicating the presence of an inborn error of purine or pyrimidine metabolism. However, altered excretions of purine and pyrimidines may also be a secondary phenomenon due to the presence of other metabolic disorders, such as a deficiency of the urea cycle [15]. Increased concentration of a single metabolite or combinations of metabolites may also result from bacterial contamination, sample conditions, medication, or dietary compounds [6].

7.1.4 Chromatograms

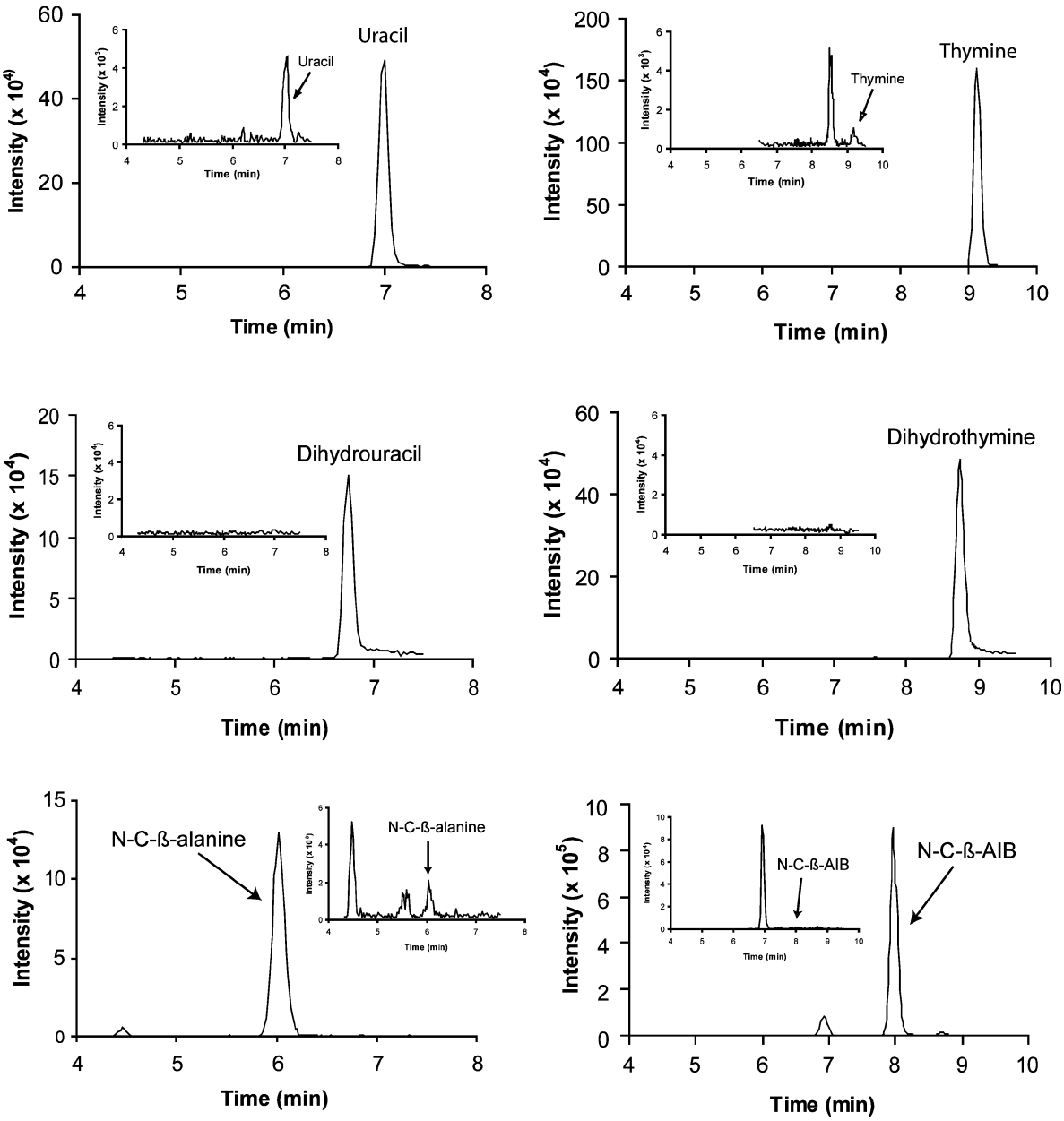

Fig. 7.1.3 High-performance liquid chromatography/electron spin ionization-tandem mass spectrometry profiles of urines from patients with a dihydropyrimidine dehydrogenase (*upper panel*), dihydropyrimidinase (middle panel) and a *β*-ureidopropionase deficiency (*lower panel*). The inserts show the profiles of a control urine, note the differences in scale. *N-C-β-alanine* N-Carbamyl-*β*-alanine, *N-C-β-AIB* N-carbamyl-*β*-aminoisobutyric acid

7.1.5 Reference Values

Reference values for purine and pyrimidine nucleosides and bases in urine from controls (≤ 3 years) are shown in Table 7.1.3.

Table 7.1.3 *Concentration of purine and pyrimidine metabolites in urine from controls* (n = *104)*

Compound	Mean ± SD (μmol/mmol creatinine)	Range (mean ± 2SD)
Uracil	11.8 ± 9.1	0–30
Thymine	0.5 ± 0.6	0–1.7
Adenine	0.6 ± 1.0	0–2.6
Hypoxanthine	14.0 ± 6.6	0.8–27
Guanine	0.8 ± 1.0	0–2.8
5-Hydroxymethyluracil	0.1 ± 0.4	0–0.9
Xanthine	18.5 ± 6.3	5.9–31
Orotic acid	1.1 ± 0.8	0–2.7
Thymidine	0.0 ± 0.1	0–0.2
Uridine	1.0 ± 0.8	0–2.6
Pseudouridine	88.5 ± 30.8	27–130
Deoxyadenosine	0.0 ± 0.1	0–0.2
Deoxyinosine	0.0 ± 0.1	0–0.2
Deoxyguanosine	0.0 ± 0.05	0–0.1
Inosine	1.3 ± 0.9	0–3.1
Guanosine	0.5 ± 0.5	0–1.5
Adenosine	1.1 ± 0.8	0–2.7
Succinyladenosine	4.0 ± 1.7	0.6–7.4
Dihydrothymine	3.1 ± 2.1	0–7.3
Dihydrouracil	6.3 ± 5.3	0–17
N-Carbamyl-β-alanine	11.0 ± 9.2	0–29
N-Carbamyl-β-aminoisobutyric acid	1.8 ± 2.3	0–6.4

■ ***Table 7.1.4*** *Concentration range of purine and pyrimidine metabolites in urine (µmol/mmol creatinine) from patients.* ADA *Adenosine deaminase,* APRT *adenine phosphoribosyltransferase,* ASA *adenylosuccinate lyase,* DHP *dihydropyrimidinase,* DPD *dihydropyrimidine dehydrogenase,* HGPRT *hypoxanthine-guanine phosphoribosyltransferase,* PNP *purine nucleoside phosphorylase,* TP *thymidine phosphorylase,* UMPS *uridine monophosphate synthase, β-*UP *β-ureidopropionase*

Compound	ADA [a]	PNP [a]	HGPRT [a]	APRT [a]	TP [b]	ASA [a]	UMPS [a]	DPD [c]	DHP [a]	β-UP [d]
Uracil					77			177–901	49–150	2–39
Thymine					48			35–679	12	2–7
Adenine				10–36						
Hypoxanthine			90–270							
Guanine										
5-hydroxymethyluracil										
Xanthine			25–100							
Orotic acid							1000–9600			
Thymidine					125					
Uridine										
Pseudouridine										
Deoxyadenosine	130–190									
Deoxyinosine		320–650								
Deoxyguanosine		200–410								
Inosine		1350–1900								
Guanosine		570–1000								
Adenosine										
Succinyladenosine						170–500				
Dihydrothymine									450–1200	77–280
Dihydrouracil									130–700	47–69
N-carbamyl-β-alanine										795–820
N-carbamyl-β-aminoisobutyric acid										490–623

[a] Data obtained from Simmonds [5]; [b] Data obtained from Fairbanks et al. [1]; [c] Data obtained from van Kuilenburg et al. [13]; [d] Data obtained from van Kuilenburg et al. [14]

7.1.7 Pitfalls

Bacterial contamination of the urine may result in strongly increased levels of uracil due to the bacterial degradation of pseudouridine. Thymine-uraciluria, which is indicative of a dihydropyrimidine dehydrogenase or dihydropyrimidinase deficiency, may also result from increased tissue degradation. However, the latter situation is also characterized by hyper-β-aminoisobutyric aciduria and hyper-β-alaninuria [6]. Under alkaline conditions, due to the presence of bacterial contamination, the deoxynucleosides may be hydrolyzed toward their corresponding nucleoside bases.

7.1.8 Follow-Up Enzyme Assays

The activity of dihydropyrimidine dehydrogenase can be measured in peripheral blood mononuclear cells, fibroblasts, and liver using radiolabeled thymine followed by separation of radiolabeled thymine and the radiolabeled reaction products with reverse-phase HPLC combined with online detection of the radioactivity [12].

The activity of dihydropyrimidinase or β-ureidopropionase can only be measured in liver or kidney. The activity of dihydropyrimidinase is determined using a radiochemical assay with subsequent separation of radiolabeled dihydrouracil from radiolabeled N-carbamyl-β-alanine with reverse-phase HPLC combined with detection of $^{14}CO_2$ by liquid scintillation counting [11]. The activity of β-ureidopropionase can be determined using radiolabeled N-carbamyl-β-alanine followed by separation of radiolabeled N-carbamyl-β-alanine from radiolabeled β-alanine by reverse-phase HPLC [10, 14].

The activity thymidine phosphorylase can be detected in leukocytes using a non-radiochemical assay in which thymine is detected at 265 nm after separation with reverse-phase HPLC [9].

The activity of hypoxanthine-guanine phosphoribosyltransferase, adenine phosphoribosyltransferase, adenosine deaminase, and purine nucleoside phosphorylase can be determined in dried blood spots using an HPLC-linked assay [3].

References

1. Fairbanks LD, Marinaki AM, Carrey EA, Hammans SR, Duley JA (2002) Deoxyuridine accumulation in urine in thymidine phosphorylase deficiency (MNGIE) J Inherit Metab Dis 25:603–604
2. Ito T, van Kuilenburg ABP, Bootsma AH, Haasnoot AJ, van Cruchten AG, Wada Y, van Gennip AH (2000) Rapid screening of high-risk patients for disorders of purine and pyrimidine metabolism using HPLC-electrospray tandem mass spectrometry of liquid urine or urine-soaked filter paper strips. Clin Chem 46:445–452
3. Jacomelli, G, Michelia, V, Peruzzi, L, Notarantonioa, L, Cerbonia, B, Sestinia, S, Pompuccia, G (2002) Simple non-radiochemical HPLC-linked method for screening for purine metabolism disorders using dried blood spot. Clin Chim Acta 324:135–139
4. Jaeken J, Van den Berghe G (1984) An infantile autistic syndrome characterised by the presence of succinylpurines in body fluids. Lancet 2:1058–1061

5. Simmonds HA (1996) Purine and pyrimidine disorders. In: Blau N, Duran M, Blaskovics ME (eds) Physician's Guide to the Laboratory Diagnosis of Metabolic Diseases. Chapman Hall Medical, London, pp 341–357
6. Van Gennip AH, Busch S, Elzinga L, Stroomer AEM, van Cruchten A, Scholten EG, Abeling NGGM (1993) Application of simple chromatographic methods for the diagnosis of defects in pyrimidine degradation. Clin Chem 39:380–385
7. Van Gennip AH, Abeling NGGM, Vreken P, van Kuilenburg ABP (1997) Inborn errors of pyrimidine degradation: clinical, biochemical and molecular aspects. J. Inherit Metab Dis 20:202–213
8. Van Kuilenburg ABP (2004) Dihydropyrimidine dehydrogenase and the efficacy and toxicity of 5-fluorouracil. Eur J Cancer 40:939–950
9. Van Kuilenburg ABP, Zoetekouw L (2005) Determination of thymidine phosphorylase activity by a non-radiochemical assay using reversed-phase high-performance liquid chromatography. J Chromatogr B Biomed Sci Appl 820:271–275
10. Van Kuilenburg ABP, van Lenthe H, van Gennip AH (1999) A radiochemical assay for β-ureidopropionase using radiolabeled N-carbamyl-β-alanine obtained via hydrolysis of [2-14C]5,6-dihydrouracil. Anal Biochem 272:250–253
11. Van Kuilenburg ABP, van Lenthe H, van Kuilenburg ABP (1999) Radiochemical assay for determination of dihydropyrimidinase activity using reversed-phase high-performance liquid chromatography. J Chromatogr B Biomed Sci Appl 729:307–314
12. Van Kuilenburg ABP, Van Lenthe H, Tromp A, Veltman PCJ, Van Gennip AH (2000) Pitfalls in the diagnosis of patients with a partial dihydropyrimidine dehydrogenase deficiency. Clin Chem 46:9–17
13. Van Kuilenburg ABP, Dobritzsch D, Meinsma R, Haasjes J, Waterham HR, Nowaczyk MJM, Marapoulos GD, Hein G, Kalhoff H, Kirk JM, Baaske H, Aukett A, Duley JA, Ward KP, Lindqvist Y, van Gennip AH (2002) Novel disease-causing mutations in the dihydropyrimidine dehydrogenase gene interpreted by analysis of the three-dimensional protein structure. Biochem J 364:157–163
14. Van Kuilenburg ABP, Meinsma R, Beke E, Assmann B, Ribes A, Lorente I, Busch R, Mayatepek E, Abeling NGGM, Van Cruchten A, Stroomer AEM, van Lenthe H, Zoetekouw L, Kulik W, Hoffmann GF, Voit T, Wevers RA, Rutsch F, van Gennip AH (2004) β-Ureidopropionase deficiency: an inborn error of pyrimidine degradation associated with neurological abnormalities. Hum Mol Genet 13:2793–2801
15. Van Kuilenburg ABP, van Lenthe, Löffler M, van Gennip AH (2004) Analysis of pyrimidine synthesis "de novo" intermediates in urine and dried urine filter paper strips with HPLC-electrospray tandem mass spectrometry. Clin Chem 50:2117–2124
16. Van Lenthe H, van Kuilenburg ABP, Ito T, Bootsma AH, van Cruchten AG, Wada Y, van Gennip AH (2000) Defects in pyrimidine degradation identified by HPLC-electrospray tandem mass spectrometry of urine specimens or urine-soaked filter paper strips. Clin Chem 46:1916–1922

7.2 Creatine and its Metabolites

Eduard A. Struys, Nanda M. Verhoeven, Cornelis Jakobs

7.2.1 Introduction

Creatine (Cr) plays an important role in energy transmission and storage in cells and tissues with high energy demands. Tissues like the brain, retina, spermatozoa and cardiac and skeletal muscle contain the enzyme Cr kinase, which catalyses the interconversion of Cr and its phosphorylated analogue, phosphocreatine. The dephosphorylation of phosphocreatine yields energy, as ADP is simultaneously converted into ATP.

The Cr pool in the body is maintained by two mechanisms: uptake of Cr from the diet and endogenous Cr synthesis [1]. Biosynthesis of Cr requires the action of two enzymes: L-arginine:glycine amidinotransferase (AGAT; EC 2.1.4.1) and guanidinoacetate methyltransferase (GAMT, EC 2.1.1.2). AGAT catalyses the transfer of the amidino group of arginine to glycine, yielding ornithine and guanidinoacetate (GA). GA is, by action of GAMT, methylated at its amidino group using S-adenosylmethionine as methyl donor, yielding Cr [2].

Many tissues contain a Na^+/Cl^--dependent Cr transporter (SLC6A8), which is responsible for active Cr transport over the plasma membrane. Tissues with no or limited Cr biosynthesis can be provided with Cr by action of this transporter.

In humans, two inborn errors in Cr biosynthesis and one in Cr transport are known: deficiencies of AGAT, GAMT and of the Cr transporter. AGAT deficiency, first described in 2001, has been reported in three related children [3,4] and a fourth unrelated child [5]. The affected patients show mental and motor retardation, severe delay in speech development and, only in one patient, a period of febrile seizures. GA is decreased in body fluids of AGAT-deficient patients.

GAMT deficiency has been known for more than 10 years now and several affected patients have been reported [6]. The severity of clinical symptoms varies widely. Affected patients show developmental delay with absence of active speech and, in older patients, autism with self injury. More severely affected patients present with severe extrapyramidal symptoms and intractable epilepsy. Biochemical diagnosis can be made by analysis of GA in the plasma or urine.

A genetic defect in the Cr transporter has been found in more than 50 patients in a period of only 5 years [7,8]. In a study of the prevalence of this defect, 6 affected patients were found in a group of 288 mentally retarded men (2.1%) [8]. The gene encoding the Cr transporter is located on the X-chromosome. Affected male patients show mild to severe mental retardation and epilepsy, with absence of speech.

Affected (heterozygote) females have a milder presentation, which probably depends on the lionisation pattern. Some carriers are without symptoms, whereas others have learning disabilities to various extents [9]. Biochemical diagnosis of affected male patients is possible by analysis of Cr excretion in urine.

After finding an abnormal metabolite pattern, the diagnosis of GAMT or AGAT deficiency can be confirmed by enzymatic assays in various cell types, and SLC6A8 deficiency can be confirmed by a functional Cr-uptake assay in fibroblasts. The genetic defects can be proven by mutation analysis of the gene involved.

Prenatal diagnosis of all three defects is possible by mutation analysis. Whether abnormalities in amniotic fluid concentrations of Cr and/or GA will be present in case of an affected foetus is unknown. The possibility of an enzyme assay in chronic villi or amniocytes has yet not been investigated.

The biochemical, enzymatic and molecular aspects of defects in Cr biosynthesis and transport have been extensively reviewed by Verhoeven et al. [10].

7.2.2 Properties of Analytes

The chemical structures of creatinine, Cr and GA are depicted in Fig. 7.2.1. Creatinine is the cyclic form of Cr, in which H_2O is repelled. Because of their molecular characteristics, creatinine, Cr and GA are hydrophilic and therefore highly soluble in water.

7.2.3 Methods

7.2.3.1 Determination of Creatinine

Determination of creatinine in urine, plasma or CSF would in theory be a simple and fast screening test for defects in Cr biosynthesis. The Jaffé method is still commonly used for routine creatinine determination. Enzymatic methods using a creatininase or creatinine deaminase are more specific, but higher costs have slowed their introduction. Creatinine concentrations in plasma samples from two patients with GAMT deficiency appeared significantly higher when measured by the Jaffé method than when measured enzymatically or by HPLC [10]. Creatinine concentrations in urine can not be used for the diagnosis of Cr biosynthesis defects, as normal concentrations can be found in affected patients [11]. Creatinine excretion per 24 h has been reported to be low and might therefore provide a diagnostic tool for the

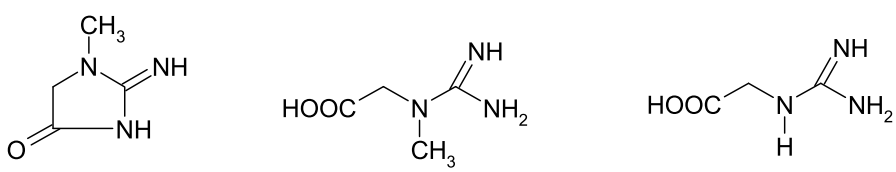

Fig. 7.2.1 Chemical structures of creatinine (*left*), creatine (Cr; *middle*), and guanidinoacetate (GA; *right*)

diagnosis of GAMT deficiency. Low urinary creatinine concentration and low 24-h urine creatinine excretion are observed in patients with vanishing muscle mass (and thus a low body Cr pool), representing an unspecific finding in several myopathies and muscular dystrophies [5]. Stöckler has reported low plasma and CSF creatinine in a patient affected with GAMT deficiency [12].

7.2.3.2 Stable-Isotope Dilution Gas Chromatography-Mass Spectrometry Method for the Determination of GA and Cr in Body Fluids

Principle

GA and Cr are determined in a single procedure based upon a selective derivatisation of the guanidino group of both GA and Cr, according to Struys et al. [13] and Almeida et al. [14]. This derivatisation is carried out in an aqueous/toluene mixture, in which the formed derivatives are "extracted" into the toluene phase. The toluene phase is subsequently blown to dryness, and the carboxylic groups of GA and Cr are derivatised with pentafluorobenzylbromide (PFBBr). The final double-derivatised molecules of GA and Cr are measured by gas chromatography (GC)-mass spectrometry (GC-MS) operating in the negative chemical ionisation selective-ion monitoring mode (Fig. 7.2.2).

Pre-Analytical

No special pre-analytical procedure needs to be carried out for the determination of GA and Cr in urine (random urine-samples are suitable), plasma, and cerebrospinal fluid (CSF).

Reagents and Chemicals

1. Toluene, p.a.
2. Hexafluoroacetylaceton.
3. Triethylamine.
4. Hexane, p.a.
5. 7% PFBBr in acetonitrile (by volume).
6. 0.5 M HCl.
7. Saturated aqueous $NaHCO_3$ solution.
8. [$^{13}C_2$]GA [internal standard, (IS); ten Brink, VU University medical centre, The Netherlands].
9. [$^{2}H_3$]Cr (IS; CDN Isotopes, Quebec, Canada).

Instrumentation

The measurement of GA and Cr is performed on a bench-top GC-MS system (e.g. Automass-2, Thermo-Finnigan; or MSD 5973 Inert, Agilent) operating in the nega-

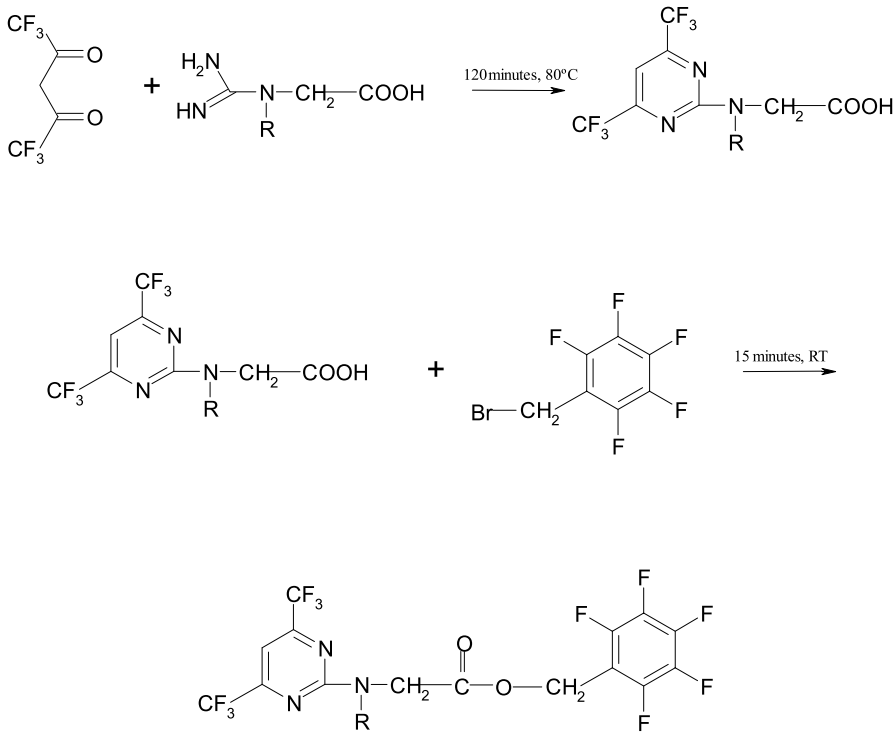

Fig. 7.2.2 Derivatisation scheme for GA and Cr. *R* = *CH*₃ creatine, *R* = *H* guanidino acetate, *RT* room temperature

tive chemical ionisation selective-ion monitoring mode, and the acquired data are obtained by the accompanying GC-MS software.

Procedure

The amounts of GA and Cr, expressed in nanomoles, and their corresponding internal standards ([$^{13}C_2$]GA and [$^{2}H_3$]Cr) in the calibration curves depend on the type of matrix (Tables 7.2.1 and 7.2.2).

Take 100 µl of plasma/CSF sample, or 50 µl of urine sample in preparation. If smaller amounts of plasma/CSF are available, add water making a total volume of 100 µl, for urine add 50 µl of water. Add 50 µl of saturated $NaHCO_3$ solution, 500 µl of toluene and 50 µl of hexafluoroacetylaceton. Derivatise for 2 h at 80°C under continuous stirring. After derivatisation, allow the vials to cool and pipette 100 µl of the toluene layer (urine/plasma) or 300 µl of the toluene layer (CSF) into a clean tube and blow to dryness at 40°C using nitrogen. To derivatise the carboxylic groups of

Table 7.2.1 *Calibration curves for guanidinoacetate (GA). CSF Cerebrospinal fluid, IS internal standards*

Calibration level	Plasma (nmol GA)	CSF (nmol GA)	Urine (nmol GA)
1	0	0	0
2	0.05	0.01	5
3	0.10	0.025	10
4	0.25	0.50	25
5	0.50	0.10	50
nmol IS	**0.25**	**0.025**	**12.5**

Table 7.2.2 *Calibration curves for creatine (Cr)*

Calibration level	Plasma/CSF (nmol Cr)	Urine (nmol Cr)
1	0	0
2	0.5	5
3	1.0	10
4	2.5	25
5	5.0	50
6	10	100
7	–	200
nmol IS	**2.5**	**25**

GA and Cr, add 100 µl of PFBBr solution (7% v/v in acetonitrile) and 10 µl of triethylamine, after which the reaction takes place at room temperature (RT) in 15 min. After the addition of 200 µl 0.5 M HCl, the derivatives formed are extracted with 1 ml hexane. The hexane layer is pipetted into a GC vial, blown to dryness at RT with nitrogen, and the dry residue is re-dissolved in 100 µl of hexane.

GC-MS Measurement

Derivatised GA and Cr are measured by GC-MS by the injection of 1 µl into the GC-MS system operating in the negative chemical ionisation mode. The injection temperature is 250°C, the transfer line temperature is 260°C and the oven temperature is programmed starting at 100°C for 1 min followed by a linear ramp of 5°C/min to 260°C. A mixture of 95% methane, 5% ammonia is used as reagent gas. A polar GC column (e.g. SGE, BPX-70) is used to allow proper chromatography, which is neces-

sary in the cases of plasma and CSF samples. The measured traces for GA are *m/z* –288 and *m/z* –290 (IS) and for Cr *m/z* –302 and *m/z* –305 (IS).

Calculation

The concentration of the analyte is calculated by interpolation of the observed analyte:IS peak area ratio into the linear regression line for the calibration curve, which is obtained by plotting the peak-area ratios against analyte concentration.

Interpretation

AGAT deficiency can be diagnosed by the decreased concentrations of GA in plasma and urine.

In patients affected with GAMT deficiency, GA is elevated in urine, plasma and CSF. In addition, Cr is decreased or in the low–normal range in urine, plasma and CSF. Creatinine in urine (expressed as excretion per 24 h) and plasma is decreased. This low urinary creatinine results in increased concentration of other metabolites (e.g. amino acids, organic acids, uric acid) when expressed per mol creatinine. During treatment by Cr supplementation, GA in plasma decreases, but does not normalise. Cr in plasma and urine becomes increased.

Male patients affected with X-linked Cr transporter defect have elevated urinary Cr concentrations only if this is expressed per mol creatinine (also mentioned Cr: creatinine ratio). In plasma, Cr concentrations are within the normal limits. Also, GA is within the reference range in both plasma and urine. Female carriers of the defect may have elevated urinary Cr excretion (expressed per mol creatinine). However this is not a consistent finding in all carriers.

Chromatograms

Example chromatograms are shown in Fig. 7.2.3.

Reference Values

Reference values for both GA and Cr are age-dependent [14], and are listed in Tables 7.2.3 and 7.2.4.

Typical Pathological Values

Examples of typical pathological values are given in Table 7.2.5. Typical pathological values for the three other children affected with AGAT deficiency have been described in non-standard units, with the exception for GA in plasma [15]. For these patients GA levels in plasma samples range from 0.01 to 0.04 μmol/l (controls 0.35–1.8). In the case of urine samples, GA is more then ten times decreased compared to

controls (values presented as μmol/l). Cr levels are expressed as the sum of Cr and creatinine and found to range from moderately lowered to low–normal.

Pitfalls

The stable-isotope dilution GC-MS measurement of GA and Cr in plasma, CSF and urine is sensitive, robust and reliable. The measurement of especially GA in CSF needs attention with regard to the chromatography. The analyses should be carried out on a GC column coated with a polar stationary phase to achieve proper separation of GA and interfering compounds.

7.2.3.3 Follow-Up Enzyme Assay

The diagnosis of GAMT deficiency and AGAT deficiency and Cr transporter deficiency can be confirmed by specific enzyme assays.

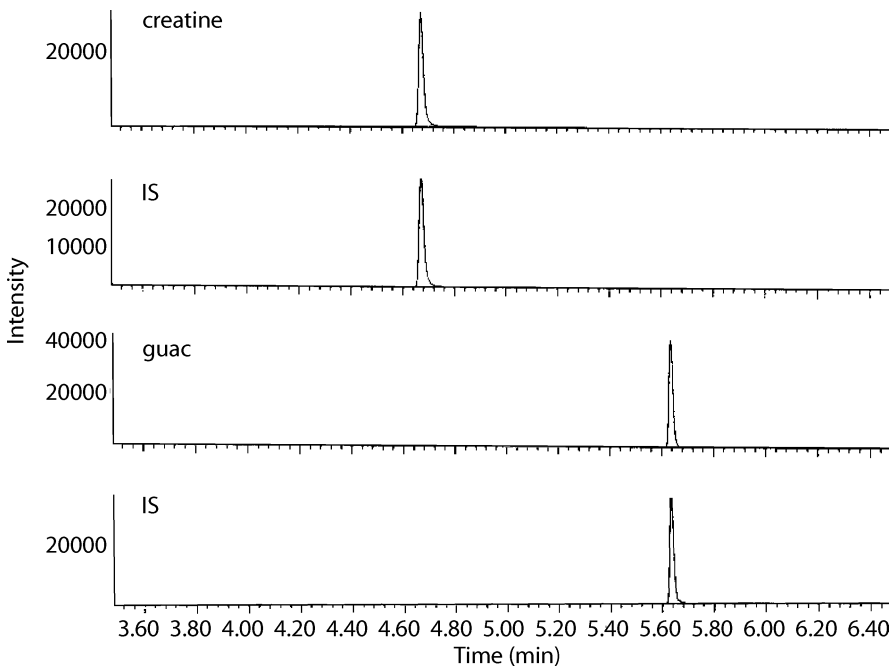

Fig. 7.2.3 Mass fragmentogram of a pooled urine sample. The *two upper traces* display the signal for Cr and its labelled internal standard (*IS*) at a retention time of 4.62 min. The *lower two traces* display the signal for GA (*guac*) and its internal standard at a retention time of 5.52 min

■ ***Table 7.2.3*** *Reference values for GA*

GA	N	Age (years)	Range
Urine (mmol/mol creatinine)	104	0–15	2–220
	40	>15	3–78
Plasma (μmol/l)	33	0–15	0.35–1.8
	21	>15	1.0–3.5
CSF (μmol/l)	10	not established	0.036–0.22

■ ***Table 7.2.4*** *Reference values for Cr*

Cr	N	Age (years)	Range
Urine (mmol/mol creatinine)	44	0–4	6–1208
	36	4–12	17–721
	47	>12	11–244
Plasma (μmol/l)	33	0–10	17–109
	32	>10	6–50
CSF (μmol/l)	34	0–10	24–53
	7	>10	38–66

■ ***Table 7.2.5*** *Pathological values for Cr and GA.* AGAT *L-Arginine:glycine amidinotransferase,* GAMT *guanidinoacetate methyltransferase*

Pathology	GA		Cr	
	Urine mmol/mol creatinine	Plasma μmol/l	Urine mmol/mol creatinine	Plasma μmol/l
GAMT deficiency ($n=8$) [10,14]	>500	>10	normal	<7
Cr transporter deficiency ($n=8$) [10,14]	normal	normal	>1400[a]	normal
AGAT deficiency ($n=1$) [5]	<0.3	<0.05	not performed	2.3

[a] Values obtained for older individuals should always be related to the proper age-matched normal values.

GAMT Deficiency

GAMT activity is measured in homogenates of cultured lymphoblasts or fibroblasts [16]. The assay is performed using [$^{13}C_2$]-GA and [$^{2}H_3$]-S-adenosylmethionine as substrates followed by the measurement of [$^{13}C_2$-$^{2}H_3$]Cr by the regular GC-MS procedure, which represents GAMT activity (Table 7.2.6).

■ ***Table 7.2.6*** *GAMT activity in controls, heterozygotes, and GAMT-deficient patients*

	GAMT activity pmol/h/mg protein	
	Lymphoblasts	**Fibroblasts**
Patients	< 5 ($n = 2$)	< 5 ($n = 5$)
Heterozygotes ($n = 2$)	69, 130	–
Controls	63–450 ($n = 10$)	60–243 ($n = 7$)

■ ***Table 7.2.7*** *AGAT activity in controls and AGAT-deficient patients*

	AGAT activity pmol/h/mg protein	
	Lymphoblasts	**Fibroblasts**
Patients ($n = 1$)	0	Not performed
Controls	21–110 ($n = 15$)	1.3–8.5 ($n = 16$)

AGAT Deficiency

AGAT activity can be determined in homogenates of lymphocytes or lymphoblasts. In this procedure [$^{15}N_2$]-L-arginine and [$^{13}C_2$-^{15}N]glycine are used as substrates [17]. The product of this enzyme reaction is [$^{13}C_2$-$^{15}N_3$]-GA, which is measured by the regular GC-MS procedure and represents AGAT activity (Table 7.2.7).

Cr Transporter Deficiency

The function of the Cr transporter is assayed using intact fibroblasts, which are cultured for 24 h in a medium that is enriched with either 25 µM or 500 µM Cr [18]. The intracellular concentration of Cr in the fibroblasts is determined using the GC-MS procedure described in detail in this chapter (Table 7.2.8).

7.2.4 Alternative Analytical Methods

Several methods are available for laboratories to determine GA and Cr in body fluids. A sensitive HPLC method for the measurement of GA and Cr plus creatinine in biological fluids has been published by Carducci et al. [19]. The method uses pre-column derivatisation with benzoin, separation on a reverse-phase column, and

■ ***Table 7.2.8*** *Uptake of Cr by fibroblasts derived from controls and patients with Cr transporter deficiency*

	Cr uptake pmol/µg protein/24 h	
	Level Cr 25 µM	**Level Cr 500 µM**
Patients ($n = 10$)	0–1	5–13
Controls	17–37	25–49

fluorescence detection. It has been proven to be useful for the diagnosis of GAMT and AGAT deficiencies; however, as Cr and creatinine are determined together, this method cannot be used for the diagnosis of the Cr transporter deficiency. Recently, liquid chromatography-tandem mass spectrometry (LC-MS/MS) methods have been described for the combined determination of GA and Cr in bloodspots, urine and plasma [20–22]. In these methods, GA and Cr are converted to their butyl-esters, enhancing sensitivity and selectivity. The decrease in sample handling and analysis time is a major advantage of these LC-MS/MS methods. With respect to analytical sensitivity, the GC-MS method [13], as described in this chapter in detail, allows detection of lowered GA in urine and plasma (important for the diagnosis of AGAT deficiency) and is the only method available thus far that is able to measure GA in CSF.

References

1. Salomons GS, Wyss M, Jakobs C (2005) Creatine. In: Coates P, Blackman MR, Cragg G, Levine M, Moss J, White J (eds) Encyclopedia of Dietary Supplements. Marcel Dekker, pp 151–158
2. Wyss M, Kaddurah-Daouk R (2000) Creatine and creatinine metabolism. Phys Rev 80:1107–1213
3. Item CB, Stöckler-Ipsiroglu S, Stromberger C, Mühl A, Alessandrì MG, Bianchi MC, Tosetti M, Fornai F, Cioni G (2001) Arginine:glycine amidinotransferase deficiency: the third inborn error of creatine metabolism in humans. Am J Hum Genet 69:1127–1133
4. Battini R, Leuzzi V, Carducci C, Tosetti M, Bianchi MC, Item CB, Stöckler-Ipsiroglu S, Cioni G (2002) Creatine depletion in a new case with AGAT deficiency: clinical and genetic study in a large pedigree. Mol Genet Metab 77:326–331
5. Salomons GS, Johnston K, Plawner L, Cooper L, Barkovich J, Verhoeven NM, Jakobs C (2005) The second family with AGAT deficiency (creatine biosynthesis defect); diagnosis, treatment and the first prenatal diagnosis. J Inherit Metab Dis 28:224
6. Stromberger C, Bodamer OA, Stöckler-Ipsiroglu S (2003) Clinical characteristics and diagnostic clues in inborn errors of creatine metabolism. J Inherit Metab Dis 26:299–308
7. Salomons GS, van Dooren SJ, Verhoeven NM, Marsden D, Schwartz C, Cecil KM, DeGrauw TJ, Jakobs C (2003) X-linked creatine transporter defect: an overview. J Inherit Metab Dis 26:309–318
8. Rosenberg EH, Almeida LS, Kleefstra T, deGrauw RS, Yntema HG, Bahi N, Moraine C, Ropers HH, Fryns JP, deGrauw TJ, Jakobs C, Salomons GS (2004) High prevalence of SLC6A8 deficiency in X-linked mental retardation. Am J Hum Genet 75:97–105

9. Mancini GM, Catsman-Berrevoets CE, de Coo IF, Aarsen FK, Kamphoven JH, Huijmans JG, Duran M, van der Knaap MS, Jakobs C, Salomons GS (2004) Two novel mutations in SLC6A8 cause creatine transporter defect and distinctive X-linked mental retardation in two unrelated Dutch families. Am J Med Genet A 132:288–295
10. Verhoeven NM, Salomons GS, Jakobs C (2005) Laboratory diagnosis of defects of creatine biosynthesis and transport. Clin Chim Acta 361:1–9
11. Verhoeven NM, Guerand WS, Struys EA, Bouman AA, van der Knaap MS, Jakobs C (2000) Plasma creatinine assessment in creatine deficiency: a diagnostic pitfall. J Inherit Metab Dis 23:835–840
12. Stöckler S, Marescau B, De Deyn PP, Trijbels JM, Hanefeld F (1997) Guanidino compounds in guanidinoacetate methyltransferase deficiency, a new inborn error of creatine synthesis. Metabolism 46:1189–11939
13. Struys EA, Jansen EE, ten Brink HJ, Verhoeven NM, van der Knaap MS, Jakobs C (1998) An accurate stable isotope dilution gas chromatographic-mass spectrometric approach to the diagnosis of guanidinoacetate methyltransferase deficiency. J Pharm Biomed Anal 18:659–665
14. Almeida LS, Verhoeven NM, Roos B, Valongo C, Cardoso ML, Vilarinho L, Salomons GS, Jakobs C (2004) Creatine and guanidinoacetate: diagnostic markers for inborn errors in creatine biosynthesis and transport. Mol Genet Metab 82:214–219
15. Carducci C, Birarelli M, Leuzzi V, Carducci C, Battini R, Cioni G, Antonozzi I (2002) Guanidinoacetate and creatine plus creatinine assessment in physiologic fluids: an effective diagnostic tool for the biochemical diagnosis of arginine:glycine amidinotransferase and guanidinoacetate methyltransferase deficiencies. Clin Chem 48:1772–1778
16. Verhoeven NM, Roos B, Struys EA, Salomons GS, van der Knaap MS, Jakobs C (2004) Enzyme assay for diagnosis of guanidinoacetate methyltransferase deficiency. Clin Chem 50:441–443
17. Verhoeven NM, Schor DS, Roos B, Battini R, Stöckler-Ipsiroglu S, Salomons GS, Jakobs C (2003) Diagnostic enzyme assay that uses stable-isotope-labeled substrates to detect L-arginine:glycine amidinotransferase deficiency. Clin Chem 49:803–805
18. Salomons GS, van Dooren SJ, Verhoeven NM, Cecil KM, Ball WS, Degrauw TJ, Jakobs C (2001) X-linked creatine-transporter gene (SLC6A8) defect: a new creatine-deficiency syndrome. Am J Hum Genet 68:1497–1500
19. Carducci C, Birarelli M, Santagata P, Leuzzi V, Carducci C, Antonozzi I (2001) Automated high-performance liquid chromatographic method for the determination of guanidinoacetic acid in dried blood spots: a tool for early diagnosis of guanidinoacetate methyltransferase deficiency. J Chromatogr B Biomed Sci Appl 755:343–348
20. Bodamer OA, Bloesch SM, Gregg AR, Stockler-Ipsiroglu S, O'Brien WE (2001) Analysis of guanidinoacetate and creatine by isotope dilution electrospray tandem mass spectrometry. Clin Chim Acta 308:173–178
21. Cognat S, Cheillan D, Piraud M, Roos B, Jakobs C, Vianey-Saban C (2004) Determination of guanidinoacetate and creatine in urine and plasma by liquid chromatography-tandem mass spectrometry. Clin Chem 50:1459–1461
22. Carducci C, Santagata S, Leuzzi V, Carducci C, Artiola C, Giovanniello T, Battini R, Antonozzi I (2006) Quantitative determination of guanidinoacetate and creatine in dried blood spot by flow injection analysis-electrospray tandem mass spectrometry. Clin Chim Acta 364:180–187

7.3 Porphyrins, Porphobilinogen, and δ-Aminolevulinic Acid

Elisabeth Irene Minder,
Xiaoye Schneider-Yin

7.3.1 Introduction

Porphyrias are inborn errors of heme biosynthesis [1, 2]. There are seven steps in this metabolic pathway (Fig. 7.3.1), each of which may be affected, leading to a specific disease entity (Table 7.3.1). Heme is synthesized in each cell, as heme is the active group of several respiratory chain enzymes. The highest heme synthesis rate, however, is found in erythrocyte precursors in the bone marrow, and the second highest is found in the hepatocytes. Whereas the liver enzymes are the same housekeeping forms as those in other tissues, heme synthesis in erythrocyte precursor cells is differentially regulated. The initial enzyme erythrocytic δ-aminolevulinic acid (ALA) synthase (ALAS) is encoded by a gene different from the housekeeping one, and several other enzymes are regulated by alternate, erythrocyte-specific promoters [3–5]. The porphyrias are divided into two groups according to their clinical presentation: the acute porphyrias and the nonacute porphyrias [6]. Acute porphyrias are acute-intermittent porphyria (AIP), porphyria variegata (PV), hereditary coproporphyria (HC), and the rare ALA dehydratase (ALAD) deficiency. Acute porphyrias are characterized by episodes of severe abdominal pain, nausea, vomiting, constipation, psychic disturbances, tachycardia, hypertension, and hyponatremia, eventually progressing to muscular weakness, paresis (including respiratory muscles), epileptic seizures, coma, and death. These acute porphyrias are characterized by increases in urinary levels of ALA and porphobilinogen (PBG) of between 5- and 20-fold during the acute crises and for up to at least 7 days thereafter. Prepubertal children are rarely affected. Skin symptoms (blisters) may or may not be present. Nonacute porphyrias are characterized by skin symptoms that are limited to light-exposed areas. Two types of photodermatosis can be distinguished: (1) blisters of 1–2 cm in diameter, filled with clear liquid, fragility of skin and miliae, or (2) acute, severely burning pain, in severe cases combined with pale swelling, fissures, and thickening of the dermis. The latter is observed mainly at the base knuckles of the hands. Discrete scars may be visible in the face. In all these forms, porphyrins are elevated in specific body fluids, but increases are eventually less dramatic than in acute porphyria episodes. The prevalent porphyrin pattern in conjunction with the clinical picture will enable diagnosis of a specific porphyria and to differentiate it from nonspecifically elevated porphyrins induced by a variety of factors such as alcohol intake and stress (see Table 7.3.1) [2].

Table 7.3.1 *Synopsis of the relatively frequent porphyrias. The diagnostic tests most significant for each porphyria have a* gray background. *The order of test to be applied depends on the clinical situation and has been outlined in the Introduction under the subheading diagnostic strategies (section 7.3.1.1).* ALA *Aminolevulinate,* ALAD *aminolevulinate dehydratase,* AIP *acute intermittent porphyria,* CEP *congenital erythropoietic porphyria,* Copro *coproporphyrin,* EPP *erythropoietic protoporphyria,* HC *hereditary coproporphyria,* HMBS *hydroxymethylbilane-synthase,* Intermediaries *heptacarboxy-, hexacarboxy-and pentacarboxyporphyrins,* MIM Nr *Mendelian Inheritance in Man number,* PCT *porphyria cutanea tarda,* Proto *protoporphyrin IX,* PV *porphyria variegata,* Uro *uroporphyrin*

		ALAD deficiency	AIP	CEP	PCT	HC	PV	EPP
MIM Nr		**125 270**	**176 000**	**263 700**	**176 090/ 176 100**	**121 300**	**176 200**	**177 000**
Affected enzyme		ALA-dehydratase	Hydroxymethylbilane synthase	Uroporphyrinogen III synthase	Uroporphyrinogen decarboxylase	Coproporphyrinogen oxidase	Protoporphyrinogen oxidase	Ferrochelatase
Clinical symptoms	Photosensitivity	None	None	Ulcers and mutilations	Blisters and fragility	Blisters and fragility	Blisters and fragility	Burning pain
	Abdominal pain	Present	Present	None	None	Present	Present	None
Urine	ALA	↑↑	↑↑	Normal	Normal–↑	↑↑	↑↑	Normal
	PBG	Normal	↑↑	Normal	Normal	↑↑	↑↑	Normal
	Uro	Normal	↑↑	↑↑	↑↑	↑↑	↑↑	Normal
	Intermediaries	Normal	↑	↑↑	↑↑	↑	↑	Normal
	Copro I	↑	↑	↑↑	Normal–↑	↑	↑	Normal
	Copro III	↑↑	↑↑	↑	Normal	↑↑	↑↑	Normal
Feces	Copro I		Normal–(↑)		Normal	(↑)	(↑)	Normal
	Copro III		Normal–(↑)		Normal	↑↑	↑↑	Normal
	Ratio		<2		<2	>2	>2	<2
	Proto		Normal–(↑)		Normal	Normal	↑↑	↑
Erythrocytes	Uro, Copro			↑↑				Normal
	Proto			↑				↑↑
Additional tests		ALAD activity ↓	HMBS activity ↓	Isomer separation	Isocoproporphyrin		Plasma scan	

In most porphyrias, excess metabolites can be detected in urine. Less polar porphyrins (i.e., coproporphyrins and protoporphyrin) are detectable in feces as they are excreted by the bile. The apolar protoporphyrin is eventually only detectable in blood. Porphyrins can easily be detected and measured by their intense fluorescence in mineral acids. The excitation wavelength is around 404 nm, and emission at about 615 nm. ALA is derivatized to a pyrrole and both, ALA and PBG, are detected by dimethylaminobenzaldehyde (DMAB), as described by Mauzerall and Granick [7].

7.3.1.1 Diagnostic Strategies

The types of test to be performed depend on the clinical situation. If the patient has an acute, severe disease and an acute porphyria is suspected, PBG should be assessed either qualitatively by a reliable screening test or quantitatively in a spot urine. Quantitative ALA can be added to uncover lead intoxication, which may be clinically undistinguishable from an acute porphyria. Furthermore, the extremely rare ALAD deficiency may show normal PBG. If increased values of PBG are present, urinary porphyrins can be determined to confirm the existence of porphyria.

If the patient is actually asymptomatic, but has a family history of acute porphyria or prior symptoms suspicious of acute porphyria, hydroxymethylbilane synthase (HMBS) activity, plasma scanning, and fecal porphyrins should be measured. These tests will reveal AIP, PV, and HC. As a small percentage of AIP families exhibit normal HMBS activity, PBG in a urine sample can be added. PBG determination can also performed as a first choice, if an acute porphyria is suspected. But if normal, it does not exclude acute porphyrias in asymptomatic phases. Furthermore, the existence of an acute porphyria is only proved if the value exceeds at least five times the upper limit of normal.

If a patient presents with blisters due to photosensitivity, a plasma scan and fecal porphyrins will not only reveal the presence of a porphyria, but will also enable the distinction between the three forms that may cause such symptoms: porphyria cutanea tarda (PCT), PV, and HC. Urinary porphyrins and eventually quantitative ALA und PBG in urine may be added in questionable cases or for monitoring of therapy.

If the patient presents with acute burning pain, the examination of choice is erythrocytic protoporphyrins. If the free protoporphyrin is significantly elevated (more than 6 μmol/l), the diagnosis of erythropoietic protoporphyria is established. Plasma porphyrins are used in patients on chronic hemodialysis who suffer from skin blisters to differentiate between PCT and pseudoporphyria; the latter does not show increased plasma porphyrins.

7.3.2 ALA and PBG

ALA and PBG are the precursors of porphyrin synthesis (Fig. 7.3.1). ALA is synthesized from glycine and succinyl-coenzyme A by ALAS. Two molecules of ALA are converted to PBG by the enzyme ALAD.

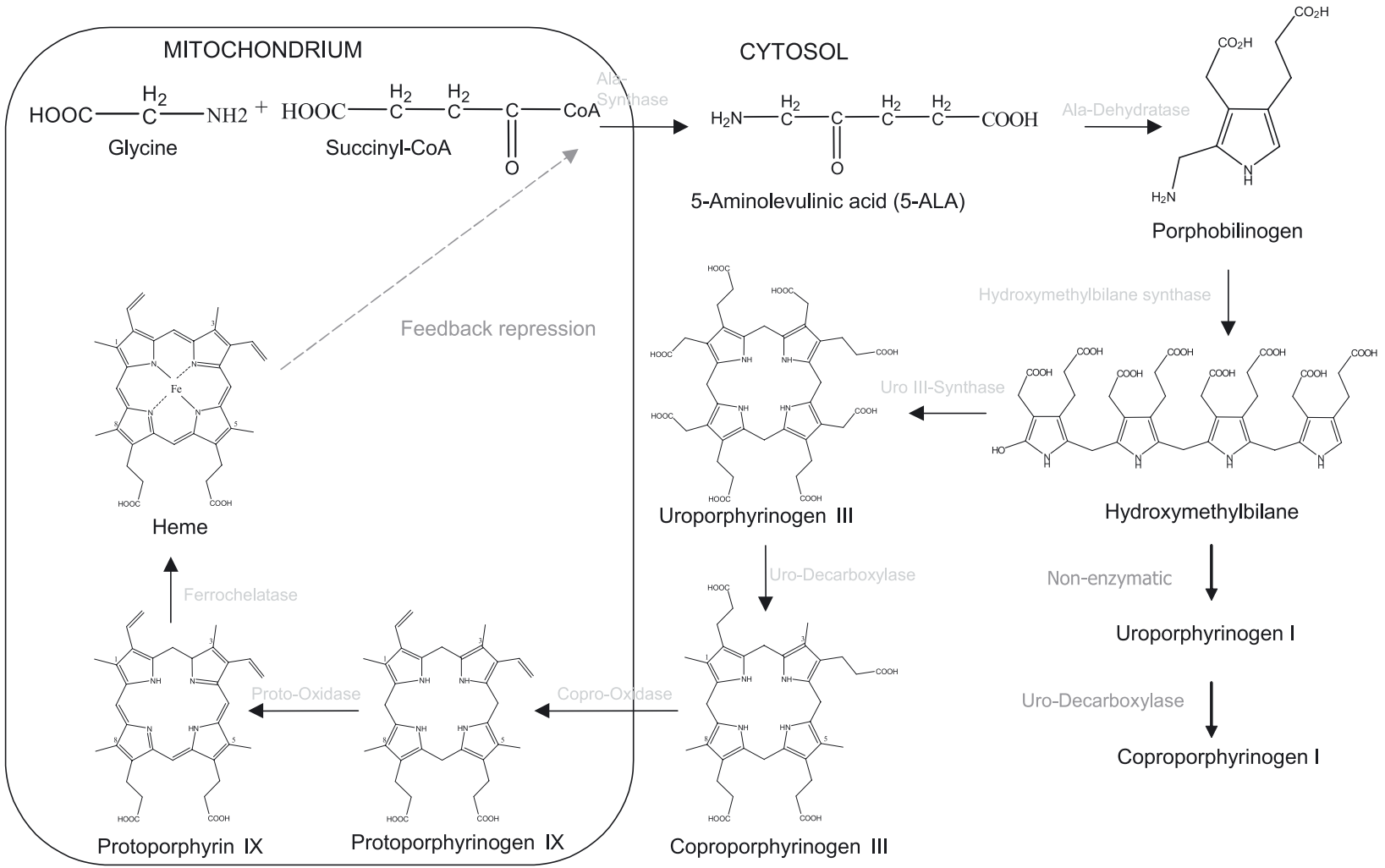
MITOCHONDRIUM
CYTOSOL
Glycine
Succinyl-CoA
Ala-Synthase
5-Aminolevulinic acid (5-ALA)
Ala-Dehydratase
Porphobilinogen
Hydroxymethylbilane synthase
Hydroxymethylbilane
Uro III-Synthase
Uroporphyrinogen III
Uro-Decarboxylase
Coproporphyrinogen III
Copro-Oxidase
Protoporphyrinogen IX
Proto-Oxidase
Protoporphyrin IX
Ferrochelatase
Heme
Feedback repression
Non-enzymatic
Uroporphyrinogen I
Uro-Decarboxylase
Coproporphyrinogen I

◄ **Fig. 7.3.1** The heme synthesis pathway starts in the mitochondrion. The next four steps proceed in the cytosol. Coproporphyrinogen oxidase is in the intermembrane space of the mitochondrion, and the last two enzymes reside at the mitochondral matrix side of the inner membrane. The product heme represses the first and rate-limiting enzyme δ-aminolevulinic acid (*5-ALA*) synthase at transcription, during the translation step, and by its transport into the mitochondrion

7.3.2.1 PBG Screening

Method

Principle

Screening tests for PBG are based on its reaction with DMAB (modified "Ehrlich's reaction"). We recommend the trace PBG test kit available from Thermo Electron (UK), which isolates PBG from urine by ion-exchange resin before the reaction with DMAB. Older screening methods, such as those of Schwartz or Hoesch, give false-positive results due to the reaction of DMAB with urea, which is abundant in urine.

Preanalytical

- Specimen

The PBG screening test should only be used in emergency situations because of its limited analytical sensitivity.

- Reagents and Chemicals

Trace PBG test kit (Thermo Electron).

- Instrumentation

None

- Calibration

None

- Quality Control

We recommend using a positive patient urine sample stabilized with 1% sodium azide and kept in aliquots at –20°C.

Analytical

The procedure is performed according to the supplier's description. For details see below under "ALA and PBG Quantitative" (section 7.3.2.2).

- Calculation

None

Postanalytical

■ Interpretation

Typical pathological values show a strong pink color. Other colors should not be interpreted. Positive tests should be confirmed by quantitative measurements of ALA and PBG.

Pitfalls

None known.

7.3.2.2 ALA and PBG Quantitative

Method

Principle

The quantitative assay for PBG and ALA (Bio Rad, Hercules, CA, USA) that is based on the classical method by Mauzerall and Granick may be used for determination of the porphyrin precursors. PBG is absorbed by the anion-exchange column and ALA by the cation-exchange column; interferences are washed out. After elution from the column, ALA is derivatized by acetyl acetone to form a pyrrole. Both ALA and PBG are determined colorimetrically with the modified Ehrlich's reagent. Instead of this broadly used standard method ALA, but not PBG may be detected and quantified using amino acid chromatography. However, our experience has shown that this method is only valid for detecting massively increased concentrations of ALA.

Preanalytical

■ Specimen

Porphyrins and porphyrin precursors are assayed most often in a 24-h urine collected without additive. Alternatively, untimed urine samples may be used and excretion standardized to creatinine. The latter is especially recommended for children and in emergency situations. Alternative specimens for porphyrins are plasma, erythrocytes, and feces, depending on the medical indication. During collection and until arrival at the laboratory, specimens should be kept cold, preferably at about 4°C, and protected from light. Specimens in the laboratory are best kept frozen, as the metabolites in body fluids are stable at –20°C for at least 3 months. Some exceptions have been noted below.

■ Reagents and Chemicals

1. Test kit ALA/PBG by column test (Bio Rad).
2. Concentrated acetic acid p.a.
3. Perchloric acid 70% p.a.
4. Modified Ehrlich's reagent (prepare freshly for each use, stable for 6 h only): 2 g 4-DMAB (part of the test kit) is solubilized in 84 ml concentrated acetic acid, with 16 ml perchloric acid added.

■ Instrumentation

1. Column rack (Bio Rad).
2. Heating device.

3. Spectrophotometer (measurement at 553 nm); alternatively, a filter photometer (at 546 nm) may be used.

Calibration

By the use of the molar extinction coefficient at 553 nm ($\varepsilon_{mM,\lambda=553}$: ALA $\varepsilon_{mM,\lambda=553} = 72$; PBG $\varepsilon_{mM,\lambda=553} = 61$) and a recovery factor according to the supplier's information. Alternatively, a standard curve may be used for ALA determination.

Quality Control

Lyphochek quantitative urine control includes a normal and an abnormal level of ALA. For PBG quality control, we recommend using a positive patient urine sample stabilized with 1% sodium azide and kept in aliquots at –20°C.

Analytical

Procedure

The procedure is performed according to the supplier's description. Briefly, the anion-exchange column is placed over the cation-exchange column. After washing of both columns with distilled water, 0.5 ml urine is placed on top of the first column and allowed to drain through both columns. ALA is retained on the cation-exchange column, and PBG on the anion-exchange column. Interferences, especially urea, are washed from the columns by adding 3 × 10 ml of distilled water. ALA is eluted from the anion column by sodium acetate buffer, and PBG from the cation column by 1 M acetic acid. ALA is derivatized by methyl acetoacetate to 2-methyl-3carbmethoxy-4-(3-propionic acid) pyrrole during 10 min heating in a boiling water bath or on a 100°C heating block. The ALA-derived pyrrole and PBG are reacted in separate tubes with modified Ehrlich's reagent containing DMAB [7], which results in a pink-colored derivative. Its absorbance is determined at 553 nm

Calculation

The $\varepsilon_{M\lambda=553}$ of PBG-derivative is 6.1×10^4; that of the ALA derivative 2-carboxyethyl-4-(3-propionic acid)pyrrole is 7.2×10^4 [7]. The dilution factor of ALA is 28, and that of PBG is 16; their recovery rates are 85% and 67%, respectively.

The supplier annotates conversion factors to transform absorbance into concentrations. These factors are composed of the dilution factor, the $\varepsilon_{mM,\lambda=553}$, and a factor for recovery of the extraction and derivatization, are 60 for conversion of ALA into mg/l or 457.56 for its conversion into µmol/l and 88 for conversion of PBG into mg/l or 388.96 for its conversion into µmol/l. Alternatively, a standard curve can be used for ALA only.

Postanalytical

Interpretation

Typical pathological values show a strong pink color. Other colors should not be interpreted. Values elevated at least fivefold are proof of acute porphyria. Lower, but still increased values may be encountered in asymptomatic porphyria patients and as a secondary phenomenon due to alcohol intake or stress. PBG elevation is apparently more specific for porphyria.

Isolated significant increases in ALA may indicate a lead intoxication, especially if combined with an increase in coproporphyrin III isomer. Alternatively, this pat-

tern may be seen in tyrosinemia type I and in the very rare ALA-dehydratase deficiency. Reference values (mean ± 2 SD) for excretion of ALA and PBG are < 50 and < 7.5 μmol/24 h, respectively, or < 2.5 and < 1.25 mmol/mol creatinine, respectively.

Pitfalls

False, isolated increases in ALA may be caused by teichoplanin and by coamoxyclav.

7.3.3 Porphyrins

Porphyrins consist of a tetrapyrrole ring with variable side chains. The physiological compounds are the reduced forms, the porphyrinogens that do not fluoresce. They react spontaneously with oxygen in the air to the strongly fluorescent porphyrins.

The first porphyrin intermediate of the biosynthetic pathway is uroporphyrinogen, which is stepwise decarboxylated by uroporphyrinogen decarboxylase to heptacarboxy-, hexacarboxy-, pentacarboxy-, and coproporphyrinogen. This latter compound proceeds, as indicated in Fig. 7.3.1, to protoporphyrinogen and protoporphyrin. The oxidized uroporphyrin and its decarboxylation products up to coproporphyrin are assayed in urine. Coproporphyrin and the further downstream intermediaries can be recovered from feces as described below.

Increased porphyrins in clear fluid such as urine may be detected directly by their pink fluorescence if exposed to long ultraviolet (Fig. 7.3.2). The specificity of this screening assay may be improved if porphyrins are extracted by talcum [8]. These isolated porphyrins may be quantified using a spectrofluorimeter. As different porphyrias show specific excretion patterns, separation of the main porphyrins is desirable. The formerly used fractionated extraction enabled to separate the uroporphyrin fraction from the coproporphyrin fraction. In addition to uroporphyrin, the first fraction includes heptacarboxy- and part of hexacarboxyporphyrins, and in addition to coproporphyrin, the second fraction includes part of hexacarboxy- and pentacarboxyporphyrins. Later on, thin-layer chromatography of methylester derivatives is used.

Nowadays, the preferred methodology is the separation and quantification of porphyrins by high-performance liquid chromatography (HPLC) with fluorescence detection. Thus, a method that detects the main isomers of specific porphyrins is recommended, as a high number of different isomers exist, especially in pathological conditions, and the relative abundance of the different isomers supports the distinction of the different porphyrias (Table 7.3.1).

7.3.3.1 Urinary Porphyrins Assessed by HPLC

Methods

Principle

Free porphyrin acids, including isomers, are separated depending on their polarity on a reverse-phase system [9, 10]. The detection by fluorescence is highly specific because both their excitation and their emission are at relatively long wavelengths.

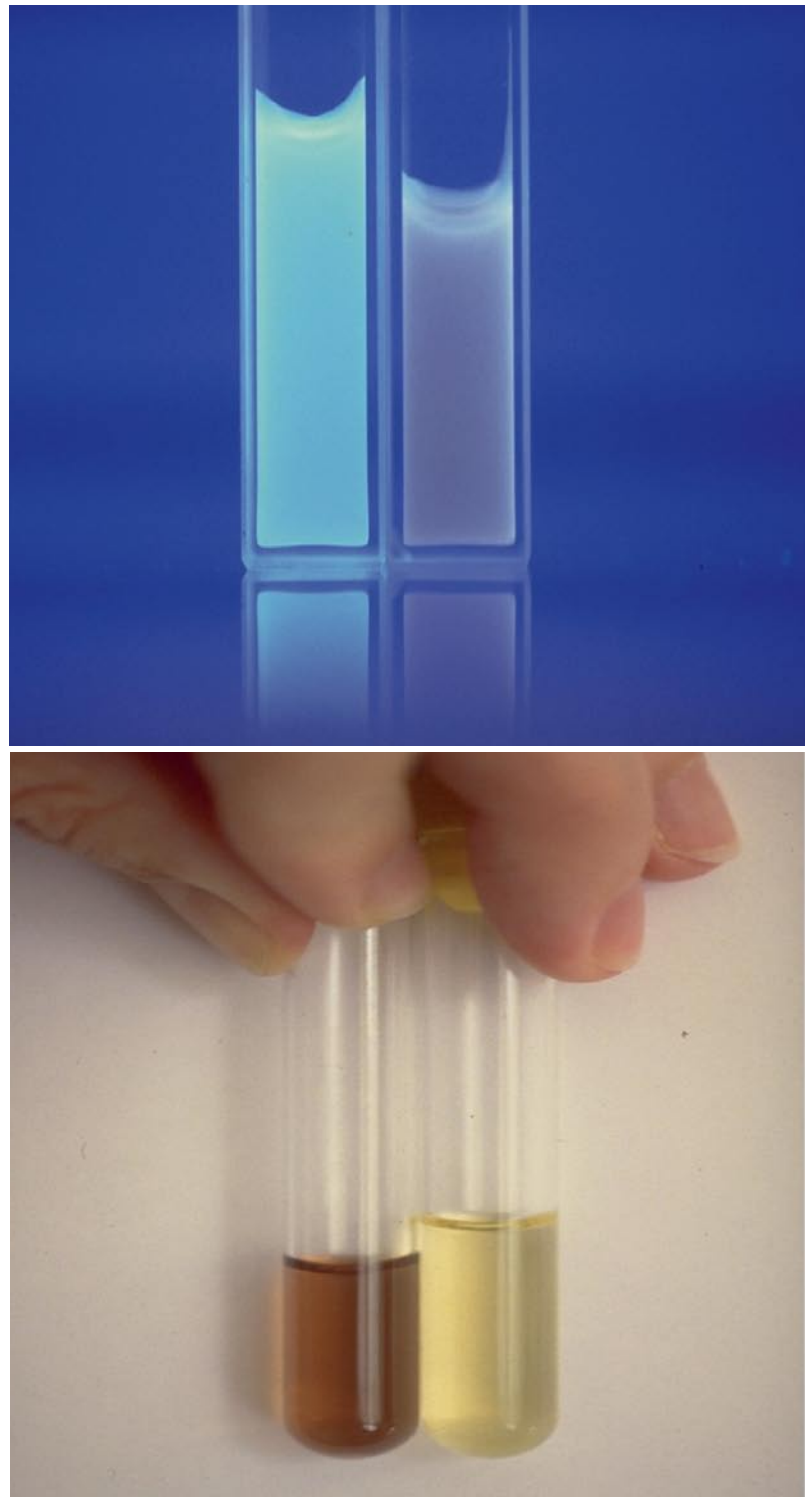

Fig. 7.3.2 Characteristic color of a porphyrin urine (*left urine on lower picture*) and typical purple fluorescence (*right urine on upper picture*) both compared to a normal urine

Preanalytical

Urine should be collected without additive. Specifically, acidified specimens should not be used. Transport and storage, as mentioned above (see section 7.3.3.2, under "Preanalytical").

Specimens

Twenty-four-hour urine collection or untimed urine samples may be assayed. For specific indications, a fecal portion (about 5–10 g), plasma, or erythrocytes may be analyzed (see below).

Reagents and Chemicals

1. 30% Hydrochloric acid (HCl).
2. Porphyrin acid marker kit (10 nmol of each uro-, heptacarboxy-, hexacarboxy-, pentacarboxy-, coproporphyrin, all I-isomers; Frontier Scientific, Logan, Utah, USA).
3. Deuteroporphyrin IX (2,4-bis-glycol; Frontier Scientific).
4. Ammonium acetate p.a.
5. Acetonitrile chromatographic grade.
6. Acetic acid (concentrate) p.a.
7. Methanol gradient, HPLC grade.

Instrumentation

1. Gradient HPLC system with fluorescence detection (excitation 404 nm, emission 618 nm).
2. Column: C1, 5 µm, 25 cm × 3.2 mm inner diameter (i.d.).
3. Buffer A: 1 M ammonium acetate, pH 5.16, containing 10 ml triethylamine and 100 ml acetonitrile per liter. The pH of the ammonium acetate buffer must be met exactly to achieve a good isomer separation.
4. Buffer B: methanol/acetonitrile 9:1.
5. Linear gradient from 0 to 80% buffer B in buffer A in 40 min, plateau at 80% for 10 min. and return to 0% in 5 min.

Calibration

Porphyrin acid marker kit (10 nmol of each uro-, heptacarboxy-, hexacarboxy-, pentacarboxy-, coproporphyrin, all I-isomers): solubilized in 5 ml 3 M HCl (stable at 4°C and light-protected for 2 weeks). 500 µl of this solution are further diluted 1:4

Table 7.3.2 *Standard (*Std*) solutions used for the determination of urinary porphyrin concentration.* IST *Deuteroporphyrin IX (2,4-bis-glycol)*

Standard	Std 1	Std 2	Std 3	Std 4
Concentration (nmol/l)	25	50	75	100
Volume standard solution (µl)	50	100	150	200
Volume IST solution (µl)	100	100	100	100
3 M HCl	850	800	750	700

with 3 M HCl for each assay (standard solution). Deuteroporphyrin IX (2,4-bis-glycol): 3.3 mg/100 ml 3 M HCl, store for up to 3 months at 4°C (IST solution). See Table 7.3.2.

Quality Control

Quality control material is available from Bio Rad or Chromsystems (Munich, Germany). We also use an abnormal patient urine stabilized with 1% azide and kept in aliquots at –20°C.

Analytical

Procedure

Samples (0.8 ml) are diluted with 0.2 ml IST solution and 0.1 ml 30% HCl, kept on ice for 15 min, centrifuged at 14,000 rpm (16,100 × *g*) and filtered (Acrodisc LC 13, Millipore) into brown HPLC autosampler tubes. Aliquots (20 µl) of standards and samples are injected into the HPLC system. Samples with high concentrations of porphyrins should be diluted with distilled water 1:10, initially.

Calculation

Calculation is based on a linear standard curve forced through zero. It is recommended to take account of all isomeric forms when calculating urinary excretion of individual porphyrins except for coproporphyrin I and III, isomers that are quantified separately. As for most of the isomers, no commercially available standards exist; we use the calibration factors of the I-isomers.

Postanalytical

Interpretation

Symptomatic porphyria patients usually show urinary porphyrin concentrations that exceed the upper limit of normal by twofold or more. Table 7.3.1 lists most of the diagnostic abnormalities of the different porphyrias. Only slightly abnormal or even fully normal values may be seen in asymptomatic patients. But alcohol overconsumption, enzyme-inducing drugs, stress, and other factors may also induce slightly abnormal values that should not be mistaken for porphyria. A characteristic sign for such a secondary effect is the isolated elevation of coproporphyrin, especially of its I-isomer.

Chromatograms

Chromatograms are shown in Fig. 7.3.3. Note the variable signal intensities on the ordinate.

Reference values

Each laboratory should establish its own reference values. Those given in Tables 7.3.3 and 7.3.4 can only be interpreted as a guide. The data given were collected by means of HPLC.

Typical Pathological Values

1. All acute porphyrias show similar urinary porphyrin patterns with predominant elevation of uroporphyrin and coproporphyrin III isomer; in addition, hepta-, hexa-, and especially pentacarboxyporphyrins are increased (see Fig. 7.3.3).

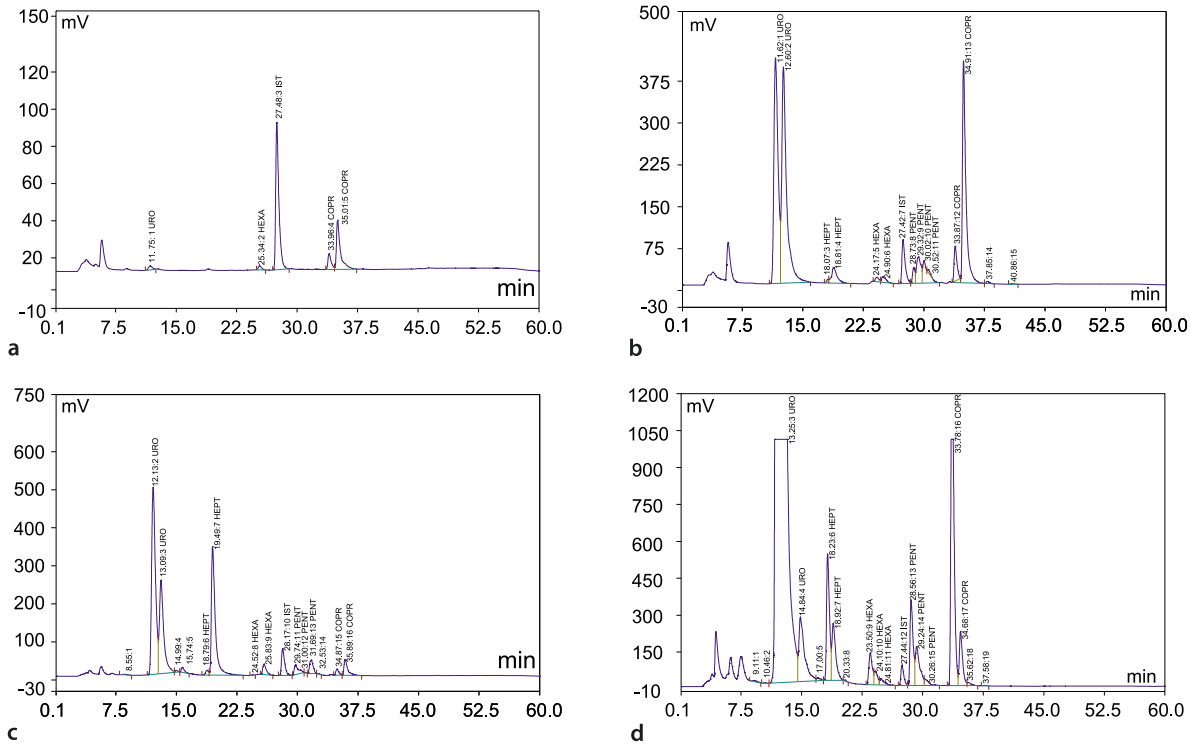

Fig. 7.3.3a–d Chromatogram of normal urine (**a**), urine from an individual with acute (in this case intermittent) hepatic porphyria (**b**), urine from an individual with porphyria cutanea tarda (**c**), and an undiluted sample from an individual with congenital erythropoietic porphyria (**d**). See typical pathological values for interpretation

2. PCT is characterized by dominantly increased uro-, heptacarboxy-, hexacarboxy-, and pentacarboxyporphyrin. Coproporphyrin may be normal or only slightly elevated.
3. Congenital erythropoietic porphyria (CEP) shows a dominance of all I-isomers.

■ Pitfalls

Chromatographic interferences are extremely rare due to the high selectivity of the applied chromatographic conditions. The most difficult interpretation problems are the discrimination between secondary effects and latent porphyria (see above, "Interpretation"). Therefore, the exclusion of porphyria in an asymptomatic individual requires additional measures to be taken (see below).

7.3.3.2 Fecal Porphyrins Assessed by HPLC

Fecal porphyrin analysis is useful to differentiate between the three acute porphyrias and to positively diagnose HC. In addition, it may support the diagnosis of PCT and of erythropoietic protoporphyria.

Table 7.3.3 *Example mean reference values for uroporphyrin, coproporphyrin I, and coproporphyrin III (these can only be interpreted as a guidance) collected by means of high-performance liquid chromatography (HPLC). The intermediary porphyrins were below the detection limit*

Age years	Uroporphyrin µmol/mol creatinine	Coproporphyrin I µmol/mol creatinine	Coproporphyrin III µmol/mol creatinine
0.00	14.26	35.68	22.75
0.25	17.24	29.22	33.12
0.50	7.80	23.80	33.78
0.75	6.66	12.22	52.59
1.00	5.96	14.02	51.47
1.50	9.77	14.38	48.79
2.25	5.67	14.96	42.24
3.00	6.39	13.33	32.67
4.00	5.64	10.32	35.73
6.00	4.40	9.45	33.41
9.00	4.25	8.10	21.62
15.00	4.89	8.11	23.88
Adults	3.9	8.4	17.8

Table 7.3.4 *Mean porphyrin reference values in adults*

Porphyrin	nmol/24 h	µmol/mol creatinine
Uroporphyrin	< 60	< 3.9
Heptacarboxyporphyrin	< 5	< 1
Hexacarboxyporphyrin	< 5	< 1
Pentacarboxyporphyrin	< 5	< 1
Coproporphyrin I	< 100	< 8.4
Coproporphyrin III	< 200	< 17.8

Methods

Principle

Porphyrins are separated from interfering pigments in stool by diethylether and then analyzed on a reverse-phase HPLC system with fluorescence detection using the same conditions as for urinary porphyrins.

Preanalytical

■ Specimens

A fecal portion of a few grams should be collected without additive. Specimens should be stored in a dark container, preferably in the cold. Storage of more than 2 days should be at –20°C.

■ Reagents and Chemicals

1. 30% HCl p.a.
2. Porphyrin acid marker kit (10 nmol of each uro-, heptacarboxy-, hexacarboxy-, pentacarboxy-, coproporphyrin, all I-isomers and Protoporphyrin IX HCl (Frontier Scientific).
3. Ammonium acetate p.a.
4. Triethylamine p.a.
5. 1,4-Dithio-DL-threitol.
6. Ammonia 32% p.a.
7. Acetonitrile, chromatographic grade.
8. Acetic acid (concentrate) p.a.
9. Methanol gradient, HPLC grade.
10. Diethylether, p.a.

■ Instrumentation

Gradient HPLC system identical to that used for urinary porphyrins. Protoporphyrin present only in feces but not in urine elutes last. If it is not eluted, the plateau phase can be prolonged for some minutes.

■ Calibration

1. Porphyrin standard: porphyrin acid marker kit (10 nmol of each uro-, heptacarboxy-, hexacarboxy-, pentacarboxy-, coproporphyrin, all I-isomers): solubilized in 2 ml 3 M HCl (stable for 2 weeks if kept at 4°C and protected from light).
2. Dithiothreitol (DTT) solution: 15 mg DTT in 14 ml 1% ammonia. Protoporphyrin IX (1.1 mg) is solubilized in 2 ml DTT solution with the aid of an ultrasonic bath within exactly 1 min. Dilute 1:10 in DTT solution (protoporphyrin standard; Table 7.3.5).

■ ***Table 7.3.5*** *Porphyrin standards used in the determination of fecal porphyrins by HPLC*

	Std 1	Std 2	Std 3	Std 4
Porphyrin standard (nmol/assay)	0.667	1.333	2.000	2.6667
Porphyrin standard (µl)	60	120	180	240
Protoporphyrin standard (nmol/assay)	3.258	6.517	13.033	19.549
Protoporphyrin standard (µl)	15	30	60	90
HCl 30% (µl)	1500	1500	1500	1500
Distilled water (µl)	2925	2850	2760	2670

Quality Control

None.

Analytical

Procedure

About 1 g of feces is weighed, dried under reduced pressure, and reweighed to calculate its dry weight. About 0.3–0.5 mg of a separate sample is weighed into a 10-ml screw-top vial. HCl (1.5 ml of 30% HCl) is added, the mixture wrapped with aluminum foil, mixed with a vortex mixer for about 30 s, placed into an ultrasonic bath for 2–3 min and again vortexed for a few seconds. Diethyl ether (4.5 ml) is added and the solution mixed again for 30 s by vortex. Three milliliters of distilled water is added carefully (the sample is warmed up by this addition). The samples are then mixed for 5 min on a mixing device and centrifuged for 5 min at 3000 rpm ($1500 \times g$). About 1.5 ml of the water phase is filtered into a brown autosampler vial for HPLC. Aliquots of 20 µl of standards and samples are injected into the HPLC system. The water phase of the samples with high concentrations of porphyrins should be diluted with 3 M HCl.

Calculation

Calculation is based on a linear standard curve forced through zero. Usually only coproporphyrin I and III and protoporphyrin are quantified. The results are converted to the amount of specific porphyrins per gram of dry feces.

Postanalytical

Interpretation

Fecal porphyrins are determined to differentiate between the three acute porphyrias, AIP, PV, and HC (Table 7.3.1). Symptomatic PV shows abundant fecal coproporphyrins, whereby the III isomer is always dominant and protoporphyrin is elevated. In symptomatic HC, only fecal coproporphyrins with dominance of the III isomers are increased. Fecal porphyrins are usually normal in AIP. They may be moderately elevated in acute porphyric attacks in AIP, but coproporphyrin I is then higher than coproporphyrin III isomer [11].

Chromatograms

Example chromatograms are found in Fig. 7.3.4. Note the variable signal intensities on the ordinate.

Reference Values

Each laboratory should establish its own reference values. Those given here can only be interpreted as a guide. To our knowledge, the age dependence of fecal porphyrin excretion has not been studied. The following values for coproporphyrin I, coproporphyrin III, and protoporphyrin represent the mean ± two standard deviations (±2SD) and were assessed in samples from adult volunteers: < 20, < 12, and < 80 nmol/g dry weight, respectively.

Typical Pathological Values

Abnormal fecal porphyrins are usually specific for a porphyric condition. PCT is characterized by normal copro- and protoporphyrin, but with a significant isocop-

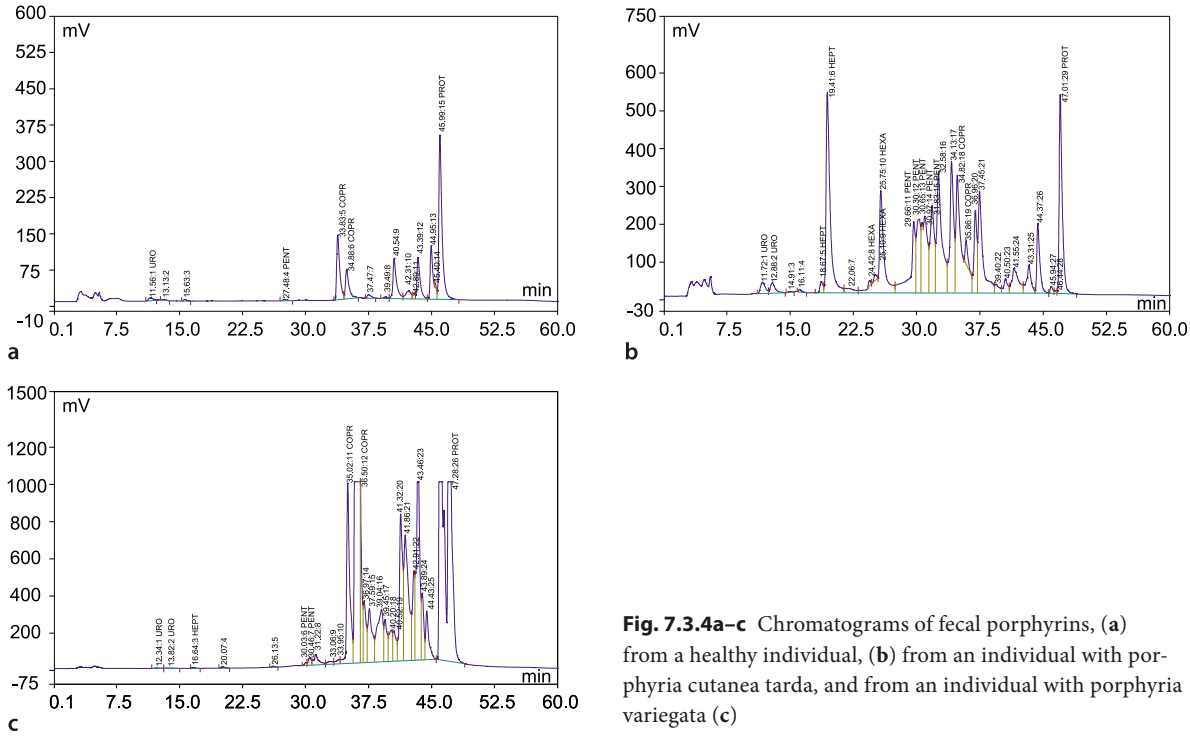

Fig. 7.3.4a–c Chromatograms of fecal porphyrins, (**a**) from a healthy individual, (**b**) from an individual with porphyria cutanea tarda, and from an individual with porphyria variegata (**c**)

roporphyrin peak that elutes between copro- and protoporphyrin (see Fig. 7.3.4). Erythropoietic protoporphyria shows an isolated increase of protoporphyrin. This sign is, however, less sensitive than elevated protoporphyrin in erythrocytes.

7.3.3.3 Plasma Scan

The plasma-fluorescence emission scan with a maximum at 627 nm is the sensitive test for PV even in asymptomatic periods.

Principle

Increased porphyrin levels in plasma can be shown by a specific fluorescence emission spectrum.

Preanalytical

Porphyrins are light sensitive. Therefore, specimens should be stored in a dark container, preferably in the cold. Storage for more than 2 days should be at –20°C.

- Specimens

Heparin- or ethylenediaminetetraacetic acid (EDTA)-treated plasma can be used.

- Reagents and Chemicals

0.9% NaCl in distilled water.

■ Instrumentation

Spectrofluorimeter with a scanning device.

■ Calibration

None.

■ Quality Control

A patient sample positive for an emission maximum may be included.

Analytical

■ Procedure

A 0.2-ml aliquot of sample is diluted with 1.8 ml NaCl solution. The solution is placed in a spectrophotometer cuvette. Excitation is set at 404 nm and an emission scan from 500 to 700 nm is collected.

■ Calculation

None.

Postanalytical

■ Interpretation

An emission maximum at 627 nm is a sensitive and specific sign for PV [12]. Other porphyrias show emission maxima around 620 nm.

■ Spectra

Spectra for fecal porphyrins are shown in Fig 7.3.5.

■ Reference Values

No peak (qualitative).

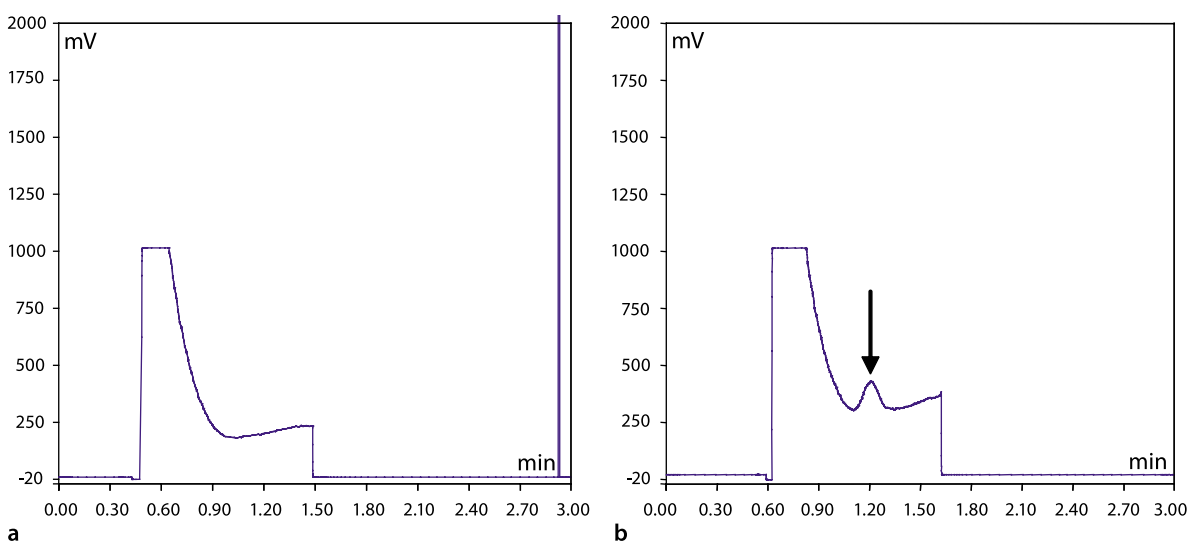

Fig. 7.3.5 Plasma scan from a healthy individual (**a**) and from an individual with porphyria variegata (**b**). Scanning velocity 200 nm/min, range 500–700. Emission maximum at 627 nm indicated by an *arrow*

■ Pitfalls

None.

7.3.3.4 Porphyrins in Plasma and Erythrocytes Assessed by HPLC

Porphyrins in plasma are mainly used to distinguish between PCT and pseudoporphyria in patients with chronic hemodialysis. CEP patients also show characteristic elevations with dominance of I-isomers, especially of uroporphyrin and its decarboxylation products, in both plasma and erythrocytes. Plasma porphyrins may be used for follow-up of the patients.

Methods: HPLC with Fluorescence Detection

Principle

Porphyrins are extracted from plasma or erythrocytes and separated according to their polarity on a reverse-phase system. Detection by their fluorescence is highly specific because both excitation and emission are at a relatively long wavelength. A high number of different isomers exist, and are especially detectable in pathological conditions.

Preanalytical

Porphyrins are light sensitive. Therefore, specimens should be stored in a dark container, preferably in the cold. Storage for more than 2 days should be at –20°C.

■ Specimens

Blood samples anticoagulated with heparin or EDTA may be used.

■ Reagents and Chemicals

1. 30% HCl.
2. Porphyrin acid marker kit (10 nmol of each uro-, heptacarboxy-, hexacarboxy-, pentacarboxy-, coproporphyrin, all I-isomers).
3. Trichloroacetic acid.
4. Ammonium acetate, p.a.
5. Acetonitrile, chromatographic grade.
6. Acetic acid, concentrate, p.a.
7. Methanol gradient, HPLC grade.

■ Instrumentation

1. Gradient HPLC system with fluorescence detection (excitation 404 nm, emission 618 nm).
2. Column: C1, 5 µm, 25 cm × 3.2 mm i.d.
3. Buffer A: 1 M ammonium acetate, pH 5.16, containing 10 ml triethylamine and 100 ml acetonitrile per liter.
4. Buffer B: methanol/acetonitrile 9:1.
5. Linear gradient from 0 to 80% B in A in 40 min, 10 min plateau at 80%, then return to 0% in 5 min.

Table 7.3.6 *Standards used in the HPLC determination of porphyrins in plasma and erythrocytes*

	Std 1	Std 2	Std 3
Concentration (nmol/l)	50	75	100
Volume standard solution (µl)	25	37.5	50
3 M acetic acid (µl)	875	863	850
Trichloroacetic acid 10%	100	100	100

Calibration

Porphyrin acid marker kit (10 nmol of each uro-, heptacarboxy-, hexacarboxy-, pentacarboxy-, coproporphyrin, all I-isomers): solubilized in 5 ml 3 M HCl (stable at 4°C and light-protected for 2 weeks; Table 7.3.6).

Quality Control

None.

Analytical

Procedure

A 500-µl aliquot of sample, 100 µl trichloroacetic acid, and 400 µl HCl 30% are mixed by vortexing and then kept on ice for at least 1 h, centrifuged at 14,000 rpm (16,100 × *g*), and filtered (Acrodisc LC 13, Millipore) into brown HPLC autosampler tubes. Aliquots (20 µl) of standards and samples are injected into the HPLC. Samples with high concentrations of porphyrins should be diluted with 3 M HCl 1:2 initially. To measure the erythrocytes they are pretreated as follows: 100 µl of 3 M acetic acid is pipetted into a tube, 50 µl of erythrocytes is added drop by drop under constant vortexing, followed by 1 min further mixing by vortex. This solution is further processed as described for plasma.

Calculation

Calculation is based on a linear standard curve forced through zero.

Postanalytical

Interpretation

1. Plasma: patients on chronic hemodialysis with PCT show typically elevated uro- and heptacarboxyporphyrins. PCT patients without renal disease may also show an identical pattern. Patients with CEP show a predominance of I-isomers.
2. Erythrocytes: patients with CEP show the same pattern as that found in their plasma.

Chromatograms

Figure 7.3.6 compares plasma porphyrin chromatograms from an individuals with PCT and an individual with CEP.

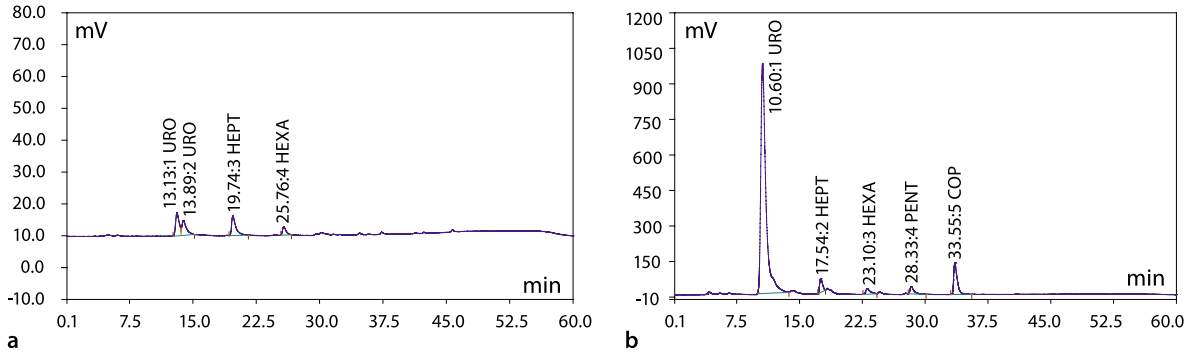

Fig. 7.3.6a,b Plasma porphyrins from an individual with porphyria cutanea tarda (**a**) and from an individual with congenital erythropoietic porphyria (**b**)

■ Reference Values

Each laboratory should establish its own reference values. Those given here can thus only be interpreted as a guide. Porphyrins in plasma are rarely detectable in healthy individuals. Patients on chronic dialysis but without signs of PCT may show some measurable values, which are given here as reference values (nmol/l, mean ± 2SD): uroporphyrin < 24.3; heptacarboxyporphpyrin < 2.7; hexacarboxyporphyrin < 1; pentacarboxyporphyrin < 1; coproporphyrin I < 1; coproporphyrin III < 1.

■ Pitfalls

None.

7.3.3.5 Porphyrins in Erythrocytes by Spectrophotometry

Porphyrins in the erythrocytes, are measured to diagnose erythropoietic protoporphyria. This determination may also be useful to differentiate between different causes of microcytic anemia.

Methods

Principle

Porphyrins are extracted and separated from heme by differential extraction and their concentration is determined fluorimetrically.

Pre-Analytical

Porphyrins are light sensitive. Therefore, specimens should be stored in a dark container, preferably in the cold. Storage for more than 2 days should be at –20°C.

■ Specimens

Blood samples anticoagulated with heparin or EDTA may be used.

Reagents and Chemicals

1. Celite, 5% g/v in 0.9% NaCl.
2. 30% HCl, p.a.
3. Protoporphyrin IX HCl, p.a.
4. Ethyl acetate, p.a.
5. Acetic acid, concentrate, p.a.
6. 1.5 M HCl.

Instrumentation

Bench-top centrifuge and spectrofluorimeter (excitation 405 nm, emission 610 nm).

Calibration

Protoporphyrin fluorescence marker (no longer available, must be replaced by protoporphyrin substance, standardized by molar extinction coefficients; see section 7.3.3.6, subheading "Calibration").

Quality Control

None.

Analytical

Procedure [13]

A 20-µl aliquot of blood is added to 100 µl of 5% Celite suspension in saline; 2 ml ethyl acetate/acetic acid 4:1 is then added. The sample is mixed for 10 s on a vortex, and centrifuged for 30 s. The supernatant is decanted into another test tube, to which 2 ml of 1.5 M HCl is added, and again agitated on a vortex for 10 s. An aliquot of the lower HCl phase is measured in a spectrofluorimeter.

Calculation

Calculation is based on the fluorescence signal of a protoporphyrin standard.

Postanalytical

Interpretation

There are three pathological conditions that are characterized by increased protoporphyin in erythrocytes: Iron deficiency, lead intoxication, and erythropoietic protoporphyria.

Reference Values

Each laboratory should establish its own reference values. That given here can only be interpreted as a guide. Free erythrocyte porphyrins reference < 4.5 µmol/l red blood cells.

Typical Pathological Values

Iron deficiency and lead intoxication result in protoporphyrin concentrations that rarely exceed 6 µmol/l. In contrast, erythropoietic protoporphyria usually manifests with protoporphyrin concentrations above this level.

Pitfalls

For a good recovery, ethyl acetate must be fresh.

7.3.3.6 Protoporphyrins in Erythrocytes Assessed by HPLC

Chromatographic determination of protoporphyrins in erythrocytes has the same indications as the spectrophotometric one. In addition, the method enables the differentiation between zinc-protoporphyrin and (metal-)free protoporphyrin. The first is elevated in iron deficiency and lead intoxication, the second in erythropoietic protoporphyria.

Methods: HPLC with Fluorescence Detection

Principle

Zinc-chelated protoporphyrin and free protoporphyrin are extracted from erythrocytes and separated according to their polarity on a reverse-phase system. Their detection by fluorescence is highly specific because both excitation and emission are at a relatively long wavelength.

Preanalytical

Porphyrins are light sensitive. Therefore, specimens should be stored in a dark container, preferably in the cold. Storage for more than 2 days should be at –20°C.

■ Specimens

Blood samples anticoagulated with heparin or EDTA may be used. We normally use washed erythrocytes (see below 7.3.3.7 HMBS Activity).

■ Reagents and Chemicals

1. Protoporphyrin IX HCl.
2. Zinc protoporphyrin IX.
3. Mesoporphyrin IX dihydrochloride.
4. Dimethylsulfoxide (DMSO).
5. Acetone p.a.
6. Tween 20 p.a.
7. Ammonium acetate p.a.
8. Acetic acid, concentrate, p.a.
9. Methanol HPLC grade.
10. DTT solution: 15 mg DTT in 14 ml 1% ammonia.
11. Internal standard solution: 0.5 mg mesoporphyrin HCl in 5 ml DMSO, kept in portions of 200 µl at –20°C.
12. Extraction solution: 2.5 ml DMSO, 25 µl Tween 20, 2.5 µl internal standard solution, with acetone at 25 ml.

■ Instrumentation

1. Isocratic HPLC system with fluorescence detection (excitation 404 nm, emission 618 nm).
2. Column: C18, 5 µm, 25 cm × 3.2 mm i.d.
3. Buffer: 140 ml 1 M ammonium acetate pH 5.16, methanol is added to 1000 ml. 1 ml DMSO is added, mixed and filtered.

Table 7.3.7 *Standard solutions used in the HPLC determination of protoporphyrins in erythrocytes*

	Std 1	Std 2	Std 3	Std 4
Concentration of standards (µM)	0.89	1.78	3.56	5.34
Volume standard solution (µl)	25	50	100	150
3 M Acetic acid (µl)	300	300	300	300
Extraction solution (ml)	3	3	3	3

Calibration

1. Protoporphyrin IX HCl (MW 562.66): 1 mg protoporphyrin IX HCl is solubilized in 20 ml DTT solution. This is kept in 200-µl aliquots at –20°C, and its concentration may be checked by the molar extinction coefficient in 1.5 M HCl ($275.1*10^3$; [14]) before use. Zinc protoporphyrin IX (0.56 mg) in 10 ml DMSO (stable at –20°C and light-protected for 3 months), 0.5 mg mesoporphyrin IX HCl (internal standard) in 5 ml DMSO, solubilized by ultrasonic bath (stable at –20°C and light-protected for 3 months).
2. Standard solution: 100 µl protoporphyrin solution, 100 µl zinc protoporphyrin solution and DMSO are mixed to achieve a volume of 5 ml. The volume of protoporphyrin solution may be corrected for decay (Table 7.3.7).

Quality Control

None. To confirm long-term reproducibility, we control the slope of the standard curves.

Analytical [15]

Procedure

A 300-µl volume of 3 M acetic acid is prelaid into glass vials, 50 µl erythrocytes are added and the suspension mixed for 1 min. Three milliliters of extraction solution is added drop by drop while constantly mixing the sample by vortex, followed by 1 min further mixing. The sample is centrifuged at 3000 rpm ($1500 \times g$) and the supernatant is evaporated under vacuum to remove all the acetone (any remaining acetone will damage the HPLC column!). The residual sample is pipetted into brown HPLC autosampler tubes. Twenty-microliter aliquots of standards and samples are injected into the HPLC. Samples with high concentrations of porphyrins should be diluted with 0.9% NaCl in distilled water to 1:10 initially.

Calculation

Calculation is based on a linear standard curve forced through zero.

Postanalytical

Interpretation

Patients with erythropoietic protoporphyria show high values of free protoporphyrin. Iron deficiency and lead intoxication augment zinc protoporphyrin.

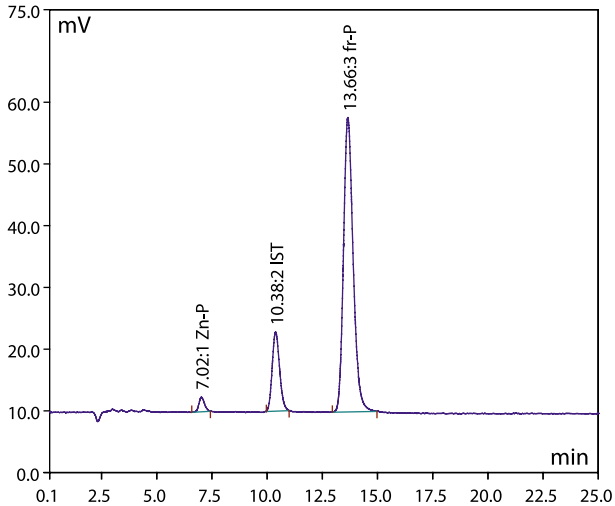

Fig. 7.3.7 Chromatogram of erythrocytic protoporphyrins from an individual with erythropoietic protoporphyria

■ Chromatograms

Example chromatograms are shown in Fig. 7.3.7.

■ Reference Values

Each laboratory should establish its own reference values. Those given below can only be interpreted as a guide. Free protoporphyrins in erythrocytes are rarely detectable in healthy individuals. Zinc protoporphyrin: < 1.3 µmol/l (mean ± 2SD), free protoporphyrin < 0.2 µmol/l (detection limit).

■ Typical Pathological Values

As stated before, increased zinc protoporphyrin is seen in iron deficiency and lead intoxication. The quantitative values are in the range of 2–6 µmol/l. Erythropoietic protoporphyria patients show an increase in protoporphyrin in the range of 6–50 µmol/l. In case of complicating liver disease, the value can increase even further.

■ Pitfalls

None.

7.3.3.7 HMBS Activity (PBG Deaminase, Uroporphyrinogen I Synthase)

HMBS activity is lowered in AIP. In the case of a newly diagnosed acute porphyria, determination of HMBS activity enables the diagnosis of AIP. We further use it in AIP family screening combined with mutation analysis.

Methods: Enzymatic Reaction

Principle

Lysed erythrocytes are incubated with the substrate PBG. The formed uroporphyrinogen is oxidized by the air oxygen to uroporphyrin, which can be determined fluorimetrically.

Pre-Analytical

HMBS is not stable at room temperature or at 4°C for more than 24 h, but it is stable at –20°C at least 3 months. Before freezing, erythrocytes have to be washed (see below). Therefore, the unfrozen sample has to be transported rapidly to the laboratory for further processing.

Specimens

Blood samples anticoagulated with heparin or EDTA may be used. As leukocytes contain significant, but variable amounts of HMBS, erythrocytes are separated from them by a sucrose gradient before freezing (see below in "Analytical").

Reagents and Chemicals

1. PBG, purest grade available (Frontier Scientific, Logan, UT, USA).
2. Uroporphyrin I fluorescence marker (5 µg/10 ml; Frontier Scientific).
3. Tris pH 7–9.
4. HCl 30% p.a.
5. Sodium hydroxide p.a.
6. Sucrose p.a.
7. Triethylamine.
8. Trichloroacetic acid p.a.
9. Acetic acid concentrate, p.a.
10. Ammonium acetate p.a.
11. Acetonitrile, chromatographic grade.
12. Methanol gradient, HPLC grade.
13. Saccharose solution: 8.5 g sucrose in 100 ml double-distilled water per patient sample.
14. Hemolysis buffer: 1.58 g Tris and 0.2 ml Triton × 100 in distilled water up to 100 ml.
15. Incubation buffer: 1.58 g Tris in distilled water, up to 100 ml, pH 8.00.
16. Substrate solution: 2.3 mg PBG in 10 ml incubation buffer.

Instrumentation

1. Water bath at 37.0°C with cover.
2. Spectrofluorimeter or gradient HPLC system with fluorescence detection (excitation 404 nm, emission 618 nm).
3. Column: C1, 5 µm, 25 cm × 3.2 mm i.d.
4. Buffer A: 1 M ammonium acetate, pH 5.16, containing 10 ml triethylamine and 100 ml acetonitrile per liter.
5. Buffer B: methanol/acetonitrile 9:1.
6. Linear gradient from 0 to 40% B in A in 10 min, then return to 0% in 5 min, and equilibration at 0% B for further 10 min.
7. 5 min.

■ ***Table 7.3.8*** *Standards used in the determination of hydroxymethylbilane synthase activity*

	Std 1	Std 2	Std 3	Std 4
Concentration (pmol/20 µl injection)	0.4816	0.9632	1.9264	2.4080
Volume standard solution (µl)	40	80	160	200
Trichloroacetic acid 10% (µl)	960	920	840	800

■ Calibration

Uroporphyrin I fluorescence standard 5 µg/10 ml = 602 pmol/ml (Table 7.3.8).

■ Quality Control

We use a portionized sample from a volunteer with low normal HMBS activity.

Analytical

Modified according to Grandchamp [16].

■ Preparation of Leukocyte-Free Erythrocytes [17]

A 4-ml sample of whole anticoagulated blood is diluted with 16 ml physiological saline. Four centrifuge tubes are filled with 20 ml saccharose solution each. Five milliliters of diluted blood is overlaid carefully on the saccharose solution of each tube. The tubes are centrifuged at 3000 rpm (1500 × *g*) for 5 min. The supernatant is completely removed and the remaining red cells are transferred to small cryotubes and frozen at –20°C.

■ Enzyme Reaction

A 100-µl aliquot of thawed erythrocytes is mixed well with 900 µl hemolysis buffer. This diluted hemolysate is used to determine hemoglobin concentration (e.g., by a routine technique).

The enzyme reaction is performed in duplicate. Incubation buffer (200 µl) is mixed with 50 µl diluted hemolysate and incubated at 37°C for 5 min, then 50 µl substrate solution is added and the tubes are kept at 37°C in the dark for a further 60 min. One null value per experiment with hemolysis buffer instead of erythrocytes is treated the same way.

The reaction is stopped by the addition of 1 ml ice-cold 10% trichloroacetic acid and the tubes are kept in ice water for 15 min. They are then centrifuged for 5 min at 14,000 rpm (16,100 × *g*) in a bench-top centrifuge. One milliliter of supernatant is aspirated with a 1-ml syringe and filtered into brown HPLC autosampler tubes. Twenty-microliter aliquots of standards and samples are injected into the HPLC system. Spectrofluorimetric determination may be used instead of HPLC.

■ Calculation

Calculation is based on a linear standard curve forced through zero. The mean value of the duplicates is corrected for the difference in the end volume (1.3 ml in samples and 1 ml in standards), and divided by the hemoglobin concentration in the hemolysate.

Postanalytical

■ Interpretation

Decreased values are a sign of AIP. Both the sensitivity and specificity are approximately 94% [18]; however, the value may be falsely normal during an acute attack [11]. Neonatal samples and individuals with a decreased erythrocyte life spans show high or increased values.

As the next enzymes of the heme pathway are active, uroporphyrinogen is converted to heptacarboxyporphyrinogen during the enzymatic reaction. This can be overcome if the incubation temperature is raised to 45°C, which inactivates uroporphyrinogen decarboxylase. Yet, 37°C is the standard temperature for enzyme activity determinations. Despite our neglect of the additionally formed porphyrins by uroporphyrinogen decarboxylase in the activity calculations, we found a highly reliable test performance.

■ Chromatograms

None.

■ Reference Values

HMBS activity 75–150 pmol/(mg hemoglobin*h) (mean ± 2SD). Each laboratory should establish its own reference values. Those given can only be interpreted as a guide.

■ Typical Pathological Values

As a heterozygous defect, HMBS activity is 50% of normal. In our experience symptomatic and asymptomatic patients with AIP show values in the range of 35–55 pmol/(mg hemoglobin*h). There may be some overlap between low normal and high porphyric values.

■ Pitfalls

As stated above, delay between blood drawing and freezing of erythrocytes can result in falsely low values. For confirmation we recommend repeating each abnormally low value. Falsely normal values are seen in AIP patients during acute porphyric crises.

7.3.3.8 ALAD Activity (Synonymous ALAD)

In ALAD deficiency, ALAD activity is decreased to a few percent of normal values. It may also be strongly inhibited in lead intoxication. The enzyme can be reactivated by DTT in lead intoxication, but reactivation fails in ALAD deficiency.

Methods: Enzymatic Reaction

Principle

Lysed erythrocytes are incubated with the substrate ALA. The formed PBG is determined by the modified Ehrlich's Reaction.

Preanalytical

ALAD is not stable at room temperature, 4°C, or at –20°C for more than 24 h. The specimen is best collected in the laboratory and the test performed immediately thereafter.

■ Specimens

Blood samples anticoagulated with heparin are used. Four 200-µl samples are prepared and immediately cooled to 4°C.

■ Reagents and Chemicals

1. ALA, purest grade available (MW 178, p.a.; Frontier Scientific).
2. $NaH_2PO_4 \cdot H_2O$ (MW 138), p.a.
3. $HgCl_2$, p.a.
4. HCl, 30% p.a.
5. Trichloroacetic acid, p.a.
6. Acetic acid, concentrate, p.a.
7. Perchloric acid, p.a. D = 1.7.
8. Buffer A: 1.78 g $Na_2HPO_4 \cdot 2H_2O$ with double-distilled water to 100 ml.
9. Buffer B: 1.38 g $NaH_2PO_4 \cdot H_2O$ with double-distilled water to 100 ml
10. Substrate solution: 0.1676 g ALA in about 65 ml buffer B is brought to pH 6.4 with solution A (about 100 ml).
11. Mercury chloride/trichloroacetic acid solution: 10 g trichloroacetic acid is solubilized in 100 ml double-distilled water (aqueous trichloroacetic acid solution). 1.35 g mercury chloride is solubilized in 100 ml aqueous trichloroacetic acid solution.
12. Ehrlich's reagent: add 2.5 g p-DMAB to a mixture of 50 ml concentrated acetic acid, 24.5 ml perchloric acid, and 4 ml mercury chloride/trichloroacetic acid solution.

■ Instrumentation

Water bath at 37.0°C with cover, and a spectrophotometer.

■ Calibration

None.

■ Quality Control

None. We use a fresh blood sample from a volunteer.

Analytical

Modified according to Berlin [19].

■ Enzyme Reaction

Three samples per patient, each with 200 µl blood, are mixed with double-distilled water prewarmed to 37°C for 10 min. To one of the tubes with the diluted hemolysate, add 1 ml mercury chloride/trichloracetic acid solution and 1 ml ALA solution for determination of the blank value. The enzyme reaction is performed in duplicate: To each of the 200-µl hemolysate samples add 1 ml prewarmed ALA solution. All three tubes are mixed and incubated for 1 h at 37°C. To stop the reaction, 1 ml mer-

cury chloride/trichloroacetic acid solution is added to the enzyme assay tubes. The three tubes are centrifuged at 20,000 × *g* for at least 10 min and the supernatant is filtered. A 1-ml sample of filtrate is mixed with 1 ml Ehrlich's reagent and then kept for 5 min at room temperature. Absorption is determined at 555 nm.

■ Calculation

$$\text{ALAD activity} = \frac{\text{absorbance} \times 100 \times 2 \times 35}{\text{hematocrit\%} \times 60 \times 0.062}$$

(ALAD activity in µmol ALA/min/l erythrocytes; "60" is the incubation time; "35" is the dilution factor; "2" represents the conversion of PBG to ALA; "0.062" is the extinction coefficient l/µmol × cm).

Postanalytical

■ Interpretation

Decreased values are a sign of lead intoxication or ALAD deficiency.

■ Reference Values

Mean ± SD = 57.1 ± 17.9. Each laboratory should establish its own reference values; those given can only be interpreted as a guide.

■ Typical Pathological Values

As ALAD deficiency is a recessive disorder, residual activities are maximally in the range of a few percent of normal.

■ Pitfalls

As stated above, delay between blood drawing and determination of the enzyme activity can result in falsely low values. For confirmation we recommend repeating each abnormally low value.

References

1. Minder EI, Schneider-Yin X (2007) The porphyrias. In: Rodés J, Benhamou JP, Blei A, Reichen J, Rizzetto M (eds) Textbook of Hepatology: From Basic Science to Clinical Practice. Blackwell, Oxford UK, pp 1343–1351
2. Minder EI, Schneider-Yin X (2002) The porphyrias. In: Blau N, Duran M, Blaskovics ME, Gibson KM (eds) Physician's Guide to The Laboratory Diagnosis of Metabolic Diseases. Springer, Berlin, Heidelberg, New York, pp 593–613
3. Bishop DF, Henderson AS, Astrin KH (1990) Human delta-aminolevulinate synthase: assignment of the housekeeping gene to 3p21 and the erythroid-specific gene to the X chromosome. Genomics 7:207–214
4. Grandchamp B, Picat C, Mignotte V, Wilson JH, Te Velde K, Sandkuyl L, Roméo PH, Goossens M, Nordmann Y (1989) Tissue-specific splicing mutation in acute intermittent porphyria. Proc Natl Acad Sci U S A 86:661–664
5. Tugores A, Magness ST, Brenner DA (1994) A single promoter directs both housekeeping and erythroid preferential expression of the human ferrochelatase gene. J Biol Chem 269:30789–30797
6. Sandberg S, Elder GH (2004) Diagnosing acute porphyrias. Clin Chem 50:803–805

7. Mauzerall D, Granick S (1995) The occurrence and determination of delta-amino-levulinic acid and porphobilinogen in urine. J Biol Chem 219:435–446
8. Doss M, Schmidt A (1972) Zwei Suchteste für Porphyrien. Z Klin Chem Klin Biochem 5:230–231
9. Lim CK, Peters TJ (1984) Urine and faecal porphyrin profiles by reversed-phase high-performance liquid chromatography in the porphyrias. Clin Chim Acta 139:55–63
10. Minder EI, Vuilleumier JP, Vonderschmitt DJ (1992) Prototype application of robot in the clinical laboratory enabling fully automated quantification of fecal porphyrins. Clin Chem 38:516–521
11. Minder EI (1993) Coproporphyrin isomers in acute-intermittent porphyria. Scand J Clin Lab Invest 53:87–90
12. Hift RJ, Meissner PN (2005) An analysis of 112 acute porphyric attacks in Cape Town, South Africa. Evidence that acute intermittent porphyria and variegate porphyria differ in susceptibility and severity. Medicine 84:48–60
13. Piomelli S, Davidow B, Guinee VF, Young P, Gay G (1973) The FEP (free erythrocyte porphyrins) test: a screening micromethod for lead poisoning. Pediatrics 51:254–259
14. Grinstein M, Wintrobe MW (1948) Spectrophotometric micromethod for the quantitative determination of the free erythrocyte protoporphyrin. J Biol Chem 172:459–467
15. Rossi E, Garcia-Webb P (1986) Red cell zinc protoporphyrin and protoporphyrin by HPLC with fluorescence detection. Biomed Chromatogr 1:163–168
16. Grandchamp B (1998) Acute intermittent porphyria. Semin Liver Dis 18:17–24
17. Blincoe C (1974) The simultaneous separation and washing of erythrocytes. Clin Chim Acta 7:297–300
18. Schuurmans MM, Schneider-Yin X, Rufenacht UB, Schnyder C, Minder CE, Puy H, Deybach JC, Minder EI (2001) Influence of age and gender on the clinical expression of acute intermittent porphyria based on molecular study of porphobilinogen deaminase gene among Swiss patients. Mol Med 7:535–542
19. Berlin A, Schaller KH (1974) European standardized method for the determination of delta-aminolevulinic acid dehydratase activity in blood. Z Klin Chem Klin Biochem 12:389–390

7.4 Trimethylaminuria

Ron A. Wevers, Udo F. H. Engelke

7.4.1 Introduction

"*What have we here? A man or a fish? Dead or alive? A fish: he smells like a fish; a very ancient and fish-like smell; a kind of not of the newest Poor John*"–William Shakespeare, The Tempest II. ii. 26-29 (A "Poor John" in those times was a salted and dried hake)

The first description of a person with a fish malodour dates back to the Mahabhatara, the Indian epic of the Bharata Dynasty [21]. The quote from William Shakespeare, opening this chapter, refers to Caliban, a savage and deformed slave and fish odour sufferer. The first clinical description of a patient with trimethylaminuria, or fish odour syndrome, is from Humbert et al. in 1970 [14]. A deficiency of trimethylamine (TMA) oxidase was found in the liver of this patient [13]. The incidence of the syndrome is as yet unknown, but more than 200 cases have been described worldwide. The disease (OMIM 602079) appears pandemic. Patients with trimethylaminuria present with an offensive body odour, usually in childhood, but sometimes as adults. They are frequently unaware of their malodour. The disorder often causes psychosocial problems, with anxiety, low self-esteem, social isolation and loneliness. School performance may suffer and the smell is highly destructive to the personal, working and career interactions of the patient. Attempts to commit suicide as a result of this condition have been documented. The severity of the syndrome is highly variable, ranging from intermittent or episodic to severe and continuous. When patients seek medical help they are sometimes referred to psychiatrists and diagnosed as obsessional. Others are advised by dermatologists or general practitioners to improve their hygiene.

Mitchell proposed a classification for various types of fish odour syndrome [21]. The primary genetic form is by far the most frequent. Some cases were described with an acquired form that seems to be precipitated by a viral infection. Insertion of viral DNA may have affected the expression of the human flavin-containing mono-oxygenase (FMO3) gene. A third form is a transient childhood form that was described first by Blumenthal et al. [8] in a child using a choline supplement. The transient form of the disease may be due to delayed FMO3 expression or immaturity of the enzyme system. A transient form associated with menstruation was first reported by Ayesh et al. [6]. It turned out that normal healthy women may have a short episode of trimethylaminuria at the onset of and during menarche. A last form is a transient type based on precursor overload. It has been shown that supplements or diets containing high levels of choline, lecithin or carnitine increase the flux through the

pathway and may lead to trimethylaminuria in individual cases. Also, the intake of TMA N-oxide, through enterobacterial metabolism, may increase the substrate load for TMA oxidase and lead to transient trimethylaminuria. In two affected breast-fed babies, the smell occurred after their mother ate eggs or fish [16].

Therapy for trimethylaminuria consists primarily of dietary management and adjustment of lifestyle. Reduction in the intake of the TMA precursors carnitine, choline, lecithin and TMA N-oxide has been successful in some, but not all patients. Patients should take a low choline diet, avoid eggs, mayonnaise, liver and other organ meats (offal), peas and soy beans, and exclude sea fish and shellfish. They should choose appropriate clothing and control room ventilation to minimise sweating. Use of an acid soap (pH 5.5–6.5) may help by decreasing TMA volatility. Treacy has reported some success of short courses of metronidazole, an antibiotic with specific activity against anaerobic bacteria, to reduce the gut microflora, thereby suppressing TMA generation [27]. Long-term use of antibiotics to reduce enteric TMA production should be avoided, but a 2-week course of metronidazole may help intermittent attacks and provide some protection for special occasions and holidays. Temporary control of the malodour may be achieved by administering lactulose, activated charcoal or neomycin, but associated diarrhoea has been reported [24,27]. For the patient and the family it is important to know that stress, menstruation and pyrexic states may exacerbate the condition.

7.4.2 Trimethylamine

TMA is a volatile aliphatic tertiary amine with a pungent odour resembling rotting fish (Fig. 7.4.1). TMA has a 100-fold greater olfactory potency than its N-oxide. The reported threshold odour for TMA is 0.9 ppm. Exposure to concentrations above 20 ppm gives moderate irritation of the respiratory system and the eyes. Dermal contact with a concentrated aqueous solution may cause severe burns [4]. Oral ingestion of 15 mg TMA hydrochloride/kg body weight induces nausea and ichthyohydrosis [9].

TMA is normally formed from dietary choline and lecithin, but also from TMA N-oxide by intestinal bacteria (Fig. 7.4.2). Choline bound to lecithin is present most abundantly in egg yolk, liver, kidney, legumes, soy beans and peas. TMA N-oxide is present in considerable amounts in marine fish, amounting to approximately 13,000 μmol/300 g fresh fish [12]. In marine fish it is thought to play a role as an osmoregulator. These fish are faced with the dehydrating force of salt water. TMA N-oxide is a major counteracting osmolyte with protein-stabilizing properties. Freshwater fish have much lower levels of methylamines. After the death of the fish TMA N-oxide may be converted into TMA by bacterial action, resulting in the characteristic smell of rotting fish.

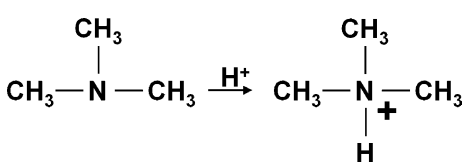

Fig. 7.4.1 Structure of trimethylamine (TMA): relative molecular mass 59.11; boiling point 2.9 C

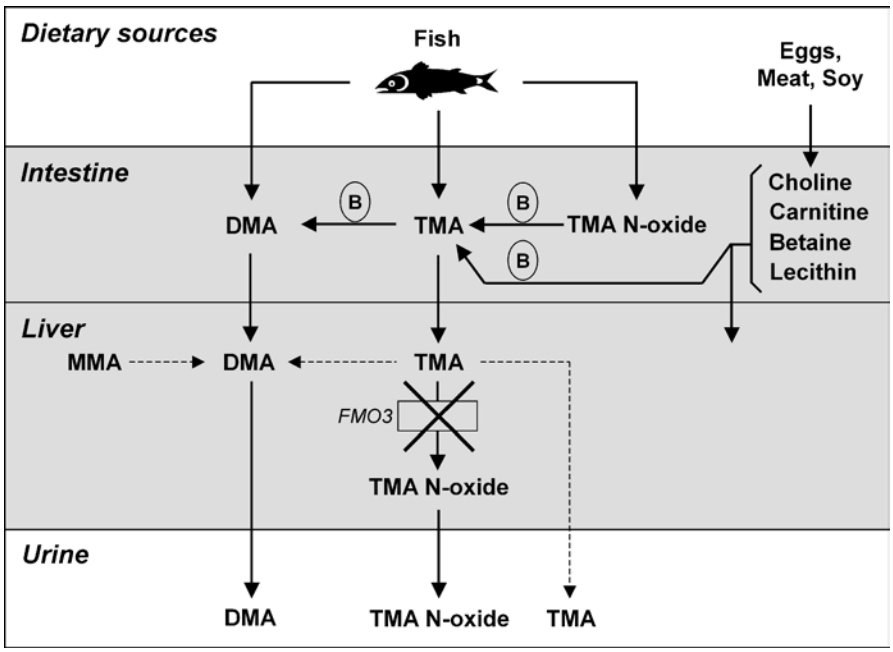

Fig. 7.4.2 The origin and metabolism of TMA in man. This figure shows the molecular defect in the flavin-containing mono-oxygenase (FMO3) in trimethylaminuria or fish odour syndrome. The *dashed line* indicates the minor metabolic pathway in healthy volunteers. Enzyme steps marked with "*B*" are in the intestinal bacterial flora. *DMA* Dimethylamine, *MMA* monomethylamine

TMA is normally cleared effectively from the human blood circulation by hepatic N-oxidation and urinary excretion of the resulting non-odourous N-oxide. TMA in human metabolism is predominantly (> 95%) N-oxidised, but N-demethylation towards dimethylamine also occurs (Fig. 7.4.2) [3,5].

TMA accumulates in urine, sweat and other body secretions of affected individuals. It may occur in the breath and being volatile it is readily released into the atmosphere.

7.4.3 Flavin-Containing Mono-oxygenases

TMA is converted into its N-oxide by an FMO in the liver (EC 1.14.13.8). Trimethylaminuria was found to relate to defects in FMO3. FMO3, is one of five human microsomal FMOs, which may have evolved in response to environmental chemicals [10,29]. FMO1 is found in foetal liver, FMO2 is expressed in adult liver and FMO3 is the main FMO in liver and brain [10]. Foetuses do not produce FMO3 after 15 weeks of gestation. Expression of FMO3 increases variably from birth, and most individuals produce significant amounts by 1–2 years [15]. The gene coding for FMO3 is on chromosome 1q23-q25. FMOs in general have a broad substrate specificity. They catalyse NADPH-dependent oxygenation of N-, S- or P-containing drugs, xenobiot-

ics and endogenous amines, and play a role in the detoxification of environmental toxins. Among the drugs that are converted by FMO3 are the anti-oestrogen drug tamoxifen, the antifungal drug ketoconazole, the H_2 blockers cimetidine and ranitidine, the beta blocker propanolol, the antipsychotic drug chlorpromazine, the opioid analgesic morphine and nonsteroidal anti-inflammatory drugs, including benzydamine and sulindac sulphide [10]. In addition, FMO3 oxidises tyramine. There have been anecdotal reports of adverse effects of eating cheese, which contains tyramine, in patients with fish odour syndrome [11,26]. Treacy et al. have reported urticaria and intolerance to sulphur-containing medication in patients [26]. It has been speculated that FMO3 deficiency may have been a contributory factor. The enzyme also is active in the metabolism of nicotine and nicotinamide. However, the pharmacologic and toxicological significance of FMO3 deficiency remains largely unknown.

7.4.4 Methods

Several methods are available in the literature for the measurement of aliphatic amines in biological samples [28]. Problems with specificity and separation and cumbersome derivatisation and/or extraction procedures have limited the use of these techniques on a larger scale in clinical practice. The lack of a simple analytical method may have led to an underestimation of the incidence of the fish odour syndrome. For diagnosing the syndrome, an analytical technique should be used that is able to simultaneously and quantitatively measure TMA and its N-oxide in the complex matrix of human urine. Two such methods are currently available for this purpose: proton nuclear magnetic resonance (NMR) spectroscopy and head-space gas analysis with gas chromatography or direct mass spectrometry (see below).

Fish odour syndrome is an autosomal recessive disease. Mutations have been found in the FMO3 gene. Molecular genetic analysis can therefore be used as a diagnostic test. Many pathogenic mutations have been described. The defect should be documented in patients with trimethylaminuria at the metabolite level and the diagnosis confirmed at the molecular genetic level. This chapter describes the available tests at the metabolite level.

7.4.4.1 Proton NMR Spectroscopy

Principle

Proton NMR spectroscopy on body fluids has been used for the diagnosis of many inherited metabolic diseases. The NMR spectrum shows an overview of proton-containing metabolites with a micromolar concentration or higher. The nine equivalent methyl group protons of TMA and of its N-oxide give characteristic resonances in proton NMR spectroscopy [1,19,20,22,25]. At pH 7.0, the TMA protons resonate as a singlet at 2.89 ppm, which only minimally shifts with pH of the sample. At pH 2.5 the exchangeable proton on the nitrogen atom of TMA changes this resonance in a doublet resonance at 2.89 ppm (Fig. 7.4.3). The methyl protons of TMA N-oxide resonate as a singlet at 3.54 ppm or at 3.27 ppm (pH 2.5 and 7.0, respectively). The recovery, linearity and reproducibility of the assay are satisfactory [19]. The method

does not require extraction, lyophilisation or derivatisation and can be performed on untreated urine within a few minutes [19]. It is an advantage of the technique that TMA and its N-oxide may both be quantified in the same spectrum. Figure 7.4.3 shows the urine NMR spectra from a patient with severe trimethylaminuria before and after a fish meal.

Pre-Analytical

Specimen

Common causes of abnormal body odour including poor hygiene, gingivitis, urinary infections and infected vaginal discharge should be excluded. Random urine specimens may be used for the assay. Severely affected patients excrete excess TMA continuously. However, patients with milder *FMO3* mutations do not have increased

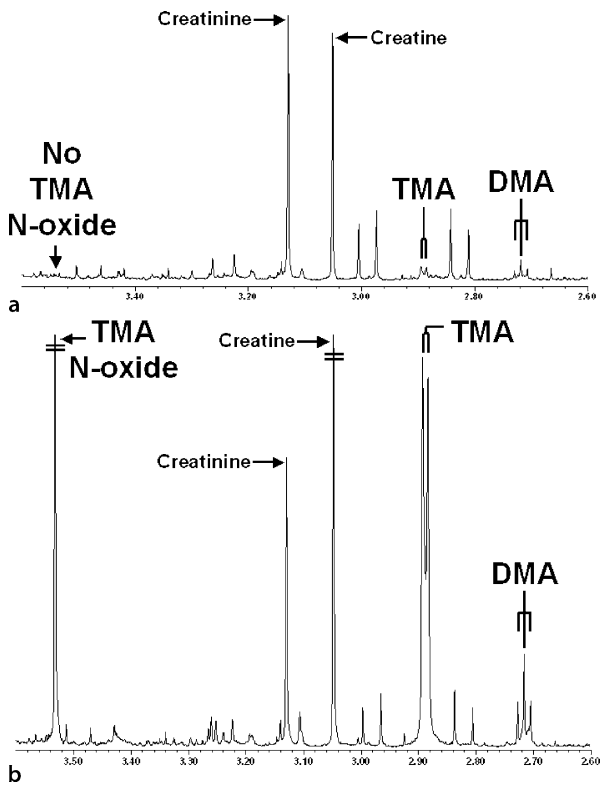

Fig. 7.4.3a,b Nuclear magnetic resonance (NMR; 500 MHz) urine spectra from a patient with severe trimethylaminuria. **a** Before eating sea fish (TMA = 44 μmol/mmol creatinine, TMA N-oxide not detectable). **b** After a 300-g sea fish meal [Nijmegen protocol: urine collection during the 6-h postprandial period; TMA = 322 μmol/mmol creatinine, TMA N-oxide:(TMA + TMA N-oxide) = 84%]. The NMR spectrum shows the presence of increased TMA in the pre-load sample as well as the absence of TMA N-oxide. After eating fish the TMA concentration is very high and the ratio is clearly abnormal

urinary TM, and a loading test may be required for the diagnoses of such cases. Samples must be acidified quickly (pH 2.0 or lower). Samples are kept frozen at –20 C or lower until analysis. Amine concentrations at these temperatures are stable for at least 3 months.

Reagents and Chemicals

A solution of 20.2 mmol/l trimethylsilyl-2,2,3,3-tetradeuteropropionic acid (TSP, sodium salt; Aldrich) in D_2O.

Instrumentation

An NMR spectrometer (300-MHz or higher field) is required for the analysis.

Calibration

Calibration may be performed based on peak area ratio (TMA:TSP and TMA N-oxide:TSP). As creatinine also gives a signal in the proton NMR spectrum (3.13 ppm at pH 2.5), it is also possible to directly calculate the TMA and TMA N-oxide concentrations per mmol creatinine.

Quality Control

For internal quality control, a urine sample from a known trimethylaminuria patient may be used. At the moment there is no official external quality control scheme available for trimethylaminuria.

Analytical

Procedure

Urine is centrifuged before analysis. A 70-µl volume of TSP in D_2O is added to 700 µl urine. This will provide a chemical shift reference as the TSP protons resonate at 0.00 ppm; it also provides a deuterium lock signal. The pH of each sample is adjusted to 2.50±0.05 with concentrated HCl. Other pH values have been used in the literature. Finally, 650 µl of sample is placed in the NMR tube (Wilmad Royal Imperial). The samples are measured on a 500-MHz spectrometer with a triple-resonance inverse ^{1}H,^{15}N, ^{13}C probe head equipped with X,Y,Z gradient coils. Spectra are acquired as 128 transients in 32,000 data points with a spectral width of 6002 Hz. The sample temperature is at 298 K. The H_2O resonance is presaturated by single frequency irradiation during a relaxation delay of 10 s while using a pulse width of 7 µs (90 excitation pulse). Automatic shimming is performed. Samples are spun at 7 Hz during the measurement. The resonance line width for TSP and relevant metabolites should be < 1 Hz. A π/2 shifted sine-bell window function is applied to the free induction decay. Fourier transformation is performed after zero-filling to 64 data points. The phase and baseline are corrected manually.

Calculation

For quantification of TMA and TMA N-oxide, the area under the curve of the TMA and TMA N-oxide resonances (both nine equivalent protons) and of the creatinine methyl group resonance (three equivalent protons) is calculated by peak integration. Correction for the number of contributing protons and dividing the TMA and

TMA N-oxide peak areas by the creatinine peak area will provide the concentration of both analytes per mmol creatinine. Often the ratio TMA:(TMA + TMA N-oxide) or the ratio TMA N-oxide:(TMA + TMA N-oxide) is used for post-analytical interpretation.

Post-Analytical Interpretation

Normal persons excrete very little TMA in the urine. However, slight TMA excretion may be observed after meals with a high content of TMA precursors like choline or lecithin, or after eating marine fish due to its high TMA N-oxide content. Healthy women may have a short episode of trimethylaminuria at the onset and during menstruation. TMA has also found to be increased in the urine of some patients using carnitine supplementation. Advanced liver and renal disease may result in TMA excretion and this constitutes the so-called secondary trimethylaminurias.

Studies using classical biochemical methods have reported reference range values varying between 1 and 7 μmol TMA/mmol creatinine [17] and 11.9±6.2 μmol/mmol creatinine (mean±1 SD) [27]. This corresponds well with the NMR data from Maschke et al. (7.7 ± 7.4 μmol/mmol creatinine; [19]. The biochemical diagnosis of trimethylaminuria is based on the detection of urinary TMA concentrations exceeding 18 μmol/mmol creatinine. The most severe cases will excrete only TMA and relatively little TMA N-oxide in a random urine sample [1]. Normal values for TMA do not exclude a milder defect in the FMO3 gene. For diagnostic purposes it may be more accurate to work with a ratio. When expressed as a ratio TMA N-oxide:(TMA + TMA N-oxide), a value > 92% should be considered normal [17,19]. In case of an abnormal ratio in a random urine sample and in patients with convincing clinical signs and symptoms, further testing should be pursued. A loading test is the next diagnostic step (see below). NMR spectroscopy of body fluids has the advantage that the spectrum gives an overview of proton-containing molecules in the sample without any preselection. This facilitates diagnosis of other inborn errors of metabolism in the same spectrum. In patients suspected to suffer from trimethylaminuria, special attention should be given to the presence of excess amounts of NN-dimethylglycine (DMG). A defect in the dehydrogenase converting DMG to sarcosine may also lead to a malodour syndrome with a fish-like smell [7]. DMG can be quantified from the NMR spectrum of the urine.

7.4.4.2 Head-Space Gas Chromatography or Head-Space Mass Spectrometry

Principle

TMA, its N-oxide and related aliphatic amines like methylamine and dimethylamine in urine may be quantified using head-space gas chromatography [28] or direct injection of the head-space gas into the gas sample injection port of a mass spectrometer [27]. These methods take advantage of the volatility of the amines and evaluate the amine-rich head-space gas generated above the sample by direct injection. The

methods are rapid and simple and allow a high sample throughput. The recovery, linearity and reproducibility of the assays are satisfactory [27,28].

Pre-Analytical

Specimen

Common causes of abnormal body odour including poor hygiene, gingivitis, urinary infections and infected vaginal discharge should be excluded. Random urine specimens may be used for the assay. Severely affected patients excrete excess TMA continuously. However, patients with milder *FMO3* mutations do not have increased urinary TMA, and a loading test may be required for the diagnoses of such cases. Urine samples are collected in airtight plastic bottles containing HCl (6 M, 15 ml) to convert TMA to the more stable TMA hydrochloride. Samples are kept frozen at –20 C or lower until analysis. Amine concentrations at these temperatures are stable for at least 3 months.

Reagents and Chemicals

All reagents are commercially available. For the gas chromatography approach, isopropylamine may be used as an internal standard [28]. It is dried over granular calcium chloride. TMA is purchased as the hydrochloride salt and TMA N-oxide as the dehydrate (Sigma, UK). TMA and TMA N-oxide are stored in desiccators over silica gel and are heated at 105 C for 2 h prior to use [28]. For head-space mass spectrometry, [$^2H_9$]-TMA is purchased from Cambridge Isotope Laboratories (UK) [27].

Instrumentation

A gas chromatograph with a flame ionisation detector equipped with a silanised glass column packed with 4% (w/w) Carbowax 20M-0.8% (w/w) potassium hydroxide on a Carbopack B graphitised carbon support (60-80 mesh; Supelco, USA). The column is conditioned by injecting 1% (v/v) aqueous ammonium hydroxide (approximately 20×10 µl) converting potassium carbonate in the packing to potassium hydroxide, thereby preventing tailing of the peaks [28].

For the isotope dilution, mass spectrometry method samples are injected directly into the gas sample injection port of the mass spectrometer [27]. These techniques do not allow concurrent analysis of TMA and TMA N-oxide in the sample. TMA N-oxide is quantified indirectly by measuring the increase in TMA after chemical reduction.

Calibration

Calibration for the head-space gas chromatography method is based on calibration curves with individual amines in distilled water. Isopropylamine is the internal standard [28]. For the isotope dilution mass spectrometry method [$^2H_9$]-TMA is used as the internal standard [27].

Quality Control

For internal quality control, a urine sample from a known trimethylaminuria patient may be used. At the moment there is no official external quality control scheme available for trimethylaminuria.

Analytical

Procedure

Urine (5 ml) urine spiked with 0.2% (v/v) isopropylamine is placed in a screw-capped 15-ml vial [28]. Pelleted potassium hydroxide (3 g) is added before sealing the vial with an airtight polytetrafluoroethylene-lined septum cap. Potassium hydroxide raises the pH of the sample to ensure that the amines are present as volatile bases. The vial is heated in an aluminium block at 90 C for 20 min. While still in this block, 2 ml head-space gas is withdrawn through the septum with a disposable syringe and injected immediately on the gas chromatography column. The operating temperatures of the column, injector port and detector unit are 70 C isothermal, 150 C and 200 C, respectively, with nitrogen carrier gas at 60 ml/min. This allows quantification of TMA and other amines. TMA N-oxide is measured after quantitative reduction into TMA. For this, titanous chloride (30%, w/v; 0.2 ml) is added to 2 ml urine in a screw-capped vial and incubated for 30 min at room temperature. The sample is then diluted ten-fold with distilled water and analysed as described above. The result represents the sum of TMA and TMA N-oxide present in the sample.

When the samples are spiked with [$^{2}H_{9}$]-TMA instead of isopropylamine, the head-space gas can also be injected directly into the gas sample injection port of a mass spectrometer for TMA quantification [27]. Electron impact mass spectra are collected over the mass range *m/z* 10–500 at a scanning rate of once per 3 s. The ion intensities of 20 consecutive scans are averaged and the ratio of the ions at *m/z* 59 and 68 is determined for TMA [27].

Calculation

Based on internal standard and the linearity of the calibration curve.

Post-Analytical Interpretation

Post-analytical considerations in general are equivalent to those for NMR spectroscopy (see above).

7.4.4.3 Loading Tests

Loading tests have been described as useful in diagnosing trimethylaminuria. A loading test is not required in severe cases of trimethylaminuria as these patients excrete significant amounts of TMA continuously. The milder cases may have fully normal TMA in urine and the diagnosis can only be made at the metabolite level after an oral challenge test. The available literature on such loading tests is largely anecdotal. Early studies have used choline loading in patients and family members [14,18,25]. Later studies used oral challenges with 300–600 mg TMA free base in a gelatine capsule [2,6]. At 900 mg there was evidence of saturation of the N-oxidation system in adults. Al-Waiz et al. have used this test to identify heterozygotes. Heterozygotes do not have the fish odour normally, but it may appear after a TMA load [2].

Healthy volunteers excrete 93.2–97.9% of the ingested TMA as TMA N-oxide. Parents of patients with trimethylaminuria excreted only 74.8–78.9% of the 600 mg TMA dose as TMA N-oxide [2]. Urine generally is collected during 6–8 h after the TMA ingestion.

FMO enzymatic activity is also involved in the formation of theobromine from caffeine. Park et al. have used this to identify heterozygotes for trimethylaminuria [23]. They determined the theobromine:caffeine ratio in the urine after administration of a cup of coffee and were able to identify heterozygotes with this test.

A further approach has been used by the author of this chapter (Wevers, unpublished data) and was used in a paper by Podadera et al. [25]. Patients were given a fish meal with 300 mg fresh sea fish and urine was collected over the 6-h period (Nijmegen protocol) or at between 2 and 12 h [25] after the meal. In a series of nine trimethylaminuria cases with confirmed pathogenic mutations in the FMO3 gene, six patients had increased TMA in a random urine sample (Nijmegen unpublished data: range 22–440 μmol/mmol creatinine; reference <18 μmol/mmol creatinine). In these patients molecular genetic confirmation is the next diagnostic step and a loading test is not strictly required. The other three cases had a normal TMA concentration in a baseline urine. After a fish meal, all three had an abnormal TMA N-oxide:(TMA + TMA N-oxide) ratio of between 30 and 84%. For healthy controls this ratio is always > 98% ($n = 4$). Figure 7.4.4 shows the excretion in two healthy volunteers and in a case of severe trimethylaminuria. Urine should be collected for 6–8 h after the fish meal. After finding an abnormal result in a loading test, molecular genetic confirmation is advised.

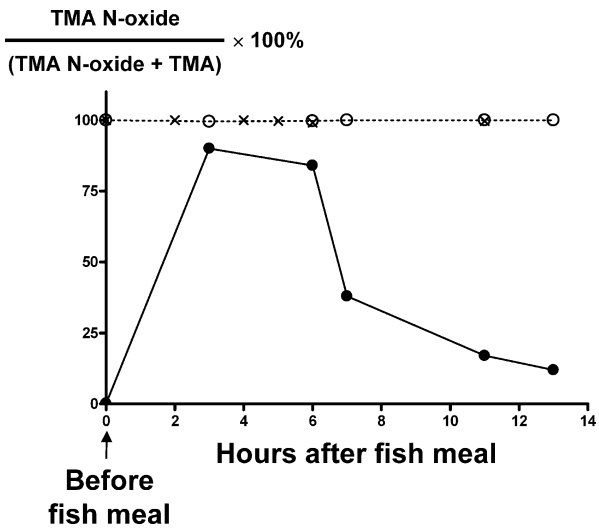

Fig. 7.4.4 Oral challenge test with a sea fish meal (300 g fresh sea fish) in two healthy volunteers (---) and one patient with the severe form of trimethylaminuria. The ability of the N-oxidation system to oxidise TMA into TMA N-oxide is expressed as the ratio TMA N-oxide:(TMA N-oxide + TMA). In this patient both the baseline value and all other data points are abnormal

References

1. Abeling NGGM, van Gennip AH, Bakker HD, Heerschap A, Engelke U, Wevers RA (1995) Diagnosis of a new case of trimethylaminuria using direct proton NMR spectroscopy of urine. J Inherit Metab Dis 18:182–184
2. 3Al-Waiz M, Ayesh R, Mitchell SC, Idle JR, Smith RL (1989) Trimethylaminuria: the detection of carriers using a trimethylamine load test. J Inherit Metab Dis 12:80–85
3. Al-Waiz M, Mitchell SC, Idle JR, Smith RL (1987) The relative importance of N-oxidation and N-demethylation in the metabolism of trimethylamine in man. Toxicology 43:117–121
4. Anonymous (1980) Workplace environmental exposure level guide. Trimethylamine. Am Ind Hyg Assoc J 41:A35–A37
5. Asatoor AM, Simenhoff ML (1965) The origin of urinary dimethylamine. Biochim Biophys Acta 11:384–392
6. Ayesh R, Mitchell SC, Zhang A, Smith RL (1993) The fish odour syndrome: biochemical, familial and clinical aspects. Br J Med 307:655–657
7. Binzak BA, Wevers RA, Moolenaar SH, Lee Y-M, Hwu W-L, Poggi-Bach J, Engelke UFH, Hoard HM, Vockley JG, Vockley J (2001) Cloning of dimethylglycine dehydrogenase and a new human inborn error of metabolism, dimethylglycine dehydrogenase deficiency. Am J Hum Genet 68:839–847
8. Blumenthal I, Lealman GT, Franklyn PP (1980) Fracture of the femur, fish odour and copper deficiency in a preterm infant. Arch Dis Child 55:229–231
9. Calvert GD (1973) Trimethylaminuria and inherited Noonan's syndrome. Lancet 1:320–321
10. Cashman JR, Zhang J (2002) Interindividual differences of human flavin-containing monooxygenase 3: genetic polymorphisms and functional variation. Drug Metab Dispos 30:1043–1052
11. Danks DM, Hammond J, Faull K, Burke D, Halpern B (1976) Trimethylaminuria: diet does not always control the fishy odor. New Engl J Med 295:962
12. Fay LB, Leaf CD, Gremaud E, Aeschlimann J-M, Steen C, Shuker DEG, Turesky RJ (1997) Urinary excretion of 3-methyladenine after consumption of fish containing high levels of dimethylamine. Carcinogenesis 18:1039–1044
13. Higgins T, Chaykin S, Hammond KB, Humbert JR (1972) Trimethylamine-N-oxide synthesis: a human variant. Biochem Med 6:392–3963
14. Humbert JR, Hammond KB, Hathaway WE, Marcoux JG, O'Brien D (1970) Trimethylaminuria: the fish odour syndrome. Lancet 2:770–771
15. Koukouritaka SB, Simpson P, Yeung CK, Rettie AE, Hines RN (2002) Human hepatic flavin-containing monooxygenase 1 (FMO1) and 3 (FMO3) developmental expression. Pediatr Res 51:236–243
16. Lee CWG, Yu JS, Turner BB, Murray KE (1976) Trimethylaminuria: fishy odours in children. N Engl J Med 295:937–938
17. 18Marks R, Dudley F, Wan A (1978) Trimethylamine metabolism in liver disease. Lancet 20:1106–1107
18. Marks R, Greaves MW, Prottey C, Hartrop PJ (1977) Trimethylaminuria: the use of choline as an aid to diagnosis. Br J Dermatol 96:399–400
19. Maschke S, Wahl A, Azaroual N, Boulet O, Crunelle V, Imbenotte M, Foulard M, Vermeersch G, Lhermitte M (1997) 1H-NMR analysis of trimethylamine in urine for the diagnosis of fish odour syndrome. Clin Chim Acta 263:139–146
20. Matsushita K, Kato K, Ohsaka A, Kanazawa M, Aizawa K (1989) A simple and rapid method for detecting trimethylamine in human urine by proton NMR. Physiol Chem Phys Med NMR 21:3–4
21. Mitchell SC, Smith RL (2001) Trimethylaminuria: the fish malodor syndrome. Drug Metab Dispos 29:4,2:517–521
22. Murphy HC, Dolphin CT, Janmohamed A, Holmes HC, Michelakakis H, Shephard EA, Chalmers RA, Phillips IR, Iles RA (2000) A novel mutation in the flavin-containing mono-

oxygenase 3 gene, FMO3, that causes fish odour syndrome: activity of the mutant enzyme assessed by proton NMR spectroscopy. Pharmacogenetics 10:439–451
23. Park CS, Chung WG, Kang JH, Roh HK, Lee KH, Cha YN (1999) Phenotyping of flavin containing monooxygenase using caffeine metabolism and genotyping of FMO3 gene in a Korean population. Pharmacogenetics 9:155–164
24. Pike MG, King GS, Pettit BR, Leonard JV, Atherton DJ (1988) Lactulose in trimethylaminuria, the fish-odour syndrome. Helv Paediatr Acta 43:345–348
25. Podadera P, Arêas JAG, Lanfer-Marquez UM (2005) Diagnosis of suspected trimethylaminuria by NMR spectroscopy. Clin Chim Acta 351:149–154
26. Treacy EP, Akerman BR, Chow LML, Youil R, Bibeau C, Lin J, Bruce G, Knight M, Danks DM, Cashman JR, Forrest SM (1998) Mutations of the flavin-containing monooxygenase gene (FMO3) cause trimethylaminuria, a defect in detoxification. Hum Molec Genet 7:839–845
27. Treacy E, Johnson D, Pitt JJ, Danks DM (1995) Trimethylaminuria, fish odour syndrome: a new method of detection and response to treatment with metronidazole. J Inherit Metab Dis 18:306–312
28. Zhang AQ, Mitchell SC, Ayesh R, Smith RL (1992) Determination of trimethylamine and related aliphatic amines in human urine by head space gas chromatography. J Chromatogr 584:141–145
29. Ziegler DM (1990) Flavin-containing monooxygenases: enzymes adapted for multisubstrate specificity. Trends Pharmacol Sci 11:321–324

8.1 A Tandem Mass Spectrometry Primer for Metabolite Disease Detection

Donald H. Chace

8.1.1 Introduction to Tandem Mass Spectrometers

Tandem mass spectrometers are just one type of mass spectrometer and there are many abbreviations and terms that are used commonly. Tandem mass spectrometers have been given many shorten names and abbreviations from tandem mass to TMS (many say they use these terms because of the challenge of pronouncing spectrometry). Unfortunately, these are incorrect abbreviations and it is essential to use tandem mass spectrometry with proper terms (TMS is and abbreviation for trimethylsilyl derivatives used in gas chromatography/mass spectrometry). The acceptable shortened name or abbreviation is tandem MS (where mass spectrometry is abbreviated and it removes the challenging spectrometry pronunciation) or MS/MS [1].

Why do we use the abbreviation MS/MS? This indicates the configuration of one of the most common types of tandem mass spectrometer, a tandem quadrupole mass spectrometer. The tandem quadrupole mass spectrometer instrument has two mass separation quadrupole devices that are separated by a collision cell or fragmentation chamber. These devices are linked in series (tandem in space). In other words a charged molecule (ion) must first pass through the first mass spectrometer (mass analyzer, MS1) and a collision cell before it reaches the second mass spectrometer (mass analyzer, MS2). The slash or dash between MS/MS (MS-MS) has been debated and it has been traditional to denote tandem in parallel instruments as MS/MS. The hyphen is utilized for other types of devices attached to the instrument such as gas chromatography (GC-MS) or liquid chromatography (LC-MS) or LC-MS/MS. Figure 8.1.1 illustrates the various configurations of tandem mass spectrometers.

These are not the only types of tandem mass spectrometers. There are numerous configurations of instruments that are based on the type of ion separation and many new terms associated with these instrument types. For example, there are instruments known as ion traps. The ion trap is a device that can measure mass, fragment a selected mass (as could be done in a collision cell) and then measure the mass of the fragment. The product ion produced by this all in one device is the same product ion that would be produced in a tandem quadrupole instrument. However, there is only one mass analyzer that functions as both the collision cell and mass measuring device. These types of instruments are sometimes referred to as tandem mass spectrometers, but are not abbreviated as MS/MS. The MS/MS analysis is done by separating the analysis in time (tandem in time) rather than two devices separated in space. A more generic term is best suited. This term is MS^n, where the n represents

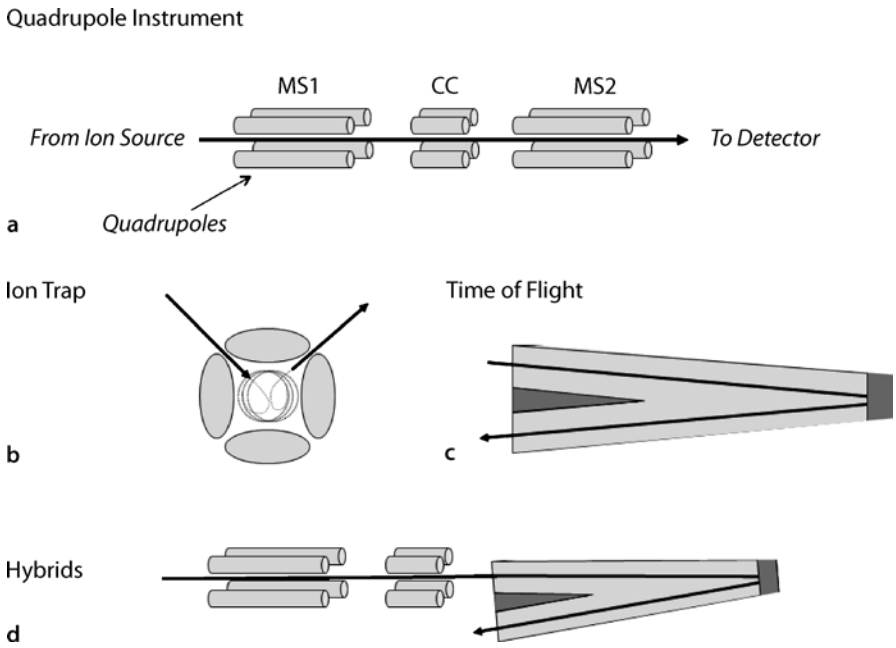

Fig. 8.1.1 Simple illustrations of a various mass spectrometers. **a** The triple-quadrupole tandem mass spectrometer (*top panel*). The middle set of quadrupoles are part of the collision cell (*CC*) and do not perform mass separation. *MS1* and *MS2* indicate the first and second quadrupole mass separation devices, respectively. The *bold arrow* shows the path of ions. **b** Ion-trap mass spectrometer (*middle left*). The charged sections of the ion trap are not elliptical as drawn, but rather hyperbolic. The diagram is also two-dimensional, whereas the ion trap is three-dimensional. The ion path is such that ions enter the device and are trapped until a specific voltage ejects these ions. **c** Time of Flight mass spectrometer with a Reflectron (*middle left*). Ions are separated by the time it takes to pass through the instrument. The Reflectron improves/focuses the ions. **d** Hybrid Tandem mass spectrometer (*bottom*). The diagram shows that a quadrupole instrument can be combined with a different type of mass spectrometer, forming a tandem hybrid instrument

the number of mass analyses. The MS analysis of a compound and its "first" fragments would be labeled MS^2 since mass of the intact, precursor ion and its fragment, product ion has two mass separations. An ion trap can, however, "trap" one of the product ions and fragment it further. This additional round of mass analysis and fragment would be called an MS^3 analyses. As you can see, an ion trap has a very important function in product ion analysis. However, it is limited in its ability to "answer questions" about the precursor ions based on its products. Simply stated, it cannot perform neutral loss or precursor ion scans as well as tandem quadrupole or tandem in space instruments. Figure 8.1.1 has a simplified diagram of an ion trap.

Finally, it is important to note there are many other instruments and configurations that are often referred to as tandem mass spectrometers. There are hybrid instruments that use another form of mass separation, time-of-flight (TOF) mass spectrometry. TOF mass spectrometry separates ions based on the time it takes to

traverse a particular ion path. They often contain a device known as a Reflectron (Fig. 8.1.1), which is essentially an ion-selective mirror or lens that helps focus the ion beam, permitting very high resolution. With the addition of a TOF instrument we have a many instrument combinations. Hence, there exists quadrupole-TOF instruments and TOF/TOF tandem instruments are available. There are even quadrupole linear ion-trap tandem mass spectrometers. All of the instruments are arranged spatially and hence are tandem in space instruments. Another type of instrument, known as a Fourier transform ion cyclotron resonance instrument, can perform tandem in time mass analysis like that of an ion trap.

8.1.2 Introduction to Clinical Analysis by MS/MS

A mass spectrometer detects the mass of ionized molecules. Many of these molecules are compounds found in biological fluids and are integral intermediates of clinical biochemistry. Mass spectrometers detect the compound(s) that enter it. It is very important that the mass spectrometer's ability to detect and measure a compound is only as good as the integrity of the compound that is injected into it. The mass spectrometer is a detector. There is a certain degree of expertise to keep the mass spectrometer operating efficiently as a detector, and some of this will be described herein. But there is an equally important expertise in sample handing and sample preparation. A poor sample preparation, poor sample quality, or inappropriate specimen type can affect the results or their meaning even if analyzed using a mass spectrometer. These are obvious statements, yet with the power of a tandem mass spectrometer, they are often overlooked. When we discuss a false result obtained by mass spectrometry, was it due to a poorly operating mass spectrometry system, sample preparation that was improper, a bad specimen, or was it a correct, true result from a patient not expressing a disease (producing particular metabolites) at the time of collection? Many techniques are required just to isolate the problems routinely encountered in an analysis of a clinical sample.

A tandem mass spectrometer and its ability to measure multiple metabolites helps overcome many of the problems associated with clinical chemistry. In terms of results, measurement of related metabolites is often better at characterizing a disease than measuring a single analyte, as often done in many classical non-mass spectrometric analyses. Yet, mass spectrometry also has its limitations and laboratories need to utilize confirmatory tests to improve the certainty of a result. Furthermore, any interpretation of a biochemical result must be done so in light of patient variables such as age, health status, and gender, for example. In other words, from the laboratory perspective, an MS/MS analysis provides some important and critical information to a medical practitioner. It is important that we explain the context of what those results are so that he/she can make a proper diagnosis. The fewer false results demonstrated in many laboratories utilizing MS/MS engender a higher degree of confidence in the analytical result among physicians. The higher the confidence in that data by the medical profession, the more likely a correct and timely diagnosis and subsequent treatment will be made.

8.1.3 Essential Principles of MS/MS

The primary use of MS/MS in most laboratories has been as a device that obtains product ion spectra, which are essentially fragmentation products. Molecules fragment in reproducible ways and follow basic physical chemistry principles. An analogy to letters and words has been used. Atoms are the letters and syllables are certain arrangements of atoms in functional groups, such as a carboxylic acid group, an amine, a hydroxyl group, ketones, and hydrocarbon chains with branch points, for example. Like words in a dictionary, the syllables are separated for pronunciation, like pro-nun-ci-a-tion. (See Fig. 8.1.2) A molecule may fragment into various pieces in the same predictable way. Product ion scans are important for learning about specific molecules and for the discovery or identification process of newly discovered compounds.

In metabolism, more specifically newborn screening for amino acids and acylcarnitines, we use two other types of MS/MS analyses: the precursor and neutral loss scans. In both types of scan, the question is asked "where did I come from?" In other words, a fragment of a molecule is detected that is unique or common to a particular molecule or family of structurally similar molecules. Because the instruments are linked in space rather than time, when a particular product is detected in the second mass spectrometer (MS2), the computer software knows what mass was being scanned in the first mass spectrometer (MS1). The difference between a precursor ion and neutral loss scan is the nature of the product. With a precursor ion scan, that product of interest is also an ion and it can be detected. With a neutral loss

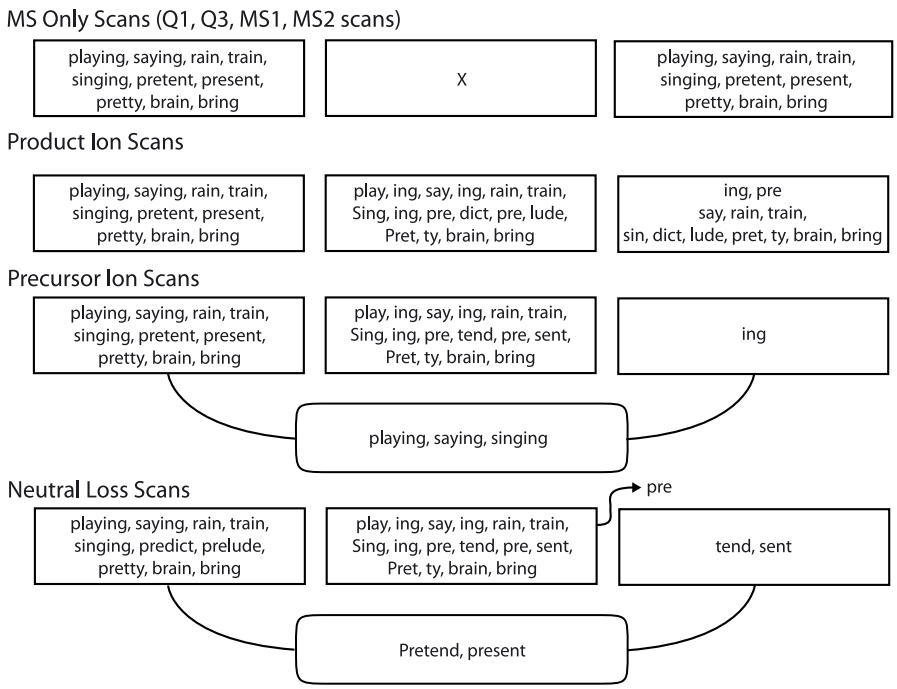

Fig. 8.1.2 Illustration of tandem mass spectrometry (*MS*) analysis using a "word" analogy

scan, the product of interest is not an ion, but a neutral uncharged molecule. It cannot be detected. However, since a molecule must fragment to a neutral and ionized fragment (i.e., split into at least two parts), the other part of the fragment is charged. Using computer software, we set the second mass spectrometer to measure the mass of any product ion that differs by the mass of the neutral molecule (which is pumped away in a vacuum). There are other functions of a mass spectrometer, such as neutral gain (rarely used) and mass spectrometry only where the mass spectrometer can be set to not fragment at all and measure all ions. See the illustration in Fig. 8.1.2 for a graphical explanation.

There is also one other type of scan that is actually a subset of all of the above scans. These are known as selected reaction monitoring (SRM) scans. These scans pick one precursor ion and one product ion and monitor that signal. You can add as many SRM scans as the software allows.

Missing from the above discussion is the collision cell or fragmentation chamber. The collision cell contains many of the electronics and features of MS1 and MS2 with a few important differences. First, the collision cell does not separate masses. It is a pass-though device where we want to keep the beam of ions tightly packed in a stream, even after the energetic fragmentation process. It is also important for these ions to maintain their certain energetic state so that they can pass through this device. This chamber can be used to regulate the energy state of the molecules so that the degree of fragmentation can be altered as well as a gas is introduced to collide with the precursor ions and cause fragmentation.

The other important aspect of MS/MS is that it can perform any of these types of scans during a particular analysis. In other words, you can perform a precursor ion scan and a neutral loss scan then repeat the entire cycle as frequently as the data sensitivity allows and for as long as the compound is present. This makes for a very versatile and powerful instrument.

Ionization is another very important component of MS/MS and all MS instruments. Molecules must be charged in order to be analyzed because the mode of analysis is by repulsion and attractive forces driving and guiding an ion down a path. It is not that different to considering the amount of force needed to keep a wandering elephant walking down a path than perhaps a turtle. For a given set of conditions, only one combination of electronic fields will permit a molecule of a certain charge and mass to pass through its chambers, at least for the quadrupole instruments. We measure mass by correlating detection with specific voltage settings. TOF instruments work a bit differently; they separate by speed and time of arrival. If we hit a bowling ball with the same force of a golf ball, the golf ball would quickly reach its target, whereas the bowling ball would move slowly toward the target. We separate mass by measuring arrival times.

Ionization is very important in that you have to have ions to detect and measure mass. Today, electrospray ionization is used; this is a process where a streaming liquid is ionized and this imparts ionization of the molecules dissolved within it. However, large amounts of liquid or uncharged molecules are not desirable in a mass spectrometer operating in a vacuum. Hence, electrospray ionization is optimized such that nearly all of the solvent/spray is removed and only charged molecules enter the mass-separation devices. You may ask how I ensure that only the molecules I am interested in make it to the mass spectrometer rather than all of the other molecules that may be present in the mix. This is an important concept, since

the ability to ionize or the efficiency of the ionization process is dependent upon the concentrations of the material in which you are interested and the concentration of all of the other materials that are present. You obtain the highest degree of ionization when less of the competitive ionization materials present. In a nutshell, this is where much thought on sample preparation and internal standardization is key. The term "ionization efficiency" is key to the quantitative aspects of mass spectrometers.

One final note that requires a discussion: it is the mass and charge of a molecule that is measured in a mass spectrometer, not simply mass. However, with most small molecules, the charge is 1 and hence an *m/z* value is *m*/1 or simply *m*. However, certain molecules have the potential to become multiply charged (i.e., proteins and peptides). Therefore multiply charged molecules could have multiple mass values at *m*/1, *m*/2, *m*/3 etc. Most metabolite analysis however is singly charged and as such simplifies this discussion.

8.1.4 Data Handling, Data Processing

For each mass value, a signal quantity at the detector is recorded as counts per second, but may also be in another form. Since there are generally many mass values acquired, there is a ion intensity for each mass. This can be displayed as a bar chart of *m/z* ratio versus signal intensity. This chart is known as a mass spectrum. Spectra come in many variants. Full scan mass spectra show a range of masses with individual values at regular intervals of 1 or even 0.1 Da. SRM measures only the precursor ion mass and its product ion. Some mass spectra are "processed" data that convert *m/z* to mass. This is often seen in protein analysis where the multiply charged mass spectra are converted to a spectrum of just mass, simplifying the spectra interpretation.

In addition to displaying data in a spectrum, data is also in the form of a list with mass and ion counts (intensity). Some mass spectrometers can do many things to spectra to improve its utility. Removing or "smoothing out" of random noise, for example, is often performed. The modified or processed data or raw data is then often shipped to another program that converts these data to concentrations or a workable form with which to make assessments.

Many mass spectrometry vendors supply software to provide the ability to perform various mathematical or statistical operations including calculation of standards curves and concentrations. In general these programs can calculate a ratio of the intensity of one peak relative to another. If that other peak or "reference" is present at a known concentration, then this ratio becomes the basis for calculation of the concentration of the unknown with various corrections and constants. There are many options to working with mass spectrometric data and, as a result, many different programs used to manipulate these data. Other programs have searchable databases to match a mass spectrum obtained with that in a library and score the closeness of a match as a numerical percentage. Other software converts an *m/z* spectrum for a protein to that of mass only due to the nature of the analysis and multiply charged proteins. That discussion is best reserved for proteomics rather than metabolomics.

8.1.5 Interpretation

In clinical chemistry, interpretation of the data can be quite simple or complex. In the case of MS/MS applications pertaining to a single analyte, all that is needed is the intensity value from the mass of a peak of interest and its internal standard. Viewing of a spectrum is not necessary. For profile methods such as full-scan acylcarnitines, amino acids, or other compound families, the interpretation is more complex. With multiple related components, calculation of the concentration of many key metabolites is required. The system generally has multiple internal standards, external standards, or both. In addition to the concentration calculations, examination of a profile is often best achieved by viewing the spectra together with the quantitative information.

8.1.6 Preparation for MS/MS Analysis

Although MS/MS improves selectivity compared to a single MS analysis for specific compounds, a certain degree of sample preparation, clean-up, and possible derivatization is necessary. As described previously, ionization is a critical step in detecting compounds of interest. Biological specimens generally have very complex components and some of them are present in very high concentration. Each of these compounds competes for the ionization process, albeit some more effectively than others. In addition, salts can create adducts that alter the mass value and ionization efficiency. Sample clean-up can improved the sensitivity and selectively greatly. As in newborn screening, several aspects of the analysis enables a higher sensitivity than otherwise could be achieved with a direct analysis of blood. First, for example, the filter paper card that is used to collect blood serves as a clean-up step if extracted with pure methanol. Altering this solvent composition (i.e., adding more water or using a more lipophilic alcohol such as ethanol) can decrease the extraction efficiency of a specimen or remove more unwanted compounds that compete for ionization. Second, esterification can increase ionization efficiency by preventing the possibly of a negative charge on the acid functionalities as well as make the compound more lipophilic. Third, the makeup of the mobile phase and slight alteration of the pH can enhance ionization. There are many methods that can be used to clean up or separate the components of interest, including high-performance liquid chromatography and column extraction.

8.1.7 Internal Standards

Perhaps no reagent is more important than the stable-isotope-labeled internal standard in any clinical assay utilizing mass spectrometry for quantification. Internal standards are important in many aspects of the analysis and are somewhat different than standards utilized in other clinical, non-mass-spectrometric assays. The ideal internal standard is an enriched isotopic version of the analyte being measure. For example, in the case of phenylalanine, a standard available may contain six ^{13}C molecules rather than ^{12}C in the aromatic ring. This has the net effect of shifting the mass of phenylalanine by six units while also maintaining nearly identical chemical

properties. A technique in mass spectrometry known as isotope-dilution mass spectrometry utilizes these standards to most accurately quantify an analyte. If a known amount of stable isotope internal standard is added to blood and mixed appropriately, it will follow all of the preparation and analytical steps as for an unlabeled analog. Typically, a standard curve of known concentration of the analyte of interest is mixed with a fixed concentration of isotope-labeled analyte and measured by mass spectrometry. A measured ratio of unlabeled to labeled analyte versus the theoretical amount of added unlabeled metabolite provides this standard curve. In other words, the labeled analyte (internal standard) becomes the reference. From the standard curve plot, calculation of the concentration is possible by extrapolation.

In some applications like newborn screening and filter paper blood spots, the internal standard that is labeled cannot be mixed with blood. It can only be present in the extraction solvents. Therefore, only the extracted metabolites can be quantitatively measured. I have denoted a term called pseudo-isotope dilution to account for the differences between traditional isotope dilution and the technique commonly used in newborn screening by MS/MS. A special analysis is capable using this technique, however, in terms of an extraction efficiency experiment. With isotope-labeled standards you can perform an experiment whereby a traditional isotope-dilution technique (internal standard added to liquid blood and spotted) is compared to pseudo-isotope dilution techniques (internal standard is added to the extraction matrix). The ratio of the results of these two analysis (pseudo/traditional) is the extraction efficiency.

Another note of importance in MS/MS is the position of the isotope label. Depending upon the type of MS/MS analysis, the position of the label is important in terms of making sure that the analyte of interest and its internal standard share the same fragments. In other words, in the case of phenylalanine for example, a label on the phenyl ring produces a fragment that is identical to the unlabeled precursor. Furthermore, the fragment (neutral loss) is the formic acid and not the phenyl ring. So both product ions are different by the labels. If the phenylalanine was labeled on the carbonyl carbon, that would be lost on fragmentation and the mass of phenylalanine would be altered and perhaps the ability to accurately quantify the mass. Therefore, extreme care is required in designing new clinical assays and new internal standards.

Not all metabolites may have an internal standard, especially in techniques that measure many substrates. In this case, we can measure the ratio of the analytes of interest to a different internal standard via a standard curve and make corrections. If no unlabeled or labeled standard is available for a compound or peak of interest, then a simple ratio of masses can be calculated. Although this may be quite reproducible, it should be recognized that there is an added degree of uncertainty about the measurement and renders the analysis qualitative, or at best semiquantitative.

8.1.8 Quality Control and Assurance

It is important to clarify a confusing issue that is commonly encountered in mass spectrometry and clinical chemistry. Mass spectrometrists define selectivity and sensitivity in quite different terms than do clinical chemists. Analytical selectivity and sensitivity are terms that should help clarify the situation. The measure of sensitiv-

ity of an instrument in terms of μmol/l or mg/dl defines detection limits from the measurement perspective. The ability to measure a particular analyte with little or no interference from other components defines selectivity from this analytical perspective. Clinically speaking, clinical sensitivity is the ability of a test to detect patients with disease where clinical selectivity has to do with the ability to distinguish one disease from another. Perhaps clinically speaking, the term "false-positive" and "false-negative" results are alternative ways of presenting the data.

There are proficiency testing programs that are geared toward clinical sensitivity or specificity by seeking to determine whether a disease can be detected versus other types of controls that are use to test sensitivity, selectivity, and most importantly, reproducibility and precision. With mass spectrometry, the controls are and should be no different than those used for other assays, with one interesting exception. Quality assurance materials prepared for MS/MS may not be useful in other assays that are less selective. The example is newborn screening where quality assurance/control QA/QC materials have a mixture of compounds present in the blood specimens. However, in less selective immunoassays, the mixture creates interferences. In addition, material is used to spike a blood sample is key and one should ensure there is no enzyme activity. We have encountered such a problem with a d/l mixture of metabolites where one form was degraded in the prepared blood.

8.1.9 Multiple Analyte Versus Single Analyte

Mass spectrometry can analyze single or multiple components in a clinical assay. Each has their advantages and disadvantages. In the case of newborn screening applications, MS/MS is used to measure the amino acid and acylcarnitine family of compounds in a single test. This has the advantage of saving dollars in the analysis. However, interpretation can be quite complex and in such a pattern, not all metabolites and the diseases they detect are created equal. The idea of a single analyte is simplest and interpretation is relatively simple, but the cost per sample may be higher. In truth, MS/MS is more ideally suited for multiple-component analysis because of its ability to selectively analyze compounds of interest, and very different compounds at the same time. For single-analyte components, other assays may be simple and less expensive and therefore MS/MS is not justified. A full-capability clinical laboratory usually has both mass spectrometry and other techniques that serve to detect a myriad of compounds and provide a confirmatory test to the assay performed on a different system.

8.1.10 A Clinical Illustration

To put the discussion described above in a practical illustration, I have included a mass spectrum from a newborn blood spot of a patient confirmed to have medium-chain acyl coenzyme A dehydrogenase (MCAD) deficiency. Figure 8.1.3 is an acylcarnitine profile obtained from a methanol extract of a dried blood spot. Stable-isotope acylcarnitine internal standards were mixed with the methanol extracting solvent at a concentration that is equivalent to 1 or 2 μmol/l of blood. The concentrations of each internal standard are marked on the illustration by the clear hexagons.

This extract was derivatized to make butyl esters of the acylcarnitines and analyzed using precursors of a 85-Da scan. The common fragment of acylcarnitine butyl esters is an ion at *m/z* 85 and all acylcarnitines share this common product. The spectra show the precursor ions or molecular ions that were being scanned at the time, detected at *m/z* 85 for both the internal standards and endogenous acylcarnitines. To the left, or lower mass values, the metabolites of interest are labeled as, for example, C3, C8, C16. Those acylcarnitines that are key to the detection of MCAD deficiency are underlined.

A key point in the examination of full-scan spectra requires a quick glance at the signal to noise ratio. This is illustrated in the spectrum and labeled as signal and noise. A simple examination will show that there is little random noise and that a peak is clearly differentiated. Also note that visually, the pattern of MCAD is clear, with a large set of peaks at C8, C6, C10:1, and C10. In fact, if you were to connect the dots it would look like a bell-shaped curve, and that is exactly the correct analogy because the activity of the MCAD enzyme is optimize for C8 and less so for C6, C10, and C10:1. C6 and C10/C10:1 can be metabolized to a smaller extent by very-long-chain acyl-coenzyme A dehydrogenase or short-chain acyl-coenzyme A dehydrogenase enzymes. This profiles is compared to the quantitative result. Regarding quantification, the relative peak intensity of the C8 is about five times that of the internal standard, which at 1 μmol/l would lead to approximately 5 μmol/l of C8. A quick glance at C3 and C16 shows that these metabolites are not deficient and hence there appears to be a know carnitine deficiency, which can be reference by the free carnitine value (data not shown). The major point here is that a mass spectrum should look like that presented in Fig. 8.1.3. The separation of M, M + 1 and M = 2 should be adequate such that M and M + 1 are differentiated and between 20 and 30% for the number of carbons detected (1.2% × Carbon number = natural abundance for ^{13}C). Between the pattern and the concentration of individual metabolites,

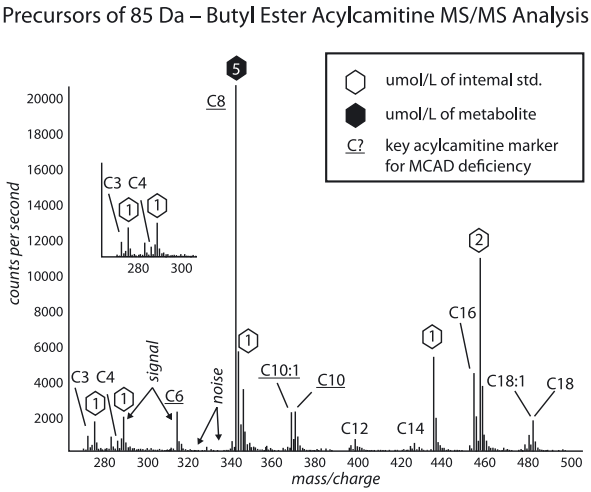

Fig. 8.1.3 Acylcarnitine profile of a blood spot from a newborn with medium-chain acyl coenzyme A dehydrogenase (*MCAD*) deficiency

detection of MCAD deficiency should be relatively easy and exhibit a degree of high accuracy and precision.

8.1.11 Brief Summary

This chapter was designed to introduce and simply illustrate how a tandem mass spectrometer is used in clinical chemistry. There are several other references for a broader description of mass spectrometer application in clinical chemistry as well as specific applications of the technology in numerous areas of metabolism and proteomics. A key point is that a tandem mass spectrometer is just one component of an entire system, which includes the specimen type, collection, sample extraction, clean-up, quantification, QA/QC, interpretation, and reporting and follow-up of abnormal results. If the mass spectrometer is operating at its peak efficiency, screening results would likely be clear and free of issues. However, if the mass spectrometer is not at its peak, questions on diagnosing the instrument problem, failed QA/QC, incorrect interpretation, and delayed results will have an adverse effect on the results and the confidence we have in them. Hence, the mass spectrometer lies at the heart of such a robust newborn screening test and other clinical tests utilizing this system.

References

1. Sparkman OD (2000) Mass Spectrometry Desk Reference, 1st edn. Global View, Pittsburgh, p 106

8.2 Molecular Genetics: Mutation Analysis in the Diagnosis of Metabolic Disorders

Johannes Zschocke, Bart Janssen

8.2.1 Introduction

"*The natural world is not famous for making life easy for human geneticists*"
D. B. Goldstein [5]

Over recent years, molecular genetic investigations have attained an important place in the diagnostic work-up of patients with known or suspected inborn errors of metabolism. Identification of a known disease-causing mutation may provide the ultimate proof of diagnosis, particularly in those disorders in which a biochemical or enzymatic diagnosis is not possible, not reliable or requires invasive procedures. This may be the case when an enzyme is expressed in specific organs only (e.g. liver or brain) or when the disease is caused by a deficiency of structural, receptor or membrane proteins. Mutation analysis may be the first follow-up method in disorders that are caused by one or a few common mutation(s) such as long-chain hydroxyacyl-coenzyme A dehydrogenase (LCHAD) deficiency. Knowledge of the mutation may provide information about the course of disease and prognosis in disorders with established genotype-phenotype correlations. Finally, knowing the causative mutations in a family may be valuable for genetic counselling and prenatal diagnosis.

DNA studies may be quite expensive, and there are several aspects that should be considered before mutation studies are requested or when the results are available:

1. Are mutation studies necessary? Enzyme studies or other phenotypic or functional investigations may be more sensitive and more (cost-)effective for reaching a diagnosis.
2. How unlikely is the diagnosis when no mutation is found? There is virtually no inborn error of metabolism for which all mutations are detected, even with the most sophisticated methods. Negative results do not usually rule out a diagnosis, and for their interpretation it is essential to know the sensitivity of the method used in the analysis. This information must be provided in the DNA analysis report.
3. How likely is the diagnosis when mutations are found? Novel DNA variants may be erroneously regarded as disease-causing when they are in fact silent. Nowadays it is easier to sequence a gene than to interpret the results correctly. Make sure that the laboratory staff is familiar with the full spectrum of mutations in the genes studied.
4. Cis or trans? When two mutations are found in a recessive disorder, inheritance in trans (on different chromosomes) should be confirmed. Two mutations may

occasionally be in cis (on the same chromosome), with another or no mutation on the second chromosome. It may be useful to confirm mutations in parental samples but beware of non-paternity.
5. How good are genotype-phenotype correlations? Is the clinical picture fully explained by the genetic findings? Is the disorder fully penetrant? Are there additional, non-genetic factors of pathogenesis?
6. Mutation data should be communicated to the family through genetic counselling. Many patients do not fully understand the genetic aspects of a metabolic disorder in their child, and genetic counselling should be offered to all. Genetic counselling is absolutely essential when other members of the family could be at risk of being affected or when prenatal diagnosis is considered an option.
7. Who benefits from the analysis? Mutation analyses in children should only be performed if there is an important medical consequence in childhood. In particular, carrier analyses in healthy siblings of children with metabolic disorders are not indicated and should not be carried out even when requested by the parents.

A range of molecular methods is available for the identification of genetic alterations. Most depend on amplification of specific genomic areas with the polymerase chain reaction (PCR). Which method is employed by a particular laboratory depends on a range of factors including experience, costs and billing. For practical purposes it is important to differentiate between mutation scanning methods, mutation screening methods, direct sequencing and genomic quantification.
1. The aim of mutation scanning methods is to detect known or novel mutations in a gene by scanning base-by-base and exon-by-exon. Abnormalities found are confirmed by direct sequencing. In this chapter we present in more detail denaturing gradient gel electrophoresis (DGGE) as a sensitive and cost-efficient mutation scanning method.
2. Mutation screening methods involve testing for specific (previously selected) mutations in a gene. This approach is relatively inexpensive and may be useful for disorders that are caused by one or few common mutations. It is important to take the origin of the patient into consideration, since the frequency of mutations differs markedly between populations. As an example for such a method we discuss restriction enzyme analysis in more detail in this chapter.
3. Direct sequencing is the gold standard of mutation detection; is also covered in this chapter. Sequencing does not usually detect large deletions or genomic rearrangements. Keep in mind that quality control schemes for DNA sequencing consistently show an error rate of at least 1% even in expert laboratories. If the results do not fit the clinical picture it may be justified to check the results in another laboratory.
4. Genomic quantification is necessary to identify large deletions or duplications that occasionally cause single gene disorders. A novel molecular method (multiplex ligation-dependent probe amplification, MLPA) has been recently developed for this purpose and is presented in this chapter.

8.2.2 Properties of the Analyte

Modern genetics started with the elucidation of the double-helical structure of the DNA molecule by James Watson and Francis Crick in 1953 [20]. It was already known

that DNA consists of the purine bases adenine (A) and guanine (G) and the pyrimidine bases thymine (T) and cytosine (C). Although the percentage of A residues differs among organisms, it always equals the percentage of T residues. Likewise, the percentage of G and C residues is equal. Human DNA consists of approximately 30% A, 30% T, 20% G and 20% C. By studying the X-ray diffraction patterns obtained by Rosalind Franklin, Watson and Crick concluded that DNA is present in the nucleus as a double helix of two antiparallel chains with A residues opposite T and G opposite C (Fig. 8.2.1). The four bases are on a deoxyribose-phosphate backbone. The units of the DNA strand are called nucleotides. Each nucleotide consists of a phosphate group

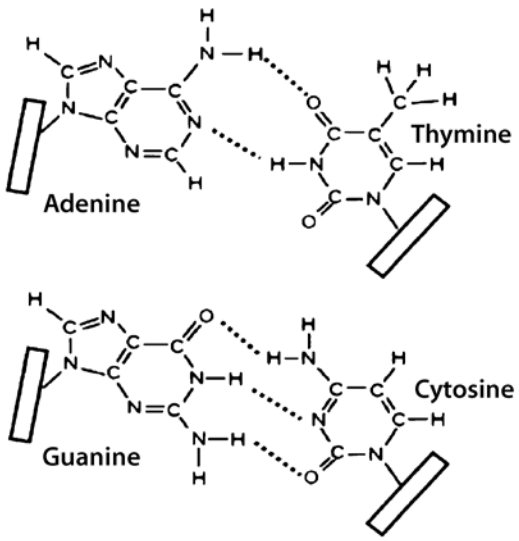

a

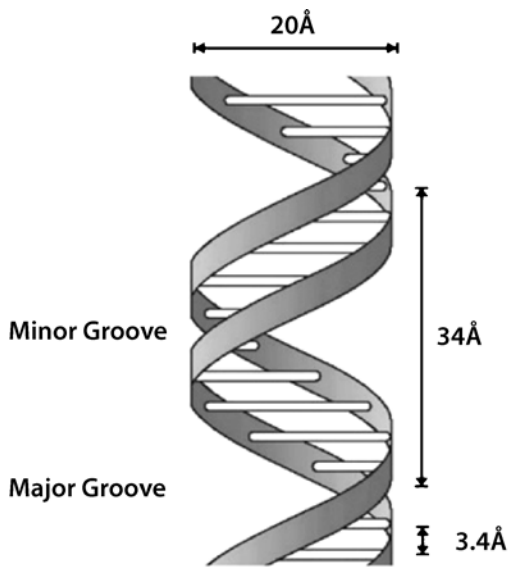

b

```
CGGCGCCGGGGACCGCTGCCACCCCGCCTAGCGCAGCGCCCCGTCCTTCCGCAGCCCAACCGCCTCTTCCCGCCCCGCCCCATCCCGCCCACGGGCTCCAGTGGGCGGGACCAGAGGAGT
CCCGCGTTCGGGGAGTATGTCAAGGCCGTGACCCGTGTATTATTGTCCGAGTGGCCGGAACGGGAGCCAACATGGCAGCGGGGTTCGGGCGATGCTGCAGG...  (intron 1,
3583 bases) ...GTCCTGAGAAGTATTTCTCGTTTTCATTGGAGATCACAGCATACAAAAGCCAATCGACAACGTGAACCAGGATTAGGATTTAGTTTTG...  (intron 2,
4155 bases) ...AGTTCACCGAACAGCAGAAAGAATTTCAAGCTACTGCTCGTAAATTTGCCAGAGAGGAAATCATCCCAGTGGCTGCAGAATATGATAAAACTGGTGAA...
(intron 3, 111 bases) ...TATCCAGTCCCCCTAATTAGAAGAGCCTGGGAACTTGGTTTAATGAACACACACATTCCAGAGAACTGTG...  (intron 4, 605 bases)
...GAGGTCTTGGACTTGGAACTTTTGATGCTTGTTTAATTAGTGAAGAATTGGCTTATGGATGTACAGGGGTTCAGACTGCTATTGAAGGAAATTCTTTGGGG...  (intron 5,
1162 bases) ...CAAATGCCTATTATTATTGCTGGAAATGATCAACAAAAGAAGAAGTATTTGGGGAGAATGACTGAGGAGCCATTGATGTGT...  (intron 6,  5108
bases) ...GCTTATTGTGTAACAGAACCTGGAGCAGGCTCTGATGTAGCTGGTATAAAGACCAAAGCAGAAAAGAAAGGAGATGAGTATATTATTAATGGTCAGAAGATGTGGATAAC
CAACGGAGGAAAAGCTAATTG...  (intron 7, 5695 bases) ...GTATTTTTTATTGGCACGTTCTGATCCAGATCCTAAAGCTCCTGCTAATAAAGCCTTTACTGGATTCAT
TGTGGAAGCAGATACCCCAGGAATTCAGATTGGGAGAAAG...  (intron 8,  3504bases) ...GAATTAAACATGGGCCAGCGATGTTCAGATACTAGAGGAATTGTCTTCGA
AGATGTGAAAGTGCCTAAAGAAAATGTTTTAATTGGTGACGGAGCTGGTTTCAAAGTTGCAATGGGAGCTTTTGATAAAACCAGACCTGTA..  (intron 9, 891 bases) ..GT
AGCTGCTGGTGCTGTTGGATTAGCACAAAGAGCTTTGGATGAAGCTACCAAGTATGCCCTGGAAAGGAAAACTTTCGGAAAGCTACTTGTAGAG...  (intron 10,  10575
bases) ...CACCAAGCAATATCATTTATGCTGGCTGAAATGGCAATGAAAGTTGAACTAGCTAGAATGAGTTACCAGAGAGCAGCTTGGGAGGTTGATTCTGGTCGTCGAAATACCTA
TTATGCTTCTATTGCAAAGGCATTTGCTGGAGATATTGCAAATCAGTTAGCTACTGATGCTGTGCAGATACTTGGAGGCAATGGATTTAATACAGAATATCCTGTAGAAAAACTAATGAG
GGATGCCAAAATCTATCAG...  (intron 11, 1321 bases)  ...ATTTATGAAGGTACTTCACAAATTCAAAGACTTATTGTAGCCCGTGAACACATTGACAAGTACAAAAA
TTAAAAAAATTACTGTAGAAATATTGAATAACTAGAACACAAGCCACTGTTTCAGCTCCAGAAAAAAGAAAGGGCTTTAACGTTTTTTCCAGTGAAAACAAATCCTCTTATATTAAATCT
AAGCAACTGCTTATTATAGTAGTTTATACTTTTGCTTAACTCTGTTATGTCTCTTAAGCAGGTTTGGTTTTTATTAAAATGATGTGTTTTCTTTAGTACCACTTTACTTGAATTACATTA
ACCTAGAAAACTACATAGGTTATTTTGATCTCTTAAGATTAATGTAGCAGAAATTTCTTGGAATTTTATTTTTGTAATGACAGAAAAGTGGGCTTAGAAAGTATTCAAGATGTTACAAAA
TTTACATTTAGAAAATATTGTAGTATTTGAATACTGTCAACTTGACAGTAACTTTGTAGACTTAATGGTATTATTAAAGTTCTTTTTATTGCAGTTTGGAAAGCATTTGTGAAACTTTCT
GTTTGGCACAGAAACAGTCAAAATTTTGACATTCATATTCTCCTATTTTACAGCTACAAGAACTTTCTTGAAAATCTTATTTAATTCTGAGCCCATATTTCACTTACCTTATTTAAAATA
AATCAATAAAGCTTGCCTTAAATTATTTTTATATGACTGTTGGTCTCTAGGTAGCCTTTGGTCTATTGTACACAATCTCATTTCATATGTTTGCATTTTGGCAAAGAACTTAATAAAATT
GTTCAGTGCTTATTATCAT
```

c

Fig. 8.2.1a–c Structure of the DNA molecule. **a** The four bases and the hydrogen bonds that bind both strands of the double helix. The sugar-phosphate backbone is represented by *open bars*. **b** The double helix with both strands depicted as ribbons. **c** the sequence of the ACADM gene. Shown are only the exonic bases. The start and stop codons are *underlined*

at the 5' carbon of a deoxyribose sugar coupled to a DNA base. Each nucleotide is coupled to the next by binding the phosphate at the 3' carbon. This defines the so-called 5'-3' orientation of the DNA strand. The two strands are held together by the hydrogen bonds between the paired bases (A-T and C-G). Due to the invariable base pairing, the information content encoded by the sequence of the DNA bases on both strands is identical: the complementary bases on opposite strands compose complementary sequences. Due to the antiparallel orientation of the strands, the complementary sequence on the opposite strand is directed in a reverse direction.

The sequence of the bases contains coded information for the synthesis of proteins. These sequences are transcribed into an RNA copy of the sequence: messenger RNA (mRNA). The mRNA is translated in the cytoplasm. The DNA also encodes structural RNAs, with functions in transcription of the DNA, processing of the transcripts and translation of the transcripts. The genetic code shown in Table 8.2.1 is simple, but efficient. At each nucleotide position, there are only four possibilities; A,

■ ***Table 8.2.1*** *The genetic code*

Amino acid		Genetic code
Alanine	Ala (A)	GCA, GCG, GCC, GCT
Arginine	Arg (R)	AGA, AGG, CGA, CGG, CGC, CGT,
Aspartic acid	Asp (D)	GAC, GAT
Asparagine	Asn (N)	AAC, AAT
Cysteine	Cys (C)	TGC, TGT
Glutamic acid	Glu (E)	GAA, GAG
Glutamine	Gln (Q)	CAA, CAG
Glycine	Gly (G)	GGA, GGG, GGC, GGT
Histidine	His (H)	CAC, CAT
Isoleucine	Ile (I)	ATA, ATC, ATT
Leucine	Leu (L)	TTA, TTG, CTA, CTG, CTC, CTT
Lysine	Lys (K)	AAA, AAG
Methionine	Met (M)	ATG
Phenylalanine	Phe (F)	TTC, TTT
Proline	Pro (P)	CCA, CCG, CCC, CCT
Serine	Ser (S)	AGC, AGT, TCA, TCG, TCC, TCT
Threonine	Thr (T)	ACA, ACG, ACC, ACT
Tryptophan	Trp (W)	TGG
Tyrosine	Tyr (Y)	TAC, TAT
Valine	Val (V)	GTA, GTG, GTC, GTT
–	Stop (X)	TAA, TAG, TGA

C, G or T. This is not sufficient to encode the 20 possible amino acids. In triplets of 3 positions, there are 64 possible combinations. Hence, the system uses triplets, called codons. The code for each protein starts with an ATG (start codon) and ends with a TAA, TAG or a TGA (stop codons). The code is almost universal; only mitochondria and ciliated protozoa have a different genetic code.

In eukaryotic organisms, the coding sequence is often interspersed by pieces of non-coding DNA, called intros. The introns are removed from the transcript immediately after transcription by a process called splicing. Hence, the mature mRNA contains the coding sequence without disruptions. At the DNA level, the stretches of coding sequence (exons) are separated from the introns by consensus splice signals. The splice sites can be predicted using the web-software provided by the Berkeley Drosophila Genome Project (http://www.fruitfly.org/seq_tools/splice.html).

DNA has several interesting properties that enable us to perform the molecular analyses described in this chapter:

1. The double helix can be separated into single strand DNA molecules by increasing the temperature or the pH. This denaturation of the DNA is reversible: during renaturation, complementary sequences bind and re-form double helices. By adding short, single-stranded synthetic DNA molecules to the denatured DNA prior to cooling to the appropriate temperature, one can bind these synthetic molecules to specific parts of target genes. Such synthetic molecules are known as "primers", "oligonucleotides" or "hybridisation probes".
2. Double stranded DNA can be enzymatically cleaved by commercially available endonucleases (restriction enzymes). These enzymes recognise specific, usually palindromic, sequences and cut specifically at those positions.
3. Single-stranded DNA can be enzymatically duplicated to double-stranded DNA by polymerases such as the thermoresistant *Taq* polymerase. Polymerases need a free 3'OH group to attach the next nucleotide to. Hence, the DNA needs to be partially double stranded. This can be achieved by binding primers to the single-stranded target DNA.
4. Double strand as well as single-strand DNA can be precipitated by ethanol.

8.2.3 Methods

8.2.3.1 DNA Isolation

Principle

The method described here is a modified version of the original protocol published by Miller et al. [12]. The aim of the procedure is to isolate large quantities of sufficiently pure DNA from lymphocytes. The basic strategy is to remove all haemoglobin by first lysing the erythrocytes. In the following steps the lymphocytes are lysed and their proteins are degraded, denatured and precipitated. Finally, the DNA is precipitated using ethanol.

Pre-analytical

Specimen

Required for this method is 2 – 10 ml of ehtylenediaminetetraacetic acid (EDTA)-treated blood. Heparinised blood can also be used, but is less preferred. The blood samples must be fresh (maximum 7 days old when kept at 4°C). Do not freeze the samples.

Reagents and Chemicals

1. Lysis buffer (33.2 g NH_4Cl; 4 g $KHCO_3$; 800 µl 0.5 M EDTA pH 7,4; dissolved in water to a final volume of 4 l; autoclave).
2. SE buffer (8.78 g NaCl; 16.82 g Na^2-EDTA; dissolve in ≈ 1.5 l water, set pH at 8.0 and fill with water to a final volume of 2 l; autoclave).
3. Proteinase K (25 mg/ml).
4. Sodium dodecylsulphate (SDS) 20%.
5. 6 M NaCl (NaCl will remain partially unresolved; autoclave).
6. 100% ethanol.
7. 70% ethanol.
8. 10 mM Tris buffer pH 7.5.

Instrumentation

Centrifuge for 50 ml tubes and a water bath.

Calibration

None.

Quality Control

None.

Analytical

Procedure

The blood is transferred into a 50-ml tube (Falcon or similar), and a similar volume (at least 10 ml) of lysis buffer is added and well mixed. The tube is left on ice for 30 – 45 min; make sure that the cells are lysed (solution should be clear). After centrifugation for 10 min at 400 × *g*, the supernatant is discarded and the pellet is resuspended in 10 ml lysis buffer. The cells are centrifuged again for 10 min at 400 × *g* and the supernatant is discarded. The pellet is resuspended in 5 ml SE buffer and centrifuged for 10 min at 400 × *g*. The supernatant is discarded and the cells are resuspended thoroughly in 5 ml SE buffer (2.5 ml SE buffer when less than 5 ml blood is used). A 20-µl volume of proteinase K (25 mg/ml) and 200 µl of 20% SDS are added to the resuspended cells. After careful homogenisation, if necessary using a pipette, the mixture is incubated overnight at 37°C.

The next day, 2 ml of 6 M NaCl (or 1 ml of 6 M NaCl for samples with 2.5 ml SE buffer) is added. The mixture is vortexed for at least 20 s with maximum speed. The proteins are precipitated in the centrifuge at 2000 × *g* and 4°C. The supernatant

is transferred to a clean tube and again centrifuged until the supernatant is clear. Meanwhile, a glass hook is made by heating the end of a Pasteur pipette in a flame. In a clean tube, two volumes of ice-cold (–10 to -20°C) 100% ethanol are carefully added to the supernatant and the tube is tilted gently. The glass hook is used to capture the precipitated DNA and to wash it in 1 ml of 70% ethanol. The DNA sample is squeezed out at the top of the tube (to remove ethanol), transferred to a dry 1.5-ml tube and air-dried for 5 min. The DNA is dissolved in 100 – 300 µl of 10 mM Tris buffer pH 7.5 by gently rocking overnight at 4°C.

Calculation of Concentration

The DNA concentration is determined by measuring the absorption at 260 nm in a 50-fold dilution of the DNA sample in an ultraviolet (UV) spectrophotometer, using the following formula:

Absorption × dilution factor × 0.05 = concentration in µg/µl.

Post-Analytical

None.

Interpretation

None.

8.2.3.2 Polymerase Chain Reaction

Principle

In 1985, Mullis and colleagues [16] described a new method for the in vitro amplification of specific DNA sequences, avoiding the need to clone DNA fragments. The polymerase chain reaction has since revolutionised molecular genetics. PCR amplification of DNA involves repeated cycles of (a) heat-denaturation of a double-stranded DNA template at approximately 94°C, (b) annealing of specific oligonucleotide primers to the single stranded DNA, and (c) extension of the annealed primers with DNA polymerase, usually at 72°C. The primers are usually around 20 base pairs (bp) long and determine target specificity. They are designed to hybridise to opposite DNA strands flanking the sequence to be amplified, with their 3' ends facing inwards. The target sequence is usually several hundred bp long. The number of sequence copies is doubled with every amplification cycle and increases exponentially as newly synthesised copies become available for primer binding. With the introduction of thermostable *Taq* DNA polymerase [9], it became the most frequently used method in molecular genetic diagnosis and research. PCR is capable of amplifying a single copy DNA sequence up to 10^{-9}-fold within a few hours or faster.

Pre-Analytical

Specimen

Genomic DNA is typically diluted to a concentration of 50 µg/ml. In principle, about 1 – 10 genome equivalents (3 – 30 pg) is sufficient to perform a PCR reaction. In routine diagnostics much larger amounts of template DNA are used (1 – 200 ng per reaction) to maximise the yield of the reaction.

Reagents and Chemicals

It is practical to use PCR reagents in 10× working solutions that will be diluted by a factor of ten for final concentration in the PCR samples. An exception is the thermostable enzyme *Taq* polymerase, which is stored at a much higher concentration. All reagents are available from numerous companies.

Reagents required for PCR:

1. PCR primers at a concentration of 2.5 – 4 µM (10× working solution).
2. *Taq* polymerase at a concentration of 5 U/µl.
3. Appropriate PCR amplification buffer (10× working solution).
4. $MgCl_2$ at a concentration of 25 – 50 mM.
5. dNTP solution 1.2 mM (each nucleotide; 10× working solution).

Instrumentation

PCR instruments are available in different specifications from numerous companies. They now usually include a heated lid, which prevents evaporation of the sample and allows PCR amplification without mineral oil. Important factors in selecting the right instrument include:

1. The speed of heating and cooling (ramping rate).
2. Temperature control.
3. Temperature uniformity across the block.
4. Versatility and ease of programming.

Calibration

There is usually no calibration required. Thermal cyclers should be checked and calibrated by the manufacturer at least once every year.

Quality control

It is recommended to include multiple positive controls (e.g. genomic DNA with and without mutation) and a negative control (water instead of template DNA) in each series.

Analytical

Procedure

The constituents of a 25-µl PCR mixture in a standard 200-µl tube are given in Table 8.2.2. Volumes can be easily adjusted proportionally for larger or smaller PCR volumes. The PCR conditions depend primarily on the melting characteristics of the primers (primers with a low melting temperature require relatively low annealing

Table 8.2.2 *Polymerase chain reaction (*PCR*) mixture in a standard 200-µl tube*

Ingredient	Volume	Final concentration
PCR buffer	2.5 µl	1×
Mg^{++}	1.5 µl	1.5 mM
dNTP	2.5 µl	120 µM each dNTP
Primers	2.5 µl each	250 – 400 nM
Taq polymerase	0.15 µl	1.5 Units
Water	11 µl	–
DNA	2.5 µl	125 ng

temperatures) and the size of the fragment to be amplified (as a rule of thumb, allow approximately 1 min elongation for each 1000-bp amplification product).

A typical PCR cycle consists of denaturation at 94°C for 5 min, 35 cycles of 94°C for 1 min, annealing for 1 min, annealing at 72 C for 1 min and final extension at 72 C for 5 min. Amplified PCR products may be stored at 4°C or frozen.

Calculation

None.

Post-Analytical

There are several methods that can be used to analyse PCR products. The most frequently used method to analyse the presence and size of PCR products is agarose gel elctrophoresis (see 8.2.3.3 Agarose Gel Electrophoresis, below)

Interpretation

Pitfalls

As PCR is a powerful method used to obtain millions of copies for each template molecule, there is a considerable contamination risk. Small amounts of PCR products from previous experiments as well as DNA molecules from other sources can cause spurious results and false interpretations. It is therefore strongly recommended to wear gloves and to pipette with tips containing aerosol filters. Moreover, PCR products should not be handled in the same room where the PCR reagents are being used.

8.2.3.3 Agarose Gel Electrophoresis

Principle

A simple way to visualise PCR products and thereby check amplification success is agarose gel electrophoresis; this method is also used to visualise the results of restriction enzyme digests. The negatively charged nucleic acid fragments migrate through an agarose gel in an electric field to the anode. The velocity of the fragments depends on their size (logarithmic): large molecules migrate slower. The fragments can be visualised in UV light (366 nm) after staining with ethidium bromide.

Pre-Analytical

Specimen

DNA (see, for example, 8.2.3.2 Polymerase Chain Reaction, above).

Reagents and Chemicals

Standard research-grade agarose is usually sufficient, but special agaroses may be used for specific applications (e.g. high-resolution gels). The electrophoresis buffer is usually prepared and stored as a 10× concentrated stock. The most commonly used buffer is Tris-borate-EDTA (TBE), or alternatively, one may use Tris-acetate-EDTA (TAE) buffer:

1. 10×TBE: 108 g Tris, 55 g boric acid and 3.72 g EDTA (pH 8.3 adjusted with HCl) dissolved in water to a final volume of 1 l.
2. 10×TAE: 48.4 g Tris, 11.4 ml acetic acid, 1.86 g EDTA dissolved in water to a final volume of 1 l.

Various loading buffers may be used for transfer of the DNA (e.g. PCR products) onto the gel. The components of a common loading buffer (5× solution) are shown in Table 8.2.3.

Table 8.2.3 *Common loading buffer (5× solution).* EDTA *Ethylenediaminetetraacetic acid,* SDS *sodium dodecylsulphate*

Ingredient	Volume	Final concentration
Glycerol	3.0 ml	30%
SDS	0.5 ml	5%
Tris-HCl	10 mg	10 mM
EDTA	4 mg	1 mM
Bromophenol blue	10 mg	0.1%
Water	10 ml	–

Various size standards are available that should be run together with the samples in order to confirm the expected size of the PCR product. Ethidium bromide (a mutagenic reagent!) is used to visualise the DNA strands; it usually sold as a concentrated stock solution (e.g. 10 mg/ml).

Instrumentation

Appropriate electrophoresis systems in various sizes are available from numerous companies. More expensive are the imaging devices, usually consisting of a UV transilluminator and a CC-camera attached to a computer. There are several types of digital image analysers commercially available. Alternatively, one may use ordinary photography (use a red filter and UV-transilluminator) to obtain an image of the gel.

Calibration

There is no calibration required.

Quality Control

None.

Analytical

Procedure

Staining of DNA in the gel after electrophoresis is usually achieved by bathing the agarose gel in ethidium bromide solution; alternatively, ethidium bromide may be added to the agarose gel (make sure that this method conforms to national safety regulations).

1. For medium-sized gels, add 1 – 3 g research-grade agarose or another agarose to 100 ml 1 × TBE buffer. Mix well and heat to boiling in a microwave oven until fully dissolved.
2. Allow the agarose to cool to approximately 50°C.
3. Pour the agarose into the gel tray, remove air bubbles if present, insert the comb and allow the gel to set at room temperature.
4. Keep at 4°C for 15 min before removing the comb to obtain the best results.
5. Mix 5 – 12 µl PCR product or restriction enzyme digest reaction mixture with 2 – 3 µl of loading buffer and load into wells. Load a suitable-sized standard in an adjacent lane if required.
6. Electrophorese at 5 – 10 V/cm (usually 100 V) for an appropriate length of time.
7. After electrophoresis, transfer the gel into ethidium bromide solution (50 µl stock solution in 1 l of tap water) and stain for 5 – 10 min. Transfer the gel onto a transilluminator and visualise the DNA with UV light, taking care to protect the skin and eyes against UV radiation. Document the result with a standard photograph or digital image analyser.

Calculation

A good approximation of the size of the products (± 5%) can be obtained by comparison with the known sizes of fragments in the size standard.

Post-Analytical

Interpretation

See the following paragraphs.

8.2.3.4 Mutation Scanning: Denaturing Gradient Gel Electrophoresis

Principle

Denaturing gradient gel electrophoresis [4] is a powerful method for identifying known or unknown mutations. It utilises differences in the melting properties of DNA fragments. Double-stranded DNA is electrophoresed on acrylamide gels that contain a gradient of increasing concentration of a denaturant agent (urea or formamide). At a given point, the duplex molecule separates at domains of low melting temperature while still being held together at domains of higher melting temperature. The opening of the duplex molecule leads to a sudden decrease of its mobility in the gel. DNA molecules that differ at only a single base display different migration patterns in the denaturing gradient gels [14]. The method on its own is relatively insensitive to mutations in the late (highest temperature) melting domains. This problem is overcome by the attachment of a 30 – 50 bp high melting temperature G + C-clamp to one PCR primer [13, 18]. Computer programs are available for the design of DGGE primers [11]. The sensitivity of the technique is further improved by the concurrent analysis of homo- and heteroduplexes; the latter always have lower melting temperatures. Designing good DGGE primers may be difficult for G + C-rich DNA fragments. A modification of the technique uses a temperature gradient gel [15]. DGGE has been used successfully for mutation scanning of numerous genes.

DGGE is a very efficient method for the identification of mutations. For small genes, all exons can be screened simultaneously on a single gel and results are obtained very rapidly. Provided that primers are well designed, sensitivity for the detection of mutations in the amplified DNA region may reach virtually 100%. In particular, heteroduplexes between wild-type and mutant alleles should always have lower melting temperatures than homoduplexes and should result in higher bands in the DGGE. Very occasionally, homozygosity in a patient may pose a problem if mutant and wild-types have identical melting characteristics. In this case, DGGE analysis in the obligatory heterozygous parents will reveal the mutation.

Pre-Analytical

Specimen

Purified DNA (see 8.2.3.1 DNA Isolation).

Reagents and Chemicals

Gradient gels are created with equal amounts of solutions containing different concentrations of the denaturing gradient, usually formamide (“high concentration” and “low concentration” solutions). The standard gel used for DGGE contains a formamide gradient from 0% (no formamide, “null solution”) to 80% (32 ml for-

mamide in a total volume of 100 ml). These solutions may be prepared as standards and should be stored in dark bottles at 4°C. Different gradient gels can be obtained by adapting the formamide concentrations in the "high concentration" and "low concentration" solutions used for creating the gradient; solutions of different strengths can be obtained by mixing 80% denaturing formamide with the "null solution" in varying proportions, as shown in Table 8.2.4.

1. "Null solution" (6% acrylamide): 75 ml 40% acrylamide, 10 ml 50× TAE buffer (see 8.2.3.3 Agarose Gel Electrophoresis), water to 500 ml (store in a dark bottle at 4°C).
2. 80% Denaturing formamide solution (6% acrylamide): 75 ml 40% acrylamide, 10 ml 50× TAE, 160 ml formamide, 168 g urea, water to 500 ml (store in a dark bottle at 4°C).

PCR primers for DGGE should be designed using dedicated software, which is commercially available. Of greatest importance is a uniform (flat) melting temperature for the whole PCR product with the exception of the GC tail introduced by means of a 40 – 60 nucleotide GC clamp. For many disorders, DGGE primer sequences are available in the literature.

Table 8.2.4 *Quantities required for "null" solution and 80% denaturing solution*

To achieve:	Mix:	
	"Null" solution	80% Denaturing solution
0%	14 ml	0 ml
5%	13.12 ml	0.88 ml
10%	12.25 ml	1.75 ml
15%	11.38 ml	2.62 ml
20%	10.50 ml	3.50 ml
25%	9.62 ml	4.38 ml
30%	8.75 ml	5.25 ml
35%	7.88 ml	6.12 ml
40%	7.00 ml	7.00 ml
45%	6.12 ml	7.88 ml
50%	5.25 ml	8.75 ml
55%	4.38 ml	9.62 ml
60%	3.50 ml	10.50 ml
65%	2.62 ml	11.38 ml
70%	1.75 ml	12.25 ml
75%	0.88 ml	13.12 ml
80%	0 ml	14 ml

Instrumentation

Vertical slab-gel electrophoresis system that allows exact and constant temperation of the gel through circulation of temperated buffer around both sides of the gel. Specialised systems are available from several companies.

Gradient former for two solutions with different concentrations of a denaturing agent, with a volume of 15 – 20 ml for each solution. The gradient former should be positioned approximately 50 cm over the workplace.

Calibration

There is no calibration required.

Quality Control

In order to recognise homozygous mutants it is essential to examine several samples of the same exon (PCR product) in adjacent lanes. It is recommended to include multiple positive controls (e.g. genomic DNA with heterozygous or homozygous mutations) and a negative control (water instead of template DNA) in each series.

Analytical

Procedure

PCR may be performed in a total reaction volume of 15 µl. Typical concentrations are given in Table 8.2.5. Typical conditions for PCR amplification and heteroduplex formation are given in Table 8.2.6.

A gel has to be prepared for further analysis of the PCR product:

1. Clean the plates with detergent and ethanol and leave to dry.
2. Assemble the plates with 1.0-mm spacers, making sure that plates and spacers are level at bottom when clamped together.
3. Prepare a gradient former by placing a stirrer into cylinder 1, which contains both the connection to the second cylinder and the outlet; make sure both valves are closed.
4. Pour the gels in a fume hood. The total gel volume depends on the electrophoresis system used. Mix acrylamide solutions with ammonium persulphate (6 µl/ml gel)

Table 8.2.5 *Typical concentrations for a PCR reaction volume.*

Ingredient	Volume	Final concentration
PCR buffer	1.5 µl	1×
Mg^{++}	0.9 µl	1.5 mM
dNTP	1.0 µl	60 µM each dNTP
2 Primers	1.0 µl each	160 nM
Taq polymerase	0.1 µl	0.5 Units
Water	9 µl	–
DNA	0.5 µl	12 ng

Table 8.2.6 *Typical conditions for PCR amplification and heteroduplex formation*

	Temperature	Time
Denaturation	94 C	5 min
38 – 40 cycles of	94 C	1 min
38 – 40 cycles of	55 C	1 min 30 s
38 – 40 cycles of	72 C	1 min 30 s
Final extension	72 C	5 min
Denaturation	94 C	1 min
Heteroduplex formation	65 C	1 h
Heteroduplex formation	35 C	1 h
Heteroduplex formation	4 C	Hold

and tetramethyl ethylene diamine (0.4 µl/ml gel). Pour the high denaturant concentration mixture into cylinder 1 and the low denaturant concentration mixture into cylinder 2.

5. Open the connection between the cylinders (observe flow in cylinder 1). Open the exit valve and slowly pour the gel (over approximately 5 min). Control the flow, particularly when the gradient former is emptying.
6. Insert the comb 5 min after pouring the gel. Gently move the comb in and out several times to enhance polymerisation.
7. Remove the combs after 30 – 60 min, rinse wells with 1 × TAE buffer. Gels may be sealed with plastic wrap and kept overnight.

Electrophoresis and visualisation of results:

1. Fill 1 × TAE buffer to comb level into the tank and preheat to 58°C. Maintain a constant temperature throughout the electrophoresis.
2. Shake off buffer from the gel pockets and rinse with 1 × TAE. Assemble the electrophoresis unit and fill reservoirs with 1 × TAE buffer. In some systems samples can be loaded before the electrophoresis unit is transferred to the tank.
3. Mix 12 µl of PCR product with 3 µl of 5 × loading buffer and load 12 – 14 µl strictly at the floor of the wells. Rinse the wells thoroughly to remove urea before loading. Several (four or more) samples of the same PCR product should be loaded in adjacent wells to allow a reliable comparison.
4. Transfer the electrophoresis unit to the tank and ensure that the buffer is at sample level. Wait 5 min until the temperature has adjusted. Electrophorese at 160 – 170 V for 4.5 h; the running times and voltage may need to be adjusted.
5. Dismantle the apparatus and pour the buffer from the top reservoir back into the tank.
6. Stain gels in ethidium bromide solution (as in 8.2.3.3 Agarose Gel Electrophoresis) for 10 min and destain in water for 10 min.
7. Transfer the gel to the UV transilluminator and photograph.

Calculation

None.

Post-Analytical

Interpretation

DGGE results in denaturation and arrest of PCR products at different positions in the gel depending on the melting temperature of the PCR product. Homozygosity in the PCR product results in a single, sharp, homoduplex band; wild-type and mutant alleles can be frequently distinguished by different positions in the gel. In contrast, heterozygosity for one or more mutation or polymorphism result in 2 – 4 sharp bands representing one or two homoduplexes (lower in the gel), and one or two heteroduplexes (higher in the gel due to a higher melting temperature). Different heterozygous mutations usually give rise to distinct band patterns; nevertheless, the exact change in a PCR product that displays an unusual pattern must be determined by DNA sequencing.

8.2.3.5 Mutation Screening: Restriction Enzyme Digestion

Principle

Restriction endonucleases are bacterial enzymes that cleave DNA at sequence specific sites. They were first discovered in 1970 [19]. Almost 2000 restriction enzymes have been identified since, and several hundred of these are commercially available [1]. Many mutations remove or create a particular restriction site in the DNA sequence. These mutations can be identified by PCR amplification, incubation of the product with the appropriate enzyme followed by visualisation of the fragments on an agarose gel.

Restriction enzymes usually cleave at palindromic sites, which are easily spotted in DNA sequences. It is preferable to use a restriction site that is created by a mutation for its analysis, since loss of a cutting site may be caused by several mutations at the same site, including polymorphisms that do not change the amino acid sequence. Positive controls should always be analysed simultaneously with the samples to test enzyme cutting efficiency and to recognise incomplete digestion of DNA. Problems can arise when the recognition site of the enzyme in question occurs more than once in the investigated DNA sequence, and this sometimes makes identification of the appropriate fragments difficult. Restriction enzymes can be expensive, and using a very expensive enzyme for the detection of one rare mutation may not be cost-efficient. However, the simplicity of the technique and its low technical demand have made it one of the most widely used methods for mutation analysis in research and clinical laboratories.

If a mutation does not create or remove a restriction site it is usually possible to artificially create restriction sites during PCR amplification. The technique is referred to as amplification-created restriction site (ACRS) analysis and was first described independently by several groups in 1989 [6, 8, 10]. It has since been applied to mutation analysis for many disorders. In the technique, one PCR primer directly

adjacent to a mutation contains a carefully chosen single-base mismatch relative to genomic DNA. During PCR amplification the mismatch is integrated into the PCR product, thereby producing a new restriction site that is either created or removed by the mutation. Presence or absence of the mutation is then detected by restriction enzyme digest. Again it is preferable to design restriction sites that are created by a mutation in order to increase specificity of the assay. The great variety of restriction enzymes available virtually guarantees that there is a choice of several ACRS primers for any mutation. A BASIC program, MISMATCH, is available for designing these primers [2]; the source code, documentation and default restriction enzyme files are on deposit in the /molbio/ibmpc subdirectory at the IuBio Archive (maintained by D. Gilbert), which is accessible by FTP at the internet address ftp.bio.indiana.edu (login as user "anonymous"; the program is relatively old and the list of restriction enzymes should be updated).

Pre-Analytical

Specimen

Purified DNA (see 8.2.3.1 DNA Isolation).

Reagents and Chemicals

Most restriction enzymes are commercially available. The enzymes are usually sold together with the appropriate reaction buffers.

Instrumentation

A water bath or heating block can be used for the incubation.

Calibration

There is no calibration required.

Quality Control

It is recommended to include multiple positive controls (e.g. genomic DNA with heterozygous and homozygous mutations) and a negative control (water instead of template DNA) in each series. A validation of the procedure can be performed by sequencing some of the wild-type and mutant PCR products, as described in 8.2.3.5 Mutation Screening: Restriction Enzyme Digest.

Analytical

Procedure

First, a PCR is performed as described in 8.2.3.2 Polymerase Chain Reaction. The product is then digested by mixing 1.5 µl of 10× enzyme reaction buffer, 8.5 µl water, 1 – 5 U enzyme and 5 µl PCR product.

The reaction is incubated for an appropriate time (usually overnight) at an appropriate temperature in a water bath. The result is visualised by agarose gel electrophoresis. A 12-µl volume of the reaction mixture is loaded onto a 2 – 3% agarose gel (higher agarose concentration for resolution of smaller fragments).

8.2.3.6 Cycle Sequencing of PCR-Amplified Genomic DNA with Universal Primers

Principle

Cycle sequencing is a modification of the traditional Sanger sequencing method. In 1977 Sanger developed a method to determine the sequence of bases in cloned DNA fragments [17]. In the original method, DNA extension is initiated at a specific site on the template DNA by using a single oligonucleotide primer complementary to the template at that position. The oligonucleotide primer is extended using a DNA polymerase, the four nucleotides, and a low concentration of a chain-terminating nucleotide: a di-deoxynucleotide of A, C, G or T. Limited incorporation of the chain-terminating nucleotide by the DNA polymerase results in a series of related DNA fragments that are terminated only at positions where that particular nucleotide (A, C, G or T) is present in the sequence. The fragments are then size-separated by electrophoresis in polyacrylamide gel, or more commonly now, in a capillary tube filled with a specific polymer. In the original method, the nucleotide order of a particular DNA template can be inferred by performing the four parallel extension reactions using one of the four chain-terminating bases in each reaction. The DNA fragments are detected by labelling the primer with a radioactive isotope or by using fluorescent dye-labelled primers. The latter has the advantage of avoiding the need for radioactivity and also that the four reactions can be combined and run in a single gel lane or capillary if the fluorescent colours can be distinguished. This approach is known as "dye primer sequencing".

More consistent results are obtained when the terminators are labelled instead of the primers, a method commonly known as "dye terminator sequencing". The complete sequencing experiment can be performed in a single reaction, instead of four single reactions, by labelling each of the dideoxynucleotide chain terminators with a separate fluorescent dye. The most commonly used method today is "dye terminator cycle sequencing". The key difference is that cycle sequencing employs a thermostable DNA polymerase that can be heated to 95°C and still retains activity. The advantage of using such a polymerase is that the sequencing reaction can be repeated over and over again in the same tube by heating the mixture to denature the DNA and then allowing it to cool to anneal the primers and polymerise new strands. Thus, less template DNA is needed than for conventional sequencing reactions. Hence, there is no need for molecular cloning of the DNA fragments and PCR products can be used almost directly.

For both dye primer and dye terminator cycle sequencing, a universal primer can be used if the appropriate recognition sequence is incorporated into the PCR product during the amplification reaction. This is easily achieved with PCR primers that contain an additional 17 – 20mer tail corresponding to the universal primer. Two different universal sequences and accordingly two different PCR primer tails are necessary for sequencing in the forward and reverse directions. Cycle sequencing with universal primers has become widely used, helped by significantly reduced primer costs and increased reliability of synthesising 40mer oligonucleotides.

Pre-Analytical

Specimen

Universal recognition sequences must be present in PCR products that are cycle sequenced with universal primers. Many laboratories routinely use universal M13 and M13 reverse tails for their forward and reverse PCR primers, respectively. We have opted for the M13 (but not M13 reverse) sequence in conjunction with a P172 sequence derived from the Bluescript SK vector. The choice of universal primers was influenced by their estimated free energy of annealing and their melting temperature [3]. The DNA sequence is incorporated as 5'-tail into the initial PCR primers, as follows:

1. M13: 5'-GTAAAACGACGGCCAGT-specific forward sequence.
2. P172: 5'-TATAGGGCGAATTGGGT-specific reverse sequence.

PCR product has to be purified before sequencing. In general, any method that removes dNTPs and primers should work. A range of kits for spin column purification or other methods are commercially available for this purpose. Poor template quality is the most common cause of sequencing problems. The use of poor-quality templates leads to noisy data or peaks under peaks, weak signals or completely unusable sequence data. The quality of the DNA can be checked by running the product on an agarose gel (see 8.2.3.3 Agarose Gel Electrophoresis). The product should have the correct size and intensity. Additional bands should be completely absent. It is recommended to use 150 – 300 ng per sequencing reaction.

Reagents and Chemicals

Universal M13 and P172 primers without the specific forward or reverse sequences are used for cycle sequencing if the respective sequences were introduced in the initial PCR reaction. For sequencing of genomic DNA up to 500 bp we recommend the BigDye Terminator v1.1 Cycle Sequencing Kit by Applied Biosystems. The kit contains premixed reagent components and requires the addition of purified PCR product and universal sequencing primer.

Other reagents:

1. PCR product purification kit (see 8.2.3.6 Cycle Sequencing of PCR-Amplified Genomic DNA with Universal Primers, subheading "Specimen").
2. Ethanol.
3. 3 M Sodium acetate, pH 5.2.
4. Hi-Di formamide (Applied Biosystems).
5. Dilution buffer for the Big-Dye terminator (Applied Biosystems).

Instrumentation

A thermal cycler (see 8.2.3.2 Polymerase Chain Reaction) is required for the cycle sequencing reaction. For fluorescent cycle sequencing we recommend instruments from Applied Biosystems (e.g. the 16-capillary ABI PRISM 3100 Genetic Analyser); other instruments are available from GC Healthcare and Beckman. For detailed instructions, refer to the respective user's manual or chemistry guide.

Calibration

Prior to the analysis, a matrix has to be generated. For detailed instructions, refer to the respective user's manual or chemistry guide. To analyse sequencing data generated with BigDye Terminator v1.1 one needs dye set/primer (mobility) files that were created for v1.0 chemistries. The dye set/primer (mobility) files for this chemistry can be downloaded from the Internet: http://www.appliedbiosystems.com/support/software.

Quality Control

None.

Analytical

Procedure

The sequencing reactions with BigDye Terminator v1.1 are set up are given in Table 8.2.7. Typical conditions for cycle sequencing are: 25 cycles of denaturation at 94 C for 30 s, Annealing at 54 – 60 C for 15 s, and extension at 60 C for 4 min.

Cycle sequencing products need to be purified, for example by ethanol precipitation prior to loading onto the sequencer. For this purpose, 80 µl water and 10 µl of 3 M sodium acetate are added to each tube or well, and the DNA is precipitated with 250 µl of ethanol. Incubate for 15 min at room temperature and spin for 20 min at maximum speed. The supernatant is removed carefully and 250 µl of 70% ethanol is added. Spin again for 15 min at maximum speed. The pellet (unusually not visible) is air-dried and may be resolved, for example in 20 µl Hi-Di formamide for transfer to the sequencing instrument. For detailed instructions, refer to the respective user's manual or chemistry guide.

Calculation

The peak intensities are automatically converted to sequence data in all instruments.

Table 8.2.7 *Recipe for the sequencing reaction solution*

Ingredient	Volume	Final concentration
PCR product (purified; 150 – 300 ng)	1.5 –5 µl	15 – 30 ng/µl
Primer (2 pmol/µl)	2.0 µl	0.4 pmol/µl
Big-Dye dilution buffer (5×)	1.5 µl	0.75×
Big-Dye terminator	1.0 µl	160 nM
Taq polymerase	0.1 µl	0.25×
Water	0.5 – 4.0 µl	–

Post-Analytical

Homozygous DNA changes are easily recognised by a change in the letter sequence generated by the automated instrument. However, in order to reliably identify heterozygous single base changes it is important to assess the height and area of individual peaks. Heterozygous mutations are best recognised by a reduction of the normal wild-type peak height and area to approximately 50%; this may be more reliable than the identification of the mutant peak. Various software programmes are now available to assist in this task; most are quite expensive.

Interpretation

Cycle sequencing of PCR-amplified genomic DNA with universal primers recognises all DNA alterations confined to the sequence between the two PCR primers used for the initial amplification reaction. Other mutations, such as mutations involving the PCR primer sites or large genomic alterations, are not usually recognised.

8.2.3.7 Genomic Quantification: Multiplex Ligation-Dependent Probe Amplification

Principle

The methods described above are suitable for studying small mutations. A homozygous deletion of a large part of a gene may be recognised by non-amplification but duplications or heterozygous deletions usually remain undetected. In case of one deleted allele and one wild-type allele, there will only be product from the wild-type, resulting in apparent homozygosity, but in fact hemizygosity for the wild-type sequence. Hence, an additional method is required to exclude large rearrangements, deletions and duplications. In the past, quantitative Southern blotting and quantitative PCR have been used for this purpose. Unfortunately, the quantitative use of these methods is not reliable. Moreover, the use of radioactivity in Southern blotting is associated with a large number of time-consuming safety regulations.

Multiplex ligation-dependent probe amplification (MLPA) is a novel method for genomic quantification that is relatively uncomplicated, reliable and fast. With MLPA, it is possible to perform a multiplex PCR reaction with simultaneous quantitative amplification of up to 45 specific sequences. Amplification products, ranging in size from 130 to 490 bp, are separated on an automatic DNA sequencer (see 8.2.3.6 Cycle Sequencing of PCR-Amplified Genomic DNA with Universal Primers, subheading “Instrumentation”). Since only one pair of PCR primers is used, MLPA reactions result in a highly reproducible peak pattern that is compared between target and control samples. The principle is explained in Fig. 8.2.2. MLPA probes are able to discriminate between sequences that differ in only one nucleotide. Although virtually everyone can develop a custom MLPA test, most MLPA kits are developed and sold by MRC-Holland (http://www.mrc-holland.com). A list of commercially available MLPA kits can be found on their website.

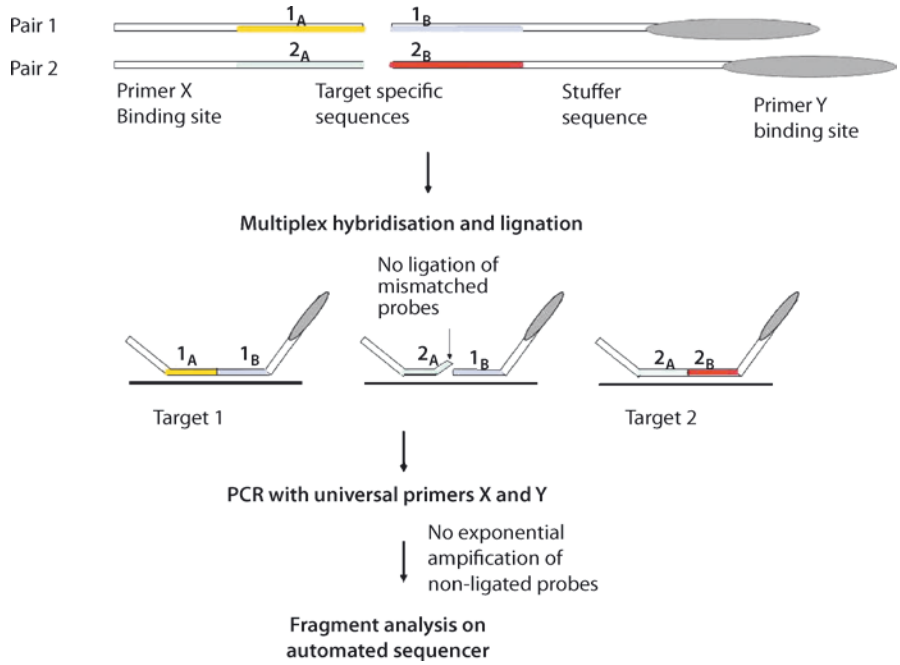

Fig. 8.2.2 Principle of genomic quantification by multiplex ligation-dependent probe amplification (MLPA). Synthetic oligonuleotides are designed to bind to exon 1 (oligo 1_A and 1_B) and 2 (2_A and 2_B). After specific hybridisation, the oligos are ligated. The ligation products undergo quantitative polymerase chain reaction using universal primers X and Y

Pre-Analytical

Specimen

DNA (see, for example, 8.2.3.2 Polymerase Chain Reaction). Some laboratories prefer to perform extra purification of the genomic DNA prior to MLPA [7]. It is not recommended to quantitatively compare DNA from different sources, such as different laboratories. The use of heparinised blood may cause a similar problem.

Reagents and Chemicals

A range of MLPA kits for various applications are commercially available by the inventors of the technique, MRC-Holland (http://www.mrc-holland.com). The "SALSA" reagents used in these kits include:

1. SALSA Probe Mix (the oligonucleotides).
2. MLPA Buffer.
3. Ligase-65 Buffer A.
4. Ligase-65 Buffer B.
5. Ligase-65 (heat-resistant ligase).
6. PCR buffer.
7. FAM primer.
8. Enzyme dilution buffer.
9. SALSA polymerase.

Not included are Hi-Di formamide (Applied Biosystems) and GS 500 ROX-Standard (Applied Biosystems).

Instrumentation

A thermal cycler (see 8.2.3.2 Polymerase Chain Reaction) is required for the cycle sequencing reaction. MRC Holland offers kits for different sequencing instruments. For more detailed instructions refer to the appropriate instrument user's manual. MLPA fragment analysis requires a fluorescent DNA analysis system. We recommend instruments from Applied Biosystems (e.g. the 16-capillary ABI PRISM 3100 Genetic Analyser); other instruments are available from GC Healthcare and Beckman.

Calibration

Fragment analysis requires different conditions compared to sequence analysis. Refer to the instrument manual for further details.

Quality Control

It is recommended to validate each kit using DNA samples with a known rearrangement.

Analytical

Procedure

In a thin-wall PCR tube, 100 ng of DNA is diluted in 5 µl of sterile water. In another tube, 1.5 µl SALSA probe mix is added to 1.5 µl MLPA buffer. The DNA tube is incubated in a thermal cycler at 98°C for 5 min and then cooled to 25°C (hold at this temperature). The premixed probe mix and buffer (3 µl) are added to the DNA without taking the DNA out of the cycler. The mixture is incubated at 95°C for 1 min. followed by incubation at 60°C for 16 h (hybridisation).

The next day, the ligase mix is prepared by adding 3 µl ligase-65 buffer A, 3 µl ligase-65 buffer B, 25 µl water and 1 µl ligase-65. The mixture has to be mixed well without vortexing. It can be kept on ice for maximally 1 h. The thermocycler is cooled to 54°C prior to adding 32 µl of ligase mix to each tube (do not take the tubes out of the cycler). After mixing, the samples are incubated at 54°C for another 15 min (ligation). After a final incubation at 98°C for 5 min, the ligation products can be stored at 4°C.

Finally, PCR is performed. First, one has to prepare the buffer mix (26 µl water and 4 µl PCR buffer) and the polymerase mix (2 µl FAM-primer, 2 µl Enzyme dilution buffer, 5.5 µl water and 0.5 µl SALSA polymerase). Both mixes are mixed well without vortexing and kept on ice. In a PCR tube, 30 µl of buffer mix is added to 10 µl of ligation product. This is preheated at 60°C in the thermocycler. A 10-µl volume of polymerase mix is added to each tube at 60°C ("hot start"). The PCR conditions are: 36 cycles of 95 C for 30 s and 60 C for 30 s, and final extension at 72 C for 1 min then hold at 4 C.

After PCR, 1.0 µl PCR product is mixed with 8.5 µl Hi-Di formamide and 0.5 µl GS 500 ROX-Standard (Applied Biosystems). The mixtures are loaded on an appropriate automated sequencer. The sequence run is performed as described in the manual.

Calculation

The peak intensities are calculated automatically. The sizes of the detected fragments are automatically determined using an internal standard.

Post-Analytical

Interpretation

We developed an algorithm for comparing peak areas that can be applied using an Excel spreadsheet. For each peak in each sample the relative peak area (RPA) is determined (i.e. the individual peak area in relation to the total of all peak areas in the sample). The mean RPA in three (usually male) control samples is determined for each fragment/exon and taken as 100%, corresponding to the normal "expected value" when no deletion or duplication is present. Standard deviations of these controls are calculated to assess the variability of the results and thus the quality of the run. For the analysis of the test samples (patients), the RPA value of each peak is compared to the mean RPA of the control samples, resulting in a percentage value denoted "RPA ratio" (norm per definition 100%). The standard deviation of single peaks should not exceed 25% to ensure reliability of the run. To minimise the risk of false-negative results and to increase the sensitivity for the detection of deletions or duplications, the results in a test sample are considered normal and reliable when the individual RPA ratios deviate by no more than 25% from the expected ratio (i.e., all RPA ratios range closely around the expected ratio of 100%). Repeated analysis is necessary when these criteria are not fulfilled.

Pitfalls

Identified deletions and duplications can be regarded reliable when they involve two or more adjacent exons. Apparent single-exon deletions are to be examined further by sequencing of that exon, to exclude polymorphic variation at the oligonucleotide binding site.

8.2.4 Follow-Up Assays

DNA studies aim to provide ultimate proof of a disease in a patient with an inherited metabolic disorder and should not usually lead to follow-up assays. Indeed, enzyme assays and other functional studies are often easier, cheaper and have a higher sensitivity than molecular studies. When possible, enzyme assays should be performed prior to the DNA test. As always: exceptions prove the rule.

References

1. Bhagwat AS (1992) Restriction enzymes: Properties and use. Methods Enzymol 216:199–224
2. Davidow LS (1992) Selecting PCR designed mismatch primers to create diagnostic restriction sites. Comput Appl Biosci 8:193–194

3. DeBellis G, Manoni M, Pergolizzi R, Redolfi ME, Luzzana M (1992) A more stringent choice of primers can improve the performance of fluorescent automated DNA sequencers. BioTechniques 13:892–897
4. Fischer SG, Lerman LS (1983) DNA fragments differing by single base-pair substitutions are separated in denaturing gels: correspondence with melting theory. Proc Natl Acad Sci U S A 80:1579–1584
5. Goldstein DB (2001) Islands of linkage disequilibrium. Nat Genet 29: 217–222
6. Haliassos A, Chomel JC, Tesson L, Baudis M, Kruh J, Kaplan JC, Kitzis A (1989) Modification of enzymatically amplified DNA for the detection of point mutations. Nucleic Acids Res 17:3606
7. Janssen B, Hartmann C, Scholz V, Jauch A, Zschocke J (2005) MLPA analysis for the detection of deletions, duplications and complex rearrangements in the dystrophin gene: potential and pitfalls. Neurogenetics 6:29–35
8. Jiang W, Kahn SM, Guillem JG, Lu SH, Weinstein IB (1989) Rapid detection of ras oncogenes in human tumors: applications to colon, esophageal, and gastric cancer. Oncogene 4:923–928
9. Kogan SC, Doherty M, Gitschier J (1987) An improved method for prenatal diagnosis of genetic diseases by analysis of amplified DNA sequences. New Engl J Med 317:985–990
10. Kumar R, Dunn LL (1989) Designed diagnostic restriction fragment length polymorphisms for the detection of point mutations in ras oncogenes. Oncogene Res 1:235–241
11. Lerman LS, Silverstein K (1987) Computational simulation of DNA melting and its application to denaturing gradient gel electrophoresis. Methods Enzymol 155:482–501
12. Maxam AM, Gilbert W (1977) A new method for sequencing DNA. Proc Natl Acad Sci USA 74:560–564
13. Miller SA, Dykes DD, Polesky HF (1988) A simple saltung out procedure for extracting DNA from human nucleated cells. Nucleic Acids Res 16:1215
14. Mullis KB, Faloona FA (1987) Specific synthesis of DNA in vitro via a polymerase-catalyzed chain reaction. Methods Enzymol 155:335–350
15. Myers RM, Fischer SG, Lerman LS, Maniatis T (1985) Nearly all single base substitutions in DNA fragments joined to a GC-clamp can be detected by denaturing gradient gel electrophoresis. Nucleic Acids Res 31:3131–3145
16. Myers RM, Lumelsky N, Lerman LS, Maniatis T (1985) Detection of single base substitutions in total genomic DNA. Nature 313:495–498
17. Rosenbaum V, Reissner D (1987) Temperature gradient electrophoresis. Thermodynamic analysis of nucleic acids and proteins in purified form and in cellular extracts. Biophys Chem 26:235–246
18. Saiki RK, Scharf S, Faloona F, Mullis KB, Horn GT, Erlich HA, Arnheim N (1985) Enzymatic amplification of β-globin genomic sequences and restriction site analysis for diagnosis of sickle cell anemia. Science 230:1350–1354
19. Sanger F, Nicklen S, Coulson AR (1977) DNA sequencing with chain-terminating inhibitors. Proc Natl Acad Sci U S A 74:5463–5467
20. Sheffield VC, Cox DR, Lerman LS, Myers RM (1989) Attachment of a 40-base-pair G + C-rich sequence (GC-clamp) to genomic DNA fragments by the polymerase chain reaction results in improved detection of single–base changes. Proc Natl Acad Sci U S A 86:232–236
21. Smith HO, Wilcox KW (1970) A restriction enzyme from Haemophilus influenzae I. Purification and general properties. J Mol Biol 51:379–391
22. Watson JD, Crick FH (1953) Molecular structure of nucleic acids: a structure for deoxyribose nucleic acid. Nature 171:737–738

Subject Index

D

E

F

H

M

N

O

P

Q

R

S

T